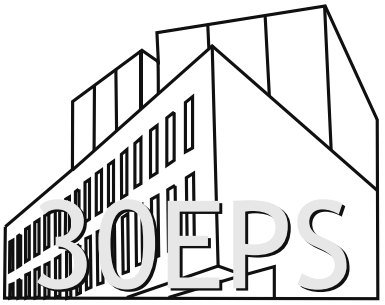

Peptides 2008

Chemistry of Peptides in Life Science Technology and Medicine

Proceedings of The Thirtieth European Peptide Symposium

Edited by
Hilkka Lankinen

Jari Vallivirta
Tomas Strandin
Jussi Hepojoki

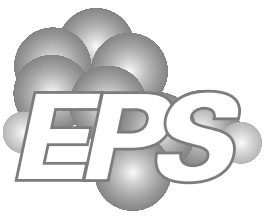

ISBN 978-952-92-7697-4 (paperback)
ISBN 978-952-92-7698-1 (PDF)

Published for The Finnish Peptide Society and the European Peptide Society

Layout and Cover design by Timo Päivärinta PSWFolders Ltd. Editing assistance by Jari Vallivirta, Tomas Strandin and Jussi Hepojoki Peptide and Protein Laboratory, Haartman Institute. Manuscripts collected by CONGREX / Blue & White Conferences Oy using Abstractlogic®

Produced in Finland

Page layout in Finland by Hilkka Lankinen and Sirpa Eskolin (Helsinki University Press)

Preface

The Thirtieth European Peptide Symposium (EPS) was arranged under the auspices of the European Peptide Society (EPS) by the Finnish Peptide Society (FIPS) in Finlandia Hall Helsinki Finland 31 August – 5 September) and preceded by the Cell Penetrating Peptides CPP) Minisymposium at Biomedicum Helsinki (30-31 August) arranged under the auspices of the European CPP network. The scientifically high esteem symposium of peptide science chemistry and technology was provided in 29 named sessions of the main symposium and its satellite meeting including 20 invited speakers 120 speakers selected from submitted abstracts and a display of 500 scientific posters. The Peptides 2008 publishes now 333 Submitted papers which base either on 39 oral or poster presentations at 30th EPS constituting The Proceedings of the Thirtieth European Peptide Symposium. In association of Peptides 2008 a few of the presentations are published also as videos (www.30eps.fi, www.pepsoc.com).

Previous publications and articles related to 30th EPS

1. 30th EPS Abstract book J. Pept. Sci. 2008 14: 8 Suppl.
2. Cell Penetrating Peptides Minisyposium Abstract book
3. Microwave Assisted Synthesis lunch session CEM Corporation.
4. The European Peptide Society Newsletter 2008 Number 38
5. The European Peptide Society Newsletter 2008 Number 39
6. The American Peptide Society Newsletter 2008 Volume 5 Number 2
7. Chemistry Today 2008 Volume 26 Number 5 Suppl.
8. Chemistry Today 2008 Volume 26 Number 6
9. Peptide societies homepage www.pepsoc.com

Scientific programme

The *European Peptide Society* honoured the life work of late Professor Dr. *Miklós Bodanszky* (1915-2007). A session dedicated to his memory included presentations provided by former students and collaborators: Professor *Jean Martinez* (Max Mousseron Biomolecule Institute (IBMM) CNRS Montpellier France) Chairman of the European Peptide Society, Distinguished professor *Sami I. Said* (Stony Brook School of Medicine New York U.S.A.), Dr. *Maria Bednarek* (Merck Research Laboratories U.S.A.), Professor *Peter Schiller* (Clinical Research Institute of Montreal Canada) and Dr. *John Tolle* (Abbot Laboratories U.S.A.). Professor *Ferenc Hudecz (*Eötvös Loránd University Budapest Hungary) Secretary of the European Peptide Society provided respects of fellow Hungarians.

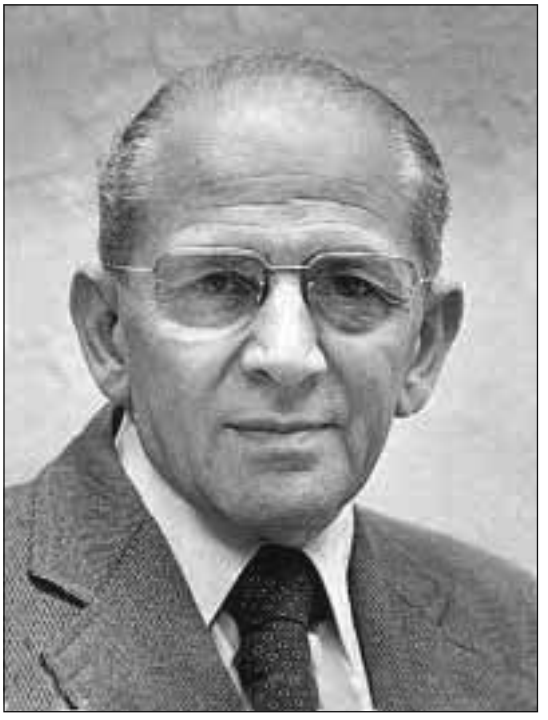

Professor Dr. *Miklós Bodanszky*

"As a lifelong friend and during my years in Cleveland's Case Western Reserve University a faculty colleague of Miklós Bodanszky I had close knowledge of his pioneering work in peptide chemistry.
He was also an exceptional human being and a true renaissance man. I wish you much success with your Symposium Session dedicated to his memory!

George Olah
Nobel laureate in Chemistry"

Professor Dr. Miklós Bodanszky

Professor ***Miklós Bodanszky*** a chemist one of the forefathers of modern peptide science died on February 7th 2007 in Princeton NJ. He made significant contributions to the file of peptide chemistry peptide antibiotic synthesis and process research. Dr. Bodanszky introduced new methods for the synthesis of peptides and small proteins with a broad variety of biological activities. He devised a new strategy now widely accepted for the construction of peptide chains from their building components and applied it in the synthesis of peptide hormones and their analogs: oxytocin vasopressin vasoactive intestinal peptide and secretin. He was the author of numerous scientific papers and of several books dealing with peptide chemistry. A native of Budapest Hungary Miklós Bodanszky received his doctorate at the Technical University of Budapest where he later became lecturer in medicinal chemistry. He left Hungary at the time of the 1956 uprising and came to the United States to join Professor V. du Vigneaud in the Department of Biochemistry at Cornell University Medical College in New York City. Subsequently he formed and led a peptide research group at the Squibb Institute for Medical Research. From 1966 until his retirement in 1983 he taught at Case Western Reserve University in Cleveland Ohio where he was the Charles Frederic Mabery Professor of Research in Chemistry. He was the first recipient of the Alan Pierce Award (now the Merrifield Award) was honored by scientific societies in the U.S. and abroad and was named a foreign member of the Hungarian Academy of Sciences. After retirement he returned to Princeton N.J. where he continued to contribute to the literature of peptide chemistry. His wife *Agnes* who was also his coworker and frequent coauthor died in 1989. He is survived by his daughter Dr. *Eva Bodanszky. J. Pept. Sci. 2008 14: 8 Suppl.*

Presentations

Professor *Kristina Luthman* (University of Uppsala Sweden) opened the "*Highlights of synthetic chemistry"* session with a textbook repertoire of know-how in inspired *"Design synthesis and use of scaffold based peptidomimetics. Conjugation Ligation and Combinatorial chemistry"*.

Professor *Kaarina Sivonen* (University of Helsinki Finland) in "*Natural peptides"* brought into attention the genetic classification and environmental importance of microbial peptide toxins in *"Biosynthesis of cyanobacterial peptide toxins"*.

Professor *Andreas Plückthon* (University of Zürich Switzerland) in "*Biochemistry of peptides*" treated peptide chemists with "*Design of a new protein domain scaffold derived from armadillo repeats"* and Professor *Anette Beck-Sickinger* (University of Leipzig Germany) with complexity of G protein coupled receptors in *"GPC-Receptors not Ligands Decide on Binding Mode in Multi-Receptor/Multi-Ligand Systems*".

Dr. Waleed Danho (The American Peptide Society) introduced "*Peptides as drugs"* to formulation and together with colleagues had calculated a good transition rate for peptides in drug research and development he encouraged to think about protein-protein interactions and metabolic drugs in front of *the next APS meeting in Indianapolis* (July 2009). Professor *Robin Offord* (Mintaka Foundation of Medical Research Université de Genève Switzerland) was directing minds to biotechnology plants as the economical peptide material mass production pipe line: "*Can biotherapeutics ever be cheap enough for developing countries? Anti-HIV chemokines as a case study*".

Professo*r Chris Dobson* (University of Cambridge U.K.) in "*Protein misfolding and amyloid disease"* associated formation of amyloid deposit into an inherent physiological balance in his excellent lead "*Life on the Edge: The Nature and Origins of Protein Misfolding Diseases"*. Professor *Andrew Miranker* (Yale University United States) discussed the capacity of proteins to self-associate in "*Elucidating molecular mechanisms on and off the pathway to amyloid deposition"*. Professor *Joachim Seelig* (University of Basel Switzerland) enlightened thermodynamics of model peptides in membranes: "*Alzheimer Peptides. The membrane-induced random coil-to-β-structure transition"* and Professor *Ernest Giralt* (Institute for Research of Biomedicine Barcelona Spain) potentials of peptide drugs in amyloid disease in "*Retro-Enantio N-Methylated Peptides as β-Amyloid Aggregation Inhibitors"*. Professor *Paul Axelsen* (University of Pennsylvania U.S.A.) brought in *"Peptide-lipid interactions"* lipid chemistry into the fore front of protein misfolding in the brains in "*Oxidatively stressed lipids and polypeptide misfolding in human disease"*. The different facets of the amyloidosis were discussed by chairmanship of Professor *Brian Austen* (University of London U.K.) who by support of Professor Paavo Kinnunen (University of Helsinki) challenged amyloidosis hypothesis and efficacy of available drugs.

In "*Peptide Materials"* Professor *Ehud Gazit* (Tel Aviv University Israel) extrapolated self assembling peptides to *Nanotechnology*. Enzyme catalysis was brought into the attention by several speakers as a viable parallel to chemical biology. Professor *Morten Meldal´*s (Carlsberg Laboratory Denmark) organizing board of 31st EPS thatched upon metalloprotein mimicry of catalysis in *"Solid phase peptide-carbene and peptide-phosphine transition metal catalysts in asymmetric synthesis and "Green" chemistry"*.

Professor *Gianni Cesareni´*s (University of Rome Tor Vergata Italy) in "*Systems biology"* discussed phosphoproteome in "*Profiling SH2 and tyrosine phosphatases target specificity"*.

Professor *Per Andrén* (University of Uppsala Sweden) in "*Analytical peptide chemistry"* raised hopes for tissue section diagnostics in *"Frontier and Perspectives – Specific and Sensitive Identification of Peptides Using Peptidomics and MALDI"*.

The CPP satellite symposium including leading experts in the field provided in 33 oral presentations the puzzles of cell penetration in delivery root membrane chemistry structure-activity vector delivery cell targeting and tissue homing aspects. Professor *Alain Prochiantz* (CNRS France) was in origins of biology in his presentation by title "Homeoprotein transduction in the development and physiology of the visual system".

Peptides 2008 Awards

The prestigious *Josef Rudinger award* was shared between Professor Dr. h.c. *Horst Kessler* Technical University of Munich Germany and Professor Dr. *Manfred Mutter* University of Lausanne Switzerland.

The highly respected *Leonidas Zervas* award was given to Professor *Anna Maria Papini* University of Florence Italy.

The Chairman of the European Peptide Society and the President of European Peptide Society Executive Committee *Jean Martinez* provided the *Award Medals and Diplomas* (the official award statements are available from EPS).

Peptides 2008 Awards were a victory to the avant-garde of structure-activity peptide chemistry in transition to modern age. The local organizers wish to congratulate the recipients for the awards and for the excellent award lectures (to be published).

The Young investigator minisymposium was applied by 43 speakers and 16 speakers preselected at the 30th EPS *Scientific Committee April Meeting* in Helsinki were attending the competition. Over 80 posters entered to the *Young investigators poster competitions* and an international committee of 26 senior peptide chemists interviewed the young investigators.

The Bert L. Schram award recipients were *Carlos Mas-Moruno* University of Barcelona Spain and *Carine Bourget* Université de Montréal Canada.

The Bert L. Scram diploma was provided to *Mattan Hurevich* The Hebrew University of Jerusalem Israel and *Dieter Verzele* Ghent University Belgium.

The Bert L. Scram poster award recipients were *Thomas Knappe* Philipps-University Marburg Germany and *Aviad Levin* The Hebrew University of Jerusalem Israel.

The Thieme Chemistries best chemistry poster award recipient was *Taku Yoshiya* Kyoto Pharmaceutical University Japan.

Many congratulations to all Peptides 2008 award recipients!

The *Sponsors* are acknowledged for continuous support and for sharing the peptide symposium by personal presence. Our special gratitude goes to the PolyPeptide Laboratories and the Bachem. The Josef Rudinger award price to Horst Kessler and Manfred Mutter were handed by Dr. *Mikael Verlander* The PolyPeptide Laboratories. The Leonidas Zervas price check to Anna Maria Papini was handed by Dr. *Dick Fritz* Bachem.

Organizers wish to thank the ESCOM Foundation and the Thieme Chemistries and the scientific committee and judges for providing valuable resources and time for the young investigator competitions. The diplomas to all recipients were provided by Prof. *David Andreu* the Scientific Officer of EPS. The ESCOM prices were given by *Dr. Elizabeth Schram* president of ESCOM foundation and *Dr. Hans Pohlman* board member. The young investigator competitions were organized by Dr. Ale Närvänen.

We also wish to thank CEM corporation for her special input as well as all who by investments supported the event (provided in separate). The forty *Exhibitors* of leading European none-European and multinational providers (listed in separate) of instruments accessories reagents and services in peptide synthesis separation techniques analytical peptide chemistry custom synthesis discovery publishing education and promotion of peptide and protein science and technology including up-coming meetings are acknowledged for all contributions to 30EPS.

A successful symposium could not be without *the participants*. The participation at 30EPS and its satellite meeting had a relatively even region wise distribution from Nordic-Baltic Mediterranean East-European Central-European and West-European countries representing altogether 32 countries (including in frequency of attendance Germany Finland Switzerland Italy France Poland U.K. Israel Sweden Spain Belgium Greece Russian Federation Hungary Greece Denmark The Netherlands Czech Republic Bulgaria The Netherlands Turkey Portugal Latvia Slovenia Austria Romania Belarus Ukraine Serbia Ireland Croatia and Slovekia). A traditional participation interest by the International peptide societies was included in attendances coming from 14 countries (Australia Canada Chile China Rep. Brazil India Iran Japan Korea Rep. New Zealand Singapore Taiwan U.S.A.). The academy based interest was of 65% and the 35% represented the industrial and company based participant registrations. The attendants from universities research institutes and companies outside Europe contributed to about 20% of the total attendance. The company representations from the U.S.A. and active attendance by the Japanese peptide chemistry research groups had greatest single effect.

Participation by the distinguished two former chairmen of the European Peptide Society Professor *Dietrich Brandenburg* Germany (1992-1998) and Professor *Raniero Rossi* Italy (1998-2002) is gratefully acknowledged.

Professor *Ferenc Hudecz* received as recognition the *European Peptide Society medal* for his long term of services of the Society given by the Executive Committee. We wish to congratulate him for successful fulfilment of high EPS officer duties. Professor *Inta Liepina* Latvia (council 2006-2008) and Professor *Chaim Gilon* Israel (council 2002-2008 and co-organizer of 28th EPS) were recognized for their services of EPS many congratulations. *The Council meeting* was held in a high attendance rate by the councillors at the Helsinki University Museum Arppeanum in former auditorium of the Chemistry Department (up to 1972) The Council dinner was served at the former Department of Geology premises in the Emperor´s Room surrounded by portraits of the Russian tsars (the first governors of Helsinki University). *The Peptide Societies Liaison meeting* was arranged at Finlandia Hall for interaction of representatives of sister societies (The minutes provided are available at peptide societies).

The *EPS contributed to travel grants* of forty scientists at 30th EPS supporting especially the attendance of young scientist.

The *Scientific committee of 30th EPS* is gratefully acknowledged for vigorous input to make the symposium to a success long before during and after the event. We are grateful to the *Local organizing committee* for giving the wide scope to the programme by suggestions of speakers and wish to thank the invited speakers and the chairs for their valuable contributions. The excellent performances throughout the symposium in preparation and during the 30EPS have been most fruitful we wish to congratulate all for a good symposium. In making of the Peptides 2008 we aim to provide you again the rewarding science exchange which characterizes EPS.

Hilkka Lankinen

On behalf of the 30th European Peptide Symposium

Sponsors

Awards
The Polypeptide Laboratories Josef Rudinger Award
The Bachem Leonidas Zervas Award
The ESCOM Science Foundation Young investigator oral and poster awards
Thieme Chemistries Young investigator poster award

Gold sponsors
The Polypeptide Laboratories symposium bags
CEM Microvawe Assisted Synthesis session

Silver sponsors
Almac Sciences U.K.
Genzyme Pharmacyticals Switzerland

Bornze sponsors and donations
Lonza Switzerland
Peptisyntha
Merck Chemicals

BCN peptides S.A. stationaries

Educational sponsors and travel grants
The European Peptide Society
The Journal of Peptide Science
The Helsinki Biomedical Graduate School
The Helsinki Graduate School in Biotechnology and Molecular Biology
Mark Cava and RSPAmino Acids
The Societas Biochemica Biophysica et Microbiologica Feannie

Media sponsors
EPS Newsletter
EPS homepage and EPS bulletin
Sister society Newsletters
Journal of Peptide Science
Thieme Chemistries
Bentham Science
Journal of Proteome
Chemistry Today
Peptides Net

Social events
Bachem and Senn Chemicals football accessories
Helsinki City city reception

The Finnish Peptide Society

Antti Vaheri Professor (Emeritus) of Virology University of Helsinki presented "*The 20 years of synthetic peptides in Finland"*. In his vivid presentation of the history from the early days referring among others to his co-identifier of fibronection *Erkki Ruoslahti* (Distinguished Professor in Biological Sciences University of California Santa Barbara U.S.A.) he listed a number of important findings to which synthetic peptides had an impact. The first international peptide meeting was attended by a long list of leading peptide scientists at Aulanko Finland in 1989. The Nobel Price awarded to Professor *Bruce R. Merrifield* in 1984 was highly appreciated as was his visit to Helsinki at the award receiving occasion.

Figure 1. *The founding meeting of the Finnish Peptide Society.* Tuomas Heiskanen Erkki Koivunen Hilkka Lankinen Ale Närvänen Tiina Pessa-Morikava Carl G. Gahmberg Carmela Kantor-Aaltonen Antti Vaheri Jorma Hermonen. Department of Biochemistry University of Helsinki (from left to right portrait of A.I. Virtanen at the back).

The Finnish Peptide Society was founded at the *Department of Biochemistry* University of Helsinki in 1997 as the peptide division of the *Societas Biochemica Biophysica et Microbiologica Fenniae.* The visits of Professor *Günter Jung* of Tübingen to Finland at mid 1990´s to become member of European Peptide Society are highly appreciated. Finland joined EPS in 2002 and as a new member was offered to arrange the 30th EPS (2008). The European Peptide Society colleagues in Finland especially at Helsinki University University of Kuopio and Perkin Elmer Wallac Turku were important for formative years of Finnish Peptide Society which organizes biannual meetings and collaborates with Graduate Schools.

Exhibitors

Company/Organization	Country
AAPPTec	UNITED STATES
Activotec	UNITED KINGDOM
AkzoNobel / Kromasil	SWEDEN
Almac Sciences	UNITED KINGDOM
Alta Bioscience	UNITED KINGDOM
American Peptide Company Inc.	UNITED STATES
Applied Biosystems	FINLAND
American Peptide Society	SWITZERLAND
Bachem AG	SWITZERLAND
BCN Peptides S.A.	SPAIN
C S Bio Co.	UNITED STATES
C. A. T. GmbH & Co KG	GERMANY
CBL Patras S.A.	GREECE
CEM Corporation	UNITED STATES
Covidien	UNITED STATES
CPC Scientific Inc.	UNITED STATES
CreoSalus	UNITED STATES
EPS 2010	DENMARK
Genzyme Pharmaceuticals	SWITZERLAND
Grace Davison Discovery Sciences	BELGIUM
Helsinki Biomedical Graduate School	FINLAND
INTAVIS AG	GERMANY
IRIS Biotech GmbH	GERMANY
Japanese Peptide Society	JAPAN
John Wiley & Sons Ltd.	UNITED KINGDOM
Jupiter Bioscience Limited	INDIA
LivChem GmbH & Co. Kg	GERMANY
Lonza	SWITZERLAND
Luxembourg Bio Technologies	ISRAEL
Merck Chemicals Ltd.	UNITED KINGDOM
NeoMPS	FRANCE
Peptisyntha SA	BELGIUM
PharmaChem / B5 srl	ITALY
Phenomenex	UNITED STATES
Polymer Laboratories Ltd. / Varian Inc.	UNITED KINGDOM
PolyPeptide Laboratories / NeoMPS	DENMARK
Polypure As	NORWAY
Protein Technologies Inc.	UNITED STATES
Rapp Polymere GmbH	GERMANY
Reanal Finechemical Private Ltd.	HUNGARY
Senn Chemicals	SWITZERLAND
Thermo Fisher Scientific Oy	FINLAND
Tianjin Nankai Hecheng S&T Co. Ltd.	CHINA
YMC Europe GmbH	GERMANY

The European Peptide Society

The Executive committee (2008)

Jean Martinez (University Montpellier France) Chairman
Ferenc Hudecz (Eötvös Loránd University Hungary) Secretary
Ettore Benedetti (University of Naples "Federico II" Italy) Treasurer
David Andreu (DCEXS-UPF-PRBB Barcelona Spain) Scientific Affairs Officer
Alex N. Eberle (University Hospital Basel Switzerland) Member

Figure 2. The Executive committee at the 30th European Peptide Society council meeting in Helsinki 2008. **From left to right:** Alex N. Eberle (Member) Ettore Benedetti (Treasurer) Jean Martinez (Chairman) David Andreu (Scientific Affairs Officer) Ferenc Hudecz (Secretary).

Acknowledgements of EPS. Certificates were provided at the opening ceremony for service as Council members to Inka Liepina, Latvia (2006-2008) and Chaim Gilon, Israel (2002-2008). Professor Ferenc Hudecz received as recognition the European Peptide Society medal for his long term of services of the Society given by the Executive Committee.

The Council 2006-2008

Ahorn. Horst J.	AUSTRIA
Austen Brian	UNITED KINGDOM
Bienert Michael	GERMANY
Cordopatis Paul	GREECE
Pristovsek Primoz	SLOVENIA
Eberle Alex N.	SWITZERLAND
Gilon Chaim	ISRAEL
Giralt Ernest	SPAIN
Hoeg-Jensen Thomas	DENMARK
Ivanov Vadim	RUSSIA
Lankinen Hilkka	FINLAND
Lavielle Solange	FRANCE
Liepina Inta	LATVIA
Penke Botond	HUNGARY
Maia Hernáni L. S.	PORTUGAL
Izdebski Jan	POLAND
Baltzer Lars	SWEDEN
Zeman Michael	SLOVAKIA
Rekaï El Djouhar	BELGIUM
Rekdal Øystein	NORWAY
Schaaper Wim	THE NETHERLANDS
Slaninová Jiřina	CZECH REPUBLIC
Toniolo Claudio	ITALY
Tourwe Dirk (retiring)	BELGIUM
Trusova Valeriya	UKRAINE
Tuscherer Gabrielle	SWITZERLAND
Vezenkov Lyubomir	BULGARIA
Vranešiæ Branka	CROATIA

The European Peptide Society Newsletter
Editor Paul Cordopatis University of Patras Greece

Journal of Peptide Science
Editor-in-chief Luis Moroder Germany

Liaison Committee Meeting

The Executive Committee of EPS

Dr. *Thomas Hoeg-Jensen* (Novonordisk)
Organizing board of 31st EPS (2010 Copenhagen)

The American Peptide Society
Robin Offord (Université de Genève Switzerland) Secretary
Ernst Giralt (Biomedical Research Institute Barcelona Spain) Council
Emanuel Escher (University of Sherbrooke Canada) Co-chair of 20th APS
Waleed Danho (Hoffmann-La Roche Inc. Discovery Chemistry New Jersey U.S.A.)
Victor Hruby (University of Arizona U.S.A.)
Felicia Etzkorn (Virginia Tech U.S.A.)

The Japanese Peptide Society
Yosiko Kiso (Kioto Pharmacytical University) Chairman
Organizer of 5th International Peptide Symposium (2010 Kioto)
Masahiko Sisido (Okayama University) Trustee (Scientific affairs)
Motoyoshi Nomizu (Tokyo University of Pharmacy and Life Sciences)

The Australian Peptide Society
John Wade (University of Queensland)

The Korean and Chinese Peptide Societies
Hahm Kyung-Soo (Chosun University Korean Rep.)
Chairman of the Korean Peptide Society

The affiliating Indian Peptide Society
V.S. Chauhan (International Centre for Genetic Engineering & Bio. New Delhi) Chairman

The scientific and travel awards committees

David Andreu Ettore Benedetti Ferenc Hudecz and *Jean Martinez* EPS
Krzysztof Rolka (University of Gdansk Faculty of Chemistry Poland) Organizer of 29th EPS
Morten Meldal (Carlsberg Laboratory SPOCC Centre Denmark) Organizer of 31st EPS
Hilkka Lankinen Ale Närvänen and Per Saris Organizers of 30th EPS

The local organizing committee

Ale Närvanen Ulf-Håkan Stenman and *Pirjo Laakkonen* (University of Helsinki Biomedicum Helsinki and University of Kuopio A.I.V. Institute)
Per Saris (University of Helsinki Dept. of Applied Chemistry and Microbiology Division of Microbiology)
Arto Annila Kai Fredrikson and *Ideo Hiwai* (University of Helsinki Dept. of Biochemistry and Dept. of Physics Inst. of Biotechnology NMR Laboratory)
Yegor Domanov and *Paavo Kinnunen* (University of Helsinki Helsinki Biophysics & Biomembrane Group)
Carl G. Gahmberg Erkki Koivunen Tanja-Maria Ranta and *Carmela Kantor-Aaltonen* (University of Helsinki Dept. of Biochemistry)
Pekka Mäntylä (University of Helsinki Dept. of Pharmacology)
Hilkka Lankinen Kalle Saksela and *Antti Vaheri* (University of Helsinki Dept. of Virology)
Marc Baumann (*Societas Biochemica Biophysica et Microbiologica Fenniae*).

Chairs of CPP symposium
*Pirjo Laakkonen (*Biomedicum Helsinki) Chairlady
Ülo Langel (University of Stockholm Sweden) Chairman
Bernard Lebleu (University of Montpellier France) Co-chairman

Chairs of 30th EPS
Hilkka Lankinen Chairlady
Ale Närvänen Chairman
Per Saris Treasurer

Judges of oral presentations: Per Saris, Jouko Vepsäläinen, Mårten Meldal, Krzysztof Rolka, Wim Schaaper and Ale Närvänen.

Poster competition judges: Brian Austen, Christian Becker, Gerardo Byk, Yegor Domanov, Ian Eggleston, Emanuel Escher, Kyung-Soo Hahm, Jari Hovinen, Vadim Ivanov, Knud Jensen, Annemieke Madder, Jason Moss, Robin Offord, Nathalie Olliver, Lazlo Otvos, Wolfgang Rapp, Paolo Rovero, Nuno Santos, Norbert Schaschke, John Wade, Tateaki Wakamiya, Erik Wallen, Jouko Vepsäläinen, Lubo Vezenkov, Alexander Zamyatnin and Ale Närvänen

EPS contributed to travel grants of 2x20 young scientists out of ~80 applicants at 30EPS.
The recipients were Antolikova, Emilia; Berliner, Karin; Claerhout, Stijn; Claudon, Paul; Cruska, Edson; Deschrijver, Tiny; Freeman, Noam; Gunasekera, Sunithi; Henrigues, Sonia; Hurevich, Mattan, Jimenez-Castells, Carmen; Kleczkowska, Patrycja; Knappe, Daniel; Kwiatkowska, Anna; Mas Moruno, Carlos; Meijneke, Tania; Pujals, Silvia; Ronga, Luisa; Sabidó Aguadé, Eduard; Valverde, Ibai; Bacsa, Bernadet; Bagheri, Moijtaba; Bonnard, Vanessa; Fraczyk, Justyna; Glowinska, Agnieszka; Hayouka, Zvi; Hershkovitz, Eyal; Jastrzabek, Konrad; Laurencin, Mathieu; Le Chevalier-Isaad, Alexandra; Malakoutikhah, Morteza; Malfi, Stefania; Melo, Manuel; Rotem, Shahar; Scieck, Alexa; Shabanpoor, Fazel; Sobolewski, Diariusz; Tiefenbrunn, Theresa; Trusova, Valeriya; Zawada, Zbigniew; Ziaco, Barbara.

Josef Rudinger Memorial Lecture

Horst Kessler studied chemistry in Leipzig and Tübingen where he received his Ph.D. degree with Eugen Müller in 1966. Shortly after his habilitation in 1969 he was appointed full professor for organic chemistry at the J. W. Goethe University in Frankfurt in 1971. In 1989 he moved to the Technische Universität München. He is also head of the Bavarian NMR Center. Guest professorships lead him to Halifax Tokyo Madison Haifa Austin and Jerusalem. In October 2008 he will become Carl von Linde Professor (Emeritus of excellence) at the Institute of Advanced Studies of the TUM. The main achievements of Professor Dr. Horst Kessler which went into the practice include design synthesis and preclinical development of Cilengitide a drug currently in clinical phase III for treatment of glioblastoma (developed by Merck KGaA Darmstadt) effi cient implant coating of Titanium implants for stimulated osseointegration (approved by Biomet Germany Berlin) and cancer imaging via "Galacto-RGD" for PET based molecular imaging (used in the Klinikum rechts der Isar in München and now worldwide to detect metastasis). His interests in the area of bioorganic and medicinal chemistry are wide on the study of biological recognition phenomena and on conformationally oriented design of biologically active molecules including peptides peptidomimetics carbohydrates and nucleic acid. Chemical synthesis of peptides sugars and their mimetics aim to conversion of peptides and small molecules into orally available drugs. Professor Kessler´s candidate drug screening technology is in advanced application of nuclear magnetic resonance (NMR). Professor Kessler develops and applies new NMR techniques to determine structure and dynamics of biomolecules especially of proteins and their complexes with ligands of low and high molecular weights. Biomaterials used on implant surface for stimulation of cell-adhesion and specifi c labeling of integrinligands for tumor diagnostics and therapy belong in the repertoire in use of his molecules in biomedicine. Horst Kessler is holder of about 625 publications 35 patents and has provided over 600 mostly invited and often plenary lectures in the fi eld his editorial board contributions throughout his carrier is in over 20 journals. Professor Dr. Kessler is the recipient of the Otto Bayer award (1986) the Max Bergmann medal for peptide chemistry (1988) the Emil Fischer medal (1997) the Max-Planck-Forschungspreis (2001) the Vincent Du Vigneaud Award of the American Peptide Society (2002) the Hans Herloff Inhoffen Medal (2002) and the Burkhart Helferich Award (2005). In 2002 he received the honorary degree of the University of Leipzig. He is a member of the "Bayerische Akademie der Wissenschaft" and the "Deutsche Akademie der Naturforscher Leopoldina". *J. Pept. Sci. 2008 14:8 Suppl.*

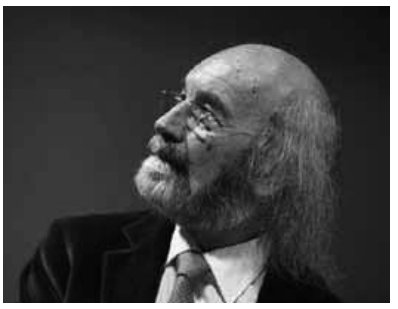

Manfred Mutter made substantial contributions to the field of Peptide Chemistry over more than 30 years. In particular his originality and scientifi c intuition have resulted in the establishment of a number of fundamental concepts which belong to today's standard tools in peptide research and which have served as a platform for numerous extensions and applications in synthetic and biomimetic chemistry. Out of more than 300 original publications reviews and book contributions the following contributions may be

highlighted: Conformational aspects in peptide synthesis: MM has been pioneer in delineating the importance of conformational changes during chain elongation and their impact on physical properties. PEG-peptides for studying conformational transitions: PEGbound peptides ('Liquid-Phase -Synthesis') allowed the conformational study of otherwise insoluble peptides for the first time (partially in collaboration with Claudio Toniolo). Templateassembled synthetic proteins (TASP) in protein de novo design: The template concept found broad application in diverse fields of peptide and protein chemistry (see chapter in Houben-Weyl). Pseudo-Prolines in peptide synthesis and biomimetic chemistry: The introduction of Pseudo-prolines as solubilising structure disruptive protection technique has become a widely used tool in the synthesis of hydrophobic peptides. In addition the tailored induction of cis-bonds into peptide backbones has opened versatile applications in biochemistry (see book chapter in C. Dugave 'Cis-trans Isomerization in Biochemistry' 2006). Switch-Peptides as folding precursors in self-assembling peptides: The recently developed concept of 'switch-peptides' for studying the molecular origin of amyloid beta based conformational transitions (see review in Biopolymers/ Peptide Science 2006) has found a broad echo in the 'amyloid-community' for its potential in biochemical/biophysical studies of degenerative diseases. Beside his innovative contributions in peptide chemistry Manfred Mutter is well known as an inspiring and motivating speaker making him one of our outstanding representatives at international conferences. Last but not least being in the process of retirement the dedication of this prestigious award represents a well-earned distinction for an outstanding scientist and a personality with a fi ne sense of humour. Professor Dr. Manfred Mutter is presently affiliated with Debiopharm S.A. CH- 1002 Lausanne Switzerland. *J. Pept. Sci. 2008 14:8 Suppl*

Leonidas Zervas Award

Anna Maria Papini introduced the "Chemical Reverse Approach" to develop post-translational modified peptides as synthetic probes to detect and fishing out specific and high affinity antibodies as biomarkers of autoimmune diseases. As a proof of concept she developed a glycopeptide-based immunoassay MS PepKit diagnostic/prognostic test for Multiple Sclerosis. Professor Papini´s main research interests are in the field of chemistry and physics of biomolecules for life sciences studying peptides and proteins involved in the molecular mechanisms of physiological and pathological conditions. She is involved in the development of synthetic & semi-synthetic strategies to co- or post-translational modified peptides in particular glycoconjugates as diagnostic and prognostic tools for human animal and plant diseases. Characterisation of biomarkers of disease activity with a particular attention to "theranostics" achieved through immunochemistry studies using conventional assays and innovative techniques for example for biosensors or electrochemical devices. Her strong commitment in synthesis of biomolecules has been focused to the development of effi cient strategies to exotic amino acids orthogonally protected for peptide synthesis (constrained amino acids glycosyl and lipophilic amino acids) cyclic peptide and peptidomimetic analogues (dicarba analogs clicked peptides) coupling reagents for solid phase chemistry (amide and ester bond formation) by conventional and alternative approaches (microwave-assisted synthesis). In 2003 she founded the first Academic Spin-off of the University of Florence EspiKem Srl Contract Research Organization involved in isolation characterisation design and synthesis of post-translational modified peptide peptidomimetic and protein antigens for in vitro diagnostics. Since 2007 she is CSO of the start-up company Toscana Biomarkers Srl that she founded as an R&D Biotech for innovative diagnostic/prognostic assays based on post-translational modified peptides. *J. Pept. Sci. 2008 14:8 Suppl*

The legacy of Miklos Bodanszky was at the 30th EPS conveyed by his students and his colleagues (from left to right): Professor **Jean Martinez** (Max Mousseron Biomolecule Institute (IBMM), CNRS, Montpellier, France), Chairman of the European Peptide Society and President of European Peptide Society Executive Committee; Professor **Peter Schiller** (Clinical Research Institute of Montreal, Canada.), Dr. **Maria Bednarek** (Merck Research Laboratories, U.S.A.), **Dr. John Tolle's** (Abbot Laboratories, U.S.A.) Professor **Sami I Said** (Stony Brook, School of Medicine, New York, U.S.A.)

Professor **Ferenc Hudecz** (Eötvös Loránd University, Department of Organic Chemistry, Budapest, Hungary), Secretary of European Peptide Society provided the early history of his country fellow.

Keyword index

Keywords are indicated in the manuscript codes between the topic area and the sequence number
*e.g. 1-**01**-001 (topic area 1 – keyword 01 – sequence number 001)*

Professor Morten Meldal (Carlsberg laboratory, Denmark) and Dr Ale Närvänen (AIV Institute, University of Kuopio, Finland) charing at 30EPS Highlights of Synthetic Peptide Chemistry.

The soccer teams of 30EPS: Europe (orange) vs. Rest of the World (white) at Helsinki Olympic Stadium, with referee Tomas Strandin. The football result was 2-1.

Submissions for Peptides 2008

ContentsPage

Keywords are indicated in the manuscript codes between the topic area and the sequence number *e.g. 1-**01**-001 (topic area 1 – keyword 01 – sequence number 001)*
Keywords are explained on page XXIII

Submitted papers: 7

Submitted papers: 87

Submitted papers: 13

Submitted papers: 103

Submitted papers: 25

Pharmacology and medical peptide chemistry orals (4-01-001 – 4-28-007)	Code	Page

Submitted papers: 7

Pharmacology and medical peptide chemistry posters (4-01-101 – 4-26-128)	Code	Page

Submitted papers: 28

Bioinformatics and systems biology orals (5-07-001)	Code	Page

Submitted papers: 1

Bioinformatics and systems biology posters (5-22-101 – 5-28-104)	Code	Page

Submitted papers: 4

Peptide biophysics and peptide-lipid interactions orals (6-07-001)	Code	Page

Submitted papers: 1

Peptide biophysics and peptide-lipid interactions orals (6-01-101 – 6-28-119)	Code	Page

Submitted papers: 19

Miscellaneous orals (17-13-001)	Code	Page
***β*-sheet antimicrobial peptide cateslytin generates rigid domains for membrane permeation** *Jean-François Frantz, Elezgaray Juan, Metz-Boutigue Marie-Hélène, Dufourc Erick*	7-13-001	614

Submitted papers: 1

Miscellaneous posters (7-01-101 – 7-07-119)	Code	Page
Degradation product of desmopressin in phosphate/citrate buffer *Nylander Bo, Malm Mattias, Walhagen Karin, Nilsson Anders*	7-01-101	616
Unusual Cleavage of Tripeptides Containing Pipecolic Acid *Islam Md Nurul, Shankar Sonu Ram, Kato Tamaki, Nishino Norikazu*	7-01-102	618
Analysis of protein-protein interaction sites without natively folded protein samples: fiction or fact? *Malešević Miroslav, Pöhlmann Angela, Lücke Christian, Träger Mario, Jahreis Günther, Hernandez-Alvarez Birte, Bordusa Frank, Fischer Günter*	7-02-103	620
Improved expressed protein ligation method for consecutive coupling of polypeptide fragments *Tömböly Csaba, Welker Ervin*	7-05-104	622
Cellular peptidomics: peptide sets produced by rat hepatocytes in vitro *Sazonova Olga, Yatskin Oleg, Khachin Dmitry, Kudryavtsev Denis, Karelin Andrei, Ivanov Vadim*	7-10-105	624

Submitted papers: 19

Submissions for Peptides 2008

Contents Page

Keywords are indicated in the manuscript codes between the topic area and the sequence number *e.g. 1-**01**-001 (topic area 1 – keyword 01 – sequence number 001)*
Keywords are explained on page XXIII

1-01-001

Cyclic opioid peptide antagonists containing (*2S*)-Mdcp or Dcp in place of Tyr[1]: Comparison with widely used μ and δ opioid antagonists

Schiller, Peter W[1,]; Lu, Yixin[2]*

[1]Clinical Research Institute of Montreal, Laboratory of Chemical Biology & Peptide Research, CANADA; [2]National University of Singapore, Chemistry and Medicinal Chemistry Program, SINGAPORE

[*]E-mail: schillp@ircm.qc.ca

Introduction

Dimethylation at the 2',6'-positions of the Tyr[1] residue in opioid peptides, as achieved by substitution of 2',6'-dimethyltyrosine (Dmt), has been shown to increase opioid agonist potency by 1-2 orders of magnitude.[1] Presumably, the potency increase is due to additional hydrophobic binding interactions of the two methyl groups with the receptor. Deletion of the N-terminal amino group of Dmt[1]-opioid peptide analogues or its replacement with a methyl group resulted in potent opioid antagonists.[2] On the basis of early structure-activity relationship studies, the phenolic hydroxyl group of Tyr[1] in opioid peptides has been thought to be indispensable for opioid activity for a long time. This was also indicated by the observation made by Bodanszky and Schiller that the unsulfated C-terminal 7-peptide of cholecystokinin had opioid activity, whereas the natural, sulfated peptide did not.[3] An interesting recent finding was the demonstration that a cyclic enkephalin analogue containing a carbamoyl (-$CONH_2$) group in place of the phenolic hydroxyl group of Tyr[1] retained high opioid agonist potency *in vitro*.[4] These various observations prompted the syntheses of analogues of Dmt, in which the –OH group was replaced by a –$CONH_2$ group and the α-amino group was either deleted [3-(2,6-dimethyl-4-carbamoylphenyl)propanoic acid (Dcp)][5] or replaced with a methyl group [(*2S*)-2-methyl-3-(2,6-dimethyl-4-carbamoylphenyl)propanoic acid ((*2S*)-Mdcp)][6] (Fig. 1). In the present paper, we compare the *in vitro* opioid antagonist properties of (*2S*)-Mdcp[1]- and Dcp[1]-analogues of cyclic opioid peptides with those of well known μ and δ opioid antagonists currently used in opioid research.

Results and discussion

The cyclic enkephalin-derived pentapeptide analogue (*2S*)-Mdcp-c[D-Cys-Gly-Phe(*p*NO_2)-D-Cys]NH_2 displayed high μ opioid antagonist activity (K_i^{μ} = 1.24 nM) in the GPI assay and weaker δ antagonist activity in the MVD assay (Table 1). In agreement with its high μ opioid antagonist activity determined in the functional assay, this compound showed high μ opioid receptor binding affinity in the rat brain membrane binding assay (K_i^{μ} = 1.02 nM) (Table 1). As indicated by the K_i ratio, it has quite high μ vs. δ receptor selectivity and high μ vs. κ selectivity. The Dcp[1]-analogue, Dcp-c[D-Cys-Gly-Phe(*p*NO2)-D-Cys]NH_2, was an about 3-fold weaker μ opioid antagonist than the corresponding Mdcp[1]-analogue and a somewhat weaker δ opioid antagonist as well. In the receptor binding assays this compound showed about 3-fold lower μ receptor binding affinity as compared to the Mdcp[1]-analogue, somewhat lower μ vs. δ selectivity and higher μ vs. κ selectivity. In agreement with the receptor binding data, both the Mdcp[1]- and the Dcp[1]-cyclic peptapeptides were relatively weak κ opioid antagonists, as determined in the GPI assay (data not shown). In comparison with the somatostatin-derived octapeptide CTOP, these two enkephalin-derived compounds showed 20-65-fold higher μ antagonist activity in the GPI assay, but similar μ receptor binding affinity. The high μ vs. δ receptor binding selectivity of CTOP was confirmed (Table 1), but no μ vs. κ receptor selectivity was observed under the binding assay conditions used in this study. CTOP and the enkephalin-derived μ antagonists described here most likely have different modes of binding to the μ opioid receptor and, therefore, both classes of compounds are of considerable

Table 1. *In vitro* opioid activity profiles of opioid antagonists

	GPI	MVD	Receptor binding[c]		K_i ratio	
Compound	K_e^{μ}, nM[a]	K_e^{δ}, nM[b]	K_i^{μ}, nM	K_i^{δ}, nM	μ/δ/κ	δ/μ/κ
(*2S*)-Mdcp-c[cGF(*p*NO_2)c]NH_2	1.24	9.78	1.02	19.0	1/19/181	
Dcp-c[cGF(*p*NO_2)c]NH_2	3.92	22.6	2.84	25.8	1/9/345	
CTOP	82.4	PA	0.745	998	1/1340/1	
(*2S*)-Mdcp-c[penGF(*p*F)Pen]F-OH	1170	0.326	5850	2.92		1/2000/1250 PA[d]
TIPP[Ψ]	inactive	2.89	3230	0.308		1/10500/>3250 PA[d]
naltrindole	–	0.636	3.86	0.182		1/21/-

[a] Determined against TAPP (H-Tyr-D-Ala-Phe-Phe-NH_2); [b] Determined against DPDPE;

[c] Displacement of [^{3}H]DAMGO (μ-selective) and [^{3}H]DSLET (δ-selective) from rat brain membrane binding sites, and of [^{3}H]U69,593 (κ-selective) from guinea pig brain membrane binding sites. [d]Partial agonist (PA).

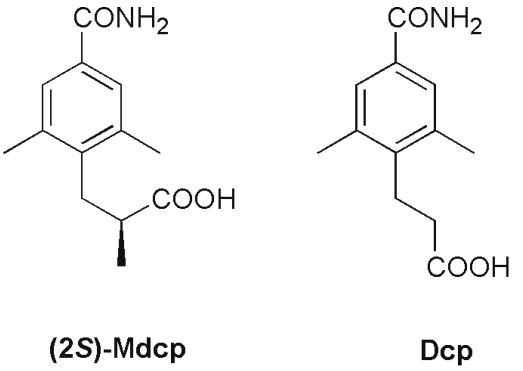

Figure 1. Structures of (*2S*)-Mdcp and Dcp.

interest as pharmacological tools. It should be pointed out that, unlike CTOP, the (*2S*)-Mdcp[1]- and Dcp[1]-pentapeptides do not carry a positive charge. Therefore, they are more lipophilic and can be expected to have an improved ability to cross the blood-brain barrier as compared to the larger and more polar CTOP molecule.

Replacement of the Tyr[1] residue in the δ-selective hexapeptide agonist H-Tyr-c[D-Pen-Gly-Phe(*p*F)-Pen]-Phe-OH[7] with (*2S*)-Mdcp led to a compound showing subnanomolar δ antagonist activity in the MVD assay, and high δ receptor binding affinity and δ selectivity in the binding assays (Table 1). In comparison with the δ antagonist TIPP[ψ] (H-Tyr-Ticψ[CH_2NH]Phe-Phe-OH), this compound has about the same high δ antagonist activity and only slightly lower δ receptor selectivity. Both (*2S*)-Mdcp-c[D-Pen-Gly-Phe(*p*F)-Pen]-(*2S*)-Phe-OH and TIPP[ψ] are more selective δ opioid antagonists than the non-peptide δ antagonist naltrindole.

Acknowledgements

This work was supported by grants from the U.S. National Institutes of Health and the National University of Singapore.

References

1. Hansen Jr DW, Stapelfeld A, Savage MA, Reichman M, Hammond DL, Haaseth RC, Mosberg HI. *J Med Chem* **35**: 684-687, 1982.
2. Lu Y, Nguyen TM-D, Weltrowska G, Berezowska I, Lemieux C, Chung NN, Schiller PW. *J Med Chem* **44**: 3048-3053, 2001.
3. Schiller PW, Lipton A, Horrobin DF, Bodanszky M. *Biochem Biophys Res Commun* **85**: 1332-1338, 1978.
4. Weltrowska G, Lemieux C, Chung NN, Schiller PW. *J Pept Res* **65**: 36-41, 2005.
5. Lu Y, Lum TK, Augustine YWL, Weltrowska G, Nguyen TM-D, Lemieux C, Chung NN, Schiller PW. *J Med Chem* **49**: 5382-5385, 2006.
6. Ghosh A, Luo J, Liu C, Weltrowska G, Lemieux C, Chung NN, Lu Y, Schiller PW. *J Med Chem* **51**: 5866-5870, 2008.
7. Hruby VJ, Bartosz-Bechowski H, Davis P, Slaninova J, Zalewska T, Stropova D, Porreca F, Yamamura HI. *J Med Chem* **40**: 3957-3962, 1997.

1-01-002

Solid phase synthesis of alkene dipeptidosulfonamide isosteres using olefin cross metathesis and the incorporation into amyloidogenic amylin(20-29)

Brouwer, Arwin J; Elgerma, Ronald C; Jagodzinska, Monika; Rijkers, Dirk TS; Liskamp, Rob MJ*

Utrecht Institute for Pharmaceutical Sciences, Utrecht University, P.O. Box 80082, NL-3508TB Utrecht, The Netherlands, Dept. of Medicinal Chemistry and Chemical Biology, THE NETHERLANDS

E-mail: a.j.brouwer@uu.nl

Introduction

The replacement of a backbone amide bond in peptides is a strategy which has been widely used to study peptide backbone interactions as well as for stabilization of peptides towards enzymatic degradation. An amide bond

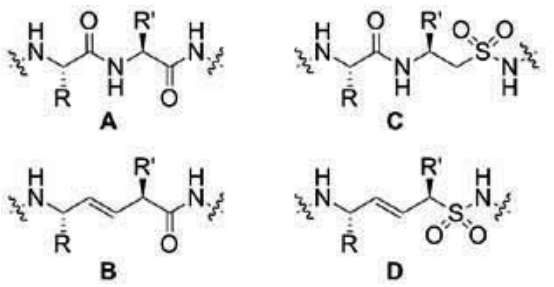

Figure 1. General structures of a dipeptide (**A**), an alkene dipeptide isostere (**B**), a peptide-peptidosulfonamide (**C**) and an alkene dipeptidosulfonamide isostere (**D**).

surrogate that mimics the geometry of the amide bond (**A**, Fig. 1) is the (E)-alkene dipeptide isostere (**B**).

This isostere has been mainly applied in the synthesis of dipeptide mimics. Only a few papers describe the incorporation of the alkene dipeptide isostere in longer peptides probably partly due to the difficulties involved in the synthesis of the isosteres. Another amide bond surrogate is the sulfonamide bond (**C**), which increases the flexibility of the backbone and is resistant to enzymatic degradation. The sulfonamide peptidomimetic is conveniently accessible[1] and has been used for incorporation into peptides.[2] A disadvantage of peptidosulfonamides (**C**, Fig. 1) might be the presence of an additional carbon atom in each amino sulfonic acid residue, which is needed for stability reasons.**3** As a result, there is no exact match of a peptidosulfonamide and its parent peptide. We envisioned that by combining the alkene dipeptide isostere with the sulfonamide a new useful peptidomimetic could be designed and synthesized: the alkene dipeptidosulfonamide isostere (**D**, Fig. 1). This isostere has the same backbone length as the parent (di) peptide, and also contains a sulfonamide moiety. For the synthesis of the alkene dipeptidosulfonamide isostere it was decided to modify a known cross metathesis (CM) procedure for the synthesis of alkenedipeptide isosteres.[4] From the available methods described in the literature, this was the most attractive one because of the relatively few reaction steps, and since its direct applicability to the synthesis of peptides containing a variety of sequences. Besides CM in solution, we were especially interested in application of CM on the solid phase, since peptides are usually synthesized on a solid support. The advantage of this approach would be that in principle any peptide sequence can be prepared using easy accessible building blocks.

Results and discussion

CM experiments in solution were performed using N-terminal olefins **1** and S-terminal olefin **2**, 2nd generation Grubbs catalyst[5] (10%) and DCM as solvent (Scheme 1). These experiments were almost directly successful and afforded alkene dipeptidosulfonamide isosteres in reasonable yields.[7] The yield of the CM reaction was clearly depending on the reactivities of the CM partners and their ratio.

Scheme 1. Synthesis of alkene dipeptidosulfonamide isosteres **4a-e** in solution and on the solid phase

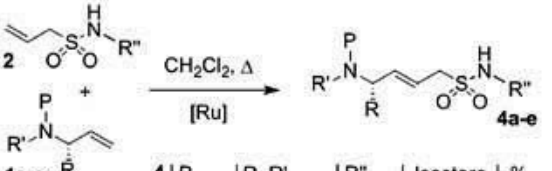

4	P	R, R'	R''	Isostere	%
a	Boc	H, H	Bn	Gly-Gly^S	12
b	Boc	CH_2Ph, H	Bn	Phe-Gly^S	39
c	Boc	$-(CH_2)_3-$	Bn	Pro-Gly^S	64
d	Fmoc	H, H	Resin	Gly-Gly^S	35
e	Fmoc	CH_2Ph, H	Resin	Phe-Gly^S	26

Although solid phase cross metathesis (SPCM) reactions have been hardly described in the literature, it has some advantages compared to CM in solution, which are reminiscent to solid phase synthesis. The olefin can be added in excess to the resin for driving the reaction to completion, and its non-desired homodimer can be easily removed by filtration. For SPCM Fmoc-protected allylamines were chosen to detemine the coupling

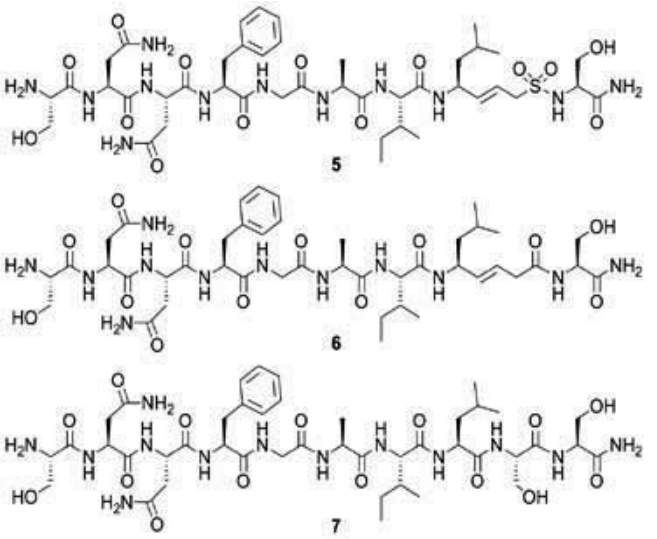

Figure 2. Structures of isostere containing amylins(20-29).

efficiency by measuring the dibenzofulvene-piperidine adduct obtained after cleavage of the Fmoc-group.

An allylsulfonamide containing TentaGel® resin was used for optimization of the SPCM reaction. Initial SPCM reactions showed very low conversions. After optimization by using two ruthenium catalysts,[5,6] different solvents, different temperatures and a lewis acid, a procedure was found with a conversion of 26% for the phenylalanine derived N-terminal olefin (**1e**), which is reasonable for SPCM.[7] Despite these modest results it was decided to apply this optimized cross metathesis procedure to the incorporation of an alkene dipeptidosulfonamide into a peptide.

Amylin(20-29) (**7**, Fig. 2) was chosen for this purpose, since this is a peptide with a high tendency to form (anti)parallel *β*-sheets, which leads to fibril formation. Amylin(20-29) is the highly amyloidogenic region of amylin, also known as human islet amyloid polypeptide, a 37-mer peptide hormone which is involved in the pathogenesis of type II diabetes. So far we have incorporated several peptidomimetic moieties in amylin(20-29) for investigation of the relations between structure and fibril formation.[8] We were interested in the structural effects upon incorporation of both the alkene dipeptidosulfonamide isostere and the alkenedipeptide isostere in amylin(20-29).

Both isosteres were successfully introduced using the SPCM reaction on the solid phase using a Rink linker. After standard SPPS, peptides **5** and **6** were cleaved from the resin and deprotected. HPLC purification afforded alkene dipeptidosulfonamide isostere **5** and alkene dipeptide isostere **6** (Fig. 1).[7] Both peptides were characterized using ESI-MS.

To study the aggregation behavior, both peptides were dissolved in 0.1% TFA/H_2O and rapid gel formation was observed (**5**: 30 min; **6**: 60 min), but clearly slower than native amylin(20-29) (<10 min). Retardation in fibril formation can be explained by removal of both a hydrogen bond donor and acceptor in the peptide backbone. The presence of amyloid fibrils with similar morphology as native amylin(20-29) was confirmed by transmission electron microscopy (TEM).[7] A combined interpretation of the CD[7] and FTIR spectra with TEM shows that a twisted *β*-sheet is the most probable secondary structure.[9]

Acknowledgments

We thank Annemarie Dechesne for measuring some of the mass spectra and Dr. George Posthuma (UMC, Utrecht) for assistance with the TEM measurements

References

1. Brouwer AJ, Monnee MCF, Liskamp RMJ. *Synthesis* **11**: 1579-1584, 2000.
2. Liskamp RMJ, Kruijtzer JAW. *Mol Diversity* **8**: 79-87, 2008 (and references cited).
3. Paik S, White EH. *Tetrahedron* **52**: 5303-5318, 1996.
4. Vasbinder MM, Miller SJ. *J Org Chem* **67**: 6240-6242, 2002.
5. Scholl M, Ding S, Lee CW, Grubbs RH. *Org Lett* **1**: 953-956, 1999.
6. Barber S B, Kingsbury JS, Gray BL, Hoveyda AH. *J Am Chem Soc* **122:** 8168-8179, 2000.
7. Brouwer AJ, Elgersma RC, Jagodzinska M, Rijkers DTS, Liskamp RMJ. *Biorg Med Chem Lett* **18**: 78-84, 2008.
8. Elgersma RC, Mulder GW, Kruijtzer JAW, Posthuma G, Rijkers DTS, Liskamp RMJ. *Bioorg Med Chem Lett* **17**: 1837-1842, 2007 (and references cited).
9. Johnson Jr WC. *Ann Rev Biophys Biophys Chem* **17**: 145-166, 1988 (and references cited).

1-01-003

Synthesis of Cyclic Peptide Chitinase Inhibitors: Natural Products with Chemotherapeutic Potential

Dixon, Mark[1]; Giuntini, Francesca[1]; Nathubhai, Amit[1]; Andersen, Ole[2]; van Aalten, Daan[2]; Eggleston, Ian[1,]*

[1]University of Bath, UNITED KINGDOM; [2]University of Dundee, UNITED KINGDOM

[*]E-mail: ie203@bath.ac.uk

Introduction

Chitinases catalyse the hydrolysis of chitin, the natural homopolymer of β(1,4)-linked N-acetyl-D-glucosamine. Chitin is a key structural component of the cell walls, exoskeletons, and eggshells of pathogenic fungi, insects, and nematodes, respectively, which all rely on the ability to hydrolyse chitin at specific points in their life cycles. Inhibitors of family 18 chitinases are now attracting considerable interest as novel fungicides and insecticides, as well as chemical tools to study human diseases as diverse as asthma and malaria. The cyclic pentapeptide natural products, argifin and argadin, are two exciting leads with μmol-nmol activity against a range of chitinases, and which pose some interesting synthetic challenges.[1] The argifin structure includes two sensitive β-linked Asp residues, as well as an unusual carbamoylated Arg side chain, while argadin contains a unique Asp β-semialdehyde residue (ASA), that is cyclised to the peptide backbone to generate a potentially labile hemiaminal. We have previously described the first syntheses of both natural products,[2,3] in which two specific side reactions were observed that limited the overall efficiency of the syntheses and their scope for use in SAR investigations. In the case of argifin, the β-Asp containing backbone of the cyclic peptide appears to be particularly prone to aspartimide formation under acidic conditions. For argadin, homoserine-containing precursors of ASA peptides prove very sensitive to backbone cleavage via acid-mediated lactone formation. We have thus developed improved routes to both compounds that allow such side reactions to be avoided. This is achieved by performing assembly, cyclisation, and key side chain derivatisations entirely on solid phase.

Results and discussion

Our revised synthetic approach to argifin is summarised in Scheme 1. The peptide backbone is assembled via attachment through an Asp α-carboxylate to 2-chlorotrityl chloride polystyrene resin, followed by standard Fmoc SPPS. After C-terminal deprotection and on-resin cyclisation, the key modified Arg side chain is installed through guanidination and acylation of an Orn residue. This indirect approach avoids the need for TFA-based deprotection of the corresponding Arg cyclic peptide in solution, which was previously found to be accompanied by significant levels of aspartimide formation.[2]

All on-resin steps proceed with high efficiency, as judged by HPLC and MS analysis, including the critical acylation, with very little diacylation observable (see inset, Scheme 1). Aspartimide formation upon cleavage from the solid support and final *tert*-butyl ester removal was eliminated by a two step protocol, employing firstly 1% TFA/DCM, followed by treatment in solution with 1M aq HCl at 60 °C. In this way, argifin was obtained in 18% yield, over a 17 step sequence, following a single HPLC purification.[4] We have also successfully applied

Scheme 1. Solid phase synthesis of argifin with (inset) HPLC analysis of on-resin acylation of Arg side chain

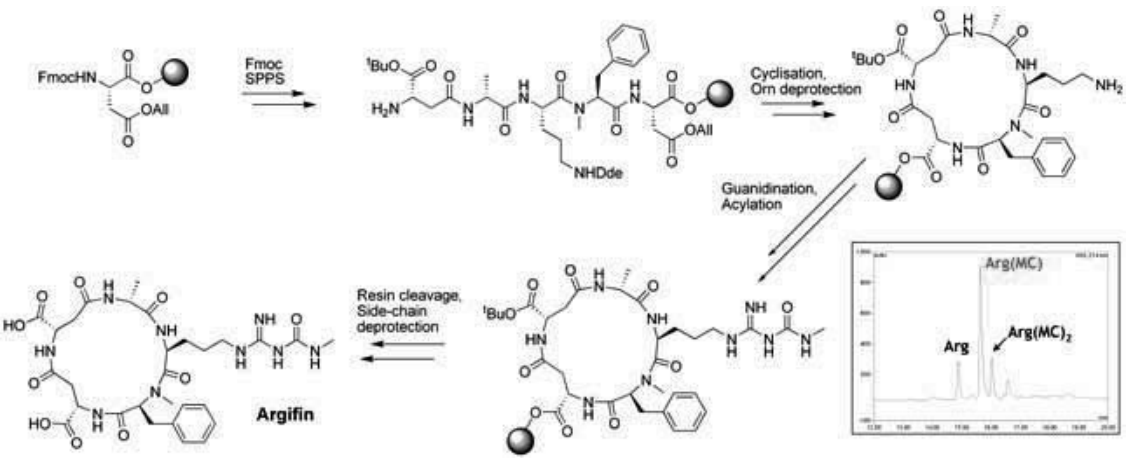

Scheme 2. Solid phase synthesis of argadin on Novasyn TG® resin

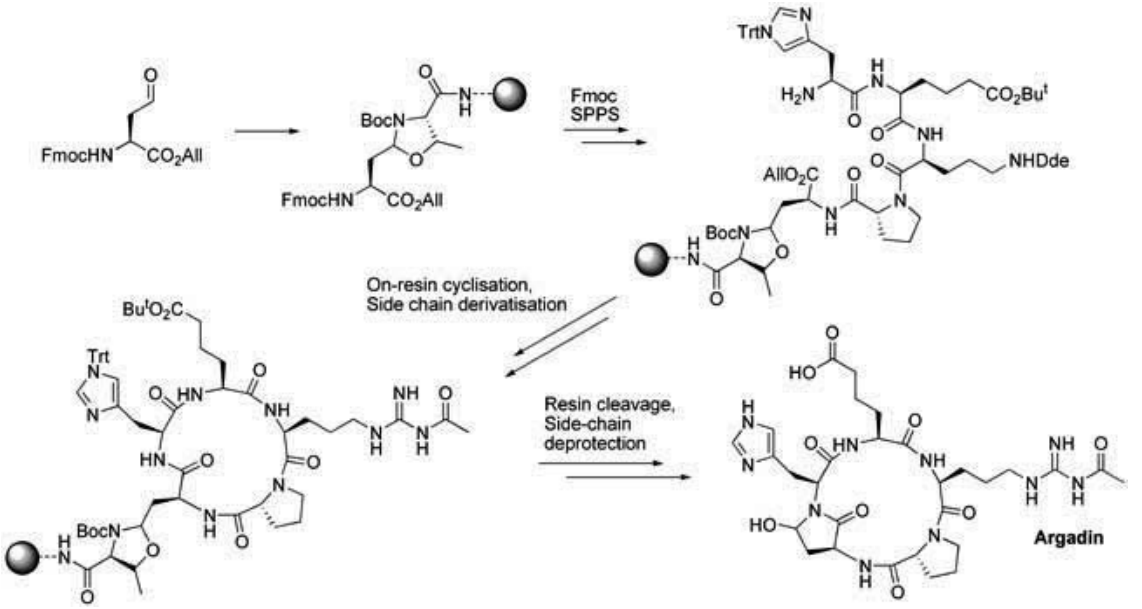

the same approach for the synthesis of family of argifin analogues in which the key Arg(MC)-MePhe motif and the flanking residues are mutated. Such compounds were also obtained in generally good overall yields (e.g, 16% for Arg(MC)→Orn(MC) mutation; 11% for MePhe→MeTyr; 8% for MePhe→Phe). Screening against a typical bacterial-type family 18 chitinase (chitinase B1 from *Aspergillus fumigatus*), confirms the critical importance of the Arg(MC) motif[5] for the development of effective inhibitors based upon the argifin scaffold, as well as a strong preference for a cis-configuration of the Arg(MC)-Xaa peptide bond.

Our new approach to argadin entails the incorporation of the problematic ASA unit at the outset of the synthesis, using its aldehyde function for immobilisation onto Novasyn TG® resin. In this way, following on-resin synthesis, the complete natural product is released directly into solution without need for further manipulations. The overall yield after 16 solid phase steps, and once again following a single HPLC purification, is 4%, which compares very favourably with the outcome from our previously reported route, wherein additional purification is required prior to introducing the ASA unit in the final step by oxidation in solution. Argadin is obtained as an approximate 5:1 mixture of diastereoisomers by this route, as previously observed.[3] We are currently exploring this methodology to establish SAR data around the argadin system, and also investigating the automation of all the on-resin steps.

Acknowledgements

This work was supported by Wellcome Trust project grant 074337 (to IME and DvA) and a BBSRC studentship (AN). DvA is supported by a Wellcome Trust Senior Research Fellowship and the EMBO Young Investigator Programme.

References

1. Andersen O, Dixon M, Eggleston I, van Aalten D. *Nat Prod Rep* **22:** 563-579, 2005.
2. Dixon M,. Andersen O, van Aalten D, Eggleston I. *Bioorg Med Chem Lett* **15:** 4717-4721, 2005.
3. Dixon M, Andersen O, van Aalten D, Eggleston I. *Eur J Org Chem* **22:** 5002-5006, 2006.
4. Dixon M, Nathubhai A, Andersen O, van Aalten D, Eggleston I. *Org Biomol Chem* **7:** 259-268, 2009. Andersen O, Nathubhai A, Dixon M, Eggleston I, van Aalten D. *Chem Biol* **15:** 295-301, 2008.

1-01-004

Dynamic Ligation of peptide electrophiles for the identification of protein-binding fragments and development of protein ligands

*Rademann, Jörg**
Department for Medicinal Chemistry, Leibniz Institute for Molecular Pharmacology, GERMANY

**E-mail: rademann@fmp-berlin.de*

Specific protein ligands are crucial for the modulation of protein activities in medicinal chemistry and chemical biology. We present a concept for the discovery and development of small molecule fragments binding to defined protein sites: Dynamic Ligation Screening enables the rapid and site-directed identification of low-affinity binders in biochemical protein acitivity and binding assays by exploiting template-assisted fragment assembly.[1]

Results and discussion

The concept was established for the development of a non-peptidic SARS coronavirus main protease (SARS-CoV Mpro) inhibitor. This enzyme has been identified as a drug target of SARS being essential for replication of the virus inside the infected host cell. Dynamic Ligation Screening was conducted with libraries of 200-6000 fragments consuming only minor amounts of enzyme: A designed peptide electrophile 2 acting as a direting probe[2,3] was incubated with one amine per well, the protease, and the fluorogenic substrate Ac-TSAVLQ-AMCA 1. The fluorogenic protease substrate 1 competed with an equilibrium of nucleophilic fragments and the peptide electrophile 2. Decreased initial rates of product formation in the fluorophore-based enzyme assay indicated the inhibitory activity of the reversibly formed ligation product (Fig. 1). One selected hit 3 was modified synthetically in order to verify the binding site (Scheme 1). Introduction. Specific protein ligands are crucial for the modulation of protein activities in medicinal chemistry and chemical biology. We present a concept for the discovery and development of small molecule fragments binding to defined protein sites: Dynamic Ligation Screening enables the rapid and site-directed identification of low-affinity binders in biochemical protein acitivity and binding assays by exploiting template-assisted fragment assembly.[1] The concept was established for the development of a non-peptidic SARS coronavirus main protease (SARS-CoV Mpro) inhibitor. This enzyme has been identified as a drug target of SARS being essential for replication of the virus inside the infected host cell. Dynamic Ligation Screening was conducted with libraries of 200-6000 fragments consuming only minor amounts of enzyme: A designed peptide electrophile 2 acting as a direting probe[2,3] was incubated with one amine per well, the protease, and the fluorogenic substrate Ac-TSAVLQ-AMCA 1. The fluorogenic protease substrate 1 competed with an equilibrium of nucleophilic fragments and the peptide electrophile 2. Decreased initial rates of product formation in the fluorophore-based enzyme assay indicated the inhibitory activity of the reversibly formed ligation product (Fig. 1). One selected hit 3 was modified synthetically in order to verify the binding site (Scheme 1).

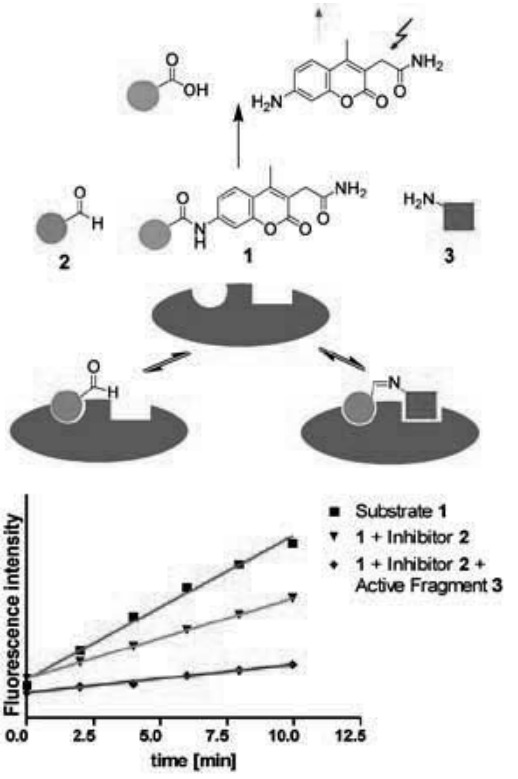

Figure 1. The concept of Dynamic Ligation Screening (DLS). Substrate 1 competes with peptide aldehyde. inhibitor 2 for the SARS-CoV main protease (blue). Active fragment 3 leads to an increased inhibition via the binding of the imine ligation product to the active site.

To obtain an entirely non-peptidic inhibitor of SARS-CoV Mpro targeting both the S´1 and S1 pockets, the dynamic ligation screening was conducted iteratively in a Fig. 1. The concept of Dynamic Ligation Screening (DLS). Substrate 1 competes with peptide aldehyde inhibitor 2 for the SARS-CoV main protease (blue). Active fragment 3 leads to an increased inhibition via the binding of the imine ligation product to the active site. To obtain an entirely non-peptidic inhibitor of SARS-CoV Mpro targeting both the S´1 and S1 pockets, the dynamic ligation screening was conducted iteratively

Scheme 1. Development of a non-peptidic SARS-CoV Mpro inhibitor via Dynamic Ligation Screening. Active Fragment 3 binding to the S1´site of the protein has been transformed into electrophilic derivatives 6-9 which were employed iteratively in reverted DLS yielding the non-peptidic inhibitor 12

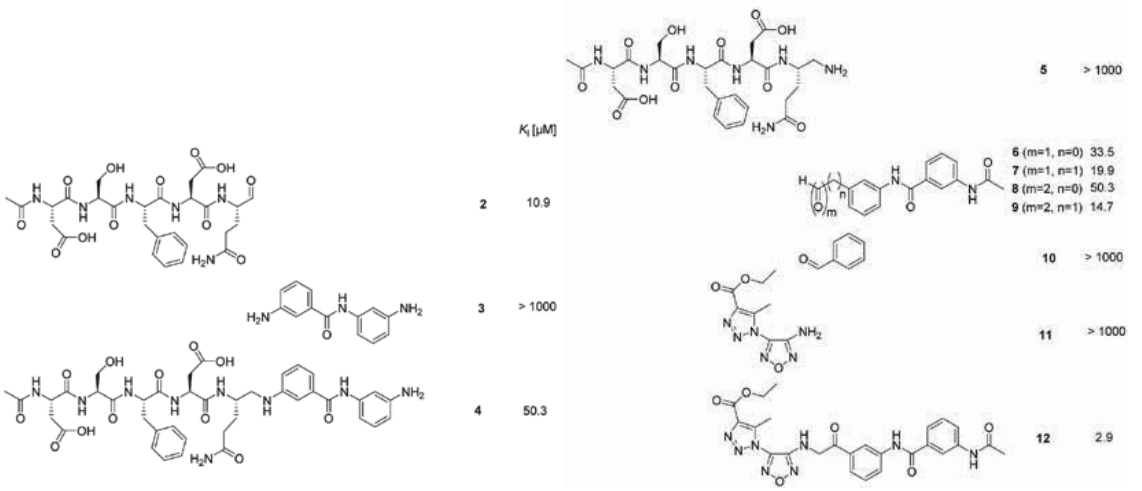

in a ”reverted” mode. Instead of peptide aldehyde 2 binding to the S-side of the binding cleft, now 2-keto aldehyde 9 presumably binding to the S´-side was employed as a directing probe (Scheme 1). This time, 110 amines selected by diversity analysis were screened. Compound 9 was incubated with one amine per well, the protease, and the fluorogenic substrate 1. In the second screen, three fragments were identified being active in presence of the directing probe 9. Most active was amine 11, which was selected for verification of the inhibitor binding by chemical synthesis. Using a 2-ketoaldehyde for the covalent linking appeared to be advantageous as the aldehyde could undergo reductive amination while the 2-keto functionality remained intact for interaction with active site cysteine 145. Amine 11 was employed for reductive amination of 2-keto aldehyde 9 using trichlorosilane as reducing agent and yielded successfully 2-amino ketone 12 as the covalent ligation product. 12 inhibited SARS-CoV Mpro with a KI value of 2.9 µM. Via an iterative scanning of different binding sites on the protein surface, moderately active peptidic inhibitors could be transformed into entirely non-peptidic inhibitors with a low µM KI. Thermodynamics of protein-assisted fragment ligations were studied for caspase-3, the cellular switch for apoptosis, the programmed cell death. As a result a model for of binding contributions of reversibly ligated fragments is developed which allows us to distinguish fragments binding additively from those binding positively cooperatively. The method can be further extended to other protein targets such as phosphatases[4] and to protein-protein interactions.

Acknowledgements

We wish to thank Samuel Beligny, Angelika Ehrlich, Franziska Hinterleitner, Dagmar Krause, Jörn Saupe, Bernhard Schmikale and Walter Verheyen for technical support. We also acknowledge discussions with Jeroen R. Mesters and Koen H. Verschueren. Work at the Leibniz Institute for Molecular Pharmacology was supported by the DFG (Ra 895/2-5).

References

1. Schmidt MF, Isidro-Llobet A, Lisurek M, El-Dahshan A, Tan J, Hilgenfeld R, Rademann J. *Angew Chem Int Ed* **47**: 3275-3278, 2008.
2. El-Dahshan A, Weik S, Rademann J. *Org Lett* **9**: 949-952, 2007.
3. Al-Gharabli S.I., Ali Shah ST, Weik S, Schmidt MF, Mesters Jr, Kuhn D, Klebe G, Hilgenfeld R, Rademann J. *ChemBioChem* **7**: 1048-1055, 2006.
4. Hellmuth K, Grosskopf S, Lum CT, Würtele M, Röder N, von Kries JP, Rosario M, Rademann J, Birchmeier W. *Proc Nat Acad Sci USA* **105**: 7275-7280, 2008.

1-01-005

Semisynthesis of Membrane-Associated Prion Proteins

Olschewski, Diana[1]; Seidel, Ralf[1]; Tatzelt, Jörg[2]; Engelhard, Martin[1]; Becker, Christian F[3,]*

[1]Max-Planck Institute of Molecular Physiology, Department of Physical Biochemistry GERMANY;
[2]Ludwig-Maximilians-Universität München, Department of Biochemistry NeuroBiochemistry GERMANY;
[3]Technische Universität München, Department of Chemistry, Protein Chemistry, GERMANY

[*]E-mail: christian.becker@ch.tum.de

Introduction

Transmissible spongiform encephalopathies (TSEs) such as Creutzfeld Jakob disease (CJD) are rare fatal neurodegenerative disorders that are characterized by the accumulation of a misfolded isoform (PrPSc) of the cellular prion protein (PrPC). PrPC is an N-glycosylated protein attached to the outer leaflet of the plasma membrane by a C-terminal glycosylphosphatidylinositol (GPI)-anchor, where it segregates into cholesterol- and spingomyelin-rich microdomains.[1] This membrane localization seems to be crucial for the de novo generation of infectious PrPSc.[2] In order to mimic the influence of membrane attachment on folding and conversion, synthesis strategies based on expressed protein ligation (EPL)[3] were devised that allowed incorporation of palmitoylated and fluorescently labelled peptides as well as of glycosylphosphatidylinositol (GPI) anchors at the C-terminus of PrP.[4,5] Following these strategies, murine PrP was modified with chemically synthesized peptides containing lipid moieties that mimic the GPI anchor and fluorescent labels for localization studies. Synthesis of these peptides was accomplished by solid phase peptide synthesis (SPPS). The resulting C-terminally modified PrP variants were successfully folded and transferred into liposomes as well as N2a cells.

Results and Discussion

An N-terminally truncated variant of murine PrP (aa 90-232) was recombinantly expressed in fusion with the GyrA intein to give -thioester group upon cleavage thatαrecombinant PrP (rPrP) with a C-terminal can be used for native chemical ligation (NCL) with membrane anchor mimics (Fig. 1A). These membrane anchor mimics consist of 16 amino acids and comprise an N-terminal cysteine residue for NCL, two lysine residues for palmitoylation, an additional lysine residue for chromophore attachment, a six amino acid TEV protease recognition site and a C-terminal polymer tag that increases solubility of the lipidated peptide (CKGENLYFQSKAAKKA-PPO3).[4] Successful NCL reactions are followed by purification via RP-HPLC and subsequent folding produces homogeneous recombinant PrP with C-terminal palmitoyl modifications (rPrPPalm). Folded rPrPPalm has a predominantly alpha-helical secondary structure, which is typical for cellular PrP and can be used for *in vitro* and *in vivo* studies (Fig. 1B,C). Fig. 1: A) Synthetic strategy for the semisynthesis of membrane associated, recombinant PrP (rPrPPalm). The palmitoylated membrane anchor is synthesized by SPPS and linked to rPrP thioester via native chemical liagtion. B) SDS-PAGE of purified rPrPPalm containing a double

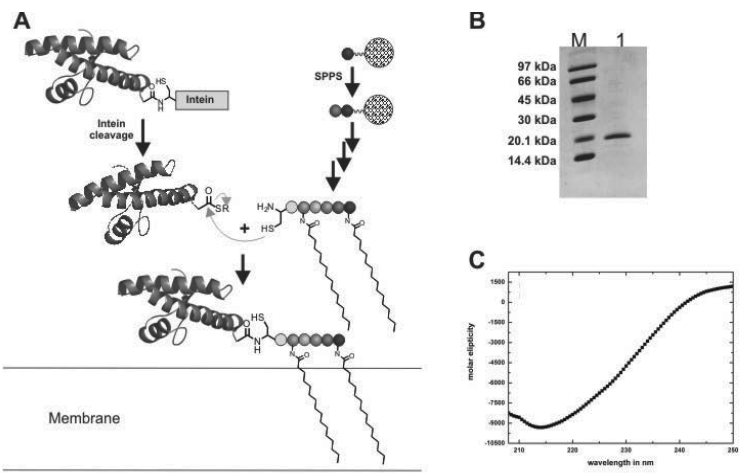

Figure 1. A) Synthetic strategy for the semisynthesis of membrane associated, recombinant PrP (rPrP^{Palm}). The palmitoylated membrane anchor is synthesized by SPPS and linked to rPrP thioester via native chemical liagtion. B) SDS-PAGE of purified rPrP^{Palm} containing a double palmitoylated membrane anchor. C) CD spectrum of folded, membrane-bound rPrP^{Palm} indicating an α-helical fold.

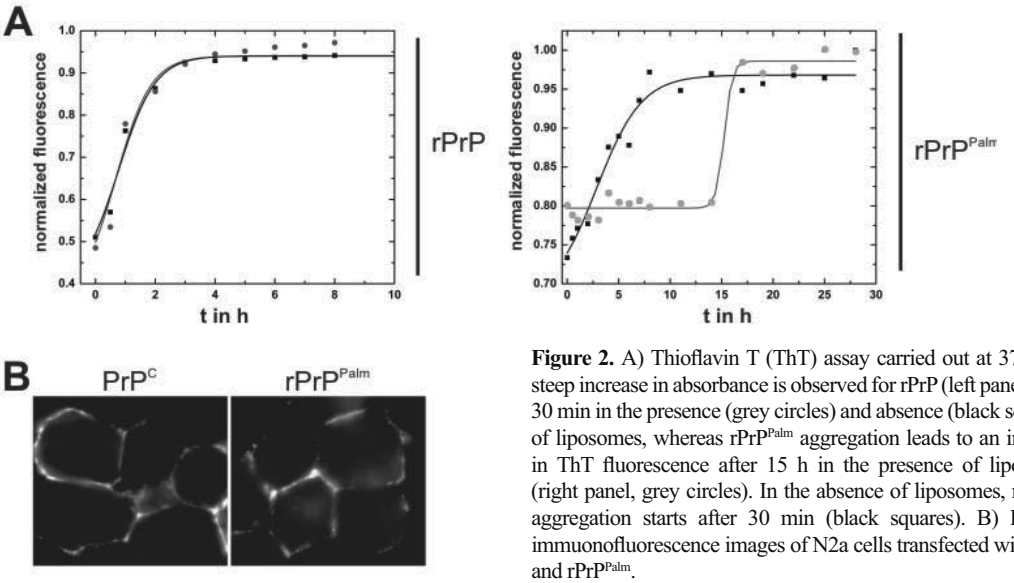

Figure 2. A) Thioflavin T (ThT) assay carried out at 37 °C. A steep increase in absorbance is observed for rPrP (left panel) after 30 min in the presence (grey circles) and absence (black squares) of liposomes, whereas $rPrP^{Palm}$ aggregation leads to an increase in ThT fluorescence after 15 h in the presence of liposomes (right panel, grey circles). In the absence of liposomes, $rPrP^{Palm}$ aggregation starts after 30 min (black squares). B) Indirect immunofluorescence images of N2a cells transfected with PrP^{C} and $rPrP^{Palm}$.

palmitoylated membrane anchor. C) CD spectrum of folded, membrane-bound rPrPPalm indicating an alpha-helical fold.

In vitro aggregation studies with rPrP and rPrPPalm clearly indicate that membrane association of PrP affects its aggregation behavior. A variety of techniques such as resistance to proteinase K digestion, Thioflavin T fluorescence and electron microscopy demonstrate that formation of fibrillar aggregates is delayed for membrane bound rPrPPalm. The lag time before fibril formation starts is dramatically increased for rPrPPalm bound to membranes as seen in the Thioflavin T assay depicted in Fig. 2A, whereas rPrPPalm in the absence of membranes shows similar aggregation behavior as rPrP. In order to study rPrPPalm *in vivo* the protein had to be successfully transferred into living cells. We achieved this by incubating mouse neuroblastoma N2a cells with rPrPPalm in the presence of a liposome-based transfection agent (Pro-Ject, Pierce). Solubilization and flotation assays confirmed successful transfer of rPrPPalm. rPrP was not transfected under similar conditions. Indirect immunofluorescence of transfected cells demonstrated that externally added semisynthetic rPrPPalm inserts into the outer leaflet of the cell membrane similar to intracellularly expressed PrPC (Fig. 2B). Fig. 2: A) Thioflavin T (ThT) assay carried out at 37 °C. A steep increase in absorbance is observed for rPrP (left panel) after 30 min in the presence (grey circles) and absence (black squares) of liposomes, whereas rPrPPalm aggregation leads to an increase in ThT fluorescence after 15 h in the presence of liposomes (right panel, grey circles). In the absence of liposomes, rPrPPalm aggregation starts after 30 min (black squares). B) Indirect immunofluorescence images of N2a cells transfected with PrPC and rPrPPalm.

Conclusion

The strategy described here allows the synthesis of folded rPrP variants with GPI anchor mimics at their C-termini (rPrPPalm) that attach to membranes and thereby afford the possibility to study rPrP in its native environment. Such membrane attachment slows the formation of fibrillar aggregates of rPrPPalm in comparison to soluble rPrP, indicating a partial -helical, cellular form of rPrPPalm. Anαprotection of the predominantly important step towards the elucidation of prion conversion and prion turn-over was achieved by a successful transfer of semisynthetic rPrPPalm into the plasma membrane of live cells.

Acknowledgements

The authors would like to thank Sascha Gentz for technical assistance and Roger Goody for continuous support. This work was funded by the Max-Planck Society and the Deutsche Forschungsgemeinschaft (SFB 596).

References

1. Critchley P, Kazlauskaite J, Eason R, Pinheiro TJT. *Biochem Biophys Res Commun* **313**: 559-567, 2004.
2. Baron GS, Caughey B. *J Biol Chem* **278**: 14883-14892, 2003.
3. Durek T, Becker, CF. *Biomol Eng* **22**: 153-172, 2005.
4. Olschewski D, Seidel R, Miesbauer M, Rambold AS, Oesterhelt D, Winklhofer KF, Tatzelt J, Engelhard M, Becker CF. *ChemBiol* **14**: 994-1006, 2007.
5. Becker CF, Liu X, Olschewski D, Castelli R, Seidel R, Seeberger PH. *Angew Chem Intl Ed* **47**: 8215-8219, 2008.

Professor Dr. Yoshiaki Kiso at 30th EPS

Dr. Elisabeth Schram at 30th EPS

1-02-006

Siamese depsipeptides: a new approach to more active compounds

Spengler, Jan1; Ruí z-Rodrí guez, Javier; Albericio, Fernando
Institute for Research in Biomedicine, Barcelona, SPAIN

Article withdrawn by authors

1-02-007

From Peptide to Non-Peptide Metalloconstructs: Dynamic Combinatorial Libraries of Oxorhenium Coordinates for the Selection of New Cyclophilin Inhibitors

Clavaud, Cécile; Le Gal, Julien; Thai, Robert; Moutiez, Mireille; Dugave, Christophe[1,]*

CEA/Saclay, iBiTecS, FRANCE

[*]E-mail: christophe.dugave@cea.fr

We recently reported on the self-assembly of peptide-oxorhenium metalloconstructs that are able to bind to the human cyclophilin A (CypA),[1] an important peptidyl-prolyl isomerase (PPIase) which plays a critical role in protein folding and is involved in the regulation of activity of several receptors and enzymes.[2] CypA possesses 2 functionally independent subsites: the S1-S1' subsite recognizes the amino acyl prolyl motif as well as amino acyl prolyl analogs, and the S2'-S3' subsite can accommodate various peptide chains and modified peptides such as the amino acyl-para-nitroanilide moiety.[2] Our strategy was mainly based on a combinatorial assembly of n modules A-(NSH_2) with m modules B-SH through the coordination of an oxorhenium core which leads to the formation of a mixture of n X m oxorhenium coordinates of general formula [A-NS_2.ReO.S-B].[1,3] In our model, A is an aminoacyl proyl surrogate which is anticipated to bind to the S1-S1' subsite while B is an amino acyl-*pNA* analog which is supposed to bind to the S2'-S3' subsite. Screening of libraries of peptide- and non peptide-oxorhenium conjugates using a fluorescence quenching assay led to the identification of some coordinates that bind to CypA with an affinity better by one order of magnitude (Kd = 10-15 μM) relative to model substrate peptides.[1] Further studies showed that these compounds are able to inhibit the PPiase activity of CypA (IC_{50} = 12 μM).[1]

We investigated the self-assembly of similar oxorhenium coordinates from mixtures of modules in a buffer in the presence of CypA, using water-soluble oxorhenium salts such as oxorhenium gluconate. We assumed that CypA would be able to favor the formation of oxorhenium coordinates that display a higher affinity for its active site and hence would enable their selection from the dynamic combinatorial library. For this purpose, we tuned the kinetically-controlled assembly of oxorhenium coordinates by adding glutathione (GSH) which can substitute reversibly the 'B-S' moiety of complexes to give the corresponding GSH adducts. In these conditions, CypA should protect more efficiently the coordinates that tightly bind to its active site whereas other oxorhenium complexes would be dissociated (Fig. 1).

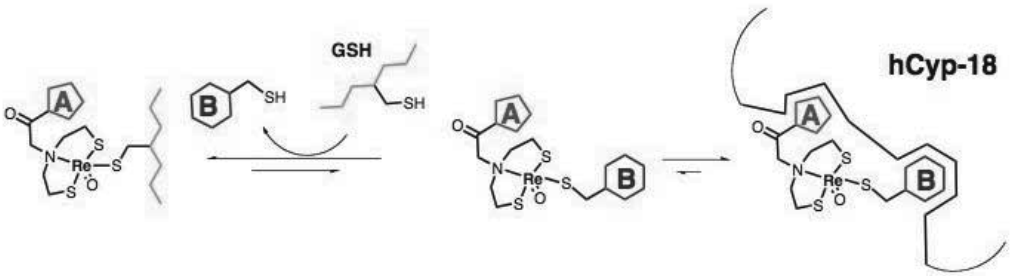

Figure 1.

Firstly, we ensured that prolonged incubation of CypA with oxorhenium gluconate does not inhibit the PPIase activity. We observed that kinetics of self-assembly of the coordinates in a 35 mM hepes buffer pH 7.6 significantly vary from one compound to another. Their sensitivity to GSH also strongly depends on the chemical nature of the constituting modules. In order to compensate biases that might hamper the detection of high affinity compounds, we chose to monitor the reaction by LC-MS in various conditions including addition of 64 μM cyclophilin (theoretical concentration of modules: 47 μM) and increasing concentrations in GSH (from 10^{-6} to 10^{-1} M). Oxorhenium complexes were easily identified due to their particular isotopic motif that reflects the combination of rhenium with 3 sulfur atoms.[2] Preliminary experiments, performed using some previously described compounds, showed that addition of GSH to low affinity compounds dramatically decreases the integrated ionic current independently of the presence of CypA. Conversely, complexes that bind to CypA are more resistant to GSH in the presence of the enzyme. Titration of the integrated ionic current in various conditions gave the C_{50} which must be corrected in order to compensate differences in the ability of oxorhenium coordinates to be ionized by ES/MS. This was done using a standard oxorhenium coordinate as a reference. For most of the metalloconstructs, the CC_{50} values were inversely proportional to the corresponding

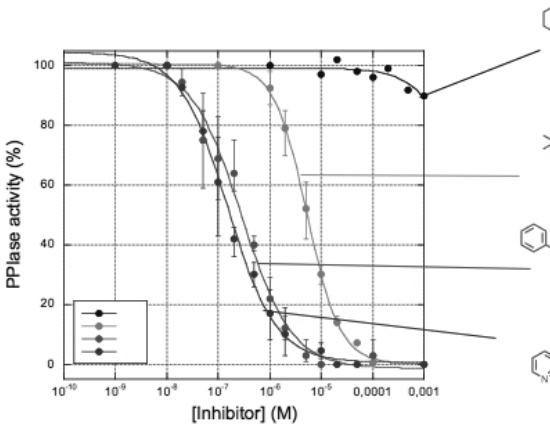

Cmpd.	CC_{50} (µM)	IC_{50} (µM)
7a	< 0.5	> 10,000
5b	1000	5.3 ± 0.2
9b	2200	0.3 ± 005
16n	1250	0.2 ± 0.02

Fugure 2.

Kd and IC_{50}. This result confirms that CypA is able to select high affinity ligands by protecting them against thiol substitution.[4]

We applied this strategy to the selection of new cyclophilin inhibitors from 16 parallel dynamic combinatorial libraries of 12 complexes (192 components). In particular, we identified 3 oxorhenium coordinates with CC_{50} in the millimolar range whereas most of other compounds (i.e. **7a**) are dissociated below 10 µM (Fig. 2).

Complexes **5b**, **9b** and **16n** bind to CypA with micro to submicromolar affinities whereas compound **10i** does not. Compounds **9b** and **16n** are able to inhibit the PPIase activity with IC_{50} of 300 and 200 nM respectively, an increase in affinity of more than 2000 fold relative to the model peptides. Moreover, these values are only 10 times more than cyclosporine A, one of the most potent inhibitor of CypA.

Although the sensitivity of the composite oxorhenium coordinates to GSH might be a major drawback to the use of such peptide metalloconstructs as inhibitors of cytosolic enzymes, they could be used as tracers for molecular imaging and radiotherapeutics.[5] In particular such compounds might be employed for the targeting of integral proteins and plasma protein using rhenium radioisotopes ($^{186/188}$Re) and ^{99m}Tc, an artificial gamma emitter currently used for routine imaging,[6] which shares numerous chemical properties with rhenium.

References

1. Clavaud C, Heckenroth M, Stricane C, Lelait M-A, Ménez A, Dugave C. *ChemBioChem* **7**: 1352-1355, 2006.
2. Dugave C. Cis-Trans Isomerization. *Biochemistry Wiley-VCH*, Weinheim, 2006.
3. Clavaud C, Heckenroth M, Stricane C, Ménez A, Dugave C. *Bioconjugate Chem* **17**: 807-814, 2006.
4. Clavaud C, Le Gal J, Thai R, Moutiez M, Dugave C. *ChemBioChem* **9**: 1823-1829, 2008.
5. Johannsen B, Pietzsch H-J. *Eur J Nucl Med* **29**: 263-275, 2002.
6. Dilworth Jr, Parrot SJ. *Chem Soc Rev* **27**: 43-55, 1998.

1-05-008

Solid phase peptide-carbene and peptide-phosphine transition metal catalysts in assymetric synthesis and "green" chemistry.

Meldal, Morten; Christensen, Christian A.; Worm-Leonhard, Kasper; Feldthusen Jensen, Jacob; Benito, Juan*

Carlsberg Laboratory, DENMARK

**E-mail: mpm@crc.dk*

Metallo enzymes are amongst the most sophisticated catalysts in nature, active at minute concentrations and exhibiting extreme chemo-, regio- stereo selectivity. The metal is essential and directly involved in the catalysis. These enzymes often present incredible turnovers in the catalytic event and this may be attributed to the evolved high affinity for the substrate, tight binding of the transition state and ready release of product combined with efficient catalytic machinery. In contrast most small artificial transition metal catalysts used in organic synthesis do not bind with high affinity to their substrates and stereoselectivity is frequently achieved by prohibiting the binding of the "wrong" isomer of the transition state. Such catalysts are used at relatively high concentration and are generally active towards one or several classes of functional groups with little dependence of the molecular framework of substrate. In order to utilize the folding capacity of peptide molecules and the diversity of amino acids to create libraries of catalysts presenting a chiral, substrate binding environment around the transition metal we have devised a range of techniques that are particularly suited for generation of solid phase bound catalyst in a combinatorial fashion. These involve the clean and efficient generation of phosphines[1,2] and carbenes[3,4] directly in the peptide backbone to draw most efficiently on the chirality and folding of the peptide. The phosphines and carbenes are introduced immediately prior to complexation with transition metal. The phosphines and carbenes have furthermore been combined with auxiliary ligands strategically placed in side chains of the peptide.

A large variety of peptidic palladium catalysts bound to support was prepared quantitatively on PEGA resin. This choice of resin was very important since the open structure of the PEGA matrix in aqueous solvents allowed preparation of catalysts that very efficiently catalyzed C-C bond formation in water. We have termed such catalysts organozymes. The solid phase peptide phosphine catalyst could be quantitatively recycled for new reactions without significant loss of palladium.

The solid phase mono and bis phosphine catalysts gave quantitative yields and decent ee's (up to 70%) in room temperature catalysis of C-allylation of malonic esters without any optimization of the catalyst structure. The carbene complexation to palladium was more vigorous and the catalysts less active at room temperature. The carbene catalysts were therefore significantly more stable than the phosphines and could be used at μw conditions. Thus, using the peptide carbene catalysts at elevated temperature, Sonogashira and Suzuki couplings were quantitative in as little as 10 min. Most importantly, the peptide carbene catalysts were completely stable and could be used at 100 °C for quantitative reactions in water. These PEGA bound peptide carbenes therefore act as true "green" solid phase catalysts. According to NMR the only compound eluting from a catalyst column was the product of reaction from equimolar amounts of starting materials. The catalyst could be used for 8 successive cycles of reaction at 0.03 equivalents of palladium without any loss of activity. In summary a novel and general methodology for the preparation and application of phosphine and carbene peptides for transition metal catalysis has been developed that provide the opportunity to prepare large libraries of peptide based transition metal catalysts. We are currently in the process of combining infrared measurement of heat of reaction

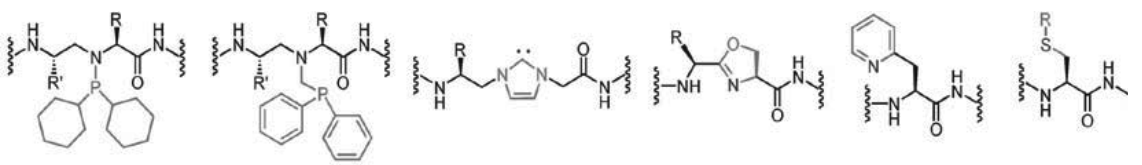

Figure 1. Transition metal binding functionality incorporated into peptides during the present work. Phosphines were introduced last by reaction with Ph_2PCH_2OH or $cHex_2PCl$ and the catalyst was formed by reaction with allyl palladium chloride. Carbenes were introduced through incorporation of a imidazolinium dipeptide building block followed by reaction with BEMP prior to complexation with $PdCl_2COD$. Oxazolines were prepared on solid support from the iodoalanine.[5] Optically pure Pya residues required the preparation and purification of a dipeptide prior to incorporation into peptides. Mono and bis carbene-pyridine building blocks were also synthesized and incorporated into peptides.

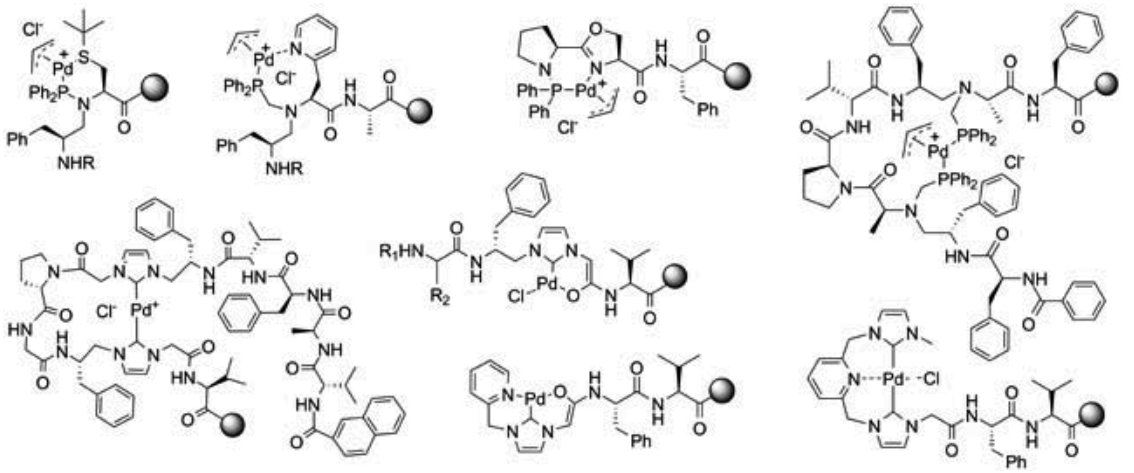

Figure 2. Typical catalyst structures used in the present work. The combination of phosphine and carbene within the same peptide was also feasible by phosphinylation followed by reaction with BEMP followed by addition of $PdCl_2COD$.

with the use of encoded beads for structure determination in order to facilitate the combinatorial assessment of catalytic activity.

References

1. Christensen CA, Meldal M. Efficient solid-phase synthesis of peptide based phosphine ligands: towards combinatorial libraries of selective transition metal catalysts. *Chem Eur J* **11**: 4121-4131, 2004.
2. Christensen CA, Meldal M. Solid-phase synthesis of a P,S-ligand system designed for generation of combinatorial peptide-based catalyst libraries. *J Comb Chem* **9**: 79-85, 2007.
3. Jensen JF, Worm-Leonhard K, Meldal M. Optically active (peptido-carbene) palladium complexes: towards true combinatorial solid phase libraries of transition metal catalysts. *Eur J Org Chem* **22**: 3785-3797, 2008.
4. Worm-Leonhard K, Meldal M. Green catalysts: Solid-phase peptide carbene ligands in aqueous transition metal catalysis. *Eur J Org Chem* **31**: 5244-5253, 2008.
5. Benito JM, Christensen CA, Meldal M. Versatile solid-phase synthesis of peptide-derived -oxazolines. Application in the synthesis of ligands for asymmetric catalysis. *Org Lett* **7**: 581-584, 2004.

1-01-101

Straightforward Synthesis of Enantiopure Tfm-amino acids from Chiral CF_3-Oxazolidines

Brigaud, Thierry[1,]; Huguenot, Florent[2]; Chaume, Grégory[1]; Caupène, Caroline[1]; Van Severen, Marie-Céline[1]*

[1]Université de Cergy-Pontoise, FRANCE; [2]Université Paris Descartes, FRANCE

[*]E-mail: thierry.brigaud@u-cergy.fr

Trifluoromethylated-amino acids (Tfm-AAs) are very attractive target molecules for the design of biologically active compounds.[1,2] Our laboratory aims to prepare enantiopure Tfm-AAs as their incorporation into key positions of peptide chains could constitute a prominent pathway to conformationally constrained and highly stable peptides. However, the preparation of these amino acids in enantiopure form remains a challenge.[3,4] We report here a straightforward synthesis of enantiopure α- and *β*-Tfm-amino acids from chiral CF_3-oxazolidines.

The Strecker-type reaction proved to be an efficient strategy for the synthesis of enantiopure *α*-Tfm-amino acids and diamines.[5]

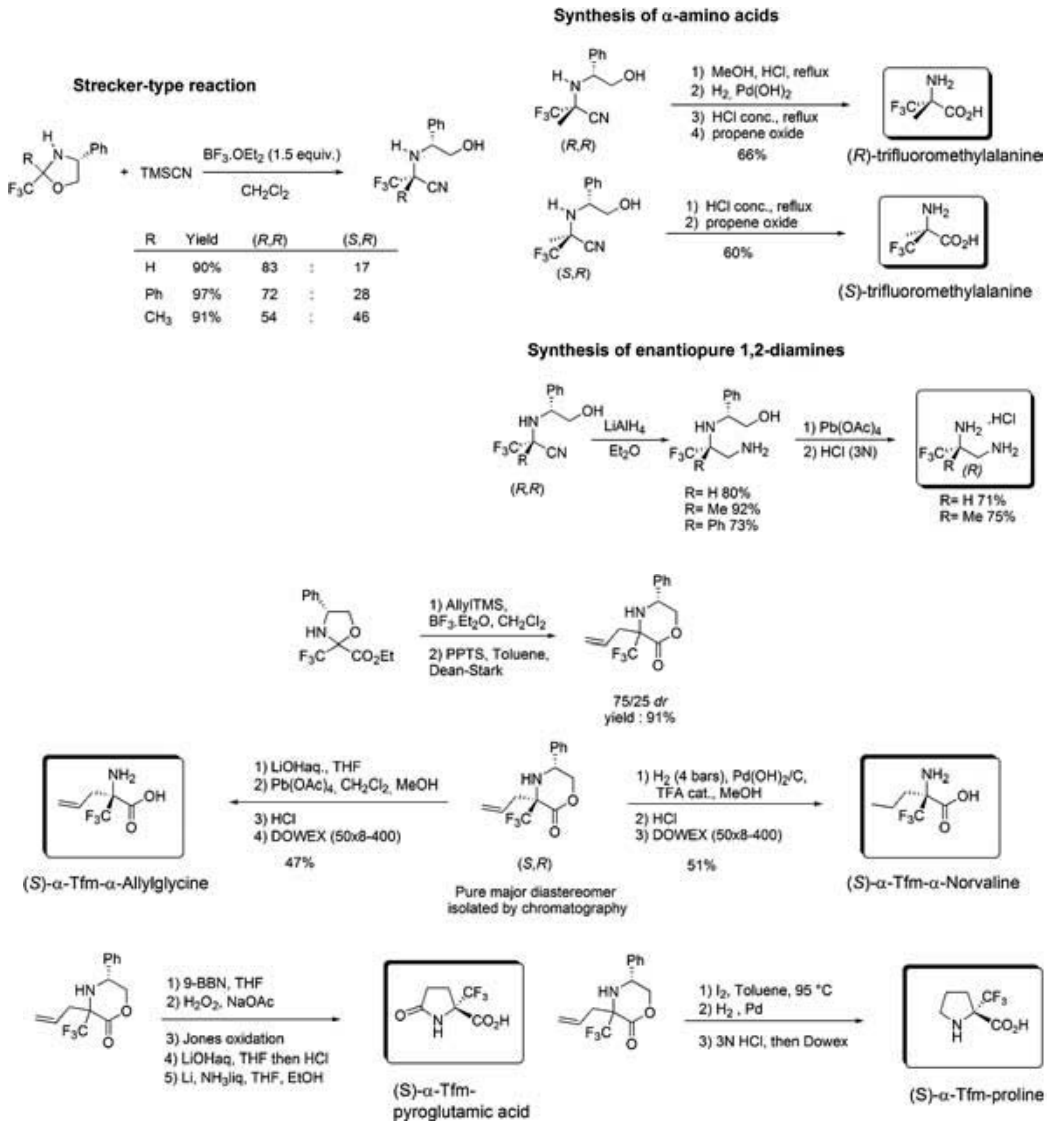

In other respect, the allylation reaction of an ethyltrifluoropyruvate based oxazolidine proved to be a very efficient strategy for the synthesis of various enantiopure α-Tfm-amino acids including cyclic aminoacids such as α-Tfm-proline[6] and α-Tfm-pyroglutamic acid.[7]

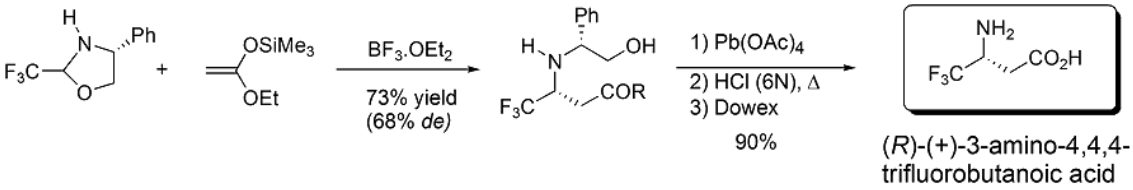

References

1. Molteni M, Pesenti C, Sani M, Volonterio A, Zanda M. *J Fluorine Chem* **125**: 1335-1343, 2004.
2. Smits R, Cadicamo CD, Burger K, Koksch B. *Chem Soc Rev* **37**: 1727-1739, 2008.
3. Qiu X-L, Meng W-D, Qing F-L. *Tetrahedron* **60**: 6711-6745, 2004.
4. Kukhar VP, Soloshonok VA. *Fluorine Containing Amino Acids: Synthesis and Properties*; Wiley: New York, 1995.
5. Huguenot F, Brigaud T. *J Org Chem* **71**: 7075-7078, 2006.
6. Chaume G, Van Severen M-C, Marinkovic S, Brigaud T. *Org Lett* **8**: 6123-6126, 2006.
7. Chaume G, Van Severen M-C, Ricard L, Brigaud T. *J Fluorine Chem* **129**: 1104-1109, 2008.
8. Huguenot F, Brigaud T. *J Org Chem* **71**: 2159-2162, 2006.

1-01-102

Highly Diastereoselective Synthesis of β²-Amino acids Using Novel Fluorinated Oxazolidine (Fox) as Chiral Auxiliary

Brigaud, Thierry; Pytkowicz, Julien; Tessier, Arnaud; Lahmar, Nour*

Université de Cergy-Pontoise, FRANCE

**E-mail: thierry.brigaud@u-cergy.fr*

β^2-amino acids are finding an increasing interest because of their biological properties.[1] Moreover, their incorporation into a peptide chain gives rise to the formation of well defined β-peptide secondary structures[2] associated with specific biological activities. For these reasons, several chiral auxiliary-based[3] or catalytic asymmetric methods have recently been reported for their preparation.

We recently reported that the alkylation reactions of an amide enolate derived from a *trans* trifluoromethylated oxazolidine (**Fox**) chiral auxiliary occur with a complete diastereoselectivity and in good yields with various electrophiles.[4]

We report here that the alkylation reactions of a homoglycine–type precursor were also performed in good yields and with a complete diastereoselectivity (Table).[5] Interestingly, the reaction with hindered halogenated compounds such as isobutyl iodide and isopropyl iodide giving rise to β^2-homoleucine and β^2-homovaline precursors were also completely diastereoselective.

The (*R*) configuration of the unique diastereomer is in good agreement with a favoured *re* face alkylation of the *Z* amide enolate. To explain the excellent diastereoselectivity, we propose the existence of a transition state presenting a F•••Na interaction.[6]

Using the benzylated diastereomerically pure amide as a representative substrate, we then performed the LAH mediated removal of the Fox chiral auxiliary followed by an oxidation in order to obtain the enantiopure β^2-homophenylalanine. The corresponding γ-amino alcohol was obtained by reduction. In any cases, the Fox chiral auiliary was conveniently recovered.

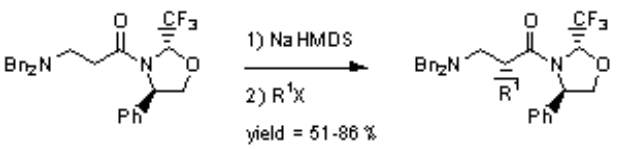

R¹	Yield (%)[a]	de[b]
Me	84	>98 %
Bn	86	>98 %
All	82	>98 %
Et	80	>98 %
*i*Bu	51	>98 %
*i*Pr	51	>98 %

[a]yield of purified product
[b]based on ^{19}F crude NMR analysis

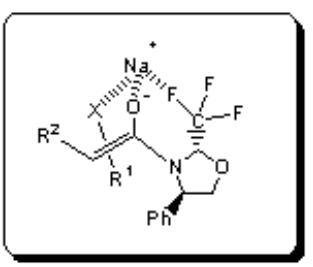

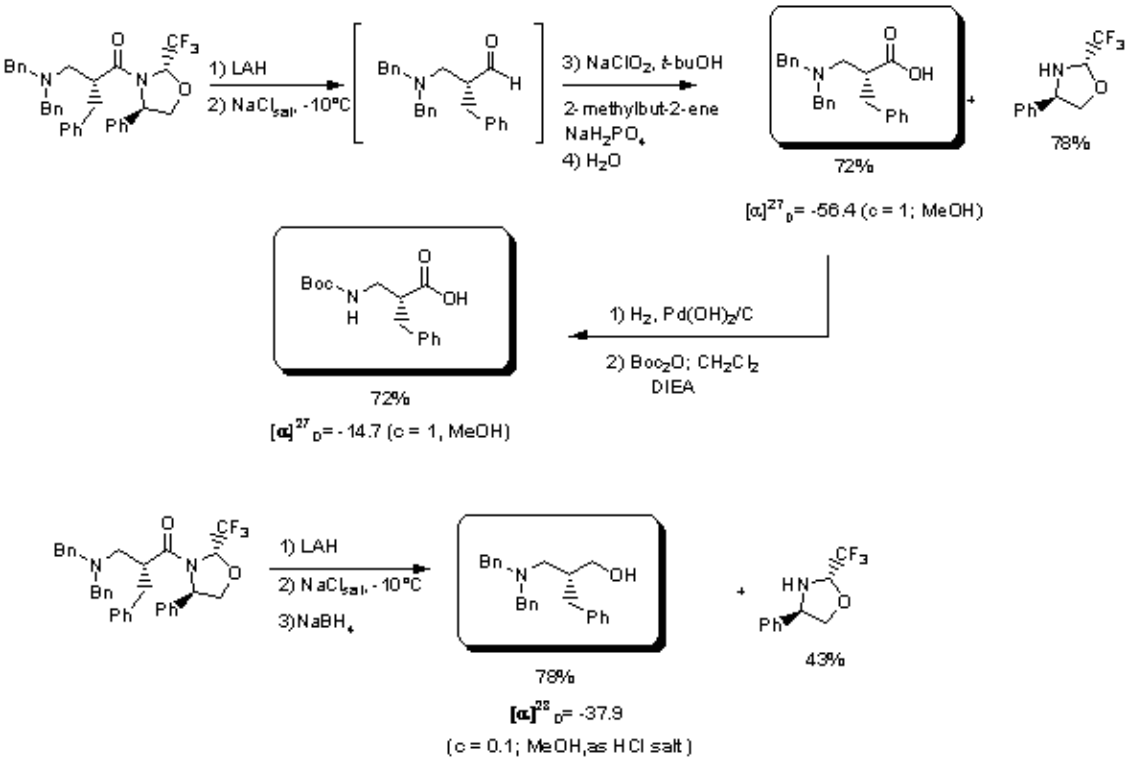

Acknowledgment

The authors thank Central Glass Company for the generous gift of trifluoroacetaldehyde hemiacetal and financial support.

References

1. Liu M, Sibi MP. *Tetrahedron* **58**: 7991–8035, 2002.
2. (a) Seebach D, Beck AK, Bierbaum D. *J Chem Biodiversity* **1**: 1111–1239, 2004.
3. (a) Beddow JE, Davies SG, Ling KB, Roberts PM, Russell AJ, Smith AD, Thomson JE. *Org Biomol Chem* **5:** 2812–2825, 2007.
   (b) Moumne R, Denise B, Guitot K, Rudler H, Lavielle S, Karoyan P. *Eur J Org Chem 2007* **12**: 1912–1920.
   (c) Moumne R, Lavielle S, Karoyan P. *J Org Chem* **71**: 3332–3334, 2006.
   (d) Ponsinet R, Chassaing G, Vaissermann J, Lavielle S. *Eur J Org Chem* **1**: 83–90, 2000.
4. Tessier A, Pytkowicz J, Brigaud T. *Angew Chem Int Ed Engl* **45:** 3677-3681, 2006.
5. Tessier A, Lahmar N, Pytkowicz J, Brigaud T. *J Org Chem* **73**: 3970-3973, 2008.
6. Sini G, Tessier A, Pytkowicz J, Brigaud T. *Chem Eur J* **14**: 3363-3370, 2008.

1-01-103

Synthesis of CF_3-Pseudoproline Units: An approach to conformationally constrained dipeptides

Chaume, Grégory; Barbeau, Olivier; Brigaud, Thierry*

University of Cergy-Pontoise, FRANCE

**E-mail: gregory.chaume@u-cergy.fr*

Conformationally constrained cyclic amino acids have recently gained considerable interest because of their ability to control the conformation of peptides for structure–activity relationships investigations as well as for the design of peptidomimetics.[1] In particular, incorporation of proline derivatives is known to restrict the amino acyl-proline *cis*/*trans* isomerization,[2] to limit the protein folding and consequently to modulate the biological activity of peptides. Based on these observations, Mutter's group introduced pseudoproline building blocks (ψPro) into a peptide sequence as reversible protecting groups for Ser, Thr and Cys.[3] The ψPro residues proved to be versatile tools for overcoming the aggregation caused by hydrophobic interactions encountered during solid-phase peptide synthesis (SPPS).[4] They also turned out to be inducers of *β*–turns containing predominantly *cis*-amide bond[5] and useful tools in peptide cyclization.[6]

Our group is interested in the stereoselective synthesis of α– and *β*–trifluoromethyl amino acids starting from chiral CF_3-oxazolidines (Fox) or imines.[7] As a complementary strategy, we have also developed the preparation of CF_3–ψPro since conformational restrictions as well as unique physical and biological properties imparted by the fluorinated group are expected from the incorporation of such kind of amino acids into a peptide chain.[8] Because the chemical stability of ψPro systems strongly depends on the electronic effects of the C_2 substituents, pseudoprolines containing a CF_3 group at the C_2 show a high degree of stability towards acidic media. This property could also make them convenient building blocks for the purification of peptides issue from SPPS.

We first focused our attention to the preparation of CF_3–pseudoprolines. Condensation of fluoral with (*S*)-serine methyl ester gave the corresponding oxazolidines **3** in good yield as a separable 1:1 (from Serine **2**) to 9:1 (from Serine **1**) diastereomeric ratio (Fig. 1). Condensation of the trifluoroacetone with (*S*)-serine methyl ester **2** afforded the more hindered oxazolidines **4** in 81% yield as a non separable 9:1 diastereomeric ratio.

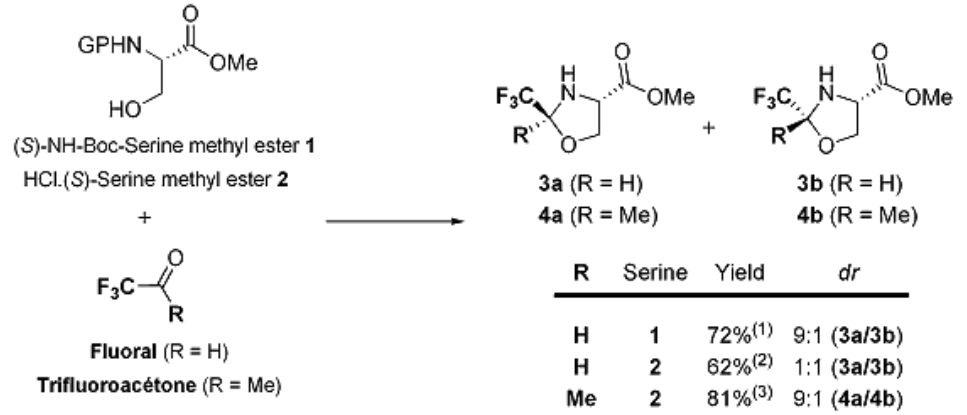

R	Serine	Yield	*dr*
H	1	72%(1)	9:1 (**3a/3b**)
H	2	62%(2)	1:1 (**3a/3b**)
Me	2	81%(3)	9:1 (**4a/4b**)

(1): PPTS (0,1 eq.), Toluene, Dean-Stark for 18h;
(2): Sodium acetate (1 eq.), Toluene, Dean-Stark for 6h;
(3): Sodium acetate (1 eq.), Toluene, 0°C to 20°C then Dean-Stark for 6h.

After separation by chromatography, oxazolidines **3a** and **3b** were separately subjected to the *N*-acylation using either acyl chloride or symmetric anhydride (Fig. 2). Despite the low nucleophilicity of the nitrogen due to the presence of the trifluoromethyl group, acylation reaction was performed in high yield. Analysis of the *cis*/*trans* ratio by ^{13}C NMR showed a 40/60 ratio with acetyl and propionyl group. In the case of benzoyl group, only the *cis* rotamer were observed probably due to steric hindrance.

We then turned our attention to the incorporation of CF_3-oxazolidines **3a** or **3b** into a peptide chain. Preparation of dipeptides incorporating the CF_3-ψPro

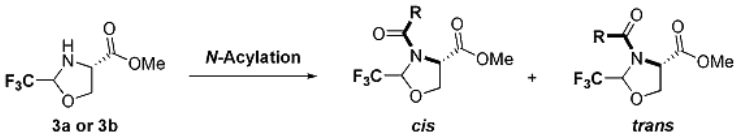

cis/trans ratio in $CDCl_3$ at 25°C

R	$(RCO)_2O$ (*cis*/*trans*)	RCOCl (*cis*/*trans*)
Me (5a)	84% (40/60)[1]	74% (40/60)[2]
Me (5b)	79% (48/52)[1]	-
Et (6a)	65% (40/60)[1]	97% (40/60)[2]
Et (6b)	89% (52/48)[1]	-
Ph (7a)	-	90% (100/0)[3]
Ph (7b)	-	96% (100/0)[3]

[1]: $(RCO)_2O$ (10 eq.), 140°C, 18h; [2]: RCOCl (3 eq.), Pyr. (3 eq.), DCM, 18h, r.t.; [3]: PhCOCl (1 eq.), 1 h, 100°C

unit at the *N*-terminal position was performed in good yield applying standard solution-phase peptide synthesis. Attempts to acylate the CF_3-ψPro nitrogen using the same conditions failed. However, acyl chloride activation of nosyl-alanine promoted the peptide coupling reaction in high yield to afford the same dipeptide **9** in 80/20 diastereomeric ratio whatever the starting oxazolidine. The *cis*/*trans* isomerization proved to be highly dependant of solvent, but X-Ray structure of **9** showed a *cis* amide bond.

In conclusion, we have successfully prepared dipeptides containing α-CF_3-pseudoproline at either C- or N-terminal position. Optimization of the peptide coupling reaction for C-terminal dipeptide is currently under investigation.

Acknowledgments

The authors thank Central Glass Company for a generous gift of fluoral and X. Le Goff of Ecole Polytechnique, Palaiseau for the X-ray structure of **9**.

References

1. Mikhailiuk P K, Afonin S, Palamarchuk G V, Shishkin O V, Ulrich A S, Komarov I V. Synthesis of trifluoromethyl-substituted proline analogues as 19F NMR labels for peptides in the polyproline II conformation. *Angew Chem Int Ed* **47**: 5765-5767, 2008.
2. Flores-Ortega A, Jimenez A I, Cativiela C, Nussinov R, Aleman C, Casanovas J. Conformational preferences of a-substituted proline analogues. *J Org Chem* **73**: 3418-3427, 2008.
3. Tuchscherer G, Mutter M. Under the influence of phi and psi. *J Pept Sci* **11**: 278-282, 2005.
4. Wohr T, Wahl F, Nefzi A, Rohwedder B, Sato T, Sun X, Mutter M. Pseudo-prolines as a solubilizing, structure-disrupting protection technique in peptide synthesis. *J Am Chem Soc* **118**: 9218-9227, 1996.
5. Dumy P, Keller M, Ryan D E, Rohwedder B, Wohr T, Mutter M. Pseudo-prolines as a molecular hinge: reversible induction of cis amide bonds into peptide backbones. *J Am Chem Soc* **119**: 918-925, 1997.
6. Skropeta D, Jolliffe K A & Turner P. Pseudoprolines as removal turn inducers: tools for the cyclization of small peptides. *J Org Chem* **69**: 8804-8809, 2004.
7. For recent entry and references, see: Ghaume G, Van Severen M-C, Ricard L, Brigaud T. Concise access to enantiopure (*S*)- and (*R*)-α-trifluoromethyl pyroglutamic acids from ethyl trifluoropyruvate-based chiral CF3-oxazolidines (Fox). *J Fluorine Chem* **129**: 1104-1109, 2008.
8. Kukhar V P, Soloshonok V A. *Fluorine containing amino acids, synthesis and properties,* Wiley, New York, 1995.

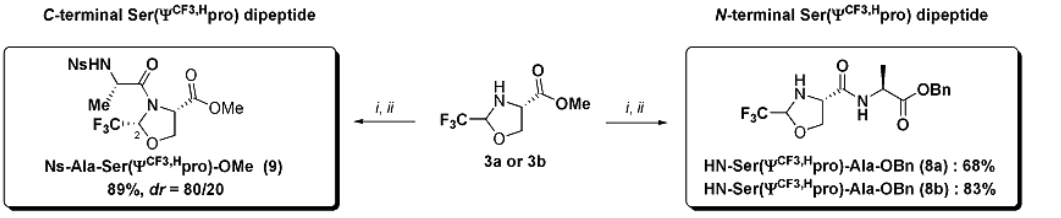

i: 1-chloro-*N*,*N*-2-trimethylpropenylamine (7 eq.), DCM;
ii: Collidine (1eq.), Ns-Ala-OH (7 eq.), DCM, 18h.

i: LiOHaq, THF;
ii: (*S*)-HCl.H_2N-Ala-OBn, HOBt, EDCI, $NaHCO_3$, DCM, 18h.

1-01-104

Synthesis of antimicrobial peptide Parasin I

Krasnoschek, Anastasia A[1]; Gluzdikov, Ivan A[1,]; Vinogradov, Valentin A[2]; Titov, Mikhail I[1]*

[1]Chemistry of Natural Compounds, Chemical Department, Saint-Petersburg State University; [2]Biovalent Ltd

RUSSIAN FEDERATION

[*]E-mail: givana1@yandex.ru

Abstract

The method of convergent synthesis of antimicrobial peptide Parasin I with use of Fmoc-solid phase peptide synthesis (SPPS) is developed. It is shown, that condensation of fragments 8-13 and 14-19 with the subsequent elongation of a chain on one amino acid more effective method, than synthesis with use of three fragments. The structure was supported by mass-spectra (MALDI-TOF) and HPLC analysis.

Keywords. convergent synthesis; antimicrobial peptide; Parasin I; SPPS.

Introduction

In 1998 Park *et al*.[1] described Parasin I – a novel cationic peptide isolated from catfish (Parasilurus asotus) epithelia. They demonstrated its strong antimicrobial activity against a wide spectrum of microorganisms and lack of any hemolytic activity. Parasin I has a molecular mass of 2000,4 Da and consist of 19 amino acids, including three arginines and five lysines, which contribute to the net charge of +8. The complete amino acid sequence of Parasin I is **Lys[1]-Gly[2]-Arg[3]-Gly[4]-Lys[5]-Gln[6]-Gly[7]-Gly[8]-Lys[9]-Val[10]-Arg[11]-Ala[12]-Lys[13]-Ala[14]-Lys[15]-Thr[16]-Arg[17]-Ser[18]-Ser[19]**.

In the literature accessible to us there are instructions on synthesis Parasin I and its some analogues in quantity of several mg by means of automatic solid phase peptide synthesizer.[2] We had been developed a method of synthesis Parasin I, suitable for scaling.

Results and discussion

General information. For reception target peptides were used amino acids of L-configuration. Cleanliness of the received substances estimated by means of analytical HPLC. An analytical highly effective liquid chromatography spent on KNAUER Smartline 2500 chromatograph, equipped spectrophotometric detector. At carrying out analytical HPLC used column Phenomenex - Luna (2), C-18, 5мкм, 4×250 mm and Diaspher - 300 - Ñ-4, 5мкм, 4×250 mm at speed of a stream eluent 1 ml/min. Detection at 214 nm and 254 nm.

Mass-spectra have been removed on MALDI-TOF Voyager-DE PerSeptive BioSystems in a mode of a delay extraction (DE). As a matrix in most cases was used the a-ciano-4-hydroxycinnamic acid.

Synthesis. During the full synthesis of Parasin I by elongation of a chain from the C-end by SPPS using Fmoc/t-Bu – chemistry on 2-chlorotritylchloride resin, addition of Arg^{11} appeared incomplete, possibly, owing to aggregation growing peptide chains on the polymeric carrier. Increasing concentration of amino acid, use of other condensing agents, increasing temperature (to 55 °C) and reaction time (about two days) did not lead to acceptable levels of joining Arg^{11}. Therefore a decision was taken to synthesize the target peptide by convergent SPPS. Breakdown of the polypeptide chain of Parasin I into fragments was carried out in order to lower the probability of collateral processes (primarily racemization) during the assembly of the target molecule. Since the chain elongation was becoming ineffective after Ala^{12}, we have halved the remaining 12-amino acid fragment making use of the favorable arrangement of the glycine residues 7 and 8. The protected peptide fragments were synthesized with high purity by SPPS using Fmoc-strategy on 2-chlorotritylchloride resin. We had been synthesized fragments 1-7, 8-13, 14-19:

FmocLys[1](Boc)Gly[2]Arg[3](Pbf)Gly[4]Lys[5](Boc)Gln[6](Trt)Gly[7]OH

FmocGly[8]Lys[9](Boc)Val[10]Arg[11](Pbf)Ala[12]Lys[13](Boc)OH

FmocAla[14]Lys[15](Boc)Thr[16](tBu)Arg[17](Pbf)Ser[18](tBu)Ser[19](tBu)OH

Completeness of passage of reaction defined by means of the Kaiser-test and the indicator bromphenol blue. The received fragments have been connected with each other by means of 1,3-diisopropylñarbîdiimide (DIC) at presence 1–hydroõó-7-azabånzotriazole (HOAt) under the Scheme 1.

Conditions of carrying out of reactions:
- Loading on resin: 0,3 mmol/g
- Time of reaction: 24 hours
- Temperature: room
- Surpluses of reagents: Table 1

Table 1. Surpluses of reagents

Reagent	mmol
Fmoc-14-19-OH	1
Fmoc-8-13-OH	3
Fmoc-1-7-OH	3
DIC	3,3
HOAt	3,3

The HPLC analysis of the obtained substance has shown the presence of a signal of an impurity. On a mass spectrum, in addition to a signal of a molecular ion of Parasin I (MW=2001,67 Da) there was a signal corresponding to a molecular ion of a fragment 8-19 (MW=1289,96 Da). This result indicates to an incomplete coupling of the fragment 1-7.

We have undertaken an attempt to consecutively elongate the chain by addition of the single amino acids after Gly[7]. The fragment condensation 8-13 + 14-19 has been carried out in the same conditions as in the first case (Scheme 2). This approach makes it possible to obtain target peptide with much higher yield. By this procedure, Parasin I was purified by RP-HPLC. The mass of the molecular ion was in good agreement with the calculated value.

Conclusions

Thus, the method convergent synthesis Parasin I has appeared is more productive, than a linear method solid-phase synthesis. Furthermore the chosen strategy allows to receive analogues native peptide, varying separate fragments of its sequence.

References

1. Park IY, Park CB, Kim MS, Kim SC. *FEBS Lett* **437**: 258-262, 1998.
2. *US Patent No* 2008/006316594 B1, 2001.

Scheme 1

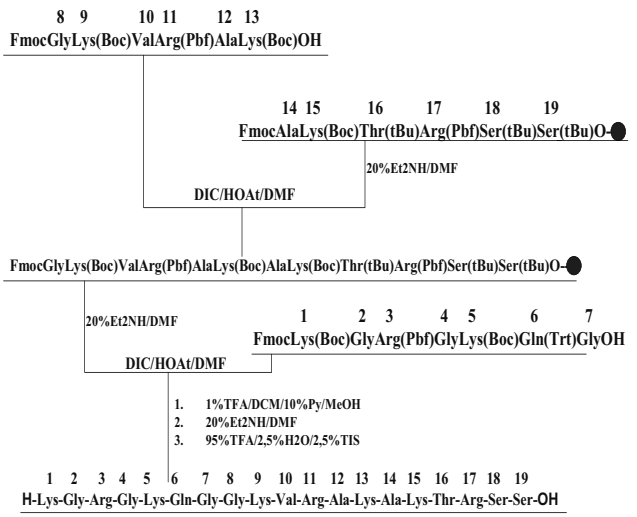

Scheme 2

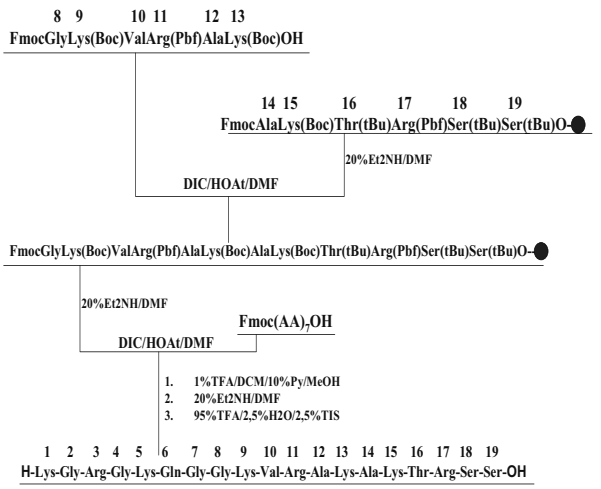

1-01-105

Synthesis of biological active cyclopeptides corresponding to 4th loop of nerve growth factor

Gudasheva, Tatiana[1]; Morozova, Anna[1]; Antipova, Tatiana[1]; Akparov, Valery[2]; Seredenin, Sergey[1]

[1]Zakusov Research Institute of Pharmacology Russian Academy of Medical Sciences, RUSSIAN FEDERATION; [2]Institute of Genetics and Selection of Industrial Microorganisms, RUSSIAN FEDERATION

[*]E-mail: sosnovka@mtu-net.ru

There is substantial evidence indicating that substances with the activity of the nerve growth factor (NGF) can be useful in the treatment of some neurodegenerative diseases, such as Alzheimer's disease, Parkinson's disease, ets. Inhibitors of NGF have potential for treatment NGF-dependent cancer. NGF was promoted as a drug in the treatment of Alzheimer's disease and neuropathies caused by diabetes and AIDS but was taken out of clinical trials because of grave side effects.[1] F.M. Longo and M. Manthorpe showed that cyclic hepta- and octapeptides involving five to six amino acid residues from the sequences of loops 1, 2, or 4 of NGF behave as agonists of NGF, by increasing the survival of neurons.[2] Our goal was to synthesize cyclopeptide NGF analogues containing only three amino acid residues from the sequence of loop 4 in order to identify the shortest active fragment.

The object of modeling was mice NGF loop 4 formed by residues 93–96: -Asp-Glu-Lys-Gln-, which is most exposed outward. Molecular modeling using the program HyperChem showed that the conformation of the *β*-turn region of loop 4 is similar to that of the four-membered cyclopeptide cyclo(-Asp- Glu-Lys-Gly-). We included in its composition the amino acid residues that belong to the central peptide fragment of the *β*-turn and the preceding residue of aspartic acid in order to elucidate its role in the activity of NGF. We chose glycine as the fourth residue instead of Gln 96. To study the effect of the peptide conformation on activity in more detail, we synthesized two more cyclopeptide homologs containing the same sequence Asp-Glu-Lys and, respectively, two and three Gly residues. Thus, we synthesized the following cyclic peptides: cyclo(-Gly-Asp-Glu-Lys-) (VII), cyclo(-Gly-Gly-Asp-Glu-Lys-) (VIII), and cyclo(-Gly-Gly-Gly-Asp-Glu-Lys-) (IX). The linear precursors H-Gly-Asp(OBut)-Glu(OBut)-Lys(Boc)-OH (I), H-Gly-Gly-Asp(OBut)-Glu(OBut)-Lys(Boc)-OH (II), and H-Gly-Gly-Gly-Asp(OBut)-Glu(OBut)-Lys(Boc)-OH(III), were obtained by the solid-phase method using the standard Fmoc/But strategy for the stepwise elongation of the chain from the N-terminal residue H-Lys(Boc)- on a polymeric support with an anchor Clt group. Highly acid-labile trityl esters can be selectively cleaved by 0.5% TFA/CH_2Cl_2. After purification by preparative HPLC, the yields of six-, five-, and four-membered linear protected peptides (I)–(III) were 52, 56, and 87%, respectively. In our conditions, hexapeptide (III) was obtained in two forms in the ratio 3:2. These compounds were identified as diastereomers since they had close retention times in HPLC and similar sets of signals in ^{1}H NMR spectra. It is evident that the formation of the second isomer was caused by the unexpectedly high degree of epimerization during the attachment of one of amino acid residues, probably aspartic acid. We explain this phenomenon by the use of the BOP reagent since, in the case of four and five-membered peptides, PyBOP was used to activate the same amino acids, and no epimerization was observed. The cyclization was performed using a diastereomer of hexapeptide, which was obtained with a high yield; we considered it to consist of L-amino acids. The cyclization of linear precursors of (I)–(III) for suppressing the intermolecular side reactions was carried out according to the Ziegler dilution principle at a concentration of the peptide 10^{-3} M in DMF (Table 1).

Table 1. Yields and analytical data for protected cyclopeptides IV-VI.

Peptides	Method of cyclization	Yield, %	Analytical HPLC (214 nm)			Data of ESI-MS		Monomer content, %
			R_t, min		Ratio of peak heights	Molecular mass, M		
			LD*	LE*		Found $[M+H]^+$	Calculated, M	
(IV)	BOP	92	12.00&12.20	11.25&11.27	1:3	756&1511	755	75
	HBTU	74	12.08 &12.15	11.26&11.27	1:3	756&1511		75
	DPPA;10^{-3}M	62	12.38	11.57	-	756		100
(V)	BOP	72	13.56&13.68	12.00&12.10	1:3	699 & 1397	698	75
	DPPA; 10^{-3}M	48	14.00	12.27	-	699		100
(VI)	BOP	81	17.02	14.93	-	1283	641	0
	DPPA;10^{-3}M	40	17.32&17.40	15.00&15.10	3:1	642&1283		25
	DPPA;10^{-4}M	10	17.48	15.35	-	642		100

*Analytical HPLC was carried out on a Reprosil 80 ODS-2 column (125 x4 mm, C_{18}, 3 um) at a flow rate of 0.5 ml/min in a gradient of acetonitrile concentration in water (30-80%, 25 min) (LD) and using the same gradient on a Diasorb 130-C16T column (4.6 x150 mm, C_{16}, 7 um) at a flow rate of 1 ml/min (LE)

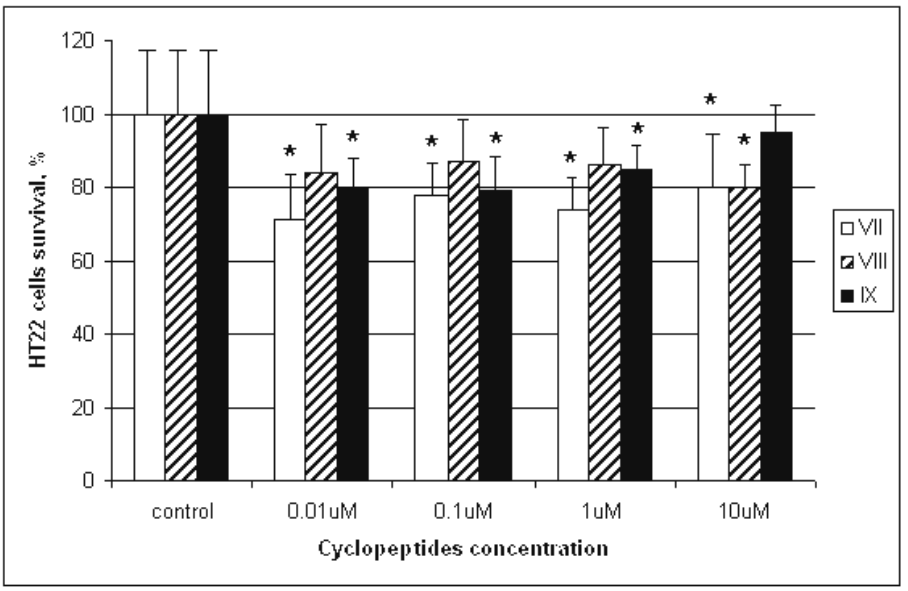

Figure 1. Survival-counteractive activity of NGF cyclopeptide analogs VII-IX. HT-22 cells were cultered as described [3]. MTT was added to wells 28h after seeding and optical density of each well was measured by spectrophotometry at 600 nm. The dates are an average of 12 independed bioassays. * $p<0.05$; Student t-test.

With the use of the BOP and HBTU reagents, the conversion of initial compounds to cyclic products was from 70 to 90% for all peptides, and 40–60% in the presence of the milder activating reagent DPPA. The products of peptide cyclization with the use of BOP, HBTU, and, in the case of the four-membered peptide, DPPA contained a dimeric cyclopeptides in addition to the monomeric cyclopeptides cyclo(-Gly-Asp(OBut)-Glu(OBut)-Lys(Boc)-) (IV), cyclo(-Gly-Gly-Asp(OBut)-Glu(OBut)-Lys(Boc)-) (V), and cyclo(-Gly-Gly-Gly-Asp(OBut)-Glu(OBut)-Lys(Boc)-) (VI). The monomers and dimers were identified by mass spectrometry. Their relative amounts in the mixture were determined from the data of analytical HPLC. The extent of dimerization depended on the nature of the activating agent and the size of the cycle. The greatest amounts of the dimer were obtained using BOP and HBTU reagents. In the case of BOP, the dimer was the only reaction product of the four-membered peptide, whereas five- and six-membered peptides formed about 25% of the dimer. As opposed to these reagents, DPPA at the same concentrations of the peptides led to pure five- and six-membered cyclopeptides; in the case of the four-membered peptide, the yield of the monomeric cyclopeptide was about 25%. At the dilution to 10^{-4} with the use of DPPA, a four-membered cyclopeptide without the dimeric contaminant was obtained. The yield in this case was 10%. All cyclic peptides were separated by preparative reversed-phase HPLC. The structures and diastereomeric purity were confirmed by the ^{1}H NMR spectroscopy data. The molecular masses of cyclopeptides were supported by mass spectrometry. The deblocking of cyclopeptides was carried out simultaneously with the removal of Boc- and But-groups by treatment with 4 M HCl in dioxane. Thus, we obtained novel low-molecular-weight analogues of NGF that reproduce the conformation of its fourth loop and contain only three amino acid residues of this loop, including two central residues of the β-turn and the preceding residue Asp93 whose role in the manifestation of the neuroprotective properties of NGF has been so far little understood. Synthesised cyclopeptides decreased survival of immortalized mice hippocampal cells HT-22 in the concentration range of 10^{-5} – 10^{-8} M. Most active was cyclotetrapeptide VII (Fig. 1).

This confirms that cyclotetrapepride conformation is close to biological active β-turn conformation. This work is supported by a grant from the Russian Foundation of Basic Research, grant No. 09-04-0104.

References

1. Apfel SC. *Ann Neurol* **51**: 8-11, 2002.
2. Longo FM, Manthorpe M. *US patent* 5,958,875, 1999.
3. Tan S, Wood M, Maher P. *J Neurochem* **71**: 95-105, 1998.

1-01-106

Enantioselective synthesis of fluorinated *p*-borono-L-phenylalanines enriched with ^{10}B atom

Hattori, Yoshihide[1]; Kurihara, Kei[2]; Asano, Tomoyuki[3]; Kirihata, Mitsunori[3]; Yamaguchi, Yoshihiro[2]; Wakamiya, Tateaki[2]

[1]Frontier Science Innovation Center, Osaka Prefecture University, Sakai, Osaka 599-8231, JAPAN; [2]Faculty of Science and Technology, Kinki University, Higashi-osaka, Osaka 577-8502, JAPAN; [3]Graduate School of Life & Environmental Sciences, Osaka Prefecture University, Sakai, Osaka 599-8231, JAPAN

[*]E-mail: vagrants@mail.goo.ne.jp

Introduction

The boron neutron capture therapy (BNCT) based on the interaction between ^{10}B isotope and thermal neutron has been highly noted in recent years as one of promising techniques for treatment of cancers. *p*-(^{10}B)Borono-L-phenylalanine (L-^{10}Bpa), in which boron atom is enriched with ^{10}B isotope, is now using clinically as an efficient ^{10}B carrier for treatment of patients in particular with malignant brain tumor and melanoma.[1]

From the standpoint of diagnosis of cancers, the magnetic resonance imaging (MRI) is noted as one of common techniques. In particular, MRI based on the measurement of ^{19}F atom is becoming a remarkable one. To create practical materials utilizing as not only the ^{10}B carrier but also MRI probe, we had already synthesized the compounds containing both ^{10}B and ^{19}F atoms in a single molecule such as *β*-[4-(^{10}B)borono-2,6-difluorophenyl]-DL-alanine [DL-^{10}Bpa(2,6F$_2$)],[2] *β*-[4-(^{10}B)borono-2-trifluoromethylphenyl]-DL-alanine [DL-^{10}Bpa(2CF$_3$)].[3]

So far as we know, the biological activity of amino acids is sometimes different between L and D forms. In fact, L-^{10}Bpa is using clinically for BNCT in recent years, since the incorporating amount of L-^{10}Bpa is higher than that of D-^{10}Bpa or DL-^{10}Bpa. In order to develop a practical method for the synthesis of L-^{10}Bpa, we recently established the enantioselective method utilizing the Negishi reaction based on the coupling of 4-(^{10}B) boronoiodobenzene derivative with 3-iodo-L-alanine derivative.[4]

In the present paper, we report the enantioselective syntheses of L-^{10}Bpa(2,6F$_2$)(**1**) and L-^{10}Bpa(2CF$_3$)(**2**) based on the Negishi reaction.

Results and Discussion

At first, the amino group of 4-bromo-2,6-difluoroaniline (**3**) was converted into the triazene group, and the bromo group was substituted into the borono group. After the iodination of the triazene group, the borono group was protected with 1,8-diaminonaphtalene, which was developed as masking agent in the Suzuki-Miyaura cross coupling by Suginome *et al*.[5] In the next step, Z-Ala(3I)-OMe was converted into Zn adduct, and then coupled with aryliodide **7** under the Negishi coupling conditions to give the precursor of L-^{10}Bpa(2,6F$_2$) (**8**). The diaminonaphtyl group of compound 8 was cleaved with 2M H_2SO_4, and Z-L-^{10}Bpa(2,6F$_2$)-OMe thus obtained was hydrolyzed with 3M HCl to give L-^{10}Bpa(2,6F$_2$) (**1**). The synthesis of L-^{10}Bpa(2CF$_3$) was accomplished in a similar manner of L-^{10}Bpa(2,6F$_2$). HPLC analysis of **1** and **2** with a chiral column revealed the optical purity to be >99%.

References

1. Kato I, Ono K, Sakurai Y, Ohmae M, Maruhashi A, Imahori Y, Kirihata M, Nakazawa M, Yura Y. *Appl Radiat Isot* **61**: 1069-1073, 2004.
2. Hattori Y, Asano T, Niki Y, Kondoh H, Kirihata M, Yamaguchi Y, Wakamiya T. *Bioorg Med Chem* **14**: 3258-3262, 2006.
3. Hattori Y, Yamamoto H, Asano T, Niki Y, Kondoh H, Kirihata M, Yamaguchi Y, Wakamiya T. *Bioorg Med Chem* **15**: 2198-2205, 2007.
4. Hattori Y, Asano T, Kirihata M, Yamaguchi Y, Wakamiya T. *Tetrahedron Lett* **49**: 4977-4980, 2008.
5. Noguchi H, Hojo K, Suginome M. *J Am Chem Soc* **129**: 758-759, 2007.

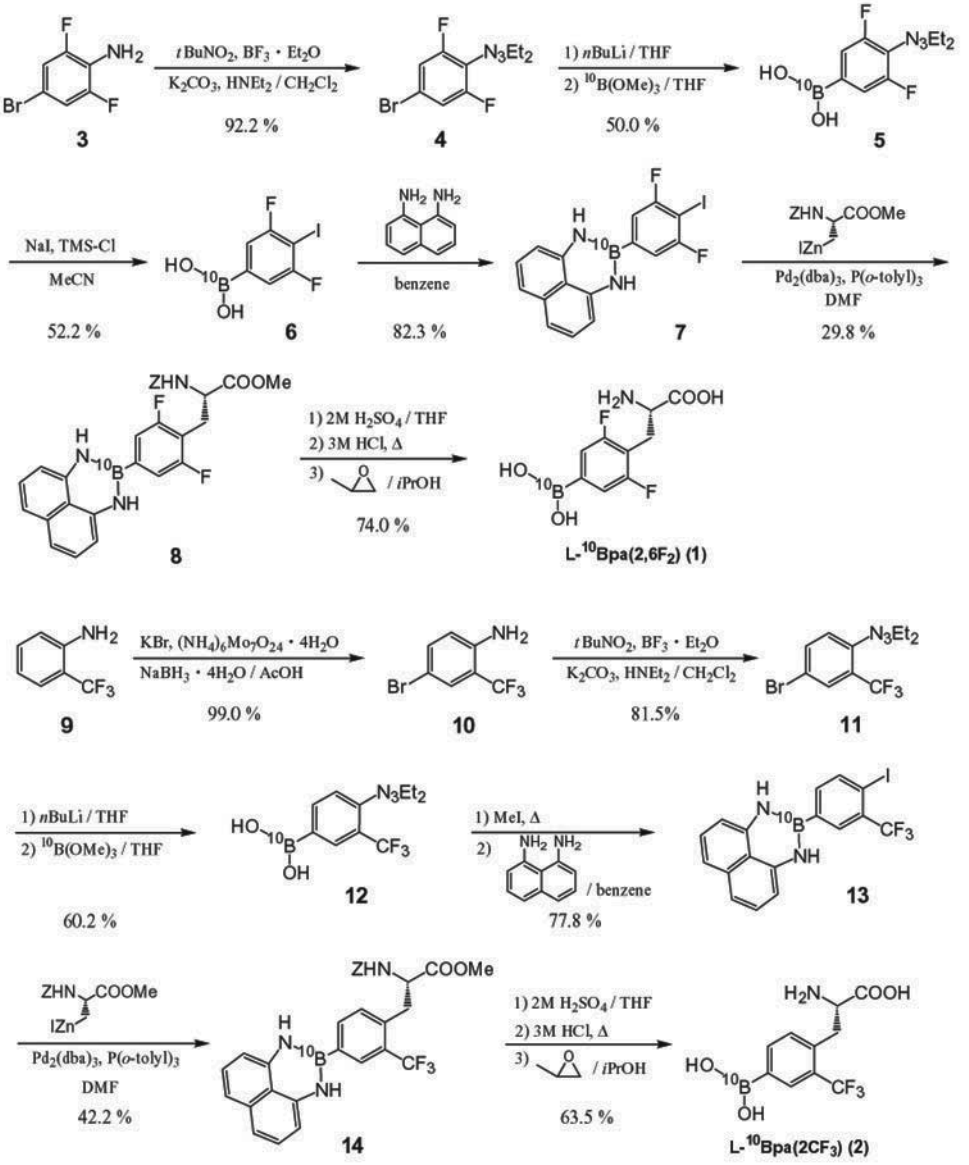

Figure 1. Enantioselective synthesis of fluorinated L-Bpas.

1-01-107

New APA inhibitors interacting with the S1 subsite bring new insights in the APA substrate specificity mediated by the calcium ion.

Claperon, Cédric[1]; Rozenfeld, Raphel[1]; Iturrioz, Xavier[1]; Okada, Mayumi[1]; Roques, Bernard[2]; Maigret, Bernard[3]; LLorens Cortes, Catherine[1]; Inguimbert, Nicolas[2,]*

[1]Collège de France, INSERM U691, FRANCE; [2]University Paris Descartes, INSERM U640, FRANCE; [3]University, CNRS UMR 7503, FRANCE

[*]E-mail: nicolas.inguimbert@univ-paris5.fr

Introduction

Aminopeptidase (APA, EC 3.4.11.7) is a membrane-bound zinc metallopeptidase involved in the maturation of brain angiotensin III, a peptide which exerts a tonic stimulatory action on blood pressure in hypertensive animals.[1] Therefore, developing inhibitors of this enzyme should result in new antihypertensive agents with possible new application in the treatment of certain forms of hypertension.[2-3] We and others have previously reported the design of such inhibitors.[4-5] Nevertheless, the improvement of the affinities of the inhibitors is relatively impaired since the three dimensional (3D) structure of the enzyme is not available. With the aim of getting insight into inhibitors optimization, a 3D model of APA was constructed in our group as an alternative.[6] Furthermore, it is well established that APA substrate specificity and enzymatic activity are calcium dependent. In order to render this model more accurate and so on to identify the amino acids residues involved in calcium binding, we have designed new inhibitors able to explore the APA S1 subsite to better understand its specificity.

We will report the synthesis of these new inhibitors, as well as an inversion of the specificity of APA S1 subsite in absence of calcium. These results and the identification of the amino acids implicated in calcium binding will be discussed on the basis of site-directed mutagenesis studies. One of the designed inhibitors, NI 926 (Ki = 70 nM) is to date the more potent inhibitor of APA activity measured without calcium. Altogether, these data should allow the improvement of APA inhibitors by structure aided design.

Inhibitors synthesis

Esterification of (S)-*N*-Boc-trityl-cysteine with trimethylsilyldiazomethane yields compound **1** which was then used for the introduction of the carboxylate side chain by a one pot reaction involving a DIBAl-H induced reduction of the methyl ester moiety leading to an aluminoxyacetal intermediate[5]. The latter intermediate was not isolated and was submitted in situ to a Wittig–Horner reaction leading to compound **2**. After reduction the *α–β*-unsaturated ester **2** give the intermediate **3** which was submitted to a saponification reaction affording the acid **4**. Coupling **4** with N-boc-diaminoethane or glycine tertiobutyl ester led to the fully protected inhibitors **5**, **7** which deprotection yield respectively the inhibitors **NI950** and **NI 926** (Fig. 1).

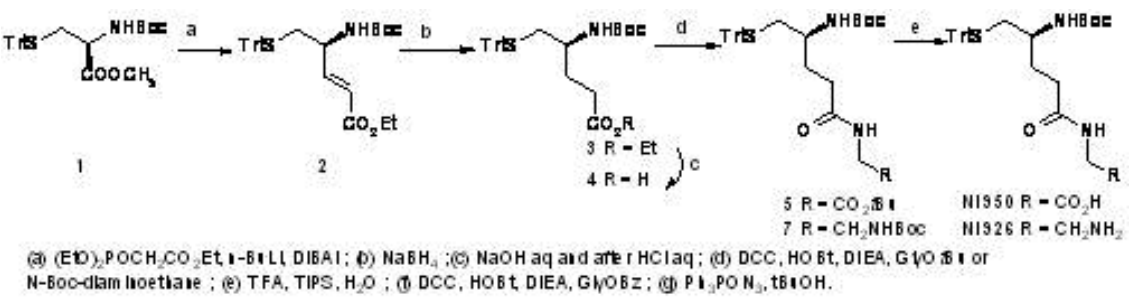

Figure 1. Synthesis of APA inhibitors.

Results and discussion

Ca^{2+} affected the affinity of APA for both acidic and basic substrates. As inhibitors differs in terms of their P1 side chains, we hypothesized that the difference between the Ki values of mutated APAs and wild-type

Table 1. Ki values of the inhibitors on Wild Type and mutated APA

		Ki values (µM)					
	Ca2+ (mM)	**WT**	**D213/E**	**D213/N**	**D213/Q**	**D218/E**	**D218/A**
LysSH	0	0.26	2.75	11.96	42.0	0.79	1.64
	4	3.1	20.74	-	-	2.7	
NI 926	0	0.07	1.16	4.3	14.1	0.11	2.3
	4	1.13	12.3	-	-	0.6	
NI 950	0	1.5	1.3	1.6	7.5	5.1	0.05
	4	0.7	1.0			0.6	

APA reflected changes in the docking of the P1 residue into the S1 subsite. Therefore, in absence of Ca^{2+} LysSH interacts with Asp 213 while NI 926 interacts with Asp 218. Furthermore, acidic specificity of APA is restored by Ca^{2+} addition. Because D218 is conserved in APN, we could hypothesized that NI 926 should also inhibit this enzyme.

Conclusion

In conclusion, this study highlights the role of Asp-213 and Asp-218 in Ca^{2+} binding and,therefore, in Ca^{2+} induced APA substrate specificity. Our data provide new insight into the organization of the APA active site, delineating the S1 subsite, precisely localizing Asp-213 and Asp-218 within this subsite and identifying the mode of interaction of these residues with the Ca^{2+} ion and that of the Ca^{2+} ion with the acidic side chain of the substrate. The role we have demonstrated for the Asp-213 and Asp-218 residues is consistent with the 3D model of APA, thus validating this model. Moreover, we have shown here the interest to have developed the APA 3D model for the design of new potent APA inhibitors, such as NI926. This model provides new insight into the organization of the S1 subsite and Ca^{2+} binding and will be a useful tool for understanding the binding of APA inhibitors interacting with both S1 and S'1 subsites and so on for the development of a new generation of APA inhibitors functioning as central-acting antihypertensive agents.

References

1. Zini S, Fournié-Zaluski M-C, Chauvel E, Roques BP, Corvol P, Llorens-Cortes C. *Proc Natl Acad Sci U S A* **93**: 11968-11973, 1996.
2. Reaux A, Fournié-Zaluski MC, David C, Zini S, Roques BP, Corvol P, Llorens-Cortes C. *Proc Natl Acad Sci U S A* **96**:13415-13420, 1999.
3. Bodineau L, Frugière A, Marc Y, Inguimbert N, Fassot C, Roques B, Llorens-Cortes C. *Hypertension* **51**: 1318-1325, 2008.
4. David-Basei C, Fournié-Zaluski M-C, Roques BP. *Expert Opin Ther Pat* **11**: 431-444, 2001.
5. Inguimbert N, Coric P, Dhotel H, Bonnard E, Llorens-Cortes C, De Mota N, Fournié-Zaluski MC, Roques BP. *J Pept Res* **65**: 175-188, 2005.
6. Rozenfeld R, Iturrioz X, Maigret B, Llorens-Cortes C. *J Biol Chem* **277**: 29242-29252, 2002.

1-01-108

Development of water-soluble click peptides by use of the *O-acyl* isopeptide method: *In situ* production of Alzheimer's amyloid *β* peptide

Taniguchi, Atsuhiko[1]; Sohma, Youhei[1]; Skwarczynski, Mariusz[1]; Nagano, Takami[1]; Okada, Takuma[2]; Ikeda, Keisuke[2]; Prakash, Halan[3]; Mukai, Hidehito[1]; Hayashi, Yoshio[1]; Kimura, Tooru[1]; Hirota, Shun[3]; Matsuzaki, Katsumi[2]; Kiso, Yoshiaki[1,]*

[1]Kyoto Pharmaceutical University, JAPAN; [2]Kyoto University, JAPAN; [3]Nara Institute of Science and Technology, JAPAN

[*]E-mail: kiso@mb.kyoto-phu.ac.jp

Introduction

A clear understanding of the pathological mechanism of amyloid *β* peptide (A*β*), especially A*β*1-42, would be of great significance in the discovery of novel drug targets against Alzheimer's disease (AD). However, the elucidation of the mechanism is a difficult issue, because the handling problems of A*β*1-42 including poor solubility and uncontrolled assembly pose significant obstacles in establishing an experimental system that clarifies the pathological function of A*β*1-42.[1] To overcome the handling problems of A*β*1-42 (**1**) in biological experiments, we applied an *O*-acyl isopeptide method,[2] in which the presence of an *O*-acyl instead of the native *N*-acyl residue at a hydroxyamino acid residue (e.g. Ser, Thr) in the backbone changed the physicochemical property derived from the native peptide, and the target peptide was generated via an *O-N* intramolecular acyl migration.[2-4] A*β*1-42 isopeptide (26-*O*-acyl isoA*β*1-42, **2**) in which Gly[25] was esterified to a hydroxyl group of Ser[26] had a much higher water-solubility than A*β*1-42 (**1**) and migrated to **1** under physiological conditions.[5] In this context, we developed a click peptide which produces intact **1** *in situ* with an action (click) via a quick and one-way conversion.

Results and discussion

We synthesized photo-click peptides **3**-**7** in which each photocleavable protective group was introduced at an amino group of Ser[26] in isopeptide **2** (Fig. 1).[6-8] The click peptides can convert to A*β*1-42 (**1**) with a photo-

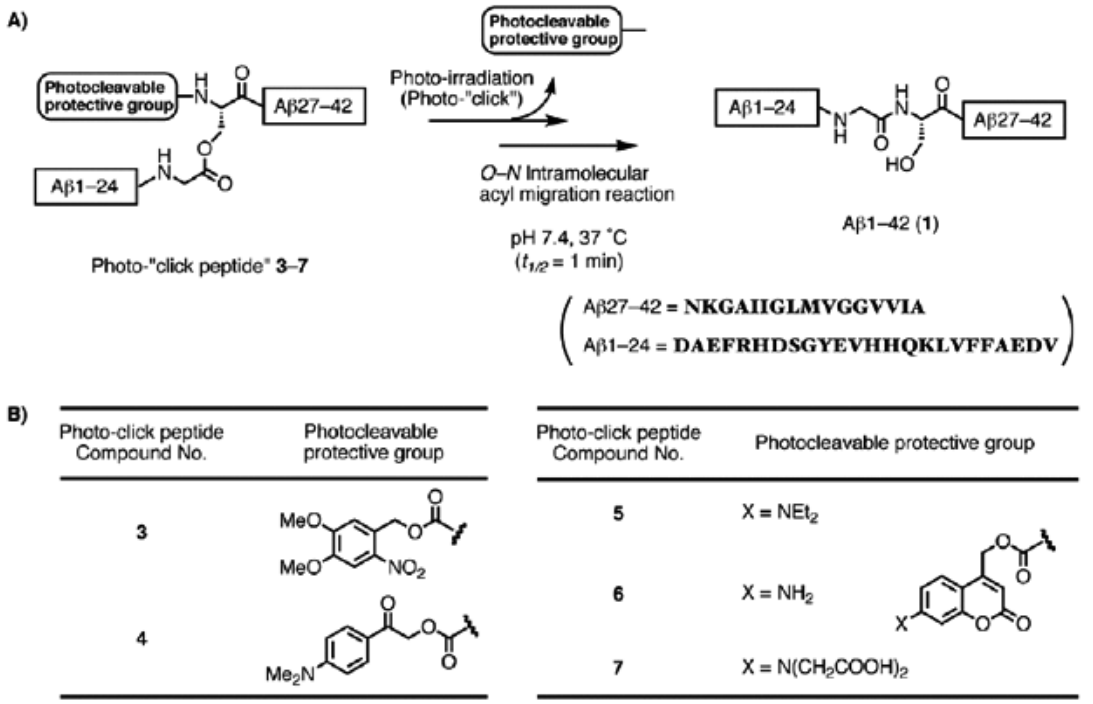

Figure 1. Photo-click peptide **3-7**: A) *In situ* production of A*β*1-42 (**1**) via an *O-N*intramolecular acyl migration triggered by photo-irradiation (photo-click) and B) photocleavable protective groups.

irradiation (photo-click) via photo-reaction and ensuing *O-N* acyl migration.

Among them, click peptide **7** with bis(carboxymethyl) amino-coumarin group had an advantageous water-solubility itself, nearly 100-fold higher than Aβ1-42 (**1**).[8] In size-exclusion chromatography, **1** formed an oligomer with incubation time at the expense of the monomer, while photo-click peptide **7** retained the monomeric form even after 6 h incubation. Additionally, in thioflavin T assay, **1** formed an amyloid fibril, while **7** has no ability of amyloid formation. These results indicated that **7** had no self-assembling (aggregative) nature in contrast to aggregative **1**. In circular dichroism (CD) spectroscopy of **1**, the conformational change from a random coil to a β-sheet structure was observed during incubation. In contrast, **7** had a stable random coil structure. We propose that the disruption of the higher order structure because of the ester bond in **7** is related to the non-self-assembling natures of the click peptide. When a solution of photo-click peptide **7** (20 μM **7** in 1% DMSO / phosphate buffered saline, pH 7.4) was photo-irradiated with UV for 2 min and incubated at 37 ºC for 30 min, Aβ1-42 (**1**) was released from **7** *in situ*. The difficulties in handling Aβ1-42 due to poor solubility and uncontrolled assembly in the biological experiment are significant problems in elucidating the function of Aβ1-42 in AD. On the other hand, since the click peptides, in general, do not exhibit these unfavorable natures during storage and handling and they can quickly release intact Aβ1-42 *in situ* after being triggered by an activation (click), the click peptides would be useful tools to establish a reliable biological experiment system in AD research.

Acknowledgements

This research was supported in part by the "Academic Frontier" Project for Private Universities: matching fund subsidy from MEXT (Ministry of Education, Culture, Sports, Science and Technology) of the Japanese Government, and the 21st Century COE Program from MEXT. A. T., Y. S. and H. P. are grateful for Research Fellowships of JSPS for Young Scientists.

References

1. Rahimi F, Shanmugam A, Bitan G. *Curr Alzheimer Res* **5:** 319-341, 2008.
2. Sohma Y, Sasaki M, Hayashi Y, Kimura T, Kiso Y. *Chem Commun* 124-125, 2004.
3. Mutter M, Chandravarkar A, Boyat C, Lopez J, Santos SD, Mandal B, Mimna R, Murat K, Patiny L, Saucede L, Tuchscherer G. *Angew Chem Int Ed* **43:** 4172-4178, 2004.
4. Carpino LA, Krause E, Sferdean CD, Schümann M, Fabian H, Bienert M, Beyermann M. *Tetrahedron Lett* **45:** 7519-7523, 2004.
5. Sohma Y, Sasaki M, Hayashi Y, Kimura T, Kiso Y. *Tetrahedron Lett* **45:** 5965-5968, 2004.
6. Kiso Y, Taniguchi A, Sohma Y. *Wiley Encyclopedia of Chemical Biology,* Vol. 1, Begley TP (Ed.), Wiley & Sons Inc, Hoboken, 2009**,** pp 379-383.
7. Taniguchi A, Sohma Y, Kimura M, Okada T, Ikeda K, Hayashi Y, Kimura T, Hirota S, Matsuzaki K, Kiso Y. *J Am Chem Soc* **128:** 696-697, 2006.
8. Taniguchi A, Skwarczynski M, Sohma Y, Okada T, Ikeda K, Prakash H, Mukai H, Hayashi Y, Kimura T, Hirota S, Matsuzaki K, Kiso Y. *ChemBioChem* **9:** 3055-3065, 2008.

1-01-109

Sulfur-containing amino acid amides of phenolic acids

Spasova, Maya[1]; Paizs, Csaba[2]; Stoykova, Boyka[1]; Milkova, Tsenka[1,]; Irimie, Florin[2]*

[1]South-West University "Neofit Rilski", BULGARIA; [2]"Babes Bolyai" University of Cluj Napoca, ROMANIA

[*]E-mail: tsenkamilkova@abv.bg

Introduction

It is known that different types of natural and synthetic compounds exhibited antioxidant activity. More than 300 heterocyclic compounds have been reported in various processed foods and beverages, e.g. brewed coffee[1,2] and some of them as pyroles, thiophenes, furans and etc. posses antioxidative activity.[3] Another important class of antioxidants is also found in roasted coffee,[4] green robusta coffee been and etc. are *N*-phenylpropenoyl amino acid amides. This finding emerged us to comprise three types antioxidants- hydroxycinamic acids, polyamines and benzothiophen –containing amino acid and converted them into *N*-phenylpropenoyl polyamine-amino acid amides.

Results and Discussion

Two kinds of *N*-hydroxycinnamoyl- polyamine -amino acid amides 4 (5) were synthesized by three-stage reaction (Scheme 1) and their abilities to scavenge radical were examined.

Evaluation of DPPH Scavenging Activity *In vitro*

The antioxidative potential of the desired hydroxycinnamoyl amides 4 (5) was studied against DPPH* (1,1-diphenyl-2-picrylhydrazyl radical) in abs. EtOH. The obtained results are summarized in Table 1. By comparison of the tested amides for DPPH radical-scavenging activity with well-known antioxidants the

Scheme.1

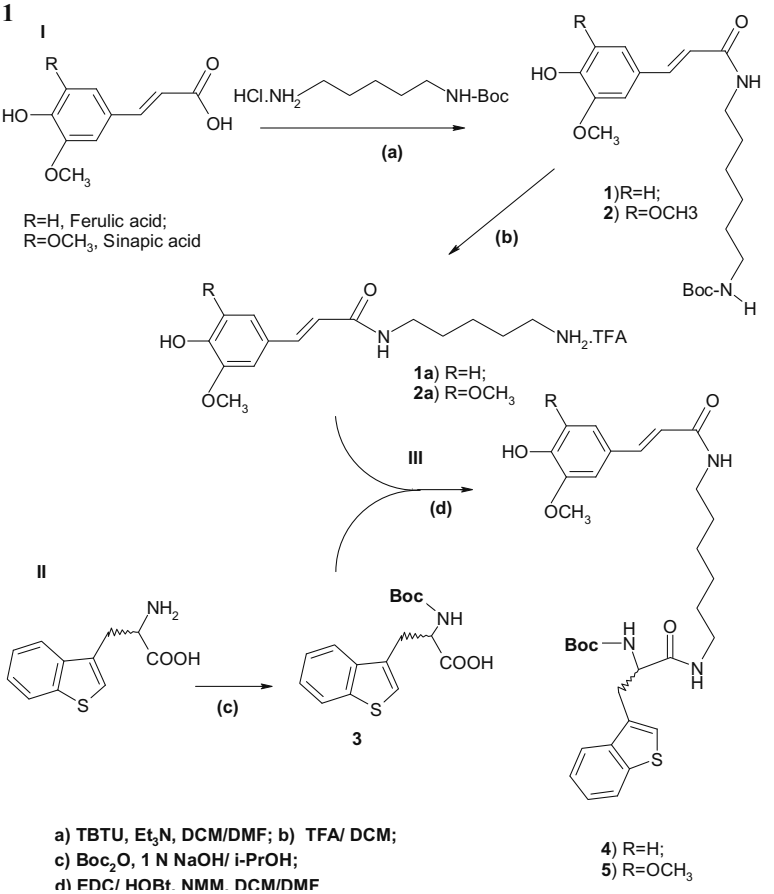

Table 1. Radical scavenging activity of hydroxycinnamoyl amides against DPPH* test

	(%) RSA					
	0.9 mM		1.8 mM		3.6 mM	
	Reaction time (min)					
AH	10'	20'	10'	20'	10'	20'
Quercetin	49.00±0.02	54.00±0.03	80.10±0.04	86.20±0.01	85.20±0.05	87.8±0
Eugenol	9.000±0.004	11.400±0.001	17.100±0.004	21.200±0.003	30.40±0.02	37.60±0.01
Isoeugenol	7.800±0.002	8.600±0.003	13.500±0.003	14.700±0.002	23.800±0.005	25.300±0.005
Sinapic acid	16.1±0.5	17.2±0.3	26.5±0.1	31.9±0.1	69.0±1.8	69.6±1.0
compound (5)	8.10±0.01	9.60±0.01	12.40±0.06	15.90±0.02	27.30±0.02	29.10±0.01
Ferulic acid	12.0±0.1	13.8±0.3	21.0±0.2	25.1±0.4	36.7±0.1	44.3±0.1
compound (4)	5.30±0.01	6.70±0.01	8.40±0.01	11.900±0.001	17.60±0.01	20.80±0.05
D,L α-Tocopherol	15.5±0.1	15.9±1.0	34.9±1.1	38.4±1.1	53.0±0.9	58.1±1.8

% RSA—percent radical scavenging activity; % RSA = [$Abs_{516nm\ (t = 0)}$ - $Abs_{516nm(t = t')}$ x $100/Abs_{516nm(t = 0)}$], as proposed by Pekkarinen et al.[5]; quercetin, eugenol, isoeugenol, tochopherol, sinapic-and ferulic- acids were used as standards.

next increasing order was found: quercetin> sinapic acid>tocopherol> ferulic acid> eugenol> compound (5)> isoeugenol, compound (4). The synthesized amides showed unsignificant free radical scavenging activity in comparison with all used standards. Only sinapoylamide (5) was found to be more potent than isoeugenol.

Acknowledgements

For the support of this work we are grateful to the National Found for Scientific Research of Bulgaria (Contracts VUH-07/05), South-West University "Neofit Rilski" Blagoevgrad, Bulgaria and to the CEEPUS mobility program.

References

1. Flament I, Chevalier C. *Chem Ind* 592-596, 1988.
2. Czerny M, Grosch W. *J Agric Food Chem* **48**: 868-872, 2000.
3. Yanagimoto K, Lee K-G, Ochi H, Shibamoto T. *J Agric Food Chem* **50**: 5480 –5484, 2002.
4. Stark T, Justus H, Hofmann T. *J Agric Food Chem* **54**: 2859-2867, 2006.
5. Pekkarinen S, Stockmann H, Schwarz K, Heinonen IM, Hopia AI. *J Agric Food Chem* **47**: 3036-3043, 1999.

1-01-110

1,3-Disubstituted 1,2,3,4-tetrahydro-*β*-carbolines as peptidomimetics of tryptophan: synthesis and conformational analysis

Slupska, Marta[1]; Misiak, Maria[1,]; Urbanczyk-Lipkowska, Zofia[2]; Kozminski, Wiktor[1]; Misicka, Aleksandra[1]*

[1]University of Warsaw, Faculty of Chemistry, POLAND; [2]Polish Academy of Sciences, Institute of Organic Chemistry, POLAND

[*]E-mail: misicka@chem.uw.edu.pl

Introduction

Tryptophan in many cases is a pharmacophore which determines the affinity of peptide ligands to their receptors. Cyclic analogues of tryptophan which introduce local constraints and reduce the flexibility of the indol moiety are very valuable tools to probe the bioactive conformation of ligands. The Pictet-Spengler reaction[1] is widely applied to the synthesis of constrained analogs of tryptophan containing 1,2,3,4-tetrahydro-*β*-carboline skeleton[2,3]. We report the synthesis of various 1,3-disubstituted 1,2,3,4-tetrahydro-*β*-carbolines as peptidomimetics of tryptophan. The reaction was studied in terms of double stereodifferentiation. L and D α-Aminoaldehydes were used as carbonyl components; methyl ester of tryptophan or dipeptides with N-terminal Trp were used as arylethylamine substrates.

Results and discussion

Dipeptides with N-terminal Trp were obtained by standard method (TBTU, HOBT) in solution. Aminoaldehydes were obtained via $LiAlH_4$ reduction of Weinreb amides derived from Cbz-protected L and D *α*-amino acids.

The Pictet-Spengler reaction was performed in CH_2Cl_2 with 5 eq. of TFA. The temperature of reaction was controlled to avoid the racemisation of aldehyde and to control the stereoselection of the reaction. As the product of reaction the mixture of *cis/trans* isomers is formed (substituents on C-1 and C-3). The ratio of diastereomers was measured by ^1H NMR before purification.

During the reaction the chirality transfer from C-2 of aminoaldehydes to the newly created stereogenic center is observed. Reactions with all (5) D-amino aldehydes are completely selective and only one isomer (*cis*) is formed;

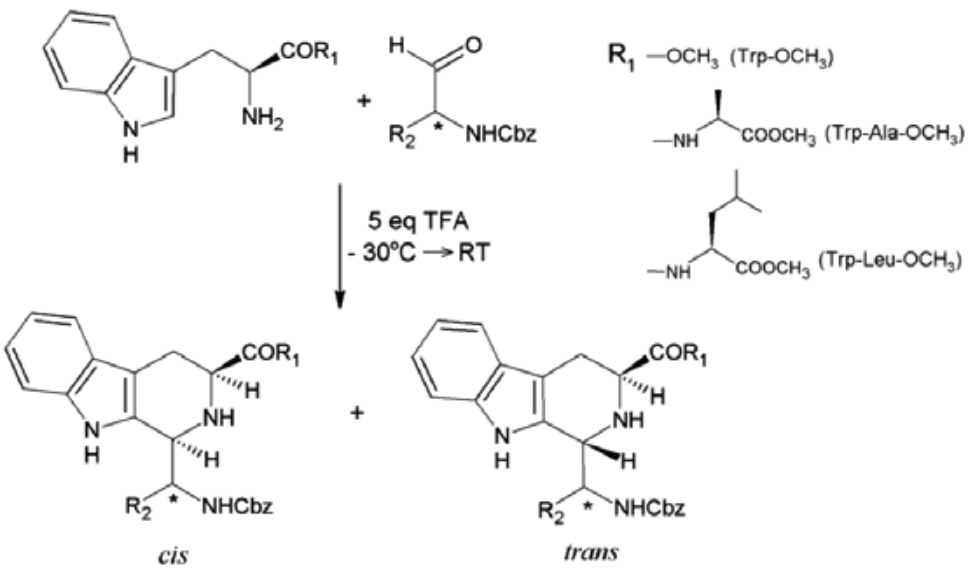

Figure 1. Synthesis of the 1,3-disubstituted 1,2,3,4,-tetrahydro-*β*-carbolines.

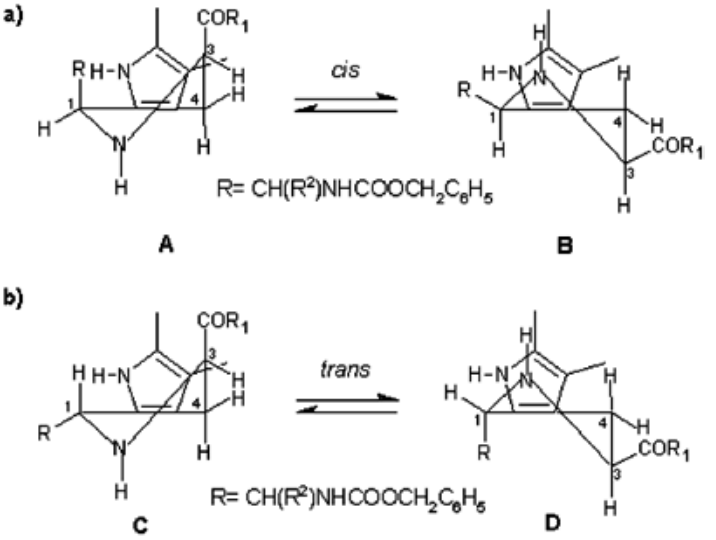

Figure 2. Possible conformations of the *cis* and *trans* 1,3-disubstituted 1,2,3,4-tetrahydro-*β*-carbolines.

reactions with L-amino aldehydes (5) lead to the mixture of products with the dominance of *trans* isomer (more that 65%). The substituent occurred on C-terminal part of Trp (R1) does not affect the selectivity of reaction. The ratio of *cis/trans* isomers is comparable for methyl ester of tryptophan and dipeptides with N-terminal Trp. The stereoselectivity of reaction is probably determined by the formation of pseudocyclic 7-membered ring with intramolecular hydrogen bond between iminium cation and Cbz-group.

The conformations of *cis* and *trans* 1,3-disubstituted 1,2,3,4-tetrahydro-*β*-carbolines were studied by 2D NMR ROESY spectra. For *cis* analogs two half chair conformations are possible: with both substituents equatorially or axially located (Fig. 2a). For all analogs (derived from Trp-*O*Me or dipeptides) the more stable is conformation with equatorially located substituents. For *trans* isomers two axial/equatorial conformations are possible (Fig. 2b). The conformational equilibrium depends on the size of substituents. Our *trans* analogs contain small (ester moiety) or bulky ones (peptide moiety). The ester group is axial whereas the peptide moieties are equatorially located. It means that the conformation of the building blocks based on 1,2,3,4-tetrahydro-*β*-carbolines before and after incorporation into the peptides could be different and this could have influence on the biologically activity. Therefore everyone has to be careful during designing and synthesis of compounds with defined orientation of pharmacophoric groups.

Acknowledgement

This work was partially supported by the University of Warsaw BW 120000-501/68-179215 grant. We thank M. Wilczek for helpful discussion.

References

1. Pictet A, Spengler T. *Chem Be*r **44**: 2030-2036, 1911.
2. Tatsui G. *J Pharm Soc Jpn* **48**: 92, 1928.
3. Snyder HR, Walker HG, Werber FX. *JACS* **28**: S177, 1949.

1-01-111

Photoinduced macrocyclizations on helical Bpa/Met oligopeptides

Moretto, Alessandro[1,]; Crisma, Marco[1]; Formaggio, Fernando[1]; Huck, Lawrence A.[2]; Mangion, Dino[2]; Leigh, William J.[2]; Toniolo, Claudio[1]*

[1]University of Padova, 35131 Padova, ICB-CNR, Padova Unit, Department of Chemistry, ITALY; [2]McMaster University, Hamilton, ON, L8S 4M1, Department of Chemistry, CANADA

[*]E-mail: alessandro.moretto.1@unipd.it

The [3-(4-benzoylphenyl)alanine] (Bpa) residue is widely used as a photoaffinity label for the study of *intermolecular* (peptide) ligand-protein (receptor) interactions, where it is thought to primarily function by hydrogen-abstraction from Met residues followed by covalent C-C bond formation of the resulting radical pair.[1,2]

We are carrying out detailed studies of this reaction in a series of five, structurally rigid, 3_{10}-helical hexapeptides of general sequences Boc-$U_xBU_yMU_z$-OMe and Boc-$U_xMU_yBMU_z$-OMe, where B = L-Bpa, U = Aib, M = L-Met, and $U_x+U_y+U_z = 4$. We aim at determining the effects of spacer length (U_y = 1-3) on the rate of the intramolecular excited state reaction (Yang photocyclization) and the chemical and 3D-structures of the resulting products. The triplet state lifetimes of the Bpa residues in the compounds, determined in a deoxygenated, dilute, CH_3CN solution by laser flash photolysis, vary in the following order: UBU_2MU, $\tau = 60$ ns; UMU_2BU, $\tau = 190$ ns; $UBUMU_2$, $\tau = 350$ ns; $UBMU_3$, $\tau = 430$ ns; and UBU_3M, $\tau = 920$ ns.

In addition to the information these data provide on the structural requirements for intramolecular excited state quenching in the molecules, they also serve to define the conditions necessary for optimal intramolecular reaction in preparative photolysis experiments. Accordingly, the products resulting from UBU_2MU have been prepared in high yields, isolated, and structurally characterized by HPLC, mass spectrometry, FT-IR absorption, NMR, and CD techniques, and for one of them by X-ray diffraction as well (Fig. 1).

Two 3_{10}-helical diastereomers, arising exclusively from the Bpa diradical regioselective attack on the Met *S*-methyl group (Fig. 2), were found.

References

1. Kauer JC, Erickson-Viitanen S, Wolfe HR Jr, Grado WF. *J Biol Chem* **261**: 10695-10700, 1986.
2. Pérodin J, Deraët M, Auger-Messier M, Boucard AA, Rihakova L, Beaulieu M-E, Lavigne P, Parent J-L, Guillemette G, Leduc R, Escher E. *Biochemistry* **41**: 14348-14356, 2002.

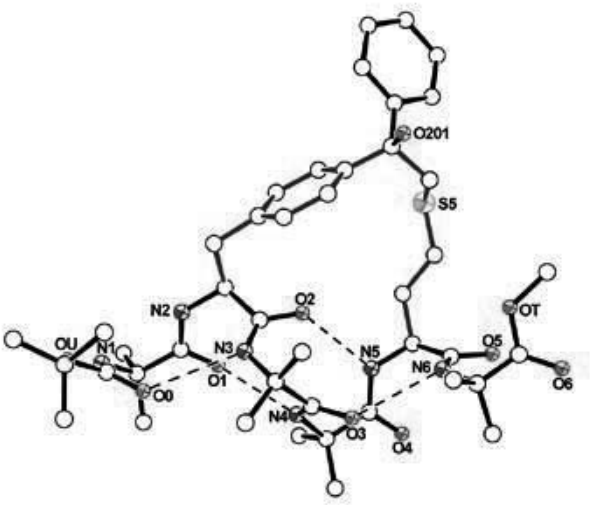

Figure 1. X-Ray diffraction structure of the major side-chain conformer of the macrocyclized hexapeptide diastereomer (product B) arising from the Yang photocyclization of Boc-Aib-L-Bpa-$(Aib)_2$-L-Met-Aib-*O*Me. The configuration of the novel side-chain chiral center is *R*. H-atoms have been omitted. Only the *N*, *O*, and *S* atoms are numbered. The three C=O•••H-N intramolecular H-bonds of the 3_{10}-helical structure are represented by dashed lines.

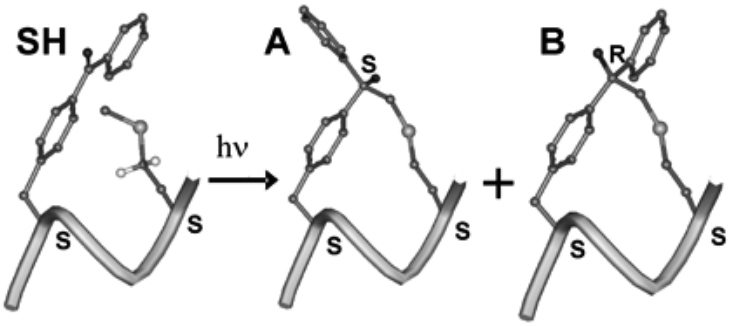

Figure 2. Cartoon showing the two diastereomeric products (**A** and **B**) afforded by the Yang photocyclization reaction on the terminally-protected hexapeptide Boc-Aib-L-Bpa-$(Aib)_2$-L-Met-Aib-OMe (**SH**). H-abstraction took place only from the Met ε-CH_3 group.

1-01-112

Peptido[2]rotaxanes with amino acids containing either functional groups or folded peptide segments in the axle

Moretto, Alessandro; Crisma, Marco; Toniolo, Claudio*

University of Padova, 35131 Padova, ICB-CNR, Padova Unit, Department of Chemistry, ITALY

**E-mail: alessandro.moretto.1@unipd.it*

Peptido[2]rotaxanes based on an achiral benzylic amide macrocycle locked onto various peptide axles as short as Gly-Xxx dipeptides were recently characterized by Leigh and coworkers.[1,2] We are currently expanding this field by synthesizing and studying the properties of new sets of peptido[2]rotaxanes. The initial set examined includes symmetrical compounds with axles built up with a central fumaric diamide station and either two amino acids containing functional groups or two folded Aib (α-aminoisobutyric acid) homo-peptides of different lengths (from 1 to 4 residues), and a benzylic amide macrocycle as the wheel (Table I).

These supramolecular systems have been characterized spectroscopically and one of them by X-ray diffraction as well (Fig. 1). The fundamental interactions between macrocycle and axle (the same interactions offering the major contribution to the template-directed preparation of this family of molecules) are intercomponent H-bonds comprising the four amide groups in the ring and the two amide bonds in the fumaric derivative.

The former group of peptido[2]rotaxanes allow us to study side-chain to side-chain interactions across the wheel of the rotaxane supramolecule or to generate catenanes by covalently linking the two side chains via disulfide bond formation or ring-closing metathesis. The latter group represents our first step towards the preparation of supramolecules with the wheel capable of traveling to a second station by wrapping up around a helical peptide axle. These investigations are currently under way in our laboratory.

References

1. Clegg W, Gimenez-Saiz C, Leigh DA, Slawin AM, Teat SJ. *J Am Chem Soc* **121**: 4124-4129, 1999.
2. Asakawa M, Brancato G, Fanti M, Leigh DA, Shimizu T, Slawin AMZ, Wong JKY, Zerbetto F, Zhang S. *J Am Chem Soc* **124**: 2939-2950, 2002.

Table I. List of peptido[2]rotaxanes synthesized

1	[Z-L-Phe-O-$(CH_2)_2$-NH-Fum]$_2$ [a]
2	[Fmoc-Aib-O-$(CH_2)_2$-NH-Fum]$_2$
3	[Z-$(Aib)_3$-O-$(CH_2)_2$-NH-Fum]$_2$ [b]
4	[Fmoc-$(Aib)_4$-O-$(CH_2)_2$-NH-Fum]$_2$
5	[Z-TOAC-O-$(CH_2)_2$-NH-Fum]$_2$
6	[Fum-TOAC-L-Lys(CO-CH_2-CH_2-S-Trt)-OBzl]$_2$
7	[Boc-L-Lys(CO-CH_2-CH_2-S-Trt)-O-$(CH_2)_2$-NH-Fum]$_2$
8	[Fmoc-L-Lys(Boc)-O-$(CH_2)_2$-NH-Fum]$_2$
9	[Fmoc-L-Lys(CO-CH_2-CH_2-CH_2-CH=CH_2)-O-$(CH_2)_2$-NH-Fum]$_2$

[a] Z, benzyloxycarbonyl; Fum, -CO-CH=; Fmoc, 9-fluorenylmethyloxycarbonyl; TOAC, 4-amino-4-carboxy-2,2,6,6-tetramethylpiperidine-1-oxyl; Trt, trityl; Bzl, benzyl; Boc, *tert*-butyloxycarbonyl.
[b] Pseudorotaxane.

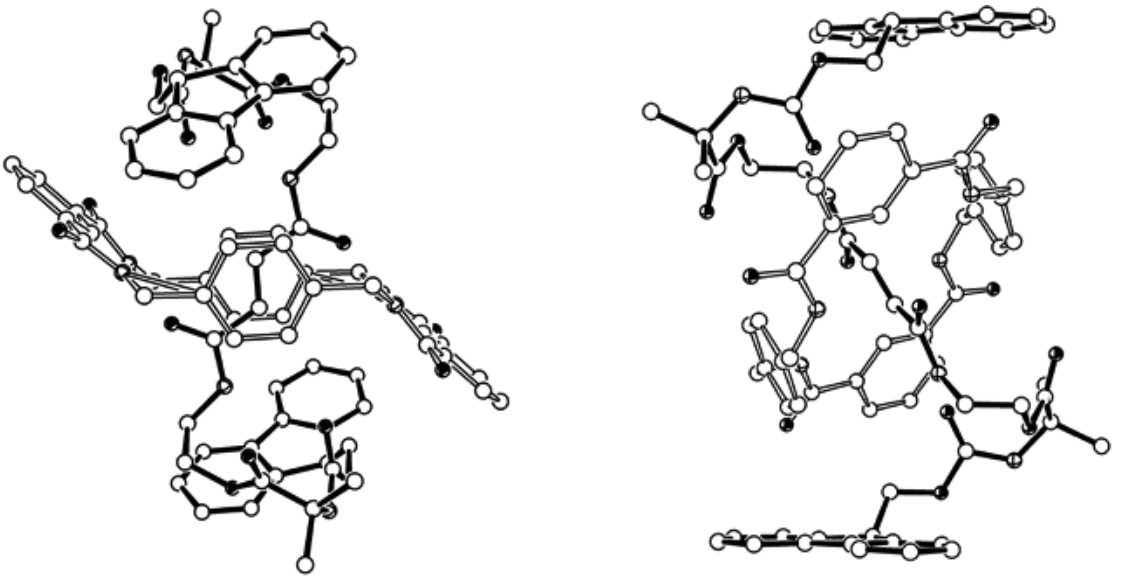

Figure 1. Two views of the X-ray diffraction structure of the peptido[2]rotaxane [Fmoc-Aib-*O*-$(CH_2)_2$-NH-Fum]$_2$ (**2**). Peptide axle is highlighted in black.

1-01-113

Synthesis of peptides containing five-member cyclic *N*-amidino-amino acids

Moskalenko, Yulia; Panarin, Eugeniy; Leko, Maria; Shkarubskaya, Zoya; Dorosh, Marina; Burov, Sergey[1,]*

Institute of Macromolecular Compounds of Russian Academy of Sciences, RUSSIAN FEDERATION

[*]*E-mail: burov@hq.macro.ru*

Introduction

Guanidine-containing compounds owing to their unique physicochemical properties can play an important role in biological recognition processes. Five-member cyclic *N*-amidino-amino acids represent hybrid structures, combining proline rigidity and high positive charge of arginine guanidine group. Their incorporation into peptide sequence requires use of substituted derivatives or effective guanidinylation technique. The aim of our study was to elaborate methods for the synthesis of peptides, containing *N*-amidino-proline, *N*-amidino-pyroglutamic acid and cyclocreatine (Fig. 1).

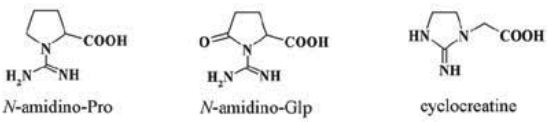

Figure 1. *N*-amidino amino acids.

Results and discussion

Recently we have presented synthesis of Mts-protected *N*-amidino-Pro[1]. Nevertheless, its application shows slow condensation rate as compared to Arg(Mts) in solid phase synthesis of short peptides (RGD analogues, 4-5 residues) or completely fails in the case of longer ones (GnRH analogue, 10 residues). On the other hand, polymer supported guanidinylation of proline by *bis*-Boc-protected carboxamidine-*1H*-benzotriazole[2] seems to be preferred route to *N*-amidino-proline containing peptides.

Three methods of *N*-amidino-pyroglutamic acid synthesis have been investigated (Fig. 2) and finally model dipeptide has been acquired on Wang polymer by the cyclization of *alpha*-guanidinoglutaric acid residue (Fig. 3). For selective Boc-deprotection on Wang resin the literature technique has been utilized.[3] It should be mentioned that ESI-MS and NMR analyses evidence for concomitant side reaction of triethylamine alkylation by polymer linker fragment.

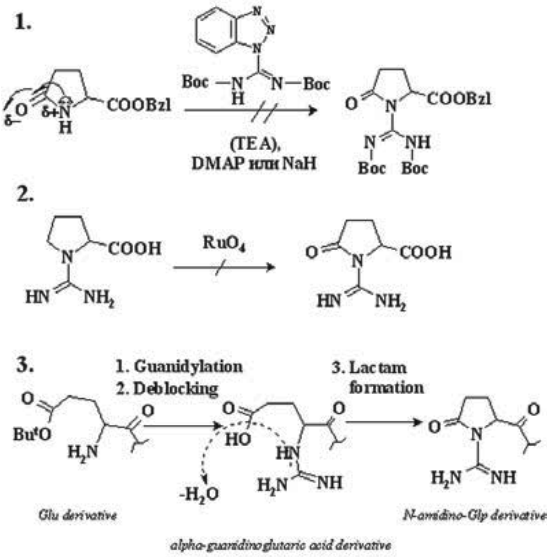

Figure 2. Synthesis of *N*-amidino-pyroglutamic acid and its derivatives.

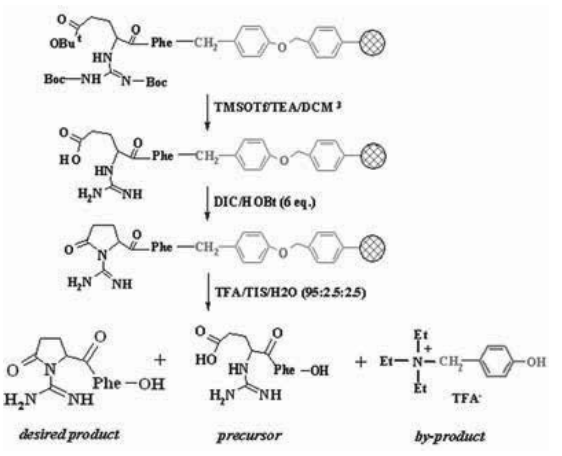

Figure 3. Solid phase synthesis of *N*-amidino-Glp-Phe.

It was shown that independently from neither cyclization time nor condensing agent effectiveness (DIC or HCTU) the lactam formation is incomplete. Separation of the end product and its precursor by means of HPLC has been successfully carried out in ammonium formate buffer at pH 6 instead of commonly used TFA buffer. HPLC analysis has shown *N*-amidino-Glp-Phe stability at acidic and physiological pH and fast ring opening in water solution at pH 9. An attempt to provide a lactam formation by *alpha*-guanidinoglutaric acid residue cyclization on longer peptide sequences (GnRH analogue, 10 residues) has been failed. This suggests that *N*-amidino-pyroglutamic acid incorporation into oligopeptide structure will require the fragment condensation.

For cyclocreatine application in peptide synthesis we suggest the use of its *p*-toluenesulfonate having good solubility in DMF and showing effective coupling by Cl-HOBt/DIC method (Fig. 4).

Though the formation of unknown by-product is observed, this technique can be easily applied in the synthesis of cyclocreatine containing peptides.

References

1. Burov SV, Moskalenko YuE, Leko MV, Dorosh MYu, Panarin EF. *Russ J Bioorg Chem* **32**: 509-516, 2006.
2. Musiol H-J, Moroder L. *Org Lett* **3**: 3859-3861, 2001.
3. Lejeune V, Martinez J, Cavelier F. *Tetrahedron Lett* **44**: 4757-4759, 2003.

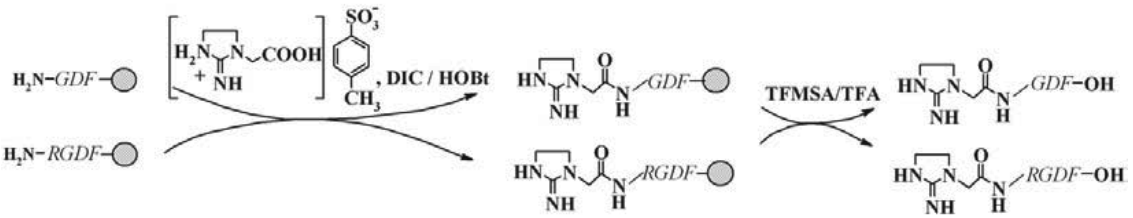

Figure 4. Synthesis of RGD peptides, containing cyclocreatine.

1-01-114

Hydrolytic action of Candida antarctica lipase B (CAL-B) and pig liver esterase (PLE) upon various carboxyl protecting groups

Thodi, Kalliopi[1]; Barbayianni, Efrosini[1]; Fotakopoulou, Irene[2]; Bornscheuer, Uwe T.[3]; Constantinou-Kokotou, Violetta[2]; Kokotos, George[1]; Moutevelis-Minakakis, Panagiota[1,]*

[1]University of Athens, Department of Chemistry, GREECE; [2]Agricultural University of Athens, Chemical Laboratories, GREECE; [3]Institute of Biochemistry Greifswald University, Department of Biotechnology and Enzyme Catalysis, GERMANY

[*]E-mail: pminakak@chem.uoa.gr

Introduction

Biocatalysts offer great alternative to chemical methods. Recently, we demonstrated that an esterase from Bacillus subtilis and lipase A from *Candida antarctica* were able to cleave *tert*-butyl, methyl, benzyl, allyl, 2-chloroethyl, 2,2,2-trichloroethyl, phenacyl, and diphenylmethyl esters from a variety of substrates including simple carboxylic acids, *N*-protected amino acids and dipeptides, under mild and selective conditions, that avoid side-reactions.[1-3] To extent our studies, we investigated the applicability of various lipases and esterases to selectively remove allyl esters from a variety of substrates. In particular, two enzymes, pig liver esterase (PLE) and lipase B from *Candida antarctica* (CAL-B), were found to be active toward allyl esters.

Results and Discussion

Allyl esters of simple carboxylic acids and *N*-protected amino acids were prepared as substrates. For comparison reasons, the hydrolysis of the corresponding methyl and ethyl esters was also studied. The results of their hydrolysis by CAL-B and PLE, using 1:4 or 1:30 enzyme/substrate ratio, are summarized in Table 1. Both enzymes removed methyl, ethyl and allyl esters from phenylacetic acid in high yields (entries 1-3, Table 1). Cinnamic and octanoic acid were isolated in moderate yields from the corresponding allyl esters in the presence of CAL-B, demanding longer reaction time (entries 5, 6, Table 1). Concerning the allyl and methyl ester of Boc-*β*-alanine and allyl ester of Boc-*γ*-aminobutyric acid, CAL-B was effective, hydrolyzing all three compounds in high yields within 1.5 hour, while PLE needed longer reaction time

Table 1. Hydrolysis of allyl and other esters by CALB and PLE

Entry	Substrate	Product	CALB/substrate 1:4		CALB/substrate 1:30		PLE/substrate 1:4	
			Time (h)	Yield[a] (%)	Time (h)	Yield[a] (%)	Time (h)	Yield[a] (%)
1	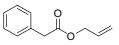		1	88	1.5	58	1	90
2			1	92	1.5	75	1	92
3	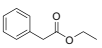		1	89	1.5	77	1	90
4	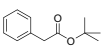		1	18	1.5	9		
5	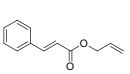		24	76				
6	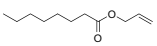	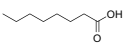	24	58				
7	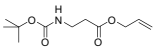	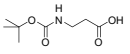	1.5	88			>24	[b]
8	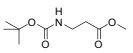	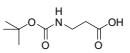	1.5	83			4	58
9	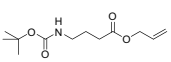	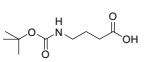	1.5	76				

[a]Yield of isolated product, [b]Not detected.

Table 2. Hydrolysis of various Z-L-glutamates by CALB and PLE

Entry	Substrate	Product	CALB/substrate 1:4		CALB/substrate 1:30		PLE/substrate 1:30	
			Time (h)	Yield[a] (%)	Time (h)	Yield[a] (%)	Time (h)	Yield[a] (%)
1	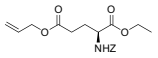	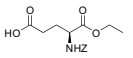	4.5	26	4.5	9	4.5	40
		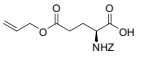	4.5	50	4.5	24	4.5	18
2	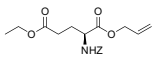	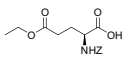	4.5	22	4.5	16	4.5	47
		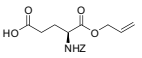	4.5	44	4.5	23	4.5	12
3	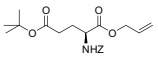	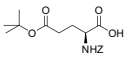	24	17				
4	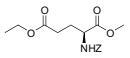	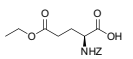					4.5	26
		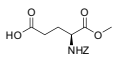					4.5	14
5	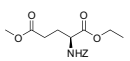	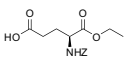					4.5	30
		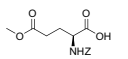					4.5	10

[a]A mixture of the products was isolated and the yield of each was determined by NMR spectroscopy.

in the case of Boc-*β*-alanine methyl ester, showing no activity at all in the case of Boc-*β*-alanine allyl ester (entries 7-9, Table 1).

Since the hydrolysis of the above mentioned esters was very quick and no selective under the conditions used, the removal of these groups using an even lower ratio of CAL-B/substrate (1:30) was examined and the results are presented in Table 1. It is clear that longer reaction times were needed and methyl ester was slower hydrolyzed by CAL-B, than allyl and ethyl esters (entries 1-3, Table 1). *Tert*-butyl phenylacetate was a very poor substrate for the lipase (entry 4, Table 1).

In order to further investigate the quick and possibly selective removal of the groups mentioned above, in case they are present in the same molecule, we synthesized a series of dicarboxylates, based on glutamic acid. The results derived using CAL-B and PLE are summarized in Table 2. In the case of *α*-ethyl, *γ*-allyl and *α*-allyl, *γ*-ethyl Z-L-glutamates (entries 1, 2, Table 2), CAL-B shows a preference for ethyl esters, either in *γ*- or in *α*-position. The reaction rate is lower when the enzyme/substrate ratio is decreased, while the selectivity for ethyl toward allyl ester is not improving. The hydrolysis of *α*-allyl, *γ*-*tert*-butyl Z-L-glutamate (entry 3, Table 2) is slow and reaches a maximum of 17% yield within 24 hours at a CAL-B/substrate ratio 1:4. PLE at an enzyme/substrate ratio 1:30, shows selectivity for allyl esters, either in *α*- or in γ-position (entries 1, 2, Table 2). Interestingly, in the case of *α*-methyl, *γ*-ethyl and *α*-ethyl, *γ*-methyl Z-L-glutamates (entries 4, 5, Table 2), there is a subtle, though noteworthy selectivity by PLE for the methyl ester of both substrates, which cannot be accomplished by chemical means, in the presence of ethyl ester.

Acknowledgments

The project is co-funded by the European Social Fund and National Resources (EPEAEK II).

References

1. Schmidt M, Barbayianni E, Fotakopoulou I, Höhne M, Constantinou-Kokotou V, Bornscheuer UT, Kokotos G. *J Org Chem* **70:** 3737-3740, 2005.
2. Barbayianni E, Fotakopoulou I, Schmidt M, Constantinou-Kokotou V, Bornscheuer UT, Kokotos G. *J Org Chem* **70:** 8730-8733, 2005.
3. Fotakopoulou I, Barbayianni E, Constantinou-Kokotou V, Bornscheuer UT, Kokotos G. *J Org Chem* **72:** 782-786, 2007.

1-01-115

Synthesis of C-terminal exenatide sequence H-Ala-Pro-Pro-Pro-Ser-NH_2

Nikolskaia, Sofia[1,]; Nurutdinov, Alexandr[1]; Gluzdikov, Ivan A[1]; Vinogradov, Valentin A[2]; Titov, Mikhail I[1]*

[1]Saint-Petersburg State University; [2]Biovalent Ltd, RUSSIAN FEDERATION

[*]E-mail: soniko4031@yandex.ru

Abstract

Synthesis of the C-terminal fragment H-Ala-Pro-Pro-Pro-Ser-NH_2 is developed. Both solid-phase and classical methods of peptide synthesis have been used, with protected serine OH-group and with free OH-group. The structure was supported by ^{1}H NMR, mass-spectra (MALDI-TOF) and HPLC analysis.

Introduction

Exenatide (synthetic exendin-4), 39-amino acid peptide is a novel drug for treatment of type 2 diabetes mellitus.[1] Exendin-4 was originally isolated from the salivary secretions of the lizard Heloderma suspectum (Gila monster). Exenatide regulates glucose level in blood. Glucoregulatory actions of exendin-4 include glucose-dependent enhancement of insulin secretion, glucose-dependent suppression of inappropriately high glucagon secretion, slowing of gastric emptying, and reduction of food intake. In additional, exendin-4 reproduces pancreas functions.[2]

Materials and methods

Boc-Pro-Pro-OH. H-Pro-OH (9.47 g, 82 mmol) and NaOH (3.29 g, 41mmol) in 8 ml water were dropped into a solution of Ná-Boc-Pro-OSu (12.90 g, 41 mmol) in 37 ml dioxane. The reaction mixture was stirred overnight at room temperature. The solution was evaporated on 2/3, brought to pH~4 by gradual additional 1M aq. H_2SO_4 and extracted with EtOAc. The organic solution was washed with aq. NaCl, dried with Na_2SO_4, filtered and evaporated. The residue crystallized from 40 ml EtOAc. Yield: 8.5 g (66%). **Boc-Pro-Pro-OSu**. Boc-Pro-Pro-OH (8.35 g, 27 mmol) and N-hydroxysuccinimide (3.41 g, 30 mmol) in 110 ml THF were treated with DCC (6.13 g, 30 mmol) in 15 ml THF. In 2 hours the dropped out urea was filtered. The solution was evaporated to dryness; the residue was crystallised from isopropyl alcohol. Yield: 6.75 g (61 %). **Boc-Pro-Pro-Pro-OH**. H-Pro-OH (3.83 g, 34 mmol) in 17 ml 1 M solution of NaOH was dropped into a solution of Boc-Pro-Pro-OSu (6.75 g, 17 mmol) in 25 ml dioxane. The reaction mixture was stirred overnight at room temperature. The solution was evaporated on 2/3, washed with ether, brought to pH~4 by gradual additional 1 M aq. H_2SO_4 and extracted with EtOAc. An organic solution was washed with aq. NaCl, dried with Na_2SO_4, filtered and evaporated. The residue crystallized from 40 ml EtOAc. Yield: 3.86 g (63%). **TFA*H-Pro-Pro-Pro-OH**. Boc-Pro-Pro-Pro-OH (3.00 g, 7 mmol) was dissolved in 10 ml TFA, in half an hour solution was evaporated to dryness. The product was dissolved in 30 ml isopropyl alcohol. A solution was evaporated, the residue was crystallised from 40 ml ether. Yield: 3. 01 g (94 %). **z-Ala-Boc-Pro-Pro-Pro-OH**. TFA*H-Pro-Pro-Pro-OH (17.8 g, 42 mmol) and DIPEA (15.3 ml, 92 mmol) in 90 ml dioxane were treated with z-Ala-OH (15.5 g, 48 mmol) in 90 ml dioxane. After stirring overnight at room temperature the dioxane was evaporated; the residue was diluted with water, washed with ether and extracted with n-butanol. An organic solution was washed with aq. NaCl, water and evaporated to dryness. The product was crystallized from MTBE, filtered, and dried on air. Yield 17.5 g (81 %). **z-Ala-Boc-Pro-Pro-Pro-Ser(tBu)-NH_2**. z-Ala-Boc-Pro-Pro-Pro-OH (17.5 g, 34 mmol) and H-Ser(tBu)-NH_2 (5.8 g, 36 mmol) in 100 ml THF were treated with DCC (8.2 g, 40 mmol) in 40 ml THF. The reaction mixture was stirred overnight at room temperature. A solution was filtered and evaporated to dryness. The product was crystallised from MTBE, filtered, and dried under vacuum. Yield: 16.2 g (72 %). **X-Ala-Boc-Pro-Pro-Pro-Ser-NH_2 (X=Z, Boc, Fmoc)**. 1 eq. TFA*H-Pro-Pro-Pro-Ser-OH and 1.2 eq. X-Ala-OH in DMF were treated with 2 eq. N-methylmorpholine. After stirring overnight at room temperature the DMF was evaporated; the residue was diluted with water and extracted by n-butanol. An organic solution was evaporated to dryness; the product was crystallised from MTBE, filtered and dried on air. Yield: 82-84 %.

Results and discussion

Preparation of Pro-Pro-Pro was a key stage in synthesis of H-Ala-Pro-Pro-Pro-Ser-NH_2. Synthesis of the

Scheme 1

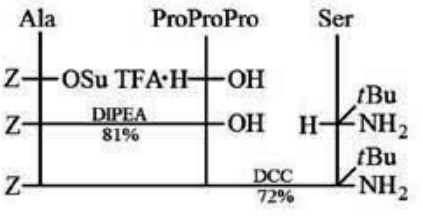

Scheme 2

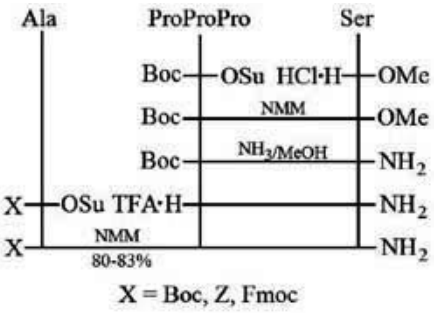

protected tripeptide was carried out by classical method in a solution by growing of a chain from the N-terminus as free diproline easily is exposed to cyclization with diketopiperazine formation. Boc-Pro-OSu was coupled with H-Pro-ONa.[3] Protected tripeptide Boc-Pro-Pro-Pro-OH was obtained as result of interaction of Boc-Pro-Pro-OSu and H-Pro-ONa. The Boc-group has been removed by action of TFA in DCM.

Various schemes of synthesis were investigated. At first (Scheme 1) z-Ala-OSu was coupled with TFA*H-Pro-Pro-Pro-OH in presence of DIPEA. The z-Ala-Pro-Pro-Pro-OH was coupled with H-Ser(tBu)-NH_2 in presence of DCC as condensing agent. z-group was removed with catalytic hydrogenolysis. Under other scheme (Scheme 2) Boc-Pro-Pro-Pro-OSu was coupled with HCl*H-Ser-OMe in the presence of NMM. The Boc-Pro-Pro-Pro-Ser-OMe was converted to Boc-Pro-Pro-Pro-Ser-NH_2 by treatment with ammonia in methanol. The Boc-group was removed by action of TFA in DCM. X-Ala-OSu was coupled with TFA*H-Pro-Pro-Pro-Ser-NH_2 in presence of NMM using of various protected groups: Boc, Z and Fmoc. Also the fragment with free OH-group of serine has been obtained by SPPS using Fmoc/tBu strategy on 2-chlorotrityl amine resin (consequence assembly of peptide chain and fragment condensation) (Fig. 1). In these schemes of synthesis the yield of the Fmoc-protected pentapeptide has not exceeded 30 %. Both solid-phase and classical methods of peptide synthesis have been used, with protected serine OH-group and with free OH-group From the received data (Table 1) follows, that synthesis of the Boc-protected fragment with free serine OH-group is more effective than others syntheses. The peptide H-Ala-Pro-Pro-Pro-Ser-NH_2 has been used for exenatide preparation.

References

1. Hargrove DM, Kendall ES, Reynolds JM, Lwin AN, Herich JP, Smith PA, Gedulin BR, Flanagan SD, Jodka CM, Hoyt JA, McCowen KM, Parkes DG, Anderson CM. *Regulatory Peptides* **141**: 113-119, 2007.
2. Nielsen LL, Young AA, Parkes DG. *Regulatory Peptides* **117**: 77-88, 2004.
3. Wunsch E, Moroder L, Gohring-Romani S, Musiol H, Gohring W, Bovermann G. *Int J Peptide Protein Res* **32**: 368-383, 1988.

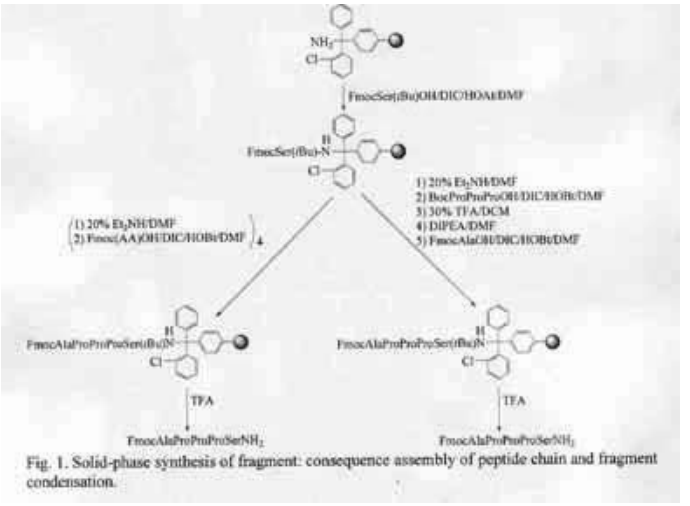

Fig. 1. Solid-phase synthesis of fragment: consequence assembly of peptide chain and fragment condensation.

Table 1. Data of RP-HPLC.

Protected fragment	Purity of a product on HPLC, %
classical method in a solution	
ZAlaProProProSer(*t*Bu)NH_2	87
BocAlaProProProSerNH_2	95
ZAlaProProProSerNH_2	78
FmocAlaProProProSerNH_2	56
Solid-phase synthesis	
FmocAlaProProProSerNH_2 (consequence assembly of peptide chain)	72
FmocAlaProProProSerNH_2 (fragment condensation)	70

1-01-116

Conjugation of glaucine to hydroxycinnamoyl amino acid amides

Spasova, Maya[1,]; Philipov, Stephan[2]; Avramov, Georgi[1]; Milkova, Tsenka[1]*

[1]South-West University "Neofit Rilski", Department of Chemistry, BULGARIA; [2]Bulgarian Academy of Sciences, Institute of Organic Chemistry, BULGARIA

[*]E-mail: mayabg2002@yahoo.com

Introduction

The increasing recognition of the participation of free radical-mediated oxidative events in the initiation and/or progression of cardiovascular, tumoural, inflammatory and neurodegenerative disorders, has given rise to the search for new antioxidant molecules. Recently we found that sinapoyl- and feruloyl amides of phenylalanine possess considerable antioxidant potential against bulk phase lipid peroxidation.[1,2] On the other hand, data exist about the photoprotective and antioxidant activity of aporphinic alkaloid glaucine.[3] Our study on the antioxidant potential of synthesized hydroxycinnamoyl amides of 3-aminomethylglaucine have shown an increasing of their radical scavenging activity against DPPH* in comparison to the starting aporphinic alkaloid.[4] It could be expected that the coupling of hydroxycinnamoyl amino acid amides to glaucine could result in enhancement of the antioxidative activity of the synthesized compounds.

Results and Discussion

Two kinds of *N*-hydroxycinnamoyl-phenylalanyl-3-aminomethylglaucine amides 3 and 4 were synthesized (Fig. 1). The amides 1 and 2 have been previously reported4 but the compounds 3 and 4 are unknown. The chemical structures of the newly synthesized amides were confirmed by UV, ^{1}H-NMR and ES-MS spectra. The values of the proton-proton vicinal coupling constants (3JH/H about 15.5 Hz) measured for the olefinic protons of feruloyl- and sinapoyl residues define E -configuration of the double bond of all studied compounds. Evaluation of DPPH Scavenging Activity In vitro DPPH* (1,1-diphenyl-2-picrylhydrazyl) assay is easy and the simplest method to measure the ability of antioxidants to intercept free radicals. The scavenging effects of hydroxycinnamic acid amides and standard antioxidant-tocopherol against DPPH* are illustrated in Table 1. The N-feruloyl – and sinapoyl-phenylalanyl-3-aminomethyl amides, have shown two times higher radical scavenging activity compared to those amides without phenylalanine rest (1 and 2). Among all tested compounds, sinapoyl-phenylalanyl-3-aminomethyl amide possessed the highest activity even of the standard antioxidant – tocopherol. Acknowledgements For the support of this work we are grateful to the National Found for Scientific Research of Bulgaria (Contracts VUH-07/05), South-West University "Neofit Rilski" Blagoevgrad, Bulgaria and to the CEEPUS mobility program.

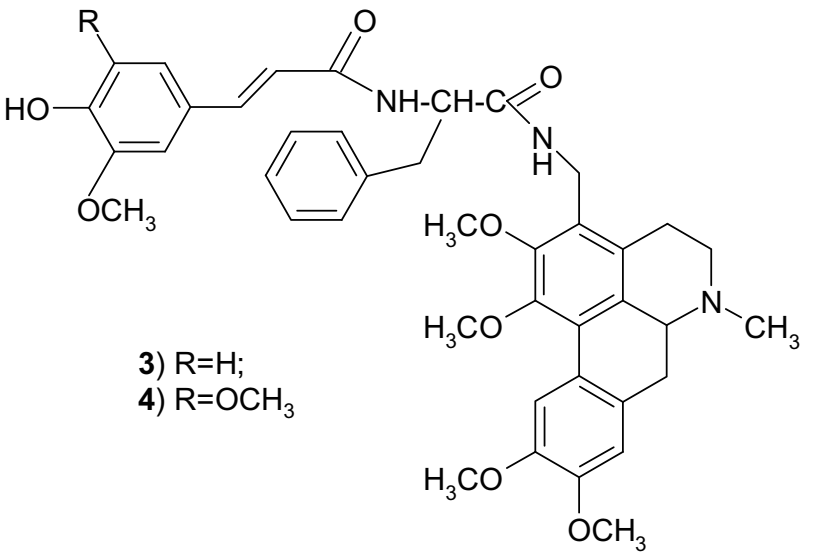

Figure 1.

Table 1. Effect of reaction period and concentration of synthesized hydroxycinnamoyl amides against DPPH*

	(%) RSA					
	0.9 mM		1.8 mM		3.6 mM	
	Reaction period (min)					
AH	10'	20'	10'	20'	10'	20'
D,L α-Tocopherol	15.5	15.9	34.9	38.4	53.0	58.1
N-(Sinapoyl)-Phe-3-aminomethylglaucine (4)	**19.7**	**25.9**	**34.4**	**43.4**	**56.5**	**62.5**
Sinapoylamide of 3-aminomethylglaucine (**1**)	8.0	10.5	14.4	18.0	26.3	31.6
N-(Feruloyl)-Phe-3-aminomethylglaucine (3)	**13.5**	**17.5**	**20.5**	**27.4**	**29.8**	**40.2**
Feruloylamide of 3-aminomethylglaucine(**2**)	8.3	10.1	16.6	19.4	31.2	36.1
3-Aminomethylglaucine	1.6	2.5	2.2	3.0	2.9	3.8

The N-feruloyl – and sinapoyl-phenylalanyl-3-aminomethyl amides, have shown two times higher radical scavenging activity compared to those amides without phenylalanine rest (**1** and **2**). Among all tested compounds, sinapoyl-phenylalanyl-3-aminomethyl amide possessed the highest activity even of the standard antioxidant –tocopherol.

References

1. Spasova M, Kortenska-Kancheva V, Totseva I, Ivanova G, Georgiev L, Milkova Ts. *J Pept Sci* **12**: 369-375, 2005.
2. Kortenska-Kancheva V, Spasova M, Totseva I, Milkova Ts. *La rivista italiana delle Sostanze grasse* **83**: 162-169, 2009.
3. Hidalgo ME, Farah M, Carrasco L, Fernández E. *J Photochem and Photobiol B* **80**: 65-69, 2005.
4. Spasova M, Philipov S, Nikolaeva-Glomb L, Galabov A, Milkova Ts. *Bioorg Med Chem* **16**: 7457-7461, 2008.
5. Pekkarinen S, Stockmann H, Schwarz K, Heinonen I.M, Hopia AI. *J Agric Food Chem* **47**: 3036 –3043, 1999.

1-01-117

Synthesis and Biological Activity of Cinnamic Acid Amides of Oxazole Containing Amino Acids

Stankova, Ivanka[1,]; Spasova, Maya[1]; Shishkov, Stoyan[2]*

[1]Department of Chemistry, South-West University ``Neofit Rilski", Blagoevgrad, BULGARIA;

[2]St Kl Ohridski Sofia University, Faculty of Biology, Laboratory of Virology, Sofia, BULGARIA

[*]E-mail: ivastankova@abv.bg

Introduction

Cinnamic acids and their derivatives (esters, amides and glycosides) attract attention in biology and medicine because of their antiviral, antioxidant, anti-inflammatoryt, antimutagenic properties.[1-4] In course of exploring new hydroxycinnamides as an antioxidative agent, we synthesized hydroxycinnamic acid amides with 2-aminomethyl-oxazole-4-carboxylic acid methyl ester. We have considered the role of heterocyclic amino acid and the effect of these structure modification on antioxidant activity. Herein, we describe the preparation of hydroxycinnamides from the corresponding acids (sinapic, p-coumaric, ferulic acids) and 2-aminomethyl-oxazole-4-carboxylic acid methyl. We also have evaluated then effectiveness of these compounds in DPPH radical-scavenging activity and their antiviral activity.

Results and discussions

The synthetic rout for preparation of p-coumaroyl-, feruloyl- and sinapoyl amides is shown in Fig. 1. Synthesis of oxazole containing glycine was prepared as described.[5] A solution of sinapic, p-coumaric, ferulic acids in dimethylformamide (DMF) was treated with triethylamine and TFA.2-aminomethyl-oxazole-4-carboxylic acid methyl ester using the coupling agent 1-[3-(dimethylamino)propyl]-3-ethyl carbodiimide hydrochloride (EDC) and 4-(dimethylamino)-pyridine (DMAP) as a catalyst, to produce the amide derivate (2 a-c).

Biological activity

Antioxidative activity of cinnamic acid amides of oxazole containing amino acid by DPPH•

The radical scavenging activities of the hydroxycinnamoyl amino acid-oxazole amides were determined by the DPPH (1,1-diphenyl-2-picrylhydrazyl) assay according to the method, proposed by Pekkarinen *et al*.[6] The synthesized hydroxycinnamoyl amides were found to be inefficient radical scavengers. Among them especially the sinapic acid amide of oxazole containing amino acid showed the highest antioxidant activity, but lower to the standards alpha-tocopherol, ferulic and sinapic acids.

Effect of the compounds (2 a-c) on the replication of HSV-1 and HSV-2

The hydroxycinnamic acid amides were explored against HSV-1, strain Da, and HSV-2, strain Bja. The compounds were applied in concentrations 100, 80, 40, 20, 10, 5, 1 and 0.5 μg/mL. Compounds 2 a-c showed low cytotoxicity – after 96 hours of cultivation MTC were determined - 20 μg/ml. The three investigated amides were applied in two-fold concentrations. The compounds had no effect on the replication of HSV-1 and HSV-2 during the multicycle virus growth. Intermolecular reactions of the acids with some cell metabolites not involved in the viral replication, were suggested.

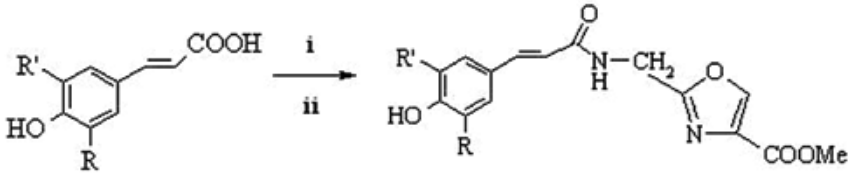

1 a-c **2 a-c**

1 a) p-coumaric acid; R, R'=H;
1 b) ferulic acid; R=OCH_3; R'=H;
1 c) sinapic acid; R, R'=OCH_3.

(i) TFA-2-aminomethyl-oxazole-4-carboxylic acid methyl ester; (ii) EDC/DMAP.

Figure 1. Synthesis of hydroxycinmamides of 2-aminomethyl-oxazole-4-carboxylic acid methyl ester.

Conclusion

Three novel hydroxycinnamic acid derivatives have been synthesized from the sinapic, p-coumaric, ferulic acids and oxazole containing TFA.glycine-4-carboxylic acid methyl ester. The hydroxycinnamoyl oxazole conjugates have been studied for their antioxidant activity by DPPH* test. The new hydroxycinnamoyl amides were found to posses activity similar to p-coumaric acid. Among them especially the sinapic acid amide of oxazole containing amino acid showed the highest antioxidant activity, but lower to the standards alpha-tocopherol, ferulic and sinapic acids. All of the tested amides do not demonstrate antiviral effect on the replication of HSV-1 and HSV-2.

Acknowledgement

We gratefully acknowledge financial support from the National Found for Scientific Research of Bulgaria (Contract Bin 4/04 and VUH-07/05).

References

1. Lee S, Han Jong-Min, Kim H, Kim E, Jeon TS, Lee WS, Cho KH. *Bioorg Med Chem Lett* **14**: 4677, 2004.
2. Hensel A, Deters M, Müller G, Stark T, Wittschier N, Hofmann T. *Planta Med* **73**: 142-150, 2007.
3. Sangku Lee, Chul-Ho Lee, Eungsoo Kim, Sang-Hun Jung, Hyeong Kyu Lee. *Bull Korean Chem Soc* **28**: 1787-1791, 2007.
4. Moon J-H, Terao J. *J Agric Food Chem*. **46**: 5062-5065, 1998.
5. Videnov G, Kaiser D, Kempter C, .Jung G. *Angew Chem* **108**: 1604-1607, 1996. *Angew Chem Int Ed Engl* **35**: 1503-1506, 1996.
6. Pekkarinen S, Schwarz K, Heinonen M, Hopia A. *J Agric Food Chem* **47**: 3036-3043, 1999.

1-01-118

Synthesis of novel hydantoin-phosphonic acids and dipeptides consist hydantoin structure with potential biological activity

Todorov, Petar[1]; Naydenova, Emilia[1,]; Pavlov, Nikola[1]; Troev, Kolio[2]*

[1]University of Chemical Technology and Metallurgy, Department of Organic Chemistry, BULGARIA; [2]Institute of Polymers, Bulgarian Academy of Sciences, BULGARIA

[*]E-mail: e_naydenova@abv.bg; pepi_37@abv.bg

Introduction

Hydantoins are synthetically valuable, compounds frequently used as precursors to α-amino acid. C-5 substituted hydantoins as well as aminophosphonic acids are also important medicines. Due to their antidepressant, anti-convulsant, cardiac anti-arrhythmic, as well as their antiviral activities and anticancer effects they have found numerous applications. The cycloalkanespiro-5-hydantoins also reveal anticonvulsive effect which however is very weak. It has been observed that the enlargement of their cyckloalkane rings increases this effect. It was found in our experiments that the involvements of an amino group into the hydantoin ring of the spirohydantoins influences their biological activity.[1] The established antiproliferative effects of the α-aminophosphonic acids combined with the low toxicity of these agents towards mammalians determines the greet interest towards novel antineoplastic agents design.[2,3] Taking into account this fact we describe herein the synthesis of novel hydantoin-phosphonic acids and dipeptides with hydantoin structure with emphasis on the structure – biological activity relationship.

Results and Discussion

The novel dipeptides (1, 2a-2d) were synthesized by liquid-phase peptide synthesis by reacting Boc- or Z-amino acids (Gly, Phe, Tyr, Leu, Ser) with 3-amino-hydantoins using TBTU/DIEA as a condensing reagent. The cycloalkanespiro-5-hydantoins with 5-, 6-, 7- and 8-membered rings were obtained from the corresponding cyclic ketones by Bucherer-Lieb reaction. Using own modified method we transformed them into 3-aminoderivatives by means of $NH_2NH_2.H_2O$. The protecting groups of peptides were removed by hydrogenation over Pd/C catalyst for benzyloxycarbonyl, and one by TFA for the butyloxycarbonyl (Fig. 1).

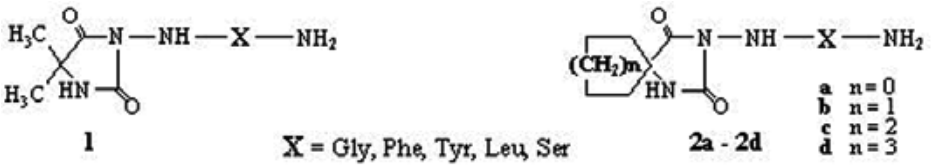

Figure 1. Structure of new dipeptides consist hydantoin structure.

The starting hydantoins were used for the preparation of the new α-aminophosphonic acids. They have been synthesized by two different methods. For the synthesize of new [(5,5-dimethyl-2,4-dioxoimidazolidine-1,3-diyl) dimethyl]diphosphonic acid (3) we used Engelmann and Pikl's procedure. As starting compounds were 5,5-dimetylhydantoin, phosphorus trichloride and formaldehyde, mixed in the molar ratio - 1:2:2. The dimethyl[(5,5-dimethyl-2,4-dioxoimidazolidin-3-yl)aminomethyl] phosphonate (4), dimethyl[(3-[(dimethoxyphosphoryl)methyl]amino-5,5-dimethyl-2,4-dioxoimidazol- idin-1-yl)methyl]phosphonate (5) and compounds 6a-6d, 7a-7d, 8a-8d were prepared with good yields via Kabachik-Fields reaction (Fig. 2).

All newly synthesized compounds were characterized by IR, ^{1}H, $^{13}C\{^{1}H\}$ and ^{31}P NMR spectroscopy, MS and TLC. The structures of novel dipeptides were proved by ES-MS. The biological trials are in the progress.

Acknowledgements

We gratefully acknowledge the financial support by the University of Chemical Technology and Metallurgy – contract №10507.

References

1. Naydenova E, Pencheva N, Popova J, Stoyanov N, Lazarova M, Aleksiev B. *Il Farmaco* **57**: 189-194, 2002.
2. Naydenova E, Topashka-Ancheva M, Todorov P, Yordanova Ts, Troev K. *Bioorg Med Chem* **14**: 2190-2196, 2006.
3. Naydenova E, Todorov P, Topashka-Ancheva M, Momekov G, Yordanova Ts, Konstantinov S, Troev K. *Eur J Med Chem* **43**: 1199-1205, 2008.

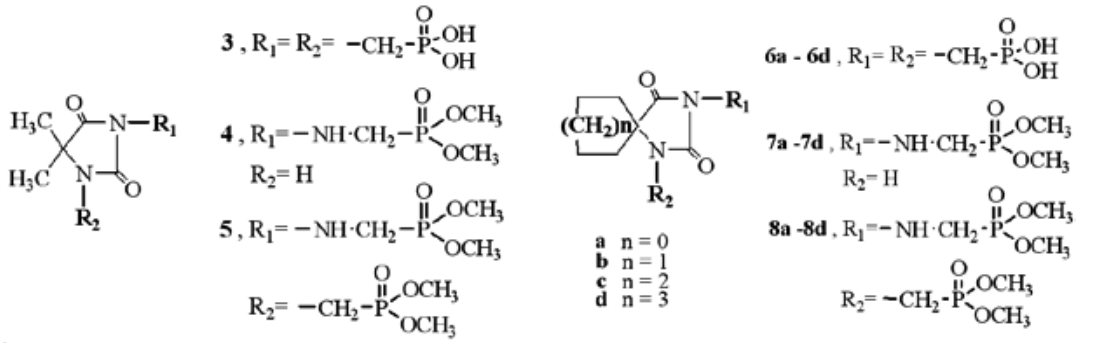

Figure 2. Structure of new hydantoin-phosphonic acids.

1-01-119

Synthesis, resolution, and absolute configuration of BpAib, a benzophenone-containing C^{α}-tetrasubstituted α-amino acid

Wright, Karen[1]; Wakselman, Michel[1]; Mazaleyrat, Jean-Paul[1]; Moretto, Alessandro[2]; Crisma, Marco[2]; Formaggio, Fernando[2]; Toniolo, Claudio[2,]*

[1]University of Versailles, F-78035 Versailles, ILV, UMR CNRS 8180, FRANCE; [2]University of Padova, I-35131 Padova, ICB-CNR, Department of Chemistry, ITALY

[*]*E-mail: claudio.toniolo@unipd.it*

Photoreactive amino acids with benzophenone side chains, the prototype of which is Bpa [3-(4-benzoylphenyl) alanine],[1] have found numerous applications as photoprobes for covalent modification of enzymes and receptors, as well as in intramolecular quenching by a nitroxide free radical in trichogin peptide analogues. However, the remarkable flexibility of the Bpa side chain[2] may question the extrapolation of results of photocross-linking experiments and photophysical data to protein mapping and intramolecular distances, respectively. To overcome this problem, we designed and synthesized a new "constrained Bpa" amino acid, BpAib, belonging to the sub-class of the $C_i^{\alpha} \leftrightarrow C_i^{\alpha}$ cyclized, C^{α}-tetrasubstituted α-amino acids (strong β-turn and helix inducers in peptides), the prototype of which is Aib.

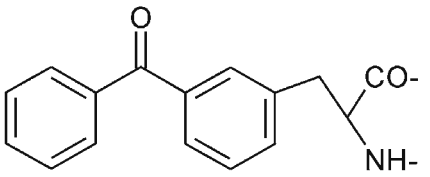

Bpa

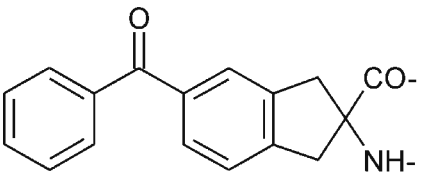

BpAib

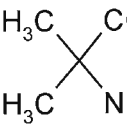

Aib

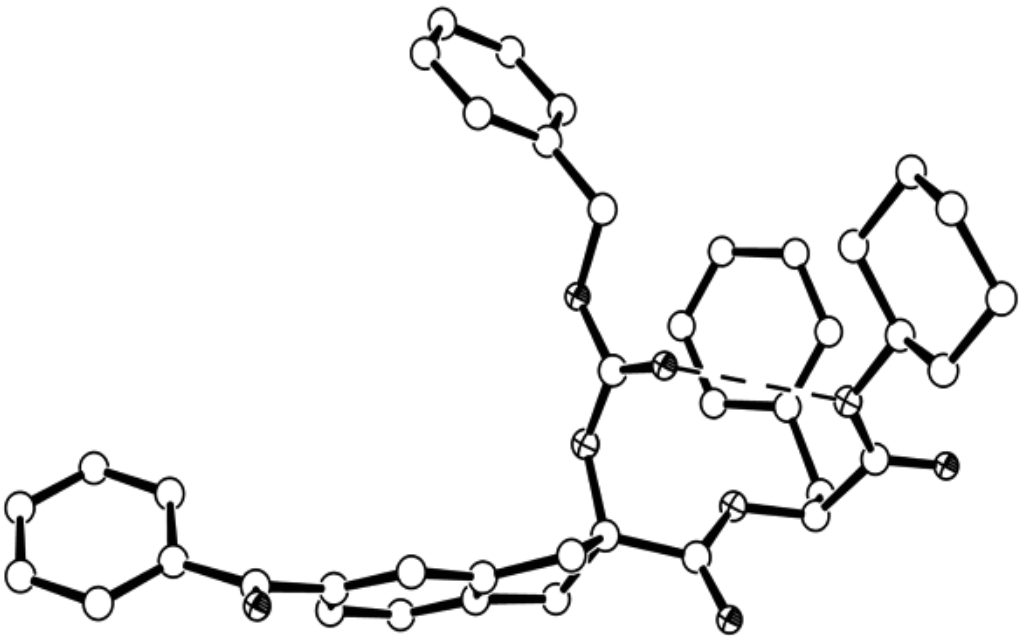

Figure 1. X-Ray diffraction structure of z-(*R*)-BpAib-(*S*)-Phe-NHChx.

Racemic Boc-BpAib-OH was prepared by bis(alkylation) of ethyl isocyanoacetate under phase-transfer conditions with 1-benzoyl-3,4-(bis)bromomethyl benzene as the alkylating agent, followed by acidic hydrolysis, N^{α}-Boc protection, and saponification of the ester function. Resolution was achieved through the terminally-blocked dipeptide Bz-BpAib-(*S*)-Phe-NHChx (Chx, cyclohexyl) with chromatographic separation of the diastereomers and acidic hydrolysis. X-Ray diffraction analysis of a z-BpAib-(*S*)-Phe-NHChx diastereomer allowed the assignment of the absolute configuration of the BpAib enantiomers (Fig. 1). Photocross-linking studies using this residue are currently in progress.

References

1. Kauer JC, Erickson-Viitanen S, Wolfe HR Jr, DeGrado WF. *J Biol Chem* **261**: 10695-10700, 1986.
2. Saviano M, Improta R, Benedetti E, Carrozzini B, Cascarano GL, Didierjan C, Toniolo C, Crisma M. *ChemBioChem* **5**: 541-544, 2004, and references cited therein.

1-01-120

Synthesis and conformational analysis of doubly spin-labelled β-peptides based on the nitroxide bearing POAC residue

Toniolo, Claudio[1,]; Formaggio, Fernando[1]; Toffoletti, Antonio[1]; Franco, Lorenzo[1]; Mazaleyrat, Jean-Paul[2]; Wakselman, Michel[2]; Wright, Karen[2]*

[1]University of Padova, I-35131 Padova, Department of Chemistry, ITALY; [2]University of Versailles, F-78035 Versailles, ILV, UMR CNRS 8180, FRANCE

[*]E-mail: claudio.toniolo@unipd.it

The nitroxide spin-labelled $\beta^{2,3}$-cyclic amino acid POAC was synthesized, resolved and its absolute configuration assigned[1] in order to be used as a spin-probe to evaluate the 12-helical β-peptide secondary structure.[2] We designed and prepared a series of β-hexapeptides, namely based on two (*3R,4R*)-POAC and four (*1S,2S*)-ACPC residues for configurational homogeneity of the amino acid components.

In these hexapeptides two POAC residues are incorporated at positions i, i+n (n = 1-4) to observe conformation-related spin-spin interactions. The peptides were synthesized by N- to -C chain elongation of N^{α}-Boc protected peptide segments in solution. Our analyses, performed by FT-IR absorption, CD, and EPR (Fig. 2) spectroscopic techniques, allowed us to conclude that the preferred conformation of the hexapeptides is closely related to the 12-helix adopted by their ACPC homo-hexapeptide counterparts.

Boc-ACPC-POAC-POAC-ACPC-ACPC-ACPC-OMe (**1**)
Boc-ACPC-POAC-ACPC-POAC-ACPC-ACPC-OMe (**2**)
Boc-ACPC-POAC-ACPC-ACPC-POAC-ACPC-OMe (**3**) (Fig. 1)
Boc-ACPC-POAC-ACPC-ACPC-ACPC-POAC-OMe (**4**)

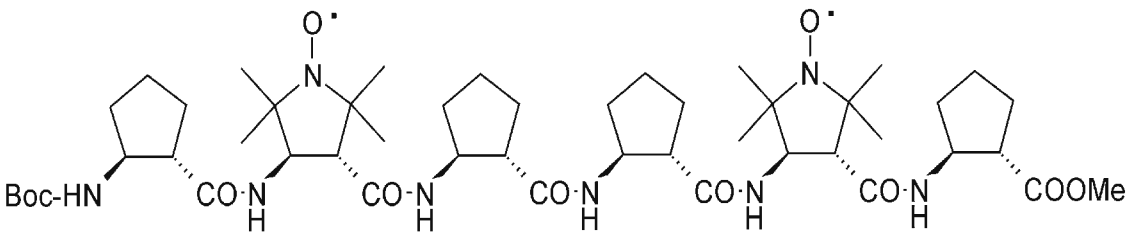

Figure 1. Chemical structure of Boc-ACPC-POAC-ACPC-ACPC-POAC-ACPC-OMe (3).

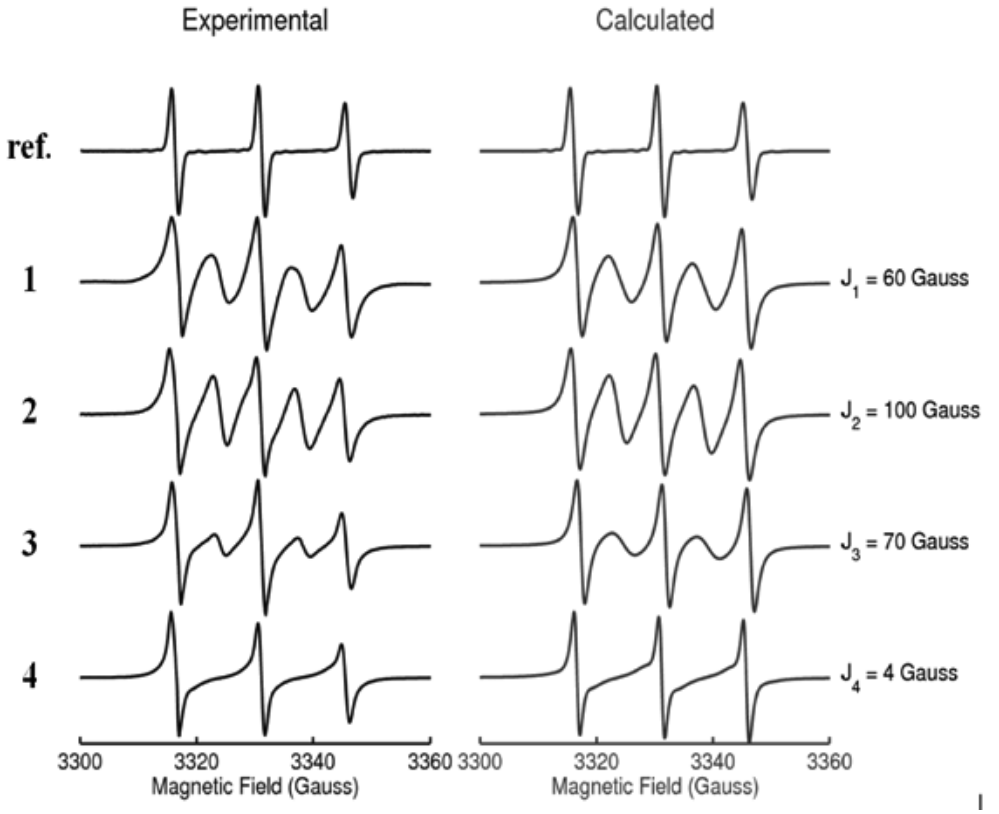

Figure 2. Experimental and calculated EPR spectra of the reference compound Fmoc-POAC-OH (**ref.**) and the POAC/ACPC hexapeptides 1-4 in chloroform solution (T=298 K).

References

1. Wright K, Dutot L, Wakselman M, Mazaleyrat J-P, Crisma M, Formaggio F, Toniolo C. *Tetrahedron* **64**: 4416-4426, 2008.
2. Appella DH, Christianson LA, Klein DA, Powell DR, Huang X, Barchi JJ Jr, Gellman SH. *Nature* **387**: 381-384, 1997.

1-01-121

N-Methylation of N^{α}-acetylated, C^{α}-ethylated, fully-extended homo-peptides: synthetic and conformational aspects

*Moretto, Alessandro; Crisma, Marco; Formaggio, Fernando; Toniolo, Claudio**

University of Padova, 35131 Padova, ICB-CNR, Padova Unit, Department of Chemistry, ITALY

**E-mail: claudio.toniolo@unipd.it*

Peptides characterized by single or multiple N-methylated, C^{α}-trisubstituted (protein) α-amino acids are one of the subject of increasing interest in medicinal chemistry. Several naturally occurring peptides, remarkably stable to proteolytic attacks, are based on N-methylated peptides. N-Methylation of the -CONH- function is a useful tool for discriminating solvent exposed from intramolecularly H-bonded secondary amide groups in peptides.

We are currently extending this reaction to linear peptides based on C^{α}-tetrasusbtituted α-amino acids. After having investigated the synthesis and conformation of the N-methylated homo-peptides from the C^{α}-methylated, helicogenic α-aminoisobutyric acid (Aib) and C^{α}-methylnorvaline [(αMe)Nva] residues,[1] in this work we examined the N-methylation reaction on homo-peptides from $C^{\alpha,\alpha}$-diethylglycine (Deg).[2,3] More specifically, we studied the peptide series Ac-$(Deg)_n$-$N(Et)_2$ with n = 1-5. Under the experimental conditions used, only mono-methylation (on the N-terminal, acetylated residue) does take place. Our FT-IR absorption, NMR, and X-ray diffraction analyses (Figs. 1 and 2) support the view that the helical conformation preferred by the original peptides is not significantly perturbed in the derivatives mono-methylated at position 1.

References

1. Moretto A, Crisma M, Kaptein B, Broxterman QB, Toniolo C. *Biopolymers (Peptide Science)* **84**: 553-565, 2006.
2. Benedetti E, Barone V, Bavoso A, Di Blasio B, Lelj F, Pavone V, Pedone C, Bonora GM, Toniolo C, Leplawy MT, Kaczmarek K, Redlinski A. *Biopolymers* **27**: 357-371, 1988.
3. Tanaka M, Imawaka N, Kurihara M, Suemune H. *Helv Chim Acta* **82**: 494-510, 1999.

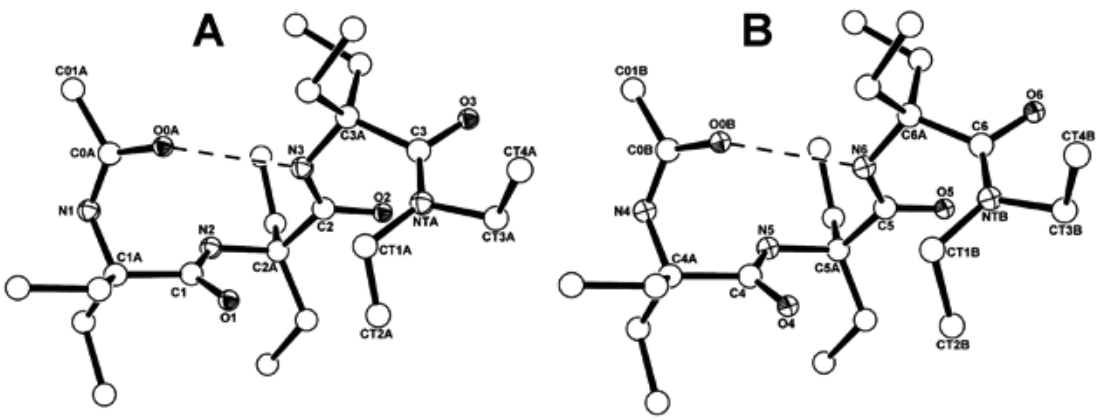

Figure 1. X-Ray diffraction structures of the two crystallographically independent molecules (**A** and **B**) in the asymmetric unit of Ac-$(Deg)_3$-$N(Et)_2$ with partial atom numbering. In each molecule the C=O•••H-N intramolecular H-bond is represented by a dashed line.

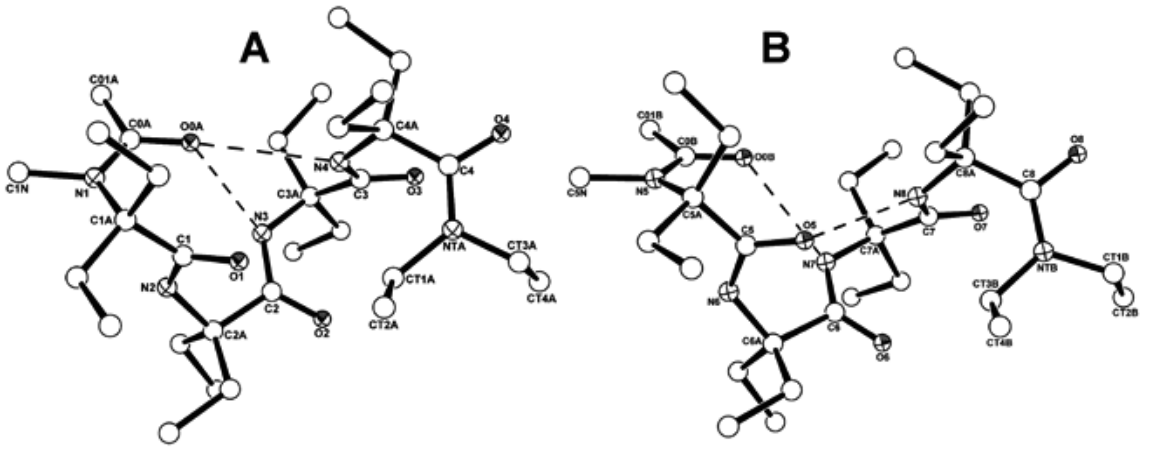

Figure 2. X-Ray diffraction structures of the two crystallographically independent molecules (**A** and **B**) in the asymmetric unit of Ac-MeDeg-$(Deg)_3$-$N(Et)_2$ with partial atom numbering. In each molecule the two C=O•••H-N intramolecular H-bonds are represented by dashed lines.

1-01-122

A substituted proline with a strong preference for helix conformation: an X-ray diffraction investigation

Moretto, Alessandro[1]; Toniolo, Claudio[1,]; Crisma, Marco[1]; Formaggio, Fernando[1]; Kaptein, Bernard[2]; Broxterman, Quirinus B[2]*

[1]University of Padova, 35131 Padova, ICB-CNR, Padova Unit, Department of Chemistry, ITALY; [2]Innovative Synthesis and Catalysis, 6160 MD Geleen, DSM Pharmaceutical Products, NETHERLANDS

[*]E-mail: claudio.toniolo@unipd.it

L-Proline is conformationally unique among coded amino acids in that its φ torsion angle is blocked (-65 ± 10°) by its characteristic five-membered pyrrolidine ring structure and the preceding ω torsion angle (tertiary amide) can undergo *cis* (0°) ↔ *trans* (180°) isomerization much easier than the secondary amides of the usual peptide bonds. In addition, its *ψ* torsion angle is commonly found either in the *right*-handed 3_{10}-/α-helical region (-30° ÷ -50°, or *cis'* conformation) or in the *left*-handed, *semi*-extended, region [-150 ±10°, or *trans'*, or poly-(L-Pro)$_n$ conformation]. Methylation at the C^{α}-position of a Pro residue was suggested to block the preceding tertiary amide (ω) torsion angle of the resulting (*α*Me)Pro to the *trans* disposition and to restrict the *φ,ψ* surface to a *single* region, that where the 3_{10}/*α*-helices are found.[1] We have synthesized a large set of N^{α}-blocked, (αMe)Pro-containing, dipeptide *N'*-alkylamides having the general formulas P-D-(*α*Me)Pro-Xxx-NH*i*Pr and P-Xxx-D-(*α*Me) Pro-NH*i*Pr, where P is Ac, *i*Bu, Z, or Boc and Xxx is D-Ala, L-Ala, Aib, Gly, D-(*α*Me)Pro, or L-(*α*Me)Pro.

The results of the X-ray diffraction analyses performed to date (Table I and Fig. 1) clearly show that the region of the conformational map overwhelmingly preferred by (*α*Me)Pro is indeed that typical of 3_{10}/*α*-helices, but the *semi*-extended, type-II poly(Pro)$_n$ helical region can also exceptionally be explored by this extremely sterically demanding, C^{α}-tetrasubstituted *α*-amino acid. In addition, the known high propensity for *β*-turn formation of the Pro residue is even enhanced in peptides based on its C^{α}-methylated derivative. To complete the picture of the preferred conformation of (*α*Me)Pro, the synthesis and crystal-state investigation of a series of terminally-protected homo-peptides from D-(*α*Me)Pro are also currently in progress in our laboratory.

References

1. Burgess A, Paterson Y, Leach SJ. *Peptides, Polypeptides, and Proteins;* Blout ER, Bovey FA, Goodman M, Lotan N (Eds), Wiley, New York, NY, 1974, pp 79-87.

Table I. 3D-Structural parameters in the crystal state for the novel (*α*Me)Pro-containing dipeptide sequences

Peptide sequence	Backbone torsion angles				Type of β-turn
	ϕ_{i+1}	ψ_{i+1}	ϕ_{i+2}	ψ_{i+2}	
Ac-L-Ala-L-(αMe)Pro-NH*i*Pr	-135	77	-58	-37	open
Boc-L-Ala-L-(αMe)Pro-NH*i*Pr	-76	130	-59	-36	open
Ac-D-(αMe)Pro-D-Ala-NH*i*Pr	53	32	66	25	III′
Ac-D-(αMe)Pro-L-Ala-NH*i*Pr	53	-129	-77	-12	II′
*i*Bu-L-Ala-D-(αMe)Pro-NH*i*Pr	-55	133	78	0	II
Ac-D-(αMe)Pro-Aib-NH*i*Pr	53	37	61	28	III′
Z-Aib-D-(αMe)Pro-NH*i*Pr	50	39	67	22	III′
	54	32	55	21	III′
Z-D-(αMe)Pro-D-(αMe)Pro-NH*i*Pr	50	34	57	28	III′

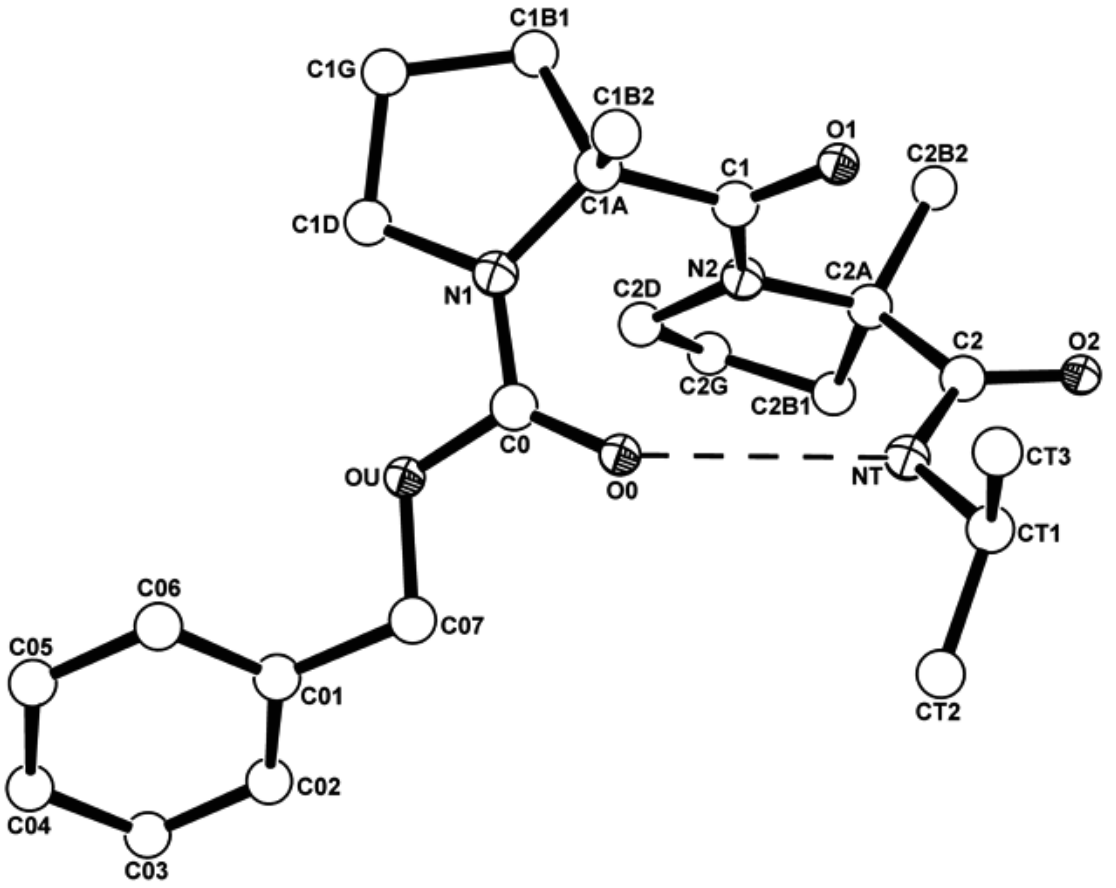

Figure 1. X-Ray diffraction structure of Z-D-(*α*Me)Pro-D-(*α*Me)Pro-NHiPr with atom numbering. The C=O•••H-N intramolecular H-bond of the type-III' *β*-turn is indicated by a dashed line.

1-01-123

Impact of ionic liquids on peptide acylation reactions

Wespe, Christian; Mrestani-Klaus, Carmen; Bordusa, Frank*
University Halle-Wittenberg, GERMANY

**E-mail: christian.wespe@gmx.de*

Introduction

Ionic liquids (ILs) are organic salts which are fluid at temperatures below 100 °C. As salts they have only marginal vapor pressures,[1] are easy to reuse, mostly chemically inert, thermally stable over a broad range of temperatures and can potentially be fine-tuned to individual task specific requirements.[2] Because of these characteristics, ILs became increasingly attractive solvents for a wide spectrum of technical and chemical applications as well. Besides these more general features, ILs were found to affect the regioselectivity of certain organic reactions. Heck[3] or Diels-Alder reactions[4] for example exhibit significant higher regioselectivities if suitable ILs are used as the solvent. Minor efforts have been made however in investigating the behavior of peptides in ILs,[5] although peptide chemistry would profit by IL-induced regioselectivity effects in a particular manner. Due to the chemical multifunctionality of the peptide reactants a protecting group hierarchy is necessary to control the course of synthesis leading to a poor atom economy of the whole reaction. In principle, the same limitation holds true for site-specific modificiations of preformed peptide targets which by chemical means proceed in a chemoselective way at best. Presently, no solvent system is known which inherently affects the regioselectivity of peptide synthesis or modification reactions.

Results and Discussion

In systematic study on the regioselectivity effect of ILs in peptide-based reactions, we first evaluated the impact of ILs on the course of peptide acylation reactions. As initial screening system, the model peptide H-GAKAY-OH containing two reactive amino groups; i.e., the N-terminal amino function and the N^{α}-amino function of the lysine side chain, and the 3-(4-hydroxyphenyl)propionic acid *N*-hydroxysuccinimide ester (Phloretin-OSu) as the acylating reagent were used. The ILs tested were selected regarding their viscosity, water miscibility and their commercial availability. Special but not exclusive attention was paid to imidazolium based ILs which are available in a broad collection of ions. Quantification of the regioselectivity inducing effect of the ILs was made by the newly introduced regioisomeric excess (re). In analogy to the well-known enantiomeric excess (ee), re was defined as the quotient of the difference in the regioisomeric products divided by the products' sum. Accordingly, negative re-values indicate a preferred N^{α}-acylation whereas positive re's imply a preference of ILs for mediating the acylation of the N-terminal amino group. Selected results obtained are shown in Fig. 1 indicating a significant inherent regioselectivity behavior of certain ILs. For dimethylimidazolium based ILs such as 1-ethyl-3-methylimidazolium dimethylphosphate [EMIM][Me_2PO_4] for example strongly positive re-values and, thus an improved N-terminal acylation of the peptide was found, while in 1-ethyl-3-methylimidazolium diethylphosphate [EMIM][Et_2PO_4] the re-value was negative indicating a preferred acylation of the lysine's side-chain amino function. By using two peptide libraries of the type H-Xaa-Ala-Lys-Ala-Tyr-OH and H-Val-Xaa-Lys-Xaa-Tyr-OH including also two elongated 16mer and 29mer polypeptides it could be shown that this surprising regioselectivity inducing effect of ILs is not restricted to the peptide H-GAKAY-OH but also holds for all other peptides independent of their individual sequence or length. Furthermore, no qualitative influence of the acyl donor structure on the regioselectivity effect was found indicating that the regioselectivity effect of ILs is of general importance in peptide acylation reactions. Besides the investigation of the general characteristics, large efforts have been made to clarify the molecular reasons of this IL-induced regioselectivity behavior. Based on Eyring kinetics, a significant influence of ILs on the activation parameters of the acylation reactions became obvious. In accordance with the course of the acylation reactions, N-terminal directing ILs kinetically favor reactions at the N^{α}-amino function while ILs showing an improved regioselectivity for the lysine side chain clearly support N^{α}-acylations. These results go along with our findings obtained from FTIR-spectroscopy which show a significant effect of ILs on the pKa-value of the peptides' reactive amino functions. Accordingly, ILs mediating the acylation of the lysine's side-chain amino function reduce the pKa of the corresponding N^{α}-amino group to a value which is even lower than that of N-terminal counterpart. The exact opposite was found for ILs directing the acyl moiety to the peptides' N-termini. As the rational behind, direct IL/peptide interactions are assumed. Their general existence was already proven by initial NMR studies. Interestingly, for imidazolium-derived ILs a correlation between the chemical shift changes of the proton signal at C2 upon addition of the peptide and the individual effect of the IL on the regioselectivity became obvious. The relevance of this interaction could be already demonstrated by the use of C2-methylated ILs which

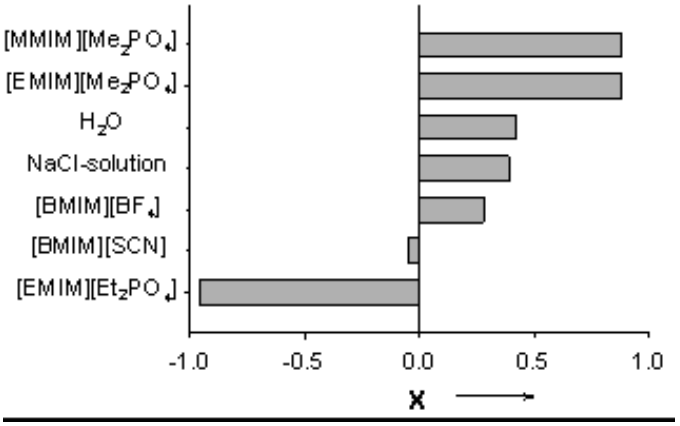

Figure 1. Effect of ILs on the regioselectivity of phloretylation reactions of GAKAY with Phloretin-OSu. Conditions: T=30 °C, pH 8.2, 80% (v/v) IL/water/NaCl-solution, 10% (v/v) DMF, 10% (v/v) MOPS-buffer (c=50 mM); c(peptide)=c(Phloretin-OSu)=1.6 mM, NaCl-solution: 5.7 M NaCl in water, errors are less than 5% (±2.5%),X: re.

exhibit a significantly weaker regioselectivity behavior compared to their original non-methylated counterparts. Detailed ^{15}N-NMR studies are needed however, to visualize the impact of those interactions on the reactivity of the peptide's individual amino functions.

Acknowledgements

This work has been supported by the Deutsche Forschungsgemeinschaft DFG (SPP 1191).

References

1. Earle MJ, Esperança JM, Gilea MA, Lopes JN, Rebelo LP, Magee JW, Seddon KR, Widegren JA. *Nature* **439**: 831-834, 2006.
2. Welton T. *Chem Rev* **99**: 2071-2083, 1999.
3. Calò V, Nacci A, Monopoli A, Ferola V. *J Org Chem* **72**: 2596-2601, 2007.
4. Janus E, Goc-Maciejewska I, Łożyński M, Pernak J. *Tetrahedron Lett* **47**: 4079-4083, 2006.
5. Valette H, Ferron L, Coquerel G, Gaumont A-C, Jean-Christophe Plaquevent J-H. *Tetrahedron Lett* **45***:* 1617-1619, 2004.

1-01-124

Synthesis of a novel α,α-disubstituted glycine, α-cyclobutylalanine

Yamada, Takashi[1,]; Okumura, Tomoko[1]; Mizukoshi, Rina[1]; Murashima, Takashi[1]; Miyazawa, Toshifumi[1]; In, Yasuko[2]*

[1]Faculty of Science and Engineering, Konan University, Department of Chemistry, JAPAN; [2]Osaka University of Pharmaceutical Sciences, JAPAN

[*]E-mail: yamada@center.konan-u.ac.jp

Introduction

Nonproteinogenic *α,α*-disubstituted glycines are of increasing importance in developing small, acyclic, conformationally restricted peptides. In particular, α-methyl-α-amino acids are valuable tools for controlling secondary structures in *de novo* designed peptides because they have fairly good reactivity among *α,α*-disubsutituted glycines. They are known to be $\alpha/3_{10}$-helices inducers, and also to be often powerful enzyme inhibitors.[1] Previously, we reported that a facile synthesis of enantiomerically pure *α*-methyl-*α*-amino acids using the Ugi reaction and the excellent chromatographic separation of diastereomers of the resulting Ugi products, as the key steps (Scheme 1).[2] As far as we were able to examine, every Fraction A (**1A**) of the Ugi products (**1**), which elutes faster than Fraction B (**1B**) in the column chromatography using silica-gel, provided the (S)-isomer of *α*-methyl-*α*-amino acid (**3**) without exception. We also reported the preparation of a novel amino acid, *α*-cyclopropylalanine (**3**: R = cyclopropyl) (*α*Cpa) as an application of this method, and the determination of chirality of *α*Cpa by X-ray crystal structural analysis[3]. Thereby, we established that the (*S*-*S*) diastereomer of the Ugi product (**1**) always elutes faster than the (*S*-*R*) one of **1** under the conditions used above, and the enantiomer of *α*-methyl-*α*-amino acid [AA(*α*Me)] (**3A**) obtained from Fraction A (**1A**) has a positive optical rotation and the (*S*)-configuration. We report here the preparation of another novel amino acid, *α*-cyclobutylalanine (**3**: R = cyclobutyl) (*α*Cba), in order to compare with *α*Cpa.

Results and discussion

Diastereomeric dipeptides (**4A** and **4B**) containing *α*Cba (**6**) was prepared in a good yield (63%) by the Ugi reaction, and the diastereomers were easily separated by open-column chromatography or preparative TLC using silica-gel (Table 1).

Hydrolysis with HCl of each diastereomer (**4A** and **4B**) followed by catalytic hydrogenolysis afforded enantiomerically pure *α*Cba (**6A** and **6B**). In this case, Fraction A (**4A**) also afforded (+)-*α*Cba (**6A**) (Scheme 2). Therefore, the configurations of **6A** and **6B** can be estimated to be (*S*) and (*R*), respectively.

Conclusion

Both enantiomers of enantiomerically pure α-cyclobutylalanine (*α*Cba) could be successfully obtained. Even in the case of *α*Cba, Fraction A of the Ugi products afforded (+)-enantiomer, and thus (*S*)-isomer. This method shown in Schemes 1 and 2 will provide a facile, practical preparation of various, chiral *α*-methyl-*α*-amino acids.

Scheme 1. Synthesis of chiral *α*-methyl-*α*-amino acids [AA(*α* Me)] (3A / 3B)

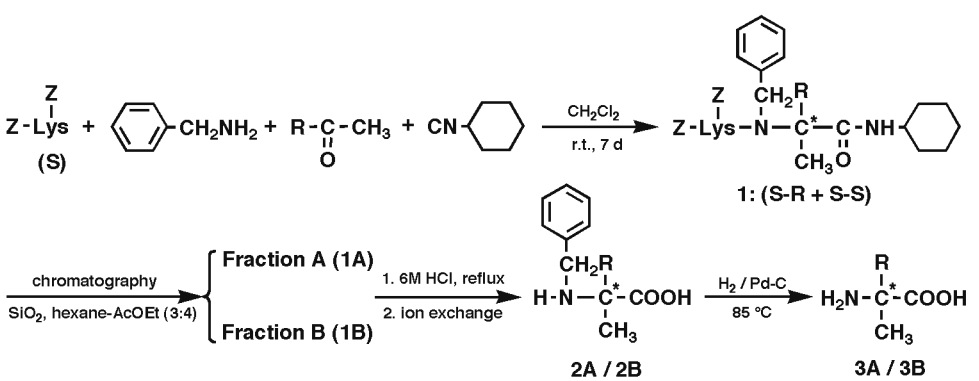

Table 1. Separation of diastereomers *(***3A** / **3B** *and* **4A** / **4B***)* by column chromatography

	Fraction	Yield (%)[a]	R_f[b]	t (min) [c]	$[\alpha]_D^{25}$ [d]
Z-L-Lys(Z)-(N-Bzl)αCpa-NH-cHex	3A	43	0.56	8.1	+ 20.4°
	3B	44	0.31	11.2	- 18.6°
Z-L-Lys(Z)-(N-Bzl)αCba-NH-cHex	4A	31	0.65	10.8	+ 8.4°
	4B	32	0.39	14.8	- 9.2°

a) Yield in isolation by SiO_2 column chromatography [elution solvent: hexane-AcOEt (3:4)].
b) TLC: Kieselgel 60 F_{254}, hexane-AcOEt (3 : 4).
c) HPLC conditions : column, Wakosil-II $5C_{18}$ (Φ4.6 mm×150 mm); mobile phase, 80% MeOH aq.; column temp., 30 °C; flow rate, 1.0 ml/min; detection, UV at 254 nm. d) c 1.0, MeOH.

Scheme 2. Synthesis of chiral α-cyclobutylalanine (**6A** and **6B**)

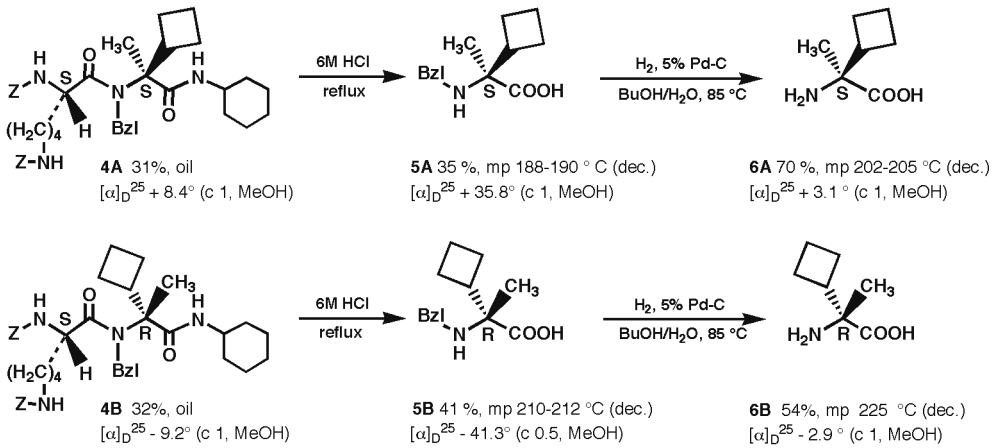

References

1. Cativiela C, Diaz-de-Villegas MD. *Tetrahedron Asym* **9**: 3517-3599, 1998.
2. Yamada T, Tsuboi D, Okano K, Kanda A, Nishi Y, Yamanishi F, Origane Y, Nakamura Y, Yanagihara R, Miyazawa T. *Peptide Science* (Symposium 1999): 147-150, 2000.
3. Yamada T, Okumura T, Mizukoshi R, Tsuboi T, Murashima T, Miyazawa T, In Y. *Peptide Science* (Symposium 2007): 129-132, 2008.

1-01-125

Photoswitchable bisintercalators – synthesis of Triostin A analogs

Zobel, Ansgar; Gaus, Katharina; Wollschläger, Katrin; Nieß, Anke; Juodaityte, Jovita; Sewald, Norbert*

Bielefeld University, Organic and Bioorganic chemistry, GERMANY

**E-mail: ansgar.zobel@uni-bielefeld.de*

Introduction

Novel highly active and specific DNA binding molecules have a considerable potential particularly with regard to applications in medical Science. The major and minor grooves of the DNA serve as recognition areas. It is of high interest for Chemical Biology to control DNA-binding abilities of synthetic molecules. A possible modulator is light in combination with photoswitchable molecules.

Triostin A is a natural bisintercalator which belongs to the quinoxaline antibiotics with antitumoral properties originally isolated from *Streptomyces* S-2-210. It consists of a bicyclic octadepsipeptide symmetrically composed of the amino acids alanine, D-serine, *N*-methyl-valine and *N*-methyl-cysteine. The cysteine sidechains form an intramolecular cystine bridge. The heteroaromatic quinoxaline moieties attached to D-serine are able to intercalate GC-specifically into duplex DNA. Placing its peptide backbone in the minor groove the Triostin A-DNA complex is stabilized additionally. The binding process to the DNA induces a change in conformation and therefore inhibits the transcription by blocking specific enzymes.

TANDEM is the synthetical analog and differs from Triostin A in the absence of *N*-alpha-methylation in the depsipeptidic backbone. This fact causes AT-selectivity of the molecule due to the change in the hydrogen bonding pattern.[1] The combination of photoswitchability and DNA binding ability is realized by substitution of the TANDEM cystine bridge with an azobenzene moiety leading to AzoTANDEM derivatives.

Peptide synthesis in solution using Fmoc/*tert*-Butyl strategy gives the depsipeptide Qxc-D-Ser-(H-Val)-Ala-^{t}Bu (**6**) which can be easily coupled to the photoisomerizable amino acid 3,3'-Diazenediyldi[(*S*)-*N*-(*tert*-butyloxycarbonyl)-*O*-methyltyrosine] (**7**).[2] The final double macrolactamization under pseudo high dilution conditions leads to the target compound *meta*-AzoTANDEM.

In order to investigate the photoswitchability, RP-HPLC measurments were carried out with irradiated and nonirradiated samples of *meta*-AzoTANDEM. In thermal equilibrium the *cis*-configuration of the bisintercalator explicitly overweighs the *trans*-configuration. The ratio is 21/79 percent (*trans/cis*). Irradiation at 300 nm for 30 min shifts this ratio to 9/91 percent (*trans/cis*) emphasizing the predominance of *cis*-configuration of the molecule in thermal equilibrium. The state can either be undone by irradiation with sunlight (ratio: 18/82 percent) or by irradiation at 420 nm which leads to the initial condition approximately (ratio: 24/76 percent).

In summary, the successful introduction of an azobenzene unit leads to a Triostin A analog whose configuration can be influenced by light. The rigidity of the depsipeptidic backbone and the substitution pattern in the azobenzene unit forces the molecule mostly into *cis*-configuration.

DNA binding abilities of *meta*-AzoTANDEM will be investigated in the future. Additionally, further Triostin A analogs will be synthesized and the photoswitchability will be tested by RP-HPLC- and NMR-analysis.

References

1. Addess KJ, Sinsheimer JS, Feigon J. *Biochemistry* **32**: 2498-2508, 1993.
2. Juodaityte J, Sewald N. *J Biotechnol* **112**: 127-138, 2004.

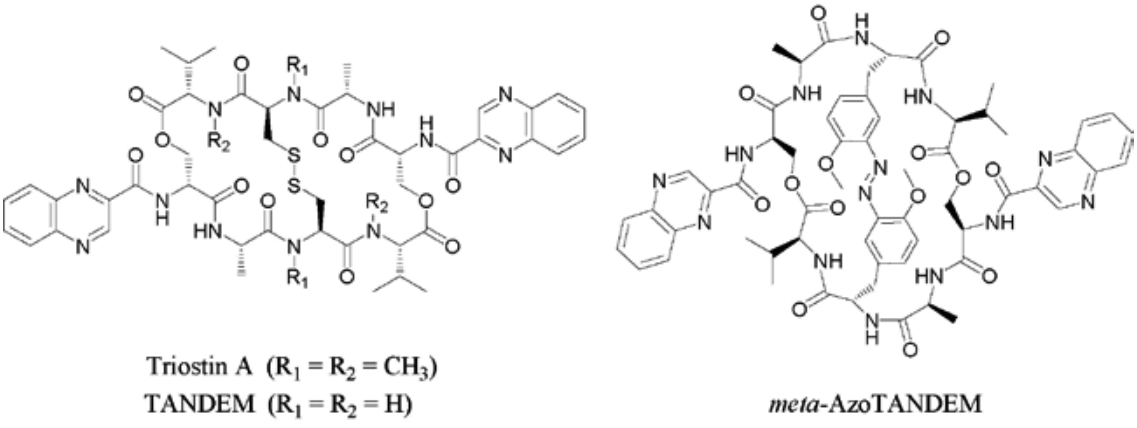

Figure 1. Chemical structures of Triostin A, TANDEM and *meta*-AzoTANDEM.

Scheme 1. Total synthesis of *meta*-AzoTANDEM

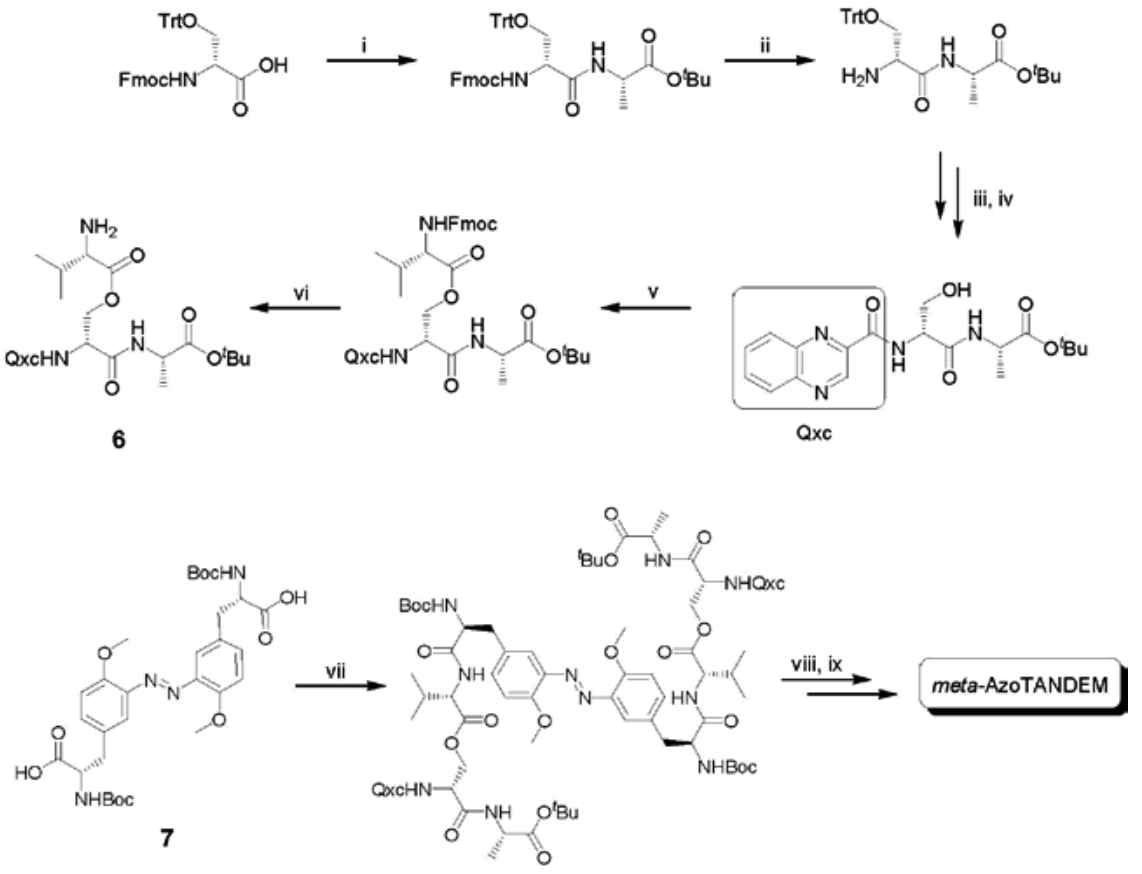

Reagents and conditions: (i) H-Ala-O^{t}Bu · HCl, HATU, HOAt, DIPEA, DMF; (ii) 20 % Diethylamine, DCM; (iii) QxcCl, Triethylamine, DCM; (iv) 2% TFA in DCM; (v) Fmoc-Val-OH, HATU, HOAt, DIPEA, DMF; (vi) 7% Piperazine in DCM; (vii) **6**, HATU, HOAt, DIPEA, DMF; (viii) 50% TFA in DCM; (ix) HATU, HOAt, DIPEA, DMF.

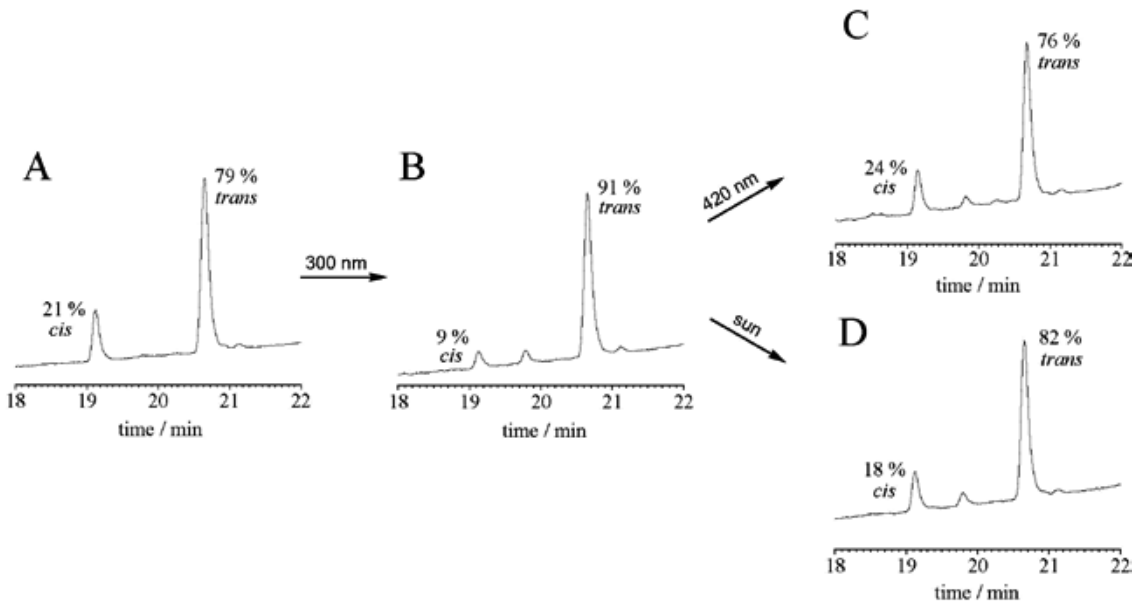

Figure 2. RP-HPLC analysis of *meta*-AzoTANDEM. Ratio of *trans/cis*-configuration in thermal eqilibrium (A), after irradiation at 300 nm (B), after irradiation at 420 nm (C), after irradiation with sunlight (D).

1-01-126

Design and synthesis of a non – peptide PAR-1 thrombin receptor antagonist, using cyclohexane as template

Androutsou, Maria-Eleni[1]; Agelis, George[1]; Magoulas, George[1]; Keppa, Pasxalina[1]; Saifeddine, Mahmound[2]; Hollenberg, Morley[2]; Matsoukas, John M[1,]*

[1]University of Patras, Department of Chemistry, GREECE; [2]University of Calgary, Department of Medicine, CANADA

[*]E-mail: imats@chemistry.upatras.gr

Introduction

Receptors that mediate thrombin action are attractive drug discovery targets because of their involvement in cardiovascular pathophysiology (dysregulation of platelet aggregation and endothelial cell function). The cellular actions of thrombin are, in large part, caused by the activation of Proteinase-Activated Receptors (PAR_s) 1, 3 and 4.[1] The serine proteinase thrombin cleaves and activates cellular PAR-1 in many pathophysiological settings associated with hemostasis, tissue injury and the proliferation of vascular smooth muscle and tumor cells. Thrombin cleaves the extracellular, N-terminal peptide chain of PAR-1 between Arg-41 and Ser-42 to expose a truncated N terminus bearing the peptide recognition motif SFLLRN.[2] Synthetic peptides containing this epitope have full PAR-1 agonist properties independent of thrombin activation. The limited stability of peptides often restricts their medical application. Therefore in the present study, we synthesized a novel non-peptide PAR-1 mimetic, based on a conformational analysis of the $S_{42}FLLR_{46}$ tethered ligand sequence of PAR-1 in order to inhibit the cellular actions of thrombin. The rational design, based on NMR constraints and Molecular Dymamics, led to compound 1 containing the spatially closed key pharmacophoric guanidyl and phenyl groups, attached to cyclohexane as a template. Compound **1**, inhibited both TFLLR-amide (10 μM) and thrombin (0.5 and 1 U/ml)-mediated calcium signaling in a cultured human HEK cell assay.[3]

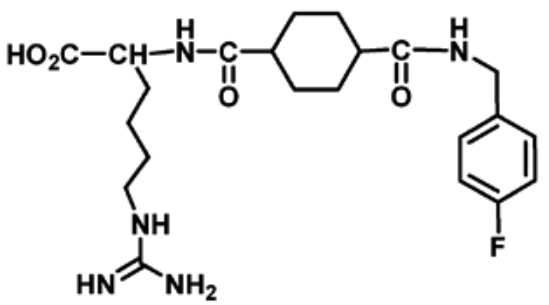

Figure 1. Chemical structure of compound **1**.

Results and Discussion

Structure activity studies (SAR_s) have shown that the peptides require at least the N-terminal pentapeptide with a free amino group at position 1, a certain aromatic residue such as phenylalanine at position 2 and a basic residue such as arginine at position 5 in order to express biological activity.[4] A resent study in our laboratory has shown that an adjacent of a fluoro group improves the biological activity by thrombin receptor-derived peptides .[5] The rational design based on NMR constrains and Molecular Dynamics, led to compound 1 containing the key pharmacophoric guanidyl and fluoro-phenyl groups attached to the cyclohexane template. The synthesis of Compound **1** was achieved using Fmoc strategy in solid phase synthesis and the purity was assessed by analytical HPLC and identified by ESI-MS, NMR. Biological evaluation showed that the synthesized compound 1 inhibited both TFLLR-amide (10 μM) and thrombin (0.5 and 1 U/ml)-mediated calcium signaling in a cultured human HEK cell assay (Fig. 2).

Acknowledgements

This research project is co-financed by E.U.-European Social Fund (75%) and the Greek Ministry of Development-GSRT (25%) with ancillary support from the Canadian Institutes of Health Research (CIHR: MH and MS).

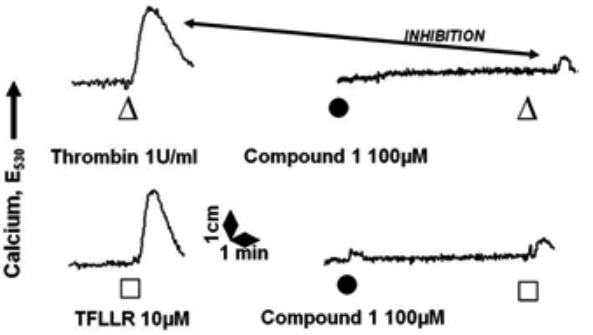

Figure 2. PAR-1 expressing HEK cells were exposed to either Thrombin (Δ) or the PAR-1 AP, TFLLR-NH_2 (□) without (left-hand tracings) or with (right-hand tracings) prior treatment of cells with Compound **1** (●). An upward deflection indicates an increase in intracellular calcium (Upward arrows: E530). A time scale is shown (1 min).

References

1. Hollenberg MD, Compton S. *J Pharm Rev* **54**: 203-217, 2002.
2. Ahn H-S, Chackalamannil S, Boykow G, Graziano M, Foster C. *Curr Pharm Design* **9**: 2349-2365, 2003.
3. Vergnolle N, Wallace J, Bunnett N, Hollenberg MD. *J Pharm Exp Ther* **288**: 358-370, 1999.
4. Matsoukas JM, Hollenberg M, Mavromoustakos T, Panagiotopoulos D, Alexopoulos K, Yamdagni R, Wu Q, Moore G. *J Prot Chem* **16**: 113-131, 1997.
5. Alexopoulos K, Fatsea P, Melissari E, Vlahakos D, Roumelioti P, Mavromoustakos T, Mihailescu S, Paredes-Carbajal CM, Mascher D, Matsoukas JM *J Med Chem* **47**: 3338-3352, 2004.

1-01-127

Stereoselective synthesis of (3S)- and (3R)-hydroxy-3-(2,6-dimethyl-4hydroxyphenyl) propanoic acid and its incorporation into a cyclic enkephalin analogue

Weltrowska,Grazyna
IRCM, Montreal,CANADA

Article withdrawn by editors


2008/2009 Catalog
Novabiochem®

1-01-128

Synthesis and Activity of Cyclic Analogues of PTH(1-11)

Caporale, Andrea[1,]; Zanta, Fabrizio[1]; Cabrele, Chiara[2]; Wittelsberger, Angela[3]; Peggion, Evaristo[1]*

[1]Univ. of Padova, Institute of Biomolecular Chemistry, CNR, via Marzolo 1, 35131 Padova., Dept. of Chemical Sciences, ITALY; [2]Univ. Regensburg, Universitaetstr. 31, 93053, Fakultaet fuer Chemie und Pharmazie, GERMANY; [3]Tufts Univ. School of Medicine, 136 Harrison Avenue, Boston, MA 02111, Dept. of Physiology, UNITED STATES

[*]E-mail: andrea.caporale@unipd.it

Introduction

Parathyroid hormone (PTH)[1] is an 84 amino acid hormone with a vital role in regulating the concentrations of ionized calcium and phosphate in the blood and extracellular fluids. It has been shown that the fragment PTH(1-34) is sufficient to bind and activate the PTH type I receptor (PTH1R). The molecular mechanisms of binding and activation have been extensively investigated, and it has been shown that the interaction of N-terminal fragments of PTH with PTH1R can increase in peptides as short as 11 amino acids by introducing certain constraints and by enhancing the α-helicity in the N-terminal portion of PTH(1-11).[1] The design of cyclic analogues represents a widely used strategy to increase peptide stability and potency. The structural constraint induced by a cycle reduces conformational flexibility and may enhance potency, selectivity, stability and bioavailability as well as membrane barrier permeability.[2] Besides backbone cyclization, also side-chain cyclization between positions that are not involved in receptor recognition can be exploited. Previous works based on D-AA-scan analysis have shown that analogues containing D-Gln at positions 6 and 10 adopted a better-defined α-helical structure.[3] Recently, Gardella and co-workers[4] reported that an analogue of PTH(1-11) cyclized between residues 6 and 10 exhibited almost the same activity of the linear analogues. In this work, two new analogues were synthesized by SPPS using side-chain cyclization either between Lys^6 and Glu^{10}(**I**) or between Ser^6 and Ser^{10}(**II**). Then, they were biologically tested and conformationally analyzed by CD and 2D-NMR.

Results and Discussion

Side-chain cyclization of **I** was accomplished on the solid support, following selective removal of the alloc and allyl protecting groups from Lys^6 and Glu^{10}, respectively.[5] For the synthesis of analogue **II** the Trt protecting groups of the Ser side chains were selectively cleaved, followed by esterification with ½ eq. adipic acid. In this synthesis, Ile^5 was introduced prior cyclization in order to avoid difficult acylation steps during the peptide-chain growth. The CD spectra revealed the presence of a well-defined helical structure, as indicated by the positive band at φ 190 nm and the negative ones at φ 208 and 222 nm. This secondary structure was also confirmed by 2D-NMR experiments, by which the chemical shift differences between the α-protons in the cyclic peptides and those for a random coil conformation[6] were obtained and compared to those reported for the linear analogue [Aib^1, Aib^3, Nle^8, Gln^{10}, Har^{11}]-PTH(1-11). All residues but the side-chain cyclized Ser^6 and Ser^{10} showed negative chemical shift differences, indicating a short helical segment in the sequence Val^2-Har^{11} (negative values ≥0.1 ppm) (Fig. 1).

Finally, both cyclic peptides were found to act as agonists, with analogue **II** being active in the low-nanomolar range. Our work shows that the combination of C$^{\alpha}$-tetra-substituted amino acids[7] with a bridge between positions 6 and 10 positively affects the α-helix structure of PTH(1-11) that maintains its ability to activate the receptor.

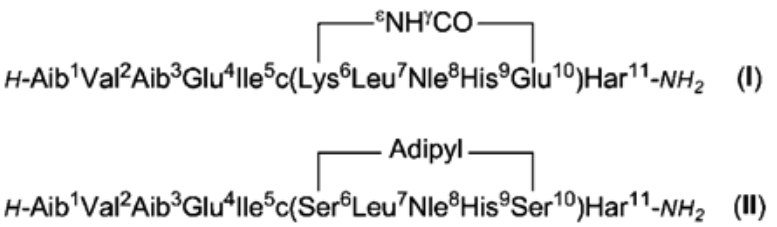

Figure 1.

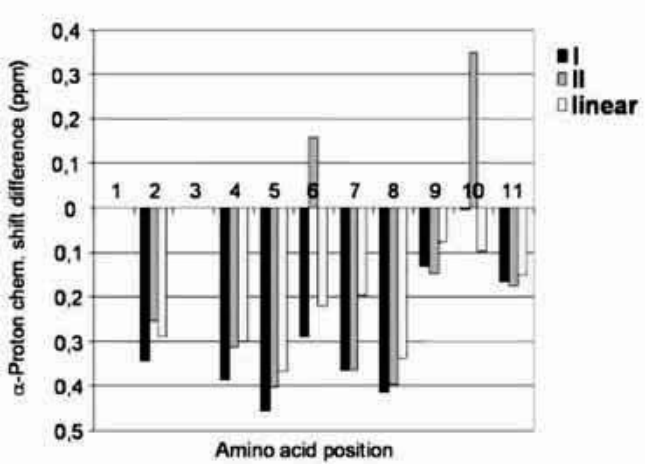

Figure 2. Chemical shift differences between the α-protons in the cyclic peptides **I** and **II** and those for a random coil conformation.[6] Comparison with differences reported for the linear analogue [Aib[1], Aib[3], Nle[8], Gln[10], Har[11]]-PTH(1-11). Regarding the positive bars at positions 6 and 10, it should be pointed out that they derive from the difference between the values of the *$^{\beta}$O*-acylated Ser residues in analogue **II** and the value attributed to an unmodified Ser residue in a random coil conformation.[6]

References

1. Chorev M. *Biopolymers (Peptide Science)* **80**: 67-84, 2005; Shimizu N, Guo J, Gardella TJ. *J Biol Chem* **276**: 49003-49012, 2001; Shimizu M, Carter PH, Khatri A, Potts JT Jr, Gardella T. *Endocrinol* **142**: 3068-3074, 2001.
2. Hruby VJ, Balse PM. *Curr Med Chem* **7**: 945-970, 2000.
3. Caporale A *et al*. *Proceedings 20th APS -Peptides for Youth- Montreal, Canada* 2007.
4. Shimizu N, Petroni BD, Khatri A, Gardella TJ. *Biochemistry* **42**: 2282-2290, 2003; Tsomaia N, Pellegrini M, Hyde K, Gardella TJ, Mierke DF. *Biochemistry* **43**: 690-699, 2004.
5. Grieco P, Gitu PM, Hruby VJ. *J Pept Res* **57**: 250-256, 2001.
6. Pastore A, Saudek V. *J Magn Reson* **90**: 165-176, 1990.
7. Barazza A, Wittelsberger A, Fiori N, Schievano E, Mammi S, Toniolo C, Alexander JM, Rosenblatt M, Peggion E, Chorev M. *J Pept Res* **65**: 23-35, 2005.

1-01-129

An Efficient Method for the Synthesis of C-terminal Amidated Enkephalins

Arabanian, Armin[1,]; Balalaie, Saeed[1]; Mohammadnejad, Mahdieh[1]; Gross, Jürgen H[2]*
[1]K.N.Toosi University of Technology, P.O.Box: 15875-4416, Tehran, Peptide Chemistry Research Group, IRAN (ISLAMIC REP.); [2]Universität Heidelberg, Im Neuenheimer Feld 270, 69120, Heidelberg, Organisch-Chemisches Institut, GERMANY

[*]E-mail: arabanian@dena.kntu.ac.ir

Following discovering enkephalins in 1975 (Hughes), it is now well established that enkephalins play several important roles in CNS in addition to their role in the process of analgesia. Composition based findings showed that endorphine which is a 31 amino acid peptide having the Met-enkephalin sequence at its C-terminus produces a powerful analgesia 100 times more potent that morphine.[1] It was shown that derivatization of the terminal carboxy function of Met-enkephalin to get alkylamides could be expected to lead to derivatives that would not only be resistant to the attack of carboxypeptidases, but would also posses higher binding affinity for the opioid receptors due to enhanced hydrophobicity at the C-terminus. It could also affect the lipophilicity of the peptides, and could affect the interaction with the opiate receptors and cause the more activity of enkephalin derivatives. Meanwhile, lengthening and shortening of the alkyl chain were found to have an adverse effect on the antinociceptive activity of the peptide.[2]

The presence of C-terminus α-amido group on the peptide chain is essential for the biological activity of many peptide hormones. Amidated peptides are usually prepared by solid-phase synthesis on benzhydrylamine resins or by the aminolysis of C-terminal peptide esters, which can be prepared by conventional peptide synthesis. Recombinant DNA technology allows the production of longer peptides by fermentation, but these products lack the C-terminal amido group. There are different methods for the synthesis of amidated C-terminal peptides, such as a) enzymatic amidation,[3] b) the combination of rDNA technology with chemical modification of C-terminus c) using of amide resins in SPPS d) using of carboxypeptidase in the presence of ammonia e) conversion of C-terminus peptides to methylester derivatives and addition of ammonia at low temperature.[4-6] All of the reported methods have some merits such as laborious reaction conditions, high price of enzymes and limitation of solubility parameters, using of ammonia or alkylamines in gas forms, and use of HF for the cleavage of peptide from the surface of amide resin. Both separation and purification of enzymes need lot of time and energy. Herein, we wish to report an efficient route for the amidation, alkylamidation and semicarbazidation of the C-terminus Met- and Leu-enkephalins using ammonium chloride, alkylammonium hydrochloride and semicarbazide hydrochloride (Scheme 1).

The shown tetrapeptide-resins **2** in Scheme 1 were synthesized manually using the standard solid phase peptide synthesis via Fmoc strategy. First of all, Fmoc-leu-OH or Fmoc-Met-OH were loaded on the surface of 2-chlorotrityl chloride resin **1** and Fmoc-protected amino acids were coupled according to known methods. The tetrapeptide-resins **2** could react with Boc-Tyr(tBu)-OH to afford the pentapeptide-resins **3**. Cleavage of the desired peptides from the surface of the resin and reaction with ammonium chloride, ethyl ammonium chloride and seimcarbazide hydrochloride led to amidated form of C-terminus enkephalins. For full deprotection of the pentapeptides, a mixture of TFA:TES:H_2O (94:5:1) was used. This novel strategy is the combination of solid and solution phase peptide synthesis and it has some advantages compared to the previously reported methods such as, mild reaction condition, cost effectiveness, and reducing of the reaction steps. All products were characterized using NMR and MALDI mass spectrometry. In conclusion, we have demonstrated a novel strategy via combination of solid and solution phase peptide synthesis using Fmoc and Boc strategy that

Scheme 1. Synthesis of C-terminal amidated enkephalins

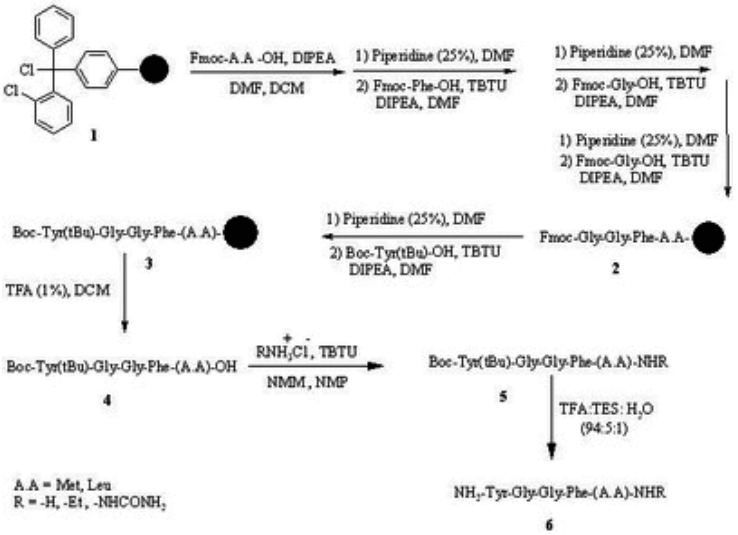

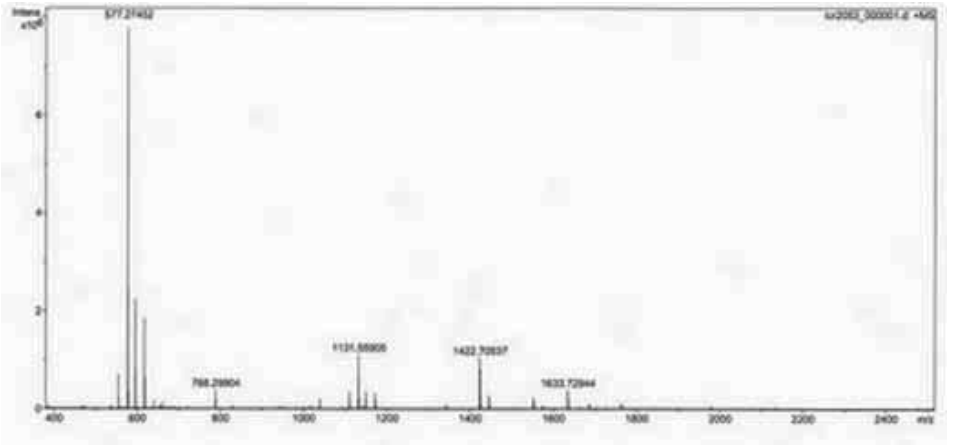

Figure 1. MALDI-MS spectrum of Leu-Enk-NH_2.

leads to the formation of C-terminus amidated Met- and Leu-enkephalin derivatives.

Acknowledgements

We thank National Research Institute for Science Policy (NRISP, Iran) for financial support. We also thank Tofigh Daru Research & Engineering Co. for kind cooperation. A part of this research work was supported by research council of K. N. Toosi University of Technology is gratefully acknowledged.

References

1. Gutstein, H B & Akil, H. In Goodman & Gilman's *The Pharmacological Basis of Therapeutics* Eds Brunton LL, Lazo JS, Parker KL (eds). McGraw-Hill Companies, New York, 548-550, 2006.
2. Martinez A, Farr A, Vos MD, Cuttitta F, Treston AM. Peptide-amidating enzymes are expressed in the stellate epithelial cells of the thymic medulla. *J Histochem Cytochem* **46:** 661-668, 1998.
3. Cerovský V, Kula M-R. C-terminal peptide amidation catalyzed by orange flavedo peptide amidase. *Angew Chem Int Ed* **37:** 1885-1887, 1998.
4. Bui CT, Bray AM, Nguyen T, Ercole F, Maeji NJ. Solid phase synthesis of C-terminal peptide amides: development of a new aminoethyl-polystyrene linker on the Multipin ™ solid support. *J Pept Sci* **6:** 243-250, 2000.
5. Stathopolos P, Papas S, Tsikaris V. C-terminal N-alkylated peptide amides resulting from the linker decomposition of the Rink amide resin. A new cleavage mixture prevents their formation. *J Pept Sci* **12:** 227-232, 2006.
6. Matsuo H, Mizuno K, Kojima M. C-terminal α-amidation enzyme and process for production thereof. *US Patent* **5,360,727**, 1994.

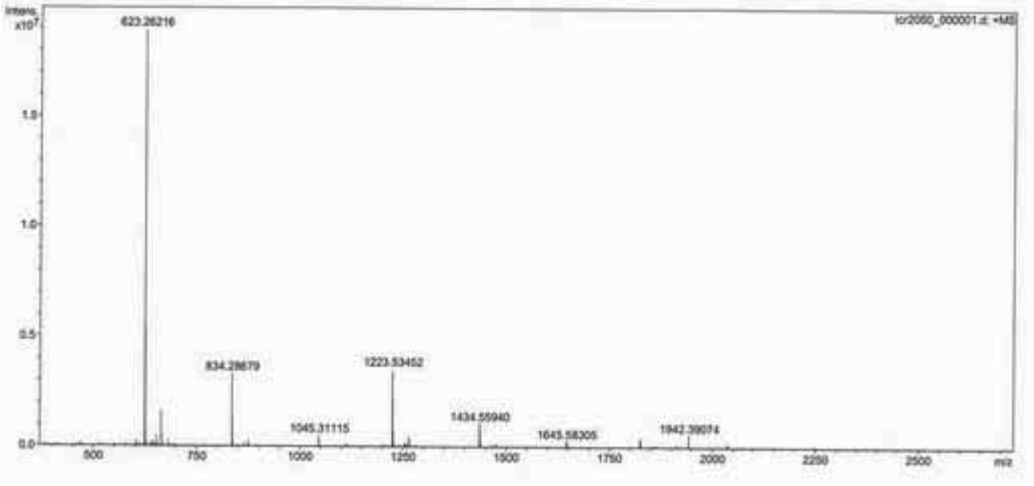

Figure 2. MALDI-MS spectrum of Met-Enk-NHC_2H_5.

1-01-130

Synthesis of Novel Gn-RH Analogues Using Ugi-4MCR

Balalaie, Saeed[1,]; Arabanian, Armin[1]; Mohammadnejad, Mahdieh[1]; Gross, Jürgen H[2]*

[1]K.N. Toosi University of Technology, P.O.Box: 15875-4416, Tehran, Peptide Chemistry Research Group, IRAN (ISLAMIC REP); [2]Universität Heidelberg, Im Neuenheimer Feld 270, 69120, Heidelberg, Organische-Chemisches Institut, GERMANY

[*]E-mail: balalaie@kntu.ac.ir

Gonadotropin-releasing hormone (Gn-RH) is secreted from the hypothalamus and its action on the pituitary gland then leads to the release of luteinizing hormone (LH) and follicle-stimulating hormone (FSH). Both of these hormones then act on the ovaries and are responsible for the pro-fertility effects of Gn-RH, primarily through the release of steroidal hormones. Gn-RH was first isolated from porcine hypothalamus and was shown to be a decapeptide I. Similar peptides have been isolated and sequenced from other species such as chicken, salmon and lamprey.[1]

The bulky hydrophobic amino acid residues in position 6 appear to be very important for the high potency of the analogues. In this way, substitution and addition of hydrophobicity at position 6 in Gn-RH analogues is an interesting subject. It was shown that the substitution could affect the biological activities of synthetic peptides. Results from a number of ongoing studies on prostate cancer patients using Goserelin, Buserelin, Tryptorelin and Leuprolide are recently been published. Synthesis of novel Gn-RH has attracted particular interest.[2] MCRs applications in all areas of applied chemistry are very popular because, they offer a wealth of products, while requiring only a minimum of effort. MCRs are applying for the synthesis of complex molecules in one –pot reactions with high bond-forming efficiency (BFE). Meanwhile, a wide variation among these starting materials opens up versatile opportunities for the synthesis of compound libraries. Among many types of MCRs, the most useful are isocyanide based MCRs (IMCRs).[3,4]

Herein, we present an efficient method for the synthesis of novel Gn-RH analogues using Ugi four-component reaction from C-terminus heptapeptide, N-terminus tripeptide, aromatic aldehydes and isocyanides (Scheme 1).

This research concerned the design and synthesis of C-terminus heptapeptide and N-terminus tripeptide as starting materials. The C-terminus heptapeptide 2 was synthesized using solid phase peptide synthesis strategy. 2-Chlorotrityl chloride and Fmoc-amino acids were used in this strategy. Meanwhile, TBTU was used as the coupling reagent for the synthesis of C-terminus

Scheme 1. Synthesis of Novel Gn-RH Analogues Using Ugi-4MCR

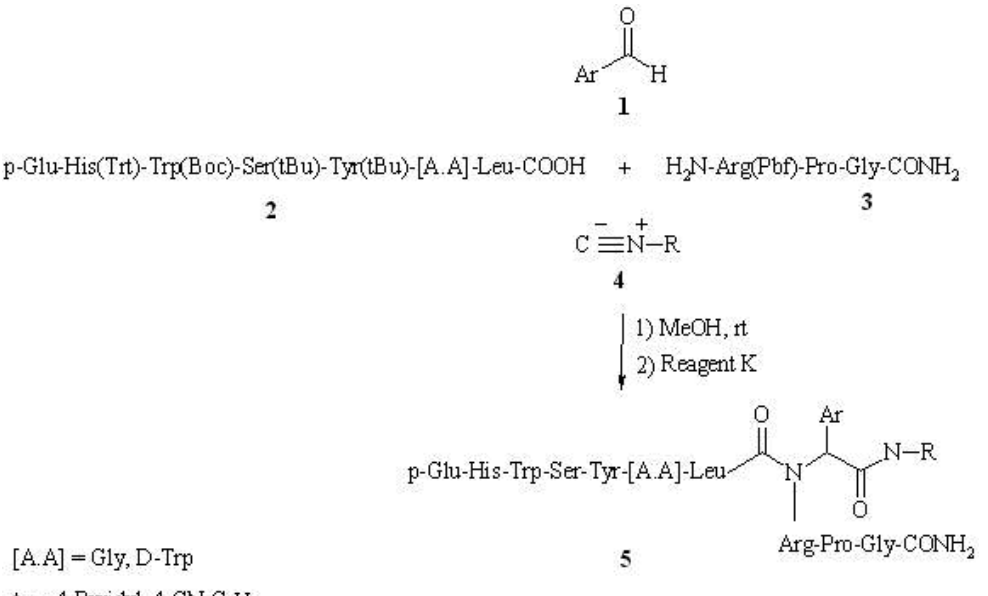

Scheme 2. Mechanism of the imine formation and Mumm rearrengment in Ugi-4MCR

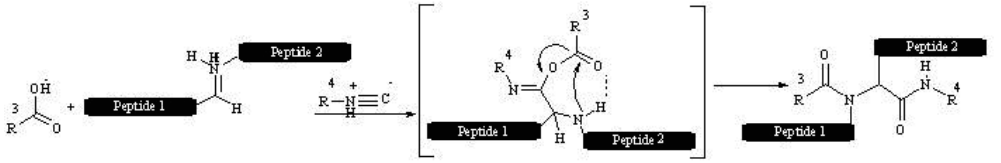

heptapeptide and N-terminus tripeptide. The tripeptide 3 was synthesized in solution phase and with Boc/Z strategy.[5] The generally accepted mechanism of the Ugi four-component coupling (4CC) reaction involves four elementary steps, the last of which is irreversible. In the first step, the aldehyde condenses with an amine group of N-terminus tripeptide to form an imine that could be converted and produce iminium salt in the presence of C-terminus heptapeptide. Next, the isocyanide is added to the iminium salt to produce a nitrilium ion. Then, a reactive *O*-acyl iminolate is formed via the α-addition of carboxylate anion to the nitrilium ion. The final step involves the *O*- to *N*-acyl transfer (Mumm rearrangement) to afford the novel Gn-RH analogues (Scheme 2).

Using Ugi-4CC created a new stereocenter in the products but, in our approach the ratio of one diasteromer is more. Two different heptapeptides were used for the synthesis of Gn-RH analogues. In case 5a, there was Gly at the position 6 in Gonadorelin analogues sequence and d-Trp in triptorelin analogues 5b. Investigation of anti-cancer activity of one of the triptorelin analogues shows better anti-cancer activity of this compound in comparison to triptorelin. The research for finding other biological activities of these new analogues is underway. The products were purified using preparative HPLC and their structures were confirmed using MALDI and ESI Mass spectrometry and also amino acid analysis data.

pGlu-His-Trp-Ser-Tyr-Gly-Leu-Arg-Pro-Gly-NH_2

(I)

Figure 1. MALDI-MS Spectrum result.

In conclusion, we introduced novel synthetic Gn-RH analogues via Ugi four-component reaction of C-terminus heptapeptide, N-terminus tripeptide, aromatic aldehydes, and isocyanides at room temperature. In this research, triptorelin and gonadorelin analogues were synthesized with good yields.

Acknowledgements

We thank National Research Institute for Science Policy (NRISP, Iran) for financial support. We also thank Tofigh Daru Research & Engineering Co. for kind cooperation. A part of this research work was supported by research council of K. N. Toosi University of Technology which is gratefully acknowledged.

References

1. Millar RP, Lu Z-L, Pawson, AJ, Flanagan CA, Morgan K, Maudsley SR. Gonadotropin-releasing hormone receptors. *Endocrine Rev* **25:** 235-275, 2004.
2. Padula AM. Gn-RH analogous – agonists and antagonist. *Animal Reproduction Sci* **50:** 115-126, 2005.
3. Dömling A. Recent development isocyanide based multicomponent reactions in applied chemistry. *Chem Rev* **106:** 17-89, 2006.
4. Hebach C, Kazmaier U. Via Ugi reactions to conformationally fixed cyclic peptides. *Chem Commun* **5:** 596-597, 2003.
5. Han S, Kim Y. Recent development of peptide coupling reagents in organic synthesis. *Tetrahedron* **60:** 2447-2467, 2004.

1-01-131

Resin Comparison and Fast Conventional Synthesis of Human SDF-1α on the *Symphony*®, *Tribute*™ and *Prelude*™

Patel, Hirendra; Chantell, Christina; Fuentes, German; Menakuru, Mahendra

[*]*Protein Technologies, Inc., UNITED STATES*

[*]*E-mail: info@peptideinstruments.com*

Introduction

Stromal cell-derived factor 1α (SDF-1α) or CXC chemokine ligand 12α (CXCL12α) is a member of the chemokine family of peptides, which is involved in basal leukocyte trafficking and homing, as well as in development.[1]

To the best of our knowledge, there are no publications on the step-wise conventional Fmoc solid phase peptide synthesis of SDF-1α. However, there is one article on the general synthesis of chemokines that includes SDF-1α.[2] In 1997, Ueda *et al.* also reported the synthesis of a SDF-1α analogue by chemical ligation.[3] The fragments of this analogue were synthesized using an *in situ* neutralization Boc chemistry protocol.

Results and discussion

In 2008, we reported that HCTU is a very reactive and relatively inexpensive coupling reagent which can be used as a substitute for the more expensive coupling reagent HATU. We used HCTU to perform fast Fmoc peptide synthesis with coupling times of 5 minutes or less.[4] In this paper, we synthesized SDF-1α using HCTU on Fmoc-Lys(Boc)-Wang-PS-LL resin (0.26 mmol/g) in 101 hours. (Fig. 1a & Table 1). The crude peptide was then purified and its mass was confirmed with MALDI-TOF (Calculated: 7963.5 m/z, Observed: 7959.9 *m/z*) (Fig. 2). Based on our previous work,[4-6] we reduced the total synthesis time to 22 hours and produced comparable results by HPLC analysis (Fig. 1a & 1b).

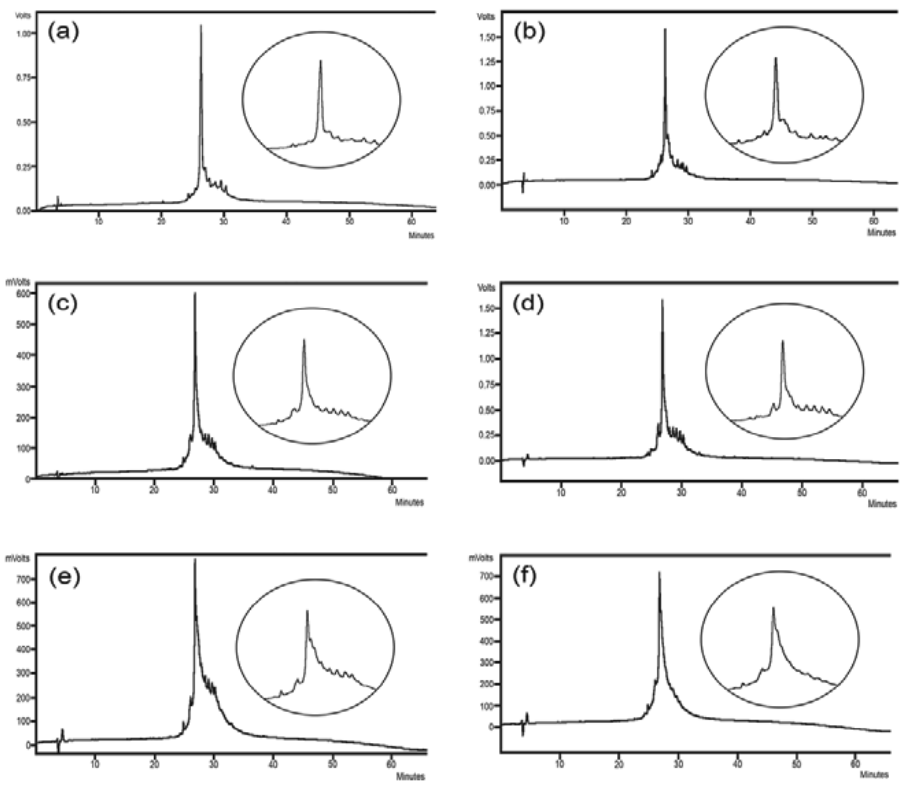

Figure 1. HPLC's of crude SDF-1α synthesized on Wang-PS resin (0.26 mmol/g) for (a) 101 hours, (b) 22 hours, (c) with DBU added to the deprotection mixture, (d) on HMPB-ChemMatrix resin (0.68 mmol/g), (e) on Wang-PS resin (0.55 mmol/g), and on (f) CLEAR resin (0.45 mmol/g). Blow-up of main peak shown in circles.

Table 1. *Summary of resin and synthesis comparison of SDF-1α*

Solid Support	Linker	Substitution (mmol/g)	Deprotecting Reagent	Deprotection Time	Coupling Time	Washes
PS	Wang	0.26	20% Pip	3 min & 17 min	2 x 30 min	3 DMF 3 DCM
PS	Wang	0.26	20% Pip	2 x 2 min	2 x 2.5 min	1 DMF 1 DCM
PS	Wang	0.26	2% DBU 20% Pip	2 x 2 min	2 x 2.5 min	1 DMF 1 DCM
ChemMatrix	HMPB	0.68	20% Pip	2 x 2 min	2 x 2.5 min	1 DMF 1 DCM
PS	Wang	0.55	20% Pip	2 x 2 min	2 x 2.5 min	1 DMF 1 DCM
CLEAR	HMPA	0.45	20% Pip	2 x 2 min	2 x 2.5 min	1 DMF 1 DCM

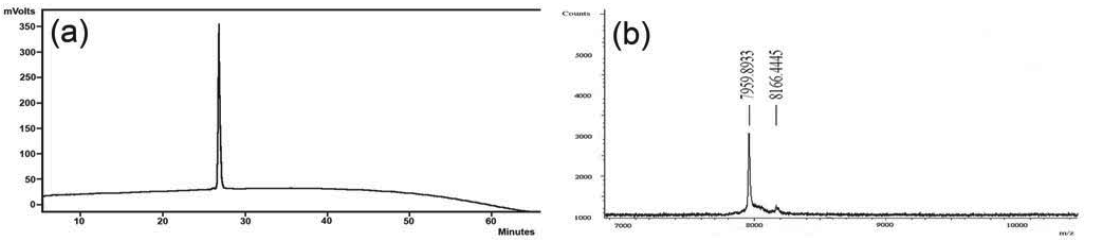

Figure 2. (a) HPLC and (b) mass spectrum of purified SDF-1α.

The effect of different bases in the deprotection mixture and different resin materials and loadings was tested for the 22 hour synthesis. 2% DBU (a more efficient base) added to the deprotection mixture did not improve the result (Fig. 1b & 1c). HMPB-ChemMatrix resin (Fig. 1d) produced a higher purity peptide than Wang-PS resin with a loading of 0.55 mmol/g (Fig. 1e) but was less pure than the lower loaded 0.26 mmol/g Wang-PS resin (Fig. 1b). This shows that at comparable loadings, ChemMatrix produces a higher purity crude peptide than polystyrene. However, resin loading seems to be more influential than the resin material, for at a loading of 0.26 mmol/g, polystyrene produces a higher purity crude peptide than the higher loaded ChemMatrix resin. This is similar to our previous findings.[4-5] CLEAR resin did not show an improvement over the Wang-PS-LL resin (Fig. 1f). As it was made of a different material and had a higher loading, it is difficult to say whether one or both variables were responsible for the result.

Methods

Fmoc solid phase peptide synthesis. Peptides were synthesized on a Protein Technologies, Inc. ***Symphony***®, ***Prelude***™ or ***Tribute***™ peptide synthesizer at the 20 µmol scale (25 µmol for the ***Symphony***®) using a 10 fold excess of Fmoc-amino acid (200 mM) relative to the resin. Resins were purchased from Novabiochem, Peptides International, or Matrix Innovation. Deprotection was performed using 20% piperidine/DMF or 2% DBU/20% piperidine in DMF. Coupling was performed using 1:1:2 amino acid/HCTU/NMM in DMF. Fmoc-amino acid, HCTU, 400 mM NMM in DMF and 20% piperidine were supplied by Protein Technologies, Inc. DBU was purchased from Sigma-Aldrich. Cleavage was carried out using 95/2/2/1 TFA/water/anisole/EDT for 2 hours.

Analysis. Crude peptides were precipitated using ice-cold ether and dissolved in HPLC grade water. Peptides were then analyzed on a Varian microsorb-MW 300 angstrom, 5 µm, C18 column, 250 x 4.6 mm over 60 minutes using a gradient of 5-95% aqueous MeCN with 0.1 % TFA at 1 mL/min. Detection was at 214 nm. The peptide masses were confirmed by MALDI-TOF mass spectrometry at the University of Arizona mass spectrometry facility.

References

1. Kunkel SL, Godessart N. *Autoimmunity Rev* **1:** 313-320, 2002.
2. Cotton G, Geffroy D. *Speciality Chemicals Magazine* **26:** 38-39, 2006.
3. Ueda H, Siani MA, Gong W, Thompson DA, Brown GG, Wang JM. *J Biol Chem* **272:** 24966-24970, 1997.
4. Hood C, Fuentes G, Patel H, Page K, Menakuru M, Park JH. *J Pept Sci* **14:** 97-101, 2008.
5. Fuentes G, Hood C, Patel H, Page K, Menakuru M, Park JH. *Proceedings of the 10th Chinese Peptide Symposium*, 2008.
6. Page K, Hood CA, Patel H, Fuentes G, Menakuru M. *J Pept Sci* **13:** 833-838, 2007.

1-01-132

Isopeptide method: an efficient preparation of difficult peptides on solid support

*Yoshiya, Taku; Taniguchi, Atsuhiko; Abe, Naoko; Ito, Nui; Sohma, Youhei; Skwarczynski, Mariusz; Kimura, Tooru; Hayashi, Yoshio; Kiso, Yoshiaki**

Kyoto Pharmaceutical University, Department of medicinal chemistry, JAPAN

**E-mail: ky02412@poppy.kyoto-phu.ac.jp*

Introduction

The synthesis of difficult sequence-containing peptides is one of the most problematic areas in peptide chemistry, and these peptides often have low solid-phase synthetic yield and purity due to their hydrophobic and aggregative properties. In 2003, we discovered that the presence of an *O*-acyl instead of *N*-acyl hydroxyamino acid residue within the peptide backbone significantly changed the secondary structure of the native peptide, and thereby decreased the unfavorable nature derived from difficult sequences.[1] This *O*-acyl isopeptide subsequently afforded the corresponding target peptide via an *O-N* intramolecular acyl migration reaction. These findings led to the development of an *O*-acyl isopeptide method.[2] The method has been successfully applied to efficiently synthesize difficult sequence-containing peptides. Several other research groups such as Mutter *et al.*, Carpino *et al.*, Borner *et al.*, Otaka *et al.*, and Martinez *et al.* have used similar principles, and thus suggesting that the method is widely advantageous for peptide preparation. Recently, we designed and prepared *O*-acyl isodipeptide units from a two-step solution phase synthesis, as a mean to avoid epimerization-induced esterification on the resin in the subsequent synthesis of *O*-acyl isopeptide.[3,4] Using the units, fully automated protocols can take advantage of the routine amide bond formation in SPPS of *O*-acyl isopeptides. Other research groups have also synthesized *O*-acyl isopeptides from corresponding units using fully automated protocols.[5,6]

Results and discussion

In the current study, toward routine preparation of amyloid *β* peptide 1-42 (A*β*1-42, **1**), we synthesized A*β*1-42 isopeptide (26-*O*-acyl isoA*β*1-42) employing ABI 431A Peptide Synthesizer with fully automated protocols using Boc-Ser(Fmoc-Gly)-OH (**2**), in which a native Gly^{25}-Ser^{26} bond was modified to a *β*-ester bond in the *O*-acyl isopeptide structure. During the synthesis, after Fmoc deprotection, the peptide-resin was coupled with the corresponding HOBt ester of an Fmoc amino acid or the unit, which was "preactivated" with DCC and HOBt in NMP, to obtain peptide-resin. Interestingly, in HPLC and MS analysis of the crude peptide (Fig. 1a), production of des-(Ser^{26})-[$Met(O)^{35}$]-A*β*1-42 (**9**) was observed instead of desired [$Met(O)^{35}$]-26-O-acyl isoA*β*1-42 (**7**) after a final TFA treatment. Herein, we report the elucidation and suppression of this side reaction by solvent effects.

Analytical HPLC was performed using a C18 reverse phase column (4.6 ~ 150 mm; YMC Pack ODS AM302) with binary solvent system: a linear gradient of CH_3CN (0-100% CH_3CN, 40 min) in 0.1% aq TFA at a flow rate of 0.9 mL min^{-1} (40 ˚C), detected at 230 nm.

We focused on the effect of solvent on SPPS during a coupling reaction of Boc-Ser(Fmoc-Gly)-OH (**2**) with protected [$Met(O)^{35}$]-A*β*27-42-resin (**4**). Unit **2** (2.5 eq) was coupled to **4** with DIPCDI (2.5 eq) and HOBt (2.5 eq) in either DMF or CH_2Cl_2. Each peptide-resin was treated with a TFA cocktail and the obtained crude

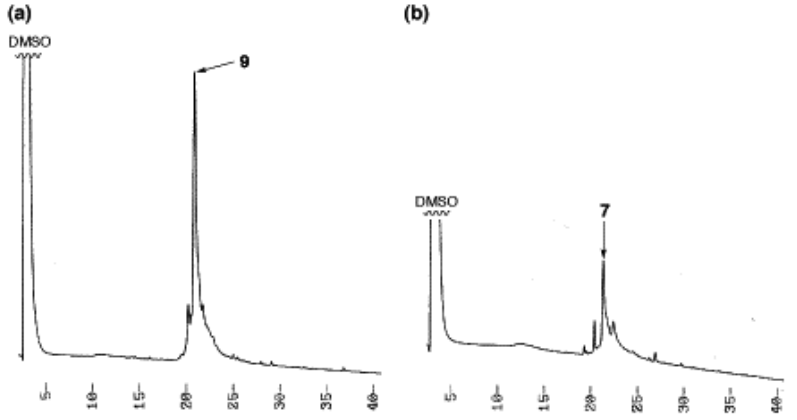

Figure 1. HPLC profiles of the crude peptide after TFA treatment in the synthesis of Aβ1-42 isopeptide 7 using O-acyl isodipeptide unit 2 with (a) fully automated protocols, in which 2 was coupled using the DCC-HOBt method in NMP, and (b) manual protocols, in which 2 was coupled using the DIPCDI-HOBt method in CH_2Cl_2.

Scheme 1. *Reagents/conditions:* (i) 20% piperidine/DMF, 20 min; (ii) Fmoc-AA-OH (2.5 eq), DIPCDI (2.5 eq), HOBt (2.5 eq), DMF, 2 h; (iii) Boc-Ser(Fmoc-Gly)-OH (**2**, 2.5 eq), DIPCDI (2.5 eq), HOBt (2.5 eq), DMF or CH_2Cl_2, 2 h; (iv) TFA-*m*-cresol-thioanisole-H_2O (92.5:2.5:2.5:2.5), 90 min; (v) NH_4I (40 eq), dimethylsulfide (40 eq), TFA:H_2O (2:1), 0 ˚C, 60 min; (vi) pH 7.4 phosphate buffered saline, overnight

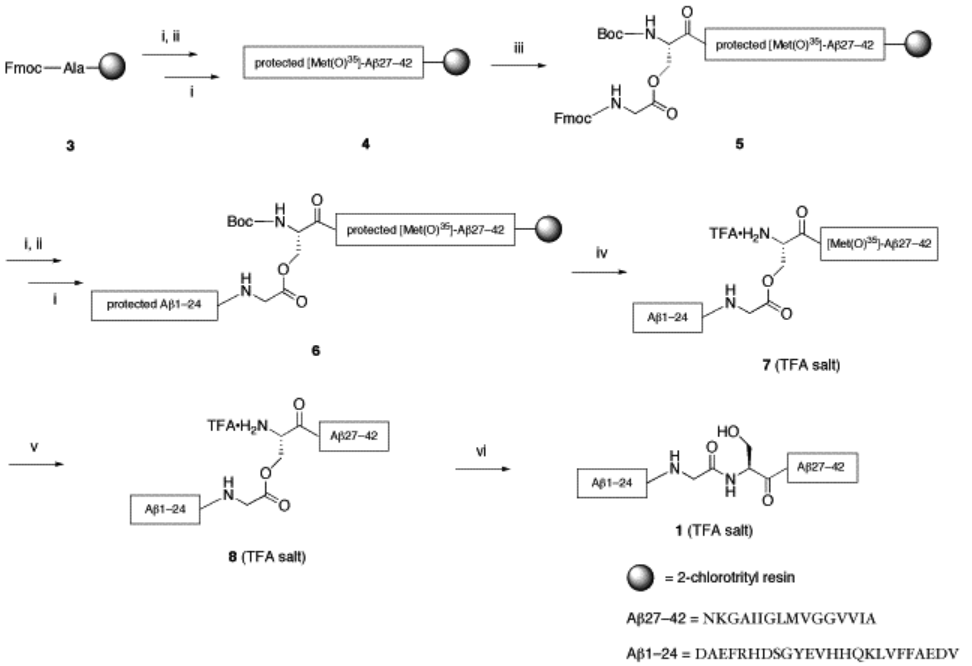

peptide was analyzed by HPLC. HPLC yield of desired 25-*N*-Fmoc-[Met(O)^{35}]-26-*O*-acyl isoAβ25-42 in the crude peptide prepared using CH_2Cl_2 was remarkably higher than that of the DMF conditions. Additionally, in MS analysis, undesired 25-*N*-Fmoc-des-(Ser^{26})-[Met(O)^{35}]-Aβ25-42 was not detected when CH_2Cl_2 was used. These results suggested that less polar CH_2Cl_2 was superior to DMF from the viewpoint of suppression of the side reaction. Based on these results, we synthesized Aβ1-42 isopeptide by the *O*-acyl isopeptide method using unit **2** and manual protocols (Scheme 1). In HPLC or MS analysis of the crude peptide, desired [Met(O)^{35}]-26-*O*-acyl isoAβ1-42 (**7**) was mainly observed and undesired des-(Ser26)-[Met(O)^{35}]-Aβ1-42 (**9**) was not detected (Fig. 1b). Thus, in the synthesis using unit **2** which was coupled in CH_2Cl_2, **7** was obtained more efficiently than in DMF. Finally, Aβ1-42 isopeptide **1** was prepared from **7** as reported.[7]

In summary, a side reaction, which resulted in the deletion of Ser^{26} in the *O*-acyl isopeptide structure, was observed during the synthesis of Aβ1-42 isopeptide using *O*-acyl isodipeptide unit. We optimized the coupling conditions to suppress the side reaction. Non-polar solvent CH_2Cl_2 was superior to DMF in suppressing the side reaction.[8] Based on this result, using CH_2Cl_2 as solvent for the coupling of the unit, we synthesized Aβ1-42 isopeptide with nearly no side reaction associated with the Ser^{26} deletion. By choice of solvent, *O*-acyl isopeptide would be efficiently synthesized using fully automated protocols. With the expansion of the use of the *O*-acyl isodipeptide units, *O*-acyl isopeptide method can be applied to wide ranges of peptide chemistry.

Acknowledgements

This research was supported in part by the Academic Frontier Project for Private Universities: matching fund subsidy from MEXT (Ministry of Education, Culture, Sports, Science and Technology) of the Japanese Government, and the 21st Century COE Program from MEXT. T. Y., A. T., and Y. S. are grateful for Research Fellowships of JSPS for Young Scientists.

References

1. Sohma Y *et al. Peptides, Peptide Revolution: Genomics, Proteomics and Therapeutics*, Kluwer Academic, The Netherlands, 2003, pp 67-68.
2. Sohma Y *et al. J Pept Sci* **12:** 823-838, 2006.
3. Sohma Y *et al. Tetrahedron Lett* **47:** 3013-3017, 2006.
4. Yoshiya T *et al. Org Biomol Chem* **5:** 1720-1730, 2007.
5. Santos SD *et al. J Am Chem Soc* **127:** 11888-11889, 2005.
6. Coin I *et al. J Org Chem* **71:** 6171-6177, 2006.
7. Sohma Y *et al. J Pept Sci* **11:** 441-451, 2005.
8. Taniguchi A *et al. J Pept Sci* **13:** 868-874, 2007.

1-01-133

The application of *N*-(4,6-dimethoxy-1,3,5-triazin-2-yl)strychninium tetrafluoroborate in SPPS as traceless enantioselective coupling reagents

Kamiński, Zbigniew J[*]*; Kolesińska, Beata*

Technical University of Lodz, Institute of Organic Chemistry, POLAND

[*]*E-mail: zbigniew.kaminski@p.lodz.pl*

Introduction

The demand for a diversity of structural features of non-proteinogenic amino acids, widely used as new building blocks, is severely restricted by the laborious procedures leading to enantiomerically homogeneous products. Typical sources, such as isolation from natural products, biotechnological methodology, or even asymmetric synthesis, although recently developed, are of limited value because of their complex or tedious synthetic procedures or restricted access to the pool of chiral auxiliaries.

Results and Discussion

Recently, we attempted to resolve this problem by designing and preparing tetrafluoroborates of chiral *N*-triazinylammonium salts which were found to be stable and highly efficient enantioselective coupling reagents useful in enantioselective (ee up to 98%) peptide synthesis from racemic amino acids in solution.[1] According to the concept, the structure of an enantioselective coupling reagent was modular and consisted of a classic achiral triazine based reagent and a chiral auxiliary. Due to the departure of the chiral auxiliary after activation, all further stages of the coupling procedure in solution were free of the disturbances caused by the presence of the stereogenic center of the chiral auxiliary (traceless). Thus, the configuration and enantiomeric purity established during the activation stage, remained essentially intact in all the syntheses involving this carboxylic component and reagent. This assured the predictability of configuration and enantiomeric enrichment for all the syntheses involving a given set of components based on a single model experiment. Moreover, after the departure of a chiral auxiliary at the activation stage, the structure, properties, and reactivity of the activated carboxylic component remained exactly the same as those obtained in a reaction involving a classic achiral reagent **2,**[2] which has opened the possibility for the routine application of traceless reagents, avoiding additional studies on the scope and limitation of the coupling procedure.

In order to verify the synthetic usefulness of traceless enantioselective coupling reagents, *N*-(4,6-dimethoxy-1,3,5-triazin-2-yl)strychninium tetrafluoroborate (**1**) was prepared and used in solid phase peptide synthesis.

Table 1. Racemization during SPPS on Val-Wang resin using *N*-(4,6-dimethoxy-1,3,5-triazin-2-yl)-strychninium tetrafluoroborate (**1**) as a coupling reagent and enantiomerically homogeneous substrates

C-component	Amine	C-component: L/D [%]	N-component: L/D [%]
Fmoc-L-Ala-OH	DIPEA	100/0	100/0
Fmic-L-Ala-OH	strychnine	100/0	100/0
Fmoc-L-Phe-OH	DIPEA	99.8/0.2	100/0
Fmoc-L-Phe-OH	strychnine	100/0	100/0
Fmoc-L-Ser(tBu)-OH	DIPEA	99.7/0.3	100/0
Fmoc-L-Ser(tBu)-OH	strychnine	99.8/0.2	100/0
Fmoc-L-His(Trt)-OH	DIPEA	99.5/0.5	100/0
Fmoc-L-His(Trt)-OH	strychnine	99.6/0.4	100/0

Experiments with enantiomerically homogeneous C-components have confirmed negligible racemization accompanying coupling mediated by *N*-(4,6-dimethoxy-1,3,5-triazin-2-yl)strychninium tetrafluoroborate under standard SPPS conditions (Table 1).

Scheme 1. After departure of chiral auxiliary in activation stage, the structure, properties activated carboxylic component remained exactly the same as those obtained in a reaction involving achiral reagent

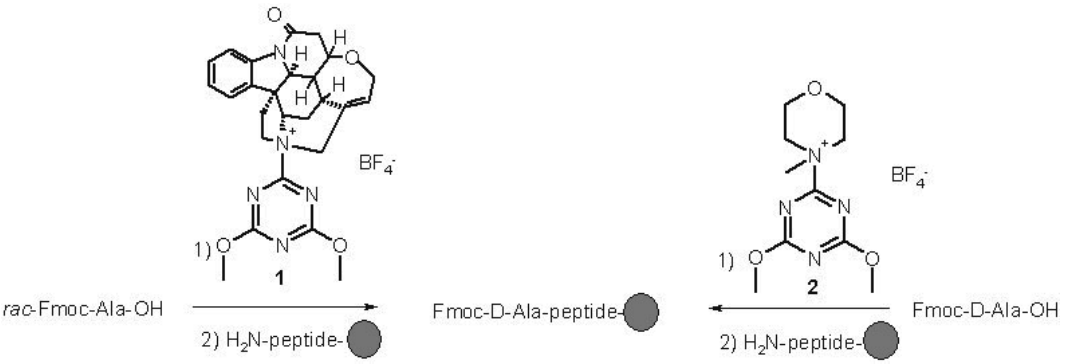

Scheme 2. Enantioselective synthesis on Wang resin

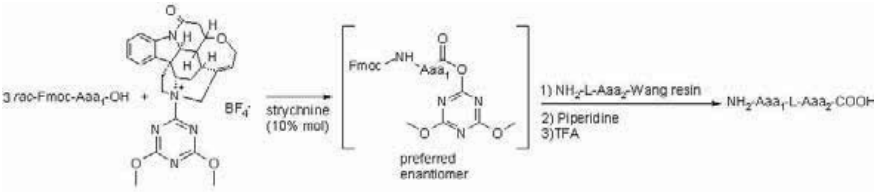

Experiments with SPPS using a threefold excess of racemic carboxylic components and a chiral traceless reagent 1 proceeded under standard conditions. The enantiomeric purity of crude peptides cleaved from the resin was determined after their hydrolytic degradation to amino acids by GC method using a ChirasilVal capillary column (Table 2).

Results confirmed that in all cases the configuration of an enantiomer incorporated into the peptide chain from the racemic substrate was identical. Enantiomeric enrichments were less uniform, although ee 84-96 for the incorporation of *rac*-Fmoc-Ala, ee 80-100 for *rac*-Fmoc-Phe and ee 78-100 for *rac*-Fmoc-Tyr confirmed the most important advantage of the application of traceless chiral N-triazinylammonium tetrafluoroborates, which is the predictability of the configuration of a preferred enantiomer and the repeatability of enantiomeric purity of the incorporated amino acid.

Acknowledgement

This work was supported by Ministry of Science and Higher Education, Grant PBZ-KBN-126/T09/15.

References

1. Kolesińska B, Kamiński ZJ. *Polish Pat Appl* **P-38476** from 04.02. 2008.
2. Kamiński ZJ, Kolesińska B, Kolesińska J, Sabatino G, Chelli M, Rovero P, Błaszczyk M, Główka ML, Papini AM. *J Am Chem Soc* **127**: 16912-16920, 2005.

Table 2. Enantiomeric composition of crude peptides prepared on H_2N-Aaa-Wang resin with a threefold excess of racemic C-component using *N*-(4,6-dimethoxy-1,3,5-triazin-2-yl)strychninium tetrafluoroborate (**1**) as a coupling reagent

Racemic C-component	NH_2-Aaa-Wang resin	Pref. conf.	L/D [%]
Fmoc-*rac*-AlaOH	NH_2-Gly~~	D	2/98
''	NH_2-L-Leu~~	D	5/95
''	NH_2-L-Phe~~	D	8/92
''	NH_2-L-Glu(OtBu)~~	D	3/97
''	NH-L-Pro~~	D	4/96
Fmoc-*rac*-Phe-OH	NH_2-Gly~~	L	90/10
''	NH_2-L-Leu~~	L	100/0
''	NH_2-L-Ala~~	L	98/2
''	NH_2-L-Glu(OtBu)~~	L	98/2
''	NH-L-Pro~~	L	96/4
Fmoc-*rac*-Tyr-OH	NH_2-Gly~~	L	89/11
''	NH_2-L-Leu~~	L	100/0
''	NH_2-L-Ala~~	L	100/0
''	NH_2-L-Phe~~	L	98/2
''	NH-L-Pro~~	L	99/1

1-01-134

Synthesis of peptides from racemic amino acids with predictable optical purity and configuration of the product by using traceless chiral triazine coupling reagents

Kolesińska, Beata; Kasperowicz, Katarzyna; Kamiński, Zbigniew J*

Technical University of Lodz, Institute of Organic Chemistry, POLAND

**E-mail: beata.kolesinska@p.lodz.pl*

Introduction

The demand for a molecular diversity of peptides used in the studies on structure-activity relationships and the construction of compound libraries have remarkably stimulated progress in the preparation of optically active analogues of proteinogenic amino acids. However, an alternative approach based on the enantiodifferentiating transformation of racemic substrates, which are usually easily available, would be valued as more advantageous and less time consuming than the classic procedure involving racemate resolution or asymmetric synthesis. Enantiodifferentiating methods would be considered as general and the most convenient in the case of constructing complex molecule libraries from chiral building blocks. Several chiral coupling reagents have been proposed for the synthesis of enantiomerically enriched peptides directly from racemic amino acids. Optically active N-hydroxysuccinimide and diacylamine derivatives, chiral DMAP analogues, N-methylimidazole, heterocyclic carbene, benzotetramisole, tertiary amines and phosphines and others were used as a chiral auxiliary.[1] So far, however, none of the coupling methods has been accepted in practice because of the unpredictable results of synthesis involving multiple stereogenic centers which are present in chiral coupling reagents and chiral substrates.

Results and Discussion

In order to design an efficient chiral auxiliary and to resolve the problem of predictability of synthetic results including purity, high yield, optimal coupling conditions, configuration and the enantiomeric composition of the final product, this paper presents a novel general approach allowing a preferred enantiomer to be selectively incorporated directly from a racemic substrate. It is based on the synthesis of a traceless coupling reagent **4** effective as an enantiodifferentiating agent only at the activation stage, and then, after the departure of the chiral auxiliary, transformed into a well-known classic achiral acylating reactive intermediate **3**. Thus, the structure, properties and reactivity of the activated carboxylic component **3** should be exactly the same as those obtained in a reaction involving a classic achiral reagent **2.**[2] Moreover, due to the departure of the chiral auxiliary after activation, all further stages of the coupling procedure should remain free of the disturbances caused by the presence of the stereogenic center of the chiral auxiliary and therefore the configuration and enantiomeric purity, once established during the activation stage, should remain essentially intact in all the syntheses involving this carboxylic component and reagent. This means that the configuration and results of enantiomeric enrichment could be predicted for all the syntheses involving a given

Scheme 1. Synthesis with achiral coupling reagent **2** or traceless coupling reagent **4** proceeds *via* the same intermediate **3**

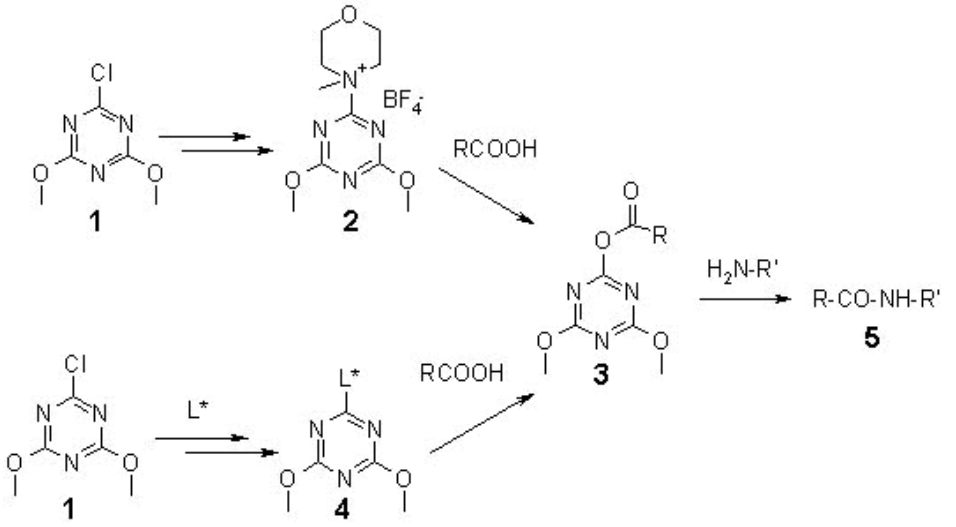

Table 1. 2 eq. Z-DL-Ala-OH+1 eq. DMT/brucine/BF_4 +1 eq. L-Phe-OMe, activation: 30 min

Entry	amine	Solvent	Yield [%]	DL/LL
1	brucine	THF	67	80/20
2	"	DMF	96	65/35
3	"	1,2-diethoxyethan	77	82/18
4	"	AcOEt	82	77/23
5	"	THF + *t*-BuOH (1:1)	89	55/45
6	"	$CHCl_3$	96	82/18
7	"	CH_2Cl_2	93	87/13
8	DIPEA	"	96	85/15
9	brucine	CH_3CN	91	95/5
10	DIPEA	"	94	90/10

set of components from a single model experiment, avoiding additional studies on the scope and limitations of the acylation procedure.

According to this concept, the reagent **4** consists of a stable binary system formed from readily accessible achiral triazine components and an appropriate tertiary amine used as a chiral auxiliary L*. The reagent **4** was prepared by the treatment of brucine tetrafluoroborate with **1** in the presence of an HCl acceptor.[3] It was found that the presence of a catalytic amount of the appropriate tertiary amine is essential to the activation of the carboxylic function.

Achiral DIPEA and brucine were selected as suitable for the process of activation. The character of the solvent was crucial for the efficient enantiodiscriminating activation of the carboxylic component and acetonitrile was selected as the most suitable.

Even if only a twofold excess of racemic *N*-protected alanine was used, high enantiomeric purity and the same D-configuration at the alanine stereogenic centre were obtained with **4** used as a coupling reagent as determined by GC on a ChirasilVal capillary column (Table 2).

Acknowledgement

This work was supported by Ministry of Science and Higher Education, Grant PBZ-KBN-126/T09/15.

References

1. a) Vedejs E, Chen X. *J Am Chem Soc* **118**: 1809, 1996.
   b) Ruble JC, Fu GC. *J Am Chem Soc* **120**: 11532-11533, 1998.
   c) Spivey AC, Fekner T, Adams H, Spey SE. *J Org Chem* **64**: 9430-9443, 1999.
   d) Miller SJ, Copeland GT, Papaioannou N, Horstmann TE, Ruel EM. *J Am Chem Soc* **120**: 1629-1630, 1998.
2. Kamiński ZJ, Kolesińska B, Kolesińska J, Sabatino G, Chelli M, Rovero P, Błaszczyk M, Główka ML, Papini AM. *J Am Chem Soc* **127**: 16912-16920, 2005.
3. Kolesińska B, Kamiński ZJ. *Polish Pat Appl* **P-38476** from 04.02. 2008.

Table 2. 2 eq. racemic carboxylic acid+1 eq. **4** + 1 eq. amino component

Entry	racemic component	acylated component	product prepared	Yield [%]	D/L
1	Z-DL-Ala	L-Phe-OMe	Z-D-Ala-L-Phe-OMe	94	96/4
2		L-Leu-OMe	Z-D-Ala-L-Leu-OMe	93	93/7
3		L-Trp-OMe	Z-D-Ala-L-Trp-OMe	88	96/4
4		L-Val-OMe	Z-D-Ala-L-Val-OMe	96	98/2
5		L-Ile-OBut	Z-D-Ala-L-Ile-OBut	95	92/8
6		L-Ser-OMe	Z-D-Ala-L-Ser-OMe	93	95/5
7		L-Tyr-OEt	Z-D-Ala-L-Tyr-OEt	89	99.6/0.4
8		L-His-OMe	Z-D-Ala-L-His-OMe	88	92/8
9		L-Pro-OMe	Z-D-Ala-L-Pro-OMe	92	97/3
10		Gly-OEt	Z-D-Ala-Gly-OEt	85	98/2
11		Aib-OMe	Z-D-Ala-Aib-OMe	88	94/6
12		NH_2-$(CH_2)_3CH_3$	Z-D-Ala-NH-$(CH_2)_3CH_3$	86	99/1
13		CH_3OH	Z-D-Ala-OCH_3	96	97/3
14	Fmoc-DL-Ala	L-Phe-OMe	Fmoc-D-Ala-L-Phe-OMe	92	96/4
15		L-Leu-OMe	Fmoc-D-Ala-L-Leu-OMe	93	92/8
16		Gly-OEt	Fmoc-D-Ala-Gly-OEt	87	96/4
17		NH_2-$(CH_2)_3CH_3$	Fmoc-D-Ala-NH$(CH_2)_3CH_3$	86	95/5

1-01-135

2-Chloro-4,6-*bis*-(2,2,2-trifluoroethoxy)-1,3,5-triazine and *N*-[4,6-(2,2,2-trifluoroethoxy)-1,3,5-triazin-2-yl)]-*N*-methylmorpholinium tetrafluoroborate as coupling reagents

*Jastrzabek Konrad, Kolesińska, Beata**; Kamiński, Zbigniew J*

Technical University of Lodz, Institute of Organic Chemistry, POLAND

**E-mail: kolesins@gmail.com*

Introduction

It has been expected that modification of substituents in the triazine ring could improve activity, stability and solubility of new triazine based coupling reagents.[1] In order to increase reactivity of triazine coupling reagents analogues with electron withdrawing 2,2,2-trifluoroethoxy substituents in the triazine ring has been prepared and their reactivity was studied.

Results and Discussion

2-Chloro-4,6-(2,2,2-trifluoroethoxy)-1,3,5-triazine (**2**) has been obtained by the treatment of cyanuric chloride (**1**) with 2,2,2-trifluoroethanol. Taking advantage of modular structure of triazine coupling reagents the entire family of *N*-(4,6-(2,2,2-trifluoroethoxy-1,3,5-triazinyl-1) ammonium tetrafluoroborates were obtained, and *N*-[4,6-(2,2,2-trifluoroethoxy)-1,3,5-triazin-2-yl)]-*N*-methylmorpholinium tetrafluoroborate (**3**) has been used in this studies.

We found **3** useful for activation of carboxylic components. The participation of triazine "superactive ester" **4** as intermediate in the condensation has been proved in the model experiments. It was expected that efficient coupling reagents should be useful for amide bond formation between broad range of substrates, work in stoichiometric quantities, be soluble and stable in most of the solvents. It should function efficiently in solution as well as in SPPS, to get high purity crude products and minimize racemization of the products.

Utility of reagents *N*-(4,6-(2,2,2-trifluoroethoxy-1,3,5-triazinyl-1)ammonium tetrafluoroborates were confirmed by peptide synthesis in solution (Table 1). It has been found that due to the presence of strongly electron withdrawing trifluooethoxy substituents in triazine ring activate carboxylic acids proceeded substantially faster than in the syntheses involving classic reagents bearing methoxy groups in the triazine ring,[2] although the isolation of final products obtained in solution was less convenient due to lowered solubility of fluorinated side-products.

In our study we focused our attention on the performance (in terms of purity of the crude and extent of racemization) testing **3** in the solid phase synthesis of model peptides with AibAib fragment, which are a good example of difficult peptide sequence.

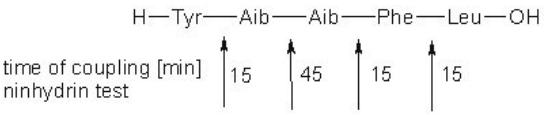

It has been found that **3** in difficult coupling of sterically hindered *α,α*-disubstituted Aib components both activation as well as aminolysis proceeded with trifluooethoxy substituted triazines **3** faster then with appropriate analogue substituted with methoxy groups in the triazine ring.

Even in the case of short 15 min coupling time prolonged to 45 min only for Aib-Aib sequence, the deletion products were diminutive and expected pentapeptide was prepared on the Wang resin with 83% yield after single coupling using threefold excess of reagents.

Scheme 1. Synthesis of *N*-[4,6-(2,2,2-Trifluoroethoxy)-1,3,5-triazin-2-yl)]-*N*-methylmorpholinium tetrafluoroborate (**3**) and activation of carboxylic component

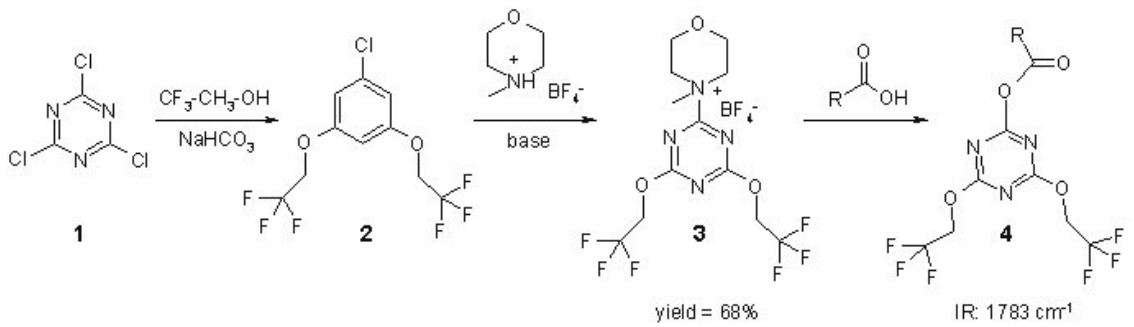

Table 1. Coupling in solution using *N*-(4,6-(2,2,2-trifluoroethoxy-1,3,5-triazinyl-1)ammonium tetrafluoroborate (**3**)

Peptide	Yield (%)	Purity (%)	enentiomeric purity [%L / %D]	
			N-terminal AA	C-terminal AA
Z-Phe-Ala-OMe	95	89	-	-
Z-Aib-Phe-OMe	97	93	-	99.2/0.8
Z-Aib-Aib-OMe	76	80	-	-
Boc-Pro-Val-OMe	92	86	100/0	99.0/1.0
Boc-Leu-Phe-OMe	84	80	98.9/1.1	97.6/2.4
Boc-Val-Aib-OMe	89	84	99.6/0.4	-
Fmoc-Phe-Leu-OMe	98	95	99.3/0.7	96.2/3.8
Fmoc-Ala-Phe-OMe	99	96	99.4/0.6	98.9/1.2
Fmoc-Phe-Aib-OMe	95	93	99.1/0.9	-
Fmoc-Thr(tBu)-Leu-OMe	93	93	95.1/4.9	98.2/1.8
Fmoc-Ser(tBu)-Leu-OMe	99	96	93.8/6.2	99.0/1.0
Z-Phe-Ala-OMe	95	89	-	-

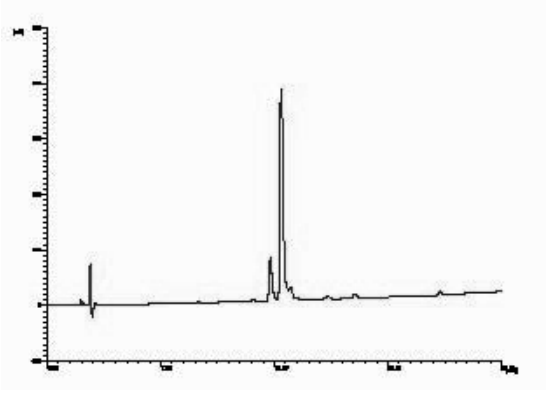

Figure 1. RP-HPLC profile of crude Tyr-Aib-Aib-Phe-Leu-OH after cleavage from resin (Vydac C-18 column, gradient acetonitrile/water).

Acknowledgement

This work was supported by Ministry of Science and Higher Education, Grant PBZ-KBN-126/T09/15.

References

1. Jastrzbek KG, Kolesińska B, Sabatino G, Rizzolo F, Papini AM, Kamiński ZJ. *Int J Pept Reas Therap* **13**: 229-236, 2007.
2. Kamiński ZJ, Kolesińska B, Kolesińska J, Sabatino G, Chelli M, Rovero P, Błaszczyk M, Główka ML, Papini AM. *J Am Chem Soc* **127**: 16912-16920, 2005.
3. Kolesińska B, Kamiński ZJ. *Polish Pat Appl* P-38476 from 04.02. 2008.

1-01-136

Solid-Phase Synthesis of the Cys-Rich Peptide Linaclotide

Albericio, Fernando[1,]; Giraud, Matthieu[2]; Gongora-Benitez, Miriam[1]; Paradis-Bas, Marta[1]; Tulla-Puche, Judit[1]; Werbitzky, Oleg[2]*

[1]Institute for Research in Biomedicine, Barcelona Science Park, Barcelona, SPAIN; [2]LONZA Ltd, CH-3930 Visp, SWITZERLAND

[*]E-mail: albericio@irbbarcelona.org

Linaclotide is a 14-residue peptide currently undergoing phase II clinical trials for the treatment of gastrointestinal diseases such as chronic constipation (CC). Linaclotide, which can be administered orally, is an agonist of the guanylate cyclase type-C receptor found in the intestine. From a structural point of view, this small peptide presents a constrained structure with the presence of three disulfide bridges between Cys1-Cys6, Cys2-Cys10, and Cys5-Cys13.

In order to achieve the large amounts required for a marketed peptide, an efficient synthesis is required. To optimize this synthesis, its fundamental limitations need to be determined and addressed. In the case of Linaclotide, the key points are related to the numerous Cys residues (some of them consecutive) in the peptide, for two reasons: the potential risk of racemization upon assembling the linear chain, and the misfolding of the three disulfide bridges. To address these points, the concourse of distinct protecting groups and folding conditions as well as the analysis of the disulfide bridges in the final folded peptide have been studied and are discussed in this presentation.

Strategies

Several strategies have been examined using distinct Cys–protecting groups (StBu, Acm, Trt, Mmt, pMeOBzl) and different resins (Wang and CTC), in addition to performing disulfide formation in solid–phase and solution. First, a total regioselective method (2+2+2) and semi–regioselective method (2+4 and 4+2) were tested. In parallel, a random/thermodynamic strategy was also studied (6 Trt and 6 Acm). Lineal peptides were synthesized manually using DIPCDI and HOBt in DMF, with preactivation for 5 min, for 1 h at RT to incorporate all the Cys residues. These conditions assure that racemisation does not occur.[1,2] Other amino acids were coupled using HCTU and DIEA in DMF for 1 h at RT. The 6 Acm (CTC resin) strategy, both in solid–phase and solution, resulted in scrambling. The Acm group always yielded unsatisfactory results using 3 strategies 4 Trt + 2 Acm (CTC resin) and 2 strategies 2 Trt + 4 Acm (CTC resin) strategies. In these cases, the quality of the first intermediate (2 or 1 disulfide formed) was not kept to the end after adding I_2 to remove the Acm and perform the formation of the last (4 Trt + 2 Acm) or two last (2 Trt + 4 Acm) disulfide bridges. In addition, the formation of the first disulfide bridge was not possible on solid–phase when 2 StBu + 2 Trt + 2 Acm (CTC resin) and 2 Mmt + 2 Trt + 2 Acm (Wang resin) were used. The Mmt group was not compatible with the CTC resin in the 2 Mmt + 2 Trt + 2 Acm strategy. For the regioselective StBu strategies, the removal of StBu depends not only on its positions in the sequence, but also on the protecting groups of the nearest residues. In the 2 StBu + 2 Trt + 2 pMeOBzl strategy, the Cys5-Cys13 disulfide bond was not easy to obtain in the first step and one of the StBu groups was difficult to remove when it was in the Cys2-Cys10 positions. The best results were achieved with Cys1-Cys6; StBu groups were removed without difficulty and the disulfide bond was the easiest to obtain in the first step. In the 2 StBu + 4 Trt strategy the Cys1-Cys6 disulfide bond gave the correct conformation to obtain the properly and completely oxidized peptide. In the random 6 Trt strategy (CTC resin) the cyclization of the free thiol peptide was carried out in solution. Three conditions were studied: **a)** the peptide was dissolved in buffer A (100 mM sodium phosphate, 2 M guanidine hydrochloride, pH 7.0) and the solution was stirred at open atmosphere at RT for 12 h; **b)** the peptide was dissolved in buffer A and 5% of DMSO was then added. The solution was stirred at open atmosphere at RT for 12 h; and **c)** the peptide was dissolved in a mixture of buffer A (50%), 2-propanol (50%) and 2 mM red glutathione were added (pH 7.4). The solution was stirred at open atmosphere at RT for 12 h. All the experiments showed a similar chromatographic profile with a main peak which corresponded to the completely oxidized peptide, as shown by the data obtained by HPLC-ES (+).

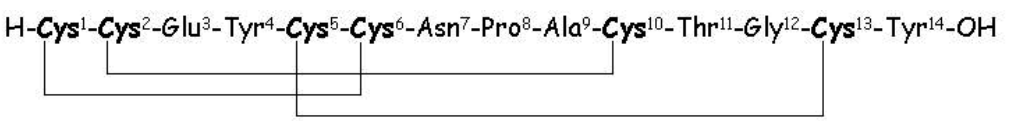

Figure 1. Structure of Linaclotide.

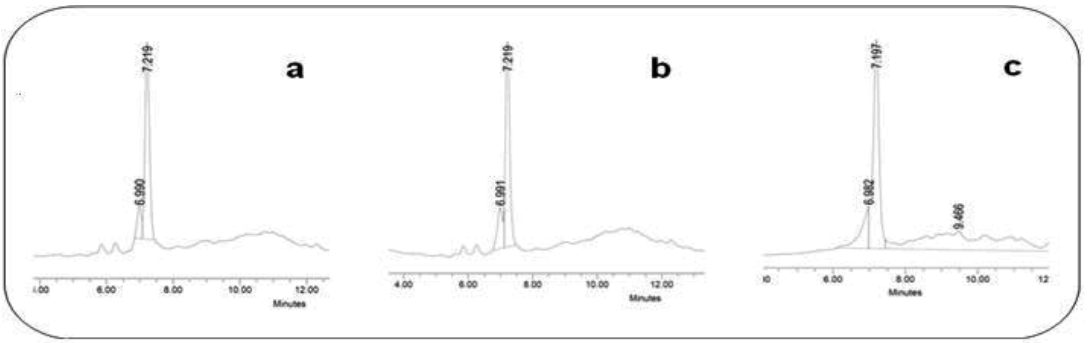

Figure 2. Chromatographic profiles of the completely oxidized peptides from 6 Trt Strategy.

Disulfide bond analysis

Linaclotide contains 14 aa with 6 Cys residues, which can form 15 theoretically possible disulfide structures. In order to confirm that the proper isomer (Cys1-Cys6, Cys2-Cys10, Cys5-Cys13) had been obtained following the 6 Trt Strategy, a disulfide bond analysis was carried out using a modified method of Wu and Watson.[3,4] The masses of the resulting peptide fragments were related to the location of the paired Cys residues that had undergone reduction, cyanylation, and cleavage. Fragments expected from the Cys1-Cys6 disulfide bond had a mw of 643.16 and 955.30; from the Cys2-Cys10 disulfide bond a mw of 120.04, 570.16 and 925.29; and from the Cys2-Cys10 disulfide bond a mw of 309.08, 515.15 and 791.25.

Conclusions

The 6 Trt strategy allowed to obtain the properly and completely oxidized peptide. The disulfide bond analysis confirmed that the suitable isomer (Cys1-Cys6, Cys2-Cys10 and Cys5-Cys13) has been achieved.

References

1. Han Y, Albericio F, Barany G. *J Org Chem* **62**: 4307-4312, 1997.
2. Angell YM, Alsina J, Albericio F, Barany G. *J Pept Res* **60**: 292-299, 2002.
3. Wu J, Watson JT. *Methods Mol Biol* **194**: 1–22, 2002.
4. Vila-Perello M, Andreu D. *Biopolymers* **80**: 697-707, 2005.

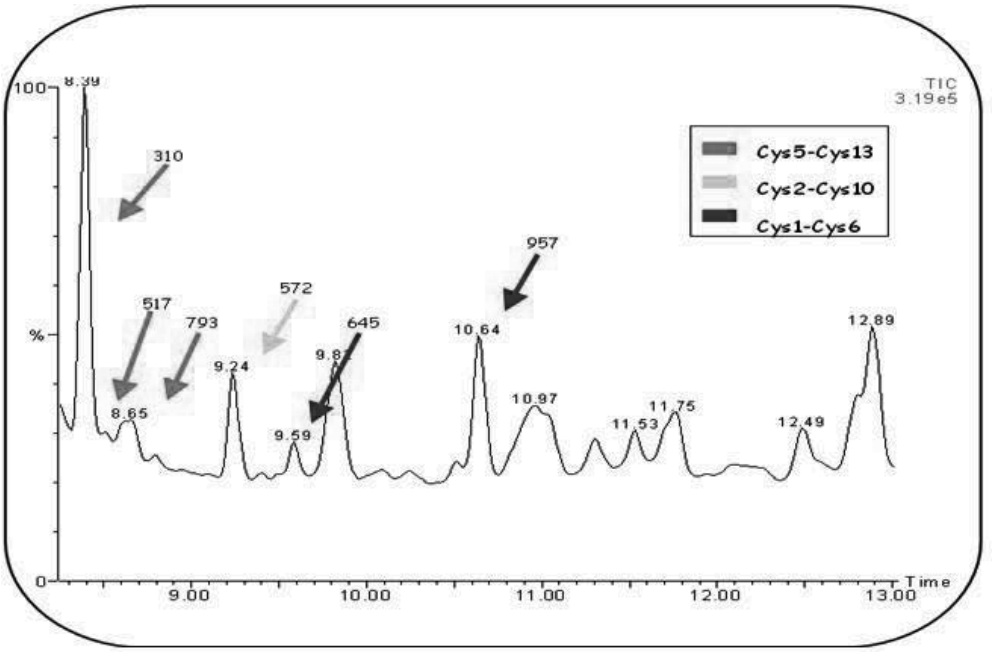

Figure 3. HPLC-ES(+) of the disulfide bond analysis.

1-05-180

Multiple, successive azide-alkyne cycloadditions as a new ligation tool

Valverde, Ibai E; Aucagne, Vincent; Delmas, Agnès F*

CNRS, CBM UPR 4301, FRANCE

**E-mail: valverde@cnrs-orleans.fr*

Introduction

Copper-catalyzed Cycloaddition of Azides on terminal Alkynes(CuAAC)affords1,4-disubstituted1,2,3-triazoles under mild conditions. In addition, the reaction provides high yields and is highly chemoselective.[1] As triazole is stable to acid and basic hydrolysis, and reductive and oxidative conditions, the reaction has been widely used in chemistry and *Biochemistry* proving to be a useful tool in combinatorial, bioconjugate or medicinal chemistry. In the peptide field, the reaction has been applied to synthesize cyclic, labeled and side-chain modified peptides including efficient synthesis of pseudo-glycopeptides.[1a] Conformational and structural studies prove that the triazole ring is an excellent trans-amide surrogate[2] and thus, can be considered as a pseudo-native amide linkage for peptide ligation.

Results & discussion

In order to explore the potential of the reaction as a way to successively assemble several peptide chains, we previously elaborated a new strategy for consecutive regiospecific triazole formation based on temporary alkyne protection by a trimethylsilyl group (TMS).[3] Despite the success of this approach, the TMS proved not to be completely stable in the presence of stoichiometric amounts of copper(I). With the aim of providing a robust and general method for iterative cycloadditions on peptides, the stability of the most commonly used silyl protective groups was examined under different reaction conditions, including classical Fmoc-SPPS. Table 1 shows the percentage of alkyne deprotection under different conditions.

As expected, TMS is the most labile group of our pool whereas triisopropylsilyl (TIPS) is completely stable to Fmoc SPPS elongation, TFA cleavage conditions and harsh CuAAC conditions (Table 1, entries **1** to **4**). As a consequence, TIPS is the most suited masking group for multiple, iterative triazole ligation to generate mimics of proteins. On the other hand and to our surprise, the triethylsilyl (TES) silver salt-mediated deprotection proved to be quasi-orthogonal with TIPS (Table 1, entry **5**). Aware that an additional dimension in alkyne protection opens the way for an easy construction of triazole based branched architectures, we decided to perform a triple consecutive CuAAC on a single template (Scheme 1). Thus, compound **1** was obtained from an azido aspartic acid functionalized with two alkynes protected by two semi-orthogonal silyl groups.

All cycloadditions proceeded quickly and quantitatively, as expected in the presence of large

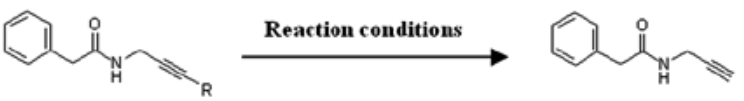

	Reaction conditions	t	R				
			TMS	TES	TBDMS	TBDPS	TIPS
1	TFA/CH_2Cl_2 (1:1)	2h	9.7%	<1%	0%	0%	0%
2	TFA/H_2O/ TIS (95:2.5:2.5)	3h	56%	43%	28%	45%	14%
3	Piperidine/DMF (2:8)	5h	0%	0%	0%	0%	0%
4	Cu(II) 2 equiv., sodium ascorbate 4 equiv. *t*BuOH/MeOH (9:1)	o/n	38%	0%	0%	0%	0%
5	Ag(I) 10 equiv., CH_2Cl_2/MeOH/H_2O (7:4:1)	8h	100%	100%	24%	<1%	<1%
6	TBAF 3 equiv., THF anhydrous	30 min	100%	100%	100%	100%	100%

Table 1. Systematic screening of trialkylsilylalkyne cleavage under different conditions

Scheme 1. Synthesis pathway to triple successive CuAAC
(i) Cu(I), tBuOH/H_2O; (ii)$AgNO_3$, CH_2Cl_2/MeOH/H_2O; (iii) TBAF, THF

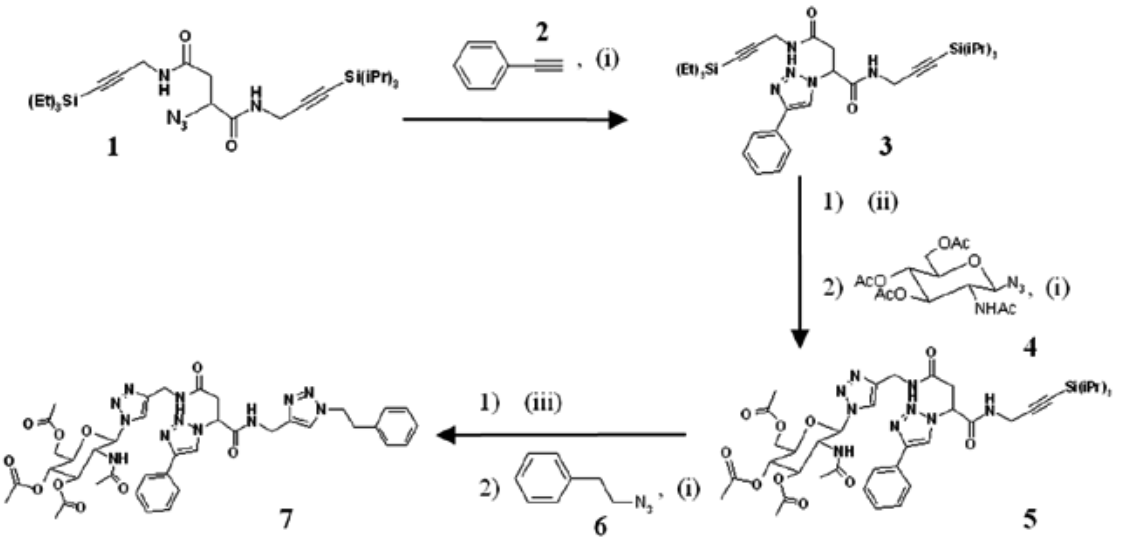

amount of catalyst, without any cleavage of the silyl groups. Deprotection of **3** was performed with $AgNO_3$ in CH_2Cl_2/MeOH/H_2O with no cleavage of TIPS which was removed during the deprotection of **5** with TBAF in THF. Such mild and chemoselective conditions proceeded in high yields and allowed a complete TES and TIPS cleavage without affecting the scaffold. Thanks to the chemoselectivity and the efficiency of all the reactions in the synthesis pathway, **7** was obtained in 60% overall yield after one final flash chromatography.

In conclusion, we succeeded in developing a robust and efficient method for successive triazole ligation using a TIPS protected alkyne compatible with in-solution or solid phase chemistry. In addition to this iterative method, another methodology for finely tuned deprotection conditions and potentially leading to branched molecular architectures was described. Both approaches were **E-mail*idated by the synthesis of a model tris-triazolo scaffold. The methodology is currently being expanded to large peptides as a new tool for the synthesis of protein analogues or for the decoration of peptide-based molecular templates.

Acknowledgements

This work was supported by a grant from the Ligue Contre Le Cancer section Centre. I. V. would like to acknowledge the Région Centre and the CNRS for a PhD fellowship.

References

1. (a) Tornøe CW, Christensen C, Meldal M. *J Org Chem* **67**: 3057-3064, 2002. (b) Rostovtsev VV, Green LG, Fokin VV, Sharpless KB. *Angew Chem Int Ed* **41**: 2596-2599, 2002.
2. (a) Bock VD, Speijer D, Hiemstra H, Van Maarseveen JH. *Org Biomol Chem* **5**: 971-975, 2007. (b) Horne WS, Yadav MK, Stout CD, Ghadiri MR. *J Am Chem Soc* **126**: 15366-15367, 2004.
3. Aucagne V, Leigh DA. *Org Lett* **8**: 4505-4507, 2006.

1-01-138

Instability of tert-butyl esters towards hydrazinolysis. Side chain hydrazide formation in peptides

Kruszynski, Marian[1,]; Schmidt, Albert; Heavner, George A; Pomerantz, Steven*

Centocor R&D, Inc, UNITED STATES

[*]E-mail: Mkruszy2@cntus.jnj.com

Introduction

C-terminal peptide hydrazides are obtained by hydrazinolysis of suitably protected peptides linked to the 2-methoxy-4-alkoxybenzyl alcohol resin (SASRIN™).[1] In Fmoc/tBu SPPS the Asp and Glu carboxylic acid side-chains have been successfully protected by the tBu ester.[2] The present work is based on observation of the unexpected peptide-hydrazide products found after hydrazinolysis of protected peptide-resin containing tert-butoxycarbonylated acidic residues (Asp(OtBu) and Glu(OtBu)): [GLP-1] [D-Ala2, Gly31-PEG11-Gly33]-SASRIN™ resin (peptide resin-I).

Results and discussion

Boc-His(Boc)-D-Ala-Glu(OtBu)-Gly-Thr(tBu)-[Phe-Thr(YMe,Mepro)]-Ser(tBu)-Asp(OtBu)-Val-[Ser(tBu)-Ser(YMe,Mepro)]-Tyr(tBu)-Leu-Glu(OtBu)-Gly-Gln(Trt)-Ala-Ala-Lys(Boc)-Glu(OtBu)-Phe-Ile-Ala-Trp(Boc)-Leu-Val-Lys(Boc)-Gly-Arg(Pmc)-Gly-PEG11–Gly-SASRIN™ was synthesized on an ABI 433A Peptide Synthesizer using Fmoc/HBTU/HOBt chemistry. Protected resin I was reacted with 10% hydrazine hydrate/DMF over 2 hours (A) or 20% hydrazine/DMF over 24 hours (B) then deprotected using acidolytic cleavage mixture. The analytical RP HPLC and HPLC MS data are shown in Fig. 1.

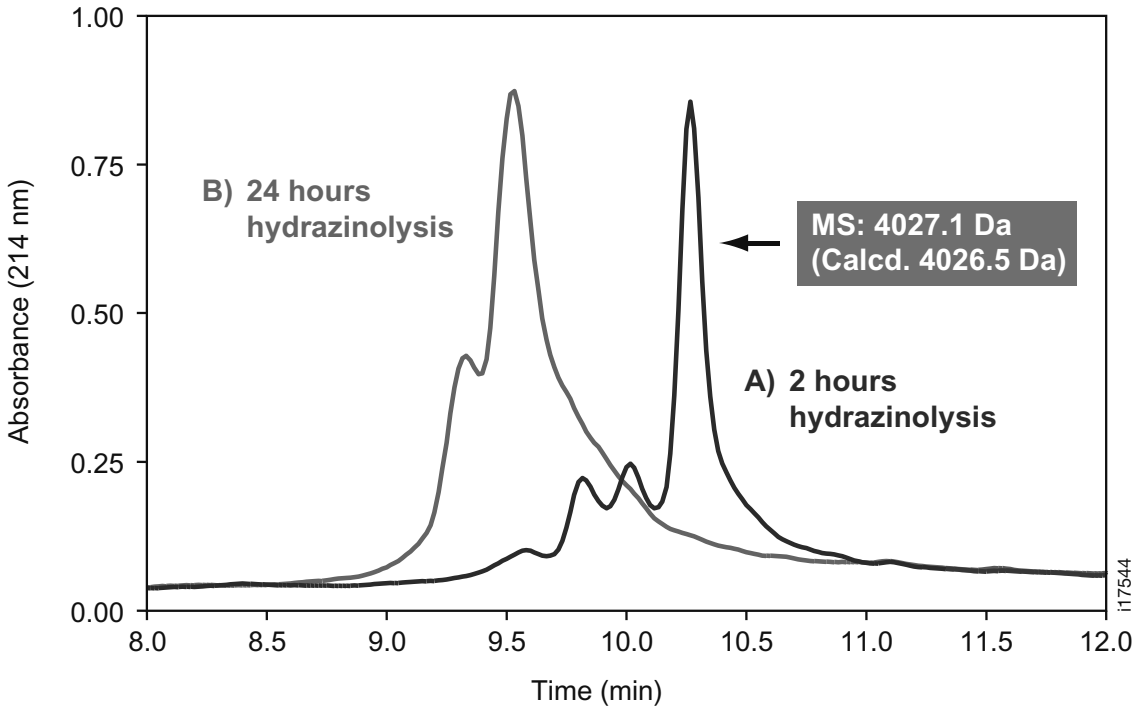

Figure 1. The crude products analyzed by reversed phase HPLC (C18) at 214 nm. A) HaEGTFTSDVSSYLEGQAAKEFIAWLVKGRG-PEG_{11}-G-$NH-NH_2$; B) Four products were identified by HPLC-MS HPLC MS of the crude peptide mixture from the 2 hours reaction gave a main peak (100%) with a mass of 4,027.1 Da, which corresponds to expected, C-terminal hydrazide (IA) (calculated molecular weight: 4,026.5 Da). The HPLC MS of the crude peptide mixture from the 24 hours reaction showed the presence of two main products: HPLC MS: 4,070.1 Da [M+42 Da] (100%) and HPLC-MS: 4,054.2 Da [M+28 Da] (82%). There were two other products with a mass of 4,041.99 Da [M+14 Da] (23%) and 4,084.5 Da [M+56 Da] (30%). The relative amounts of products were evaluated based on the HPLC MS main peak treated as 100% and are general estimates only. The MALDI MS/MS spectrum of the 4068.9 Da peak of peptide B fraction is shown in Fig. 2.

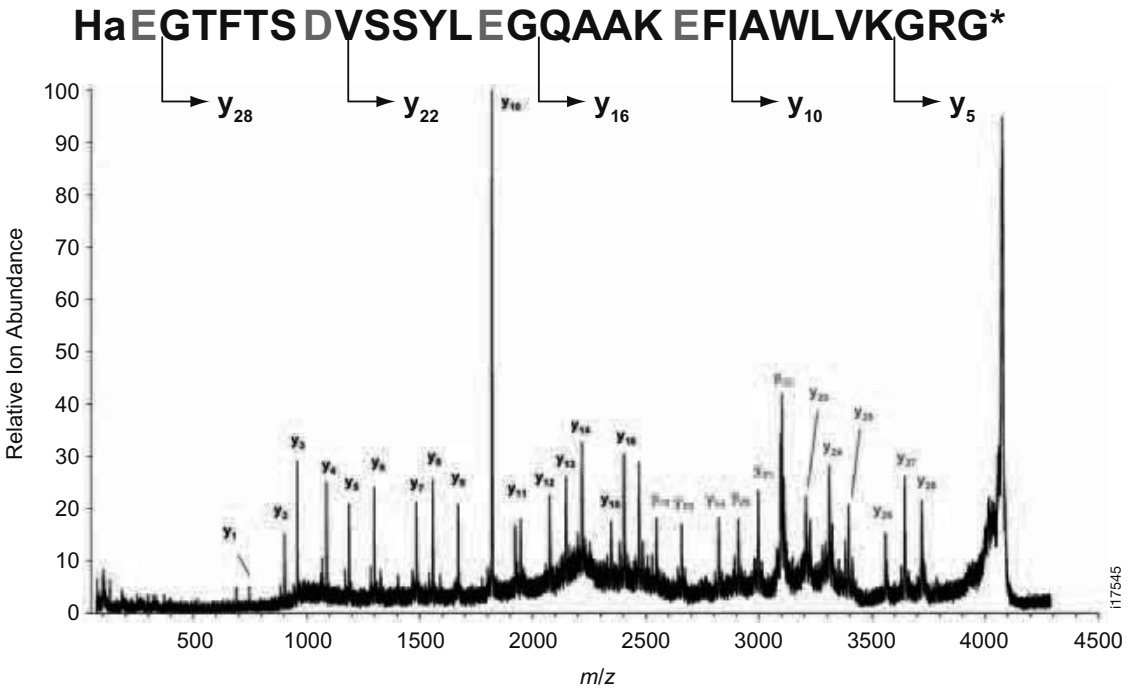

Figure 2. The MALDI MS/MS spectrum (metastable decomposition mode) of the 4068.9 Da peak of peptide B fraction. Species in red are +14 Da above predicted values, and species in green are +28 Da . Abbreviations: *) –PEG11-Gly-hydrazide. Ions for y17 through y22 of the 4068.9 Da are all shifted by +14 Da, while ions for y23 through y28 are all shifted by +28 Da. These results indicate [M+14 Da] "adduct" at Glu15 (y17) and another [M+14 Da] "adduct" at Asp9 (y23). It was found that tert-butyl esters of Asp and Glu side chains are not stable to hydrazinolysis, leading to formation oh hydrazides [Asp(NH-NH_2) and Glu(NH-NH_2). It is believed, that tBu esters compared to primary alkyl esters, offer a degree of steric shielding which make them resistant to attack by a wide range of nucleophiles.3 Our observation, to the best of our knowledge, has not been previously documented in the literature. We found the relative stability of different protecting groups to hydrazinolysis is *O*-Mpe > *O*-tBu > *O*-PhiPr. This makes possible the synthesis of site-specific peptide hydrazides in peptides containing multiple Asp and Glu residues. However, significant epimerization of Asp(OtBu) occurred upon exposure to 20% hydrazine/DMF solution. Two pseudoproline derivatives used for synthesis of peptide resin-I were chemically stable to hydrazinolysis. These findings could be used for the synthesis of protected or free peptide α- and α-hydrazides.

References

1. Mergler M, Nyfeler R *Peptides: Chemistry and Biology*, Smith JA, Rivier JE (Eds), ESCOM, Leiden, 1992, p. 551; Dick F, Hassler O. In *Peptides*, 1992, Schneider CH, Eberle AN (Eds), ESCOM, Leiden, 1992, p. 273.
2. Chang C-D *et al*. *Int J Peptide Protein Res* **15**: 9-66, 1980.
3. In *Methods of Organic Chemistry* (Houben-Weyl), *Synthesis of Peptides and Peptidomimetics* (Workbench Edition), Murray Goodman (Editor-in-Chief); Arthur Felix, Luis Moroder, Claudio Toniolo, (Eds); Georg Thieme Verlag Stuttgart – New York 2004, Volume E 22, p 209.

1-01-139

CLEAR-OX™: Synthesis of Disulfide-Bridged Peptides Under Mild Conditions

Darlak, Krzysztof[1,]; Cecil, Matthew R.[1]; Czerwinski, Andrzej[1]; Darlak, Miroslawa[1]; Long, DeAnna W[1]; McGrew, Danny[1]; Morgan, Timothy L[1]; Valenzuela, Francisco[1]; Barany, George[2]*

[1]Peptides International, UNITED STATES; [2]University of Minnesota, UNITED STATES

[*]E-mail: kd@pepnet.com

Introduction

The recently introduced polymer-supported oxidant, CLEAR-OX™, which combines the advantages of solid-phase chemistry with the versatility of solution-phase reactions, has proven to be a very valuable tool in the preparation of disulfide-bridged peptides.[1, 2] About 10-15% of all current peptide-based active pharmaceutical ingredients (APIs) contain one or more disulfide linkages. The oxidative synthetic step alone presents a set of unique challenges, especially when multiple disulfide bridges are involved or sensitive amino acid residues are present in the sequence. CLEAR-OX is comprised of the well-proven aqueous-compatible CLEAR resin for peptide synthesis as the support, and the robust DTNB [5,5'-dithiobis(2-nitrobenzoic acid)] moiety, aka Ellman's reagent, as the oxidant. More specifically, a lysine-preformed cyclic DTNB[3] is covalently attached to CLEAR with a β-alanine spacer. Previous work has established improved yields and purities for a number of peptides for which disulfide-bridge formation was mediated by CLEAR-OX, and also stressed the extraordinary mildness and operational convenience of the process. To additionally demonstrate some of the benefits that CLEAR-OX may offer, we report here the synthesis and oxidation under varying conditions of several peptides of biological interest. These include two bicyclic toxins, where in each case oxidation with CLEAR-OX gave the desired product with the correct disulfide arrangement.

Methods

Peptides used for these oxidation studies were synthesized either manually or with an automated solid-phase synthesizer (Pioneer™ or Prelude™) using standard Fmoc/*t*-Bu protection strategies on either polystyrene or CLEAR resins with HCTU/NMM activation. Peptides were cleaved from the resins with TFA: anisole: water: triisopropylsilane (88:5:5:2, v/v/v/v) for 2 h at room temperature under inert atmosphere, and were subjected directly to oxidations without purification. Solution oxidations were performed with peptide concentrations of 1 mg/ml in degassed 0.1 M ammonium acetate buffer at pH 7.0-7.5, using either 0.1 M $K_3Fe(CN)_6$ for 1 h or air for 16-24 h. Oxidations with CLEAR-OX resin were performed with peptide concentrations of 5-7 mg/ml and 2-3-fold molar excess of CLEAR-OX in degassed 0.1 M ammonium acetate buffer in acetonitrile (1:1, v/v), at pH 4.6 or 6.8. Progress of the oxidation was noted as the color of the resin changed from yellow to deep orange. Reaction completion was confirmed by an Ellman's test.[4] In all cases, oxidation products were analyzed by RP-HPLC and confirmed by ESI-MS.

Results and Discussion

Data for selected peptides are presented in Tables I and II. For all tested peptides, oxidations resulted in the expected disulfide products. CLEAR-OX mediated oxidations

Table I. Summary of Oxidation Results

#	Peptide Sequence	HPLC Purity (%)				
		Reduced Crude Dithio	Crude Oxidized Product CLEAR-OX pH 4.6	CLEAR-OX pH 6.8	$K_3Fe(CN)_6$ pH >7	Air pH >7
1	H-CNGRC-NH_2	58	68	36	61	--
2	H-CARAC-NH_2	25	52	37	24	--
3	H-XCYwKVCT-NH_2	55	68	63	47	--
4	H-PFCNAFTGC-NH_2	56	72	71	76	--
5	H-GRCCHPACGKNYSC-NH_2	60	34	38	--	44
6	H-GCCSDPRCAWRC-NH_2	37	42	48	--	34

In **3**, X = D-Nal. For conotoxins **5** and **6**, the nested disulfide arrangement pairs the first and third Cys, and the second and fourth Cys, from amino terminus; products co-eluted with reference standards.

were straightforward to carry out, since products could be separated from the polymer-bound oxidant by simple filtration. Oxidations were carried out with as low as two-fold excess of CLEAR-OX to obtain satisfactory yields, and were complete within 1-2 h. The optimum pH value was found to be 4.6. Solubility problems with the reduced peptides were overcome by the addition of acetonitrile to the CLEAR-OX cyclization mixtures.

It is well known that solution oxidations require that the target peptide be sufficiently dilute to reduce intermolecular dimerization and oligomerization. In this regard, it is encouraging that oxidations using CLEAR-OX were successful at considerably higher concentrations than solution oxidations, thus allowing for reduced solvent use in larger scale reactions. A further benefit for CLEAR-OX relates to its efficacy when sensitive residues, *e.g.* Trp, are present. These observations and conclusions extended to two bicyclic peptides, namely conotoxin MI (**5**) and conotoxin ImI (**6**). In summary, the CLEAR-OX oxidation method is recommended due to its convenience, mildness, and versatility.[5]

Acknowledgements

Supported by NIH/SBIR GM058987.

References

1. CLEAR resins are protected under *US Patent*s **5,910,554** and **5,656,707** granted to the Regents of the University of Minnesota.
2. Darlak K, Long DW, Czerwinski A, Darlak M, Valenzuela F, Spatola AF, Barany G. *J Pept Res* **63**: 303-312, 2004.
3. Annis I, Chen L, Barany G. *J Am Chem Soc* **120**: 7226-7238, 1998.
4. Ellman GL. *Arch Biochem Biophys* **82**: 70-77, 1959.
5. CLEAR-OX™ is commercially available from Peptides International.

Table II. Selected CLEAR-OX Mediated Oxidation Results

#	Scale (g)	Purity of Dithio Cleaved Peptide (%)	Crude Yield g (%)	Crude Oxidized HPLC (%)	Final Yield* mg (overall %)	Final Purity* (%)
1	2.0	58	1.60 g (80%)	73	433.90 mg (27%)	99
2	2.0	25	1.43 g (72%)	54	123.47 mg (9%)	96
3	2.0	55	1.02 g (51%)	64	84.46 mg (8%)	95
4	2.0	56	1.37 g (69%)	62	70.85 mg (5%)	96

* Purification was performed in a two-stage reverse-phase chromatography process

1-01-140

Solid-phase synthesis of 5-arylhistidines via a microwave-assisted Suzuki-Miyaura cross-coupling

Cerezo, Vanessa[1]; Verdié, Pascal[2]; Amblard, Muriel[2]; Martinez, Jean[2]; Planas, Marta[1]; Feliu, Lidia[1,]*

[1]University of Girona / LIPPSO, SPAIN; [2]University of Montpellier / Faculté de Pharmacie, FRANCE

[*]E-mail: lidia.feliu@udg.edu

Introduction

Unnatural amino acids are increasingly becoming important substrates in modern drug design, synthesis and discovery research. Their incorporation into biologically active peptides may lead to peptidomimetics with restricted conformational flexibility, increased proteolytic stability, and enhanced selectivity and biological activity.[1] Among them, biaryl amino acids have been the focus of intense synthetic efforts owing to the broad spectrum of activities shown by peptides containing biaryl motifs.[2] In particular, 5-arylhistidines occur naturally in the active site of the heme-copper oxidases and in cytotoxic and antifungal marine peptides.[3,4]

Despite their interest, the preparation of 5-arylhistidines still remains an important synthetic challenge, including as key step the arylation of the position 4(5) of the imidazole ring. In the course of our synthetic studies on biaryl aminoacids, we focused our interest on studying a methodology toward the preparation of 5-arylhistidines. Recently, we have reported the synthesis of these amino acid derivatives in solution via a microwave-assisted Suzuki-Miyaura cross-coupling of a 5-bromohistidine with various arylboronic acids.[5] In the present study we describe an efficient solid-phase synthesis of 5-arylhistidines by arylation of the position 4(5) of the imidazole ring via a microwave-assisted Suzuki-Miyaura cross-coupling.[6]

To investigate the feasibility of the solid-phase arylation of the imidazole ring of a histidine residue, the tripeptidyl Rink amide resins **1a** and **1b** were chosen as model. They were prepared following Fmoc/tBu strategy by sequential coupling and deprotection steps using standard conditions.

Results and discussion

Arylation of the histidine residue of resins **1a** and **1b** via a microwave-assisted Suzuki-Miyaura cross-coupling was first optimized by using phenylboronic acid as arylating reagent (Fig. 1). Several reaction parameters were modified such as the solvent, the reagent concentration, the time and the temperature. For each experiment, aliquots of resin were subjected to the corresponding reaction conditions and, after acidolytic cleavage, the obtained crude product mixture was analyzed by LC-MS. To promote the SEM group removal during the cleavage step, stirring and 3 h of TFA exposure were found to be essential. Treatment of resins **1a** and **1b** with $PhB(OH)_2$ (4 eq.), $Pd_2(dba)_3$ (0.2 eq.) and KF (4 eq.) at 170 °C for 15 min under microwave irradiation led to the highest percentage of arylated product (85% including **2** and SEM-protected **2**) and no starting material was detected. The crude product mixture proved to contain H-His-Leu-Leu-NH_2 (10%), derived from the reductive dehalogenation of bromohistidines **1a** and **1b**.

We explored the applicability of the Suzuki-Miyaura reaction to the coupling of 5-bromohistidine tripeptidyl resins **1a** and **1b** with other arylboronic acids possessing substituted benzene, pyridine, and thiophene rings. All reactions afforded the desired 5-arylhistidine tripeptides **3-8** in purities ranging from 52 to 83% (including the corresponding SEM-protected peptide derivatives). Couplings with 5-methyl-2-methoxyphenylboronic acid and 3-nitrophenylboronic acid gave the highest percentages of arylated product (83 and 80%, respectively, calculated from the non-protected and SEM-protected biaryl tripeptide). In addition to the presence of starting material (2-15%), all the crude reaction mixtures contained also H-His-Leu-Leu-NH_2 (4-36%). In the case of the 3-pyridylboronic acid it was necessary to repeat the reaction three times to obtain **7** with 52% purity. The 5-arylhistidine tripeptides were purified by reverse-phase preparative HPLC and fully characterized by mass spectrometry, and ^{1}H- and ^{13}C-NMR. 2D-COSY and HMQC experiments were carried out to completely assign all the proton and carbon signals.

The extension of the above methodology to the synthesis of peptides containing tyrosine-histidine cross-links was studied (Fig. 1). Resins **1a** and **1b** were treated with a tyrosine boronic acid derivative (4 eq.), $Pd_2(dba)_3$ (0.2 eq.) and KF (4 eq.) in DME/EtOH/H_2O (9:9:2) under microwave irradiation at 140 ºC for two periods of 30 min and 1 h, respectively. Under these conditions, the 5-(3-tyrosyl)histidine peptide **9** was formed (18%) together with its acid derivative (49%). Similarly to previous reactions, it was also observed the formation of H-His-Leu-Leu-NH_2 (19%) and the presence of starting material (12%). To promote complete hydrolysis, the resin obtained from the Suzuki-Miyaura reaction was exposed to LiOH (5 eq.) in THF/H_2O (7:1) leading to 67% of the corresponding 5-(3-tyrosyl)histidine acid derivative.

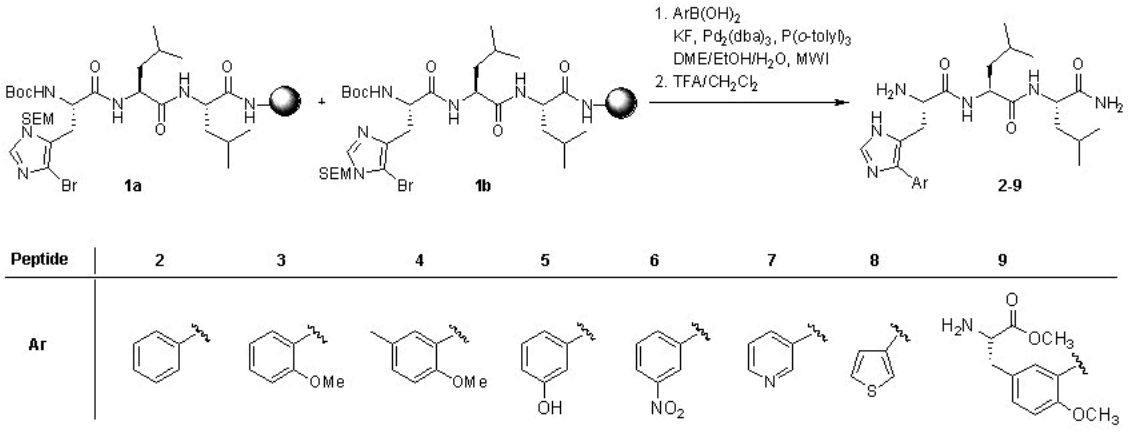

Figure 1. Microwave-assisted arylation of resins **1a** and **1b** with various arylboronic acids.

Acknowledgements

Vanessa Cerezo is the recipient of a predoctoral fellowship from the University of Girona. This work was supported by grant AGL2006-13564-C02-02/AGR from MEC of Spain.

References

1. Pavar MC, Hanif K, Azam A, Lata S, Qadar Pasha MA, Pasha S. Structure-activity relationship study between ornithyl-proline and lysyl-proline based tripeptidomimics as angiotensin-converting enzyme inhibitors. *Bioorg Med Chem Lett* **16**: 2117-2121, 2006.
2. Feliu L, Planas M. Cyclic peptides containing biaryl and biaryl ether linkages. *Int J Pept Res Ther* **11**: 53-97, 2005.
3. Bewley CA, He H, Williams DH, Faulkner DJ. Aciculitins A-C: cytotoxic and antifungal cyclic peptides from the lithistid sponge *Aciculites orientalis*. *J Am Chem Soc* **118**: 4314-4321, 1996.
4. Tomson F, Bailey JA, Gennis RB, Unkefer CJ, Li Z, Silks LA, Martinez RA, Donohoe RJ, Dyer R B, Woodruff WH. Direct infrared detection of the covalently ring linked His-Tyr structure in the active site of the heme-copper oxidases. *Biochemistry* **41**: 14383-14390, 2002.
5. Cerezo V, Afonso A, Planas M, Feliu L. Synthesis of 5-arylhistidines via a Suzuki-Miyaura cross-coupling. *Tetrahedron* **63**: 10445-10453, 2007.
6. Cerezo V, Amblard M, Martinez J, Verdié, Planas M, Feliu L. Solid-phase synthesis of 5-arylhistidines via a microwave-assisted Suzuki-Miyaura cross-coupling. *Tetrahedron* **64**: 10538-10545, 2008.

1-01-141

Novel peptide-hetorocycle conjugates: derivatives of 3-(benzimidazol-5-yl)alanine

*Ratajska, Małgorzata; Kluczyk, Alicja; Cebrat, Marek; Stefanowicz, Piotr; Bartosz-Bechowski, Hubert; Szewczuk, Zbigniew**

Faculty of Chemistry, Wroclaw University, POLAND

**E-mail: szewczuk@wchuwr.pl*

Introduction

In a search for new bioactive peptides we investigate methods for introducing heterocyclic motifs into peptide side chains. Our strategy for synthesis of peptides containing novel heterocyclic amino acids is based on direct chemical transformation of the amino acid side chains.[1,2] Considering the biological importance and complexing abilities of benzimidazoles,[3,4] we developed a direct efficient solid-phase synthesis of benzimidazole-peptide conjugates, expecting these new compounds to express novel biological properties. The peptide-heterocycle hybrids are obtained by the on-resin reaction between aldehydes and peptides containing a *β*-(3,4-diaminophenyl)alanine residue, developed by us specifically for introducing such modifications into peptides.[1] The character of the aldehyde used for benzimidazole synthesis and the stoichiometry of the reaction determine the structure of the final product.

Results and discussion

We developed an efficient and straightforward solid phase synthesis method of substituted and fused benzimidazole scaffolds conjugated with peptides. The application of the stoichiometric amount of aldehyde leads to 2`-substituted 3-(1H-benzimidazol-5-yl)alanine-containing peptides, whereas the increase in aldehyde content results in 1`,2`-disubstituted derivatives as well as a small amount of triple substituted benzimidazoles.[5] The compatibility of our method with the Fmoc solid phase peptide synthesis protocols was proven by the synthesis of analogues of immunosuppressory fragments of ubiquitin and HLA-DQ.[6,7] The reaction with dialdehydes results in more extended conjugated ring systems, giving novel amino acid residues containing tricyclic systems, in the case of *o*-phthalic aldehyde - the pyrido[1,2-a]benzimidazole derivative.

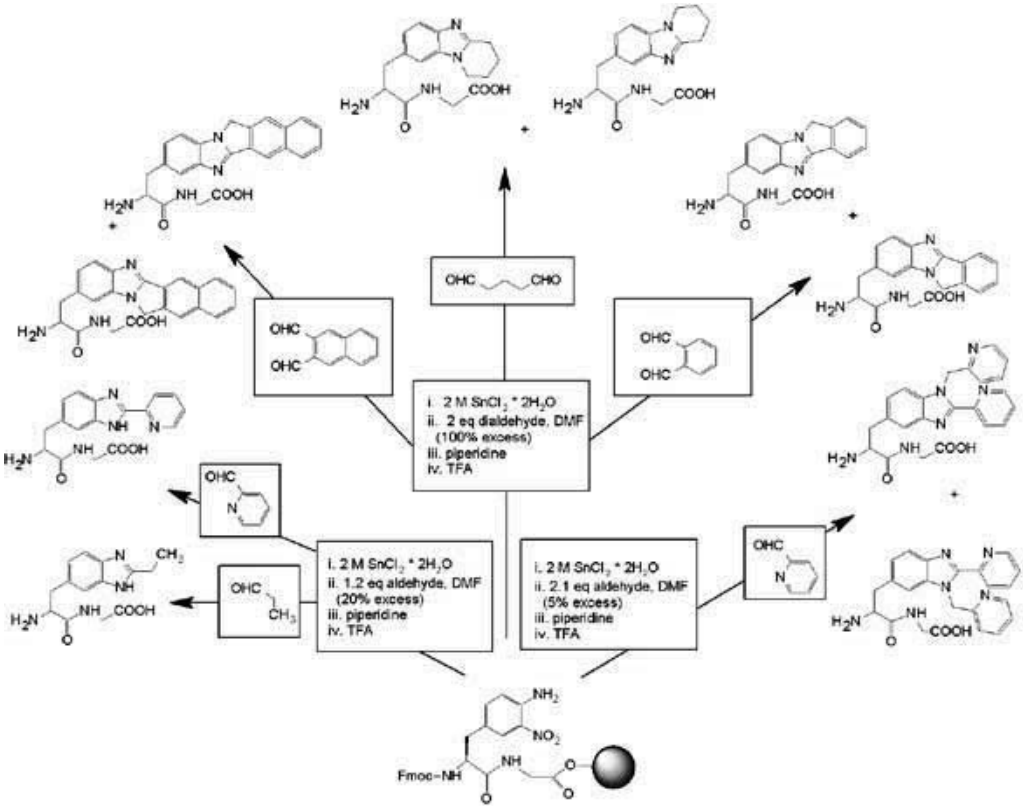

Figure 1. On-resin benzimidazole scaffold formation.

The disubstituted novel benzimidazole amino acids are formed as pairs of isomers. The same is observed for peptides containing polycyclic benzimidazoles due to clockwise and counter clockwise ring closure. The isomers were separated by preparative HPLC and their structures were unambiguously assigned by the two-dimensional NMR spectra due to significant contacts generated by the CH_2 protons from the *N*-substituent in position 1 of benzimidazole skeleton and the specific chemical shift change of the protons of the benzene ring. The results of the high resolution ESI-MS/MS experiments revealed the fragmentation pattern of the of benzimidazole-peptide conjugates with characteristic immonium and benzyl type ions stable in broad range of collision energy.

Acknowledgements

Supported by grant number N N 204 249934 from the Ministry of Science and Higher Education (Poland).

References

1. Staszewska A, Stefanowicz P, Szewczuk Z. *Tetrahedron Lett* **46:** 5525-5528, 2005.
2. Koprowska-Ratajska M, Kluczyk A, Stefanowicz P, Bartosz-Bechowski H, Szewczuk Z. *Amino Acids* **36**: 309-315, 2009.
3. Vourloumis D, Takahashi M, Simonsen KB, Klaus B, Ayida BK, Barluenga S, Winters GC, Hermann T. *Tetrahedron Lett* **44:** 2807-2811, 2003.
4. Devereux M, O'Shea D, Kellett A, McCann M, Walsh M, Egan D, Deegan C, Kedziora K, Rosair G, Müller-Bunz HJ. Inorg. Biochem. **101:** 881-892, 2007.
5. Wu Z, Rea P, Wickham G. *Tetrahedron Lett* **41:** 9871–9874, 2000.
6. Szewczuk Z, Stefanowicz P, Wilczynski A, Siemion IZ, Cierniewski CS, Kralisz U, Wieczorek Z. *Biopolymers* **40:** 571-583, 1996.
7. Szewczuk Z, Stefanowicz P, Wilczynski A, Staszewska A, Siemion IZ, Zimecki M, Wieczorek Z. *Biopolymers* **74:** 352-362, 2004.

1-01-142

Inhibitors of DapE and ArgE enzymes as new antimicrobial agents: Synthesis and characterization

Hlaváček, Jan[1,]; Pícha, Jan[1]; Vanek, Václav[1]; Jirácek, Jiri[1]; Slaninová, Jiřina[1]; Fučík, Vladimír[1]; Gilner, Danuta[2]; Holz, Richard C[2]*

[1]Institute of Organic Chemistry and Biochemistry CAS, 166 10 Prague 6, CZECH REPUBLIC; [2]Loyola University Chicago, 1068 W.Sheridan Rd., Chicago, IL, 60626, UNITED STATES

**E-mail: honzah@uochb.cas.cz*

Introduction

Inhibition of microbial enzymes catalyzing metabolic processes essential for bacteria might lead to cessation of bacterial development. In our search for potential antimicrobial drugs, we have investigated two microbial enzymatic systems: N^{α}-acetyl-L-ornithine deacetylase (ArgE)[1,2] and the dapE-encoded N^{α}-succinyl-L,L-diaminopimelic acid desuccinylase (DapE),[3,4] both of which appear to be promising targets for potent and selective enzyme inhibitors based on modification of N^{α}-acetyl-L-ornithine (Orn) and N^{α}-succinyl-L,L-diaminopimelic acid (SDAP).

Results and Discussion

In this study, we have synthesized and characterized N^{α}-protected derivatives of Orn: R-CO-Orn-OH 1a-1j, 2a-2f and of DAP: HO_2C-CH(NH-CO-R)-$(CH_2)_3$-CH(NH_2)-CO_2H 3a-3d (Table 1) as potential inhibitors of ArgE or DapE, respectively. These molecules were hypothesized to be inhibitors of these enzymes due to the stability of the corresponding amide bonds against enzymatic degradation. The derivatives 1a-1j were formed by acylation of H-Orn(Boc)-Wang polystyrene resin using the corresponding carboxylic acids in DMF and DIC/HOBt as the coupling reagents, in the presence of DIEA. Removal of N^{δ}-Boc protecting group and detachment of the R-CO-Orn-OH derivatives from the resin were performed simultaneously by a 95% TFA-TIS-anisole (95:2.5:2.5) mixture. The derivatives 2a-2f were prepared in solution from H-Orn(Z)-OMe. Its reaction with triphosgene afforded a corresponding isocyanate that was refluxed in pyridine with a series of alcohols to obtain protected derivatives of Orn. A final deprotection step was performed by hydrogenation on Pd/C and saponification with 1 M NaOH, followed by desalting on a Dowex 50 x 2 ion exchanger. For the synthesis of DAP derivatives 3a-3d, the soluble $N^{\alpha},N^{\alpha'}$-bis-Boc-DAP$(OH)_2$ was prepared first, which was converted to the corresponding bis-benzyl ester. Then, both of the amino groups were deprotected by TFA and only one of them was again protected by a Z group. Thus, the selective acylation of the second amino group was achieved using the corresponding anhydrides at elevated temperature. Finally, the temporary protecting groups were removed by catalytic hydrogenation on a Pd/C catalyst. In preliminary kinetic studies, several of these compounds were found to be moderately strong inhibitors of ArgE or DapE and also showed efficacy towards the bacterial strain Bacillus subtilis. IC50 values were determined for Orn and DAP derivatives for both ArgE and DapE using spectrophotometric assays (Table 1). For ArgE, the hydrolysis of Ac-Orn-OH (2 mM in 50 mM Chelex-100 treated potassium phosphate buffer, pH 7.5; 25 °C) was monitored at 214 nm. For DapE, the hydrolysis of L,L,D,D-SDAP (3 mM in 50 mM Chelex-100 treated potassium phosphate buffer, pH 7.5; 25 °C) was monitored at 225 nm. Most of the compounds tested provided IC50 values in the mM range towards ArgE, indicating that they are moderately strong inhibitors. ClAc-Orn-OH (1 g) was the best inhibitor tested towards ArgE providing an IC50 value of 85 mM. The TFAc- (1f) and EtOCO- (2b) Orn derivatives provided IC50 values of 200 and 250 mM, respectively. Ac-D-Orn-OH (1a) showed slight inhibition of ArgE providing an IC50 value of 410 mM. None of the compounds tested in Table 1 were inhibitors of DapE. Antimicrobial activity was tested qualitatively by the drop diffusion method on LB agar (SIGMA). Quantitative minimal inhibitory concentration (MIC) was established by following the growth of bacteria in suspension. The test organisms used were *Bacillus subtilis* 168 and *Escherichia coli*. Bacteria were grown in LB broth and in mid exponential phase added to a solution of the compounds tested, and incubated at 37 °C for 20 h in a final volume of 0.2 ml. Preliminary studies indicate a very weak inhibitory activity for N^{α}-substituents of Orn. The highest inhibitory potency was displayed by Ac-D-Orn-OH (1a), ClAc- (1g), DClAc- (1h), and TClAc-Orn-OH (1i) towards *Bacillus subtilis* 168 (Table 1). No inhibitory activity was detected towards *Escherichia coli*. These data correlate well with the IC50 values determined for ArgE, suggesting that i) these compounds are capable of getting across the cell membrane and ii) that ArgE is the bacterial enzymatic target.

Acknowledgements

This research was supported by the Research Project Z40550506, the Grant Agency of the Czech Academy of Sciences (No. IAA400550614) and the National Science Foundation (CHE-0652981, RCH).

Table 1. Analytical data and inhibitory activities of Orn 1a-1j, 2a-2f and DAP 3a-3d derivatives

Compound	Formula[a] Calc./found (m/z)	HPLC RT (min)[b]	ArgE IC50 (mM)	DapE	*B. subtilis* µg[c]
1a[d],R = CH_3	$C_7H_{14}N_2O_3$ 174.2/175.1	2.85	0.41 ± 0.1	f	26.0[e]
1b, R = $(CH_3)_3C$	$C_{10}H_{20}N_2O_3$ 216.3/217.1	11.02	~5.4	4.2	19.5[f]
1c, R = $(CH_3)_2CH$	$C_9H_{18}N_2O_3$ 202.3/203.1	11.22	1.21 ± 0.2	f	26.2[g]
1d, R = $CH_3(CH_2)_2$	$C_9H_{18}N_2O_3$ 202.3/203.1	11.12	0.42 ± 0.08	f	26.1[g]
1e, R = CH_3CH_2	$C_8H_{16}N_2O_3$ 188.2/189.1	7.05	0.76 ± 0.04	f	26.0[f]
1f, R = CF_3	$C_7H_{11}N_2O_3F_3$ 228.2/229.1	4.34	0.20 ± 0.04	f	23.9[e]
1g, R = CH_2Cl	$C_7H_{13}N_2O_3Cl$ 208.6/209.2	7.32	0.085 ± 0.007	f	21.7[e]
1h, R = $CHCl_2$	$C_7H_{12}N_2O_3Cl_2$ 243.1/243.9	7.41	0.34 ± 0.03	f	41.2[e]
1i, R = CCl_3	$C_7H_{11}N_2O_3Cl_3$ 277.5/278,9	7.68	0.45 ± 0.03	f	28.2[e]
1j[d], R = CCl_3	$C_7H_{11}N_2O_3Cl_3$ 277.5/278,9	7.72	0.32 ± 0.02	f	36.2[f]
2a, R = CH_3O	$C_7H_{14}N_2O_4$ 190.1/191.0	4.12	1.01±0.11	-	26.0[g]
2b, R = C_2H_5O	$C_8H_{16}N_2O_4$ 204.2/205.1	5.54	0.25±0.07	-	28.1[e]
2c, R = $(CH_3)_2CHCH_2O$	$C_{10}H_{20}N_2O_4$ 232.3/233.2	9.51	1.16±0.14	-	32.0[f]
2d, R = $(CH_3)_2CHO$	$C_9H_{18}N_2O_4$ 218.2/219.2	7.56	1.40±0.09	-	26.0[f]
2e, R = $CH_3(CH_2)_2O$	$C_9H_{18}N_2O_4$ 218.2/218.9	7.58	0.71±0.05	-	26.2[g]
2f, R = $(CH_3)_3CO$	$C_{10}H_{20}N_2O_4$ 232.3/233.3	9.17	0.54±0.05	-	29.0[g]
3a, R = CH_3	$C_9H_{16}N_2O_5$ 232.3/233.3	2.70	~ 2.63	17	h
3b, R = $HO_2CCH{=}CH$	$C_{11}H_{16}N_2O_6$ 272.2/273.2	9.38	~0.48	f	h
3c, R = $HO_2C(CH_2)_3$	$C_{12}H_{20}N_2O_6$ 288.38/229.2	3.77	~2.11	f	h
3d, R = $HO_2CCH_2C(CH_3)_2CH_2$	$C_{14}H_{24}N_2O_6$ 316.4/317.3	4.02	~1.28	f	h

[a] Determined with ESI MS technique; [b] For HPLC a TSP instrument with an SP 8800 pump, an SP 4290 integrator, TSP Spectra 100 UV detector and 5 µm Supelco 15 x 0.4 cm column, 20 min gradient 0-50% ACN in 0.05% TFA and for compounds **1a**, **2a-2d** an isocratic analysis with 0.05% TFA were used; [c] Maximal quantity of compound applied in agar plate; [d] Compound with D-Orn; [e] Weak inhibitor; [f] No inhibition; [g] Very weak inhibitor; [h] Measurement in progress.

References

1. Ledwidge R., Blanchard JS. *Biochemistry* **38**: 3019-3024, 1999.
2. Javid-Majd F, Blanchard JS. *Biochemistry* **39**: 1285-1293, 2000.
3. Lin YK, Myhrman R, Schrag ML, Gelb MH. *J Biol Chem* **263**: 1622-1627, 1988.
4. Bienvenue DL, Gilner DM, Davis RS, Bennett B, Holz RC. *Biochemistry* **42**: 10756-10763, 2003.
5. McGregor W, Swierczek SI, Bennett B, Holz RC. *J Am Chem Soc* **127**: 14100-14107, 2005.

1-01-143

Self-assembling Antimicrobial Cyclic Pseudopeptides including Aza-β³-Amino Acids

Laurencin, Mathieu[1,]; Legrand, Baptiste[2]; Mouret, Liza[2]; Zatylny-Gaudin, Céline[3]; Henry, Joël[3]; Bondon, Arnaud[2]; Fleury, Yannick[4]; Baudy-Floc'h, Michèle[1]*

[1]UMR CNRS 6226, Université de Rennes 1, ICMV, FRANCE; [2]UMR CNRS 6026, Université de Rennes 1, RMN-ILP, FRANCE; [3]UMR 100 IFREMER, Université de Caen Basse-Normandie, LBBM, FRANCE; [4]EA 3882, Université de Bretagne Occidentale., LUBEM, FRANCE

[*]E-mail: matam96@hotmail.com

Introduction

Antibiotic resistance of pathogens against conventional antibiotics is increasing at a rate that far exceeds the pace of new development of drugs. So, antimicrobial peptides, both synthetic and from natural sources, have raised interest as potential useful drugs in the future. Small antimicrobial cyclic hexapeptides completely composed of L-aminoacids[1] or alterning L and D aminoacids[2] had already been described with both bacteria and fungi activities. However, due to proteolytic degradation, peptides are not ideal candidates for pharmaceutical development. That is why numerous researches try to develop non natural peptidic analogues for enhancing metabolic stability, bioavailability, and biological absorption. In this class of peptidomimetics, pseudopeptides consisting exclusively or including aza-β^3-amino acids have emerged as a promising new class of compounds that favour hydrogen bond formation and can enhance biological activities when compared to natural parent peptides.[3] We have designed "mixed" cylic pseudopeptides composed of α- and aza-β^3-amino acids that target bacterial cell wall and induce the death of the pathogens.

Results and Discussion

In our laboratory, we have developed the synthesis of Fmoc-aza-β^3-amino acids those bear natural proteinogenic side chains (like aza-β^3-lysine) or hydrophobic non proteinogenic side chains specially designed for antimicrobial application (like aza-β^3-1-naphthylalanine). The synthesis of these cyclic pseudo-peptides is very suitable with automated solid phase synthesis in Fmoc chemistry. So, we can build and test a lot of different cyclic antimicrobial pseudopeptides. Among the twenty first synthesised cyclopseudopeptides, some of them have broad spectrum antibactericidal activities on gram positive and gram negative bacteria with low minimum inhibitory concentrations (MIC). On the other hand, this type of molecules is not hemolytic and cytotoxic at antimicrobial activity levels.[4]

Table 1. Structure and biological activities of cyclopseudopeptides P1 and P2. (MIC: Minimum Inhibitory Concentration in µM; ND: Not Determined)

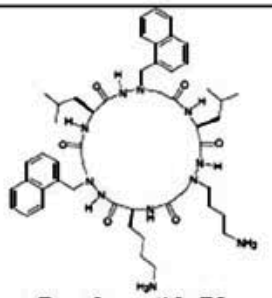

Pseudopeptide P1

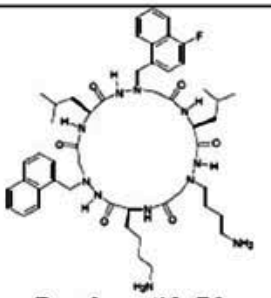

Pseudopeptide P2

	MIC 48h on *Staphylococcus aureus*	MIC 48h on *Enterococcus faecalis*	MIC 48h on *Streptococcus equinus*	MIC 48h on *Bacillus megaterium*	MIC 48h on *Escherichia coli*	MIC 48h on *Pseudomonas aeruginosa*	% Hemolysis at 100µM
P1	25	50	6,25	3,12	50	50	1,5
P2	12,5	25	6,25	3,12	25	25	5
melittin	25	12,5	3,12	6,25	6,25	50	100

Scheme 1: Schematic representation of possible interactions of antimicrobial cyclopseudopeptides.

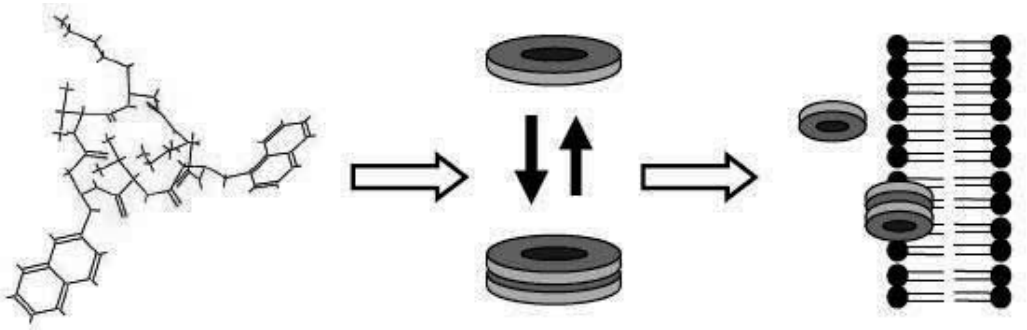

To explain the mechanism of action of our pseudopeptides that act on the microbial membranes we performed NMR studies. We have demonstrated that in solution cycles auto-associate at high concentrations and we investigate their behaviour in presence of small unilamellar lipidic vesicules (SUV).[5]

CD spectrum and fluorescence studies have revealed that cyclopseudopeptide P1 adopt a well defined structuration in presence of SDS micelles or anionic SUV and a stacking of bulky aromatic side chains in these conditions. Therefore this phenomenon of self-association seems to be facilitated at the lipid interface.

References

1. Dathe M, Nikolenko H, Klose J, Bienert M. *Biochemistry* **43**: 9140-9150, 2004.
2. Ferandez-Lopez S, Kim HS, Choi E, Delgado M, Granja Jr, Khazanov A, Kraehenbuehl K, Long G, Weinberger DA, Wilcoxen KM, Ghadiri MR. *Nature* **412**: 452-455, 2001.
3. Dali H, Busnel O, Hoebeke J, Bi L, Decker P, Briand J.P., Baudy-Floc'h M., Müller S. *Mol Immunol* **44**: 3024-3036, 2007.
4. Baudy-Floc'h M, Laurencin M, Zatylny-Gaudin C, Henry J. *CNRS Patent,* **N° 07/07108**, 2007.
5. Da Costa G, Mouret L, Chevance S, Le Rumeur E, Bondon A. *Eur Biophys J* **36**: 933-942, 2007.

1-01-144

Controlling α-helical secondary structure of oligopeptides and its use as a chiral catalyst

Tanaka, Masakazu[1,]; Nagano, Masanobu[1]; Demizu, Yosuke[1]; Doi, Mitsunobu[2]; Kurihara, Masaaki[3]; Suemune, Hiroshi[1]*

[1]Kyushu University, Graduate School of Pharmaceutical Sciences, JAPAN; [2]Osaka University of Pharmaceutical Sciences, JAPAN; [3]National Institute of Health Sciences, Division of Organic Chemistry, JAPAN

[*]E-mail: mtanaka@phar.kyushu-u.ac.jp

Introduction

Replacement of α-hydrogen atom of L-α-amino acids results in *α,α*-disubstituted amino acids. A *α,α*-disubstituted amino acid (dAA), a chiral *α*-aminoisobutyric acid (Aib), is well-known, and is widely used to construct helical secondary structures of oligopeptides.[1] Helical secondary structures constructed using Aib usually show not *α*-helices but 3_{10}-helices, which form an intramolecular hydrogen-bonding ring composed of ten atoms, and one helical turn consisting of three amino acid residues. We designed and synthesized a chiral cyclic *α,α*-disubstituted amino acid (*S,S*)-Ac(5)c(dOM), in which the *α*-carbon atom is not a chiral center but chiral centers existing at the side chain. Homooctapeptide composed of (*S,S*)-Ac(5)c(dOM) formed a left-handed α-helix both in solution and in the solid state.[2] Furthermore, when the cyclic amino acid (S,S)-Ac(5)c(dOM) was incorporated into L-Leu-hexapeptide, the hexapeptide Cbz-{L-Leu-L-Leu-(*S,S*)-Ac(5)c(dOM)}$_2$-OMe preferentially formed right-handed *α*-helices in the crystal state, whereas the hexapeptide Cbz-{L-Leu-L-Leu-Aib}$_2$-OMe having Aib formed a right-handed 3_{10}-helix.[3] The finding that the propensity of cyclic amino acid Ac(5)c(dOM) is to form *α*-helix over 3_{10}-helix, encouraged us to use the cyclic amino acid containing *α*-helical oligomer as an asymmetric catalyst for epoxidation.

Results and Discussion

We synthesized a chiral cyclic amino acid (*S,S*)-Ac(5)c(dOM) starting from dimethyl L-(-)-tartrate, and (1*S*,3*S*)-Ac(5)c(OM), which has one MeO substituent at the *γ*-position of cyclopentane, starting from L-malic acid. As helical peptides, we prepared L-Leu-based oligopeptides with cyclic amino acids: Boc-{L-Leu-L-Leu-dAA}$_n$-*O*Me {n = 1, 2, 3 and 4; dAA = (*S,S*)-Ac(5)c(dOM) or (1*S*,3*S*)-Ac(5)c(OM)} by solution-phase methods. Initially, we studied the preferred conformation of hexa-, nona-, and dodecapeptides using IR, ^{1}H NMR, and CD spectra. These oligopeptides seemed to preferentially form helical secondary structures in solution.

We examined the asymmetric epoxidation of chalcone using these helical oligopeptides as chiral catalysts. The α-helical polyleucine oligomer-catalyzed asymmetric epoxidation of chalcone was reported by Julia, Colonna and co-workers.[4] They studied the generality of substrates, reaction conditions, effect of the length of oligomers, and reaction mechanisms.[5] We performed the epoxidation of chalcone in THF from 0 °C to room temperature, using urea-H_2O_2 complex (1.3 eq.) as an oxidant, DBU (5.5 eq.) as a base, and 25 mol% of oligomer as a chiral catalyst. The epoxidation reaction proceeded smoothly, but the enantiomeric excess of product was maximal 40% ee when the oligomer Boc-{L-Leu-L-Leu-(*S,S*)-Ac(5)

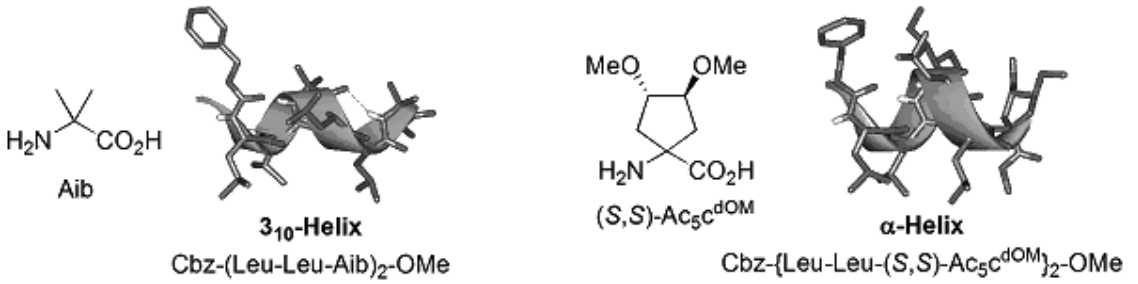

Figure 1. Structures of Aib and (*S,S*)-Ac(5)c(dOM), and helical structures.

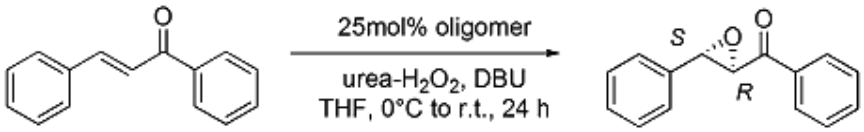

Figure 2. Julia-Colonna asymmetric epoxidation of chalcone.

c(dOM)}$_n$-OMe was used as a chiral catalyst. In contrast, the use of nonapeptide with (1*S*,3*S*)-Ac(5)c(OM) as a chiral catalyst afforded epoxide of good enantiomeric excess (>80% ee) in excellent chemical yield. The detailed results and the mechanisms of enantio-face selection will be reported elsewhere.

Acknowledgements

This work was supported in part by a Grant-in-Aid (B) from JSPS, by a Grant-in Aid for Scientific Research on Priority Areas (No. 20037054, "Chemistry of Concerto Catalysis E from MEXT, and also by a Grant-in-Aid from the ASAHI GLASS Foundation. The present address of Y.D. and M.T. is Nagasaki University. M.N. thanks the JSPS for Research Fellowships.

References

1. Karle IL, Balaram P. *Biochemistry* **29**: 6747-6756, 1990; Tanaka M. *J Synth Org Chem Jpn* **60**: 125-136, 2002.
2. Tanaka M, Demizu Y, Doi M, Kurihara M, Suemune H. *Angew Chem Int Ed* **43**: 5360-5363, 2004.
3. Demizu Y, Tanaka M, Nagano M, Kurihara M, Doi M, Maruyama T, Suemune H. *Chem Pharm Bull* **55**: 840-842, 2007; Tanaka M. *Chem Pharm Bull* **55**: 349-358, 2007.
4. Banfi S, Colonna S, Molinari H, Juli ES, Guixer J. *Tetrahedron* **40**: 5207-5211, 1984.
5. Kelly DR, Roberts SM. *Peptide Science* (Biopolymers) **84**: 74-89, 2006; Licini G, Bonchio M, Broxterman QB, Kaptein B, Moretto A, Toniolo C, Scrimin P. *Peptide Science* (Biopolymers) **84**: 97-104, 2006.

1-01-145

Helical-screw handedness of peptides composed of diastereomeric cyclic amino acids

Nagano, Masanobu[1,]; Tanaka, Masakazu[1]; Doi, Mitsunobu[2]; Kurihara, Masaaki[3]; Suemune, Hiroshi[1]*

[1]Graduate School of Pharmaceutical Sciences, Kyushu University, JAPAN; [2]Osaka University of Pharmaceutical Sciences, JAPAN; [3]National Institute of Health Sciences, JAPAN

[*]E-mail: nagano@lyra.phar.kyushu-u.ac.jp

Introduction

Helical-screw handedness in proteins is believed to result from the α-carbon chiral center of L-α-amino acids.[1] Recently, we have reported that the helical-screw sense of oligopeptides can be controlled without a chiral center on the peptide-backbone by chiral centers at the side chain; that is, we designed and synthesized an optically active cyclic α,α-disubstituted amino acid (*S,S*)-Ac(5)c(dOM), in which the α-carbon atom is not a chiral center but chiral centers exist at the side chain. Conformational analysis of the (*S,S*)-Ac(5)c(dOM) peptides revealed that the hexapeptide formed left-handed 3_{10}-helices, and the octapeptide assumed a left-handed α-helix both in solution and in the solid state.[2] On the other hand, homohexapeptide composed of chiral bicyclic amino acid; (*R,R*)-Ab(5,6=)c, in which chial centers similarly exist only at the side chain, formed both right-handed and left-handed 3_{10}-helical structures in solution and in the solid state.[3]

Herein we designed two new diastereomeric cyclic α,α-disubstituted amino acids; (1*S*,3*S*)- and (1*R*,3*S*)-1-amino-3-(methoxy)cyclopentanecarboxylic acid [Ac(5)c(OM)] having chiral centers both at the α-carbon atom and at the side chain, and studied the preferred conformation of their homopeptides.

Results and Discussion

The cyclic amino acids (1*S*,3*S*)- and (1*R*,3*S*)-Ac(5)c(OM) were synthesized starting from L-(-)-malic acid; that is, after esterification of malic acid, the secondary alcohol was converted to a methyl ether. Then, reduction of diester and iodination of alcohol gave a diiodide. Bisalkylation of dimethyl malonate with the diiodide gave a cyclic diester. Monohydrolysis of the diester, followed by Curtius rearrangement, produced separable mixtures of (1*S*,3*S*)- and (1*R*,3*S*)-Ac(5)c(OM). We prepared both diastereomeric (1*S*,3*S*)- and (1*R*,3*S*)-homooligomers by solution-phase methods, respectively. Conformational studies using 1H NMR, FT-IR, and X-ray crystallographic analysis revealed that the dominant conformation of (1*S*,3*S*)-Ac(5)c(OM) tetra- and hexapeptides was both right-handed and left-handed 3_{10}-helical stuructures in solution and in the solid state. Thus, (1*S*,3*S*)-Ac(5)c(OM) peptides seemed to have only a little bias for one-handed helical-screw sense. The detailed conformational analysis of elongated (1*S*,3*S*)-Ac(5)c(OM) homooligomers and (1*R*,3*S*)-Ac(5)c(OM) homooligomers will be reported elsewhere.

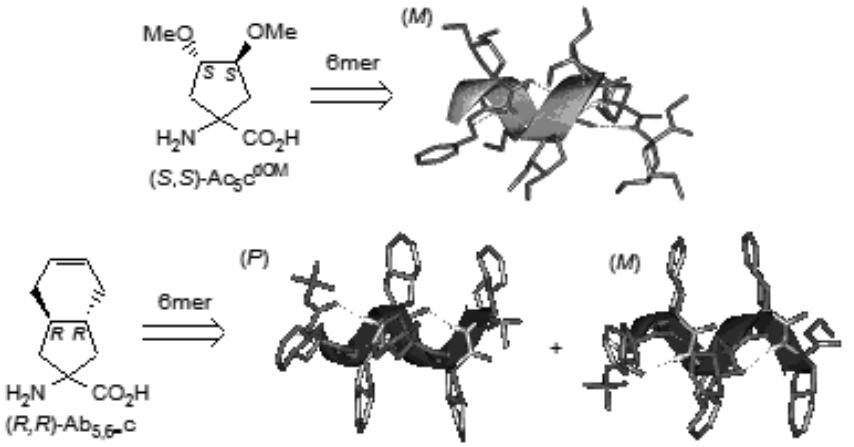

Figure 1. Secondary structures of peptides composed of chiral cyclic amino acids.

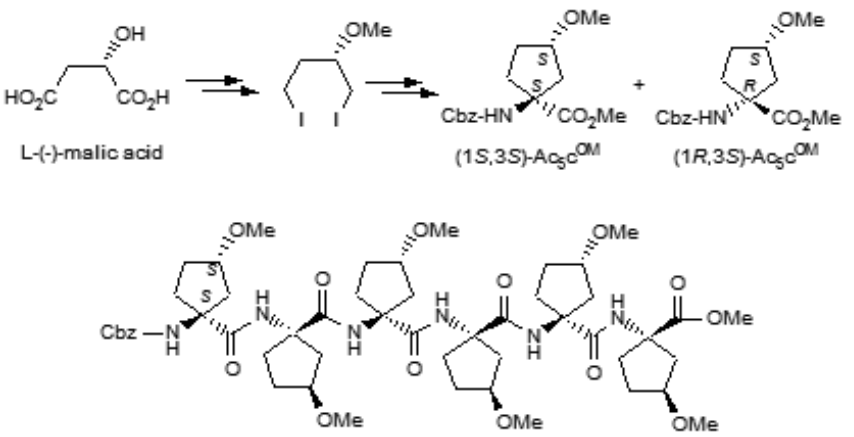

Figure 2. Synthesis of cyclic amino acids, (1*S*,3*S*)- and (1*R*,3*S*)-Ac(5)c(OM), and structure of (1*S*,3*S*)-Ac(5)c(OM) hexapeptide.

Acknowledgements

This work was supported in part by a Grant-in-Aid (B) from JSPS, a Grant-in Aid for Scientific Research on Priority Areas (No. 20037054, Chemistry of Concerto Catalysis) from MEXT, and also by a Grant-in-Aid from the ASAHI GLASS Foundation. The present address of M.T. and Y.D. is Nagasaki University. M.N. thanks the JSPS for Research Fellowships.

References

1. Branden C, Tooze J. *Introduction to Protein Structure*, Garland, New York, 1991, p 1.
2. Tanaka M, Demizu Y, Doi M, Kurihara M, Suemune H. *Angew Chem Int Ed* **43**: 5360-5363, 2004.
3. Tanaka M, Anan K, Demizu Y, Kurihara M, Doi M, Suemune H. *J Am Chem Soc* **127**: 11570-11571, 2005.

1-01-146

Multi-tethered and orthogonally protected piperazine, diazepane and pyrrolidone building blocks for fast "around-the-scaffold" drug design

Gellerman, Gary[1,]; Hazan, Eran[1]; Kovaliov, Marina[1]; Albeck, Amnon[2]; Shatzmiler, Shimon[1]*

[1]Ariel University Center of Samaria, Dep. of Biological Chemistry, ISRAEL; [2]Bar Ilan University, Dep. of Chemistry, ISRAEL

[*]E-mail: garyg@ariel.ac.il

Introduction

Piperazines, diazepanes and their keto analogs are amongst the most important scaffolds in today's drug discovery. In recent years combinatorial chemistry around these core structures has become an important tool for generation of new lead structures in drug discovery processes and it gives access to diverse chemical entities with novel structures and properties.[1] The libraries of small molecules are generally prepared on solid support, simplifying tedious purification steps of the intermediates and facilitating the entire synthesis.

The piperazine, diazepane and pyrrolidone templates are defined in medicinal chemistry as a "privileged scaffold" - molecular backbone with versatile binding properties representing a frequently-occurring binding motif, and providing potent and selective ligands for a wide range of biological targets.[2,3]

Apparently, the majority of the methodologies are not stereospecific and complex mixtures of stereoisomers are generated.[4]

The strategy that we chose to overcome this obstacle is to use the "privilege" backbone, initially prepared in optically pure form, bearing various tethers with orthogonally protected groups applicable via Solid Phase Organic Chemistry (SPOC). Such approach preserves the important chiral centers and the related diversity in potential hits.

Here we report on synthesis of novel "privileged" core structures containing 2-ketopiperazine, DKP, 2-kediazepane and even 2-aminopyrrolidone motifs of the general structures I-V respectively (Scheme 1). These chiral building blocks can be applied in "around-the-scaffold" modification strategy and efficient multi-cyclic optimization processes by SPOC in Fmoc (Fmoc/ Alloc/ protection) mode, introducing valuable physico-chemical properties in three independent diversity points yielding compounds amenable to Lipinski rule of five and ADMETox requirements.[5] Furthermore, being chiral and controllable in the length and the nature of the side arms, our scaffolds will likely yield piperazine, diazepane and pyrrolidone libraries with high-resolution coverage of medicinal space around these privileged motifs.

Scheme 1

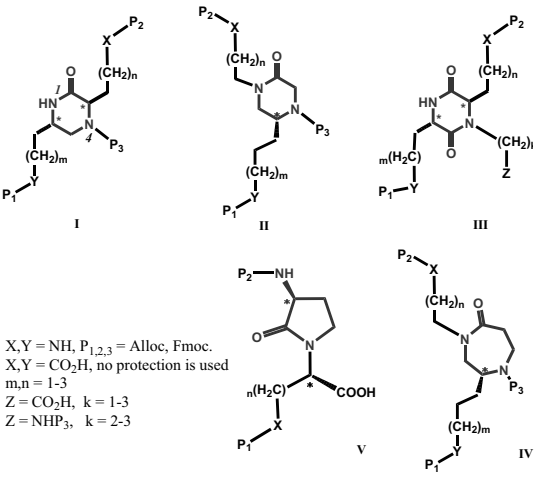

Results and Discussion

The orthogonally protected multi-tethered, optically pure 2-ketopiperazine, DKP, 2-ketodiazepane and 2-aminopyrrolidone scaffolds for Fmoc combinatorial chemistry presented in the work are prepared from accessible chiral amino acid precursors, by sequentially applying reductive alkylation, dipeptide coupling and regioselective ring formation.[6,7] The synthetic routs reported in this work are general and applicable for preparation of diverse scaffolds controlling chirality, arm position and length. In addition, the nature of functional moieties at the arms and protection mode for further diversification in three independent directions can be determined. The key step of the synthesis involves standard reductive alkylation between optically pure amino acid synthons (Scheme 2) that bear suitable protecting groups for Fmoc solid phase synthetic methodologies. Subsequent ring closure in the intermediate compounds, followed by Boc removal and Fmoc protection, afforded the desired scaffolds. All intermediates as well as final compounds were characterized (MS, IR, H^1&C^{13} NMR, COSY, EA) and in some cases were even used in the next step without purification (reductive alkylation). The compounds were purified by flash chromatography (petrol ether/ethyl acetate/MeOH) on silica gel yielding usually yellowish or colorless oils. The final compounds were obtained in reasonable overall yields (36% - 52%). The synthetic routes and techniques are simple and convenient

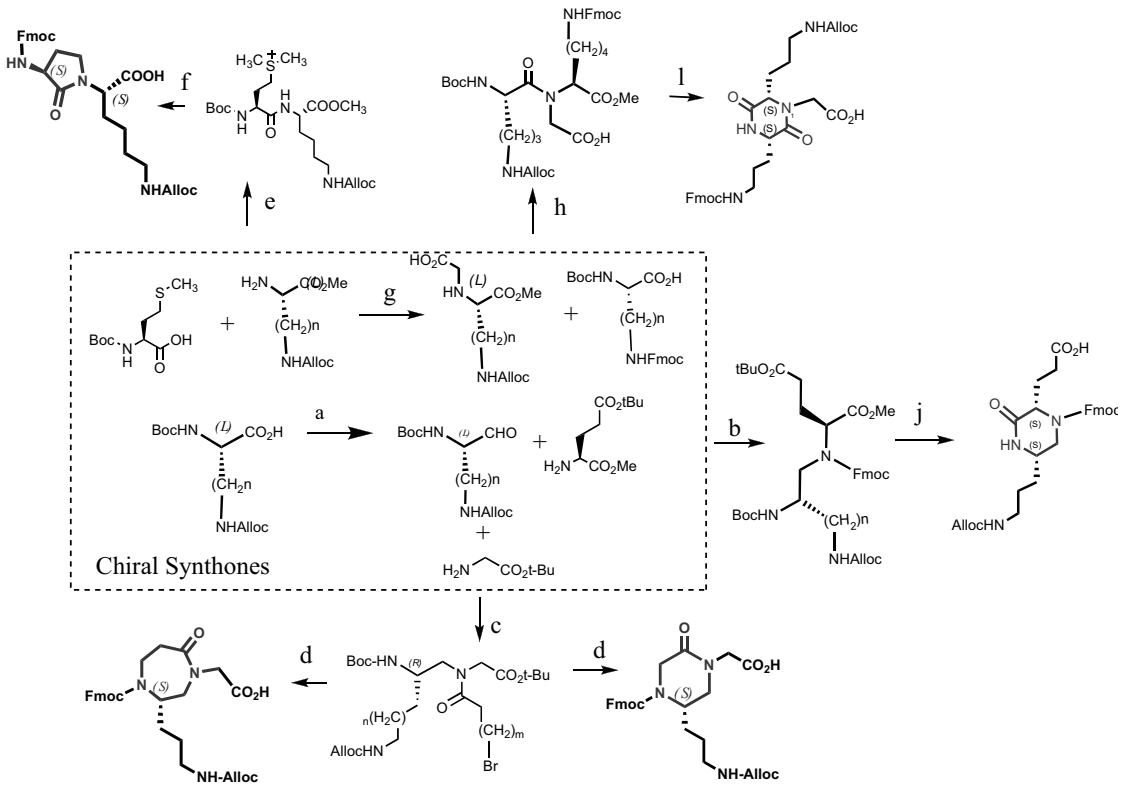

Scheme 2 a. (1) NH(OMe)Me, i-BuOCOCl, NMM, THF, RT, 18 h; (2) $LiAlH_4$, THF, RT; **b.** (1) $NaBH_3CN$, AcOH, MeOH, 1:99; RT; (2) Fmoc-Cl, TEA, DCM, 0 °C-RT, over night; j. (1) TFA, DCM (1:1), 0 °C-RT, 2h; (2) TEA, 2-butanol:Toluene (4:1), refluxe, 18 h; **c.** (1) Na(Ac)3BH, DCE, 4A M.S, N_2, 0 °C, over night.; (2) $ClCO(CH_2)mBr$, aq.EtOAc- $NaHCO_3$, 0 °C, 20 min; d (1) Cs_2CO_3, DMF, 65 °C, 2 h; **d.** DCM/TFA, 1 h; (2) DCM, 0 °C, DIPA, Fmoc-Cl. over nigh; **e.** (1) DIC, HOBT: (2): CH3I: **f.** (1): NaH, DMF/CH2Cl2 1:1: (2): Formic acid 98%: (3) FmocCl, DIEA, DCM; **g.** $HCOCO_2H$, NaCNCH3, MeOH:AcOH (99:1), RT, 24 h; **h.** HATU, TEA, DMF, 60 °C, 6 h; l. (1) 4N HCl in dioxane, 0 °C, 24 h; (2) NMM, 2-butanol, refluxe, 10 h

and can be applicable in preparation of other medicinally relevant building templates like benzodiazepine, diazocane, thiazinane their keto derivatives. Our goal is to prepare sufficient "pool" of these building blocks for its implementation in fast convergent "around-the-scaffold" drug discovery.

References

1. Thorpe DS. Combinatorial chemistry: starting the second decade. *Pharmacogenomics J* **1**: 229–233, 2001.
2. (a) Fischer PM. Diketopiperazines in peptide and combinatorial chemistry. *J Pept Sci* **9**: 9–35, 2003; (b) Dinsmore CJ, Beshore DC. Recent advances in the synthesis of diketopiperazines. *Tetrahedron* **58**: 3297-3312, 2002. (c). Shorvon S. Pyrrolidone derivatives. *Lancet* **358**: 1885-1892, 2001.
3. Szardenings AK, Burkoth TS, Campbell DA. A simple procedure for the solid phase synthesis of diketopiperazine and diketomorpholine derivatives. *Tetrahedron* **53**: 6573-6593, 1997.
4. Doemling A. Convergent and Fast Route to Piperazines via IMCR. *Org Chem Highlights* **2005**, June 5, 1-8.
5. Walters WP, Murko AA, Murko MA. Recognizing molecules with drug-like properties. *Curr Opin Chem Biol* **3**: 384-387, 1999.
6. Gellerman G, Elgavi A, Salitra Y, Kramer M. Facile synthesis of orthogonally protected amino acid building blocks for combinatorial N-backbone cyclic peptide chemistry. *J Pept Res* **57**: 277-291, 2001.
7. (a) Gazal S, Gellerman G, Gilon C. Novel Gly building units for backbone cyclization: synthesis and incorporation into model peptides. *Peptides* **24**: 1847–1852, 2003; (b) Gellerman G, Hazan E, Albeck A, Shatzmiler S. Facile Synthesis of Orthogonally Protected Optically Pure Keto- and Diketopiperazine Building Blocks for Combinatorial Chemistry. *Int J Pept Res Ther* **14**: 183-192, 2008.

1-01-147

The studies on the solid phase synthesis and selective detection of peptide-derived Amadori products by mass spectrometry

Kapczynska, Katarzyna; Stefanowicz, Piotr; Kijewska, Monika; Pasikowski, Pawel; Szewczuk, Zbigniew*

University of Wroclaw, Faculty of Chemistry, POLAND

**E-mail: stp@chem.uni.wroc.pl*

Introduction

Peptide- and proteins-derived Amadori products attract an increasing attention as the negative consequences of glycation are more frequently diagnosed and better understood. Structural proteins with a long turnover time, like collagen and crystalline,[1] as well as relatively short-lived hormones and regulatory peptides[2,3] undergo the process of glycation *in vivo*. Therefore, glycated proteins and especially their fragments could be used as markers of diabetes mellitus, the aging process, and Alzheimer's disease. The dynamic progress in the studies on the biochemical consequences of the Maillard reaction requires the development of a fast, convenient, and general method of glycated peptides synthesis and analysis.

Results and discussion

Several procedures of site selective peptide-based Amadori products synthesis have been published recently.[4,5] We designed and optimized a novel strategy of peptide-derived Amadori products synthesis on the solid support. This method uses a fully protected lysine derivative (*Nα*-9-fluorenylmethoxycarbonyl-*Nε*-tert-butyloxycarbonyl-*Nε*-*N*-(2,3:4,5-di-*O*-isopropyliden-1-deoxy-*β*-D-fructopyranose-1-ylo)lysine, Fmoc-Lys(*i,i*-Fru,Boc)-OH), which is a building block permitting to introduce the glycated lysine moiety into the peptide chain according to the standard Fmoc protocol. Cleavage time was extended to 8 hours because of the lower isopropylidene groups lability in comparison to other protecting groups used in the Fmoc protocol (Fig. 1). Therefore, the new procedure does not require a high temperature and gives good yields and relatively pure products free of diglycated peptides which are difficult to separate because retention times of mono-, di- and nonglycated peptides are similar. A series of glycated polypeptides derived from fragments of bovine serum albumin were obtained by the standard Fmoc protocol. Analytical data are shown in the Table 1. The glycation site and the structure were confirmed by electrospray mass spectrometry and enzymatic hydrolysis. Using synthetic peptide-derived Amadori products we developed a new and straightforward method of selective detection of these compounds in the complex mixtures. The proposed approach is based on the convolution mapping analysis[6] modified by using more than one neutral loss for a particular molecule. Such mathematical operations on mass spectra allow to reveal the signal originated from a peptide-derived Amadori product and to identify it. This approach gives the results similar to those obtained by neutral loss scanning but it is free of the triple quadrupol mass spectrometers' disadvantages, namely relatively low sensitivity in the scan mode.

Table 1. Analytical data of synthetic peptide-derived Amadori products

GLYCATED PEPTIDE	R_t [min][a]	Crude yield [%]	HPLC purity [%][b]	Formula / Predominant ion	*m/z* calc/ found[c]
DTISK(Fru)LKE	16.50	78.9	85	$[MH_2]^{2+}$	591.8092 / 591.8110
Ac-NDTISK(Fru)LKE	17.17	78	88	$[MH_2]^{2+}$	676.8438/ 676.8457
DTISKLK(Fru)E	13.00	88.1	92	$[MH_2]^{2+}$	690.8650/ 690.8623
DTEK(Fru)NIK(Fru)KNT	12.83	87.1	83	$[MH_2]^{2+}$	771.8914/ 771.8913

[a] C18 column Vydac (250x4.6 mm): gradient 0–80% B in A in 60 min, A: water+0.1% TFA, B: acetonitrile+0.1% TFA.
[b] Purity based on the integral of the crude product absorption at λ 220 nm on RP-HPLC.
[c] ESI-MS spectrum, MicrOTOFQ (Bruker Daltonics).

References

1. Jerums G, Panagiotopoulos S, Forbes J, Osicka T, Cooper M. *Arch Biochem Biophys* **419:** 55-62, 2003.
2. McKillop AM, Abdel-Wahab YH, Mooney MH. *Diabetes Metab* **28:** 61-69, 2002 .
3. McKillop AM, Abdel-Wahab YH, Mooney MH, O'Harte FP, Flatt PR. *Regulatory Peptides* **113:** 1-8, 2003.
4. Stefanowicz P, Kapczyńska K, Kluczyk A, Szewczuk Z. *Tetrahedron Lett* **48:** 967-969, 2007.
5. Frolov A, Singer D, Hoffmann R. *J Pept Sci* **12:** 862-867, 2007.
6. Hoffman MD, Sniatynski MJ, Rogalski JC, Yves Le Blanc JC, Kast J. *J Am Soc Mass Spectrom* **17:** 307-317, 2006.

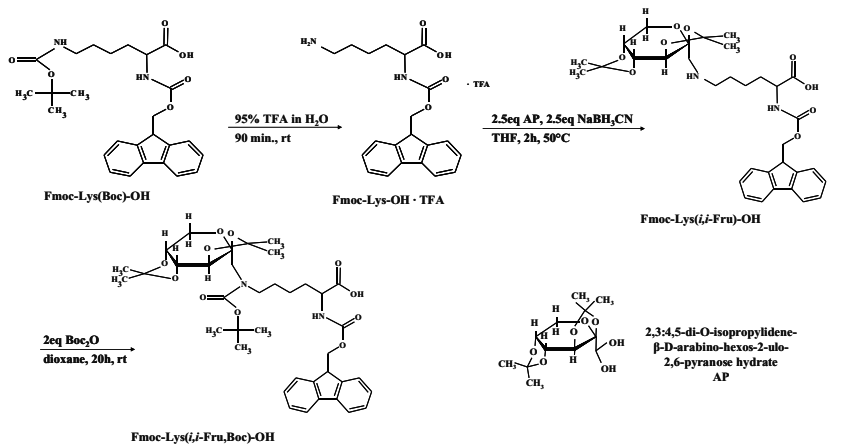

Figure 1. *Synthesis of Fmoc-Lys(i,i-Fru,Boc)-OH*

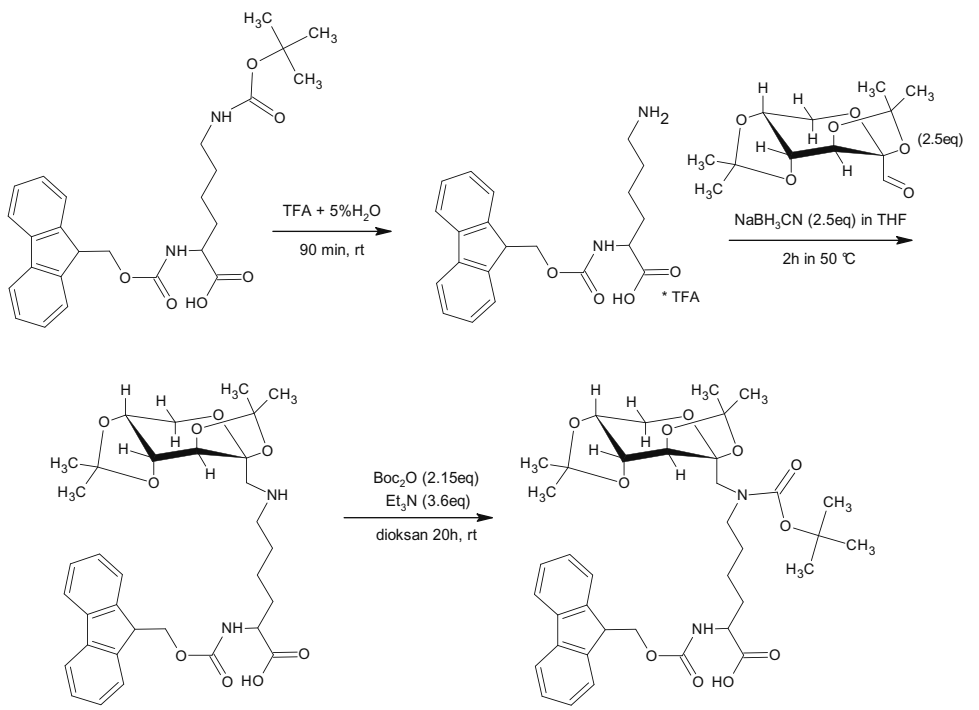

1-01-148

Synthesis, modeling studies and biological activities of a non-peptide AT_1 receptor angiotensin II

Agelis, George[1]; Matsoukas, Minos-Timotheos[1,]; Resvani, Amalia[1]; Kelaidonis, Konstantinos[1]; Keppa, Pasxalina[1]; Tselios, Theodore[1]; Vlahakos, Demetrios[2]; Matsoukas, John M[1]*

[1]University of Patras, Chemistry, GREECE; [2]"ATTIKON" University Hospital, GREECE

[*]E-mail: minws13@hotmail.com

Introduction

The Renin-Angiotensin System (RAS) plays a significant role in blood pressure regulation. A sequence of enzyme reactions leads to the release of Ang II, an octapeptide which is characterized by numerous biological aspects. Ang II is a drastic vasoconstrictor, as well as a growth factor implicated in cardiac, and vascular hypertrophy. Most of the known physiological actions of Ang II are mediated by the AT_1 receptor which is part of the G protein-coupled receptor family, and has been extensively studied towards its structural characteristics and 3D model. Interactions between AT_1 and Ang II have been recorded over the years based on binding experiments using mostly radiolabeled Ang II and the receptor itself, expressed in culture cells.

Structure Activity Relationships (SAR)[1] and Molecular Modelling studies on Losartan and Ang II led to design and synthesis of V8, a potent non-peptide AT_1 receptor antagonist, bearing the basic pharmacophoric groups (imidazole, tetrazole, phenyl).

Results and Discussion

This research focuses on the conformational properties of the analogue V8 that differ in the substitution pattern around the imidazole ring when compared to Losartan[2,3]. Thus, the alkyl chain and hydroxymethyl group possess different topographical position in an attempt to optimize the mimicry of lipophilic superimposition of the butyl chain with isopropyl group of Ile[5] in AngII and to probe the significance of the position of hydroxymethyl group.

The representative conformers were generated using the Grid Scan method. The final lower energy conformations were grouped into clusters using the root mean square (RMSD) energy convergence criterion. Populations of the various conformers that represent local minima at the potential energy surface were identified and obtained from each cluster. Global minima was compared and superimposed with EXP3174, Losartan's bioactive conformation (Fig. 1). Molecular Modeling Simulations and SAR studies indicate that reorientation of butyl and hydroxymethylene groups on the imidazole template of Losartan retains high binding to AT_1 receptor as prototype compound and that the spacing of these substituents are of primary importance.The antagonist V8 seems to have similar potency with Losartan in our *in vivo* and *in vitro* biological studies (Fig. 2).

In conclusion, high potency, short regioselective and cost effective synthesis renders compound V8 as attractive candidate for advanced toxicological evaluation as a drug against hypertension and cardiovascular diseases.

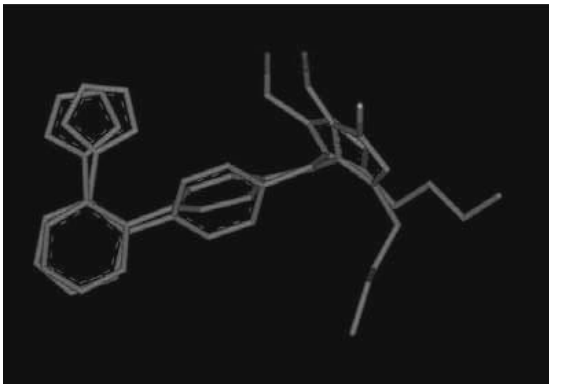

Figure 1. Superimposition between global minimum structure and Losartan.

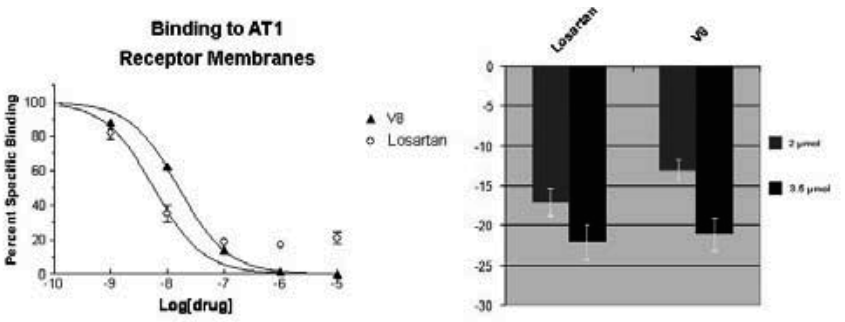

Figure 2. Binding affinity of V8 and Losartan to AT_1 receptor and percentage changes in mean blood pressure of each compound in anesthetized rabbits made hypertensive by constant infusion of AngII.

Acknowledgments

Present work was supported by the Ministry of Development, General Secretariat for Research and Technology (Grant PRAXE B) and ELDRUG SA.

References

1. Matsoukas JM, Agelis G, Wahhab A, Hondrelis J, Panagiotopoulos D, Yamdagni R, Wu, Q, Mavromoustakos T, Maia LHLS, Ganter R, Moore GJ. *J Med Chem* **38**: 4660-4669, 1995.
2. Duncia JV, Chiu AT, Carini DJ, Gregory GB, Johnson AL, Price WA, Wells GJ, Wong PC, Calabrese JC. *J Med Chem*, **33**: 1312-1329, 1990.
3. Wexler RR, Greenlee WJ, Irvin JD, Goldberg MR, Prendergast K, Smith R.D, Timmermans PBMWM. *J Med Chem* **39**: 625-656, 1996.

1-01-149

Synthesis of human and rat obestatin

Seytablaeva, Sevil; Titov, Mikhail I*

St Petersburg State University, Chemical Department, RUSSIAN FEDERATION

**E-mail: s-sevil@yandex.ru*

Abstract

We describe and compare two various schemes of synthesis of rat and human obestatins by both solid-phase and solution methods.

Introduction

Obestatin is a recently described 23 amino-acids peptide derived from preproghrelin. It was identified by bioinformatic prediction.[1] Obestatin decreases food intake and body weight gain, decelerates gastric emptying, promotes sleep in rat,[2] inhibits water drinking.[3]
The sequence of corresponding **rat** obestatin:
HPheAsnAlaProPheAspValGlyIleLysLeuSerGlyAlaGln
TyrGlnGlnHisGlyArgAlaLeuNH$_2$
differs from **human obestatin** by three amino acids:
HPheAsnAlaProPheAspValGlyIleLysLeuSerGly
ValGlnTyrGlnGlnHisSerGlnAlaLeuNH$_2$.

Materials and methods

N$^{\alpha}$-Fmoc-protected amino-acids, 1-hydroxybenzotriazole (HOBt), *N,N'*-diisopropilcarbodiimid (DIC), 2-chlorotrityl chloride resin were purchased from Iris Biotech GmBH (Germany).

Peptides synthesis and purification. Stepwise synthesis of fragments was carried out using the orthogonal Fmoc/ tBu strategy utilizing a 2-chlorotrityl-chloride resin with DIC/ HOBt. Completeness of the reaction was monitored by the Kaiser test and the Bromphenol Blue test. C-terminal amino-acid of each fragment was loaded on the 2-chlorotrityl chloride resin in DCM in the presence of excess DIPEA, unreacted functional sites were capped with methanol, again in presence base. The fragment was built using standard solid phase chemistry by removing the N-terminal Fmoc group with diethylamine in DMF for 20 min and then adding a solution of the next Fmoc amino-acid (2-times excess) that has been preactivated with DIC/HOBt. The fragments were cleaved from resin using 1% TFA in DCM. Peptide fragments were precipitated by the addition of water and isolated in high yield by filtration. The purity of cleaved fragments was monitored by analytical reversed-phase HPLC and MALDI-TOF-MS (Table 1).

Thus we have obtained by solid-phase peptide synthesis following fragments:

BocPheAsn(Trt)AlaProPheAsp(OBu^t)ValGlyOH
FmocIleLys(Boc)LeuSer(Bu^t)GlyOH
FmocValGln(Trt)Tyr(But)Gln(Trt)GlnHis(Trt)Ser(Bu^t)
Gln(Trt)AlaOH
FmocAlaGln(Trt)Tyr(Bu^t)Gln(Trt)GlnHis(Trt)GlyArg
(Pbf)AlaOH.
Fragments H-AA14-23-NH$_2$ were synthesized in solution (Fig. 1).

Results and Discussion

Synthesis of obestatins was developed on the basis of solution and solid phase synthesis of protected peptide fragments followed by their assembly into the final product in solution (Scheme 1) or using solid phase and further condensation with H-Leu-NH$_2$ in solution (Schemes 2).

The solution assembly begins with the coupling of H-AA14-23-NH$_2$ to the C-terminus of Fmoc-AA9-13-OH using DCC/ HOBt. The Fmoc-group was removed and the amine product was isolated by precipitation with diethyl ether. The full-length peptides were achieved by coupling H-AA9-23-NH$_2$ with Boc-AA1-8-OH (Fig. 2). The free peptides were obtained by treating the protected peptide with mixture of TFA:H$_2$O:TIPS (95:2.5:2.5) for 2 h at room temperature. Products were purified on a Knauer HPLC system (WellChrom HPLC-Pump K-1800,

Table 1.

Peptides	Expected MW	Found MW
HPheAsnAlaProPheAspValGlyOH	865.95	865.4
HIleLysLeuSerGlyOH	516.64	516.2
HValGlnTyrGlnGlnHisSerGlnAlaOH	1088.15	1088.1
HAlaGlnTyrGlnGlnHisGlyArgAlaOH	1058.13	1057.9
Obestatin-rat	2516.89	2516.3
Obestatin-human	2546.67	2546.3

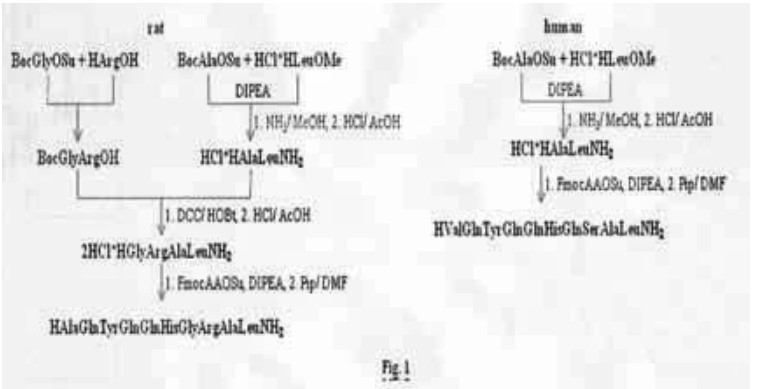

Fig. 1

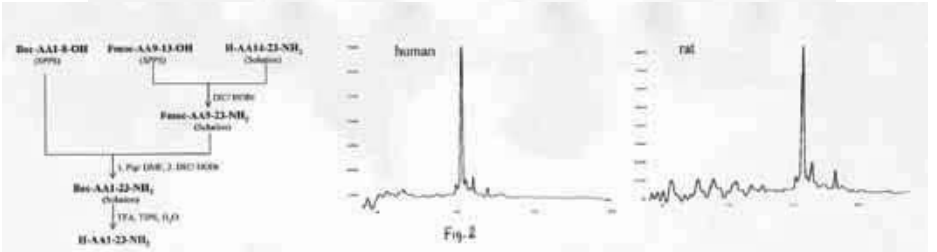

Fig. 2

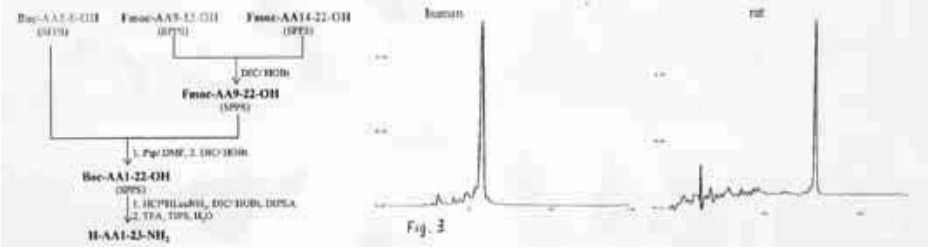

Fig. 3

UV Detector 2500) with column Diasorb-130-C 16T (50 ~250 mm; 11 μm) from BCM using a linear gradient of 10-50% B in A [A, 0,1% (vol/vol) TFA in water; B, 0,1% (vol/vol) TFA in acetonitrile] over 120 min and a flow rate of 60 ml/min for rat obestatin and linear gradient of 35-80% B in A [A, 0,1% (vol/vol) TFA in water; B, 0,1% (vol/vol) TFA in acetonitrile] over 120 min and a flow rate of 60 ml/min for human obestatin, and isolated by lyophilization with 32% yield and over 95% purity (rat) and 35% yield and over 95% purity (human). The major peak was assigned to desired peptide based on its mass as determined by MALDI-TOF-MS (Table 1).

The solid phase assembly begins with the coupling of Fmoc-AA9-13-OH (3-times excess) to H-AA14-22-OH loaded on 2-chlorotrityl chloride resin (loading: 0, 16 mmol/g) using DIC/ HOBt. The Fmoc- group was removed, after washing of loaded resin Boc-AA1-8-OH was coupled to H-AA9-22-OH. The fragment Boc-AA1-22-OH was cleaved from resin using 1% TFA in DCM. The full-length peptide was achieved by coupling of Boc-AA1-22-OH with $HLeuNH_2$ (4-times excess) using DIC/ HOBt in solution (Fig. 3). The free peptides were obtained by treating the protected peptides with mixture of TFA:H_2O:TIPS (95:2,5:2,5) for 2 h at room temperature. Peptides were purified on a Knauer HPLC system (WellChrom HPLC-Pump K-1800, UV Detector 2500) with column Diasorb-130-C 16T (50 ~250 mm; 11 μm) from BCM using a linear gradient of 35-80% B in A [A, 0,1% (vol/vol) TFA in water; B, 0,1% (vol/vol) TFA in acetonitrile] over 120 min and a flow rate of 60 ml/min for human obestatin and linear gradient of 15-50% B in A [A, 0,1% (vol/vol) TFA in water; B, 0,1% (vol/vol) TFA in acetonitrile] over 120 min and a flow rate of 60 ml/min for rat obestatin, and isolated by lyophilization with 54% yield and over 95% purity (human) 58% yield and over 95% purity (rat). The major peak is assigned to desired peptide based on its monoisotopic mass as determined by MALDI-TOF (Table 1).

References

1. Zhang JV, Ren PG, Avsian-Kretchmer O, Luo CW, Rauch R, Klein C, Hsueh AJ. Obestatin, a peptide encoded by the ghrelin gene, opposes ghrelin's effects on food intake. *Science* **310**: 996-999, 2005.
2. Szentirmai E, Krueger JM. Obestatin alters sleep in rats. *NeuroScience Lett* **404**: 222-226, 2006.
3. Samson WK, White MM, Price C, Ferguson AV. Obestatin acts in brain to inhibit thirst. Water and electrolyte homeostasis. *Am J Physiol Regul Integr Comp Physiol* **292**: R637-R643, 2007.

1-02-150

Versatile methods for synthesizing acyl-tetramic acids peptide analogs.

Davidov, Gali[1]; Mozes, Tamar[1]; Khandadash, Raz[1]; Diestel, Randi[2]; Sasse, Florenz[2]; Byk, Gerardo[1,]*

[1]Bar Ilan University/Dept. of Chemistry, Laboratory of Nano-Biotechnology, ISRAEL; [2]Department of Chemical Biology, Helmholtz Centre for Infection Research, GERMANY

[*]E-mail: bykger@mail.biu.ac.il

Introduction

C-3 Acyl-tetramic acids are key structural motifs in many natural products.[1-5] They exhibit a wide range of biological activities including antibiotic, antiviral, antifungal, cytotoxic and enzyme inhibitory activities. Thus, the synthesis of such compounds represents a worthwhile and challenging goal for the organic chemist. In this work we have improved significantly the acylation of tetramic acid derivatives in solution using microwave allowing the access to a variety of acyltetramic derivatives. Additionally, we present here a new solid phase mircrowave assisted synthesis of acyl-tetramates on pre-synthesized peptides and amino acids. Preliminary biological data indicates that some derivatives are potential candidates for anti-cancer treatment.

Results and discussion

1.a Acylation of tetramic acid in solution and generation of a new tetramic acid analog scaffold: Acylation of tetramic acid is usually performed in a two steps process through Fries rearrangement using DCC as reagent.[6] We have changed DCC by BOP reagent and carried out the reaction under microwave energy (Biotage Initiator station), our procedure have shortened the reaction time to 25 min. at 800 °C in dichloromethane (Fig. 1A).

1.b Acylation of tetramic acid analogs using diglycolic anhydride to form a scaffold building block: This acylation was carried out using a slightly different method. Diglycolic anhydride was directly reacted in solution with various tetramic acid derivatives adding DMAP and TEA (one equivalent of each component). The reaction was performed under microwave energy and was shortened from 25 to 5 min for Val and Leu scaffold, and 10 min for Phe scaffold, at 800 °C. This strategy opens the gate to acyl-tetramate building blocks that can be directly coupled to peptides as any classical amino acid.

2. Acylation of tetramic acid on solid phase: In order to extend the scope of our improved acylation methodology we have developed a synthetic protocol for generating the acyl-tetramic function on solid support. For this purpose, amino acids or peptides were synthesized on the solid support and reacted with diglycolic anhydride at their N-terminus. The tetramic acid was acylated by treating the solid supported diglycolic-acid-peptide/amino acid with a series of tetramic acids using BOP reagent under microwave energy (Fig. 2).

3. Coupling of the building block scaffold to aliphatic amines: In order to demonstrate the versality of the new building blocks, they were coupled in solution to aliphatic amines hexylamine and tetradecylamine, activated by BOP and TEA in acetonitrile solution at room temperature, interestingly the boc protecting group spontaneously cleaved during purification and the final products were always unprotected (Table 1). Additionally, building blocks were coupled to solid supported peptide Arg-Arg-Lys-Lys using conventional BOP coupling to generate acyl-tetramic-peptides (Table 1).

3. Biological assays: derivative TMM-1062 was active against L929 (IC50: 23 µg/ml). Compound GLD-1031A showed slight antibacterial activities, and cytotoxic activity against both mammalian cell lines. The IC50 of GLD-1031A ranged between 18 and 30 µg/ml. Phenotypic screening with GLD-1031A showed a striking alteration of the Endoplasmic Reticulum network (Fig. 3).

Conclusions

We have shown the improved synthesis of acyltetramic analogs by two strategies, the first includes the improvement of the acylation process by using BOP reagent combined with the use of microwave energy for the acylation. This strategy was demonstrated by the acylation on solid pahse of solid supported amino acids and peptides. The second strategy includes the generation of a new acyl-tetramic acid building block scaffold that was coupled to amines, amino acids and peptides in solution and solid phase to generate new analogs bearing the acyl-tetramate scaffold. The products were preliminary tested for toxicity of different cancer cell lines and some of them demonstrated a potential for cancer therapy.

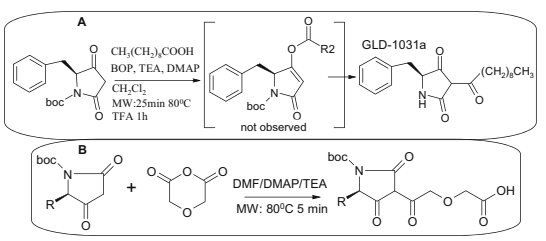

Figure 1. *Microwave assisted synthesis of acyltetramic acid derivatives*. A: improvement of classical procedure. B: Acylation of tetramic acid using diglycolic anhydride to generate building blocks. R= i-Pr; i-Bu; Bn.

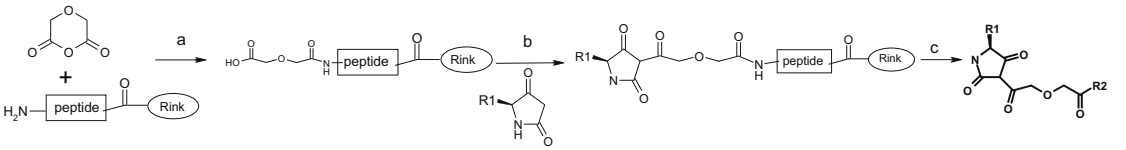

#	R1	R2	#	R1	R2
GLD-1081	Bn	Ala-NH_2	GLD-1158	i-Pr	Gly-NH_2
GLD-1146	Bn	Gly-NH_2	GLD-1159	i-Pr	Ala-NH_2
GLD-1148	Bn	Val-NH_2	GLD-1213	i-Pr	Phe-NH_2
GLD-1163	Bn	Phe-NH_2	GLD-1204	H	Gly-NH_2
GLD-1151	i-Bu	Gly-NH_2	GLD-1208	H	Ala-NH_2
GLD-1156	i-Bu	Ala-NH_2	GLD-1207	H	Phe-NH_2
GLD-1112	i-Bu	Phe-NH_2	GLD-1211	H	Val-NH_2
GLD-1211	i-Bu	Val-NH_2	GLD-1126	i-Bu	Arg-Arg-Lys-Lys-NH_2
GLD-1157	i-Pr	Val-NH_2	GLD-1092	Bn	Arg-Arg-Lys-Lys-NH_2

Figure 2. Upper panel: Solid phase synthesis of a series of acyltetramic acid amino acids and peptides. a) DMF/diglycolic anhydride/DMAP/TEA 1 h; b) DMF/tetramic acid analog/BOP/DMAP microwave 800 °C/25 min; c) TFA/DCM (1:1) 1 h, filtration. Lower panel: synthesized products with their R1 and R2 values.

Table 1. *Use of acyltetramic building block in solution and solid phase.* Reaction and list of synthesized compounds

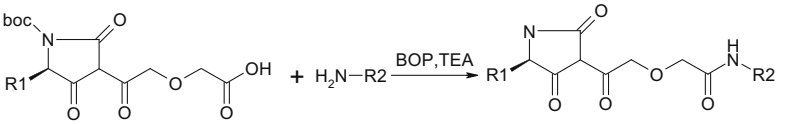

#	R1	R2	Phase of reaction
TMM-1062	i-Pr	n-hexyl	solution
TMM-1095	Bn	n-hexyl	solution
TMM-1097	Bn	n-tetradecyl	solution
TMM-1083	i-Pr	Arg-Arg-Lys-Lys-NH_2	solid
TMM-1094	Bn	Arg-Arg-Lys-Lys-NH_2	solid
TMM-1089	i-Bu	Arg-Arg-Lys-Lys-NH_2	solid

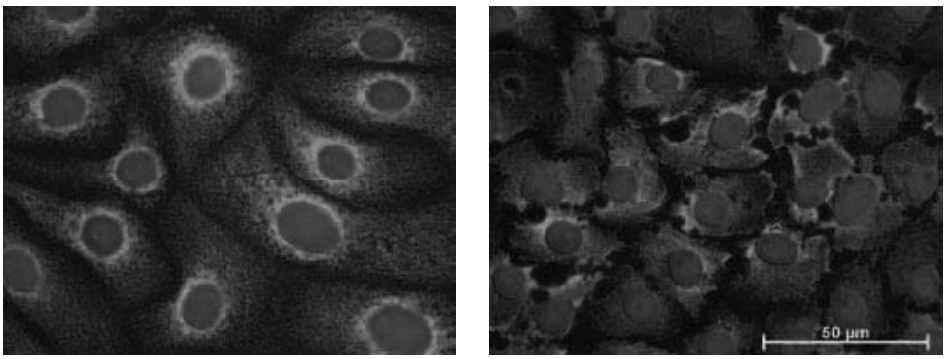

Figure 3. A-498 kidney cancer cells were incubated with tetramic acid GLD1031A (right) and stained for nuclei (blue) and Endoplasmic Reticulum (green). Clear morphological changes are observed when the treated cells are compared to control cells (left).

Acknowledgements

This work was supported by the Marcus Center for Medicinal Chemistry.

References

1. Royles B.JL. *Chem Rev* **95**: 1981-2001, 1995.
2. Hopmann C, Kurz M, Bronstrup M, Wink J, LeBeller D. *Tetrahedron Lett* **43**: 435-438, 2002.
3. Yamada S, Yaguchi S, Matsuda K. *Tetrahedron Lett* **43**: 647-651, 2002.
4. Wolf D, Schmitz IJ, Qiu F, Kelly-Borges M. *J Nat Prod* **62**: 170-172, 1999.
5. Lang G, Cole ALJ, Blunt JW, Munro MHG. *J Nat Prod* **69**: 151-153, 2006.
6. Schobert R, Jagusch C. *Tetrahedron* **61**: 2301-2307, 2005.

1-03-151

Mild and Selective Boc Deprotection on Acid Cleavable Rink-Amide MBHA Resin

Freeman, Noam S; Gilon, Chaim*

The Hebrew University of Jerusalem, Institute of Chemistry, ISRAEL

**E-mail: freeman@chem.ch.huji.ac.il*

Introduction

A number of reagents have been reported for t-butoxycarbonyl (Boc) deprotection on acid-sensitive resins.[1-3] To the best of our knowledge, all attempts to remove Boc on acid-labile resin have resulted in some cleavage from the resin.

Tin tetrachloride ($SnCl_4$) has been shown to be an excellent mild and selective reagent for deprotection of Boc from amino acids and guanidines in solution.[4,5]

We examined the removal of the Boc group with $SnCl_4$ during solid phase peptide synthesis on acid sensitive Rink-amide MBHA resin.

Results and discussion

Solution phase procedures for $SnCl_4$ Boc deprotection call for 2 equivalents of the reagent (corresponding to 1 Boc group present) in organic solvent.[4] Assuming the Boc group will be similarly removed on solid support, we first examined these conditions on resin bound Fmoc-phenylalanine to evaluate the extent of cleavage from the resin. Rink-amide MBHA resin bound Fmoc-phenylalanine was treated with 2 consecutive (no intermediate washings) portions of 2 equivalents of fresh $SnCl_4$, 0.02 M in dry DCM, for 15 minutes each. Fmoc substitution test[6] of the resin bound Fmoc-phenylalanine suggested that these conditions do not cause any apparent cleavage from the resin.

To ensure selectivity of the $SnCl_4$ Boc deprotection, Fmoc-Lys(PG)-OH (PG= Boc, Z, Alloc and Dde) was coupled to the resin and Boc deprotection was applied using the above conditions. Kaiser[7] and Cloranil[8] tests gave positive free amine indications only in the presents of the Boc protecting group. For the other protecting groups the tests were completely negative.

We next wanted to assure that the applied conditions are sufficient for complete Boc deprotection and that this procedure does not cause contamination to the desired product. As a model, a tetra-peptide sequence Lys-Val-Phe-Ala-NH_2 was chosen. Two parallel tetra-peptides were synthesized on Rink-amide MBHA resin (1) using Boc chemistry applying the above conditions for $SnCl_4$ Boc deprotection and (2) using Fmoc chemistry with standard piperidine Fmoc deprotection. Side chain amine of lysine was protected with Fmoc for the Boc-Chemistry peptide (Boc-Lys(Fmoc)-OH) and with Boc for the Fmoc-chemistry peptide (Fmoc-Lys-(Boc)-OH). Amino acid couplings for both peptides were achieved by standard HOBT/HBTU/DIEA coupling protocols. Peptide yields were determined by quantitative Fmoc substitution test of the peptidyl-resin prior to final Fmoc deprotection and cleavage. The Fmoc-chmistry peptide was obtained in 84% yield (including Fmocilated impurities) whereas the Boc-chemisrty peptide was obtained in 61% yield (desired product only) indicating that each cycle of Boc deprotection (three cycles of two $SnCl_4$ portions each) caused a decrease of about 7.5% in yield. Crude HPLC of both tetra-peptides were almost identical indicating high purity synthesis and complete Boc deprotection (Fig. 1).

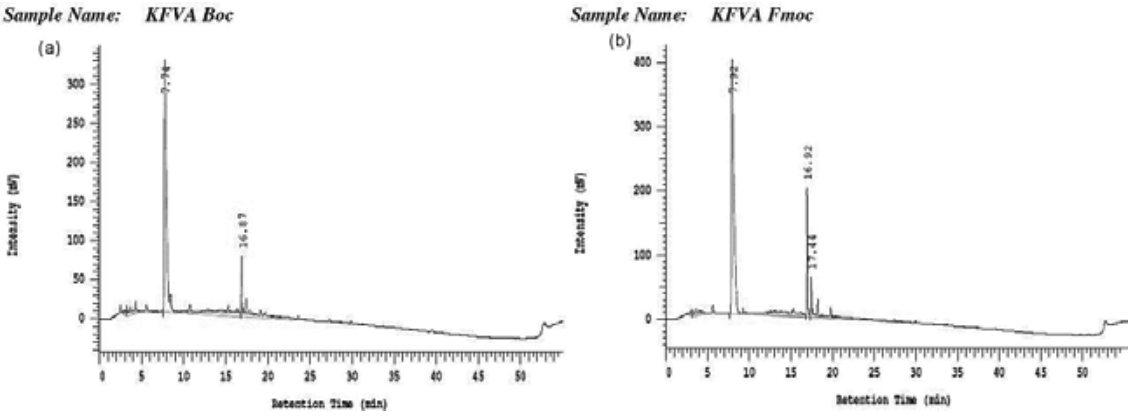

Figure 1. Analytical HPLC (220 nm) chromatograms of crude Lys-Val-Phe-Ala-NH_2 peptide synthesized using (a) Boc chemistry with $SnCl_4$ Boc deprotection and (b) Fmoc chemistry with piperidine Fmoc deprotection.

In attempt to find optimal conditions for $SnCl_4$ Boc deprotection, Fmoc-Lys(Boc)-OH was coupled to the resin and the loading was determined. Boc deprotection was applied and subsequent to the appropriate washings, the loading test was determined again to evaluate the degree of cleavage from the resin. The free amine was then protected with Fmoc (using Fmoc-OSu/TEA in DCM over night) and the loading was determined once more to ensure complete Boc deprotection. Factors that were examined included number of $SnCl_4$ equivalents, $SnCl_4$ concentration in CDM, number of cycles (1 or 2 consecutive) and time of cycle. Preliminary results clearly indicate that the resin bound Fmoc-Lys is considerably more susceptible to cleavage from the resin by $SnCl_4$ treatment. Currently, best conditions for complete Boc deprotection, with minimal cleavage from the resin, are 2 consecutive 5 minute cycles of 2 equivalents of $SnCl_4$, 0.012 M in DCM. Changes in $SnCl_4$ concentration in DCM hardly affected the results. This is in agreement with the proposed mechanism suggesting the formation of a complex between the free amine and the Sn. Low concentration is recommended, however, since any encounter with water will form strong acid (HCl) which will promote cleavage from the resin.

Conclusions

We present a simple, inexpensive, and efficient method for selective Boc deprotection from acid sensitive Rink-amide MBHA resin with minimal loss of substrate by cleavage. Preliminary results suggest that extent of cleavage from the resin varies depending on the C-terminal amino acid. Temporary Boc protection on Rink amide MBHA resin avoids the dangers and inconveniences of HF cleavage reactions that are routinely used for cleavage of Boc-chemistry resins. This deprotection procedure may not be ideal for repetitive cycles during peptide synthesis in Boc strategy on acid-labile resin. However, it can be very useful as a selective deprotection step in solid phase syntheses of small molecules wherein only few Boc removals are required. Finally, this method provides an economical alternative to large-scale Fmoc-chemistry SPS considering that Boc intermediates tend to be cheaper and more stable than Fmoc ones.

References

1. Zhang AJ, Russell DH, Zhu JP, Burgess K. *Tetrahedron Lett* **39**: 7439-7442, 1998.
2. Trivedi HS, Anson M, Steel PG, Worley J. *Synlett* **12**: 1932-1934, 2001.
3. Lejeune V, Martinez J, Cavelier F. *Tetrahedron Lett* **44**: 4757-4759, 2003.
4. Frank R, Schutkowski M. *Chemical Communications* **22**: 2509-2510, 1996.
5. Miel H, Rault S. *Tetrahedron Lett* **38**: 7865-7866, 1997.
6. Novabiochem®. *Novabiochem Catalog* **2006/2007**, 3.4.
7. Kaiser E, Colescott R L, Bossinger CD, Cook PI. *Anal Biochem* **34**: 595-598, 1970.
8. Christensen T. *Acta Chem Scand Ser B* **33**: 763-766, 1979.

1-03-152

A potent and non-explosive substituent for classical benzotriazole-based additives: Oxyma Pure

Subirós-Funosas, Ramon[1]; El-Faham, Ayman[2]; Albericio, Fernando[3,]*

[1]Universitat de Barcelona, Facultat de Química, SPAIN; [2]University of Alexandria, Faculty of Science, EGYPT; [3]Institute for Research in Biomedicine, SPAIN

[*]E-mail: fernando.albericio@irbbarcelona.org

One of the most critical aspects in peptide chemistry is undoubtedly the proper selection of the coupling reagent so that yield, purity and racemization can reach the optimal level. Benzotriazoles and their derivatives can be extensively found among these reagents, either as additives (together with carbodiimides) or as stand-alone coupling reagents. The first compound of this family to establish itself as an additive in peptide chemistry was 1-hydroxybenzotriazole (HOBt)[1] in the early 70's, and more recently its more potent aza counterpart (HOAt)[2] has gained in popularity. Unexpectedly, explosive properties of benzotriazole-based additives have been reported, thereby limiting their transport and hindering their commercial availability.[3] To introduce a non-explosive and efficient replacement for these commonly used additives, we report an in depth study on ethyl 2-cyano-2-(hydroxyimino)acetate, under the commercial name of Oxyma Pure (Fig. 1), which showed promising results in suppressing racemization in studies published a few years ago.[4]

Racemization was examined in two peptide models: Z-Phg-Pro-NH_2 and Z-Phe-Val-Pro-NH_2 in solution phase, comparing HOAt, HOBt, Oxyma Pure and HOP (*N*-hydroxy-2-pyridone).[5] Results are shown in Table 1. Regarding the stepwise coupling of Z-Phg-OH onto H-Pro-NH_2, HOP rendered the dipeptide in considerable yield, although an enormous percentage of racemization was observed, even without preactivation. As expected, HOAt suppressed racemization to a greater extent than HOBt (3.3% vs. 9.3%). The performance of Oxyma Pure was impressive, with only 1.0% of DL epimer observed. Even after 2 min of preactivation (conditions that showed no starting Z-Phg-OH), the low percentage of racemization was maintained. A similar trend was observed in the more sensitive [2+1] segment coupling of Z-Phe-Val-OH onto H-Pro-NH_2. Oxyma Pure suppressed racemization more than HOBt and was comparable with HOAt, which performed slightly better. Nevertheless, Oxyma Pure afforded the tripeptide in the highest yield.

The relative potency of HOAt, HOBt and Oxyma Pure in affording Leu-enkephalin (H-Tyr-Leu-Leu-Phe-Leu-NH_2) analogues was also tested by replacing the two consecutive Leu amino acids for more bulky residues. The synthesis of the Aib (α-aminoisobutyric acid) derivative must be highlighted because of its high sterical hindrance.[6] Once tripeptide H-Aib-Phe-Leu-resin was quantitatively assembled, we studied the incorporation of Aib and Tyr, with 3 min of preactivation to ensure comparability of active ester formation. Results at a range of coupling times are shown in Table 2. In all cases, Oxyma Pure afforded the highest degree of purity, with a much higher percentage of pentapeptide than that observed with HOAt and especially with HOBt. A 4 hour double coupling for Aib and standard 1 hour for Tyr rendered the pentapeptide in 92% purity.

In addition to the coupling efficiency of Oxyma Pure, a major issue to be addressed was its decomposition behaviour, which ideally should not follow the typical profile of an explosive compound: namely fast decomposition simultaneously releasing high pressure. The likeliness of an explosive event was studied by means of DSC and ARC experiments. Differential Scanning Calorimetry (DSC) tests provided information about the relative decomposition kinetics. Consistent with their reported explosive character, HOBt and HOAt decomposed in a short range of temperatures, while the decomposition of Oxyma pure was much slower and in a constant manner. Complementary to this test, we applied an adiabatic calorimetry assay, ARC, which accurately gave the decomposition onset temperatures and also the pressure released. Although the decomposition of Oxyma Pure began at a lower temperature than HOBt and HOAt (120 ºC vs. 190 ºC and 218 ºC), implying that it is not recomendable to work with Oxyma Pure below 70 ºC, the pressure released (and so the potential explosive character) was much lower (62 bar vs. 170-180 bar).

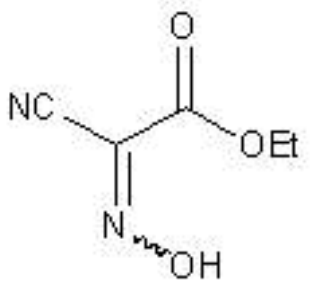

Figure 1. Structure of ethyl 2-cyano-2-(hydroxyimino)acetate (Oxyma Pure).

Table 1. Yield and racemization during formation of Z-Phg-Pro-NH_2 and [2+1] Z-Phe-Val-Pro-NH_2 in DMF (solution phase synthesis).[a]

Entry	Coupling Reagent	Z-Phg-Pro-NH_2		Z-Phe-Val-Pro-NH_2	
		Yield (%)	DL (%)	Yield (%)	LDL (%)
1	HOAt/DIC	81.4	3.3	86.1	2.1
2	HOBt/DIC	81.9	9.3	78.8	8.9
3	Oxyma Pure/DIC	89.9	1.0	--	--
4	Oxyma Pure/DIC [b]	88.2	1.1	89.8	3.8
5	HOP/DIC	88.2	17.4	88.5	45.1
6	HOP/DIC [b]	83.4	26.1	--	--

[a] Couplings were conducted without preactivation, except on entries 4 and 6. [b] 2 min of preactivation was used

Table 2. Percentage of H-Tyr-Aib-Aib-Phe-Leu-NH_2 and related deletion peptides during solid phase assembly in various coupling conditions using a series of additives.[a]

Coupling time	Entry	Coupling Reagent	pentapeptide (%)	des-Aib (%)	des-Tyr (%)	tripeptide (%)
30 min	1	HOAt/DIC	11.3	86.1	1.8	0.8
	2	HOBt/DIC	3.0	91.0	0.9	5.1
	3	Oxyma Pure/DIC	28.0	70.5	1.1	0.4
1 hour	4	HOAt/DIC	28.7	71.3	--	--
	5	HOBt/DIC	9.8	86.9	1.6	1.7
	6	Oxyma Pure/DIC	55.7	44.3	--	--
1 hour double coupling	7	HOAt/DIC	55.0	45.0	--	--
	8	HOBt/DIC	18.9	80.6	0.5	--
	9	Oxyma Pure/DIC	69.0	31.0	--	--

[a] HPLC-MS showed the right mass for the pentapeptide at 611.4

In summary, in all cases Oxyma Pure performed more efficiently than HOBt, and in certain experiments was even superior to HOAt, as highlighted in the synthesis of a demanding pentapeptide. Moreover, Oxyma Pure was considerably less likely to undergo an explosive event compared to the two benzotriazole-based additives. On the basis of this observation, we conclude that Oxyma Pure is a safe and effective alternative.

Acknowledgements

This work was partially supported by CICYT (CTQ2006-03794/BQU), the *Generalitat de Catalunya* (2005SGR 00662), the Institute for Research in Biomedicine, and the Barcelona Science Park. RS-F thanks *the Ministerio de Educación y Ciencia* for a FPU PhD fellowship. We also thank the Calorimetry Platform at the Barcelona Science Park for their support in the DSC and ARC experiments.

References

1. König W, Geiger R. *Chem Ber* **103**: 788-798, 1970; ibid, 2034-2040.
2. Carpino LA. *J Am Chem Soc* **115**: 4397-4398, 1993.
3. Wehrstedt *et al*. *J Hazard Mat* **A126**: 1-7, 2005.
4. a) Izdebski J. *Pol J Chem* **53**: 1049-1057, 1979.
   b) Itoh M. *Bull Chem Soc Japan* **46**: 2219-2221, 1973.
5. a) El-Faham A, Albericio F. *Org Lett* **9**: 4475-4477, 2007.
   b) El-Faham A, Albericio F. *J Org Chem* **73**: 2731-2737, 2008.
6. Carpino L A, El-Faham A, Minor CA, Albericio F. *J Chem Soc Chem Comm* **1994**, 201-203.

1-03-153

Site-specific PEGylation of human IgG1-Fab using a rationally designed trypsin variant

Liebscher, Sandra[1,]; Trost, Eva[2]; Hoess, Eva[2]; Bordusa, Frank[1]*

[1]Martin-Luther-University Halle-Wittenberg, Institute of Biochemistry Kurt-Mothes Str. 3, 06120 Halle/Saale, GERMANY; [2]Roche Diagnostics GmbH, Nonnenwald 2, 82372 Penzberg, GERMANY

[*]E-mail: s.liebscher@enzyme-halle.mpg.de

Introduction

Site-specific covalent modification of proteins is a powerful tool in fundamental and applied research as well. Especially for medical purposes selective derivatization procedures become more and more essential. Particularly polymer-modified protein pharmaceuticals have revolutionized drug development leading to protein therapeutics with highly improved stability and pharmacokinetic.[1] The first and so far only PEGylated Fc-free antibody against TNFα is Certolizumab pegol which is presently in the approval procedure at European Medicines Agency.[2] Despite the extraordinary interest in selectively modified proteins there is however a lack of generally usable and flexible methods, which restore full biological function of the protein to be modified. In the present contribution we describe the suitability of the genetically optimized trypsin variant K60E/N143H/E151H/D189K for C-terminal derivatization of proteins with synthetic functionalities under native conditions. The trypsin variant possesses restricted zinc-inducible proteolytic activity towards the rare recognition sequence YRH with an occurance of less than 0.5% in native proteins. Placing of this sequence at the C-terminal region of respective proteins via standard mutagenesis provides suitable precursor targets for site-specific modification via a biocatalytic transamidation reaction. C-terminal PEGylation of human IgG1 Fab with 20 kDa PEG via this noval approach proceeds efficiently with a total yield of isolated modified antibody fragment of 40%. Interestingly, no undesired cleavage reactions could be detected.

Results and discussion

The fourfold trypsin variant was generated by site directed mutagenesis and subsequently screened towards its specificity by using a peptide library of the general structure Bz-AAX$_{aa}$X$_{bb}$X$_{cc}$AAG-OH. In wild-type enzyme, D189 is situated on the bottom of the S1-subsite being responsible for the enzyme´s native specificity towards basic residues due to the formation of a salt bridge.[3] The replacement of D189 with Arg prevents this native cleavage activity. To create a unique recognition sequence we further introduced Asp at the bottom of the S1´-subsite inducing a specificity for Arg at the P1´-position.[4] Finally, metal ion induceable specificity for P2´-His containing substrates was created by two artificial His-residues placed at the border of the S2´-subsite.[5] The initial hydrolysis rate of Bz-AAYRHAAG-OH was more than 13-fold increased in the present of $ZnCl_2$ due to the artificial metal binding site at the S2´-subsite. The synthetic utility of this trypsin variant with nearly quantitative product yields was already shown for the N-terminal modification of proteins via the common substrate mimetic concept. The practicability of the fourfold trypsin variant for the C-terminal modification procedure was initially evaluated in model reactions with 1 mM Bz-AAYRHAAG-OH, 5 mM H-RHAK(CF)-OH (CF…6-carboxyfluorescein) and 20 µM trypsin variant in the presence of 100 µM $ZnCl_2$ (100 mM HEPES, 100 mM NaCl, 10 mM $CaCl_2$, pH 7.8). Via a transamidation reaction the product Bz-AAYRHAK(CF)-OH was formed in a yield of about 60%. To evaluate the function of the approach for the C-terminal modification of human

Figure 1. Conversion from IgG1 to the PEGylated Fab-fragment. The human IgG1-Fab-fragment is first elongated by the recognition sequence YRH and a Strep II fusion. After expression and purification, the Fab-fragment is incubated with RH-PEG20,000 and the trypsin variant K60E/N143H/E151H/D189K in the present of zinc ions. Via a transamidation reaction the desired product Fab-PEG20,000 is formed with an isolated product yield of 40%.

IgG1-Fab, the antibody fragment was recombinantly adapted to the needs of the biocatalyst by introducing the aforementioned recognition sequence YRH at the proteins C-terminus followed by a final Strep-tag motif to simplify the purification of the construct via affinity chromatography. The purified Fab-fragment (100 μM) was then incubated with RHAK(MCa)-PEG20,000 (MCa…6-methyl-coumarin, 500 μM) in presence of the trypsin variant K60E/N143H/E151H/D189K (10 μM) and 100 μM $ZnCl_2$ at 30 °C (100 mM TRIS, 150 mM NaCl, 10 mM $CaCl_2$, pH 7.8). According to the two step mechanism of the transamidation reaction, the recognition and cleavage of YRH motif leads at first to the acylation of the biocatalyst resulting in the formation of a covalent acyl-enzyme-intermediate. In the second step, the acyl-enzyme-intermediate becomes nucleophilic attacked by the N-terminal amino function of RH-PEG20,000 leading to the final PEGylated Fab-fragment. A schematic representation from the IgG1 to the PEGylated Fab-fragment is shown in Fig. 1.

The time course of the product formation was resolved by fluorescence-based HPLC analysis. Within 30 min, the desired transamidation product was formed with an isolated product yield of 40%. The formation of the desired PEGylated Fab-fragment was competed by the corresponding hydrolysis reaction based on the nucleophilic attack of water resulting in an incomplete product formation. The synthesis reaction was stopped by the addition of 1 mM EDTA leading to an inactivation of the zinc ion-dependent enzyme. PEGylated product was isolated by gelfiltration and analyzed by SDS-PAGE. The modified Fab-fragment shows an obvious shift in molecular mass. The corresponding protein band was clearly stained by the addition of iodine indicating the desired PEGylation. The isolated product was furthermore characterized by mass spectroscopy. The regioselectivity of the derivatisation reaction was validated by patial digestion with the endoproteinase Lys-C. Via mass spectrometry of the digestion mixture it was shown that the PEGylation was situated at the C-terminus of the Fab-fragment exclusively. PEGylated Fab-fragment was investigated by Biocore measurements. The stability of the complex was not influenced by the derivatization reaction.

References

1. Harris JM, Chess RB. *Nat Rev Drug Discov* **2**: 214-221, 2003.
2. Sandborn WJ, Feagan BG, Stoinov S, Honiball PJ, Rutgeerts P, Mason D, Bloomfield R, Schreiber S; PRECISE 1 Study Investigators. *N Engl J Med* **357**: 228-238, 2007.
3. Perona JJ, Tsu CA, Craik CS, Fletterick RJ. *J Mol Biol* **230**: 919-933, 1993.
4. Kurth T, Grahn S, Thormann M, Ullmann D, Hofmann HJ, Jakubke HD, Hedstrom L. *Biochemistry* **37**: 11434-11440, 1998.
5. Willett WS, Gillmor SA, Perona JJ, Fletterick RJ, Craik CS. *Biochemistry* **34**: 2172-2180, 1995.

1-03-154

Resin Comparison and Fast Conventional Synthesis of Human SDF-1α on the *Symphony*®, *Tribute*™ and *Prelude*™

Patel, Hirendra; Chantell, Christina; Fuentes, German; Menakuru, Mahendra
*Protein Technologies Inc, UNITED STATES**

Article is on p. 78-79 (1-01-131)

1-03-155

Fast Fmoc-deprotection reagent for peptide synthesis

Rawer, Stephan[1,]; Vidal-Wagner, Juan[1]; Henklein, Peter[2]*

[1]Applied Biosystems Deutschland GmbH, PSM support europe, GERMANY; [2]Universitätsmedizin Charité Berlin, Institut für Biochemie, GERMANY

[*]E-mail: Stephan.Rawer@appliedbiosystems.com

Introduction

The commun reagent for Fmoc-deprotection in solid phase peptide synthesis is 20% piperidine in DMF or NMP.[1] Piperidine is declared as a drug precursor by EU Council Regulation (EEC) No 111/2005.[2] Therefore there is a strong legal control of its distribution, and very much time-consuming paperwork to fill-in. Although exist are studies on stronger deprotection reagents, used for difficult cleavage, and smoother reagents, described to avoid side reactions for base sensitive sequences and suppression of aspartimide formation only a few literature is found on an actual subtitute for piperidine.[3] In our previous presentation we showed studies of alternative bases for Fmoc-deprotection by kinetic measurements in solution.[4]

Results and discussion

Recently we developed a new Fmoc-deprotection reagent, which is reacting faster than piperidine as shown by kinetic studies in solution.

The new reagent was tested and compared in the kinetic experiment by recording the dibenzofulvene formation and decrease at 301 nm (Fig. 1). As showing in the kinetic curves, Mix1 is simlar and the new reagent mix is faster reacting than 20% piperidine.

Further the new reagent was compared to piperidine and Mix1 by synthesis' on a model peptide (IIKKSTALLG). It is a well known by monitoring that this peptide shows difficult Fmoc-deprotections at the last two amino acids. To observe the differences, we shortened and fixed the Fmoc-deprotection time to 3 min. After cleavage with 95% TFA, 2,5% H_2O and 2,5% TIS, the ultimate quality of the peptides was assessed by using MALDI mass spec techniques. The crude peptide synthesized with the new reagent shows less Fmoc-deletion peptides in comparison to piperidine and Mix 1.

The new reagent mixture shows a better performance in rapid deprotection against piperidine. No deletion peptides were detected and the last 2 cycles are literally 100% effective Fmoc-deprotection with the new reagent.

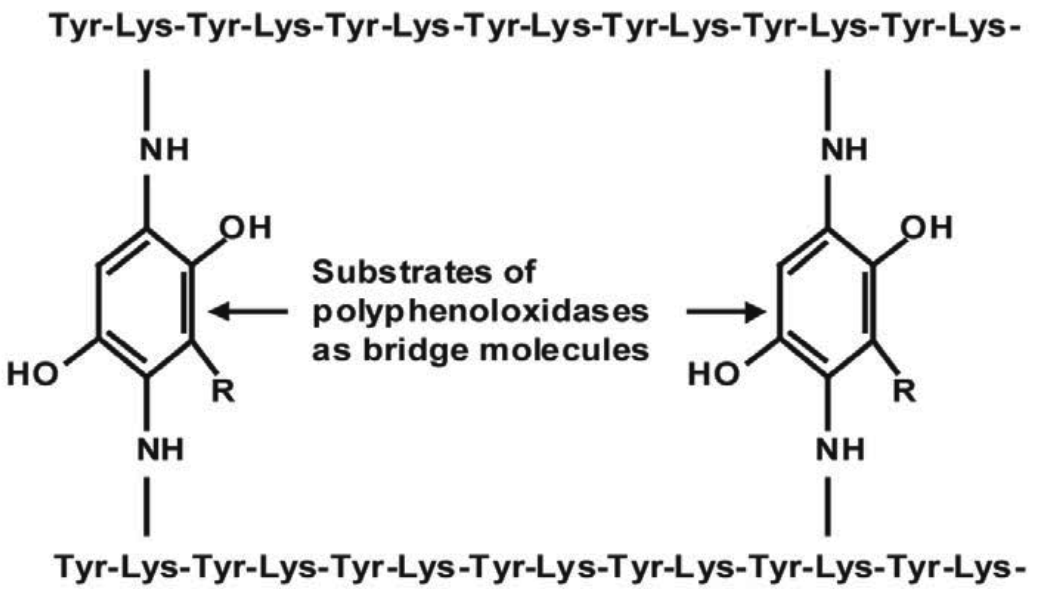

Figure 1. UV kinetic of the deprotection of Fmoc-Ala-OH in solution at the wavelength of 307 nm. start of measurement: 10 sec after mix. Deprotection: with 20% piperidine, mix 1 and the new reagent.

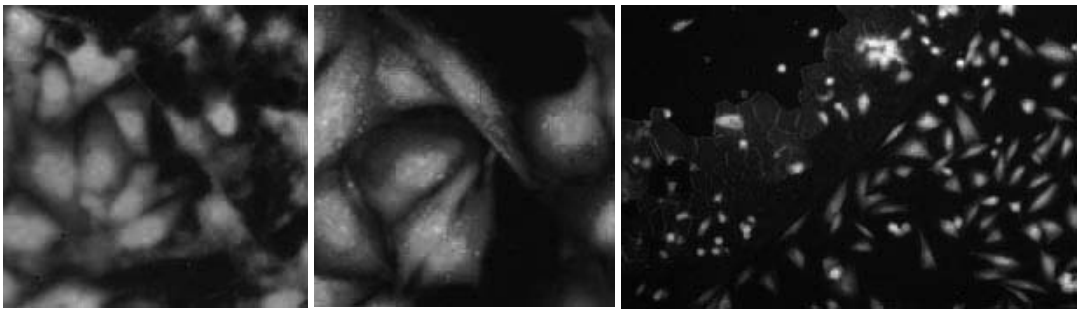

Figure 2. MALDI-MS analysis of crude KINSTALL-peptides: new reagent, mix 1 and 20% piperidine. No [MH+Fmoc]+ and no [MH-Ile+Fmoc]+ peak was observed with the new reagent.

References

1. Goodman M, Felix A, Moroder L, Toniolo C. (Eds), *Synthesis of Peptides and Peptidomimetics, Houben-Weyl, Vol E22a.* Georg Thieme Verlag, Stuttgart New York, 2004, 64ff .
2. *Official Journal of the European Union* L 22, 26.01.2005.
3. Hachmann J, Lebl M. *J Comb Chem* **8**: 149, 2006
4. Rawer S, Roeder R, Henklein P. *Peptides 2006* (Proceedings of the 29th European Peptide Symposium, Gdańsk, Poland). Rolka K, Rekowski P, Silberring J (Eds), Kenes International, Geneva, Switzerland, 2007, pp 780-781.

1-03-156

A Non-Explosive Replacement for Benzotriazole-based Coupling Reagents

El-Faham, Ayman[1]; Subirós-Funosas, Ramon[2]; Albericio, Fernando[3,]*

[1]Faculty of Science, Alexandria University, Department of Chemistry, EGYPT; [2]Institute for Research in Biomedicine, SPAIN; [3]Faculty of Chemistry, University of Barcelona, Department of Organic Chemistry, SPAIN

[*]E-mail: fernando.albericio@irbbarcelona.org

Peptide synthesis is based on the proper combination of protecting groups and a suitable coupling method.[1] Almost all peptide bonds formed are currently carried out in the presence of 1-hydroxybenzotriazole (HOBt)[2] or its derivatives (HOAt,[3] Cl-HOBt[4]). Recent reports have confirmed the explosive properties of HOBt derivatives.[5] Thus, a replacement for HOBt is required for the preparation of peptides for research purposes and more importantly, for the production of peptide-based APIs. Here we report on several alternatives for the uronium salts based on HOBt and its parent additives, incorporating a proton acceptor.

To determine the compatibility of the new coupling reagents with peptide synthesis in both manual and automatic mode, their solubility and stability in solution and in solid state was tested (Table 1). The Oxyma Pure derivative **6b** (**COMU**) gave a color which made the reaction able to be followed to completion. Up to 1.5 M solution of COMU could be prepared, whereas the maximum concentration of HATU and HBTU were 0.43 M and 0.46 M respectively.

The efficiency of the new coupling reagent (**6b**) for the coupling of hindered amino acid was examined using the model system **Fmoc-Val-OH** + **H-Val-NH$_2$** (Table 2).

Table1. Hydrolytic stability of immonium-type coupling reagents in DMF.

Time (min)	HATU (Yield %)		COMU (**6b**) (Yield %)	
	2 eq.	1 eq.	2 eq.	1 eq.
5	83.0	70.0	95.1	82.0
10	87.6	76.0	96.0	86.0
20	90.5	80.0	98.0	90.1
30	92.5	82.0	98.5	94.5
60	93.0	82.0	100.0	96.0
120	94.0	83.0	100.0	98.0

To study the configuration retention induced by the new coupling reagents, several previously studied model peptide systems [Z-Phg-Pro-NH$_2$ and Z-Phe-Val-Pro-NH$_2$] were examined.[6] These models involve stepwise coupling and [2+1] segment coupling as well. For the more sensitive coupling of Z-Phg-OH onto H-Pro-NH$_2$ to give Z-Phg-Pro-NH$_2$, HDMODC **6a** and COMU **6b** have a greater conservation of chirality than the HATU and HBTU analogs.

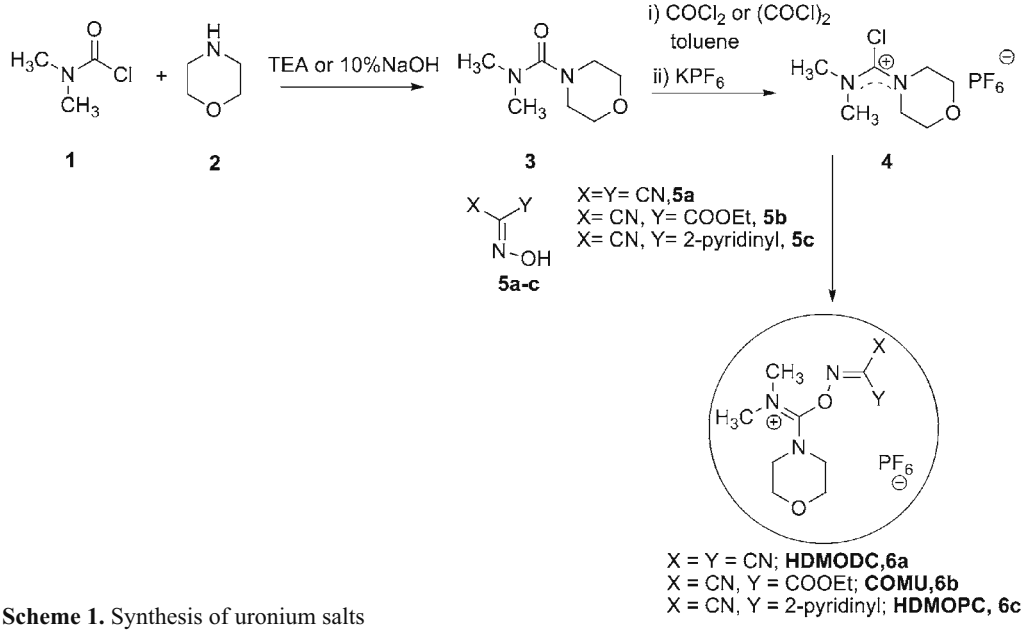

Scheme 1. Synthesis of uronium salts

Table 2. Extent of coupling of Fmoc-Val-Val-NH_2 using distinct coupling reagents and different eq of DIEA in DMF

Coupling Reagent	5 h	24 h	48 h
HATU	99 %	95 %	76 %
HBTU	100 %	98 %	86 %
HOTU	100 %	95 %	84 %
COMU(**6b**)	100 %	100 %	93 %

In a more demanding example, H-Tyr-Aib-Aib-Phe-Leu-NH_2 was manually assembled on Fmoc-Rink Amide-AM-resin using the corresponding amino acid/activator (3 eq.) and DIEA (6 eq. or 3 eq.). 30 min coupling times were applied except for Aib-Aib, for which 1 h was used. The best results were obtained with **6b** (COMU) (Table 4).

Table 3. Yield and racemization during the formation of Z-Phg-Pro-NH_2 and Z-Phe-Val-Pro-NH_2 in DMF (Solution Phase Synthesis)[a]

AA	Coupling Reagent	Base (eq.)	Yield (%)	LDL (%)
Z-Phg-Pro-NH_2	HATU	DIEA (2)	78.4	3.1
	HBTU	DIEA (2)	80.2	8.2
	HOTU	DIEA (2)	78.9	0.17
	COMU (6b)	DIEA (2)	88.2	0.12
	HDMODC (**6a**)	DIEA (2)	90.1	0.40
	HDMOPC (**6c**)	DIEA (2)	86.0	13.6
Z-Phe-Val-Pro-NH_2	HATU	DIEA (2)	85.8	13.9
		DIEA (1)	83.2	11.0
		TMP (2)	78.0	5.3
	HBTU	DIEA (2)	78.6	27.7
		DIEA (1)	81.2	16.3
		TMP (2)	91.2	14.2
	HOTU	DIEA (2)	88.7	23.6
		TMP (2)	80.3	7.4
		TMP (1)	91.3	7.5
	COMU (6b)	DIEA (2)	89.8	19.3
		TMP (2)	90.3	7.0
		TMP (1)	88.0	3.5
	HDMODC (**6a**)	TMP (2)	90.0	17.9
	HDMOPC (**6c**)	TMP (2)	87.2	43.6

[a]Tetrapeptide (des-Aib) was confirmed by peak overlap in the presence of an authentic sample. The crude H-Tyr-Aib-Aib-Phe-Leu-NH_2 was analyzed by HPLC [Symmetry Waters C_{18}(4.6 x 150 mm, 4 μm), linear gradient over 30 min of 20 to 80 % CH_3CN in H_2O/0.1 % TFA, flow rate 1.0 ml/min, t_R penta = 8.82 min, t_R des-Aib = 9.10 min.]. HPLC-MS showed the right mass for the pentapeptide at 612.0.Des-Aib and pentapeptide were coinjected with authentic samples.

Table 4. The % of des-Aib (4-mer) (Tyr-Aib-Phe-Leu-NH_2) during solid-phase assembly of pentapeptide (Tyr-Aib-Aib-Phe-Leu-NH_2)

Coupling Reagent	Base (eq.)	Penta (%)	Des-Aib (%) tetra
HATU	DIEA (2)	83.0	17
HBTU	DIEA (2)	47.0	53
HTOC	DIEA (2)	99.0	1.0
COMU (6b)	**DIEA (2)**	**99.7**	**0.26**
HDMODC (**6a**)	DIEA (2)	95.3	4.7
HDMOPC (**6c**)	DIEA (2)	41.3	58.3

Conclusions

In conclusion, here we describe new families of uronium-type coupling reagents that differ in their carbocation skeleton structure as well as the leaving group. The presence of the morpholino group has a marked influence on the polarity of the carbon skeleton, which affects the solubility and stability as well as the reactivity of the reagent. These results should be taken into account when coupling reagents are placed in open vessels, such as in some automatic synthesizers. Remarkably, the Oxyma Pure derivative (**6b**) gave equally good results as the aza derivatives and performed extremely well in the presence of only 1 eq. of base.

References

1. (a) Lloyd-Williams P, Albericio F, Giralt E. *Chemical Approaches to the Synthesis of Peptides and Proteins.* CRC, Boca Raton, FL, U S A, 1997; (b) Goodman M. Ed. *Synthesis of Peptides and Peptidomimetics. Houben-Weyl, Methods of Organic Chemistry, Vol. E22a.* Thieme, Stuggart•New York, 2002; (c) Amblard M, Fehrentz J-A, Martinez J, Subra G. *Mol Biotech* **33**: 239-254, 2006.
2. (a) Albericio F, Carpino LA. *Solid-Phase Peptide Synthesis. Methods in Enzymology, Vol* **289**, Fields GB (Ed), Academic Press, Orlando, 1997, pp 104-126; (b) Humphrey JM, Chamberlin AR. *Chem Rev* **97***:* 2243-2266, 1997; (c) Kamiński ZJ. *Biopolymers* **55**: 140-165, 2000; (d) Albericio F, Chinchilla R, Dodsworth DJ, Najera C. *Org Prep & Proc Int* **33**: 203-303, 2001; (e) Han S-Y, Kim Y-A. *Tetrahedron* **60**: 2447-2467, 2004; (f) Montalbetti CAGN, Falque V. *Tetrahedron* **61**: 10827-10852, 2005.
3. Dourtoglou V, Ziegler J C, Gross B. *Tetrahedron Lett* **19**: 1269-1272, 1978.
4. Albericio F, Bofill JM, El-Faham A, Kates SA. *J Org Chem* **63**: 9678-9683, 1998.
5. Wehrstedt *et al*., *J Hazard Mat* **A126**: 1-7, 2005.
6. a) El-Faham A, Albericio F. *Org Lett* **9**: 4475-4477, 2007. b) El-Faham A, Albericio F. *J Org Chem* **73**: 2731-2737, 2008.

1-03-157

Efficient Chemical Synthesis of Amides and Peptides using Phosphonic Acid/Alkylene Oxide Chemistry

Bayryamov, Stanislav[1]; Danalev, Dantcho[2,]; Vassilev, Nikolay[3]*

[1]1Institute of Organic Chemistry with Centre of Phytochemistry, Bulgarian Academy of Sciences, Laboratory of Biocatalysis, BULGARIA; [2]University of Chemical Technology and Metallurgy, Organic Chemistry, BULGARIA; [3]1Institute of Organic Chemistry with Centre of Phytochemistry, Bulgarian Academy of Sciences, BULGARIA

[*]E-mail: dancho_danalev@yahoo.com

The peptide bond formation is one of the most important phenomena in the nature. The basic aim of this reaction to realize a transmission of genetic information "from the language of nucleic acids to that of the proteins" is possible due to one big alliance between ribosome, i-RNA and t-RNA, including specific amino acids. At the end of last century Thomas Cech revealed the phenomena that RNA molecules (ribozymes) are enzymes as well as proteins.[1] A new mechanism of phosphoryl transfer is proposed, including 1,2-diol system with participation of vicinal syn-2'-OH group in the ribose cycle from the RNA molecule. In 2000 Moore and Steirz revealed that in a distance of 20 Å around its reactive site any protein miss.[2] The conclusion is that ribosome is the biggest known ribozyme, and peptidyltransferase reaction is catalyzed by the ribosome RNA. During the process of amino acids activation aminoacyl adenillate is obtained. This fact gave us the idea to convert the nature reaction to a low-molecular level and to realize a new approach for synthesis of amino acid amides and peptides by means of 1,2-diol system properties and H_3PO_3. The reaction of latter with amino acid leads to its activation results to obtaining of 1,4-dioxo-5-alkyl-1,3,2-oxaza phospholane, which was similar to urethane *N*-carboxy anhydrides.[3] The biochemical reactions run in a water media at normal temperature with high rate, low energy consumption, regio- and stereo specific. The yields of the aim products are quantitative. That's why a lot of scientists search for similar conditions and reagents to mimic the nature in a practice, i.e. to create biomimetic reactions. Since 1960 a lot of publication revealed that five member acylphosphates could be intermediates during the process of phosphoenolpyruvate ester obtaining.[4-6] *N*-phosphoryl amino acids could autocatalized a lot of bioorganic reactions at mild conditions resulting to peptides, esters, etc. obtaining. In 1995 a series of in silico experiments allowed isolation and characterization of very important intermediate in all these reactions - an activated intra molecular pentacoordinated phosphocarboxyl mixed anhydride.[7] Hua *et al*. study a series of *N*-phospho-*α*-amino acids reactions in a water-alcohol media at mild conditions. They reveal that these compounds could auto activate *N*-phosphoryl peptides, *N*-phospho-*α*-amino acid esters obtaining and intra molecular *N*-*O*-phosphoryl

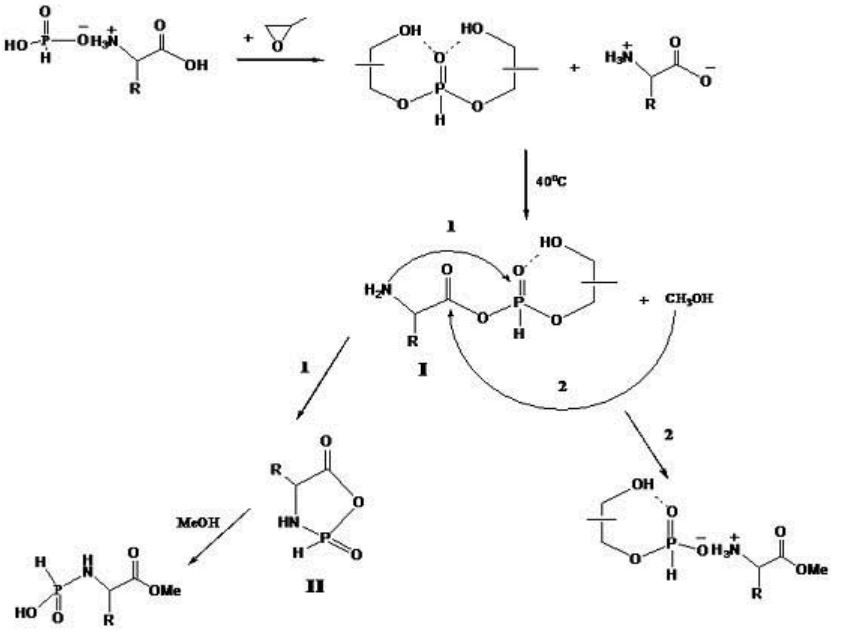

Figure 1. A possible progress of amino acid esters obtaining reaction catalyzed by H_3PO_3

group transfer.[4,8] Studying the reaction of amino acid phosphorylation Zeng *et al*. are isolated successfully N-dialkoxyphosphoryl peptides at the presence of dialkyl phosphite.[9] A previous investigation on the reaction of amino acid esters catalyzed by phosphorous acid was done. Our approach allows synthesizing of different amino acid derivatives without preliminary protection of amino acid functional groups. Their blocking was made in situ during the reaction. The activation of *α*-carboxyl function as an electrophile run at the same time as α-amino group protection as a nucleophile that ensure only the aim condensation reaction. The reaction was made in the presence of hydroxypropyl ester of H_3PO_3 in situ obtained by means of H_3PO_3 and propylen oxide. The reaction possible mechanism is presented on the Fig. 1.

A series of methyl esters of Gly, Ala, Thr и Phe was synthesized by our group by the method described above.[10]

Herein we describe the synthesis of dipeptide derivatives H-Phe-Gly-NH_2, H-Phe-NH-Bz, H-Phe-NH-Bu, H-Phe-Phe-OMe. The newly synthesized products were analyzed by ^{1}H и ^{13}C-NMR, and 2D-NMR.

H-Phe-NH-Bu: ^{1}H-NMR ($CDCl_3$) – 0.9-0.96 (m 3H, CH_3 - Bu), 1.27-1.48 (m 6H, CH2 - Bu), 1.67-1.7 (q 1H, αCH - Phe), 2.06 (s 1H, αNH - Phe), 4.21-4.29 (m 2H, βCH2 - Phe), 7.27-7.73 (m 5H, Ar - Phe), 8.08 (s 1H, NH - Bu); ^{13}C-NMR ($CDCl_3$) – 14.09 (CH3), 28.92-30.37 (CH2 - Bu), 38.75 (CH2 - Phe), 68.16 (αCH - Phe), 128.8-130.9 (Ar - Phe), 167.74 (C=O).

H-Phe-NH-Bzl: ^{1}H-NMR ($CDCl_3$) – 2.02 (s 1H, αNH - Phe), 2.92-2.97 (m 1H, βCH2a - Phe), 3.14-3.17 (m 1H, βCH2b - Phe), 3.83 (q 1H, αCH - Phe), 4.56 (s 2H, CH2 - Bzl), 7.01-7.25 (m 10H, Ar – Phe, Bzl), 8.02 (s 1H, NH - Bzl); $_{13}$C-NMR ($CDCl_3$) – 39.9 (CH2 - Phe), 44.4 (CH2 - Bzl), 54.6 (αCH - Phe), 126.6-141.6 (Ar – Phe, Bzl), 172.3 (C=O).

H-Phe-Gly-NH_2: ^{1}H-NMR ($CDCl_3$) – 3.1-3.13 (m 1H, βCH2a - Phe), 3.14-3.16 (m 1H, βCH2b - Phe), 3.49 (s 2H, CH2 - Gly), 3.53-3.57 (q 1H, αCH - Phe), 3.66 (s 1H, αNH - Phe), 4.52 (d 2H NH2-amide), 7.00-7.23 (m 5H, Ar - Phe), 8.05 (s 1H, αNH - Gly); 13C-NMR (CDCl3) – 44.29 (CH2 - Gly), 67.22 (CH2 - Phe), 68.17 (αCH - Phe), 125.43-129.26 (Ar - Phe), 166.13 (C=O, amide), 174.92 (C=O).

H-Phe-Phe-OMe: ^{1}H-NMR ($CDCl_3$) – 2.12 (s 1H, αNH - Phe), 2.94 (m 1H, βCH2a - Phe), 3.10 (m 1H, βCH2a - Phe), 3.21 (m 1H, βCH2b - Phe), 3.31 (m 1H, βCH2b - Phe), 3.67 (s 3H, OCH3), 4.01 (q 1H, αCH - Phe), 4.81 (q 1H, αCH - Phe), 7.10-7.23 (m 10H, Ar - Phe), 8.05 (s 1H, NH – Phe/Phe); ^{13}C-NMR ($CDCl_3$) – 37.7 (CH2 - Phe), 41.4 (CH2 - Phe), 51.0 (OCH3), 52.9 (αCH - Phe), 53.5 (αCH - Phe), 126.6-140.0 (Ar - Phe), 171.9 (C=O, ester), 172.2 (C=O, Phe/Phe). The reaction was made in a series of solvents with the aim of its different applications. General procedure for the obtaining of dipeptide derivatives: H-Phe-OH (1 mol) and H_3PO_3 (1 mol) were dissolved in a mixture of MeCN/H_2O or DMSO and 2.5 moles of oxyrane were added. After heating for 20-30 min at 40 °C the amino component was added. The reaction mixture was stirred for 12 h. At the end of the reaction time 1N NaOH was added. The reaction mixture was stirred for 3-4h. The obtained product was extracted with EtOAc (3x20 ml) and washed with 5% $NaHCO_3$ (3x20 ml) and H_2O till pH 7. The organic layer was dried and the solvent was evaporated under vacuum.

References

1. Ramirez F. *Acc Chem Res* **1**: 168-174, 1968.
2. Ugi I, Marquarding D, Klusacek H, Gillespie P, Ramirez F; ibid. **4**: 288-296, 1971.
3. Fuller W, Cohen M, Sabankareh M, Mlair R. *JACS* **112**: 7414-7416, 1990.
4. Clark VM, Kirby AJ. *J Am Chem Soc* **85**: 3705-3706, 1963.
5. Benkovic SJ, Schray KJ. *Biochemistry* **7**: 4090-4096, 1968.
6. Schray KJ, Benkovic SJ. *J Am Chem Soc* **93**: 2522-2529, 1971.
7. Zhao YF, Ju Y, Li YM, Wang Q, Yin YW, Tan B. *Int J Pept Protein Res* **45**: 514-518, 1995.
8. Li YM, Zhao YF. *Phosphorus, Sulfur, and Silicon and the Related Elements* **78**: 15-21, 1993.
9. Zeng JN, Xue CB, Chen QW, Zhao YF. *Bioorganic chemistry* **17**: 434-442, 1989.
10. Videva VS, Bairyamov SG, Devedjiev IT. *Bulg Chem Commun* **39**: 276-280, 2007.

1-03-158

Solid Phase Synthesis of Aza-Peptides Using Activated *N*'-Substituted Ddz Protected Hydrazines

Freeman, Noam S; Hurevich, Mattan; Gilon, Chaim*

Hebrew University of Jerusalem, Institute of Chemistry, ISRAEL

**E-mail: freeman@chem.ch.huji.ac.il*

Introduction

Aza-peptides are peptide analogues in which one or more of the α-carbons, bearing the side chain residues, has been replaced by a nitrogen atom.[1,2] Aza-amino acid residues conserve the pharmacophores necessary for biological activity while inducing conformational changes and increased resistance to proteolytic degradation. These properties cause aza-peptides to be an attractive tool for structure-activity relationship studies and drug design.[3]

The2-(3,5-dimethoxyphenyl)propan-2-yloxycarbonyl (Ddz) group is an attractive protecting group which can be removed under extremely mild conditions.[4] The Ddz protecting group is normally removed with dilute TFA solutions (0.2-3%) in few minutes. However, Ddz can also be selectively removed by photolysis or by Lewis acids such as $Mg(ClO_4)_2$ or $ZnCl_2$. These extremely mild conditions offer an additional degree of orthogonality and enable Ddz to replace Fmoc in the SPPS using the Fmoc/t-Bu chemistry strategy.[5]

We present two general methods for the synthesis of *N*'-substituted 2-(3,5-dimethoxyphenyl)propan-2-yl carbazates (*N*'-substituted Ddz protected hydrazines). We then evaluate the application of *N*'-substituted Ddz hydrazines in solid phase aza-peptide synthesis using acid labile Rink-amide methylbenzhydrilamine (MBHA) resin with mild Lewis acid mediated Ddz deprotection.

Results and discussion

N'-substituted Ddz protected hydrazines were prepared in satisfying yields using two general synthetic pathways: (1) Reduction of the Ddz hydrazones, derived from the reaction of commercially available 2-(3,5-dimethoxyphenyl) propan-2-yl carbazate (Ddz hydrazide) **1** with either aldehyde or ketone. (2) Nucleophilic substitution of alkyl-halide with Ddz hydrazide (Fig. 1).

A general approach for solid phase synthesis of aza-peptides has been developed based on the in-situ activation of *N'*-substituted Ddz protected hydrazines with phosgene[6] followed by introduction to N-terminus peptidyl-resin. Procedures for activation and coupling as activated aza-amino acids are similar to those reported for *N*'-alkyl Fmoc carbazates[7] with minor modifications. The Ddz protecting group was removed conveniently and selectively with $Mg(ClO_4)_2$ in ACN at 50 °C[5] followed by coupling of the next amino acid with triphosgene[8] and routine peptide elongation (Fig. 2).

Conclusion

We present the synthesis of novel *N*'-substituted Ddz hydrazines in which the *N*-substituents are mainly derived from the side chains of amino acids. We demonstrate the incorporation of these aza-amino

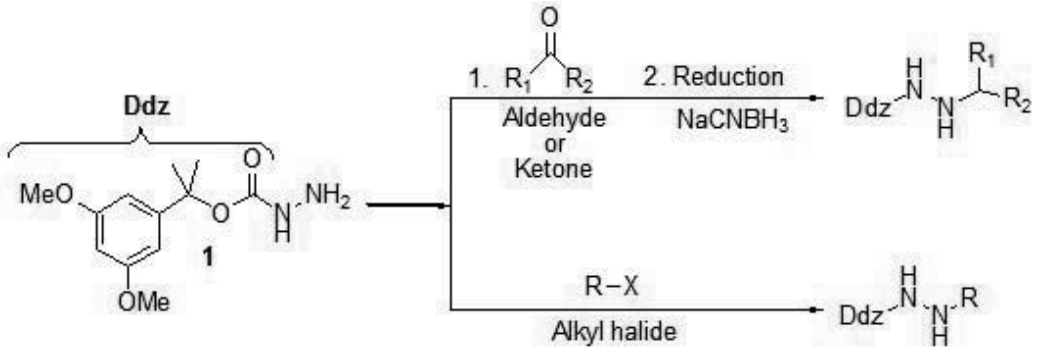

Figure 1. Synthetic scheme of *N*'-Alkyl,*N*-Ddz hydrazines.

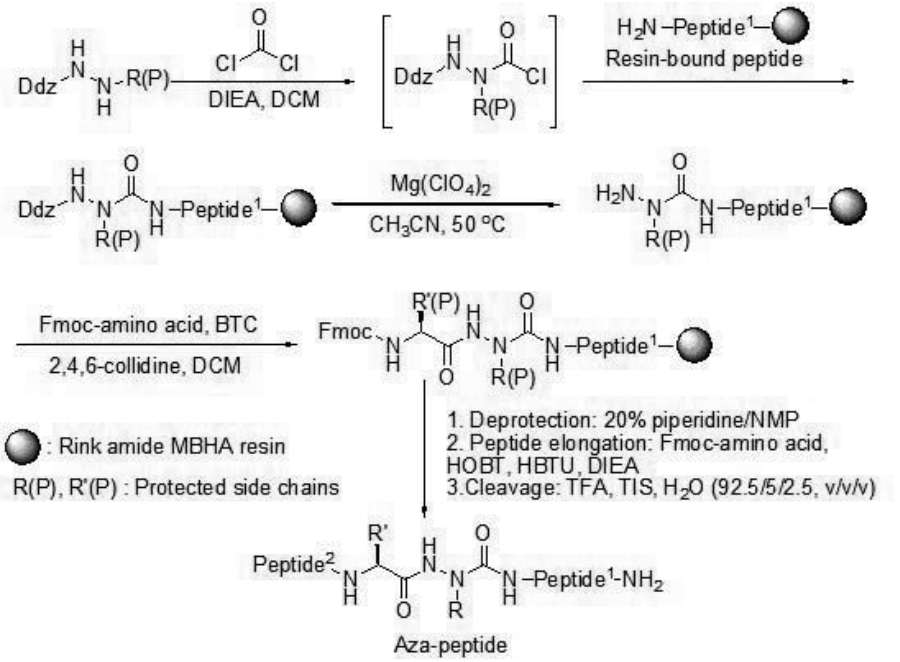

Figure 2. General protocol for solid phase synthesis of aza-peptides using *N*'-substituted Ddz hydrazines.

acid precursors into peptides to afford aza-peptides using standard SPPS Fmoc chemistry. This convenient procedure for solid phase synthesis of aza-peptides using Ddz orthogonal protection facilitates the generation of novel peptidomimetics such as branched aza-peptides and cyclic aza-peptides. In addition, Ddz deprotection is orthogonal with both the Fmoc and Boc chemistry side-chain protecting groups, making the solid phase Ddz-aza-peptide synthesis compatible with both the Fmoc and the Boc strategies.

References

1. Gante J. *Synthesis* **6**: 405-413, 1989.
2. Zega A, Urleb U. *Acta Chim Slov* **49**: 649-662, 2002.
3. Zega A. *Curr Med Chem* **12**: 589-597, 2005.
4. Birr C, Lochinger W, Stahnke G, Lang P. *Justus Liebigs Ann Chem* **763**: 162-172, 1972.
5. Wildemann D, Drewello M, Fischer G, Schutkowski M. *Chem Commun* **18**: 1809-1810, 1999.
6. Gibson C, Goodman SL, Hahn D, Holzemann G, Kessler H. *J Org Chem* **64**: 7388-7394, 1999.
7. Boegli D, Lubell WD. *J Comb Chem* **7**: 864-878, 2005.
8. Falb E, Yechezkel T, Salitra Y, Gilon C. *J Pept Res* **53**: 507-517, 1999.

1-03-159

Improved synthesis of relaxin-2

Barlos, Kostas; Vasileiou, Zoe; Gatos, Dimitrios; Barlos, Kleomenis*

University of Patras, 26500 Patras, Department of Chemistry, GREECE

E-mail: barlos@cblpatras.gr

Introduction

Insulin and insulin like peptides (INSL) are important because of their potential pharmaceutical applications. Among the INSLs, human relaxin-2 (RLN2) was tested in clinical trials against a variety of indications. RLN2 is consisted of two peptide chains, A (RLN2-A) and B (RLN2-B) joined by two intermolecular cysteine bridges. Chain A contains an additional intramolecular disulfide bond. The synthesis of RLN2 is complicated, not only because the two chains must be connected in the correct way but also because of the high insolubility of chain-B. The high insolubility of chain-B and of the intermediate smaller peptides is also indicated by the difficult coupling and deprotection steps during its solid phase synthesis. Attempts to synthesize the peptide by the condensation of protected fragments gave also low yield and purity for the same reasons. Analytical HPLC of crude chain-B obtained show broad peaks and are therefore of low analytical value. The HPLC-purification of chain-B is also very difficult. To overcome the solubility problems, extended or shortened B-chains are synthesized to study the folding and other biological properties of RLN2.[1]

Results and discussion

To improve the synthesis of RLN2 a better method of preparing RLN2-B was absolutely necessary. However, this could not be possible without discovering a system to dissolve it easily and to overcome the difficult steps of its synthesis. During several attempts to synthesize RLN2, either by the step by step or by the fragment condensation approach, we steadily identified by LC-MS a Met-sulfoxide side product. The interesting on this was that it eluted as a sharp peak indicating its better solubility, as compared to RLN2. This was a very promising observation, so we assumed that oxidation of one of the Met-residues and the conversion of RLN2-B to the corresponding Met(*O*)-RLN2 could significantly improve its solubility. In addition, we expected similar improvement in the solubility of the intermediate fragments during the peptide elongation. This change in solubility could allow a) better analysis of intermediates and so the possibility to optimize the synthesis and b) easier purification by HPLC and handling of the crude synthetic RLN2-B.

Met^{25}(*O*)-RLN2-B was prepared by the Fmoc/tBu-based methodology using the 2-chlorotrityl resin (Fig. 1). Even in the first not optimized synthesis the crude product obtained was of 68% purity. It was good soluble in various aqueous solutions and its purification by HPLC occurred easily and we were able to obtain it in 46% yield. Oxidation of Met^{25}(*O*)-RLN2-B with DMSO gave almost quantitatively the corresponding cyclic derivative. Met^{4}(*O*)-RLN2-B and Met$^{4,\ 25}$(*O*)-RLN2-B were also prepared by similar methods. These derivatives show also increased solubility. Even more soluble is the corresponding oxidized derivative of Met^{25}(*O*)-RLN2-B.

The combination of RLN2-A with Met^{25}(*O*)-RLN2-B was performed by mixing them in the linear and oxidized form under various conditions and rates. In Fig. 2b is shown the analytical HPLC obtained after reacting

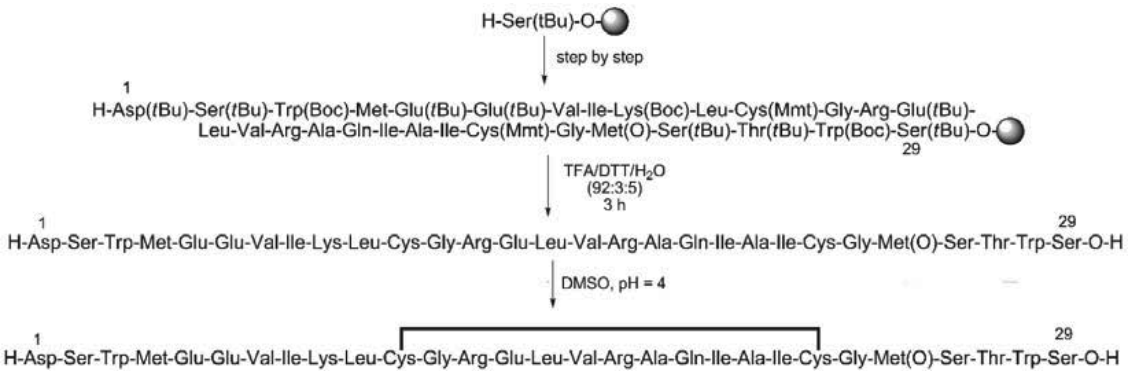

Figure 1. Synthesis of Met^{25}(*O*)-human relaxin-2 B-chain and of its cyclic derivative.

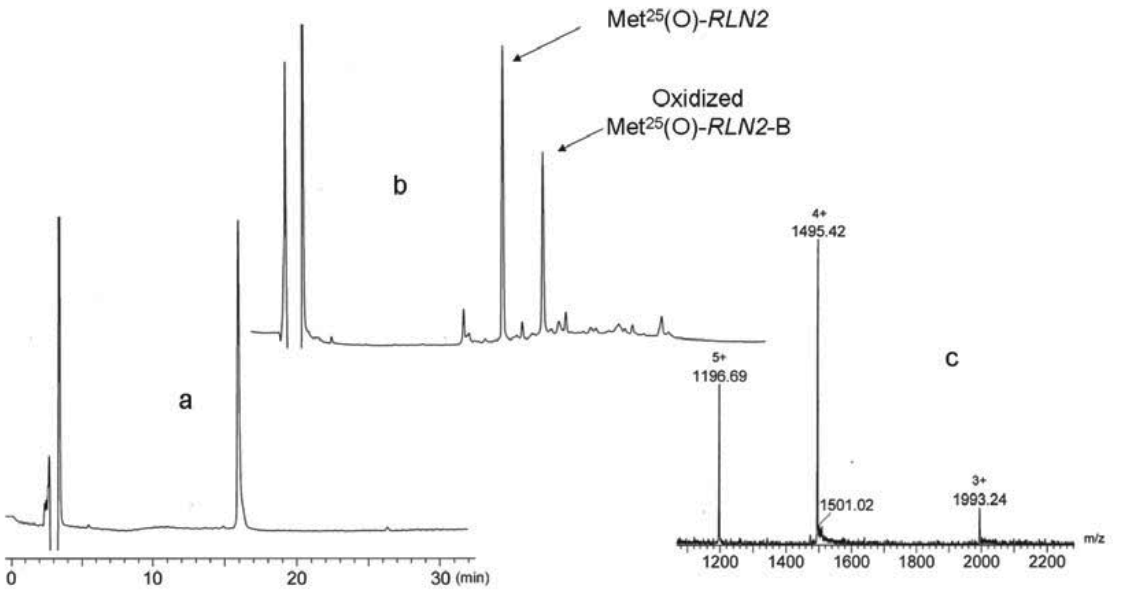

Figure 2. (a) Analytical HPLC of purified human relaxin-2 (b) the product mixture obtained by the combination of oxidized RLN2-A with Met[25](*O*)-RLN2-B for 24 h at RT , detection at 214 nm (c) ES-MS of human relaxin-2.

oxidized chain A with a 2.5 molar excess of Met[25](*O*)-RLN2-B for 24 h at RT. As solvent, 6N-Gd.HCl was used and the pH of the mixture was set at 10.5 by adding sodium glycinate. These conditions were described by Wade *et al*.[1] The obtained relaxin derivative was easily transformed to the corresponding native relaxin by reduction with ammonium iodide.

In conclusion, the synthesis of Met[25](*O*)-RLN2-B is performed in high yield and purity. This derivative and other Met(*O*)-containing analogs show increased solubility, as compared to native relaxin chain-B. That allowed its simple purification and application in chain combination experiments and in the preparation of relaxin analogs.

Acknowledgements

The work was funded by CBL-Patras S.A.

References

1. Wade J, Tregear G. *Methods Enzymol* **289:** 637-646, 1997.

1-03-160

Synthesis of peptides from racemic amino acids with predictable optical purity and configuration of the product by using traceless chiral triazine coupling reagents

*Kolesińska, Beata**

Technical University of Lodz Institute of Organic Chemistry, POLAND

**E-mail: address beata.kolesinska@p.lodz.pl*

Introduction

The demand for a molecular diversity of peptides used in the studies on structure-activity relationships and the construction of compound libraries have remarkably stimulated progress in the preparation of optically active analogues of proteinogenic amino acids. However, an alternative approach based on the enantiodifferentiating transformation of racemic substrates, which are usually easily available, would be valued as more advantageous and less time consuming than the classic procedure involving racemate resolution or asymmetric synthesis. Enantiodifferentiating methods would be considered as general and the most convenient in the case of constructing complex molecule libraries from chiral building blocks. Several chiral coupling reagents have been proposed for the synthesis of enantiomerically enriched peptides directly from racemic amino acids. Optically active N-hydroxysuccinimide and diacylamine derivatives, chiral DMAP analogues, *N*-methylimidazole, heterocyclic carbene, benzotetramisole, tertiary amines and phosphines and others were used as a chiral auxiliary.[1] So far, however, none of the coupling methods has been accepted in practice because of the unpredictable results of synthesis involving multiple stereogenic centers which are present in chiral coupling reagents and chiral substrates.

Results and Discussion

In order to design an efficient chiral auxiliary and to resolve the problem of predictability of synthetic results including purity, high yield, optimal coupling conditions, configuration and the enantiomeric composition of the final product, this paper presents a novel general approach allowing a preferred enantiomer to be selectively incorporated directly from a racemic substrate. It is based on the synthesis of a traceless coupling reagent **4** effective as an enantiodifferentiating agent only at the activation stage, and then, after the departure of the chiral auxiliary, transformed into a well-known classic achiral acylating reactive intermediate **3**. Thus, the structure, properties and reactivity of the activated carboxylic component **3** should be exactly the same as those obtained in a reaction involving a classic achiral reagent **2**.[2] Moreover, due to the departure of the chiral auxiliary after activation, all further stages of the coupling procedure should remain free of the disturbances caused by the presence of the stereogenic center of the chiral auxiliary and therefore the configuration and enantiomeric purity, once established during the activation stage, should remain essentially intact in all the syntheses involving this carboxylic component and reagent. This means that the configuration and results of enantiomeric enrichment could be predicted for all the syntheses involving a given set of components from a single model experiment, avoiding additional studies on the scope and limitations of the acylation procedure.

According to this concept, the reagent **4** consists of a stable binary system formed from readily accessible achiral triazine components and an appropriate tertiary amine used as a chiral auxiliary L*.

The reagent **4** was prepared by the treatment of brucine tetrafluoroborate with **1** in the presence of an HCl

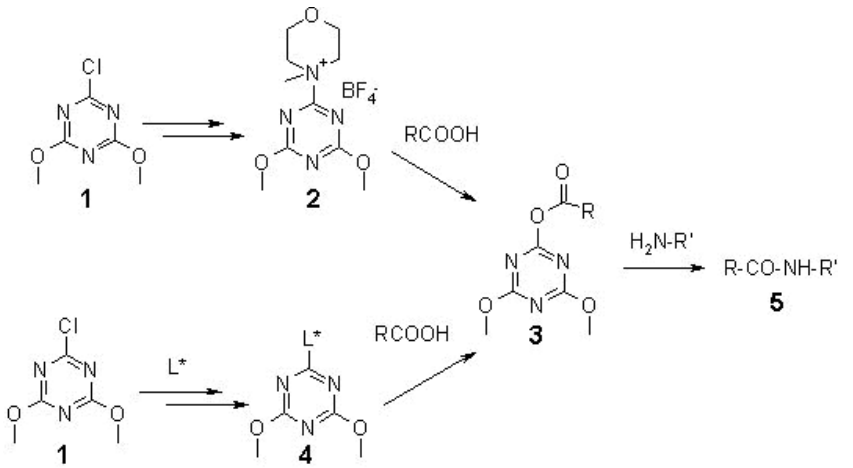

Entry	amine	Solvent	Yield [%]	DL/LL
1	brucine	THF	67	80/20
2	"	DMF	96	65/35
3	"	1,2-diethoxyethan	77	82/18
4	"	AcOEt	82	77/23
5	"	THF + *t*-BuOH (1:1)	89	55/45
6	"	$CHCl_3$	96	82/18
7	"	CH_2Cl_2	93	87/13
8	DIPEA	"	96	85/15
9	brucine	CH_3CN	91	95/5
10	DIPEA	"	94	90/10

acceptor[3]. It was found that the presence of a catalytic amount of the appropriate tertiary amine is essential to the activation of the carboxylic function. Achiral DIPEA and brucine were selected as suitable for the process of activation. The character of the solvent was crucial for the efficient enantiodiscriminating activation of the carboxylic component and acetonitrile was selected as the most suitable.

Even if only a twofold excess of racemic N-protected alanine was used, high enantiomeric purity and the same D-configuration at the alanine stereogenic centre were obtained with **4** used as a coupling reagent as determined by GC on a ChirasilVal capillary column.

Acknowledgement

This work was supported by Ministry of Science and Higher Education, Grant PBZ-KBN-126/T09/15.

References

1. a) Vedejs E, Chen X. *J Am Chem Soc* **118**: 1809-1810, 1996; b) Ruble JC, Fu GC. *J Am Chem Soc* **120**: 11532-11533, 1998; c) Spivey AC, Fekner T, Adams H, Spey SE. *J Org Chem* **64**: 9430-9433, 1999; d) Miller SJ, Copeland GT, Papaioannou N, Horstmann TE, Ruel EM. *J Am Chem Soc* **120**: 1629-1630, 1998.
2. Kamiński ZJ, Kolesińska B, Kolesińska J, Sabatino G, Chelli M, Rovero P, Błaszczyk M, Główka ML, Papini AM. *J Am Chem Soc* **127**: 16912-16920, 2005.
3. Kolesińska B, Kamiński ZJ. *Polish Pat Appl* **P-38476** from 04.02. 2008.

Table 2. 2 eq. racemic carboxylic acid+1 eq. DMT/brucine/BF_4+1 eq. amino component.

Entry	racemic component	acylated component	product prepared	Yield [%]	D/L
1	Z-DL-Ala	L-Phe-OMe	Z-D-Ala-L-Phe-OMe	94	96/4
2		L-Leu-OMe	Z-D-Ala-L-Leu-OMe	93	93/7
3		L-Trp-OMe	Z-D-Ala-L-Trp-OMe	88	96/4
4		L-Val-OMe	Z-D-Ala-L-Val-OMe	96	98/2
5		L-Ile-OBut	Z-D-Ala-L-Ile-OBut	95	92/8
6		L-Ser-OMe	Z-D-Ala-L-Ser-OMe	93	95/5
7		L-Tyr-OEt	Z-D-Ala-L-Tyr-OEt	89	99.6/0.4
8		L-His-OMe	Z-D-Ala-L-His-OMe	88	92/8
9		L-Pro-OMe	Z-D-Ala-L-Pro-OMe	92	97/3
10		Gly-OEt	Z-D-Ala-Gly-OEt	85	98/2
11		Aib-OMe	Z-D-Ala-Aib-OMe	88	94/6
12		NH_2-$(CH_2)_3CH_3$	Z-D-Ala-NH-$(CH_2)_3CH_3$	86	99/1
13		CH_3OH	Z-D-Ala-OCH_3	96	97/3
14	Fmoc-DL-Ala	L-Phe-OMe	Fmoc-D-Ala-L-Phe-OMe	92	96/4
15		L-Leu-OMe	Fmoc-D-Ala-L-Leu-OMe	93	92/8
16		Gly-OEt	Fmoc-D-Ala-Gly-OEt	87	96/4
17		NH_2-$(CH_2)_3CH_3$	Fmoc-D-Ala-NH$(CH_2)_3CH_3$	86	95/5

1-03-161

Backbone cyclization of peptides via *N*-functionalized phosphorylated tyrosine

Reissmann, Siegmund; Zoda, Mohammad Safa

Friedrich-Schiller-university, GERMANY

E-mail: siegmund.reissmann@uni-jena.de

Peptide ligands for SH2- and PTP domains containing phosphotyrosine are of great interest to influence the activity of kinases, phosphatases and other functional proteins.[1] Backbone cyclization can help to stabilize these ligands against proteolytic degradation and to preform their bioactive conformation.[2] Till now backbone cyclization has been mainly performed with bifunctional and only in few cases with trifunctional amino acids, but never with phosphorylated tyrosine. Modelling of a ligand for the *N*-terminal SH2-domain of the phosphatase SHP-1 resulted in a sequence which requires *N*-functionalized phosphorylated tyrosine in the peptide chain.

The assembly of such peptides requires preformed building units because of the low coupling yields by acylation of *N*-functionalized amino acids. Since the necessary reductive alkylation of phosphotyrosine and derivatives provides only very low yields we used *N*-functionalized pseudodipeptides with the unprotected phenolic hydroxyl group. Thus we synthesized building units of the common structures:

Fmoc-Aaψ[CO-N(CH_2)n-(X)-NH-Alloc)Tyr(OH)-OH.

Reductive alkylation[3] of Tyr(But)-OBut with the corresponding Alloc-NH-aldehydes provides products from sufficient purity and in sufficient yield (60 to 80%), independently from length and properties of the chain (Fig. 1). Depending on the steric hindrance of coupling reactions by the N-terminal amino acid these pseudodipeptides were synthesized either in solution (Abu, Fig. 2) or at SASRIN-resin with repeated couplings

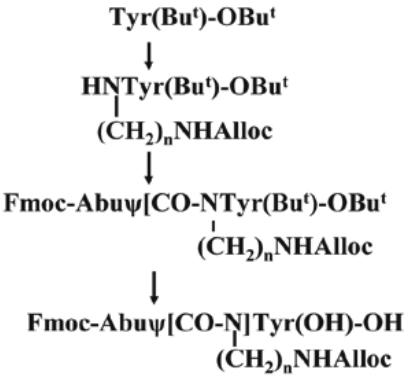

Figure 1. Synthesis of dipeptide building units in solution.

and with a large excess of the bulky amino acid derivative [Asn(Trt)]. The building units were purified at each step by flash chromatography (3 times) and analytically characterized by HPLC, ESI-MS and NMR.

We could not succeed with the synthesis of the corresponding preformed dipeptide units with allyl esters like Fmoc-Aaψ[CO-N(CH_2)m-COOAll)Tyr(OH)-OH. Also all approaches to form an alternative pseudopeptide bond[4] Fmoc-Aaψ[CH_2-N(CO-(CH_2)n-COOAll)] Tyr(OH)-OH proceeded unsuccessfully.

We checked our strategy on the synthesis of modelled

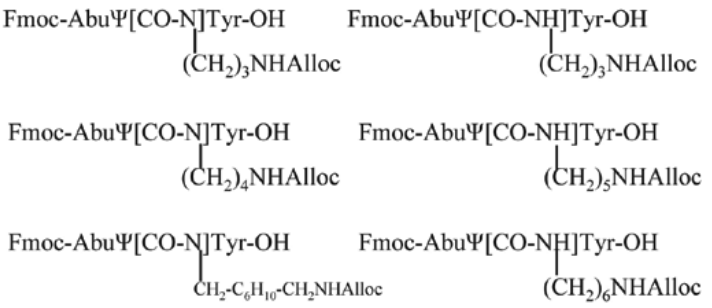

Figure 2. Synthesized pseudodipeptides.

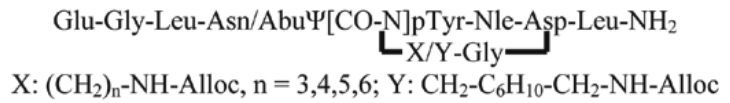

Figure 3. Synthesized octapeptide ligands with backbone cyclization.

octapeptide-ligands for the *N*-terminal SH2-domain of the phosphatase SHP-1. Condensation of the dipeptide units were performed with PyBOP, stepwise coupling to the peptide fragments with unprotected phenolic hydroxyl group via pentafluoro phenylesters. For backbone cyclization we used PyBOP as coupling reagent. But, from the free phenolic hydroxy group result various side reactions, including *O*-acylation and *N-O* migration of the amino acid coupled to *N*-alkyl tyrosine. After finishing the assembly the obtained cyclic octapeptides were consecutively phosphorylated, deblocked, removed from the resin, precipitated with ether and purified by semipreparative HPLC. Global phosphorylation of linear and cyclic octapeptides was carried out at RINK-amide resin (loading: 0.7 and 0.4 meq/g) with di-t-butyl-*N,N*- and di-benzyl-phosphoramidites under argon in DMF and subsequent oxidation.[5] Repeated phosphorylation enhances the yield only marginally. Phosphorylated and unphosphorylated octapeptides can be obtained simultaneously Besides these two products some fragments, phosphonates, incomplete deblocked octapeptides and linear peptides could be detected in the crude product. By the described route the following octapeptide ligands were synthesized (Fig. 3).

Acknowledgements

The project was financially supported by the “DFG” (Re 853/10-1).

References

1. Burke TR, Zhang Z-Y. Protein-tyrosine phosphatases: structure, mechanism, and inhibitor discovery. *Biopolymers (Peptide Science)* **47**: 225-241, 1998.
2. Reissmann S, Imhof D. Development of Conformationally Restricted Analogues of Bradykinin and Somatostatin Using Constraint Amino Acids and Different Types of Cyclization (rev). *Current Medical Chem* **11**: 2823-2844, 2004.
3. Müller B, Besser D, Kleinwächter P, Arad O, Reissmann S. *J Pept Res* **54**: 383-393, 1999.
4. Besser D, Müller B, Agricola I, Reissmann S. *J Pept Sci* **6**: 130-138, 2000.
5. Perich JW. *Synthesis of Phosphopeptides. Houben-Weyl* **E22**: 375-424, 2003.

1-03-162

Studies on the synthesis of the kazal-type inhibitor LEKTI domain 6

Vasileiou, Zoe[1]; Barlos, Kostas[1]; Gatos, Dimitrios[1,]; Adermann, Knut[2]; Forssmann, Wolf-Georg[2]; Barlos, Kleomenis[1]*

[1]Department of Chemistry, University of Patras, 26500 Patras, GREECE; [2]IPF PharmaCeuticals GmbH, D-30625 Hannover, GERMANY

[*]E-mail: d.gatos@upatras.gr

Introduction

LEKTI (Lympho-Epithilial Kazal-Type Inhibitor) is a novel multidomain proteinase inhibitor consisting of 15 potential serine proteinase inhibitory domains. Defects within the gene encoding LEKTI have been associated with several skin diseases and atopic disorders, including Netherton syndrome and atopic dermatitis.[1] Therefore, LEKTI represents a potential drug candidate for treating these disorders. In order to develop an efficient method to synthesize the domain 6 of LEKTI, consisting of 68 amino acid-residues and two disulfide bonds (Fig. 1), two main approaches were investigated: a) the condensation of large protected fragments in solution and b) the native chemical ligation of unprotected fragments in aqueous buffer.

Results and Discussion

The required fragments [Cys^{12}(Acm)]-(1-25)-thioester and the [Cys^{48}(Acm)]-(26-68) were prepared by the Fmoc/tBu-based methodology using the 2-chlorotrityl resin. Protected 1-25 and 1-22 fragments were prepared by stepwise SPPS with the Asn$^{13, 21}$ residues left unprotected. In order to regioselectively form the two disulfide bonds, Cys^{12,48} residues were side-chain protected by the Acm group, whereas Cys^{26,45} were protected by the very acid-labile Mmt group. Fragment 1-25, was converted to the corresponding *C*-thioester by reacting it with excess of methyl mercaptoacetate using DIC/HOBt as the condensing agent. The thioesterification reaction was unusually fast, being complete in 15 min at RT. Similarly, the 26-68 protected fragment was prepared by condensing fragment 26-38 on the resin bound 39-68 fragment with the Asn$^{30, 43}$ and Ser^{46} being side-chain Trt-protected. Thioester 1-25 and *N*-Cys 26-48 peptides were obtained in 52 and 31 % yield, respectively, after deprotection and HPLC purification.

Following the fragment condensation approach, the 1-22 and 23-68 protected fragments were condenced in solution. The 23-68 fragment was used either in the free carboxylate form or after protecting it with the Clt group. Best results were obtained by preactivating the C-component (1.1 molar excess) with EDAC/HOBt for 1h at RT and adding then the N-component in the activated mixture. DCM was used as the solvent, where both fragments were freely soluble. A typical LC-MS analysis of the reaction mixture, after deprotection is shown in Fig. 2a. In the alternative native chemical ligation (NCL) approach, purified 1-25 thioester peptide and the *N*-Cys 26-68 segment (1.1 molar excess) were ligated in phosphate buffer at pH = 7.5, containing 5 % thiophenol and 1 % TCEP at RT. The reaction was fast, being complete in 1 h at RT (Fig. 2b).

Purified linear [Cys^{12,48}(Acm)]-LEKTI-6 was subjected to a two-step oxidation procedure, involving a DMSO oxidation step to form the first Cys^{26}-Cys^{45} disulfide bond, followed by iodine oxidation to form the Cys^{12}-Cys^{48} bond. The DMSO oxidation proceeded smoothly and was completed within 3.5 h at RT without the formation of any remarkable side product. In contrary, the oxidative removal of Acm and the formation of the second disulfide bond gave a rather complicated product mixture. Besides the required product and its corresponding sulfoxide, other main components identified were the complete deprotected and reduced LEKTI and the *S*-iodide-LEKTI. Interestingly, we found that large excess of iodine and short reaction time lead to a product mixture with a much higher purity in LEKTI and Met(O)^{47}-LEKTI. The LEKTI-sulfoxide was cleanly and quantitatively reduced with ammonium iodide. LEKTI-6 was thus obtained in >99% purity.

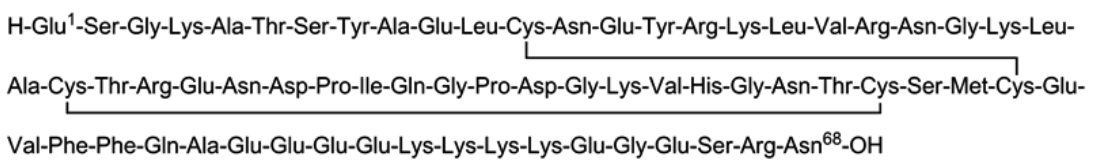

Figure 1. Primary structure of LEKTI domain 6.

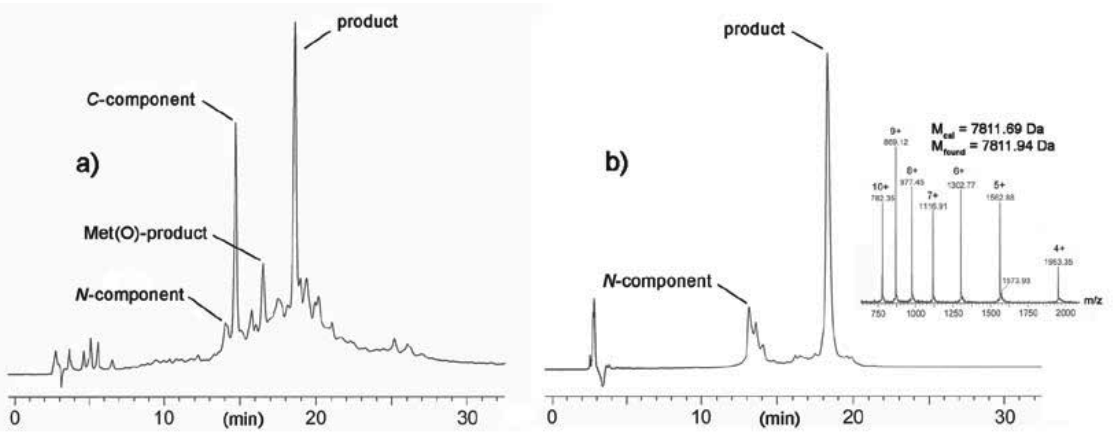

Figure 2. (a) HPLC analysis of the mixture obtained from fragment condensation in solution, after deprotection and (b) HPLC analysis of the chemical ligation mixture at 1 h and ES-MS of purified [Cys^{12,48}(Acm)]-LEKTI-6(1-68).

In conclusion, LEKTI domain 6 was obtained in good yield either by the condensation of protected fragments in solution or by ligation methods. The condensation method is economically more attractive, but ligation is easier to control. The formation of the two disulfide bonds by DMSO followed by oxidative removal of *S*-Acm with iodine proceeds with excellent regioselectivity.

Acknowledgments

The work was funded by CBL-Patras S.A.

References

1. Magert H, Standker L, Kreutzmann P, Zucht H, Reinecker M, Sommerhoff C, Fritz H, Forssmann W-G. *J Biol Chem* **274:** 21499-21502,1999.

1-03-163

Azide as a protecting group for lysine side chains on the solid phase peptide synthesis oriented toward the peptide condensation by the thioester method

Katayama, Hidekazu[1,]; Hojo, Hironobu[1]; Ohira, Tsuyoshi[2]; Nakahara, Yoshiaki[1]*
[1]Tokai University, Department of Applied Biochemistry JAPAN; [2]Kanagawa University, Department of Biological Science, Faculty of Scie, JAPAN

[*]E-mail: katay@hotmail.co.jp

Introduction

The solid phase peptide synthesis (SPPS) is usually limited to approximately less than 50 residues long. For the synthesis of longer peptides, condensation methods of two or more peptide segments are used. Thioester method is one of the condensation methods of peptide segments.[1] In this method, any residue at the ligation point can be used, although the protecting groups for amino and thiol groups are required. For protection of thiols, acetoamidomethyl group can be used due to its stability under both basic and acidic conditions. Inconveniently, Boc groups should be introduced to the amino groups in the peptide segments used for this method after the cleavage from the resins and the purification steps. To overcome this problem, a less hydrophobic protecting group for amines stable under both acidic and basic conditions was desired. Azide moiety was a good candidate for such purpose. In this study, to investigate the usefulness of azide for an amino protecting group, we have synthesized two crustacean pigment dispersing hormones (PDHs), NSELINSLLGIPKVMTDA-amide (PDH-I) and NSELINSLLGLPKFMIDA-amide (PDH-II),[2] by the thioester method using the azido peptides as building blocks.

Results and Discussion

Fmoc-Lys(N_3)-OH was synthesized from Fmoc-Lys-OH by the copper(II)-catalyzed diazo transfer method,[3] and introduced to the C-terminal segments, H-Ile-Pro-Lys(N_3)-Val-Met-Thr-Asp-Ala-NH_2 and H-Leu-Pro-Lys(N_3)-Phe-Met-Ile-Asp-Ala-NH_2, by the ordinary Fmoc-based SPPS. To synthesize the common N-terminal peptide segment (Fmoc-Asn-Ser-Glu-Leu-Ile-Asn-Ser-Leu-Leu-Gly-SR), Fmoc-Asn-Ser-Glu-Leu-Ile-Asn-Ser-Leu-Leu-Gly-(Et)Cys-NH_2 was synthesized by the Fmoc-SPPS and then the C-terminal *N*-ethylcysteine was converted to the thioester using 4-mercaptophenylacetic acid by our novel thioesterification reaction developed previously.[4] The N- and C-terminal segments were dissolved in dimethylsulfoxide containing 3-hydroxy-4-oxo-3,4-dihydro-1,2,3-benzotriazine (HOOBt), and the coupling reaction was initiated by addition of diisopropylethylamine (DIEA). The condensation was almost completed within 5 h, and the Fmoc group of the desired product was removed by piperidine. The crude peptide was precipitated by diethylether, and the azide group was reduced to amino group by Zn powder in 50% aqueous AcOH solution. The desired products were purified by reversed-phase HPLC with yields of 47%

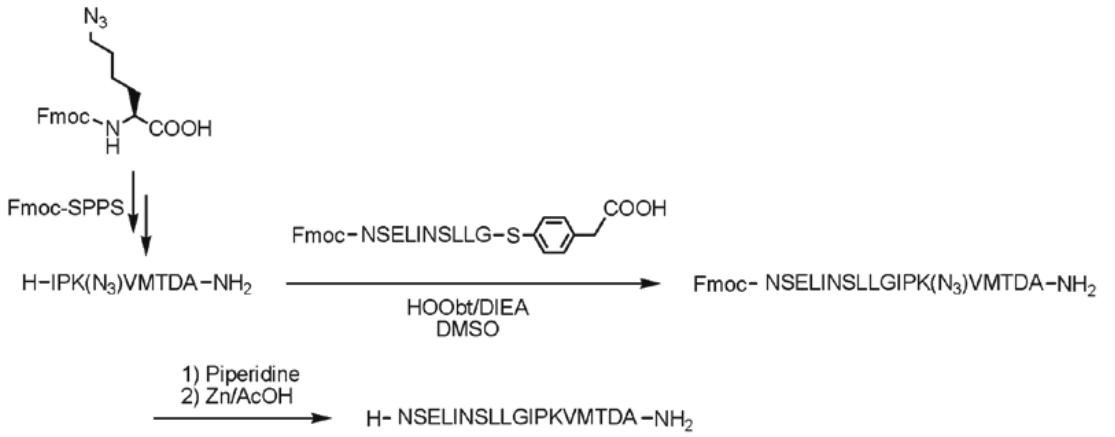

and 57% for PDH-I and -II, respectively.[5] The *in vivo* biological assay[2] of the synthetic peptides was carried out. Thirty minutes after injection of each peptide to the eyestalk-ablated prawns, melanophores were enlarged compared from those of saline-injected animals, indicated that the synthetic PDHs were fully active. Currently, we are examining the synthesis of large glycoproteins using this azide-based strategy.

References

1. Hojo H, Aimoto S. *Bull Chem Soc Jpn* **64**: 111-117, 1991.
2. Yang W-J, Aida K, Nagasawa H. *Gen Comp Endocrinol* **114**: 415-424, 1999.
3. Speers AE, Cravatt BF. *Chem Biol* **11**: 535-546, 2004.
4. Hojo H, Onuma Y, Akimoto Y, Nakahara Y, Nakahara Y. *Tetrahedron Lett* **48**: 25-28, 2007.
5. Katayama H, Hojo H, Ohira T, Nakahara Y. *Tetrahedron Lett* **49**: 5492-5494, 2008.

1-03-164

Peptide thioester preparation and peptide ligation using cysteinyl prolyl ester (CPE) autoactivating unit

Kawakami, Toru[1,]; Aimoto, Saburo*
Institute for Protein Research, Osaka University, JAPAN

[*]E-mail: kawa@protein.osaka-u.ac.jp

Introduction

Peptide thioester is a key building block in ligation strategy for polypeptide synthesis. In the thioester method, partially protected peptide thioesters are used as building blocks and are condensed in the presence of silver ions as an activating reagent for the thioester.[1] Chemoselective ligation of the unprotected peptide thioester with a peptide having a cysteine residue at the N-terminus is performed in an aqueous buffer solution in native chemical ligation.[2] During the course of our studies related to new ligation methodology, we have been focusing on an *N* to *S* acyl shift reaction of a cysteine-containing peptide, resulting in an *S*-peptide (peptide thioester).[3] On the other hand, in 1985, Zanotti *et al*. reported that a diketopiperazine thioester, *cyclo*(-Cys($COCH_2Ph$)-Pro-) (**1**) was formed when a *p*-nitrophenyl (Np) ester, $PhCH_2CO$-Cys(S*t*Bu)-Pro-ONp (**2**), was treated with tributylphosphine under aqueous conditions.[4] The thioester **1** would be formed via the intramolecular *N*-*S* acyl shift reaction followed by diketopiperazine (DKP) formation. Based on these observations, we found that a peptide having a cysteinyl prolyl ester (CPE) at the C-terminus (CPE-peptide) **3** is transformed into a peptide thioester of DKP **4** via the intramolecular reaction in neutral aqueous conditions.[5] In this paper, the peptide thioester formation and the ligation of the CPE-peptide are described (Fig. 1).

Results and Discussion

When a peptide, Fmoc-His-Pro-Ile-Arg-Gly-Cys-Pro-OCH_2CONH_2 (**3a**), was treated with sodium 2-mercaptoethanesufonate in a sodium phosphate buffer (pH 8.8) in the presence of tris(2-carboxyethyl)phosphine, the corresponding peptide thioester, Fmoc-His-Pro-Ile-Arg-Gly-$SCH_2CH_2SO_3H$ (**5a**), was obtained in a yield of 72% after 6 h at 37 °C. Hydrolysis of the thioester **5a** gradually proceeded in prolonged reaction time. In the buffer below pH 8, the thioester was relatively stable to hydrolysis, though the thioester formation was slower. The CPE-peptides (Fmoc-His-Pro-Ile-Arg-*Xaa*-Cys-Pro-OCH_2CONH_2) containing a different amino acid residue of *Xaa* (*Xaa* = Gly, **3a**; Ala, **3b**; Val, **3c**; and Ser, **3d**) were transformed into the peptide thioesters. In a phosphate buffer at pH 8.2 and 37 °C, the rates of the thioester formation were very similar though the *Xaa* was different in each CPE-peptide, and the yield of the thioester reached ca. 70% within 6 h. After that, the thioesters having Gly, **5a**; Ala, **5b**; and Ser **5d** at the (*Xaa* residues were gradually hydrolyzed, while Val-thioester **5c** was relatively stable after 24 h. Epimerization occurred at the C-terminal amino acid residues of the thioester. The D-amino acid content increased with the reaction time. For example, in the case of Ser-thioester **5d**, it increased from 12% (2 h) to 34% (8 h). When isolated thioester **5d**

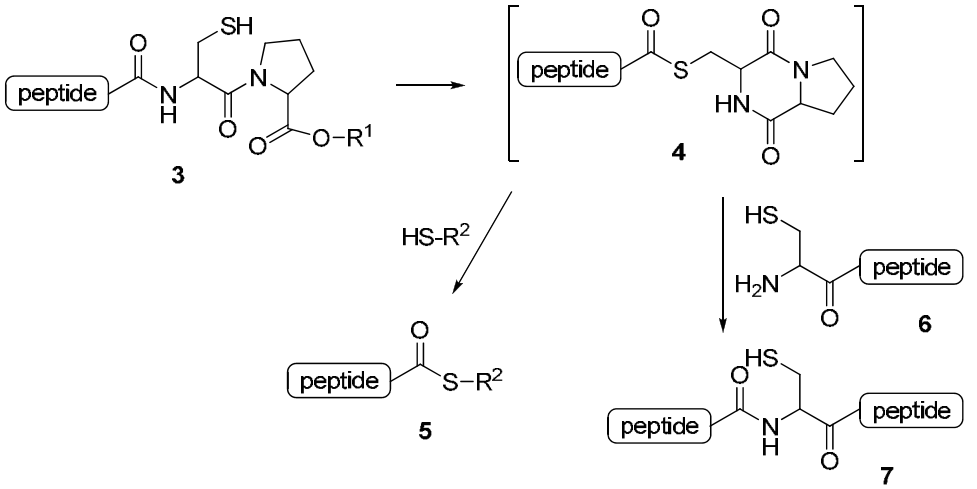

Figure 1. Peptide thioester formation and ligation of CPE-peptide.

was treated under the same reaction conditions, it was epimerized along with hydrolysis: After 8 h, thioester **5d** was epimerized in 39%, and hydrolyzed in ca 30%. In the case of Val-thioester **5c**, the D-Val residue was contained in less than 4% after 24 h. The epimerization occurs after the thioester formation.

The CPE-peptide is transformed into the DKP-thioester automatically in the neutral buffer solutions. Therefore, when it is mixed with a cysteinyl peptide, the ligation reaction occurs.[5] When CPE-peptide **3a** was reacted directly in one-pot with Cys-Asp-Ile-Leu-Leu-Gly-NH_2 (**6a**) in a tricine buffer (pH 8.2) containing 20 mM tris(hydroxypropyl)phosphine and 6 M guanidine for 24 h, the ligated product, Fmoc-His-Pro-Ile-Arg-Gly-Cys-Asp-Ile-Leu-Leu-Gly-NH_2 (**7a**), was formed and purified by RP-HPLC in 60% yield.[5] The ligation of CPE peptides **3b** and **3c** with **6a** gave Fmoc-His-Pro-Ile-Arg-Ala-Cys-Asp-Ile-Leu-Leu-Gly-NH_2 (**7b**) in 56% and Fmoc-His-Pro-Ile-Arg-Val-Cys-Asp-Ile-Leu-Leu-Gly-NH_2 (**7c**) in 49%, respectively, and the D-amino acid content in the product was less than 4% in the both cases.

In summary, the peptide containing Cys-Pro-Ester (CPE) unit at the C-terminus (CPE-peptide) is automatically activated into the thioester, and undergoes ligation with a Cys-peptide in one-pot under neutral conditions. Although at the high pH conditions the hydrolysis and epimerization of the thioester occur after the thioester formation, these side reactions are suppressed when the thioester reacts rapidly with a Cys-peptide. Thus, the ligation reaction proceeds with minimum epimerization. The CPE-peptide can be easily prepared by standard Fmoc solid phase peptide synthesis because it has no thioester moiety, and it is applied to the chemoselective ligation reactions.

Acknowledgements

This research was supported, in part, by Grants-in-Aid for Scientific Research from the Ministry of Education, Culture, Sports, Science and Technology, Japan.

References

1. Hojo H, Aimoto S. Polypeptide synthesis using the S-alkyl thioester of a partially protected peptide segment. Synthesis of the DNA-binding domain of c-Myb protein (142-193)-NH_2. *Bull Chem Soc Jpn* **64**: 111-117, 1991.
2. Dawson PE, Muir TW, Clark-Lewis I, Kent SBH. Synthesis of proteins by native chemical ligation. *Science* **266**: 776-779, 1994.
3. Nakamura K, Sumida M, Kawakami T, Vorherr T, Aimoto, S. Generation of an S-peptide via an N-S acyl shift reaction in a TFA solution. *Bull Chem Soc Jpn* **79**: 1773-1780, 2006.
4. Zanotti G, Pinnen F, Lucente G. Cyclization under mild conditions of cysteine containing peptides. *Tetrahedron Lett* **26**: 5481-5484, 1985.
5. Kawakami T, Aimoto S. Peptide ligation using a building block having a cysteinyl prolyl ester (CPE) autoactivating unit at the carboxy terminus. *Chem Lett* **36**: 76-77, 2007.

1-03-165

Synthesis of cysteine-rich peptides

Kádár, Kinga[1,]; Panyi, György[2]; Varga, Zoltán[2]; Tóth, Gábor K[1]*

[1]University of Szeged, Department of Medical Chemistry, HUNGARY; [2]University of Debrecen, Department of Biophysics and Cell Biology, HUNGARY

[*]E-mail: k_kinga2000@yahoo.com

Introduction

The chemistry used to oxidize the free thiol (-SH) bonds to the corresponding disulfide (-*S*-*S*-) bond in a controlled fashion remains a significant challenge is spite of many advances in peptide chemistry. The primary reason of this lies in the difficulties involved in the formation of multiple regioselective disulfide bonds.[1,2]

In this work we focused on the elucidation of synthetic strategies for the preparation of multiple disulfide containing peptide venoms regulating the ion channels of immune cells- Anuroctoxin (35 amino acids, 4 disulfide bonds) and Tc32 (35 amino acids, 3 disulfide bonds)-, and a neuropeptide with regulatory functions- Orexin A (33 amino acids, 2 disulfide bonds).

Materials and methods

For the synthesis of the peptides we used the Boc/Bzl-chemistry and for the Cys side-chain protection we chose the 4-methylbenzyl group. The solid supports used were MBHA or PAM resins.

For the synthesis of these naturally occuring Cys-rich peptides we had chosen the oxidative folding being the most simple of the methods available. This means that, if we efficiently manipulate the oxidative conditions, we can exploit the information retained in the basic amino acid sequence of the peptide.

Results and discussion

Anuroctoxin:

Anuroctoxin, isolated from the mexican scorpion *Anuroctonus phaiodactylus*, was classified into subfamily 6 of the α-KTx scorpion toxins, is a high affinity blocker of Kv1.3 channels of human T-lymphocytes and it does not block the Ca^{2+}-activated IKCa1 K^+ channels; these two channels play different but important roles in T-lymphocyte activation.[3]

Several folding experiments lead to the same cyclic form of the peptide toxin- the native one.

The fastest folding happened in redox buffer, but the most selective method had proven to be 10% DMSO (v/v) in NH_4OAc buffer (pH 6.5).

The main folding product was isolated (Fig. 1) and it's regioselectivity was verified with biological measurements and it had proven to be the native isomer (Fig. 2).

Orexin A:

Orexin A is a neuropeptide with strongly conserved structure. Investigations suggest the involvement of this peptide into many physiological and behavioural activities that are involved in or associated with feeding behaviour, and other functions like modulation of neuroendocrine function or the sleep-awake cycle.[4]

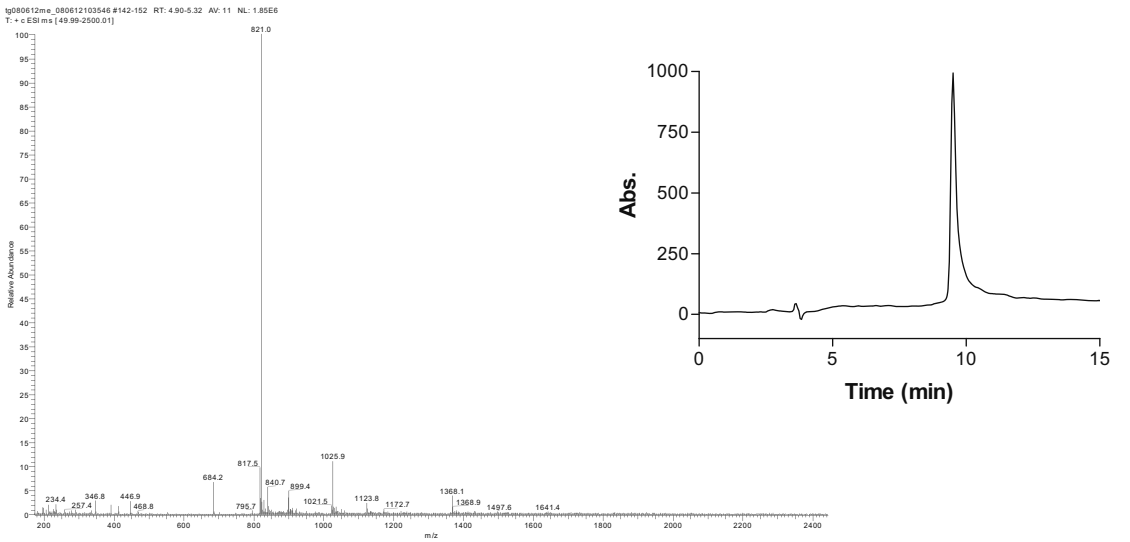

Figure 1. The MS spectrum and HPLC profile of the purified peptide toxin.

In the literature several synthesis methods using different side-chain protection for the cysteines (Trt,Acm) can be found, but these are all time and reagent consuming, therefore our synthesis can be a valuable alternative.

Varying the folding conditions we could isolate the correctly folded isomer as the major reaction product. The correct structure was proven by coelution of the synthesized isomer and the commercially available Orexin A.

Tc32:

Tc32, isolated and characterized from the venom of the brazilian scorpion *Tityus cambridgei*, was classified as the first example of a new subfamily of K^+-channel specific peptides (α-KTx18.1). It recognizes with high affinity the Kv1.3 channels essential to the normal functioning of cells belonging to the immune systeme, rather than the voltage-gated K^+-channels of the Shaker B type.[5]

From folding in alkaline buffer with Clear-Ox resin was isolated the first and second isomer of Tc32 which proved to be inactive in biological measurements.

Even with the variation of the experimental conditions – such as pH (2.7-10), buffer (Gly-NaOH, Tris-HCl, NH_4OAc), peptide concentration (0.5 mg/ml, 1.0 mg/ml), redox reagents (air, DMSO, Clear-Ox resin, cystine/cysteine), denaturants (8M Guanidine HCl)-, we isolated several pure peptide with correct masses, but we could not generate the desired disulfide connectivities. We must conclude that the synthesis with oxidative folding failed.

In the new synthesis we used an orthogonal protection scheme: Cys7, Cys26- Meb; Cys12, Cys16, Cys31, Cys33- Acm. The Cys7-Cys26 disulfide bond was formed in NH_4OAc buffer pH 7.5 with Clear-Ox resin. The other two bridges were formed with iodine in 50% AcOH, the oxidation reaction happened simultaneously with the Acm-deprotection.

But the third isolated isomer had proven to be another misfolded form of the toxin Tc32.

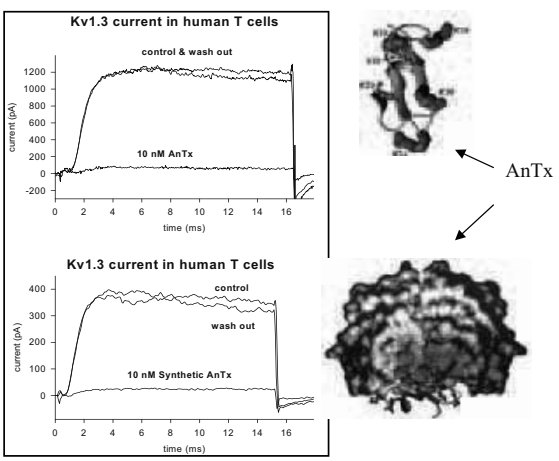

Figure 2. The regioselectivity was proven with biological measurements.

Conclusions

In the case of Anuroctoxin we isolated the native form of the peptide toxin with high selectivity and we optimized the folding conditions, so within an hour the majority of the linear peptide folds in the cyclic form with all four disulfide bonds in the correct form.

For the synthesis of Orexin A we optimized the folding conditions and, using a polymer-supported oxidant- the Clear-Ox resin-, within two hours we could isolate the correctly folded isomer as the major reaction product.

But oxidative folding does not always give the correctly folded isomer. The best proof for this is the Tc32 scorpion toxin which albeit our tryings always gave the misfolded isomers if we used the linear unprotected peptide. Therefore a new chemical synthesis using different side-chain protection needed to be taken into consideration.

The synthesis of a new orthogonally protected Tc32- using two different Cys-protecting groups-, did not concluded the correctly folded peptide, so a new protection scheme driven by the rationality of the obtained isomers has to be applied.

References

1. Boulègue C, Musiol HJ, Prasad V, Moroder L. Synthesis of cystine-rich peptides. *Chemistry Today* **24**: 425-471, 2006.
2. Tóth GK, Pataricza J, Janáky T, Mák M, Zarándi M, Papp JG, Penke B. Synthesis of 2 peptide scorpion toxins and their use to investigate the aortic tissue regulation. *Peptides* **16**: 1167-1172, 1995.
3. Bagdány M, Batista CVF, Valdez-Cruz NA, Somodi S, Rodriguez de la Vega RC, Licea AF, Varga Z, Gáspár R, Possani LD, Panyi G. Anuroctoxin, a new scorpion toxin of the α-KTx 6 subfamily, is highly selective for Kv1.3 over IKCa1 ion channels of human T lymphocytes. *Mol Pharmacol* **67**: 1034-1044, 2005.
4. Söll R, Beck-Sickinger AG. On the synthesis of Orexin A: a novel one-step procedure to obtain peptides with two intramolecular disulphide bonds. *J Pept Sci* **6**: 387-397, 2000.
5. Batista C V F, Gómez-Lagunas F, Rodríquez RC, Hajdu P, Panyi G, Gáspár R, Possani LD. Two novel toxins from the Amazonian scorpion *Tityus cambridgei* that block Kv1.3 and Shaker B K+-channels with distinctly different affinities. *Biochimica et Biophysica Acta* **1601**: 123-131, 2002.

1-03-166

Glycopeptides - a synthetic challenge

Tóth, Gábor K[1]; Kádár, Kinga[1,]; Hegyi, Orsolya[1]; Csikós, Orsolya[1]; Kalmár, László[2]; Kerékgyártó, János[2]*

[1]University of Szeged, Department of Medical Chemistry, HUNGARY; [2]University of Debrecen, Department of Biochemistry HUNGARY

[*]E-mail: k_kinga2000@yahoo.com

Introduction

The arising interest in glycoproteins comes from the increasing awareness of their importance in many diverse biochemical processes including cell growth regulation, binding to cells, intercellular communication and tumor metastasis.

The rational preparation of the glycosylated peptides is one of the most challenging tasks of peptide chemistry, especially of those having oligosaccharide moieties. There are two main strategies for the synthesis of glycopeptides: the synthon and global (convergent) method.[1] Both of them can be implemented in liquid or solid-phase. Since the glycosylation could appear on *O* and *N* atoms of the amino acid side-chain, due to the different reactivity of the glycosidic linkage different chemical strategies will necessitate.

In this paper we compare several chemical strategies for the preparation of two model peptides (Leu-Lys-Asn*-Gly-Gly-Pro, Gly-Val-Glu-Asp-Ile-Ser*-Gly-Leu-Pro-Ser-Gly, *site of glycosylation).[2] As glyco-part several mono, di and trisaccharide including chitobiose, galactosyl-xylose, mannosyl-*N*-acetyl-glycosyl-N-acetylglucosamine were used and several of the used strategies led to successful preparation of these glycoconjugates.

Materials and methods

The common core region of the most N-glycosylated glycoproteins is the following trisaccharide: *β*-D-Man-(1→4)-*β*-D-GlcNAc-(1→4)-D-GlcNAc attached to the amide nitrogen of an Asn-unit.

In order to investigate the coupling reaction between glycosylamines and selectively protected peptides, with respect to the size of each component and choice of protection for the carbohydrate hydroxyl functions, the preparation of the fully *O*-benzylated glycosyl azides GlcNAc(*β*1-N_3), GlcNAc(*β*1-4)GlcNAc(*β*1-N_3) and Man(*β*1-4)GlcNAc(*β*1-4)GlcNAc(*β*1-N_3) representing the reducing terminal of the core structure of N-glycans were prepared.[3] Chemoselective reduction of the azido fuction of glycosyl azides resulted in fully *O*-benzylated glycosylamines.

The coupling reactions by *in situ* trapping of the amines with selectively protected activated aspartic acid and Leu-Lys-Asp*-Gly-Gly-Pro hexapeptide resulted in our target carbohydrate-aspartic acid and carbohydrate - hexapeptide derivatives, respectively.

The peptides were prepared after the standards of Boc/Bzl and Fmoc/tBu chemistries. The amino acid protection and the cleavage conditions were adapted after the rationality of the synthesis in each case.

Results and discussion

The Fmoc-Leu-Lys(Fmoc)-Asp-Gly-Gly-Pro-NH_2 peptide was prepared for post-synthetic glycosylation (Fig. 1), but all these reactions concluded in a series of undesired side-reactions.

In order to avoid these side-reactions (e.g. aspartimide formation) we designed and synthesized a new selectively protected, resin bound peptide for post-synthetic glycosylation. The solid support used was H-Pro-2-chlorotrityl-chloro resin, the aspartic acid side-chain was protected as allylester and the respective

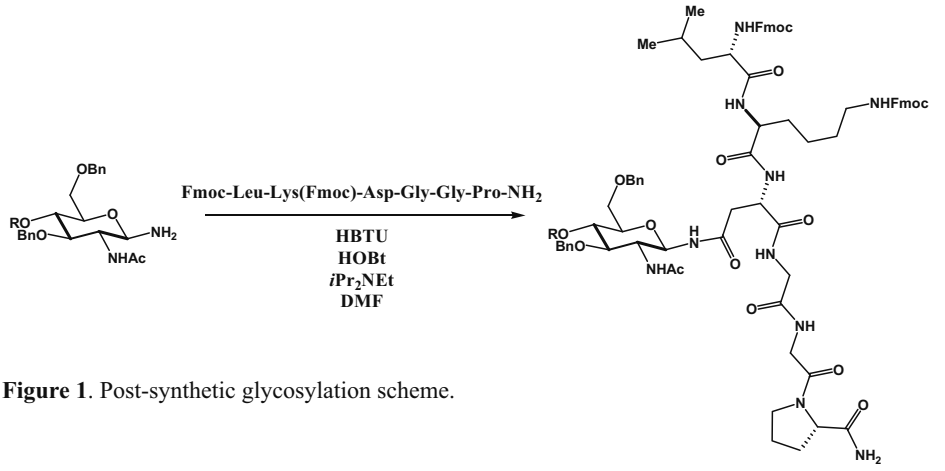

Figure 1. Post-synthetic glycosylation scheme.

Figure 2. Carbohydrate-aspartic acid building block synthesis scheme.

backbone nitrogen was Hmb protected. After removal of the allylester, the glycosylation of the peptide was performed.

The following carbohydrate-hexapeptide derivatives were prepared using the appropriate carbohydrate-aspartic acid derivatives as building blocks:

H-Leu-Lys-GlcNAc(β1-N)Asn-Gly-Gly-Pro-OH, H-Leu-Lys-GlcNAc(eq.1-4)GlcNAc(β1-N)Asn-Gly-Gly-Pro-OH, H-Leu-Lys-Man(β1-4)GlcNAc(β1-4) GlcNAc(β1-N)Asn-Gly-Gly-Pro-OH.

The building blocks used in the synthesis were prepared from the reaction between the glycosylamines and the activated aspartic acids (Asp*) as shown in Fig. 2.

The peptides were manually synthesized on Boc-Pro-Merrifield resin (0.64 mM/g). The amino acids were incorporated using the Boc/Bzl strategy, including the glycosylated aspartic acid derivatives.

Cleavage from the resin was made using: 10% HBr/acetic acid in TFA with 2% DTT for 120 min.

The monosaccharide-hexapeptide derivative was successfully isolated.

During the cleavage from the resin of the disaccharide-hexapeptide derivative we observed the loss of a monosaccharide unit. We had tried to optimize the cleavage conditions by reducing on a hand the amount of HBr/acetic acid and on the other hand the reaction time, but it had not concluded in better results.

In order to avoid the loss of a glyco-unit during cleavage from the resin, we had incorporated a base-labile fluorene derived linker between the resin and the amino acid sequence. The *N*-[(9-hydroxymethyl)-2-fluorenyl] succinic acid (HFMS) handle was synthesized according to Rabanal (Fig.3).[4]

Partial deterioration of the carbohydrate moiety can also be observed during cleavage from resin in alkaline conditions.

Cleavage from the resin of the trisaccharide-hexapeptide derivative with HBr/acetic acid resulted in low yield of the trisaccharide-hexapeptide derivative.

Conclusions

The glycosylated aspartic acid derivatives after catalytic hydrogenation are suitable building blocks for solid phase peptide synthesis.

For the preparation of carbohydrate-hexapeptide conjugates by post-synthetic glycosylation of the suitable protected hexapeptide appropiate reaction conditions were elaborated in order to minimize undesired side reactions. Both the ^{1}H- and ^{13}C-NMR spectra revealed that the anomerization of the amines could be avoided under the applied reaction conditions.

Acknowledgement

This work was supported by the following grant: OTKA 71753.

References

1. Arsequell G, Valencia G. Recent advances in the synthesis of complex N-glycopeptides. *Tetrahedron: Asymetry* **10**: 3045-3094, 1999.
2. Hudáky P, Stráner P, Váradi Gy, Tóth G, Perczel A. Cooperation between a salt bridge and the hydrophobic core triggers fold stabilization in a Trp-cage miniprotein. *Biochemistry* **47**: 1007-1016, 2008.
3. Kerékgyártó J, Ágoston K, Batta Gy, Kamerling J P, Vliegenthart F G. Synthesis of fully and partially benzylated glycosil azides via thioalkyl glycosides as precursors for the preparation of N-glycopeptides. *Tetrahedron Lett* **39**: 7189-7192, 1998.
4. Rabanal F, Giralt E, Albericio F. Synthesis and applications of a new base-labile fluorene derived linker for solid-phase peptide synthesis. *Tetrahedron* **51**: 1449-1458, 1995.

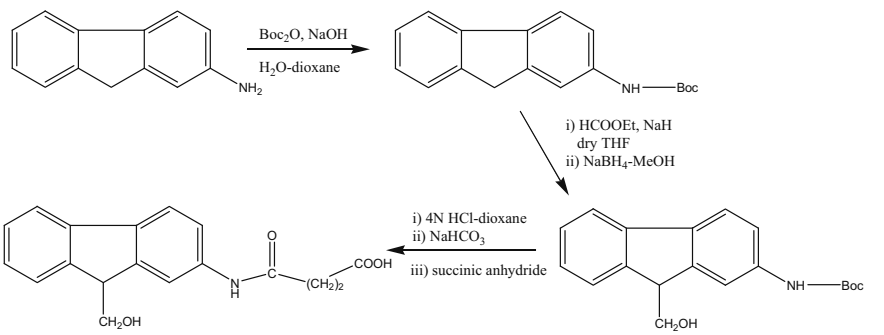

Figure 3. HFMS handle synthesis scheme.

1-03-167

Peptide synthesis in water using Boc-amino acid nanoparticles

Hojo, Keiko[1,]; Ichikawa, Hideki; Fukumori, Yoshinobu; Kawasaki, Koichi*

Kobe Gakuin University, Faculty of Pharmaceutical Sciences, JAPAN

[*]E-mail: hojo@pharm.kobegakuin.ac.jp

Introduction

Development of green sustainable chemistry is currently regarded as a challenge in Science and technology to reduce the use of organic solvents and, instead, utilize less toxic solvents. Water and aqueous-based solvent systems are the solvents of choice for replacing the traditional solvents commonly used in synthetic chemistry. During the last few years, we have focused on developing an organic solvent-free peptide synthesis method using aqueous solvents.[1,2] One of the most important, and sometimes difficult, aspects of peptide synthesis is to choose the best amino acid derivatives in order for the synthetic reaction to proceed. Currently, Boc- and Fmoc-amino acids are routinely used as building blocks for peptide synthesis. However, they are sparingly soluble in water. Utilization of nanoparticle-based technology is an emerging strategy to tackle formulation problems associated with poorly water-soluble drugs.[3] Recently, we succeeded in developing a solid-phase synthesis method in water using water-dispersible Fmoc-amino acid nanoparticles.[4] This novel technology uses suspended nanoparticle reactants for the coupling reaction. Here, we investigated the feasibility of this method for in-water solution-phase synthesis of peptides using water-dispersible Boc-amino acid nanoparticles.

Results and Discussion

We prepared aqueous dispersions of Boc-amino acid nanoparticles using a planetary ball mill in the presence of PEG as a dispersion agent. The grinding media was composed of zirconium oxide beads. The sizes of the resulting water-dispersible nanoparticles were determined by dynamic light scattering analysis, and were found to be between 400~700 nm. Scanning electron microscope images revealed formation of nano-sized particles. To evaluate the feasibility of using the water-dispersible Boc-amnio acid nanoparticles as building blocks for peptide synthesis, we performed in-water coupling reactions using these nanoparticles and demonstrated total synthesis of Leu-enkephalinamide (Fig. 1). The in-water coupling reaction was carried out for 12 hrs using 4-(4,6-dimethoxy-1,3,5-triazin-2-yl)-4-methylmorpholinium chloride (DMT-MM)[5,6] in the presence of *N*-methylmolpholine (NMM) (Fig. 2). The Boc group was removed by treatment with 4.0 mol/L HCl-dioxane solution. All the coupling reactions using water-dispersible nanoparticles resulted in good yields (over 80%), and the purity of the reaction products were satisfactory (over 90% in HPLC analysis), even when the products were simply washed after the reaction was over and underwent no further purification. Thus, Leu-

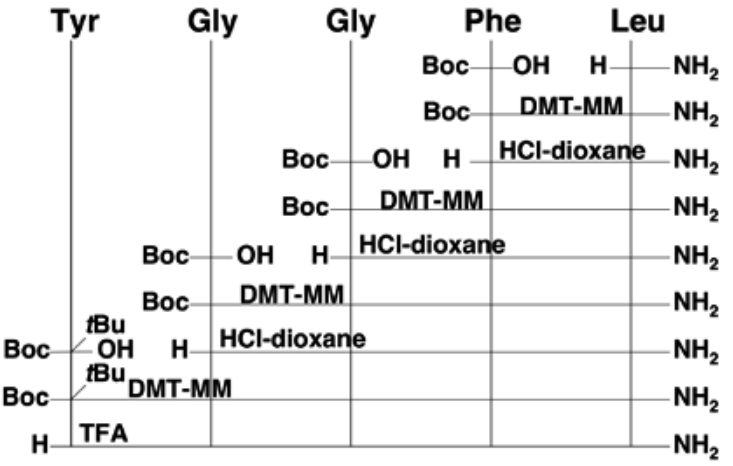

Figure 1. Synthetic scheme for Leu-enkephalinamide.

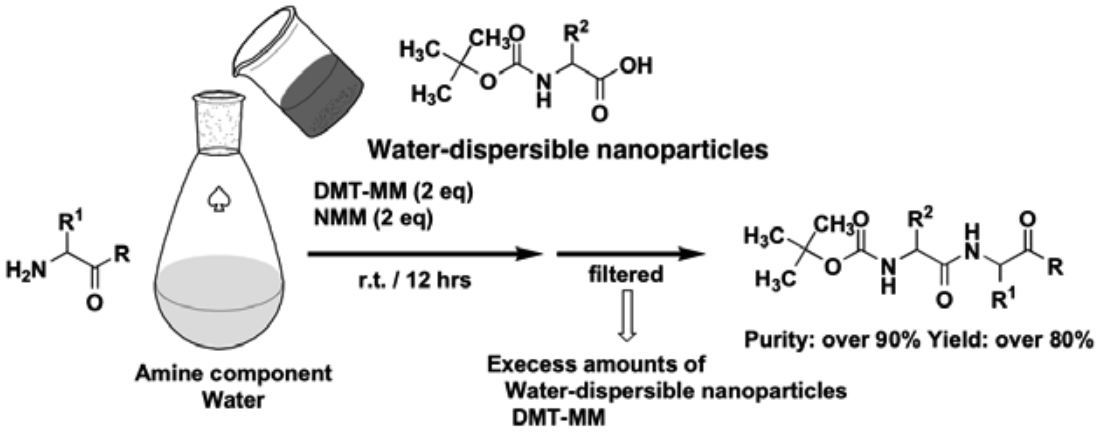

Figure 2. Coupling reaction in water using water-dispersible nanoparticles.

enkephalinamide was successfully synthesized in water according to the Boc chemistry.

Conclusion

We developed a new water-based peptide synthesis method that utilizes aqueous nanocolloidal reactants as building blocks. The application of water as a solvent in peptide synthesis provides both opportunities and challenges in developing water-soluble or water-dispersible building blocks or reagents, and thus promises to contribute to the future development of green sustainable chemistry.

Acknowledgements

This work was supported in part by Grant-in-Aid for Scientific Research and by eAcademic Frontier f Project for Private Universities: matching fund subsidy from the Japanese Ministry of Education, Culture, Sports, Science and Technoligy, 2006-2010.

References

1. Hojo K, Ichikawa H, Fukumori Y, Kawasaki K. Development of a method for solid-phase peptide synthesis in water. *Int J Pept Res Ther* **14**: 373–380, 2008.
2. Hojo K, Maeda M, Kawasaki K. Solid-phase peptide synthesis in water. III. A water-soluble N-protecting group, 2-[phenyl(methyl)sulfonio]ethoxycarbonyl tetrafluoroborate, and its application to peptide synthesis. *Tetrahedron* **60**: 1875-1866, 2004.
3. Rabinow BE. Nanosuspensions in drug delivery. *Nat Rev Discov* **3**: 785-795, 2004.
4. Hojo K, Ichikawa H, Maeda M, Kida S, Fukumori Y, Kawasaki K. Solid-phase peptide synthesis using nanoparticulate amino acids in water. *J Pept Sci* **13**: 493-497, 2007.
5. Kamiński ZJ, Paneth P, Rudzinski J. A study on the activation of carboxylic acids by means of 2-chloro-4,6-dimethoxy-1,3,5-triazine and 2-chloro-4,6-diphenoxy-1.3.5-triazine. *Org Chem* **63**: 4248-4225, 1998.
6. Kunishima M, Kawachi C, Morita J, Terao K, Iwasaki F, Tani S. 4-(4,6-Dimethoxy-1,3,5-triazin-2-yl)-4-methyl-morpholinium chloride: an efficient condensing agent leading to the formulation of amide and esters. *Tetrahedron* **55**: 13159-13179, 1999.

1-03-168

Solid-phase synthesis of 4,5,8-trihydroxy-9,10-anthraquinone-1-yl-(tuftsin and retro-tuftsin) derivatives

Kukowska-Kaszuba, Magdalena[1,]; Dzierzbicka, Krystyna[1]; Mackiewicz, Zbigniew[2]*

[1]Gdańsk University of Technology,11/12 G. Narutowicza Street, 80-952 Gdańsk, Department of Organic Chemistry, POLAND; [2]University of Gdańsk, 18/19 J. Sobieskiego Street, 80-952 Gdańsk, Department of Polypeptides Chemistry, POLAND

[*]E-mail: magda1805@o2.pl

Introduction

Anthraquinone derivatives constitute a very large group of compounds which have found a clinical application in treatment of different types of cancer. However, these compounds also show a lot of negative effects what limited their application. Both high cardiotoxic activity and multidrug-resistant (MDR) led scientists to research rather novel analogues void of disadvantages and possess better pharmaceutical properties. Mitoxantrone is a well-known anthracycline antibiotic that has become the model for drug design.[1-4]

On the other hand, tuftsin (H-Thr-Lys-Pro-Arg-OH) is a tetrapeptide of biological origin that can activate several elements of immune system such as granulocytes and macrophages. It indicates not only immunological stimulating factor but also antibacterial, antifungal, antiviral and antineoplastic properties. However, tuftsin is unstable in plasma and it has become the aim of new analogues formation that are more resistant to proteolytic degradation.[5,6]

Encouraged by the results obtained, we synthesized a new series of compounds containing tuftsin analogues at the first position of anthraquinone moiety. Modification of the tuftsin chain was based on the introduction of simple amino acids such as glycine and isoleucine into the peptide chain at the ε-amino group of lysine. Hence we hope that the covalent bond combining two molecules, tuftsin and anthraquinone, allowed us to obtain the conjugates with potential anticancer properties.

Results and discussion

In the present study, we described a simple procedure for obtaining tuftsin–anthraquinone conjugates **3a-f** (Scheme 1) using Fmoc/*t*-Bu strategy. The method ensured selective removal of all side chain protecting groups and cleavage of peptidyl-anthraquinone from the resin. Entering protected amino acids were activated with DIC and HOBt in the presence of 1% Triton in DMF, DCM and NMP mixture. The modification of tuftsin chain was achieved by introducing a lysine residue protected at the ε-amino group with a Mtt group. Orthogonal protection ensured the obtainment of tuftsin analogues containing isopeptide bond.

The condensation between leuco-1,4,5,8-tetrahydroxyanthraquinone[7] (**1**) and N-termini of peptide-resin (**2a-f**) was achieved during reaction in DMF under nitrogen and heated to reflux for 24h. Then peptidyl-anthraquinone-resin was oxidized in air at room temperature.[2] Simultaneous deprotection of the peptide side chain and liberation from the resin was achieved using standard TFA cocktail. The final products (**3a-f**) were purified by RP-HPLC and characterized by MS and ^{1}H–NMR.

Scheme 1. Synthesis of the tuftsin-anthraquinone conjugates

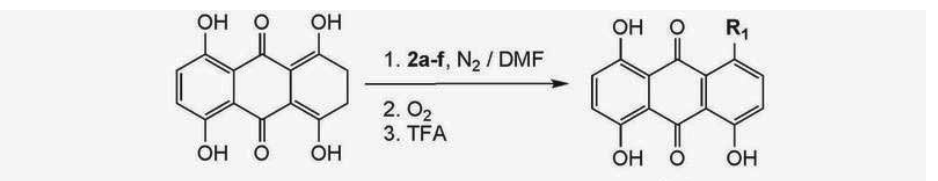

1 **3a-f**

2a. H-Thr(*t*-Bu)-Lys-Pro-Arg(Pbf)-O-polymer
2b. H-Thr(*t*-Bu)-Lys(Boc-Gly)-Pro-Arg(Pbf)-O-polymer
2c. H-Thr(*t*-Bu)-Lys(Boc-Ile)-Pro-Arg(Pbf)-O-polymer
2d. H-Arg(Pbf)-Pro-Lys-Thr(*t*-Bu)-O-polymer
2e. H-Arg(Pbf)-Pro-Lys(Boc-Gly)-Thr(*t*-Bu)-O-polymer
2f. H-Arg(Pbf)-Pro-Lys(Boc-Ile)-Thr(*t*-Bu)-O-polymer

R= Thr-Lys-Pro-Arg-OH (**a**)
Thr-Lys(Gly)-Pro-Arg-OH (**b**)
Thr-Lys(Ile)-Pro-Arg-OH (**c**)
Arg-Pro-Lys-Thr-OH (**d**)
Arg-Pro-Lys(Gly)-Thr-OH (**e**)
Arg-Pro-Lys(Ile)-Thr-OH (**f**)

Acknowledgements

This work was supported by the Polish State Committee for Scientific Research (Grant No. NN 405064134) and University of Gdańsk (Grant BW No. 8000-5-0126-8).

References

1. Dzierzbicka K, Kolodziejczyk AM. Anthracenedione Analogues – Synthesis and Biological Activity. *Pol J Chem* **79:** 1-29, 2005.
2. Giles GI, Sharma RP. Solid phase synthesis of anthraquinone peptides and their evaluation as topoisomerase I inhibitors. *J Pept Sci* **11:** 417-423, 2005.
3. Gatto B, Zagotto G, Sissi C, Cera C, Uriarte E, Palu G, Capranico G, Palumbo M. Peptidyl anthraquinones as potential antineoplastic drugs: synthesis, DNA binding, redox cycling, and biological activity. *J Med Chem* **39:** 3114-3122, 1996.
4. Dzierzbicka K, Sowinski P, Kolodziejczyk AM. Synthesis of analogues of anthraquinones linked to tuftsin or retro-tuftsin residues as potential topoisomerase inhibitors. *J Pept Sci* **12:** 670-678, 2006.
5. Wardowska A, Dzierzbicka K, Mysliwski A. Tuftsin - new analogues and properties. *Post Biochem* **53:** 60-65, 2007.
6. Siemion IZ, Kluczyk A. *Tuftsin: on the 30-year anniversary of Victor Najjar's discovery. Peptides* **20:** 645-674, 1999.
7. Chang P, Cheng ChCh. An improved practical synthesis leuco-1,4,5,8-tetrahydroxy-anthraquinone. *Synthetic Com* **25:** 1893-1900, 1995.

1-03-169

Solid phase synthesis of tuftsin derivatives conjugated to 1,4-dihydroxyanthraquinone

Kukowska-Kaszuba, Magdalena[1,]; Dzierzbicka, Krystyna[1]; Mackiewicz, Zbigniew[2]*

[1]Gdańsk University of Technology, 11/12 G. Narutowicza Street, 80-952 Gdańsk, Department of Organic Chemistry, POLAND; [2]University of Gdańsk, 18/19 J. Sobieskiego Street, 80-952 Gdańsk, Department of Polypeptides Chemistry, POLAND

[*]E-mail: magda1805@o2.pl

Introduction

Large number of anthraquinones have been synthesized and some of them have found a clinical application in treatment of leukemia or solid tumor. However, it also demonstrates cardiotoxic activity as a consequent of reactive oxygen species (ROS) generation what limited their application. In recent years peptidyl-anthraquinones have had a great influence on medical Sciences. Amino acid or peptide linked to anthraquinones have given promising results in cancer therapy as topoisomerase I or II (topo) inhibitors. Their mechanism of action is based on stabilizing the DNA-topo cleavable complex and consequently stops correct replication and transcription. Encouraging results described in literature show a new group of peptidyl-anthraquinones.[1-3] In our studies, we used tuftsin analogues as peptidyl chain. Tuftsin (H-Thr-Lys-Pro-Arg-OH) is a natural peptide that indicates not only immunological stimulating factor but also antibacterial, antifungal, antiviral and antineoplastic properties. In spite of its wide range of activity, the peptide is unstable in plasma and it has become the aim of new analogues formation that are more resistant to proteolytic degradation.[1,2,4,5]

Results and discussion

Continuing our studies of synthetic terapeutic agents, we obtained a series of anthraquinones substituted by tuftsin derivatives, **1a-i** (Fig.1) using the solid phase chemistry. N-terminal elongation of the peptide chain was based on a two-step procedure involving deprotection and coupling. The condensation between leuco-compound6 and N-termini of peptide-resin was achieved during reaction in DMF under nitrogen, stirred and heated for 24h. A threefold excess of leucoanthraquinone was used in reaction with peptidyl-resin and then peptidyl-anthraquinone-resin was oxidized in air at room temperature.[3,7] Next, dried peptidyl-anthraquinone-resin was treated with a cocktail of TFA to cleave from resin ensuring simultaneous removal of the side chain protecting groups. 4-Hydroxy-anthraquinone-1-yl-tuftsin/retro-tuftsin analogues were purified by solid-phase extraction (SPE) and characterized by MS, ^{1}H-NMR, elemental analysis, analytical RP-HPLC. The conjugates were obtained in good yield (31-45%) and >95% purity. All tuftsin conjugates were sent to assay their biological activity.

Number	Peptide Sequences	
1a	H-Thr-Lys(Gly)-Pro-Arg-OH	Tuftsin analogues
1b	H-Thr-Lys(Val)-Pro-Arg-OH	
1c	H-Thr-Lys(βAla)-Pro-Arg-OH	
1d	H-Thr-Lys(Ile)-Pro-Arg-OH	
1e	H-Arg-Pro-Lys(Gly)-Thr-OH	Retro-tuftsin analogues
1f	H-Arg-Pro-Lys(Val)-Thr-OH	
1g	H-Arg-Pro-Lys(Ala)-Thr-OH	
1h	H-Arg-Pro-Lys(βAla)-Thr-OH	
1i	H-Arg-Pro-Lys(Ile)-Thr-OH	

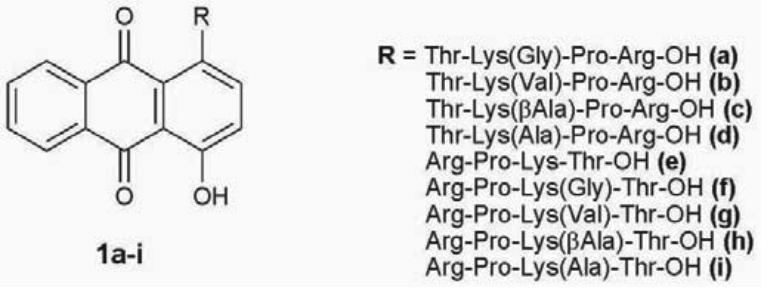

Figure 1. Synthetized conjugates of tuftsin derivatives linked to 1,4-dihydroxyanthraquinone.

Acknowledgements

This work was supported by the Polish State Committee for Scientific Research (Grant No. NN 405064134) and University of Gdańsk (Grant BW No. 8000-5-0126-8).

References

1. Dzierzbicka K, Kolodziejczyk A. Anthracenedione Analogues - Synthesis and Biological Activity. *Pol J Chem* **79**: 1-29, 2005.
2. Kukowska M, Dzierzbicka K, Mackiewicz Z. Peptidyl anthraquinone conjugates and its biological activity. *Wiad Chem* **60**: 523-545, 2006.
3. Giles GI, Sharma RP. Solid phase synthesis of anthraquinone peptides and their evaluation as topoisomerase I inhibitors. *J Pept Sci* **11**: 417-421, 2005.
4. Wardowska A, Dzierzbicka K, Mysliwski A. Tuftsin - new analogues and properties. *Post Biochem* **53**: 60-65, 2007.
5. Mező G, Szekerke M, Sarmay G, Gergely J. Synthesis and functional studies of tuftsin analogs containing isopeptide bond. *Peptides* **11**: 405-415, 1990.
6. Mothilal KK, Inbaraj J, Gandhidasan R, Murugesan R. Photosensitization with anthraquinone derivatives: optical and EPR spin trapping studies of photogeneration of reactive oxygen species. *J Photochem Photobiol* A **162**: 9-16, 2004.
7. Greenhalgh CW, Hughes N. The reaction of leucoquinizarins with alkylenediamines. *J Chem Soc (C)*, 1284-1288, 1968.

1-04-170

Microwave-assisted solid-phase peptide synthesis: shifting off the limitations affecting conventional synthetic strategies

Rizzolo, Fabio[1,2,]; Sabatino, Giuseppina[1,2]; Fridkin, Mati[3]; Chelli, Mario[1,2]; Rovero, Paolo[1,4]; Papini, Anna Maria[1,2]*

[1]Interdepartimental Laboratory of Peptide & Protein Chemistry & Biology (PeptLab), Polo Scientifico e Tecnologico of the University of Firenze, Italy ; [2]Dept. of Organic Chemistry `Ugo Schiff', and CNR-ICCOM, University of Firenze, ITALY; [3]Weizmann Institute of Science, Dept. of Organic Chemistry, Rehovot, ISRAEL; [4]Dept. of Pharmaceutical Sciences, University of Firenze, ITALY

[*]E-mail: fabio.rizzolo@gmail.com

Introduction

Solid-phase peptide synthesis (SPPS) revolutionized peptide chemistry, achieving rapidly a leading position in the field of organic synthesis. However this approach exhibits some limitations especially severe in case of syntheses of difficult sequences. Such difficulties closely depend on the nature of the peptide chain and can be mainly summarised as a result of internal aggregation of resin-bound peptide during its elongation (i.e. amyloidogenic sequences) and because of presence of bulky-modified or unnatural amino acids (i.e. glycosylated and citrullinated peptides). Both situations reduce reagent penetration and decrease significantly reaction rates in acylation and deprotection steps.

Recently, the growing interest in microwave-assisted SPPS (MW-SPPS) is justified by several advantages in terms of yield and time-consuming compared to conventional protocols.[1] Considering limitations affecting SPPS, we reported the application of microwave energy to the solid-phase syntheses of various difficult sequences.

Results and discussion

Peptide drugs and diagnostics can be very complex molecules difficult to be produced in adequate quantities, particularly if presenting various modifications (i.e. post translational modifications) and constrained unnatural amino acids. We describe optimized protocols to obtain higher pure crude peptides of different difficult sequences using a microwave-assisted synthetic strategy. Our case studies include amyloidogenic sequences, citrullinated and glycosylated peptides, as well as multiple antigen peptides (MAPs).

All peptides were synthesized using a Liberty™ Microwave Peptide Synthesizer (CEM Corp.), a monomode microwave apparatus combined with a temperature control system, with standard protocols as follows: coupling reactions with a 0.5 M solution of TBTU in DMF and a 2M solution of DIEA in NMP; N^{α}-Fmoc deprotection with a 20% piperidine solution in DMF. Cleavage of peptides from the resin and final side-chain deprotections were usually performed in 3 hours at room temperature using ad hoc cleavage cocktails.

Amyloidogenic peptides have been frequently reported as difficult sequences to be obtained by SPPS. In fact the formation of sequence-specific secondary structures reduces reagents penetration and decreases reaction rates in both coupling and deprotection steps, strongly affecting the final yield and purity of the crude peptide. The application of microwave energy in SPPS possibly leads to de-aggregation of the peptide backbone, thus allowing the reagents to reach the N-terminus sites of growing chains more easily, improving deprotection and coupling steps. In fact, starting from Fmoc-Ser(tBu)-Wang Resin (0.132 g, 0.76 mmol/g), SAA 47-76 (a 29-mer amyloidogenic peptide)[2] was obtained as a crude with 60% RP-HPLC purity. After purification, we obtained 20 mg of >98% pure peptide.

CSF114(Glc), an *N*-glucosylated peptide developed by PeptLab as useful Multiple Sclerosis (MS) antigenic probe, is proposed as antigenic probe in an assay for the screening of specific autoantibodies as biomarkers of MS patients' sera[3] It is characterised by a β-hairpin structure bearing the minimal epitope (a β-D glucopyranosyl moiety linked to the Asn residue on the tip of the turn) fundamental for autoantibody recognition in ELISA. Up to now this glycopeptide was obtained in solid-phase by a building-block approach, incorporating the glycosylated asparagine (orthogonally protected for Fmoc/tBu strategy) into the target peptide sequence during elongation of the peptide chain. The main difficulties associated with this glycopeptide synthesis are both in obtaining the building block Fmoc-Asn(Glc*O*Ac4)-OH in large scale, and in low coupling efficiency of the sterically hindered sugar-bound asparagine derivative. Using MWs (Discover, CEM Corp.) we obtained the building block in large scale[4] and starting from Fmoc-Lys(Boc)-Wang (0.149 g, 0.67 mmol/g) by MW-SPPS we improved the yield in crude CSF114(Glc), allowing more rapid and efficient purification steps by RP-HPLC. The final glycopeptide was obtained with a purity >98% (fundamental for reliable ELISAs on MS patients' sera), in higher yield compared to conventional protocol.[5]

Multiple Antigen Peptide (MAP) concept was introduced by Tam[6] as a valuable approach for generating

antibodies to peptides and developing synthetic vaccines. The MAP system consists of a small immunogenic inert core matrix of lysine residues with α- and ε-amino groups for anchoring multiple copies of the same or different synthetic peptides. The main limitation in the SPPS of MAPs is represented by the low yield in coupling of amino acid residues due to the sterically hindered branch of polylysines characterizing the solid support $Fmoc_4$-Lys_2-Lys-*β*Ala-Wang resin (0.29 mmol/g, 0.345 g). The MAP of 21×4 residues - EPK391 - was obtained by MW-SPPS with a purity >85% after a simple and fast SPE purification, with a final yield of 14% and used as an efficient diagnostic ELISA for Rheumatoid Arthritis (RA).[7]

Anti-cyclic citrullinated peptide antibodies are highly specific and sensitive markers accepted as diagnostics of RA showing a sensitivity in up to 70% RA patients.[7] Using various functionalised Wang resin (0.6-0.7 mmol/g) and microwave-assisted strategy we succeeded the synthesis of a library of citrullinated peptides termed TBX (containing multiple copies of citrulline residues), improving yield in terms of purity of crude peptides as reported in Table 1.

Considering concrete and increasing demand of difficult peptides, benefits obtained by MW-SPPS can be justified to set up reliable synthetic protocols, down-streaming purification and analytical steps, overcoming some limitations usually affecting conventional SPPS.

Acknowledgements

We gratefully acknowledge the fruitful cooperation of EspiKem S.r.l. (Florence, Italy) and Ente Cassa di Risparmio di Firenze.

References

1. Paolini I, Rizzolo F, Papini AM. *Chemistry Today* **26**: 36, 2008.
2. Yavin EJ, Preciado-Patt L, Rosen O, Yaron M, Suessmuth RD, Levartowsky D, Jung G, Lider O, Fridkin M. *FEBS Letters* **472**: 259-262, 2000.
3. Lolli F, Mulinacci B, Carotenuto A, Bonetti B, Sabatino G, Mazzanti B, D'Ursi AM, Novellino E, Pazzagli M, Lovato L, Alcaro MC, Peroni E, Pozo-Carrero MC, Nuti F, Battistini L, Borsellino G, Chelli M, Rovero P, Papini AM. *Proc Nat Acad Sci USA* **102**: 10273-10278, 2005.
4. Paolini I, Nuti F, Pozo-Carrero MC, Barbetti F, Kolesińska B, Kamiński ZJ, Chelli M, Papini AM. *Tetrahedron Lett* **48**: 2901-2904, 2007.
5. Rizzolo F, Sabatino G, Chelli M, Rovero P, Papini AM. *Int J Pept Res Ther* **13**: 203-208, 2007.
6. Tam JP. *Proc Nat Acad Sci USA* **85**: 5409-5413, 1988.
7. Alcaro MC. Lolli F, Papini AM *et al*. *Chemistry Today* **25**: 14, 2007.

Table 1

Peptide	HPLC purity (%)		Peptide	Yield of crude peptide (%)	
	Non MW-assisted	MW-assisted		Non MW-assisted	MW-assisted
TB1	52	83	TB1	87	95
TB2	35	76	TB2	86	86
TB3	55	30	TB3	67	88
TB4	56	78	TB4	82	92
TB5	59	76	TB5	85	94
TB6	28	35	TB6	87	88
TB7	43	47	TB7	91	94

1-04-171

Solid-phase peptide synthesis at elevated temperatures - A comparison of conventional and microwave heating technology

Bacsa, Bernadett[1,]; Horváti, Kata[2]; Bősze, Szilvia[2]; Andreae, Fritz[3]; Kappe, C Oliver[1]*

[1]Karl-Franzens-University, CDLMC and Institute of Chemistry, AUSTRIA; [2]Hungarian Academy of Sciences, Eötvös Loránd University, Research Group of Peptide Chemistry, HUNGARY; [3]piCHEM Forschungs- und Entwicklungs GmbH, AUSTRIA

[1,]E-mail: bernadett.bacsa@gmail.com*

Introduction

A number of reports in the literature have advocated the use of microwave technology to obtain peptides not only faster but also in higher purity as compared to conventional room temperature SPPS. It has recently been suggested that due to the very high dipole moment of an amide bond, irradiation of peptides with microwave energy may lead to a de-aggregation of the peptide backbone via direct interaction of the peptide chain with the electric field (nonthermal microwave effects).[1] Microwave effects of this type would not be reproducible by conventional heating at the same measured bulk reaction temperature. Herein a detailed evaluation of microwave-assisted Fmoc solid-phase peptide synthesis involving several difficult sequences under strictly controlled conditions is presented. Using recently developed fast responding internal fiber-optic temperature probes,[2] the reaction temperatures experienced in microwave-assisted peptide couplings have been carefully monitored and optimized. Adequate control experiments between microwave and conventional heating at the same reaction temperature have been performed in order to distinguish between thermal and nonthermal microwave effects.

Results and discussion

For optimization studies a model peptide (H-Gly-Ile-Leu-Thr-Val-Ser-Val-Ala-Val-NH_2) was selected which suffers from poor synthetic efficiency under standard SPPS conditions. Synthesis of the nonapeptide was performed using various combinations of solid supports (polysterene, Tentagel, ChemMatrix), solvents (DMF, NMP, NMP/DMSO, LiCl/NMP), excess of coupling reagents (10, 5, 3 molar) and different coupling and cleavage temperatures (60-90 °C) employing Fmoc/*t*Bu orthogonal protection strategy. Microwave-assisted SPPS was performed using a dedicated 300 W single-mode manual microwave peptide synthesizer (Discover SPS). Using RAM-ChemMatrix resin, the desired peptide could be synthesized in very high purity (ca. 95%) virtually free from any impurities such as deletion sequences experienced with Polystyrene and Tentagel resins. An additional advantage is the fact that here a 3-fold excess of Fmoc-amino acid was sufficient to allow the generation of a high purity peptide at 86 °C applying a 10 min coupling time. Applying the optimized reaction conditions for the preparation of the model peptide, a comparison of microwave-heated with conventionally-heated coupling and deprotection reactions *at the exact same temperature* were conducted. For this purpose the same solid-phase reaction vessel used in the Discover SPS for microwave-assisted couplings and deprotections was applied in a conventional manual solid-phase synthesizer keeping all other reaction parameters the same. As can be seen from Fig. 1. that there is a surprisingly close match in terms of peptide purity between the results obtained using conventional heating and microwave heating at the same coupling and deprotection temperatures.

The general effectiveness of elevated temperature SPPS was tested on other difficult and longer peptide sequences, the generation of the Cecropin A(1-7)–Mellitin(2-9) hybride peptide (H-Lys-Trp-Lys-Leu-Phe-Lys-Lys-Ile-Gly-Ala-Val-Leu-Lys-Val-Leu-NH_2) and the Magainin-II-amide peptide derivative (H-Cys-Gly-Ile-Gly-Lys-Phe-Leu-His-Gly-Ala-Lys-Lys-Phe-Gly-Lys-Ala-Phe-Val-Gly-Glu-Ile-Met-Asn-Ser-NH_2) was attempted. The synthesis of the both modell peptide was performed on ChemMatrix resin applying the microwave-assisted DIC/HOBt coupling and piperidine/DMF deprotection conditions optimized for nonapeptide GILTVSVAV utilizing 3-fold excess of activated Fmoc-amino acids at 86 °C coupling temperature (10 min reaction time) and 3 min deprotection cycles at 86 °C provided the Cecropin A(1-7)–Mellitin(2-9) hybride peptide in remarkable 91% purity. The identical experiment using conventional heating at 86 °C for coupling and deprotection led to a similar peptide purity (87 %). Applying the optimized coupling/deprotection SPPS conditions described above Magainin-II-amide peptide derivative was obtained on ChemMatrix resin in 54% purity using microwave conditions, compared to 48% purity applying conventional heating at the same temperature. This demonstrates the absence of any significant nonthermal microwave effect, even for longer peptide sequences. Standard room temperature SPPS was not successful in providing this peptide in a reasonable purity.

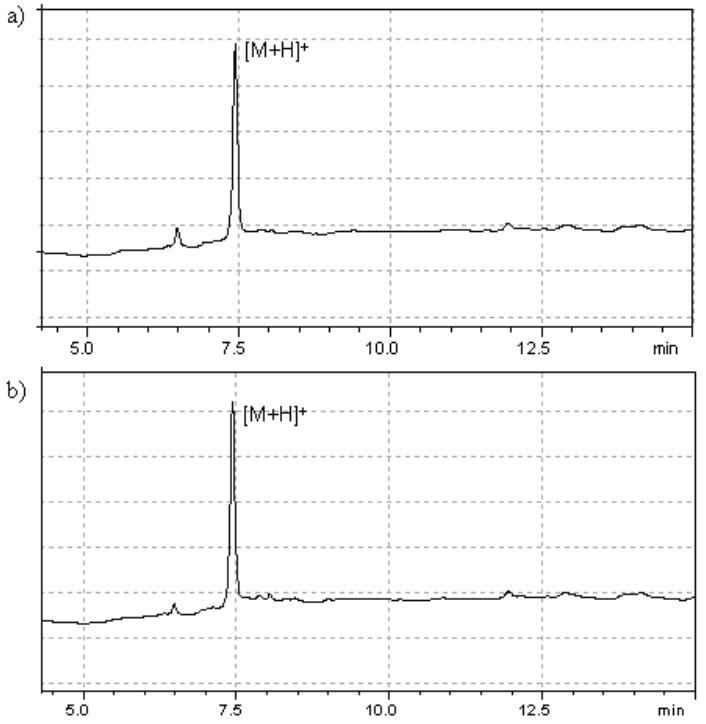

Figure 1. Comparison of peptide purities of GILTVSVAV peptide synthesized on ChemMatrix resin using 3 eq. of Fmoc-amino acids under (a) conventional and (b) microwave conditions at 86 °C.

In order to investigate the effect of temperature on amino acid racemization during the SPPS of model peptide GILTVSVAV resulting from the room temperature and microwave-assisted SPPS at 86 °C were analyzed for amino acid racemization following standard protocols. Gratifyingly, for all 6 different amino acids in the sequence there was no detectable racemization (< 0.26 %) in both the nonapeptide sample synthesized at 25 °C and the peptide prepared under microwave conditions at 86 °C. As expected from recently published racemization studies concerning microwave-assisted SPPS at elevated temperatures,[3] a significant amount of racemization was found for both His (ca. 7% D-His) and Cys (ca. 2% D-Cys) in the synthesis of the 24-mer using the DIC/HOBt coupling conditions at 86 °C. Importantly, the racemization levels were very similar comparing peptide samples obtained from microwave and conventionally heating experiments at 86 °C. This again indicates that the mode of heating in SPPS at elevated temperature does not have an effect on peptide purity and racemization and therefore supports the notion that nonthermal microwave effects are not involved.[4]

Acknowledgements

This work was supported by a grant from the Christian Doppler Society (CDG). We also thank Thorsten Radolf for performing the MS experiments.

References

1. Collins JM, Leadbeater NE. *Org Biomol Chem* **5**: 1141-11450, 2007.
2. Herrero MA, Kremsner JM, Kappe CO. *J Org Chem* **73**: 36-47, 2008.
3. Palasek SA, Cox ZJ, Collins JM. *J Pept Sci* **13**: 143-148, 2007.
4. Bacsa B, Horváti K, Bõsze Sz, Andreae F, Kappe CO. *J Org Chem* **73**: 7532-7542, 2008.

1-04-172

Microwave mediated peptide synthesis in comparison to conventional peptide synthesis

Henklein, Peter[1]; Röder, René[2]; Rapp, Wolfgang[3,]*

[1]Charité Universitätsmedizin-Berlin, Instute of Biochemistry GERMANY; [2]Charité Universitätsmedizin-Berlin, Institute of Biochemistry GERMANY; [3]Rapp Polymere GmbH, GERMANY

[*]E-mail: rapp-polymere@t-online.de

Introduction

During the last few years microwave assisted peptide synthesis has become popular. Improved kinetic rates, faster synthesis times and purer peptides are reported. There is also an ongoing discussion about an additional "microwave induced effect". We have reported the impact of the polymer matrix, activation method and temperature to improve cycle times, kinetic rates and product quality.[1-4] As a result polymer microspheres in combination with elevated temperatures allowed finally the synthesis of β-endorphin in less than 5h.[5] Rivier et. al have summarized the results applying elevated temperature to SPPS.[6] Based on this background model peptides were synthesized on batch and continuous flow synthesizers with and without microwave irradiation and on a microwave system.

Results and discussion

A double walled glass column was used in the MilliGen 9050 flow through system. Water of 60 °C was pumped through the jacket to achieve approximately 50 °C inside the column. For applying microwave energy the MilliGen 9050 was combined with the CEM Discover. A glass column was placed in the microwave chamber of the Discover. Temperature feedback, measured on the surface of the column adjusts the microwave power automatically to keep the temperature inside the column at 50 +/-5 °C. All experiments were performed under identical conditions only varying the acylation time. The peptides are analyzed by HPLC, HPLC/MS and MALDI-MS. For peptide 1 and 2 an acylation time of 20 min gave the best results. Further reduction of acylation below the optimal acylation time results in a significant drop in peptide purity despite microwave irradiation (Table 1, entry 5 and 7 for 1 and 10 for 2). For the difficult peptide 2 we have not found any improvement by microwave irradiation (Table 1, entry 8-10; 11 and 12 yields only in the aminosuccinylated peptide M-18. The difficult WW2 sequence (Table 1, entry 13-17) was synthesized on ChemMatrix and TentaGel R RAM resins on the ABI 433A at rt and the CEM Liberty at elevated temperature.

Conclusion

All investigated examples show clearly that synthesis performed under microwave irradiation gave no benefit over the synthesis performed with conventional heating. In all cases microwave irradiation has only a thermal effect. Peptides with difficult sequences can not be synthesized with higher purities by microwave irradiation. The same results can be achieved by using other energy sources for elevated reaction temperatures. We have not found any "nonthermal microwave induced" effect. This is in accordance with results of other authors.[7] The obtained yields of the peptides are only depending on the reaction temperature and the nature of the used resin for the SPPS.

References

1. Rapp W, Bayer E. *Innovations and Perspectives in Solid Phase Synthesis, Peptides, Polypeptides and Oligonucleotides* (Epton R. Ed). Intercept Ltd., Andover, 1992, p 259.
2. Bayer E, Goldammer C. *Peptides, Chemistry and Biology* (Smith JA, Rivier JE. Eds), *Proceedings of the 11th American Peptide Symposium*. Escom, Leiden, 1992, p 589.
3. Rapp W, Bayer E. In *Peptides 1992* (Schneider CH, Eberle AN. Eds), *Proceedings of the 22nd European Peptide Symposium*. Escom, Leiden, 1993, p 25.
4. Rapp W. *Combinatorial Peptide and Nonpeptide Libraries* (Jung G. Ed). VCH Weinheim-New York-Basel-Cambridge Tokyo, 1996, pp 425-464.
5. Rapp W, Fritz H, Bayer E. *Peptides, Chemistry and Biology* (Smith JA, Rivier JE. Eds), *Proceedings of the 12th American Peptide Symposium*. Escom, Leiden, 1992, p 529.
6. Rivier J. *Solid Phase Synthesis at elevated Temperature. Houben-Weyl E22A*; Goodman M, Felix A, Moroder L, Toniolo C (Eds), Thieme Stuttgart-New York, 2002, pp 806-813.
7. Herrero A, Kremsner JM, Kappe O. *J Org Chem* **73**: 36-47, 2008.

Table 1. Microwave assisted versus conventional synthesis. Peptide 1: GNNDESNISFKEK, peptide 2: ADGSLDYNHLV, peptide 3: ATAVSEWTEYKTANGKTYYYNNRTLESTWEKPQELK.

entry	synthesizer	peptide	energy source	Temp [°C]	resin	coupling time [min]	crude purity [%]
1	MiliGen 9050	peptide 1	water bath	60	TentaGel S PHB	20	87
2	MiliGen 9050/ CEM Discover	peptide 1	microwave	50+/-5	TentaGel S PHB	20	82
3	MiliGen 9050	peptide 1	water bath	60	TentaGel S PHB	10	81
4	MiliGen 9050/ CEM Discover	peptide 1	microwave	50+/-5	TentaGel S PHB	10	82
5	MiliGen 9050/ CEM Discover	peptide 1	microwave	50+/-5	TentaGel S PHB	6	52
6	ABI 433A	peptide 1	r.t.	r.t.	TentaGel S PHB	15	62
7	CEM/Liberty	peptide 1	microwave	50	TentaGel S PHB	5	11
8	MiliGen 9050	peptide 2	water bath	60	TentaGel S RAM	20	48 + (M-18)[a]
9	MiliGen 9050/ CEM Discover	peptide 2	microwave	50+/-5	TentaGel S RAM	20	31 + (M-18)[a]
10	MiliGen 9050/ CEM Discover	peptide 2	microwave	50+/-5	TentaGel S RAM	10	25 + (M-18)[a]
11	ABI 433A	peptide 2	r.t.	r.t.	TentaGel S RAM	15	(M-18)[a]
12	CEM/Liberty	peptide 2	microwave	50	TentaGel S RAM	5	(M-18)[a]
13	ABI 433A	peptide 3	r.t.	r.t.	ChemMatrix	15	32
14	CEM/Liberty	peptide 3	microwave	50	TentaGel R RAM	5 min [b]	47
15	CEM/Liberty	peptide 3	microwave	75	TentaGel R RAM	5 min [b]	46
16	CEM/Liberty	peptide 3	microwave	50	ChemMatrix	5 min [b]	32
17	CEM/Liberty	peptide 3	microwave	75	ChemMatrix	5 min [b]	52

[a](M-18) = aspartimide
[b]10 min after AA 17

1-04-173

Enhanced microwave assisted on-bead disulfide bond formation method: Synthesis of α-Conotoxin MII

Galanis, Athanassios S [1,2,]; Albericio, Fernando[1]; Grøtli, Morten[2]*

[1]University of Barcelona, Barcelona Scientific Parc, SPAIN; [2]University of Gothenborg, Department of Chemistry, SWEDEN

[*]E-mail: athanassios.galanis@irbbarcelona.org

Introduction

Disulfide bonds play an important role in the folding and stability of many biologically important peptides and proteins. Intramolecular disulfide bonds serve to covalently cross-link portions of the polypeptide chain that are apart in the linear sequence but come together in three dimensions. Despite extensive research, the controlled formation of intramolecular disulfide bridges still remains one of the main challenges in the field of peptide chemistry.[1,2]

Conotoxins form a large family of peptide toxins from cone snail venoms that act on a broad spectrum of ion channels and receptors.[3] The subgroup α-conotoxins specifically and selectively bind to subtypes of nicotinic acetylcholine receptors (nAchRs), which are targets for treatment of several neurological disorders. The aim of this work is to develop an improved method able to generate conotoxins in high yield and purity. This will overcome a key barrier currently preventing the efficient synthesis of small focused libraries in order to investigate the structure-activity relationship (SARs) of those peptides. The development of general synthetic strategies for the preparation of conotoxins and analogues are essential to efficiently approach important questions within the area of neurobiology.

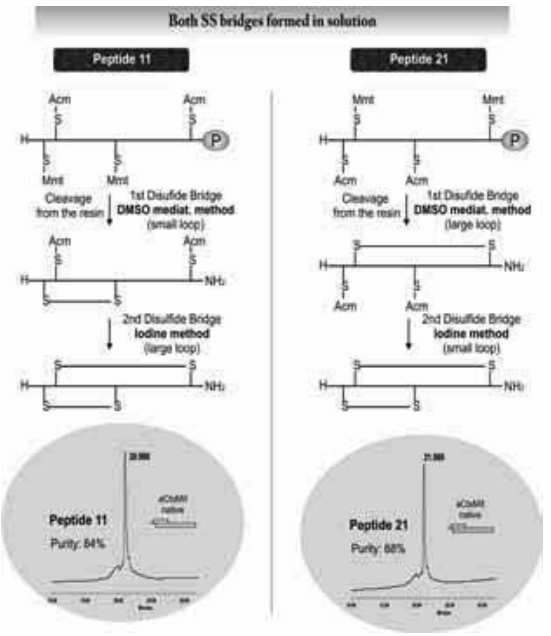

In order to optimize the α-CtxMII synthesis, both classical SPPS and microwave assisted synthesis of the linear peptide precursor were compared. Furthermore, several cyclization methods for disulfide bond formation were evaluated. Among them a recently reported on-bead method[4] was investigated and modified in order to improve the yields of the α-CtxMII synthesis. The use of the microwave assisted heating for enhancing the disulfide formation using a solid phase displacement strategy is discussed.

Results and Discussion

The peptide chain elongation of the α-CtxMII was carried out using conventional 9-fluorenylmethyloxycarbonyl (Fmoc)/tert butyl (tBu) solid phase chemistry. In order to increase the yields and to reduce the time of the peptide synthesis we also applied microwave assisted heating.

In order to achieve selective SS bond formation, side chain protection of cysteine was provided by ortogonal pairwise combination of 4-methoxytrityl (Mmt) and acetamidomethyl (Acm) protecting groups. The two different pairwise protecting groups were sequencing in appropriate positions to form either the large or the small disulfide bridge. The formation of the disulfide bridges were performed after the cleavage of the peptides from the resin using common oxidation methods (Fig. 1). The final products, when the small or the large loop formed first were in purity of 83.77% (peptide 11) and 87.74% (peptide 21), respectively.

In order to investigate formation of the first disulfide bridge on solid support one of the Mmt groups was replaced by a StBu group (Fig. 2). Pursuing this procedure, StBut was removed by treating the resin with 30% mercaptoethanol. The produced free thiol group was then reprotected with 5â€ nitropyridin sufenyl (5-Npys) group. The cyclization step was followed by treatment of the resin with 1% TFA in the presence of 5% triisopropylsilane (TIC) as scavenger. In this step Mmt group is removed from the other Cys and the free thiol group reacts with the 5-Npys-activated cysteine to give the desirable disulfide bond. We modified this method

Figure 1. Orthogonal synthesis of α-Conotoxin MII by in solution oxidations. Peptide 11 (left) which small loop closed firstly and 21 (right) which long loop closed firstly. Both disulfide bridges have been formed in solution.

applying microwave assisted heating in every step. At the last step the resin-bound peptides were irradiated once by 1% TFA for 7 min to remove Mmt group, followed by 2 to 6 times repetitive microwave heating pulses (5 min each) in DCM at 60 °C, in order to complete the cyclization (Fig. 2).

Consecutively, the monocyclic intermediates were oxidized after their cleavage from the RAM-TentaGel resin. The oxidation of crude peptides was then carried out with diluted I_2. The second cyclization step in solution, following the first loop closing by the displacement technique, was almost completed for both peptides (97 - 98%). Purities were 79% (overall yield: 67%) and 65% (overall yield: 65%) for the crude 12 and 22 peptides respectively without any purification of the monocyclic intermediates (Fig. 3).[5]

Conclusion

A novel, rapid synthetic strategy for the synthesis of α-CtxMII has been developed. We clearly demonstrate the advantage of forming disulfide bridges by applying microwave assisted heating. This technique demonstrates the advantage of preparing the first disulfide bridge while the peptides are resin bound, producing the monocyclic intermediate in high purity and major reduced time. This step is critical to provide the dicyclic native peptide, that was performed by a followed classical in solution oxidation by iodine strategy. Our strategy should be useful for preparing a range of small disulfide rich peptides of biological importance.

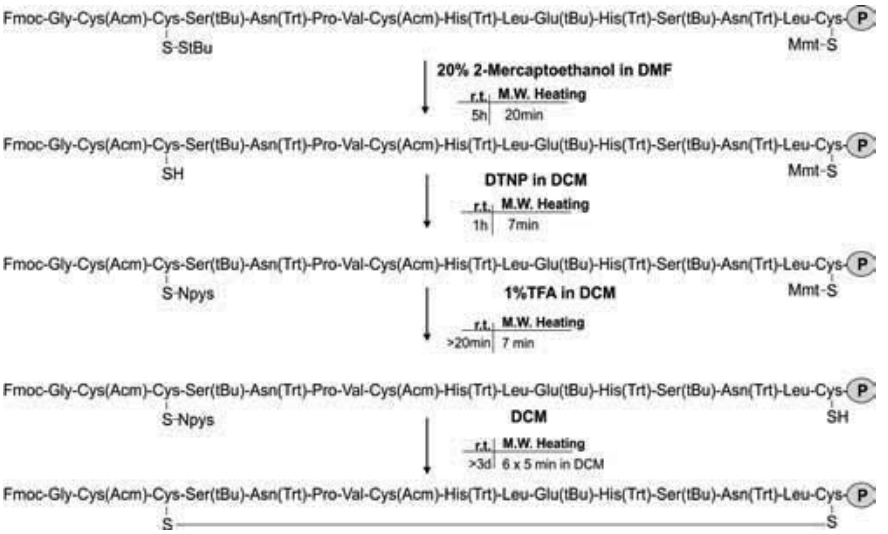

Figure 2. First reported S-S bridge formation on-bead, using microwave assisted heating. Example of this method for the formation of the long loop of the aCtxMII.

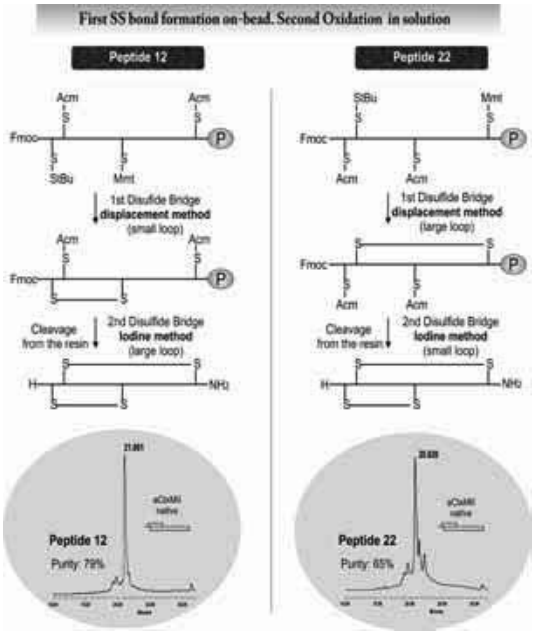

Figure 3. Orthogonal synthesis of α-Conotoxin MII using the microwave assisted displacement method for the first cyclization step on-bead as described above. Second cyclization was performed in solution.

References

1. Annis I, Hargittai B, Barany G. *Methods Enzymol.* **289**: 198-221, 1997.
2. Andreu D, Albericio F, Sole NA, Munson MC, Ferrer M, Barany G. *Peptide Synthesis and Purification Protocols*; Humana Press (Pennington MW, Dunn BM. Eds) 1994, pp 91-169.
3. Harvey SC, McIntosh JM, Cartier GE, Maddox FN, Luetje CW. *Mol Pharmacol* **51**: 336-342, 1997.
4. Galande K, Weissleder R, Tung C-H. *J Comb Chem* **7**: 174-177, 2005.
5. Galanis AS, Albericio F, Grotli M. *Biopolymers (Peptide Science)* **1**: 23-34, 2009.

1-04-174

Solid phase peptide synthesis in aqueous environment using microwave assistance heating

Galanis, Athanassios S[1,2,]; Albericio, Fernando[1]; Grřtli, Morten[2]*

[1]University of Barcelona, Barcelona Science Park, SPAIN; [2]University of Gothenborg, Department of Chemistry, SWEDEN

[*]E-mail: athanassios.galanis@irbbarcelona.org

Introduction

Since the first reports on the use of microwave heating more than 20 years ago, microwave assisted organic synthesis (MAOS) has become an important tool for rapid and efficient synthesis of organic molecules.[1] Microwave assisted heating has also been applied to peptide synthesis in order to reduce coupling times and to improve the yields for the synthesis of difficult sequences.[2] As far as water as solvent is concerned, numerous recent publications report the combination of water as an environmentally benign solvent for chemical transformations with the use of microwave irradiation as an efficient heating method.[3] Herein, we describe our attempts towards microwave assisted solid-phase peptide synthesis in water. A variety of common amino acids derivatives and coupling reagents have been studied in order to optimize coupling reactions in water by microwave assisted heating. We also describe the total synthesis of a small peptide using water as solvent. The solid phase synthesis using the environmental friendly aqueous medium dramatically reduces the cost of the synthesis and could be broadly applied in research or in industrial production of peptides.

Results & Discussion

Herein, we report the development of an efficient method for aqueous solid phase peptide synthesis of Leu-Enkephalin (YGGFL) using commercial available amino acids derivatives. The cornerstone of this work is the use of the microwave assisted heating for the coupling reactions of each amino acid derivative on the solid support. The benefit of the dipolar polarisation mechanism of the polar peptides backbone in combination with the polar water medium provides the energy source aiming to improve the coupling efficiency.[4] Apart of the effects of the microwave radiation, a further crucial point for the reactions progress is the improved solubility of the hydrophobic Boc derivatives in the applied high temperatures.

In order to evaluate the SPPS in water using microwave assisted heating, the synthesis of Leu-Enkephalin was used as a model system. Preliminary experiments were performed evaluating the coupling reactions in water for each residue of Leu-Enkephalin. Thus, corresponded oligopeptides were synthesized by classical SPPS using organic solvents. Those bound on resin oligopeptides were used as starting material for the coupling of each Leu-Enkephalin residue, using the Boc- and Fmoc *N*-protecting derivatives. Furthermore, the N^{α}-azido modified amino acids comprise the Leu-Enkephalin sequence were synthesized and were evaluated. Azido-group has been proposed as an alternative N^{α}-protecting group that provides improved hydrophilicity to amino acids derivatives. Rink - Amide TentaGel and ChemMatrix resins were used for the preliminary experiments due to their swelling abilities

COUPLING REACTION IN WATER				RESULTS		
a.a. +	A	→	B	x:	% A	% B
x-Phe-OH EDC / HOSu +	H_2N-L-(P)	2 x 7 min; 70 °C m.w. →	x-FL-(P)	Fmoc	nd	58.3 %
				Boc	nd	78.4 %
				N_3	nd	48.4 %
x-Gly-OH EDC / HOSu +	H_2N-FL-(P)	2 x 7 min; 70 °C m.w. →	x-GFL-(P)	Fmoc	4.5 %	69.0 %
				Boc	0.3 %	93.7 %
				N_3	38.9 %	32.6 %
x-Gly-OH EDC / HOSu +	H_2N-GFL-(P)	2 x 7 min; 70 °C m.w. →	x-GGFL-(P)	Fmoc	0 %	59.1 %
				Boc	0 %	100 %
				N_3	68.9 %	21.1 %
x-Tyr-OH EDC / HOSu +	H_2N-YGFL-(P)	2 x 7 min; 70 °C m.w. →	x-YGGFL-(P)	Fmoc	2.2 %	74.6 %
				Boc	0.9 %	83.5 %
				N_3	31.6 %	27.0 %

Table 1. Coupling reactions of each derivative of Leu-Enkephalin sequence. Boc, Fmoc and azido acids derivatives were reacted in water to bound on resin oligopeptides pre-synthesized by classical SPPS method (shown at column A). The yields of the final product (% B) and the remaining unreacted oligopeptide (% A) are represented. The yields were obtained after the properly treatment and cleavage from the resin of the resultant products

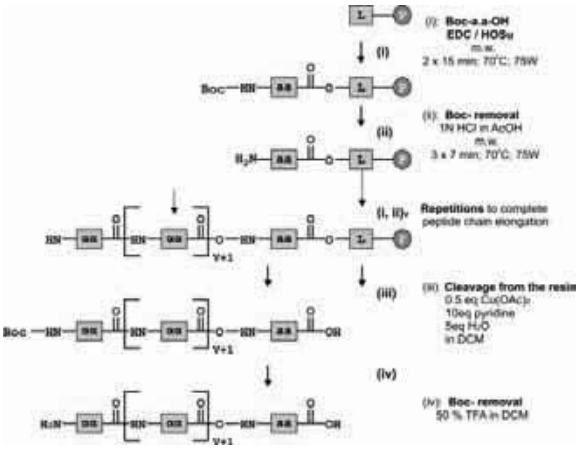

Figure 1. Synthetic protocol for SPPS in water using microwave assisted heating.

and the workup properties in aqueous environment. After evaluation of several coupling reagents and optimization of the coupling conditions two coupling reactions for each derivative were carried out with 5-fold excess of the Boc-a.a. / EDC / HONB coupling mixture, using a CEM microwave reactor, for 7 min at 70 °C

Boc-protected amino acids gave in general a much higher coupling efficiency compared to Fmoc- or Azido-protected amino acids. (Table 1). We expected the Azido acids to give much higher yields than observed due to their more hydrophilic nature compared to Boc- and Fmoc-protected amino acids. Fmoc-protected amino acids provide lower yields than Boc-derivatives, probably due to the bulky and more hydrophobic character of Fmoc-group.

We then attempted the stepwise microwave assisted solid-phase peptide synthesis in water of Leu-Enkephalin using Boc-protected amino acids (Fig. 1). The Hydrazino-benzoyl-AM-NovaGel resin was used as solid support due to its orthogonal properties with the Boc-strategy, the swelling properties in water and the mild cleavage conditions. Coupling reactions were carried out as described before.

The target compound was obtained in high yield and purity (Fig. 2) after cleavage of the peptide from the resin. Only traces of byproducts have been detected correspond mainly to failure sequences. The strategy of SPPS in water using MW assisted heating and the Boc- and EDC/HONB strategy provided results comparable to the classical strategies using organic solvents.

Conclusion

We have demonstrated that it is possible to carry out aqueous solid phase peptide synthesis with high coupling efficiency by applying microwave assisted heating in combination with commercial available Boc-protected amino acids and appropriate coupling agents. This synthetic approach is a rapid strategy of low cost that provides high yield and purity. The method is environmental friendly using low toxicity reagents and avoiding the use of large amount of organic solvents. We aspire that this work will be the provenance for developing "green- peptide- chemistry". The scope, limitations and application of this approach to the synthesis of larger and more complex peptides are under investigation.

Acknowledges

A.S.G. acknowledges a MARIE-CURIE Intra-European-Fellowship- Project No 040451.

References

1. Kappe CO. *Angew Chem Int Ed Engl* **43**: 6250-6284, 2004.
2. Bacsa B, Desai B, Dibo G, Kappe CO. *J Pept Sci* **12**: 633-638, 2006.
3. Polshettiwar V, Varma RS. *Chem Soc Rev* **37**: 1546-1557, 2008.
4. Siskin M, Katritzky AR. *Science* **254**: 231-237, 1991.

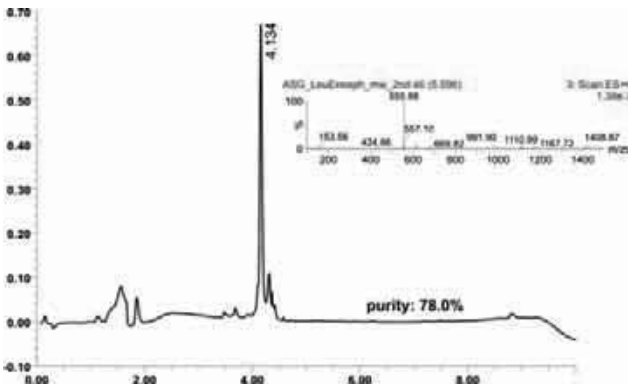

Figure 2. Analytical HPLC and MS of the crude Leu-Enk peptide synthesized in water.

1-04-175

Synthetic antifreeze glycopeptide analogues: synthesis, structural, and functional studies

Heggemann, Carolin[1]; Budke, Carsten[2]; Thomas, Koop[2]; Sewald, Norbert[1,]*
[1]Organic and Bioorganic chemistry, Bielefeld University, GERMANY; [2]Physical Chemistry, Bielefeld University, GERMANY

[*]E-mail: norbert.sewald@uni-bielefeld.de

Introduction

Glycosylated peptides are involved in various biological processes such as cell adhesion and differentiation. In contrast to mucin-type *O*-glycan peptides present on the membrane of mammalian cells, antifreeze glycopeptides (AFGPs) are a sparsely investigated example of glycosylated peptides. AFGPs consist of a varying number of repeating units of AAT with minor sequence variations, where the threonine hydroxyl group is glycosylated with the disaccharide *β*-D-galactosyl-(1→3)-*α*-*N*-acetyl-D-galactosamine. Although it is known that the *N*-acetyl group at the C2 position of the galactosamine, the *α*-configured glycosidic bond to the threonine hydroxyl group, and the *γ*-methyl group are essential, the adsorption mechanism is not yet understood.[1] Solid phase peptide synthesis employing the glycosylated threonine building blocks is an excellent method for the preparation of AFGPs, especially for those peptides containing sequence variations. The introduction of the bulky glycosylated amino acid is facilitated by the use of HATU and microwave-assistance during the coupling cycles.

Scheme 1. Different mono- and diglycosylated peptides with and without sequence variations. Using this method we synthesized different peptides including sequence variations and variable carbohydrate moieties. The peptides were structurally analyzed by CD and NMR. The experiments led to the conclusion that the structure in solution is highly flexible as almost all protons undergo fast deuterium exchange at room temperature. The CD curves of all peptides have basically the same shape indicating either a polyproline II helical structure or a random coil. However, the maxima and minima differ. The introduction of proline into the chain surprisingly reduces the CD effect

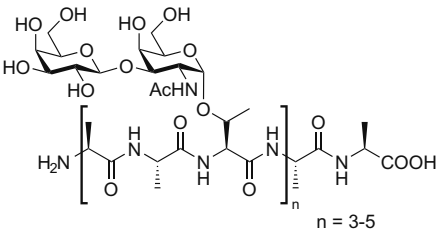

1-3

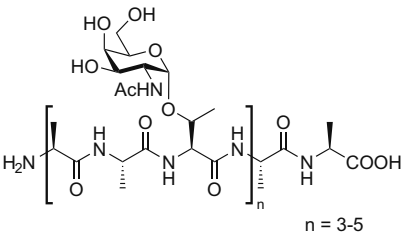

4-6

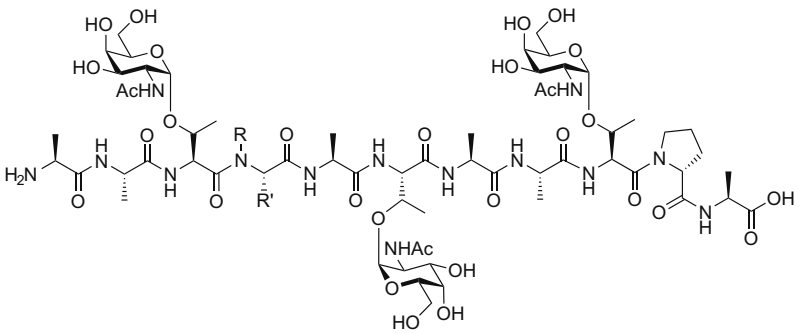

R, R' = , Pro **7**

R = H, R' = H , Gly **8**

R = H, R' = , Ser **9**

Scheme 2. CD spectra of different AFGP analogues (c = 0.2 mg/mL, Millipore water, 0.2 mm cuvette, 10 °C). All peptides have been tested according to their microphysical properties. The antifreeze activity of the AFGP analogues has been tested by observing the recrystallization inhibition. The activity increased with the chain lengths of the peptides. As expected, the native analogues containing the disaccharide unit were more active than the monoglycosylated analogues. In addition, the proline containing analogues **7-9** were significantly less active than **4**[2]

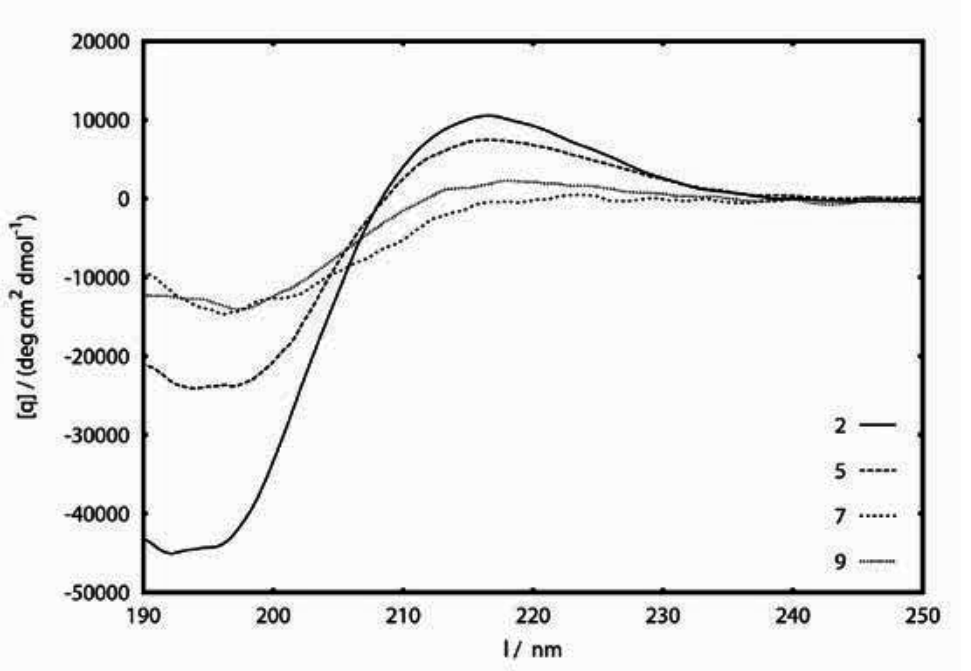

Acknowledgment

This work was supported by the DFG (SFB 613).

References

1. Tachibana Y, Fletcher GL, Fujitani N, Tsuda S, Monde K, Nishimura S. *Angew Chem* **116**: 874-880, 2004.
2. Heggemann C, Budke C, Schomburg B, Wißbrock M, Koop T, Sewald N. *Amino Acids* **38**: 213–222, 2010.

1-04-176

LC-ESI-MS Characterization and Prep-RP-HPLC purification of FMDV Synthetic Viral Peptides

Ozdemir, Zafer Omer[1,]; Topuzogullari, Murat; Karabulut, Erdem; Mustafaeva, Zeynep*

Chemical and Metallurgical Faculty, Yildiz Technical University, Bioengineering Dept., TURKEY

[*]E-mail: ozdemirz@gmail.com

Peptide synthesis has become an important part of drug and biotechnology industries and researches on the last decades.[1] Synthesis is partly complicated job of the desired peptide sequence. There are different methodologies[2] for synthesis of peptides (t-Boc, F-moc, etc.), but the vital parts of the producing synthetic peptide are the characterization and purification steps. Because characterization and purification are the answer for the question of "What is the result of synthesis?"

Materials and Methods

All chemicals used in this study were obtained from commercial sources. Wang resins, amino acids and coupling reagents are purchased from NovaBiochem. The other chemicals are purchased from Sigma-Aldrich. In this study, we characterized synthetic capsid peptides of FMDV (Foot and Mouth Disease Virus) with LC-ESI-MS (Shimadzu LCMS-2010 EV) and purified them with reversed phase HPLC by using a Shim-pack PRC ODS column (20 mm ID and 250 mm length). ESI (Electro Spray Ionization) is one of the medhods[3,4] for ionisation of molecules in MS analysis. Acetonitrile was used as the organic mobile phase in methods for both LC-MS and preparative HPLC. Mobile phase additives was trifluoroacetic acid or formic acid. All the peptides were synthesised in our research laboratory with Liberty Automated Microwave Synthesis Workstation (CEM), by using Solid Phase F-moc Chemistry in DMF media. After synthesis, cleavage of peptides was accomplished with appropriate cocktail for VP1 200-213 sequence; 95% TFA, 2,5 % Water, 2,5 % EDT, and for VP1 135-161 sequence; 94% TFA, 2 % Water, 2 % Phenol, 2 % Thioanisole. After cleavage peptides are precipitated with cold (-20 °C) ether. Peptide sequences and chromatograms are shown in Fig. 1-3.

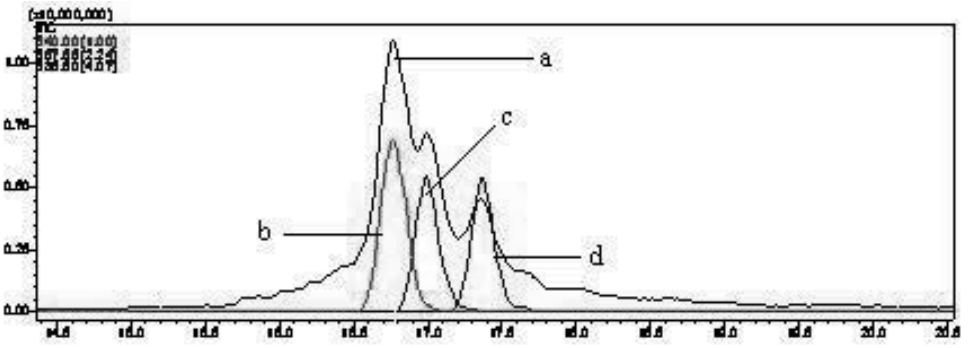

Figure 1. a) Total ion chromatogram (TIC) of VP1 200-213 (WDRHKQRIIAPAKQLG) peptide mixture after synthesis, b) selected ion ($[M+3H^+]^{3+}$=640) chromatogram for VP1 200-213. There is no deletions, c) selected ion ($[M+3H^+]^{3+}$= 587,85) chromatogram for VP1 200-213 without one arginine in the sequence, d) selected ion ($[M+3H^+]^{3+}$=535,80) chromatogram for VP1 200-213 without two arginines in the sequence.

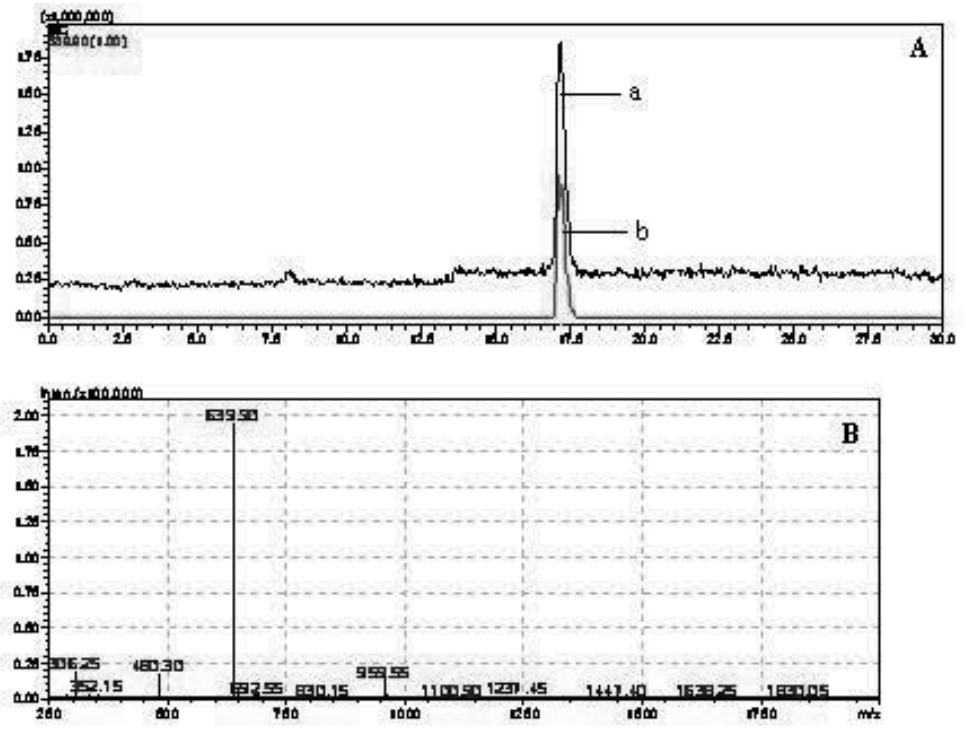

Figure 2. **A.** a) TIC of VP1 200-213 peptide after purification, b) selected ion ($[M+3H^+]^{3+}$=639,90) chromatogram for VP1 200-213. **B**. Mass spectrum of VP1 200-213 between the retention times of 16-8-17,8 min. 639,90 ($[M+3H^+]^{3+}$) is the triple charged ion of VP1 200-213. 480,3; 959,95 are quadruple and double charged ions of the peptide.

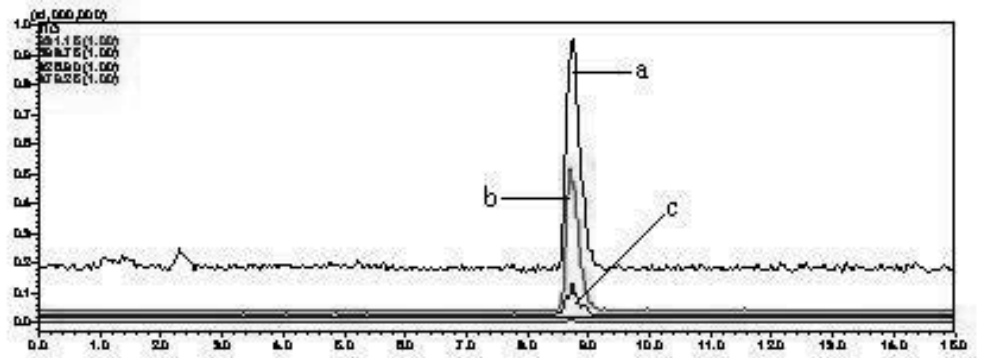

Figure 3. a) TIC of purified VP1 135-161 (SKYSTTGERTRGDLGALAARVATQLPA) peptide, b) selected ion ($[M+3H^+]^{3+}$= 931,15) chromatogram for VP1 135-161, c) selected ion ($[M+3H^+]^{4+}$= 698,75) chromatogram for VP1 135-161.

Acknowledgments

This research was supported by grant from Turkish Republic Prime Ministry State Planning Organization (25-DPT-07-04-01).

References

1. Kimmerlin T, Seebach D. *J Pept Res* **65**: 229-260, 2005.
2. Sewald N, Jakubke H. *Peptides: Chemistry and Biology.* Wiley-VCH Verlag GmbH & Co. KGaA, 2002, ISBNs: 3-527-30405-3.
3. Hop CE, Bakhtiar R. *Biospectroscopy* **3**: 259-280, 1997.
4. Chapman Jr. *Mass Spectrometry of Proteins and Peptide*, Sale, Manchester, UK, 2000.

1-05-177

Insights into β2–microglobulin amyloidogenesis using site–directed–isotope labelling, Fourier transformed infrared spectroscopy and native chemical ligation

Briand, Benoit[1,]; Beyermann, Michael[1]; Fabian, Heinz[2]*

[1]Leibniz-Institut für Molekulare Pharmakologie, GERMANY; [2]Robert-Koch Institut, GERMANY

[*]E-mail: briand@fmp-berlin.de

Introduction

Dialysis–related amyloidosis, a disease arising from long–term dialysis is characterised by gradual accumulation of β2-microglobulin (β2m) amyloid fibrils in bones and ligaments. Although β2m is known to form amyloid fibrils in vitro under acidic pH conditions, seeding of preformed amyloid fibrils or as an effect of ionic strength, the mechanism underlying aggregation of soluble β2m into insoluble fibrils under physiological conditions is largely unknown. Interestingly, Eakin and co. recently showed that the chemical basis of the amyloidogenesis process is a backbone isomerisation of the conserved Pro 32.[1] Our aim is to understand the molecular mechanism associated with β2m amyloidogenesis using Fourier transformed infrared (FTIR) spectroscopy and site–directed–isotope labelling, a method in which the vibration of the labelled residue is shifted from its original position in the spectrum. We already demonstrated that FTIR spectroscopy along with site directed–isotope–labelling is a promising approach to obtain information on the microenvironment of tyrosine side chain residues.[2] To use this approach in the case of β2m amyloidogenesis, we decided to synthesise an isotopically labelled β2m at crucial residues such as Pro 32 that should undergo drastic variations in their microenvironments during the misfolding. With its 99 residues, β2m is over the limits of a reasonable synthesis using SPPS but the two suitably positioned cysteines in its sequence offer the possibility of a chemical synthesis using native chemical ligation. Thus, we were able to realise the chemical synthesis of an isotopically labelled β2m in a good yield using a three segments strategy with disconnections at the two cysteines and thiazolidine as a masked cysteine for the middle segment. The synthetic β2m obtained was in full agreement with the characteristic β2m FTIR spectra. Future FTIR measurements using our isotopically labelled β2m should give new insights into the molecular basis of β2m amyloidogenesis.

References

1. Eakin CM, Berman AJ, Miranker AD. *Nature Struct Mol Biol* **13**: 202-208, 2006.
2. Tremmel S, Beyermann M, Oschkinat H, Bienert M, Naumann D, Fabian H. *Angew Chem Int Ed* **44**: 4631-4635, 2005.

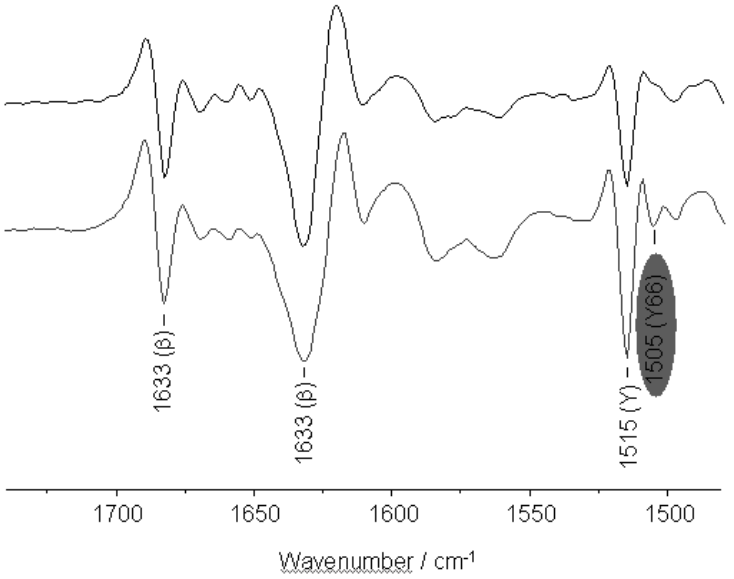

recombinant β_2-m

chemically synthesized β_2-m, site-specifically $^{13}C_1$(4)-Tyr66 labeled

1-05-178

Thiocarbamate-linked peptides by chemoselective peptide ligation

*Besret, Soizic; Ollivier, Nathalie; Blanpain, Annick; Melnyk, Oleg**

Institut de Biologie, Institut Pasteur de Lille, CNRS, Universités de Lille 1 et 2, FRANCE

**E-mail: oleg.melnyk@ibl.fr*

Thiol-based ligation chemistries are highly efficient tools for the synthesis of complex scaffolds. We show here that transthioesterification of the phenylthiocarbonyl (PTC) group by the thiol group of cysteine is an efficient process which leads to the formation of an alkylthiocarbamate bond (Scheme 1).[1]

The PTC group can be easily introduced into peptides on α or ε amino groups using commercially available phenylthiochloroformate (PTC-Cl). Typically, the peptide was first assembled using standard Fmoc/*tert*-butyl solid-phase methods. Phenylthiochloroformate was reacted in anhydrous THF with the amino group of a peptidyl resin in the presence of Et_3N. Deprotection and cleavage in TFA furnished the thiocarbamate-peptide in good yield after purification (45-55%). Depending of the sequence, the reaction time with PTC-Cl must be kept to a minimum (typically 30 min) and *N*-methylmorpholine must be used instead of Et_3N to avoid hydantoin formation.

PTC-peptides react chemoselectively with cysteinyl peptides to give an alkylthiocarbamate bond. *S,N*-shift of the alkylaminocarbonyl group from the Cys side chain to the α amino group did not occur. Ligation proceeds similarly with peptides derivatized by Ac-Cys at the N-terminus or having an internal Cys residue. Typically, the reaction was performed at pH 7.5 in a 0.1 M sodium phosphate buffer in the presence of thiophenol and benzylthiol under argon (50 mM peptide concentration). Using these experimental conditions, thiocarbamate 6 (Scheme 2) was isolated with a 66% yield after RP-HPLC purification. Subsequently, we found that thiophenol and benzylthiol were not necessary for the ligation to proceed efficiently. No ligation product was detected when the same reaction was performed with the Ser analog of peptide 4 H-SILKEPVHGV-NH_2, showing the requirement of a Cys residue for the ligation to proceed. This ligation method was also successfully applied to the synthesis of a cyclic peptide (the PTC group was introduced on an ε amino group by selective on-resin deprotection of a Lys(Mtt) residue)[2] or for the synthesis of di- or tetravalent multiple antigenic peptides (the PTC group was introduced on the lysine trees). The thiocarbamate linkage is stable at or below pH 7.5 and thus is compatible with most experimental procedures used in biochemical or biological studies.

In conclusion, thiocarbamate ligation is a novel thiol-based site-specific ligation method which complements the peptide chemist's tool box for creating original scaffolds.

Scheme 1. Principle of thiocarbamate ligation

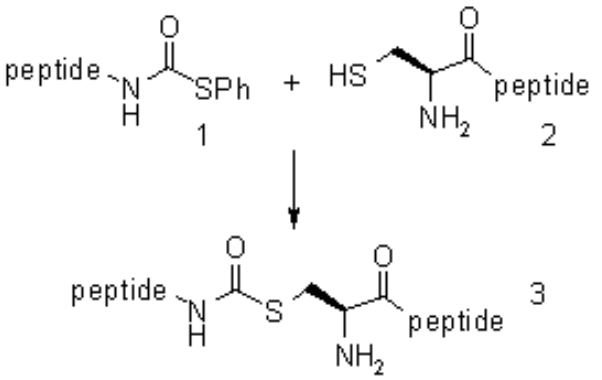

Scheme 2. Thiocarbamate ligation between Cys-peptide 4 and PTC-peptide 5

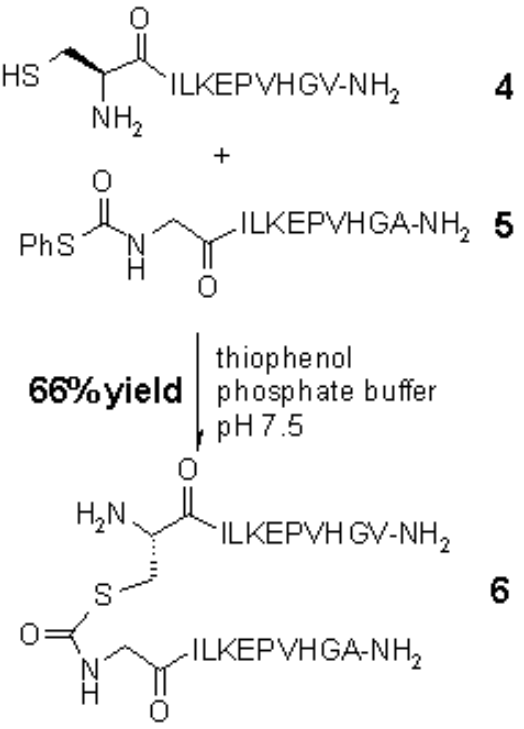

Acknowledgements

We gratefully acknowledge financial support from CNRS, Institut Pasteur de Lille, Université de Lille 1 and Université de Lille 2. This work was performed in the Chemical Systems Biology platform located at the Institute of Biology (IFR 142).

References

1. Besret S, Ollivier N, Blanpain A, Melnyk O. *J Pept Sci* **14**: 1244-1250, 2008.
2. Bourel L, Carion O, Gras-Masse H, Melnyk O. *J Pept Sci* **6**: 264-270, 2000.

1-05-179

Synthesis of azapeptides by chemical ligation

Ollivier, Nathalie; Besret, Soizic; Blanpain, Annick; Melnyk, Oleg*
Institut de Biologie de Lille, CNRS-UMR 8161, FRANCE

**E-mail: Nathalie.Ollivier@ibl.fr*

The substitution of amino acids by aza amino acids in peptides is a way to improve their stability towards proteases, to modulate their conformation or biological activities. Azapeptides are usually synthesized on solid phase by coupling protected aza amino acids precursors to the peptidyl resin. Alternately, the chemoselective formation of an azapeptide bond between unprotected peptide fragments would allow the incorporation of aza amino acids in large structures in a convergent way. We disclose here a novel site-specific ligation method which leads to the formation of an azaGly residue at the ligation site, as Gly is a frequent amino acid in peptides or proteins (Fig. 1).

Two strategies were examined. The first one is based on the reaction between a C-terminal peptide thioester and an N-terminal azaGly peptide (Fig. 1A). The second one involves the reaction of a C-terminal peptide hydrazide with a N-terminal phenylthiocarbonyl (PTC) peptide (Fig. 1B).

Peptide thioesters (R = $(CH_2)_3NHSO_2(CH_2)_3CONH_2$) were synthesized using the Fmoc/*tert*-butyl chemistry and the Kenner sulfonamide linker. After peptide elongation, a solid-phase Mitsunobu alkylation of the acylsulfonamide bond with $HO(CH_2)_3SSi(iPr)_3$ resulted, after thiol unmasking, in the formation of a supported thioester through an intramolecular *N,S*-acyl shift.[1] The C-terminal peptide thioester was deprotected and cleaved from the resin using standard procedures. The azaGly peptide was prepared by coupling Boc-NHNHCOImd, obtained by reacting Boc-$NHNH_2$ with carbonyldiimidazole, to the peptidyl resin. Hydrolysis of the azaGly peptide bond occurred rapidly in aqueous acids such as water containing 0.05% TFA. The azaGly peptide was saved by performing the purification in a pH 7.0 triethylamine acetate buffer.

Thioester Ac-ILKEPVHGA-SR was reacted with peptide H_2NNHCO-GILKEPVHGA-NH_2 in *t*BuOH/water/AcOH in the presence of $AgNO_3$ to give ligated product Ac-ILKEPVHGA-azaG-GILKEPVHGA-NH_2 (28% yield after purification). However, formation of the ligation product resulted in a partial racemization of Ala residue (30%).

Method B was envisioned as a way to circumvent the racemization problem encountered with C-terminal peptide thioesters, since peptide hydrazides can be synthesized using racemization-free methods. The synthesis of PTC-peptides was recently disclosed by us.[2] The PTC group is easily introduced on the solid phase after peptide elongation using phenylthiochloroformate/Et_3N in THF. Cleavage of the PTC-peptide from the resin was performed in TFA using standard experimental conditions.[2] Peptide hydrazide was prepared by nucleophilic cleavage of a peptide assembled and deprotected on a Novasyn TG HMBA resin using standard procedures. Activation of the PTC-GILKEPVHGA-NH_2 with silver ions in the presence of the peptide hydrazide Ac-FSLKEPAVHQA-$NHNH_2$ in *t*BuOH/water/AcOH as before led to the clean formation of the ligated product Ac-FSLKEPAVHQA-azaG-GILKEPVHGA-NH_2 (41% yield after purification) as expected without racemization of Ala residue (Fig. 2).

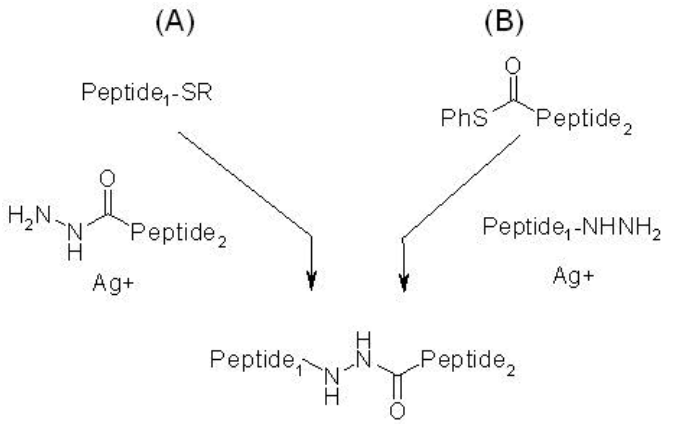

Figure 1. Azapeptides can be assembled chemoselectively using either C-terminal peptide thioesters or N-terminal phenylthiocarbonyl peptides.

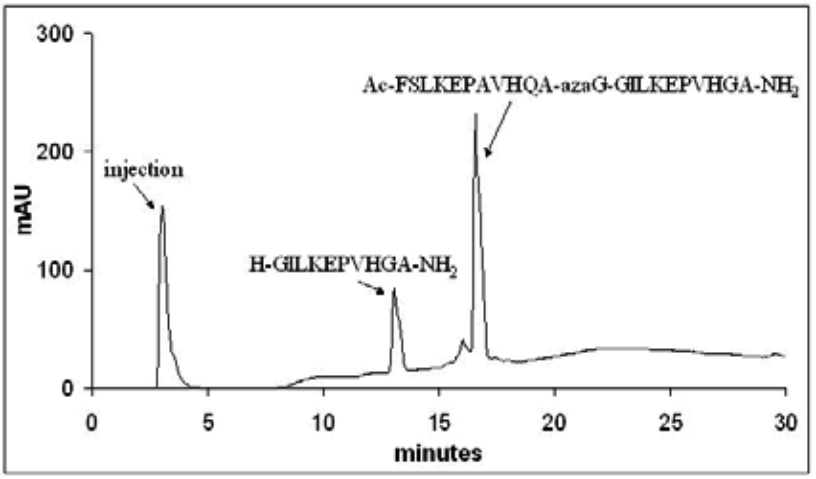

Figure 2. Ligation between PTC-GILKEPVHGA-NH_2 and Ac-FSLKEPAVHQA-$NHNH_2$ in *t*BuOH/water/AcOH. The RP-HPLC was performed after 24 h at 18 °C.

In conclusion, the silver catalyzed reaction of PTC-peptides with C-terminal peptide hydrazides or of C-terminal peptide thioesters with azaGly-peptides allows the convergent and chemoselective synthesis of peptides incorporating an azaGly residue. Adjusting carefully the apparent pH in the *t*BuOH/water solvent mixture is crucial to reach good yields and chemoselectivity for both methods. Method B based on the reaction between a C-terminal peptide hydrazide and a PTC-peptide is preferred due to the absence of racemization, and because both type of fragments can be synthesized easily using standard Fmoc/*tert*-butyl SPPS methods. Application of the method for the synthesis of larger polypeptides is underway.

Acknowledgements

We gratefully acknowledge financial support from CNRS, Institut Pasteur de Lille, Université de Lille 1 and Université de Lille 2. This work was performed in the Chemical Systems Biology platform located at the Institute of Biology.

References

1. Ollivier N, Behr JB, El-Mahdi O, Blanpain A, Melnyk O. Fmoc solid-phase synthesis of peptide thioesters using an intramolecular *N,S*-acyl shift. *Org Lett* **7**: 2647-2650, 2005.
2. Besret S, Ollivier N, Blanpain A, Melnyk O. Thiocarbamate-linked peptides by chemoselective peptide ligation. *J Pept Sci* **14**: 1244-1250, 2008.

1-05-181

Synthesis of peptide thioester by Fmoc chemistry through hydroxyl side chain anchoring

*Lelièvre, Dominique; Barta, Pavel; Aucagne, Vincent; Delmas, Agnès F**

CNRS, CBM, FRANCE

**E-mail: delmas@cnrs-orleans.fr*

Introduction

Since developed by Kent and co-workers in 1994,[1] native chemical ligation (NCL) methods have been used to synthesize various natural polypeptides and proteins. Up to now the preparation of the C-terminal peptide thioester using Fmoc chemistry remains the limiting stage of this methodology. Among several available approaches, the strategy which involves the side chain anchoring of trifunctional amino acids[2] seems the most attractive to the synthesis of long peptide thioesters. In order to prepare a 53-mer peptide thioester with a serine at the antepenultimate C-terminal position, we set out to extend the side chain anchoring strategy to the hydroxyl side chain of serine. The 53-mer peptide thioester corresponds to the N terminal fragment of mitogaligin, a cytotoxic 97-residue protein, we have planned to produce by native chemical ligation.

Results and Discussion

Our approach was inspired by the methodology initially developed by Hanessian,[3] and applied by Mayer and co-workers[4] to the on-resin head-to-tail cyclization of peptides. It involves: (a) the β-hydroxyl reaction of Ser or Thr to the trichloroacetimidate derivative of Wang resin, (b) a stepwise elongation using Fmoc chemistry, (c) the selective allyl ester deprotection, (d) the solid phase carboxyl activation to couple an amino thioester, (e) a final TFA treatment to release the deprotected peptide from the resin.

To demonstrate the feasibility of this technique, we carried out the synthesis of a model peptide Ac-Ser-Arg-Ser-Thr-S$(CH_2)_2$-CO_2Et[5] starting with a trichloroacetimidate Wang polystyrene resin. The etherification (step a) was performed using BF3·Et_2O as catalyst. When using Wang-PEGA resin, a well-known resin to synthesize long peptides,[6] this step required camphorsulfonic acid (CSA) instead of BF3.Et_2O. A special care was taken to minimize epimerization which can occur during the installation of the thioester moiety (step d). The challenge was to achieve quantitative conversion without affecting the stereochemical integrity of the Cα of the C-terminal serine (step d). The epimerization which can possibly occur was evaluated using the commercially available H-Thr(tBu)-NH_2 instead of H-Thr(tBu)-S$(CH_2)_2$-CO_2Et. The two reference peptide amides Ac-SRST-NH_2 and Ac-SRsT-NH_2 were easily synthesized by standard Fmoc chemistry using a Rink resin and characterized by analytical HPLC and MS. Several coupling reagents were tested under different conditions using HATU/DIEA or HOAt/DCC. No significant epimerization (<1%) and good conversion (> 99%) were observed when the amino acid derivative and the coupling reagents were successively added to the resin bed. Ac-SRST-S$(CH_2)_2$-CO_2Et was then prepared using H-Thr(tBu)-S$(CH_2)_2$-CO_2Et (5 eq.) / DIEA (8 eq.) and HOAt/DCC (5 eq.) in CH_2Cl_2/DMF (8/2) leading to a 94 % conversion. Repeating the same protocol was necessary to reach completion without any detectable epimerization.Finally, HPLC-purified peptide thioester was engaged in the native chemical ligation with cysteine-containing peptide H-CTWSL-OH. After 22 h, the ligation nearly reached completionaffording peptide Ac-SRSTCTWSL-OH judging by HPLC. Such low reaction kinetics is well-known for peptide thioesters containing a C-terminal β–branched residue like threonine.

In conclusion, our results show that the side chain anchoring through reaction of a β-hydroxyl amino acid with a trichloroacetamidate Wang resin is a valuable methodology to prepare peptide thioesters by standard Fmoc chemistry. The risk of epimerization has been prevented by using efficient procedures for the on-solid phase α–COOH activation. This work extends the strategy based on side chain anchoring of tri-functional amino acids already described and will be adapted in the next future to the synthesis of large peptide thioesters.

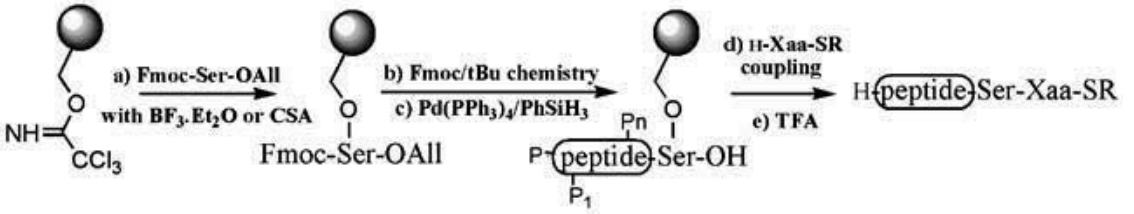

References

1. Dawson PE, Muir TW, Clarklewis I, Kent SBH. *Science* **266**: 776-779, 1994.
2. Wang P, Miranda LP. *Int J Pept Res Ther* **11**: 117-123, 2005.
3. Hanessian S, Xie F. *Tetrahedron Lett* **39**: 733-736, 1998.
4. Yan LZ, Edwards P, Flora D, Mayer JP. *Tetrahedron Lett* **45**: 923-925, 2004.
5. Lelièvre D, Barta P, Aucagne V, Delmas AF. *Tetrahedron Lett* **49**: 4016-4019, 2008.
6. Cremer GA, Tariq H, Delmas AF. *J Pept Sci* **12**: 437-442, 2006.

1-07-182

Oxidative folding of conopeptides in an ionic liquid

Miloslavina, Alesia[1,]; Stark, Annegret[2]; Leipold, Enrico[3]; Heinemann, Stefan H[3]; Imhof, Diana[1]*

[1]Friedrich-Schiller-University Jena, Center for Molecular Biomedicine, Department of Biochemistry GERMANY; [2]Friedrich-Schiller-University Jena, Institute of Technical and Environmental Chemistry, GERMANY; [3]Friedrich-Schiller-University Jena, Center for Molecular Biomedicine, Department of Biophysics, GERMANY

[*]E-mail: alesia.miloslavina@uni-jena.de

Introduction

During the last decade, the interest in using the structural tuneability of ionic liquid (IL) solvent properties for the optimisation of chemical reactions has increased immensely. Ionic liquids were promising in various applications owing to their unique properties that primarily have been exploited to improve the (eco-) efficiency of chemical processes.[1] Due to their composition of cations (e.g. 1,3-dialkylimidazolium, *N*-alkylpyridinium) and anions (e.g. halides, acetate, trifluorosulfonate), solvation of substances occurs by ions only. Few examples of ILs application as reaction media for oxidative processes[2] or in peptide synthesis[3] have already been described. Therefore, we focused our attention to apply ILs for the oxidative folding procedure of cysteine-rich conopeptides. The characterization of conotoxins comprises a real analytical and chemical challenge that includes peptide sequencing, modification and oxidation of the thiol-groups of cysteines. Different strategies for solid phase peptide synthesis and oxidative folding were already published in the literature, however, a major drawback of all these reports is the low yield of the desired products.[4] The synthesis of multiple disulfide-bridged peptides can be achieved either by direct oxidative folding or by orthogonal protection strategies.[5] However, in our experience, due to aspects such as the number of reaction steps required, the overall yield of reaction product and formation of by-products (e.g. misfolded peptides), the direct oxidative folding of the non-protected linear precursor is preferred for conopeptides. The key to successful synthesis and isolation certainly is the efficient and correct folding of the reduced peptide.

Results and discussion

During our research we found that the final oxidation of linear cysteine-rich conopeptides to their bioactive multiply disulfide-bridged products can be performed in an IL as reaction medium. The method features a very good solubilisation of rather hydrophobic peptides, a high-concentration approach and requires no redox-active agents, finally leading to higher yields at reduced separation effort. For that purpose, four conotoxins of different hydrophobicity were used to prove this novel method: μ-SIIIA, μ-PIIIA, δ-EVIA and δ-SVIE. The corresponding linear precursors were synthesised on Tentagel R-RAM according to the Fmoc-strategy and characterised with RP-HPLC, MALDI-TOF mass spectrometry and amino acid analysis. The reduced peptides were then subjected to conventional direct oxidative folding in buffer solution containing either GSH (glutathione, reduced)/GSSG (oxidised) in isopropanol[4] (method A) or cysteamine/cystamine/GSH in methanol[6] (method B) (Fig. 1, (ii) and (iii)). All results were compared with the results obtained by oxidative folding with air in a biocompatible IL, 1-ethyl-3-methylimidazolium acetate [C2mim(OAc)] (method C), (Fig. 1 (iv)). A variety of other ILs were also tested for their applicability for the oxidative folding of hydrophobic conopeptides, such as δ-EVIA and δ-SVIE, however, only [C2mim(OAc)] was useful for further investigations. This was due to parameters like appropriate viscosity of the reaction solution, good solubility of the hydrophobic peptides and formation of the desired oxidised product. As depicted in Fig. 1 ((ii) and (iii)), although the desired oxidised peptide was formed by all methods a variety of unwanted side-products occurred to a rather high extent if using

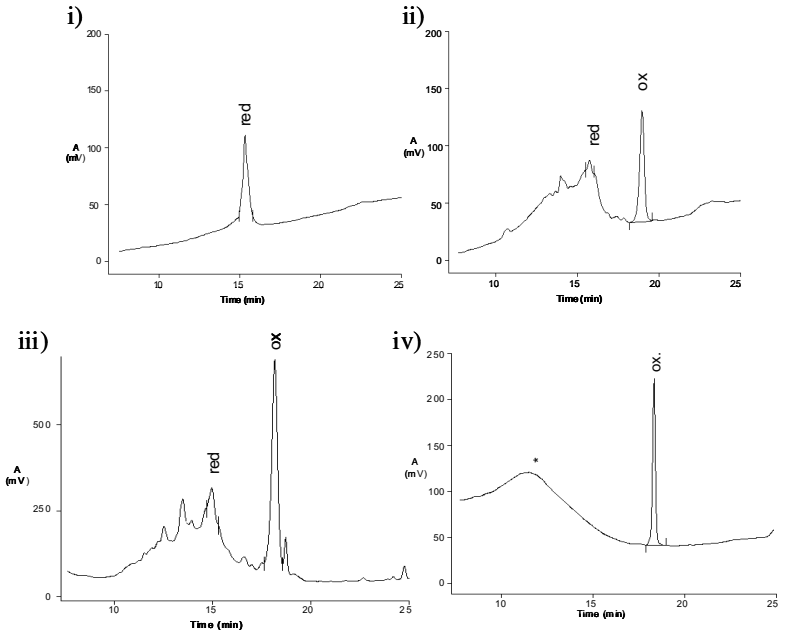

Figure 1. HPLC elution profiles of δ-EVIA (reduced (i) and oxidised (ii-iv) forms), after oxidative folding according to methods A (ii), B (iii) and C (iv), t = 1 h. *Peak from the ionic liquid [C_2mim](OAc). HPLC conditions: gradient: 25%-75% eluent B in 30 min, eluent A: 0.1% TFA/water, eluent B: 0.1% TFA/acetonitrile, flow rate: 1 ml/min (λ = 220 nm) Method iv) provides a novel method for the efficient oxidation of linear cysteine-rich conopeptides to their bioactive counterparts, while at the same time side-product formation is minimised compared to conventional methods. This method enables the efficient formation of both hydrophilic as well as poorly water soluble conotoxins and therefore improves accessibility to different classes of conotoxins.

buffer solutions with redox-active agents. Our results further indicate that for the four peptides investigated, the selectivity of the direct oxidative folding (ii, iii) was not significantly changed under the two different buffer conditions used. Additionally, for hydrophobic peptides such as δ-EVIA and δ-SVIE, (ii) and (iii) oxidising methodologies proved to be disadvantageous due to their low solubility in aqueous solutions.

Acknowledgements

This work was financially supported by the Carl-Zeiss-Stiftung, S.T.I.F.T. and the Friedrich Schiller University Jena.

References

1. Stark A, Seddon KR. *Ionic Liquids. Kirk-Othmer Encycl Chem Tech* (Seidel A. Ed). John Wiley & Sons, Hoboken. 2th edn. **26**: 836-920, 2007.
2. Jiang N, Ragauskas AJ. *Tetrahedron Lett* **48**: 273-276, 2007 .
3. Vallette H, Ferron L, Coquerel G, Guillen F, Plaquevent JC. *ARKIVOC* 200-211, 2006.
4. Mcintosh JM, Hasson A, Spira ME, Gray WR, Li WQ, Marsh M, Hillyard DR,Olivera BM. *J Biol Chem* **270**: 16796-16802, 1995.
5. Moroder L, Musiol HJ, Götz M, Renner C. *Biopolymers* **80**: 85-97, 2005.
6. DeLa Cruz R, Whitby FG, Buczek O, Bulaj G. *J Pept Res* **61**: 202-212, 2002.

1-08-183

Exogenous delivery and molecular evolution: peptides based on C^{α}-methylated α-amino acid as asymmetric catalysts in the syntheses of simple sugars

Moretto, Alessandro[1,]; Formaggio, Fernando[1]; Toniolo, Claudio[1]; Broxterman, Quirinus B.[2]; Weber, Arthur L[3]; Pizzarello, Sandra[4]*

[1]University of Padova, 35131 Padova, ICB-CNR, Padova Unit, Department of Chemistry, ITALY; [2]Innovative Synthesis and Catalysis, 6160 MD Geleen, DSM Pharmaceutical Products, NETHERLANDS; [3]Moffet Field, CA 94035-1000, SETI Institute, Ames Research Center, UNITED STATES; [4]Arizona State University, Tempe, AZ 85018-1604, Department of Chemistry and Biochemistry UNITED STATES

[*]E-mail: alessandro.moretto.1@unipd.it

Introduction

It is known that chiral amino acids, as well as their dipeptides, may catalyze the asymmetric condensation of glycolaldehyde in water (Fig. 1).[1,2]

On the basis of the particularly large erythrose enantiomeric excesses (*ee*) obtained when utilizing the chiral L-Val-L-Val catalyst and given the possibility of an abundant delivery of other types of amino acids to the early Earth, we have studied the catalytic effect on this synthesis of the peptides based on C^{α}-methylated *α*-amino acids, such as Iva (isovaline or C^{α}-methyl, C^{α}-aminobutyric acid) and C^{α}-methylvaline, (*α*Me)Val, that are abundant in meteorites.

Resuts and discussion

Results of the catalysis experiments (Table I) showed that all C^{α}-methylated peptides to the tetramer level exhibit significant chiral influence on the synthesis of tetroses and mimic the effect of the L-Val-L-Val catalyst in having a larger erythrose ee than threose *ee*, as well as in their configuration relationship with the sugars (the product erythrose acquires *ee* of configuration opposite to that of the catalyst in case of peptides, while it is the same for amino acids). Interestingly, the largest *ee* (45% for erythrose) was obtained with the Iva homo-tetrapeptide under mild conditions. The homo-dipeptides of both Iva and (αMe)Val also produced a significant *ee* (41% for erythrose) that appears to increase with time.

Because C^{α}-methylated amino acids are non-racemic in meteorites, do not racemize in aqueous environments, and are known to be (3_{10})-helix formers in peptides with as few as four residues,[3] these results suggest that meteoritic, C^{α}-methylated, *α*-amino acids may have contributed to molecular evolution upon delivery to the early Earth by catalytically transferring their asymmetry to other prebiotic molecules.

References

1. Pizzarello S, Weber A. *Science* **303**: 1151, 2004.
2. Weber A, Pizzarello S. *Proc Natl Acad Sci U S A* **103**: 12713-12717, 2006.
3. Toniolo C, Crisma M, Formaggio F, Peggion C. *Biopolymers (Peptide Science)* **60**: 396-419, 2001.

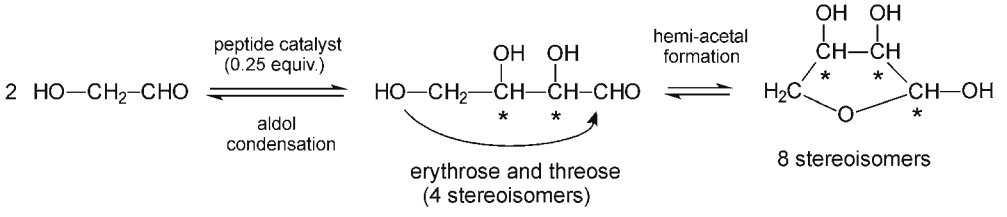

Figure 1. The reaction investigated.

Table 1. Tetroses produced by the peptide-catalyzed condensation of glycolaldehyde with C^{α}-methylated amino acid peptide catalysts, in sodium acetate buffer at pH 5.4

Catalyst	Time/T °C	D-thr ee%	D-ery ee%	~Yield %
$(D\text{-Iva})_2$	18hr/25	10	-41	2
	3hr/50	7	-34	6
$(D\text{-Iva})_4$	3hr/50	14	-38	10
	18hr/25	20	-45	10
	5ds/25	18	-34	4
$[L\text{-}(\alpha Me)Val]_2$	18hr/25	-10	20	5
	12hr/50	-10	28.5	7
	12hr/50+2ms/25	-13	37.5	25
$[L\text{-}(\alpha Me)Val]_4$	8hr/50	-12	26	10

1-09-184

The application of N-Alkyl cysteine (NAC)-assisted thioesterification reaction to the synthesis of polypeptides by the thioester method

Hojo, Hironobu; Ozawa, Chinatsu; Katayama, Hidekazu; Nakahara, Yuko; Nakahara, Yoshiaki*

Tokai University, JAPAN

**E-mail: hojo@keyaki.cc.u-tokai.ac.jp*

Peptide thioester is a key compound in the synthesis of proteins by the thioester method as well as the native chemical ligation. The peptide thioester has been mainly prepared by the Boc method using an established protocol. Due to the increasing interest in the post-translational modifications, such as glycosylation, peptide thioester synthesis by the Fmoc method, which do not use harsh acidic conditions, is desired. Recently, we have developed a novel SPPS thioesterification, in which N-alkyl cysteine (NAC) residue at the C-terminus of a peptide is used as a *N*- to *S*-acyl transfer device as shown in Fig. 1. As this method is fully compatible with the Fmoc method, the synthesis of glycopeptide thioester can be easily accomplished by the method. In this paper, we synthesized glycopeptide dendrimer, the sequence of which is derived from the MUC1 mucin carrying cancer-related carbohydrate (T-antigen), by the sequential application of the NAC method as shown in Fig. 2. First, the glycopeptide thioester 5 was synthesized by the Fmoc method using the NAC method. Fmoc-*N*-ethyl-*S*-trityl cysteine (Fmoc-(Et)Cys(Trt)) was introduced into CLEAR amide resin. Then, a glycine, the C-terminal amino acid in the MUC1 sequence, was introduced using Fmoc-Gly activated by HATU and DIEA. The remaining amino acids were introduced by a peptide synthesizer (Applied Biosystems, 433A) using the FastMocTM protocol, except that Fmoc-Thr carrying the benzyl-protected Gal-GalNAc moiety (T-antigen) was activated by HBTU was introduced manually. The obtained resin was treated with Reagent K to achieve deprotection of the peptide part. After precipitation by diethyl ether, the crude peptide was further treated with low-acidity TfOH<> to remove benzyl groups of the carbohydrate portion. The obtained peptide, which was in an equilibrium between the amide 7 and thioester 6 forms, was then dissolved in a 5% 3-mercaptopropionic acid (MPA) solution to obtain the glycopeptide thioester 5. After 2 d, the NAC-containing peptide was almost converted to the thioester 5 without significant decomposition of the carbohydrate and the thioester portions. The yield of the purified glycosylated peptide thioester 5 was 20% based on the initial loading amount of Gly on the resin. This yield was significantly higher than those of glycosylated peptide thioesters prepared by modified Fmoc strategy using a resin, which immobilizes a peptide via a thioester linkage. This result demonstrated the practical applicability of the NAC method for glycopeptide thioester synthesis. The lysine trimer carrying NAC 4, in which the N- to S- acyl transfer activity is blocked by the Trt group, was synthesized by the Fmoc SPPS method using 2-chlorotrityl alcohol resin. Next, the glycopeptide dendrimer 1 was synthesized by the thioester method<> according to Scheme 1. The glycopeptide thioester 5 and dendrimer core 4 were dissolved in DMSO containing HOOBt and DIEA. AgCl was then added to initiate the coupling reaction. RPHPLC analysis of the solution indicated that the thioester 5 was almost consumed within 6 h and the new peak corresponding to the desired tetramer 3 appeared. The tetramer 3 was precipitated by ether, and used in the next reaction without further purification. The Trt group of the C-terminal NAC residue was removed by TFA containing 5% 1,2-ethanedithiol (EDT), and thioesterification was carried out by 5% aq MPA treatment. The reaction proceeded without significant side reactions within 4 d. Then the desired tetrabranched thioester 2 was isolated by RPHPLC in high purity. Finally, the thioester 2 was condensed with ethylenediamine by the thioester method to obtain the octamer. After isolation by gel filtration chromatography (GFC), the isolated product was analyzed by SDS-PAGE, MALDI-TOF mass (Fig. 3), and amino acid composition analyses, demonstrated that the product 1 was obtained in high purity. The NAC-assisted thioesterification reaction proved to be an efficient method to obtain highly pure glycopeptide thioester in good yield. The consecutive application of the NAC method to the peptide and tetrameric dendrimer successfully gave a highly pure octabranched glycopeptide dendrimer with molecular weight larger than 20 kDa, which will be a candidate for unambiguous cancer vaccines. The biological study using the dendrimer is now in progress.

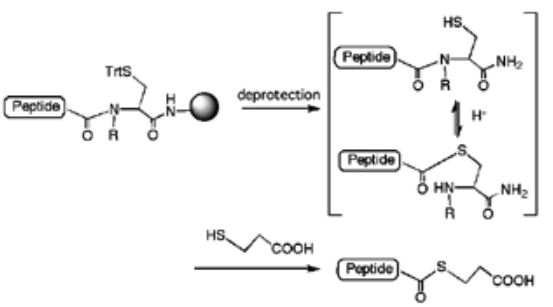

Figure 1. Novel thioesterification reaction using NAC.

References

1. Hojo H, Onuma Y, Akimoto Y, Nakahara Y, Nakahara Y. *Tetrahedron Lett* **48**: 25-28, 2007.
2. Nakamura K, Ishii A, Ito Y, Nakahara Y. *Tetrahedron* **55**: 11253-11266, 1999.
3. Tam JP, Heath WF, Merrifield RB. *J Am Chem Soc* **108**: 5242-5251, 1986.
4. Hojo H, Haginoya E, Matsumoto Y, Nakahara Y, Nabeshima K, Toole BP, Watanabe Y. *Tetrahedron Lett* **44**: 2961-2964, 2003.
5. Hojo H, Matsumoto Y, Nakahara Y, Ito E, Suzuki Y, Suzuki M, Suzuki A, Nakahara Y. *J Am Chem Soc* **127**: 13720-13725, 2005.
6. Hojo H, Aimoto S. *Bull Chem Soc Jpn* **64**: 111-117, 1991.
7. Aimoto S. *Biopolymer (Peptide Science)* **51**: 247-265, 1999.

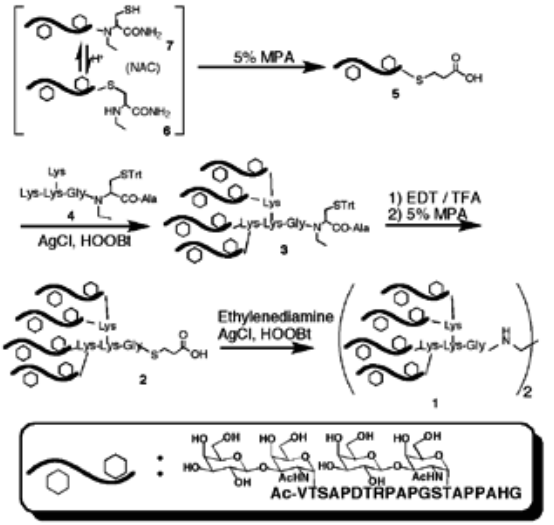

Figure 2. Synthetic route for glycopeptide dendrimer 1 using the NAC method.

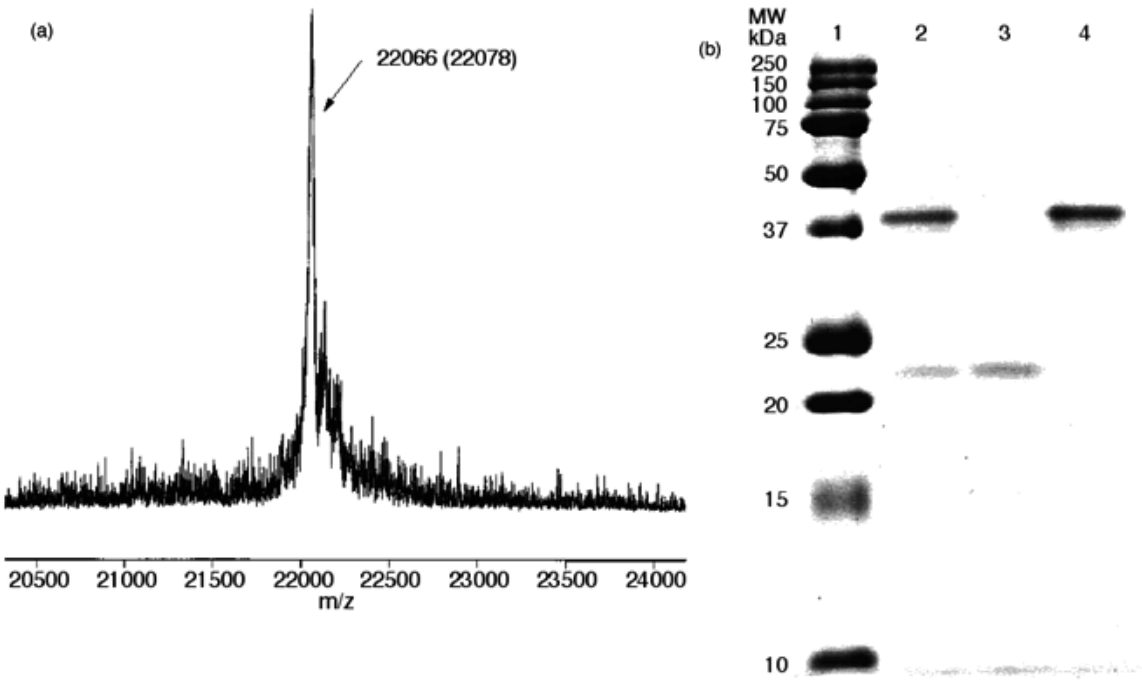

Figure 3. (a) MALDI-TOF mass spectrum of 1 and (b) SDS-PAGE of the glycopeptide dendrimer. Lane 1: m.w. standard; lane 2: coupling mixture for the preparation of the product 1; lane 3: purified tetramer 2; lane 4: purified octamer 1.

1-09-185

Construction of *O*-glycoside peptide libraries by Fmoc-SPPS using the building block strategy

Kawasaki, Takayasu; Miyajima, Midori; Kawahira, Noboru; Hirata, Akiyoshi; Ohyama, Takafumi; Nokihara, Kiyoshi[1,]*

HiPep Laboratories, JAPAN

[*]*E-mail: noki@hipep.jp*

Introduction

Labeled peptide libraries consisting of α-helices, β-loops and β-sheets peptides have been successfully constructed for peptide arrays focusing on a protein-detection system.[1-3] It is known that more than half the proteins in mammalian cells are post-translationally modified and these play an important role in various bio-recognition processes. Glycoproteins are particularly important in cell-adhesion, infection and defense systems. Peptide libraries for arrays have been expanded to incorporate glycopeptides, which are more difficult to synthesize and purify than the parent peptides. The present paper describes efficient construction of structured and labeled *O*-glycoside peptides by the Fmoc-SPPS using the building block strategy.

Results

Previous preparations introduced sugar units at the N^{ε}–Lys position resulting in glycopeptides of a non-natural type[4] which are unsuitable for the construction of a large diversity of products. Hence we needed to devise a strategy to improve construction of a glycopeptide library with natural glycosylated amino acids. Two strategies are known for glycopeptide syntheses, the post-modification method and the building block method. As shown in Fig. 1 the former method gave lower productivity, while the latter was favorable for high throughput library construction with excellent yields. Consequently four variants of glycosylated Fmoc-Thr (glucoside, mannoside, galactoside and lactoside) were prepared in good yield (Table 1). The resulting building blocks were incorporated into secondary structured peptides with a diversity in the number (one or two), type and position(s) of sugar units and backbone amino acid sequence (Fig. 2). After incorporation of the glycosyl group(s) a fluorescent dye was attached and purified. CD spectra indicated the sugar moieties did not significantly influence the peptide secondary structures.

Discussion

In this research, *O*-glycosylated peptides have been efficiently synthesized by the building block strategy using the Fmoc-SPPS. The present protocol has been used to prepare ca. one hundred glycopeptides that have been tested against various carbohydrate-binding proteins. Introduction of the glycoside moieties does not influence the secondary structure of the peptides. Thus these peptides can be used in arrays as part of our protein detection system (designated PepTenChip®).

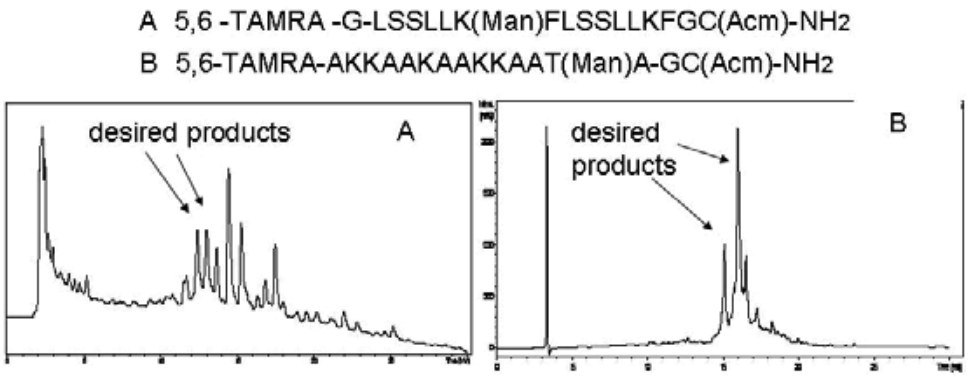

Figure 1. Representative HPLC profiles of crude labeled *O*-glycoside peptides by the post-modification method (left: A) and the building block method (right: B). The mixture of 5,6 TAMRA has been incorporated. Column: HiPep-Cadenza C18 (3.0 ~150 mm); Eluent: 0.1% TFA / 0.1% TFA in 90% ACN= 70/30-10/90% in 30 min (A); 90/10-30/70% in 30 min (B).

Table1. Preparation of glycoside building blocks and glycopeptide library in the present work. Their homogeneity has been characterized by ion-trap LCMS. Solvents used were A: ACN/H2O= 7/6, 0.1%TFA; B: AcOEt/pet. Ether = 8/2. Diversity* C: Number of glycoside attached building blocks; D: Position of glycoside; E: Backbone amino acids

Fmoc-Thr(*O*-glycoside)	Yield (%)	Purification Method	2nd structure	Peptides prepared	Diversity*		
					C	D	E
Glc	60	A RP-Prep TLC					
Gal	70	B Silica-gel Column	α-helix	30	4	4	2
Man	70	B Silica-gel Column	β-sheet	32	4	4	2
Lac	80	A RP-Prep TLC	β-loop	25	4	2	2

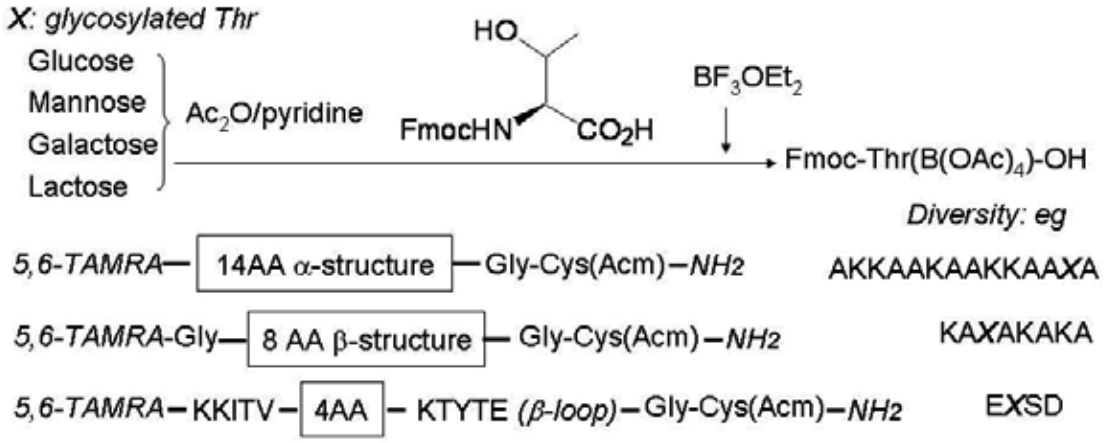

Figure 2. Syntheses of building blocks and architecture of designed labeled glycopeptide libraries. Boxes indicate the diversity of the amino acid sequence, sugar species with one or two sugars and their position. X indicates *O*-glycosyl Thr. Cys can be used for anchoring on substrates after removal of Acm.

Acknowledgements

The authors thank Ono, N., Suzuki, K., Miyazato, N., Kodama, Y., Tetsuya Sogon, T. for their assistance. This work was partially supported by the R and D Program for New Bio-industry Initiatives, National Agriculture and Food Research Organization and Bio-Venture Project of Okinawa Prefecture (2004-6), Ministry of Internal Affairs and Communications.

References

1. Takahashi M, Nokihara K, Mihara H. *Chem Biol* **10**: 53-60, 2003.
2. Usui K, Ojima T, Takahashi M, Nokihara K, Mihara H. *Biopolymers* **76**: 129-139, 2004.
3. Usui K, Takahashi M, Nokihara K, Mihara H. *Molecular Diversity* **8**: 209-218, 2004.
4. Usui K, Ojima T, Tomizaki K, Mihara H. *NanoBiotechnology* **1**: 191-199, 2005.
5. Yang Y-Y, Ficht S, Brik A,Wong C-H. *J Am Chem Soc* **129**: 7690-7701, 2007.
6. Norgren AS, Norberg T, Arvidsson PI. *J Pept Sci* **13**: 717-727, 2007.

1-13-186

Micrawave-assisted synthesis and characterization of biodegradable poly(1-Azabicyclo[4.2.0]octane) as a potential carrier system for antigenic peptide and proteins

Karabulut, Erdem[1,]; Ozdemir, Zafer Omer; Saricay, Yunus; Mustafaeva, Zeynep*

Yildiz Technical University, Bioengineering Department, Istanbul, TURKEY

[*]*E-mail: erdkarabulut@gmail.com*

In this study we offer a new method to synthesize positively charged poly(1-azabicyclo[4.2.0]octane)-common name is polyconidine- and its water-soluble polyampholyte derivative synthesized with bromoacetic acid using microwave irradiation as a model carrier sytem for biological macromolecules like peptides, proteins etc.

1-Azabicylo[4.2.0]octane containing unsubstituted four-membered azetidine ring was synthesized using microwaveassisted synthesis method and used as monomer in cationic ring-opening polymerization. Different alkyl halide derivatives were used as initiators to start polymerization. Microwave-assisted synthesis of polyconidine derivatives was carried out by bromoacetic acid using microwave irradiation. Characterization of polyconidine and its derivatives was achieved by size-exclusion chromatography (SEC) with on line quadruple detection system, ATR FT-IR and UV Spectroscopy.

In recent years there have been made so many research which are intended for developing functional biopolymer systems. In most of the studies until now, it is emphasized on the synthesis, characterization and the diversity of biologically featured polyelectrolytes.[1] Since polyelectrolytes have positive and/or negative charges they are intended to use in biological systems. The synthesis and modification of a biodegredable polyelctrolyte, poly(1-Azabicyclo[4.2.0]octane) (PC) which has an heteroatom in its structure was explained.

A polymeric tertiary amine is available by cationic ring-opening polymerization of 1-Azabicylo[4.2.0] octane (C). The polymerization of bicyclic monomer containing azetidine ring, C, proceeds without appreciable transfer and/or termination. The synhthesis and homopolymerization of this monomer was first published in 1960.[1] 2-(2-Hydroxyethyl) piperidin was used as starting compound instead of 2-(β-Hydroxyethyl) pyridine. Several authors studied the mechanism and kinetics of the polymerizaton.[1-2] More recently the NMR spectra and some details about the structure and properties of this polymer was published.[3] In all of these studies the synthesis of C and its polymers was carried out by conventional organic synthesis methods. The synthetic application of azetidine polymerization is limited, however, due to the difficulties with monomer synthesis. The closure of 4-membered ring is much more difficult than the closure of 3-,5-, or higher member rings.[4-6] So after a long-term work scientists have obtained only a small amount of final product conidine.[7-8]

Thereafter, polymers and their derivatives having different molecular weights were synthesized and the characterization of these polymers were done by SEC with on line quadruple detection system (light-scattering, UV, refraktive index and viscosity), ATR FT-IR and UV spectroscopy

It is determined that molecular weights of the polymers were affected by the change in the amount and the type of initiators used and also from the polymerization media.

PC and its bromoacetic acid derivative are considered to be a new developed synthetic polyelectrolytes for using in liver organisms. PC was synthesized in 1960's by using conventional organic synthesis methods. Investigations have showed that PC is not a toxic polymer system. In this study we have developed a new synthesis method using microwave energy. Microwave-assisted organic synthesis is a newly developed method. After 1990's this method has been started to be used for organic synthesis and polymer synthesis. Quaternization of PC with bromoacetic acid makes its water-soluble polyampholyte derivative because of its carboxy groups. This charge equilibrium is also very important for polymer characteristic. Charges in the polymer chains determine polymer attitude in physiological fluids. The number of carbaxy groups makes stick conformation of polymer chains. The cationic polymerization of cyclic amines which are known to provide living systems with small anions like F-, Cl- or Br-. Because of this it was decided to use initiators presented in Table 1. Mw, polydispersity values, Mark-Houwink-Kuhn constants and hydrodynamic radius vaules obtained from SEC with on line quadruple detection system of PC's which are initiated with four different initiators were shown in Table 1. All of the initiator/monomer rates were 1/1000. Since the counter ions can stop the chain growth the amount of initiators were released very small. Polydispersity values of each polymers were close one another. This condition is appropriate for living type polymerization because polydispersity values of living type polymers are closer to one.

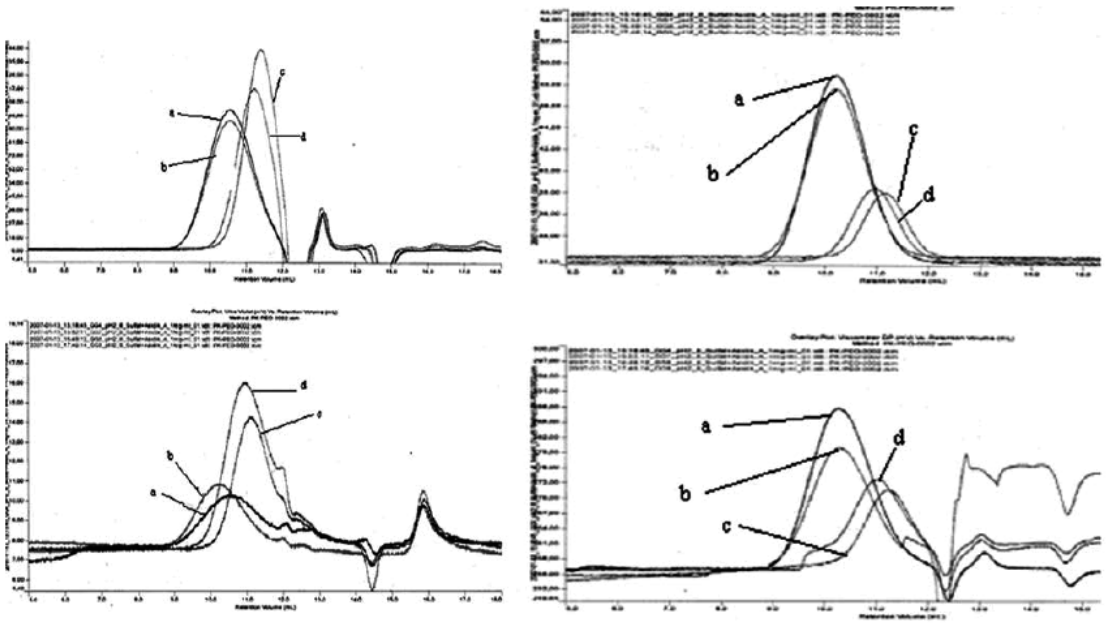

Figure 1. Refractive index, UV, light scattering and viscosity chromatograms of polyconidine samples which started with different initiators (mole ratios are 1/1000 of initiator and monomer). Methyl iodide (a), trimethysilane bromide (b), t-buthyl bromide (c), benzoil chloride (d).

Table 1. Physicochemical values (Mn, Mw, Mw/Mn intrinsic viscosity, Rh, a, Mark-Houwink log K) obtained from size-exclusion chromatography (SEC) with on line quadruple detection system

Initiator	CH_3I	Benzoyl chloride	TMS-Br	t-butyl bromide
Peak RV (ml)	10.523	11.192	10,523	11,367
Mn (Daltons)	20279	9831	20953	6304
Mw	29556	12626	31802	8032
Mz	39436	16114	43694	10086
Mp	26914	10713	28578	6916
Mw/Mn	1457	1,284	1,518	1,274
IV (dl/g)	0.4747	0,3024	0,4300	0,1713
Rh (nm)	5.876	3,756	5,808	2,736
Mark-Houwink a	0.607	0,556	0,651	0,613
Mark-Houwink logK	-3,029	-2,856	-3,287	-3,151
Initiator/monomer rate	1:1000	1:1000	1:1000	1:1000

References

1. Lavagnino ER, Chauvette RR, Cannon WN, Kornfield EC. Conidine-synthesis, polymerization and derivatives. *J Amer Chem Soc* **82**: 2609, 1960.
2. Schulz RC, Schmidt M, Schwarzenbach E, Zöller J. Some new polyelectrolytes. *Macromol Chem, Macromol Symp* **26**, 221-231, 1989.
3. Zaikov GE, Livshits VS. Biodegradable polymers for medical purposes. *Khim-farm Zh* No. 4, 416-427, 1984.
4. Penczek S, Cypryk M, Duda A, Kubisa P, Slomkawski S. Living ring-opening polymerizations of heterocyclic monomers. *Prog Polym Sci* **32***:* 247-282, 2007.
5. Mühlbach K, Schulz RC, Polymers of 1-Azabicyclooctane[4.2.0]. Part 3. Modification of polystyrene-block-poly-1-azabicyclooctane[4.2.0]. *Acta Polymer* **46**: 130-133, 1995.
6. Nekrasov AV, Berestetskaya TZ. Kinetics and mechanism of copolymerization of conidine and β-propiolactone. *Polymer Science U.S.S.R*. **26**: 1165-1169, 1984.
7. Mühlbach K, Schulz RC. Polymers of 1-azabicyclo[4.2.0] octane, 1, Structure of monomer and homopolymer. *Makromol Chem* **189**: 1267, 1988.
8. Matyjaszewski K. Cationic polymerization of 1-azabicyclo[4.2.0]octane 1, Alkylation. *Makromol Chem* **185**: 37-49, 1984.

1-15-188

New Building Blocks Useful For The Synthesis Of Ribosylated Peptides

Bonache, M Angeles[1,]; Nuti, Francesca; Le Chevalier Isaad, Alexandra; Peroni, Elisa; Chelli, Mario; Papini, Anna Maria*

University of Firenze, PeptLab, Dipartimento di Chimica Organica, ITALY

[*]E-mail: angelesbonache@hotmail.com

Introduction

Several autoimmune diseases have been associated with post-translational modifications (PTMs). Glycosylation is one of the most important PTM of secreted proteins and plays a crucial role in several immune functions.[1] Glycosylation defects can be associated with disease conditions. Not only sugars but also their configuration and linkage to amino acids in glycoproteins are essential to investigate their role in regulating diverse physiological and pathological processes. In previous studies, we demonstrated that the presence of a *β*-D-glucopyranosyl moiety, N-linked on an Asn residue at position 7 in CSF114(Glc), is fundamental for autoantibody recognition in Multiple Sclerosis patients' sera. CSF114 is a structure-based designed peptide sequence of 21-amino acids able to expose at the best PTMs (e.g. sugars, citrullines, lipids) because of a type I' *β*-turn.[2] We identified Asn(*β*-Glc) as minimal epitope for Multiple Sclerosis autoantibody recognition, after evaluating in Competitive and SP-ELISA a CSF114-type glycopeptide library based on glyco-amino acid diversity. To this aim, several glycosylated building blocks orthogonally protected for SPPS were developed in large scale, e.g. Glc, Man, GlcbGlc, Gal, GlcNAc, glycomimetics, etc., on the side chains of Ser, Thr, Asp, Glu, HyPro.[3-4] Due to the high specific protein-protein communication that can be possibly mediated by sugars in pathological conditions, we can hypothesize that using a screening based on a sugar scan we can identify specific autoantibodies in human sera, as diagnostic/prognostic tools.

Results

In order to obtain ribosylated peptides, we synthesized for the first time Fmoc-L-Asn[(2,3-*O*-Isopropyliden,5-OAc)α-Rib]-OH **(6α)** and Fmoc-L-Asn[(2,3-*O*-Isopropyliden,5-OAc)β-Rib]-OH **(6β)** introduced in the CSF114 type I' *β*-turn structure to test them as possible synthetic probes. The new CSF114-ribosylated peptides will contribute to the library of glycopeptides - based on glycoamino acid diversity - used to fishing out families of autoantibodies specific for different forms of Multiple Sclerosis or other sugar-mediated autoimmune diseases. The new building blocks **6α** and **6β** were synthesized starting from D-ribose (**1**). The 2,3-*O*-Isopropyliden-1,5-diacetate protected ribosyl derivative (**2**) was obtained after condensation of **1** with acetone and subsequent acetylation with Ac_2O in pyridine. Azide moiety was introduced by Me_3SiN_3 via $SnCl_4$ catalysis affording a mixture of the anomers **3α:3β** (36:64). Even if it was possible to easily separate the two anomers by FCC and characterize them as pure compounds, the following reduction reaction was performed on the β-anomer in the presence of Palladium black, obtaining in any case

Scheme 1

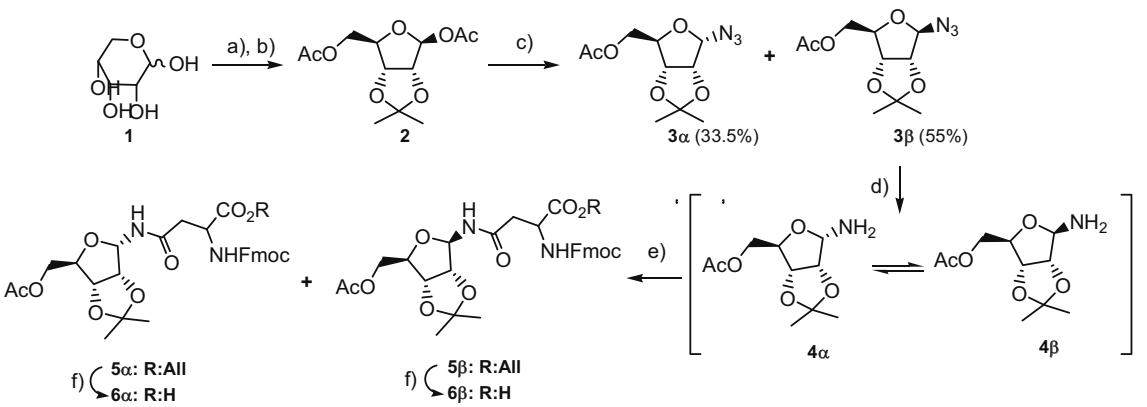

Reagents and conditions: a)Acetone, $CuSO_4$, H_2SO_4. b) Ac_2O, Pyridina (Yield: 68%). c) Me_3SiN_3, $SnCl_4$, CH_2Cl_2 (Yield: 61%). d) H_2, Pd black, EtOH (Yield: 99%). e) Fmoc-Asp-OAll, TBCR/BF_4, CH_3CN (Yield: 40%). f) $Pd(PPh_3)_4$, Ph_3SiH, CH_2Cl_2 (Yield 97%).

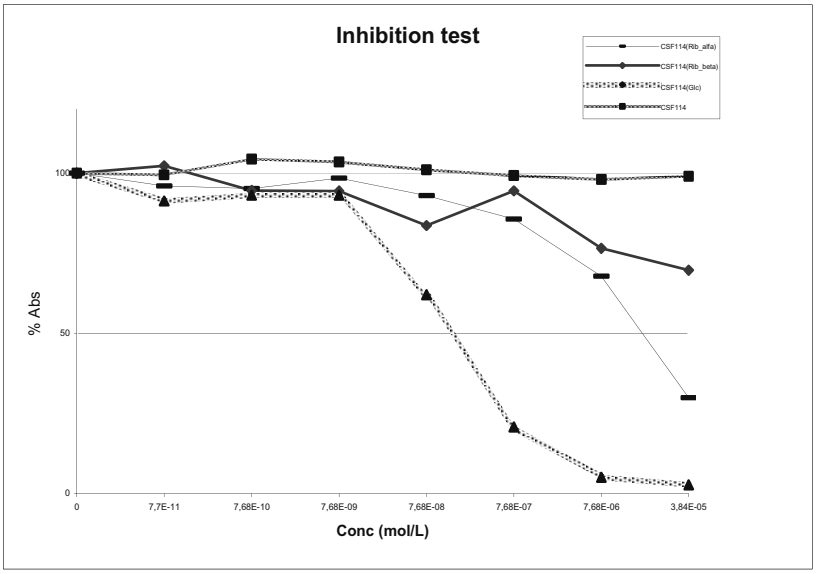

Figure 1

a mixture of amines **4α:4β** (the equilibrium was detected by ^{1}H-NMR). Coupling reaction of the anomeric mixture of the ribosyl amines **4α:4β** to Fmoc-Asp-OAll (via the Triazine-Based Coupling Reagent, DMT-NMM / BF4),[4] formed the desired N-glycosidic bond. The two pure anomers **5α** and **5β** of the new protected ribosylated asparagine derivatives, N$^{\alpha}$Fmoc protected and *C*$^{\alpha}$-protected as allyl esters, were obtained after an effcient separation by FCC from the corresponding anomeric mixture 40:60. Subsequent removal of the allyl group with $Pd(PPh_3)_4$ and triphenylsilane afforded the anomerically pure desired building blocks **6α** and **6β** (Scheme 1).

The building blocks **6α** and **6β** orthogonally protected were introduced independently at position 7 in a MW-assisted Fmoc/tBu-SPPS of the CSF114 peptide sequence. After cleavage, deprotection of the amino-acid side chains and of the hydroxyl functions of ribose, and purification by RP-HPLC, we obtained [Asn^7(αRib)]CSF114 (**IIIα**) and [Asn^7(βRib)]CSF114 (**IIIβ**). Autoantibody titre in MS patients' sera was evaluated by competitive ELISA with the new CSF114-type ribosylated peptides **IIIβ** and **IIIα** and compared with CSF114(Glc) (**II**) and the corresponding unglycosylated sequence CSF114 (**I**). Competive ELISA showed that both the ribosylated peptides **IIIα** and **IIIβ** are not able to inhibit anti-CSF114(Glc) autoantibodies in MS patients' sera (Fig 1). These data confirmed our previous results.[2] Therefore, Asn(*β*-Glc) is up to now the unique minimal and fundamental epitope recognizing specific and high affinity autoantibodies in a relapsing-remitting form of MS.

Acknowledgments

We acknowledge Ente Cassa di Risparmio di Firenze, FIRB Internationalisation 2005 RBIN04TWKN. M.A.B. thanks Alfonso Martin Escudero Foundation (Spain) for the financial support of her post-doctoral fellowship.

References

1. Daniels MA, Hogquist KA, Jameson SC. *Nat Immunol* **10**: 903-910, 2002.
2. (a) Papini AM, Rovero P, Chelli M, Lolli F. *PCT International Patent Application* **WO 03/000733,** *2008*.
(b) Lolli F, Mulinacci B, Carotenuto A, Bonetti B, Sabatino G, Mazzanti B, D'Ursi AM, Novellino E, Pazzagli M, Lovato L, Alcaro MC, Peroni E, Pozo-Carrero MC, Nuti F, Battistini L, Borsellino G, Chelli M, Rovero P, Papini AM. *Proc Natl Acad Sci U S A* **102**: 10273-10278, 2005.
(c) Carotenuto A, D'Ursi AM, Mulinacci B, Paolini I, Lolli F, Papini AM, Novellino E, Rovero P. *J Med Chem* **49**: 5072-5079, 2006.
3. Paolini I, Nuti F, Pozo-Carrero MC, Barbetti F, Kolesińska B, Kamiński ZJ, Chelli M, Papini AM. *Tetrahedron Lett* **48**: 2901-2904, 2007.
4. Kamiński ZJ, Kolesińska B, Kolesińska J, Sabatino G, Chelli M, Rovero P, Błaszczyk M, Główka ML, Papini AM. *J Am Chem Soc* **127**: 16912-16920, 2005.

1-16-189

Parallel small scale peptide synthesis meets a fast, low-cost purification method for the production of high quality peptide microarrays to analyze DNA-protein interactions

Dauber, Marc[1]; Schnoelzer, Martina[2]; Hoheisel, Joerg[1]; Jacob, Anette[1,]*

[1]German Cancer Research Center, Functional Genome Analysis, GERMANY; [2]German Cancer Research Center, Protein Analysis, GERMANY

[*]E-mail: a.jacob@dkfz.de

Introduction

Synthetic peptides are versatile tools for all kind of biological applications, e.g. for the analysis of protein-protein or protein-DNA interactions, epitope binding, enzyme activity, phosphorylations and so on. For most of these applications only small amounts of a great many of different peptides in high quality are required. Whereas parallel synthesis of peptides in a small scale is relatively easy to achieve, purification in a high-throughput format is not. Standard purification of peptides involves ether precipitation and HPLC, which is time consuming, cost intensive and not very practicable for high-throughput applications.

Thus, herein, a small scale peptide synthesis (0,1 µmol) in 384-microwell plates was optimized and combined with a fast but yet efficient, low-cost "Fmoc-on" purification method1, which can be well integrated into the synthesis process. As an example, over 300 peptides synthesized and purified in such a way were used to produce microarrays which were finally employed for the analysis of binding domains of transcription factors, relevant for breast cancer.

Results and discussion

Peptides were synthesized in 384-microwell plates by an Autospot robot (Intavis, Köln, Germany) according to standard solid phase Fmoc-chemistry. After synthesis, peptides were cleaved from the resin with their N-terminal Fmoc-group still on and an aliquot of each product was analyzed by MALDI-TOF MS for quality control. In order to optimize "Fmoc-on" purification protocols and to demonstrate purification efficiency crude 20 mer Fmoc-products whose MALDI spectra show only very small amounts of by-products were in some cases additionally spiked with the respective acetylated 19 and 17 mers, thereby simulating a higher amount of long truncated sequences. However, in general, crude products cleaved from the resin were directly transferred by extraction into another 384-microwell plate filled with purification material. Purification takes place due to the high affinity of the terminal Fmoc-group to this material. Under conditions where the full-length products stay on this material all truncated sequences are washed away. Subsequently, the purified products can be eluted with the Fmoc-group still on. Or, as an alternative, the Fmoc-

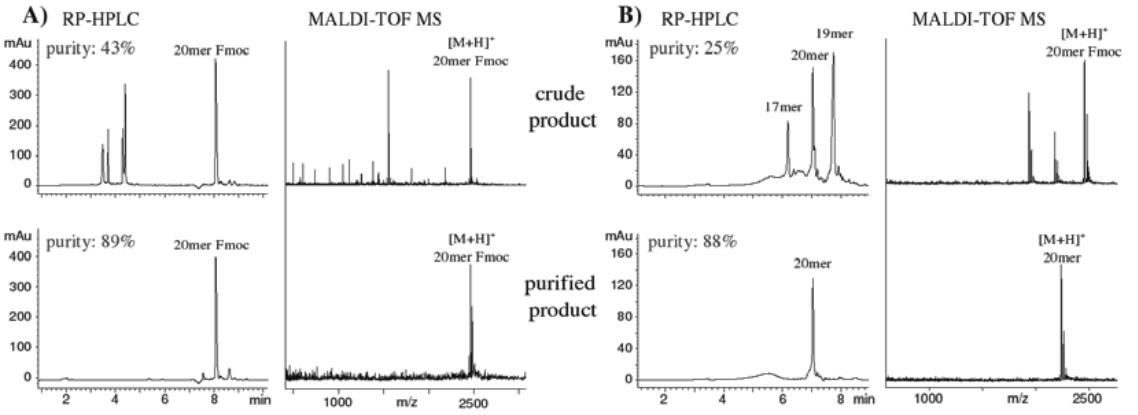

Figure 1. Demonstration of typical results by means of the purification of Fmoc-VWGEPGTNGQHAFYQLIHQG. For both purification processes good purities (89 and 88%, respectively) as well as very good recoveries (98 and 92%) were achieved. Furthermore, HPLC as well as MALDI spectra demonstrate quantitative cleavage of the Fmoc-group on the purification material.

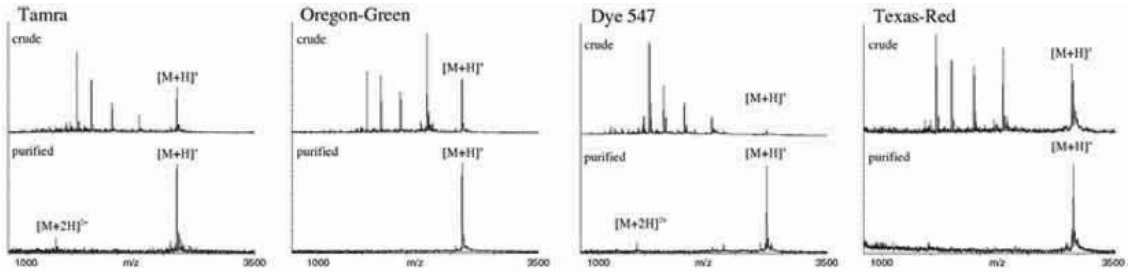

Figure 2. Demonstration of the purification efficiency by means of MALDI-TOF MS spectra.

group can be cleaved directly on the purification material with 20%piperidine in dichloromethane and the fully deprotected purified peptides are eluted. In order to verify the efficiency of the purification method and recovery of the full-length products from the purification material, aliquots of the crude products cleaved from the resin and the respective purified products were analyzed by RP-HPLC and MALDI-TOF MS.

Parallel purification in 384-microwell plates can also be carried out for peptides carrying a fluorescent dye instead of the N-terminal Fmoc protection group. For a "proof of principle" the peptide VWGEPGTNGQHAFYQLIHQG was synthesized four times and labeled with different dyes at the N-terminus. After cleavage from the resin, crude dye-labeled products were purified as described.

In order to study binding sites of transcription factors, related to breast cancer, a microarray with peptides covering the sequences of NF-*k*B, HUMETS1A, HUMAP2 and Y-box was produced. Peptides were designed as 20mers with an overlap of 13 amino acids. Thus, 304 peptides with an additional cysteine at the N-terminus were synthesized, purified as described above and spotted on maleimide activated glass slides.

References

1. Brandt O, Hoheisel J, Jacob A. **PCT/EP2005/005807**, 2005.

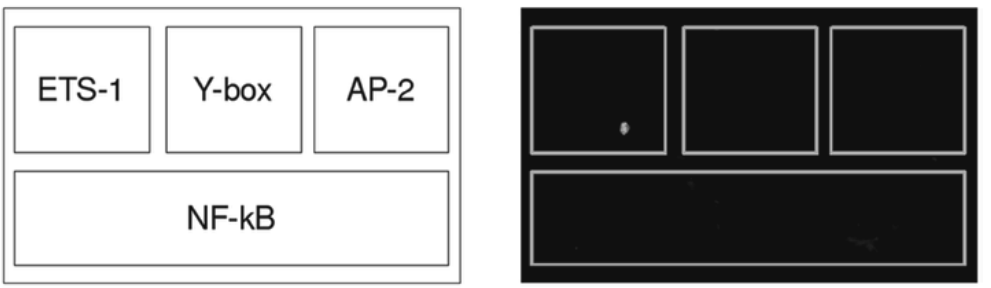

Figure 3. On the left side: Layout of a microarray consisting of 304 peptides covering the sequences of NF-kB, HUMETSIA1A (ETS-1), HUMAP2 (AP-2) and Y-box. On the right side: Incubation with a Cy3/Cy5 labeled DNA double strand which binds to ETS-1.

1-20-190

Synthesis of desmycosin analogs containing peptides at 4'-position

Karpenko, Victoria[1,]; Sumbatyan, Natalia[1]; Korshunova, Galina[2]; Bogdanov, Aleksei[1]*

[1]Chemistry Department of Moscow State University, Moscow, RUSSIAN FEDERATION; [2]A.N. Belozersky Institute of Physico-Chemical Biology, Moscow State University, RUSSIAN FEDERATION

[*]E-mail: victoriya_msu@mail.ru

Introduction

Desmycosin (Des) is an antibiotic-macrolide related to a group of tylosin (Tyl) which structure is based on 16-member lactone with carbohydrate substitutes attached (Fig. 1, **I, II**). Macrolides are well known translation inhibitors, they bind to ribosomal tunnel (RT) in a way that their lactone ring is located orthogonally to the long axis of the RT, covering most of its cleft; hence, the mechanism of protein synthesis inhibition by macrolides relies on the mechanical obstruction they provide to the passage of nascent polypeptide chain through the RT.[1,2,3]

Recently we have designed and synthesized a number of peptide derivatives of macrolides where the peptide part modeled the growing chain, while the antibiotic served as an "anchor" for positioning the peptide at the specific site of RT.[4,5] Two types of such peptide – macrolide conjugates are possible: with peptide fragments directed to peptidyl transferase center (PTC) or to the exit of the RT. Peptide – macrolide conjugates are of interest both as antibacterial agents and potential probes for investigation of nascent peptide chain topography in the RT.

It is revealed that some nascent peptides can specifically interact with RT and affect the functions of the ribosome. For example, arrest of translation in case of SecM and TnaC nascent peptides occurs at the proline codon, underscoring the importance of the C-terminal proline residue that, in the stalling complex, resides in the PTC active site.[6] However, structural reasons of proline interaction in PTC are still unclear.

Now we report a new type of peptide - macrolide conjugates in which peptide binds by its α-amino function through a spacer to the 4'-hydroxyl group of the mycaminose residue of Des. Peptide fragments of these desmycosin derivatives contain proline residues that assumed to be located in the PTC region of ribosome when complexes of the desmycosin peptide derivatives with bacterial ribosomes are formed.

Results and discussion

Tylosin (Fig. 1, **I**) contains two carbohydrate substitutes: disaccharide formed of mycaminose and mycarose residues at position 5 of the lactone ring, and mycinose residue at position 14; desmycosin (Fig. 1, **II**) differs from tylosin by the absence of the mycarose residue. Disaccharide and mycaminose residues of the antibiotics are located along the walls of the RT and are directed to PTC moreover disaccharide extention of tylosin reaches into PTC when macrolide is bound to bacterial ribosome. To construct peptide derivatives of macrolide in which proline residues are supposed to interact with PTC region

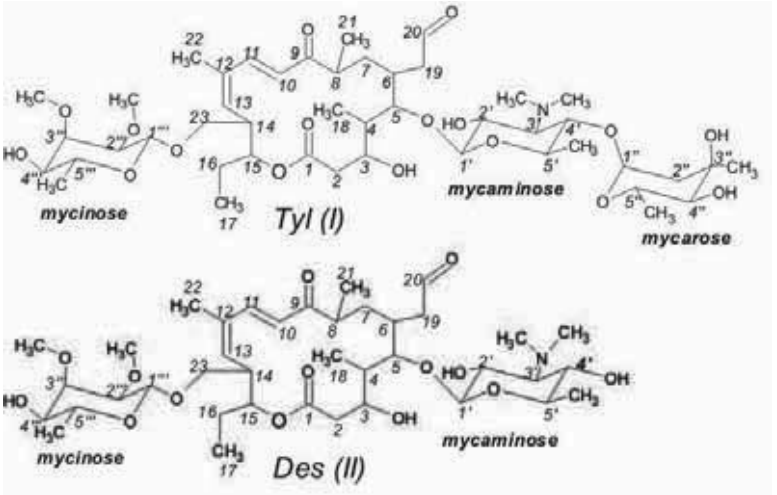

Figure 1. Structures of Tylosin and Desmycosin.

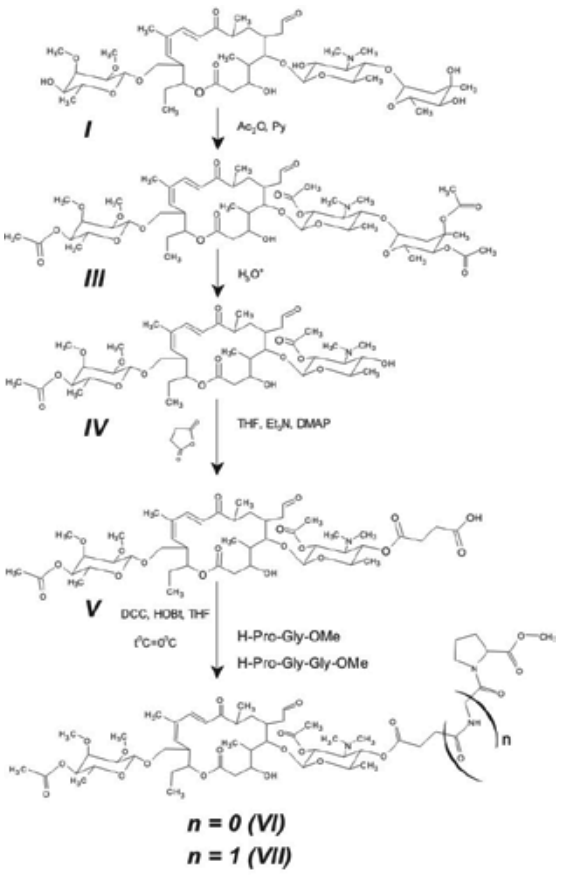

Figure 2. A scheme of desmycosin analogs synthesis.

we decided to dispose peptide fragments in place of mycaminose moiety of tylosin.

Two proline-containing peptides are chosen for modification of antibiotics: H-Gly-Pro-OMe and H-Gly-Gly-Pro-OMe. Boc-protected peptides were obtained by HOBt/DCC-method in solution; Boc-group was removed with trifluoroacetic acid.

The synthesis of peptide-macrolide conjugates included the following steps (Fig. 2). The first step of the synthesis was acetylation of 2'-, 2"-, 4"- and 4"'-OH-groups of Tyl by Ac_2O (compound **III**) in pyridine following by hydrolysis in 1 N sulphuric acid resulted in 2'-, 4"'- diacetylated Des (compound **IV**).[7] Free 4'-OH group of mycaminose was used for reaction with succinic anhydride leading to formation of reactive carboxyl group (compound **V**). A reaction between 4'-hydroxyl group of desmycosin and cyclic anhydrides resulting in opening of cycle has not been described previously. That is why we selected the most appropriate conditions for the reaction according to the method described:[8] 4 eq. of succinic anhydride and 3.5 eq. of Et_3N were added to 1 eq. of 2'-, 4"' diacetylated Des in THF in the presence of catalytic quantity of DMAP; after stirring at the room temperature ^{O}C for 6 h reaction mixture was evaporated; the product was purified by silicagel chromatography in chloroform - methanol (6:1). The yield was 64%. ÒLC: R_f (chloroform – ethanol – acetic acid, 85:10:2) = 0.31. HPLC: τ = 6.2 min (20-80 % B for 30 min; À: 0.05% TFA, B: 0.05% TFA in CH_3CN). MALDI MS: m/z calcd. for $C_{47}H_{73}NO_{19}$ 955.97; found 956.40. The position of succinic residue in the desmycosin derivative (C-4' of Des) was confirmed with NMR spectroscopy (^1H, COSY, HSQC, HMBC). NMR-experiments showed a chemical shift of functionally significant protons at the 4'-position (from 2.52 ppm in **IV** to 3.45 ppm in **V**).

The next step was a reaction between the carboxyl group of compound **V** with α-amino groups of peptide methyl esters H-Gly-Pro-OMe and H-Gly-Gly-Pro-OMe, resulting in compounds **VI** and **VII**. Compound **VI** was purified by column silicagel chromatography in chloroform - methanol (6:1): the yield was 32%. ÒLC: R_f (chloroform – ethanol – acetic acid, 85:10:2) = 0.75. HPLC: τ = 6.7 min (20-80 % B for 30 min; À: 0.05% TFA, B: 0.05% TFA in CH_3CN). MALDI MS: m/z calcd. for $C_{55}H_{85}N_3O_{21}$ 1124.16; found 1124.50. Compound **VII** was purified by column silicagel chromatography in chloroform - methanol (6:1): the yield was 30%. ÒLC: R_f (chloroform – ethanol – acetic acid, 85:10:2) = 0.80. HPLC: τ = 6.5 min (20-80 % B for 30 min; À: 0.05% TFA, B: 0.05% TFA in CH_3CN). MALDI MS: m/z calcd. for $C_{57}H_{88}N_4O_{22}$ 1181.22; found 1181.70.

Conclusions

Synthesis of the new type of peptide - macrolide conjugates in which peptide binds by its α-amino function through a carboxyl containing spacer to the 4'-hydroxyl group of the mycaminose residue of Des was elaborated. Two new desmycosin analogs containing proline peptide moieties at the 4'-position were obtained.

Acknowledgements

This work was supported by the Russian Foundation for Basic Research (grant RFBR 07-04-0092).00000

References

1. Hansen JL, Ippolito JA, Ban N, Nissen P, Moore PB, Steitz TA. *Moll Cell* **10**: 117-128, 2002.
2. Streitz T. *FEBS Lett* **579**: 955-958, 2005.
3. Yonath A. *Annu Rev Biochem* **74**: 649-679, 2005.
4. Sumbatyan NV, Korshunova GA, Bogdanov AA. *Biochemistry (Moscow)* **68**: 1156-1158, 2003.
5. Korshunova G, Sumbatyan N, Fedorova V, Kuznetsova I, Shishkina A, Bogdanov A. *Russian J Bioorg Chem* **33**: 218-226, 2007.
6. Mankin A. *TRENDS in Biochem Sci* **31**: 11-13, 2006.
7. Kirst HA, Debono M, Toth JE, Truedell B, Willard KE. *J Antibiotic* **39**: 1108-1122, 1986.
8. Marshall A, Chobanian H. *Org Syntheses* **82**: 43-50, 2005.

2-05-001

Non Peptide Mimetics: A New Generation of Drugs

Matsoukas, John M[1,]; Agelis, George[1]; Androutsou, Maria-Eleni[1]; Kalavrizioti, Dimitra[2]; Kelaidonis, Konstantinos[1]; Keppa, Pasxalina[1]; Magoulas, George[1]; Matsoukas, Minos-Timotheos[1]; Resvani, Amalia[1]*

[1]University of Patras, Department of Chemistry, GREECE; [2]University of Patras, Department of Medicine, GREECE

**E-mail: imats@chemistry.upatras.gr*

Introduction

The discovery of Losartan, a non peptide Angiotensin II Receptor antagonist and our Ring Cluster Angiotensin II Receptor Conformation, were announced in 1989 during the Gordon Research Conference on Angiotensin and the Renin – Angiotensin – System (RAS).[1] The drug was discovered in the Laboratories of Dupont and the announcement at the Conference was the approval for Clinical trials which led to the first Angiotensin II nonpeptide Receptor antagonist followed by another eight Sartans, now in medical use. Previous Angiotensin II peptide antagonists such as Sarilesin and Saralasin failed to become drugs due to its peptide nature rendering them susceptible to proteolytic enzymes which hydrolyze them. The announcement was the result of many years work on Angiotensin and the RAS System, since it was discovered 80 years ago[1]. Breakthroughs in this evolution was the discovery of Captopril by Miguel Ondetti in 1975 and Losartan by Timmermans in 1989.[2]

In this article the main steps followed in our laboratories in Patras, which led to the Discovery of our Elsartans (Patent Pending) are presented. Briefly the main steps are: 1. Peptide (The Tool), 2. Peptide Model (The Ligand – Receptor Interaction), 3. Cyclic Peptide (The Drug Lead), 4. Non Peptide Mimetic (The Drug). Also, the strategic steps are described, in the design and synthesis in our Laboratories of peptide and non peptide mimetics for important Peptides and Proteins such as Myelin Epitopes (MBP, PLP, MOG) implicated in Multiple Sclerosis,[3] Thrombin Receptor Activating Peptides (TRAP) implicated in Angiogenesis and Cancer[4] and Gonadotropin Releasing Hormone (GnRH) implicated in Fertility and Cancer.[5]

Results and Discussion

Peptide Mimetics for Angiotensin II, Myelin Epitope Peptides, Thrombin Receptor Activating Peptides and Gonadotropin Releasing Hormone have been designed and synthesized as a result of SAR, NMR and Modeling studies. A peptidomimetic is a compound that mimics or blocks the biological effects of a peptide or a protein motif, with the potential to act as a drug molecule. Whatever is the nature of its chemical structure, a peptide mimetic is a synthetic compound which aims to serve as a therapeutic agent for pathological conditions. The pharmacological access of these molecules can be correlated with the extent of their mimicry of the peptides that cause the pathological damage. Strategies and examples are described for designing peptide mimetics. A rational design has been set out, which aids in the synthesis and the development of peptide mimics. This involves the following steps (Fig. 1):

1. Identification of the minimal peptide amino acid sequence responsible for activity. This amino acid will determine the lead compound.

2. Development of the possible bioactive conformation of the minimal peptide sequence which mimics the parent peptide or protein using a combination of NMR Spectroscopy and Molecular Modeling.

3. Design and Synthesis of cyclic peptide analogues, which retain or suppress activity of the parent peptide. Cyclic analogues are more stable in proteolytic enzymes (Fig. 2).

4. Design and Synthesis of peptide and non peptide molecules, which retain critical pharmacophoric groups of the peptide, for medical applications (Fig. 3).

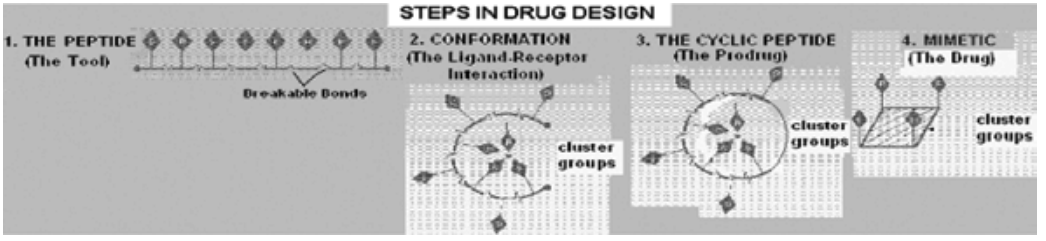

Figure 1. Strategic Steps in Drug Design.

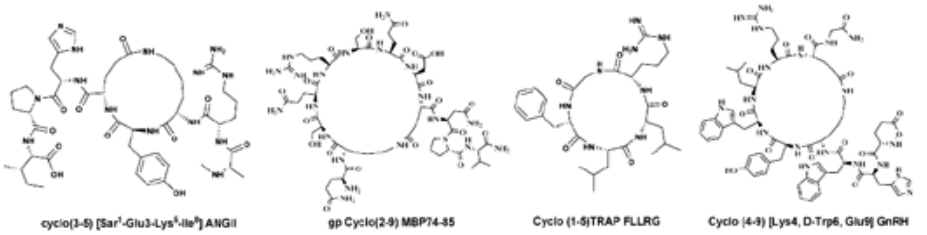

Figure 2. Active cyclic analogues for Angiotensin II, gpMBP 74-85, $S_{42}FFLR_{46}$ (TRAP) and GnRH.

Figure 3. From Angiotensin to Takeda lead drug and to Losartan.

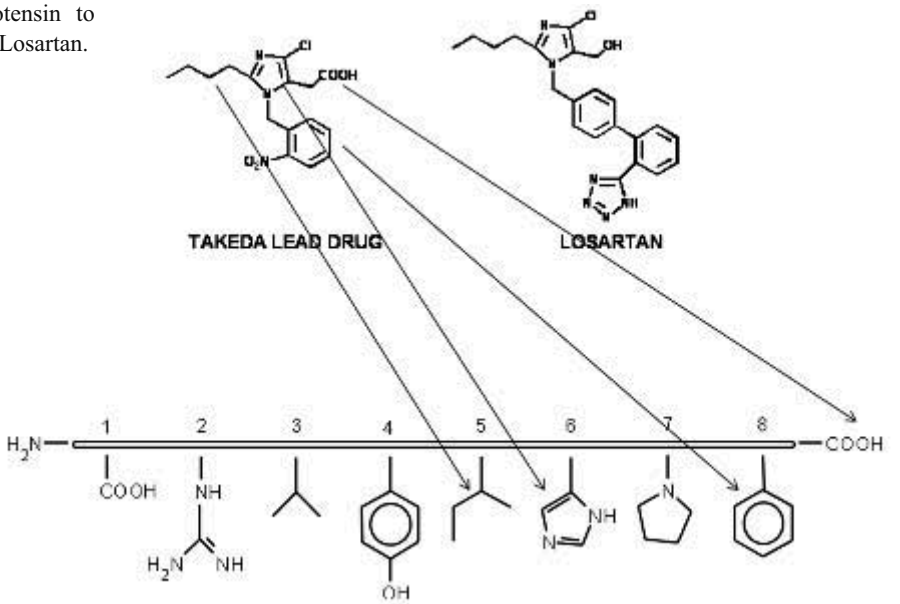

Example of design and synthesis of a peptide mimetic from a peptide is Losartan, which was the first Sartan in the market. The identification of pharmacophoric groups of Angiotensin II (Tyr, His, Phe, COO^-) in combination with Modeling Studies and Fermandjian¢s Model led to the first weak ANG II antagonist, Takeda¢s lead drug and then to Losartan.

Acknowledgements

Present work was supported by the Ministry of Development, General Secretariat for Research and Technology (Grants PRAXE A and B, EPAN), ELDRUG S.A. and Medicinal Chemistry Post Graduate Program.

References

1. Matsoukas JM, Hondrelis J, Keramida M, Mavromoustakos T, Makriyannis A, Yamdagni R, Wu Q, Moore GJ. *J Biol Chem* **269**: 5303-5311, 1994.
2. Wexler RR, Greenlee WJ, Irvin JD, Goldberg MR, Prendergast K, Smith RD, Timmermanns PBMWM. *J Med Chem* **39**: 625-656, 1996.
3. Katsara M, Deraos G, Tselios T, Matsoukas JM, Apostolopoulos V. *J Med Chem* **51**: 3971-3978, 2008.
4. Meyer JD, Manning MC, Vander Velde DG. *J Pept Res* **60**: 159-168, 2002.
5. Keramida M, Tselios T, Mantzourani E, Papazisis K, Mavroumoustakos T, Claussen C, Agelis G, Deraos S, Habibi H, Matsoukas JM *J Med Chem* **49**: 105-110, 2006.

2-05-002

Chemotactic Drug Targeting (CDT)
Synthesis and in vitro application of chemotactic drug delivery systems

Bai, Katalin Boglárka[1,]; Láng, Orsolya[2]; Szabó, Ildikó[1]; Köhidai, László[2]; Hudecz, Ferenc[3]; Mező, Gábor[1]*

[1]Eötvös L University, Research Group of Peptide Chemistry, Hungarian Aca, HUNGARY; [2]Semmelweis University, Department of Genetics, Cell- and Immunobiology, HUNGARY; [3]Eötvös L. University, HUNGARY

[*]E-mail: katalin.b.bai@gmail.com

Introduction

In the field of targeted drug delivery, numerous bioconjugates have been developed to enhance the efficiency and specificity of novel antitumor therapeutics. These kind of drug delivery systems (DDSs) usually consist of a carrier, a drug and targeting moieties.During the past decade, several carrier systems have been envolved depend on the target organ. Forasmuch the receptor mediated endocytosis may provide the appropriate pathway for cellular uptake, targeting moieties have amended the structure of DDSs. Our aim was to develop targetable oligopeptide-based chemotactic drug delivery systems (CDDS) for the treatment of cancer. These CDDSs consist of a peptide carrier molecule (Tp20), targeting sequences with chemotactic properties (TKPR, For-TKPR, TKPPR, For-TKPPR), enzyme-labile spacer sequences (GFLGC) and drug molecules (Dau) in Fig. 1. Tp20 was used as carrier molecule which is a tetramer of a tuftsin analogue (TKPPR). This tuftsin analogue remains the advantageous properties of the original molecule (TKPR) and beside these, it can bind to the tuftsin receptor (neuopilin 1) with more than 4 times higher binding activity than tuftsin. The chemotactic targeting sequences were also tuftsin and tuftsin derivatives. Daunomycin (Dau) a member of the anthracycline family was incorporated as anticancer drug. Dau is commonly used to treat specific types of leukemia (acute myeloid and acute lymphocytic leukemia). However, Dau could cause severe toxicity, the most frequent side effects include cardiotoxicity, nephrotoxicity, and bone marrow resulting in immunsupression. Dau was coupled to the carrier *via* Cathepsin B-cleavable spacer sequence (GFLG). This linker is frequently used in drug conjugates and could be cleaved in the lysosomes.

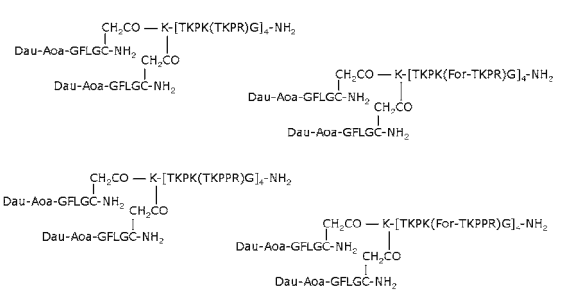

Figure 1. Structure of the Dau-containing conjugates.

Results and Discussion

Carriers with tuftsin-like targeting moieties in branches (Fig. 1.) were synthesized by SPPS using mixed Boc and Fmoc strategies. Tp20 carrier was built up on MBHA resin using standard Boc chemistry. After the synthesis of the carrier backbone, a Boc-Lys(Boc)-OH was attached to the *N*-terminus. The Fmoc groups were removed and the targeting sequences were built up on Lys side chains using Fmoc\Bzl strategy.[1] After completion of the synthesis of the chemotactic branches, the Boc-groups from *N*-terminal Lys were removed and chloroacetylation was performed. The chloroacetylated peptides were removed from the resin with liquid HF in the presence of appropriate scavengers. The GFLGC spacer peptide was synthesised on Rink Amide MBHA resin using Fmoc chemistry. After the synthesis a Boc-Aoa was coupled to the *N*-terminus. The peptide was cleaved from the resin with TFA in the presence of scavengers. Dau was coupled to the spacer in solution forming oxime bond. The chloroacetylated peptides were dissolved in 0.1M Tris buffer (pH 8.2) and Dau-Aoa-GFLGC-NH_2 was added to the solution in solid form at RT. The conjugation reaction was monitored by analytical HPLC. The crude products were purified by RP-HPLC and the pure compounds were characterized by analytical HPLC and ESI-MS. Four conjugates were prepared: (Dau-Aoa-GFLGC{CH_2CO}-NH_2)-K(Dau-Aoa-GFLGC{CH_2CO}-NH_2)-[TKPK(X)G]$_4$-NH_2, where X=chemotactic peptides: TKPR, For-TKPR, TKPPR, For-TKPPR. *In vitro* biological assays (chemotaxis, cellular uptake and MTT-assay) were investigated with the conjugates and their components on MonoMac6 human tumor cell line. The drug-oligopeptide conjugates as well as the corresponding branched oligopeptides were tested in chemotaxis assay on MonoMac6 cells. In case of TKPR branches, the branched peptide had chemoattractant effect at the lowest concentration (10^{-10} M), and it was slightly repellent at the higher concentration range. When Dau-Aoa-spacer was coupled to the peptide, significant chemoattractant behavior appeared at the whole concentration range. In this case the coupling of the Dao-Aoa-spacer considerably amended the biological properties of the branched peptide. In case of the formylated branches, the branched peptide had chemoattractant effect at the whole concentration range except at 10^{-8} M where it was repellent. The conjugation with Dau-Aoa-spacer

decreased the effect of the molecule, it had a slight chemoattractant effect at the lower concentration range. In case of TKPPR branches, the acetylated branched peptide showed a bi-phasic effect, it could trigger chemorepellent effect at the higher concentration range, but it exhibited significant attractant chemotactic activity at the lower concentration range. The coupling of the Dau-Aoa-GFLGC-NH_2 to the branched peptide resulted increased effects. When For-TKPPR branched peptide was studied, significant attractant behaviour was detected at 10^{-6} and 10^{-9} M, which effect was retained and increased the conjugation with Dau-Aoa-spacer. Cellular uptake of the conjugates was studied. The mean fluorescence intensity of cells was quantitated by flow cytometry. We observed concentration-dependent accumulation of fluorescence signal within the cells indicating rapid internalization of each conjugate. A high level of internalization of the conjugates with For-TKPR branches was observed, while the internalization of the other conjugates was less pronounced. MTT-assay was also carried out using the conjugates and the free daunomycin to determine the IC_{50} values. The For-TKPR and TKPPR branched conjugates were more effective molecules than the free drug but the other two conjugates were also efficient. (Table 1).

In conclusion, most of the conjugates had advatageous chemotactic properties, they can be internalized rapidly and could trigger toxic effect on the cells, so thus our results suggest that these novel oligopeptide-based chemotactic drug delivery systems might be potential candidate for targeted cancer chemotherapy.

Acknowledgements

This work was supported by grants from the Hungarian National Science Fund (OTKA T 049814), ETT 202/2006 and GVOP-3.2.1.-2004-04-0005/3.0 and GV.

References

1. Mező G, Láng O, Jakab A, Bai KB, Szabó I, Schlosser G, Láng J, Kõhidai L, Hudecz F. *J Pept Sci* **12**: 328-336, 2006.

Table 1. IC_{50} values of the prepared conjugates compared with daunomycin

	Dau	***TKPR***	***For-TKPR***	***TKPPR***	***For-TKPPR***
IC_{50}(μM)	2.5	2.8	1.0	1.9	8.5

2-05-003

Solid-Phase synthesis of pyrrolo[3,2-*e*][1,4]diazepin-2-ones peptide turn mimics

Deaudelin, Philippe; Lubell, William D[1,*]

Université de Montréal, CANADA

[*]*E-mail: william.lubell@umontreal.ca*

Known as «privileged structures» for their capacity to bind to multiple receptor types with high affinity, the 1,4-benzodiazepin-2-ones[1] have served as oxytocin antagonists,[2] blockers of protein-DNA interactions[3] and enzyme inhibitors.[4] The less common pyrrolodiazepinones have exhibited interesting biological activities, such as inhibition of HIV-1 reverse transcriptase,[5] as well as antitumor and antibiotic activities (**3**).[6] Because of the spectrum of applications of aryldiazepinone derivatives as well as their potential to mimic the gamma-turn conformation (**2**),[7] we have developed a solid-phase method for the synthesis of pyrrolo[3,2-*e*][1,4]diazepin-2-ones **1**.

Our approach was developed based on the recently described diastereoselective Pictet-Spengler approach for the synthesis of 1,3,5-tri- and 1,3,4,5-tetrasubstituted pyrrolo[3,2-*e*][1,4]diazepin-2-ones in solution.[7] 4-Oxoproline resin **6** was prepared from Wang resin (1.3 mmol/g) by way of the corresponding bromide as previously described for the solid-supported synthesis of 4-aminopyrrole-2-carboxylates.[8] Wang bromide resin was treated with *N*-(PhF)-4-hydroxyproline cesium salt. The alcohol was oxidized by treating 4-hydroxyproline resin with oxalyl chloride, dimethylsufoxide and triethylamine in DCM to give 4-oxoproline resin **6**. Ketone **6** was treated with *N*-benzylamine and a catalytic amount of *p*-toluenesulfonic acid in THF at 50 °C to give 4-benzylaminopyrrole resin **7**. 9-Phenylfluorene (PhFH) that departed in the pyrrole formation was used to calculate the loading of resin **7** (1.0 mmol/g). Amine acylation was performed using Fmoc(Boc)LysCl, which was generated *in-situ* with triphosgene and 2,4,6-collidine in THF, to give the aminoacylaminopyrrole resin **8**. The Fmoc cleavage was achieved by treating protected amine **8** with a 20% (v/v) piperidine/DMF solution to give the corresponding amine resin **9**. In the key Pictet-Spengler reaction, resin **9** was placed in a sealed tube and treated with benzaldehyde in a 0.1 M TFA/toluene solution containing sodium sulphate and the mixture was heated to 70 °C. This one-pot procedure caused cyclization, Boc deprotection and resin cleavage to afford diazepinone **10** which was purified by chromatography on silica gel and isolated as a pure diastereoisomer in 41 % overall yield. The *cis* relative stereochemistry of **10** was assigned based on results obtained in solution.[7]

The solid-supported synthesis of pyrrolodiazepinone **10**, proof-of-concept has been accomplished. Work is now in progress to develop this methodology for making diazepinone libraries by employing different amines, amino acids and aldehydes in the synthetic sequence.

Acknowledgments

This work was funded by the Natural Sciences and Engineering Research Coucil of Canada (NSERC), the Fonds Québecois de la Recherche sur la Nature et les Technologies (FQRNT) and the Canadian Institute of Health Research (CIHR).

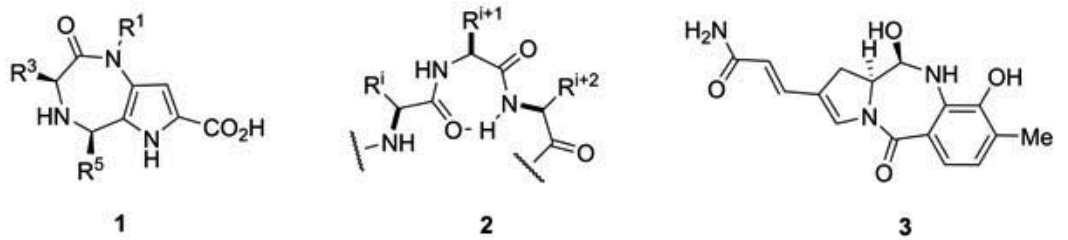

1 **2** **3**

Figure 1. Representative diazepinones and gamma-turn structures.

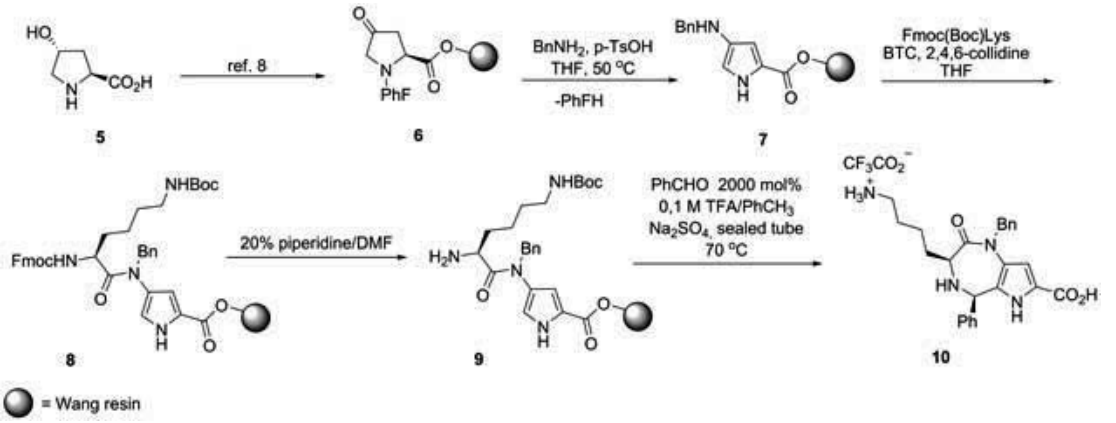

Figure 2. Synthesis of pyrrolo[3,2-*e*][1,4]diazepin-2-one **10**.

References

1. Horton DA, Bourne GT, Smythe ML. *Chem Rev* **103**: 893-930, 2003.
2. Wyatt PG, Allen MJ, Chilcott J, Hickin G, Miller ND, Woolard PM. *Bioorg Med Chem Lett* **11**: 1301-1305, 2001.
3. Stevens SY, Bunin BA, Plunkett MJ, Swanson PC, Ellman JA, Glick GD. *J Am Chem Soc* **118**: 10650-10651, 1996.
4. Micale N, Vairagoundar R, Yakovlev AG, Kozikowski AP. *J Med Chem* **47**: 6455-6458, 2004.
5. De Lucca GV, Otto MJ. *Bioorg Med Chem Lett* **2**: 1639-1644, 1992.
6. Kaneko T, Wong H, Doyle TW, Rose WC, Bradner WT. *J Med Chem* **28**: 388-392, 1985.
7. Deaudelin P, Lubell WD. *Org Lett* **10***:* 2841-2844, 2008.
8. Brouillette Y, Rombouts F Jr, Lubell WD. *J Comb Chem* **8**: 117-126, 2006.

2-07-004

Synthesis of a Series of Cyclic i-to-i+4 Side Chain-to-Side Chain 1,4-Disubstituted [1,2,3] triazolyl-Bridged PTHrP(11-19) Derivatives

Le Chevalier Isaad[*]*, Alexandra*[1]*; Scrima, Mario*[2]*; Cantel, Sonia*[3]*; Levy, Jay*[4]*; Rovero, Paolo*[5]*; D'Ursi, Anna Maria*[2]*; Chorev, Michael*[6]*; Papini, Anna Maria*[1]

[1]*University of Firenze, PeptLab, Department of Organic Chemistry, ITALY;* [2]*University of Salerno, Department of Pharmaceutical Sciences, ITALY;* [3]*University of Montpellier, Max Mousseron Institute of Biomolecules, FRANCE;* [4]*University of Indiana, Department of Chemistry, UNITED STATES;* [5]*University of Firenze, PeptLab, Department of Pharmaceutical Sciences, ITALY;* [6]*Harvard Medical School, Laboratory for Translational Research, Department of Medicine, Brigham and Women's Hospit, UNITED STATES*

[*]*E-mail: alexandra.isaad@gmail.com*

Introduction

Side chain-to-side chain cyclization is used to stabilize a bioactive conformation and to reduce proteolytic degradation. Among the numerous modes of cyclization, bioisosteric modifications and cyclizations that do not require orthogonal protection schemes, are of great interest. The recently introduced Cu(I)-catalyzed azide–alkyne 1,3-dipolar Huisgen's cycloaddition[1] as also known as copper-catalyzed azide–alkyne click chemistry reaction[2] presents a promising opportunity to develop a new paradigm for intramolecular cyclization.[3] The peptidomimetic nature of the 1,4-disubstituted [1,2,3] triazolyl entity suggests it could replace successfully the classical lactam-type side chain-to-side chain bridge providing similar structural constraints and enhanced proteolytic resistance. In fact the incorporation of the 1,4-disubstituted [1,2,3]triazolyl moiety as an isosteric peptide bond surrogate in some pseudopeptides demonstrated that it could supports a variety of secondary structural elements such as *α*-helical coiled-coils, a *β*-turn mimetic, and an extended *β*-sheet-like hollow tubular assemblies, that increase the biological activity.[4] We report the design and synthesis of these novel class of constraint cyclic peptides as compared with the corresponding model peptide lactam.

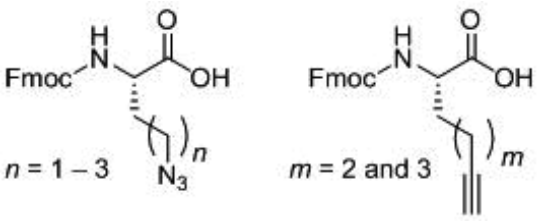

Figure 1. N$^{\alpha}$-Fmoc-ω-azido and Nα-Fmoc-ω-alkynyl-α-amino acids as building blocks for Fmoc/t-Bu solid phase peptide synthesis.

Results

The preparation of N^{α}-Fmoc-*ω*-azido-*α*-amino acids was afforded by either diazo-transfer of the N^{α}-protected *ω*-amino-*α*-amino acid or a multistep strategy from the N^{α}-protected *ω*-hydroxy-*α*-amino acid. The N^{α}-Fmoc-*ω*-ynyl-*α*-amino acids were prepared by alkylation of Ni(II) complexes of the Schiff bases derived from glycine and a chiral inducer with alk-ω-yne bromides. In general, these alkylations occure with conservation of configuration at the C$^{\alpha}$, the Si-face of the glycine enolate being largely favoured. Therefore, we have postulated the retention of the (S)-configuration in the newly synthesized amino acids.[5] These building blocks (Fig. 1) were used in solid phase synthesis of linear peptides to replace Lys13 and Asp17 by *ω*-azido- and *ω*-ynyl-*α*-amino acid residues, generating the linear peptide precursors I'-VIII' that are derived from the putative helical sequence of human parathyroid hormone related protein, Ac-PTHrP(11-19) NH_2. The series of i-to-i+4 side chain-to-side chain [1,2,3]-triazolyl containing cyclo-nonapeptides (I-VIII) was generated by cleavage from the resin and side chain deprotection, followed by solution phase intramolecular Cu(I)-catalyzed azide–alkyne 1,3-dipolar Huisgen's cycloaddition generating cyclopeptides in which side chains in positions i and i+4 were bridged by either 1,4- or 4,1-disubstituted-[1,2,3]triazolyl moieties (I, III, V and VII, and II, IV, VI and VIII, respectively). The [1,2,3] triazolyl ring is flanked by alkyl chains (CH2)m and (CH2)n (where m≠n, n and m=1-4 and m+n=4, 5, 6, and 7) on residues i and i+4, respectively (Tab.1) (manuscript in preparation).

Discussion

The availability of these series of i-to-i+4 side chain-to-side chain cyclopeptides will enable thorough conformational analysis to gain insight on the impact of the ring size, orientation and position of the [1,2,3] triazolyl moiety within the bridging structure on the conformational preference of these cyclopeptides, This will allow us to identify the permutations that best mimic

at the helical nature of the parent cyclo[Lys13,Asp14] PTH(11-19) lactam analogue. Moreover, these studies will offer guidelines for the use of this new class of intramolecular side chain-to-side chain cyclization in the rational design of conformationally stabilized helical peptides crucial for the development of novel biomaterial and peptide-based drugs.

Acknowledgements

We thank the travel grant EPS, the FIRB Internationalisation 2005 RBIN04TWKN and also Fondazione Ente Cassa di Risparmio di Firenze (Italy) for financially supporting the PeptLab of the University of Florence.

References

1. Huisgen R. in *1,3-Dipolar Cycloaddition Chemistry*, Wiley, New York, 1984, pp 1-176; Rostovtsev VV, Green LG, Fokin VV, Sharpless KB. *Angew Chem Int Ed Engl* **41**: 2596-2599, 2002; Tornøe CW, Christensen C, Meldal M. *J Org Chem* **67**: 3057-3064, 2002.
2. Kolb HC, Finn MG, Sharpless KB. *Angew Chem Int Ed Engl* **40**: 2004-2221, 2001.
3. Cantel S, Isaad Ale C, Scrima M, Levy JJ, DiMarchi RD, Rovero P, Halperin JA, D'Ursi AM, Papini AM, Chorev M. *J Org Chem* **73**: 5663-5674, 2008.
4. Horne WS, Yadav MK, Stout CD, Ghadiri MR. *J Am Chem Soc* **126**: 15366–15367, 2004; Angell Y, Burgess K. *J Org Chem* **70**: 9595–9598, 2005; Horne WS, Stout CD, Ghadiri MR. *J Am Chem Soc* **125**: 9372–9376, 2003.
5. Le Chevalier Isaad A, Papini AM, Chorev M, Rovero P. *Eur J Org Chem* **31**: 5308–5314, 2008.

Table 1. Series of linear precursors (I'-VIII') and 1,4-disubstituted [1,2,3]triazolyl bridge- containing cyclopeptides (I-VIII)

Linear Precursors		1,4-disubstituted-[1,2,3]Triazolyl-Containing Cyclononapeptides	
I'	N^{α}-Ac-Lys-Gly-Nva(δ-N_3)-Ser-Ile-Gln-Pra-Leu-Arg-NH_2	I	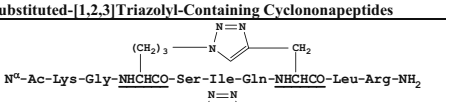
II'	N^{α}-Ac-Lys-Gly-Pra-Ser-Ile-Gln-Nva(δ-N_3)-Leu-Arg-NH_2	II	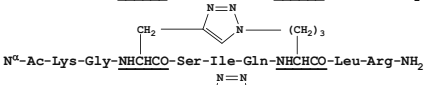
III'	N^{α}-Ac-Lys-Gly-Nle(ε-N_3)-Ser-Ile-Gln-Pra-Leu-Arg-NH_2	III	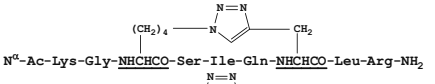
IV'	N^{α}-Ac-Lys-Gly-Pra-Ser-Ile-Gln-Nle(ε-N_3)-Leu-Arg-NH_2	IV	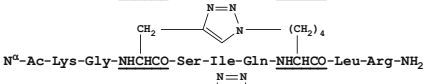
V'	N^{α}-Ac-Lys-Gly-hAla(γ-N_3)-Ser-Ile-Gln-Nle(δ-yl)-Leu-Arg-NH_2	V	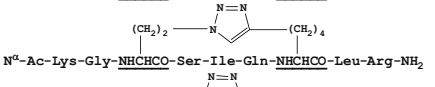
VI'	N^{α}-Ac-Lys-Gly-Nle(δ-yl)-Ser-Ile-Gln-hAla(γ-N_3)-Leu-Arg-NH_2	VI	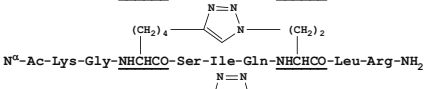
VII'	N^{α}-Ac-Lys-Gly-Nva(δ-N_3)-Ser-Ile-Gln-Nle(δ-yl)-Leu-Arg-NH_2	VII	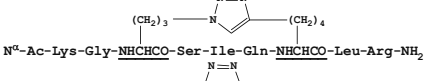
VIII'	N^{α}-Ac-Lys-Gly-Nle(δ-yl)-Ser-Ile-Gln-Nva(δ-N_3)-Leu-Arg-NH_2	VIII	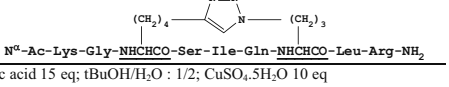

Reaction Conditions For Cyclization: HPLC purified linear peptide 1 eq; ascorbic acid 15 eq; $tBuOH/H_2O$: 1/2; $CuSO_4.5H_2O$ 10 eq

2-07-005

Modulating Biology with Cryptic Cell Penetrating Peptides

Howl, John; Jones, Sarah*

University of Wolverhampton, Molecular Pharmacology Group, RIHS, UNITED KINGDOM

**E-mail: J.Howl@wlv.ac.uk*

Introduction

To date, numerous cell penetrating peptides (CPP) have been developed as highly efficient vectors for the intracellular delivery of chemically diverse bioactive cargoes. The general utility of this strategy requires CPP with both minimal toxicity towards target cells and negligible biological activity. Thus, commonly employed vectors such as penetratin, Tat, transportan, and a variety of other amphipathic and/or polybasic sequences, have proven valuable tools for the intracellular delivery of bioactive cargoes that profoundly influence cellular function. A more general consideration of the multi-domain architecture of many human proteins indicates that similar amphipathic/polybasic sequences may be crucial to both trafficking events and biological function. For example, arginine is commonly located at the site of protein interfaces. Both arginine and lysine are also targets for a range of post-translational modifications that include methylation and acetylation that consequently modulate signal transduction events. Finally, many bioactive peptides such as mastoparan (INLKALAALAKKIL) are also polycationic in nature. Such considerations prompted our current efforts to identify cryptic CPP sequences within human proteins that can both translocate the eukaryotic plasma membrane and also directly influence cellular biology. The starting point for the development of biologically-active cryptic CPP was the QSAR-based prediction algorithm recently described by Ülo Langel's group.[1] This strategy has enabled the study of cryptic CPP in which multiple pharmacophores for cellular penetration and biological activities are discontinuously organised within the primary sequence. We have recently re-introduced the term rhegnylogic to distinguish this class of CPP from the more usual sychnologic tandem combination of CPP and cargo.[2]

Results and Discussion

As indicated in Table 1, we have employed QSAR prediction analyses to identify putative CPP within the primary sequence of proteins that include cytochrome *c* (Cyt *c*) the human type 1a calcitonin receptor (hCTR1a) and endothelial nitric oxide synthase (eNOS).

Cryptic CPP sequences are selectively located within both amino and carboxyl helical domains of cytochrome *c* (Cyt *c*), a signalling protein integral to apoptotic events. Detailed characterisation of these peptides has identified a series of efficient CPP vectors that differentially target intracellular organelles. Of these, Cyt $c^{77\text{-}101}$ (Table 1) is the most efficient translocating sequence and also possesses moderate apoptogenic potency when exogenously applied to astrocytoma cell lines.[3] These molecular properties mimic the propensity of Cyt *c* to translocate biological membranes as a mediator of both mitochondrial apoptosis and inflammation. Moreover, recent chimeric combination of Cyt *c*-derived CPP and other biologically-active sequences has generated more potent apoptogenic peptides.

Members of the type 2 G protein-coupled receptor family bind peptide ligands that are structurally related to calcitonin. The 20 amino acid sequence, hCTR1a$^{174\text{-}193}$ (Table 1), predicted as a highly probable CPP by QSAR analysis, is located within the first intracellular loop of the hCTR1a. This sequence includes a splice variant 16 AA insert that modulates the G protein coupling specificity of the native receptor. hCTR1a$^{174\text{-}193}$ (1 μM) independently stimulated cAMP formation in ECV304 cells and also augmented calcitonin-induced cAMP synthesis by the direct activation of heterotrimeric G proteins.[2]

Related studies have identified a cryptic CPP within nitric oxide synthase, eNOS$^{492\text{-}507}$, located within a helical domain known to tightly bind calmodulin. Significantly,

Table 1. Examples of cryptic CPP identified by QSAR analyses of native proteins. For experimental purposes, all sequences are synthesized as peptide amides. Cationic residues are illustrated in bold type

SEQUENCE	SOURCE
GT**K**MIFVGI**KKK**EE**R**ADLIAYL**KK**A	Cyt $c^{77\text{-}101}$
RKLTTIFPLNW**KYRK**ALSLG	hCTR1a$^{174\text{-}193}$
RKKTF**K**EVANAV**K**ISA	eNOS$^{492\text{-}507}$

this peptide potently inhibits the proliferation, migration and tube-forming capacity of primary endothelial cells and exhibits potent anti-angiogenic properties *in vivo*.

Conclusions

These data confirm that cryptic CPP can modulate many aspects of cell biology and are, therefore, a valuable new class of bioactive peptide. We have suggested that the term bioportide is a useful descriptor of this class of biologically active CPP.[3]

Acknowledgment

We gratefully acknowledge the collaborative support provided by Ülo Langel and co-workers.

References

1. Hällbrink M, Kilk K, Elmquist A, Lundberg P, Lindgren M, Jiang Y, Pooga M, Soomets U, Langel Ü. *Int J Pept Res Ther* **11**: 249-259, 2005.
2. Jones S, Östlund P, Langel Ü, Zorko M, Nicholl I, Howl J. *Peptides 2006* (*Proceedings of the 29th European Peptide Symposium, Gdańsk, Poland*). Rolka K, Rekowski P, Silberring J (Eds), Kenes International, Geneva, Switzerland, 2007, pp 430-443.
3. Howl J, Jones S. *Int J Pept Res Ther* **14**: 359–366, 2008.

2-17-006

Manipulation and measurement of intracellular calpain activity by new cell penetrating peptide conjugate

Bánóczi, Zoltán[1,]; Farkas, Attila[2]; Alexa, Anita[2]; Tantos, Ágnes[2]; Tompa, Péter[2]; Friedrich, Péter[2]; Hudecz, Ferenc[1]*

[1]Eötvös L. University, Hungarian Academy of Sciences, Research Group of Peptide Chemistry, HUNGARY;
[2]Biological Research Center, Hungarian Academy of Sciences, Institute of Enzymology, HUNGARY

[*]E-mail: banoczi@elte.hu

Introduction

Calpains are intracellular cysteine proteases and are of considerable interest because of their implication in various physiological and pathological events. For studying the functions of calpains there is a need to manipulate the enzyme activtiy and also to detect the changes. The enzymetic activity could be eliminated by inhibitors or the knock-out of the responsible gene(s) or could be increased by overexpression of calpain gene. For detection the activity of intracellular calpain a proper cell-penetrating substrate is needed. Our aims were to prepare new cell-penetrating conjugates with calpain activating capacity based on the calpastatin A and C related peptides[1] and with calpain specific substrate based on our optimised substrate peptide sequence.[2]

Results

The calpastatin A and C related peptides were conjugated to the C-terminal of penetratin via amide, thioether or disulfide bonds (Fig. 1).

The conjugates were prepared either by tandem solid phase peptide synthesis (conjugate with amide bond) or in solution (conjugates with thioether and disulfide bond) using the purified peptide fragments.[3] As we have demonstrated earlier, the calpastatin A and C peptides activate the isolated m-calpain *in vitro*.[4] This effect was the most pronounced when a 1:1 (mol/mol) mixture of both peptides was used for incubation with calpain. Using the same assay,[4] therefore we have performed a comparative study to investigate the effect of conjugation on the enzyme activation effect of calpastatin A plus C peptides. We found that all conjugates regardless on the type of linkage between the two partners activated the isolated m-calpain. We observed also that this effect of the conjugates was significantly higher than that of the free peptides. The internalisation of the conjugates labelled with fluorophores by COS-7 cells and the kinetics of the cellular uptake were studied by fluorescent microscopy and also by FACS analysis as a function of time. In order to study the intracellular calpain-activating potency of conjugate, COS-7 cells were treated with the 1:1 (mol/mol) mixture of penetratin-calpastatin A and C conjugates containing amide bond. The calpain activity was measured after cytolysis of treated/untreated cells. In case of measurements immediately after cytolysis, calpain activity was only noticeable at 10 mM $CaCl_2$ concentration. However, the calpain activity in the cell lysate of cells treated with the conjugate mixture was clearly higher at both low and high $CaCl_2$ concentrations as compared to the untreated control. We observed essentially the same tendency in the case of experiments performed after 30 min of the cytolysis.

A new cell-penetrating calpain substrate (Fig. 2), $TPLKSPPPSPRER_7$, was built up on resin and the DABCYL chromophore was attached to its N-terminal amino group. This peptide was cleaved from the solid support, and after the temporary protection of e-amino group of Lys residue, the EDANS fluorophore was coupled to the carboxy group of Glu residue.[5] We found that the substrate conjugate is a better substrate (k_{cat}= 0.2 s^{-1} and K_M/k_{cat}=5000 M^{-1} s^{-1}) than the free peptide substrate (DABCYL-TPLKSPPPSPR-EDANS) (k_{cat}= 0.17 s^{-1} and K_M/k_{cat}=680 M^{-1} s^{-1}).[2] We observed that in comparison with the free peptide the conjugate internalised into COS-7 cells already at low concentration.

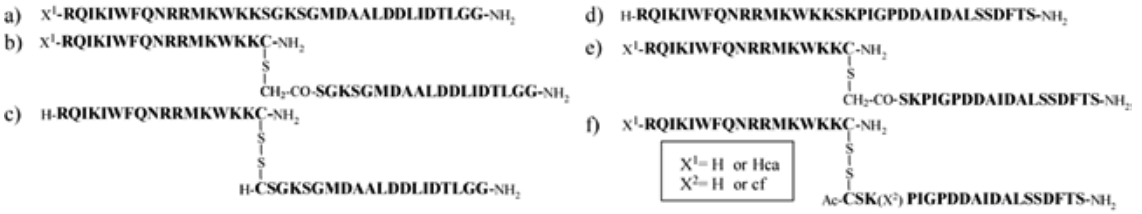

Figure 1. Outline of the structure of the penetratin-calpastatin A (a-c) and penetratin-calpastatin C (d-f) conjugates with or without fluorescent probes. (Hca=4-[7-hydroxycoumaryl] acetic acid, cf=5(6)-carboxyfluorescein).

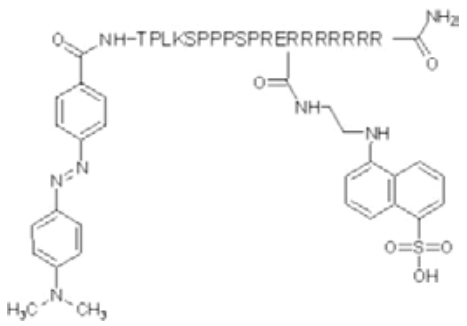

Figure 2. Structure of cell-penetrating calpain substrate.

Considering that the cell-penetrating substrate conjugate seemed to be a good substrate *in vitro* and could translocate into COS-7 cells, we extended our studies to evaluate its applicability for measurements of intracellular calpain activity. First we used the cell-penetrating substrate to determine calpain activity in the lysate of Drosophila melanogaster S2 cells. In order to prove the calpain cleavage of substrate, lysate of cells overexpressing calpain was used. We found that the substrate was readily cleaved in the cell lysate and this could be inhibited by Calpain inhibitor I (N-Acetyl-L-leucyl-L-leucyl-L-norleucinal). The increase of the fluorescence intensity was the largest in presence of Ca^{2+}. We observed the same phenomenon in case of normal cells. Than S2 cells were treated with the solution of cell-penetrating substrate conjugate followed by lyses. The activity of endogenous calpain in the lysate was measured after Ca^{2+} activation. In the absence of Ca^{2+} ion, only the base-line fluorescence intensity was detected. The addition of Ca^{2+} initiated the increase in the fluorescence intensity indicating of the activation of calpain. In the third experiment, the activity of endogenous calpain was measured in living cells. First S2 cells were treated with cell-penetrating substrate; then ionomycin was added to the cells and the fluorescence intensity was monitored. Results show that the fluorescence intensity is decreased due to the sedimentation of cells. After the addition of 10 μM ionomycin, the fluorescence intensity slightly increased, indicating calpain activation and substrate cleavage.

Conclusions

The calpain enzymes are promising target for the treatement of various diseases. New cell-penetrating constructs reported here with calpain activating capacity or with substrate properties may open a new perspective in the studies of calpain function. These compounds as simple tools can be utilised to manipulate or to measure of calpain activity without the application of gene technology even in living cells.

Acknowledgements

These studies were supported by grants from the Hungarian Research Fund (OTKA K 68285, NK-60-723), from the Hungarian Ministry of Education (Medichem2, NFKP 1/A/005/2004), and from GVOP-2.2.1.-2004-04-0005/2.0, GVOP-3.2.1-2004-04-0352/3.0, GVOP-3.2.1-2004-04-0005/3.0.

References

1. Tompa P, Mucsi Z, Orosz G, Friedrich P. Calpastatin subdomains A and C are activators of calpain. *J Biol Chem*. **277**: 9022-9026, 2002.
2. Tompa P, Buzder-Lantos P, Tantos A, Farkas A, Szilágyi A, Bánóczi Z, Hudecz F, Friedrich P. On the sequential determinants of calpain cleavage. *J Biol Chem*. **279**: 20775-20785, 2004.
3. Bánóczi Z, Tantos A, Farkas A, Tompa P, Friedrich P, Hudecz F. Synthesis of cell-penetrating conjugates of calpain activator peptides *Bioconjugate Chem* **18**: 130-137, 2007.
4. Tompa P, Mucsi Z, Orosz Gy, Friedrich, P. Calpastatin subdomains A and C are activators of calpain. *J Biol Chem* **277**: 9022-9026, 2002.
5. Bánóczi Z, Alexa A, Farkas A, Friedrich P, Hudecz F. Novel cell-penetrating calpain substrate. *Bioconjugate Chem* **19**: 1375-1381, 2008.

2-17-007

Modification of the chemical structure of cell-penetrating peptides : impact on cargo delivery

Aussedat, Baptiste[1]; Dupont, Edmond[2]; Sagan, Sandrine[1]; Joliot, Alain[2]; Lavielle, Solange[1]; Chassaing, Gérard[1]; Burlina, Fabienne[1,]*

[1]Université P. et M. Curie, UMR CNRS 7613, FRANCE; [2]ENS, UMR CNRS 8542, FRANCE

[*]E-mail: fabienne.burlina@upmc.fr

Cell-penetrating peptides (CPPs) are receiving a lot of attention because they are able to deliver inside cells bioactive cargoes that are poorly internalized by themselves such as oligonucleotides, peptides and proteins. Previous studies performed on CPPs have led to the identification of several amino acids which promote cellular uptake. These include the cationic residues Lys and Arg and the hydrophobic Trp residue.[1,2] Our aim was to further characterize the functional and structural determinants for cargo delivery. For this, we have synthesized linear and dendrimeric pseudo-peptide carriers bearing ammonium, guanidinium, indol and/or myristyl groups (Fig. 1). Our approach has then been to study the impact of these modifications on the amount of internalized cargo, its intracellular degradation and localization.[3] The cargo which corresponds to a peptide inhibitor of protein kinase C (PKCi = Biotin-GGGGCRFARKGALRQKNV) was linked to the carriers by a disulfide bridge.

The amount of PKCi cargo delivered inside cells was determined using a method based on MALDI-TOF mass spectrometry (Fig. 2).[3] We observed no difference between the delivery efficiency of carriers functionalized by ammoniums or guanidiniums (carriers L1 and L3). In addition, changing the spatial arrangement of the guanidiniums had no impact (carrier D1). Interestingly, it was found that cationic residues can be partially replaced by indols maintaining the same efficiency of

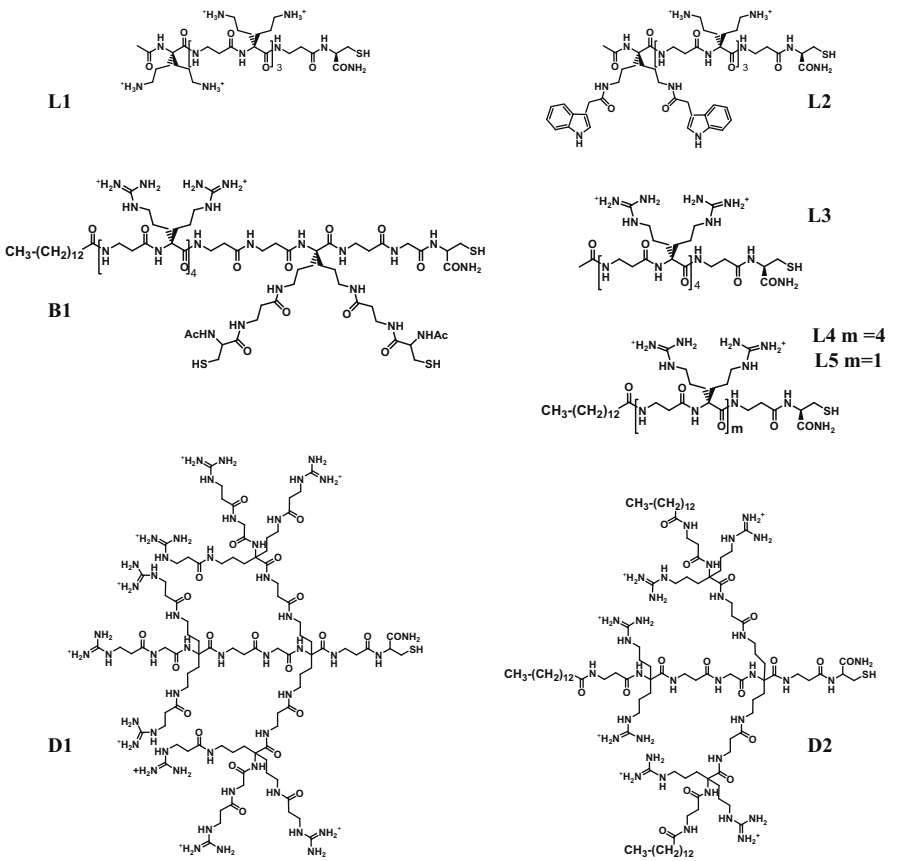

Figure 1. Structure of the pseudo-peptide carriers.

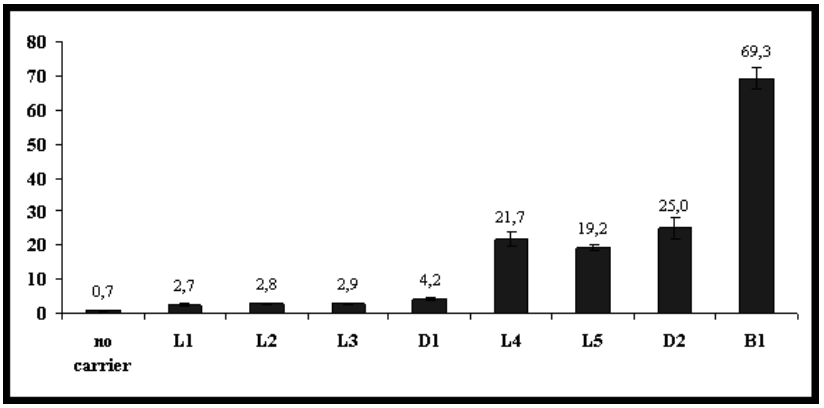

Figure 2. Amount (pmol) of intact PKCi cargo delivered by the different carriers measured by MALDI-TOF mass spectrometry. Carrier-cargo conjugates (7.5 μM) were incubated for 75 min at 37 °C with 1 million CHO cells.

delivery (carriers L1 and L2). A strong improvement was observed upon mono-myristoylation of the carrier (carrier L4) but increasing the number of myristyl groups (D2) had no significant effect. Based on these results, we designed compound B1 by combining the structure of the efficient myristoylated carrier L4 with a branched domain to attach three cargoes. With this functionalization, the intracellular concentration of cargo was tripled (14.5 μM using conjugate L4-PKCi and 46.2 μM using conjugate B1-$(PKCi)_3$) using the same extracellular concentration of conjugate (7.5 μM). This shows that carrier L4 is itself internalized with the same efficiency in both cases despite the structural changes between both conjugates. This study also led to the identification of the efficient minimalist pseudo-peptide carrier L5 which corresponds to a unique myristoylated bis-arginine residue. The profile of degradation of the internalized cargo was analyzed by MALDI-TOF mass spectrometry. The intact cargo was the most abundantly detected species with all carriers. Partial cleavage after basic residues of the cargo was also always observed. In contrast, cleavage after Ala residues was only observed when the cargo was delivered by myristoylated carriers. These data thus revealed differences in the trafficking or distribution of the internalized cargo depending on the nature of the transporters.

Finally, the intracellular localization of the PKCi cargo was examined by confocal microscopy. The biotinylated PKCi cargo was revealed using fluorescent streptavidin. The intracellular distribution of the cargo was found to vary strongly with the carrier used. With all the non-myristoylated pseudo-peptide carriers, a faint fluorescence signal was detected mainly in endosomes but also in the cytosol and sometimes the nucleus. This pattern was close to the one obtained with classical CPPs. Myristoylated carriers gave different cargo localizations. With L4 and L5 the staining was mostly found in perinuclear vesicular structures and visible throughout the cytosol. Carrier B1 led to more intense diffuse cytolic labelling, together with the detection of some nuclear staining. In contrast with carrier D2, the staining was restricted to the vicinity of the plasma membrane.

In conclusion, some of the new carriers were found to be very efficient in particular when myristoylation was combined with the attachment of multiple cargoes on the carrier. This study also gave the evidence that distinctive intracellular localization and degradation profiles of the cargo can be obtained by changing the chemical structure of the carrier. Our aim is now to identify more clearly the intracellular organelles that can be accessed with these carriers.

Acknowledgements

We would like to thank Prof. A. Prochiantz and Dr. G. Bolbach for fruitful discussions. We thank for financial support the ANR (Prob-DOM) and the Fondation pour la Recherche Médicale (fellowship for B.A.).

References

1. Derossi D, Chassaing G, Prochiantz A. Trojan peptides: the penetratin system for intracellular delivery. *Trends Cell Biol* **8**: 84-87, 1998.
2. Wender P A, Mitchell DJ, Pattabiraman K, Pelkey E T, Steinman L, Rothbard JB. The design, synthesis, and evaluation of molecules that enable or enhance cellular uptake: peptoid molecular transporters. *Proc Natl Acad Sci U S A* **97**: 13003-13008, 2000.
3. Aussedat B, Dupont E, Sagan S, Joliot A, Lavielle S, Chassaing G, Burlina F. Modifications in the chemical structure of Trojan carriers: impact on cargo delivery. *Chem Commun* 1398-1400, 2008.

2-19-008

Surface-bound cationic antimicrobial peptides: The effect of immobilization upon the activity spectrum and the mode of action

Bagheri, Mojtaba; Beyermann, Michael; Dathe, Margitta*

The Leibniz-Institute of Molecular Pharmacology, GERMANY

**E-mail: bagheri@fmp-berlin.de*

Introduction

Accumulation of bacteria and their growth on surfaces, particularly biomedical ones, lead to biofilm formation which causes serious threat to human health. Biofilms are extremely resistant to conventional antibiotics.[1] Thus, the development of bactericidal surfaces which inhibit colonization of pathogens is highly important. Surfaces coated with cationic antimicrobial peptides are one opportunity to combat this threat. How (i) the immobilization of antimicrobial peptides at different chain positions, (ii) the length of spacer between the active sequences and the solid surface, and (iii) the density of loaded peptides on the surfaces influence the biocidal activity towards bacteria needs to be investigated.[2]

In this study, we took the advantages of three synthesis resins TentaGel S NH_2, HypoGel 400 NH_2, and HypoGel 200 NH_2 (Rapp Polymere GmbH, Germany) characterised by PEG spacers of different length (molecular mass between 200-6000 Da) and the same distribution of size (diameter 150 µm) to immobilize two highly active α-helical antimicrobial peptides, the model KLAL peptide;[3] KLALKLALKALKAALKLA-NH_2, and magainin 2-derived MK5E;[4] GIGKFIHAVKKWGKTFIGEIAKS-NH_2 at C- and N-terminus and via different side-chain positions. Standard solid phase peptide synthesis (SPPS), thioalkylation,[5] and oxime-forming ligation[6] strategies were used to immobilize the peptides at the C- and N-terminus and side-chain via the ε-amino group of lysine residues. We tested the antimicrobial activities of these resin beads-bound peptides toward Gram-positive *B.subtilis* and Gram-negative *E.coli* bacteria. Furthermore, to evaluate the membrane permeabilizing activity of the immobilized peptide, the interaction of the C-terminally TentaGel S NH_2-bound peptides with large unilamellar vesicles (LUVs) composed of POPC and POPG lipids was studied fluorimetrically by measuring the time dependent decrease in self-quenching of entrapped calcein (excitation at 490 nm, emission at 514 nm).

Results and Discussion

To make the immobilization of both KLAL and MK5E peptides as simple as possible, we coupled the peptides C-terminally by SPPS, and at the N-terminus and side-chains via thioalkylation (for KLAL), and oxime-forming ligation (for MK5E) strategies. The density of immobilized peptides was determined by measuring the absorption of the cleaved Fmoc- chromophore upon exposure of the peptide-loaded resins (which were treated firstly with an excess amount of Fmoc-Cl) by exposure to 20% piperidine in DMF. Depending upon the resin capacity and the coupling strategies, peptide loading between 0.1 and 0.25 µmol/mg for C-terminally and about 0.03 µmol/mg for N-terminally and side-chain immobilized peptides was obtained (Table 1, 2).

Table 1. The antimicrobial activities of KLAL and MK5E peptides immobilized on TentaGel S NH_2 resin towards *B. subtilis* and *E. coli* along with the densities of immobilized peptides. (a) The determination of the amount of immobilized peptides was based on the absorption of the Fmoc-chromophore at 301 nm (ε=6000 M^{-1} cm^{-1}). (b) The MIC of the immobilized peptides was calculated on the basis of the amount of resin causing growth inhibition and the density of the peptides on the resin. MIC = MBC. (c) The numbers give the chain position of immobilization. K stands for the lysine residue. (d) not determined

Peptide	Position of immobilization	Antimicrobial activity				Density of peptide (µmol/mg)[a]
		B. subtilis (DSM 347)		*E. coli* (DH 5α)		
		MIC of resin (mg/ml)	MIC[b] (mM)	MIC of resin (mg/ml)	MIC (mM)	
KLAL	C-terminus	2	0.20	25	2.47	0.099
	N-terminus	5	0.14	25	0.70	0.028
	K 5[c]	5	0.12	25	0.60	0.024
	K 9	2	0.06	25	0.70	0.028
	K 12	5	0.15	25	0.75	0.030
	Random	5	0.15	25	0.77	0.031
MK5E	C-terminus	5	0.67	5	0.67	0.133
	N-terminus	10	0.26	15	0.39	0.026
	K 4	nd[d]	nd	5	0.19	0.039
	K 10	5	0.17	5	0.17	0.033
	K 14	5	0.13	5	0.13	0.025

Table 2. Antimicrobial activities and peptide densities of C-terminally immobilized KLAL and MK5E peptides on HypoGel 400 NH_2, HypoGel 200 NH_2 resins towards *B.subtilis* and *E.coli* bacteria

Peptide	Antimicrobial activity (HypoGel 400 NH_2/HypoGel 200 NH_2)				Density of peptide (μmol/mg)
	B.subtilis (DSM 347)		*E.coli* (DH 5α)		
	MIC of resin (mg/ml)	MIC (mM)	MIC of resin (mg/ml)	MIC (mM)	
KLAL	10/15	1.51/3.71	55/70	8.31/17.29	0.151/0.247
MK5E	10/15	1.80/3.79	15/10	2.70/2.53	0.180/0.253

We observed that tethering conserved the activity spectrum of the soluble peptides towards *E.coli* and *B.subtilis* in the millimolar range (Table 1, 2) compared to micromolar concentrations of the free peptides.[3,4] TentaGel S NH_2-bound peptides were more active towards bacteria than the peptides immobilized at HypoGel resins. This can be explained by the PEG spacer of TentaGel resin which is sufficiently long to span the cell wall of bacteria and to interact with the cytoplasmic target membrane. A comparison of the biocidal activities of HypoGel 200 and 400 NH_2 characterized by comparable spacer lengths but different surface densities of peptides show that an increase in the amount of loaded peptide at the resin is not sufficient to compensate for the spacer length-related activity decrease (Table 2).

In addition, slight differences in the antimicrobial activities of KLAL and MK5E bound at different chain positions on TentaGel S NH_2 were observed (Table 1) suggesting that the activity is less dependent upon the position of immobilization.

Moreover, the TentaGel S NH_2-bound KLAL and MK5E can interact with and permeabilize the lipid bilayers composed of POPC and POPG. The kinetics of the dye release from mixed POPC/POPG LUVs induced by immobilized peptides is presented in Fig. 1. Although different in the degree, each of the resin-tethered peptides induced disruption of the bilayers in a dose-dependent manner. Non-modified TentaGel S NH_2 was not membrane active (data not shown). These results suggest that C-terminal immobilization via a large PEG chain conserved the bilayer permeabilizing ability of the soluble KLAL and MK5E peptides presented before.[3,4]

In conclusion, we found that immobilization of helical antimicrobial peptides conserved the antimicrobial activity spectrum and the membrane permeabilizing mode of action. The length of the spacer and the amount of target-accessible peptide are the most critical parameters for the activity whereas the chain position of immobilization seems to be less crucial for the activity. Finally, surface immobilization might provide a powerful strategy to get information on the mode of peptide action.

References

1. Davies D. *Nat Rev Drug Discov* **2**: 114, 2003.
2. Haynie SL, Crum GA, Doele BA. *Antimicrob. Agents Chemother* **39**: 301-307, 1995.
3. Dathe M, Meyer J, Beyermann M, Maul B, Hoischen C, Bienert M. *Biochim Biophys Acta* **1558**: 171-186, 2002.
4. Dathe M, Nikolenko H, Meyer J, Beyermann M, Bienert M. *FEBS Lett* **501**: 146-150, 2001.
5. Takahashi M, Nokihara K, Mihara H. *Chem Biol* **10**: 53-60, 2003.
6. Kochendoerfer GG. *Curr Opin Chem Biol* **9**: 555-560, 2005.

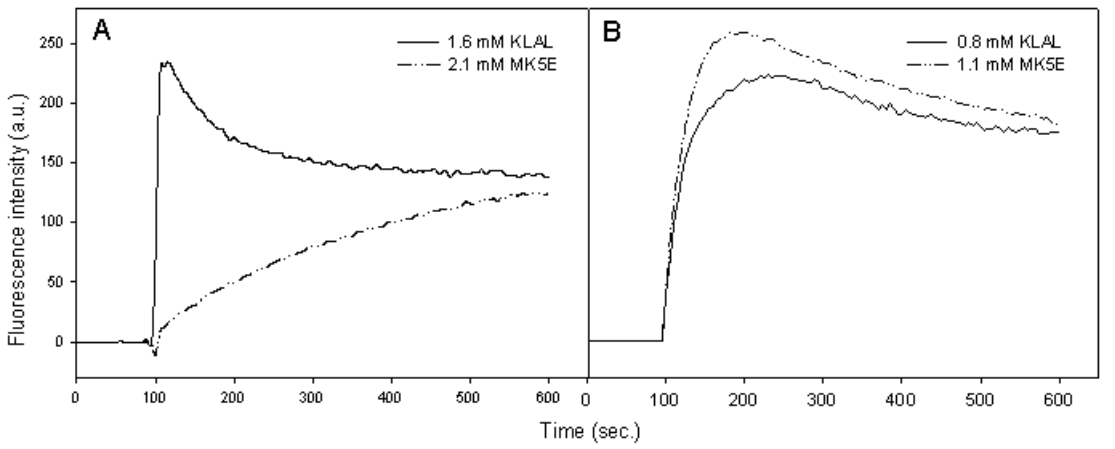

Figure 1. Kinetics of dye release from (A) POPC/POPG (3/1 mol/mol), and (B) POPC/POPG (1/3 mol/mol) LUVs induced by C-terminally TentaGel S NH2-bound model KLAL peptide, and MK5E. The dye release was monitored as increase in the fluorescence intensity at 514 nm. The lipid concentration was 25 μM.

2-19-009

Design and synthesis of cell-penetrating nucleopeptides

Geotti-Bianchini, Piero[1,2,]; Beyrath, Julien[2]; Chaloin, Olivier[2]; Formaggio, Fernando[1]; Bianco, Alberto[2]*

[1]Università di Padova, Dipartimento di Scienze Chimiche, ITALY; [2]UPR 9021 IBMC-CNRS Strasbourg, Laboratoire d'Immunologie et Chimie Thérapeutiques, FRANCE

[*]E-mail: piero.geotti@unipd.it

It is well known that synthetic oligonucleotides cannot be used for *in vivo* applications due to several problems, e.g. their rapid enzymatic hydrolysis and their extreme difficulty to cross cell membranes. In order to overcome these limitations different class of analogues have been designed.

Peptide nucleic acids, proposed by Nielsen in 1991,[1] have gained much attention as oligonucleotide mimics with very good affinity and selectivity. On the other side, such molecules have poor water solubility and do not penetrate efficiently through biological membranes.

We therefore focused our attention on nucleopeptides, a different class of nucleotide analogues containing nucleoamino acids, i.e. amino acids carrying nucleobases at their side chains. In nucleopeptides, backbone conformation controls the relative orientation and distance of the nucleobase side chains, thus modifying the nucleobase ability to interact with complementary sequences.[2]

Our workproject aimed at investigating the effects of backbone structuration in sequential nucleopeptides on peptide-peptide and peptide-oligonucleotide base pairing properties. For this purpose, we designed a library of sequential nucleopeptides with a polyalanine backbone in which nucleoamino acids are placed every third residue and two lysine residues are set at the N- and C- terminus in order to increase water solubility and allow for peptide further functionalization at the N-terminal ε-amino group. Each member of the library carries four times one of the DNA nucleobases (thymine, adenine, cytosine, guanine) and can be either underivatized, or biotinylated, or fluorescently labelled with fluorescein isothiocyanate (FITC) (Fig. 1).

N^{α}-Boc-protected β-alanyl nucleoamino acids carrying the four DNA bases have been synthesized in solution by alkylation of the protected nucleobases with the lactone of the Boc-protected serine at low temperature in the presence of a strong, non nucleophilic base.[3]

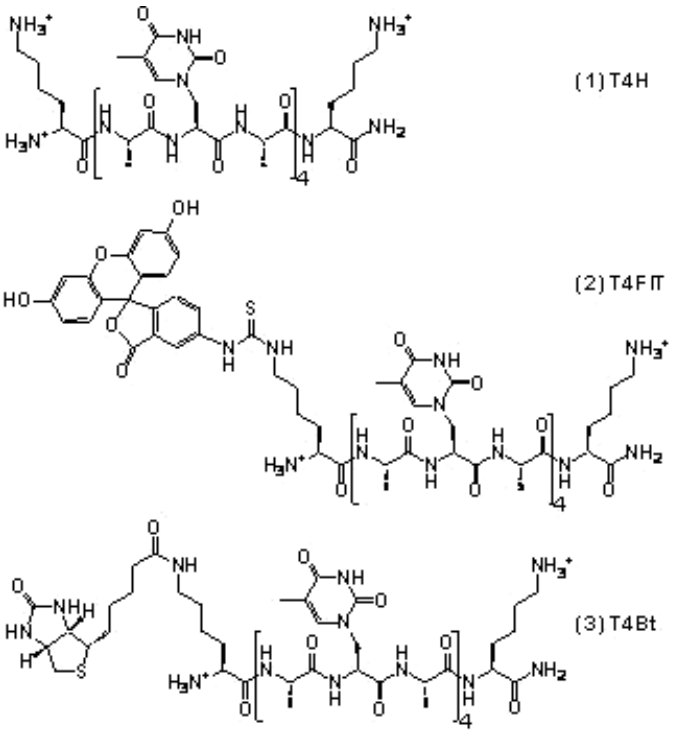

Figure 1. Molecular structures of the thymine based nucleopeptides: (1) T4H, underivatized peptide; (2) T4FIT, peptide derivatized with FITC; (3) T4Bt, biotinylated peptide.

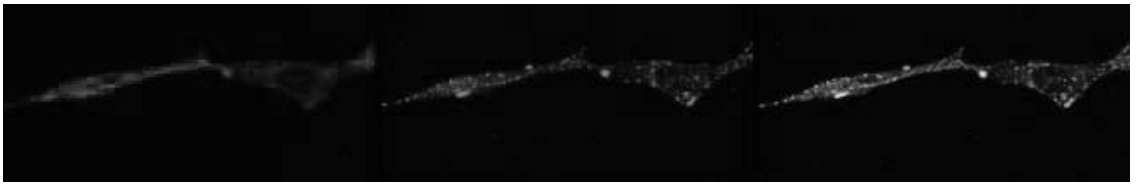

Figure 2. Confocal images of Renca cells incubated with 50 μM T4FIT for 12 h. Left: membrane and cytosol staining with FM4-64; middle: peptide fluorescence; right: merge.

Subsequently, the nucleopeptides have been synthesized on solid-phase following the Boc/Bzl strategy on a MBHA resin (30 μmol scale). After completion of the peptide sequence resin beads were split in three parts: one was not further derivatized, one was biotinylated, one was allowed to react with FITC. Nucleopeptides were cleaved with TFA/TMSOTf/*p*-cresol overnight, precipitated from cold Et_2O, purified by RP-HPLC and characterized by MALDI-MS.

The nucleopeptide pairing properties have been investigated through surface plasmon resonance. Streptavidin was immobilized on a gold chip and it complexed irreversibly the biotinylated nucleopeptides. Underivatized complementary peptides were allowed to flow on the chip and a kinetic binding analysis yielded the thermodynamic dissociation constants. In the case of the biotinylated adenine based peptide towards the non derivatized thymine based peptide a dissociation constant of about 30 μM has been observed. Similar affinities towards the bound adenine based peptide were found for complementary RNA oligonucleotides (U_4, U_8), while the affinity of complementary DNA oligonucleotides (dT_8, dT_{10}) was about ten times higher.

Cytotoxicity tests have shown that thymine based nucleopeptides T4H, T4Bt and T4FIT do not affect cell viability of different tumor and lymphoid cell lines at concentrations up to 100 μM and for incubation times up to 24 hours.

To test the cell penetration ability of our compounds, Renca cells have been incubated for up to 12 hours with fluorescent and biotinylated thymine based nucleopeptides at concentrations in the range 0.5-50 μM. After membrane and nucleus staining cells were observed at the epifluorescence and confocal microscope; peptides were detected either by direct fluorescence (T4FIT) or with fluorescently labelled streptavidin (T4Bt). Spot like fluorescence is detected in the cytosol and in the nucleus, while some diffuse fluorescence is observed in the cytosol (Fig. 2).

Mechanistic data on cell uptake of the fluorescent thymine based nucleopeptide were collected. Uptake is concentration, time and energy dependent, since coincubation with NaN_3 and 2-deoxy-D-glucose significantly reduces the increase of fluorescence with time. The internalized nucleopeptides colocalize significantly with transferrin, a classic clathrin mediated endocitosys marker.

Taken together, these data suggest endocytosis as the major entry pathway for the nucleopeptides, although possibly other non-endocitotic routes can be involved. In conclusion, the properties of our nucleopeptides make them interesting candidates as nucleic acid modulators.

Aknowledgements

This work has been supported by the CNRS. P. G.-B. is grateful to the Università italo-francese (UIF-UFI) for supporting his international PhD (VINCI program 2005). Confocal images were recorded at RIO Cellular Imaging Platform of Esplanade (Strasbourg, France).

References

1. Nielsen PE, Egholm M, Berg RH, Buchardt O. Sequence-selective recognition of DNA by strand displacement with a thymine-substituted polyamide. *Science* **254**: 1497-1500, 1991.
2. (a) Lohse P, Oberhauser B, Oberhauser-Hofbauer B, Baschang G, Eschenmoser A. Chemie von α-Aminonitrilen. XVII. Oligo(nukleodipeptamidinium)-Salze. *Croat Chem Acta* **69**: 535-562, 1996;
(b) Diederichsen U. Pairing properties of alanyl peptide nucleic acids containing an amino acid backbone with alternating configuration. *Angew Chem Int Ed* **35**: 445-448, 1996.
3. Chaltin P, Lescrinier E, Lescrinier T, Rozanski J, Hendrix C, Rosemeyer H, Busson R, Van Aershot A, Herdewijn T. Selection of new sequence-selective unnatural peptides binding to double stranded deoxyribonucleic acids (dsDNA) by means of a gel-retardation experiment for library analysis. *Helv Chim Acta* **85**: 2258-2283, 2002.

2-19-010

Human cystatin C interactions with amyloidogenic molecules

Juszczyk, Paulina[1]; Szymańska, Aneta[1]; Rodziewicz-Motowidło, Sylwia[1]; Jankowska, Elzbieta[1]; Ładewska, Anna[1]; Spodzieja, Marta[1]; Kołodziejczyk, Aleksandra S[1]; Paraschiv, Gabriela[2]; Przybylski, Michael[2]; Grzonka, Zbigniew[3]

[1]Faculty of Chemistry, University of Gdańsk, POLAND; [2]University of Konstanz, GERMANY; [3]University of Gdańsk, POLAND

[*]E-mail: paulina_juszczyk@wp.pl

The devastating effects of amyloidogenic proteins and peptides on human health are still not fully understood. Numerous experiments have determined many physiological ligands of amyloidogenic proteins. The search for the new molecules binding to amyloids could help to understand the aggregation pathway, cellular toxicity of amyloids or neuroprotective properties of protein ligands. Therefore, it is necessary to develope sensitive analytical methods that enable to clarify details of interactions between amyloidogenic molecules. Recent developments show that selective proteolytic excision combined with mass spectrometric peptide mapping (Epitope-Excision-MS) present high potential for the determination of epitope for antigen-epitope mapping and for the identification of antibody paratope sequences.[1] In this work we present identification of the biding sites between already prooved complexes of human cystatin C (hCC) and: A) amyloid beta peptide (Aβ),[2] B) serum amyloid A (SAA)[3] and C) anti-cystatin C antibody (mAb anti-hCC).[4] Our results might be of paramount importance for the development of new inhibitors for aggregation processes of all examined cystatin C ligands. The determination of the interacting sites could also be useful in designing new tools for diagnostics in many neurodegenerative disorders. Our studies will allow to speculate whether amyloidogenic molecules association is bona fide phenomenon or just accidental interaction. Information about location of hCC binding sites in three different complexes brought us to the hypothesis that cystatin may be not only protease inhibitor in human body but it can also play more important role like stabilization of the balance in amyloidogenic molecules distribution in human body. It seems that C-terminal part of the protein is essential for complexing amyloidogenic molecules as well as for binding of monoclonal antibodies. This part of hCC is able to inhibit aggregation of amyloid beta peptide,[5] decrease pro-inflammatory properties of serum amyloid A[3] and by interaction with monoclonal antibodies is influencing 3D domain swapping of cystatin C.[4] Our still progressing studies revealed that the Aβ- binding site identified in hCC, residues (101-117), is located in the C terminal part within the L2 loop and β5 strand of hCC which comprise the external part of the protein and are exposed to the environment. The C-terminal binding epitope enables interactions of the Aβ peptide with the L2-β5 part without any restriction. The binding sites for SAA-hCC complex are located in C-terminal parts of both proteins, namely resides (96-109) in hCC and (87-105) in SAA. In the case of monoclonal antibodies epitope is located inside the binding site of Aβ, residues (107-114) [Fig.1]. The identification of the binding site in hCC may be of high importance for oligomerisation and fibrillisation studies of hCC and its amyloidogenic mutant L68Q which, due to its structural similarity to hCC can be assumed to have a similar binding epitope for all three proteins. The knowledge of the binding epitope may be used for future *in vitro* studies of hCC fibril formation, since fibrils can be easily formed with the L68Q hCC mutant by 3D domain swapping, but not by native hCC. Our results might be crucial for the development of new inhibitors for aggregation processes of all examined cystatin C ligands. The interaction of hCC with other amyloidogenic proteins may be an important neuroprotective mechanism in brain, and may attenuate their oligomerisation and play a regulating role in different amyloidosis. The identification of the binding site in hCC should be very important for oligomerisation studies of new oligomerisation inhibitors may be designed based on the cystatin C, and hCC-epitope. It seems somewhat paradox that interaction of two potentially amyloidogenic molecules might give a lead to control or inhibit neuropathological changes in amyloidogenic diseases.

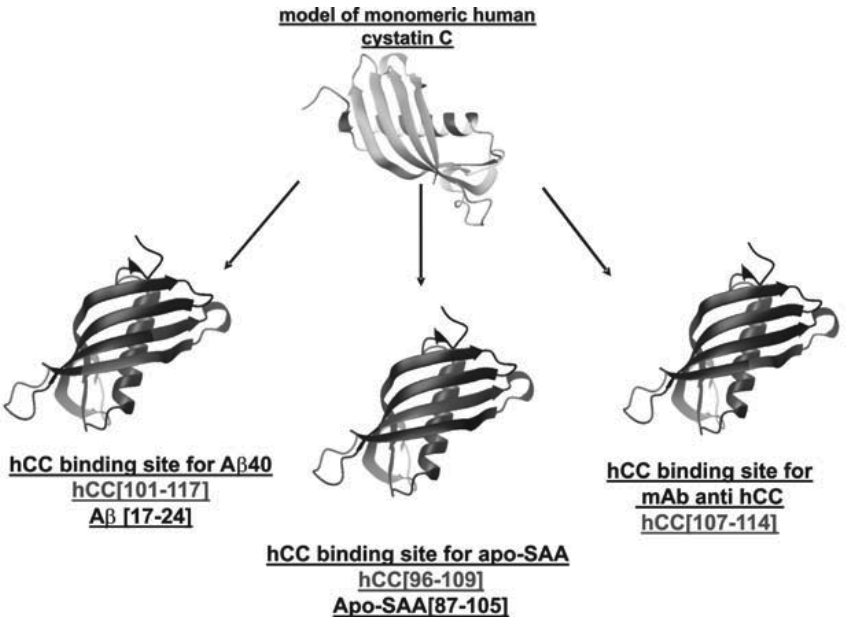

Figure 1. Location of binding sites for complexes of hCC with Aβ, apo-SAA and mAb anti-hCC.

Acknowledgements

University of Gdañsk grant BW 8000-5-121-8 to Paulina Juszczyk.

References

1. Stefanescu R, Iacob RE, Damoc EN, Marquardt A, Amstalden E, Manea M, Perdivara I, Maftei M, Paraschiv G, Przybylski M. *Eur J Mass Spectrom* (Chichester, Eng) **13**: 69-75, 2007.
2. Sastre M, Calero M, Pawlik M, Mathews PM, Kumar A, Danilov V, Schmidt SD, Nixon RA, Frangione B, Levy E. *Neurobiol Aging* **25**: 1033-1043, 2004.
3. Bokarewa M, Abrahamson M, Levshin N, Egesten A, Grubb A, Dahlberg L, Tarkowski A. *J Rheumatol* **4**: 1293-1301, 2007.
4. Nilsson M, Wang X, Rodziewicz-Motowidlo S, Janowski R, Lindstrom V, Onnerfjord P, Westermark G, Grzonka Z, Jaskólski M, Grubb A. *J Biol Chem* **279**: 24236-24245, 2004.
5. Selenica ML, Wang X, Ostergaard-Pedersen L, Westlind-Danielsson A, Grubb A. *Scand J Clin Lab Invest* **67**: 179-190, 2007.

2-23-011

Mimetibodies™, A New Platform Technology for the Development of Biologically Active Peptides that Prolongs the Half-Life

*Heavner, George A**

Centocor, Inc., Discovery Technology Research, UNITED STATES

**E-mail: gheavner@cntus.jnj.com*

In the past 40 years, researchers have identified biologically active peptides with specific activity and receptor subtype specificity. The small size of these peptides has often left them susceptible to proteolysis and golmerular filtration, resulting in short *in vivo* half-lives that have precluded their use as human therapeutics. Monoclonal antibodies are one of the most rapidly growing class of drugs, having extremely high affinity and specificity, coupled with long pharmacokinetic profiles due to their molecular size and active recycling mechanisms through Fc receptor binding. We have developed a novel platform for display and delivery of bioactive peptides that links the biological properties of the peptide with the pharmacokinetic properties of an antibody and have applied this platform to several therapeutic peptide classes.

The initial mimetibody constructs involved the replacement of two of the CDRs on each Fab arm of an antibody with two identical, active peptide sequences. The first mimetibody was constructed on an IgG1 framework using an erythropoietic mimetic peptide (EMP-1),[1] a peptide identified from phage display that has similar activity to erythropoietin but no sequence homology. This construct (Fig. 1, #1) was more active on a molar basis than the EMP-1 peptide but significantly less active than erythropoietin (EPO). Several iterations of redesign involved removal of portions of the IgG framework and re-engineering the presentation of the active peptides. The improvements that resulted from this redesign are illustrated by compounds #2 and #3 (CNTO 528). Although EMP-1 is several orders of magnitude less potent than erythropoietin *in vitro*, CNTO 528, that involved no amino acid substitutions in the EMP-1 sequence, was only 10 fold less potent than erythropoietin in stimulating the growth of UT-7_{EPO} cells. The structure of CNTO 528 is shown in Fig. 2.

A first-in-human study was conducted with CNTO 528. Individuals that were given either a single i.v. dose of 0.3 or 0.9 mg/kg or three i.v. doses of 0.09 mg/kg had elevated levels of hemoglobin at 30 days. By comparison, a therapeutic dose of erythropoietin results in a maximal increase in hemoglobin at day 4 with a return to baseline at day 7. Additional re-engineering led to CNTO 530, a compound with a longer half-life in animals and a higher potency than CNTO 528 in the UT-7 assay.[2]

We have successfully applied the mimetibody platform to a variety of therapeutic areas, one example being GLP-1.[3] The GLP-1 mimetibody maintained the bioactivity of GLP-1, had a half-life in mice of 30 hours and was shown to improve glucose control and reduce food intake

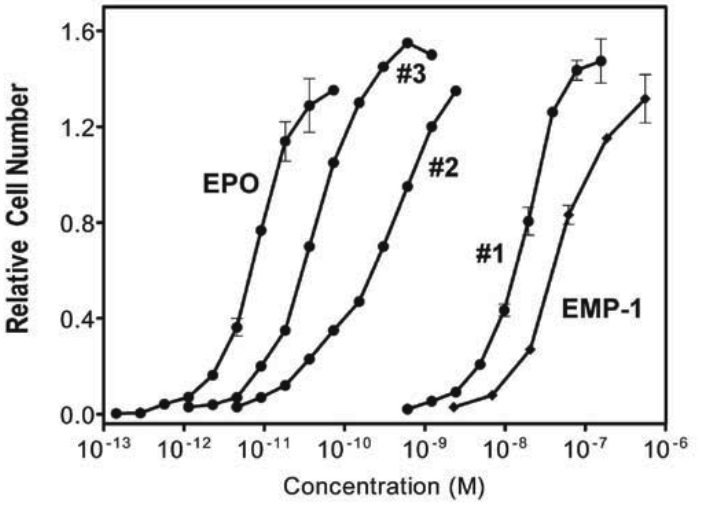

Figure 1. Proliferation of the erythropoietic-dependent cell line UT-7 in response to erythropoietin and various erythropoietic molecules.

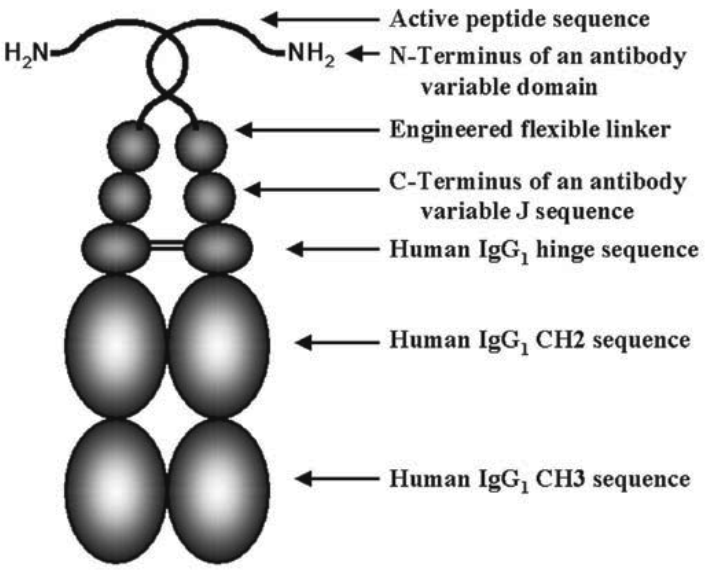

Figure 2. Schematic of the structure of the erythropoietic mimetibody CNTO 528.

and body weight in DIO (diet induced obese) mice. The mimetibody platform has proven to be robust and widely applicable. It can extend the half-life relative to the parent peptide; it can increase activity as demonstrated by the significantly increase the activity of the EMP-1 peptide without changes in the peptide sequence; and it has been shown in human studies to result in compounds that are both safe and efficacious.

References

1. Wrighton NC, Farrell FX, Chang R, Kashyap AK, Barbone FP, Mulcahy LS, Johnson DL, Barrett RW, Jolliffe LK, Dower WJ. Small peptides as potent mimetics of the protein hormone erythropoietin. *Science* **273**: 458-463, 1996.
2. Bugelski PJ, Capocasale RJ, Makropoulos D, Marshall D, Fisher PW, Lu J, Achuthanandam R, Spinka-Doms, T., Kwok, D., Graden, D., Volk, A., Nesspor, T., James, I.E. and Huang, C. CNTO 530: Molecular pharmacology in human UT-7EPO cells and pharmacokinetics and pharmacodynamics in mice. *J Biotechnol* **134**: 171-180, 2008.
3. Picha KM, Cunningham MR, Drucker DJ, Mathur A, Ort T, Scully M, Soderman A, Spinka-Doms T, Stojanovic-Susulic V, Thomas BA, O'Neil KT. Protein Engineering Strategies for Sustained Glucagon-Like Peptide-1 Receptor–Dependent Control of Glucose Homeostasis. *Diabetes* **57**: 1926-1934, 2008.

2-25-012

A novel nucleolar localization signal sequence derived by structural minimization of an animal toxin

Rádis-Baptista, Gandhi[1]; G. de la Torre, Beatriz[2]; Andreu, David[2,]*

[1]Federal University of Pernambuco, Recife, Department of Biochemistry BRAZIL; [2]Pompeu Fabra University, Department of Experimental and Health Sciences, SPAIN

[*]E-mail: radisbra@yahoo.com

Introduction

Localization sequences are specific signals that sort proteins to precise cellular compartments. Among those, cell-penetrating peptides (CPPs) are natural or synthetic sequences, cationic and amphipathic, capable of translocating eukaryotic membranes, occasionally localizing to the nucleus. Animal venoms, for their part, are a rich source of bioactive peptides that on occasion can be turned into useful drugs. Snakes, scorpions or spiders produce and secrete a valuable diversity of toxins capable of interacting with distinct molecular targets in the cell. A limited number of animal toxins is known to translocate the cytoplasmic membrane and localize into distinct cell compartments. One example is crotamine,[1] a rattlesnake toxin of 42 amino acids that selectively translocates into cells at specific phases of cell cycle, and localizes to the nucleus. In solution, crotamine adopts an αββββ fold, stabilized by three disulfide bonds,[2] similar to β-defensin 2 and Na^+-channel scorpion toxin.

Results and discussion

Structure-based deconstruction of complex, highly folded peptides has been used to identify minimal traits essential for activity[3] and to design therapeutically useful versions. When applied to crotamine, with the goal of defining minimal motifs for translocation, one particularly interesting result of this type of minimalistic analysis was a peptide where the N-terminal (residues 1-9) and C-terminal (residues 38-42) regions were spliced together, with or without an Ahx spacer [YKQCHKKGGXKKGSG, X=Ahx (**1**) or nil (**2**)]. To explore peptide uptake and targeting, **1** and **2** were labeled with rhodamine B and analyzed by time-lapsed confocal microscopy on live HeLa cells (Fig. 1). At 15 μM, and as early as 15 min, the peptides translocated the membrane and localized to the nucleus, specifically to the nucleolus (Fig. 1A), where they bound various stages of nucleolar organization, including pre-mitotic re-associating, self-organizing and cytokinetic nucleoli, as well metaphasic

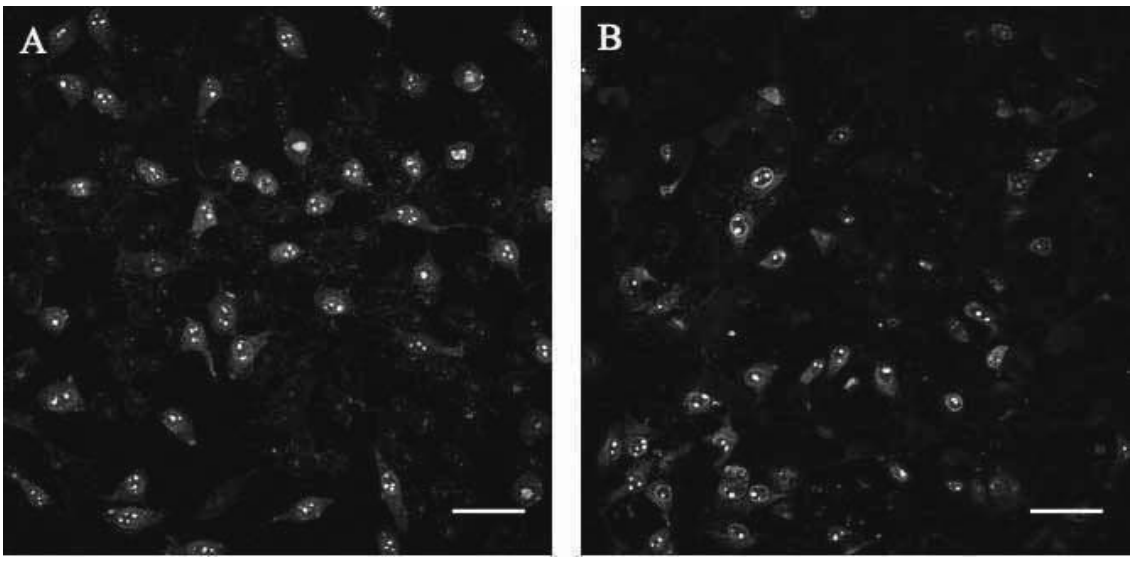

Figure 1. Penetration and nucleolar localization of peptides **1** and **3**. HeLa cells grown to 50-60% confluence (37 ^{0}C, 5% CO2) were incubated with rhodamine B-labeled **1** (15 μM, panel A) or **3** (50 μM, panel B) and uptake and compartmentalization monitored for 60 min by confocal microscopy. Images represent a focal plane section of the nuclear volume; bar = 50 μM.

chromosomes. The similar behavior of **1** and **2** suggests that the flexible Ahx spacer is not required for (neither does it interfere with) cellular penetration and nucleolar homing.

The relative chemical similarity between the spliced N- and C-terminal segments prompted us to investigate an inverted (GSGKKXGGKKHCQKY, retro-**1**) sequence, which was found equally able to translocate into HeLa cells, albeit at concentrations ≥ 50 μM. Interestingly, an His→Ile replacement in this retro sequence resulted in an analogue (GSGKKXGGKKICQKY, **3**, Fig. 1B) with uptake and localization properties similar to **1** and **2**, suggesting that peptides **1**-**3** share an intrinsic nucleolar homing trait. In all cases, the peptides were found by an MTT assay to be non-toxic to HeLa cells up to 100 μM. To gain further insight on the process of cell penetration and nucleolar compartmentalization, the D-enantiomer of **1** (ykqchkkGGXkkGsG) was made. When tested on HeLa cells, it failed to translocate, localizing instead on the plasma membrane (images not shown) and thus suggesting that internalization of the *all*-L peptides **1**-**3** is mediated by some receptor capable of chiral discrimination.

Taken together, the above results appear to define a novel CPP family with fairly simple structural features (e.g. allowing sequence reversion) that nonetheless translate into precise nucleolar localization. A detailed biophysical elucidation of the structural features underlying the penetrating mechanism of these new CPPs is under way. Meanwhile, it is worth noting that the nucleolus is one of the most prominent structural and functional elements of the nucleus, with a role conventionally associated to ribosome biogenesis. Recently, additional biological functions mediated by nucleoli have been unveiled, including roles in viral infection, regulation of tumor supression and oncogenic activities, stress sensing, aging control, and modulation of telomerase activity.[4] We expect that our new CPPs will find use as probes for investigating protein traffic at the nucleolar level, and/or as carriers of drugs and other cargos into this important subnuclear organelle.

Acknowledgements

G.R-B. thanks Fundación Carolina (Madrid, Spain) for a visiting scholarship and the Federal University of Pernambuco, Brazil, for a temporary leave from teaching duties. Research supported by the Spanish Ministry of Education and Science (grant BIO2005-07592-CO2-02 to D.A.).

References

1. Kerkis A, Kerkis I, Rádis-Baptista G, Oliveira EB, Vianna-Morgante M, Pereira LV, Yamane T. *FASEB J* **18**: 1407-1409, 2004.
2. Nicastro G, Franzoni L, Chiara C, Mancin AC, Giglio Jr, Spisni A. *Eur J Biochem* **270**: 1969-1979, 2003.
3. Vila-Perelló M, Tognon S, Sánchez-Vallet A, García-Olmedo F, Molina A, Andreu D. *J Med Chem* **49**: 448-451, 2006.
4. Olson MO, Dundr M. *Histochem Cell Biol* **123**: 203-216, 2005.

2-29-013

N-acylation of anti-LPS peptides renders micellar and tubular nanostructures with enhanced LPS-neutralizing activity

Mas-Moruno, Carlos[1]; Cascales, Laura[2]; Cruz, Luis J.[1]; Mora, Puig[2]; Perez-Paya, Enrique[2]; Albericio, Fernando[1,]*

[1]Institute for Research in Biomedicine, Barcelona Science Park, Barcelona, SPAIN; [2]Department of Medicinal Chemistry, Centro de Investigacion Principe, Valencia, SPAIN

[*]E-mail: albericio@irbbarcelona.org

Introduction

Sepsis and its acute state, septic shock, are the first cause of mortality in intensive care units and a leading cause of mortality worldwide.[1] In 2006, septicemia was the 10th foremost cause of death in the U.S.[2] Sepsis is produced by a bacterial endotoxin, the lipopolysaccharide (LPS), a major component of the cell wall in Gram-negative bacteria.[3] Therefore, peptides that interact with LPS can provide the basis for the development of new antisepsis agents. In the present study, we have focused on three LPS-binding proteins: i) the Limulus anti-LPS factor (LALF), ii) the bactericidal permeability-increasing protein (BPI), and iii) the serum amyloid P (SAP). Several *N*-acylated peptides derived from LALF-14c were synthesized, cyclized and evaluated for anti-LPS activity. An increase in activity of at least 10-fold was observed for C16-LALF-14c over the parent peptide, C2-LALF-14c.[4] On the basis of TEM images, this enhancement could be associated with the capacity of peptides to form nanostructures. TEM studies revealed that long fatty acyl chains promote the formation of micellar and fibrilar superstructures. This nanostructure-biological activity correlation has been corroborated with other anti-LPS peptides, BPI and SAP, which also displayed improved activities.[4]

Results and discussion

The optimal acyl chain length for LPS interaction was studied after conjugation of LALF-14c (G[CKPTFRRLKWKYKC]G), the LPS-binding domain of LALF,[5] with different aliphatic acids: from acetic acid (C2) to palmitic acid (C16). The synthesis of these peptides was carried out on solid-phase (SP) using a Fmoc/tBu strategy. Acylation of the free amino N-terminus was achieved using PyBOP/HOAt/DIEA as coupling reagents. After cleavage, the linear peptides were purified and cycled in solution using DMSO. Finally, the cyclic peptides were treated with HP-20 Diaion resin. This treatment yielded the cyclic peptides with excellent purities. This methodology proved to be very useful to overcome the problems in solubility presented by the peptides with a greater number of carbon units.[4] The LPS-neutralizing activity of the resulting peptides was evaluated using the Limulus amebocyte lysate assay (LAL)[6] (Fig. 1). The initial increase in the acyl chain length from C2- to C6-LALF-14c did not represent an improvement in LPS-neutralizing activity. In contrast, this activity clearly improved for the peptides bearing longer acyl chains, i.e. from C8- to C16-LALF-14c. In particular, C16-LALF-14c showed a 10-fold increase in LPS-neutralizing activity when compared to the original acetylated peptide.

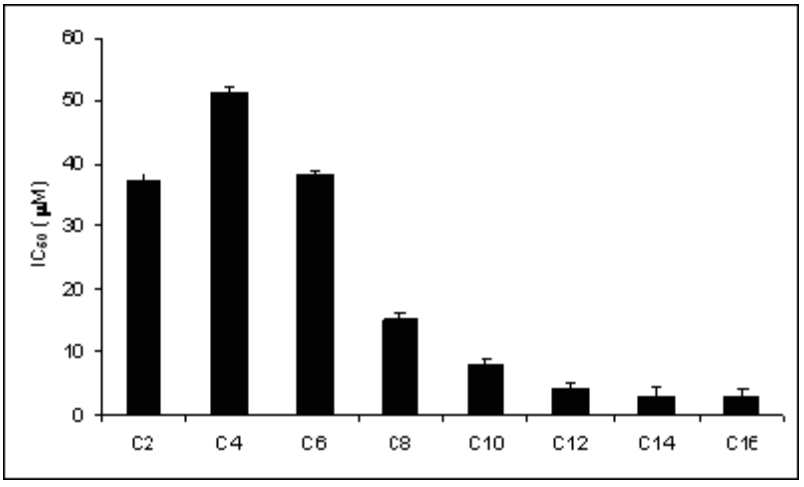

Figure 1. LPS-neutralizing activity (IC_{50}) of LALF-14c-derived peptides. IC_{50} values are represented as mean values ± SD.

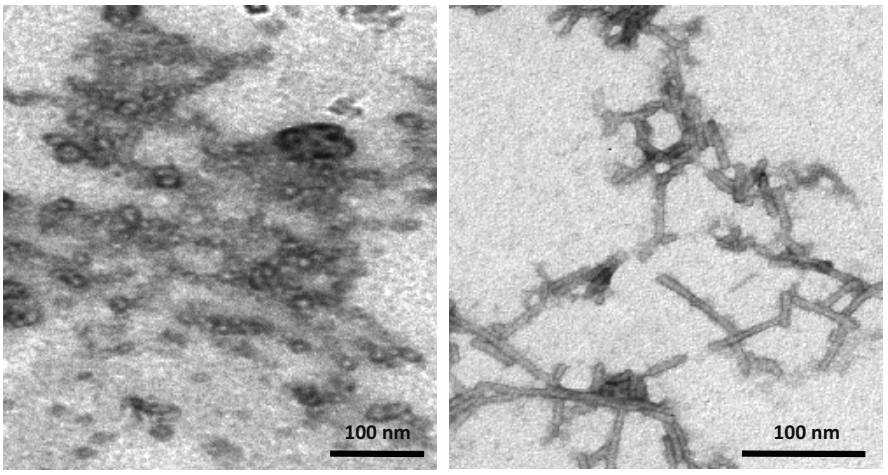

Figure 2. TEM images of C16-LALF-14c (left) and C16-BPI (right). One representative micrograph is shown for each peptide. Peptides were dissolved in PBS at 5 mg/mL and stained with 2% uranyl.

To study the effect that *N*-acylation could have in the conformation of the peptides, a comparative analysis of the conformational behavior of C2- and C16-LALF-14c was carried out using Transmission Electron Microscopy (TEM). TEM images (Fig. 2) showed that C16-LALF-14c formed micelles at 5 mg/mL, whereas C2-LALF-14c did not form any defined structure. The spheroidal micelles were 15-20 nm in diameter and several of these structures accumulated into aggregates of multiple monomers. The minimal acyl chain length required for micelle formation was also determined. Under assay conditions, C2- and C4-LALF-14c did not form micelles. The tendency to form such nanostructures was low for peptides C6- to C10-LALF-14c, and only C12- to C16-LALF-14c showed a great abundance (images not shown). This behaviour correlates well with the values of activity presented before.

To determine whether this phenomenon could be translated to other LPS neutralizing peptides, 2 different anti-LPS proteins were selected: BPI and SAP. Hence, the active sequences from BPI (IKISGKWKAQKRFLKM) and SAP (QALNYEIRGYVIIKP) were synthesized and *N*-acetylated or palmitoylated on SP. BPI-derived peptides were easily synthesized using an automatic peptide synthesizer. However, the synthesis of SAP was more challenging due to the hydrophobic sequence Val-Ile-Ile. In this case, Microwave (MW)-assisted solid-phase synthesis was necessary. The biological activity of these peptides was calculated using the LAL test. C2-BPI and C2-SAP, with IC_{50} values of 16 and 8 μM, respectively, had a greater activity than the original C2-LALF-14c. Nevertheless, *N*-terminal palmitoylation of these peptides rendered again enhanced LPS-neutralizing activities. C16-BPI displayed an inhibitory activity of 60 nM and C16-SAP was almost 2 times more active (5 μM) than C2-SAP. These results are in agreement with those previously obtained for LALF and confirm that acyl chain incorporation modulates the activity of different anti-LPS peptides. The effect of *N*-acylation on these peptides was also explored with TEM. Again, no aggregates or defined structures were observed for the acetylated peptides. In contrast, in both C16-BPI and C16-SAP peptides, clear fibril-like nanostructures were detected. C16-BPI displayed defined tubular structures that were 50-140 nm long and 9-12 nm wide (Fig. 2). In contrast, C16-SAP showed fibrils prone to self-associate and aggregate (images not shown). These images show the extent of the aggregation properties of these new LALF, BPI and SAP lipopeptides.

Acknowledgements

This work was partially supported by Fundacio La Marato de TV3 and CICYT (BIO2004-998, CTQ2006-03794/BQU).

References

1. Riedemann NC, Guo RF, Ward PA. *Nat Med* **9**: 517-524, 2003.
2. Heron MP, Hoyert DL, Xu J, Scott C, Tejada-Vera B. *National Vital Statistics Reports* **56**: 1-52, 2008.
3. Cohen J. *Nature* **420**: 885-891, 2002.
4. Mas-Moruno C, Cascales L, Cruz LJ, Mora P, Perez-Paya E, Albericio F. *ChemMedChem* **3**: 1748-1755, 2008.
5. Ried C, Wahl C, Miethke T, Wellnhofer G, Landgraft C, Schneider-Mergener J, Hoess A. *J Biol Chem* **271**: 28120-28127, 1996.
6. *US Department of health and human services, PHS Food and Drug administration.* Guideline on validation of the limulus amebocyte lysate test as an end-product endotoxin test for human and animal parental drugs, biological products and medical services. 1987.

2-01-101

New Amide Analogues Of Antistasin Isoform 2 And 3

Danalev, Dantcho[1,]; Vezenkov, Lyubomir*

University of Chemical Technology and Metallurgy, Organic Chemistry, BULGARIA

[*]E-mail: dancho_danalev@yahoo.com

During the last years the number of deaths due to hemostatic impairments such as coronary thrombo-embolisms, myocard heart attack, etc. has become equal to those caused by cancer formations. Haemostasis is a key process whose correct functioning is an important defence mechanism of the human organism. It is a blood coagulation process activated in case of injury of the blood system. If it is functioning correctly vascular-motor and cell reactions are triggered and the blood coagulation cascade is activated. Coagulation is a defence function of the organism that has to be strictly regulated. After the bleeding is stopped, a number of limiting self-regulatory mechanisms are initiated. They act competitively and their role is to: - stop further coagulation; - to prevent the thrombus formation in the organism; - restrict the coagulation to the injured are. Besides the mechanisms limiting the formation of thrombocytes, the availability of plasma proteins is also important in this respect as they deactivate the serine proteinase of the coagulation, i.e. they act as inhibitors. The main function of blood coagulation is the conversion of the soluble fibrinogen into insoluble fibrin clot. This process is accompanied by a series of enzyme reactions described in 1964 as an enzyme cascade.[1] A major role in them plays a number of serine proteinases which are known as: • Blood clotting factors - extrinsic system: Factor III, Factor VII - intrinsic system: Factor XII, high molecule kininogen, prekalikrein, Factor XI, Factor IX, Factor VIII - common pathway: Factor XI, Factor V, Phospholipids, Factor II, Factor I, Factor XIII Factors of the fibrinolysis Factors of the control mechanisms (inhibitors) According to the avalanche theory coagulation can be considered as an auto bioenhancing process. As a result the inhibition of proteinases located in the centre of the process would prevent the avalanche formation of strong enzyme substrates down the chain. Proof of this thesis is the fact that the inhibition of Factor Xa prevents the activation of 138 thrombin molecules.[2] That is why the main target in the creation of anticoagulants is the inactivation of Factor Õà. In the last 20 years a number of proteins and peptides with different molecule mass and well established anticoagulation activity have been isolated from the salivary glands of several bloodsucking animals. Many of the strongest anticoagulants isolated from bloodsucking animals are found in the saliva of different types of leeches. In 1987 Tuszynski *et al*. reported for 119 amino acids protein isolated form the salivery glands of Mexican leech Haementeria officinalis with strong anticoagulant properties which they named antistasin.[3] One year later kinetic investigations of Nutt *et al*. reveal that antistasin is a potent, slow, tight-binding Factor Xa inhibitor.[4,5] A large part of the natural anticoagulant peptides and proteins isolated later, show partial or complete similarity between their active centres and other parts of their molecules and those of antistasin. Thus it becomes the founder of the largest group of natural anticoagulants - antistasin type inhibitors. Two years later Condra *et al*.[6] reported that they isolate three isoforms of antistasin corresponding to its C-terminus which save good anticoagulant activity:

isoform 1:Arg-Pro-Lys-Arg-Lys-Leu-Ile-Pro-Arg / IC_{50}=5 nM
isoform 2:Arg-Pro-Lys-Arg-Lys / IC_{50}=500 nM
isoform 3 :Arg-Pro-Lys-Arg / IC_{50}=740 nM

During last few years a data in the literature for short peptides with strong anticoagulant activity increased. A lot of authors publish a data for tripeptide sequences as D-Phe-Arg-Pro; D-Arg-Gly-Arg; Tyr-Ile-Arg; Phe-Ile-Arg, which show anticoagulant activity in nanomolar range.[7-9] In 2004 we synthesized and characterized a series of hybrid structure between isoform 2 and 3 of antistasin and mentioned above tripeptides.[10] The aim of these compounds creation was to obtained new structures with better anticoagulant activity and good selectivity towards different enzymes included in the blood coagulation cascade as well as to reveal the role of some amino acids in the different positions of the molecule. We concluded interesting structure-activity relationships. At the same work we reported for the synthesis of one hexapeptide replacing its C-terminal COOH function with $CONH_2$: D-Phe-Pro-Arg-Pro-Lys-Arg-NH_2. The latter showed 12 times better activity than its analogues with N-terminal COOH group and 40 times higher activity than natural isoform 3 of antistasin. Based on the fact mention above herein we reported the synthesis of all previously obtained hybride structures but replacing there C-terminal COOH function with amide:

Tyr-Ile-Arg-Pro-Lys-Arg-NH_2
Tyr-Ile-Arg-Pro-Lys-Arg-Lys-NH_2
Phe-Ile-Arg-Pro-Lys-Arg-NH_2
Phe-Ile-Arg-Pro-Lys-Arg-Lys-NH_2
D-Arg-Gly-Arg-Pro-Lys-Arg-NH_2
D-Arg-Gly-Arg-Pro-Lys-Arg-Lys-NH_2

All compounds were synthesized by SPPS by means of Rink amide resin/Fmoc-strategy. The structures were proved by ES/MS and anticoagulant activity according to the APTT was determined. Their IC_{50} are found too and they are in a nM range. All newly synthesized peptides have 10 to 200 times higher activity than C-terminal COOH analogues and 20 to 500 times higher activity than natural isoforms of antistasin. Some analogues show better activity than natural isoform 1. The kinetic investigations towards the enzymes from blood coagulation cascades in relation to the specificity of new hybride structures and the toxicity studies are in progress.

In a conclusion we revealed that:

1. Lys^{113} is very important for the substrate-enzyme interaction.

2. The replacement of C-terminal COOH with $CONH_2$ results to many times increasing of anticoagulant activity.

3. The replacement of L- with D-amino acid in P3 position is not a key factor for anticoagulant activity increasing.

4. The availability of aromatic amino acid in P3 position is not crucial for anticoagulant activity availability.

References

1. Gould R, Shafer J. *Perspectives in Drug Discovery and Design* **1**: 419, 1993.
2. Richard C, Becker MD, Frederick A, Spencer MD. *Curr Interv Card Rep* **3**: 251, 2001.
3. Tuszynski GP, Gasic TB, Gasik GJ. *J Biol Chem* **262**: 9718-9723, 1987.
4. Mao SS, Przysiecki CT, Krueger JA, Cooper CM, Lewis SD, Joyce J, Lellis C, Garskyi VM, Sardana M, Shafer JA. *J Biol Chem* **273**: 30086-30091, 1998.
5. Dunwiddie CT, Nutt EM, Vlasuk GP, Siegl PK, Shaffer LW. *Thromb Haemost* **67**: 371-376, 1992.
6. Condra C, Nutt EM, Petroski CJ. *Thromb Haemost* **61**: 437-441, 1989.
7. Bajusz S, Szell E, Bagdy D, Barabas E, Horvath G, Dioszegi M, Fittler Z, Szabo G, Juhasz A, Tomori E, Szilagyi G. *J Med Chem* **33**: 1729-1735, 1990.
8. Marlowe CK, Sinha U, Gunn AC, Scarborough RM. *Bioorg Med Chem Lett* **10**: 13-16, 2000.
9. Ostrem JA, Al-Obeidi F. *Biochemistry* **37**: 1053-1059, 1998.
10. Danalev D, Vezenkov L, Grigorova B. *J Pept Sci* **10**: 27-36, 2004.

2-01-102

Synthesis of the S129-I229 fragment of the extracellular domain of the VEGF receptor 1 embedding the ligand binding site.

Goncalves, Victor[1]; Gautier, Benoit[1]; Huguenot, Florent[1]; Leproux, Pascale[2]; Garbay, Christiane[1]; Vidal, Michel[1]; Inguimbert, Nicolas[1,]*

[1]University Paris Descartes, INSERM U648, FRANCE; [2]CNRS UMR 8638, University Paris Descartes, FRANCE

[*]E-mail: nicolas.inguimbert@parisdescartes.fr

Introduction

The interaction of the vascular endothelial growth factor (VEGF) with its cellular receptors exerts a central role in the regulation of angiogenesis. Among these receptors, the VEGF receptor 1 may be implicated in pathological angiogenesis.[1] However, no structural data, describing the interaction between this receptor and small molecule antagonists, is currently available. Domain deletion experiments carried on the VEGFR1 extracellular portion have shown that the second immunoglobulin-like domain, from the N-terminus (VEGFR1 d2), is necessary and sufficient to bind VEGF[2]. Indeed, VEGFR1 d2 alone binds VEGF only 60-fold less tightly than the full length protein. The structure of this domain (VEGFR1 129-229) has been solved, by NMR[2] or by X-ray crystallography in complex with VEGF[3] and PlGF.[4] Because of the importance of the human VEGFR1 d2 as a potential target in the development of angiogenesis modulators, the availability of this protein domain, and mutants, should be useful in the screening and structure aided design of novel specific ligands. Up to now, the 101-amino acid polypeptide chain of VEGFR1 d2 has been only produced by gene expression in Escherichia coli.[3] As an alternative we engaged a study to produce this protein by SPPS.

Stepwise synthesis of the VEGFR1 d2 domain

During SPPS, the excessive hydrophobicity of the growing protected polypeptide chain gives rise to low coupling yields and undesirable side products. In order to overcome this problem we used the N-dimethoxybenzyl (Dmb) amino acid and pseudoproline (dimethyloxazolidine) dipeptide building blocks which have been proposed for the synthesis of difficult aggregation prone sequences.[5-6] The peptide was synthesized using Fmoc protected aminoacids and Novasyn TGA resin on an automated ABI 433A peptide synthesizer with double coupling for difficult sequences and by incorporation of four oxazolidine pseudoproline dipeptide derivatives and two Dmb glycines. The elongation proceeded smoothly for the coupling of the first fifty residues but was rather difficult for the last part.

VEGFR1 d2 Purification and folding

The crude was submitted to purification by RP-HPLC on a C18 column and 12.5 mg VEGFR1 d2 were obtained (measured mass of 11523.0 ± 1.0 Da (calculated mass: 11523.17 Da). Then, the peptide was dissolved at 0.2 mg/mL in a 0.1 M Tris, 2.2 M guanidine, pH 8.0 buffer for 1 h and submitted to air oxidation at 4 °C for 24 h. A minimum concentration of 1.8 M of guanidine was necessary to avoid aggregation of the unfolded peptide. The folding process was monitored by analytical RP-HPLC (Fig. 2). The solution was then dialyzed against a 50 mM Na_2HPO_4, 150 mM NaCl buffer at pH 6.5 for 24h at 4 °C. The peptide was concentrated and filtered with an Amicon Ultra centrifugation tube equipped with a molecular-weight cut-off filter of 10000 Da. RP-HPLC analysis indicated that the desired peptide was retained and that most of the impurities had been eliminated. The mass of the folded peptide, determined by ESI Q-Tof mass spectroscopy, was of 11521.0 ± 1.0 Da in agreement with the formation of a disulfide bridge during the folding process (Fig. 2).

H-^{129}**Ser-Asp-Thr-Gly-Arg-Pro-Phe-Val-Glu-Met-Tyr-Ser-Glu-Ile-Pro-Glu-Ile-Ile-His-Met-Thr-Glu-**^{151}Gly-Arg-
Glu-Leu-Val-Ile-Pro-Cys-Arg-Val-Thr-**Ser**-Pro-**Asn**-Ile-**Thr**-Val-Thr-Leu-Lys-Lys-**Phe**-Pro-Leu-Asp-Thr-Leu-Ile-Pro-
Asp-^{181}Gly-Lys-**Arg-Ile-Ile-Trp**-Asp-Ser-**Arg**-Lys-Gly-Phe-Ile-Ile-Ser-Asn-Ala-Thr-Tyr-**Lys-**^{201}**Glu-Ile**-Gly-Leu-Leu-
Thr-Cys-Glu-Ala-Thr-Val-Asn-Gly-His-Leu-Tyr-Lys-Thr-Asn-Tyr-Leu-Thr-His-Arg-Gln-Thr-Asn-Thr-^{229}Ile-OH

Figure 1. Synthesis sequence of the 101-residue VEGFR1 d2. Sites substituted by dimethyloxazolidine dipeptides and (Dmb)-glycines are written in red and underlined. Proline residues are written in red. Double-coupled residues are in bold.

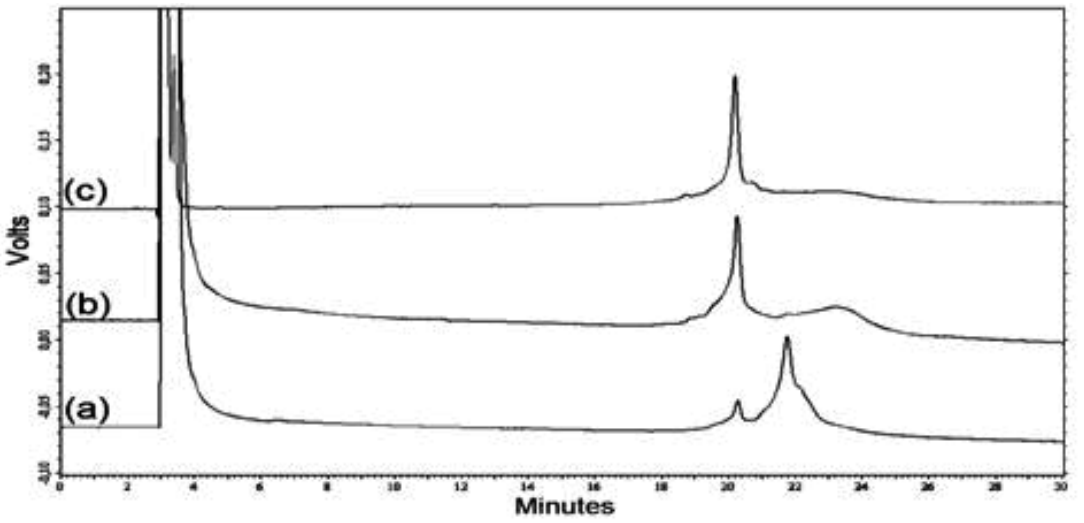

Figure 2. Folding and purification of VEGFR1 d2. RP-HPLC elution profiles of analytical samples recovered after (a) 0h and (b) after 18 h of air oxidation and (c) after dialysis and utrafitration.

Elisa based assays

In order to confirm that VEGFR1 d2 has adopted its bioactive conformation, we employed an ELISA-based assay to confirm the ability of VEGFR1 d2 to bind VEGF165[7]. A fixed amount of VEGFR1 d2 was coated on a high-binding microplate and was put in presence of different doses of biotinylated VEGF165 (btVEGF165). After wash steps, the remaining btVEGF165 bound to VEGFR1 d2 was detected by chemiluminescence thanks to a streptavidin-horseradish peroxidase conjugate allowing to determine an IC50 of 1.62 nM for 250 ng of immobilized VEGFR1 d2 (Fig. A). Furthermore, the binding of btVEGF165 on this receptor domain could be inhibited by the addition of unlabelled VEGF165 with an IC50 of 0.52 nM. Alternatively, VEGFR1 d2 inhibited dose dependently the btVEGF165 interaction with the full length extracellular domain of VEGFR1 (VEGFR1 ECD) with an IC50 of 0.6 µM in the conditions of the experiment. In this case, VEGFR1 ECD was adsorbed on the microplate and put in presence of a fixed quantity of biotinylated VEGF165 and different amounts of VEGFR1 d2.

Conclusion

The biological evaluation of VEGFR1 d2 activity, in combination with ESI Q-Tof mass spectroscopy, allowed us to confirm the correct folding of the protein domain. Based on the saturation assay, the Kd of VEGFR1 d2 for biotinylated VEGF165 was 1.62 nM. This result is in good agreement with previous studies indicating that this region of VEGFR1 was responsible for the binding of VEGF. Indeed, for comparison, the Kd of btVEGF165 for the full length VEGFR1 ECD is estimated at 757 pM.[7] To conclude, we expect to improve the yield of this synthesis by using a systematic double coupling of β-branched residues and those directly following. In a near future we expected to be able to incorporate unnatural fluorescent amino acids in the peptide sequence, and to use the VEGFR1d2 as a screening template for VEGFR1d2 antagonist.[8]

References

1. Carmeliet P. *Nature* **438**: 932-936, 2005.
2. Starovasnik MA, Christinger HW, Wiesmann C, Champe MA, de Vos AM, Skelton NJ. *J Mol Biol* **293**: 531-544, 1999.
3. Wiesmann C, Fuh G, Christinger HW, Eigenbrot C, Wells JA, de Vos AM. *Cell* **91**: 695-704, 1997.
4. Christinger HW, Fuh G, de Vos AM, Wiesmann C. *J Biol Chem* **279**: 10382-10388, 2004.
5. Johnson T, Quibell M, Owen D, Sheppard RC. *J Chem Soc Chem Commun* **4**: 369-372, 1993.
6. Wöhr T, Wahl F, Nefzi A, Rohwedder B, Sato T, Sun X, Mutter M. *J Am Chem Soc* **118**: 9218-9227, 1996.
7. Goncalves V, Gautier B, Garbay C, Vidal M, Inguimbert N. *Anal Biochem* **366**: 108-110, 2007.
8. Goncalves V, Gautier B, Coric P, Bouaziz S, Lenoir C, Garbay C, Vidal M, Inguimbert N. *J Med Chem* **50**: 5135-5146, 2007.

2-01-103

In-vivo and *in-vitro* activities of new L-Valine derivatives: structure-activity relationships

Tsekova, Daniela[1,]; Tancheva, Lyubka[2]; Makakova, Emilia[3]; Alov, Petko[4]; Pajeva, Ilza[4]; Petkov, Vesselin[2]*

[1]University of Chemical Technology and Metallurgy, Department of Organic Chemistry, BULGARIA; [2]Bulgarian Academy of Sciences, Institute of Neurobiology, BULGARIA; [3]University of Sofia, Chemistry Faculty, BULGARIA; [4]Bulgarian Academy of Sciences, Center of Biomedical Engineering, BULGARIA

[*]E-mail: d_tsekova@abv.bg

Introduction

Four derivatives of L-Valine were studied as potential pharmacological agents. L-Valine is bound to either nicotinic (m-pyridinic) acid (M) or isonicotinic (p-pyridinic) acid (P) from N-side and to an alkyl spacer consisting of 3 or 6 methylene groups from C-side. The compounds belong to the group of low molecular weight gelators (LMWG) and have very high ability to form intermolecular H-bonds, involving also solvent molecules in their supramolecular complexes formation.[1,2] Constructed by the natural L-α-aminoacid – Valine, which is connected by amide (peptide) bonds with neighbouring groups (different from the natural L-α-aminoacids), these compounds are representatives of the class of peptidomimetics. The other ingredient of the molecule is either nicotinic or isonicotinic acid, which are expected to determine their specific biological activities. There are number of reports in the literature for pronounced biological activities of similar compounds derivatives of nicotinic and isonicotinic acids- anti-anxiety, anxiolytic properties anti-inflammatory, antituberculosis and anti-depressant activities.[3-6] But up to now similar analogs have not been used as lead structures for drug synthesis.

Results and discussion

• TOXISITY

In vitro (citotoxicity): The four compounds are nontoxic at concentrations 250 µÌ. Using for control Vit. C it was found that their citotoxicity was even lower then that of Vit C.
In vivo: lack of acute and prolonged toxicity was observed.
- LD50 (lethal dose) is over 2000 mg/kg (p.os and i.p.).
- NOEL (no observed effect level) was estimated as 40 mg/kg i.p.
- Limac (limit of acute toxicity) was found at 80 mg/kg i.p. Dissection of the animals at the 5, 7 and 14 day of the treatment did not show prolonged toxicity.

Table 1. Calculated pKa data for the four compounds

Compound	P3	P6	M3	M6
pKa_1	3,19	3,08	3,14	2,93
pKa_2	3,8	3,71	3,74	3,62
pKa_3	11,33	11,35	11,76	11,78
pKa_4	11,94	11,95	12,37	12,38
pKa_5	15,73	15,96	15,75	15,97
pKa_6	16,64	16,58	16,65	16,59

• PHARMACOLOGICAL ACTIVITIES

- ED50 (the effective doses) of the compounds were about 250 mg/kg b.w. i.p., which means that therapeutic index (LD50/ED50) is higher than 8.
- A significant analgesic effect of M6 and P6 (250 mg/kg) was found most pronounced on the1st hour for Ð6 and on the 3rd hour for Ì6. M3 and P3 showed weak analgesic effect after 5 days treatment.
- The four compounds posses some depressing effect on the orientation most pronounced for M3, followed by P3.
- Decreasing of neuromuscular coordination after a 5-day treatment more pronounced for P3 and M3 analogues was recorded.
- A good dose-dependent effect on learning and memory of the treated animals was established with compounds M6 and P6. The effect of compound Ì6 was stronger.[7]

• PHYSICO-CHEMICAL CHARACTERISTICS

related with the properties of the compounds as putative drugs (pKa, log P, chelating effect).
- Applying ACD Labs, data for pKa were calculated and they are presented in Table 1.

Some of the results calculated and presented in the Table 1 were conformed experimentally.[8] As it is visible from the Table 1, the four compounds at physiological ðÍ 7,4 exist in their unionized form, therefore they keep in the molecule places with high affinities to H-bonds and complexes formation. In acidic solution at pH lower then 3 they exist in their double ionized form RH_2^{2+} and because of that they are completely soluble in stomach environment.
- Solubility of the substances in water and in octanol (as a representative of lipids) was studied and log P was estimated. It was found that their solubility in octanol is much higher than in water, for M6 and P6 it was about 80-100 times, while for M3 and P3 was about 30-50 times. Estimation of log P was performed on the basis of experiments and ACD Labs calculations. Theoretically and experimentally determined octanol/water logP values of the compounds correlate with their CNS-effects. M6 and P6 had higher logP than M3 and P3 and showed better antinociceptive and anticonvulsant activity *in vivo*.
- There are variety of theoretical models for chelate complexes formation, which includes oxigen and nitrogen atoms from the amide groups and pyridine rings in the molecules in different space orientations. Tests for chelating activity toward Fe^{2+} show that most effective are M6 and M3 at all studied concentrations.[8]

It is possible any of the found biological activities to be connected with their ability to make complexes.

Conclusions

We can say that studied compounds revealed at in-itro and in-vivo experiments promising activities for drug development on their basis and that encourages future studies in this direction.

Materials and method

In-vivo: Male Albino mice ICR with initial body weight 18–20g (10 in groups). Toxicological studies: Parameters of acute toxicity.- Limac, NOEL, LD50, Prolonged toxicity – after 5, 7 and 14 days. Reversibility of the toxic damages – till the 14th day after acute administration of the compounds. Neuropharmacological: Analgesic (antinociceptive) effect- test for chemical irritation with 1% acetic acid solution;. "Rota-rod" test (Neuromuscular coordination); "Hole board" test (Orientation), Passive avoidance step down test (Learning and memory). *In-vitro*: Toxicity: F4N- mouse erythro-leukimic cells, obtained by erythroidal cells, transformed by the Friend virus were used. Physico-chemical studies: UV spectrophotometry (VARIAN CARY100 Scan UV-VIS) and ACD Labs.

Acknowledgements

We thank for the funding provided by UCTM –Sofia, Bulgaria, Research Contract 10508.

References

1. Tsekova DS, Escuder B, Miravet JF. *Cryst Growth Des* **8**: 11-13, 2008.
2. Miravet JF, Escuder B. *Chem Commun* 5796-5798, 2005.
3. Belenky P, Bogan KL, Brenner C. *Trends Biochem Sci* **32**: 12-19, 2007.
4. Niren NM. *Cutis* **77**: 11-16, 2006.
5. Dömling A, Achatz S, Beck B. *Bioorg Med Chem Lett* **17**: 5483-5486, 2007.
6. Timmins GS, Deretic V. *Mol Microbiol* **62**: 1220-1227, 2006.
7. Tantcheva L, Petkov VV, Karamukova G, Abarova S, Y. Chekalarova, Tsekova D, Escuder B, Miravet JF, Lyubomirova K. *Bulg Chem Comm* **38**: 54-57, 2006.
8. *MS Thesis* Makakova E. Sofia University, Chemistry Faculty, Sofia, Bulgaria, 2008.

2-01-104

N-Methylation of cyclic enkephalin analogues

Berezowska, Irena; Weltrowska, Grazyna; Wilkes, Brian C; Lemieux, Carole; Chung, Nga N; Schiller, Peter W*

Clinical Research Institute of Montreal, Lab.of Chemical Biology and Peptide Research, CANADA

**E-mail: irena.berezowska@ircm.qc.ca*

Introduction

Substitution of *N*-methylated amino acids in biologically active peptides enhances their stability against enzymatic degradation and introduces conformational constraints in the peptide backbone, resulting in enhanced conformational integrity. Furthermore, *N*-methylated peptides have a decreased capacity to engage in hydrogen-bonding with water molecules and, consequently, a better ability to cross biological barriers. This is exemplified by the naturally occurring peptide cyclosporine which is orally active. In an effort to improve both the agonist potency and the blood-brain barrier permeability of the cyclic enkephalin peptides H-Tyr-c[D-Cys-Gly-Phe-D(or L)-Cys]NH_2,[1] we synthesized and pharmacologically characterized analogues that contain 2',6'-dimethyltyrosine (Dmt) in place of Tyr1 and are *N*-methylated at Phe4 and/or Cys5.

Results and Discussion

Attempts to prepare *N*-methylated Cys derivatives by direct methylation using CH_3I/NaH or CH_3I/KO*t*Bu afforded products in poor yield. Fmoc-D- or L-Cys(NMe)-OH with *tert*-butyl side chain protection was finally prepared in good yield using the oxazolidinone procedure.[2] Linear precursor peptides were prepared by solid-phase synthesis and disulfide bond formation was performed in solution using $K_3Fe(CN)_6$ as oxidizing agent.

Monomethylation at the Phe[4] residue or at the D- or L-Cys5 residue resulted in compounds that retained subnanomolar μ receptor binding affinity and subnanomolar or low nanomolar δ and κ receptor binding affinities (Table 1). The receptor binding affinities are in agreement with the agonist potencies determined in the guinea pig ileum (GPI) and mouse vas deferens (MVD) assays (IC_{50} values in the subnanomolar to 1 nM range). The two dimethylated analogues also displayed subnanomolar μ receptor binding affinity and high κ receptor binding affinity. One of them, H-Dmt-c[D-Cys-Gly-Phe(NMe)-D-Cys(NMe)]NH_2, showed 6-fold preference for μ receptors over δ receptors, whereas the other one was essentially non-selective. The very high agonist potencies observed with the two dimethylated analogues in the GPI assay reflect their high μ and κ receptor affinities determined in the binding assays. In comparison with the two unmethylated parent peptides, all methylated analogues show similarly high ì receptor binding affinities and agonist potencies in the GPI assay, but somewhat lower μ receptor binding affinities and δ agonist potencies.

A molecular mechanics (energy minimization) study was performed on the "bare" peptide ring structures lacking the exocyclic Dmt residue and the phenyl moiety in the 4-position side chain. For the D- and L-Cys5 parent peptides 69 and 109 low-energy conformers within 3 kcal/mol of the lowest-energy ring structure were found. *N*-methylation at the D- and L-Cys5 residue reduced the number of low-energy conformers to 28 and 16, respectively, and, similarly, for both isomers *N*-methylated at the 4-position 28 low-energy conformers were identified. For the analogues *N*-methylated at both the 4- and the 5-position merely 4 low-energy conformers were obtained for the L-isomer and 9 for the D-isomer. Thus, mono- and dimethylation produced a progressive decrease in conformational flexibility, with the L-Cys(NMe)-containing analogues being structurally more rigid than the corresponding D-Cys(NMe)-containing ones. It can be concluded that progressive conformational restriction of the peptide ring structure in these compounds does not have a major effect on *in vitro* opioid activity.

Acknowledgements

This work was funded by the National Institute on Drug Abuse, NIH (grant DA-004443).

References

1. Schiller PW, Eggimann B, DiMaio J, Lemieux C, Nguyen TM-D. Cyclic enkephalin analogs containing a cystine bridge. *Biochem Biophys Res Commun* **101**: 337-343, 1981.
2. Ruggles EL, Flemer Jr S, Hondal RJ. A viable synthesis of *N*-methyl cysteine. *Bioplymers* (*Peptide Science*) **90**: 61-68, 2008.

Table 1. *In vitro* opioid activity profiles of *N*-methylated cyclic enkephalin analogues

	Receptor binding[a]			GPI	MVD
Compound	**K_i^{μ}, nM**	**K_i^{δ}, nM**	**K_i^{κ}, nM**	**IC_{50}, nM**	**IC_{50}, nM**
Dmt-c[cGF(NMe)c]NH_2	0.496	2.29	0.447	1.07	1.11
Dmt-c[cGF(NMe)C]NH_2	0.354	2.36	0.855	0.457	0.884
Dmt-c[cGFc(NMe)]NH_2	0.504	0.525	0.942	1.81	0.352
Dmt-c[cGFC(NMe)]NH_2	0.586	0.776	1.03	1.36	0.196
Dmt-c[cGF(NMe)c(NMe)]NH_2	0.876	5.51	1.42	1.34	3.72
Dmt-c[cGF(NMe)C(NMe)]NH_2	0.641	1.79	0.875	0.394	1.95
Dmt-c[cGFc]NH_2	0.412	0.202	0.666	0.586	0.0530
Dmt-c[cGFC]NH_2	0.282	0.306	0.677	0.812	0.115

[a]Displacement of [^{3}H]DAMGO (μ-selective) and [^{3}H]DSLET (δ-selective) from rat brain binding sites, and of [^{3}H]U 69,59 (κ-selective) from guinea pig brain binding sites.

2-01-105

A useful scaffold for β-turn scan in peptides. Enkephalin and morphiceptin analogues containing a 4-aminopyroglutamic acid residue.

Kaczmarek, Krzysztof[1,]; Chung, Nga N[2]; Schiller, Peter W[2]*

[1]Technical University of Lodz, Institute of Organic Chemistry, POLAND; [2]Clinical Research Institute of Montreal, Quebec, Laboratory of Chemical Biology and Peptide Res, CANADA

[*]E-mail: kjkaczm@p.lodz.pl

Introduction

Different types of turns are important elements of secondary structure in peptides and proteins. The most common ones are different kinds of β-turns involving four consecutive amino acid residues. The dipeptide unit containing the second and the third residues of such turns exists in the *cis*-conformation. Our *cis*-peptide bond motif 4-aminopyroglutamic acid **1** promotes the β-turn type VI/VI', and can be treated as a hybrid of glycine and alanine. This feature prohibits its utilization as a replacement for any possible dipeptide unit. In order to convert our compound into a more valuable tool for probing the existence of a particular peptide bond in the *cis*-conformation, we have elaborated the synthesis of N-monoalkylated derivatives of 4-aminopyroglutamate residue **2** through a reductive alkylation reaction performed on solid support. Following this idea, we have obtained analogues with *N*-benzylated and *N*-(p-hydroxy)benzylated 4-aminopyroglutamate residues as scaffolds for the Phe-Ala and Tyr-Ala dipeptides units, respectively. This communication is a summary of our long-term project aimed at enkephalin and morphiceptin analogs and contains new results as well as the results previously presented at European and Polish Peptide Symposia.

Results and discussion

We have proposed[1-2] a convenient synthesis of 4-amino-pyroglutamic acid derivatives based on Michael type addition of in situ generated Z-dehydroAla-OMe to enolates prepared from diethyl acylaminomalonates. The crude mixture of the 4 stereoisomers of Z-4-aminopyroglutamic acid was separated through fractional crystallization as Z-*cis* and Z-*trans* racemates. Each of racemates was separately converted into the mixture of diasteomeric salts with cinchonidine and then separated again through fractional crystallization. After removal of the Z-group and introduction of Fmoc protection, we obtained the optically pure derivatives of all four stereoisomers: Fmoc-APy-OH, Fmoc-apy-OH, Fmoc-aPy-OH and Fmoc-Apy-OH. All of them were incorporated into enkephalin amide (positions 1-2, 2-3, 4-5) and morphiceptin (positions 1-2, 3-4). The solid-phase peptide syntheses were performed on a MBHA and/or Rink Amide resin according to standard protocols. After deprotection, the N-terminal amino group of the 4-aminopyroglutamate residue was alkylated by means of 4-(4-benzyloxy)benzaldehyde (*N*-terminal 1-2 analogs) or benzaldehyde (C-terminal 4-5 and 3-4 analogs, respectively) and $NaBH_3CN$ in trimethyl orthoformate, according to a described procedure.[3] The next amino acid (Fmoc-Gly-OH or Fmoc-Pro-OH) was double coupled, because one could expect difficulties in the acylation of the *N*-benzylated amino group due to increased steric hindrance. The biological results obtained with the 4 enkephalin analogs modified in position 2-3 in the guinea pig ileum (GPI) and mouse vas deferens (MVD) assays are shown in the Table 1. Compounds 2-4 are essentially inactive in both assays at concentrations up to 10 μM. However, they are very weak δ partial agonists at this concentration (24%, 38% and 9%, respectively) and compound 2 was very weak μ partial agonist at this concentration (32%). Surprisingly, compound 1 is a weak μ antagonist in the GPI assay with a Ke value of 2940 nM. All N-terminal analogs were essentially inactive, showing no significant agonist or antagonist activity in the guinea pig ileum (GPI) and mouse vas deferens (MVD) assays at concentrations up to 10 μM. A

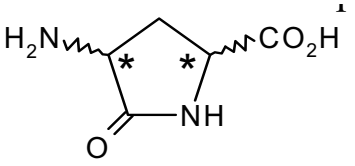

1

(2S,4R)-aPy, (2R,4S)-Apy - trans
(2S,4S)-APy, (2R,4R)-apy - cis

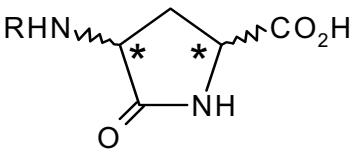

2

R= H, Bzl, (4-OH)-Bzl, ...

Table 1. Guinea pig ileum (GPI) and mouse vas deferens (MVD) assay of opioid peptide analogues. Mean of 3-6 determinations ± SEM. [a]agonist TAPP (H-Tyr-D-Ala-Phe-Phe-NH_2 Determined against the μ [b]P.A. = partial agonist (value in parentheses indicates maximal inhibition of the contractions (%) obtained at a concentration of 10 μM)

Compound	GPI IC_{50}[nM]	MVD IC_{50}[nM]
H-Tyr-(*2S,4R*)-aPy-Phe-Leu-NH_2	K_e = 2940±480 nM[a]	>10 000 inactive
H-Tyr-(*2S,4S*)-APy-Phe-Leu-NH_2	>10 000 (P.A. 32%)[b]	>10 000 (P.A. 24%)[b]
H-Tyr-(*2R,4S*)-Apy-Phe-Leu-NH_2	>10 000 inactive	>10 000 (P.A. 38%)[b]
H-Tyr-(*2R,4R*)-apy-Phe-Leu-NH_2	>10 000 inactive	>10 000 (P.A. 9%)[b]

morphiceptin analog containing the (*S,S*)-motif residue and enkephalin analogs containing (*R,R*) and (*2S,4R*) motifs were totally inactive in the GPI assay, whereas four others only slightly inhibited the electrically evoked contractions to the extent of 8-13% at a concentration of 10 μM. Thus, the latter compounds are extremely weak partial μ agonists. In the MVD assay all analogs were completely inactive at concentrations up to 10 μM except one. The morphiceptin analog containing the *N*-alkylated (*R,R*)-motif residue showed 19% inhibition of the contractions at 10 μM, indicating that it is a very weak partial δ agonist. The most interesting results were obtained in the GPI and MVD assays with analogs modified at the C-terminus (Chart 1).

One of the enkephalin analogues, [N(Bzl)-(*R,R*)-apy$^{4-5}$]- enkephalin amide, has about the same μ agonist potency as Leu-enkephalin in the GPI assay, but is seven times less potent in the MVD assay, indicating that it is less δ-selective than Leu-enkephalin. Two other enkephalin analogs, [N(Bzl)-(*S,S*)-APy$^{4-5}$]- and [N(Bzl)-(*2S,4R*)-aPy$^{4-5}$]-enkephalin, showed weak μ agonist activity in the GPI assay and were inactive in the MVD assay. The fourth enkephalin analog and three morphiceptin analogs were completely inactive at concentrations up to 10 μM in both assays. Only the morphiceptin analog containing the N(Bzl)-(*2S,4R*)-aPy$^{3-4}$ residue turned out to be a weak μ and δ agonist. NMR and molecular modeling studies of the last series of analogs are in progress and the results will be published in a separate communication.

Acknowledgments

This work was supported in part by the Ministry of Science and Higher Education(Poland) grant 2 P05F 345 and NIH (U.S.) grant DA-04443.

References

1. Kaczmarek K, Kaleta M, Chung NN, Schiller PW, Zabrocki J. *Acta Biochim Pol* **48**: 1159-1163, 2001.
2. Kaczmarek K, Chung NN, Schiller PW, Zabrocki J, *Peptides 2002* (*Proceedings of the 27th European Peptide Symposium*), Benedetti E, Pedone C (Eds), Eldizioni Ziino, Napoli, 2002, pp 158-159.
3. Szardenings AK, Burkoth TS, Look GC, Campbell DA. *J Org Chem* **61**: 6720-6722, 1996.
4. Kaczmarek K, Chung NN, Schiller PW. *Peptides 2006* (Proceedings of the 29th European Peptide Symposium, Gdańsk, Poland). Rolka K, Rekowski P, Silberring J (Eds), Kenes International, Geneva, Switzerland, 2007, pp 868-869.

Chart 1. Guinea pig ileum (GPI) and mouse vas deferens (MVD) assays of N-alkylated 4-5 enkephalin and 3-4 morficeptin analogs

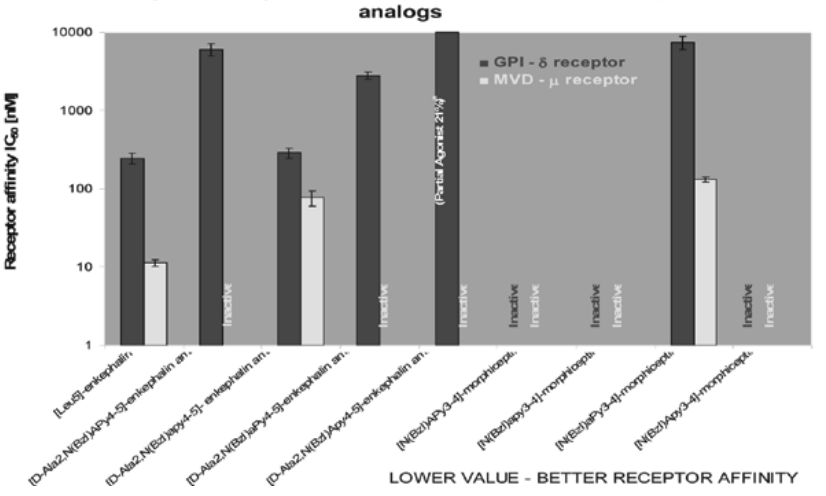

2-01-106

Modifications of the Myelin Basic Protein epitope MBP87-99 divert Th2 to Th1: Immune responses in peripheral blood mononuclear cells (PBMC) from Multiple Sclerosis patients.

Deraos, George[1]; Chatzantoni, Kokona[2]; Matsoukas, Minos-Timotheos[1]; Katsara, Maria[1]; Tselios, Theodore[1]; Deraos, Spyros[1]; Papathanasopoulos, Panagiotis[3]; Vynios, Dimitrios[1]; Apostolopoulos, Vasso[4]; Mouzaki, Athanasia[2]; Matsoukas, John M[1,]*

[1]University of Patras, Chemistry, GREECE; [2]University of Patras, Medical School, GREECE; [3]University of Patras, Medical School, GIBRALTAR; [4]Burnet Institute, Immunology and Vaccine Lab, AUSTRALIA

[*]E-mail: imats@chemistry.upatras.gr

Abstract

Derangement of cellular immunity is central in the pathophysiology of multiple sclerosis (MS) and it is often manifested by abnormal patterns of cytokine production. Herein we investigated cytokine secretion in peripheral blood mononuclear cells (PBMC) of 18 MS patients and 15 controls, and attempted to correlate cytokine polarization with the nature of the antigenic stimulus. To this end, we synthesized two novel citrullinated peptide analogs, linear [Cit91, Ala96, Cit97]MBP87-99 and cyclo(87-99)[Cit91, Ala96, Cit97]MBP87-99 that resulted from citrullination of 91, 97 Arg residues in MBP87-99 epitope antagonists, linear [Arg91, Ala96] MBP87-99 and cyclo(87-99) [Arg91, Ala96]MBP87-99 peptides respectively. We cultured PBMC from MS patients and control subjects with the citrullinated peptides and, also, with other non-citrullinated MBP peptides, and investigated the effect of the peptides on cytokine secretion. We suggest that citrullination of self-antigens may potentially trigger disease in susceptible individuals. This finding may open new avenues in drug design and synthesis of new substances that inhibit citrullination and, thus, arrest epitope spreading and worsening of MS. Introduction Multiple sclerosis (MS) a is a chronic disorder of the central nervous system which is predominantly characterized by local T cell and macrophage infiltration, leading to demyelination and loss of neurologic function.[1] MS is an autoimmune disease triggered by CD4+ T cells, although auto antibodies cannot be excluded. Antigens within the myelin sheath, such as, myelin basic protein (MBP), proteolipid protein and myelin oligodendrocyte glycoprotein[2,3] have been described as the main constituents of which self reactive CD4+ T cells and auto-antibodies are directed against. Altered peptide ligands (APL) are usually defined as analogs derived from the native, wild type peptide, which, carry amino acid mutations at T cell receptor (TCR) contact residues.[4] Some of these APL (also known as - mutant or antagonist peptides) are able to specifically antagonize and/or inhibit T cell activation induced by the wild type immunogenic (agonist) peptide4. Furthermore, peripheral blood mononuclear cells (PBMC) from healthy and MS patients cultured with P6 and P7 significantly increased the Th2/Th1 cytokine ratio. Numerous studies have implicated the role of citrullination of self-peptides in the pathogenesis of autoimmune diseases including MS 2. Citrullination is the conversion of Arg to citrulline (Cit) resulting in the positive charge of Arg side chain into neutral. Thus, given the high amount of citrullinated MBP protein in MS patients brain tissue, a preferential response to MBP newly formed citrullinated peptides may be present and could contribute to disease. Herein, we describe the conversion of linear and cyclic MBP87-99 APLs, P6 and P7 respectively, to their citrullinated analogs cP6 ([Cit91, Ala96, Cit97]MBP87-99) and cP7 (cyclo(87-99)[Cit91, Ala96, Cit97]MBP87-99), and their effects on cytokine stimulation by PBMC isolated from MS patients and control subjects. It is demonstrated that the APLs, P6 and P7, in their citrullinated form (cP6 and cP7) results in the polarization of Th1 cytokines in MS patients PBMC. Hence, indicating that citrullination of MBP peptides may trigger disease. Furthermore, molecular modeling was used to gain insights into the actions noted by the citrullinated peptides.

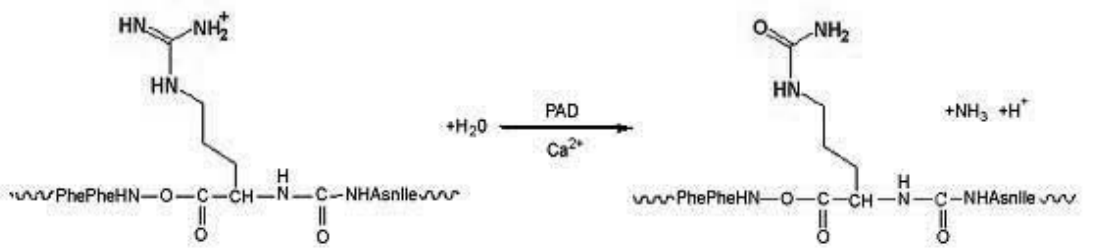

Results

Cytokine secretion investigations were included in the evaluation study herein of linear and cyclic APL (P6 and P7) and were compared to their citrullinated converted analogs (cP6 and cP7). The results of the present study strongly support the long suspected importance of citrullination as a major mechanism in triggering autoimmune / inflammatory diseases such as MS. In particular, culture of PBMC from MS patients with citrullinated analogs, cP6 and cP7, increased the secretion of IL-2 and IFN-α and simultaneously decreased the secretion of IL-10, charectheristic of Th1 polarization. On the contrary, the non-citrullinated linear APL peptide P6 induced the production of IL-10 and reduced the production of IL-2 and IFN-α characteristic of Th2 polarization. Cyclic APL peptide P7, however, stimulated IFN-α but simultaneously IL-10 was also induced. These findings, indicate that citrullination of APL (antagonistic) peptides from MBP87-99 immunodominant peptide, leading to Th1 dominance, may have implications in exacerbations or triggering disease.

References

1. Holmoy T, Hestvik AL. Multiple sclerosis: immunopathogenesis and controversies in defining the cause. *Curr Opin Infect Dis* **21**: 271-278, 2008.
2. Polman, C. H.; Uitdehaag, B. M. New and emerging treatment options for multiple sclerosis. *Lancet Neurol* **2**: 563-566, 2003.
3. Steinman L. Multiple sclerosis: a coordinated immunological attack against myelin in the central nervous system. *Cell* **85**: 299-302, 1996.
4. Evavold BD, Sloan-Lancaster J, Allen PM. Tickling the TCR: selective T-cell functions stimulated by altered peptide ligands. *Immunol Today* **14**: 602-609, 1993.

2-01-107

Solid-Phase Synthesis and Effects of Amino Acid and Peptide Analogs of Non-Protein Amino Acid Canavanine on Nociception

Dzimbova, Tatiana[1,]; Djambazova, Elena[2]; Bocheva, Adriana[2]; Pajpanova, Tamara[1]; Golovinsky, Evgeny[1]*

[1]Institute of Molecular Biology, BULGARIA; [2]Medical University, Dept. of Pathophysiology, BULGARIA

[*]E-mail: tania_dzimbova@abv.bg

Introduction

Non-protein amino acids have been widely used as components of peptides to enhance biological activity, proteolytic stability, and bioavailability. It is well known that unnatural amino acids with guanidine functionality exhibit diverse pharmacological effects when introduced in biologically active systems. Our previous efforts were focused on the preparation and the characterization of unnatural amino acids, particularly those containing a basic functionality in the side chain. We have synthesized numerous unnatural amino acids, structural analogues of arginine and lysine, which demonstrated certain biological effects.[1,2] Recently, as part of our ongoing research focused on the search of novel arginine mimetics, we developed an efficient approach for solid-phase synthesis of unnatural oxyamino acid nor-canaline (NCan) and oxyguanidino acid nor-canavanine (NCav) (Fig. 1). Next we studied the possibilities of introducing NCan and NCav into the molecule of biologically active peptides. We also studied their antinociceptive activity on the most frequently used models based on tests with thermal and mechanical irritation.

Results and Discussion

A representative scheme on Fig.2 summarizes synthetic route for obtaining the target compound NCav. For the protection of amino group of serine a phenacetyl protecting group was used.[3] For this end, we found that enzymatic protecting group techniques are efficient methods for the selective protection/deprotection of the amino acid. After loading of Ser to the resin, activation of hydroxyl group was achieved using the MeSO2Cl.[4] The introduction of aminooxy group was obtained under Mitsunobu conditions with N-hydroxylphthalimide.[5,6] Removing of the phthalimide group leads to protected nor-canaline derivative. Obtained compound could be cleaved from the resin with 95% TFA. Enzymatic hydrolysis under the action of penicillin amidase provided globally-unprotected desired product. Reactions could be continued on the solid-phase support using 1-H-pyrazol-1(N,N`-bis-Boc)- carboxamidine for guanilation of nor-canaline[7] afforded the protected nor-canavanine derivative. Cleavage of the derivative from the resin followed by enzymatic hydrolysis of *N*-protected group provided the final nor-canavanine.

Encouraged by the previous findings, we adopted the similar solid support approach for the synthesis of model peptides containing nor-canaline. We successfully applied Mitsunobu conditions to introduce aminooxy group in the model tetrapeptide containing Ser-residue (Fig.3).

Next we examined for analgesic activity obtained new compounds. The antinociceptive effects were evaluated using the paw pressure (PP), the hot plate (HP) and tail

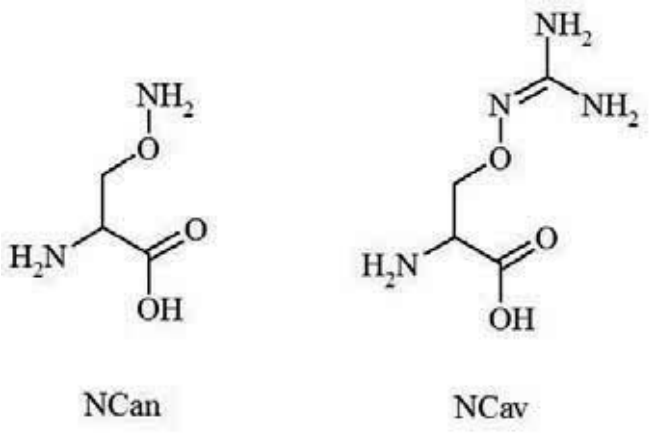

Figure 1. Nor-Canaline (NCan) and nor-Canavanine (NCav).

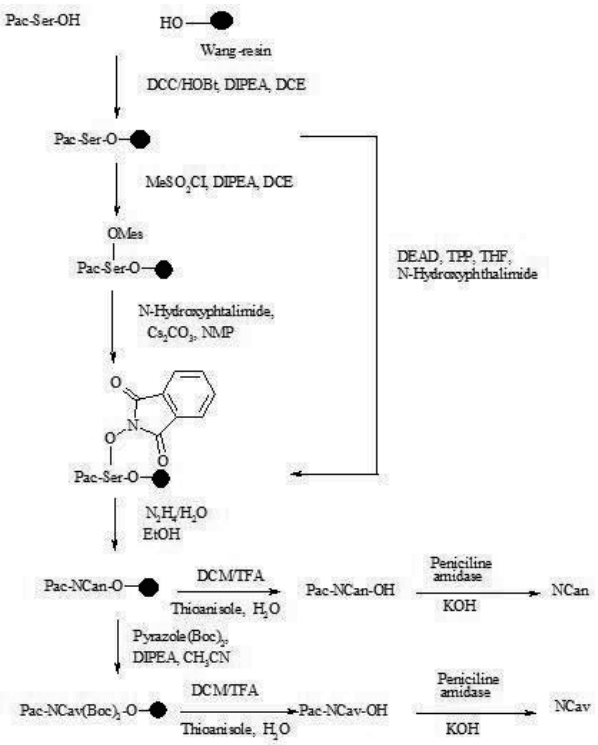

Figure 2. Solid-phase synthesis of NCan and NCav.

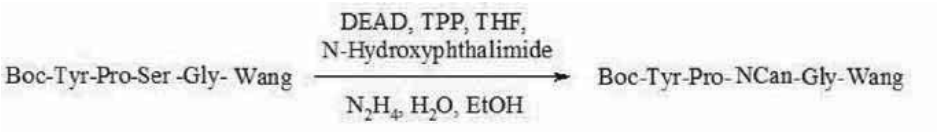

Figure 3. Solid-Phase synthesis of NCan containing peptide.

flick (TF) tests. Our data shows that nor-canavanine and model peptide exerted naloxone-reversible antinociception by paw-pressure test. Conclusions In conclusion, the practical synthesis of aminooxy and guanidinooxy containing amino acid analogues has been reported herein. These NCav analogues can be synthesized on a solid phase support, easily and in a good yield. In addition, aminooxy group could be introduced in peptides containing Ser. NCav showed pronounced analgesic effects. Most probably the stronger and prolonged antinociceptive effects are due to enhanced bioavailability and metabolic stability of the molecule.

Acknowledgments

This work was partially supported by the National Science Fund of the Bulgarian Ministry of Education and Science, Grant MU-FS-13/07.

References

1. Videnov G, Aleksiev B, Stoev M, Pajpanova T, Jung G. *Liebigs Ann Chem* **9**: 941-945*,* 1993.
2. Dzimbova T, Pajpanova T, Tabacova S, Golovinsky E. *5th Hellenic Forum on Bioactive Peptides*, TYPORAMA, Greece, Cordopatis P (Ed.) pp 223, 2007.
3. Fuganti C, Grasseli P, Casati P. *Tetrahedron Lett* **22**: 3191-3194, 1986.
4. Richter LS, Desai M. *Tetrahedron Lett* **38**: 321-324, 1992.
5. Tomczuk B, Tianbao L, Sol RM, Fedde C, Wang A, Murphy L, Crysler C, Dasgupta M, Eisennagel S, Spulino J, Bone R. *Bioorg Med Chem Lett* **13**: 1495-1498, 2003.
6. Barlos K, Papaioannou D, Sanida C. *Liebigs Ann Chem* **2**: 287-291, 1986.
7. Drake B, Patek M, Lebl M. *Synthesis* **6***:* 579-582, 1994.

2-01-108

Synthesis of β^2-amino acids and their application in endomorphin analogues

Tymecka, Dagmara[1,]; Kosson, Piotr[2]; Lipkowski, Andrzej W.[2]; Misicka, Aleksandra[1]*

[1]Faculty of Chemistry, University of Warsaw, POLAND; [2]Medical Research Centre, Polish Academy of Sciences, POLAND

[*]E-mail: dulok@chem.uw.edu.pl

Introduction

A major challenge in opioid peptide chemistry is the synthesis of novel compounds mimicking the endogenous peptide ligands. These new peptidomimetics should be biologically active and more stable against enzymatic degradation than their parent ligands. One of the possibilities is the introduction of β-amino acids into the peptide's sequence. Monosubstituted β-amino acids (β^2- or β^3-) due to their similarity in structure to α-amino acids, moreover their tendency to give folded structures even in short peptides and to the stability towards mammalian peptidases may be very useful in the creation of the new potentially active compounds.[1] We focused our attention on developing a method for the synthesis of different β^2-amino acids (as homologues of α-amino acids) as elements for the synthesis and the SAR study of endomorphin analogues. As templates: endomorphin-1, -2 and its D-Ala^2-analogue (TAPP) have been used.[2,3] Small library has been created in which α-amino acids in every position with exception of Pro were substituted by their respective β^2-analogues.

ENDOMORPHIN-1 (EM-1) H-Tyr-Pro-Trp-Phe-NH_2
ENDOMORPHIN-2 (EM-2) H-Tyr-Pro-Phe-Phe-NH_2
TAPP H-Tyr-D-Ala-Phe-Phe-NH_2

Results

The fully protected β^2-amino acids were obtained in two-step method based on the conversion of methyl cyanoacetate to the desired products (Fig. 1). The first step of the procedure was the alkylation of methyl cyanoacetate with a various alkyl halides (for aliphatic path) or the Knoevenagel condensation of methyl cyanoacetate and aromatic aldehydes (for aromatic path). The second step, which involved reduction and then *N*-Boc protection of the resulting first step-products, was performed in one-pot. $CoCl_2$-$NaBH_4$ combination was used as a reducing agent in MeOH as a solvent.[4] The fully protected β^2-homo-amino acids (Boc-β^2hXaa-OMe) were formed in satisfactory overall yields (37-58%).

In two cases - β^2hPhe and β^2hAla - the resulting racemic mixtures were successfully separated into amino acid enantiomers via diastereomeric amides using (*S*)-(-)-1-phenylethylamine as the resolving agent. All of peptides were synthesized in the solution (fragment condensation strategy). The final analogues were isolated by HPLC method. In four cases (analogues 2,3 and 9,10) we were not able to separate the diastereoisomers and bindings assays were performed for diastereomeric mixtures. The receptor affinities of the obtained opioid tetrapeptides containing β^2-amino acids for μ-opioid receptor were measured and compared to those of endomorphins and TAPP (Table 1).

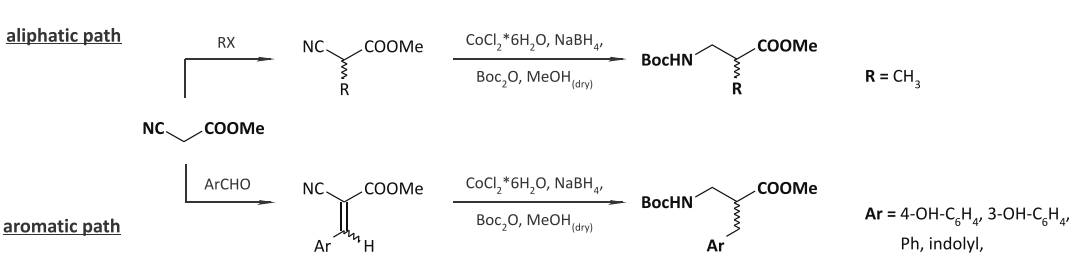

Figure 1. Synthesis of *N*-Boc-protected β^2-amino acid esters.

Table 1. Binding affinities of endomorphins and their analogues.

No	Peptide sequence	IC_{50} μ ± S.E.M. [nM][a]
1	**H-Tyr-Pro-Trp-Phe-NH_2 (EM-1)**	**4.07 ± 3.8**
2	H-(***R,S***)-**β²hTyr**-Pro-Trp-Phe-NH_2	151.3 ± 3.7
3	H-(***R,S***)-**β²h-*m*-Tyr**-Pro-Trp-Phe-NH_2	**6.2 ± 4.4**
4	H-Tyr-Pro-(***R* or *S***)-**β²hTrp**-Phe-$NH_{2\ more\ polar}$	>1000 ± 2.8
5	H-Tyr-Pro-(***R* or *S***)-**β²hTrp**-Phe-$NH_{2\ less\ polar}$	no response
6	H-Tyr-Pro-Trp-(***R***)-**β²hPhe**-NH_2	162.0 ± 2.9
7	H-Tyr-Pro-Trp-(***S***)-**β²hPhe**-NH_2	77.6 ± 3.1
8	**H-Tyr-Pro-Phe-Phe-NH_2 (EM-2)**	**6.5 ± 2.8**
9	H-(***R,S***)-**β²hTyr**-Pro-Phe-Phe-NH_2	467.7 ± 2.5
10	H-(***R,S***)-**β²h-*m*-Tyr**-Pro-Phe-Phe-NH_2	128.8 ± 3.5
11	H-Tyr-Pro-(***R***)-**β²hPhe**-Phe-NH_2	97.7 ± 4.4
12	H-Tyr-Pro-(***S***)-**β²hPhe**-Phe-NH_2	>1000 ± 2.6
13	H-Tyr-Pro-Phe-(***R***)-**β²hPhe**-NH_2	72.4 ± 1.9
14	H-Tyr-Pro-Phe-(***S***)-**β²hPhe**-NH_2	**38.0 ± 2.6**
15	**H-Tyr-D-Ala-Phe-Phe-NH_2 (TAPP)**	**5.1 ± 3.5**
16	H-(***R* or *S***)-**β²hTyr**-D-Ala-Phe-Phe-$NH_{2\ more\ polar}$	338.8 ± 5.1
17	H-(***R* or *S***)-**β²hTyr**-D-Ala-Phe-Phe-$NH_{2\ less\ polar}$	77.6 ± 2.4
18	H-(***R* or *S***)-**β²h-*m*-Tyr**-D-Ala-Phe-Phe-$NH_{2\ more\ polar}$	11.2 ± 6.3
19	H-(***R* or *S***)-**β²h-*m*-Tyr**-D-Ala-Phe-Phe-$NH_{2\ less\ polar}$	48.9 ± 2.3
20	H-Tyr-(***R***)-**β²hAla**-Phe-Phe-NH_2	954.9 ± 2.9
21	H-Tyr-(***S***)-**β²hAla**-Phe-Phe-NH_2	>1000 ± 2.8
22	H-Tyr-D-Ala-(***R***)-**β²hPhe**-Phe-NH_2	95.4 ± 2.5
23	H-Tyr-D-Ala-(***S***)-**β²hPhe**-Phe-NH_2	15.5 ± 2.5
24	H-Tyr-D-Ala-Phe-(***R***)-**β²hPhe**-NH_2	1.9 ± 2.4
25	H-Tyr-D-Ala-Phe-(***S***)-**β²hPhe**-NH_2	7.76 ± 4.0

[a] μ-ligand: [^{3}H] DAMGO

Conclusions

Incorporation of *β*-homo-amino acids in endomorphin sequence changed (through additional -CH_2- in the peptide backbone) the relationship of the distance between the pharmacophore elements of endomorphins and TAPP (Tyr[1], Phe[3]/Trp[3] and/or Phe[4]).

In results:

- μ-affinity of the analogues containing (*R*)- and (*S*)-*β*²hPhe (or *β*²hTrp for EM-1) in position 3 or 4 in endomorphins was decreased,
- *μ*-affinity of the analogues containing >)-*β*²hPhe in position 3 (only isomer *S*) or 4 in the TAPP compound was retained. This may suggest that the TAPP molecule is more flexible (than endomorphins) and can easier adopt the biologically active conformation with additional changes in the structure, especially in the 4th position,
- substitution of Tyr>[1] in opioid peptides with respective β²-homo-amino acids requires simultaneous change of position of hydroxyl group on aromatic ring from *para* (*β*²hTyr) to *meta* (*β*²h-*m*-Tyr) position. Such change gives the possibility for mimicking the tyramine moiety, which occurs in the alkaloid-opioid system.

Acknowledgements

Project supported by EU grant Normolife (LSHC-CT-2006-037733).

References

1. Juaristi E, Soloshonok VA. *Enantioselective synthesis of β-amino acids 2nd Edition*, John Wiley & Sons Inc, 2005.
2. Zadina JE, Hackler L, Ge L-J, Kastin AJ. *Nature* **386**: 499-502, 1997.
3. Schiller PW, Nguyen TM-D, Chung NN, Lemieux C. *J Med Chem* **32**: 698-703, 1989.
4. Caddick S, Judd DB, de KLewis AK, Reich MT, Williams MRV. *Tetrahedron* **59**: 5417-542, 2003.

2-01-109

Non-Protein Amino Acid Analogues of Melanocyte Inhibiting Factor (MIF-1): Synthesis and Effects of Nociception

Kalauzka, Rositsa[1]; Dzimbova, Tatiana[1,]; Djambazova, Elena[2]; Bocheva, Adriana[2]; Pajpanova, Tamara[1]*

[1]Institute of Molecular Biology, BULGARIA; [2]Medical University, Dept. of Pathophysiology, BULGARIA

[*]E-mail: tania_dzimbova@abv.bg

Introduction

MIF-1 (L-Prolyl-L-Leucyl-Glycine amide, PLG) is a brain peptide, presented in hypothalamic tissue, as well as the C-terminal tripeptide of the neurohypophiseal hormone oxytocin and inhibits the release of melanocyte-stimulating hormone (MSH) in some systems. Recently, some chemical modifications of MIF-1 to enhance opiate agonist/antagonist actions as well as binding activity of analogues have been reported. On the other hand, the concept of structural modification in peptide fragments to confer them specific properties is of current interest in the study and design of new bioactive targets. A well known example is the incorporation of unnatural amino acids into the molecule of natural biologically active peptides leading to analogues with significant theoretical and practical importance. With this idea in mind we studied possibilities of introducing unnatural amino acids canaline (Can), nor-canaline (NCan), canavanine (Cav), nor-canavanine (NCav) and sLys into MIF-moiety in order to achieve a better analgesic effect. We also studied their antinociceptive activity on the most frequently used models based on tests with thermal and mechanical irritation during acute pain.

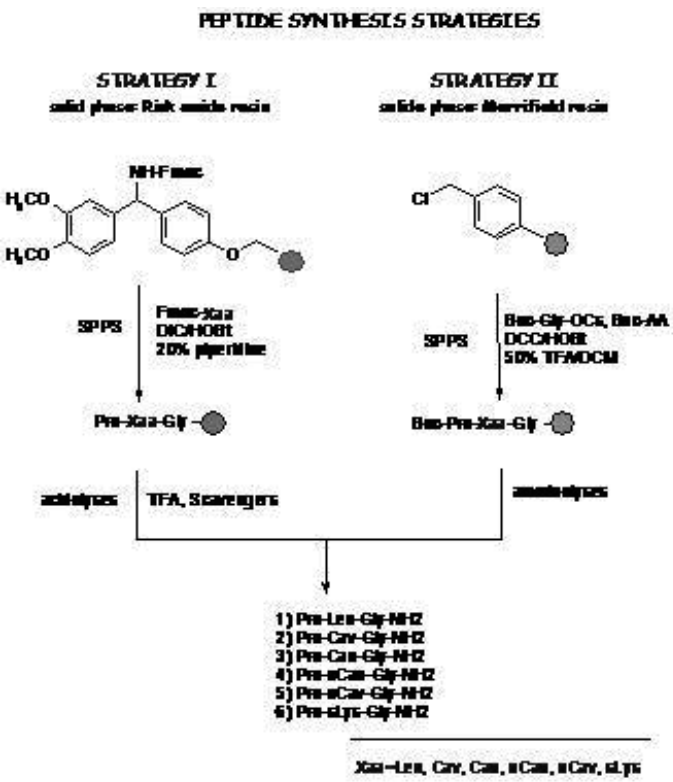

Figure 1. Solid-phase synthesis of MIF-1 analogues.

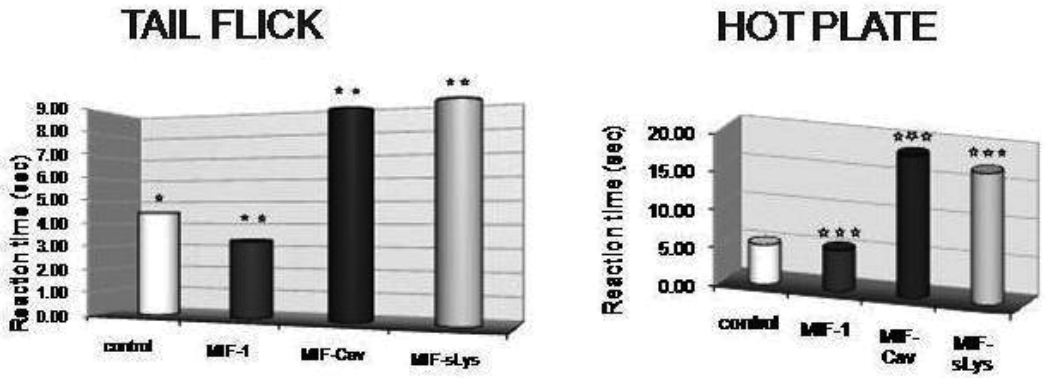

Figure 2. Effects of MIF-1 and analogues (1 S.E.M.; *P±mg/kg, i.p.) on nociception.

Results and Discussion

To obtain the peptide mimetics manual stepwise solid phase techniques was applied (Fig. 1). The modification included MIF-1 analogues 1-6 where Leu was replaced with Cav, Can, nCav, nCan and sLys. The peptides were synthesized on a Rink-amide resin using Fmoc-strategy with DIC/HOBt activation and Merrifield resin using Boc-strategy with DCC/HOBt activation. The crude peptides were purified by preparative TLC and their purity was checked by analytical HPLC. The precise molecular mass was confirmed by ESI-MS.

Antinociceptive effects were evaluated using tail flick (TF) and hot plate (HP) tests. The experiments were carried out on male Wistar rats (180-200g) housed at 12 h light/dark cycle. Food and water were available ad libitum. All experiments were carried out between 09.00 a.m./12.00 p.m. Each group included 8-10 rats. MIF-1 and analoguese (all in dose 1 mg/kg) were dissolved in sterile saline (0.9% NaCl) solution and were injected intraperitoneally (i.p.). The experimental procedures were carried out in accordance with the institutional guidance and general recommendations on the use of animals for scientific purposes. The results were statistically assessed by one-way analysis of variance (ANOVA).

Data are presented as mean <0.01, ** P<0.01 versus control; +P<0.01, P<0.01 versus each of peptides. It was found that substitution of Leu in position 2 of MIF-molecule by unnatural amino acids increased the pain threshold. The analgesic effect with Cav-substitution was highest, whereas parent MIF-1 showed only a minute increase of pain-threshold.

Conclusions

In conclusion it could be suggested that:

o The newly synthesized analogues exhibit naloxone-reversible antinociceptive activity.

o Opioid receptors, especially μ-receptor are involved in antinociceptive action.

o Substitution of leucine in position 2 of MIF-1 molecule by non-protein amino acids (sNle and Cav) significantly increased the analgesic effect of the newly synthesized MIF-1 analogue.

Acknowledgments

This work was partially supported by the National Science Fund of the Bulgarian Ministry of Education and Science, Grant MU-FS-13/07.

References

1. Kastin AJ, Olson RD, Ehrensing RH, Berzas MC, Schally AV, Coy DH. *Pharmac Biochem Behav* **11**: 721-723, 1979.
2. Erchegyi J, Zadina JE, Qui X-D, Kersch D-C, Ge L-J, Brown MM, Kastin AJ. *Pept Res* **6**: 31-38, 1993.
3. Pajpanova T, Bocheva A, Golovinsky E. *Methods Find Exp Clin Pharmacol* **21**: 591-594, 1999.

2-01-110

Design And Synthesis Of New Peptide Mimetics With Potential *β*-secretase Inhibition Activity

Ivanov, Ivan[1]; Danalev, Dantcho[1]; Vezenkov, Lyubomir[2,]*

[1]University of Chemical Technology and Metallurgy, Organic Chemistry, BULGARIA; [2]University of Chemical Technology and Metalurgy, Organic Chemistry, BULGARIA

[*]E-mail: lvezenkov@yahoo.com

Alzheimer's disease (AD) is affected around 20 millions people worldwide. The last forecast shows that during the next 20-30 years their number will double because of the human life span increasing. The transformation of amyloid *β* (Aβ) soluble form into insoluble *β*-fibers is a critical stage in the AD progression.The process of Aβ formation starts with four cleavages of this protein catalyzed by different proteinases named *α*, *β* and *γ*-secretases. The cleavage in Aβ1 and Aβ11 is catalyzed by the enzyme *β*-secretase. Last ten years are plenty of different investigations on the *β*-secretase inhibition process. The investigation of Tung *et al*. revealed that the shortest peptide structure with *β*-secretase inhibition activity is EVDLA.[1] Their experiments show the role of different amino acids for the inhibition activity. They investigate the activity of derivatives based on the sequence Boc-VDLAVE(P3')F(P4')-OH. They succeed to increase *β*-secretase inhibition activity replacing C-terminal amino acids at P3' and P4' position by benzylamin. The other potential residue they determined is pyridinylmethylamine (IC^{50}=70 nM).[1] Because of better activity of the compounds with benzylamine C-terminus in our new structures the same fragment as C-terminal residue was used.

Based on the information mentioned above the design of peptide mimetics including minimal substrate subunits with C-terminal benzylamine and 3,4-dimethoxybenzylamide functions was done. Ten peptide mimetics with potential *β*-secretase inhibition activity were synthesized by means of peptide synthesis in solution according to the schemes 1 and 2: DLA/or*β*-AV-NH-Bzl; Boc-LDLA/or *β*-AV-NH-Bzl; DLDLA/or *β*-AV-NH-Bzl; Boc-LDLA/or *β*-AV-3,4-dimethoxybenzylamide; DLDLA/or *β*-A)

Scheme 1. Synthesis of DLDL A (or *β*-A)V-NH-BZl

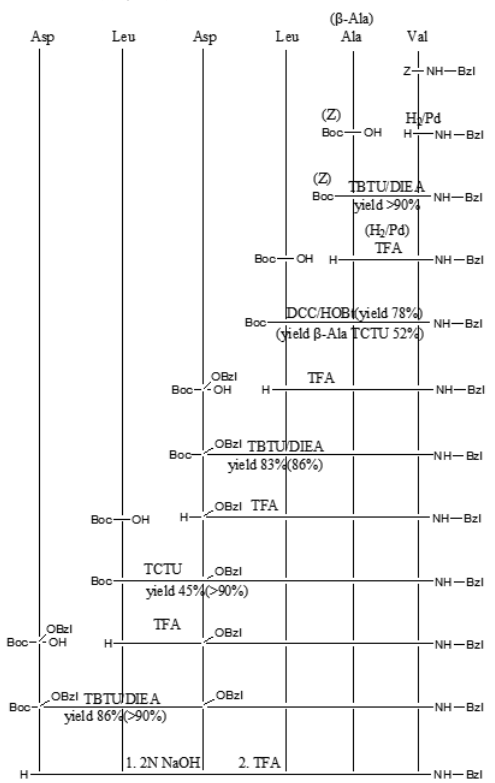

Scheme 2. Synthesis of DLDL A (or *β*-A)V-3,4-dimethoxybenzylamide

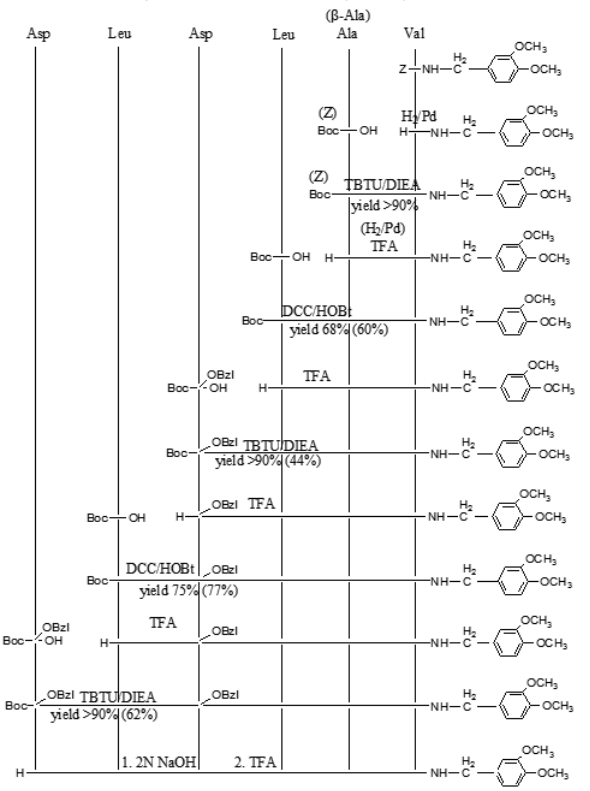

Table 1. Melting points and $[\alpha]^{22}_{546}$ of the newly synthesized products.

N	Product	M.p. [°C]	$[\alpha]^{22}_{546}$ [°]
1	Z-Val-NH-Bzl	167-169	- 40
2	Boc-Ala-Val-NH-Bzl	164-166	- 120
3	Z-*β*-Ala-Val-NH-Bzl	184-186	-
4	Boc-Leu-Ala-Val-NH-Bzl	139-141	- 130
5	Boc-Leu-*β*-Ala-Val-NH-Bzl	169-171	- 40
6	Boc-Asp(OBzl)-Leu-Ala-Val-NH-Bzl	121-123	- 0.2*
7	Boc-Asp(OBzl)-Leu-*β*-Ala-Val-NH-Bzl	124-126	+ 40
8	Boc-Leu-Asp(OBzl)-Leu-Ala-Val-NH-Bzl	197-199	-
9	Boc-Leu-Asp(OBzl)-Leu-*β*-Ala-Val-NH-Bzl	200-201	-
10	Boc-Asp(OBzl)-Leu-Asp(OBzl)-Leu-Ala-Val-NH-Bzl	193-195	-
11	Boc-Asp(OBzl)-Leu-Asp(OBzl)-Leu-*β*-Ala-Val-NH-Bzl	191-193	- 10
12	Asp-Leu-Ala-Val-NH-Bzl	119-121	- 50
13	Asp-Leu-*β*-Ala-Val-NH-Bzl	152-154	+ 30
14	Boc-Leu-Asp-Leu-Ala-Val-NH-Bzl	125-127	+ 30
15	Boc-Leu-Asp-Leu-*β*-Ala-Val-NH-Bzl	123-125	+ 20
16	Asp-Leu-Asp-Leu-Ala-Val-NH-Bzl	117-119	+ 40
17	Asp-Leu-Asp-Leu-*β*-Ala-Val-NH-Bzl	114-116	+ 60
18	Z-Val-3,4-dimethoxybenzylamide	144-146	-
19	Boc-Ala-Val-3,4-dimethoxybenzylamide	151-153	- 90
20	Z-*β*-Ala-Val-3,4-dimethoxybenzylamide	187-189	-
21	Boc-Leu-Ala-Val-3,4-dimethoxybenzylamide	183-185	- 60
22	Boc-Leu-*β*-Ala-Val-3,4-dimethoxybenzylamide	169-171	- 20
23	Boc-Asp(OBzl)-Leu-Ala-Val-3,4-dimethoxybenzylamide	178-180	- 10
24	Boc-Asp(OBzl)-Leu-*β*-Ala-Val-3,4-dimethoxybenzylamide	191-193	+ 36
25	Boc-Leu-Asp-Leu-Ala-Val-3,4-dimethoxybenzylamide	136-138	-
26	Boc-Leu-Asp-Leu-*β*-Ala-Val-3,4-dimethoxybenzylamide	210-212	-
27	Asp-Leu-Asp-Leu-Ala-Val-3,4-dimethoxybenzylamide	amorphus	-
28	Asp-Leu-Asp-Leu-*β*-Ala-Val-3,4-dimethoxybenzylamide	217-219	-

For all compounds $[\alpha]^{22}_{546}$ [°] is for C 1 MeOH except *C 0.5 MeOH.

V-3,4-dimethoxybenzylamide. All newly synthesized compounds were characterized by TLC, mp and $[\alpha]_{546}{}^{22}$ (Table 1). Their structures were proved by ES-MS. The purity of all compounds was monitored by TLC in the systems: $CHCl_3$:AcOH 9:1 (v/v); n-BuOH:AcOH:H_2O 3:1:1 (v/v/v) and pyridine:n-BuOH:AcOH:H_2O 1:1,5:0,3:1,2 (v/v/v/v) Initially fragment condensation for all aim peptides was tried. Because a lot of secondary product obtaining during of these reactions all newly compounds were synthesized by stepwise addition of amino acids from C- to N-terminus. The best results according to the condensation agent and yields are presented on the schemes. The biological trials of all newly synthesized compounds are in progress.

Acknowledgements

This work is supported with Ministry of Education grant BY-16.

References

1. Tung JS, Davis DL, Anderson JP, Walker DE, Mamo S, Jewett N, Hom RK, Sinha S, Thorsett ED, John V. *J Med Chem* **45**: 259-262, 2002.

2-01-111

Oostatic peptides containing D-amino acids: Activity and degradation in the flesh fly *Neobellieria bullata*

Bennetová, Blanka[1,]; Slaninová, Jiřina[2]; Cerný, Bohuslav[3]; Vlasáková, Vera[4]; Holík, Josef[4]; Tykva, Richard[2]; Hlaváček, Jan[2]*

[1]Institute of Entomology, CAS, 370 05 Ceské Budejovice, CZECH REPUBLIC; [2]Institute of Organic Chemistry and Biochemistry CAS, 166 10 Prague 6, CZECH REPUBLIC; [3]1st Faculty of Medicine, Charles University, 116 16 Prague 2, CZECH REPUBLIC; [4]Institute of Experimental Botany, CAS,142 20 Prague 4, CZECH REPUBLIC

[*]E-mail: blanka@entu.cas.cz

Introduction

Oostatic peptide H-Tyr-Asp-Pro-Ala-Pro-OH (1a) is the C-terminus shortened analogue of decapeptide H-Tyr-Asp-Pro-Ala-Pro-Pro-Pro-Pro-Pro-Pro-OH (1b) that was originally isolated from mosquito *Aedes aegypti.*[1] The 1a inhibits development of eggs in the flesh fly *Neobellieria bullata* by decreasing the egg hatchability and changing its structure.[2-3] In this study, our interest was focused on the oostatic activity of analogues of pentapeptide 1a, containing corresponding D-amino acid residues (2a-2f) and elucidation of their degradation in the flesh fly *Neobellieria bullata* using tritium labeled compounds 4a-4c, prepared from $^{\Delta}$Pro precursors 3a-3c:[4,5] H-Tyr-Asp-Pro-Ala-D-Pro-OH (2a), H-Tyr-Asp-Pro-D-Ala-Pro-OH (2b), H-Tyr-Asp-D-Pro-Ala-Pro-OH (2c), H-Tyr-D-Asp-Pro-Ala-Pro-OH (2d), H-D-Tyr-Asp-Pro-Ala-Pro-OH (2e), H-D-Tyr-D-Asp-D-Pro-D-Ala-D-Pro-OH (2f), H-Tyr-Asp-$^{\Delta}$Pro-Ala-Pro-OH (3a), H-Tyr-Asp-$^{\Delta}$Pro -D-Ala-Pro-OH (3b), H-Tyr-D-Asp-$^{\Delta}$Pro Ala-Pro-OH (3c), H-Tyr-Asp-[^{3}H]Pro-Ala-Pro-OH (4a), H-Tyr-Asp-[^{3}H]Pro-D-Ala-Pro-OH (4b), H-Tyr-D-Asp-[^{3}H]Pro-Ala-Pro-OH (4c).

Results and Discussion

Peptide sequences 2a-2f and 3a-3c were assembled on 2-chlorotrityl polystyrene resin, compatible with C-terminal Pro residue, using Fmoc/OtBu strategy. Fmoc deprotection was performed by 20% piperidine in DMF and the coupling by DIC/HOBt in DMF. The simultaneous side-chain deprotection and detachment of peptides from the resin were carried out by a TFA/TIS (10:1) mixture for 30 min. Radiolabeled peptides 4a-4c were obtained by addition of tritium to double bond of $^{\Delta}$Pro residue in peptides 3a-3c, in the presence of $PdO/BaSO_4$. The oostatic activity assay of peptides 2a-2f has shown a significant decrease of hatchability in the 1st gonotrophic cycle in comparison with parent 5P (1a) and no hatchability in the 2nd gonotrophic cycle. Morphology changes in ovaries are linked to a large resorption (2d-2f) of the eggs of treated fly. Even low resorption (2a-2c) interferes with the eggs development, so that hatching is impossible (Table 1). Histological pictures of degenerative morphological changes (resorption) in female reproductive system of *Neobellieria bullata* (2nd gonotrophic cycle) with time show normal follicular cells in egg chamber forming a layer around oocyte and trophocytes (A), proliferation and disintegration of follicular cells (B), remains of

Table 1. Decrease of larval hatching in the 1st and resorption of oocytes in the 2nd gonotrophic cycle[a]

Peptide		Hatchability, %	Resorption[b], %
H-Tyr-Asp-Pro-Ala-Pro-OH	1b	20	20
H-Tyr-Asp-Pro-Ala-D-Pro-OH	2a	40	40
H-Tyr-Asp-Pro-D-Ala-Pro-OH	2b	30	30
H-Tyr-Asp-D-Pro-Ala-Pro-OH	2c	30	10
H-Tyr-D-Asp-Pro-Ala-Pro-OH	2d	50	80
H-D-Tyr-Asp-Pro-Ala-Pro-OH	2e	40	99
all-D-(H-Tyr-Asp-Pro-Ala-Pro-OH)	2f	20	88

[a] No hatchability in the 2nd gonotrophic cycle was observed.
[b] The difference to 100% is equal to yolk in egg. Resorption hampers the egg evolution, which results in zero hatchability.

Table 2. Metabolites of [^{3}H]Pro3-5P (4a), [^{3}H]Pro3, D-Ala4-5P (4b) and [^{3}H] Pro3, D-Asp2-5P (4c) after injection into body of Neobellieria bullata

Amino Acid residue	Time after injection in min	Metabolite, % Pro	Pro-Ala-Pro	5P
L-Ala4 (4a)	5	86.7	13.3	-
	30	93.2	6.8	-
D-Ala4 (4b)	5	26.7	13.3	60
	30	27.6	31.0	42
D-Asp2 (4c)	5	-	-	-
	30	53	5	42

the nuclear material originating from both trophocyte and follicular cells nuclei (C) and resorption of the egg chamber content (D), after application of peptide 2d (Fig. 1). Results of the degradation of labeled pentapeptides 4a, 4b and 4c in the hemolymph of *Neobellieria bullata* are depicted in Table 2. While the 4a is degraded very fast, its analogs 4b and 4c are degraded much slower, due to elimination of enzymatic cleavage of peptide bonds between central Pro^3 residue and either D-Ala^4 (and Pro^5) or D-Asp^2 (and Tyr^1) residues in the neighborhood. Just 30 min after injection, the peptides 4b and 4c are still present in ovaries as detected by radio-HPLC (over 40%). UV-HPLC (Fig. 2) found the Pro-D-Ala-Pro and Pro to be main degradation products of 4b. The introduction of D-amino acids preserves oostatic activity of corresponding 5P and enhances a devastation of developing eggs in *Neobellieria bullata*. Apparently, the oostatic effect can be evoked without involvement of specific receptors. Therefore an autonomous function of ovaries in a process of active intake by passing 5P through inter-spaces of follicular cells could be suggested. Contrary to standard 5P, D-isomers treated were degraded much slowly, so that prolonged existence of D-isomers in the flesh fly body resulted in more ovaries influenced, thus enhancing the oostatic effect.

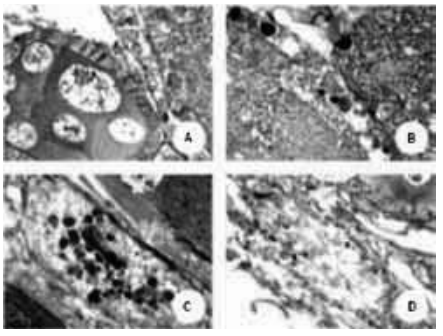

Figure 1. Histology of *Neobellieria bullata.*

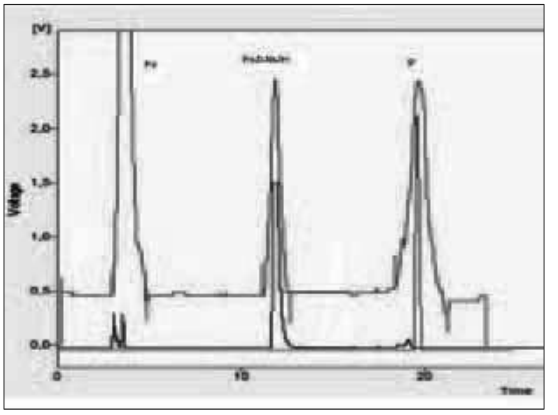

Figure 2. Radio detection: Upper line, UV detection of standards: Pro, Pro-D-Ala-Pro, 5P.

Acknowledgements

Supported by the Research Project Z4 055 0506 and the Grant Agency of the Czech Republic (Grant No. 203/06/1272)

References

1. Borovsky D, Carlson DA, Griffin PR, Shabanowitz J, Hunt DF. *FASEB J* **4**: 3015-3020, 1990.
2. Hlavácek J, Bennettová B, Barth T, Tykva R. *J Pept Res* **50**: 153-158, 1997.
3. Hlavácek J, Tykva R, Bennettová B, Barth T. *Bioorg Chem* **26**: 131-140, 1998.
4. Tykva R, Hlavácek J, Vlasáková V, Cerný B, Borovičková L, Bennettová B, Holík J, Slaninová J. *J Chrom B* **848**: 258-263, 2007.
5. Hlavácek J, Cerný B, Bennettová B, Holík J, Tykva R. *Amino Acids* **33**: 489-497, 2007.

2-01-112

Incorporation of Aza-β^3-Amino Acid into 26RFa$_{(20-26)}$, the Endogenous Ligand of GPR103: Structural Analysis

Tasseau, Olivier[1]; Legrand, Baptiste[2]; Bondon, Arnaud[2]; Leprince, Jérôme[3]; Vaudry, Hubert[3]; Baudy-Floc'h, Michèle[1,]*

[1]University Rennes, UMR CNRS 6226, ICMV, FRANCE; [2]University Rennes, UMR CNRS 6026, RMN-ILP, FRANCE; [3]University Rouen, Inserm U413, IFRMP, FRANCE

[*]E-mail: michele.baudy-floch@univ-rennes1.fr

Introduction

Aza-β^3-peptides, mixing α- and aza-β^3-amino acids (the aza analogs of β^3-amino acids), represent a novel and exciting type of peptidomimetics.[1] In particular, we have shown that aza-β^3-amino acid induces a N-N or hydrazino turn, stabilized by an eight-membered-ring intramolecular hydrogen bond between the carbonyl acceptor group of the residue i-1 and the amide proton of the residue i+1. Interestingly, this N-N turn promotes a well-defined γ-turn formation (hydrogen bond between the CO of the residue i-2 and the hydrazidic proton of the aza-β^3-moeity) when an α-amino acid is foregoing.[2] 26RFa, a novel neuropeptide of the RFamide superfamily, exhibits high affinity for GPR103 and induces a potent orexigenic effect (increase in food intake) in mice.[3] In biomimetic environment, 26RFa encompasses an α-helix between Pro4 and Arg17 residues and a canonical γ-turn centered on Ser23. 26RFa$_{(20-26)}$, whose sequence is strictly conserved across species, is about 100 times less potent than 26RFa. This heptapeptide shows important distortions of the γ-turn that may be responsible for its weak potency.[4] So, this heptapeptide constitutes an interesting target to form peptidomimetics. The aim of this study was to restore the γ-turn formation in 26RFa$_{(20-26)}$ (GGFSFRF-NH$_2$) by the presence of an aza-β^3-amino acid. The resulting 3D structure of each 26RFa$_{(20-26)}$ mimetic was studied under NMR restraints in water and DMSO.

Results and Discussion

The synthetic route for the preparation of the Fmoc-protected aza-β^3-amino acid involves the use of condensation, reduction and reductive amination of glyoxilic acid and N^{β}-Fmoc protected-N^{α}-substituted hydrazine. In the case of N^{β}-Fmoc-aza-β^3-γ-hydroxy-homothreonine (Fmoc-aza-β^3-Hyht),[5] optically pure enantiomer was obtained with 90% yield and 99% of optical purity (Scheme).

26RFa$_{(20-26)}$ mimetics were prepared by solid phase synthesis on automatic synthesizer on Rink amide resin. Fmoc strategy and HOBt/HBTU activation allowed obtaining the crude protected aza-β^3-peptide with longer coupling cycles for aza β^3-amino acids insertion. Cleavage from the resin and removal of the side chain protecting groups were performed with same conditions of standard peptide solid phase synthesis. Free aza-β^3-peptides were purified by HPLC in reversed-phase and characterized by MALDI-TOF mass spectrometry. All aza-β^3-peptides presented in the Fig. 1 could be prepared by this way.

NMR-studies in water (D_2O:H_2O) and DMSO-d6 were carried out from Tocsy and Roesy experiences at 298K in order to approach 3D conformation. In water, the comparison between 26RFa$_{(20-26)}$ and aza-β^3-peptide chemical shifts of the amide NH$_{i+1}$, immediately after aza-β^3-amino acids (NH$_i$) shown downfield shift for ψG21, ψF22, ψHyht23, ψF22-24 aza-β^3 analogues (for example 8.54 ppm, in the case of ψF22 analogue;

Scheme 1. Synthesis of protected N$^{\beta}$-Fmoc-aza-β^{-3}γ-hydroxy homoTheronine (Fmoc-aza-β^{3}Hyht

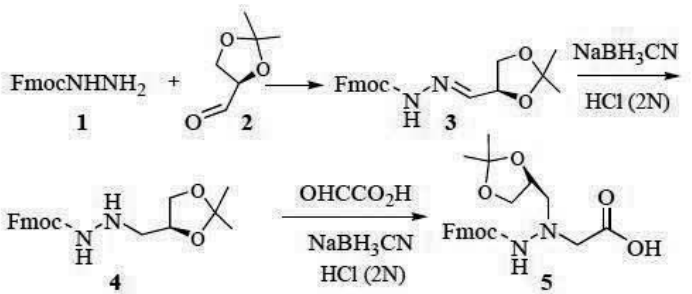

Scheme 1. Synthesis of protected N$^{\beta}$-Fmoc-aza-β^{3}γ-hydroxy homoThreonine (Fmoc-aza-β^{3}Hyht)

Name	Synthetized Peptidic analogues
ΨG20	aza-β^{3}G-G-F-S-F-R-F-NH$_2$
ΨG21	G-aza-β^{3}G-F-S-F-R-F-NH$_2$
ΨF22	G-G-aza-β^{3}F-S-F-R-F-NH$_2$
ΨHyht23	G-G-F-aza-β^{3}Hyt-F-R-F-NH$_2$
ΨF24	G-G-F-S-aza-β^{3}F-R-F-NH$_2$
ΨR25	G-G-F-S-F-aza-β^{3}R-F-NH$_2$
ΨF26	G-G-F-S-F-R-aza-β^{3}F-NH$_2$
ΨF22-24	G-G-aza-β^{3}F-S-aza-β^{3}F-R-F-NH$_2$

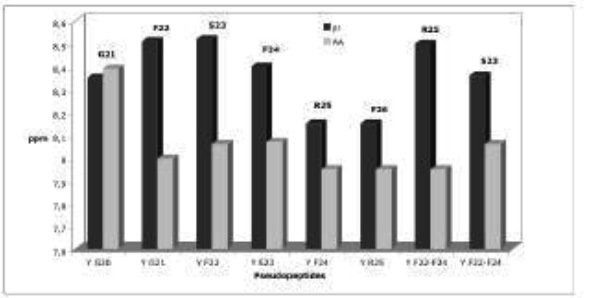

Figure 1. Chemical Shift Variation of the NHi+1 in H_2O/D_2O

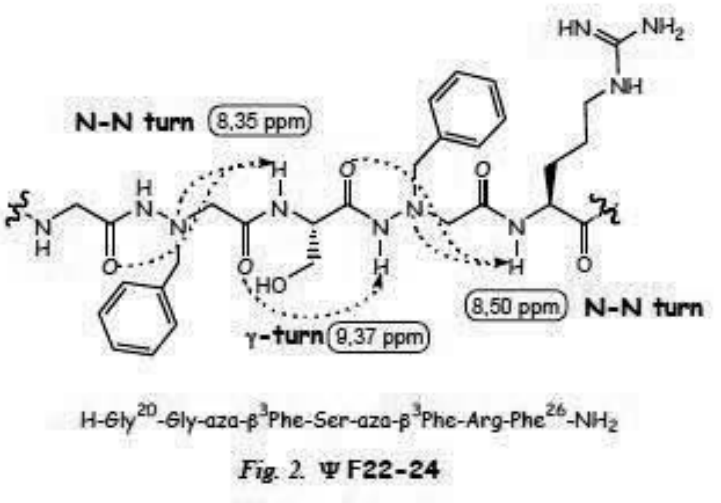

Figure 2. Ψ F22–24

expected value at 8.00 ppm, Fig. 1) indicating that H_{i+1} could be involved in intramolecular hydrogen bonds to form an N-N turn between O_{i-1} and H_{i+1}.

In DMSO, a downfield chemical shift of the hydrazidic N-H (~9.3 ppm, expected value at 7.80 ppm) was observed in each analogue. This downfield chemical shift could reveal the formation of a seven-membered-ring intramolecular hydrogen bond (γ-turn) between hydrazinic NH_i and $C{=}O_{i-2}$ induced by the aza-β^3-amino acid unit (Fig. 2).

Biological data are not in accordance with the NMR studies since «mixed» $26RFa_{(20\text{-}26)}$ ψ24 and ψ22-24 analogs, which restored a γ-turn in position 23, did not exhibit any activity. The improved potency observed for ψG20, ψG21 and ψHyht23 derivatives could be attributed to a more effective interaction with GPR103 due to hydrogen bonding.

References

1. Busnel O, Bi L, Dali H, Cheguillaume A, Chevance S, Bondon A, Muller S, Baudy-Floc'h M. *J Org Chem* **26**: 10701-10708, 2005.
2. Dali H, Busnel O, Hoebeke J, Bi L, Decker P, Briand JP, Baudy-Floc'h M, Müller S. *Mol Immunol*, **44**: 3024-3036, 2007.
3. Chartrel N, Dujardin C, Anouar Y, Leprince J, Decker A, Clerens S, Do-Régo JC, Vandesande F, Llorens-Cortes C, Costentin J, Beauvillain JC, Vaudry H. *Proc Natl Acad Sci U S A* **100**: 15247-15252, 2003.
4. Chartrel N, Bruzzone F, Leprince J, Tollemer H, Anouar Y, Do-Régo JC, Segalas-Milazzo I, Guilhaudis L, Cosette P, Jouenne T, Simonet G, Vallarino M, Beauvillain JC, Vaudry H. *Peptides* **27**: 1110-1120, 2006.
5. Busnel O, Bi L, Baudy-Floc'h M. *Tetrahedron Lett* **46**: 7073-7075, 2005.

2-01-113

An investigation of the functional requirements of Apidaecin Ib C-terminal fragment by means of peptoid-peptide hybrids

Gobbo, Marina[1]; Benincasa, Monica[2]; Bolognini, Erika[1]; Rossi, Valentina[1]; Rocchi, Raniero[1,]; Gennaro, Renato[2]*

[1]University of Padova, Department of Chemical Sciences, ITALY; [2]University of Trieste, Department of Biochem. Biophys. Macrom. Chemistry, ITALY

[*]E-mail: raniero.rocchi@unipd.it

Introduction

Pro-Arg rich peptides constitute an important class of antimicrobial peptides isolated from mammalian and insect sources.[1] They kill bacteria by acting on one or more intracellular targets, without damaging the cytoplasmatic membrane. Their particular killing mechanism and their low toxicity against mammalian cells make them attractive for the development of new antibiotics. Structure-activity relationships studies have been carried out on short Pro-Arg rich antimicrobial peptides isolated from insects and the characterization of various natural isoforms of the 18-residues peptide apidaecin Ib (GNNRPVYIPQPRPPHPRL) allowed to identify an evolutionary conserved region in the C-terminal part of the molecule. Even a single point mutation in this region results in reduction or loss of antimicrobial activity. We recently described the synthesis of some apidaecin Ib peptoid-peptide hybrids in which each arginine was replaced by the corresponding *N*-alkylglycine residue (*N*Arg).[2] The afforded modification made the resulting peptoid-peptide hybrids more resistant to proteolysis but moving the [*N*Arg]residue from the N- to the C-terminal end of the molecule progressively reduced the antibacterial activity. To study whether the antimicrobial activity of the peptoid-peptide hybrids might be affected by the size of the peptoid residue we synthesized a series of novel apidaecin analogues containing a *N*-guanidino-n-butylglycine (*N*Har) or N *N*-guanidinoethylglycine (*N*Nar) residue either in position 12 or 17 (Fig. 1). Moreover to increase the resistance to proteolysis of the trypsin sensitive Arg[17] - Leu[18] bond, the C-terminal leucine was replaced by the *N*-isobutylglycine (*N*Leu) residue.

Results and Discussion

Peptoid-peptide hybrids were automatically assembled on solid phase, using a modification of Zuckerman's sub-monomer method to introduce the *N*-alkylglycine residue.[2] Peptides were obtained in 80-85% yield, but during the synthesis of the [*N*Leu[18]]apidaecin analogue an extensive detachment, as diketopiperazine, of the C-terminal dipeptide occurred during the Fmoc deprotection in spite using of a chloro-trityl resin.[3] After purification and characterization by HPLC and ESI-MS, the conformational features of peptoid-peptide hybrids were investigated. The CD spectra of apidaecin analogues in buffer (pH 7.4) closely resemble those of the parent peptide. They are characterized by a broad negative band centered at 200 nm, that suggests the presence of largely unordered structures. In 90% aqueous trifluoroethanol and in micellar SDS the spectra show a red-shifting and a broadening of the negative band, with reduction of the CD band intensity. This pattern, which

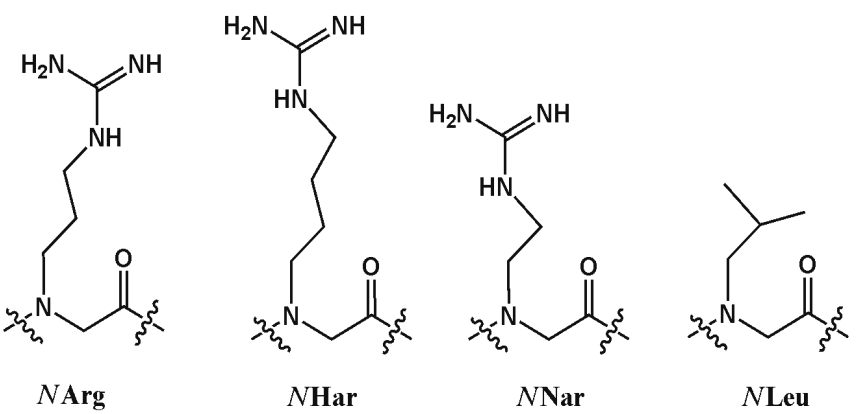

Figure 1. *N*-alkyl glicine residues used in the synthesis of peptoid-peptide hybrids of Apidaecin Ib.

Table 1. Minimum Inhibitory Concentration (MIC) of apidaecin and its analogues

PEPTIDE	*E. coli ML35*	*E. coli ATCC 25922*	*K. pneumoniae 22*	*S. enteritidis PD1*	*S. typhimurium ATCC 14028*
Apidaecin Ib	8	8	64	8-16	4-8
[*N*Arg12]apidaecin	16	16	> 128	32	16
[*N*Nar12]apidaecin	16-32	32	> 128	64-128	32
[*N*Har12]apidaecin	16-32	32-64	> 128	64-128	32
[*N*Arg17]apidaecin	> 128	> 128	> 128	> 128	> 128
[*N*Nar17]apidaecin	> 128	> 128	> 128	> 128	> 128
[*N*Har17]apidaecin	> 128	> 128	> 128	> 128	> 128

is more pronounced for the [*N*Leu^{18}]apidaecin, can be correlated to an increase of the type β-turn percentages in the conformational mixture. The antimicrobial activity of apidaecin peptoid-peptide hybrids was tested by the broth microdilution assay in 50% MHB and the results are summarized in Table 1.

The introduction of a peptoid residue at the C-terminal end of apidaecin significantly increases its stability against enzymic degradation but dramatically decreases the antimicrobial activity. This finding suggests that a defined conformation in this part of the molecule, probably involving the N-H bond of the C-terminal dipeptide, is needed for the interaction of apidaecin with its intracellular targets. The same type of modification in the middle part of the moleculein causes only a slight decrease of activity, which depends also from the size of the peptoid residue.

References

1. Sitaram N. Antimicrobial peptides with unusual amino acid composition and unusual structures. *Curr Med Chem* **13**: 679-696, 2006.
2. Gobbo M, Biondi L, De Cian V, Reddi E, Rocchi R, Bertoloni G. *Peptides 2006* (Proceedings of the 29th European Peptide Symposium, Gdańsk, Poland). Rolka K, Rekowski P, Silberring J (Eds), Kenes International, Geneva, Switzerland, 2007, pp 440-441.
3. Steinauer R, White P. *Innovation and perspective in solid phase synthesis, 3rd International Symposium*, Epton R (Ed). Mayflower Worldwide Ltd., Birmingham, 1994, pp 689.

2-01-114

Pipecolic Acid Disrupts Collagen Triple Helix Structure in Model Peptides

Shankar, Sonu Ram[1]; Islam, Md. Nurul[1]; Tanaka, Yuji[2]; Kato, Tamaki[1]; Nishino, Norikazu[1,]*

[1]Graduate School of Life Science and Systems Engineering, Kyushu Institute of Technology, JAPAN; [2]Department of Biological Substances and Life Science, Kyushu Kyoritsu University, JAPAN

[*]E-mail: nishino@life.kyutech.ac.jp

Introduction

Collagen is group of proteins with ubiquitous occurrence among vertebrates. Research spanning more than 50 years has provided details about its structure.[1] It is characterized by triple helical assembly of three left handed helices with polyproline II (PPII) type conformation. Peptide chain is represented as $(Xaa\text{-}Yaa\text{-}Gly)_n$, where Xaa and Yaa positions are frequently occupied by imino acids proline (Pro) and hydroxyproline (Hyp) respectively. Based on high frequency of tripeptide units with imino acid residues, $(Pro\text{-}Pro\text{-}Gly)_{10}$ and other collagen model peptide with natural and synthetic amino acid residues have been synthesized to understand structure and stability of triple helix at molecular level.[2] Computational studies have shown that with substitution of L-azetidine carboxylic acid (Aze), a lower ring homologue of proline, in model peptides, stability of triple helix is reduced.[3] Pipecolic acid (Pip), higher ring homologue of Proline, found in plants, fungus as well as vertebrates, is part of many natural bioactive molecules such as rapamycin, FK506 etc. It has also been incorporated in many synthetic peptides.[4] It has been substituted for proline to modify the conformation and biological activity of the peptides. Substitution of Pro with Pip has assisted in synthesis of enzyme inhibitors and conformationally restricted peptides, to improve the pharmacological profile of drugs and also to study interaction of enzyme with peptides. Computational and crystal studies of dipeptides have shown that Pip is compatible with PPII conformation.[5] In this study Pip has been introduced as substituent for Pro in reference model peptide $(Pro\text{-}Pro\text{-}Gly)_{10}$ to understand its propensity and effect on triple helix association as well as PPII type conformation of peptide chain which will assist in understanding of factors in stabilization of collagen model peptides.

Results and discussion

Pipecolic acid was synthesized by intramolecular cyclization of 2-amino-6-bromohexanoic acid.[6] Dipeptides and tripeptides were synthesized by the aid of DCC/HOBT and HBTU/HOBt as coupling reagents respectively (Fig. 1). Peptide segments were anchored on Barlos resin and manual solid phase synthesis was applied for elongation. Treatment with AcOH/TFE/DCM (2:2:6) and RP-HPLC purification was carried out to obtain desired model peptides with all Xaa and/or Yaa positions of $(Pro\text{-}Pro\text{-}Gly)_{10}$ replaced with Pip residues to make $(Pip\text{-}Pip\text{-}Gly)_{10}$ (1), $(Pip\text{-}Pro\text{-}Gly)_{10}$ (2) and $(Pro\text{-}Pip\text{-}Gly)_{10}$ (3). 50 µM Solution of these peptides were made in 0.1 M phosphate buffer (pH 7), equilibrated at 4 °C for more than 48 h and analyzed by circular dichroism (CD) spectroscopic measurements (Fig. 2a). CD spectra of collagen is characterized by large negative ellipticity around 200 nm and positive ellipticity around 225 nm. At 4 °C, peptide 1 neither show negative minimum nor the positive maximum similar to reference collagen model peptide. The result shows that substitution of all proline with Pip destabilizes the PPII conformation. In case of Peptides 2 and 3, negative ellipticity was observed but not positive maxima. These facts shows that one substitution in every tripeptide unit allows PPII like conformation of peptide chain, but still, their association into triple helix cannot take place.

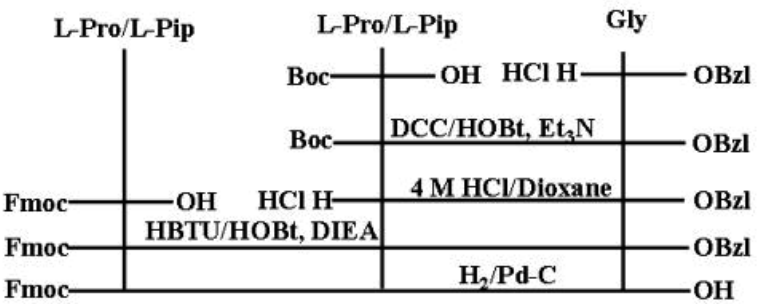

Figure 1. Strategy for synthesis of tripeptide segments.

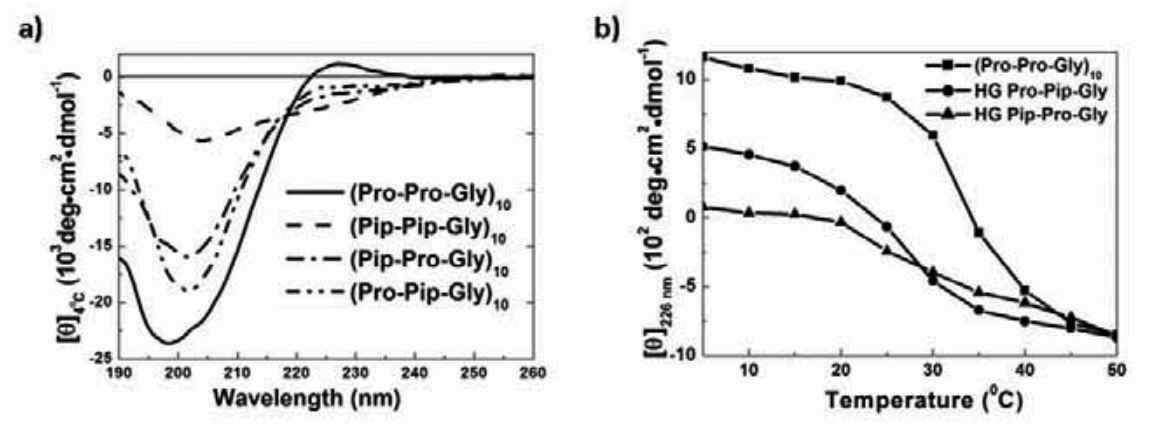

Figure 2. a) CD spectra of homotrimers at 4°C (Pro-Pro-Gly)$_{10}$ (—), (Pro-Pip-Gly)$_{10}$ (— •• —), (Pip-Pro-Gly)$_{10}$ (—•—) in phosphate buffer and (Pip-Pip-Gly)$_{10}$ (——) in 4% TFE/ phosphate buffer. **b)** Thermal denaturation curves of model peptides (Pro-Pro-Gly)$_{10}$(—■—) HG Pro-Pip-Gly (—•—) and HG Pip-Pro-Gly (—▲—) in phosphate buffer. Peptide concentrations were 50 μM.

We also examined the role of one Pip residue in the collagen model peptide by synthesizing host guest peptides (Pro-Pro-Gly)$_5$-(Pro-Pip-Gly)-(Pro-Pro-Gly)$_4$ (denoted as HG Pro-Pip-Gly) (4) and (Pro-Pro-Gly)$_5$-(Pip-Pro-Gly)-(Pro-Pro-Gly)$_4$ (denoted as HG Pip-Pro-Gly) (5). They were analyzed by CD spectroscopy as described earlier. In both the cases, there were positive ellipticities observed. The difference was observed in thermal denaturation of peptides. While 4 showed mild cooperative denaturation, 5 did not show any such transition (Fig. 2b). This shows that substitution of Pip in Yaa position allows triple helix formation but not in in Xaa position.

Destabilization in case of 1, evident from its deviation from PPII type conformation, can be primarily attributed to the steric hindrance between neighboring Pip residues. Bulkiness of Pip residue may further obstruct hydration of carbonyl groups. Rigidness of Pip in chair conformation, torsion angles and Xaa position being more exposed to the solvent, can be reasons of greater destabilization of triple helix in 5 compared to 4 and lower PPII content in 2 compared to 3. This can also explain higher propensity of Pip for Yaa position and other features of Pip containing collagen model peptides. In conclusion, in spite of being homologue of proline, Pip residues in the collagen model peptides disrupt triple helix structure.

References

1. a) Ramachandran GN, Kartha G. *Nature* **176**: 593-595, 1955. b) Okuyama K, Tanaka N, Ashida T, Kakudo M, Sakakibara S, Kishida Y. *J Mol Biol*. **65**: 371-373, 1972.
2. Sakikabara S, Inouye K, Shudo K, Kishida Y, Kobayashi Y, Prockop DJ. *Biochim Biphys Acta* **303**: 198–202, 1973.
3. Zagari A, Némethy G, Scheraga HA. *Biopolymers* **30**: 967-974, 1990.
4. a) Ireland RE, Gleason JL, Gegnas LD, Highsmith TK. *A J Org Chem* **61**: 6856-6872, 1996. b) Nishino N, Jose B, Okamura S, Ebisusaki S, Kato T, Sumida Y, Yoshida M. *Org Lett* **5**: 5079–5082, 2003.
5. Jhon JS, Kang YK. *J Phys Chem* **111**: 3496-3507, 2007.
6. Watanabe LA, Haranaka S, Jose B, Yoshida M, Kato T, Moriguchi M, Sodaf K, Nishino N. *Tetrahedron*: *Asymmetry* **16**: 903–908, 2005.

2-01-115

Analgesic Effects of MIF-1's Analogues

Bocheva, Adriana[1]; Kalauzka, Rositsa[2]; Pajpanova, Tamara[2]

[1]Medical University, Dept. of Pathophysiology, BULGARIA; [2]Institute of Molecular Biology, BULGARIA

[*]E-mail: tania_dzimbova@abv.bg

Introduction

The problem of the efficient therapy of pain and epilepsy are important not only from clinical but from social and economic point of view. Over the past 50 years pharmacological and pharmaceutical Sciences have sought in vain for a highly efficacious centrally acting analgesic, lacking abuse potential. Such drugs could replace the opioids as standard drugs against severe pain. For example, morphine and amphetamine, are both powerful analgesics with high abuse potential, but their long-term application as an analgesics, lead to tolerance/dependence and imunossupression. This opens the avenue to target for the development of new types of analgesic drugs. Peptide and protein therapeutics are logical targets, in spite of problems associated with their low bioavailability, rapid metabolism, and lack of oral activity. Our special interest was focused on "Designed synthesis" and screening of new "peptide mimetics": in particular MIF-related compounds.[1] MIF-1 (prolyl-leucyl-glycinamide, PLG) also known as melanocyte stimulating hormone release inhibiting factor is the C-terminal tripeptide of oxytocin has pronounced CNS effects. PLG also has been evaluated clinically and found to be beneficial in treating Parkinson's disease and major depression.[2] The aim of this study was to investigate the analgesic effects of of MIF-1 and its analogues modified at position 2 with unnatural amino acids Cav, sLys, sLeu, sIle and sNle during acute pain.

Results and Discussion

The analogues of MIF-1 – Cav2- MIF, sLys2- MIF, sLeu2- MIF, sIle2- MIF and sNle2- MIF were synthesized according the procedure previously reported.[3] To investigate the analgesic effects of MIF-1 and analogues most frequently used models for studying antinociceptive activity are based on test with thermal and mechanical irritation were applied. Antinociceptive effects were evaluated using tail flick (TF), hot plate (HP) and paw pressure (PP) test. Tail-flick test (TF): The tail-flick response was elicited by applying radiant heat to the dorsal surface of the tail. A cut-off tail flick latency of 20 s. was used to avoid tissue damage. The intensity of heat stimulus in the tail-flick test was adjusted so that the animal flicked its tail within 3 to 5 sec. Hot plate test (HP): The latency of response to pain was measured from the moment of placing an animal on a metal plate (heated to 55 ± 0.5 °C) to the first signs of pain (paw licking, jump). The cut off time was 30 sec. Paw pressure test (PP): The changes in the mechanical nociceptive threshold of the rats were measured by the using an analgesiameter (Ugo Basile). The pressure was applied to the hind-paw and the pressure (g) required to elicit nociceptive responses such as squeak and struggle was taken as the mechanical nociceptive threshold. A cut-off value of 500 g was used to prevent damage of the paw. To determine whether analgesic activity of the synthesized MIF-1 analogues are mediated by the opioid system a competitive antagonist of opiate receptors as naloxone (Nal) was used. Naloxone was injected 20 min. before each of investigated peptides. The experiments were carried out on male Wistar rats (180-200 g) housed at 12 h light/dark cycle. Food and water were available ad libitum. All experiments were carried out between 09.00 a.m./12.00 p.m. Each group included 8-10 rats. MIF-1

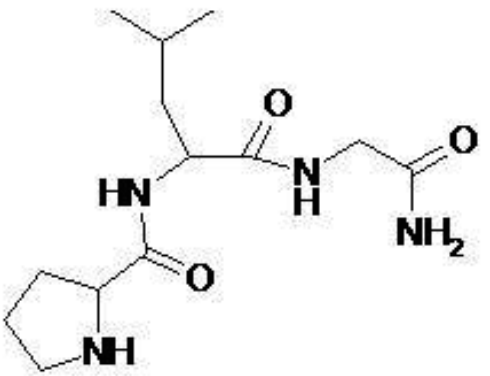

Figure 1. Effects of MIF-1 and analogues S.E.M.; *P± (1 mg/kg, i.p.) on nociception Data are presented as mean <0.01, ** P<0.01 versus control; +P<0.01, ++ P<0.01 versus each of peptides. sLys2-MIF and sNle2-MIF exerted antinociceptive effects on hot-plate, tail-flick and paw pressure tests. More stronger was the effect of sNle-, Lys- and Cav-MIF. The present results show that Cav, sNLe and Ile analogues exerted significant antinociceptive effects, which is antagonized by NAL (1 mg/kg i.p.).

and naloxone (all in dose 1 mg/kg) were dissolved in sterile saline (0.9% NaCl) solution and were injected intraperitoneally (i.p.). The experimental procedures were carried out in accordance with the institutional guidance and general recommendations on the use of animals for scientific purposes. The results were statistically assessed by one-way analysis of variance (ANOVA).

Conclusions

In conclusion it could be suggested that:

o The newly synthesized analogues exhibits naloxone-reversible antinociceptive activity.

o Opioid receptors, especially μ-receptor are involved in antinociceptive action.

o Substitution of leucine in position 2 of MIF-1 molecule by non-protein amino acids (sNle and Cav) significantly increased the analgesic effect of the newly synthesized MIF-1 analogue.

Acknowledgments

This work was partially supported by the National Science Fund of the Bulgarian Ministry of Education and Science, Grant MU-FS-13/07

References

1. Kastin AJ, Olson RD, Ehrensing RH, Berzas MC, Schally AV, Coy DH. *Pharmac Biochem Behav* **11**: 721-723, 1979.
2. Erchegyi J, Zadina JE, Qui DC, Kersch X-D , Ge L-J, Brown X-D, Kastin A. *Pept Res* **6**: 31-38, 1993.
3. Pancheva S, Kalauzka R, Popgeorgieva E, Pajpanova T. *Peptides 2004* (*Proceedings of the Third Intern. and Twenty-Eighth European Peptide Symposium, Prague, Czech Republic*). Flegl EM, Slaninova S, Fridkin M, Gilon C (Eds), Kenes Intern., Geneva, Switzerland, 2005, pp 950-951.

2-01-116

Synthesis and antiproliferative activity against breast and colon cancer cells of peptidomimetics based on Substance P C–terminal region hexapeptide

Glezakos, Petros; Stahtea, Xanthi; Sarigiannis, Yiannis; Karamanos, Nikos; Stavropoulos, George[1,]*
University of Patras, Department of Chemistry, GREECE

[*]E-mail: G.Stavropoulos@chemistry.upatras.gr

Introduction

The last years our research group has focused his efforts on the synthesis of small peptides, based on Substance P C-terminal fragments. It has been shown they increase the secretion of tumor necrosis factor α (TNF-α) and prevent the proliferation of several cancer cell lines.[1] We have also shown the antiproliferative activity of tri- and tetra-peptoids in breast and prostate cancer cells.[2,3]

The aim of this study was to design and prepare more potential antagonist of cancer cells proliferation. Thus, the synthesis of hexa-peptoids containing the residues D-Trp and Tic and the peptoid residues HN-N(R)-CH_2CO, NPhe and NAla in their sequence afforded active compounds, according to their effect on cancer cells proliferation.

Results and Discussion

All the syntheses were carried out stepwise by SPPS, using the Fmoc/But methodology on the solid support 2-chlorotrityl chloride resin,[4] and DIC/HOBt as coupling reagent. The analogs were purified (HPLC) and identified (ESI-MS). The synthesized compounds have the following structures in comparison with Substance P C-terminal fragments:

Cells were routinely grown at 37 °C in a humidified atmosphere of 5% (v/v) CO_2. The MDA-MB-231 breast cancer cells were cultured in EMEM supplemented with 10% FBS, while the HT-29 colon cancer cells were grown in DMEM medium containing 10% FBS. Cell proliferation was determined by WST-1 assay.[5,6] Cells were treated with various concentrations of peptoids for 48h, in the presence and absence of serum. The mean value of three experiments is shown at the Fig. bellow.

Conclusions

We report the synthesis of a series of hydrazino-peptoids, analogs of SP_{5-10} hexapeptide containing residues like HN-N(R)-CH_2CO, NPhe and NAla, and also D-Trp and Tic. The D-Trp is incorporated in positions 5 of the hexapeptoids 1-3 and in positions 4 and 6 of the hexapetoids 4-6.

The biological assays showed that all peptoids significantly inhibited the proliferation of HT-29 and MDA-MB-231 cells in a dose-dependent manner in absence of serum, even at low concentrations. Especially the hydrazino-peptoids containing Tic, an unusual

Substance P	Arg^1-Pro^2-Lys^3-Pro^4-Gln^5-Gln^6-Phe^7-Phe^8-Gly^9-Leu^{10}-Met^{11}-NH_2
1	Glp^1-$NPhe^2$-Gly^3-[NH-N(Bzl)-CH_2-CO]^4-D-Trp^5-Leu^6-OH
2	Glp^1-$NAla^2$-Gly^3-[NH-N(Bzl)-CH_2-CO]^4-D-Trp^5-Leu^6-OH
3	Glp^1-Tic^2-Gly^3-[NH-N(Bzl)-CH2-CO]^4-D-Trp^5-Leu^6-OH
4	Glp^1-$NPhe^2$-Gly^3-D-Trp^4-[NH-N(Bzl)-CH_2-CO]^5-D-Trp^6-OH
5	Glp^1-$NAla^2$-Gly^3-D-Trp^4-[NH-N(Bzl)-CH_2-CO]^5-D-Trp^6-OH
6	Glp^1-Tic^2-Gly^3-D-Trp^4-[NH-N(Bzl)-CH2-CO]^5-D-Trp^6-OH

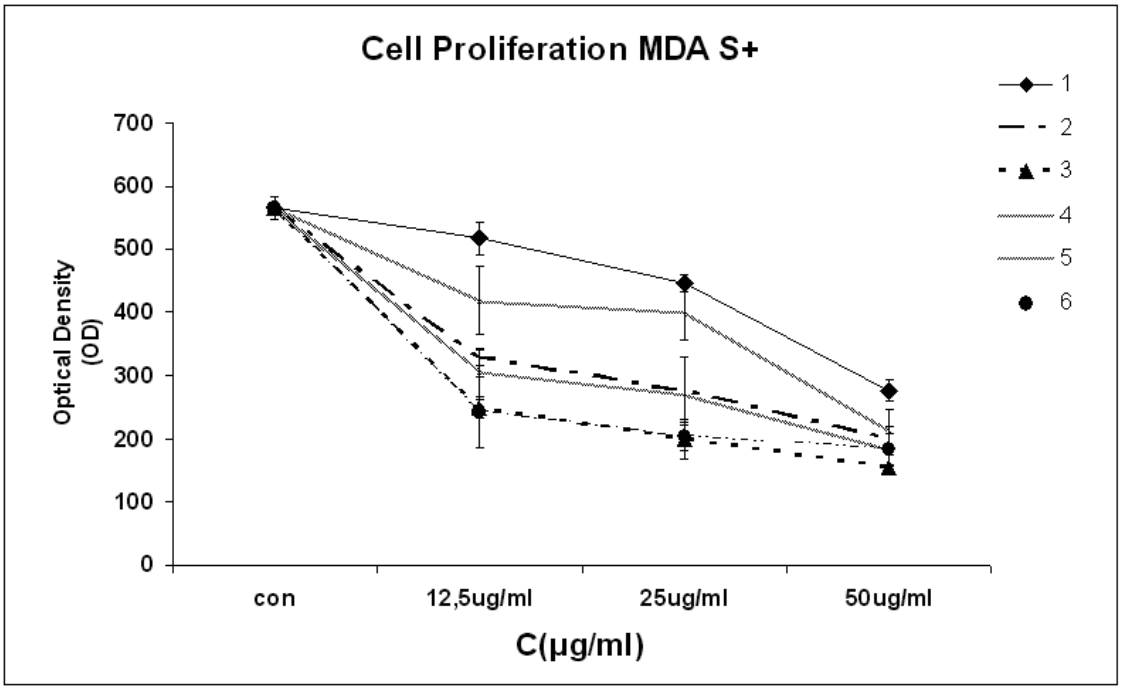

Figure 1. Increasing concentrations of peptoids in MDA breast cancer cells in presence of serum on cell proliferation.

amino acid, exhibit a significant antiproliferative activity on breast and colon cancer cells, suggesting that they may have powerful anti-tumor activity. The biological assays showed that hydrazino-peptoids act as potent antiproliferative agents in breast and colon cancer cells and further studies are warranted to evaluate their inhibitory effects in the view of new analogues.

References

1. Ho WZ, Stavropoulos G, Lai JP, Hu BF, Magafa V, Anagnostides S, Douglas SD. *J Neuroimmunol* **82**: 126-132, 1998.
2. Vakalopoulou P, Makrodouli H, Stavropoulos G. *J Pept Sci Suppl* **10**: 264, 2004.
3. Sarigiannis Y, Anastasopoulos Ch, Vakalopoulou P, Stavropoulos G. *Peptides 2006* (*Proceedings of the 29th European Peptide Symposium, Gdańsk, Poland*). Rolka K, Rekowski P, Silberring J (Eds), Kenes International, Geneva, Switzerland, 2007, pp 692-693.
4. Barlos K, Chatzi O, Gatos D, Stavropoulos G. *Int J Pept Res* **37**: 513-520, 1991.
5. Stahtea X, Roussidis A, Kanakis I, Tzanakakis G, Mavroudis D, Kletsas D, Karamanos N. *Int J Cancer* **121**: 2808-2814, 2007.
6. Kousidou O, Mitropoulou T, Roussidis A, Kletsas D, Theocharis A, Karamanos N. *Int J Oncol* **26**: 1101-1109, 2005.

2-01-117

Macrocyclic phosphino dipeptide isostere inhibitors of β secretase (BACE1) with improved serum stability

Manzenrieder, Florian[1,]; Huber, Timo[1]; Kuttruff, Christian[1]; Dorner-Ciossek, Cornelia[2]; Kessler, Horst[1]*

[1]Technical University Munich, GERMANY; [2]Boehringer-Ingelheim Pharma GmbH & Co.KG, GERMANY

[*]E-mail: Florian.Manzenrieder@ch.tum.de

Introduction

BACE1 is a molecular target for therapeutic intervention in Alzheimer's disease. In 2000 and 2002, Tang *et al*. reported nanomolar inhibitors of the aspartyl protease BACE1.[1] Subsequently, X-ray structures of these inhibitors in complex with BACE1 were available, showing the main features of the enzyme-inhibitor interactions. Based on the observation that the P1 and P3 side chains of Tang's pseudo peptidic inhibitors are in close proximity we investigated the cyclization at these positions. We have recently shown that the phosphino dipeptide (PDP) isostere is a suitable replacement of the hydroxy ethylene isostere in OM00-3 retaining full activity.[2] Consequently, we were interested to develop a macrocyclic inhibitor with P1 and P3 cyclized side chains containing a PDP isostere with view to enhancement of human serum stability. In our search for conformationally restrained PDP isostere BACE1 inhibitors we presumed that the P1 and P3 cyclization would lock the active conformation of the linear pseudo peptidic inhibitor in the N-terminal region including the PDP isostere (Fig. 1). A detailed analysis of the crystal structure of OM00-3 bound to BACE1 revealed that the ideal macrocycle should consist of a 13-membered cycle. It was promising that a low-energy conformation of our macrocyclic inhibitor was able to perfectly emulate the bioactive conformation of OM00-3. Superposition and docking of this low-energy conformation to BACE1 indicated that the macrocycle would not clash with the enzyme.

Synthesis

Synthesis of the Fmoc-(*S*)-homoallylglycin fragment was accomplished according to a route depicted by Rojo *et al*.[3] Next, we used a three component condensation to gain access to the desired PDP isostere fragment. In this work the Matziari protocol[4] was slightly modified as we used the carboxymethyl ester instead of a free acid analog. The synthesis of the peptidic precursor molecule for ring closing metathesis was accomplished on solid support. The prepared fragments were then assembled on solid support and the linear peptide was cleaved from the resin. The metathesis reaction was accomplished in solution using the 2nd generation catalyst developed by Grubbs *et al*. It turned out that hydrogenation with Pd/C in the DCM/*tert*-butanol mixture led to clean hydrogenation of the olefin and removal of the Fmoc group. The final reaction to obtain the desired macrocyclic derivative was to remove the protecting groups still attached (Scheme 1). It was possible to separate all of the four diastereomers which were named after their chronological appearance from the HPLC-column as follows: **2 P-1** to **P-4**.

Biological evaluation and enzymatic stability of macrocyclic inhibitors of BACE1

The inhibitory effects of these macrocyclic phosphino peptides against BACE1 were examined by a biochemical assay using the ectodomain of BACE1. The results and analytical data are shown in Fig. 2. The most active compound is **2-P1** and has an activity of 47 nM. The aim of this study was to analyze the effect of cyclization on enzymatic stability, therefore the present investigation used fresh human serum preparations. Compounds **1** and **2-P1** were treated with fresh human serum of a single donor and the amount of intact ligand was determined by quantitative HPLC and HPLC-MS analysis over time. The linear inhibitor is rapidly degraded with a half-life of about 14.8 min. As assumed,

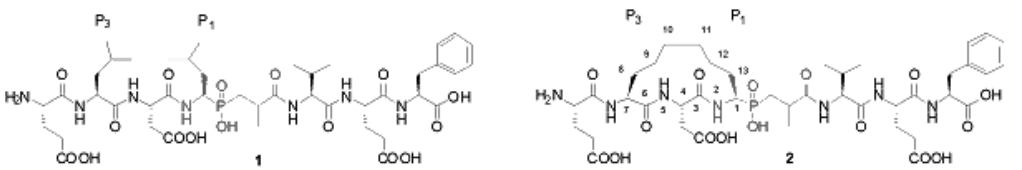

Figure 1. Linear inhibitor **1** and macrocyclic inhibitor **2**.

Scheme 1. Strategy to synthesize **2** via key fragments; assembly on solid support; metathesis, reduction and deprotection

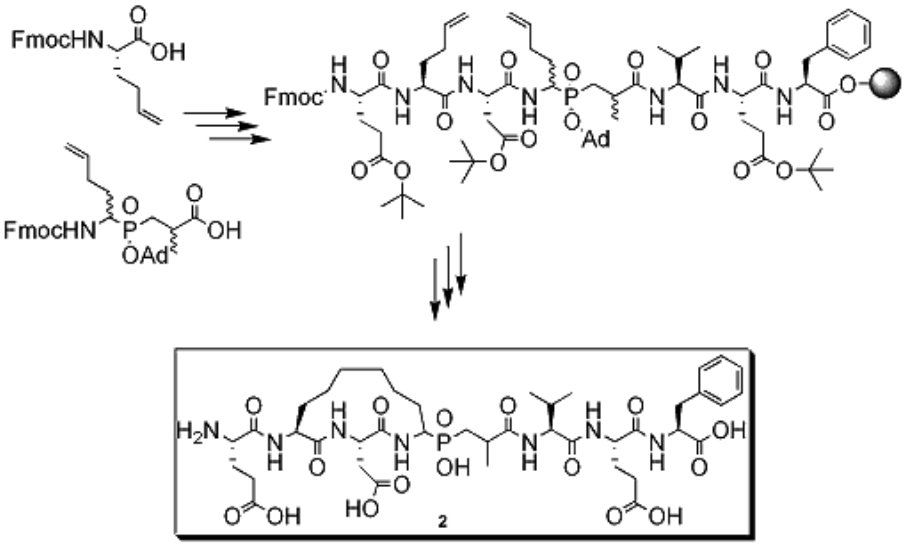

Table 1. IC_{50} values of the isolated diastereomers against BACE1

Compound	Inhibition IC_{50}(nM)[a]	half life time (min)
QM-003	6(±0.7)[b]	–
1	12(±2)[b]	14.8
2-P1	47(±10)	43.9
2-P2	320(±30)	–
2-P3	522(±50)	–
2-P4	808(±70)	–

[a] Values are means of 2 experiments, standard deviation is given in paretheses.
[b] Data taken from previous measurement with the full-domain of BACE1.

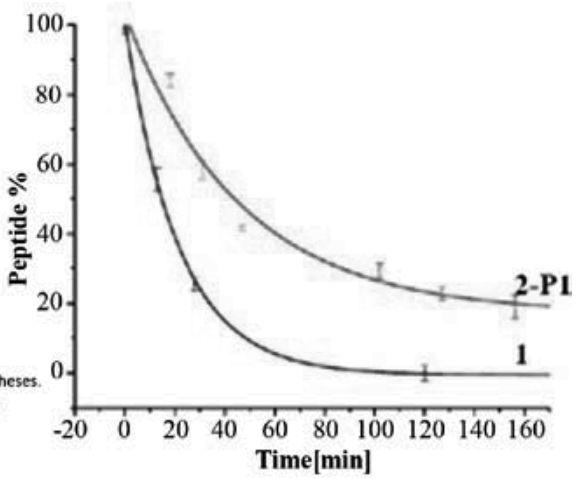

Figure 2. Test results for the macrocyclic inhibitor (left) and stability in human serum (right).

the cyclic inhibitor was more stable and degraded with a half-life of about 43.9 min. In total the stability increased by a factor of approximately three (Fig. 2).

Conclusion

We report the synthesis of a potent macrocyclic PDP isostere inhibitor with prolonged human serum stability.

References

1. Hong L, Turner RT, Koelsch G, Shin D, Ghosh AK, Tang J. *Biochemistry* **41**: 10963-10967, 2002.
2. Manzenrieder F, Frank AO, Huber T, Dorner-Ciossek C, Kessler H. *Bioorg Med Chem* **15**: 4136-4143, 2007.
3. Rojo I, Martin JA, Broughton H, Timm D, Erickson J, Yang HC, McCarthy Jr. *Bioorg Med Chem Lett* **16**: 191-195, 2006.
4. Matziari M, Yiotakis A. *Org Lett* **7**: 4049-4052, 2005.

2-01-118

Design and synthesis of cyclotheonamide analogs with a basic P3 residue as inhibitors of human *β*-tryptase

Schaschke, Norbert[1,]; Sommerhoff, Christian P[2]*

[1]Universität Bielefeld, Fakultät für Chemie, GERMANY; [2]Klinikum der LMU, München, Abteilung Klinische Chemie und Klinische Biochemie, GERMANY

[*]E-mail: norbert.schaschke@uni-bielefeld.de

Introduction

Tryptases constitute a family of serine proteases with trypsin-like activity that are expressed virtually exclusively in mast cells. Among them, tryptase *β* is the most prominent member in terms of both expression and proteolytic activity. After being released into surrounding tissues by mast cell degranulation, *β*-tryptase is thought to play a pivotal role in the pathogenesis of allergic and inflammatory disorders, and thus inhibiting its proteolytic activity represents a promising approach for therapeutic intervention.[1] Tryptase *β* has an extended substrate specificity: Beside the basic S1 ligand, which is essential for substrate recognition and processing, the protease shows an additional preference for basic residues in P3 position.[2] To take advantage of this substrate specificity for inhibitor design, cyclotheonamides provide good structural prerequisites. As shown by the X-ray structure of cyclotheonamide A in complex with trypsin, these cyclic pentapeptides adopt an extended conformation stabilized by macrolactamization, thus allowing to address the S1', S1, S2, and S3 pock*et al*ong the active-site cleft in a substrate-like manner.[3] The S1 ligand, (*S*)-3-amino-6-guanidino-2-oxo-hexanoic acid, interacts via its guanido function with Asp 189 at the bottom of the S1 pocket. In addition, the ketone covalently modifies the *γ*-oxygen of Ser 195 by hemiketal formation.

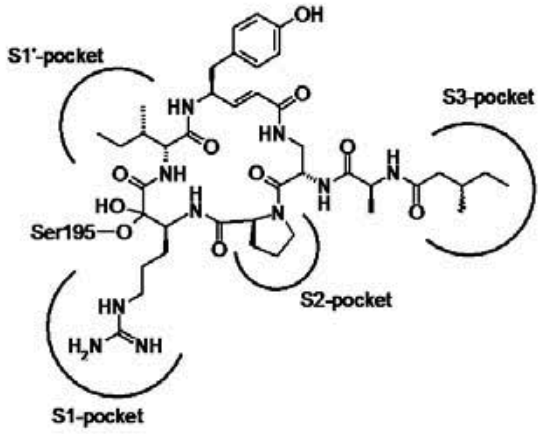

Figure 1. Proposed binding mode of cyclotheonamide E4 based on the X-ray structure of trypsin in complex with cyclotheonamide A.

Results and discussion

In this study we have focused on cyclotheonamide E4 (Fig. 1) that has been isolated from a marine sponge of the genus *Ircinia*.[4] The cyclic peptide scaffold was modified at two positions: (i) the S1 ligand was replaced by β-homolysine to obtain reversible protease inhibitors, and (ii) the *α*-amino function of (*S*)-2,3-diamino propionic acid was used as anchoring point for basic P3 ligands of different chain lengths to exploit interactions with the negatively charged Glu 217 of tryptase. Several analogs (Fig. 2) were synthesized by a combination of solid phase and solution phase chemistry as reported recently[5] and subsequently characterized by RP-HPLC and ESI-MS. Their inhibitory properties are summarized in Table 1. As a measure for selectivity among the trypsin-like serine proteases inhibitory data for both human *β*-tryptase and bovine trypsin are reported. The kinetic measurements show that inhibitors **1**-**5** block the enzymatic activity of trypsin and *β*-tryptase in a reversible fashion. Furthermore, the distance scan revealed the optimal chain length to address Glu 217 within the S3 pocket. Whereas 4-amino butyric acid (inhibitor **2**) is apparently too short to exploit interactions with Glu 217, *ω*-amino acids with a chain length of 5, 6, and 7 C-atoms (inhibitors **3**, **4**, and **5**, respectively) represent well suited basic S3 ligands. In conclusion, by implementing information derived from substrate specificity screening into the cyclotheonamide E4 scaffold highly potent and selective *β*-tryptase inhibitors were obtained.

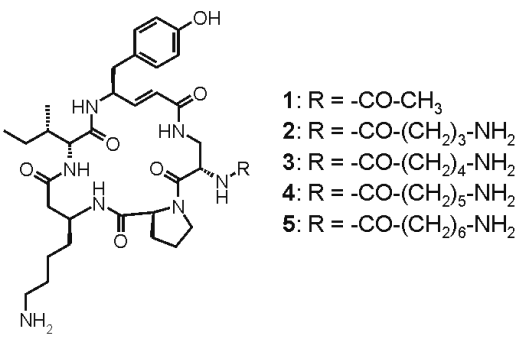

Figure 2. Structures of the synthesized cyclotheonamide E4 analogs **1**-**5**.

Table 1. Inhibitory properties of the cyclotheonamide E4 analogs **1**-**5**.

Inhibitor	K_i [μM]	
	β-Tryptase	Trypsin
1	380	230
2	1	150
3	0.012	24
4	0.016	40
5	0.023	132

Acknowledgements
The study was supported by the DFG (grant: SCHA 1012/1).

References

1. Sommerhoff CP, Schaschke N. *Curr Pharm Design* **13**: 313-332, 2007.
2. Harris JL, Niles A, Burdick K, Maffitt M, Backes B J, Ellman JA, Kuntz I, Haak-Frendscho M, Craik C S. *J Biol Chem* **276**: 34941-34947, 2001.
3. Lee A Y, Hagihara M, Karmacharya R, Albers MW, Schreiber SL, Clardy J. *J Am Chem Soc* **115**: 12619-12620, 1993.
4. Murakami Y, Takei M, Shindo K, Kitazume C, Tanaka J, Higa T, Fukamachi H. *J Nat Prod* **65**: 259-261, 2002.
5. Schaschke N, Sommerhoff CP. *Peptides 2006* (*Proceedings of the 29th European Peptide Symposium, Gdańsk, Poland*). Rolka K, Rekowski P, Silberring J (Eds), Kenes International, Geneva, Switzerland, 2007, pp 354-355.

2-01-119

The potent antiproliferative activity of small hydrophobic peptides containing adamantyl group

Miyazaki, Anna[1]; Tsuda, Yuko[1]; Miyawaki, Youhei[1]; Fukushima, Shoji[1]; Yokoi, Toshio[1]; Vántus, Tibor[2]; Bökönyi, Györgyi[2]; Szabó, Edit[2]; Horváth, Anikó[2]; Kéri, György[2]; Okada, Yoshio[1,]*

[1]Faculty of Pharmaceutical Sciences, Kobe Gakuin University, Kobe, 651-2180, JAPAN; [2]PathoBiochemistry Research Group of Hungarian Academy of Science and Semmelweis University H-1088 Budapest, HUNGARY

[*]E-mail: okada@pharm.kobegakuin.ac.jp

Introduction

The somatostatin (SRIF) is a cyclic tetradecapeptide, which exerts inhibitory effects on the secretory processes in the endocrine and exocrine systems, anti-inflammatory and the cell proliferation through somatostatin receptors (SSTR1-SSTR5). SSTRs are distributed throughout human body, not only in normal cells but also in tumor cells. Keri *et al.* reported that TT-232, [D-Phe-c(Cys-Tyr-D-Trp-Lys-Cys)-Thr-NH_2], had potent antiproliferative activity without antisecretory action.[1] Based on this report, we tried to design and synthesize somatostatin analogues with more potent antiproliferative activity. Furthermore the stability and cell permeability of analogues need for high bioavailability. Focusing on active sequence, Tyr-D-Trp-Lys we synthesized the cyclic peptides containing pyrazinone ring[2] as well as linear peptides with or without a Boc group at N-terminus, and in some cases the C-terminal Lys was substituted with hydrophobic and bulky groups (Fig. 1).

Results and discussion

Their antiproliferative activities on A431 cells on which the SSTRs are expressed, were examined by MTT assay (Fig. 2). In the cyclic analogues, the replacement by Dmt or Phe resulted in severe loss of antiproliferative activity compared with the compounds containing a Tyr, although the ligand-receptor interaction might be activated by hydrophobicity. By contraries of opioid mimetics,[3] the Dmt substitutions in somatostatin analogues might bring unfavorable functions; therefore we suggested that the structures of the binding site of SSTRs were quite different from those of opioid receptors in spite of comprising the same G protein-coupled receptor family, or the binding site of SSTRs was not accommodated by the added bulkiness of Dmt. In the linear analogues, the compounds containing adamantylamine (**10, 11, 16** and **17**) exhibited the most potent antiproliferative activity, even greater than TT-232. Especially **10** and **11** with a Boc group exhibited very high antiproliferative activity on SW480 cells, equally (data not shown). The result indicated that the activity might be attributed to Tyr-D-Trp sequence coupled with a hydrophobic and bulky residue both at the N-terminus and at the C-terminus, and thus increased hydrophobicity in the whole molecule. Our data further suggests that not only hydrophobicity but also aliphatic properties and rigidity are important at the C-terminus. Furthermore we also studied DNA fragmentation by FACS analysis and cellular morphology of compound **10** (data not shown).[4] The results demonstrated that these somatostatin analogues induced cell death by apoptosis.

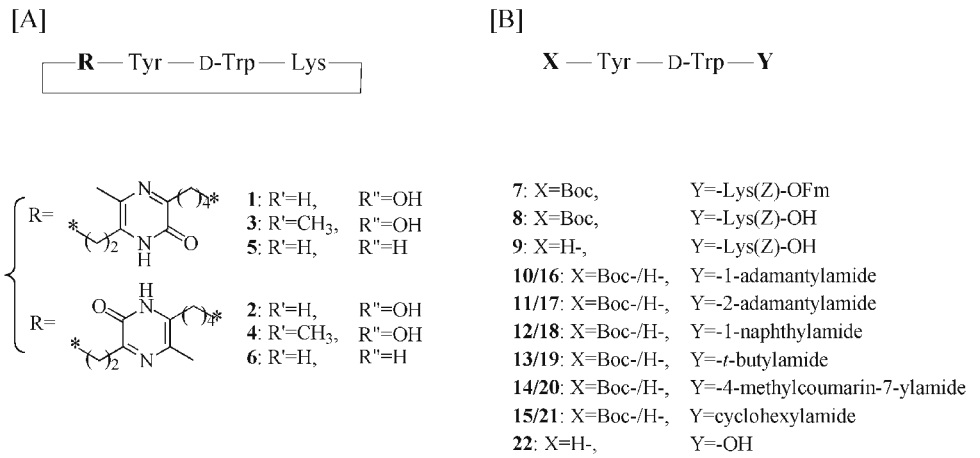

Figure 1. Structures of somatostatin analogues **1-22**.

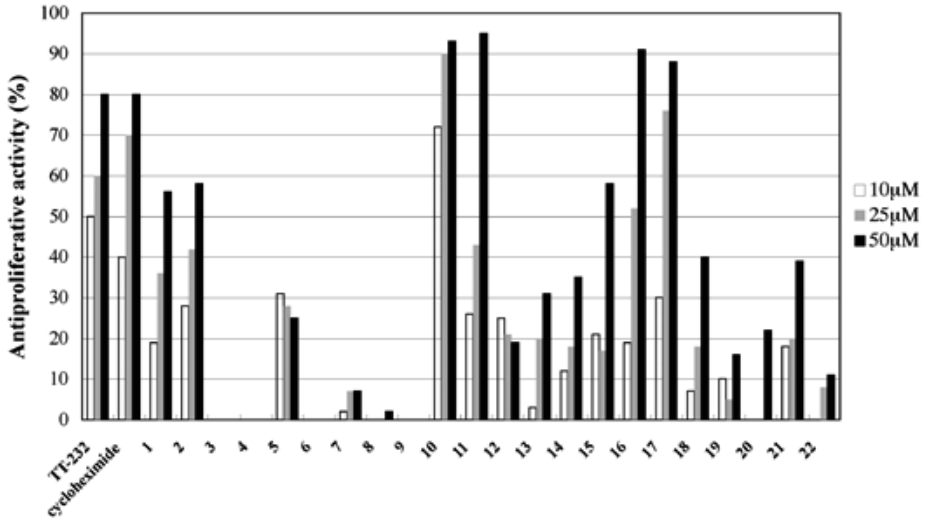

Figure 2. Antiproliferative activities of somatostatin analogues on A431 by MTT test.

Acknowledgements

This work supported in part by KAKENHI (Grant 17790026), by a Grant-in-Aid (C) from Kobe Gakin University, and by NEXT gAcademic Frontier h Project (2006) and in part by Hungarian Grants JAP-6/02, OTAKA 49478, 60197, Cell Kom Ret-06/2006. T. V. is a Bolyai Postdoctorial Felow of the Hungarian Academy of Sciences.

References

1. Kéri G, Mezô I, Vadász Z, Horváth A, Idei I, Vántus T, Balogh Á, Bökönyi G, Bajor T, Teplán I, Tamás J, Mák M, Horváth J, Csuka O. Structure-activity relationship studies of novel somatostatin analogs with antitumor activity. *Pept Res* **6**: 281-288, 1993.
2. Miyazaki A, Yokoi T, Tachibana Y, Enomoto R, Lee E, Bökönyi G, Kéri G, Tsuda Y, Okada Y. Design and synthesis of novel type somatostatin analogs with antiproliferative activities on A431 tumor cells. *Tetrahedron Lett* **45**: 6323-6327, 2004.
3. Jinsmaa Y, Miyazaki A, Fujita Y, Li T, Fujisawa Y, Shiotani K, Tsuda Y, Yokoi T, Ambo A, Sasaki Y, Bryant SD, Lazarus LH, Okada Y. Oral bioavailability of a new class of μ-opioid receptor agonists containing 3, 6-bis[Dmt-NH(CH_2)$_n$]-2(1*H*)-pyrazinone with central-mediated analgesia. *J Med Chem* **47**: 2599-2610, 2004.
4. Miyazaki A, Tsuda Y, Fukushima S, Yokoi T, Vántus T, Bökönyi G, Szabó E, Horváth A, Kéri G, Okada Y. Synthesis of somatostatin analogues containing C-terminal adamantane and their antiproliferative properties. *J Med Chem* **51**: 5121-5124, 2008.

2-02-120

Antimicrobial peptides tailored for plant protection

Ferre, Rafael[1]; Monroc, Sylvie[1]; Badosa, Esther[2]; Cabrefiga, Jordi[2]; Besalú, Emili[3]; Feliu, Lidia[1]; Montesinos, Emilio[2]; Bardají, Eduard[1]; Planas, Marta[1,]*

[1]University of Girona / LIPPSO, SPAIN; [2]University of Girona / CIDSAV, SPAIN; [3]University of Girona / IQC, SPAIN

[*]E-mail: marta.planas@udg.es

Introduction

Bacterial diseases of plants are currently one of the major factors limiting worldwide crop production, and their control is mainly based on copper compounds and antibiotics.[1,2] Although antibiotics are highly efficient, they are not authorized in several countries and resistance has been developed in plant pathogens. This work focused on finding new control agents against economically important plant pathogenic bacteria such as *Erwinia amylovora*, *Pseudomonas syringae* and *Xanthomonas vesicatoria* for which the available methods are not sufficiently effective. We have synthesized combinatorial libraries of linear undecapeptides and cyclodecapeptides, which have been screened for antibacterial activity and eukaryotic cytotoxicity. The main features expected for these peptides are low environmental impact, broad spectrum of activity, reasonable bacterial selectivity, and low eukaryotic cytotoxicity.

Results and discussion

A 125-member library of linear undecapeptides was designed based on the alpha-helical wheel diagram of the peptide H-K[1]KLFKKILKF[10]L-NH_2 (BP76) that inhibited *in vitro* growth of the plant pathogenic bacteria *E. amylovora*, *X. vesicatoria*, and *P. syringae* at low micromolar concentrations.[3,4] Amino acids possessing various degrees of hydrophobicity and hydrophilicity were incorporated at positions 1 (Lys, Tyr, Leu, Phe or Trp) and 10 (Lys, Tyr, Val, Phe or Trp), and N terminus derivatization was also studied (H, acetyl, tosyl, benzoyl or benzyl group) (Fig. 1). Library screening for *in vitro* growth inhibition of the above bacteria identified 27, 40 and 113 sequences with MIC values below 7.5 μM against *E. amylovora*, *P. syringae* and *X. vesicatoria*, respectively. Some peptides were as potent as BP076 and, remarkably, 18 of them were more potent than BP076 against *X. vesicatoria* (MIC<2.5 μM). N-terminus derivatization led to an important decrease of the antibacterial activity against *E. amylovora* and *P. syringae*, but afforded peptides with identical or improved MIC values against *X. vesicatoria*. High activity was observed for peptides bearing a Lys at position 1. The toxicity to eukaryotic cells of the most active peptides was tested by their ability to lyse human red blood cells. While the presence of a Lys at position 1 was associated with low hemolysis, N-terminal derivatization or presence of hydrophobic amino acids at position 10 led to high hemolytic peptides. In particular, peptides containing Trp were the most hemolytic. Peptides with an optimal balance between antibacterial and hemolytic activities were tested *in vivo* by evaluating their preventive effect of inhibition of *E. amylovora* infection in detached apple and pear flowers, and in immature pear fruits (Table 1). All peptides significantly reduced the severity of infections caused by *E. amylovora* in flowers at 100 and 200 μM, except for peptide BP077 at 100 μM. The best peptide was BP100, showing efficacies in flowers of 63-76% at 100 μM. These percentages were only slightly lower than those obtained with streptomycin at 70 μM, currently used in field sprays for fire blight control. In immature pear fruits, all peptides showed a lower efficacy in reducing the severity of infections caused by *E. amylovora* than in flowers. Peptide BP100 was also the most active but significantly less effective than streptomycin.

Head-to-tail cyclic peptides of 4 to 10 residues consisting of alternating hydrophilic (Lys) and hydrophobic (Leu and Phe) amino acids were synthesized.[5,6] Their general formula is c(X_n-Y-X_m-Gln) where X is Lys or Leu, Y is L-Phe or D-Phe, m = n = 1, or m = 3 and n = 0-5. Their antibacterial activity against *E. amylovora*, *P. syringae* and *X. vesicatoria* was evaluated and their cytotoxic effects were determined by measuring the hemolytic activity. Results showed that linear peptides were inactive against the three bacteria tested. Cyclic peptides were active only toward *X. vesicatoria* and *P. syringae* and sequences bearing a L-Phe showed higher antibacterial and hemolytic activities than their D-Phe diastereomers. Peptide c(KLKLKFKLKQ) (BPC10L) was the most active, with MIC values of 6.25 and 12.5 μM against *X. vesicatoria* and *P. syringae*, respectively, but it displayed a high hemolytic activity. Based on this sequence, a library of 56 cyclic decapeptides was prepared and screened for antibacterial activity and eukaryotic cytotoxicity, and led to the identification of peptides with improved MIC against *P. syringae* (3.1 to 6.2 μM) and *X. vesicatoria* (1.6 to 3.1 μM). Notably, peptides active against *E. amylovora* (MIC of 12.5 to 25 μM) were found, constituting the first report of cyclic peptides with activity towards this bacteria. A second library based on the structure c($X^1X^2X^3X^4$LysPheLysLysLeuGln) with X being Lys or Leu yielded peptides with optimized activity profiles. The activity against *E. amylovora* was further improved (MIC of 6.2 to 12.5 μM) and the best peptides, c(KKLKKFKKLQ) (BPC194) and c(KLKKKFKKLQ) (BPC198), displayed a low eukaryotic cytotoxicity at concentrations 30-120 times higher than the MIC values.

Table 1. Linear peptides with the best biological activity profile

Peptide	Sequence	MIC intervals (μM)			Hemolysis (%)	
		E. amylovora	*P. syringae*	*X. vesicatoria*	50 μM	150 μM
BP076	KKLFKKILKFL-NH_2	2.5-5.0	2.5-5.0	2.5-5.0	3	34
BP077	Ac-KKLFKKILKFL-NH_2	5.0-7.5	5.0-7.5	<2.5	6	40
BP100	KKLFKKILKYL-NH_2	2.5-5.0	2.5-5.0	5.0-7.5	3	22
BP125	Ts-KKLFKKILKKL-NH_2	>7.5	2.5-5.0	2.5-5.0	2	8
BP126	Bz-KKLFKKILKKL-NH_2	5.0-7.5	2.5-5.0	2.5-5.0	2	14

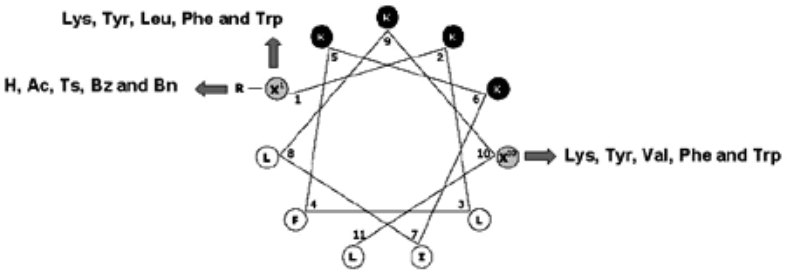

Figure 1. Edmunson wheel projection of the 11-mer peptides of the 125-member library

In conclusion, the most promising peptides described here can be considered as lead compounds to be further tested in *ex vivo* and in *in vivo* assays, and as good candidates for the development of effective antibacterial agents for use in plant protection.

References

1. Agrios G N. *Plant Pathology 4th Edition*, Academic Press, Calofornia, U S A , 1998.
2. Vidaver A K. Uses of antimicrobials in plant agriculture. *Clin Infect Dis* **34**: S107-S110, 2002.
3. Ferre R, Badosa E, Feliu L, Planas M, Montesinos E, Bardají E. Inhibition of plant-pathogenic bacteria by short synthetic cecropin A-melittin hybrid peptides. *Appl Environ Microbiol* **72**: 3302-3308, 2006.
4. Badosa E, Ferre R, Planas M, Feliu L, Besalú E, Cabrefiga J, Bardají E, Montesinos E. A library of linear undecapeptides with bactericidal activity against phytopathogenic bacteria. *Peptides* **28**: 2276-2285, 2007.
5. Monroc S, Badosa E, Besalú E, Planas M, Bardají E, Montesinos E, Feliu L. Improvement of cyclic decapeptides against plant pathogenic bacteria using a combinatorial chemistry approach. *Peptides* **27**: 2575-2584, 2006.
6. Monroc S, Badosa E, Feliu L, Planas M, Montesinos E, Bardají E. De novo designed cyclic cationic peptides as inhibitors of plant pathogenic bacteria. *Peptides* **27**: 2567-2574, 2006.

2-02-121

Selection of chromogenic and fluorogenic substrates of neutrophil serine proteases using combinatorial chemistry approach

Lesner, Adam[1,]; Wysocka, Magdalena[1]; Guzow, Katarzyna[2]; Wiczk, Wiesław[2]; Rolka, Krzysztof[1]*

[1]Gdańsk University Faculty of Chemistry, Bioorganic chemistry Department, POLAND; [2]Gdańsk University/Faculty of Chemistry, POLAND

[*]E-mail: adas@chem.univ.gda.pl

Proteinase 3 (PR3) along with elastase and cathepsin G (CG) is synthesized and stored in azurohilic granules of polymorphonulcear neutrophiles. Those members of chymotrypsin clan of serine protease family are involved in several important physiological processes like degradation of the components of the extracellular matrix (elastin, collagen, laminine),[1] control of cytokine activity (TNF-α, IL-1β),[2] platet activation and antimicrobial activity.[3] They are secreted as active enzymes by neutrophiles in inflammatory site.[4] Recent work reveals that only proteinase 3 is involved in regulation of cell proliferation and apoptosis. Moreover this protease is a target in the autoimmune severe disease called the Wegener's granulocytosis.[5] This makes this 30 kDa protease an excellent target for drug discovery. However, due to high sequence identity with human neutrophil elastase (HNE) and almost identical primary specificity with HNE1 it's difficult to discriminate the effects of the action of those two proteases. In our recent work[6] the synthesis and kinetic investigation of tripeptide library ABZ-X3-X2-X1-ANB-NH_2 that in position X3 and X2 consisted of all proteinogenic amino acid residues, except Cys and in position X1 = Ala, Abu, Val, Nva, Ser, Thr, Ile, Leu, Nle, the ANB-NH2 stand for amide of 5-amino-2-nitro benzoic acid. The obtained substrate ABZ-Tyr-Tyr-Abu-ANB-NH_2 was used as a starting structure for

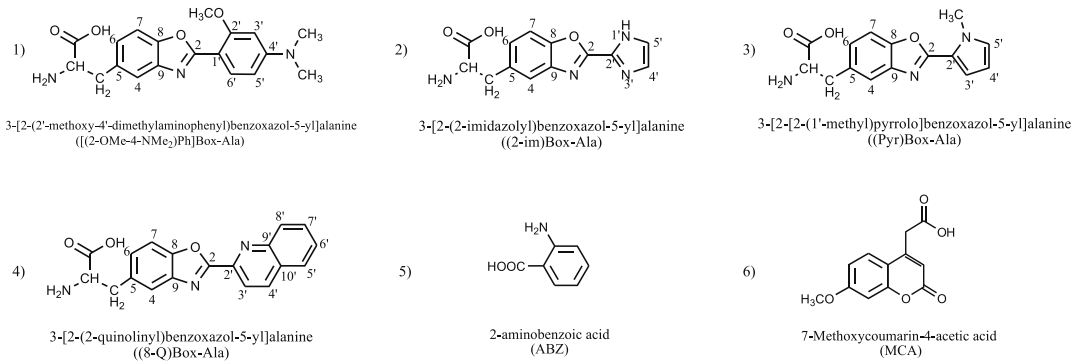

Figure 1. The chemical structure of fluorofores introduced at N-termini of peptide.

further investigation. The ABZ moiety was replaced by series of benzoxazole-L-alanine derivates that chemical structures are present in Fig. 1.

The commonly used fluorofores ABZ and MCA was used as a reference compounds. The introduced set of fluorofores at N-termini and ANB-NH_2 at C-termini of peptides synthesized served as donor and acceptor, respectively. Such substituents allow the fluorescence resonance energy transfer (FRET) within the peptides synthesized. Moreover all benzoxazole-L-alanine derivates displayed a good overlapping of its emission spectrums with the absorption spectrum of the acceptor (ANB-NH_2). Substrate activity assay of such peptides against proteinase 3, cathepsin G and human neutrophil elastase revealed the sequence that is selectively and efficiently hydrolyzed by proteinase 3.

It also worth to stress out that all substrates displayed dual chromogenic-fluorogenic properties. Physicochemical parameters of such substrates determined are listed in Table 1. The highest substrate activity among all studied substrates against proteinase 3 was displayed for peptide 3 with the smallest substituent (pyrrole ring) within this set (Fig. 2). Residual proteolytic susceptibility is displayed by large 2'-methoxy-4'-

Table 1. Physicochemical parameters of proteinase 3 substrates

No	sequence: X-Tyr-Tyr-Abu-ANB-NH_2	MW calculated/ determinated	t_R [min]*	F_1/F_0	Energy transfer efficiency [%]
1	[(2-OMe-4-NMe_2)Ph]Box-Ala	929.4/930.4	20.42	11.8	91
2	(2-im)Box-Ala	846.3/847.3	12.49	14.1	93
3	(Pyr)Box-Ala	859.3/860.3	19.94	10.2	90
4	(8-Q)Box-Ala	907.3/908.3	22.12	8.6	88
5	ABZ	689.4/690.9	20.45	7.4	86
6	MCA	808.3/809.3	25.08	5.2	80

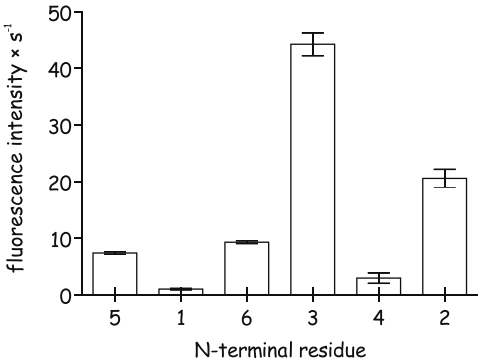

Figure 2 . Activity of proteinase 3 substrates with different N-terminal substituents.

dimethyl-aminophenyl group There is a good correlation between size of the benzoxazole derivates size and activity against proteinase 3. Substrate with the highest activity was subjected for further studies.

The compound numbers corresponds to Fig. 1. The sensitivity assay was performed for substrate 3. The results obtained indicate that fluorescence of substrate (Pyr)Box-Ala-Tyr-Tyr-Abu-ANB-NH_2 could be easily detected at a concentration of proteinase 3 as low as 2.9 $\times 10^{-11}$ M that is 10 fold lower that for ABZ containing peptide that was report previously by our group. PR3 is released for azurophil granules along with HNE and CG. Prolonged (up to 24 hours) incubation with CG or HNE of compound 3 results no visible proteolysis. Such data indicate that peptide 3 is selectively hydrolyzed only by PR3 in presence of other neutrophil proteases like HNE or CG. In conclusion, the sensitive and selective substrate of proteinase 3 was developed that contained new molecular probe that serve as a fluorofore. This peptide displays dual chromogenic and fluorogenic properties and using this substrate we were able to detect as less as 28.7 pM of proteinase 3.

Acknowledgements

This work was supported by University of Gdañsk (grants No. BW 8000-5-0397-8 and BW 8000-5-451-8).

References

1. Rao NV, Wehner NG, Marshall BC, Gray WR, Gray BH, Hoidal JR. *J Biol Chem* **266**: 9540-9548, 1991.
2. Renesto P, Halbwachs-Mecarelli L, Nusbaum P, Lesavre P, Chignard M. *J Immunol* **152**: 4612-4617, 1994.
3. Gabay JE, Scott RW, Campanelli D, Griffith J, Wilde C, Marra MN, Seeger M, Nathan CF. *Proc Natl Acad Sci U S A* **86**: 5610-5614, 1989.
4. Wiedow O, Wiese F, Christophers E. *Arch Dermatol Res* **287**: 632-635, 1995.
5. Kantari C, Pederzoli-Ribeil M, Amir-Moazami O, Gausson-Dorey V, Moura IC, Lecomte MC, Benhamou M, Witko-Sarsat V. *Blood* **110**: 4086-4095, 2007.
6. Wysocka M, Lesner A, Guzow K, Mackiewicz L, Legowska A, Wiczk W, Rolka K. *Anal Biochem* **378**: 208-215, 2008.

2-02-122

Selection of peptomeric inhibitors of bovine α-chymotrypsin and cathepsin G based on trypsin inhibitor SFTI-1 using combinatorial chemistry approach

Dębowski, Dawid[1]; Łęgowska, Anna[1]; Wysocka, Magdalena[1]; Lesner, Adam[1]; Rolka, Krzysztof[1,]*

[1]Faculty of Chemistry, University of Gdańsk, Sobieskiego 18, 80-952 Gdańsk, POLAND

[*]E-mail: krzys@chem.univ.gda.pl

Introduction

The sunflower trypsin inhibitor SFTI-1 is considered to be a very attractive template for design of new inhibitors with a potential use as pharmacological agents because it possesses the combination of two desirable features: small size (only 14 amino acid residues in length) and high inhibitory activity against trypsin and cathepsin G.[1] The introduction of *N*-substituted glycine residue (peptoid monomer) mimicking Phe in this position of monocyclic SFTI-1 with disulfide bridge only, yielded potent chymotrypsin inhibitor (Ka = 3.8 x 10^8 M^{-1}).[2] As a result, we obtained a peptide-peptoid hybrid polymer called *peptomer* that beside retaining its high inhibitory activity, displayed another valuable attribute - proteolytic resistant P_1-P_1' reactive site. Herein, we present the impact that a replacement of further naturally occurring residues in SFTI-1 with *N*-substituted glycine derivatives has on inhibitory activity against chymotrypsin and cathepsin G. We focus our attention on the Ile7-Pro8-Pro9-Ile10 region of the sequence that makes an important contribution to structural integrity and rigidity of SFTI-1. This region includes *cis*-Pro8 residue, conserved among the members of Bowman-Birk family. Based on our previous results and also published by other groups, we obtained the library consisting of 360 peptomers. The general formula of the synthesized library is shown in Fig. 1.

Results and Discussion

Synthesis was conducted manually by the solid-phase method using Fmoc/*t*Bu chemistry. Peptide library was synthesized by the portioning-mixing method. Incorporations of *N*-substituted glycine derivatives

Gly-Arg-Cys-Thr-Nphe[5]-Ser-X_1-X_2-X_3-X_4-Cys-Nphe-Pro-Asp

where:

X_1 = X_4 = Ile, Nleu, Nnle;

X_2 = Pro, Npip, Namp, Naem, Noct;

X_3 = Nnle, Abu, Pro, Trp, Npip, Namp, Naem, Noct

Figure 1. General formula of the library of the SFTI-1 analogues.

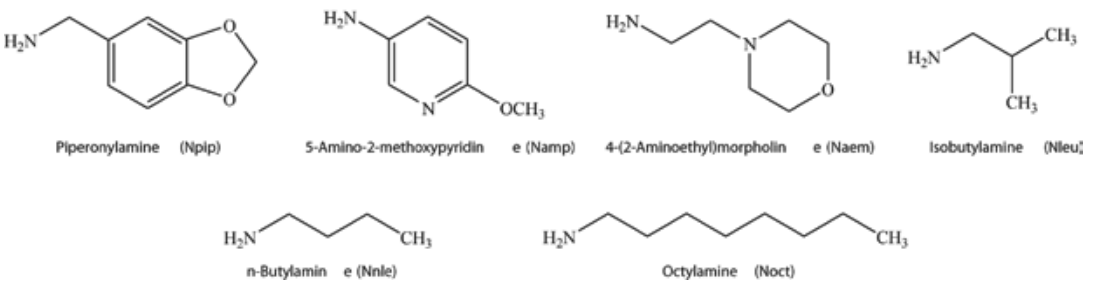

Figure 2. List of primary amines used for the preparation of *N*-substituted glycine residues. Abbreviations of peptoid monomers obtained are shown in brackets.

Table 1. Association equilibrium constants of the selected peptomeric analogue of SFTI-1 with the experimental enzymes

Inhibitor*	K_a [M^{-1}]	
	bovine α-chymotrypsin	cathepsin G
SFTI-1 wild	$(5.2 \pm 1.7) \times 10^6$ [4]	$(5.7 \pm 0.3) \times 10^6$
[Phe^5]SFTI-1	$(2.0 \pm 0.2) \times 10^9$ [5]	$(3.7 \pm 0.2) \times 10^6$
[$Nphe^5$] SFTI-1	$(3.9 \pm 0.3) \times 10^8$ [2]	N/A
[$Nphe^{5,12}$]SFTI-1	$(9.3 \pm 0.8) \times 10^7$	$\sim 10^5$
[$Nphe^{5,12}$,$Naem^8$]SFTI-1	$(1.3 \pm 0.3) \times 10^8$	N/A
[$Nphe^{5,12}$,$Npip^{8,9}$,$Nnle^{10}$]SFTI-1	$\sim 10^5$	$(2.1 \pm 0.1) \times 10^7$

*All analogues are monocyclic with disulfide bridge only

were performed using submonomer strategy. Chemical formulas of primary amines used for incorporation of peptoid monomers are shown in Fig. 2.

Disulfide bridge formation was achieved using iodine-mediated oxidation in MeOH/AcOH. The deconvolution procedure was performed by the iterative method in solution. Association equilibrium constants (K_a) were determined as described previously[3]. Deconvolution of the peptomer library revealed that three analogues: [$Nphe^{5,12}$,$Naem^8$]SFTI-1, [$Nphe^{5,12}$,$Naem^8$]SFTI-1 and [$Nphe^{5,12}$,$Npip^{8,9}$,$Nnle^{10}$]SFTI-1 displayed the highest inhibitory activity against bovine α-chymotrypsin and cathepsin G, respectively. The values of K_a of these selected analogues together with reference compounds determined with both enzymes were summarized in Table 1.

Reports published up to date postulated that well conserved *cis*-Pro in position 8 of Bowman-Birk inhibitors is essential for maintaining their activity. In contrary, the results presented here clearly indicate that certain substitutions of this amino acid residue can be tolerated, yielding potent inhibitors. It is also worth noticing that the introduced modifications produced not only potent but also selective chymotrypsin and cathepsin G inhibitors.

Acknowledgements

This work was supported by Ministry of Science and Higher Education (grant No. 2889/H03/2008/34).

References

1. Luckett S, Garcia RS, Barker JJ, Konarev AV, Shewry PR, Clarke AR, Brady RL. High-resolution structure of a potent, cyclic proteinase inhibitor from sunflower seeds. *J Mol Biol* **290**: 525-533, 1999.
2. Stawikowski M, Stawikowska R, Jaśkiewicz A, Zabłotna E, Rolka K. Examples of peptide-peptoid hybrid serine protease inhibitors based on the trypsin inhibitor SFTI-1 with complete protease resistance at P1-P1' reactive site. *ChemBioChem* **6**: 1057-1061, 2005.
3. Łegowska A, Bulak E, Wysocka M, Jaśkiewicz A, Lesner A, Debowski D, Rolka K. Peptomeric analogues of trypsin inhibitor SFTI-1 isolated from sunflower seeds. *Bioorg Med Chem* **16**: 5644-5652, 2008.
4. Zabłotna E, Kazmierczak K, Jaskiewicz A, Kupryszewski G, Rolka K. Inhibition of bovine α-chymotrypsin by cyclic trypsin inhibitor SFTI-1 isolated from sunflower seeds and its two acyclic analogues. *Letters of Peptide Science* **9**: 131-134, 2002.
5. Zabłotna E, Jaskiewicz A, Łęgowska A, Lesner A, Rolka K. Design of Serine Proteinase Inhibitors by Combinatorial Chemistry using Trypsin Inhibitor SFTI-1 as a Starting Structure. *J Pept Sci* **13**: 749-755, 2007.

2-02-123

Using a random peptide library to screen for antimicrobial activity against *Pseudomonas aeruginosa*

Mikut, Ralf[1]; Hilpert, Kai[2,]*

[1]Karlsruhe Institut of Technology, Institut for Applied Computer Science, Karlsruhe, GERMANY; [2]Karlsruhe Institut of Technology, Institute of Biological Interfaces, Karlsruhe, GERMANY

[*]E-mail: kai.hilpert@ibg.fzk.de

The introduction of antibiotics into the human health care had a strong influence of the treatment strategy and consequently on the surviving rate of patients with severe bacterial infections. In our time, many medical procedures, for example surgeries, are strongly depended on antibiotics as a prophylaxis to prevent infections. However, it is known since the 1940s that bacteria can become resistant. At that time until the 1960s several new classes of antibiotics were discovered, therefore the resistance toward one of the antibiotics was not seen as critical. In the recent years, it has become clear that we are now facing an era of multidrug resistance in our hospitals and communities. According to the 2004 report of the National Nosocomial Infection Surveillance (NNIS),[1] the rate of resistance to methicillin (a marker for multidrug resistance) of *Staphylococcus aureus* (well known as MRSA) has increased to 59%. Thus, it is important to develop new classes of antibiotics and novel strategies to treat antibiotic resistant infections. Cationic antimicrobial peptides are recognized to be an alternative to conventional antibiotics.[2] It was shown that these peptides can kill Gram-positive as well as Gram-negative bacteria. Some of them are also effective against fungi, enveloped viruses and eukaryotic parasites.[3] They differ in structure, but most of them are cationic and amphiphilic and smaller than 60 amino acids. An overview of 1137 proteins/peptides believed to be antimicrobial can be found at http://www.cnbi2.com/cgi-bin/amp.pl?allpeptides=1AMPs. A total random peptide library consisting of 200 9mer peptides was tested for antimicrobial activity against *Pseudomonas aeruginosa*.[4] With help of a computer program 200 random sequences were created, consisting of all 20 proteinogenic amino acids except cysteine (Fig. 2). The peptides were synthesized on cellulose using the SPOT technology and tested by using a screening system recently described.[5,6] Here, we compared the amino acid distribution of this random peptide library with the available natural antimicrobial peptides. The amino acid distribution of the natural library is shown in Fig. 1 using all 1045 sequences matched to 146 clusters (http://www.cnbi2.com/cgi-bin/amp.pl?allpeptides=1AMPs). The amino acid distribution of the random peptide library was nearly uniform (Fig. 2). Some examples of generated sequences are given in Table 1. The antimicrobial activity against *Pseudomonas aeruginosa* of the 200 random peptides was very poor.[4] Analyzing the data with our newly developed routine,[7] we identified in a preprocessing step, 15 peptides with unusual curves of the luminescence values, that were automatically excluded. The remaining 185 peptides of the random library have estimated IC75 values at relative concentrations of 1.55 0.43 (best peptide: 0.31) in contrast to the control peptides (Bac2a) with 0.12 0.03.

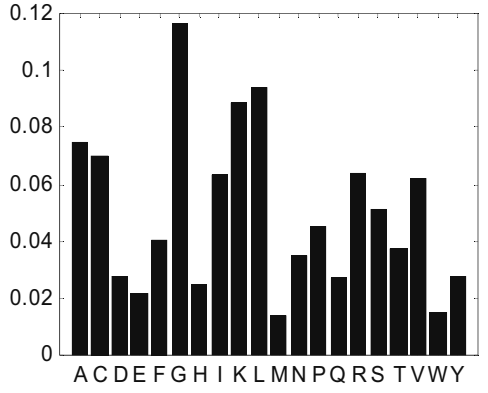

Figure 1. Mean amino acid distribution in the library with 1137 proteins/peptides.

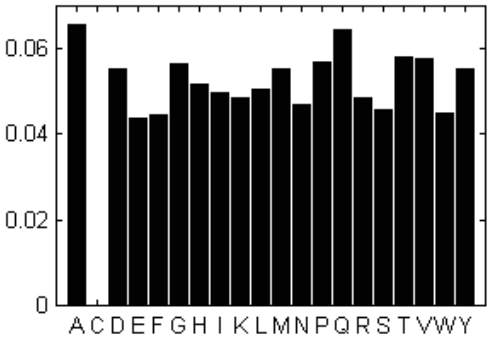

Figure 2. Mean amino acid distribution in the random library.

VGTDVTKIQ	NTHEAMLMS
FNAPNWNLW	WALWNYERP
YPDIYRTAT	SPDDGKFYP
HSTNLWIGI	SALMVYNRF
GHKFYAMAK	TYAGRTTKF
DYKIGAITI	YVAWQTQKT
LSYQLRHEE	YNAHKMHYY
LDKTASPVN	LRTEIFPWK
RSQLRVASH	SFHWRMGVI
WQQYSARHA	RMWAWQDAV
LNGDEQQEQ	QTHMVMGKQ
YLYYGGRKT	AFHIVIEVA
SPVAYVRGQ	SWAITEGGF
YAKDGTSQV	ETTDYNPDY
KNQGQTKMV	GVFPFWPLR
TQPQITLDV	VMLTMVWDR
IKQVNVVQK	DIGELMMAH
DMPELEGYV	PDDQAIPDF
TGFDLAYYK	IHYMSSLDR
SSFVRRGAP	PVFVETADE
TGGWHQPYW	FQQRMEVIE
MFMFAHPMW	EWQVSPATH
RYEKHIAHN	KHLKERDEW
VHHDVRPVR	HEWRMQRGT
AHVMYKAIP	TSQGNGRVL
TILKHEVGT	IKSGSTPTQ
HTIPLNLVW	GDPIPRYFT
FLIFHEFEP	DFLILGFNF
SEIDGDMYV	PEKGYGWVM

Table 1. Examples for generated sequences, all peptides are C-terminally amidated

In conclusion, with a library of 200 peptides, the chance to find antimicrobial peptides is rather low. Consequently, the random generation of a library would require a much larger number of peptides. An alternative is the generation of semi-random libraries based on design rules, like amino acid distribution of natural antimicrobial peptides to increase the probability of antimicrobial peptides.

References

1. Centers for Disease Control and Prevention (CDC), 2004, http://www.cdc.gov/ncidod/dhqp/pdf/nnis/2004NNISreport.pdf.
2. Marr AK, Gooderham WJ, Hancock REW. Antibacterial peptides for therapeutic use: obstacles and realistic outlook. *Curr Opin Pharmacol* **6**: 468-472, 2006.
3. Hancock REW. Cationic peptides: effectors in innate immunity and novel antimicrobials. *Lancet Infect Dis* **1**: 156-164, 2001.
4. Cherkasov A, Hilpert K, Jenssen H, Fjell CD, Waldbrook M, Mullaly SC, Volkmer R, Hancock REW. Use of artificial intelligence in the design of small peptide antibiotics effective against a broad spectrum of highly antibiotic-resistant superbugs. *ACS Chem Biol* **4**: 65-74, 2009.
5. Hilpert K, Winkler DFH, Hancock R. Peptide arrays on cellulose support: SPOT synthesis - a time and cost efficient method for synthesis of large numbers of peptides in a parallel and addressable fashion. *Nat Protocols* **2**: 1333-1349, 2007.
6. Hilpert K, Hancock REW. Use of luminescent bacteria for rapid screening and characterization of short cationic antimicrobial peptides synthesized on cellulose using peptide array technology. *Nat Protoc* **2**: 1652-1660, 2007.
7. Mikut R, Reischl M, Ulrich AS, Hilpert K. Data-Based Activity Analysis and Interpretation of Small Antibacterial Peptides. *Proceedings of 18th Workshop Computational Intelligence*, Karlsruhe University Press, 2008.

2-03-124

Conformational Preferences of Cyclopeptides Formed by i-to-i+4 Side Chain-to-Side Chain Cyclization via 1,4-Disubstituted [1,2,3]Triazolyl Moiety

Mario Scrima[1]; Alexandra Le Chevalier Isaad[2-3]; Manuela Grimaldi[1]; Paolo Rovero[2-4]; Anna Maria Papini[2-3]; Michael Chorev[5]; Anna Maria D'Ursi[1,]*

[1]Dipartimento di Scienze Farmaceutiche, Via Ponte Don Melillo 11C, Salerno, I-84084, ITALY; [2]Laboratory of Peptide & Protein Chemistry & Biology, Polo Scientifico e Tecnologico, University of Firenze, I-50019 Sesto Fiorentino, ITALY; [3]Dipartimento di Chimica Organica, Polo Scientifico e Tecnologico, University of Firenze, Via della Lastruccia 13, Sesto Fiorentino, I-50019, ITALY; [4]Dipartimento di Scienze Farmaceutiche, University of Firenze, Via Ugo Schiff 3, Polo Scientifico e Tecnologico, Sesto Fiorentino, I-50019, ITALY;

[5] Laboratory for Translational Research, Harvard Medical School, One Kendal Square, Building 600, Cambridge, Massachusetts 02139, USA

[*]E-mail: dursi@unisa.it

Introduction

The cyclization through intramolecular side-chain-to-side-chain covalent bond formation is a strategy to stabilize the bioactive conformations of linear peptides and to improve their metabolic stability, potency and selectivity.

We have recently published preliminary study reporting the synthesis and the conformational analysis of a model i-to-i+4 side chain-to-side chain 1,4-disubstituted-[1,2,3]triazolyl-bridged cyclopeptide [Ac-Lys-Gly-Xaa(&[1])-Ser-Ile-Gln-Yaa(&[2])-Leu-Arg-NH_2][(&[1](CH_2)4-1,4-[1,2,3]triazolyl-CH_2&[2])]$_1$ (Scheme 1, **III**) that was designed to mimic a i-to-i+4 side chain-to-side chain lactam-bridged cyclopeptide, Ac-Lys-Gly-Lys(&[1])-Ser-Ile-Gln-Asp(&[2])-Leu-Arg-NH_2]. This was a truncated version of parathyroid hormone-related protein (PTHrP), [Lys[13](&[1]),Asp[17](&[2])]PTHrP(1-34)NH_2, which was reported to be α-helical and a potent agonist of the parathyroid hormone receptor 1 (PTHR1).[2-3]

Here we present CD and NMR conformational analysis of new analogs of cyclopetide **III** - cyclopeptides **I** and **II** (Scheme 1) -. These cyclopeptides included 1,4- (**I**) or 4,1- (**II**) disubstituted-[1,2,3]triazolyl moieties respectively, flanked alternatively by alkyl chains $(CH_2)_3$ and $(CH_2)_1$ on the N- and C-terminal sides of the backbone.

Results and discussion

CD and NMR spectra of [1,2,3]triazolyl-containing peptides (I and II) were recorded in water and in HFA/water (50/50 v:v). CD spectra in water as well as in water/HFA mixture (Fig. 1) presented negative bands at 208 and 222 nm. The quantitative estimation of CD curves using DICHROWEB website according to ContinLL algorithm evidenced a significant presence of β-turn structures.

Scheme 1. 1,4-disubstituted-[1,2,3]Triazolyl-Containing Cyclononapeptides Fragment corresponding to the ω-Azido-containing α-amino acyl residues in the cyclopeptide are highlighted in red. Fragment corresponding to the ω-Ethynyl-containing α-amino acyl residues in the cyclopeptide are highlighted in blue

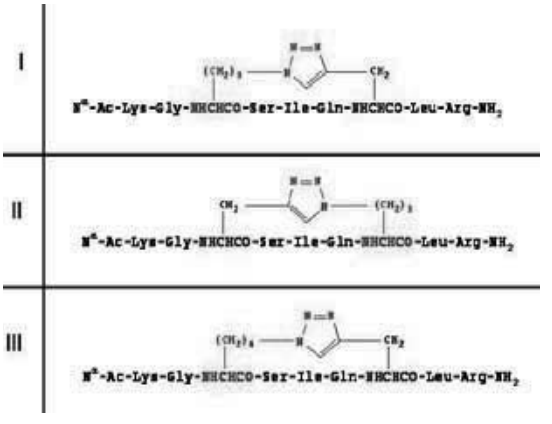

2D 1H COSY, TOCSY and NOESY of [1,2,3]triazolyl containing cyclopeptides **I** and **II** allowed the collection of NOE data (Fig. 1) to calculate 3D models (Fig. 2). NOESY spectra of cyclopeptides in water include few significant NOE connectivities suggesting a minor contribution of ordered structures. On the contrary NOESY spectra in water/HFA mixture evidence a high number of sequential and medium range NOEs. In particular sequential α-N(i,i+1) and NH-NH(i,i+1) NOE connectivities, as well as medium range α-N(i,i+2), NH-NH(i,i+2), NH-NH(i,i+3) NOE connectivities.

Analysis of NMR structures of cyclopeptide **I** in water shows the presence of γ-turn conformations in the ^{12}Gly-^{15}Ile segment; conversely type **I** β-turn and γ-turn are present in the C-terminal segment of cyclopeptide **II**. Fig. 3 shows the bundles of 20 superimposed conformers representing the backbones of cyclopetides **I** and **II** in HFA/water. NMR structures of compounds **I** and **II** evaluated by PROMOTIF procedure, evidence folded but non regular secondary structures. A minor contribution of regular secondary structures points, for cyclopeptide **II**, to a detectable presence of γ-turn conformations.

The comparison of low energy NMR structures of cyclopetide **I** and **II** with the previously mentioned cyclopetide **III** and with the lactam parent peptide, evidence a low degree of similarity among the superimposed conformers. The structural differences can be dependent on the shortening of the linker, which is composed of 3+1 or 1+3 (compound **I** and **II**) methilen moieties, instead of 4+1 methilen moieties (compound **III**). The present results indicate that rings of smaller dimensions lead to the distortion of the conformations so that the helical regularity typical of bioactive cyclo lactam is lost. In conclusion in the choice of the right ring size of triazolil cyclopeptides resembling the conformational properties of cyclo lactam, a reduction of the ring size is not advisable.

References

1 Cantel S, Le Chevalier-Isaad A, Scrima M, Levy JJ., DiMarchi RD, Rovero P, Halperin JA, D'Ursi AM, Papini AM, Chorev M. *J Org Chem* **73**: 5663-5674, 2008.

2 Chorev M, Roubini E, McKee RL, Gibbons SW, Goldman ME, Caulfield MP, Rosenblatt M. *Biochemistry* **30**: 5968-5974, 1991.

3 Maretto S, Mammi S, Bissacco E, Peggion E, Bisello A, Rosenblatt M, Chorev M, Mierke DF. *Biochemistry* **36**: 3300-3307, 1997.

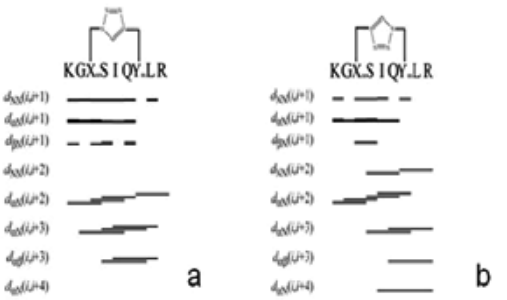

Figure 1. NOE connectivities as derived from NOESY spectra of cyclopeptides **I** (a) and **II** (b) in HFA/water 50/50 v:v.

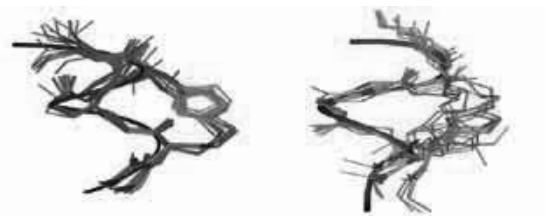

Figure 2. NMR structure bundles of cyclopeptides **I** (left) and **II** (right) as derived from HFA/water 50/50 v:v NOESY spectra at 600 MHz and 300K.

2-03-125

Solid-phase synthesis and biological activity of linear tuftsin and retro-tuftsin derivatives

Kukowska-Kaszuba, Magdalena[1,]; Dzierzbicka, Krystyna[1]; Mackiewicz, Zbigniew[2]*

[1]Gdańsk University of Technology, 11/12 G. Narutowicza Street, 80-952 Gdańsk, Department of Organic Chemistry, POLAND; [2]University of Gdańsk, 18/19 J. Sobieskiego Street, 80-952 Gdańsk, Department of Polypeptides Chemistry, POLAND

[*]E-mail: magda1805@o2.pl

Introduction

Tuftsin (H-Thr-Lys-Pro-Arg-OH) is a natural peptide that is liberated from Fc-domain of the heavy chain of immunoglobulin G by the action of two specific enzymes (leukokininase, spleen tuftsin endocarboxypeptidase). Being a tetrapeptide of biological origin is extremely important compound because it can activate several elements of immune system such as granulocytes and macrophages. Tuftsin indicates not only immunological stimulating factor but also antibacterial, antifungal, antiviral and antineoplastic properties.[1,2] Presented immunomodulator also co-administrates along with different antibiotics in the treatment of opportunistic infections. In spite of its wide range of activity, tuftsin is unstable in plasma and it has become the aim of new analogues formation that are more resistant to proteolytic degradation. Numerous different modifications of the tuftsin chain which have improved the biological activity have been reported to date.[3] Modifications include changing the length and sequence of the central chain. The highly interesting results were dependent on peptide resistance against enzymatic cleavage. Recent research has proved that retro-tuftsin analogues significantly surpass tuftsin in both stability and activity. To date, many retro-tuftsin analogues that have demonstrated very encouraging results have been synthesized but there is still wide scope for further research. Moreover tuftsin analogues containing an isopeptide bond have shown increased resistance in relation to tuftsin.[2-5]

Results and discussion

Encouraged by the results obtained, we prepared linear tuftsin derivatives **1a-i** (Table 1) that fall into two series: tuftsin and retro-tuftsin analogues. Each group includes analogues containing a modification at the ε-amino group of lysine. The introduction of an additional residue (alanine, β-alanine, valine, glycine and isoleucine) into the tuftsin or retro-tuftsin chain at the ε-amino group of lysine allowed us to form the isopeptide bond. All the peptides were synthesized using a Fmoc-technique. Tuftsin derivatives were confirmed by MS, amino acid analysis, elemental analysis and RP-HPLC analysis.[4]

In the second part of our study, we performed the pilot tests to determine the *in vitro* activity of nine synthetic peptides (**1a-i**). The activity of the pentapeptides was investigated against reference strains of bacteria (*S. aureus, S. epidermidis, R. equi, E. Coli, P. aeruginosa, E. faecalis*), yeast (*C. albicans*) and fungi (*A. niger*). The biological activity of tuftsin analogues was investigated at Medical University of Gdańsk using microbroth dilution method according to the procedures outlined by the National Committee for Clinical Laboratory Standards. The activity of our peptides was compared to synthesized tuftsin which exhibit well known activity.[5,6] The concentrations of peptides prepared for the test were: 1000, 500, 250, 250, 125, 62.5, 31.25 and 15.6 μg/ml. Peptides **1a-i** at a concentration of 500 μg/ml, after 24 h incubation at 37 °C, limited the growth of *R. equi* and *E. faecalis*. However the development of these bacteria, after 36 h incubation, was observed at 40% respectively in relation to the growth at low concentration. Peptides **1a-i** at the concentration of 250 μg/ml, after a 3 day incubation, inhibited the growth of *R. equi* and *S. epidermidis* at 25% and 29% respectively. No inhibitory effect was observed with other microorganisms. All the peptides were either less effective or lacked any activity in relation to tuftsin. Presented results suggest that the modification of the tuftsin chain at the ε-amino group of lysine probably plays a key role in the stabilization of the peptide but does not any influence on the enhancement of biological activity. However we envisage using more strains of microorganisms to investigate the biological properties of tuftsin analogues.

Table 1. Sequence of tuftsin and retro-tuftsin derivatives

Number	Peptide Sequences	
1a	H-Thr-Lys(Gly)-Pro-Arg-OH	**Tuftsin analogues**
1b	H-Thr-Lys(Val)-Pro-Arg-OH	
1c	H-Thr-Lys(βAla)-Pro-Arg-OH	
1d	H-Thr-Lys(Ile)-Pro-Arg-OH	
1e	H-Arg-Pro-Lys(Gly)-Thr-OH	**Retro-tuftsin analogues**
1f	H-Arg-Pro-Lys(Val)-Thr-OH	
1g	H-Arg-Pro-Lys(Ala)-Thr-OH	
1h	H-Arg-Pro-Lys(βAla)-Thr-OH	
1i	H-Arg-Pro-Lys(Ile)-Thr-OH	

Acknowledgements

This work was supported by the Polish State Committee for Scientific Research (**Grant No. NN 405064134**) and University of Gdańsk (Grant BW No. 8000-5-0126-8).

References

1. Siemion IZ, Kluczyk A. Tuftsin: on the 30-year anniversary of Victor Najjar's discovery. *Peptides* **20:** 645-674, 1999.
2. Mező G, Szekerke M, Sarmay G & Gergely J. Synthesis and functional studies of tuftsin analogs containing isopeptide bond. *Peptides* **11:** 405-415, 1990.
3. Wardowska A, Dzierzbicka K & Mysliwski A. Tuftsin - new analogues and properties. *Post Biochem* **53:** 60-65, 2007.
4. Kukowska-Kaszuba M, Dzierzbicka K, Mackiewicz Z. Synthesis of linear tuftsin analogues modified at the ε-amino group of lysine. *Tetrahedron Lett* **49:** 5718-5720, 2008.
5. Dzierzbicka K, Rakowski T, Kolodziejczyk AM. Tuftsin - endogenous immunomodulator. *Post Biochem* **46:** 327-335, 2000.
6. Blok-Perkowska D, Muzalewski F, Konopinska D. Antibacterial properties of tuftsin and its analogs. *Antimicrob Agents Chemother* **25**: 134-136, 1984.

2-03-126

Biocatalyst-Catalyzed Peptide Synthesis Using Inverse Substrates as Acyl Donor[1,2]

Sekizaki, Haruo; Fuchise, Tomoyoshi; Kojoma, Mareshige; Toyota, Eiko*
Faculty of Pharmaceutical Sciences Health Sciences University of Hokkaido, JAPAN

**E-mail: sekizaki@hoku-iryo-u.ac.jp*

Introduction

Previously we reported that the *p*-amidinophenyl esters behave as specific substrates for trypsin and trypsin-like enzymes.[3] Such a substrate is termed an "inverse substrate".[3] Inverse substrates allow the specific introduction of an acyl group carrying a non-specific residue into the trypsin active site. The characteristic features of inverse substrate suggested that they are useful for enzymatic peptide synthesis. Thus development of general method for the preparation of a variety of inverse substrates would be valuable. We designed non-conjugated compounds of amidino group and phenol ring for more stable inverse substrate than the conjugated amidino phenol esters.

Results and Discussion

Herein, we presented a facile synthetic method for two series of new type inverse substrates; *N-tert*-butoxycarbonyl (Boc)-amino acid *p*- and *m*-(amidinomethyl)phenyl esters, by using Brian's catalytic hydrogenation of {[(acetoxy) imino]-2-aminoethyl}phenyl esters (**4**, **9**) as a key step, as shown in Chart 1.[4] We analyzed the kinetic behavior of trypsin towards these synthetic esters, and conclude that all new synthetic inverse substrates examined in this study could be expected as acyl donor components in trypsin-catalyzed peptide synthesis. Indeed, they were found to be readily coupled with an acyl acceptor such as L-alanine *p*-nitroanilide to produce dipeptide. An α-aminoisobutylic acid containing dipeptide was especially obtained in satisfactory yield (**11c**) using inverse substrate (**5c**) and bovine trypsin or SG (Streptomyces griseus) trypsin. The optimum condition for the coupling reaction was studied by changing the organic solvent (DMF or DMSO), pH (5, 6, 7, 8, 9 or 10), and acyl acceptor concentration (2.5, 5, 10, 20, 25 or 25 mM). The best condition was selected as follows: acyl donor, 1 mM; acyl acceptor (L-Ala-*p*NA), 20 mM; trypsin, 10 mM; 50% DMSO-MOPS (50 mM, pH 8.0, containing 20 mM $CaCl_2$); 25 °C. The progress of the coupling reaction was monitored by HPLC under the following conditions: Shim-pack CLC-ODS (M) (column i.d. 4.6 x 250 mm), isocratic elution at 1ml/min, 0.1% aqueous trifluoroacetic acid/ acetonitril. An aliquot of the reaction mixture was injected and the eluate was monitored at 310 nm. The results of SG trypsin-catalyzed coupling reaction as listed in Table 1.

Table 1. Yields of SG Trypsin-catalyzed Peptide Synthesis

Enzyme	Acyl donor (No.)	Reaction time (hr)	Product (No.)	Yield (%)
SG trypsin	*N*-Boc-L-Ala-O*p*AM (**5a**)	24	*N*-Boc-L-Ala-L-Ala-*p*NA (**11a**)	74
SG trypsin	*N*-Boc-D-Ala-O*p*AM (**5b**)	24	*N*-Boc-D-Ala-L-Ala-*p*NA (**11b**)	74
SG trypsin	*N*-Boc-Aib-O*p*AM (**5c**)	48	*N*-Boc-Aib-L-Ala-pNA (**11c**)	90
SG trypsin	*N*-Boc-L-Ala-O*m*AM (**10a**)	24	*N*-Boc-L-Ala-L-Ala-*p*NA (**11a**)	64
SG trypsin	*N*-Boc-D-Ala-O*m*AM (**10b**)	24	*N*-Boc-D-Ala-L-Ala-*p*NA (**11b**)	64
SG trypsin	*N*-Boc-Aib-O*m*AM (**10c**)	48	*N*-Boc-Aib-L-Ala-*p*NA (**11c**)	16

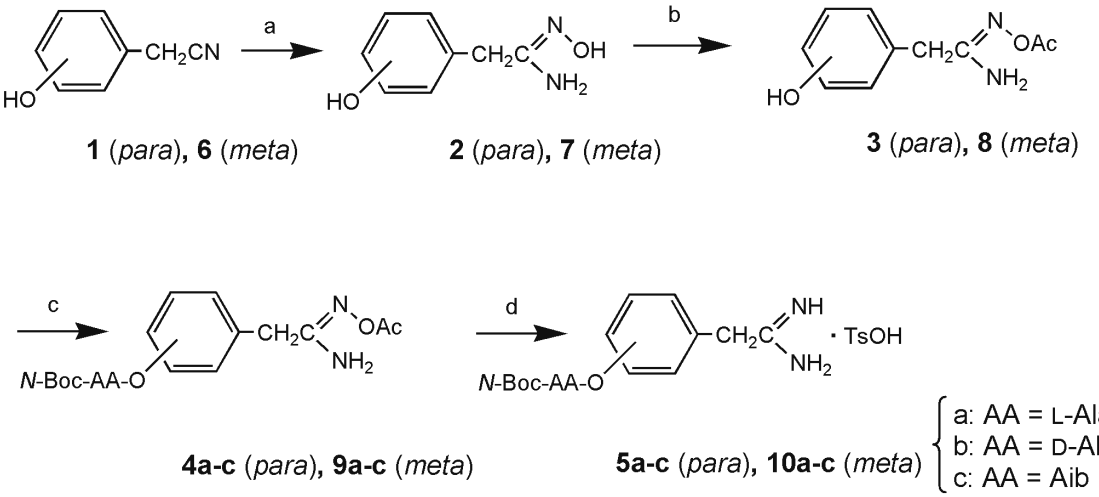

Reagents: a) NH_2OH HCl, K_2CO_3 / H_2O-EtOH; b) Ac_2O / pyridine; c) *N*-Boc-AA-OH, DMAP, DCC / DMF-EtOAc
d) H_2, Pd-C / EtOH

Chart 1

References

1. Sekizaki H, Itoh K, Shibuya A, Toyota E, Tanizawa K, *Chem Pharm Bull* **55**: 1514-1517, 2007.
2. Sekizaki H, Itoh K, Shibuya A, Toyota E, Kojoma M, Tanizawa K. *Chem Pharm Bull* **55**: 688-691, 2008.
3. Tanizawa K, Kasaba Y, Kanaoka Y. *J Am Chem Soc* **99**: 4485-4488, 1977.
4. Judkins BD, Allen GD, Cook TA, Evans B, Sardharwala TE. *Synth Commum* **26**: 4351-4367, 1996.

2-03-127

Synthesis of Conjugates of MDP and nor-MDP linked to Tuftsin Derivatives as Potential Immunomodulators

Dzierzbicka, Krystyna[1]; Wardowska, Anna[2]; Kukowska-Kaszuba, Magdalena[1,]; Mysliwski, Andrzej[2]*

[1]GdańskUniversity of Technology, 11/12 G. Narutowicza Street, 80-952 Gdańsk, Department of Organic Chemistry, POLAND; [2]Medical University of Gdańsk, Dêbinki 1 Street, 80-210 Gdańsk, Department of Histology and Immunology, POLAND

[*]E-mail: magda1805@o2.pl

Introduction

Muramyl dipeptide (MurNAc-L-Ala-D-isoGln; MDP) is the minimal bioactive structure of bacterial peptidoglycan (PGN).[1,2] MDP stimulates various functions of macrophages and increases the non-specific resistance of the host against numerous microorganisms. The another immunomodulator is tuftsin, a natural tetrapeptide of sequence H-Thr-Lys-Pro-Arg-OH (TKPR), present in the blood of humans and other mammals, capable of stimulating certain white blood cells (monocytes, macrophages, and neutrophils).[3,4]

Continuing our program of syntheses of muramyl dipeptide (MDP) and nor-muramyl dipeptide (nor-MDP) conjugates as potential immunomodulators, we designed novel conjugates of MDP or nor-MDP with tuftsin derivatives containing isopeptide bond between ε-amino group of lysine and carboxylic group of simple amino acids such as alanine and valine. Tuftsin analogues containing isopeptide bond showed increased chemical resistance and activity in relation to tuftsin. The introduction of the additional residue at ε-amino group of lysine by NHCO- formation caused that isopeptide bond became stronger than peptide bond in central chain.[5,6]

Results and Discussion

1-Benzyl-MDP and 1-benzyl-nor-MDP described in previous papers[7,8] were used for synthesis of conjugates with tuftsin derivatives (H-Thr-Lys(Y)-Pro-Arg-OMe, Y=Ala,Val) (Fig. 1). Acylation of the Thr amino group of partially protected pentapeptides by MDP or nor-MDP was performed using the mixed anhydride method. The protected conjugates were isolated and purified with a preparative TLC. The protected pentapeptides (Boc-Thr-Lys(ZY)-Pro-Arg(NO_2)-OMe, Y=Ala, Val) were synthesized by the conventional chemical procedure using also mixed anhydride method, isolated by column chromatography and purified with preparative TLC on silica gel. Finally, from peptides the Boc group was removed by treatment with TFA to give trifluoroacetate (TFAxThr-Lys(ZY)-Pro-Arg(NO_2)-OMe, Y=Ala,Val) which was used for synthesis of conjugates with MDP or nor-MDP. The final products **1a-h** were hydrogenolysed in 50 % methanolic acetic acid containing palladium black, purified with preparative TLC and were lyophilized to give hygroscopic solids. The immunostimulatory potency of the synthesized compounds was investigated at Medical University of Gdańsk, Poland. Results of biological tests of compounds **1a-h** containing isopeptide bond will be reported in the future.

Acknowledgments

This work was supported by the Polish State Committee for Scientific Research (Grant No. N N 405 181135).

References

1. Dzierzbicka K, Kolodziejczyk AM. Muramyl peptides – synthesis and biological activity. *Pol J Chem* **77:** 373-395, 2003.
2. Traub S, von Aulock S, Hartung T, Hermann C. MDP and other muropeptides – direct and synergistic effects on the immune system. *J Endotoxin Res* **12:** 69-85, 2006.
3. Najjar VA, Nishioka K. Tuftsin: a natural phagocytosis stimulating peptide. *Nature* **228:** 672-673, 1970
4. Wardowska A, Dzierzbicka K, Mysliwski A. Tuftsin – new analogues and properties. *Post Biochem* **53:** 60-65, 2007.
5. Mező G, Szekerke M, Sarmay G, Gergely J. Synthesis and functional studies of tuftsin analogs containing isopeptide bond. *Peptides* **11:** 405-415, 1990.
6. Granoth R, Vadai E, Burstein Y, Fridkin M, Tzehoval E. Tuftsin-THF-γ2 chimeric peptides: potential novel immunomodulators. *Immunopharmacol* **37:** 43-52, 1997.
7. Dzierzbicka K, Trzonkowski P, Sewerynek P, Kolodziejczyk AM, Mysliwski A. Synthesis and biological activity of tuftsin, its analogue and conjugates containing muramyl dipeptides or nor-muramyl dipeptides. *J Pept Sci* **11:** 123-135, 2005.
8. Dzierzbicka K. Synthesis of new conjugates of MDP and nor-MDP with retro-tuftsin derivatives as potential immunomodulators. *Pol J Chem* **82:** 1431-1439, 2008.

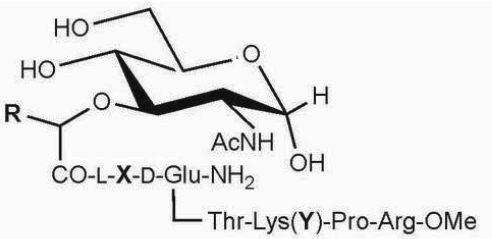

Comp.	R	X	Y
1a	CH_3	Ala	Ala
1b	CH_3	Ala	Val
1c	H	Ala	Ala
1d	H	Ala	Val
1e	CH_3	Val	Ala
1f	CH_3	Val	Val
1g	H	Val	Ala
1h	H	Val	Val

Figure 1. Synthesized conjugates of MDP or nor-MDP with tuftsin derivatives.

2-04-128

On-resin microwave-assisted ring closing metathesis for rapid synthesis of Octreotide dicarba-analogues

Di Cianni, Alessandra[1,2,]; D'Addona, Debora[1,2]; Rizzolo, Fabio[1,2]; Papini, Anna Maria[1,2]; Ginanneschi, Mauro[1,2]*

[1]Interdepartimental Laboratory of Peptide & Protein Chemistry & Biology (PeptLab), Polo Scientifico e Tecnologico of the University of Firenze, ITALY; [2]Dept. of Organic Chemistry 'Ugo Schiff", University of Firenze, ITALY

[*]E-mail: aledicianni@gmail.com

Introduction

Somatostatin (SRIF) induces its biological effects on both endocrine and exocrine secretion, all inhibitory in nature, by a family of structurally related, G-protein-coupled, transmembrane receptors located in pituitary, pancreas, gastrointestinal tract, thyroid and immune cells. Somatostatin receptors (sstr) have also been localized in varius tumor cells.[1,2] However, the use of somatostatin itself for medical treatment is limited by its short half-life *in vivo* (3 min). In order to overcome this severe drawback, many linear and ciclic hexa-, epta- and octapeptide analogues have been in so far prepared and tested as a drug inhibiting the cellular proliferation.[3] Among these analogues, the cyclic octapeptide octreotide strongly binds $hsst_2$ receptor subtype (and, in less extent, $hsst_5$ subtype) *in vitro*, and it is still used in clinical protocols though with alternate results.[4] The amino acid sequence of octreotide shows the same disulphide bridge of the parent somatostatin that can be subjected to the attacks of oxidizing and reducing agents. Moreover, the disulfide bridge can't be employed in the radiolabeling procedure with ^{188}Re and ^{99m}Tc because of the bridge opening. This prompted us to search a more stable tether bridging the active motif of somatostatin and octreotide. We synthesised via RCM (Ring Closing Metathesis) several Octreotide dicarba-analogues lacking the disulfide bridge, of the general formula H-D-Phe^2-c[Hag^4-Phe^7-D-Trp^8-Lys^9-X^{10}-Hag^{14}]-Thr(ol)^{15}-OH (SRIF numbering) (Fig. 1).[5,6] The premier reaction of RCM was performed in an oil bath under severe experimental conditions. The microwaves assisted version was, instead, efficient for the cyclopeptides yield and required very short reaction times.

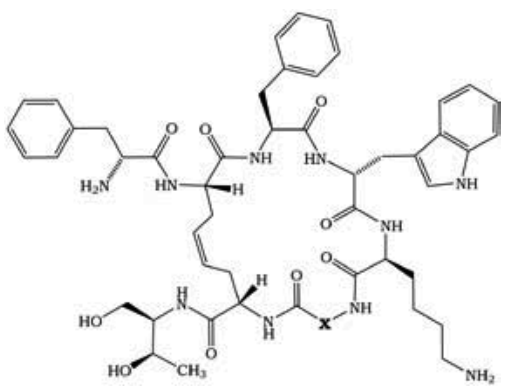

Figure 1. Unsaturated dicarba-analogues.
X= **1**: Thr; **2**: Phe; **3**: Tyr(Bzl).

Results

We previously synthesized the three dicarba-analogues on H-Thr-ol(tBu)-2-chlorotrityl resin. The synthesis was stopped to the allylglycine residue, in order to overcome steric problems in the cyclization reaction, due to the presence of a bulky residue (D-Phe) at the end of the sequence that probably disfavours the correct orientation of the two allylglycine side chain. The N-terminal residue was anchored after the cyclization step.

The cyclization between the two allylglycine residues was performed with catalysts I and II (Fig. 2). The resin aliquots containing the peptides 1-3 were swollen for 2 h in anhydrous DCM. The vessel was heated to 45 °C and a DCM solution of catalyst (0.5 mole eq. calculated on the basis of 0.5 mmol/g of peptide) was added. Catalyst II helved the reaction time and increase the yield of about 10% respect to the cyclization with catalyst I (Table 1).[5,6] The same reaction was performed with a CEM Discover Microwaves instrument with milder conditions (30 minutes swelling, commercial solvent, 0.04 mole eq. of catalyst respect to the substitution of the resin 0.5 mmol/g).[7,8] All microwave reactions were conducted in a sealed glass tube; the pressure was monitored and did not exceed 95 psi. After each reaction, the instrument was runned with a cooling method, in order to start the next experiment at the same temperature of the first one (Table 2). After the complete elimination of ruthenium side-products by SPE, the purification by RP-HPLC was easier.

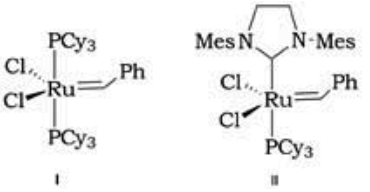

Figure 2. 1st and 2nd generation Grubbs catalyst.

After each reaction, the instrument was runned with a cooling method, in order to start the next experiment at the same temperature of the first one (Table 2).

Table 1. Cyclization of the linear hepta-peptides **1, 2, 3** with I and II. [a]Overall yield of isolated pure compounds, calculated on the basis of an average peptide loading of 0.5 mmol/g of resin. [b]Calculated on the basis of peaks area in analytical RP-HPLC

Compounds	Catalyst (hours of reflux)	% yield[a]	Cyclic/ linear ratio[b]
1	I (48)	25	85:15
1	II (24)	35	90:10
2	I (52)	10	30:70
2	II (48)	20	50:50
3	I (48)	3	50:50
3	II (24)	13	80:20

Table 2. Microwave-assisted RCM on peptides **1, 2, 3.** [a]Calculated on the basis of peaks area in analytical RP-HPLC

Compounds	Microwave methods (time. Minutes)	Catalysts	Cyclic/ linear ratioa
1	150W, 100 °C, (10)	I	70:30
2	150W, 100 °C, (10)	I	50:50
3	150W, 100 °C, (10)	I	65:35
1	150W, 100 °C, (10)	II	95:5
2	150W, 100 °C, (10)	II	97:3
3	150W, 100 °C, (10)	II	95: 5
1	150W, 100 °C, (3)	II	98:2
2	150W, 100 °C, (3)	II	97:3
3	150W, 100 °C, (3)	II	95: 5
1	150W, 100 °C, (3)	I	70:30
2	150W, 100 °C, (3)	I	50:50
3	150W, 100 °C, (3)	I	65:35
1	100W, 80 °C, (3)	II	98:2
2	100W, 80 °C, (3)	II	97:3
3	100W, 80 °C, (3)	II	95: 5

Table SEQ Table * ARABIC 1: Cyclization of the linear hepta-peptides **1, 2, 3** with I and II.
[a] Overall yield of isolated pure compounds, calculated on the basis of an average peptide loading of 0.5 mmol/g of resin. b Calculated on the basis of peaks area in analytical RP-HPLC.

Table SEQ Table * ARABIC 2: Microwave-assisted RCM on peptides **1, 2, 3.**

[a] Calculated on the basis of peaks area in analytical RP-HPLC.

After the complete elimination of ruthenium side-products by SPE, the purification by RP-HPLC was easier.

Discussion

We evaluated the efficacy of microwaves on RCM by using catalysts I and II. We found that microwave is useful in difficult sequence as that represented by compound 2. Comparing the results in Table 1 and 2 is clear that catalyst II work more efficiently than catalyst I but with the use of microwaves synthesis is possible to achieve good yield with I too. Moreover, the short reaction time in the microwaves assisted RCM is important for the stability of the catalyst and for avoiding severe anhydrous conditions.

Acknowledgement

This work was supported by Ente Cassa di Risparmio di Firenze and MIUR funds (Prin 2005).

References

1. Burgus R, Brazeau P, Vale W. Isolation and Determination of the Primary Structure of Somatostatin (a Somatotropin Release Inhibiting Factor) of Bovine Hypothalamic Origin. *Advances in Human Growth Hormone Research, U S A Government Printing Office DHEW* Publ No (NIH) **74-612**: 44-158, 1973.
2. Patel JC. Molecoular Pharmacology of Somatostatin Receptor Subtypes. *J Endocrinol Invest* **20**: 348-367, 1997.
3. Janecka A, Zubzycka M, Janecki T. Somatostatin analogs. *J Pept Res* **58**: 91-107, 2001.
4. Lamberts SWJ, van der Lay AJ, de Herder WW, Hofland LJ. Octreotide. Drug Therapy. *New Engl J Med* **334**: 246-254, 1996.
5. Carotenuto A, D'Addona D, Rivalta E, Chelli M, Papini AM, Rovero P, Ginanneschi M. Synthesis of a Dicarba-Analog of Octreotide Keeping the II' β-Turn of Pharmacophore in Water Solution. *Letters in Organic Chemistry* **2**: 274-279, 2005.
6. D'Addona D, Carotenuto A, Novellino E, Piccand V, Reubi JC, Di Cianni A, Gori F, Papini AM, Ginanneschi M. Novel sst5-Selective Somatostatin Dicarba-analog. Synthesis and Conformation-Affinity Relationships. *J Med Chem* **51**: 512-520, 2008.
7. Kappe CO. Controlled Microwave Heating in Modern Organic Synthesis. *Angew Chem Int Ed Engl* **43**: 6250-6284, 2004.
8. Robinson AJ, Elaridi J, Van Lierop BJ, Mujcinovic S, Jackson WR. Microwave-assisted RCM for the Synthesis of Carbocyclic Peptides. *J Pept Sci* **13**: 280-285, 2007.

2-04-129

Efficient microwave-assisted synthesis of myelin epitopes MOG_{35-55} and MOG_{97-108} using CLTR-Cl resin

Friligou, Irene; Androutsou, Maria- Eleni; Agelis, George; Matsoukas, John M; Tselios, Theodore*

University of Patras, Department of Chemistry, GREECE

**E-mail: imats@chemistry.upatras.gr*

Introduction

MS is a chronic inflammatory and demyelinating disease of the CNS believed to be mediated by an autoimmune T cell response directed at proteins of the myelin sheath, such as myelin basic protein (MBP), proteolipid protein (PLP) and MOG.[1,2] There is evidence that MOG_{35-55} is encephalitogenic in chronic EAE (Experimental Autoimmune Encephalomyelitis, the best well studied animal model of MS) while MOG_{97-108} is the immunodominant HLA-DR4-restricted T cell epitope *in vivo*[3]. In this study, we synthesized the above epitopes with Microwave Enhanced Solid Phase Peptide Synthesis using the CEM Liberty automated microwave peptide synthesizer and CLTR-Cl resin. Microwave enhanced peptide synthesis is 10 to 20 times faster compared to traditional methods and produces cleaner peptides with higher yields. In peptide synthesis the solid support is able to absorb microwave energy very rapidly and easily transfer this energy to the reaction components. The *N*-terminal amine group and peptide backbone are polar, causing them to constantly try to align with the alternating electric field of the microwave. During peptide synthesis this can help break up the chain aggregation owing to intra and interchain association and allow for easier access to the solid phase reaction matrix.[4]

Results and Discussion

Microwave energy represents a fast and efficient way to enhance both the Fmoc deprotection and coupling reactions in Fmoc/tBu solid phase peptide synthesis (SPPS). Unlike conventional heating, microwave energy directly activates any molecule with a dipole moment and allows for rapid heating at the molecular level. Two epitopes (35-55, 97-108) of human MOG (Myelin Oligodendrocyte Glycoprotein), which are implicated in Multiple Sclerosis (MS), were synthesized with Microwave Enhanced Solid Phase Peptide Synthesis utilizing 2-chlorotrityl chloride resin (CLTR-Cl). The first N^{α}-Fmoc (9-fluorenylmethyloxycarbonyl)-protected amino acid (1 eq.) was coupled to the resin in 1h in the presence of diisopropylethylamine (DIPEA) (4.5 eq.) in dichloromethane (DCM). The remaining peptide chain was assembled with microwave energy by sequential couplings of the appropriate each time residue (0.2M in DMF) in the presence of *N,N'*-diisopropylcarbodiimide (DIC) (0.5M in DMF) and 1-hydroxybenzotriazole (HOBt) (0.5M in DMF). The Fmoc protecting group was removed by treatment with piperidine (25% in DMF). The total synthesis was carried out in 18 and 13.5 hours respectively. The maximum temperature reached during both the deprotection and coupling reactions was 80 °C except for the coupling of FmocHis(Tr)OH (50 °C). The protected peptide resin was then cleaved with the splitting solution DCM/AcOH/TFE 7/2/1 for 1.5 h at RT. The resin was filtered, the solvent was removed on a rotary evaporator and the obtained oily product precipitated from cold dry diethylether as a white amorphous solid. The deprotection of the peptide was achieved with 65% trifluoroacetic acid (TFA) in DCM in the presence of triethylsilane (TES), anisole and water as scavengers for 4 h at RT, crude purity ~60%. The solvent was removed on a rotary evaporator and the obtained oily

Scheme 1. (a) RP-HPLC of final crude MOG_{35-55}. [Nucleosil C18, 250x4,6mm, 5ìm. TR: 15.1min. Conditions: 5% (B) to 100% (B) in 30min, Flow rate: 1ml/min, (A):TFA solution in H_2O 0,08% (v/v), (B):TFA solution in AcN 0,08% (v/v)] (b) ESI-MS of MOG_{35-55}. Ì: 2592 , Ì+2Ç$^{+}$: 1297, M+3H^{+}: 865, M+4H^{+}: 649, M+5H^{+}: 519.4

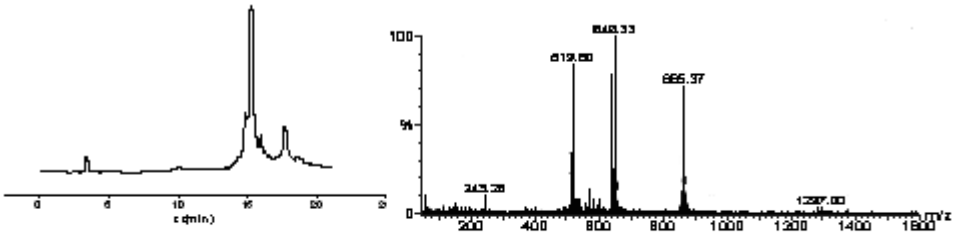

Scheme 2. (a) RP-HPLC of final crude MOG_{97-108}. [Nucleosil C18, 250x4,6 mm, 5ìm. TR: 13.5 min. Conditions: 5% (B) to 100% (B) in 30 min, Flow rate: 1 ml/min, (A):TFA solution in H_2O 0,08% (v/v), (B):TFA solution in AcN 0,08% (v/v)] (b) ESI-MS of MOG_{97-108}. Ì: 1561.63 , Ì+2Ç$^{+}$: 781.82

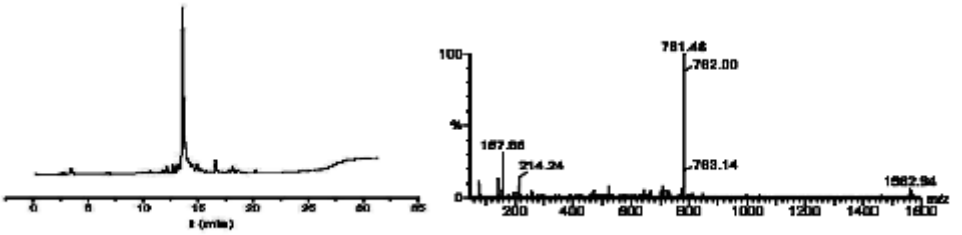

product precipitated from cold dry diethylether as a white solid. The purity of the final products was verified by RP-HPLC and their identification was achieved by ESI-MS (Schemes 1, 2).

Acknowledgements

This research project is co-financed by E.U.-European Social Fund (75%) and the Greek Ministry of Development-GSRT (25%). Special thanks to Eldrug SA for providing access to Cem Liberty automated microwave peptide synthesizer.

References

1. Tselios TV, Lamari FN, Karathanasopoulou I, Katsara M, Apostolopoulos V, Pietersz GA, Matsoukas JM, Karamanos NK. *Anal Biochem* **347**: 121-128, 2005.
2. Matsoukas JM, Apostolopoulos V, Kalbacher H, Papini AM, Tselios T, Chatzantoni K, Biagioli T, Lolli F, Deraos S, Papathanassopoulos P, Troganis A, Mantzourani E, Mavromoustakos T, Mouzaki A. *J Med Chem* **48**: 1470-1480, 2005.
3. Forsthuber TG, Shive CL, Wienhold W, de Graaf K, Spack EG, Sublett R, Melms A, Kort J, Racke MK, Weissert R. *J Immun* **167**: 7119-7125, 2001.
4. Palasek SA, Cox ZJ, Collins JM. *J Pept Sci* **13**: 143–148, 2007.

2-04-130

Microwave-Assisted Solid Phase Synthesis of Backbone Cyclic Glycopeptide Libraries

Nuti, Francesca[1,2,]; Qvit, Nir[3,4]; Rizzolo, Fabio[1,2], Hurevich, Mattan[4]; Peroni, Elisa[1,2]; Rovero, Paolo[1,5]; Gilon, Chaim[4]; Papini, Anna Maria[1,2]*

[1]Interdepartimental Laboratory of Peptide & Protein Chemistry & Biology, Polo Scientifico e Tecnologico of the University of Firenze, ITALY; [2]Dept. of Organic Chemistry `Ugo Schiff', and CNR-ICCOM, University of Firenze, ITALY; [3] Dept. of Chemical and Systems Biology, Stanford University School of Medicine, Stanford, CA, UNITED STATES; [4]Institute of Chemistry, The Hebrew University of Jerusalem, Jerusalem, ISRAEL; [5]Dept. of Pharmaceutical Sciences, University of Firenze, ITALY

[*]E-mail: nuti.francesca@gmail.com

Introduction

In previous studies, A.M. Papini *et al*.[1] developed CSF114(Glc) [characterized by a type I' β-turn surrounding the minimal epitope Asn(β-Glc)] detecting specific and high affinity autoantibodies in Multiple Sclerosis (MS) patients' sera by ELISA. A conformation-activity relationship study of a library of glucosylated peptides characterized by different β-turn types revealed the importance of the β-turn structure in the glycopeptide antigen-autoantibody interaction. Starting from the sequence of CSF114(Glc), we replaced the dipeptide at the tip of the β-turn, i.e. Asn7-Gly8, with the sequence Pro7-Asn8, obtaining [Pro7,Asn8(Glc),Thr10]CSF114. This sequence stabilizes a type I β-turn motif between residues 6-9 and displays higher affinity for MS autoantibodies.[2a] Moreover, we synthesized the shorter sequence [Pro7,Asn8(Glc),Thr10] CSF114(5-11) (I) including (a) the minimal epitope region and (b) a Thr residue fixed at position 10, thus reproducing the N-glycosylation consensus sequence Asn-Xxx-Thr. Interestingly, the type I β-turn structure increases antibody affinity also in the shorter heptapeptide I as measured by competitive ELISA.[2b] According to the results obtained with the linear heptapeptide in MS autoantibody recognition, we applied the Backbone Cyclicization (BC) method to develop two backbone cyclic libraries of glycopeptides based on the sequence of the active linear heptapeptide. Backbone Cyclization is a method introduced by C. Gilon *et al*.[3] that allows obtaining cyclic peptides without changing the original sequence or the chemical character of any amino acid residues required for bioactivity, in order to enhance activity, stability to metabolic degradation, selectivity and bioavailability.

Results and discussion

We applied the potential of BC in Multiple Sclerosis autoantibody recognition to develop new Synthetic GlycoPeptide probes, mimetic of native autoantigens. In particular, we undertook a Sequence-based Cycloscan for a systematic screening of a broad range of peptides starting from the linear heptapeptide I, characterized by a type I β-turn structure previously demonstrated to increase Multiple Sclerosis antibody affinity.[2b] Cycloscan is an hierarchical scan of Backbone Cyclic GlycoPeptide Libraries (BC-GPL) based on the shortest active lead and it is used for fast discovery of bioactive BC Leads. We designed two libraries based on the heptapeptide [Pro7,Asn8(Glc),Thr10]CSF114(5-11) (I). The first library contains a Gly-Building Unit [Fmoc-*N*α(*N*ω(Alloc(n-alkyl))Gly-OH(G-BU)][4] at the C-terminus and is connected to the N-terminus by dicarboxilic acid linker of various lengths (n=2,3,4,6). In the second library, His9 of the heptapeptide is replaced by G-BU modified with various alkyl chains (n=2,3,4,6). Sixteen BC-GlycoPeptides were synthesized combining for the first time the MW-SPPS (Liberty CEM Coorporation, NC) and Tea-bags methodology (MW/Tbags SPPS). In particular we optimized the reaction conditions for both coupling of the dicarboxilic acid and cyclization thanks to TBTU activation by MW conditions. We succeeded in obtaining, after purification by RP-HPLC, only seven peptides in sufficient yield with 95% purity, which were screened by competitive ELISA on MS patients' sera. In particular the two BC-GlycoPeptides demonstrated in competitive ELISA high activity for anti-CSF114(Glc) antibodies.

References

1a. Lolli F, Mulinacci B, Carotenuto A, Bonetti B, Sabatino G, Mazzanti B, D'Ursi AM, Novellino E, Pazzagli M, Lovato L, Alcaro MC, Peroni E, Pozo-Carrero MC, Nuti F, Battistini L, Borsellino G, Chelli M, Rovero P, Papini AM. *Proc Natl Acad Sci U S A* **102**: 10273-10278, 2005.

1b. Lolli F, Mazzanti B, Pazzagli M, Peroni E, Alcaro MC, Sabatino G, Lanzillo R, Brescia Morra V, Santoro L, Gasperini C, Galgani S, D'Elios MM, Zipoli V, Sotgiu S, Pugliatti M, Rovero P, Chelli M, Papini AM. *J Neuroimmunol* **167**: 131-137, 2005.

1c. Papini AM. *Nat Med* **11**: 13, 2005.

1d. Papini AM, Rovero P, Chelli M, Lolli F. U S A & *Australian Patent & PCT* **WO 03/000733 A2**.

2a. Carotenuto A, D'Ursi AM, Mulinacci B, Paolini I, Lolli F, Papini AM, Novellino E, Rovero P. *J Med Chem* **49**: 5072-5079, 2006.
2b. Carotenuto A, Alcaro MC, Saviello MR, Peroni E, Nuti F, Papini AM, Novellino E, Rovero P. *J Med Chem* **51**: 5304-5309, 2008.
3a. Gilon C, Halle D, Chorev M, Selinger Z, Byk G. *Biopolymers* **31**: 745-750, 1991.
3b. Gilon C, Hornik V. *US Patent Application 2002*: **US 95-569042 19951207.**
4. Bitan G, Muller D, Kasher R, Gluhov EV, Gilon C. *J Chem Soc Perkin Trans* 1, 1501-1510, 1997.

2-05-131

Synthesis and folding of the circular cystine knotted cyclotide cycloviolacin O2

Leta Aboye, Teshome[1,]; Clark, Richard J[2]; Craik, David J.[2]; Göransson, Ulf[1]*

[1]Uppsala University, Division of Pharmacognosy, Department of Medicinal, SWEDEN; [2]The University of Queensland, Institute for Molecular BioScience, Australian Res, AUSTRALIA

[*]E-mail: Teshome.Aboye@fkog.uu.se

Introduction

The cyclotides is a family of bioactive plant proteins that contain a head-to-tail cyclized backbone and a knotted arrangement of their three disulfide bonds, as shown in Fig. 1. These structural features are unique for cyclotides and define the cyclic cystine knot (CCK) motif. Cyclotides typically comprise 28 to 31 amino acids, and they form the largest family of circular proteins currently known. The CCK motif provides cyclotides with exceptional chemical and biological stability.[1] Over the last years, these peptides has emerged as an attractive scaffold for engineering of peptides for pharmaceutical, medical and agricultural applications.[2]

Cyclotides are divided into two subfamilies, Möbius and bracelets. The bracelets display higher sequence diversity and higher potency, and thus emerge as the prime target for cyclotide engineering. However the broad application of cyclotide engineering has ben hampered by the fact that the bracelet subfamily has been inaccessible for efficient chemical synthesis. In this work,[3] we show a strategy based on Fmoc chemistry and native chemical ligation[4] for the synthesis of these circular plant peptides, and the first method for successful and direct oxidative folding of bracelet cyclotides.

Results and discussion

The prototypic bracelet cyclotide cycloviolacin O2 was synthesized by manual solid phase peptide synthesis using Fmoc chemistry. The fully protected linear peptide (30 residues, CSCKSKVCYRNGIPCGESCVWIPCISSAIG) was cleaved off the resin. Native chemical ligation was then used for cyclisation; the required C-terminal thioester was introduced on crude protected peptide,[5] followed by deprotection and cyclisation, as outlined in Fig. 2.

Folding conditions were optimized to achieve maximum yield of correctly folded product, i.e. the native form. Concentrations of cosolvents, detergents, salt, redox agents as well as the effects of temperature and duration of reaction, were examined. Under most conditions misfolded products were predominant. However, using 35% DMSO as cosolvent gave a yield of ~40%, which was further optimized, with redox agents, to >50%.

The development of an Fmoc based approach using standard SPPS building blocks and procedures and oxidative folding conditions for bracelet cyclotides is a potential landmark in the exploitation of cyclotides as they greatly increase the structural diversity accessible by synthesis. Hence, the current results are a significant step

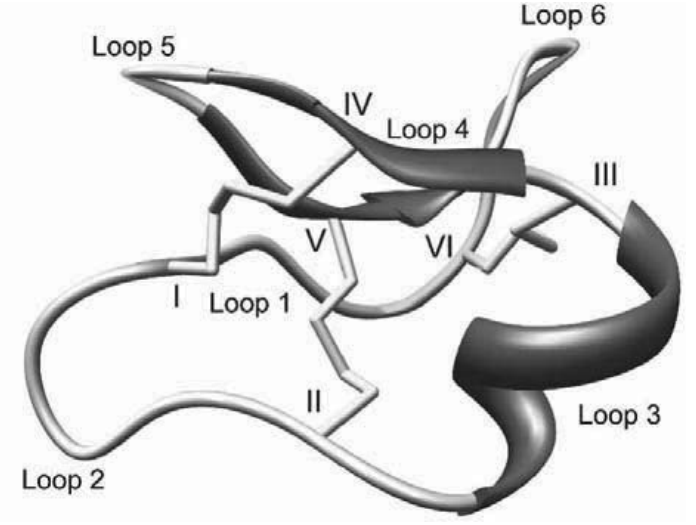

Figure 1. Cyclotide structure. Note the cyclic peptide backbone, and the cystine knot, which arises as two disulfide bonds (I-IV, III-VI) and their interconnecting backbone segments form a ring that is penetrated by the third disulfide bond (II-V). The bracelet subfamily is characterised by a helical loop 3, and, in most cases, a cluster of positively charged residues in loop 5.

to the overall goal for bioengineering on the cyclotide scaffold for utilization of their diversity of sequences and extraordinary structural stability for pharmaceutical and agricultural applications.

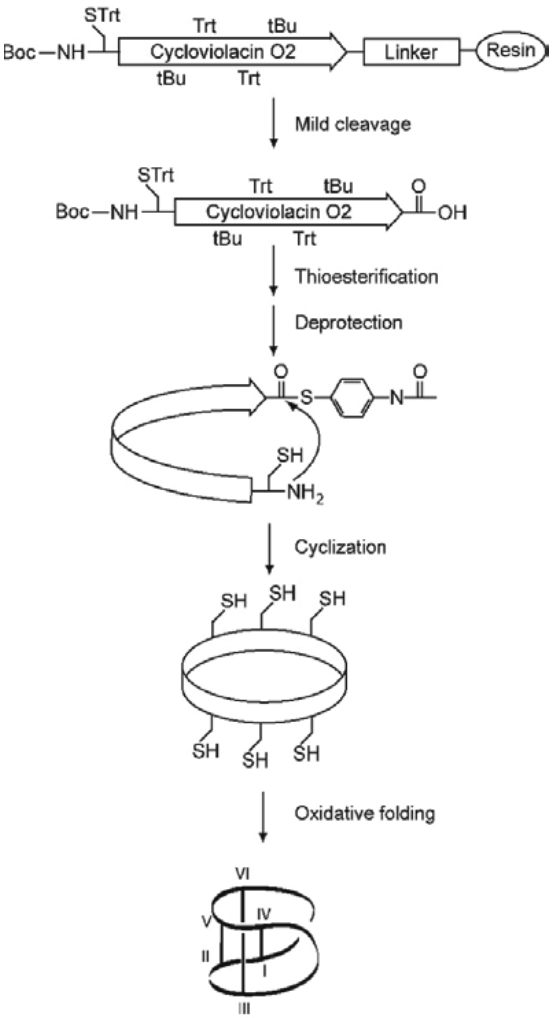

Figure 2. The linear peptide was synthesized by manual SPPS using Fmoc-Gly preloaded NovaSyn TGT resin. Protected peptide was cleaved from the resin by treatment of resin-peptide with AcOH/TFE/DCM) (1/1/8) followed by thioester formation using Peptide/PyBOP/4-acetamidothiophenol/DIPEA (1:5:15:1100) in 20 ml of DCM. The thioester was cyclized in Tris buffer at pH 7.4 and oxidatively folded with an optimized folding buffer at pH 8.5.

Acknowledgements

This study was supported by the Swedish International Development Cooperation Agency (SIDA), Dept for Research Cooperation (SAREC) (T.L.A. and U.G.); The Royal Swedish Academy of Sciences and Swedish Research Council (U.G.). Work on cyclotides at the University of Queensland is supported by grants from the Australian Research Council and the National Health and Medical Research Council.

References

1. Colgrave, M. L.; Craik, D. J. *Biochemistry* **43**: 5965-5975, 2004.
2. Craik, D. J.; Clark, R. J.; Daly, N. L. *Expert Opin Investig Drugs* **16**: 595-604, 2007.
3. Leta Aboye, T.; Clark, R. J.; Craik, D. J.; Göransson, U. *ChemBioChem* **9**: 103-113, 2008.
4. Dawson, P. E.; Muir, T. W.; Clark-Lewis, I.; Kent, S. B. *Science* **266**: 776-779, 1994.
5. Eggelkraut-Gottanka, R.; Klose, A.; Beck-Sickinger, A.; Beyermann, M. *Tetrahedron Lett* **44**: 3551-3554, 2003.

2-05-132

Modification of the regenerative chemokine SDF1 α to allow fluorescence imaging

Bellmann-Sickert, Kathrin[1]; Baumann, Lars[1]; Beck-Sickinger, Annette G[2,]*

[1]Leipzig University, Translational Center for Regenerative Medicine, GERMANY; [2]Leipzig University, Institute of Biochemistry GERMANY

[*]E-mail: beck-sickinger@uni-leipzig.de

The chemokine SDF1 α (CXCL12) is known to be involved in a lot of metabolic processes like cancer metastasis, HIV infection and rheumatoid arthritis on the one hand and formation of the bone marrow, embryogenesis and organogenesis on the other hand. SDF1 α is constitutively expressed in many tissues, but, atypically for homeostatic chemokines, its expression can also be upregulated by inflammatory or immune stimuli. It is then able to attract hematopoietic stem cells that are needed within regeneration of the injured tissue, especially after ischemia. This process is called chemotaxis. The chemokine forms a gradient with the highest concentration at the site of inflammation. Cells expressing the corresponding chemokine receptor, are then conducted along this gradient. SDF1 α mediates chemotaxis and cell signalling via the chemokine receptor CXCR4, which is, like all chemokine receptors, a seven transmembrane G-protein coupled receptor (GPCR).[1] In order to study interactions between the receptor and its ligand or analogues of it, it is useful to label the ligand. Since we wished to investigate specific binding and internalization of SDF1 α, our aim was to label it with a fluorescence tag. For that, we chose 5,6-carboxyfluorescein (CF).

Since SDF1 α consists of 68 amino acids and two disulfide bonds, the synthesis of labelled analogues is very challenging. Solid phase peptide synthesis (SPPS) results in very low yields, while recombinant expression and labelling afterwards often produces unspecifically labelled products. Therefore, we chose a mixture of both methods. We synthesized the C-terminal part SDF1 $\alpha_{50\text{-}68}$ by SPPS and specifically bound CF to lysine in position 56. The N-terminal part SDF1 $\alpha_{1\text{-}49}$ was expressed as a C-terminal thioester. For that, the cDNA of SDF1 $\alpha_{1\text{-}49}$ was cloned into the pTXB1 vector in front of an intein and a chitin binding domain. The fusion protein consisting of these three domains was then expressed and purified by a chitin column. SDF1 $\alpha_{1\text{-}49}$ could finally be cleaved as a thioester from the bound fusion protein by addition of the thiol mercaptoethane sulfonic acid sodium salt (MESNa). Since the C-terminal part SDF1 $\alpha_{50\text{-}68}$ starts with a cysteine residue, both SDF1 $\alpha_{1\text{-}49}$ and SDF1 $\alpha_{50\text{-}68}$ could be ligated by native chemical ligation (NCL) (Fig. 1).[2] Within that process the sulfhydryl group of the cysteine attacks the C-terminal thioester and that way conjugates both parts by a transthioesterification. The final step is an S-N-acyl shift, which forms the more stable amide out of the thioester bond at the conjugation

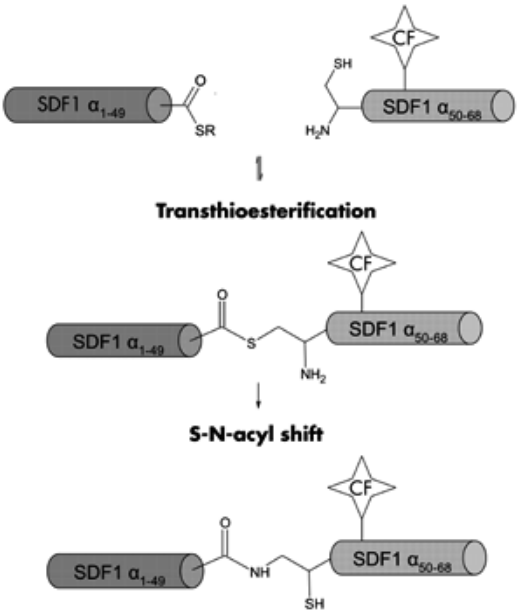

Figure 1. Mechanism of native chemical ligation.

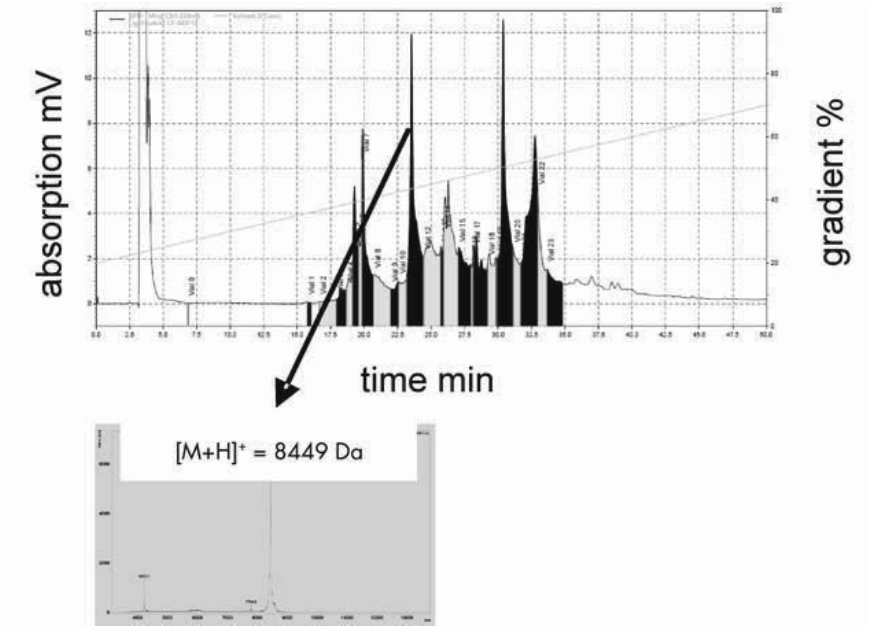

Figure 2. RP-HPLC and MALDI-ToF-MS of [K^{56}(CF)]SDF1 α.

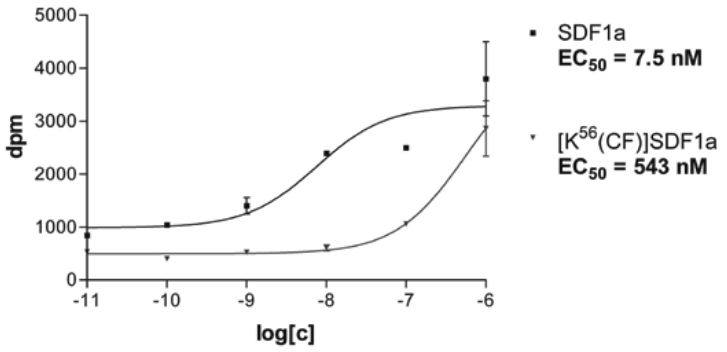

Figure 3. Signal transduction assay of SDF1 α and [K^{56}(CF)]SDF1 α.

site. The ligation product was finally refolded by dialysis against a cysteine/cystin redox system and decreasing urea concentrations. Purification of the ligated and refolded product [K^{56}(CF)]SDF1 α yielded a single peak after semipreparative reversed phase high performance liquid chromatography (RP-HPLC). Its identity could be verified by matrix assisted laser desorption ionization time of flight mass spectrometry (MALDI-TOF-MS). The measured mass of 8449.0 Da is consistent with the calculated one (8449.0 Da) (Fig. 2).

Signal transduction of the CF-labeled analogue was tested by an IP3 assay. Within this assay, formation of inositol-3-phosphate (IP3) out of [^{3}H]-labelled myo-inositol, induced by stimulation of the GPCR, is investigated. While SDF1 α shows half maximal IP3 formation at 7.5 nM, [K^{56}(CF)]SDF1 α has an EC50 value of 543 nM, meaning a 72-fold decrease in binding (Fig. 3). But since the curve of [K^{56}(CF)]SDF1 α reaches the maximum of that one for SDF1 α, it still is able to fully activate the receptor.

In conclusion, we succeeded in the synthesis and biological characterization of a fluorescein-labelled SDF1 α-analogue. Further studies will concentrate on fluorescence microscopy.

References

1. Kucia M, Jankowski K, Reca R, Wysoczynski M, Bandura L, Allendorf DJ, Zhang J, Ratajczak J, Ratajczak MZ. CXCR4-SDF-1 signalling, locomotion, chemotaxis and adhesion. *J Mol Histol* **35**: 233-245, 2004.
2. David R, Richter MP, Beck-Sickinger AG. Expressed Protein Ligation. Method and Applications. *Eur J Biochem* **271**: 663-677, 2004.

2-07-133

P5U and urantide modified at position 7 with Tpi

Auriemma, Luigia[1]; Campiglia, Pietro[2]; Gomez-Monterrey, Isabel Maria[3]; Novellino, Ettore[3]; Sorrentino, Raffaella[3]; Carotenuto, Alfonso[3]; Grieco, Paolo[3,]*

[1]Dept. Pharmaceutical and Tox. Chemistry, University of Naples Federico II, ITALY; [2]University of Salerno, ITALY; [3]University of Naples Federico II, ITALY

[*]E-mail: pagrieco@unina.it

Introduction

Urotensin II (U-II) is a disulfide bridged peptide hormone recently identified as the ligand of a Gprotein-coupled receptor. Human U-II (H-Glu-Thr-Pro-Asp-cyclo[Cys-Phe-Trp-Lys-Tyr-Cys]-Val-OH has been descibed as the most potent vasoconstrictor compound identified to date and it appears to be involved in the regulation of cardiovascular homeostasis and pathology. U-II Cterminal cyclic heptapeptide portion (CFWKYCV), which is essential for the biological activity, has been highly conserved in evolution from fish to mammalians. Recently, we have reported a superagonist (P5U) and a full antagonist (UrantideTM) at rat UT receptor with a partial activity at human receptor.[1,2] In order to elucidate the most important substructural features responsible for agonist/antagonist activity of this important peptide-hormone we decided to explore the position 7 replacing the residue Trp (Fig. 1) with the unnatural amino acid Tpi or DTpi (1,2,3,4 tetrahydronorharman-3-carboxylic acid) (Table 1), using P5U and Urantide as our lead compounds.

Methods

Peptides were synthesized using a convetional Fmoc-based solid-phase strategy in a manual reaction vessel. Disulfide bridge was obtained by oxidation using DMSO 10% of a solution (1 ml/mg of linear peptide) 0.05 M of NH_4HCO_3.The purification of final products was achieved using a semipreparative RP-HPLC. Analytical HPLC indicated a purity greater than 97%, and molecular weights were confirmed by ESI-MS. The peptides were tested for their ability to induce efficacious contractions in the rat isolated thoracic aorta. As reference compounds we used P5U and Urantide. Table 2 shows the biological activity of the analogues tested in this study. The binding experiments relating to compounds 3 and 4 are ongoing.

Table 1

Structure of Synthesized Peptides	
P5U	H-Asp-c[Pen-Phe-Trp-Lys-Tyr-Cys]-Val-OH
Urantide	H-Asp-c[Pen-Phe-DTrp-Orn-Tyr-Cys]-Val-OH
1	H-Asp-c[Pen-Phe-DTpi-Orn-Tyr-Cys]-Val-OH
2	H-Asp-c[Pen-Phe-Tpi-Lys-Tyr-Cys]-Val-OH
3	H-Asp-c[Pen-Phe-DTpi-Lys-Tyr-Cys]-Val-OH
4	H-Asp-c[Pen-Phe-Tpi-Orn-Tyr-Cys]-Val-OH

Table 2

Biological Activity			
Peptide	pEC_{50}	pA_2	pKi
P5U	8.93±0.07	---	9.7±0.07
Urantide	---	8.3	8.3±0.04
1	---	6.275	7.43
2	7.92	---	8.16
3	7.68	---	---
4	---	6.303	---

Discussion and Conclusion

With aim to investigate the importance of Trp residue in position 7 of Urantide and P5U sequences we have replaced this residue with the unnatural and constrained amino acid Tpi. The replacement of Trp7 with Tpi in the sequence of Urantide lead to compounds 1 and 4 with antagonist activity although less potent. The compounds 2 and 3 showes to be agonists but less potent when compared to the hUT-II(4-11) and P5U. The conformational behavior of the new analogues in membrane mimetic environment (SDS and DPC micelles) by spectroscopic and computational methods is currently in progress. On the basis of the NMR and simulation results, we will design other analogues of Urantide and P5U aiming to improve their pharmacological profiles and to increase their potency.

References

1. Grieco P, Carotenuto A, Campiglia P, Zampelli E, Patacchini R, Maggi CA, Novellino E, Rovero P. *J Med Chem* **45**: 4391-4394, 2002.
2. Patacchini R, Santicioli P, Giuliani S, Grieco P, Novellino E, Rovero P, Maggi CA. *British J of Pharmacol* **140**: 1155-1158, 2003.
3. Grieco P, Carotenuto A, Campiglia P, Marinelli L, Lama T, Patacchini R, Santicioli P, Maggi CA, Rovero P, Novellino E. *J Med Chem* **48**: 7290-7297, 2005.

2-07-135

Novel antimicrobial peptides from the venom of solitary bees

Ceřovský, Václav[1,]; Hovorka, Oldřich; Cvačka, Josef; Voburka, Zdeněk; Slaninová, Jiřina; Fučík, Vladimír; Borovičková, Lenka; Bednárová, Lucie; Buděšínský, Miloš*

[*]*E-mail:* Cerovský@*uochb.cas.cz*

Introduction

Among linear cationic α-helical antimicrobial peptides (AMPs), those isolated from the venom of hymenoptera represent a remarkable group. These peptides are stored in venom reservoirs together with a complex mixture of enzymes, neurotoxins and low-molecular-mass compounds. Regardless of different compositions, the main function of venoms is to subdue the prey and defense against predators. The venom peptides of hymenoptera that are best characterized include the mastoparans, chemotactic peptides and kinins isolated from hornets and wasps, hemolytic melittin, neurotoxic apamine from honeybees, cytolytic bombolitins from bumble bees and ponericins isolated from Ponerinae ants. Some of these peptides[1-3] exhibit potent antimicrobial activity against broad range of bacteria. Here we describe the structural characterization and biological activities of novel AMPs named melectin (MEP)[4] and lasioglossins (LL-I, LL-II, L-III) which we isolated from the venom of cleptoparasitic bee *Melecta albifrons* and a solitary bee *Lasioglossum laticeps*, respectively.

Results and discussion

Bee specimens of *Melecta albifrons* were collected in the urban area of northwest Prague and the *Lasioglossum laticeps* in the northeast area of the Czech Republic. The venom reservoirs of five individuals were removed by dissection and their content extracted with a mixture (25 μl) of acetonitrile/water (1 : 1) containing 0.1% TFA. The extracts were fractioned by HPLC (Fig. 1). The major peptide components corresponding to peaks MEP, LL-I, LL-II and LL-III were analyzed by ESI-QTOF mass spectrometry and by Edman degradation. Their primary sequences were established as follows: MEP, H-Gly-Phe-Leu-Ser-Ile-Leu-Lys-Lys-Val-Leu-Pro-Lys-Val-Met-Ala-His-Met-Lys-NH_2; LL-I, H-Val-Asn-Trp-Lys-Lys-Val-Leu-Gly-Lys-Ile-Ile-Lys-Val-Ala-Lys-NH_2; LL-II, H-Val-Asn-Trp-Lys-Lys-Ile-Leu-Gly-Lys-Ile-Ile-Lys-Val-Ala-Lys-NH_2 and LL-III, H-Val-Asn-Trp-Lys-Lys-Ile-Leu-Gly-Lys-Ile-Ile-Lys-Val-Val-Lys-NH_2.

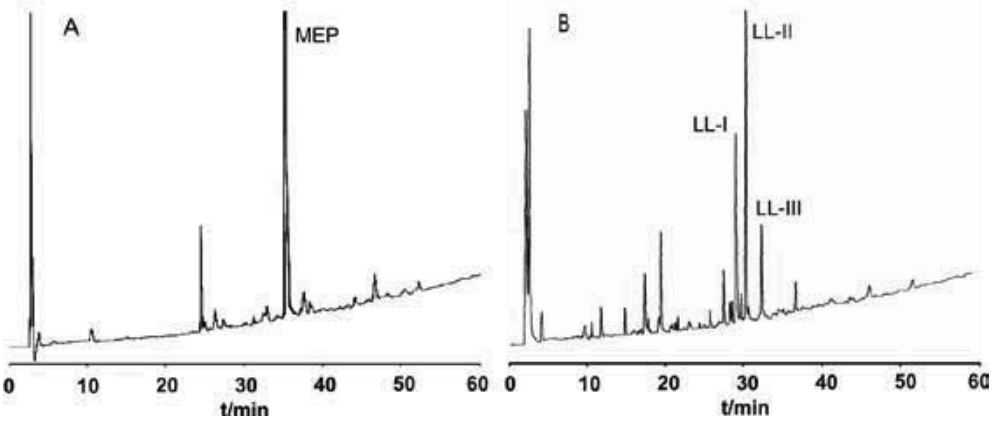

Figure 1. RP-HPLC profiles of *Melecta albifrons* (A) and *Lasioglossum laticeps* (B) venom extracts at 222 nm on Vydac C-18, 250 x 4.6 mm column. An elution gradient of solvents from 5 % to 70 % of acetonitrile in water/0.1% TFA was applied for 60 min at a 1 ml/min flow rate.

Melectin and lasioglossins were prepared by standard Fmoc chemistry method with DIPCI/HOBt as coupling reagents on a Rink Amide MBHA resin in polypropylene syringes with a bottom Teflon filter. For the further studies they were purified by preparative HPLC. All of these peptides proved to be quite effective antimicrobial agents with low hemolytic activity (Table 1).

Table 1. Antimicrobial and hemolytic activities of synthetic MEP, LL-I, LL-II and LL-III vs. indolicidin and tetracycline

Peptide	Antimicrobial activity MIC (μM)				Hemolytic activity LC_{50} (μM)
	B.s.	S.a.	E.c.	P.a.	
MEP	0.8	6.8	2.0	18.5	>100
LL-I	0.8	14.3	1.7	15.8	>200
LL-II	0.7	9.0	1.4	14.4	>200
LL-III	0.8	3.9	1.4	18.7	>200
Indolicidin	1.0	>100	13.0	>100	>200
Tetracycline	12.5	0.4	1.5	75.7	>200

B.s., Bacillus subtilis; S.a., Staphylococcus aureus; E.c., Escherichia coli;P.a., Pseudomonas aeruginosa

As CD spectroscopic measurements and NMR study of melectin and lasioglossins in the presence of TFE or SDS confirmed the presence of a significant amount of α-helical structure, we assume that these peptides can adopt an amphipathic α-helical conformation within bacterial cell membrane which is a prerequisite for their antimicrobial activity. In Edmundson wheel projection (Fig. 2), nearly all of the hydrophilic amino acid residues are situated on one side of the α-helix, whereas the hydrophobic amino acid residues (underlined) are on the opposite side. These novel antimicrobial peptides firstly identified in solitary bee venom possessing high antimicrobial and low hemolytic activity, may serve as new templates for the development of effective antibiotic peptides.

Acknowledgements

The work was supported by the Czech Science Foundation, grant No. 203/08/0536 and by the research project No. Z40550506 of the Institute of Organic Chemistry and Biochemistry Academy of Sciences of the Czech Republic.

References

1. Souza BM, Mendes MA, Santos LD, Marques MR, César LM, Almeida RN, Pagnocca FC, Konno K, Palma MS. *Peptides* **26**: 2157-2164, 2005.
2. Cerovský V, Slaninová J, Fucík V, Hulacová H, Borovičková L, Jezek R, Bednárová L. *Peptides* **29**: 992-1003, 2008.
3. Orivel J, Redeker V, Le Caer JP, Krier F, Revol-Junelles AM, Longeon A, Chaffotte A, Dejean A, Rossier J. *J Biol Chem* **276**: 17823-17829, 2001.
4. Cerovský V, Hovorka O, Cvacka J, Voburka Z, Bednárová L, Borovičková L, Slaninová J, Fucík V. *ChemBioChem* **9**: 2815-2821, 2008.

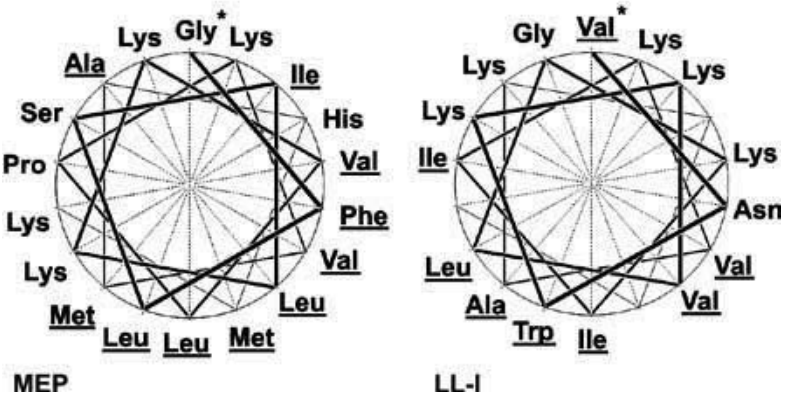

Figure 2. Helical wheel projection of MEP and LL-I. * N-terminal amino acids.

2-07-136

Antimicrobial activity of analogues of the peptide isolated from the venom of social wasp Polistes major major inhabiting the Dominican Republic

*Jezek, Rudolf; Sebestik, Jaroslav; Safarik, Martin; Fučík, Vladimir; Borovičková, Lenka; Ceřovský, Václav; Slaninová, Jiřina**

Inst.Org.Chem.Biochem. Acad. Sci. Czech Rep, CZECH REPUBLIC

**E-mail: slan@uochb.cas.cz*

Introduction

Wasp venoms are complex mixtures of proteins, peptides and other low molecular mass components. The composition is specific for every wasp species. Some of the venom peptides exhibit also antimicrobial activity. Recently we have described isolation and biological activities of several new peptides from the venom of social wasp Polistes major major found in Dominican Republic.[1] We have also reported the synthesis of their analogues in order to investigate structure-activity relationship with respect to the antimicrobial and hemolytic activities.[2] Here we present the activities of a few further analogues of one of the peptides called PMM having the following structure: H-Ile-Asn-Trp-Lys-Lys-Ile-Ala-Ser-Ile-Gly-Lys-Glu-Val-Leu-Lys-Ala-Leu-NH_2. The parent sequence (1-17) or its truncated analogues (2-17; 3-17; 8-17; 9-17; 10-17) were modified on the N-end with palmitic acid (Pal) or 9-acridinyl (Acr) or 9-(1,2,3,4-tetrahydro)acridinyl (Tac) groups. The amino acids in position 8 and/or 12 were replaced by Lys, Ser or Ala. The structure and activities of the analogues synthesized are given in Table 1.

Results and Discussion

The analogues were synthesized manually by solid-phase method using Nα-Fmoc chemistry protocol on a Rink Amide MBHA resin. Protected amino acids were coupled in 4-fold excess in DMF as solvent and DIPC/HOBt (7 eq/5 eq) as coupling reagents. The course of coupling was monitored using 1% solution of Bromophenol Blue (with the exception of Acr-Ile, Tac-Ile and Acr_2-Lys). The peptides were deprotected and cleaved from the resin with a mixture of TFA/H_2O/TIS (95 : 2.5 : 2.5) for 3.5 h and precipitated with tert-butyl methyl ether. Acr- and Tac-amino acids needed prolonged coupling times and 10 times lower concentration in the reaction mixture; the best solvent for the coupling was found to be tetrahydrofuran. Crude peptides were purified by preparative RP-HPLC using a Vydac C-18 column (250 x 10 mm) at a 3.0 ml/min flow rate; the peaks of palmitoylated peptides were wider compared to common peptides. The purity of all the peptides was checked using analytical HPLC and was higher than 95%. The MS were as expected.

The palmitoylated peptides contrary to the literature[3] were found to have very low antimicrobial activity

Table l. Structure and activities of the new analogues

analogue	structure	MIC [μM]				hemolysis
		B.s.	*S.a.*	*E.c.*	*P.a.*	LC50 [μM]
Pal-1	Palmitoyl-PMM(10-17)	>100	-	>100	-	>>200 (n=2)
Pal-2	Palmitoyl-PMM(9-17)	>100	>100	>100	>100	>>200 (n=2)
Pal-3	Palmitoyl-PMM(8-17)	>100	-	>100	-	50.0±5,4 (n=2)
Pal-4	Palmitoyl-PMM(3-17)	50	>100	100	>100	16.9±1,8 (n=3)
Pal-5	Palmitoyl-PMM(2-17)	75	>100	100	>100	9.3±0,2 (n=3)
Pal-6	Palmitoyl-PMM(1-17)	>100	>100	>100	>100	91.4±8,9 (n=3)
PMM	**see above in the text**	**1.3**	**2**	**2.5**	**15**	**80**
S-S	[Ser^{12}]-PMM	1.13	1.25	2.25	20	48.8±4,7 (n=3)
K-S	[Lys^8,Ser^{12}]-PMM	1.13	1.25	2	10	44.7±5,6 (n=3)
A-S	[Ala^8,Ser^{12}]-PMM	1.13	1.25	2.25	20	51.0±7,2 (n=3)
A-K	[Ala^8,Lys^{12}]-PMM	0.88	1.25	2.25	20	59.3±6,9 (n=3)
S-K	[Lys^{12}]-PMM	1.13	1.25	2.25	10	67.4±12,5 (n=3)
K-K	[Lys^8,Lys^{12}]-PMM	0,88	1.25	1.13	10	50.5±10,7 (n=3)
Tac-I	[Tac-Ile^1]-PMM	1.0	3	1.5	80	19.0
Acr-I	[Acr-Ile^1]-PMM	1.0	8	1.5	100	22.2
Acr_2-K	[Acr_2-Lys^1]-PMM	2	>100	4	>100	66.5

B.s., Bacillus subtilis; S.a., Staphylococcus aureus; E.c., Escherichia coli; P.a., Pseudomonas aeruginosa.

against all 4 types of bacteria (Table 1). The prolongation of the peptide chain using a fatty acid even canceled the activity of the very active compound PMM (Pal-6 analogue). The long palmitic acid may hinder the interaction of the N-end of PMM with the bacterial cell membrane. Hemolytic activity of the palmitoylated analogues differed significantly being in the range of 9.3 μM (high hemolysis) to >200 μM (no hemolysis).

Substitution of amino acid residues Ser^{8} or Glu^{12} subsequently for alanine, serine or lysine, i.e. the enhancement of the positive charge of the peptides, neither improved nor deteriorated the activity of the peptides significantly, unfortunately their undesired hemolytic activity was two times enhanced.

Also analogues of the PMM with substituted N-terminal amino group with bulky aromatic Acr or Tac^{4} did not show improved biological activities in comparison to the mother compound. It is however quite interesting that the antimicrobial activity against *B.s.* and *E.c.* was not at all deteriorated, however the activity was decreased against *S.a.* in the case of Acr analogues and against *P.a.* in the case of both Tac and Acr analogues. Their hemolytic activity was however rather high.

Acknowledgements

The work was supported by the Czech Science Foundation, grant No. 203/08/0536 and the research project of the Inst. *Org Chem* Biochem. AVCR, v.v.i., No. Z40550506.

References

1. Čerovský V, Pohl J, Yang Z, Alam N, Attygale AB. Identification of three novel peptides isolated from the venom of the neotropical social wasp Polistes major major. *J Pept Sci* **13**: 445–450, 2007.
2. Čerovský V, Slaninova J, Fucík V, Hulacova H, Borovičková L, Jezek R, Bednarova L. New potent antimicrobial peptides from the venom of Polistinae wasps and their analogs. *Peptides* **29**: 992-1003, 2008.
3. Makovitzki A, Avrahami D, Shai Y. Ultrashort antibacterial and antifungal lipopeptides. *Proc Nat Acad Sci USA* **103**: 15997-16002 2006.
4. Demeunynck M, Charmantray F, Martelli A. Interest of acridine derivatives in the anticancer chemotherapy. *Curr Pharm Design* **7**: 1703-1724, 2001.

2-07-137

Antimicrobial properties of new mastoparan analogues

Ruczynski, Jaroslaw[1,]; Parfianowicz, Brygida[1]; Olkowicz, Mariola[1]; Mucha, Piotr[1]; Skupien, Magdalena[1]; Rekowski, Piotr[1]; Wisniewska, Katarzyna[2]; Dabrowska-Szponar, Maria[2]*

[1]University of Gdańsk, Faculty of Chemistry, POLAND; [2]Medical University of Gdańsk, Department of Medical Microbiology, POLAND

[*]E-mail: ruczynski@chem.univ.gda.pl

In recent years antimicrobial peptides (AMP), both synthetic and from natural sources, have attached much attention as a novel class of antibiotics in particular against antibiotic-resistant pathogens. One of the most promising AMP are peptides belong to the mastoparan family. Mastoparan (MP) is an antimicrobial cationic tetradecapeptide with following primary structure INLKALAALAKKIL-NH_2.[1] This amphiphilic α-helical peptide, originally isolated from the venom of wasp *Paravespula lewisii*, shows a variety of biological activities such as inhibition of the growth of Gram-positive bacteria, activation of mast cell degradation and histamine release, activation of phospholipase A_2 and C or erythrocyte lysis. MP is turned out to enhance the permeability of artificial and biological membranes and activate GTP-binding regulatory proteins by a mechanism analogous to that of G-protein-coupled receptors. MP is also well known as a part of chimeric peptide transportan (TP) – a cell penetrating peptide (CPP), consisting *N*-terminal fragment 1-12 of galanin (GAL) and MP at the *C*-terminus linked with Lys residue.[2]

In present study we have designed and synthesized several new chimeric mastoparan analogues composed of MP and other biologically active peptides (galanin, RNAIII inhibiting peptide) and containing natural or unnatural structures (Table 1). Next we examined each of these hybrid constructs as well as natural peptides for they antimicrobial activities against three reference strains: *Staphylococcus aureus* (NCTC 4163), *Escherichia coli* (NCTC 8196) and *Pseudomonas aeruginosae* (NCTC 6749). The susceptibility of microorganisms to the peptides was determined by the broth microdilution assay according to the procedures outlined by the National Committee for Clinical Laboratory Standards.[3]

Studies have shown that antimicrobial activities of synthesized peptides against Gram-positive bacteria (*S. aureus*) were greater than for Gram-negative bacteria (*E. coli* and *P. aeruginosae*). In case of *S. aureus* the most active analogues were: MP, TP10 and MP-RIP with the MIC values ranged from 8 to 16 μg/ml. Relative strong activities showed: [des-Lys^7]TP10-[Lys^2,Ile^4]RIP, MP-[Lys^2,Ile^4]RIP, RIP-MP and [Lys^2,Ile^4]RIP-MP. MIC values for these peptides were in range of 32-64 μg/ml and they were lower than that for TP. However MIC values for TP10-RIP, TP10-[Lys^2,Ile^4]RIP, TP, Galp, [Lys^{13}(GAc)]TP, [Lys^{13}(UAc)]TP and [Lys^{13}(AdC)]TP reached about 128 μg/ml. In case of *E. coli*, only two analogues: MP and MP-[Lys^2,Ile^4]RIP showed significant MIC values (about 32 and 64 μg/ml respectively). However all MIC values for *P. aeruginosa* were above 128 μg/ml.

As we expected hybrid constructs benefit from the properties of mastoparan and inhibit bacterial proliferation. We have found that MIC value for analogue MP-RIP is similar to that for MP and other conventional antimicrobial agents and that the MP-RIP analogue kills *S. aureus* cells at concentration that did not damage human cells. We suggest that this hybrid may benefit from the properties of RIP and may be a potent therapeutic agent against straphylococcal infections. RIP and its synthetic analogue [Lys^2,Ile^4]RIP have been shown to be effective inhibitors of diseases caused by various strains of *S. aureus*. RIP does not directly kill bacteria proliferation but interferes with their signal transduction, thus making them non-pathogenic.[4]

Interesting activities exhibited also other two analogues: MP-[Lys^2,Ile^4]RIP and [des-Lys^7]TP10-[Lys^2,Ile^4]RIP. Hybrids containing [Lys^2,Ile^4]RIP analogue were generally less effective inhibitors of growth of the bacteria than hybrids containing non-modified RIP structure. In case of [des-Lys^7]TP10-[Lys^2,Ile^4]RIP deletion of Lys^7 residue caused a decrease in MIC value as compared to analogue containing non-modified RIP structure. However an increase in MIC values in case of MP(4-14)-RIP and MP(4-14)-[Lys^2,Ile^4]RIP confirms the hypothesis that the first three *N*-terminal residues in MP structure are essential for high activity against bacteria. Among synthesized eleven analogues of TP and TP10 carying nucleobase, nucleoside or benzimidazole derivatives inactive were eight. Other three analogues: [Lys^{13}(GAc)]TP, [Lys^{13}(UAc)]TP and [Lys^{13}(AdC)]TP have shown weak antibacterial activities comparable to the non-modified TP structure.

Acknowledgements

This work was supported by the University of Gdańsk grant BW 8000-5-0133-8.

Table 1. A comparison of MIC values of synthesized peptides

Peptide	Molecular weight	MIC [μg/ml]		
		S. aureus	*E. coli*	*P. aeruginosae*
MP	1478.9	8	32	256
retro-MP	1478.9	>256	256	256
MP–retro-MP	2940.9	>256	>256	>256
RIP	913.0	>256	>256	>256
MP–RIP	2374.9	16	256	>256
RIP–MP	2374.9	32	128	>256
MP(4-14)	1138.5	>256	>256	>256
MP(4-14)–RIP	2034.5	>256	>256	>256
[Lys^2,Ile^4]RIP	881.0	>256	>256	>256
MP(4-14)–[Lys^2,Ile^4]RIP	2002.5	256	>256	>256
MP–[Lys^2,Ile^4]RIP	2343.0	64	64	>256
[Lys^2,Ile^4]RIP–MP	2343.0	64	256	>256
Galp	2809.5	128	>128	>128
TP	2840.5	128	>128	>128
[Lys^{13}(2-APAc)]TP	3016.0	>256	>256	>256
[Lys^{13}(AAc)]TP	3015.7	>128	>128	>128
[Lys^{13}(CAc)]TP	2991.6	>128	>128	>128
[Lys^{13}(GAc)]TP	3030.8	128	>128	>128
[Lys^{13}(TAc)]TP	3006.6	>128	>128	>128
[Lys^{13}(UAc)]TP	2992.7	128	>128	>128
[Lys^{13}(AdC)]TP	3129.6	128	>128	>128
[Lys^{13}(UrC)]TP	3108.8	>128	>128	>128
TP10	2181.8	16	128	256
[Lys^7(BnzAc)]TP10	2339.8	256	>256	>256
[Lys^7(NBnzAc)]TP10	2466.8	>256	>256	>256
[Lys^7(PBnzAc)]TP10	2417.4	>256	>256	>256
TP10–RIP	3077.8	128	>256	>256
TP10–[Lys^2,Ile^4]RIP	3045.8	128	>256	>256
[des-Lys^7]TP10–[Lys^2,Ile^4]RIP	2917.6	64	256	>256
Gentamicin	477.6	0.5	1.0	0.25

AL - galanin;
Galp - GAL(1-13)-MP (galparan);
MP - mastoparan;
RIP - RNA III inhibiting peptide (YSPWTNF-NH_2);
TP - GAL(1-12)-Lys-MP (transportan);
TP10 - GAL(7-12)-Lys-MP (transportan-10);
AdC - adenosine-5'-carboxylic acid;
UrC - uridine-5'-carboxylic acid;
AAc - 9-adeninylacetic acid;
GAc - 9-guaninylacetic acid;
TAc - 1-thyminylacetic acid;
UAc - 1-uracilacetic acid;
CAc - 1-cytosinylacetic acid,
2-APAc - 2-aminopurine-9-acetic acid;
BnzAc - benzimidazole-1-acetic acid;
NBnzAc - 2-nonylbenzimidazole-1-acetic acid;
PBnzAc - 2-(2-pyridyl)benzimidazole-1-acetic acid.

References

1. Xu X, Yang H, Yu H, Li J, Lai R. The mastoparanogen from wasp. *Peptides* **27**: 3053-2057, 2006.
2. Pooga M, Hallbrink M, Zorko M, Langel Ü. Cell penetration by transportan. *FASEB J* **12**: 67-77, 1998.
3. *NCCLS: National Committee for Clinical Laboratory Standards.* Methods for dilution antimicrobial susceptibility test for bacteria that grow aerobically **13** (25), 1993.
4. Giacometti A, Cirioni O, Gov Y, Ghiselli R, Del Prete MS, Mocchegiani F, Saba V, Orlando F, Scalise G, Balaban N, Dell'Acqua G. RNA III inhibiting peptide inhibits in vivo biofilm formation by drug-resistant Staphylococcus aureus. Antimicrob. Agents. Chemother. **47**: 1979-1983, 2003.

2-07-138

Influence of bulky 3,3-diphenylalanine isomers at position 2 of AVP analogues on their conformation

Kwiatkowska, Anna; Sikorska, Emilia*

Faculty of Chemistry, University of Gdańsk, Departament of Organic Synthesis, POLAND

E-mail: aniak@chem.univ.gda.pl

Introduction

Vasopressin (AVP) belongs to the neurohypophyseal hormone family. It plays a very important role in the control of urine concentration and the blood pressure in mammals. It is suggested that main structural elements of the AVP-like hormones are β-turns at positions 3,4 and/or 4,5, whereas β-turns at positions 2,3 and/or 3,4 are characteristic of oxytocin-like peptides.[1] Moreover, it is known that a proper orientation of the Tyr[2] side chain is necessary for agonistic activity.[2] One modification that can alter the preferred orientation of the side chain is the change of configuration from L to D.[3] Also lack of a phenol group in the aromatic side chain at position 2, which is crucial for transduction, results in loss of agonistic properties.

In this study, we present the results of conformational analysis of four vasopressin (AVP) analogues modified at position 2 with the 3,3-diphenylalanine (Dip) isomers. These are: [Mpa[1],Dip[2],Val[4],D-Arg[8]]VP (I), [Mpa[1],D-Dip[2],Val[4],D-Arg[8]]VP (II), [D-Dip[2],D-Arg[8]]VP (III) and [Mpa[1],D-Dip[2]]AVP (IV). All the peptides exhibit strong antidiuretic effect, except for peptide I. In turn, analogue I exhibits enhanced affinity to human OT receptor. Analogues II, III and IV reveal also antiuterotonic activity. Moreover, analogue II is also a blocker of V_{1a} receptors.

Results and Discussion

Biological activity of vasopressin rests on its ability of binding to respective transmembrane receptors. Hence, incorporation a bulky residue into the AVP sequence produces very often an inactive analogue, because the bulkiness results in difficulties with location of the analogue inside a not large enough receptor cavity. Therefore, high activity of the AVP analogues modified with bulky 3,3-diphenylalanine (Dip) isomers is surprising and worth of conformational investigations.

NMR spectra of analogues II and IV display two distinct sets of residual proton resonances indicating that the peptides adopt two conformations being in equilibrium.Their appearance is due to the *cis/trans* isomerization of the Cys[6]-Pro[7] peptide bond. In each case, the major conformation possesses all peptide bonds in trans configuration. The contributions of *cis* isomer are 2% and 6% for peptide II and IV, respectively. With the remaining AVP analogues, only one set of proton resonances appears in the NMR spectra.

Inspection of the NOE patterns suggests that the AVP analogues adopt preferentially a reverse structure in the their cyclic part. The amide proton coefficient calculated for Asn[5] is located near -2.5 [ppb/deg] for each peptide, thus indicating a strong hydrogen bond, HN^5-CO^2, and a β-turn at position 3,4. The $H_N(6)$-$H_N(7)$ and $H_\alpha(7)$-$H_N(9)$ connectivities in the NOESY spectra of peptides II and III also suggest bent structures in the C-terminal part.

Three-dimensional structures of the analogues were determined using two-dimensional NMR spectroscopy and molecular dynamics simulations with time-averaged restraints. The simulations were carried out with the parm99 force field in AMBER8.0 package.[4] The initial solvent configuration around the peptide was obtained by filling cubic box with DMSO molecules. The overall box size was enlarged by about 10 Å in each direction. Chloride ions were used to neutralize the system. To equilibrate the solution density, the initial simulations were carried out at 303 K, in a periodic box, until the density was close to that of the solvent. In the next step, a LES (locally enhanced sampling) system was used for each system separately. A total of five copies of each peptide in the DMSO solution were generated by ADDLES module of the AMBER 8.0 program. Then a MD-LES with ensemble-averaged distance and dihedral angle restraints derived from the NMR spectroscopy was made. A 9 Å cutoff radius was chosen. The simulations were carried out at 303 K in a periodic box of constant volume, with the Particle-mesh Ewald (PME) procedure. The time step was 2 fs. The total duration of the run was 4 ns. The coordinates were collected every 2000th step. The conformations obtained during the last 25 ps of the MD-LES simulations were considered in further analysis. As a result, 100 conformations for each peptide were analyzed.

Main structural elements of the peptides studied are reverse structures. All the peptides tend to create β-turn at position 3,4. Analogues I and II show enhanced propensity to form β-turn in the 3-5 fragment probably owing to replacement of the polar Gln with hydrophobic Val at position 4. Analogue II, in contrast to I, creates also a βII'-turn at position 2,3. A high probability of a βII'-turn between residues 1 and 4 is provided by a D-amino

acid at position 2. Moreover, the C-terminus of analogue II is involved in either β-turn or γ-turn at positions 7,8 or 8, respectively. Besides, they differ from each other with variant mutual location of the aromatic side chains (Fig. 1) which has essential influence on activity.

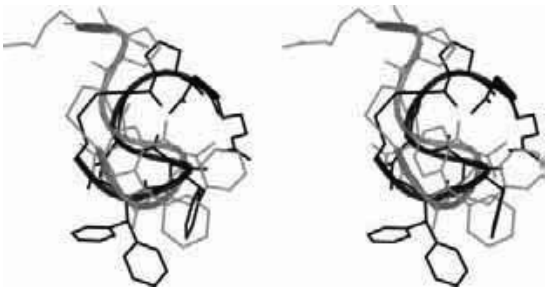

Figure 1. Comparison of average structures of analogue I (black line) and analogue II (gray line). RMSD1-6= 1.492 Å for Cα.

The majority of the structures obtained for analogue IV form βII'-turn in the Mpa^{1}-Gln^{4} fragment, characteristic of oxytocin-like hormones. Analogues III and IV, similar as II, create β-turn at position 7,8, which seems to be crucial for antagonistic activity towards OT receptors in the case of the presented peptides.

Acknowledgment

This work was supported in part by the State Committee for Scientific Research, Poland, grant No. KBN 2385/B/H03/2008/34.

References

1. Liwo A, Tempczyk A, Ołdziej S, Shenderovich MD, Hruby VJ, Talluri S, Ciarkowski J, Kasprzykowski F, Łankiewicz L, Grzonka Z. Exploration of the conformational space of oxytocin and arginine-vasopressin using the electrostatically driven Monte Carlo and molecular dynamics methods. *Biopolymers* **38**: 157-175, 1996.
2. Hruby VJ, Chow MS, Smith DD. Conformational and structural considerations in oxytocin-receptor binding and biological activity. *Annu Rev Pharmacol Toxicol* **30**: 501-534, 1990.
3. Hruby VJ, Upson DA, Yamamoto DM, Smith CW, Walter R. Active site studies of neurohypophyseal hormones. Comparison of oxytocin and arginine vasopressin analogs containing 2-D-tyrosine. *J Am Chem Soc* **101**: 2717-2721, 1979.
4. Case DA, Darden TA, Cheatham III TE, Simmerling CL, Wang J, Duke RE, Luo R, Merz KM, Wang B, Pearlman DA, Crowley M, Brozell S, Tsui V, Gohlke H, Mongan J, Hornak V, Cui G, Beroza P, Schafmeister C, Caldwell JW, Ross WS, Kollman PA. *AMBER **8***, University of California, San Francisco, 2004.

2-07-139

N-terminal modification of arginine vasopressin with *CIS*-1-amino-4-phenyl-cyclohexane carboxylic acid: Highly potent oxytocin receptor antagonists

Prahl, Adam[1,]; Kwiatkowska, Anna[1]; Śleszyńska, Małgorzata[1]; Derdowska, Izabela[1]; Sobolewski, Dariusz[1]; Borovičková, Lenka[2]; Slaninová, Jiřina[2]; Lammek, Bernard[1]*

[1]Faculty of Chemistry, University of Gdańsk, Departament of Organic Synthesis, POLAND; [2]Academy of Sciences of the Czech Republic, Institute of Organic Chemistry and Biochemistry CZECH REPUBLIC

[*]E-mail: ap@chem.univ.gda.pl

Introduction

Arginine vasopressin (AVP) is a cyclic nonapeptide with multiple functions. The design of analogues, which are very active either as agonists or antagonists and truly selective for individual receptors, still remains an area of great interest. The most straightforward approach for peptide modification is introduction of bulky or sterically restricted elements into the peptide chain with the aim to restrict the conformational flexibility of the molecule.

We decided to check how substitution of position 2 with bulky *cis*-1-amino-4-phenyl-cyclohexane-1-carboxylic acid (*cis*-Apc, see Fig. 1) would reflect in the values of biological potency of the analogues. The *cis*-Apc differs from 1-aminocyclohexane-1-carboxylic acid (Acc) previously used in our laboratory[1] by the presence of phenyl moiety and was chosen in order to find out how the enlargement of the side chain and change of its character for aromatic one will influence the activity of resulting analogues. We synthesized four new analogues of AVP: [*cis*-Apc^2]AVP (**I**), [Mpa^1,*cis*-Apc^2]AVP (**II**), [*cis*-Apc^2,Val^4]AVP (**III**), [Mpa^1,*cis*-Apc^2,Val^4]AVP (**IV**) and determined some of their pharmacological properties.

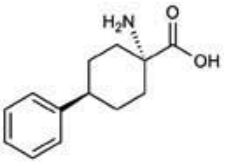

Figure 1. Structure of cis-1-amino-4-phenyl-cyclohexane-1-carboxylic acid.

Results and Discussion

The new analogues of AVP were synthesized manually using Fmoc-chemistry on polystyrene resin (TentaGel S Ram-resin, capacity 0.22 mmol/g), according to standard procedures.[2] The purity and identity of each peptide were determined by HPLC and by MALDI TOF mass spectrometry (molecular ion). The values of the molecular ions were as expected and the purity was higher than 98%.

The activities of new analogues were determined in the *in vitro* rat uterotonic test in the absence of magnesium

Table 1. Pharmacological Properties of the New AVP Analogues

Analogue		Activity				
		Oxytocic Uterus *in vitro* test no Mg^{2+}	Pressor IU/mg or pA_2	Antidiuretic IU/mg 60 min	(200 min)	Affinity to human OTR[nM]
AVP[a]		17	412	465	(465)	5.5±0.4
[Acc^2]AVP[b]		pA_2~5.6	56.6	750-900	(~9 300)	
[*cis*-Apc^2]AVP	(**I**)	pA_2=7.47±0.30	pA_2=6.73	~10	(~2000)	110±26
[Mpa^1,Acc^2]AVP[b]		pA_2=6.1 and 0.7 IU/mg	17.2±0.8	~4500	(50 000)	
[Mpa^1,*cis*-Apc^2]AVP	(**II**)	pA_2=8.46±0.20	pA_2=7.41	~45	(~9000)	5.4±1.2
[*cis*-Apc^2,Val^4]AVP	(**III**)	pA_2=8.22±0.11	pA_2=6.85	~15	(~2000)	88.8±30.2
[Mpa^1,*cis*-Apc^2,Val^4] AVP	(**IV**)	pA_2=8.40±0.19	pA_2=7.04	~20	(~4500)	9.1±0.7

[a]Values taken from reference[4]; [b] Values taken from reference[1]

ions, in the pressor test using rats in urethane anesthesia, and in the antidiuretic assay using conscious rats. Test details have been described earlier.[1] Binding affinities to the human oxytocin receptor were determined as described[3] using tritiated oxytocin from NEN Life Science, Boston, MA, USA.

The results of pharmacological evaluation of the new analogues **I** – **IV**, together with the relevant data for AVP and some related peptides, are shown in Table 1. The antidiuretic potency of all these analogues is lower than that of AVP if calculated on the basis of the threshold doses. On the other hand, the peptides exhibit significantly prolonged activity as can be seen from the activities calculated on the antidiuresis half time level 200 min. In regard to the uterotonic test, the compounds **II** – **IV** are highly potent blockers of oxytocin receptors, while peptide I exhibited moderate antioxytocic potency. The *cis*-Apc[2] substitution by itself is sufficient to evoke substantial antioxytocic activity of analogues. Moreover, combination of *cis*-Apc modification with either deamination of position 1 (analogue **II**) or replacement of the Gln[4] residue by aliphatic Val[4] (analogue **III**) or both modifications (analogue **IV**) greatly increase the antioxytocic potency of resulting peptides, as compared to parent compound [*cis*-Apc[2]]AVP. As far as the pressor test is concerned, it is clear that the *cis*-Apc[2] modification converted AVP and its analogues in all four cases (compounds **I**– **IV**) into weak or moderately potent antagonists.

These, in our opinion interesting findings demonstrate the usefulness of our approach in the design of new highly active and selective analogues with desired pharmacological properties.

Acknowledgments

Partial funding for this work was provided by Polish State Committee for Scientific Research under the grant No. 1312/T09/2005/29 and 2385/B/HO3/2008/34 and by research project No. Z4055905 of the Academy of Sciences of the Czech Republic.

References

1. Kowalczyk W, Prahl A, Derdowska I, Dawidowska O, Slaninová J, Lammek B. Highly potent 1-aminocyclohexane-1-carboxylic acid substituted V2 agonists of arginine vasopressin. *J Med Chem*. **47**: 6020-6024, 2004.
2. Bodanszky M, Bodanszky A. *The Practice of Peptide Synthesis.* Springer-Verlag, Berlin, Germany, 1984, p 83.
3. Gimpl G, Burger K, Fahrenholz F, Cholesterol as modulator of receptor function. *Biochemistry* **36**: 10959-10974, 1997.
4. Lebl M, Jošt K, Brtnik F, Tables of Analogs in *Handbook of Neurohypophyseal Hormone Analogs*. CRC Press Inc, Boca Raton, FL, Vol. II, Part 2, pp 127-267, 1987.

2-07-140

Influence of (2S,4R)-4-(2-naphthylmethyl)-pyrrolidine-2-carboxylic acid in position 2 of arginine vasopressin and its analogues on pharmacological properties

Derdowska, Izabela[1,]; Kwiatkowska, Anna[1]; Prahl, Adam[1]; Sobolewski, Dariusz[1]; Borovičková, Lenka[2]; Slaninová, Jiřina[2]; Lammek, Bernard[1]*

[1]Faculty of Chemistry, University of Gdańsk, Departament of Organic Synthesis, POLAND; [2]Academy of Sciences of the Czech Republic, Institute of Organic Chemistry and Biochemistry CZECH REPUBLIC

[*]E-mail: iza@chem.univ.gda.pl

Introduction

Arginine vasopressin (AVP), a neurohypophyseal hormone and neuromodulator, is a cyclic nonapeptide with a disulfide bridge between Cys residues at positions 1 and 6. It exerts its biological effects upon binding to three receptor subtypes termed: V_{1A}, V_{1B} (V_3), and V_2, Furthermore, AVP to some extent can interact with the oxytocin (OT) receptor.[1,2]

Biological activity of peptides is determined by their structure and conformation. Conformational restriction of bioactive peptides is therefore a well-established strategy to change their pharmacological profile.

Peptide flexibility can be restricted by a local constraint, e.g. by introducing amino acids with limited conformational freedom, which has an impact on specific orientations of the peptide backbone and the side chains. In this work, we decided to check the influence of the bulky aromatic conformationally constrained imino acid, (*2S,4R*)-4-(2-naphthylmethyl)-pyrrolidine-2-carboxylic (Nmp) acid (Fig. 1) , at position 2 of the AVP and some of its analogues on the pharmacological properties. The synthesized analogues have the following structures: [Nmp^2]AVP (**I**), [Mpa^1,Nmp^2]AVP (**II**), [Nmp^2,D-Arg^8] AVP (**III**), [Mpa^1,Nmp^2,D-Arg^8]AVP (**IV**).

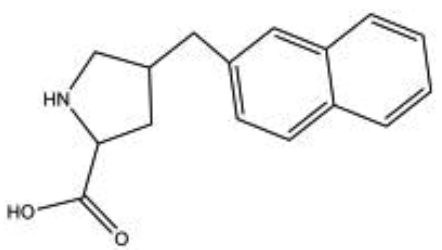

Figure 1. Structure of (*2S,4R*)-4-(2-naphthylmethyl)-pyrrolidine-2-carboxylic acid (Nmp).

Results and Discussion

The new analogues of AVP were synthesized manually using Fmoc-chemistry on polystyrene resin (TentaGel S Ram-resin, capacity 0.22 mmol/g), according to standard procedures.[3] The purity and identity of each peptide were determined by HPLC and by MALDI TOF mass spectrometry (molecular ion). The values of the molecular ions were as expected and the purity was higher than 98%. The activities of new analogues were determined in the *in vitro* rat uterotonic test in the absence of magnesium ions, the pressor test using urethane anesthetized rats and in the antidiuretic assay using conscious rats (for details see ref.[4]). Binding affinities to the human oxytocin receptor were determined using tritiated oxytocin from NEN Life Science, Boston, MA, USA.

The results of pharmacological evaluation of the new analogues **I** – **IV**, together with relevant data for AVP and some related peptides, are shown in Table 1. All new compounds exhibited moderate antioxytocic activities in the uterotonic test (pA_2 values ranging from 6.95-7.61) and were weak antagonists of AVP in the pressor test (pA_2 values ranging from 5.70- 6.31). The antidiuretic potency was negligible, in the case of analogues **I** and **II** about 1000 times lower than AVP at the threshold level (60 min) and about 10 times or more lower at the effect level 200 min. The remaining two peptides (**III** and **IV**) showed no antidiuretic activity at the highest dose tested.

These results together with the data of activities of analogues having in position 2 α-2-indanylglycine,[5] *cis*-1-amino-4-phenyl-cyclohexane-1-carboxylic acid,[6] 2-aminoindane-2-carboxylic acid[7] or more bulky 3,3-diphenylalanine enantiomers[4] offer interesting new information about structure – activity relationship of AVP analogues and may be profitably used for the design of new analogues with better pharmacological profiles.

Table 1. Pharmacological Properties of the New AVP Analogues

Analogue	Activity			
	Oxytocic Uterus *in vitro* no Mg^{2+} IU/mg or pA_2	Pressor IU/mg or pA_2	Antidiuretic IU/mg 60 min - 200 min	Affinity to human OTR [nM]
AVP[a]	17	412	465	
[D-Arg[8]]VP[a]	0.4	4.1	114 - 257	
[Mpa[1]]AVP[a]	27-63	346-370	1300 - 1745	
[Nmp[2]]AVP **(I)**	pA_2=7.30±0.27	pA_2=5.70	b	375±109
[Mpa[1], Nmp[2]]AVP **(II)**	pA_2=7.61±0.11	pA_2=6.31	b	47.2±5.4
[Nmp[2],D-Arg[8]]AVP **(III)**	pA_2=6.95±0.15	pA_2=5.80	c	1440±160
[Mpa[1],Nmp[2],D-Arg[8]]AVP **(IV)**	pA_2=7.53±0.08	pA_2=6.15	c	118±15

[a] Values taken from reference[8]; [b] Antidiuretic activity about 1000 times lower than AVP at the threshold level (60 min) and about 10 times or more lower at the effect level 200 min; steeper dose response curve; [c] No antidiuretic activity up to the dose 1 x 10^{-2} mg/kg of experimental animal

Acknowledgments

Partial funding for this work was provided by Polish State Committee for Scientific Research under the grant No. 1312/T09/2005/29 and 2385/B/HO3/2008/34 and by research project No. Z40550506 of the Academy of Sciences of the Czech Republic.

References

1. Jard S, Barberis C, Audigier S, Tribollet E. Neurohypophyseal hormone receptor systems in brain and periphery. *Prog Brain Res* **72**: 173-187, 1987.
2. Gimpl G, Fahrenholz F. The oxytocin receptor system: structure, function, and regulation. *Physiol Rev* **81**: 629-683, 2001.
3. Bodanszky M, Bodanszky A. *The Practice of Peptide Synthesis*. Springer-Verlag: Berlin, Germany, p 83, 1984.
4. Kowalczyk W, Prahl A, Derdowska I, Sobolewski D, Olejnik J, Zabrocki J, Slaninová J, Lammek B. Analogues of neurohypophyseal hormones, oxytocin and arginine vasopressin, conformationally restricted in the N-terminal part of the molecule. *J Med Chem* **49**: 2016-2021, 2006 .
5. (a) Proceedings of 30th Peptide Symposium (2-07-139). Lammek B, Kwiatkowska A, Derdowska I, Prahl A, Sobolewski D, Śleszyńska M, Borovičková L, Slaninova J. *Proceedings of 30th Peptide Symposium* (2-07-142); (b) Kwiatkowska A, Sleszyńska M, Derdowska I, Prah A, Sobolewski D, Slaninovà J, Lammek B. These Proceedings and Abstracts of the 30th European Peptide Symposium, 31 August-5 September 2008, Helsinki, Finland. *J Pept Sci* **14:** 8 Suppl, 94, 2008; (c) Kwiatkowska A, Derdowska I, Prahl A, Sobolewski D, Slaninovà J, Lammek B. ibid p. 94.
6. (a) Prahl A, Kwiatkowska A, Śleszyńska M, Derdowska I, Sobolewski D, Borovičková L, Slaninova J, Lammek B. Proceedings of 30th Peptide Symposium (2-07-139); (b) Kwiatkowska A, Sleszyńska M, Sobolewski D, Prahl A, Derdowska I, Slaninovà J, Lammek B. Abstracts of the 30th European Peptide Symposium, 31 August-5 September 2008, Helsinki, Finland. *J Pept Sci* **14**: 8 Suppl, 93, 2008.
7. Kowalczyk W, Sobolewski D, Prahl A, Derdowska I, Borovičková L, Slaninová J, Lammek B. The effects of N-terminal part modification of arginine vasopressin analogues with 2-aminoindane-2-carboxylic acid: a highly potent V2 agonist. *J Med Chem*. **14**: 2926-2929, 2007.
8. Lebl M, Jošt K, Brtnik F. *Tables of Analogs in Handbook of Neurohypophyseal Hormone Analogs*. CRC Press Inc, Boca Raton, FL, Vol II, Part 2, pp 127-267, 1987.

2-07-141

New analogs of the antimicrobial Gramicidin S

Ciarkowski, Jerzy[1,]; Mickiewicz, Beata[1]; Kamysz, Elżbieta[1]; Kamysz, Wojciech[2]; Rodziewicz-Motowidło, Sylwia[1]*

[1]University of Gdańsk, Faculty of Chemistry, POLAND; [2]Lipopharm.pl, Zblewo, Faculty of Pharmacy, Medical University of Gdańsk, POLAND

[*]E-mail: jurek@chem.univ.gda.pl

Introduction

Gramicidin S (GS) is a peptide antibiotic cyclo-(Val-Orn-Leu-D-Phe-Pro)$_2$ isolated from *Bacillus brevis*.[1] It forms a two-stranded antiparallel β-sheet imposed by two II' β-turns[2] with the D-Phe-Pro sequences at the corners and hydrophobic and hydrophilic residues on the opposite sides of the β sheet as a structural feature required for the antimicrobial activity of GS3. Despite its wide Gram+/- antimicrobial spectrum, GS is useless in therapy because of its high hemotoxicity in humans.[3] It was found, however, that the analogs of GS-14 (GS with Lys-Leu inserted into each strand) got more antimicrobial selectivity when their amphipatic moments were perturbed by swapping Lys with the adjacent Leu/Val, or by configuration reversal at Lys.[4] In this study we report on effects of similar perturbations put on GS original c-decapeptide, using the following examples: c(Val-Lys-Leu-D-His-Pro)$_2$, GS_1, as the mother compound; and its three analogs, viz. c(Val-**D-Lys**-Leu-D-His-Pro-Val-Lys-Leu-D-His-Pro) – Lys2 converted to D, GS_2; c(**Lys-Val**-Leu-D-His-Pro-Val-Lys-Leu-D-His-Pro) – Val1-Lys2 swapped, GS_3; and c-(Val-**Leu-Lys**-D-His-Pro-Val-Lys-Leu-D-His-Pro) – Lys2-Leu3 swapped, GS_4; all possessing reduced ring-sequence symmetry. Having solved their structures by 2D-NMR and having tested their activities/selectivities, we could make no structure-toxicity correlations since only GS_1 had relatively favorable bio-profile, as already published,[4] while the other – did not.

Results and discussion

The proton chemical shifts were assigned using TOCSY and the sequences were confirmed using ROESY spectra. For GS10_1 and GS10_2 there were signals indicative of two major and minor components. Moderate ROE between αH_i and NH_{i+1} indicated *trans* geometry for all peptide bonds. Additionally, lack of any chemical exchange signals ruled out *cis-trans* isomerism. Fig. 1 summarizes the ROE patterns, the values of vicinal coupling constants $^3J_{HN\alpha H}$ and the temperature coefficients for the peptides. The strong crosspeaks for the αH_i-NH_{i+1} and βH_i NH_{i+1} protons pairs suggest formation of β turns in peptides structures. However, low temperature coefficients of the amide protons (< -3.0x10^{-3} ppb) would indicate lack of regular structure of the peptides.

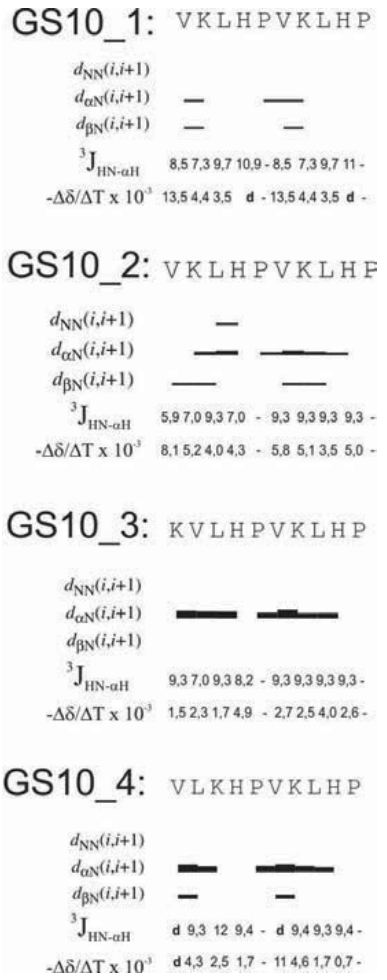

Figure 1. Summary of ROE connectivities, $^3J_{HN\alpha H}$ [Hz] couplings and NH temperature coefficients ($-\delta\delta/\delta$T [ppb/K]). The height of the bars reflects strength of ROE correlation; d – difficult to measure.

Detailed studies show that GS_1 forms a two-stranded antiparallel β-sheet with the D-His-Pro sequences making two II' β turns. Very similar structure but with shorter β sheet is formed by the GS10_4 peptide. The other analogs GS10_2 and GS10_3 do not form a regular β-hairpin structure (Fig. 1). The configuration of amino acid seems important since changing Lys2 for D-Lys2 (GS10_2) causes bending of the backbone and destabilizes the

conformation. Destabilization of the β-sheet in GS10_3 is probably caused by the repulsion of two remote residues Lys1 and D-His4 resulting in disturbing ring symmetry. Our biological studies show that only GS10_1 has similar to Gramicidin S activity. The other analogs are completely inactive. Better understanding of structural features responsible for the action of these peptides is thus crucial for the design of valuable analogs.

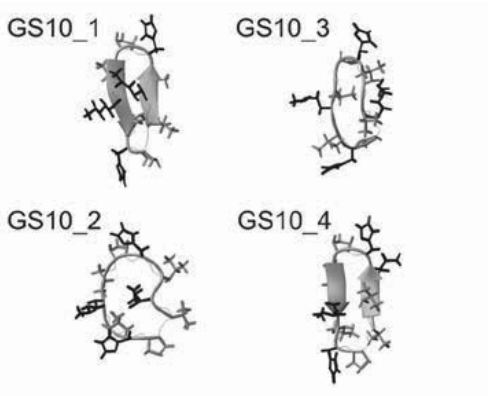

Figure 2. NMR-resolved conformations of GS analogs.

Methods

Synthesis: Peptides were synthesized manually by the Fmoc/t-Bu strategy using 2-chlorotrityl resin and fragment ligation. The crude peptides were purified by solid-phase extraction. The peptides were eluted from the cartridge with varied acetonitrile-water mixtures in the presence of 0.05% trifluoroacetic acid. The purity of each fraction was determined by thin layer chromatography (TLC) and reverse-phase high performance liquid chromatography (RP HPLC). The peptides were characterized by matrix-assisted laser desorption ionization – time-of-flight mass spectrometry (MALDI-TOF). *NMR*: 500 MHz 2D-NMR spectra were measured on Varian 500 MHz spectrometer. 1D in 22, 30, 40, 50 °C and 2D: DQF-COSY, TOCSY (80 ms), ROESY (200 ms) and NOESY (100 ms). Samples were dissolved in D_2O/H_2O (1:9, v/v). Peptides initial structures we resolved using the DYANA[5] program with simulated-annealing algorithm. Taken from DYANA, the torsion angles and distance restraints were used in the Time-Averaged Constraints Molecular Dynamics calculations in AMBER program.

Acknowledgements

The calculations were carried out in TASK Gdańsk, Poland. This work was supported by the Ministry of Science and Education of Poland, grant no: BW/8000-5-0111-8 (JC, SR-M). The NMR was done in Intercollegiate NMR Lab by Pawel Sowinski, Gdańsk, Poland.

References

1. Gause GF, Brazhnikova MG. *Nature* **154**: 703, 1944.
2. Rackovsky S, Scheraga HA. *Proc Natl Acad Sci U S A* **77**: 6965-6967, 1980.
3. Kondejewski LH, Farmer SW, Wishart DS, Kay CM, Hancock REW, Hodges RS. *J Biol Chem* **271**: 25261-25268, 1996.
4. Kondejewski LH, Farmer SW, Wishart DS, Hancock REW, Hodges RS. *Int J Pept Protein Res* **47**: 460-466, 1996.
5. Güntert P, Mumenthaler C, Wütrich K. *J Mol Biol* **273**: 283-298, 1997.

2-07-142

Analogues of arginine vasopressin modified in the *N*-terminal part of the molecule with *α*-2-indanylglycine. Highly active and selective antiuterotonic agents

Lammek, Bernard[1,]; Kwiatkowska, Anna[1]; Derdowska, Izabela[1]; Prahl, Adam[1]; Sobolewski, Dariusz[1]; Śleszyńska, Małgorzata[1]; Borovičková, Lenka[2]; Slaninová, Jiřina[3]*

[1]Faculty of Chemistry, University of Gdańsk, Departament of Organic Synthesis, POLAND; [2]Academy of Sciences of the Czech Republic, Institute of Organic Chemistry and Biochemistry CZECH REPUBLIC; [3]Faculty of Chemistry, University of Gdańsk, Institute of Organic Chemistry and Biochemistry CZECH REPUBLIC

[*]E-mail: rekug@ug.gda.pl

Introduction

Many of vasopressin agonists and antagonists have been designed and synthesized in the course of extensive investigation of structure – activity relationship.[1,2] A great deal of evidence shows that the conformation of the N-terminal part of arginine vasopressin analogues is crucial for their pharmacological activity.[2]

Incorporation of unnatural non-proteinogenic *α*-amino acids into peptides is a promising approach in peptide modification. The conformationally restricted amino acid derivatives are of particular interest. We decided to check how substitution of position 2 with bulky *α*-2-indanylglycine (Igl, see Fig. 1) would reflect in the values of biological potency of the analogues. We designed, synthesized and determined some pharmacological properties of four new analogues of AVP where the above mentioned modification was combined with Mpa[1] and/or Val[4] substitutions. These peptides have the following structure: [Igl[2]]AVP (**I**), [Mpa[1],Igl[2]]AVP (**II**), [Igl[2],Val[4]]AVP (**III**), [Mpa[1],Igl[2],Val[4]]AVP (**IV**).

Results and discussion

The new analogues of AVP were synthesized manually using Fmoc-chemistry on polystyrene resin (TentaGel S Ram- resin, capacity 0.22 mmol/g), according to standard procedures.[3] The purity and identity of each peptide were determined by HPLC and by MALDI TOF mass spectrometry (molecular ion). The values of the molecular ions were as expected and the purity

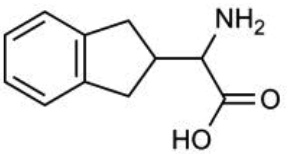

Figure 1. Structure of a-2-indanylglycine (Igl).

Table 1. Pharmacological Properties of the New AVP Analogues

Analogue	Activity			
	Oxytocic Uterus *in vitro* test no Mg^{2+}	Pressor IU/mg or pA_2	Antidiuretic IU/mg 60 min (200 min)	Affinity to human OTR[nM]
AVP[a]	17	412	465	
[Val[4]]AVP[a]	-	32	738	
[Mpa[1]]AVP[a]	27-63	346-370	1300-1745	
[Igl[2]]AVP **I**	pA_2=7.19±0.10	0	b	1005±282
[Mpa[1],Igl[2]]AVP **II**	pA_2=7.94±0.20	0	b	202±16
[Igl[2],Val[4]]AVP **III**	pA_2=7.68±0.16	0	b	745±175
[Mpa[1],Igl[2],Val[4]]AVP **IV**	pA_2=7.75±0.10	0	b	745±175

[a] Values taken from ref 2; [b] negligible antidiuretic activity; about 1000 times lower than AVP at the threshold level (60 min) and about 10 times or more lower at the effect level 200 min; steeper dose response curve

was higher than 98%. The activities of new analogues were determined in the *in vitro* rat uterotonic test in the absence of magnesium ions, in the pressor test using urethane anesthetized rats, and in the antidiuretic assay using conscious rats (for details concerning all test, see ref.[4]). Binding affinities to the human oxytocin receptor were determined as described in[5] using tritiated oxytocin from NEN Life Science, Boston, MA, USA.

The results of pharmacological evaluation of the new analogues **I** – **IV**, together with relevant values for AVP and for some related peptides, are shown in Table 1. All new compounds exhibited only negligible antidiuretic activity, about 1000 times lower than that of AVP at the threshold level (60 min) and about 10 times or more lower at the effect level 200 min. Peptides having α-2-indanylglycine (Igl) in position 2 were moderate (**I**) or high (**II**, **III**, **IV**) oxytocin antagonists. It should be pointed out that single substitution, e.g. replacement of Tyr in AVP molecule with Igl, results in moderately potent and highly selective antagonist of oxytocin (**I**). The most potent antioxytocic peptide was obtained by combination of Igl^2 modification with deamination of position 1 ([Mpa^1,Igl^2]AVP, analogue **II**, pA_2=7.94±0.22). In regard to pressor activity, all new peptides were devoid of any activity in the concentration range tested.

These results are even more interesting when we recall our previous findings describing the activities of analogues of AVP having in position 2 related non-proteinogenic amino acid 2-aminoindane-2-carboxylic acid or more bulky 3,3-diphenylalanine enantiomers.[4,6] The analogues showed very different pharmacological profile. Combination of modification in position 2 and additional substitution in position 1, 4 and 8 may give peptides with desired activity. Our new Igl^2 substituted peptides proved that the presence of the sterically restricted amino acid residue may result in highly active and exceptionally selective antioxytocic agents.

Acknowledgments

Partial funding for this work was provided by Polish State Committee for Scientific Research under the grant No. 1312/T09/2005/29 and 2385/B/HO3/2008/34 and by research project No. Z4055905 of the Academy of Sciences of the Czech Republic.

References

1. Manning M, Sawyer WH. Discovery, development, and some uses of vasopressin and oxytocin antagonists. *J Lab Clin Med* **114**: 617-632, 1989.
2. Lebl M, Jošt K, Brtnik F. *Tables of Analogs in Handbook of Neurohypophyseal Hormone Analogs*. CRC Press Inc, Boca Raton, FL, Vol. II, Part 2, pp 127-267, 1987.
3. Bodanszky M, Bodanszky A. *The Practice of Peptide Synthesis*. Berlin, Germany, p 83, 1984.
4. Kowalczyk W, Prahl A, Derdowska I, Sobolewski D, Olejnik J, Zabrocki J, Slaninová J, Lammek B. Analogues of neurohypophyseal hormones, oxytocin and arginine vasopressin, conformationally restricted in the N-terminal part of the molecule. *J Med Chem* **49**: 2016-2021, 2006.
5. Gimpl G, Burger K, Fahrenholz F. Cholesterol as modulator of receptor function. *Biochemistry* **36**:10959–10974, 1997.
6. Kowalczyk W, Sobolewski D, Prahl A, Derdowska I, Borovičková L, Slaninová J, Lammek B. The effects of N-terminal part modification of arginine vasopressin analogues with 2-aminoindane-2-carboxylic acid: a highly potent V2 agonist. *J Med Chem* **14**:2926-2929, 2007.

2-07-143

Cyclic enkephalin analogs containing two alkylurea units

Łuczak, Sylwia[1,]; Ciarkowski, Jerzy[1]; Rodziewicz-Motowidło, Sylwia[1]; Czaplewski, Cezary[1]; Wójcik, Jacek[2]; Nowakowski, Michał[2]; Kwasiborska, Maria[2]; Izdebski, Jan[3]; Oleszczuk, Marta[4]; Schiller, Peter W[5]; Chung, Nga N[5]*

[1]Faculty of Chemistry, University of Gdańsk, 80-952 Gdańsk, POLAND; [2]Laboratory od Biological NMR, Institute of Biochemistry and Biophisics, PAS, 02-106 Warsaw, POLAND; [3]Peptide Laboratory, Department of Chemistry, Warsaw University, 02-093 Warsaw, POLAND; [4]Department of Biochemistry University of Alberta, Edmonton, CANADA; [5]Laboratory of Chemical Biology and Peptide Research, IRCM, Montreal, CANADA

[*]E-mail: sluczak@chem.univ.gda.pl

Introduction

Structure-activity results for eight enkephalin analogs derived from the combinations of D-Lys and D-Orn in position 2, with Lys, Orn, *α,γ*-diaminobutyric Dab and *α,β*-diaminopropionic Dap acid in position 5 are presented. Both diamino acids (Daa) are coupled *ω-ω'* by means of the urea bridge and accordingly the compounds are restrained by 17- to 21-membered rings, see Table. In addition, the NH ethylurea at the C-terminus was introduced, in contrast to the amide group in former analogs[1,2]

Results and discussion

1H NMR chemical shifts of the peptides in water were fully assigned and their sequence was confirmed. Several cross-peaks between the protons of amidoalkylurea and the preceding residues have been observed in each case, suggesting that the unit may be involved in specific interactions with residues 4 and/or 5. The peptides are more active than enkephalin in the GPI and similarly active to it in the MVD assay. The differences in activity of these peptides and respective C-amidated analogues[3] are shown if available in Table. Only one ethylureaamide is more active in the GPI while three of them are more active in the MVD assay than the respective amide. Two different NMR-structure refinement methods were used, each stemming from different principles: the calculations using molecular dynamics with time-averaged restraints (TAV-MD)[3,4] and those using weighed fits of low-energy conformations[1,2]. Despite both methods end up with apparently divergent results, one could find per any compound a family from the statistical fitting that could reasonably stick to the unique family from TAV-MD (Fig. 1) It demonstrates that the rms values vary relatively widely (0.56 to 1.78 Å), indicating the most similar results from both methods for D-Lys2/Orn5 and the most diverse ones for D-Lys2/Dab5, respectively. Regarding the method of statistical weighing alone, it is seen that for D-Lys2/Dap5 (6 families) and D-Orn2/Dab5 (4 families) - both being locked by 18-membered rings - they give less conformational diversity than for D-Lys2/Orn5 (12 families) or D-Orn2/Lys5 analogs (4 families) being on the other end (both with 20-membered rings). A correlation of increasing conformational spread i.e. flexibility with increasing ring size would be expected, yet the D-Orn2/Dap5 analog (4 families), with the smallest

Table 1. GPI and MVD assay of enkephalin analogues, IC50 [nM] and comparison of their activities with those of respective amides[1,2]

Compound	Ring size	GPI		MVD	
		IC_{50}	IC_{50}(amide)[1,2]/ IC_{50}(current)	IC_{50}	IC_{50}(amide)[1,2]/ IC_{50}(current)
D-Lys^2/Dap^5	18	1.97	0.107	1.81	0.360
D-Lys^2/Dab^5	19	5.55	not studied[1,2]	6.00	not studied[1,2]
D-Lys^2/Orn^5	20	18.1	not studied[1,2]	22.7	not studied[1,2]
D-Lys^2/Lys^5	21	20.2	1.015	2.6	2.763
D-Orn^2/Dap^5	17	11.3	0.145	14.1	0.886
D-Orn^2/Dab^5	18	3.36	0.610	11.6	0.750
D-Orn^2/Orn^5	19	6.87	0.681	16.5	1.224
D-Orn^2/Lys^5	20	16.1	0.658	28.2	1.464
[Leu^5]enkephalin		246	-	11.4	-

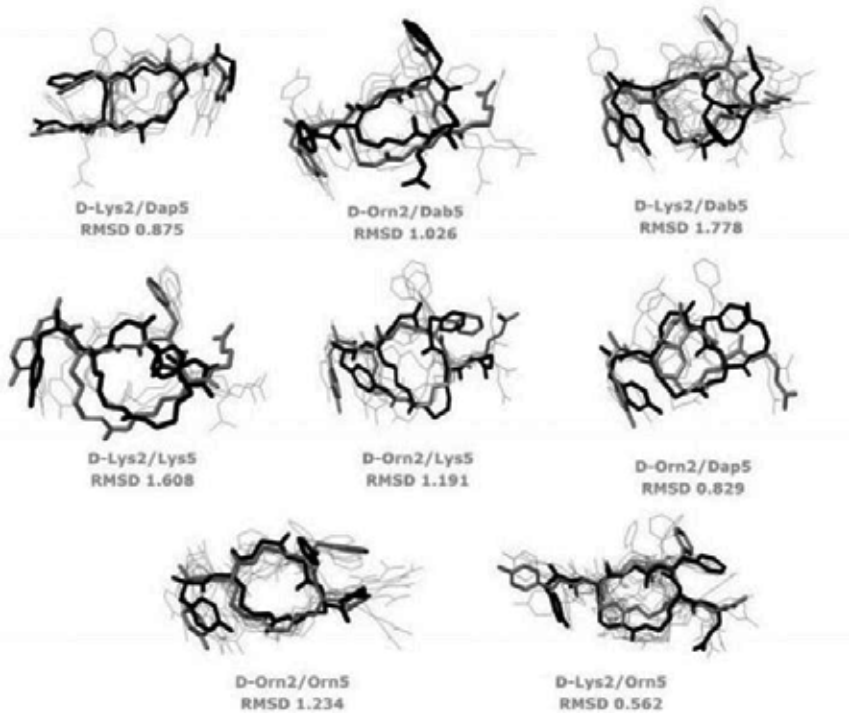

Figure 1. The most similar structures from statistical fitting (gray) overlaid onto those from the MD-TAV (black). Other families obtained in the statistical weighing are also shown (light gray).

17-membered ring, is also quite conformationally spread. Given relatively low diversity in activity and selectivity (despite being highly active per se, compare Table) in the current series, one can hardly make any structure-activity correlations. Despite the results from the statistical weighing may appear more physical giving, as expected and in contrast with the TAV-MD method, diverse conformational families for small flexible peptides like these, both methods may be not particularly amenable for comparisons and thereby the results of TAV-MD not necessarily be worse than the former. One has to remember that the statistical fitting uses stiff-geometry ECEPP force field[5] while the other method flexible-geometry AMBER force field[3]. Hence, the former can easier get stalled in local minima on the energy hypersurface due to harder barriers among them, while the latter, especially in the course of MD, is more ready to pass them in a soft-geometry force field.

Methods

Details of the synthesis, bioassay and NMR will be described elsewhere while both methods to structure calculation from NMR have been widely used, see e.g. Ref.[4] for TAV_MD and Refs.[1,2] for weighed fit of low-energy conformations. Comparison of structures resulting from both methods is drawn briefly. The TAV-MD method yielded less diverse conformations (one family) contrary to 4-12 conformational families obtained from statistical weighing. Hence, a representative conformer of each compound resulting from TAV-MD method was systematically overlaid onto consecutive diverse conformers yielded by the statistical fitting. Best fit for each compound is shown in Fig. 1.

Acknowledgements

Supported by the Polish Ministry of Science and Higher Education (grant 3T09A 02328 for JI; grant DS/8372-4-0138-8 for SR-M & JC).

References

1. Filip K, Oleszczuk M, Wójcik J, Chung NN, Schiller PW, Pawlak D, Zieleniak A, Parcinska A, Witkowska E, Izdebski. J. *J Peptide Sci* **11**: 347-352, 2005.
2. Pawlak D, Oleszczuk M, Wójcik J, Pachulska M, Chung NN, Schiller PW, Izdebski J. *J Peptide Sci* **7**: 128-140, 2001.
3. Case DA, Darden TA, Kollman PA. *AMBER 8*, University of California, San Francisco, 2004.
4. Zieleniak A, Rodziewicz-Motowid³o S, Rusak £, Chung NN, Czaplewski C, Witkowska E, Schiller PW, Ciarkowski J, Izdebski J. *J Peptide Sci* **14**: 830-837, 2008.
5. Liwo A, Tempczyk A, O³dziej S, Shenderovich MD, Talluri S, Ciarkowski J, Kasprzykowski S, £ankiewicz L, Grzonka Z. *Biopolymers* **38**: 157–175, 1996.

2-07-144

Analogues of bradykinin B_2 receptor antagonist

Sobolewski, Dariusz[1,]; Neugebauer, Witold[2]; Côté, Jérôme[2]; Bélanger, Simon[2]; Gobeil Fernand Jr[2]; Lammek, Bernard[1]; Prahl, Adam[1]*

[1]Faculty of Chemistry, University of Gdañsk, Sobieskiego 18, 80-952 Gdañsk, POLAND; [2]Department of Pharmacology, Faculty of Medicine, Sherbrooke University, Sherbrooke, Québec, J1H 4N5, CANADA

[*]E-mail: dareks@chem.univ.gda.pl

Introduction

Synthesis of bradykinin (Arg-Pro-Pro-Gly-Phe-Ser-Pro-Phe-Arg; BK) analogues for structure-activity studies started shortly after the announcement of the structure of this hormone in 1960. However, the first report on bradykinin analogues able to antagonize the effects of BK in standard kinin assays came 25 years later, with the description of the [D-Phe^7]BK and [Thi^{5,8},D-Phe^7]BK.[1] Hundreds of analogues with single or multiple substitutions were later designed and synthesized in many laboratories to study the role of amino acid residues in all positions of BK, as well as the influence of various combinations of substitutions on pharmacological activity of the resulting compounds. A major improvement in the potency of BK antagonists was achieved in 1991, when potent B_2 blockers, carrying conformationally constrained amino acid residues in their *C*-terminal ends have been synthesized.[2] In our laboratory we also explored several structural factors that might affect the antagonistic properties of BK analogues. For instance, we reported that acylation of the *N*-terminus of several known B_2 antagonists with various bulky acyl groups has consistently improved their antagonistic potency in rat blood pressure assay.[3-5] Bearing in mind successful manipulations consisting of substitution of sterically restricted amino acids in the *C*-terminal part of BK analogues that resulted in highly potent and selective B_2 antagonists, we have now decided to use Icatibant (HOE-140), the most potent peptidic human bradykinin B_2 receptor antagonist, as a starting structure and substitute its position 7, 8 or 9 with chosen D-amino acid residues and/or nonproteinogenic amino acid residues, e.g. *N*-cyclohexylglycine (Nchg), 4-phenylpiperidine-4-carboxylic acid (Ppc), (S)-piperidine-3-carboxylic acid (Nip) and 1-aminocyclohexane-1-carboxylic acid (Acc) (analogues I, III, V, VII, IX, XI, XIII, XV, XVII, respectively). In the next nine peptides we combined these changes with acylation of the *N*-terminus with 1-adamantaneacetic acid (Aaa), which previously was demonstrated to improve antagonistic properties (analogues II, IV, VI, VIII, X, XII, XIV, XVI, XVIII).

Results and discussion

The eighteen new peptides (I-XVIII) were synthesized by Fmoc strategy, purified and characterized. Their molecular ion values were as expected and their purity was better than 98%. All new analogues were tested on the human umbilical vein for their antagonistic potency as well as for their affinity to human bradykinin B_2 receptor expressed on human embryonic kidney 293T cells (HEK-293T cells). Pharmacological data of peptides I-XVIII are presented in Table 1.

Only three compounds containing Nchg^8, Nchg^9 or Ppc^9 (peptides I, III, V, respectively) exhibited noticeable antagonistic activities on human bradykinin receptors thus still less potent then HOE-140 sequence. Each of them with Aaa^0 showed lower activity then parent peptide. Analogues: D-Arg-Arg-Pro-Hyp-Gly-Thi-Ser-D-Phe-Acc-Arg (XVII) and Aaa-D-Arg-Arg-Pro-Hyp-Gly-Thi-Ser-D-Phe-Acc-Arg (XVIII), although strongly potent antagonists against BK-induced blood pressure lowering responses in rats,[4] did not show noticeable antagonistic activity on BK-induced contraction of the isolated human umbilical vein, a well-established B_2R bioassay system, suggesting a species dependent activity of the compounds.

Acknowledgments

Partial funding for this work was provided by Polish Ministry of Science and Higher Education under grant number 0380/H03/2006/31 and by The Canadian Institute of Health Research (MOP-66998).

References

1. Vavrek RJ, Stewart JM. *Peptides* **6:** 161-166, 1985.
2. Hock FJ, Wirth K, Albus U, Linz W, Gerhards HJ, Wiemer G, Henke S, Breipohl G, Konig W, Knolle J, Scholkens B. *Br J Pharmacol* **102:** 769-773, 1991.
3. Lammek B. *Pol J Chem* **68:** 913-920, 1994.
4. Labudda-Dawidowska O, Wierzba TH, Prahl A, Kowalczyk W, Gawiński Ł, Plackova M, Slaninová J, Lammek B. *J Med Chem* **48:** 8055-8059, 2005.
5. Labudda O, Wierzba T, Sobolewski D, Kowalczyk W, Sleszyńska M, Gawiński L, Plackova M, Slaninová J, Prahl A. *J Pept Sci* **12:** 775-779, 2006.

Table 1. Pharmacological properties of the new Icatibant (HOE-140) analogues

Peptide		Bioassays on the human Umbilical Vein (hUV)		Affinity to human bradykinin B_2 receptor
		pIC_{50} [a]	α^{E} [b]	pIC_{50} [c]
D-Arg-Arg-Pro-Hyp-Gly-Thi-Ser-D-Tic-Oic-Arg	**HOE-140**	8.65 ± 0.03	0	8.30 ± 0.15
D-Arg-Arg-Pro-Hyp-Gly-Thi-Ser-Nchg-Thi-Arg	**I**	7.66 ± 0.02*	1.20	7.78 ± 0.18
Aaa-D-Arg-Arg-Pro-Hyp-Gly-Thi-Ser-Nchg-Thi-Arg	**II**	<6.0	0.52	<6.0
D-Arg-Arg-Pro-Hyp-Gly-Thi-Ser-D-Phe-Nchg-Arg	**III**	6.93 ± 0.13	0	6.13 ± 0.04
Aaa-D-Arg-Arg-Pro-Hyp-Gly-Thi-Ser-D-Phe-Nchg-Arg	**IV**	6.81± 0.21	0	6.82 ± 0.18
D-Arg-Arg-Pro-Hyp-Gly-Thi-Ser-D-Phe-Ppc-Thi-Arg	**V**	6.76± 0.14	0	6.15 ± 0.02
Aaa-D-Arg-Arg-Pro-Hyp-Gly-Thi-Ser-D-Phe-Ppc-Thi-Arg	**VI**	<6.0	0	<6.0
D-Arg-Arg-Pro-Hyp-Gly-Thi-Ser-Ppc-Ppc-Thi-Arg	**VII**	<6.0	0	<6.0
Aaa-D-Arg-Arg-Pro-Hyp-Gly-Thi-Ser-Ppc-Ppc-Thi-Arg	**VIII**	<6.0	0	<6.0
D-Arg-Arg-Pro-Hyp-Gly-Thi-Ser-Ppc-Thi-Arg	**IX**	<6.0	0	<6.0
Aaa-D-Arg-Arg-Pro-Hyp-Gly-Thi-Ser-Ppc-Thi-Arg	**X**	<6.0	0	<6.0
D-Arg-Arg-Pro-Hyp-Gly-Thi-Ser-Nip-Thi-Arg	**XI**	<6.0	0	<6.0
Aaa-D-Arg-Arg-Pro-Hyp-Gly-Thi-Ser-Nip-Thi-Arg	**XII**	<6.0	0	<6.0
D-Arg-Arg-Pro-Hyp-Gly-Thi-Nip-D-Phe-Thi-Arg	**XIII**	<6.0	0	<6.0
Aaa-D-Arg-Arg-Pro-Hyp-Gly-Thi-Nip-D-Phe-Thi-Arg	**XIV**	<6.0	0	<6.0
D-Arg-Arg-Pro-Hyp-Gly-Thi-Ser-D-Phe-Nip-Arg	**XV**	<6.0	0	<6.0
Aaa-D-Arg-Arg-Pro-Hyp-Gly-Thi-Ser-D-Phe-Nip-Arg	**XVI**	<6.0	0	<6.0
D-Arg-Arg-Pro-Hyp-Gly-Thi-Ser-D-Phe-Acc-Arg	**XVII**	<6.0	0	<6.0
Aaa-D-Arg-Arg-Pro-Hyp-Gly-Thi-Ser-D-Phe-Acc-Arg	**XVIII**	<6.0	0	<6.0

[a] negative decadic logarithm of the molar concentration of an antagonist that reduces a specified BK response to 50% of its former value; [b] residual agonistic activity of the compound expressed as a fraction of that produced by BK (10 mM); [c] negative decadic logarithm of the molar concentration of an agent that causes a 50% reduction in the specific binding of the radioligand [^{3}H]BK. *Indicating pEC_{50} value.

2-07-145

Metal ion interactions within the 1-16 N-terminal region of β-Amyloid

Damante, Chiara Antonia[1,]; Ősz, Katalin[2]; Nagy, Zoltán[2]; Pappalardo, Giuseppe[3]; Grasso, Giulia[3]; Impellizzeri, Giuseppe[1]; Rizzarelli, Enrico[1]; Sóvágó, Imre[2]*

[1]University of Catania, Department of Chemical Sciences, ITALY; [2]University of Debrecen, Department of Inorganic and Analytical Chemistry, HUNGARY; [3]CNR, Institute of Biostructures and Bioimaging, ITALY

[*]E-mail: chiarauni@tiscali.it

Introduction

Alzheimer's disease (AD) is the most prevalent neurodegenerative disease worldwide leading to dementia. The hallmark of this disorder is the formation of deposits of intracellular neurofibrillary tangles of protein tau and extracellular amyloid plaques in the brain.[1] The major component of these insoluble aggregates is a 39-43 residue peptide known as amyloid-β peptide (Aβ). Transition metals, such as copper(II) and zinc(II), can contribute either directly or indirectly to the pathogenesis of AD. Indeed, metals may play a series of fundamental roles considering the multiple aspects of the disease process: they are involved in the regulation of APP gene expression,[2] the regulation of APP mRNA translation, the proteolytic processing of APP to generate Aβ into the plaques, the modulation of matrix metalloprotease activity which affects Aβ turnover.[3] Moreover, both copper(II) and zinc(II) have been shown to promote the aggregation process and the cytotoxicity of Aβ.[4,5] The peptide region responsible for zinc(II) or copper(II) binding has been mapped within the 1-16 amino acid sequence of Aβ (Aβ(1-16)). However the Aβ(1-16) complexes formed in the presence of an excess of metal ions (either copper(II) or zinc(II)) revealed to be insoluble in aqueous solution. Here we report a detailed study on the zinc(II) and copper(II) complexes with a new polyethylene glycol peptide conjugate (Aβ(1-16)PEG). It turned out that PEG conjugation enhanced the solubility in water of copper(II) or zinc(II) complexes allowing their investigation at different metal ion to peptide ratios, ranging from 1:1 to 4:1. We employed a combined potentiometric and spectroscopic approach to determine the coordination features of both zinc(II) and copper(II) complexes with the peptide fragment. The obtained results were further validated by limited proteolysis experiments.

Results and discussion

The potentiometric titrations carried out at different metal ion to ligand ratios, demonstrate that the Aβ(1-16)PEG can bind up to four copper(II) ions per peptide molecule forming mono-,di-, tri- and tetra-nuclear complexes (Fig. 1). In the presence of an excess of zinc(II), the Aβ(1-16)PEG is able to bind up to three zinc(II) equivalents. The curve distribution diagrams resulted in an intricate entanglement due to the formation of many complex species. In addition the presence of coordination isomers makes it difficult to structurally characterize all the metal complexes.

Circular Dichroism (CD) measurements carried out on copper(II) complexes at 1:1 metal ion to peptide ratio, indicate no detectable dichroic activity below pH 6. This finding suggests that the *N*-terminal amino group of the peptide is the major copper(II) binding site starting with the involvement of terminal amino and carboxylate functions of aspartyl residue in the coordination. The deprotonation of side chain imidazole functions results in the formation of macrochelates of which several isomers exist, because one or more histidyl residues can occupy the remaining coordination sites. In the case of the zinc(II), ^{1}H-NMR experiments, carried out at pH 7 and either in the presence or absence of zinc(II), indicate that the His13 and His14 residues are the mainly responsible for metal anchoring. The carboxylate group of the Glu11 assists the coordination of the metal ion. In addition, the fourth position in the zinc(II) coordination sphere can be probably assigned to the imidazole ring of His6.

Both copper(II) and zinc(II) complexes with Aβ(1-16) PEG were also studied by means of limited proteolysis carried out at various metal to peptide ratios. Such a study was carried out in order to evaluate an eventual metal-induced structuring of the peptide, which is in turn related to the preferred binding site of the different metal ion within the primary sequence of the polypeptide. Results obtained from trypsin digestion show that the cleavage of the Arg5-His6 peptide bond is slower in the presence of copper(II) than in the absence of this metal ion. The slower cleavage is due to the decreased accessibility of the putative peptide bond caused by copper(II)-induced folding of the region 1-6 of Aβ(1-16)PEG. This result suggests that the copper(II) is preferentially located within this amino acid region, by contrast the zinc(II), which does not alter the cleavage rate with trypsin, would reside quite far from this site.

Acknowledgments

This work was supported by MiUR PRIN 2006-33492, 2005-035582, FIRB RBNE03PX83 and FIRB RBIN04L28Y (E.R.), the MTA (Hungary) - CNR (Italy)

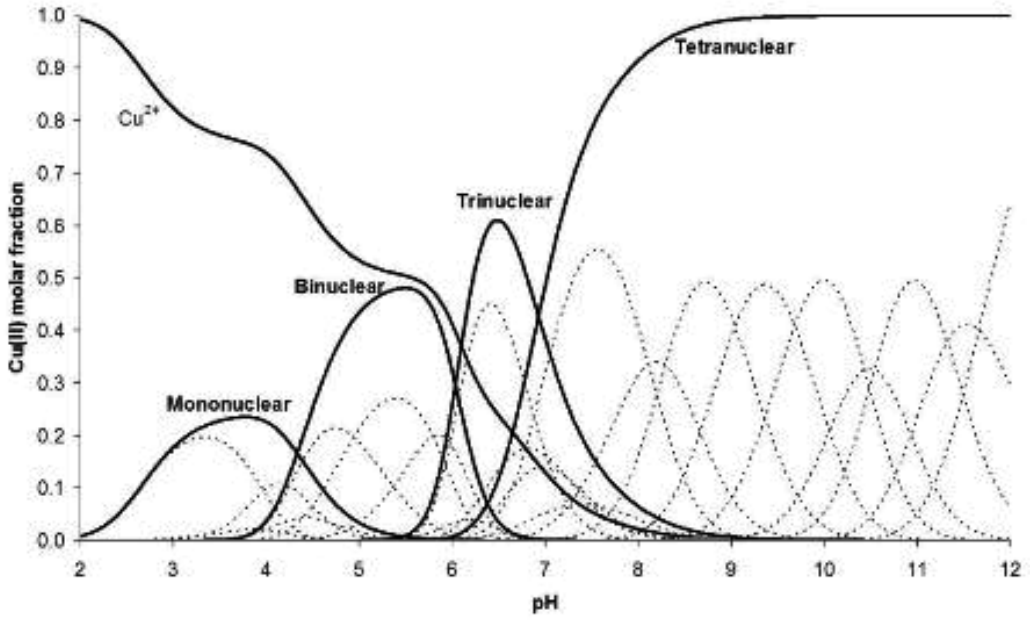

Figure 1. Species distribution diagram of the complex species formed in the copper(II)−Aβ(1-16) PEG system (c_L = 2.0 x 10^{-3} mol dm^{-3}, $c_{Cu(II)}$ = 8.0 x 10^{-3} mol dm^{-3}).

bilateral program and OTKA T048352 and D048488 (Hungary).

References

1. Selkoe DJ. *Nature* **399:** A23-31,1999.
2. Armendariz AD, Gonzales M, Loguinov AV, Vulpe CD. *Physiol Genomics* **20:** 45-54, 2004.
3. Filiz G, Price KA, Caragounis A, Du T, Crouch PJ, White AR. *Eur Biophys J* **37:** 315-321, 2008.
4. Multhaup G, Masters CL. *Met Ions Biol Syst* **36:** 365-387, 1999.
5. Bush AI. *Trends Neurosci* **26:** 207-214, 2003.

2-07-146

Antibacterial activity and resistance to proteolytic degradation of trichogin GA IV and selected analogues

Toniolo, Claudio[1]; De Zotti, Marta[1]; Formaggio, Fernando[1]; Stella, Lorenzo[2]; Kim, Mi-Hyun[3]; Park, Yoonkyung[3]; Hahm, Kyung-Soo[4]

[1]University of Padova, 35131 Padova, ICB-CNR, Padova Unit, Department of Chemistry, ITALY; [2]University of Rome "Tor Vergata", 00133 Rome, Department of Chemical Sciences and Technologies, ITALY; [3]Chosun University, 501-759 Gwangju, Research Center for Proteineous Materials, KOREA (REP.); [4]Chosun University, 501-759 Gwangju, Department of Cellular and Molecular Medicine, KOREA (REP.)

[1]E-mail: claudio.toniolo@unipd.it

Introduction

Trichogin GA IV is the most extensively investigated member of the class of lipopeptaibols that are linear peptide antibiotics of fungal origin, characterized by the presence of a variable, but remarkable, number of Aib residues, a fatty acyl group at the N-terminus, and a 1,2-amino alcohol at the *C*-terminus.[1]

Results and discussion

Several analogues of trichogin GA IV with amino acid substitutions or deletions were designed and synthesized, which allowed determination of the minimal inhibition concentration against Gram-positive and Gram-negative bacteria and various pathogenic fungal cells. The natural peptide exhibits a specific activity against *S. aureus* and only a marginal hemolytic effect. Interestingly, trichogin GA IV is active also against several methicillin-resistant *S. aureus* strains. Studies on synthetic analogues demonstrated that substitution of the C-terminal leucinol by Leu-OMe and substitution of one Aib residues by the EPR label TOAC do not perturb significantly the biological activity of the peptide. On the other hand, removal of three or seven N-terminal residues eliminated any antibacterial activity.

Table 1. Amino acid sequences of trichogin GA IV and its synthetic analogues

Trichogin GA IV	*n*-Oct-Aib-Gly-Leu-Aib-Gly-Gly-Leu-Aib-Gly-Ile-Lol
Tric-OMe	*n*-Oct-Aib-Gly-Leu-Aib-Gly-Gly-Leu-Aib-Gly-Ile-Leu-OMe
Tric-TOAC	*n*-Oct-TOAC-Gly-Leu-Aib-Gly-Gly-Leu-Aib-Gly-Ile-Leu-OMe
Tric-8	*n*-Oct-Aib-Gly-Gly-Leu-Aib-Gly-Ile-Leu-OMe
Tric-4	*n*-Oct-Aib-Gly-Ile-Leu-OMe

n-Oct = *n*-octanoyl, Lol = leucinol, Aib = α-aminoisobutyric acid, TOAC = 4-amino-4-carboxy-2,2,6,6-tetramethylpiperidine-1-oxyl, OMe = methoxy.

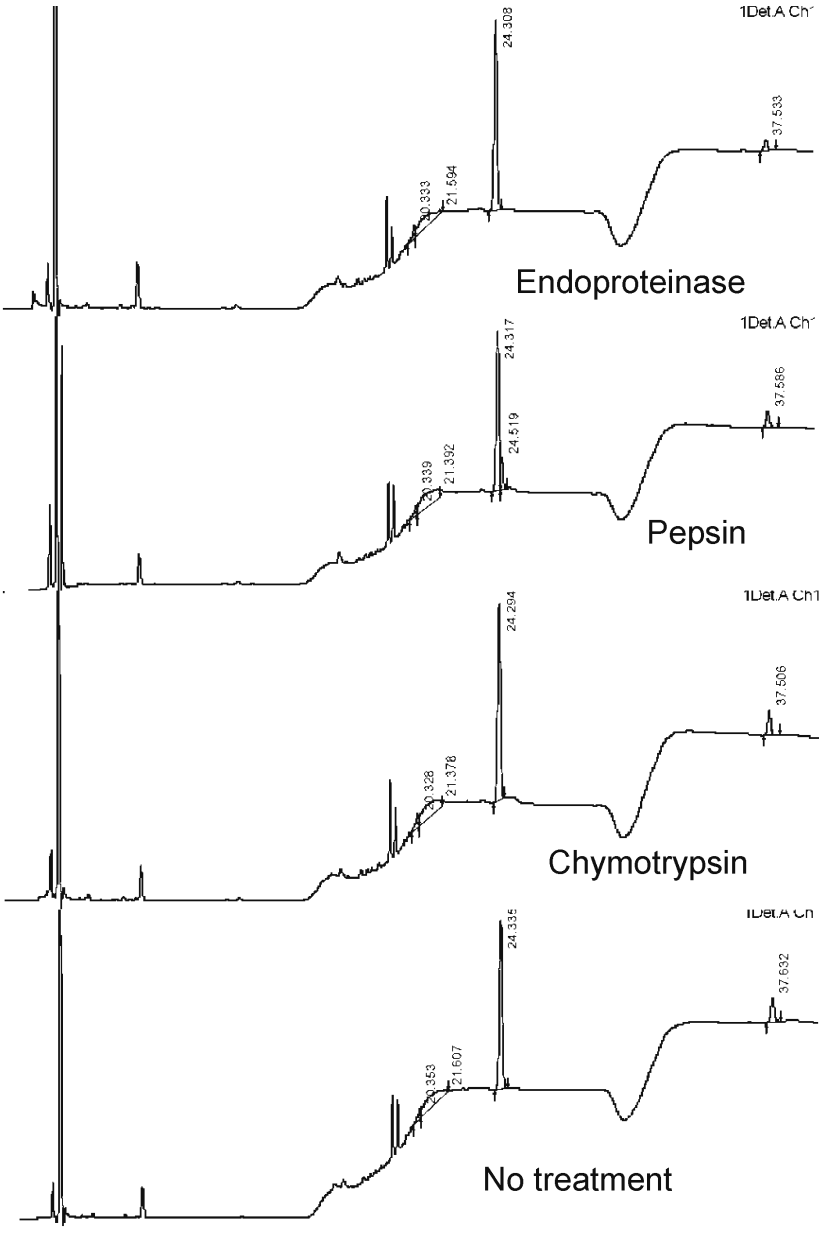

Figure 1. HPLC elution profiles of trichogin GA IV after proteolytic enzyme treatment [1 : 250 enzyme/peptide, w/w; 37 °C, overnight].

Finally, studies of proteolytic degradation on trichogin GA IV (Fig. 1) and selected analogues where the three Aib residues are replaced by Leu demonstrated that the presence of several non-coded Aib residues endows the natural peptaibol with remarkable resistance to proteolysis. The present results indicate that trichogin GA IV is a promising lead compound for the development of new, selective and protease-resistant, antibacterial drugs.

References

1. Peggion C, Formaggio F, Crisma M, Epand RF, Epand RM, Toniolo C. *J Pept Sci* **9**: 679-689, 2003.

2-07-147

The chiral sequence of a natural peptide inhibitor of HIV-1 integrase elucidated

De Zotti, Marta[1]; Toniolo, Claudio[1,]; Formaggio, Fernando[1]; Kaptein, Bernard[2]; Broxterman, Quirinus B[2]; Felock, Peter J[3]; Hazuda, Daria J[3]; Singh, Sheo B[4]; Brückner, Hans[5]*

[1]University of Padova, 35131 Padova, ICB-CNR, Padova Unit, Department of Chemistry, ITALY; [2]6160 MD Geleen, DSM Pharmaceutical Products, Innovative Synthesis and Catalysis, NETHERLANDS; [3]Rahway, NJ 07065, Merck Research Laboratories, UNITED STATES; [4]West Point, PA 19486, Merck Research Laboratories, UNITED STATES; [5]University of Giessen, 35392 Giessen, Department of Food Sciences, GERMANY

[*]E-mail: claudio.toniolo@unipd.it

Integramide A, an efficient inhibitor of the coupled reaction of HIV-1 integrase, is a 16-mer linear peptide characterized by nine C^{α}-methylated α-amino acids (five Iva, isovaline, and four Aib, α-aminoisobutyric acid, residues) that was isolated from fungal extracts of *Dendrodochium sp.* The amino acid sequence was fully elucidated by the Merck groups a few years ago[1] (Fig. 1). On the other hand, the chiral sequence was only partially determined. In particular, the precise stereochemistry of the Iva14-Iva15 dipeptide (known to contain one D- and one L-residue) near the *C*-terminus was not reported.

To solve this unsettled stereochemical issue and to assess integramide A primary structure-bioactivity relationship, we performed by solution methods the total chemical independent syntheses of both L-D and D-L 16-mer diastereomers and compared their properties with those of the natural inhibitor. For an unambiguous, complete stereochemical assignment of integramide A we relied heavily on HPLC (Fig. 2) and NMR (Fig. 3) techniques.

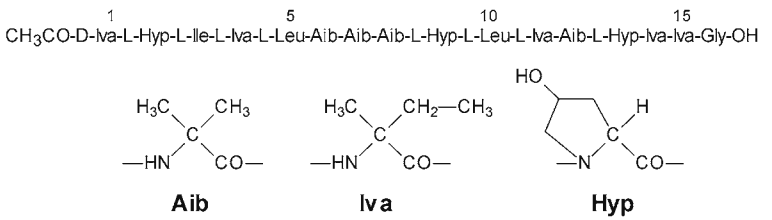

Figure 1. Amino acid sequence of integramide A and chemical structures of Aib, Iva, and Hyp.

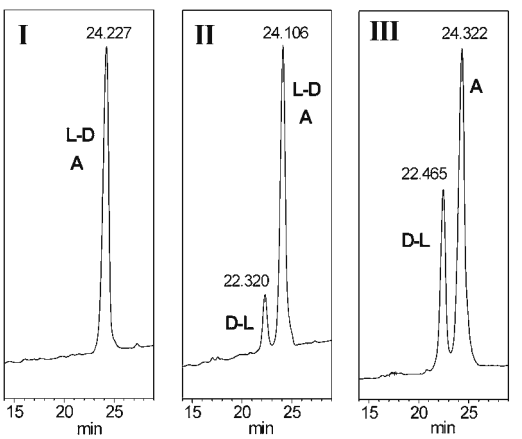

Figure 2. HPLC profiles for artificial mixtures of the natural integramide A (**A**), and the two synthetic diastereomers L-Iva14-D-Iva15 (**L-D**) and D-Iva14-L-Iva15 (**D-L**): mixture of L-D and A (**I**); mixture of L-D, D-L, and A (**II**); mixture of D-L and A (**III**).

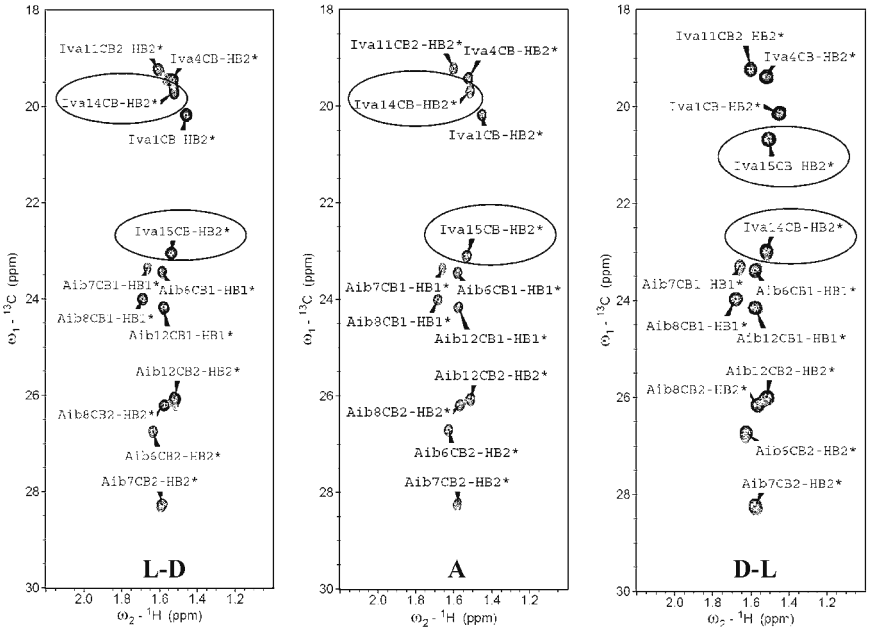

Figure 3. Comparison among the aliphatic regions of the $^{\beta}$C-selective HMQC spectra of the natural integramide A (**A**), and the two synthetic diastereomers L-Iva14-D-Iva15 (**L-D**) and D-Iva14-L-Iva15 (**D-L**) in TFE,d_2 solution at 300 K. The peaks of the Iva14 and Iva15 residues are highlighted.

Our results clearly indicate that the chirality sequence of the Iva14-Iva15 dipeptide of the natural product is L-D. The stereochemical inversion in the two integramide A diastereomers, evaluated as inhibitors of HIV-1 integrase in the coupled reaction of proviral DNA into the host cell DNA, is in general not detrimental, but it is even slightly beneficial against the strand transfer reaction.

References

1. Singh SB, Herath K, Guan Z, Zink DL, Dombrowski AW, Polishook JD, Silverman KC, Lingham RB, Felock PJ, Hazuda DJ. *Org Lett* **4**: 1431-1434, 2002.

2-07-148

Biological studies of the peptide *Hy-a1* and analogs

Crusca Jr, Edson[1,]; Rezende, Adrielle[1]; Marchetto, Reinaldo[1]; Castro, Mariana S[2]; Fontes, Wagner[2]; Cilli, Eduardo M[1]*

[1]UNESP - São Paulo State University, Institute of Chemistry, BRAZIL; [2]UnB - University of Brasília, BRAZIL

[*]E-mail: crusca@iq.unesp.br

Introduction

Antibiotic resistant bacterial strains represent a global health problem with a strong social and economic impact.[1] Thus, there is an urgent need for the development of antibiotics with novel mechanisms of action. Castro's group isolated and determined the sequence of the peptide *Hy-a1* (IFGAILPLALGALKNLIK) of skin secretion from the frog *Hypsiboas albopunctatus* which showed antimicrobial activity. The aim of the present work was evaluated 4 analogues to supply information about the relationship structure-biological activity. All analogues contain a single substitution in position 6, Leu by Trp, to fluorescent studies, and differ in N-terminus: 1) no modification (W^6-*Hy-a1*); 2) one group acetyl (no charge - (Ac^0-W^6-*Hy-a1*); 3) one aspartate (negative charge - (D^0-W^6-*Hy-a1*); 4) one lysine (positive charge - (K^0-W^6-*Hy-a1*). The peptides were synthesized by SPPS using the Fmoc chemical approach. The biological activities were assayed by measuring growth inhibition of two types of Gram-positive and two Gram-negative bacteria.

Results and discussion

The synthesis and purification of peptides by HPLC was efficient and a high purity level (≥96%) was obtained. The biological activity of these peptides showed that the peptide with tryptophan in position 6 has higher MIC that wild type peptide. The peptides contain at the N-terminal region the group acetyl or a residue of Asp showed MIC values of ≥128 μM for *E. coli* and *P. aeruginosa*, although less than 8 μM for the Gram-positive bacteria (Table 1). Different results were observed when the residue added was Lys (Table 1). In this case, the activity against whole bacteria was sustained or increased. These results showed that the N-terminal region of the peptide *Hy-a1* develop key roles in its antibacterial action in different types of bacteria. A similar mechanism has been observed for some antimicrobial peptides.[2,3] Overall, in cytolysins was observed that the hydrophobic sequence and the first two residues of the amphipathic *α*-helix probably lining the pore[4] is involved in the process of binding to the membrane.

To evaluate the relationship between the biological activity and structure, conformational properties were investigated by CD techniques in water and in zwitterionic micelles (LPC). The CD experiments demonstrated that in water (pH 5.0) the peptides have a random structure (Fig. 1A), but in LPC micelles they acquired an ordered structure (Fig. 1B) composed mainly by *α*-helix. Therefore, according to these data there is not one straight relationship between structure and antibacterial activity.

However, numerous studies about antimicrobial peptides have connected the positive charge, hydrophobibity and amphipathic structures with the activity and selectivity. Although in this study, we have demonstrated that the *N*-terminus of the peptides is important for selectivity. These results provide useful information for the design of peptides with selective targets.

Table 1. Antibacterial activity

Peptide (uM)	*E. coli*	*S. aureus*	*P. aeruginosa*	*B. subtilis*
Hy-a1	32	8	64	8
W^6-Hy-a1	32	8	32	2
Ac^0-W^6-Hy-a1	128	4	>128	4
K^0-W^6-Hy-a1	4	4	16	4
D^0-W^6-Hy-a1	>128	8	>128	4

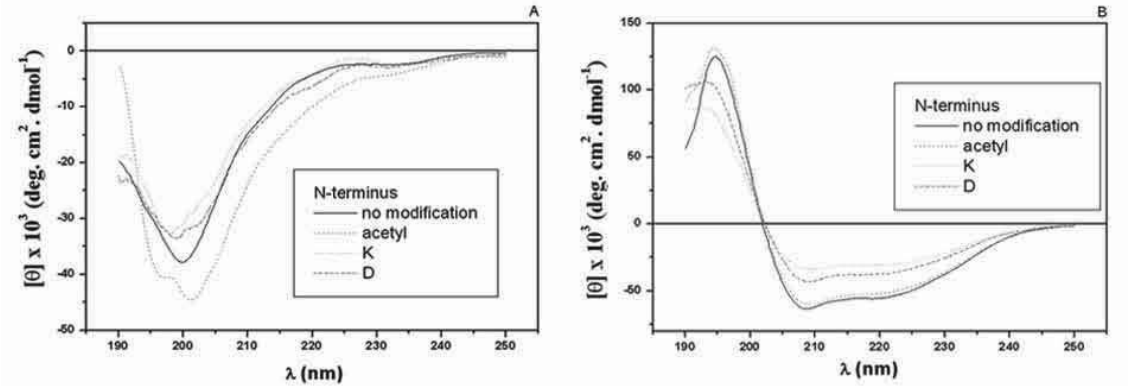

Figure 1. Far-UV CD spectra of analogues of peptide *Hy-a1* in aqueous solution (A) and zwitterionic detergent LPC at 10 mM (B).

Acknowledgements

This work was supported by grants from FAPESP/CNPq. We also wish to thank Dra. Leila M. Beltramini for generously supplying CD data.

References

1. Cohen ML. *Science* **257**: 1050-1055, 1992.
2. Machado A, Sforça ML, Miranda A, Daffre S, Pertinhez TA, Spisni A, Miranda MT. *Biopolymers (Peptide Science)* **88**: 413-426, 2007.
3. Yang ST, Jeon JH, Kim Y, Shin SY, Hahm KS, Kim JI. *Biochemistry* **45**: 1775-1778, 2006.
4. Mancheño JM, Martín-Benito J, Martínez-Ripoll M, Galvilanes JG, Hermoso JA. *Structure* **11**: 1319-1328, 2003.

2-07-149

Application of non-sequential pharmacophore concept for design of antimicrobial peptide dendrimers

Urbanczyk-Lipkowska, Zofia[1]; Polcyn, Piotr[1]; Janiszewska, Jolanta[2]

[1]Institute of Organic Chemistry PAS, 01-224 Warsaw, POLAND; [1]Industrial Chemistry Research Institute, 01-093 Warsaw, POLAND

[*]E-mail: ocryst@icho.edu.pl

Introduction

One of the most promising types of molecular architecture allowing construction of polyvalent structures are dendrimers. Dendrimers are relatively new class of macromolecules with radial distribution of branched elements around the central core and perfect structure. Location of a high number of functional groups at the surface allows to present multiple pharmacophoric units to the receptors, with immediate application for design of a new generation drugs or vaccines, tools for studying autoimmune diseases or understanding gene delivery mechanism. Here we present another possible application of dendrimeric compounds – preparation of drug molecules, which mimic active conformations of various macromolecular ligands. We focused on low molecular weight basic dendrimeric peptides which mimic sequence-related active conformations of recently discovered natural antimicrobial peptides. This so called – "non-sequential pharmacophore" concept resulted in de novo design of new structural classes of dendrimeric compounds with high antimicrobial potency against Gram(-) and Gram(+) bacteria and fungi.[1,2] Present communication reports on synthesis, and antimicrobial properties of a new dendrimeric peptides built around several new scaffolds.

Materials and methods

Two families of amphiphilic peptide dendimers 37 – 40 and 49 – 52, (Fig. 1) in the form of hydrochlorides, built around new three- and tetravalent cores obtained from basic natural amino acids, were synthesized using standard peptide synthesis procedures. Correct molecular mass, charge structure and purity of the final compound, were confirmed by elemental analysis, ESI MS and NMR spectra.

Results of antimicrobial tests show that 4-branched derivatives 49 - 52 containing more lypophilic Phe-(2-Cl-Z)-Lys sequence are ca. 10 times more potent that compounds 37 - 40 with 3-branches and terminal (2-Cl-Z)-Lys fragment (Table 1). There is also noticeable increase in activity against Gram(-) *E. coli* strains. Interestingly, the highest activity is observed against methicillin resistant strains both, from Gram(+) *S. aureus* ATCC 43300 and Gram(-) *E. coli* ATCC BAA-198. It appears that new central scaffolds afford better interactions between negatively charged microbial membranes and designed cationic dendrimers than just Lys alone.[1]

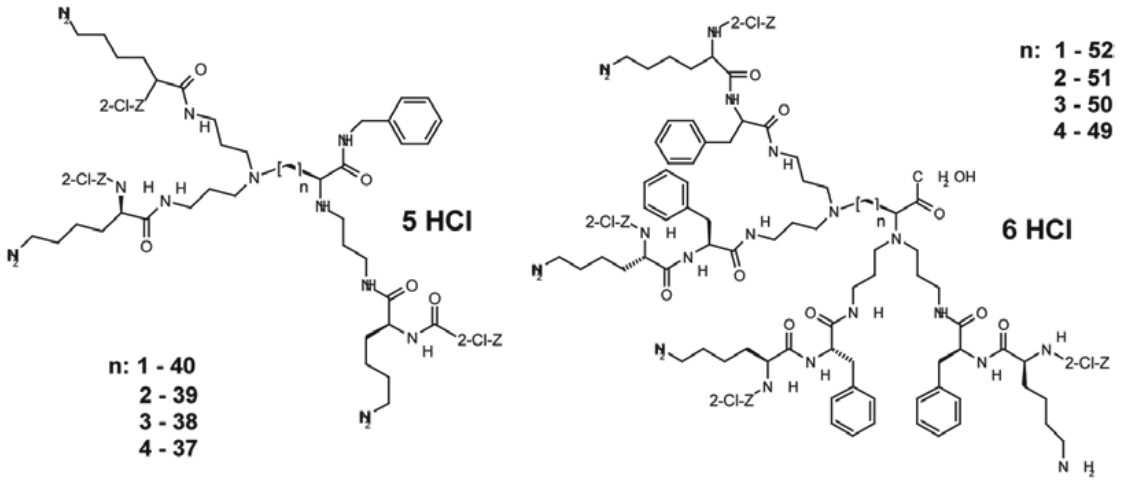

Figure 1. Chemical structure of dendrimers.

Table 1. Minimal inhibitory concentration (MIC, (μM dm^{-3})

Strain	Minimal inhibitory concentrations, MIC (μM dm^{-3})							
	37	**38**	**39**	**40**	**49**	**50**	**51**	**52**
S. aureus ATCC 25923	21.6	10.9	11.7	2.8	3.4	27.3	1.3	1.7
S. aureus ATCC 43300	21.6	10.9	103	11.8	1.7	13.6	7.3	3.4
E. coli ATCC 25922	86	21.8	48	11.8	6.8	27.3	7.3	7.3
E. coli ATCC BAA-198	43	10.9	>88	>89	3.4	13.6	6.9	6.8
C. albicans ATCC 90028	>86	10.9	103	417	6.8	54	6.9	6.8
C. crusei ATCC 6258	43	5.4	44	44	3.4	27.3	3.4	6.8

Results and discussion

Multi-drug resistance against classic antibiotics, is one of the most serious problems in contemporary medicine. Therefore, design of antimicrobial compounds with a new structures, that are "not known" to bacteria and possibly new mechanism of action (inhibition of cell wall construction vs. membrane lytic activity) is a one of the possible solutions to this problem. The presented design of dendrimeric compounds containing amino acids with application of the more branched scaffolds resulted with significant increase of antimicrobial potency against Gram(+), Gram(-) bacteria and *C. albicans* and "switched on" activity against multiresistant reference strains from both groups. These small dendrimers express low hemotoxicity and due to their structure are resistant to enzymatic degradation. This makes this group of dendrimeric compounds a prospective target for further development.

Acknowledgements

Grant from the Ministry of Science and Higher Education – No 3T09B 115 28 and the EC grant Normolife (LSHC-CT-2006-037733) are acknowledged.

References

1. Janiszewska J, Swieton J, Lipkowski AW, Urbanczyk-Lipkowska Z. *Bioorg Med Chem Lett* **13**: 3711-3713, 2003.
2. Janiszewska J, Urbanczyk-Lipkowska Z. *J Mol Microbiol Biotechnol* **13**: 221-225, 2007.

2-07-150

Enhancement of Antimicrobial Activity of a Natural Antimicrobial Neuropeptide of *Sepia officinalis*.

Laurencin, Mathieu[1,]; Duval, Emilie[2]; Zatylny-Gaudin, Céline[2]; Henry, Joël[2]; Baudy-Floc'h, Michèle[1]*

[1]UMR CNRS 6226, Université de Rennes 1, ICMV, FRANCE; [2]UMR 100 IFREMER, Université de Caen Basse-Normandie, LBBM, FRANCE

[*]E-mail: matam96@hotmail.com

Introduction

A wide variety of organisms produce antimicrobial peptides as part of their first line of defence. The survival of marine invertebrates in seawater which contains many invading microorganisms (up to 10^6 bacteria/mL and 10^9 virus/mL) suggests that their innate immune system is effective and their circulating hemolymph contains biologically active substances such as antimicrobial peptides. Several antimicrobial peptides of marine origin were isolated and characterized but the research for antimicrobial compounds stemming from marine invertebrates stays under exploited towards the scale of the source.[1] However, antimicrobial activity is not the main function of some of these peptides. It was reported that some neuropeptide or peptidic hormones display some structural similarities with antimicrobial peptides. Recently, Brogden and coworkers reviewed this type of neuropeptide like substance P, enkelytin and neuropeptide Y that exhibit antimicrobial activities.[2] In the Cuttlefish *Sepia officinalis* we observed an antibacterial activity for the neuropeptide: H-ALSGDAFLRF-NH_2 (**AD**).[3] This decapeptide belonging to the FMRFamide family involved in regulation of reproduction and chromatophore function is able to inhibit the growth of marine *Vibrio* bacteria. As pathogenic organisms, the Center for Disease Control and prevention (CDC) estimates that there are 8,000 infections and 60 deaths each year that are the result of *Vibrio* infections.

Results and Discussion

To improve this antimicrobial activity, we first introduce a Lysine residue instead of Aspartic residue. The antimicrobial activity of this new peptide (**AK**) has been improved by augmentation of the positive net charge (+1 to +3). Moreover preliminary results have shown that the incorporation of aza-β^3-amino acid analogues could create original hybrid pseudopeptides with superior activity.[4] Therefore some α-amino acids were replaced by aza-β^3-amino acids for enhancing the biodisponibility and the antimicrobial activity of this natural sequence. The natural peptide is not efficient against *Staphylococcus aureus* whereas the peptidic (**AK**) and two of the pseudopeptidic analogues (**K-1Nal** and **K-2Nal**) revealed interesting Minimum Inhibiting Concentration (MIC). The MIC of the pseudopeptide **K-1Nal** is comprised between 8-16 µM. We have shown that depending on the substituted residue and on the structuration, these modifications could lead either to no activity or to a drastic enhancement of the antimicrobial activity, demonstrating that aza-β^3-amino acids can facilitate the burying in lipidic bilayer of antimicrobial peptides that acts on bacterial membranes.[5]

Circular dichroism studies have revealed for these amphiphilic peptides **AD** and **AK** changes from a random coil conformation in phosphate buffer to an helical structuration in more hydrophobic environment 50% trifluoroethanol (TFE) and in bacterial membrane mimetic environment 30 mM SDS micelle. For pseudopeptide **K-1Nal**, CD spectrum in TFE and SDS present the characteristic shape of close stacking of aromatic α-L-naphthylalanines.[6] These results suggest that pseudopeptide **K-1Nal** adopts a well defined structuration at membrane contact drive by the stacking of aromatic residues.

Acknowledgements

We thank SERB Laboratories and the "Region Bretagne" for their financial support.

References

1. Tincu JA, Taylor SW. *Antimicrob Agents Chemother* **48**: 3645-3654, 2004.
2. Brogden KA, Guthmiller JM, Salzet M, Zasloff M. *Nat Immunol* **6**: 558-564, 2005.
3. Henry J, Zatylny C, Boucaud-Camou E. *Peptides* **20**: 1061-1070, 1999.
4. Dali H, Busnel O, Hoebeke J, Bi L, Decker P, Briand JP, Baudy-Floc'h M, Müller S. *Mol Immunol* **44**: 3024-3036, 2007.
5. Baudy-Floc'h M, Zatylnyj-Gaudin C, Henry J, Duval E, Laurencin M. *SERB patent* **N° FR 07 09054**, 2007.
6. Dathe M, Nikolenko H, Klose J, Bienert M. *Biochemistry* **43**: 9140-9150, 2004.

Table 1. Sequences and activities of the natural peptide and of five synthetic analogues.
(MIC: Minimum Inhibitory Concentration in µM: NA: No activity detected)

Name	Primary sequence	MIC on *Escherichia coli* ATCC 10536	MIC on *Staphylococcus aureus* ATCC 6538P
AD	H-ALSGDAFLRF-NH_2	584	NA
AK	H-ALSG**K**AFLRF-NH_2	72	289
Aβ^3	H-A-**aza-β^{3}L**-S-**aza-β^{3}G**-D-**aza-β^{3}A**-F-**aza-β^{3}L**-R-**aza-β^{3}F**-NH_2	NA	NA
Aβ^{3}K	H-ALSG-**aza-β^{3}K**-AFLRF-NH_2	NA	NA
K-1Nal	H-ALSG**K**A-**aza-β^3-1-Nal**-LR-**aza-β^3-1-Nal**-NH_2	32	16
K-2Nal	H-ALSG**K**A-**aza-β^3-2-Nal**-LR-**aza-β^3-2-Nal**-NH_2	129	32

Scheme 1. *CD spectrum of the peptidic analogue **AK** and of the pseudopeptidic analogue **K-1Nal** in phosphate buffer, 50% TFE and 30 mM SDS.*

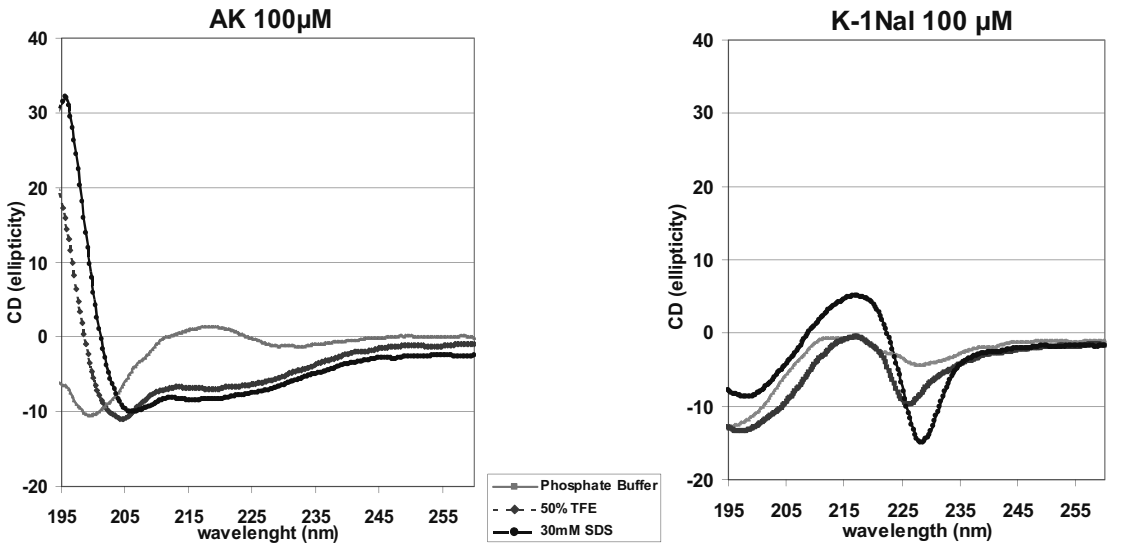

2-07-151

New bradykinin B_2 antagonists – influence of *C*-terminal modifications on their pharmacological properties

Ślęszyńska, Małgorzata,[*1]; *Kwiatkowska, Anna*[1]; *Sobolewski, Dariusz*[1]; *Wierzba, Tomasz*[2]; *Katarzyńska, Joanna*[3]; *Zabrocki, Janusz*[3]; *Borovičková, Lenka*[4]; *Slaninová, Jiřina*[4]; *Prahl, Adam*[1]

[1]*Faculty of Chemistry, University of Gdańsk, Gdańsk, POLAND;* [2]*Department of Physiology, Medical Academy of Gdańsk, Gdańsk, POLAND;* [3]*Institute of Organic Chemistry, Technical University of Łódź, Łódź, POLAND;* [4]*Institute of Organic Chemistry and Biochemistry Academy of Sciences of the Czech Republic, Prague, CZECH REPUBLIC*

[*]*E-mail: slesza@chem.univ.gda.pl*

Introduction

The bradykinin (BK) B_2 receptor had not been clearly defined until 1985 when the first generation of antagonists based on [D-Phe^7]BK was prepared.[1] In those early compounds (e.g. [Thi^{5,8},D-Phe^7]BK), the partial agonist or an antagonist character was attained by structural change caused by non-natural conformation of D-Phe^7. The added rigidity at this position in subsequent peptide antagonists showed that the spatial orientation of the *C*-terminal region of the peptide molecule was critical for antagonism. We reported previously that acylation of the *N*-terminus of several known B_2 antagonists with various bulky acyl groups (e.g. 1-adamantaneacetyl, 1-adamantanecarbonyl, 4-tert-butylbenzoyl, palmitoyl, etc.) has consistently improved their antagonistic potency in rat blood pressure assay (up to 33 times).[2] In the present study we describe the synthesis and some pharmacological properties of eight new analogues of BK. Two peptides were designed by substitution of position 7 or 8 of the Stewart's antagonist ([D-Arg^0,Hyp^3,Thi^{5,8}, D-Phe^7]BK)[3] with pipecolic acid (Pip), analogues **I** and **III**, respectively. The next two analogues were obtained by replacement of the D-Phe residue in position 7 of the Stewart's peptide with β^2-isoproline (β^2-iPro) or β^3-homoproline (β^3-hPro), analogues **V** and **VII**, respectively. The aforementioned compounds were also *N*-acylated with 1-adamantaneacetic acid (Aaa), resulting in analogues **II, IV, VI** and **VIII**.

Results and Discussion

The new analogues were synthesized manually using Fmoc chemistry, purified and characterized. The purity of each peptide was determined by HPLC and the values of the molecular ions were as expected. Biological activity of the compounds was assessed in the isolated rat uterus test (RUT) and by their ability to inhibit the vasodepressor response to exogenous BK in conscious rats (blood pressure test; BPT). Pharmacological data of the analogues and that of Stewart's antagonist used as a positive control are summarized in Table 1. From the presented results it is clear that replacement of the residue at position 8 by Pip is advantageous for B_2 antagonistic potency of the resulting analogue, which retains its antagonistic properties also in the RUT. A similar, though less distinct effect was noticed following Pip^7 substitution. Analogue **I** is another example of B_2 antagonist with non-aromatic conformationally constrained amino acid residue at this position, that supports our previous results.[4] Peptide **V** (weak B_2 agonist at low doses and weak antagonist at high doses in BPT) and peptide **VII** (weak B_2 antagonist in BPT) differ by the presence of proline derivatives with only slight distinction in structure. Already such a minor structural difference has a significant impact on bioactive conformation of the molecules and consequently influences their interaction with B_2 receptors. These findings seem to support our previous results obtained for modification of position 7 of the BK analogues with the 1-naphthyl-D-alanine and 2-naphthyl-D-alanine residues.[5] Our earlier hypothesis concerning acylation of the *N*-terminus of BK antagonists with bulky groups is not valid for each pair of the new analogues. The acylated compounds, with the exception of the pair **VII** and **VIII**, were less potent than the non-acylated ones (analogues **II, IV, VI** and **I, III, V,** respectively). In the case of RUT, acylation resulted in the decrease of the agonistic activity (compare peptides **I** and **II**, **VII** and **VIII**), but in slight increase of the antagonistic potency (compare peptides **III** and **IV**). Consequently, we can assume that the analogue-receptor interaction of numerous B_2 antagonists acylated with bulky substituents is modified owing to the more rigid structure of the *C*-terminal part of the molecule which results in an interference with the effective signal transduction. Two of the new analogues (**III** and **IV**) are potent B_2 antagonists in both assays. However, those peptides which showed a strong (**I** and **II**) or moderate (**VII** and **VIII**) antagonistic potency in BPT showed agonistic properties in RUT. This supports the idea of the presence of different subtypes of B_2 receptors in the uterus and blood vessels as postulated by various investigators.[6-8] Because of

Table 1. Pharmacological properties of the new analogues of BK

Analogue		Uterotonic potency: % of activity of BK or pA_2	Vasodepressor potency		
			ED_{20} [μg/min]	ED_{50} [μg/min]	ED_{90} [μg/min]
[D-Arg^0-Hyp^3,Thi^{5,8},D-Phe^7]-BK Stewart's antagonist		pA_2 = 7.70 ± 0.13	0.43 ± 0.03	3.19 ± 0.33	52.60 ± 10.59
[D-Arg^0-Hyp^3,Thi^{5,8},Pip^7]-BK	**I**	18.3%	0.23 ± 0.04	2.05 ± 0.26	44.98 ± 10.64
Aaa[D-Arg^0-Hyp^3,Thi^{5,8},Pip^7]-BK	**II**	0.5%	1.30 ± 0.46	40.67 ± 14.38	4456 ± 1575
[D-Arg^0-Hyp^3,Thi^5,D-Phe^7,Pip^8]-BK	**III**	pA_2 = 7.43 ± 0.26	0.10 ± 0.016	0.73 ± 0.09	11.35 ± 1.76
Aaa[D-Arg^0-Hyp^3,Thi^5,D-Phe^7,Pip^8]-BK	**IV**	pA_2 = 7.99 ± 0.25	0.16 ± 0.03	1.43 ± 0.22	28.99 ± 6.15
[D-Arg^0-Hyp^3,Thi^{5,8},*β*iPro^7]-BK	**V**	<0.01%	agonist	weak antagonist	weak antagonist
Aaa[D-Arg^0-Hyp^3,Thi^{5,8},*β*iPro^7]-BK	**VI**	<0.01%	agonist	weak antagonist	weak antagonist
[D-Arg^0-Hyp^3,Thi^{5,8},*β*hPro^7]-BK	**VII**	1.9%	15.94 ± 2.37	127.02 ± 34.11	1441 ± 413
Aaa[D-Arg^0-Hyp^3,Thi^{5,8},*β*hPro^7]-BK	**VIII**	0.1%	3.58 ± 0.80	76.05 ± 23.29	6141 ± 2483

Notes: In the uterotonic test, agonistic activity was calculated as percentage of the BK activity (set to 100%); antagonistic activity was calculated as pA_2 (negative common logarithm of analogue concentration shifting the log dose–response curve for BK by a factor of 0.3 to the right: the calculations were made from the linear portions of the curves); ED_{20}, ED_{50} and ED_{90} represent doses of BK antagonist (μg/min) that inhibit the vasodepressor response to 250 ng of BK by 20, 50 and 90%, respectively.

the presence of non-proteinogenic amino acid residues in the molecules of the new analogues, one should also consider the possibility that the metabolism also accounts for the differences in the activities just discussed.

Acknowledgements

This work was supported by the Polish State Committee for Scientific Research, grant no. PB 0380/H03/2006/31.

References

1. Vavrek RJ, Stewart JM. Competitive antagonists of bradykinin. *Peptides* **6**: 161-164, 1985.
2. Lammek B. Design and synthesis of B_2-antagonists of bradykinin. *Pol J Chem* **68**: 913-920, 1994.
3. Schachter LR, Uchida Y, Londridge DJ, Łabèdz T, Whalley ET, Vavrek RJ, Stewart JM. New synthetic antagonists of bradykinin. *Br J Pharmacol* **92**: 851-855, 1987.
4. Labudda-Dawidowska O, Wierzba TH, Prahl A, Kowalczyk W, Gawiński Ł, Plackova M, Slaninova J, Lammek B. New Bradykinin Analogues Modified in the C-terminal Part with Sterically Restricted 1-Aminocyclohexane-1-carboxylic Acid. *J Med Chem* **48**: 8055-8059, 2005.
5. Prahl A, Wierzba T, Winklewski P, Wszędybył M, Cherek M, Juzwa W, Lammek B. Influence of C-terminal Modifications of Bradykinin Antagonists on Their Activity. *Collect Czech Chem Commun* **62**: 1940-1946, 1997.
6. Steranka L, Manning D, Dehas C, Ferkany J, Borosky S, Connor J, Vavrek R, Stewart J, Shyder S. Bradykinin as a pain mediator: receptors are localized to sensory neurons have analgesic actions. *Proc Natl Acad Sci U S A* **85**: 3245-3249, 1988.
7. Plevin R, Owen P. Multiple B_2 kinin receptors in mammalian tissues. *Trends Pharmacol Sci* **9**: 387-389, 1988.
8. Milan A, Mulatero P, Williams TA, Carra R, Schiavone D, Martuzzi R, Rabbia F, Vegilo F. Bradykinin B_2 receptor gene (-58T/C) polymorphism influences baroreflex sensitivity in never treated hypertensive patients. *J Hypertens* **23**: 63-69, 2005.

2-07-152

Design, synthesis and biological activities of temporin A and temporin L analogues

Malfi, Stefania[1,]; Auriemma, Luigia[1]; Saviello, Maria Rosaria[1]; Marcozzi, Cristina[1]; Carotenuto, Alfonso[1]; Campiglia, Pietro[2]; Gomez-Monterrey, Isabel Maria[1]; Mangoni, Maria Luisa[3]; Gaddi, Ludovica Marcellini Hercolani[3]; Novellino, Ettore[1]; Grieco, Paolo[1]*

[1]University of Naples Federico II, ITALY; [2]University of Salerno, ITALY; [3]University of Rome, ITALY

[*]E-mail: stefania.malfi@unina.it

Introduction

Temporins A and L are antimicrobial peptides isolated from the skin of Red European frog '*Rana temporaria*'. Actually, they are the smallest natural antimicrobial amide-peptides characterized by short sequence (10-14 residues) with a net positive charge at neutral pH value. Temporins are active against a broad spectrum of microorganism: Temporin A (TA) (FLPLIGRVLSGIL-NH_2) is preferentially active against Gram-positive bacterial strains; Temporin L (TL) (FVQWFSKFLGRIL-NH_2) has the highest activity among all temporins against fungi, and bacteria, including resistant Gram-negative strains, but it shows hemolytic activity too. TA exerts its antimicrobial activity by its ability to form a transmembrane pore via a 'barrel-stave' mechanism or to form a 'carpet' on the membrane surface via the 'carpet-like' model.[1] Mangoni *et al*.[2] reported that the ability of temporins to destroy microbial cells is independent of membrane composition, since they lysed artificial vesicles built from zwitterionic and acidic phospholipids as well.[2] We investigated the preferential conformation of TL and TA in SDS and DPC solutions, which are considered as good models of bacterial and eukaryotic cell membranes, respectively. On the bases of the NMR results, we designed and synthesized new TA and TL analogues (Table 1) to understand the exact mechanism of the action and to find new potent antimicrobial agents without hemolytic activity.

Synthesis and nmr analysis

The temporins A, L and their analogues were synthetized in solid phase by the classical strategy via Fmoc using Rink-Amide resin. Finally, the peptide chains were cleaved from the resin using TFA 90% TIS 5% H2O 5% mixture. The crude peptides were purified by RP-HPLC and characterized by ESI-MS. CD and NMR analysis[3] revealed that both peptides adopt a random coil conformation in water solution and prefer a helical conformation in membrane mimetic environments. The two analyzed peptides show in both SDS and DPC solutions structures which can be described as a stable amphipatic α-helix. In Fig. 1, we report the NMR structures. Subtle differences could be observed in the conformational preferences of the two peptides in the different membrane mimetic environments. In particular, helical character of TL significantly increases passing from SDS to DPC micelles. TA conformational behaviour observed in SDS and DPC solutions was very similar. Slight differences are localized in the *N*-terminal region of the peptide. In fact, this region shifts from a β-turn structure revealed in SDS micelle to an α-helix structure in DPC. Overall spectroscopic data indicate that the propensity in forming α-helical structures is the following: TL in DPC solution > TL in SDS solution ≥TA in DPC solution ≥TA in SDS solution. Furthermore, using paramagnetic probes to define the location of temporins with respect to the micelle, we could predict a 'carpet-like' mechanism for the antimicrobial, and a 'barrel-stave' model for the hemolytic action of the peptides.[1]

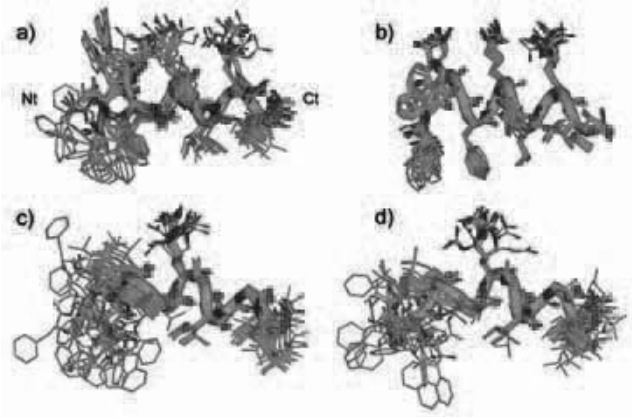

Figure 1. Superposition of the 20 lowest energy conformers of TL in SDS (a), TL in DPC (b), TA in SDS (c), TA in DPC (d). Structures were superimposed using the backbone heavy atoms of residues 3-11. Heavy atoms are shown with different colors (carbon, green; nitrogen, blue; oxygen, red). Hydrogen atoms are not shown for clarity. Backbone atoms of the lowest energy conformer were evidenced as a ribbon. Nt: N-terminal, Ct: C-terminal.

Table 1. New compounds designed by NMR studies

Temporin L	**FVQWFSKFLGRIL-NH_2**
Temporin A	**FLPLIGRVLSGIL-NH_2**
Pro^3-TL	**FVPWFSKFLGRIL-NH_2**
Gln^3-TA	**FLQLIGRVLSGIL-NH_2**

Results and discussion

Based on the NMR and simulation results we designed new analogues of TL and TA with the aim of improving the pharmacological profile compared to the parent peptides (Table 2). Since the main difference observed between the TA and TL secondary structures both in SDS and DPC micelle solutions was the presence of a turn conformation in the *N*-terminal region of TA, likely induced by the Pro3 residue, we firstly investigated this position both in TA and in TL. We replaced the Gln3 of TL with a Pro obtaining the Pro3-TL analogue (Table 1). Biological data (Table 2) showed a little increase of antimicrobial activity respect to that of the parent TL, with a decreased hemolytic activity. Analogously, we designed and synthesized a chimera derivative of TA in which Pro3 was replaced by the Gln residue found in TL, obtaining the Gln3-TA analogue (Table 1). Gln3-TA analogue showed higher hemolytic activity and a little increase of antimicrobial activity compared to the parent peptide TA (Table 2).

Conclusion

Our results point to a different molecular mechanism underlying antimicrobial and hemolytic actions of TA and TL. In particular, the 'carpet-like' and the 'barrel-stave' models were employed to interpret the antimicrobial and hemolytic activities of temporins, respectively. Biological activity of new rationally designed analogues confirms our hypothesis. In particular, with respect to the native TL, the analogue Pro3-TL has shown an increased antimicrobial potency and a decreased hemolytic activity which make it an interesting molecule for further structure-function relationship studies.

References

1. Shai Y. Mode of action of membrane active antimicrobial peptides. *Biopolymers (Peptide Science)* **66**: 236-248, 2002.
2. Mangoni ML, Rinaldi AC, Di Giulio A, Mignogna G, Bozzi A, Barra D, Simmaco M. *Eur J Biochem* **267**: 1447-1454, 2000.
3. Carotenuto A, Malfi S, Saviello MR, Campiglia P, Gomez-Monterrey I, Mangoni ML, Gaddi LM, Novellino E, Grieco P. Different Molecular Mechanism Underlying Antimicrobial and Hemolytic Actions of Temporins A and L. *J Med Chem* **51**: 2354- 2362, 2008.

Table 2. Antimicrobial and hemolytic activities of temporin analogues

	MIC (μM)[a]			
	TL	*Pro^3-TL*	*TA*	*Gln^3-TA*
Gram-negative				
Escherichia coli D21	12	12	>24	>24
Enterobacter faecalis ATCC 29212	6	6	12	6
Pseudomonas aeruginosa ATCC 15692	24	24	>24	>24
Pseudomonas syringae pv tobaci	6	6	>24	>24
Yersinia pseudotuberculosis YPIII	3	3	12	6
Gram-positive				
Bacillus megaterium Bm11	1.5	1.5	1.5	0.75
Staphylococcus aureus Cowan I	3	1.5	1.5	1.5
Staphylococcus aureus ATCC 25923	3	3	3	1.5
Staphylococcus capitis, 1	1.5	1.5	1.5	1.5
Staphylococcus epidermidis ATCC 12228	3	1.5	3	1.5
Streptococcus pyogenes ATCC 21547	6	6	12	6
Yeasts				
Candida albicans ATCC 10231	12	6	12	6
Saccharomyces cerevisiae	6	6	6	6
Saccharomyces pombe	6	3	3	3
	% hemolysis			
Peptide concentration (μM)				
3	13	6	3	9
6	48	10	4.5	18
12	92	42	6	70
24	94	92	28	92

2-07-153

Comparative structural studies of potent neuroprotective peptides of the humanin family

Benaki, Dimitra[1]; Zikos, Christos[2]; Evangelou, Alexandra[3]; Slaninová, Jiřina[4]; Vlassi, Metaxia[1]; Livaniou, Evangelia[3]; Mikros, Emmanuel[5]; Pelecanou, Maria[1,]*

[1]NCSR "Demokritos", Institute of Biology, GREECE; [2]Biomedica Life Sciences, GREECE; [3]NCSR "Demokritos", Institute of Radioisotopes & Radiodiagnostic, GREECE; [4]Czech Academy of Sciences, Institute of Organic Chemistry & Biochemistry CZECH REPUBLIC; [5]University of Athens, Department of Pharmacy, GREECE

[*]E-mail: pelmar@bio.demokritos.gr

Introduction

The Humanin family of peptides is a new and continuously growing class of agents targeting neuroprotection. The parent peptide Humanin (HN) discovered in 2001[1] was found to suppress *in vitro* neuronal cell death related to Alzheimer's disease insults. Most importantly, new more potent HN derivatives have demonstrated *in vivo* activity by reversing learning and memory deficits experimentally induced in rats and mice,[2] extending also their rescue activity to other degenerative diseases.[3] The sequence and the relative potency of the most important members of the HN family, which offers hope for the development of new therapeutic strategies against neurodegenaration, are summarized in Table 1. CL, the most potent derivative of HN family, is a hybrid peptide composed of the 9 amino acid Activity-Dependent Neurotrophic Factor (ADNF9), SALLRSIPA, *C*-terminally fused to the mHNG17 peptide. Although HN has been connected in the literature with various signaling pathways, its mechanism of action remains unknown. In this study structural characteristics based on CD and NMR studies of this family are presented and compared with the hope to correlate structure with activity.

Results and discussion

CD Experiments: The parent peptide HN as well as its potent derivatives are characterized by high flexibility in aqueous solution at physiological pH. In unbuffered (pH around 3.0) aqueous solutions and high (>0.5 mg/mL) concentrations the CD spectra of HN, HNG and CL remain invariable, while mHNG17 displays a transition from random coil (min. at 198 nm) to β-sheet (min. 216 nm) (Fig. 1A). As the pH is raised to 7 HN and HNG gradually display variations related to an oligomerization process, while the CL spectra remain invariable (Fig. 1B). In the more lipophilic environment attained by the addition of TFE in aqueous solution, all the peptides adopt α-helical conformation stabilized at appr. 30% TFE. Secondary structure estimation based on CD data revealed that under the specific experimental conditions HN has the higher α-helical percentage of 33%, while HNG and CL have 15% and 20% respectively, suggestive of a higher flexibility for these two derivatives in solution.

NMR Experiments: HN in 30% TFE adopts α-helical structure that extends from Gly5 to Leu18[4] while in HNG, the helical region is shorter and extends from

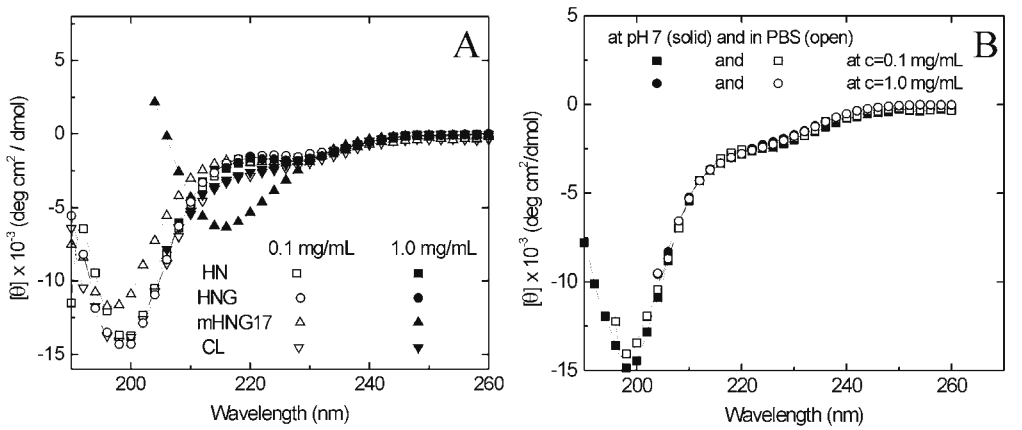

Figure 1. (A) CD spectra of the peptides studied in unbuffered aqueous solutions (pH approx. 3.0) of 0.1 and 1.0 mg/mL. (B) CD of CL at pH 7 and in PBS at 0.1 and 1.0 mg/mL.

Table 1

Peptide	*Sequence*	*Effective Concentration*
HN	MAPRGFSCLLLLTSEIDLPVKRRA	10 μM
HNG	MAPRGFSCLLLLT**G**EIDLPVKRRA	10 nM
modified_HNG17 (mHNG17)	P**A**G**A**SRLLL_T**G**EIDLP	10 pM
Colivelin (CL)	SALLRSIPA-P**A**G**A**SRLLLLT**G**EIDLP	100 fM

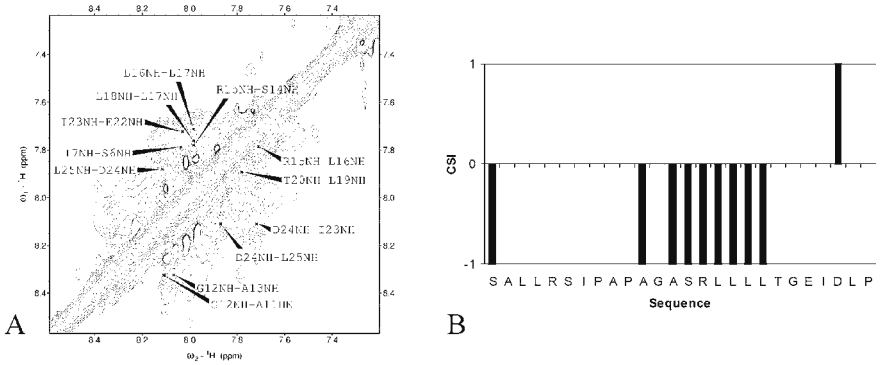

Figure 2. (A) NH-NH region of a 500 MHz NOESY spectrum of CL (mix. time 200 ms) in 40% TFE at 298 K. (B) Deviations of α-proton chemical shift from random coil values observed for CL in the same solution. The negative values are consistent with the presence of α-helices.

Gly5 to Thr13, as expected by the presence of Gly14.[5] NMR spectra of CL were collected for solutions of 40% TFE and they were fully assigned. The almost complete set of NH(i)-NH(i+1) nOe connectivities for residues Ala11-Thr20 (Fig. 2A), the presence of αH(i)-NH(i+3) and αH(i)-βH(i+3) nOes, and the CSI data (Fig. 2B) are indicative of α-helical structure formation along the central part of the sequence leaving the ADNF9 *N*-terminal part in unordered form. The NMR study of mHNG17 was hampered by the gradual precipitation observed in solution at the higher concentrations required.

In summary, the CD and NMR studies reveal in aqueous solution molecules with highly flexibility - a property that may facilitate interactions with functional counterparts - able however to adopt helical conformations in more lipophilic environment - a property that may be crucial for membrane passage and secretion. With the exception of CL, at pH 7 all peptides have a tendency for self-association - a property that has been linked in the literature to the mechanism of their neuroprotective action - with the tendency being more pronounced for mHNG17.

Materials and methods

Synthesis: HN and derivatives were synthesized in our lab, following the Fmoc-solid phase peptide synthesis approach on an in-house prepared o-Cl-trityl-amidomethyl polystyrene resin.[6] The peptides were purified with semi-preparative RP-HPLC and were more than 95% pure.

CD spectropolarimetry: CD experiments were recorded on a Jasco J-715 instrument.

NMR spectroscopy: NMR experiments were recorded on a Bruker DRX-500 MHz Avance spectrometer.

References

1. Hashimoto Y, Niikura T, Tajima H, Yasukawa T, Sudo H, Ito Y, Kita Y, Kawasumi M, Kouyama K, Doyu M, Sobue G, Koide T, Tsuji S, Lang J, Kurokawa K, Nishimoto I. *Proc Natl Acad Sci U S A* **98**: 6336-6341, 2001.
2. (a) Krejcova G, Patocka J, Slaninova J. *J Pept Sci* **10**:636-9, 2004; Tajima H, Kawasumi M, Chiba T, Yamada M, Yamashita K, Nawa M, Kita Y, Kouyama K, Aiso S, Matsuoka M, Niikura T, Nishimoto I. *J Neurosci Res* **79**:714-723, 2005; (b) Kunešová G, Hlaváček J, Patočka J, Evangelou A, Zikos C, Benaki D, Paravatou-Petsotas M, Pelecanou M, Livaniou E, Slaninova J. *Peptides* **29**: 1982-1987, 2008.
3. (a) Matsuoka M, Hashimoto Y, Aiso S, Nishimoto I. *CNS Drug Reviews* **12**: 113-122, 2007; (b) Chiba T, Yamada M, Sasabe J, Terashita K, Aiso S, Matsuoka M, Nishimoto I. *Biochem Biophys Res Commun* **343**: 793-798, 2006.
4. Benaki D, Zikos C, Evangelou A, Livaniou E, Vlassi M, Mikros E, Pelacanou M. *Biochem Biophys Res Commun* **329**: 152-160, 2005.
5. Benaki D, Zikos C, Evangelou A, Livaniou E, Vlassi M, Mikros E, Pelacanou M. Biochem Biophys Res Commun **349**: 634-642, 2006.
6. Evangelou A, Zikos C, Livaniou E, Evangelatos GP. *J Pept Sci* **10**: 631–635, 2004.

2-07-154

In vitro and *in vivo* antitumor effect of symmetric GnRH-III dimer derivatives

Szabó, Ildikó[1,]; Bősze, Szilvia[1]; Orbán, Erika[1]; Vincze, Borbála[2]; Gaál, Dezső[2]; Csuka, Orsolya[2]; Hudecz, Ferenc[3]; Mező, Gábor[1]*

[1]Eötvös L University, Research Group of Peptide Chemistry, HUNGARY; [2]National Institute of Oncology, HUNGARY; [3]Eötvös L University, HUNGARY

[*]E-mail: szaboi8@gmail.com

Introduction

The hypothalamic decapeptide gonadotropin-releasing hormone (GnRH-I; 0.05) on both cell lines). There was no significant increase of the antiproliferative effect by the further elevation of the peptide concentration. Balb/c mice implanted by HT-29 xenograft were used for the study of the *in vivo* antitumor effect. The first treatment in all cases was ten days after the tumor implantation. The i.p. administration was carried out every day for 6 weeks. The application of dimers at 40 mg/kg body weight resulted in 50% inhibition of the tumor growth during the treatment and even 40% inhibition was observed 20 days after the last injection. None of the mice died during the experiment. Furthermore, no significant difference between the inhibitory effect of the dimers was observed. In conclusion, the new GnRH-III based dimer derivatives have increased antitumor activity and less endocrine effect than GnRH-III itself providing more selective antitumor agents. The GnRH-III dimers might be also used in targeted chemotherapy as targeting moieties for drug delivery.

Acknowledgement

This work was supported by grants from the Hungarian National Science Fund (OTKA K 043576 and T 049814), "Medichem 2" 1/A/005/2004 and GVOP-3.2.1.-2004-04-0005/3.0 and ETT 202/2006.

References

1. Lovas S, Pályi I, Vincze B, Horváth J, Kovács M, Mezö I, Tóth G, Teplán I, Murphy RF. *J Peptide Res* **52**: 384-389, 1998.
2. Kovács M, Seprödi J, Koppán M, Horváth JE, Vincze B, Teplán I, Flerkó B. *J Neuroendocrinol* **14**: 647-655, 2002.
3. Kovács M, Vincze B, Horváth JE, Seprodi J. *Peptides* **28**: 821-829, 2007.
4. Mező G, Czajlik A, Manea M, Jakab A, Farkas V, Majer Z, Vass E, Bodor A, Kapuvári B, Boldizsár M, Vincze B, Csuka O, Kovács M, Przybylski M, Perczel A, Hudecz F. *Peptides* **28**: 806-820, 2007.

2-07-155

Identifi cation, chemical synthesis, and antimicrobial activity of TBD-1 – the fi rst β-defensin isolated from reptiles

Knappe, Daniel[1]
Institute for Bioanalytical Chemistry, Center for Biotechnology and Biomedicine, Leipzig University, GERMANY

Article is on p. 336-337 (2-07-160)

2-07-156

Delta Sleep Inducing Peptide (DSIP), its analogues and Deltaran®: biological activity and mode of action

Mikhaleva, Inessa[1]; Prudchenko, Igor[1]; Nurbakov, Alfred[2]; Sapozhnikov, Alexander[3]; Ivanov, Vadim[4,]*

[1]Shemyakin-Ovchinnikov Institute of Bioorganic chemistry RAS, Peptide department, RUSSIAN FEDERATION; [2]Shemaykin-Ovchinnikov Institute RAS, Peptide department, RUSSIAN FEDERATION; [3]Shemyakin-Ovchinnikov Institute of Bioorganic chemistry RAS, RUSSIAN FEDERATION; [4]Shemyakin- Ovchinnikov Institute of Bioorganic chemistry RAS, RUSSIAN FEDERATION

[*]E-mail: imikha@ibch.ru

Introduction

DSIP is known since the late 70's.[1] For the last decade we have been engaged in broad studies on this endogenous neuromodulator in respect of both chemical aspects and physiological responses. In coarse of structure-activity investigations a large group analogues was analyzed under various test models. We found several derivatives with enhanced and selective biological activities. This peptide has emerged as a promising effective therapeutic agent due to strong and unique adaptive and stress protective activity revealed during the study. Based upon our findings we developed DSIP-related antistress and antialcoholic drug "Deltaran™" registered in Russia in 1998. Clinical trials demonstrated significant efficiency and did not revealed any side effects and contra-indications. DSIP physiological effects, structure-function relationships and specific mechanisms underlying its action still remain to be learned. Biochemical, cellular and subcellular mechanisms of DSIP actions are under our attention for some years.

Results

Previously we investigated some biochemical events underlying the stress protective efficiency of DSIP and its derivatives.[2,3] In continuation of these studies we have attempted to evaluate the putative DSIP influence on classical cellular processes utilizing stress-protective heat shock proteins (HSPs) and apoptosis in various cell lines. For HSP70 detection indirect immunofluorescence staining of fixed and permeabilized cells was used with anti-HSP70 monoclonal antibodies and secondary FITC-conjugated antibodies. For apoptosis detection propidium iodide staining was applied. Samples were analyzed in Beckman Coulter Epics XL flow cytometer. In murine thymocytes, known to express adrenergic receptors, DSIP remarkably increased both apoptosis and HSP70 level in 10-6M -10-8M concentrations. DSIP was also found to increase HSP70 in CTLL-2 cells. CTLL-2 cells were incubated with DSIP and the agonists of two different adrenergic receptors subtypes: α-adrenergic (phenylephrine) and *β*-adrenergic (isoproterenol) for 16 hours. The effect of DSIP was similar to those of the adrenergic receptor agonists (Fig. 1). In K562 cells that do not express adrenergic receptors there was no increase of HSP70 level and apoptosis after incubation with DSIP. We have found that DSIP even down regulates the

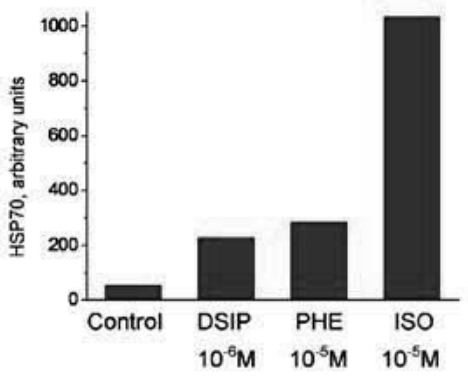

Figure 1. Effect of DSIP, phenylephrine (PHE) and isoproterenol (ISO) on the level of intracellular HSP70 in CTLL-2 cells after 16 hours incubation.

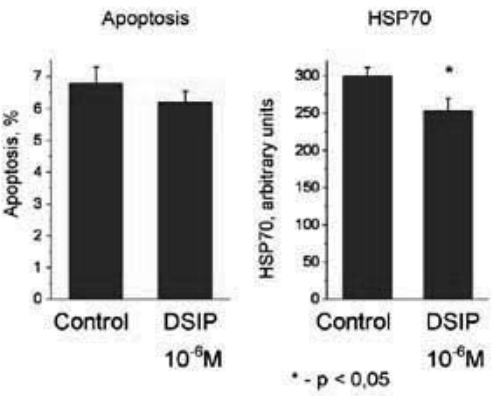

Figure 2. Effect of DSIP on apoptosis and the level of intracellular HSP70 in K562 cells after 16 hours incubation in high-density culture.

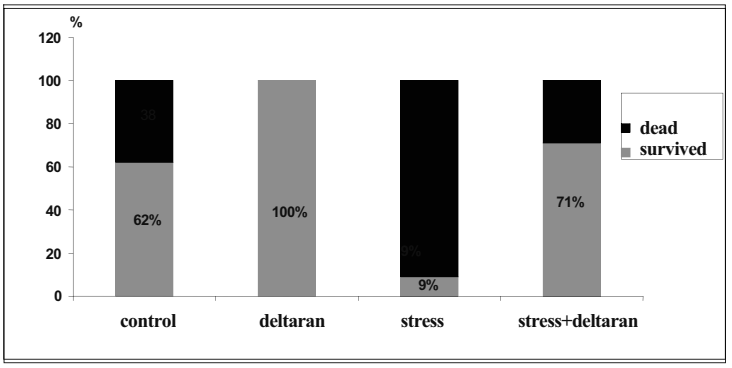

Figure 3. Effects of deltaran under experimental ischemia and ischemia+ stress in rats. Animals receiving deltaran survived experimental brain ischemia (occlusion of both carotid arteries) in 100% cases versus 38% lethality in those not exposed to this drug (first 2 columns). Only 9% of rats survived when rats were additionally subjected to emotion stress for 18 hours before ischemia (column 3), but 71% of rats survived in this case under deltaran treatment (ip., 40 μg/kg, column 4).

increase of intracellular HSP70 level during incubation of cells in high density cell culture (Fig.2). It seems possible that DSIP affects K562 cells in a different way.[4] Cellular effects of DSIP and related peptides action are under way.

We have also continued the investigations of biological properties, structure-functional relationships and biomedical profile of DSIP along with its analogues and drug deltaran. Recently we have demonstrated the sigmificant capacity of deltaran to mitigate the severity of experimental brain ishemia and prevent the negative effect of emotional stress in rats subjected to ishemia (Fig.3). Experimental animals treated by deltaran proved to have enhanced (+65%) coefficients of blood supply (local brain flow/ EEG) than untreated rats due to antioxidative action and decreasing excitotoxicity in brain structures involving emotional processing.[5] In suitable experimental models DSIP and analogues are tested on their possible efficacy as onco-protective additives to classical anti-tumor remedies. Some derivatives of this family appear to be promising as perspective compounds capable to reduce the toxicity of cytostatic treatment and enhance its efficacy.We are in progress to analyze the structural requirements for the derivatives with preferred pharmacological profile.

Acknowledgements

This work was supported by the Moscow City Government.

References

1. Schoenenberger GA, Monnier M. *Proc Natl Acad Sci U S A* **74**: 1282-1286, 1977.
2. Khvatova EM, Samartzev VN, Zagoskin PP, Prudchenko IA, Mikhaleva II. *Peptides* **24**: 307-311, 2003.
3. Popovich IG, Voitenkov BO, Anisimov VN, Ivanov VT, Mikhaleva II, Zabezhinski MA, Alimova IN, Baturin DA, Zavarzina NY, Rosenfeld SV, Semenchenko AV, Yashin AI. *Mech Ageing Dev* **124**: 721-731, 2003.
4. Nurbakov AA, Mikhaleva II, Sapozhnikov AM. *Bull Exp Biol Med* **147**: 39-41, 2009.
5. Koplik EV, Umryuchin PE, Konorova IL, Terechina OL, Mikhaleva II. *Zh Nevrol Psikhiatr* Im S S Korsakova **107**: 50-54, 2007. Russian.

2-07-157

Antiviral (HSV) activities of selected insect peptides

Kuczer, Mariola[1,]; Dziubasik, Katarzyna[1]; Midak-Siewirska, Anna[2]; Zahorska, Renata[2]; Łuczak, Mirosław[2]; Konopińska, Danuta[1]*

[1]Faculty of Chemistry, University of Wroclaw, POLAND; [2]Department of Microbiology, Medical University of Warsaw, POLAND

[*]E-mail: km@wchuwr.pl

Introduction

The *Herpesviridae* are a large family of DNA viruses that can cause skin infections, mucous membranes, tumor, and other serious diseases in animals and humans. One of the major problem of the modern medicine is a relatively small number of efficacious antiviral drugs. Therefore, identification of new biologically active substances which might be used as antiviral agents is very important.[1]

Natural products isolated from arthropods are an important source of bioactive compounds. In the last decade, a number of peptides with a large variety of biological activities was isolated from insects.[2-5] However, relatively little data are available on molecules from insects with the antiviral activities.

The subject of our investigation was a search for new biological properties of a series of known antiviral or antitumor insect peptides, such as alloferon (HGVSGHGQHGVHG) (I), Any-GS (DILRGNa) (VI), and a series of their analogs. Alloferon (I) has been isolated from the blow fly *Calliphora vicina.*[4] *In vitro*, alloferon demonstrates the stimulatory activity on natural killer lymphocytes and *in vivo* this peptides has antiviral and antitumor capabilities. Pentapeptide Any-GS (VI) has been isolated from the wild silkmoth *Antheraea yamamai.*[6] This peptide suppresses proliferation of the rat hepatoma cells.[5] We obtained the following peptides: 1/ alloferon (I) and its analogs modified at position 1, [des-His[1]]-(II), [Lys[1]]-(III), [Arg[1]]-(IV), [Ala[1]]-alloferon (V), 2/ Any-GS (VI) and its shortened derivatives, [1-4]-(VII), [2-5]-(VIII), [3-5]-Any-Gs (IX) and the analogs of Any-GS modified at position 1 such as: [Asn[1]]-(X), [Arg[1]]-(XI), [Gln[1]]-(XII), [Gly[1]]-(XIII), [Ala[1]]-Any-GS (XIV).

Peptides I-V were synthesized by the classical solid phase method according to the Fmoc-procedure. Other peptides (VI-XIV) were synthesized by classical solid-phase method according to the Boc-procedure. Amino acid were assembled either on a Wang (peptide acids) or MBHA resin (peptide amide). All peptides were purified by preparative HPLC.

During the biological investigations of the peptides, we performed a search for their *in vitro* antiviral activity against *Herpes Simplex Virus* type 1 McIntrie (HSV-1_{MC}) and cytotoxic activity using a Vero cell line. Cytotoxic activity of peptides was assessed by a light microscopy and quantified by the MTT (3-[4,5-dimethyl-thiazol-2-yl]-2,5-diphenyl tetrazoliumbromide) assay *in vitro* using a Vero cell line. Antiviral activity was assessed against *Herpes Simplex Virus* type 1 McIntire (HSV-1_{MC}) *in vitro* using a Vero cell line. In these studies the cell cultures were infected with HSV-1_{MC}1$TCID_{50}$/cell. The tested compounds were added at their maximum non-toxic concentrations to the cell culture with the virus. The antiviral activity of tested peptides was determined initially using a cytopathic effect (CPE). The inhibition of the viral CPE was assessed by a light microscopy. Virus titers were determined according to the Reed-Muench formula and expressed in $TCID_{50}$/ml at particular stages of the experiments. Antiviral activity of tested peptides was finally expressed as a reduction ratio of the virus titers by comparison with the virus control.

Results and discussion

The antiviral bioassay shows that investigated peptides evidently inhibits *in vitro* the replication of HSV-1_{MC} virus at their maximum non-toxic concentrations after 24 hours and 48 hours (Tables 1 and 2).

We found that alloferon at the concentration 90 µg/ml after 24 h of incubation inhibits *in vitro* the replication of virus HSV-1_{MC} by 2 log but after 48 h of incubation its inhibitory effect is weaker (1.5 log). A similar activity was observed for analogs of alloferon (peptides II-V) after 24 h. However, these peptides after 48 h of incubation demonstrate a weak inhibitory effect on the replication of virus HSV-1.

Any-GS (VI) at the concentration 52.5 µg/ml inhibits *in vitro* the replication of HSV-1_{MC} after 24 h and 48 h by 1.5 log and 1 log, respectively (Table 2). A similar activity was observed for its shortened derivatives (peptides VII-IX). Analogs of Any-GS modified at position 1 of the peptide chain reduce the virus titer by 2 log to 1 log after 24 h and than this effect was becoming weaker. They reduce the virus titer by 0.5 log to 1 log.

Moreover, alloferon, Any-GS, and their investigated analogs did not show any cytotoxic activity against the Vero cells at their maximum tested concentrations. Microscopic observations showed that no changes occurred in the Vero cell growth or morphology in the

Table 1. Influence of alloferon and its analogs on the replication *in vitro* of HSV-1_{MC} virus

Peptides	Concentration (μg/ml)	Effect after 24 hours incubation			Effect after 48 hours incubation		
		Virus titer ($TCID_{50}$/ml)		Inhibition ($logTCID_{50}$/ml)	Virus titer ($TCID_{50}$/ml)		Inhibition ($logTCID_{50}$/ml)
		Control	Sample		Control	Sample	
I	90	$8*10^3$	$1.1*10^2$	2	$1.8*10^4$	$8*10^2$	1.5
II	27.5	$1.7*10^3$	$0.7*10^1$	2.5	$3*10^3$	$3*10^2$	0.5
III	38.7	$1.7*10^3$	$7*10^1$	1.5	$3*10^3$	$3*10^2$	1
IV	40	$1.7*10^3$	$1.3*10^1$	2	$3*10^3$	$3*10^2$	1
V	27.5	$1.7*10^3$	$3*10^1$	2	$3*10^3$	$3*10^2$	1

Table 2. Influence of Any-GS and its analogs on the replication *in vitro* of HSV-1_{MC} virus

Peptides	Concentration (μg/ml)	Effect after 24 hours incubation			Effect after 48 hours incubation		
		Virus titer ($TCID_{50}$/ml)		Inhibition ($logTCID_{50}$/ml)	Virus titer ($TCID_{50}$/ml)		Inhibition ($logTCID_{50}$/ml)
		Control	Sample		Control	Sample	
VI	52.5	$8*10^3$	$3*10^2$	1.5	$1.8*10^4$	$1*10^3$	1
VII	57.5	$8*10^3$	$1.8*10^2$	1.5	$1.8*10^4$	$3*10^2$	2
VIII	51	$8*10^3$	$1.3*10^2$	2	$1.8*10^4$	$5*10^2$	1.5
IX	57.5	$8*10^3$	$1.2*10^3$	1	$1.8*10^4$	$1.1*10^3$	1.5
X	48.8	$1.7*10^3$	$7*10^1$	1.5	$3*10^3$	$8.3*10^2$	0.5
XI	62.5l	$1.7*10^3$	$1.6*10^1$	2	$3*10^3$	$2.1*10^2$	1
XII	26.5	$1.7*10^3$	$3*10^1$	2	$3*10^3$	$3*10^2$	1
XIII	33.7	$1.7*10^3$	$3*10^1$	2	$3*10^3$	$1.1*10^2$	1
XIV	40	$1.7*10^3$	$2.8*10^1$	2	$3*10^3$	$8*10^2$	1.5

presence of tested peptides. MTT assay also proved that they had no effect on cell proliferation.

Basing on these effects, it is difficult to discuss the structure/function relationship of the peptides studied. However these effects may constitute a basis for future antiviral drugs but it needs further studie.

References

1. Dzieciatkowski T, Rola A, Majewska A, Solarska M, Luczak M. *Post Mikrobiol* **46:** 211-221, 2007.
2. Bulet P, Stocklin R. Prot. Pept. Lett. **12:** 3-11, 2005.
3. Kuczer M, Rosinski G, Konopinska D. *J Pept Sci* **13:** 16-26, 2007.
4. Chernysh S, Kim S. I, Bekker G, Pleskach V. A, Filatova N. A,. Anikin V. B, Platonov V. G, Bulet P. *Proc Nat Acad Sci USA* **99:** 12628-12632, 2002.
5. Yang P, Abe S, Zhao Y, An Y, Suzuki K. *J Insect Biotech Sericol* **73:** 7-13, 2004.
6. Suzuki K, Minagawa T, Minakawa T, Kumagai T, Naya S, Endo Y, Osanai M, Kuwano E. *J Insect Physiol* **36:** 855-860, 1990.

2-07-158

Creation of novel spider toxin analogs to adopt as probes for visualization of glutamate receptors

Wakamiya, Tateaki; Nishimaru, Takahiro; Mori, Kiyoe; Yamaguchi, Yoshihiro*

Kinki University, Faculty of Science and Technology, JAPAN

**E-mail: wakamiya@chem.kindai.ac.jp*

Introduction

L-Glutamate (Glu) is known to be a major excitatory neurotransmitter not only in the mammalian central nervous system but also in the ganglia of arthropods. Spider toxins inhibit these Glu-mediated neurotransmission through the binding with glutamate receptors (GluRs), though the details about the binding have not been clarified yet. In order to elucidate the binding mode between spider toxins and GluRs, we focused on the visualization of GluRs by complex formation with fluorescent-labeled analogs of NPTX-594 (**1**).[1] In a previous paper, we observed that Abg-[*des*-Lys-(NPTX-594)] (**2**), a NPTX-594 analog in which the Lys residue of **1** was replaced with the *N*-(4-aminobutyl)glycine (Abg) residue, showed three times more potent biological activity than natural product.[2] Further, we can inform that there are several variations in the terminal aromatic residue of natural spider toxins.[1,3] In the present study, therefore, we planned to substitute the Dhpa residue in the analog **2** with several aromatic residues to create novel fluorescent-labeled NPTX-594 analogs, i.e., Dhpa was replaced with the coumarin-type acyl residues (analog **3**), the phenylacetyl residues having alkyne side chains that can be converted into suitable fluorophores based on the click chemistry (analogs **4**, **5**) and the coumarin-type acyl residues having the mercapto group to form disulfide bond with the Cys residue in GluRs (analogs **6**, **7**).

Results and Discussion

The syntheses of all analogs were basically carried out in a similar manner as reported in a previous paper,[4] e.g., the analog **3** was obtained as shown below, and its biological activity was evaluated by cricket bioassay (Table 1).[2]

To synthesize the analogs **4** - **7**, the Z group of the compound **11** was removed by catalytic hydrogenation, and the resulting amine component was coupled with Popa-OH or Oopa-OH by DCC/HOBt method and Mhca-OH or Mcpa-OH by EDC.HCl/HOBt method, respectively. The results of their cricket bioassay are summarized in Table 2.

In conclusion, the analogs except **5** created in the present study are adoptable as probes for visualization of glutamate receptors. We are currently undertaking the study on the binding of each analog to GluRs, and the results will be reported soon elsewhere.

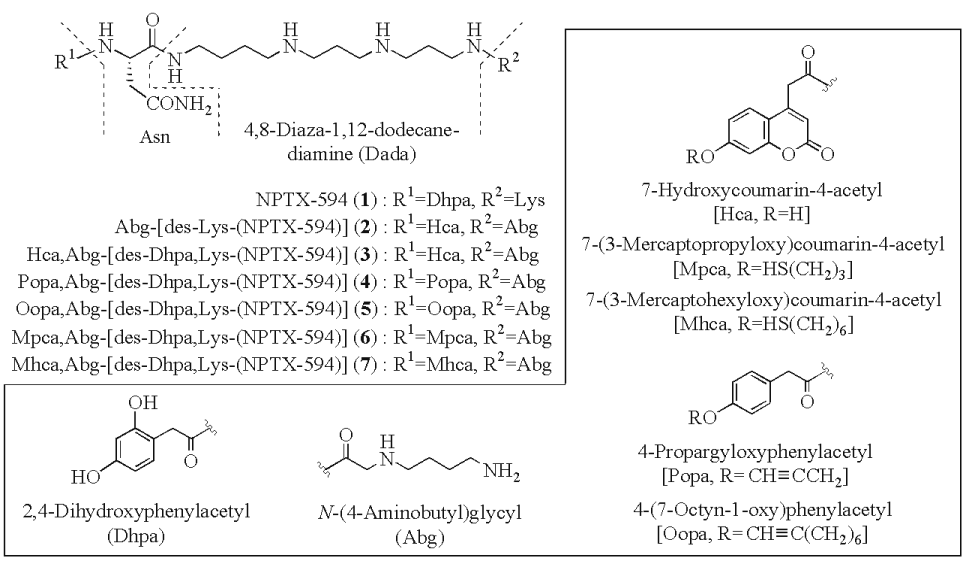

Figure 1.

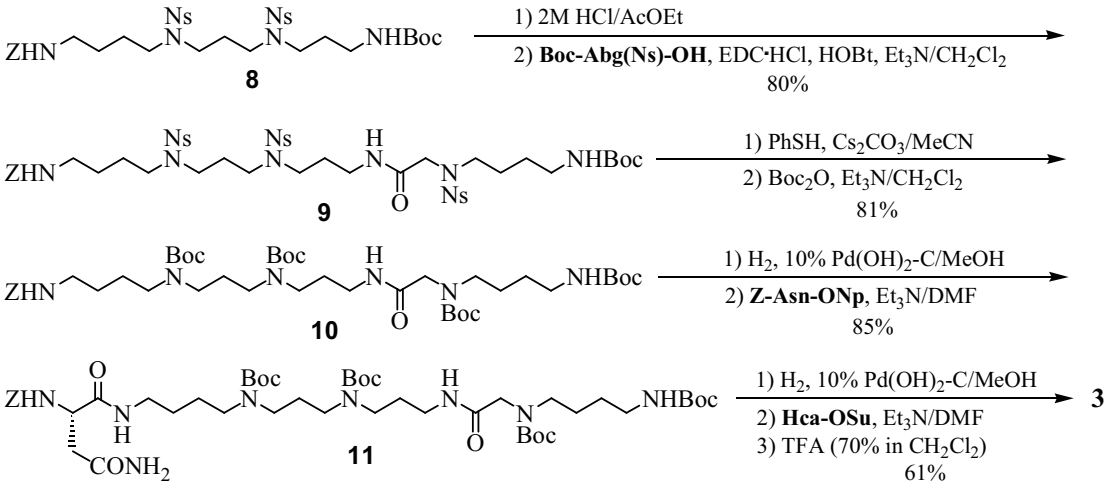

Table 1. Cricket bioassay of the analog **3**

Compounds	ED_{50} (nmol/g b.w.)	95% Confidence Interval (nmol/g b.w.)
NPTX-594 (1)	0.175	0.132 - 0.219
3	0.136	0.107 - 0.179

Table 2. Cricket bioassay of the analogs **4 -7**

Compounds	ED_{50} (nmol/g b.w.)	95% Confidence Interval (nmol/g b.w.)
NPTX-594 (1)	0.276	0.205 - 0.357
4	0.956	0.680 - 1.38
5	16.7	11.8 - 43.7
6	0.385	0.257 - 0.531
7	0.750	0.561 - 1.01

References

1. Wakamiya T, Yamamoto A, Kawaguchi K, Kinoshita T, Yamaguchi Y, Itagaki Y, Naoki H, Nakajima T. *Bull Chem Soc Jpn* **74**: 1743-1749, 2001.
2. Wakamiya T, Kinoshita T, Hattori Y, Yamaguchi Y, Naoki H, Corzo G, Nakajima T. *Bull Chem Soc Jpn* **77**: 331-340, 2004.
3. Hisada M, Fujita T, Naoki H, Itagaki Y, Irie H, Miyashita M, Nakajima T. *Toxicon* **36**: 1115-1125, 1998.
4. Nishimaru T, Sano M, Shimamoto K, Nakajima T, Yamaguchi Y, Wakamiya T. *Peptide Science* (Symposium) Nro 43: 153-154, 2006.

2-07-159

Neurotensin analogs with high affinity and selectivity at human neurotensin receptor 1

Bednarek, Maria A; Tang, Rui; Davis, Amber; Weinberg, David H*

Merck Research Laboratories, UNITED STATES

E-mail: maria_bednarek@merck.com

Introduction

Neurotensin (NTS), pGlu[1]-Leu[2]-Tyr[3]-Glu[4]-Asn[5]-Lys[6]-Pro[7]-Arg[8]-Arg[9]-Pro[10]-Tyr[11]-Ile[12]-Leu[13]-OH, was first isolated in 1973 from bovine hypothalmi and characterized as a tridecapeptide with potent hypotensive activities in anesthetized rats[1]. Subsequent studies in various preclinical models have also implicated neurotensin in several other physiological functions including regulation of analgesia, gastric motility, and modulation of food intake.

Three receptors have been identified which are able to bind neurotensin. Two of these, NTSR1 and NTSR2, are 7 transmembrane domain G protein-coupled receptors, while the third, NTSR3, is a single transmembrane domain protein identical to the trans-Golgi network transmembrane protein sortilin. NTSR1 is expressed primarily in the brain and intestine. NTSR2 is also expressed in the brain, but in regions distinct from NTSR1.

A detailed pharmacological understanding of the receptors has been hampered by a lack of straightforward *in vitro* signal transduction systems. Cell lines which express NTSR1 give reliable and robust readouts and the signaling pathway has been well characterized. In contrast, signaling via NTSR2 is species and system dependent. NTSR3 binds multiple ligands and no signaling pathway has been described for this receptor so far. It is yet not known what physiological role binding of neurotensin to NTSR3 might play.

Herein structure-function studies on NTS are reported which resulted in hNTSR1 peptide agonists of enhanced selectivity with respect to hNTSR2.

Results and Discussion

Analogs of neurotensin (NTS) listed in Tables 1 and 2 were prepared by solid phase syntheses (433A ABI peptide synthesizers). They were subsequently evaluated for their binding affinities to the human neurotensin receptors 1 and 2 in the competitive binding assays using the radiolabeled ligand [^{125}I]Tyr[3]-NTS (hNTSR1 activation data are not reported). Of those peptides, an analog of NTS with Ala in place of Arg[8] (**12**) was a high binding affinity binder to hNTSR1 (IC_{50} about 4 nM) but a rather weak ligand for hNTSR2 (IC_{50} > 1000 nM).

Table 1.

Analogs of neurotensin (NTS)
pGlu[1]-Leu[2]-Tyr[3]-Glu[4]-Asn[5]-Lys[6]-Pro[7]-Arg[8]-Arg[9]-Pro[10]-Tyr[11]-Ile[12]-Leu[13]-OH

No.	Compound	Binding Assay, IC_{50} (nM)		
		hNTS1R	hNTS2R	R2/R1
1	NTS	0.05 ± 0.008	0.87 ± 0.03	17
2	Ac-(4-13)	0.045 ± 0.003	0.51 ± 0.02	10
3	Ac-(5-13)	0.039 ± 0.003	0.19 ± 0.04	5
4	Ac-(6-13)	0.023 + 0.002	0.28 ± 0.05	12
5	Ac-(7-13)	0.12 ± 0.02	1.1 ± 0.4	9
6	Ac-(8-13)	0.33 ± 0.07	2.7 ± 0.8	8
7	Ac-(9-13)	7 ± 1.5	190 ± 50	27
8	(8-13)	0.002 ± 0.0001	0.02 ± 0.002	10
9	(1-12)-NH_2	760 ± 310	>10000	>13
10	(1-11)-NH_2	1900 ± 1600	>10000	>5
11	Gly$^{\delta}$	10.5 ± 6	650 ± 120	60
12	Ala$^{\delta}$	4.4 ± 2	>1000	>220
13	Pro$^{\delta}$	1.8 ± 0.4	920 ± 240	510
14	D-Ala$^{\delta}$	5.6 ± 2.1	510 ± 70	90
15	*D-Pro*$^{\delta}$	*2.5 + 0.6*	*1300 + 80*	*520*
16	D-NMe-Ala$^{\delta}$	0.31 ± 0.27	76 ± 23	240

Table 2.

Analogs of NT(8-13): **Arg^{8}**-Arg^{9}-Pro^{10}-Tyr^{11}-Ile^{12}-Leu^{13}-OH

No.	X^{8}	Affinity Binding Assay, IC_{50} (nM)		
		hNTS1R	hNTS2R	R2/R1
8	Arg^{8}, NTS(8-13)	0.002 ± 0.0001	0.02 ± 0.002	10
17	Ala^{8}	0.02 + 0.006	4.6 ± 0.2	230
18	Pro^{8}	0.06 ± 0.04	3.8 ± 1.2	63
19	D-Pro^{8}	0.06 ± 0.05	4.7 ± 0.5	78
20	D-NMe-Ala^{8}	0.15 ± 0.06	6.8 ± 0.7	45
21	Ac-Ala^{8}	1.9 ± 0.14	950 ± 150	500
22	*Ac-D-Pro*^{8}	*0.23 + 0.08*	*250 + 20*	*1080*

Several other analogs of NTS, in which conformationally constrain or flexible, hydrophobic amino acids were in position 8, also showed similar *in vitro* pharmacological profiles at hNTSR1 and hNTSR2. Additionally, reversal of amino acid chirality in position 8 had a rather negligible effect on peptide binding to hNTSR1 and hNTSR2. For example, Pro^{8}-NTS (**13**) and D-Pro^{8}-NTS (**15**) were both about 2 nM ligands at hNTSR1 and weak micromolar binders to hNTSR2 (IC_{50} > 900 nM). They displayed therefore about 500-fold selectivity for hNTSR1 versus hNTSR2.

pGlu^{1}-Leu^{2}-Tyr^{3}-Glu^{4}-Asn^{5}-Lys^{6}-Pro^{7}-*Pro*^{8}-Arg^{9}-Pro^{10}-Tyr^{11}-Ile^{12}-Leu^{13}-OH (**13**)
pGlu^{1}-Leu^{2}-Tyr^{3}-Glu^{4}-Asn^{5}-Lys^{6}-Pro^{7}-D-*Pro*^{8}-Arg^{9}-Pro^{10}-Tyr^{11}-Ile^{12}-Leu^{13}-OH (**15**)

The shorter analog of NTS which encompasses in its structure the *C*-terminal residues 8 through 13, Arg^{8}-Arg^{9}-Pro^{10}-Tyr^{11}-Ile^{12}-Leu^{13}-OH, NTS(8-13), (**8**), was confirmed[2] to possess *in vitro* pharmacological properties at hNTSR1 practically indistinguishable from those of the full-length NTS (**1**). Peptide **8** was an efficient binder to hNTSR2 as well, and thus, not receptor subtype selective. Replacement of Arg^{8} in NTS(8-13) with Ac-Ala or Ac-D-Pro (**21**,**22**) led to single-nanomolar ligands at hNTSR1 and moderate affinity binders to hNTSR2. Of those compounds, Ac-D-Pro^{8}-NTS (**22**) was more than 1000-fold selective with respect to hNTSR2.

Ac-D-*Pro*^{8}-Arg^{9}-Pro^{10}-Tyr^{11}-Ile^{12}-Leu^{13}-OH (**22**)

References

1. Carraway R, Leeman SE. Isolation of a new hypotensive peptide, neurotensin, from bovine hypothalami. *J Biol Chem* **248**: 6854-6861, 1973.
2. Carraway R, Leeman SE. Structural requirements for the biological activity of neurotensin, a new vasoactive peptide. *Pept Chem Struct Biol Proc. 4th Am Pept Symp* **679-85**, 1975.

2-07-160

Sequence analysis and solid phase synthesis of turtle β-defensin TBD-1

Knappe, Daniel[1,]; Stegemann, Christin[1]; Kolobov, Jr, Alexander[2]; Shamova, Olga[2]; Kokryakov, Vladimir N[2]; Hoffmann, Ralf[1]*

[1]Institute of Bioanalytical Chemistry, Center of Biotechnology and Biomedicine, Leipzig University, GERMANY; [2]Institute of Experimental Medicine, Russian Academy of Medical Sciences, 197376 Saint-Petersburg, RUSSIAN FEDERATION

[*]E-mail: daniel.knappe@bbz.uni-leipzig.de

Introduction

Antimicrobial peptides are produced by all higher organisms as an important component of their host defence. Defensins represent a major subfamily with currently more than 300 members identified, mostly in mammals and birds. They are typically active against Gram-positive and Gram-negative bacteria, fungi and viruses and link innate to adaptive immunity. Here, we describe the solid phase peptide synthesis of a new β-defensin isolated from the European pond turtle *Emy orbicularis* and sequenced by tandem mass spectrometry. Furthermore, the antimicrobial activities of the native and synthesized peptides were studied.

Isolation and *de novo* sequencing

Cationic peptides were isolated from leukocytes of the European pond turtle with acetic acid and purified to homogeneity by combining different gel electrophoretic and chromatographic techniques. The peptide with a monoisotopic mass of 4540.3 Da was active against *Escherichia coli, Listeria monocytogenes, Staphylococcus aureus*, and *Candida albicans* (Table 1). The mass increase of 6 Da after reduction as well as 348.05 Da after alkylation with iodoacetamide revealed six cysteine residues connected by three intramolecular disulfide bridges. After digestion with trypsin, Arg-C and Lys-C the complete 40-residue sequence YDLSKNCRLRGGICYIGKCPRRFFRSGSCSRGNVC CLRFG-NH2 was obtained by combining partial sequences retrieved from fragment ion spectra recorded on MALDI-TOF/TOF, ESI-QqTOF and ESI-IT mass spectrometers using post-source decay (PSD), collision-induced dissociation (CID) or electron-transfer dissociation (ETD) in combination with N-terminal derivatization with 4-sulfophenylisothiocyanate (SPITC)[1] or 2-sulfobenzoic acid cyclic anhydride (SACA)[2] and guanidation of lysine residues.[1]

Peptide synthesis and formation of disulfide bonds

To confirm the sequence of TBD-1 two peptides corresponding to residues 1-18 and 19-40 were synthesized by the Fmoc/^{t}Bu-strategy on solid phase using a multiple peptide synthesizer (Syro 2000, MultiSynTech, Germany) on 4-sulfamino-butyryl aminomethyl resin (Novabiochem, Germany) and TentaGel R resin (Rapp Polymere, Germany), respectively. Cysteine residues were incorporated with three orthogonal side-chain protecting groups, i.e., acetamidomethyl (Acm), *tert*-*tert*-butyl (^{t}Bu), and trityl (Trt) in order to form disulfide bridges between Cys1-Cys5 (Acm), Cys2-Cys4 (^{t}Bu), and Cys3-Cys6 (Trt). After TFA cleavage the two partially protected peptides were purified by RP-HPLC and ligated in 6 mol/L guanidine hydrochloride buffer containing 0.1 mol/L sodium phosphate and 1% thiophenole. After purification by RP-HPLC the first disulfide bond was formed between Cys3 and Cys6 by air oxidation for six days. Quantitative oxidation was confirmed by ESI-MS displaying the expected mass and isotope pattern. Iodine/DMSO oxidation[3] and a thermodynamically controlled

Table 1. Antimicrobial activities of native TBD-1 determined in an agar diffusion assay as minimal inhibitory concentration (MIC) in µmol/L (n.d.: not determined, +: active)

	E. coli	*Klebsiella pneumoniae*	*S. aureus*	*L. monocytogenes*	*Bacillus subtilis*	*Candida albicans*
Native TBD-1	0.65	n.d.	5.6	0.65	n.d.	5.2
Synthetic TBD-1	+	+	+	n.d.	+	n.d.

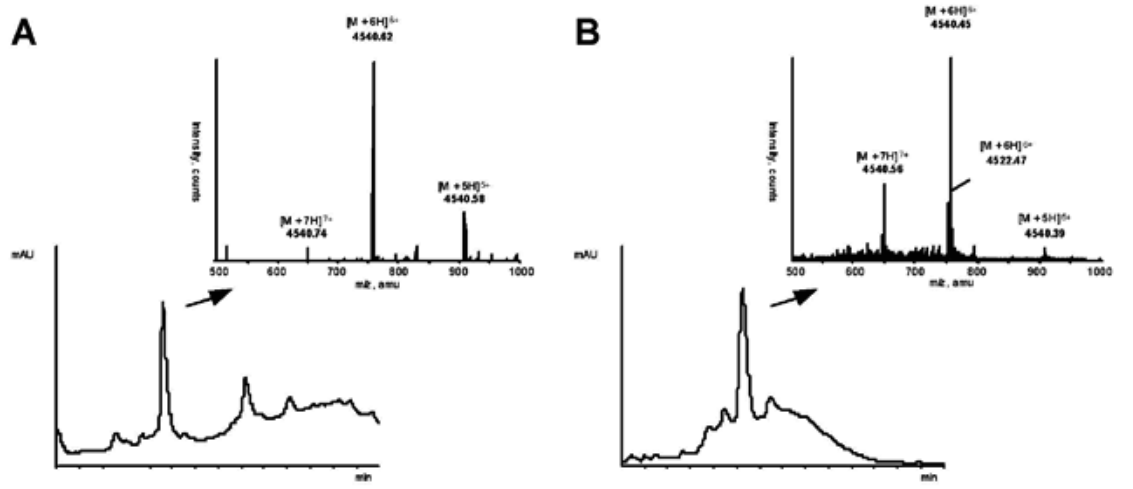

Figure 1. RP-HPLC chromatograms (bottom) of the final TBD-1 peptides obtained by the iodine/DMSO- (panel A) or one-pot-oxidation strategy (panel B) and electrospay mass spectra (top) of the obtained main fractions.

DMSO one-pot-oxidation[4] were applied alternatively to selectively remove ^{t}Bu and Acm protecting groups and form the two remaining disulfide bonds specifically (Fig. 1).

The overall yield for the iodine oxidation was only 1% pure peptide calculated from the amounts of the purified ligation product, whereas 10% were obtained for the temperature-controlled one-pot-oxidation strategy. However, this product was contaminated with TBD-1 analogues possessing different disulfide patterns coeluting with or eluting very close to the targeted peptide (Fig. 1B). Both native and synthesized TBD-1 showed antimicrobial activities in a radial agar diffusion assay (Table 1) against a panel of Gram-positive and Gram-negative bacteria as well as *C. albicans*. The activity of the synthetic peptide confirmed both the correct sequence analysis of TBD-1 and its correct synthesis on solid phase including the disulfide pattern.

Discussion

The first reptile *β*-defensin isolated from leukocytes of turtle was successfully sequenced by a combination of different mass spectrometrical techniques and successfully synthesized on solid phase by native chemical ligation. The typical disulfide pattern of *β*-defensins was specifically formed by two alternative oxidation strategies, which was finally confirmed by the antimicrobial activities against *K. pneumoniae, E. coli, B. subtilis,* and *S. aureus*.

Acknowledgements

Financial support by the European Fond for Regional Structure Development (EFRE, European Union and the Free State Saxonia) is gratefully acknowledged.

References

1. Samyn B, Debyser G, Sergeant K, Devreese B, Van Beeumen J. A case study of de novo sequence analysis of N-sulfonated peptides by MALDI TOF/TOF mass spectrometry. *J Am Soc Mass Spectrom* **15**: 1838-1852, 2004.
2. Chen P, Nie S, Mi W, Wang XC, Liang SP. De novo sequencing of tryptic peptides sulfonated by 4-sulfophenyl isothiocyanate for unambiguous protein identification using post-source decay matrix-assisted laser desorption/ionization mass spectrometry. *Rapid Commun. Mass Spectrom* **18**: 191-198, 2004.
3. Schulz A, Kluver E, Schulz-Maronde S, Adermann K. Engineering disulfide bonds of the novel human beta-defensins hBD-27 and hBD-28: Differences in disulfide formation and biological activity among human beta-defensins. *Biopolymers (Peptide Science)* **80**: 34-49, 2005.
4. Cuthbertson A, Indrevoll B. A method for the one-pot regioselective formation of the two disulfide bonds of alpha-conotoxin SI. *Tetrahedron Lett* **41**: 3661-3663, 2000.

2-07-161

Trichogin GA IV is able to bind Ca(II) and lanthanide ions

Gatto, Emanuela[1]; Stella, Lorenzo[1]; Bocchinfuso, Gianfranco[1]; Palleschi, Antonio[1]; Formaggio, Fernando[2]; Toniolo, Claudio[2]; Venanzi, Mariano[1,]*

[1]University of Rome "Tor Vergata", Department of Chemical Sciences and Technologies, ITALY; [2]University of Padova, 35131 Padova, ICB-CNR, Padova Unit, Department of Chemistry, ITALY

[*]E-mail: venanzi@uniroma2.it

Introduction

Conformationally-constrained oligopeptides are promising candidates as novel smart materials, because of their ability to fold into specific structures, to transport ions and small molecules, to transfer or storage energy or electrons. In particular, peptide complexes with metal ions are actively explored for potential application in medical diagnostics, drug discovery, imaging, and bioanalytical assays.

We are currently studying the ion binding properties of trichogin GA IV, the prototype of a family of peptide antibiotics named lipopeptaibols, showing interesting antimicrobial activity. We report here on the interactionof Ca(II), Gd(III) and Tb(III) ions with a leucine methyl ester analogue of trichogin GAIV, the sequence of which is *n*-Oct-Aib-Gly-Leu-Aib-Gly-Gly-Leu-Aib-Gly-Ile-Leu-OMe (TrGA).

Results and Discussion

X-Ray diffraction studies on TrGA showed that the first few residues at the N-terminus adopt a right-handed 3_{10}-helix, while the rest of the peptide chain forms a distorted, right-handed α-helix. We have recently shown that an equilibrium between helical conformers and more compact, folded conformers takes place in solution with a transition dynamics in the microsecond time scale.[1]

CD titrations of TrGA with Ca(II), Gd(III) and Tb(III) indicate that ion binding promotes a conformational transition, as clearly shown by the related CD spectra at different ion-peptide total molar concentration ratios (r=[Me]/[TrGA]) reported in Fig. 1. At high r values the CD curves of the ion-peptide complexes showed a positive maximum at λ=214 nm, typical of type II β-turns, suggesting a high population of bent structures. The quasi-isodichroic point, found for all systems between 198 and 202 nm, indicates that an equilibrium between extended helical conformations and β-turn rich structures actually takes place. Interestingly, while the peptide complex with Ca(II) showed molar ellipticities at 214-216 nm around 1·104 deg·cm^{2}·dmol^{-1}, Tb(III) and Gd(III) exhibit definitely higher molar ellipticities ([θ]= 4·104 and 6·104 deg·cm2·dmol-1, respectively), as a result of the larger conformational effect caused by binding of the three-fold charged lanthanide ions. Moreover, we found that TrGA did not bind K+ or Na+, emphasizing the selectivity of the peptide-ion interaction.

Titration of Tb(III) with TrGA showed an enhanced luminescence intensity of the lanthanide ion, ascribable

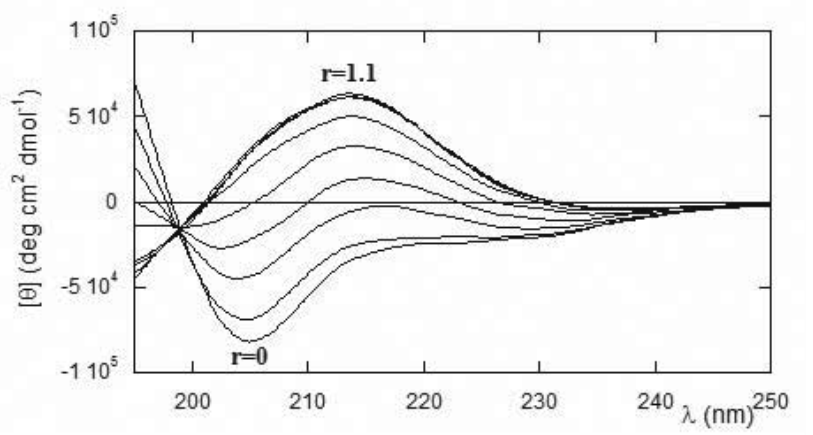

Figure 1. CD spectra of trichogin GA IV at different ion/peptide ratios (r=[Gd(III)]/[TrGA]) in acetonitrile.

to the release of water molecules from the Tb(III) coordination shell upon formation of the ion-peptide complex. The characteristic emission of Tb(III), featuring three narrow bands between 480 and 600 nm, makes this ion extremely useful for sensing and molecular recognition processes. A combined approach of molecular mechanics and molecular dynamics simulations reveals that ion-binding gives rise to a peptide loop involving the *C*-terminal helix.

These results indicate that trichogin GAIV can be used to enhance the contrast properties of Gd(III) in magnetic resonance imaging and the emission intensity f Tb(III) as luminescent probe, making these complexes promising tools for biochemical assays and biomedical imaging.

Acknowledgement

This project was supported by the Italian Ministry of University and Research (PRIN 2006).

References

1. Venanzi M, Gatto E, Bocchinfuso G, Palleschi A, Stella L, Formaggio F, Toniolo C. *ChemBioChem* **7**: 43-45, 2006.

2-07-162

Three-dimensional structure and mechanism of action of an antifungal peptide generated from hemocyanin cleavage in a penaeid shrimp

Petit, Vanessa[1]; Blond, Alain[1]; Djediat, Chakib[2]; Peduzzi, Jean[1]; Dupont, Joëlle[3]; Bachère, Evelyne[4]; Destoumieux-Garzón, Delphine[4]; Rebuffat, Sylvie[1,]*

[1]Muséum National d'Histoire Naturelle, UMR 5154 CNRS, FRANCE; [2]Muséum National d'Histoire Naturelle, Service de microscopie électronique, FRANCE; [3]Muséum National d'Histoire Naturelle, Unité Toxonomie - Collections, FRANCE; [4]Université Montpellier II, UMR 5119 CNRS Ifremer, FRANCE

[*]E-mail: rebuffat@mnhn.fr

Introduction

An antifungal peptide, PvHCt, which corresponds to the 23 amino acid *C*-terminal sequence of the shrimp respiratory protein hemocyanin, has been previously identified in the plasma of the penaeid shrimp *Litopenaeus vannamei*.[1] It has a broad spectrum of antifungal activity (minimum inhibitory concentrations (MICs) in the range 3-50 μM), the shrimp pathogen *Fusarium oxysporum* being particularly sensible. This activity would be based on the inhibition of spore germination.[1] PvHCt is generated by proteolytic cleavage in response to a microbial challenge. Similarly, a *C*-terminal fragment of hemocyanin displaying antimicrobial activity has been isolated from crayfish plasma.[2] These peptides are believed to contribute to the crustacean defence. The phenomenon of *in vitro* antimicrobial peptide generation from a respiratory pigment already observed with hemoglobin,[3] thus appears not to be restricted to mammals.

To contribute to the elucidation of the mechanism of PvHCt antifungal activity, we determined its three-dimensional structure by circular dichroism (CD), NMR and molecular modelling. We examined its effects on the *F. oxysporum* spore ultrastructure by transmission electron microscopy (TEM) and investigated the subsequent permeabilization of *F. oxysporum* cell membranes, using SYTOX Green uptake.

Results and discussion

CD experiments showed that PvHCt is unfolded in aqueous environment, while it has a high α-helix content in organic solvent and in dodecylphosphocholine (DPC) micelles used to mimic biological membranes. PvHCt solution structure consists of an α-helix spanning the region G8 to G18, which is stabilized by hydrogen bonds involving CO(i) and NH(i+4) groups. This peptide has a marked amphipathic character and shows well-defined basic and aromatic sectors (Fig. 1).

PvHCt inhibits both spore germination (50 μM) and hyphal growth (100 μM) of *F. oxysporum*. TEM showed that PvHCt induces changes of the ultrastructure of *F. oxysporum* spores with a disorganization of the cytoplasm, a significant decrease of lipid bodies and structural changes of the plasma membrane. *F. oxysporum* cell membrane permeabilization by PvHCt was shown using SYTOX Green, an organic compound that fluoresces upon interaction with nucleic acids after penetration into cells with compromised plasma membranes.[4] *F. oxysporum* spores and hyphae showed strong SYTOX Green fluorescence in the cytosol, especially localized in the nuclei (Fig. 2).

Therefore, TEM and fluorescence microscopy experiments show that PvHCt permeabilizes the plasma membrane of the fungus *F. oxysporum*, presumably by forming pores or channels.

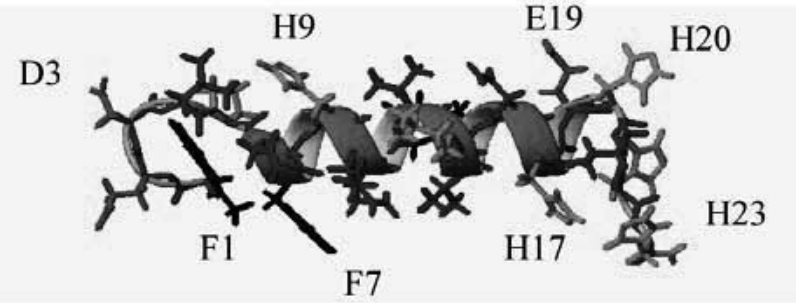

Figure 1. Helical PvHCt structure displaying the side chain orientation.

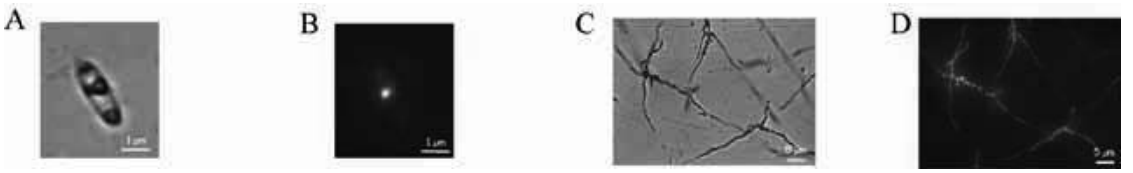

Figure 2. Detection of PvHCt-induced SYTOX Green uptake by fluorescence microscopy. *F. oxysporum* spore (A: Light-field microscopy; B: Fluorescence microscopy) and *F. oxysporum* hyphae (C: Light-field microscopy; D: Fluorescence microscopy) treated with PvHCt in the presence of SYTOX Green.

Acknowledgments

We thank the NMR, TEM and photonic microscopy (CeMIM) facilities of the National Museum of Natural History (Paris) for access to the instruments. We are grateful to Marc Gèze for the fluorescence microscopy experiments.

References

1. Destoumieux-Garzón D, Saulnier D, Garnier J, Jouffrey C, Bulet P, Bachère E. *J Biol Chem* **276**: 47070-47077, 2001.
2. Lee SY, Lee BL, Söderhäll K. *J Biol Chem* **278**: 7927-7933, 2003.
3. Mak P, Wójcik K, Wicherek L, Dubin A. *Peptides* **25**: 1839-1847, 2004.
4. Thevissen K, Terras FR, Broekaert WF. *Appl Environ Microbiol* **65**: 5451-5458, 1999.

2-07-163

Structural studies on human neuropeptide FF

Thuau, Romain[1]; Ségalas-Milazzo, Isabelle[1]; Chartrel, Nicolas[2]; Coadou, Gaël[1]; Lameiras, Pedro[1]; Davoust, Daniel[1]; Guilhaudis, Laure[1,]*

[1]Université de Rouen, UMR 6014 CNRS, IFRMP 23, FRANCE; [2]Université de Rouen, INSERM U413, IFRMP 23, FRANCE

[*]E-mail: laure.guilhaudis@univ-rouen.fr

Introduction

Neuropeptide FF (NPFF), a member of the RFamide family of peptides, appears to play an important role in pain modulation.[1] It has been reported to possess pronociceptive and analgesic activities as well as pro- and anti-opioid effects according to its mode of administration. These contradictory effects seem to result from its capacity to bind two different G protein-coupled receptors: NPFF1 and NPFF2 even though many studies favor NPFF2 as NPFF physiological receptor. Structure activity relationship (SAR) studies using NPFF analogs and derived peptides have shown that the *C*-terminal part of the molecule (PQRF-NH_2) is essential for affinity.[2] However, some of the key features for ligand recognition by NPFF receptors are still missing to design highly selective molecules. NPFF binding to its receptors occurs in the membrane environment and membrane contact is proposed to induce structural modifications onto the peptide, providing a bioactive conformation recognized by the receptor.[3] In order to provide further insight into ligand recognition, we have investigated the solution conformation of human NPFF (hNPFF) by circular dichroism (CD), NMR spectroscopy and molecular modeling in different media. Water and water/organic solvent mixtures were used to mime the extracellular medium while dodecylphosphocholine (DPC) micelles served as a membrane mimetic medium.

Results and discussion

CD and NMR showed that (1) in the presence of methanol or trifluoroethanol, turn-like elements are present in the *C*-terminal region of hNPFF structure, and (2) a secondary structure is stabilized in DPC micelles/water mixture, a membrane-interface mimetic environment. The 3D structure of hNPFF bound to DPC micelles was thus solved by molecular modeling under NMR restraints. 71 distance restraints supplemented with 4 φ angles were used for the calculations. Analysis of the dihedral angles revealed a good convergence for residues 4-8 (Fig. 1). The average φ/ψ values as well as the hydrogen bond pattern indicated that hNPFF membrane-induced structure was composed of two interlaced β-turns encompassing residues Q4 to R7 and P5 to F8 respectively.

It has been shown by structure-activity relationships

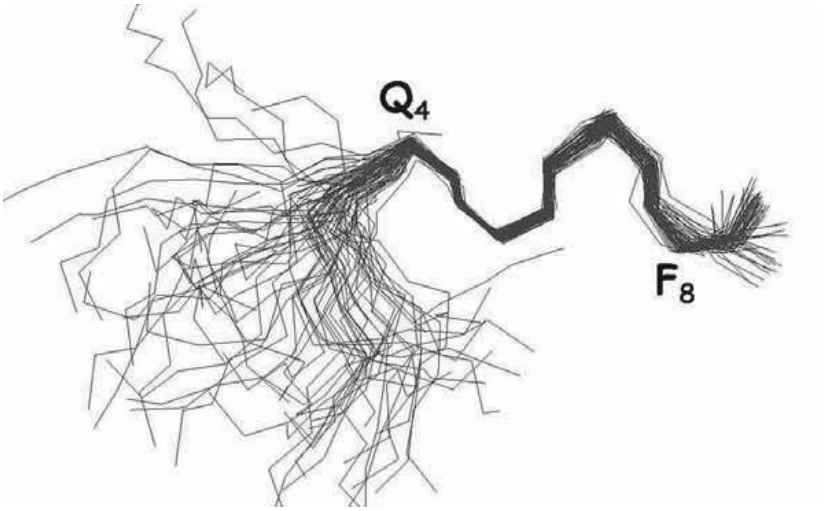

Figure 1. Superimposition of hNPFF 66 final structures between residues Q4 and F8 on backbone atoms (N, Cα, C').

studies[2,4] that PQRF-NH_2 is a core structure essential for binding to NPFF receptors. The β-turn involving residues P5 to F8 of hNPFF could, therefore, constitute a secondary structure important for receptor recognition. The *C*-terminal tetrapeptide is not sufficient to exhibit agonistic activity and the presence of the last six residues is necessary to observe a moderate activity towards NPFF2. In DPC/water mixture, hNPFF structure is composed of two interlaced type β-turns (Q4-R7 and P5-F8) which provide an amphipathic character to the *C*-terminal hexapeptide with hydrophobic side-chains on one side and hydrophilic side-chains on the other side. Such a correlation suggests that hNPFF "membrane bound" 3D structure could constitute a valuable starting point to generate hNPFF pharmacophoric models. These models may help the rational design of new agonists or antagonists for NPFF receptors.

Acknowledgements

NMR spectrometers were supported by grants of the Conseil Régional de Haute-Normandie (France). NMR and Molecular Modelling facilities were provided by the Centre de Ressources Informatiques de Haute-Normandie. The authors also thank the CRUNCh network for financial support.

References

1. Yang HY, Tao T, Iadarola MJ. *Neuropeptides* **42**: 1-18, 2008.
2. Vyas N, Mollereau C, Chevé G, McCurdy CR. *Peptides* **27**: 990-996, 2006.
3. Schwyzer R. *Biopolymers* **31**: 785-792, 1991.
4. Yoshida H , Habata Y, Hosoya M, Kawamata Y, Kitada C, Hinuma S. *Biochim Biophys Acta* **1593**: 151-157, 2003.

2-07-164

Structural comparison of μ-opioid receptor selective peptides and peptidomimetics revealed four important conformational parameters of bioactivity

Borics, Attila; Tóth, Géza*

Biological Research Center of the Hungarian Academy of Sciences, Institute of Biochemistry HUNGARY

**E-mail: aborics@brc.hu*

Introduction

Structural determinants of binding to the μ-opioid receptor (MOR) – an important target in analgesia - attracts great scientific attention. Many natural and synthetic peptides and peptidomimetics[1-4] were shown previously to bind to the MOR selectively and several pharmacophores were determined but there is no consensus about what structure is responsible for such biological activity.[5] No high resolution structure or reliable model of this receptor is available and the binding site is not exactly known despite numerous site-directed mutagenesis studies. This suggests that the determination of structural aspects of μ-opioid activity should focus on the ligands. MOR ligands with similar affinity should possess at least one common structural feature in which they differ from other ligands of different affinity. Comparative structural analysis of such ligands, considering adequate representation of binding conditions may reveal key features of bioactivity.

In this study ten MOR ligands (Table 1), including β-amino acid[6] or β-turn inducing pseudo dipeptide[7] (Fig. 1) containing endomorphin-1 and 2 analogues were examined using molecular dynamics (MD). This small pool of ligands can be divided into three groups of different MOR affinity. Conformational preference of the elements of these groups was determined in aqueous and DMSO media. Compared to water DMSO has higher viscosity and a lower relative permittivity which may be a closer approximate of the physical properties of biological environments. Furthermore, structure destabilizing effect of DMSO may help reveal intrinsic conformational preferences. Since the spatial orientation of pharmacophore groups determine the ability of ligands to bind to the receptor and this orientation is primarily governed by backbone and side-chain conformations, in our analysis we focused on these structural parameters.

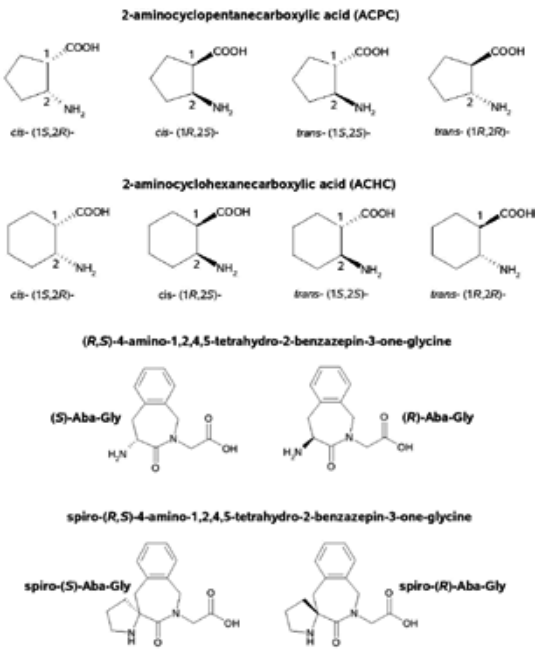

Figure 1. Alicyclic β-amino acids (upper) and β-turn inducing pseudo-dipeptides (lower).

Results

The populations of structures identified by the analysis of specific intramolecular H-bonds did not show direct correlation with biological data, neither in H_2O nor in DMSO. Although, it was found that these peptides may adopt bent structure with high propensity, in accordance with earlier observations.[3-4] Analysis of side chain rotamer populations revealed, that trans conformation of the χ^1 dihedral angle of the Tyr^1 side chain, *gauche*- conformation of χ^1 of the aromatic side chain in the third position and the relatively high flexibility of the 4th aromatic side chain is advantageous for binding to the μ-opioid receptor. Table 2 shows the graphic representation of how well each ligand conforms to these aforementioned criteria of bioactivity. In H_2O there is only weak correlation, but for results obtained by simulations in DMSO very good correlation was found between structural and biological data.

Conclusions

The following four parameters were confirmed as potential conformational requirements of MOR activity: 1. trans conformation of Tyr^1 χ^1, 2. *gauche*- conformation of Ar^3 χ^1, 3. flexibility of Ar^4 χ^1, 4. bent backbone structure. Constellation of these parameters results most likely in high MOR affinity. Incorporation of these parameters as chemical constraints may be a profitable strategy in the design of new μ-opioid ligands. Results presented

here confirm previous observations of structure and activity.[3-4] Results indicate that the physical conditions or the environment of binding to the μ-opioid receptors are better approximated by DMSO than by H_2O.

Methods

MD simulations were performed using the AMBER 9 program package and the AMBER ff99 force field parameter set. Parameters for unnatural amino acid residues were supplemented from the generalized AMBER force field (gAFF). Partial charges were determined on the HF/6-31G(d) level using the RESP method. Peptides were immersed in a truncated octahedral box of TIP3P water or DMSO[8] molecules where box sides were at least 10 Å from the closest atom of the solute. Charged N-termini of peptides were neutralized by Cl^- ions. All systems were subjected to steepest descent energy minimization followed by 100 ps NVT molecular dynamics having the peptide restrained to the center of the box to allow solvent density to equilibrate. 50.25 ns NPT molecular dynamics was then performed for each system at constant temperature (300 K) and pressure (1 bar), with the following parameters: the time step was 2 fs; the SHAKE algorithm was used to constrain all bonds to their correct length; temperature was regulated with the weak coupling algorithm and pressure was maintained using isotropic scaling. Non-bonded interactions were calculated using the PME method with all cutoff values set at 10 Å. The dielectric constant of the system was set to 78.0 and 48.0 for water and DMSO, respectively. For each peptide three simulations were started either from extended, γ-turn or β-turn or bent structures. The coordinates of the system were stored after every 2 ps and trajectories were combined having their first 250 ps excluded which were regarded as equilibration period. This resulted in 150 ns trajectories of 75000 sampled conformations for each peptide.

Acknowledgments

This work was supported by Hungarian OTKA PD-73081 and LSHC-CT-2006-037733 "NORMOLIFE" grants.

References

1. Zadina JE, Hackler L, Ge LJ, Kastin AJ. *Nature* **386**: 499-502, 1997.
2. Tóth G, Keresztes A, Tömböly Cs, Péter A, Fülöp F, Tourwé D, Navratilova E, Varga É, Roeske WR, Yamamura HI, Szűcs M, Borsodi A. *Pure Appl Chem* **76**: 951-957, 2004.
3. Hruby VJ, Agnes RS. *Biopolymers* **51**: 391-410, 1999.
4. Janecka A, Kruszynski R. *Curr Med Chem* **12**: 471-481, 2005.
5. Leitgeb B. *Chem Biodivers* **4**: 2703-2724, 2007.
6. Keresztes A, Szűcs M, Borics A, Kövér K, Forró E, Fülöp F, Tömböly Cs, Péter A, Páhi A, Fábián G, Murányi M, Tóth G. *J Med Chem* **51**: 4270-4279, 2008.
7. Tömböly Cs, Ballet S, Feytens D, Kövér K, Borics A, Lovas S, Al-Khrasani M, Fürst Zs, Tóth G, Benyhe S, Tourwé D. *J Med Chem* **51**: 173-177, 2008.
8. Fox T, Kollman PA. *J Phys Chem B* **102**: 8070-8079, 1998.

	peptide	sequence	receptor affinity (K_i^{MP}/nM)	selectivity (K_i/K_i)
1	EM-1	H-Tyr-Pro-Trp-Phe-NH_2	0-10	>1000
2	EM-2	H-Tyr-Pro-Phe-Phe-NH_2	0-10	>1000
3	DAMGO	H-Tyr-D-Ala-Gly-*N*-Me-Phe-Gly-ol	0-10	1000-100
4	(1*S*,2*R*)-ACHC[2]-EM-2	H-Tyr-(1*S*2*R*)-ACHC-Phe-Phe-NH_2	0-10	1000-100
5	Tyr-W-MIF-1	H-Tyr-Pro-Trp-Gly-NH_2	10-100	1000-100
6	(*R*)-spiro-Aba[2]-Gly[3]-EM-2	H-Tyr-(*R*)-spiro-Aba-Gly-Phe-NH_2	10-100	>1000
7	Morphiceptin	H-Tyr-Pro-Phe-Pro-NH_2	10-100	1000-100
8	(1*R*,2*R*)-ACPC[2]-EM-1	H-Tyr-(1*R*2*R*)-ACPC-Trp-Phe-NH_2	10-100	100-10
9	(1*R*,2*S*)-ACHC[2]-EM-2	H-Tyr-(1*R*2*S*)-ACHC-Phe-Phe-NH_2	100-1000	>1000
10	(*S*)-Aba[2]-Gly[3]-EM-2	H-Tyr-(*S*)-Aba-Gly-Phe-NH_2	100-1000	<10

Table 1. μ-Opioid receptor ligands of different affinity and selectivity

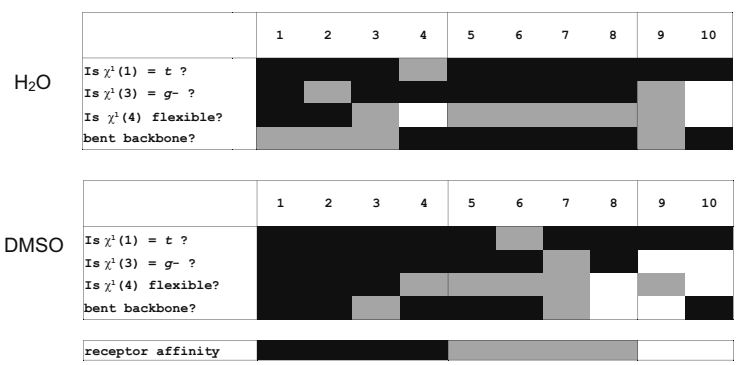

Table 2. Visual representation of the conformity of the obtained structural parameters to the newly introduced criteria of μ-opioid activity

Numbering of compounds is in accordance with the numbering in Table 1. For receptor affinity as well as for the conformity with structural requirements the colors represent: black = high, grey = moderate, white = low / none.

2-07-165

Novel chitosan-pexiganan conjugate for the treatment of infected diabetic foot ulcers: synthesis and characterization by FTIR and AAA

Batista, Mary[1]; Adeva, Alberto[2]; Gallemí, Marçal[3]; Gomes, Carlos[4]; Gomes, Paula[3,]*

[1]CIQUP, University of Porto and LAQUIPAI, University of Porto, PORTUGAL; [2]Barcelona Science Park, University of Barcelona, SPAIN; [3]CIQUP, University of Porto, PORTUGAL; [4]LAQUIPAI, University of Porto, PORTUGAL

[*]E-mail: pgomes@fc.up.pt

Pexiganan (or MSI-78) is a 22-amino acid linear analogue of magainin-2, a natural antimicrobial peptide isolated from the skin of the African clawed frog, Xenopus laevis.[1] Pexiganan is remarkably effective against more than 3000 species of Gram positive and Gram negative bacteria that cause infections on skin and soft tissues, including methicillin-resistant Staphylococcus aureus (MRSA), and has no propensity to induce bacterial resistance. The large and ever-growing incidence of diabetes in Northwestern countries, together with the lack of valuable topical antimicrobials to treat infected diabetic foot ulcers, explains the recent (October 2007) acquisition by the U.S. Pharma Corporation MacroChem of the exclusive option to license pexiganan worldwide.[2] This was followed by the latest press release on new Phase III clinical trials promoted by this company that confirm the efficacy of pexiganan to be statistically equivalent to that of oral antibiotic therapy (ofloxacin).[3] In view of the above, we decided to breakthrough to the preparation of a novel chitosan-pexiganan conjugate with potential application in the topical treatment of infected diabetic foot ulcers. Such conjugate will hopefully combine the excellent antimicrobial properties of pexiganan with the well-known biocompatibility and skin-injury-healing ability of chitosan.[4-6] To this purpose, we prepared a pexiganan analogue having an additional *C*-terminal Ala-Ala-Cys stretch in order to covalently attach the peptide to the biopolymer through regiosselective thiol-amine crosslinking promoted by Sulfo-EMCS,[7] as depicted on Scheme 1.

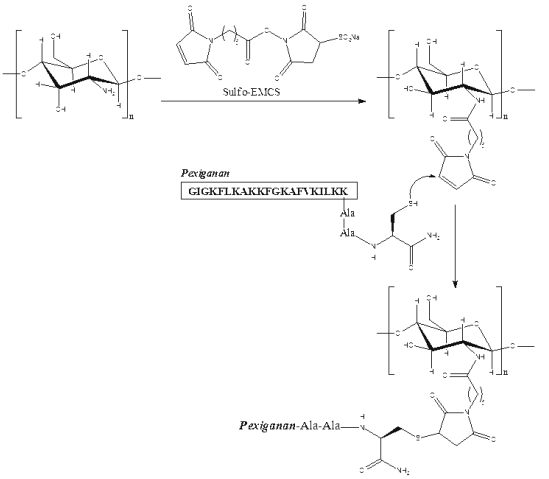

Scheme 1. Covalent attachment of Pexiganan-Ala_2Cys to chitosan amino groups by means of the Sulfo-EMCS cross-linker

The target peptide was synthesized manually on a Fmoc-Rink-MBHA resin by standard Fmoc/tBu SPPS, isolated from the crude mixture by preparative HPLC and characterized by analytical HPLC, AAA and MALDI-TOF MS (data not shown). Chitosan was reacted with Sulfo-EMCS by similar methods as those described for identical amine surface modifications,[8] the polymer solution dialysed against PBS over 1 day and them immediately reacted with the peptide. The final mixture was dialyzed against PBS over 2 days and then against deionized water over 3 days, after which it was freeze-dried and characterized by FT-IR spectroscopy (Fig. 1) and amino acid analysis (Table 1). The FT-IR spectrum of the peptide conjugate (Fig. 1B), while still displaying the characteristic bands due to the polysacharide chains (O–H bending at 1252 cm^{-1}, *C–O* stretching at 1079 cm^{-1}, *C–O–C* stretching vibration in the glucopyranose ring at 1036 cm^{-1} and the specific bands of the $\beta(1\rightarrow4)$ glycoside bridge at 1153 cm^{-1} and 899 cm^{-1}),[9,10] it also exhibits significant differences as compared to the spectrum of chitosan (Fig. 1A). Namely, the large and intense *O–H* + *N–H* stretching band has its maximal absorption shifted down to 3289 cm^{-1} (=-87 cm^{-1}), which certainly reflects the significant contribution from N–H stretching vibrations due to the primary amino groups from the N-terminal amino acid and Lys side-chains (10 groups/peptide chain) and to the amide bonds (25 secondary plus 1 primary amide groups/peptide chain); this interpretation is reinforced by the changes registered in the amide I and amide II bands, whose relative intensities are dramatically changed from Fig. 1A to Fig. 1B, as these are the two most intense bands in the spectrum of the conjugate, but not in the spectrum of unmodified chitosan; the wavenumbers for the amide I and amide II bands are also different in the conjugate, where they appear at 1653 (=+8 cm^{-1}) and 1541 cm^{-1} (=-16 cm^{-1}), respectively. Finally, differences in the *C–H* stretching region are also noteworthy: in contrast to what is observed in the spectrum of chitosan, that of the conjugate exhibits three perfectly defined bands at 3060, 2950 e 2892 cm^{-1}, attributed to *C–H* stretching vibrations

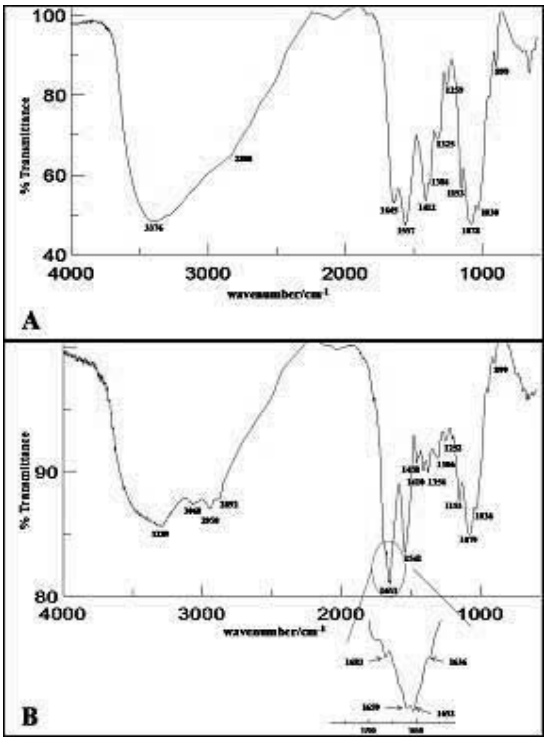

Figure 1. FTIR spectra (solid suspensions in KBr; 32 scans) of chitosan (A) and the pexiganan-chitosan conjugate (B).

Table 1.

Amino acid residue[a)]	Concentration[b)] /mM	relative proportion	
		Experimental	*Expected*[c)]
Gly	0.4240	3.25	3
Ala	0.5230	4.00	4
Val	0.1271	0.97	1
Ile	0.2461	1.88	2
Leu	0.2596	1.99	2
Phe	0.3899	2.98	3
Lys	1.661	8.93	9

a) Cys was not considered, as its quantitation by AAA is not reliable;

b) in injected sample, after known dilutions of the original hydrolysate;

c) from the Pexiganan-Ala-Ala-Cys amino acid sequence.

in, respectively, aromatic, methylene and methyl groups, most probably from the side chains of the aromatic amino acid Phe (3/peptide chain) and of aliphatic amino acids such as Leu, Ile, Val, Ala and Lys. *C–C* (aliphatic and aromatic) stretching vibrations are hindered by amide I and II bands, but a *C–C* in-ring stretching, typical of aromatics, can still be distinguished at 1458 cm^{-1}.

AAA was done on the acid hydrolysate of the peptide-chitosan conjugate, providing successful identification of the expected amino acid residues in correct proportions (Table 1). Calculations from AAA quantitation allowed determining that the polymer's degree of substitution (i.e., extent of peptide's attachment to the polymer matrix) was of about 60% (not shown). Ongoing biological studies involving this novel conjugate will be timely reported.

References

1. Ge Y, McDonald D L, Holroyd K J, Thornsberry C, Wexler, H & Zasloff M. In vitro antibacterial properties of Pexiganan, an analog of Magainin. Antimicrob. Agents Chemother. **43**: 782-8, 1999.
2. http://www.entrepreneur.com/tradejournals/article/168795681.html
3. (a) http://www.bio-medicine.org/medicine-technology-1/MacroChem-Announces-Presentation-of-Pexiganan-Phase-3-Study-Results-for-Topical-Treatment-of-Diabetic-Foot-Infection-1515-1/; (b) Batista MKS, Marçal Gallemí M, Adeva A, Gomes CAR, Gomes P. *Synthetic Commun* **39** (7): 1228-1240, 2009.
4. Ping H, Davies SS, Illum S. In vitro evaluation of the mucoadhesive properties of chitosan microspheres. *Int J Pharm* **166:** 75-88, 1998.
5. Bernkop-Schnürch A. Chitosan and its derivatives: potential excipients for peroral peptide delivery systems. *Int J Pharm* **194:** 1-13, 2000.
6. Berger J, Reist M, Mayer J M, Felt O, Peppas N A, Gurny R. Structure and interactions in covalently and ionically crosslinked chitosan hydrogels for biomedical applications. *Eur J Pharm Biopharm* **57:** 19-34, 2004.
7. Masuko T, Minami A, Iwasaki N, Majima T, Nishimura S-I, Lee YC. Thiolation of chitosan. Attachment of proteins via thioether formation. *Biomacromolecules* **6:** 880-884, 2005.
8. Xiao S-J, Wieland M, Brunner S. Reactions of surface amines with heterobifunctional cross-linkers bearing both succinimidyl ester. *J Coll Interface Sci* **290:** 172-183, 2005.
9. Batista MKS, Pinto LF, Gomes CAR, Gomes P. Novel highly-soluble peptide-chitosan polymers: synthesis and spectral characterization. *Carbohydr Polym* **64:** 299-305, 2006.
10. Gomes P, Gomes CAR, Batista MKS, Pinto LF, Silva P. Synthesis, structural characterization and properties of water-soluble N-(γ-propanoyl-amino acid)-chitosans. *Carbohydr Polym* **71:** 54-65, 2008.

2-07-166

Synthesis and biological activities of endomorphin-2 analogues containing Pro mimics

Tsuda, Yuko[1]; Miyazaki, Anna[2]; Yamada, Takashi[3]; Isozaki, Kaname[4]; Shimohigashi, Yasuyuki[4]; Ambo, Akihiro[5]; Sasaki, Yusuke[5]; Minour, Katsuhiko[6]; In, Yasuko[6]; Ishida, Toshimasa[6]; Okada, Yoshio[2]

[1]Kobe Gakuin University, Faculty of Pharmaceutical Sciences/LSC, JAPAN; [2]Kobe Gakuin Universit, Faculty of Pharmaceutical Sciences, JAPAN; [3]Konan University, Faculty of Science and Engineering, JAPAN; [4]Kyushu University, Faculty and Graduate School of Science, JAPAN; [5]Tohoku Pharmaceutical University, JAPAN; [6]Osaka University of Pharmaceutical Sciences, JAPAN

[*]E-mail: tsuda@pharm.kobegakuin.ac.jp

Introduction

Endomorphin-2 (EM-2: H-Tyr-Pro-Phe-Phe-NH_2) has high affinity and selectivity for the mu-opiod receptor.[1] We focus on the role of Pro residue, which imposes strong restraints on the conformation of the peptide backbone chain or induces *cis-trans* isomerization around the X-Pro bond. We substituted Pro with Azetidine-2-carboxylic acid (Aze) or Piperidine-2 or 4-carboxylic acids [Pip(2) or Pip(4)] to increase or decrease the rigidity. In this paper, we deal with the synthesis of EM-2 analogues containing Aze, Pip(2) or Pip(4) and the evaluation of the biological functions of the analogues on the opioid receptors. Furthermore we describe the conformational properties of EM-2 and [Dmt[1]]EM-2 in DMSO by using NMR spectroscopy and molecular modeling calculations.

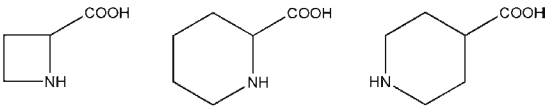

Figure 1. Structures of Azetidine-2-caroxylic acid (Aze) and Piperidine carboxylic acid [Pip(2) and Pip(4)].

[Dmt[1]]EM-2. On the other hand, [Dmt[1], L-Pip(2)[2]]EM-2 was potent and selective μ-agonist (GPI: IC_{50}=0.42 nM, MVD: IC_{50}>10,000 nM). Those findings showed the substitution of Pro could modulate the biological profile of EM-2.

Table 1. Biological activity of EM-2 analogues containing Pro mimics

Peptide	Biological Activity (IC_{50}:nM)	
	mu-Opioid Receptor[a]	delta-Opioid Receptor[b]
EM-2	5.79	344
[Dmt[1]]EM-2	0.07	1.87
[Pip(4)[2]]EM-2	213	>10,000
[L-Pip(2)[2]]EM-2	24.9	>10,000
[D-Pip(2)[2]]EM-2	200	5,055
[Aze[2]]EM-2	35.4	>10,000
[Dmt[1],Pip(4)[2]]EM-2	6.39	>10,000
[Dmt[1],L-Pip(2)[2]]EM-2	0.42	>10,000
[Dmt[1],D-Pip(2)[2]]EM-2	5.77	9.12
[Dmt[1],Aze[2]]EM-2	1.29	5.75

[a]The GPI and [b]MVD prerarations were used for assay

Results and discussion

The synthesis of peptides was achieved according to the procedure of Okada Y. *et al*.[2] The final products were identified by MALDI-TOF mass spectrometry and elemental analyses, TLC and so on. The receptor binding activity of peptides was assessed by radio-ligand receptor binding assay using μ- and δ-opioid receptors from COS-7 cell membranes expressing each opioid receptor. For the evaluation of the biological function of peptides, the GPI and the MVD tests were performed.

The substitutions of Pro in EM-2 (IC_{50}=8.65 nM) gave the μ-receptor binding activity in a nanomolar range with exception of Pip(4), which reduced the μ-receptor binding activity by16.5-fold. All of them were moderate μ-selective agonist. Furthermore, the substitution of Pro in [Dmt[1]]EM-2 (IC_{50}=0.35 nM) with Aze, Pip(2) or Pip(4) yielded the μ-binding activity with the IC_{50} values in range of 4.04 and 0.42 nM. [Dmt[1], Aze[2]]EM-2 was μ-/δ-agonist (GPI: IC_{50}=1.29 nM, MVD: IC_{50}=5.75 nM), although its biding activity was not higher than that of

To explain the influence of the Pro residues on the biological function, the conformational properties of EM-2 and [Dmt[1]]EM-2 in DMSO were investigated by using NMR spectroscopy and molecular modeling calculations.

The 1D and 2D ^{1}H-NMR spectra were recorded on a Varian unity INOVA500 spectrometer with a variable temperature-control unit. The 2D spectra (COSY, TOCSY and ROESY) were acquired in the phase-sensitive mode by using standard pulse available in the Varian software library. All peak assignments of ^{1}H-NMR spectra were performed by the combination of the connectivity information via scalar coupling in phase-sensitive TOCSY experiments and the sequential ROE network along the peptide backbone proton. Both EM-2 and [Dmt[1]]EM-2 have a *cis/trans* equilibrium in DMSO. The *cis/trans* ratios were 1/2 and 7/3, respectively. EM-2 predominantly took *trans*-conformers, while [Dmt[1]] EM-2 predominantly took *cis*-conformers.

With the use of the proton-proton distance derived from ROESY cross peaks, possible fifty 3D conformers were

generated by means of dynamical simulated annealing calculations. The energy-minimized thirty conformers were classified in several groups according to the folding patterns of their backbone structures. In DMSO solution, all *cis/trans* EM-2 conformers adopted the open structures in which extended backbone was twisted at the Pro^2-Phe^3 sequence, whereas *cis* [Dmt^1]EM-2 conformers showed the ensemble of F1- and F2-type folded structures with turning at the Pro^2-Phe^3 sequence and *trans* [Dmt^1] EM-2 seemed to be converged into the open structures. It indicated the incorporation of Dmt made easy to take the folded conformers. But it remains to be seen which conformer is bioactive. The conformational analyses of [Dmt^1, Aze^2]EM-2 and [Dmt^1, $Pic(2)^2$]EM-2 in H_2O or aqueous dodecylphosphocholine(DPC) micelles are in progress.

References

1. Zadina JE, Hackler L, Ge L-J, Kastin AJ. *Nature* **386**: 499-502, 1997.
2. Okada Y, Fujita Y, Motoyama T, Tsuda Y, Yokoi T, Li T, Sasaki Y, Ambo A, Bryant SD, Lazarus LH. *Bioorg Med Chem Lett* **11**: 1983-1994, 2003.

2-07-167

Biological evaluation of new arginine vasopressin (AVP) analogues containing non natural amino acids

Magafa, Vassiliki[1]; Pappa, Eleni V[1]; Borovičková, Lenka[2]; Pairas, George[1,]; Slaninová, Jiřina[2]; Cordopatis, Paul[1]*

[1]University, GREECE; [2]Institution, CZECH REPUBLIC

[*]E-mail: gpairas@upatras.gr

Introduction

Arginine-Vasopressin (AVP), a neurohypophyseal nonapeptide hormone [cycle 1-6 (H-Cys[1]-Tyr[2]-Phe[3]-Gln[4]-Asn[5]-Cys[6]-Pro[7]-Arg[8]-Gly[9]-NH_2)], elicits a variety of responses both centrally and peripherally by acting on three distinct G-protein coupled receptors: V_{1a} (vascular), V_{1b} (pituitary) and V_2 (renal). It also binds to the oxytocin (OT) receptor.[1] In addition to its well-known antidiuretic activity, AVP has also complex cardiovascular actions and adrenocorticotropic hormone (ACTH) releasing activity. Binding of AVP to the V_{1a} receptor subtype also stimulates glycogenolysis in the liver and promotes platelet aggregation. It is generally accepted that the structure of the *N*-terminal part of neurohypophyseal hormone analogues is important for their pharmacological activity. The configuration and the hydrophobicity of the aromatic amino acid in position 2 are important for the antagonistic activity and elimination of the *N*-terminal amino group plays an important role in the prolongation of the activity. On the other hand, the *C*-terminal Gly-NH_2 is important for agonistic activity, but it can be deleted or replaced by a wide variety of substituents with excellent retention of V_{1a}-and OT-antagonistic potency.[2] In continuing our work aimed at the design of selective AVP analogues, we synthesized twelve new analogues of AVP containing mercapto propionic acid (Mpa) or *S*-salicylic acid (Sal) in position 1, D-Tyrosine(Ethyl) [D-Tyr(Et)] or D-1,2,3,4-tetrahydro-isoquinoline-3-carboxylic acid [D-Tic] in position 2, L-arginine (Arg) in position 3 and L-*α*-*t*-butylglycine [Gly(Bu^t)] or L-*α*-(2-thienyl)-alanine [Thi] in position 4 or 9. The *C*-terminus was either free, amidated or modified by NHEt group.

Results and discussion

The new **AVP** analogues were synthesized by Fmoc/Bu^t solid phase methodology utilizing the Rink Amide MBHA,[3] the [3-((Ethyl-Fmoc-amino)-methyl)-1-indol-1-yl]-acetyl AM resin[4] and the 2-chlorotrityl-chloride resin[5] to provide the *C*-terminal amide, ethylamide and carboxylic acid, respectively. The cyclization was performed in DMSO/H_2O (2:8, v/v) for 24-36 h. All analogues were purified by gel filtration chromatography on Sephadex G-15 using 15% acetic acid as the eluent. Final purification was achieved by preparative HPLC on reversed-phase support C-18 with a linear gradient from 5 to 75% acetonitrile (0.1% TFA) for 30 min at a flow rate of 1.5 ml/min and UV detection at 220 and 254 nm. Electron-spray MS were in agreement with the expected results.

The new analogues were tested for their potency in three pharmacological tests: the uterotonic *in vitro* test in the absence of magnesium ions on an isolated strip of rat uterus, pressor test on phenoxybenzamine treated male rats and antidiuretic test on conscious male rats in

Table 1. Biological Activities of AVP Analogues

	Analogue	Activity				
		Pressor (IU/mg)	**Anti-pressor (pA_2)**	**Uterotonic *in vitro* (IU/mg)**	**Anti-Uterotonic *in vitro* (pA_2)**	**Binding Affinity to Human OTR IC_{50} (nM)**
	AVP	465		17		
1.	[Mpa[1], Thi[4]]AVP-NH_2	0.05	0	0.36	0	209 ± 42
2.	[Sal[1], Thi[4]]AVP-NH_2	0	0	0.15	0	1 783 ± 47
3.	[Sal[1], Arg[3], Thi[4]]AVP-NH_2	0	0	0.03	0	>10 000
4.	[Mpa[1], D-Tyr(Et)[2], Arg[3], Thi[4]]AVP-NH_2	0	0	0.13	0	>10 000
5.	[Sal[1], D-Tyr(Et)[2], Arg[3], Thi[4]]AVP-NH_2	0	0	0.14	0	>10 000
6.	[Mpa[1], D-Tyr(Et)[2], Arg[3], Gly(Bu^t)[4]]AVP-NH_2	0	0	0.10	0	>10 000
7.	[Mpa[1], D-Tyr(Et)[2], Arg[3], Gly(Bu^t)[4]]AVP-NHEt	0	0	0	0	>10 000
8.	[Mpa[1], D-Tyr(Et)[2], Arg[3], Gly(Bu^t)[4]]AVP-COOH	0	0	0	0	>10 000
9.	[Mpa[1], D-Tic[2], Gly(Bu^t)[9]]AVP-NH_2	0	~5.6	0	7.70 ± 0.23	1 926 ± 53
10.	[Mpa[1], D-Tic[2], Thi[9]]AVP-NH_2	0	~5.6	0	7.64 ± 0.20	1 143 ± 246
11.	[Sal[1], D-Tic[2], Thi[9]]AVP-NH_2	0	0	0	0	6 318 ± 670
12.	[Mpa[1], D-Tic[2], Thi[9]]AVP-COOH	0	0	0	7.14 ± 0.35	895 ±58
	Analogues 6, 7, and 8 were also tested for antidiuretic/diuretic activity, however they showed no activity at all					

a Burn's variation.[6] Parallel, determination of binding affinity of the analogues to cloned human oxytocin receptors on HEK cell membranes using tritiated oxytocin from NEN Life Science, Boston, MA, USA was performed. The biological activities of the new analogues are summarized in Table 1.

As can be seen from Table 1, replacement of Gln[4] by Thi leads to substantial decrease of the pressor and uterotonic activities. Replacement of Mpa[1] by Sal further decreases the activities. Additional modifications by the introduction of Arg in position 3 (analogue 3) and D-Tyr(Et) in position 2 (analogues 4 and 5) combined with modifications at position 4 by Thi (analogue 5) or Gly(Bu^t) (analogue 6), or modifications at the *C*-terminal amide (analogues 7 and 8) did not improve the biological activities. Introduction of Arg into position 3 seems to have the most deteriorating effect especially as far as the binding affinity to OTR is concerned. Replacement of Gly at position 9 by Gly(Bu^t) or Thi, combined with introduction of D-Tic in position 2 and deamination (analogues 9 and 10) led to slight decrease of oxytocin antagonistic activity if compared to [Mpa[1], D-Tic[2]]AVP analogue (pA_2 8.00). Additional modification in position 1 by Sal led to the inactive analogue 11, while deamidation of the *C*-terminus only decreased the antagonistic activity (compare analogues 10 and 12). The Sal is probably so constraint molecule that its introduction into position 1 is incompatible with biological activities.

Acknowledgements

We thank the European Social Fund (ESF), Operational Program for Educational and Vocational Training II (EPEAEK II), and particularly the Program PYTHAGORAS I, for funding the above work. The work was also supported by the research project No. Z40550506 of the Academy of Sciences of the Czech Republic.

References

1. Barberis C, Mouillac B, Durroux T. Structural bases of vasopressin/oxytocin receptor function. *J Endocrinol* **156:** 223-229, 1998.
2. Manning M, Sawyer WHJ. Design, synthesis and some uses of receptor-specific agonists and antagonists of vasopressin and oxytocin. J *Recept Res* **13:** 195-214, 1993.
3. Rink H. Solid-phase synthesis of protected peptide fragments using a trialkoxy-diphenyl-methylester resin. *Tetrahedron Lett* **28:** 3787-3790, 1987.
4. Estep KG, Neipp CE, Stephens Stramiello LM, Adam MD, Allen MP, Robinson S, Roskamp EJ. Indole Resin: A Versatile New Support for the Solid-Phase Synthesis of Organic Molecules. *J Org Chem* **63:** 5300-5301, 1998.
5. Barlos K, Chatzi O, Gatos D, Stravropoulos G. 2-Chlorotrityl chloride resin: Studies on anchoring of Fmoc-amino acids and peptide cleavage. *Int J Peptide Protein Res* **37:** 513-520, 1991.
6. Slaninova J. Fundamental Biological Evaluation. *Handbook of Neurohypophyseal Hormone Analogs*. Jošt K, Lebl M, Brtní F (Eds.), Part 1, vol. 2, CRC Press, Boca Raton, FL, pp 83-107, 1987.

2-07-168

Structure-activity relationship studies of pituitary adenylate cyclase-activating polypeptide: Ala-scan of the *N*-terminal domain

Bourgault, Steve[1,]; Vaudry, David[2]; Doan Ngoc, Duc[1]; Laburthe, Marc[3]; Couvineau, Alain[3]; Vaudry, Hubert[2]; Fournier, Alain[1]*

[1]Institut National de la Recherche Scientifique, Institut Armand-Frappier, CANADA; [2]Université de Rouen, INSERM U413, FRANCE; [3]Faculté de Médecine Xavier Bichat, INSERM U773, FRANCE

[*]E-mail: steve.bourgault@iaf.inrs.ca

Introduction

Pituitary adenylate cyclase-activating polypeptide (PACAP) is a neuropeptide with a wide distribution in the central nervous system (CNS) and peripheral tissues. PACAP biological activities have already been described in the cardiovascular and immune systems, the urogenital and respiratory tracts, the endocrine glands and the CNS.[1] PACAP exists in two *C*-terminally α-amidated isoforms containing 27- or 38-amino acids. The *C*-terminal short form, PACAP27, shows a 68% sequence identity with VIP, with which it shares common receptors. Pharmacological and molecular investigations showed the existence of three types of PACAP/VIP receptors: VPAC1 and VPAC2 that recognize both PACAP and VIP with similar high affinity and PAC1 which shows high affinity for PACAP and low affinity for VIP. Previous structure-activity relationship studies revealed that the 28-38 *C*-terminal segment seems to facilitate the binding of the peptide. Besides, *C*-terminally truncated PACAP27 analogs, from PACAP(1-26) to PACAP(1-23), appeared as potent agonists on PAC1 receptor showing, however, a small decrease of their potency.[2] On the other hand, the *N*-terminal domain of PACAP plays a crucial role for the activation of the selective PAC1 receptor. For instance, removal of the first two residues, His^1 and Ser^2, suppresses the PAC1 agonistic activity and subsequent deletions of the *N*-terminal residues of PACAP38 conducted to the identification of the potent PAC1 antagonist, PACAP(6-38)[3]. Nevertheless, the molecular requirements of the *N*-terminal domain of PACAP responsible for PAC1 receptor activation are still not clearly understood. Therefore, we carried out an Ala-scan of the *N*-terminal portion of both PACAP isoforms. A total of 14 analogs focusing on the first seven residues (His1-Ser2-Asp3-Gly4-Ile5-Phe6-Thr7) were synthesized and biologically characterized using binding and Ca^{2+} mobilization assays with Chinese hamster ovary (CHO) cells stably expressing the human PAC1 receptor.

Results and discussion

The concentrations of unlabelled peptide producing 50% of binding inhibition of the acetyl-$_{125}$I-PACAP27 probe (IC_{50}) were 8.3 for PACAP27 and 6.1 nM for PACAP38

Table 1. Pharmacological properties of PACAP and PACAP analogs on CHO transfected cells stably expressing the PAC1 receptor

Peptides	*Binding*	*Calcium mobilization*	
	IC_{50} ± S.E.M.[a] (nM)	EC_{50} ± S.E.M.[b] (nM)	*Efficacy* ± S.E.M.[c] (%)
PACAP27	**8.3 ± 1.5**	**5.6 ± 1.1**	**102.2 ± 2.5**
[Ala[1]]PACAP27	335 ± 132	174 ± 46	70.0 ± 3.9
[Ala[2]]PACAP27	5.1 ± 1.4	6.8 ± 1.5	98.1 ± 3.0
[Ala[3]]PACAP27	602 ± 164	538 ± 363	18.4 ± 4.6
[Ala[4]]PACAP27	9.1 ± 2.9	20.8 ± 2.0	104.9 ± 1.6
[Ala[5]]PACAP27	60.7 ± 22.6	39.8 ± 3.8	99.2 ± 1.5
[Ala[6]]PACAP27	1330 ± 341	462 ± 121	65.3 ± 4.2
[Ala[7]]PACAP27	17.7 ± 5.5	8.75 ± 1.7	112.3 ± 3.1
PACAP38	**6.1 ± 1.1**	**2.1 ± 0.4**	**100.0 ± 1.9**
[Ala[1]]PACAP38	49.3 ± 13.5	11.0 ± 3.0	82.6 ± 3.7
[Ala[2]]PACAP38	7.9 ± 1.4	5.1 ± 1.1	104.7 ± 3.3
[Ala[3]]PACAP38	97.2 ± 27.7	>10 000	N.D.
[Ala[4]]PACAP38	9.8 ± 3.2	7.4 ± 2.2	90.2 ± 3.9
[Ala[5]]PACAP38	34.4 ± 10.9	9.6 ± 2.1	78.3 ± 2.8
[Ala[6]]PACAP38	208 ± 62	17.3 ± 6.1	50.4 ± 3.2
[Ala[7]]PACAP38	4.0 ± 1.3	0.8 ± 0.2	100.7 ± 3.3

a Concentration producing 50% of binding inhibition
b Concentration producing 50% of the maximum effect
c Percentage of efficacy as compared to the maximal value obtained with PACAP38

(Table 1). Substitutions of the hydroxylic residues, Ser[2] or Thr[7], with Ala did not affect the affinity of PACAP for the PAC1 receptor. In contrast, incorporation of Ala in position 3 or 6 drastically decreased the binding affinities of both PACAP isoforms. Replacement of His[1] by Ala gave a 40-fold decrease of the affinity of PACAP27, while the equivalent modification reduced by 8-fold the affinity of PACAP38.

PACAP27 and PACAP38 were efficient to induce calcium mobilization in stably transfected CHO cells expressing the human PAC1 receptor. As suspected from their low binding affinities, [Ala[3]] and [Ala[6]] of both PACAP isoforms were partial agonists showing very weak potency. Incorporation of Ala at positions 1, 2, 4, 5 and 7 did not alter strongly the activation properties of PACAP38. Surprisingly, replacement of Thr[7] by Ala increased significantly the potency of PACAP38. In the same way, [Ala[7]]PACAP27 exhibited a higher efficacy compared to the native peptide. On the other hand, the *C*-terminal shorter isoform was less tolerant to substitutions of residues His[1] and Ile[5]. Especially, [Ala[1]] PACAP27 was 15-fold less potent compared to [Ala[1]] PACAP38 to induce calcium mobilization.

Previous structure-activity studies established that the *N*-terminal domain of PACAP is the major molecular determinant responsible for the activation of the PAC1 receptor. For instance, fragments (3-38) to (6-38) are potent PAC1 antagonists.[3] Moreover, residues Phe[6] and Thr[7] are highly conserved within the structurally related VIP-glucagon-secretin peptides superfamily, suggesting an essential role for these amino acids in the regulation of the biological functions of these peptides[1]. Therefore, our structure-activity relationship studies focused on the first seven residues. Our results suggested that the carboxylic acid function of residue Asp[3] and the phenyl group of Phe[6] constituted the main pharmacophores of the *N*-terminal domain of PACAP regarding the binding and activation of the PAC1 receptor. The secondary structure of PACAP27 is mainly characterized by the presence of a stable alpha-helix, which is extended from residue Ile[5] to the *C*-terminus. The presence of this helical structure represents an essential prerequisite for biological activity.[4,5] Therefore, the increasing of biological potency observed for analogs containing Ala at position 7 might be ascribed to a stabilization effect on the helical structure produced by the incorporation of Ala. Finally, our results clearly demonstrated that residues 28-38 appeared to play a favorable role for the affinity towards the PAC1 receptor, as shown with PACAP38 analogs, which mostly exhibited a better affinity and a stronger potency as compared to their PACAP27 counterparts.

References

1. Vaudry D, Gonzalez BJ, Basille M, Yon L, Fournier A and Vaudry H. *Pharmacol Rev* **52**: 269-324, 2000.
2. Gourlet P, Vandermeers A, Vandermeers-Piret MC, Rathe J, De Neef P, Robberecht P. *Regul Pept* **62**: 125-130, 1996.
3. Robberecht P, Gourlet P, De Neef P, Woussen-Colle MC, Vandermeers-Piret MC, Vandermeers A, Christophe J. *Eur J Biochem* **207**: 239-246, 1992.
4. Inooka H, Ohtaki T, Kitahara O, Ikegami T, Endo S, Kitada C, Ogi K, Onda H, Fujino M, Shirakawa M. *Nat Struct Biol* **8**: 161-165, 2001.
5. Bourgault S, Vaudry D, Botia B, Couvineau A, Laburthe M, Vaudry H, Fournier A. *Peptides* **29**: 919-932, 2008.

2-09-169

The siderophore microcin family: from the genetic systems to the antimicrobial peptides

Vassiliadis, Gaëlle; Peduzzi, Jean; Rebuffat, Sylvie[1,*]
Muséum National d'Histoire Naturelle, UMR 5154 CNRS, FRANCE

[*]*E-mail: rebuffat@mnhn.fr*

Introduction

Microcins are low molecular weight antimicrobial peptides secreted by enterobacteria and involved in microbial competitions within the intestinal tract. They are synthesized following the ribosomal pathway. We have isolated the first siderophore peptide, microcin E492 (MccE492),[1] which has a potent bactericidal activity mainly directed against *Escherichia coli*. The post-translational modification consists of a glucosylated linear trimer of *N*-(2, 3 dihydroxybenzoyl)-L-serine (DHBS), which is reminiscent of enterobactin/salmochelins,[2] linked to the *C*-terminal serine *via* an *O*-glycosidic bond (Fig. 1A). This microcin is also produced under an unmodified form (u-MccE492). Two genes (*mceC* and *mceD*) were found to be involved in the acquisition of the post-translational modification and a model of biosynthesis was proposed.[3] In order to identify novel siderophore microcins, we analyzed the genetic systems of several microcinogenic strains.[4] Based on the genetic organization of the microcin gene clusters, three microcins, which had never been isolated until now, MccM[5], MccH47 and MccI47[6], were hypothesized to carry a post-translational modification similar to that of MccE492, thus forming putatively the siderophore microcin family.

Results and discussion

The gene clusters encoding MccM, MccH47 and MccI47 were found in the genomic DNA of four *E. coli* strains (Nissle 1917 [the probiotic agent Mutaflor® used against intestinal diseases], H47, CA46, CA58) and are closely interwoven (Fig. 2). Interestingly, MceC, MchA and McmL on the one hand, MceD, MchS1 and McmK on the other hand, show strong amino acid sequence identity. MceC and MceD have been shown to be involved in the post-translational modification acquisition of MccE492. We thus hypothesized that MccM, MccH47 and MccI47 could display the same post-translational modification as MccE492.

We isolated for the first time MccM and MccH47 from different recombinant and native strains. We showed by gene complementation experiments and mass

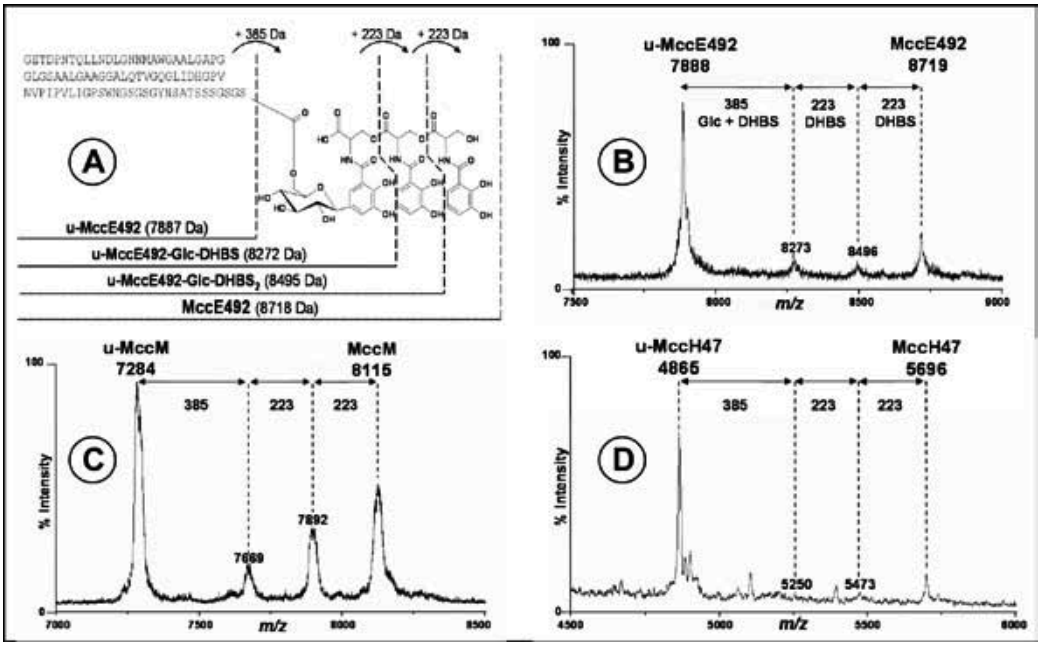

Figure 1. Structure of the MccE492 post-translational modification (A). MALDI-TOF spectra of MccE492 (B), MccM (C) and MccH47 (D) showing different ions corresponding to their unmodified, intermediate and modified forms.

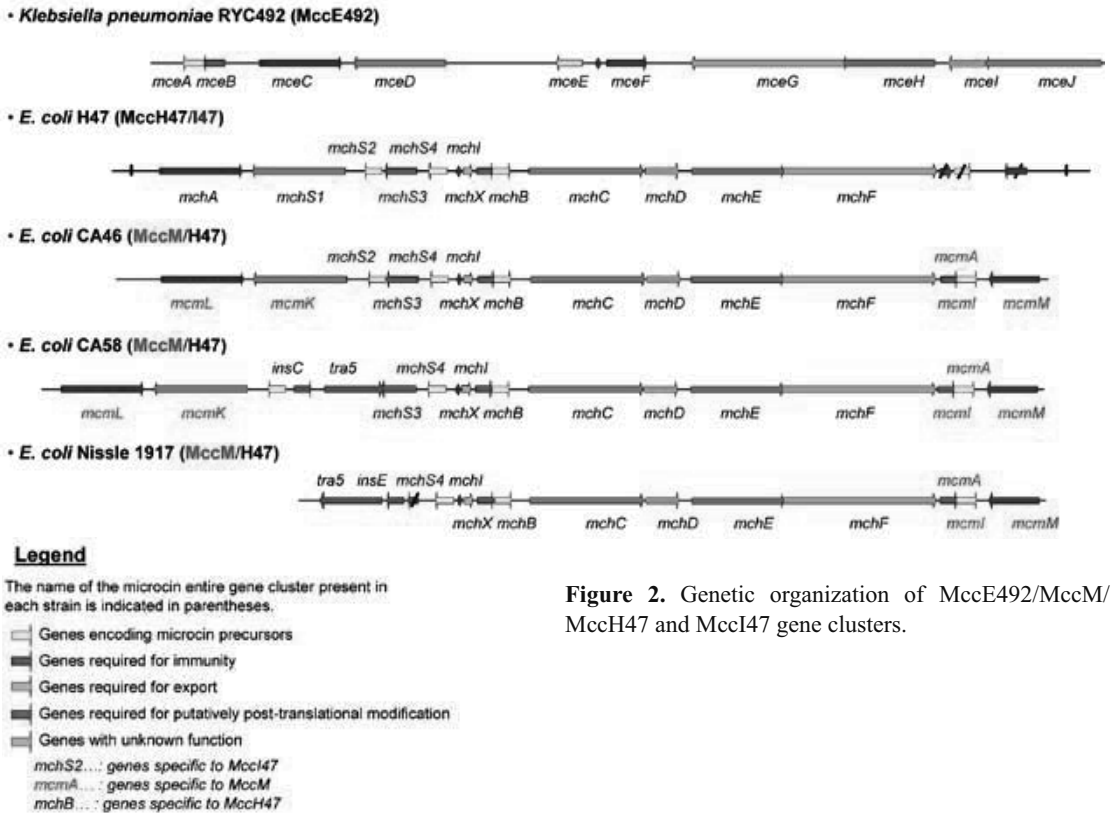

Figure 2. Genetic organization of MccE492/MccM/MccH47 and MccI47 gene clusters.

spectrometry (Fig. 1B, C, D) that they carry the same post-translational modification as MccE492, and thus form the siderophore microcin family. We also showed that *mchA*/*mcmL* and *mchS1*/*mcmK* play the same role in the post-translational modification acquisition of MccM/MccH47 as *mceC* and *mceD* for MccE492, respectively.

We also determined the sequence of the isolated MccM and its maturation site. The resulting amino acid sequences correspond to those that could be deduced from *mcmA*. The spectrum of antibacterial activity of MccM and MccH47 was studied and both microcins showed an activity against only phyllogenetically close gram-negative bacteria.

Finally, we showed that siderophore membrane receptors FepA, Fiu and Cir and the associated protein TonB are required for MccM/MccH47 activity.

References

1. Thomas X, Destoumieux-Garzón D, Peduzzi J, Afonso C, Blond A, Birlirakis N, Goulard C, Dubost L, Thai R, Tabet JC, Rebuffat S. *J Biol Chem* **279**: 28233-28242, 2004.
2. Bister B, Bischoff D, Nicholson GJ, Valdebenito M, Schneider K, Winkelmann G, Hantke K, Sussmuth RD. *Biometals* **17**: 471-481, 2004.
3. Vassiliadis G, Peduzzi J, Zirah S, Thomas X, Rebuffat S, Destoumieux-Garzón D. *Antimicrob Agents Chemother* **51**: 3546-3553, 2007.
4. Duquesne S. Destoumieux-Garzón D, Peduzzi J, Rebuffat S. *Nat Prod Rep* **24** : 708-734, 2007.
5. Patzer SI, Baquero MR, Bravo D, Moreno F, Hantke K. *Microbiology* **149**: 2557-2570, 2003.
6. Poey ME, Azpiroz MF, Lavina M. *Antimicrob Agents Chemother* **50**: 1411-1418, 2006.

2-10-172

Peptidomics of grape

Borchikiv, Alexander[1]; Zamyatnin, Alexander[2,]*

[1]Universidad Tecnica Federico Santa Maria, Departamento de Informatica, Valparaiso, CHILE; [2]A.N.Bach Institute of Biochemistry Russian Academy of Sciences, Moscow, RUSSIAN FEDERATION

[*]E-mail: aaz@inbi.ras.ru

Introduction

It is known that natural oligopeptides may regulate nearly all vital processes. Several hundreds such substances with wide spectrum of functional activity were described for different plants earlier. But there was no information on real existence of these substances in grape before. So, the structural-functional study of putative grape *Vitis vinifera* uncharacterized protein sequences was performed with the purpose of identification of grape regulatory oligopeptides. A special method of computer analysis was developed for this.[1] This method has allowed to reveal new potentially active regulatory oligopeptide structures not detected previously. Grape protein primary structures, computer database EROP-Moscow (**E**ndogenous **R**egulatory **O**ligo **P**eptides)[2] containing the information on structure and function of all known plant oligopeptides, and special computer programs were used. Uncharacterized grape protein amino acid residue sequences were selected in public TrEMBL-SwissProt database. All these data (54390 sequences) have been compared with the sequences of all of EROP-Moscow plant oligopeptides (476 entries).

Results and discussion

As a result we have found out 40 grape protein structures homologues to many known plant regulatory oligopeptides. Structures and functions of these plant oligopeptides were described for buckwheat *Fagopyrum esculentum*, common sunflower *Helianthus annuus*, common tobacco *Nicotiana tabacum*, cowpea *Vigna unguiculata*, dahlia *Dahlia merckii*, Japanese morning glory *Pharabitus nil*, kidney bean / French bean *Phaseolus vulgaris*, mouse ear-cress *Arabidopsis thaliana*, violet-flowered petunia *Petunia inflata*, soybean *Glycine max*, rubber tree *Hevea brasiliensis*, tomato *Lycopersicon esculentum*, and others. Coincidence value (homology) of grape and other plant primary structures was from 46.8 to 100 % (Fig. 1). 26 different oligopeptide sequences and 25 new putative grape oligopeptides were elucidated among them. Several structures were identical, e.g., No 1 and 2 or 4 and 5. Many of them had no sequence coincidence outside oligopeptide site, e.g., No 28 and 29, but some of them were characterized by single substitutions in pre-region, e.g., No 15/16 and 17 (pre-regions of all grape uncharacterized sequences have not been shown in Fig. 1). It is necessary to note that one primary structure No 28/29 was described earlier (amino acid residue sequence coincidence is 100%) for mouse-ear cress *Arabidopsis thalania*.[3] All other primary structures of putative grape oligopeptides were new. It has appeared also that 23 putative oligopeptide primary structures contained cysteine residues (from 2 to 8) forming potentially from 1 to 4 S—S bonds. Their position in all possible grape oligopeptides was the same as in plant oligopeptides obtained from other sources (without deletions or insertions). It has been shown that 1 or 2 grape uncharacterized proteins were homologs for from 1 to 13 different plant oligopeptide structures possessing different functions such as antibacterial, antifungal, enzyme inhibition, and others (Fig. 1 demonstrates one homolog with the maximal similarity and possessing one functional type only). Most of them were antimicrobial agents and several of them were putative rapid alkalinization factors. The similarity of putative grape primary structures with the known oligopeptides possessing known function type could be basis for the prediction their potential functional properties in further experimental investigations.

Conclusions

1). The first primary structures of grape oligopeptides were found out.
2). Their structures could participate in different plant regulatory processes, i.e., to be poly-functional regulators.
3). It is necessary to use different experimental models for the development our complete knowledge on regulatory role of both putative grape and other plant oligopeptides.

Acknowledgements

This study was supported by Chilean National Science and Technology Research Fund FONDECYT, Grant No. 1080504.

References

1. Zamyatnin AA. *Biofizika* **53**: 725-733, 2008.
2. Zamyatnin AA, Borchikov AS, Vladimirov MG, Voronina OL. *Nucl Acids Res* **34**: D261-D266, 2006.
3. Schultz CJ. *J Biol Chem* **279**: 45503-45511, 2004.

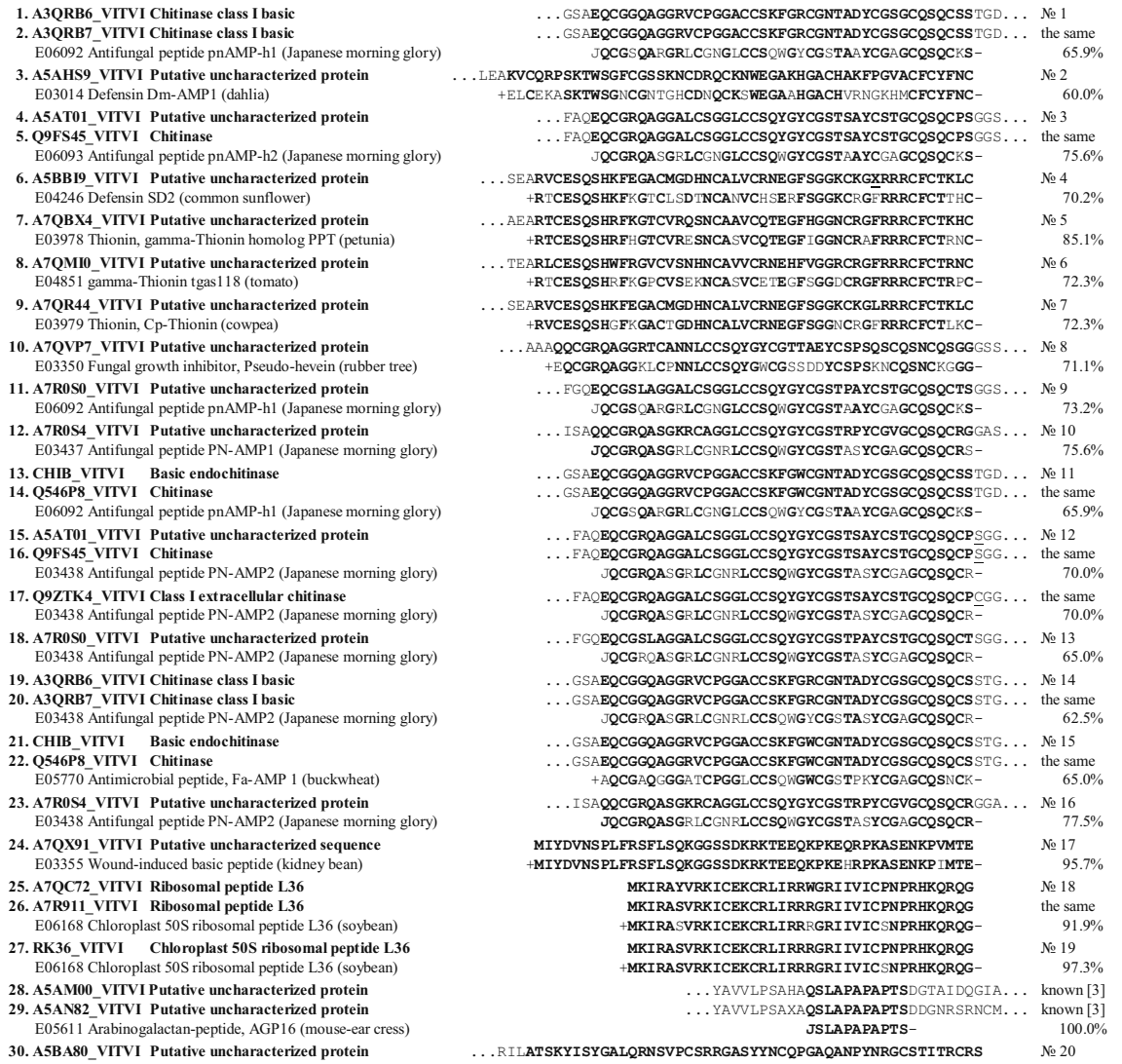

Figure 1. Sequence alignment of SwissProt-TrEMBL uncharacterized grape proteins and EROP-Moscow plant oligopeptides. Left numbers point grape protein sequences, right numbers point possible grape oligopeptides (in bold), % — percentage of coincidence of grape uncharacterized grape sequences with known plant sequences. Standard one-letter code was used for amino acid residues. Additional abbreviations: "+" — *N*-terminal ($^{+}NH_3$— group), "—" — C-terminal (—COO^{-} group).

2-11-173

The effect of the so called "*β*-sheet breakers" (BSBs) on A*β* 1-42 aggregates

Soós, Katalin[1,]; Hetényi, Anasztázia[2]; Fülöp, Lívia[1]; Laczkó, Ilona[3]; Martinek, Tamás[2]; Penke, Botond[1]*

[1]University of Szeged, Med.Chem.Dep., HUNGARY; [2]University of Szeged, Institute of Pharmaceutical Chemistry, HUNGARY; [3]Biological Research Center of the Hungarian Academy of Science, Istitute of Biophysics, HUNGARY

[*]E-mail: soska@mdche.szote.u-szeged.hu

Introduction

Inhibition of aggregation of amyloid *β*-peptide (A*β*) seems to be a critical step in the therapeutic approach to prevent amyloidosis in Alzheimer's disease. The term "*β*-sheet breaker" (BSB) had been introduced by Soto C. *et al*. in 1998. They designed inhibitors where 17-20 (LVFF) of A*β* served as a template for the synthesis of BSB peptides. Incubation of A*β* (l-42) for seven days with an equimolar or 20-fold molar excess of the pentapeptide LPFFD resulted in 34 and 72% inhibition of the fibrillogenesis, respectively. This peptide also induced a disassembly of preformed amyloid fibrils *in vitro*.[1] We have synthesized the "Soto peptide (LPFFD)" and its several derivatives including LPYFD pentapeptide as well as a big number of peptidomimetics. Their neuroprotective effect was studied by MTT cell viability test. Their mechanism of binding to fibrillar A*β* has been studied by NMR spectroscopy, diffuse light-scattering method, time dependent *ξ*-potential measurement, CD and transmission electron microscopy (TEM). The goal of the present study was to improve our understanding of processes that are initiated by the binding of short neuroprotective peptides to fibrillar A*β* 1-42.

Result and discussion

In MTT assay by monitoring the mitochondrial reduction activity, the short peptides were co-incubated with A*β*1-42 aggregate and both LPFFD and LPYFD peptides were able to inhibit the cytotoxic effect of A*β* 1-42 to a considerable extent (Table 1). It is worthy of the toxicity of A*β* peptides depends strongly on their aggregation state. Our studies with NMR spectroscopy show that short neuroprotective peptides as LPFFD bind to the surface of A*β* aggregates and decrease the specific surface area of fibrillar A*β* which is accessible for the cell-membrane-bound receptors, can obviously lead to a decreased toxicity (Fig.1).

Also an increase was observed in the absolute value of the *ξ*-potential in the negative region, a phenomenon which partially might prevents the interaction of A*β* with negatively charged cell membrane features and decreases also the toxicity of A*β*. The result of diffuse light-scattering experiments strongly suggest a significant time- dependent increase in the particle size of A*β* in both phosphate buffer and PBS, and the rate correlates very well with the change in the bound fraction in the NMR spectroscopy experiments The TEM images corroborate these observations because interfibrillar association can be clearly observed even within 10 min of mixing the fibrillar A*β* 1-42 samples with either LPFFD or ThT. TEM pictures show flocculation (precipitation due to weak attracting forces between destabilized particles) process of A*β*–LPFFD complex. This interfibrillar association is not simply electrostatically driven, but that specific noncovalent cross-linking interaction might responsible for the phenomenon. The CD spectrum of A*β* 1-42, aging for one week, revealed some changes: the amount of ordered conformational elements were increased. After 2 weeks, the red-shifted CD spectrum reflected the accumulation of twisted *β* sheet (the negative band at ~226 nm). The experiment was followed by the addition of the short peptide, in two–fold molar excess, to the fibrillar A*β* solution. After incubation of solution for another week, the CD spectral analysis demonstrated a somewhat higher amount of slightly twisted cross-*β* sheet.

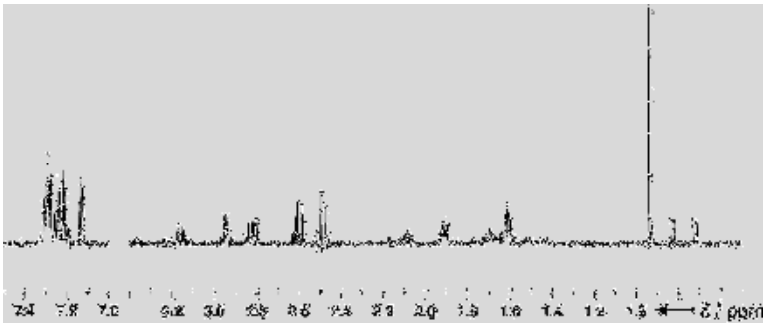

Figure 1. ^{1}H NMR difference spectrum of LPFFD upon binding to firillar A*β* 1-42-OH.

Table 1. Comparison of the results on the neuroprotective effects of the studied peptides with their fractions bound to fibrillar Aβ(1–42) in NMR experiments.

Ligand	MTT cell viability test[a] [%]	Bound fraction[b] [%]
LPYFD-NH_2	92	19
FRHDS-NH_2	89	26
RIIGL NH_2	86	9
LPFFD	84	17
GGGGG-NH_2	64	0

Table 1a) Taken from references[2,3,4]; data are referenced to a cell viability of 52% for fibrillar Aβ 1-42. (b) Values were obtained at the first measurement point

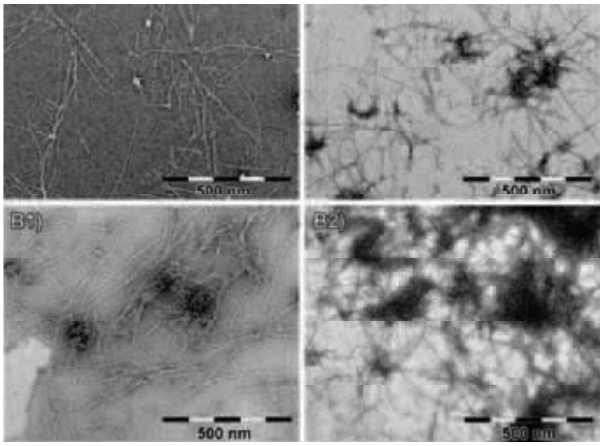

Figure 2. TEM images that indicate the effects of LPFFD on the flocculation process for fibrillar Aβ 1-42. For fibrillar Aβ 1-42 sampled at t=0 (A1) and 6 h (A2); for LPFFD- Aβ 1-42 sampled at t=0 (B1) and 6 h (B2). the samples were prepared in phosphate buffer (10 mM, pH 7.4) with 130 mM NaCl (PBS).

The most important result of these studies with different methods show that the Soto peptide LPFFD and the similar small peptides/peptidomimetics can not prevent Aβ aggregation in the molar ration of 1:1 to 1:10.

Methods

Peptide synthesis: Aβ 1-42 was synthesized as reported earlier.[5] LPFFD-OH, LPYFD-NH_2, and GGGGG-NH_2 were synthesized by solid phase synthesis using Boc chemistry and HF cleavage. The ^{1}H NMR spectroscopy measurements were performed with a WATERGATE solvent suppression scheme, for the relaxation delay 2s was used.[6] At ξ–potential measurements: all experiments were performed with a Malvern Zetasizer Nano ZS instrument equipped with a He-Ne laser.[6] At TEM experiments specimens were studied with a Philips CM 10 transmission electron mmicroscope.[6] CD measurements were performed on a Jobin-Yvon Mark VI dichrograph using a quartz cell of 0.1 cm path length.[7]

Acknowledgements

This work was supported by grants from NKTH-RET (08/2004) and OTKA (NK -73672).

References

1. Soto C, Sigurdsson EM, Morelli L, Kuma RA, Castano EM, Frangione B. β-sheet breaker peptides inhibit fibrillogenesis in a rat brain model of amyloidosis: Implications for Alzheimer's therapy. *Nat Med* **4**: 822-826, 1998.
2. Datki Z, Papp R, Zádori D, Soós K, Fülöp L, Juhász A, Laskai G, Hetényi C, Mihalic E, Zarándi M, Penke B. *In vitro* model of neurotoxicity of Aβ 1-42 and neuroprotection by a pentapeptide: irreversible events during the first hour. *Neurobiol Dis* **17**: 507-515, 2004.
3. Szegedi V, Fülöp L, Farkas T, Rózsa E, Robotka Z, Kis Z, Penke Z, Horváth S, Molnár Z, Datki Z, Soós K, Toldi J, Budai D, Zarándi M, Penke B. Pentapeptides derived from Aβ1-42 protect neurons from the modulatory effect of Aβ fibrils – an *in vitro* and *in vivo* electrophysiological study. *Neurobiol Dis* **18**: 499-408, 2005.
4. Fülöp L, Zarándi M, Datki Z, Soós K, Penke B. β-Amyloid-derived pentapeptide RIIGLa inhibits Aβ1-42 aggregation and toxicity. *Biochem Biophys Res Commun* **324**: 64-69, 2004.
5. Zarándi M, Soós K, Fülöp L, Bozsó Z, Datki Z, Tóth G. K, Penke B. Synthesis of Aβ(1-42) and its derivatives with improved efficiency. *J Pept Sci* **13**: 94-99, 2007.
6. Hetényi A, Fülöp L, Martinek T. A, Wéber E, Soós K, Penke B. Ligand-induced flocculation of neurotoxic fibrillar Aβ by noncovalent crosslinking. Chem. Bio. Chem. **9**: 748-757, 2008.
7. Laczkó I, Vass E, Soós K, Fülöp L, Zarándi M, Penke B. Aggregation of Aβ(1-42) in the presence of short peptides: conformational studies. *J Pept Sci* **14**: 731-741, 2008.

2-11-174

Designing trehalose-conjugated peptides for the inhibition of Alzheimer's Aβ oligomerization and neurotoxicity

De Bona, Paolo[1]; Giuffrida, Maria Laura[2]; Copani, Agata[2]; Pignataro, Bruno[3]; Attanasio, Francesco[4]; Cataldo, Sebastiano[3]; Pappalardo, Giuseppe[4,]; Rizzarelli, Enrico[1]*

[1]University of Catania, Department of Chemical Sciences, ITALY; [2]University of Catania, Department of Pharmaceutical Sciences, ITALY; [3]University of Palermo, Department of Physical Chemistry "F. Accascina", ITALY; [4]National Research Council, Istitute of Biostructures and Bioimaging, ITALY

[*]E-mail: giuseppe.pappalardo@ibb.cnr.it

Introduction

Alzheimer disease (AD) is a progressive fatal neurodegenerative disorder, characterized by a decline of cognitive functions including memory, orientation and language. The critical step of this pathology is the Amyloid-*β* peptide (A*β*) aggregation and fibril formation, that are considered the major contributing factors to neurodegeneration and dementia.[1] Molecules able to interfere with A*β* aggregation might show protective effects toward the A*β* correlated toxicity *in vitro* and *in vivo*. In several cases these molecules are peptide derivatives based on the A*β*(16-20) sequence which represents the self-recognition motif for the aggregation process. One of the best characterized peptide inhibitors of A*β* fibrilogenesis is the LPFFD peptide (iA*β*5p).[2] This peptide has also been reported to inhibit the A*β* toxicity, both in vitro and *in vivo*, however its pharmacological use is prevented by the low stability in the biological system.[3] To overcome this disadvantage, three trehalose conjugated derivatives of the LPFFD peptide have been synthesized (Fig. 1).

Result and Discussion

All the peptides synthesis were performed using the microwave-assisted solid phase peptide synthesis strategy on a Liberty Peptide Synthesiser. Trehalose was covalently linked to the *α*-carboxylic function in the case of the Th-CT derivative or to the carboxylic group of the aspartate side chain to give the Th-SC derivative. To synthesize the N-terminal derivative (Th-NT) we introduced a succinic acid spacer at the *N*-terminus of the pentapeptide to provide a carboxylic group useful for the trehalose conjugation. Trehalose conjugation was performed using a DMF solution of 6-amino-6-deoxy-trehalose containing HOBt, TBTU, DIPEA as activator reagents. All the synthesized compounds were tested as inhibitors of A*β* fibrillogenesis and the effects of these glycopeptides on the self-aggregation and morphology of A*β* aggregates were investigated by Scanning Force Microscopy (SFM). The biological stability of all compounds was also tested. Inhibition of A*β* aggregation was investigated by incubating a disaggregated A*β*(1-42) in 20 mM NEM buffer (pH 7.4) in the absence or in the presence of a 5-fold molar excess of each of the compounds for 3 days at 37 °C. Then, the presence of amyloid fibrils was determined according to the ThT fluorescence assay.[4] In these conditions, the fibrils content was reduced of 60% (Fig. 2A) when the A*β*(1-42) was incubated in the presence of LPFFD peptide. Similar effects were observed for the conjugated peptides Th-CT and Th-NT, while the Th-SC glycopeptide was less effective. The above findings were confirmed by dynamic Scanning Force Microscopy. A mixture of structures were observed in all the samples (data not shown) indicating

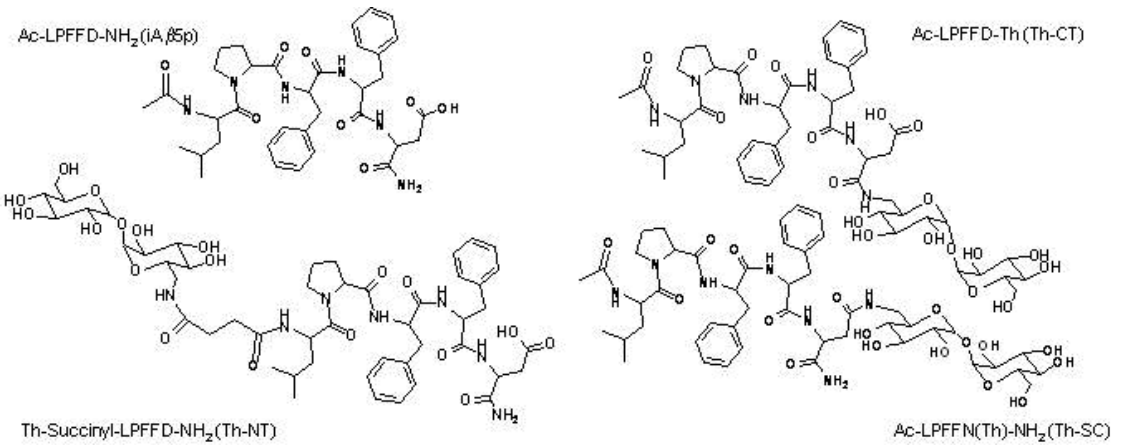

Figure 1. Representative structures of synthesized compounds tested as inhibitors of A*β*'s fibrillogenesis.

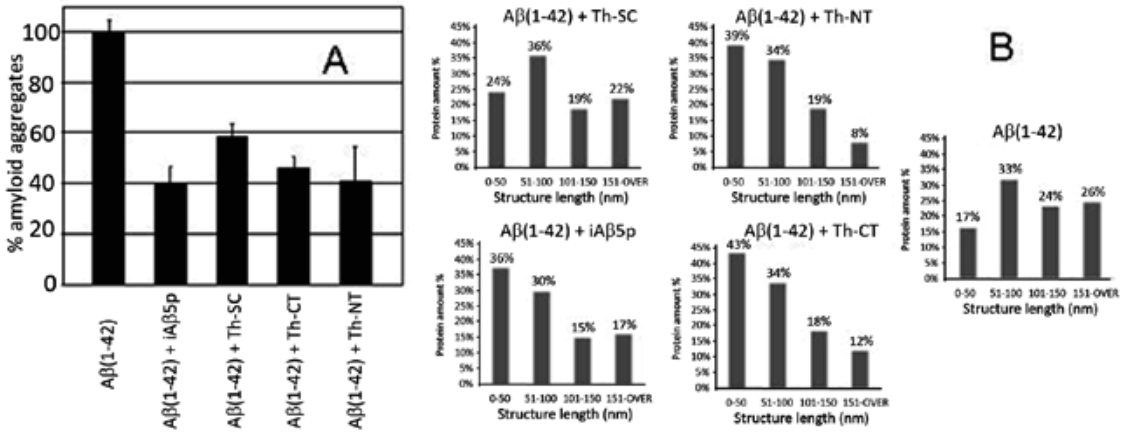

Figure 2. Thioflavin T (ThT) fluorescence emission at 485 nm of samples containing A*β*(1-42) (100 μM) incubated in the absence or in presence of candidate inhibitors in NEM buffer (**A**) and statistical distribution of fibrils length as obtained from SFM analysis for all samples (**B**).

the presence of both globular systems (3-6 nm tall; 20-50 nm wide) and linear aggregates (3-6 nm tall; up to hundreds of nanometers long) formed by the association of globular systems. A statistical analysis was performed in order to understand the effect of the above conjugates on the percentage of A*β* proteins leading to elongated structures as reported in Figure 2B. Our data show that in the control sample about 50% of proteins are involved in the formation of linear aggregates longer than 100 nm. As a result of the co-incubation with iA*β*5p, Th-NT and Th-CT, about one half of these proteins were no longer involved in the formation of such aggregates being mainly present under the form of low-weight globular systems.

Finally, the stability toward proteolytic degradation of all compounds was evaluated by incubating them (200 μM) at 37 °C in 10% rat brain homogenate. Samples were taken at different times and the amount of intact peptide was estimated by HPLC after removing the bulk of proteins by methanol precipitation. As shown in table 1, the conjugated peptides have enhanced stability toward proteolytic degradation than the unmodified peptide iA (Table 1).

Table 1. *In vitro* half-life (time needed for 50% degradation of the peptide) for all the peptide derivatives.

Peptide derivative	Stability in rat brain homogenate
iA<beta>5p	18 min
Th-CT	42 min
Th-NT	35 min
Th-SC	34 min

We show that trehalose conjugation could be an useful strategy to render a bioactive peptide more soluble and stable in the biological system, thereby, promoting it as a potential drug. In our case, trehalose conjugation does not reduce the inhibitor activity when the glucidic moiety is bound to *N*-terminus or to the *C*-terminus position, but notably it induces enhanced stability toward enzymatic degradation. Studies are in progress to better correlate peptide structure with inhibition of A*β*'s cytotoxicity.

Acknowledgements

This work was supported by MIUR PRIN 2006-33492, 2005-035582, FIRB RBNE03PX83 and FIRB RBIN04L28Y.

References

1. Hardy J, Selkoe DJ. *Science* **297**: 353-356, 2002.
2. Chacon MA, Barria MI, Soto C, Inestrosa NC. *Mol Psychiatry* **9**: 953-961 2004.
3. Adessi C, Frossard M-J, Boissard C, Fraga S, Bieler S, Rucole T, Vilbois F, Robinson SM, Mutter M, Banks WA, Soto C. *J Biol Chem* **278**: 13905-13911 2003.
4. LeVine H III. *Methods Enzymol* **309**: 274-284, 1999.

2-11-175

Conformational studies of cyclolinopeptide A analogues modified by β-prolines

Mazur, Adam; Katarzyńska, Joanna; Zabrocki, Janusz; Jankowski, Stefan[1,]*

Technical University of Lodz, Institute of Organic Chemistry, POLAND

[*]E-mail: stefan.jankowski@p.lodz.pl

Introduction

Cyclolinopeptide A, (CLA), a cyclic nonapeptide cyclo(–Pro[1]-Pro[2]-Phe[3]-Phe[4]-Leu[5]-Ile[6]-Ile[7]-Leu[8]-Val[9]–), possesses strong immunossupresive and antimalarial activity as well as the ability to inhibit cholate uptake into hepatocytes. The mechanism of cyclolinopeptide A activity is similar to that of cyclosporine A.[1,2]

The object of our studies are six CLA analogues with Pro[1] and Pro[2] residues replaced by β^2-isoproline (**A**) or β^3-homoproline (**B**):

1 cyclo(–βhPro[1]-Pro[2]-Phe[3]-Phe[4]-Leu[5]-Ile[6]-Ile[7]-Leu[8]-Val[9]–)
2 cyclo(–Pro[1]-βhPro[2]-Phe[3]-Phe[4]-Leu[5]-Ile[6]-Ile[7]-Leu[8]-Val[9]–)
3 cyclo(–βhPro[1]-βhPro[2]-Phe[3]-Phe[4]-Leu[5]-Ile[6]-Ile[7]-Leu[8]-Val[9]–)
4 cyclo(–βiPro[1]-Pro[2]-Phe[3]-Phe[4]-Leu[5]-Ile[6]-Ile[7]-Leu[8]-Val[9]–)
5 cyclo(–Pro[1]-βiPro[2]-Phe[3]-Phe[4]-Leu[5]-Ile[6]-Ile[7]-Leu[8]-Val[9]–)
6 cyclo(–βiPro[1]-βiPro[2]-Phe[3]-Phe[4]-Leu[5]-Ile[6]-Ile[7]-Leu[8]-Val[9]–)

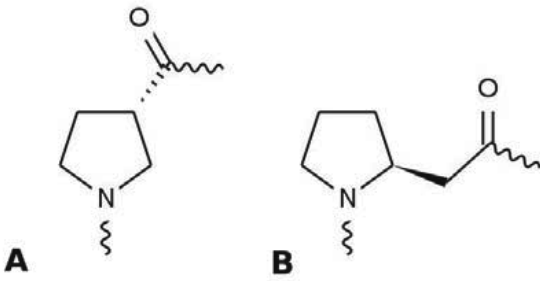

Figure 1.

NMR Spectroscopy

NMR measurements were carried out on Bruker Avance II Plus 700 MHz spectrometer in DMSO-d_6 at 25 °C. All peptides exist as mixtures of four isomers due to *cis/trans* isomerization of the Xxx-Pro bonds. For major isomers the geometry of proline-proline bonds and their percentage were determined by means of NMR: **1** (*trans*, 74%), **2** (*cis*, 95%), **3** (*trans*, 39%), **4** (*trans*, 46%), **5** (*cis*, 69%) and **6** (*cis*, 67%).[4] NOESY spectra were assigned, integrated and then applied for verification of the calculated structures for major isomers of peptides **1**-**6**. Cross-peak volumes were classified into three categories: strong (1.8-3.0 Å), medium (1.8-3.5 Å) and weak (1.8-4.5 Å). Pseudo-atom corrections (0.9 Å for CH_2, 1.0 Å for CH_3 and 2.2 Å for $(CH_3)_2$ were applied for experimental upper bounds.

Molecular dynamics

A starting coordinates of a cyclic peptides were constructed using default simulated annealing protocol implemented within XPLOR-NIH program. MD simulation was performed using the GROMACS 3.3.2 package and GROMOS 53A6 force field. Solvent was treated explicitly as a truncated octahedron box of ~800 DMSO molecules. The box vector length was set at 55 Å, which is large enough to prevent cyclic peptide interactions with its periodic image. The system was subjected to energy minimization with 5000 steps of the conjugate gradient algorithm and subsequent NPT molecular dynamics (200 ps), with restrained cartesian coordinates of peptide atoms. Total simulation time was 500 ns. In order to maintain temperature of 300 K and pressure of 1 bar, Berendsen weak coupling was used, with coupling constants of 0.1 ps for the temperature and 1 ps for the pressure. Coulomb interactions were evaluated using Particle-Mesh Ewald algorithm with switching distance of 1.0 Å. A twin range cut-off of 1.0/1.4 Å for the van der Waals interactions was applied. Integration time step was 2 fs and all bonds were constrained by means of SHAKE algorithm.

Structure analysis

NOE distance bounds were checked for the last 300 ns of trajectory using $< r^{-6} >$ distance averaging. NOE violations higher than 0.5 Å were not observed. Structures were clustered on the basis of the root mean square difference (RMSD) of backbone atoms positions with cutoff of 1.0 Å.

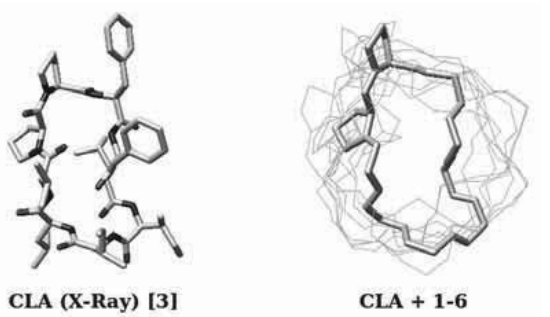

Figure 2. Central structures of main cluster (right) superimposed on the X-Ray structure of unmodified CLA (left).

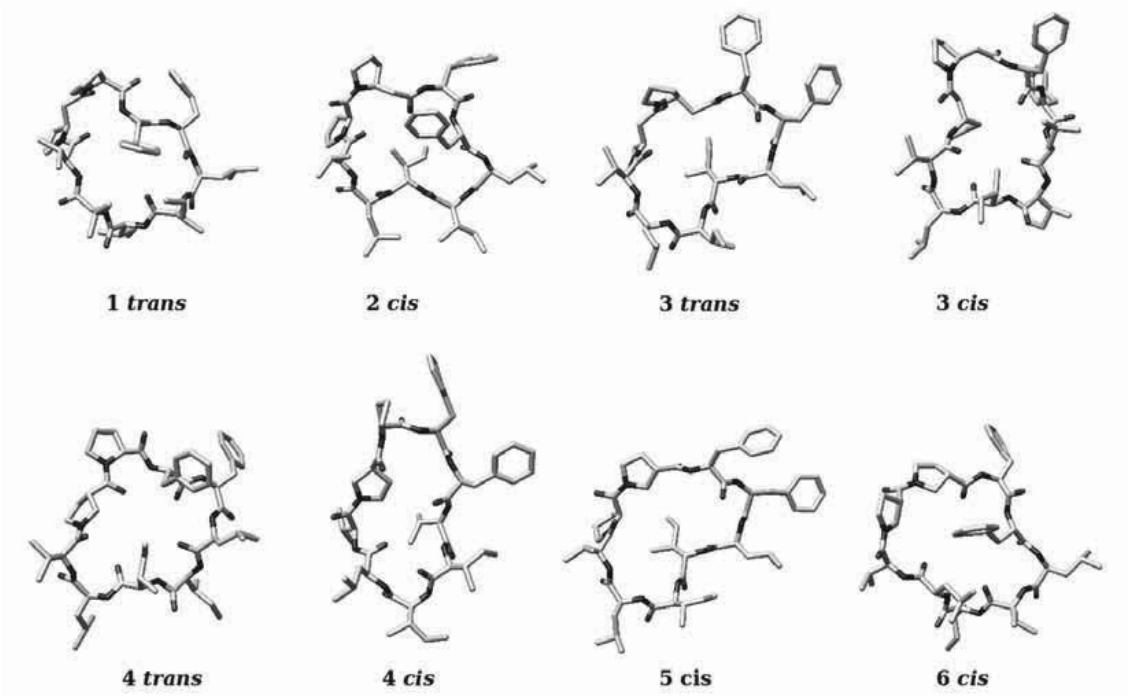

Figure 2. NMR structures of major isomers of peptides 1-6.

Conclusions

The expansion of CLA backbone by one or two carbon atoms remove mutual orientation of Phe aromatic rings and their edge-to-face orientation, which is observed for CLA. The lack of spatial proximity of benzene rings is not transmitted into significant decrease of immunosuppressive activity of CLA analogues,[4] as would be expected on the basis of previous findings.[1,2] The replacement of Pro by β-Pro is a useful tool for fine-tuning of CLA immunosuppressive activity and undesirable toxicity.

Acknowledgements

This work was supported by the Ministry of Science and Higher Education. Grants No 2 505F 035 and N N204 1970 33. AM is a grant holder of "Mechanizm WIDDOK" programme supported by European Social Fund and Polish State (contract number Z/2.10/II/2.6/04/05/U/2/06). Computer time was provided by Interdisciplinary Centre of Mathematical and Computational Modeling University of Warsaw (grant G28-23).

References

1. Benedetti E, Pedone C. *J Pept Sci* **11:** 268-272, 2005.
2. Picur B, Cebrat M, Zabrocki J, Siemion IZ. *J Pept Sci* **12:** 569-574, 2006.
3. Di Blasio B, Rossi F, Benedetti E, Pavone V, Pedone C, Temussi PA, Zanotti G, Tancredi T. *J Am Chem Soc* **111:** 9089-9098, 1989.
4. Katarzyńska J, Mazur A, Bilska M, Adamek E, Zimecki M, Jankowski S, Zabrocki J. *J Pept Sci* **14**:1283-1294, 2008.

2-11-176

The synthesis and structural study of iso-A*β*(1-42)

Bozsó, Zsolt[1,]; Penke, Botond[1]; Juhász, Gábor[2]; Szegedi, Viktor[2]; Laczkó, Ilona[3]; Soós, Katalin[1]; Simon, Dóra[1]; Fülöp, Lívia[1]*

[1]University of Szeged, Department of Medical Chemistry, HUNGARY; [2]Bay Zoltán Foundation for Applied Research, BAYGEN, HUNGARY; [3]Biological Research Center, Institute of Biophysics, HUNGARY

[*]E-mail: zbozso@yahoo.com

Introduction

A*β*(1-42) is prone to aggregate in aqueous solution. Because of that, the solubility of the peptide is poor and it cannot be stored for prolonged time in solution. Sohma and Kiso[1] attached Gly[25] to the hydroxyl side chain of the Ser[26] via an ester bond in their synthesis using Fmoc-chemistry. The solubility of the '*O*-acyl isopeptide' is greater than the A*β*(1-42), because it will not form fibrils as A*β*(1-42) does. It also can be stored in acidic solution for days. This 'isopeptide' will be rearranged at pH 7.4 to A*β*(1-42) through an *O*→*N* acyl shift.

As we know, structural studies on iso-A*β*(1-42) were not done. The purified peptide was examined with CD-spectroscopy, transmission electron microscopy (TEM), atomic force microscopy (AFM) and dynamic light scattering (DLS).

Results and Discussion

The A*β*(1-42) peptide is difficult to synthesize, because of its high tendency for aggregation during the synthesis.[2] Both the couplings and the Fmoc-removal can be troublesome, due to the steric hindrance. The incorporation of the ester-bond disturbs the structure, thus ease the synthesis after the 25th residue. If the peptide would be synthesized using Boc-chemistry the removal of the *α*-amino protecting group would be less problematic, because the 50% TFA/DCM mixture solubilizes well the peptide chain. Also diketopiperazine formation was reported during the synthesis of iso-A*β*(1-42) using Fmoc-chemistry.[3] Although this problem was solved by Coin and his coworkers,[3] the use of Boc-chemistry can suppress the side reaction too, since the neutralization step is much shorter than the time needed for the removal of the Fmoc-group. Thus a Boc-strategy was devised for the synthesis of iso-A*β*(1-42). The key step of the synthesis was that Ser[26] was incorporated using 2-Cl-Z-Ser(OtBu)-OH. The side chain protecting group of Ser[26] was removed by treating the peptide resin with 50% TFA/DCM (5+25 min). Following the neutralization step (5% DIEA/DCM, 2×1 min), the free hydroxyl group was acylated with Boc-Gly-OH using DCC/NMI activation (1:1, 10×excess, 2×4 h). Synthesis was then completed applying a standard Boc-protocol. The HPLC chromatogram of the crude peptide is presented on Fig. 1A.

CD spectroscopy and TEM revealed that even when iso-A*β*(1-42) dissolved in a pH 2 solution it has some *β*-sheet content and small aggregates are present. CD experiment also showed that further aggregation of the 'isopeptide' does not happen in the pH mentioned above. It was realized using AFM that if the 'isopeptide' dissolved in d.i. water before adjusting the pH to 7.4, particles with smaller size can be obtained, than if it is taken up straight into a pH 7.4 buffer. It was shown with CD spectroscopy that pretreatment of the 'isopeptide' with HFIP decreases its *β*-sheet content. Based on these findings the peptide was first treated with HFIP overnight, then dissolved in d.i. water and finally the pH was adjusted to 7.4 with an appropriate buffer. At this pH the *O*→*N* acyl shift has occurred. A*β*(1-42) formed from iso-A*β*(1-42) aggregates well (Fig. 2A) and during

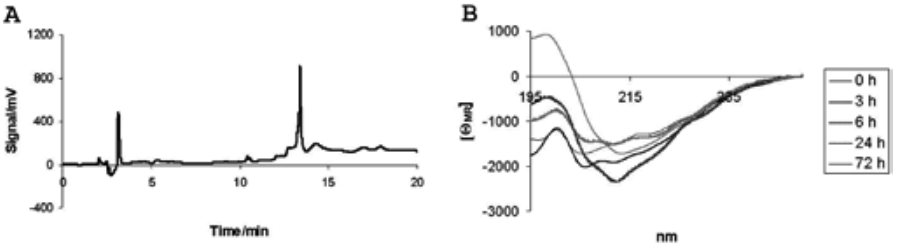

Figure 1. A: HPLC chromatogram of the crude iso–A*β*. The peptide was treated with HFIP prior injection. Conditions: 16–48% ACN/water in 20 min, 0.1% TFA, 1.2 ml/min, c18 (100 Å, 5 μ) **B:** The aggregation of the peptide followed by CD-spectroscopy.c=100 μM.

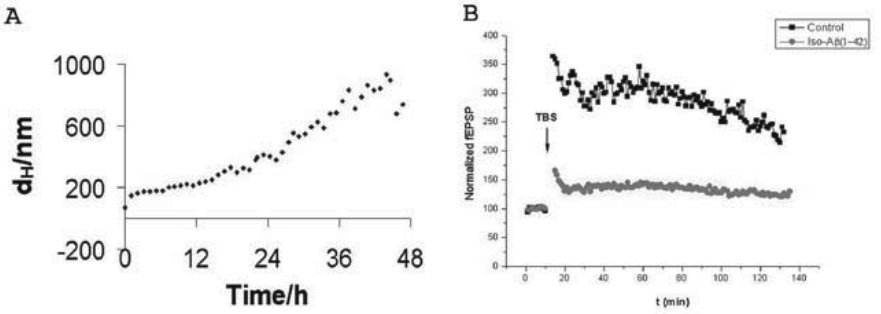

Figure 2. A: The aggregation of the peptide followed by DLS. c=100 μM. **B:** The effect of the peptide on long term potentiation in *ex vivo* electrophysiology experiment.

the aggregation its *β*-sheet content has increased (Fig. 1B). The peptide obtained from the 'isopeptide' has the same effect in *ex vivo* electrophysiology experiment as A*β*(1-42) has, namely hinders the long term potentiation, thus it decreases synaptic plasticity and the capability of learning (Fig. 2B). Our results confirmed that this peptide can be used as a precursor of iso-A*β*(1-42).

References

1. Sohma Y, Hayashi Y, Kimura M, Chiyomori Y, Taniguchi A, Sasaki M, Kimura T, Kiso Y. *J Pept Sci* **11**: 441-451, 2005.
2. Zarándi M, Soós K, Fülöp L, Bozsó Z, Datki Z, Tóth GK, Penke B. *J Pept Sci* **13**: 94-99, 2007.
3. Coin I, Dölling R, Krause E, Bienert M, Beyermann M, Sferdean CD, Carpino LA. *J Org Chem* **71**: 6171-6177, 2006.

2-11-177

Oligopeptide-porphyrin interactions: the effects of the porphyrin metalation and axial ligation on peptide matrix conformation

Setnicka, Vladimir[1,]; Hlaváček, Jan[2]; Urbanova, Marie[1]*

[1]Institute of Chemical Technology, Prague, CZECH REPUBLIC; [2]Institute of Organic Chemistry and Biochemistry Academy of Sciences of the Czech Republic, CZECH REPUBLIC

[*]E-mail: vladimir.setnicka@vscht.cz

Introduction

Peptide-porphyrin complexes are of interest because they serve as models of the biologically important porphyrin-conjugating proteins[1] involved in a variety of natural processes. For example, chlorophyll-protein complexes play an important role in the primary photophysical stages of photosynthesis, and hemoglobin is essential for oxygen transport processes. Interactions occurring between the porphyrins and the polypeptide templates, which are oppositely charged to the porphyrin, have also been extensively investigated[1,2] for their possible application to biomedicine and the photodynamic therapy (PDT)[3] of cancer diseases. Such binding, mainly driven by electrostatic interaction, may lead, in some cases, to subtle structural changes in peptide-porphyrin conjugates and, thus, influence their biological activity. For these reasons peptide-porphyrin complexes have been the subjects of numerous spectroscopic studies.[4-6]

In this work, we utilized vibrational circular dichroism (VCD) spectroscopy to study non-covalent interactions between the cationic tripeptide L-lysyl-L-alanyl-L-alanine (KAA) and the anionic porphyrin *meso*-tetrakis(4-sulfonatophenyl)porphyrin (TPPS), as well as between KAA and the three metal derivatives of TPPS (copper(II), iron(III), and manganese(III)), each of which has a different number of axial ligands. Using VCD, together with ECD spectroscopy, we studied the subtle conformational changes induced in the peptide part of porphyrin-KAA complexes by interaction with TPPS derivatives in aqueous solution at near-neutral pH values. In particular, we focused on the effect of the metalation and axial ligation of TPPS derivatives on the peptide conformation of such complexes. While the influence of TPPS on the porphyrin part of peptide-porphyrin complexes has been well-studied using a variety of methods,[4-6] its effect on peptide matrices is less understood and has only been investigated in the last decade.[7]

Results and Discussion

VCD and ECD spectra of pure KAA and its complexes with metal-free and various metallated TPPS derivatives are shown in Fig. 1 and 2, respectively. The VCD spectrum of pure KAA in the amide I' (C=O stretching vibration) region shows a negative couplet consisting of an intense negative band at 1647 cm^{-1} and a weak positive band at 1673 cm^{-1} (Fig. 1, solid line). The ECD spectrum consists of a strong negative band at ~ 188 nm and a

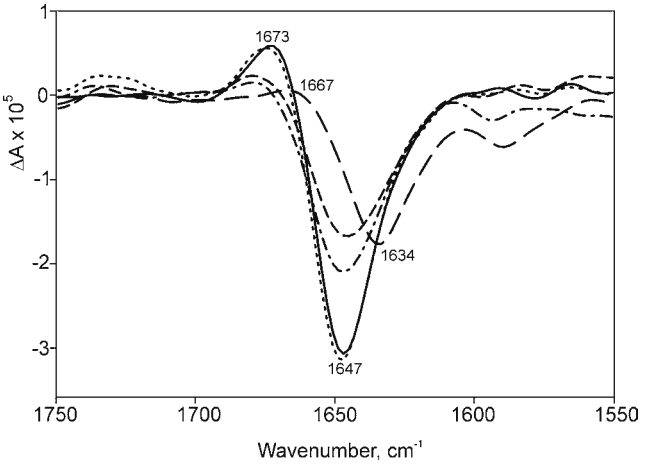

Figure 1. VCD spectra in amide I' region of KAA alone (solid line) and in the presence of metal-free TPPS (long dash), Cu(II)TPPS (short dash), Fe(III)TPPS (dash-dot), and Mn(III)TPPS (dot); *c*(KAA) = 0.14 mol L^{-1}. The molar concentration ratio peptide/porphyrin = 1/1 and pH ~ 7.4. Spectra were recorded at 8 cm^{-1} resolution using a demountable cell consisting of two CaF_2 windows separated by a 25 μm Teflon spacer.

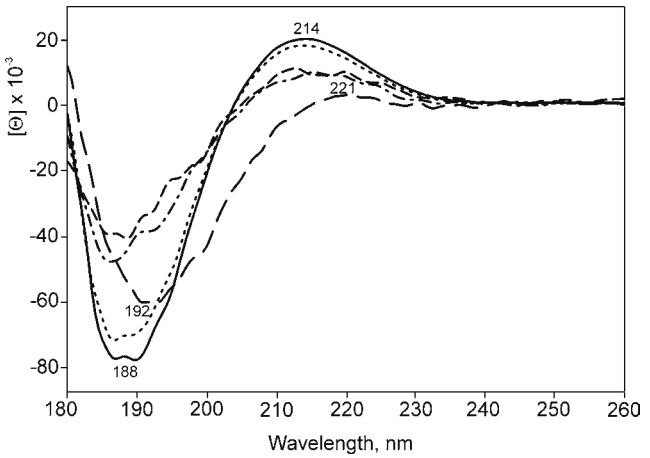

Figure 2. ECD spectra of KAA alone (solid line) and in the presence of metal-free TPPS (long dash), Cu(II)TPPS (short dash), Fe(III)TPPS (dash-dot), and Mn(III)TPPS (dot); c(KAA) = 0.14 mol L^{-1}.

weak positive band at ~ 214 nm (Fig. 2, solid line). These band shapes, both in VCD and ECD, revealed that KAA adopts a left-handed polyproline II (PPII) conformation[7,8] (a left-handed 3_1 helix of *trans* peptides) when dissolved in aqueous solution at near-neutral pH values. Because it is a very short peptide, such a conformation is best viewed as an ordered left-handed turn or left-handed twist, which, at least locally, has similarities to that of a left-handed helical PPII.

When mixed with metal-free TPPS in a molar ratio of 1/1 under the same conditions, the VCD intensities were markedly reduced in the amide I' region and a new negative band was observed at 1634 cm^{-1} (Fig. 1, long dashed line); both findings indicating[7,8] that ionic interaction between KAA and TPPS completely destabilizes the left-handed 3_1 helical segments of PPII, and results in a new type of well-organized structure, which shows spectral similarities to the β-sheet structure. Because of high sensitivity of VCD to the local structure, we hypothesize that a local β-sheet-like conformation is present in this case.

Although VCD was found to be more sensitive than ECD for determining such subtle peptide conformation changes, ECD also confirmed the existence of the new conformation (Fig. 2, long dashed line). In addition, absorption in the Soret region shows a dimeric form[4,5,7] of TPPS bound to the KAA (band at 407 nm, not shown). Thus, we conclude that metal-free TPPS, bound to the KAA as a dimer, altered the PPII conformation of KAA in its entirety, forming a new local β-sheet-like structure.

In the case of the metal derivatives of TPPS studied, only variations in the VCD intensities in the amide I' region were observed (Fig. 1). Compared to the results for pure KAA, the binding of Cu(II)TPPS, which has no axial ligand, resulted in the greatest decrease in amide I' VCD intensity (short dashed line). Nevertheless, the shape of a VCD spectrum characteristic for a PPII conformation was maintained, thereby indicating the presence of an "extended" PPII conformation in the Cu(II)TPPS-KAA complex. The conformation is best viewed as an "extended" left-handed turn or twist. Conversely, Mn(III)TPPS, which has two axial ligands, did not significantly affect the PPII conformation of KAA in the Mn(III)TPPS-KAA complex (dotted line). The ECD spectra fully supported these VCD findings.

Taken together, the different binding abilities of the metal derivatives of TPPS can be explained by differences in their number of axial ligands; the fewer axial ligands the TPPS metal derivative has, the greater the impact of that derivative on the KAA conformation. We attribute this finding to the steric effects and size of the porphyrin dimers being bound to KAA.

Acknowledgements. This work was supported by grant no. 203/06/P371 of the Grant Agency of the Czech Republic.

References

1. Lang K, Mosinger J, Wagnerová DM. *Coord Chem Rev* **248**: 321-350, 2004.
2. Pasternack RF, Gibbs EJ , Villafranca JJ. *Biochemistry* **22**: 2406-2414, 1983.
3. Sternberg ED, Dolphin D, Bruckner C. *Tetrahedron* **54**: 4151-4202, 1998.
4. Gurrieri S, Aliffi A, Bellacchio E, Lauceri R, Purrello R. *Inorg Chim Acta* **286**: 121-126, 1999.
5. Nezu T, Ikeda S. *Bull Chem Soc Jpn* **66**: 25-31, 1993.
6. Fukushima Y. *Bull Chem Soc Jpn* **69**: 1719-1726, 1996.
7. Urbanova M, Setnicka V, Kral V, Volka K. *Biopolymers (Peptide Science)* **60**: 307-316, 2001.
8. Keiderling TA, Silva RAGD, Yoder G, Dukor RK. *Bioorg Med Chem* **7**: 133-141, 1999.

2-11-178

Conformational and thermal stability of sequential cationic oligopeptides (Lys-Ala-Ala)$_n$ in aqueous solution

Setnicka, Vladimir[1]; Hlaváček, Jan[2]; Urbanova, Marie[1,]*

[1]Institute of Chemical Technology, Prague, CZECH REPUBLIC; [2]Academy of Sciences of the Czech Republic, Institute of Organic Chemistry and Biochemistry CZECH REPUBLIC

[*]E-mail: marie.urbanova@vscht.cz

Introduction

Sequential polycationic oligopeptides containing positively charged aminoacids (Lys, Arg, Orn) were found to be suitable models of biologically important small-sized proteins – histones – located in the chromosomes of eucaryotic cells. They interact with negatively charged molecules such as DNA,[1] polyuronic acids[2] and porphyrin derivatives[3,4] and thus influence a broad range of biological functions: transcription or packing of DNA, gene regulation and others.

In this study, sequential cationic oligopeptides of the different length of peptide chain, H-(L-lysyl-L-alanyl-L-alanine)$_n$-OMe, (KAA)$_n$, n = 1, 2 and 3, were synthesized and their solution conformations were investigated over a range of temperatures using a combination of spectroscopic techniques with emphasis to vibrational (VCD) and electronic (ECD) circular dichroism spectroscopies. Singular value decomposition (SVD) method of factor analysis (FA) was applied to help understand the thermal stability and thermally induced conformational changes.

Results and Discussion

The solvent-corrected VCD spectra of tripeptide KAA and hexapeptide (KAA)$_2$ measured in the amide I' region at different temperatures are presented in Fig. 1. At 20 °C, the VCD spectra of both oligopeptides show a negative couplet (intense negative band at ~ 1645 cm^{-1} followed by a broad weak positive band at ~ 1670 cm^{-1}), which is characteristic of polyproline II (PPII) conformation,[4,5] a left-handed 3_1 helix of *trans* peptides. The presence of PPII conformation was supported by position of the amide I' IR band observed at ~ 1650 cm^{-1} and also by UV-ECD spectra showing a strong negative band at ~ 188 nm and a weak positive band at ~ 215 nm (data not shown). In addition, we optimized the structures of both peptides using the semi-empirical PM3 and AM1 methods. The average dihedral angles in the upper left square of the Ramachandran plot were obtained (φ ~ -103° and ψ ~ 151°). These values are close to the canonical PPII conformation (φ ~ -79° and ψ ~ 150°).

The VCD of both peptides is shown to be significantly reduced in intensity by temperature increase. While the hexapeptide shows a more drastic intensity changes in amide I' region, the shape of a VCD spectra characteristic for a PPII conformation was maintained for both the peptides even at 90 °C, thereby indicating considerable conformational stability of the KAA sequence independently on a chain length. It is reasonable to assume that the loss of the VCD signal at higher temperatures is consistent with a loss of PPPII structure in these peptides. Thus, a disordered conformer becomes more populated at the expense of the PPII-conformer at higher temperatures. However, the PPII remains the most predominant conformation within the range of temperatures studied.

In order to support this hypothesis, the two sets of temperature-dependent VCD spectra were each analyzed for the spectral regions shown in Fig. 1 by the singular value decomposition method of factor analysis. The first two component spectra (factors) describe more than 95% of the total bandshape change and, therefore, became the focus of our attention. In general, the first component spectra (not shown) and their coefficients (loadings) C1 shown in Fig. 2 represent the average intensity of the VCD pattern, which varied slightly. The second components, which have a derivative shape (not shown), contribute to the major thermal spectral variation as indicated by a monotonic change of the second coefficients C2. The only break in the course of the coefficient dependence was observed for the both peptides between 80 and 90 °C, which is understandable because of wider distribution of conformers and a higher destabilization of the most predominant PPII conformation of short peptide sequences at these temperatures. Non-significant loadings of the third component (coefficient C3, not shown) indicate negligible contribution to the intensity from other conformations whose populations would grow in during the thermal process.

Thus, we found that temperature as well as peptide chain length impact the conformation of these sequential peptides, dissolved in aqueous solution at near-neutral pH values, to a very low degree. Our data suggest that PPII is the dominant conformation, which may be in a thermodynamic equilibrium with a more extended, disordered structure at higher temperatures. However,

the population of other highly ordered structures is negligible. This conclusion was confirmed by SVD analysis of temperature-dependent UV-ECD spectra measured on KAA, $(KAA)_2$, and $(KAA)_3$.

Acknowledgements

This work was supported by grant no. 203/06/P371 of the Grant Agency of the Czech Republic. The authors also wish to thank Prof. Jiri Bok and Prof. Vladimir Baumruk (Institute of Physics of Charles University) for providing the factor analysis software.

References

1. Gurrieri S, Aliffi A, Bellacchio E, Lauceri R, Purrello R. *Inorg Chim Acta* **286:** 121-126, 1999.
2. Bystricky S, Sticzay T, Kohn R, Blaha K. *Collect Czech Chem Commun* **51:** 2919-2923, 1986.
3. Nezu T and Ikeda S. *Bull Chem Soc Jpn* **66:** 25-31, 1993.
4. Urbanova M, Setnicka V, Kral V and Volka K. *Biopolymers* **60:** 307-316, 2001.
5. Keiderling TA, Silva RAGD, Yoder G and Dukor RK. *Bioorg Med Chem* **7:** 133-141, 1999.

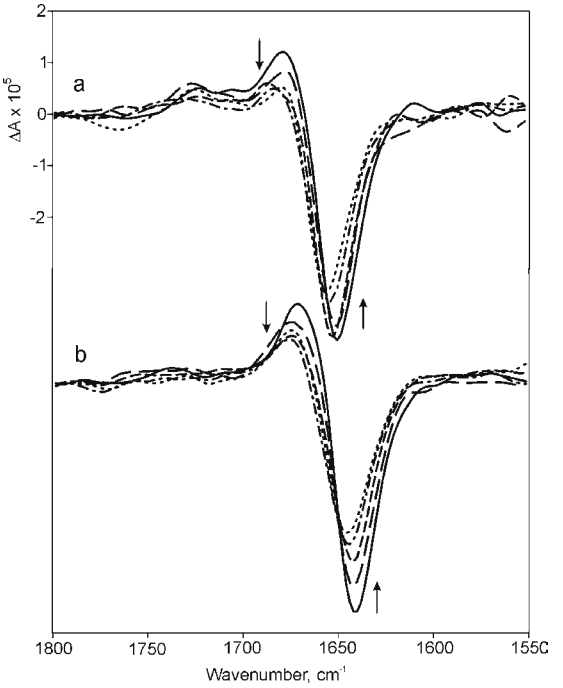

Figure 1. Temperature-dependent VCD spectra of KAA (a) and $(KAA)_2$ (b) in deuterated phosphate buffer at pH = 7.2. (Solid line: 20 °C, long dash: 40 °C, short dash: 60 °C, dash-dot: 80 °C, dotted: 90 °C). Arrows indicate direction of signal changes with increasing temperature. Spectra were recorded at 8 cm^{-1} resolution using a demountable cell consisting of two CaF_2 windows separated by a 25 μm Teflon spacer.

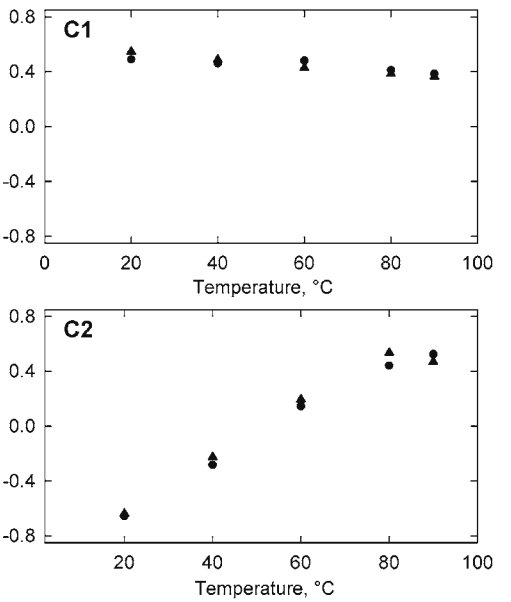

Figure 2. SVD/FA loadings determined from the amide I' VCD spectra for KAA (circles) and $(KAA)_2$ (triangles). Coefficients of the first (C1) and second (C2) component spectra are plotted.

2-12-179

Spin-label aided investigation of feline immunodeficiency virus Gp36 derived peptide in presence of membrane models.

Grimaldi, Manuela[1]; D'Errico, Gerardino[2]; Scrima, Mario[1]; Esposito, Cinzia[1]; Giannecchini, Simone[3]; Bendinelli, Mauro[4]; Rovero, Paolo[5]; Marsh, Derek[6]; D'Ursi, Anna Maria[1,]*

Università di Salerno, Dipartimento di Scienze Farmaceutiche, ITALY; [2]Università di Napoli "Federico II", Dipartimento di Chimica, ITALY; [3]Università di Firenze, Dipartimento di Sanità Pubblica, ITALY; [4]Università degli Studi di Pisa, Centro Retrovirus, Dipartimento di Biomedicina, ITALY; [5]Università di Firenze, Dipartimento di Scienze Farmaceutiche, ITALY; [6]Abt. Spektroskopie, Goüttingen, Max-Planck-Institut für biophysikalische Chemie, GERMANY

[*]E-mail: dursi@unisa.it

Introduction

P59 is a 20-mer potent antiviral peptide, corresponding to the residues 767-786 of the membrane-proximal external region (MPER) of feline immunodeficiency virus (FIV) Gp36 ectodomain (Fig. 1).[1] The lipoylated analogue, lipo-P59, displays a similar antiviral activity, which is preferentially preserved by cellular substrates. A mechanism has been proposed in which the peptide, being positioned on the surface of the cell membrane, inhibits its fusion with the virus; the lipophilic chain of lipo-P59 is thought to insert into the membrane interior, thus anchoring the peptide at the surface. In the present work, the ability of P59 and lipo-P59 to interact with lipid surfaces was investigated by using spin-labelling EPR.[3] Two phospholipids were examined, the zwitterionic dimyristoyl phosphatidylcholine and the anionic dimyristoyl phosphatidylglycerol. To support EPR data 2D TOCSY and NOESY NMR spectra were recorded in DPC/SDS 90/10 mixed micelles using 5 doxil stearic and 16 doxil stearic acids as spin labels. NMR data confirm the results of ESR experiments, leading to the specific identification of the aminoacids involved in the peptide/lipid-surface interaction.

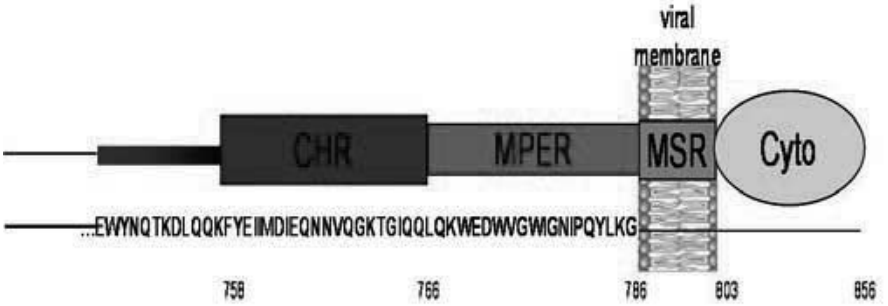

Figure 1. Schematic representation of the *C*-terminal region of gp36. P59 sequence is highlighted in bold. Domains are indicated as follows: CHR, *C*-terminal α-helix region; MPER, membrane proximal external region; MSR, membrane-spanning region; Cyto, cytoplasmic region.

Results and discussion

EPR spectra of DMPC and DMPG membranes containing phosphatidylcholine (5-PCSL), and phosphatidylglycerol (5-PGSL) spin-labeled on the 5-C atom of the sn-2 chain were recorded at different temperatures. Indeed the peptide-lipid interaction can depend upon the state (gel or fluid phase) of the lipid bilayer. The spectra were recorded in the presence and in the absence of the peptides P59 or lipo-P59. Fig. 2 shows selected ESR spectra from the zwitterionic DMPC lipid samples; significant perturbations by the peptides are detectable (compare solid and dashed lines). For both membranes a sharp decrease in 2Amax is evident, corresponding to the increase in lipid chain mobility on transition from the gel to the fluid phase of the bilayer. In the fluid membrane phase, 2Amax is larger in the presence of peptide than in its absence, i.e., the mobility of the spin-labelled chains is decreased by interaction of the peptide with the membrane. The effect is stronger for P59 than for the lipoylated analogue. For both membranes a sharp decrease in 2Amax is evident, corresponding to the increase in lipid chain mobility on transition from the gel to the fluid phase of the bilayer. In the fluid membrane phase, 2Amax is larger in the presence of peptide than in its absence, i.e., the mobility of the spin-labelled chains is decreased by interaction of the peptide with the membrane. The effect is stronger for P59 than for the lipoylated analogue.

NMR spin-label studies. The positioning of the peptide relative to the surface and interior of the DPC/SDS mixed micelles was studied using 5-doxyl, 5-DSA and 16 doxyl stearic acid, 16-DSA. These paramagnetic probes are expected to cause broadening of the NMR signals and

decrease of resonance intensities from residues inside but close to the surface (5-DSA), or deeply buried in the micelle (16-DSA), respectively. TOCSY spectra of P59 and lipo-P59 in the presence and absence of the spin labels were recorded keeping constant all other conditions. The comparison of the NH/α region of TOESY spectra of P59 and lipo-P59, acquired in the presence and in absence of 5-doxyl stearic acid, evidences that NH/α signals of Trp773 and Trp776 are sensibly decreased in intensity. Additionally Asp772, Val774, Gly775, Asn779 are slightly affected by the presence of 5-doxylstearic acid. Additionally. lipo-P59 evidenced a decrease of NH/α signals relative to Aod residue, carrying the lipophilic chain, and Ile779 16-doxylstearic acid did not yield any significant effect on P59 and lipo-P59 TOCSY spectra. Previous NMR studies revealed that P59 assumes in micellar environment an amphipathic helical structure encompassing the residues from Trp770 to Ile780 (21). The polar or charged residues are positioned on one side, (Fig. 5), with the opposite side occupied by hydrophobic residues. In particular on the hydrophobic face the tryptophans side chains are present. Our results suggest that the peptide is localized at the polar-apolar interface of membranes (38, 59) through the interaction of Trp side chains , in particular those belonging to Trp773, Trp776. The neighboring residues take part to the interaction.

Conclusions

ESR and NMR experiments using spin-labelled lipids demonstrate that the P59 and lipo-P59 peptides associate with lipid bilayers by binding at the membrane surface. Additionally, the lipoyl chain of lipo-P59 inserts between those of the lipid bilayer. This stabilises the bilayer against the surface-active, solubilising tendency of P59 without the chain, anchors the peptide more strongly to the membrane thus enhancing long-term antiviral activity, and may also increase the capacity to bind to the membrane. The mechanism of binding P59 to phospholipid membranes is primarily amphipathic, and mainly driven by Trp interfacial hydrophobic interactions.

References

1. (a) Jiang S., Lin K., Strick N, Neurath AR. *Nature* **365**: 113, 1993; (b) Jin B, Jin S, Ryu R, Ahn K, Yu YG. *Res Hum Retrovir* **16**: 1797-1804, 2000.
2. Earp LJ, Delos SE, Park HE, White JM. *Curr Top Microbiol Immunol* **285**: 25-66, 2005.
3. D'Errico G, D'Ursi AM, Marsh D. *Biochemistry* **47**: 5317-5327, 2008.

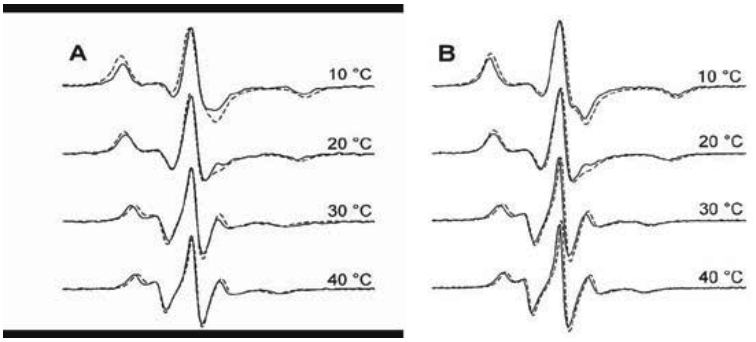

Figure 2. ESR spectra of 5-PCSL in dimyristoyl phosphatidylcholine bilayer membranes, in the presence (solid line) and in the absence (dashed line) of 1:1 wt/wt peptide at the temperatures indicated. (A) P59. (B) lipo-P59.

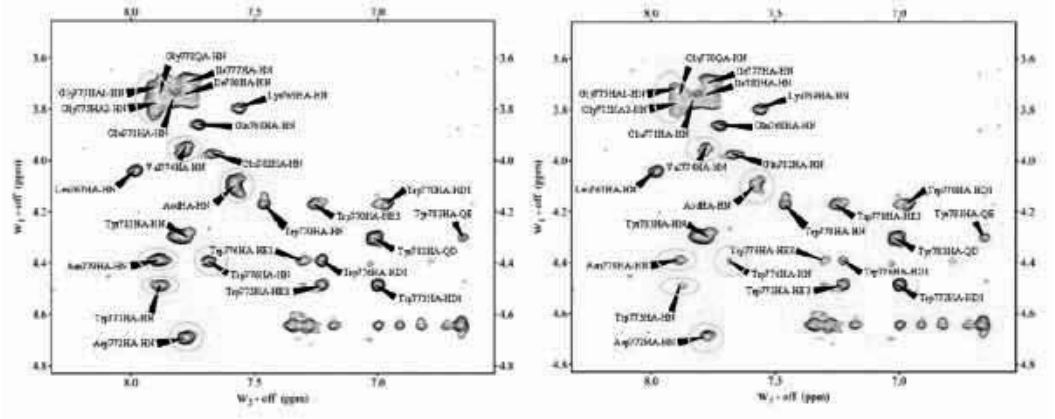

Figure 3. NH/α region of lipo-P59 TOCSY spectra recorded in the absence (left) and in the presence (right) of 5-doxyl stearic acid. Signals affected by spin label are highlighted by yellow circle.

2-12-180

Effect of flavonoids on Aβ-25-35 -DLPC vesicle interaction

Tedeschi, Annamaria[1]; Lauro, Maria Rosaria[1]; Grimaldi, Manuela[1]; D'Errico, Gerardino[2]; D'Ursi, Anna Maria[1,]; Aquino, Rita Patrizia[1]*

[1]Università di Salerno, Dipartimento di Scienze Farmaceutiche, ITALY; [2]Università di Napoli „Federico II", Dipartimento di Chimica, ITALY

[*]E-mail: dursi@unisa.it

Introduction

Neuronal cell death in Alzheimer diseases (AD) is partly induced by the interaction of the amyloid-β peptide (Aβ), the major component of amyloid deposits, with the plasma membrane of target cells.[1] Unstructured Aβ has been shown to undergo a membrane-induced conformational change to either primarily β-structure or helical structure, depending, among other factors, on the fluidity of cell membrane.[2] Flavonoids are a group of naturally occurring, benzo-γ-pyrone derivatives, ubiquitous in plants. They are endowed with tumor prevent activity and act as antioxidants through a membrane mediated molecular mechanism involving the membrane ion transport. With the aim to clarify the molecular basis of the interaction between amyloid peptides and cellular membranes, we investigated the interaction between a cytotoxic fragment of Aβ(1-42), -Aβ(25-35) - and DLPC phospholipid bilayer membranes. We investigated the ability of Flavonoids to affect the Aβ(25-35) peptide-DLPC vesicles interaction. The effect of inclusion of Flavonoids, Quercetin, Naringenin, Rutin, and Naringin in the bilayer composition was studied by Electron Paramagnetic Resonance (EPR) spectroscopy using 5-PCSL and 14-PCSL spin-labels. The encapsulation of the selected Flavonoids into DLPC vesicles, was investigated by Fluorescence Microscopy (FM) in different Flavonoid-phospholipid molecular ratios.

Results and discussion

EPR spectroscopy of spin-labelled lipids is among the most powerful tools for investigating membrane-peptide interaction; particularly, the site of the association (membrane surface or bilayer interior) can be unambiguously identified. The EPR experiments were carried out using nitroxide spin labels attached to different positions of the acyl chain: 1) 5-PCSL in which the doxyl groups is situated closer to the lipid polar head-group to allow to monitor the membrane polar domain. 2) 14-PCSL in which the doxyl group is attached near to the end of the acyl chains to allow to monitor the membrane hydrophobic domain. Electron Paramagnetic Resonance (EPR) experiments were recorded in flavonoid containing DLPC vesicles, in the presence and in the absence of Aβ(25-35) peptide. EPR spectra of pure DLPC vesicles were recorded for comparison. EPR measurements were recorded employing 5-PCSL and 14-PCSLspin labels. The analysed EPR parameter is the outer hyperfine splitting, 2Amax, which is correlate to the membrane fluidity. EPR spectra of 14-PCSL in quercetin containing DLPC vesicles were recorded in the presence and in the absence of Aβ(25-35) peptide. EPR spectra of 14-PCSL in quercetin containing DLPC vesicles show a narrow three-line spectral component (Fig. 1). This pattern is typical of a hydrophobic microenvironment characterized by high rotational mobility. Addiction of

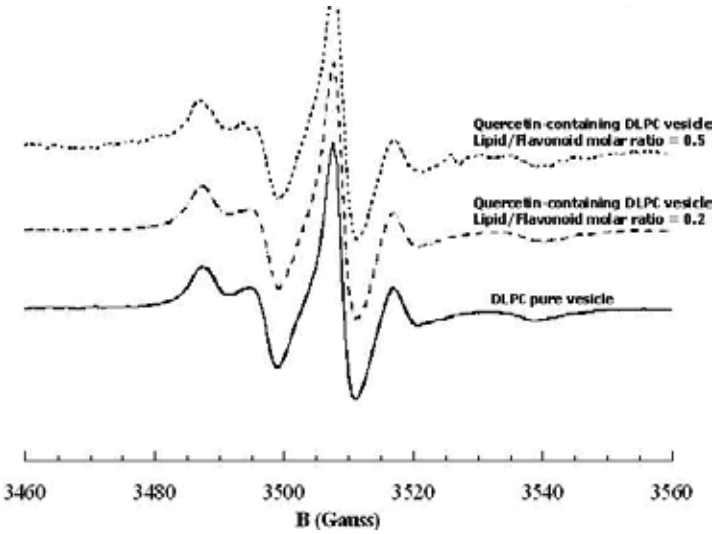

Figure 1. EPR spectra of DLPC vesicles in the presence of quercetin. Spectra differ for the lipid/Flavonoid molar ratios.

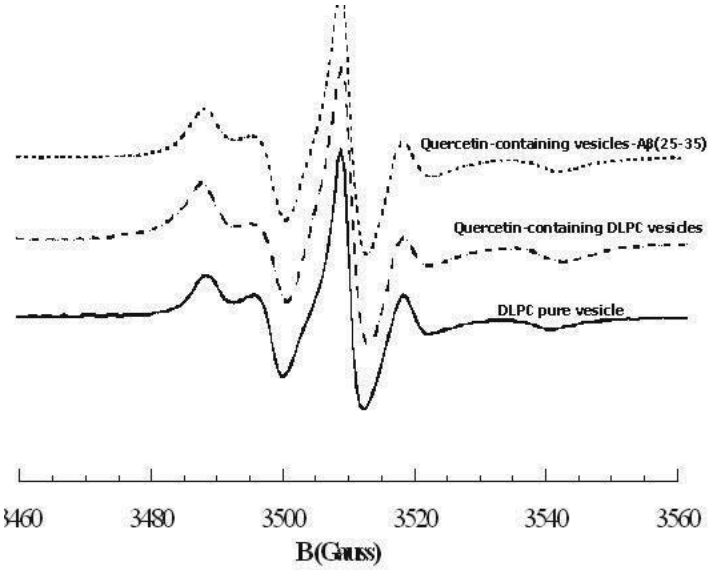

Figure 2. Comparison of EPR spectra of DLPC vesicles containing quercetin in the absence and in the presence of Aβ(25-35) peptide.

Aβ(25-35) does not modify this effect. These results indicate that host molecules – quercetin and Aβ(25-35) – have not tendency to be positioned into the hydrophobic domain of bilayer. EPR spectra of 5-PCSL performed in all examined membrane systems show a sharp three-line spectral component corresponding to the fluid lipid bilayer regions of the reconstituted vesicles in which the lipids have reduced rotational mobility. The insertion of quercetinin into the 5-PCSL spin-labelled DLPC vesicles, leads to broader spectrum with increasing of the outer hyperfine splitting constant, corresponding to an increased motional restriction of the spin-label (Fig. 2). Interestingly, the spin label motional restriction correlates with Flavonoids/phospholipid ratio (Fig. 2). The significant perturbation of the 5-PCSL spectrum due to the insertion of flavonoids and of Aβ(25-35), indicate a motional properties reduction of the doxyl group situated near the bilayer polar domain, suggesting that the host molecules insert in bilayer in the headgroup polar domain. EPR spectra of 5-PCSL were recorded in Quercetin-containing DLPC bilayers, in the presence of Aβ(25-35). Also in this case 2Amax increasing was observed, indicating a dramatic decrease in lipid fluidity of bilayer. The comparison of 5-PCSL EPR spectra of quercetin containing vesicles in the absence and in the presence of Aβ(25-35) peptide shows that the spectra are very similar, indicating that Aβ(25-35) is not able to modify the rigidity increase due to flavonoid compound.

Conclusions

Our EPR study of 5-PCSL and 14-PCSL in quercetin containing DLPC vesicles, in the absence and in the presence of Aβ(25-35), indicate that Flavonoids, in DLPC bilayers, tend to be positioned on the external layer, of the hydrophobic membrane. With such localization they yield a pronounced vesicle-rigidifying effect. This effect is not reverted by Aβ(25-35). Our findings provide a possible molecular explanation of the known neuroprotective effect of flavonoid, suggesting that they could be innovative pharmaceutical tools reverting a β-amiloid toxicity mechanism based on cell membrane destabilization.

References

1. Harrison RS, Sharpe PC, Singh Y, Fairlie DP. *Rev Physiol Biochem Pharmacol* **159**: 1-77, 2007.
2. Sipe JD, Cohen AS. *J Struct Biol* **130**: 88-98, 2000.

2-12-181

Aβ16-35 peptide: structural features in membrane mimicking systems

*Grimaldi, Manuela; Scrima, Mario; Esposito, Cinzia; Tedeschi, Annamaria; D'Ursi, Anna Maria**

Università di Salerno, Dipartimento di Scienze Farmaceutiche, ITALY

**E-mail: dursi@unisa.it*

Introduction

β Amyloid peptides A*β*(1–40) and A*β*(1–42) are the main components of plaques found in the postmortem brain of Alzheimer patients and considered the hallmark of Alzheimer disease. Depending upon conditions, A*β* (1–40) and A*β* (1–42) undergo conformational transition from soluble monomers to highly toxic *α*-sheet oligomers which form mature fibril aggregates.[1,2] Several conformational and biological analyses have been carried out on A*β* (1–40) and A*β* (1–42) as well as on their numerous derived fragments, to understand the role of the single portions in the fibrillation process. Here, we present a structural study of the fragment A*β* (16–35), in membrane mimicking, micelle systems. A*β* (16–35) includes two important A*β* fragments: A*β* (25–35) – which has been extensively studied as it is the minimal sequence preserving the toxicity of full length A*β* (1–42)[3] – and A*β* (17–21) which is known to play a critical role in the aggregation/disaggregation processes. A great deal of data have been highlighting the role of the cell membranes in toxicity mechanism of *β*-amyloid peptide; hence great interest is focused on the investigation of *β*-amyloid derived peptides in membrane mimicking systems.[4] In the present study, A*β* (16-35) was analyzed by CD and NMR spectroscopy in Sodium Dodecyl Sulphate (SDS) membrane mimicking micelle systems. The positioning of A*β* (25–35) on the micelle surface was investigated by spin-label aided techniques. NMR and CD studies in micelle solutions (CD) experiments of A*β*(16-35) were recorded in water and in pure SDS, micelle solution. CD spectrum of A*β* (16-35) recorded in pure SDS micelles evidences a positive shift of the minimum (208 nm) with respect to the signal obtained in water; this result suggests that A*β*(16-35) undergoes a conformational transitions to turn helical structures moving from water to micelle systems. 2D TOCSY and NOESY spectra of A*β*(16-35) were recorded in water, and in SDS pure micelles, at 600 MHz. NOE data are summarized in bar diagrams reported in Fig. 1. Bar diagrams evidence regular NOE patterns for spectra recorded in SDS micelles. Structure calculation: 3D structures of A*β*(16-35) were calculated on the basis of NOEs interprotonic distances, using DYANA software. The structure bundles of A*β*(16-35) in SDS micelle system (Fig. 2) evidence good definition of the structures, with low displacement among the conformers, in the superimposed regions. Analysis of backbone dihedral angles according to PROMOTIF procedure, shows that A*β*(16-35) assumes *α*-helical conformations along the segments 17Leu-24Val and 28Lys-34Leu.

Spin-labels experiments NMR spin-label studies: The positioning of the peptide relative to the surface and interior of the SDS micelles was studied using micelles containing the spin labelled compounds 5-doxyl, (5-DSA) and 16 doxyl stearic acids, (16-DSA). TOCSY and NOESY spectra of A*β*(16-35) in the presence and absence of the spin labels were recorded keeping constant all other conditions. The comparison of the NH/*α* region of TOESY spectra of A*β*(16-35), acquired in the presence and in the absence of 5-doxyl stearic acid, evidences that only NH/*α* signal of 19Phe is decreased in intensity. Conversely in the presence of 16-DSA 17Leu, 20Phe, 25Gly, 28Lys are significantly perturbed.

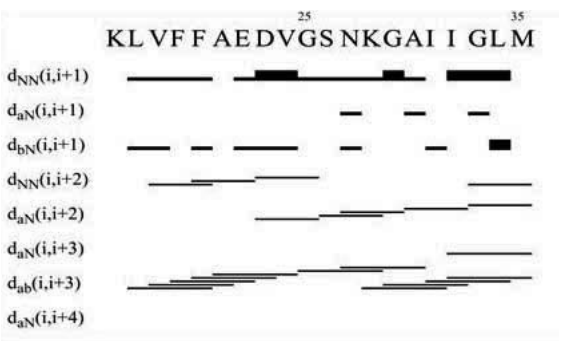

Figure 1. NOE data of A*β*(16-35) as derived from NOESY spectra recorded in SDS micelle solution at 600 MHz, 300 K.

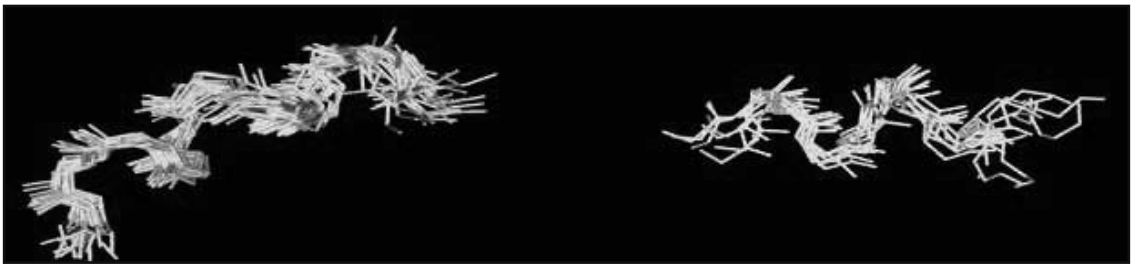

Figure 2. NMR structure bundles of 17Leu-24Val (left) and 28Lys-34Leu (right) regions of Aβ(16-35) in SDS micelle solution.

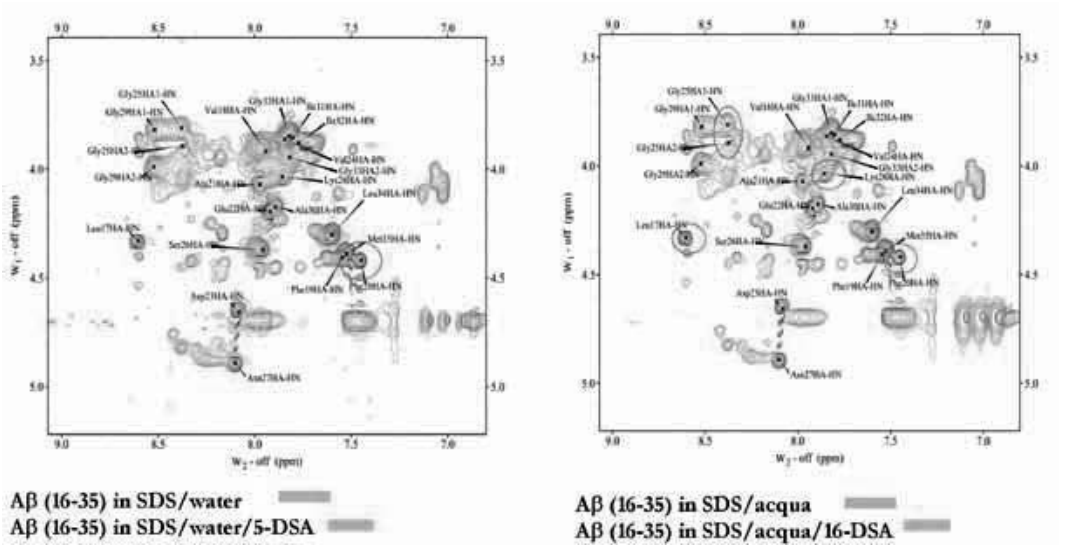

Figure 3. TOCSY spectra of Aβ(16-35) recorded in SDS micelle solution in presence of 5 doxil stearic acid (left) and 16 doxil stearic acid (right).

Conclusions

Aβ(16-35) was analyzed in SDS charged micelles. This highly negative charged surface, yields a structure stabilizing effect. Spin labels aided investigations indicate that the Aβ(16-35) fragment has tendency to interact with the inner core of the micelle rather than with its outer surface.

References

1. Sipe JD, Cohen AS. *J Struct Biol* **130**: 88-98, 2000.
2. Harrison RS, Sharpe PC, Singh Y, Fairlie DP. *Rev Physiol Biochem Pharmacol* **159**: 1-77, 2007.
3. D'Ursi AM, Armenante MR, Guerrini R, Salvadori S, Sorrentino G, Picone D. *J Med Chem* **47**: 4231-4238, 2004.
4. Matsuzaki K. Physicochemical interactions of amyloid beta-peptide with lipid bilayers. *Biochim Biophys Acta* **1768**: 1935-1942, 2007. Review.

2-14-182

Towards a Vaccine Against Multiple Sclerosis

Katsara, Maria[1]; Deraos, George[2]; Matsoukas, John M[2]; Apostolopoulos, Vasso[1,]*

[1]Burnet Institute, Austin campus, Immunology and Vaccine Laboratory, AUSTRALIA; [2]University of Patras, Chemistry, GREECE

[*]E-mail: vasso@burnet.edu.au

Introduction

Multiple sclerosis (MS) is an inflammatory, autoimmune, demyelinating disease of the central nervous system, of which CD4+ T cells of the Th1 subset, play a significant role.[1-3] Since the efficacy of current treatments are limited,[4] there is an increasing need for developing more potent therapeutic agents for MS. The design of peptide mutants (altered peptide ligands) of disease-associated myelin epitopes which, can alter immune responses, is a promising approach for the treatment of MS. Studies have shown that T cell responses in patients are associated with recognition of MBP81-105 (QDENPVVHFFKNIVTPRTPPPSQGK),[5] with the shorter peptide MBP83-99 displaying the strongest binding to HLA-DR2.[5] In addition, MBP83-99 peptide binds strongly to H2-IAs and a peptide binding motif suggested similar binding features as with HLA-DR2.[6] Cyclic peptides are of interest in immunotherapeutic studies since their linear counterparts have limited stability.[7] Moreover, cyclic peptides have been shown to bind to HLA-DR4 with similar affinity to their linear counterpart.[8] Therefore, we designed and synthesized a number of peptide analogs by mutating the principal TCR contact residue based on MBP83-99 epitope. The synthesis of all peptides (linear, cyclic, mutants), were carried out by the Fmoc/tBu methodology, utilizing the 2-chlorotrityl chloride resin.[9] Cyclization was achieved using *O*-benzotriazol-1-yl-N,N,N',N'-tetramethyluronium tetrafluoroborate and 1-hydroxy-7-azabenzotriazole, 2,4,6 collidine allowing fast reaction and high yield cyclization product.[10] The purification was achieved using RP-HPLC and the peptide purity was assessed by analytical HPLC and ESI-MS. Reduced mannan has been shown to induce a Th2 phenotype after immunization of mice[11,12] and secretion of Th2 cytokines by murine macrophages and dendritic cells in the presence of reduced mannan.[11,13] The use of reduced mannan to further divert immune responses to Th2 when conjugated to MBP83-99 peptides, constitutes a novel strategy for immunotherapy of the disease.

Results and discussion

Immunization of SJL/J mice with the native MBP83-99 peptide or the mutant peptide analogs - [A91]MBP83-99, [E91]MBP83-99, [F91]MBP83-99, [Y91]MBP83-99, [R91, A96]MBP83-99, emulsified in complete Freund's adjuvant (CFA), induced IFN-γ, and only [R91, A96]MBP83-99 mutant peptide was able to induce IL-4 secretion by T cells. Importantly, T cells against the native MBP83-99 peptide cross-reacted with all peptides except [Y91]MBP83-99 and [R91, A96]MBP83-99. The double mutant [R91, A96]MBP83-99 was able to antagonize IFN-γ production in vitro by T cells against the native MBP83-99 peptide. Antibodies generated to [R91, A96]MBP83-99 did not cross-react with whole MBP protein (14). Thus, [R91, A96]MBP83-99 is able to induce IL-4 and antagonize IFN-γ responses (Table 1). When all analogs were conjugated to reduced mannan, immune responses were diverted from Th1 to Th2 in SJL/J mice and generated antibodies which did not cross react with native MBP protein - in particular [Y91] MBP83 99 mutant peptide mutant (Table 1). Thus, this peptide is a promising candidate for the immunotherapy of MS.[6] In order to design more stable peptides for immunotherapeutic studies, a number of cyclic mutant peptides were designed and synthesized by mutating TCR contact sites of the MBP83 99 epitope. A number of cyclic analogs were tested in their ability to antagonize IFN-γ responses and cyclo(83-99)[A91]MBP83-99 mutant peptide was found to be the most efficient antagonist. We demonstrated that cyclo(83-99)[A91] MBP83-99 peptide emulsified in CFA enhanced IL-4 and antibody responses *in vivo*. Moreover, immunization of mice with cyclo(83-99)[A91]MBP83-99 peptide conjugated to reduced mannan further enhanced IL-4 responses compared to cyclo(83-99)MBP83-99 peptide (Table 1).[10] Thus, cyclization of peptides which offer greater stability and enhanced responses are novel leads for the immunotherapy of MS. In conclusion, MBP83-99 peptide generates strong IFN-γ and no IL-4 responses in SJL/J mice. It is clear that the mutation at position 91 generates IL-4 (Th2) cytokine in addition to IFN-Î³ (Th1). Mannosylation of the mutated peptides using reduced mannan was clearly able to divert immune responses from IFN-Î³ to IL-4 and IL-10. Mannosylation of linear and cyclic peptides with single or double mutation are promising new peptide leads, and, constitutes a promising approach for the immunotherapy of MS.

Acknowledgements

MK was supported by the Ministry of Development Secretariat of Research and Technology of Greece (Grant Aus. 005) and Du PrÃ© grant from MSIF. VA was supported by an NH&MRC of Australia R. Douglas Wright Fellowship (223316).

Table 1. Summary of immune responses induced to MBP_{83-99} linear and cyclic mutant peptide analogs

Peptide analog	IFN-γ	IL-4	IL-10	Ab*	Cross reaction with bovine MBP protein
CFA (Linear)					
MBP_{83-99}	+/-	-	#	-	-
$[A^{91}]MBP_{83-99}$	-	-	#	+	++
$[E^{91}]MBP_{83-99}$	-	-	#	++	-
$[F^{91}]MBP_{83-99}$	+	-	#	++	-
$[Y^{91}]MBP_{83-99}$	-	-	#	-	-
$[R^{91}, A^{96}]MBP_{83-99}$	+	+	#	+	-
Reduced Mannan (Linear)					
MBP_{83-99}	++	-	#	+++	+++
$[A^{91}]MBP_{83-99}$	-	+++	#	+	++
$[E^{91}]MBP_{83-99}$	-	+++	#	+++	+
$[F^{91}]MBP_{83-99}$	++	+++	+++	+/-	-
$[Y^{91}]MBP_{83-99}$	-	+++	+++	+++	-
$[R^{91}, A^{96}]MBP_{83-99}$	-	+++	#	+++	+++
CFA (Cyclic)					
MBP_{83-99}	++	-	#	++	#
$[A^{91}]MBP_{83-99}$	++	++	#	++	#
Reduced Mannan (Cyclic)					
MBP_{83-99}	++	-	#	++	#
$[A^{91}]MBP_{83-99}$	-	+++	#	+	#

- negative, +/- weak, + moderate, ++ strong, +++ very strong, *antibody, #not tested

References

1. Martin R, Howell M, Jaraquemada D, Flerlage M, Richert J, Brostoff S. *J Exp Med* **173**: 19-24, 1991.
2. Ota K, Matsui M, Milford E, Mackin G, Weiner H, Hafler D. *Nature* **346**: 183-187, 1990.
3. Steinman L. *Cell* **85**: 299-302, 1996.
4. Katsara M, Matsoukas JM, Deraos G, Apostolopoulos V. *Acta Biochim Biophys Sin* (*Shanghai*) **40**: 636-642, 2008.
5. Valli A, Sette A, Kappos L, Oseroff C, Sidney J, Miescher G, Hochberger M, Albert ED, Adorini L. *J Clin Invest* **91**: 616-628, 1993.
6. Katsara M, Yuriev E, Ramsland P, Deraos G, Tselios T, Matsoukas JM, Apostolopoulos V. *Mol Immunol* **45**: 3661-3670, 2008.
7. Katsara M, Tselios T, Deraos S, Deraos G, Matsoukas MT, Lazoura E, Matsoukas JM, Apostolopoulos V. *Curr Med Chem* **13**: 2221-2232, 2006.
8. Matsoukas JM, Apostolopoulos V, Kalbacher H, Papini AM, Tselios T, Chatzantoni K, Biagioli T, Lolli F, Deraos S, Papathanassopoulos P, Troganis A, Mantzourani E, Mavromoustakos T, Mouzaki A. *J Med Chem* **48**: 1470-1480, 2005.
9. Barlos K, Gatos D. *Biopolymers* 51: 266-78, 1999.
10. Katsara M, Deraos G, Tselios T, Matsoukas JM, Apostolopoulos V. *J Med Chem* **51**: 3971-3978, 2008.
11. Apostolopoulos V, Barnes N, Pietersz G, McKenzie I. *Vaccine* **18**: 3174-3184, 2000.
12. Apostolopoulos V, Pietersz G, Loveland B, Sandrin M, McKenzie I. *Proc Natl Acad Sci U S A* **92**: 10128-10132, 1995.
13. Sheng KC, Pouniotis D, Wright, M, Tang CK, Lazoura E, Pietersz G, Apostolopoulos V. *Immunology* **118**: 372-383, 2006.
14. Katsara M, Yuriev E, Ramsland P, Deraos G, Tselios T, Matsoukas JM, Apostolopoulos V. *J Neuroimmunol* **200**: 77-89, 2008.

2-14-183

Synthesis and biological evaluation of novel peptides influencing angiogenesis

Horváth, Anikó[1,]; Knedlitschek, Gudrun[2]; Okada, Yoshio[3]; Miyazaki, Anna[3]; Vántus, Tibor[4]; Seprődi, János[4]; Varga, András[5]; Tanai, Henriette[4]; Bökönyi, Györgyi[4]; Hiebl, Bernhard[6]; Kéri, György[5]*

[1]Hungarian Acedemy of Sciences and Semmelweis University Department of Medicinal Chemistry, PathoBiochemistry Research Group, HUNGARY; [2]Institute for Biological Interfaces, Forschungszentrum Karlsruhe, Department of Tumor Progression, GERMANY; [3]Department of Medicinal Chemistry, Kobe-Gakuin University, Faculty of Pharmaceutical Sciences, JAPAN; [4]Hungarian Academy of Sciences and Semmelweis University, Department of Medicinal Chemistry, PathoBiochemistry Research Group, HUNGARY; [5]Academy of Sciences and Semmelweis University, Department of Medicinal Chemistry, PathoBiochemistry Research Group, HUNGARY; [6]Institute for Biological Interfaces, Forschungszentrum Karlsruhe, Department of Tumor Progression, HUNGARY

[*]E-mail: aniko@puskin.sote.hu

Introduction

Angiogenesis is a fundamental process by which new blood vessels are formed and which is highly regulated in healthy individuals. However, many diseases are driven by unregulated angiogenesis. Excessive angiogenesis is associated with cancer, rheumatoid arthritis, psoriasis, while insufficient angiogenesis results in ischemia or atherosclerosis. Many new angiogenic modulators have been developed in the last years, mostly to inhibit angiogenesis but only few peptide-based angiogenic stimulators have been reported. There are data in the literature suggesting roles of small peptides as angiogenic modulators like Ringseis *et al*. reporting effects on endothelial cell function.[1] Endostatin, an endogenous inhibitor of angiogenesis, among its proteolitic fragments contains both, an inhibitor and a stimulator of angiogenesis.[2] We assumed that fragments of heptapeptide D-Phe-Cys(-)-Tyr-D-Trp-Lys-Cys(-)-Thr-NH_2, TT-232 (**1**), a strong antitumor agent, could also act as angiogenic modulators. The heptapeptide was developed in our laboratory[3] and has been used recently in a clinical trial (phase II).

Results

We synthesized, characterized and tested partially protected di- and tripeptide fragments of compound **1** such as Tyr-D-Trp-2-adamanthylamide (**2**), Boc-Tyr-D-Trp-cyclohexylamide (**3**), D-Phe-Cys(Acm)-Tyr-OMe (**4**) and Boc-D-Phe-Cys(Acm)-Tyr-OMe (**5**). The peptides were synthesized by step-wise solution phase peptide synthesis. The appropriately protected amino acids were coupled in the presence of activating agents (DCC, HOBt) and the reaction was monitored by TLC. After completion, the reaction mixture was purified by extraction, crystallization or high performance liquid chromatography (HPLC). The final products

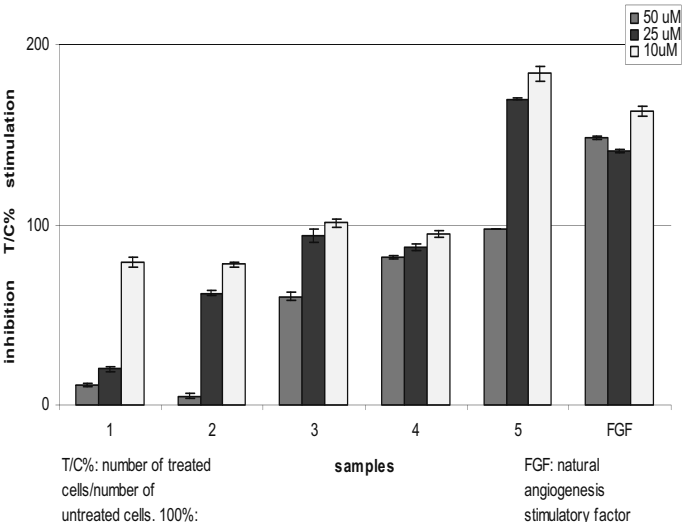

Figure 1. Effect of the new molecules on endothelial cell proliferation.

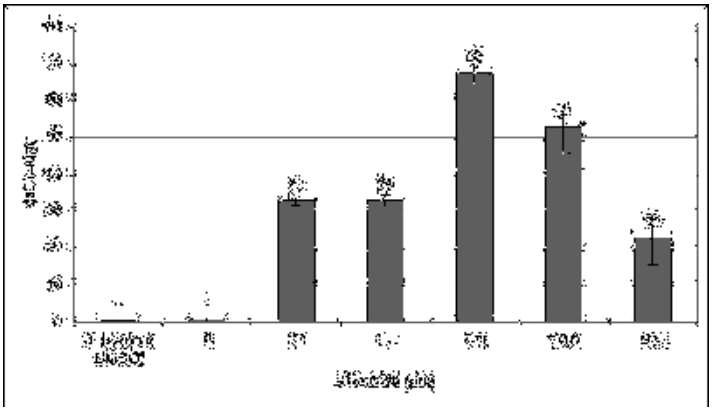

Figure 2. SHA-2-22 activity in rat aortic ring model.

were characterized by HPLC chromatography, MS and NMR. Tripeptides were synthesized similarly using characterized and appropriately protected dipeptides. In vitro biological activity of the peptides was tested on Kaposi Sarcoma (KS) tumor cells, derived from immortalized endothelial cells. The cells were incubated with test molecules at different doses for 48 hours. Visualization of the biological activity was achieved by employing a spectrofotometric assay using a tetrazolium salt (MTT).[4] The result of the assay is summarized in Fig. 1. The assay was carried out by using three controls, to appropriately monitor the stimulatory or inhibitory effects of the new molecules. One of the controls was the untreated cells, another one was the cells treated with the antiangiogenic compound **1** and the third one was the cells treated with native pro-angiogenic factor, Fibroblast Growth Factor (FGF). All results were expressed as the amount of treated cells compared to that of the non treated ones (T/C %). As it was expected, compound **1** showed a strong inhibition of cell proliferation (90 % at the doses of 50 μM), pro-angiogenic factor (FGF) showed an elevated cell number (60%) at a dose of 1 nM. Among the tested new analogs compound **4** was almost ineffective, compound **3** showed some inhibition (40%, at the dose of 50 μM), while compound **2**, a dipeptide amide comprising a unique adamanthyl group at the *C*-termini of the molecule showed similarly strong inhibition as compound **1**. The most interesting effect was achieved by compound **5**, which, at a dose of 10 μM, showed 80 % increase in cell proliferation.

Preliminary results indicate an angiogenesis promoting potential of compound **5** as assayed by the aorta ring assay,[5] which by using vascular explants reproduces more accurately the environment in which angiogenesis occurs. The result of this assay is summarized in Fig. 2.

Conclusion

Among the protected peptide fragments of antitumor agent TT-232 there are endothelial cell proliferation inhibiting (**2**) and promoting (**5**) compounds. The inhibitory activity of compound **2** is similar to that of the parent peptide (**1**), while compound **5** was shown to exhibit angiogenesis promoting properties. These peptides are promising molecules as angiogenesis modulating new drugs.

Acknowledgement

This work is sponsored by the 6th Framework Program of the European Community within the NMP3-CT-2005-0137811 "Vascuplug" contract and the National Research Foundation OTKA 49487 and 60197grants and T-488/2006 ETT grant.

References

1. Ringseis R, Matthes B, Lehmann V, Becker K, Schöps R, Ulbrich-Hofmann R, Eder K. *Biochim Biophys Acta* **1721**: 89-97, 2005.
2. Morbidelli L, Donnini S, Chillemi F, Giachetti A, Ziche M. *Clin Cancer Res* **9**: 5358-5369, 2003.
3. Kéri G, Erchegyi J, Horváth A, Mezõ I, Idei M, Vántus T, Balogh A, Vadász Z, Bökönyi G, Seprõdi J, Teplán I, Csuka O, Tejeda M, Gaál D, Szegedi Z, Szende B, Roze C, Kalthoff H, Ullrich A. *Proc Natl Acad Sci U S A* **93**: 12513-12518, 1996.
4. Hansen M, Nielsen S, Berg K. *J Immunol Methods* **119**: 203-206, 1989.
5. Nicosia RF, Ottinetti, Lab Invest. **63**: 115-122, 1990.

2-15-184

A RGD tetracyclopeptide as a new tool for specific tumor cell targeting

Schmidt, Julien[1]; Robert, Bruno[2]; Garambois, Veronique[2]; Rocheblave, Luc[3]; Martinez, Jean[3]; Pelegrin, Andre[2]; Cavelier, Florine[3]; Vives, Eric[2,]*

[1]Institut de Recherche en Cancerologie de Montpellier, FRANCE; [2]Institut de Recherche sur le Cancer de Montpellier, FRANCE; [3]Institut des Biomolecules Max Mousseron, FRANCE

[*]E-mail: evives@valdorel.fnclcc.fr

$\alpha_V\beta_3$ integrins are overexpressed in neocapillaries and in some tumor cells of various origins and are involved in tumor angiogenesis. The tripeptide sequence RGD can recognize different integrin receptors. The specificity depends on the conformation of this sequence. Various peptides or pseudopeptides containing the RGD sequence have been designed during the last decade to target $\alpha_V\beta_3$ receptors known to promote tumor angiogenesis.

Numerous laboratories designed RGD peptides with high affinity as an antagonist for $\alpha_V\beta_3$ receptors. Currently, the cyclic pentacyclopeptide c[RGDf(NMe)V] termed Cilengitide (EMD121974), is evaluated in different clinical trials as an antiangiogenic agent. The cyclic c[RGDfE] derivative is however preferred as a targeting moiety for different kinds of molecules such as drugs, fluorescent agents or radioelements since it can be coupled covalently and specifically through the acidic group of the E residue side chain.[1]

Herein, we describe a novel cyclopeptide containing only four amino acids, R,G,D and K, closed through an urea bond between the α-amino group of the arginine R residue and the ε-amino group of the closing lysine (K) residue. This tetracyclopeptide c[RGDK] can still be easily coupled to various drugs or fluorescent probes via the remaining extra cyclic acidic function of the K residue. Using different approaches, we demonstrate that this new peptide shows an higher affinity for $\alpha_V\beta_3$ receptors than the c[RGDfE].

Materials and Methods

Synthesis: The linear RGDK peptide was synthesized manually on solid phase following the fmoc chemistry. After the sequential removal of the *N*-terminal fmoc group and the alloc group of the lysine residue side chain, the semi-protected peptide was released from the 2-chlorotrityl resin following standard procedures. The cyclization between the two amines occurs through the formation of an urea bond using N,N'-carbonyldiimidazole. Under this form, the semi-protected tetracyclopeptide can therefore be either labeled with a fluorochrome as previously described[2] or directly linked as an activated targeting motif to any biologically active peptide or peptide-based scaffolds. Alternatively, the semi-protected tetracyclopeptide can be fully deprotected to afford the cyclic c[RGDK] peptide antagonist.

Biological evaluation: the c[RGDK] was evaluated as an inhibitor for the binding to purified $\alpha_V\beta_3$ receptors of a radiolabeled natural ligand, namely the echistatin, and was compared with the c[RGDfE] under the same conditions. The conjugated peptide c[RGDK]-$(KLAKLAK)_2$ was incubated at concentrations ranging from 10 nM to 100 µM on SKmeL28 cells expressing a high level of $\alpha_V\beta_3$ receptors. Since $(KLAKLAK)_2$ is known to be a proapoptotic peptide, the viability of the cells was measured by an MTS test 4 days later. As a negative control, a tetracyclopeptide c[RGEK], known to not bind to integrin receptors, was identically attached to the $(KLAKLAK)_2$ peptide. This latter conjugate, but also the $(KLAKLAK)_2$ or the c[RGDK] peptides alone, were incubated at the highest concentration for the same duration. *In vivo* therapy: 2 mg per day of c[RGDK] were injected intraperitoneally in C57Bl6 mice injected intravenously with 700 000 melanoma B16 cells. The treatment started on day 1. Mice were sacrificed on day 20 and lungs were collected, weighted and the degree of lung metastasis visually evaluated.

Results

HPLC profiles showed the quantitative cyclisation of the tetracyclopeptides closed through an urea bond. Tetracyclopeptides could thus be obtained in large quantity and coupled to various entities without further purification.

The solid-phase receptor binding assay, performed on $\alpha_V\beta_3$ purified receptors, shows a lower IC50 for c[RGDK] than c[RGDfE] in competition with radiolabeled echistatin, indicating a better affinity for this receptor.

The incubation of SKmeL28 cells with c[RGDK]-$(KLAKLAK)_2$ derivative shows a decrease of cell viability in a dose-dependant manner. All the control peptides had no effect on cell viability confirming the specific targeting properties of the c[RGDK] peptide towards $\alpha_V\beta_3$ receptors and the efficient internalization of the conjugated pro-apoptotic peptide. Internalization has also been confirmed by fluorescent microscopy (data not shown).

The *in vivo* therapy shows a significant inhibition of lung metastasis formation. Most of the mice treated daily with the c[RGDK] show less metastasis than those treated with the c[RGEK] peptide (Fig. 1). This was

also confirmed by lower weight (1,5 fold) of the lungs compare to the control groups.

Discussion

The tetracyclopeptide c[RGDK] shows a better affinity affinity for $\alpha_v\beta_3$ than the c[RGDfE] of reference. This peptide can be coupled to several entities thanks to its extracyclic acidic function following standard coupling procedures used in peptide synthesis. When linked to the well-known pro-apoptotic peptide $(KLAKLAK)_2$, the c[RGDK] demonstrates its targeting behavior and its efficient internalization into cells. Finally, this peptide shows *in vivo* inhibition of lung metastasis formation. In the future, multimerization of this peptide onto different scaffolds will be evaluated and *in vivo* experimentation will be further developed. We thus expect to obtain an higher affinity of the c[RGDK] targeting unit.

References

1. Thumshirn G, Hersel U, Goodman SL, Kessler H. Multimeric cyclic RGD peptides as potential tools for tumor targeting: solid-phase peptide synthesis and chemoselective oxime ligation. *Chemistry* **9**: 2717-2725, 2003.
2. Schmidt J., Rocheblave L., Martinez J., Pèlegrin A., Cavelier F. and Vivès E. Synthesis of new cyclic RGD peptides for specific tumor cell targeting. *Peptides 2006* (Proceedings of the 29th European Peptide Symposium, Gdańsk, Poland). Rolka K, Rekowski P, Silberring J (Eds), Kenes International, Geneva, Switzerland, pp 600-601, 2007.

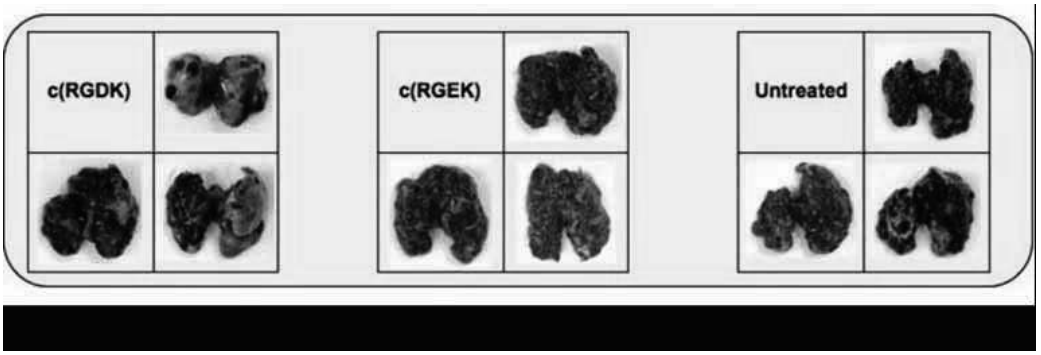

Figure 1.

2-16-185

Identification of biologically active peptides from the N-terminal domain of laminin alpha 2 chain

*Hayashi, Takemitsu; Urushibata, Shunsuke; Kobayashi, Kazuki; Ishikawa, Masaya; Hozumi, Kentaro; Kikkawa, Yamato; Nomizu, Motoyoshi**

Tokyo University of Pharmacy and Life Sciences, JAPAN

**E-mail: y031200@educ.ps.toyaku.ac.jp*

Introduction

Laminins, a major component of the basement membrane, consist of α, β, and γ chains and have various biological activities including promotion of cell adhesion, growth, migration, differentiation, and angiogenesis.[1] So far, five α (α1-α5), three β (β1-β3), and three γ (γ1-γ3) chains have been identified and at least 15 isoforms of laminin have been discovered by various combinations of each subunit. These laminin isoforms are tissue- and/or developmental stage-specifically expressed. Laminin α2 chain is mainly localized in the basement membranes of skeletal muscle and peripheral nerve. All α chains share a unique C-terminal G-domain, which consists of five laminin G-modules and the domains are similar in length. But N-terminal short arms differ in the length considerably. Biological functions of the laminin α2 chain N-terminus including integrin binding and heparin/heparan sulfate binding were found previously.[1] Additionally, failure of laminin α2-chain N-terminus leads muscular dystrophies and nerve defects.[1] Here, we focused on the N-terminal region of the mouse laminin α2 chain (position 1-1566) and screened the biologically active sequences using 142 peptides.

Results and Discussion

We synthesized one hundred and forty two peptides (A2-1 to A2-142), which covered the mouse laminin α2 chain N-terminus. All peptides were manually synthesized by 9-fruorenylmethoxycarbonyl (Fmoc) strategy with a C-terminal amide and purified by reverse-phase HPLC. Peptides were generally 12 amino acids in length and overlapped with neighboring peptides by 4 amino acids. If the N-terminal amino acid was either glutamate or glutamic acid, one amino acid was extended at the N-terminus to avoid pyroglutamine formation. Cysteine residues were omitted. Two peptides (A2-53 and A2-55) were not dissolved in aqueous solutions. Cell attachment activity of the peptides was evaluated using a peptide-coated plastic plate assay and a peptide-conjugated Sepharose bead assay using HT-1080 human fibrosarcoma cells. In the prate assay, AG73 (RKRLQVQLSIRT) was used as a positive control. AG73 is known previously as a strongest cell attachment peptide derived from the mouse laminin α1-chain G-domain.[2] As a negative control, we also used a scrambled peptide AG73T (LQQRRSVLRTKI). Five peptides (A2-20: LEFTSARYIRLR, A2-31: YYDETVASRNLSLN, A2-62: RKDFMIVLTNLE, A2-63: TNLERVLMQITYN, and A2-122: DILYDIHYILIK) showed strong cell attachment activity comparable to that of AG73. Six peptides (A2-7, A2-8, A2-44, A2-56, A2-112, and A2-114) also showed cell attachment activity, but weaker than that of AG73. Rest of the peptides did not show cell attachment activity in the plate assay. In the peptide-conjugated Sepharose bead assay, we used A13 (RQVFQVAYIIIKA) as a positive control. A13 is known previously as strong cell

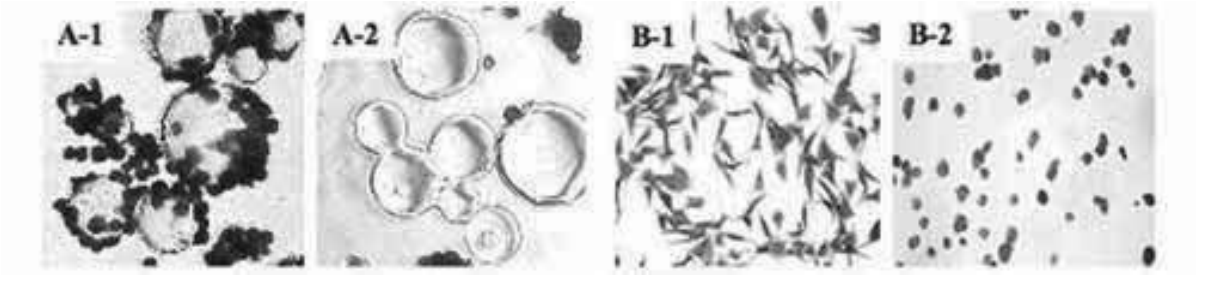

Figure 1. Adhesion of HT1080 cells on peptide-conjugated Sepharose beads. HT-1080 human fibrosarcoma cells were allowed to attach to peptide-conjugated Sepharose beads for 1h, then stained with crystal violet. (A-1) A2-62; (A-2) etanolamine (negative control). Cell spreading of human foreskin fibroblasts. Human foreskin fibroblasts were allowed to attach to peptide-coated plastic plate for 2h, then stained with crystal violet. (B-1) A2-8; (B-2) A2-20 (no spreading). Original magnification 200x.

attachment active peptide in the bead assay derived from the mouse laminin α1-chain N-terminus.[3] Ethanolamine-coupled bead was used as a negative control. Three peptides (A2-21: IRLRFQRIRTLN, A2-62, and A2-112: GGKLKYAIYFEA) showed strong cell attachment activity comparable to that of A13 (Fig. 1). Two peptides (A2-20 and A2-69) showed weaker cell attachment activity than that of A13. Rest of the peptides did not show cell attachment activity in the bead assay. Totally, thirteen peptides promoted cell attachment activity in either the plate or bead assays, and three peptides were active in both assays. Eight peptides were active only in the plate assay, whereas two peptides were active only in the bead assay. The differential activities may be due to conformational changes and/or poor coating efficiencies on the plate. N-terminal region of laminin α2-chain is consisted of three globular domains and EGF repeat regions. Eleven of thirteen cell attachment active peptides were localized in the globular domains. So the globular domains seem to be critical region for interacting with cells. Additionally, we valued cell-spreading activity of the cell attachment peptides in peptide-coated plastic plate assay using human foreskin fibroblasts. We used EF1 (DYATLQLQEGRLHFMFDLG) as a positive control. EF1 is known previously as a strong cell spreading activity derived from laminin α1 chain G-domain.[4] Two peptides (A2-8: YHYVTITLDLQQ and A2-44: AQSSYWTYGNIQD) promoted extensive cell spreading similar to that of EF1 (Fig. 1). Three peptides (A2-31, A2-56, and A2-63) promoted weaker cell spreading than that of EF1. It has been reported that EF1 promotes the cell spreading and the cell spreading activity are mediated by interacting to integrin.[4] So these cell-spreading peptides may be interacting with integrin. Further, we evaluated heparin-binding activity of the cell attachment peptides using a biotinylated heparin. We used AG73 as a positive control and AG73T as a negative control. Two peptides (A2-20 and A2-112) showed heparin binding activity. These results suggest that the two peptides have potential to interact with heparin-like cell surface molecules such as syndecan. The peptide approach is powerful for identifying active sites and characterizing the cellular receptors. So these bioactive peptides are useful for investigating the biological activities on N-terminal region of laminin α2-chain.

References

1. Suzuki N, Yokoyama F, Nomizu M. Functional Sites in the Laminin Alpha Chains. *Connective Tissue Res* **46**: 142-152, 2005.
2. Nomizu M, Kim WH, Yamamura K, Utani A, Song SY, Otaka A, Roller PP, Kleinman HK, Yamada Y. Identification of Cell Binding Sites in the Laminin α1 Chain Carboxyl-terminal Globular Domain by Systematic Screening of Synthetic Peptides. *J Biol Chem* **270**: 20583-20590, 1995.
3. Makino M, Okazaki I, Nishi N, Nomizu M. Biologically Active Sequences in Laminin, a Multifunctional Extracellular Matrix Protein. *Connective Tissue Res* **31**: 227-234, 1999.
4. Suzuki N, Nakatsuka H, Mochizuki M, Nishi N, Kadoya Y, Utani A, Oishi S, Fujii N, Kleinman HK, Nomizu M. Biological Activities of Homologous Loop Regions in the Laminin α Chain G Domains. *J Biol Chem* **278**: 45697-45705, 2003.

2-16-186

New integrin ligands based on isoDGR sequence

Otto, Elke[1]; Heckmann, Dominik[1]; Zahn, Grit[2]; Stragies, Roland[2]; Kessler, Horst[1,]*

[1]TU Muenchen, GERMANY; [2]Jerini AG, GERMANY

[*]E-mail: elke.otto@ch.tum.de

Introduction

Integrins are heterodimeric transmembrane glycoproteins which are found in many animal species ranging from sponges to mammals. These cell adhesion receptors regulate cell-cell and cell-extracellular matrix interactions,[1] thus mediate the physical anchoring and the bidirectional transmembrane signalling. Hence they are involved in fundamental cellular processes such as migration, proliferation, differentiation, and apoptosis. The peptide sequence Arg-Gly-Asp (RGD) is by far the most prominent ligand to promote specific cell adhesion through integrin stimulation. It is known to bind integrins, e.g. $\alpha_5\beta_1$ (Fibronectin, Vitronectin, Fibrinogen), $\alpha_V\beta_3$ (Fibronectin, Vitronectin), and $\alpha_{IIb}\beta_3$ (Fibronectin, Vitronectin, Fibrinogen) among many others. Fibronectin (Fn) is a large glycoprotein which is secreted as a disulfide-bonded dimer consisting primarily of three types of repeating modules (Fig. 1). It is an ubiquitous and abundant ECM protein, which plays an important role in haemostasis, thrombosis, inflammation, wound repair, angiogenesis, and embryogenesis.

Recently, it was shown that a mutation of the RGD sequence in the Fn-III-10 to RGE sequence still exhibits binding, although RGE binds no integrin. However, these fibrils have a slightly different phenotype than wild-type Fibronectin. Takahashi *et al*.[2] observed that only an $\alpha_V\beta_3$-selective compound is able to block the 'irregular' Fn assembly. This suggests that $\alpha_V\beta_3$ is, to some extend, able to bind to fibronectin at another binding site.[2] A hypothetical model for these unexpected results was proposed by Curnis *et al.*[3] The NGR (Asn-Gly-Arg) sequence, present at four positions in the fibronectin molecule (Fig. 1), is able to undergo a rearrangement into *iso*DGR (*iso*Asp-Gly-Arg). The mechanism of Asn-deamidation has already been known for a long time and has widely been considered to be a process of degradation, acting as a biochemical clock that limits protein lifetimes *in vivo*.[4] This non-enzymatic *iso*Asp formation can be enzymatically repaired to RGD by the protein-L-isoAsp-O-methyltransferase.[3] However, Curnis *et al.* have been the first to show that the deamidation process can also increase protein function and does not necessarily lead to functional degradation.[3] This new sequence was found to show activity on $\alpha_V\beta_3$ and - with less potency – on $\alpha_5\beta_1$. This new sequence could be interpreted as a kind of retro sequence of RGD. This retro sequence approach had already been investigated by Wermuth *et al.* in 1996,[5] but only a few compounds out of their synthesized library showed a mild activity towards $\alpha_V\beta_3$.

Cyclic peptides are well known to adopt stable conformations, which can be determined using NMR techniques. Biologically active peptides incorporating the *iso*DGR sequence can serve as model compounds for the various NGR-containing modules of Fn and may help to elucidate the structure-activity and the structure-selectivity relationships of the *iso*DGR sequence. Additionally, these compounds form a new class of peptidic integrin ligands, whose application potential in biology and medicine is under investigation.

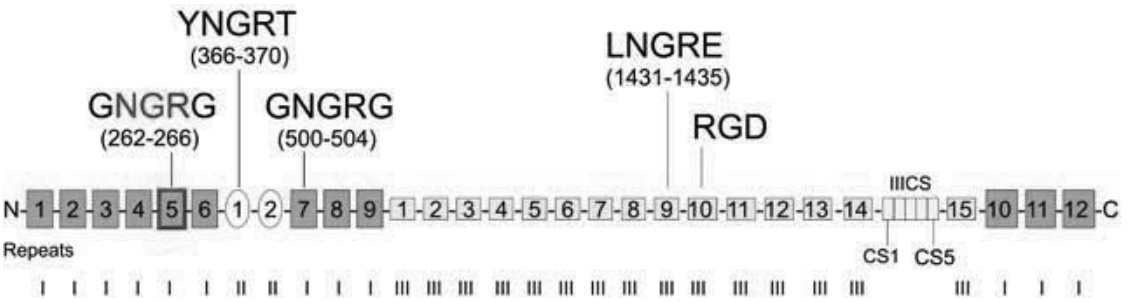

Figure 1. Schematic representation of fibronectin fragments. The three types of repeating homologous modules of which each subunit consists are termed Fn-I (blue rectangles), Fn-II (ovals), and Fn-III (squares) repeats. The modules which contain NGR and RGD sequences are indicate.[2]

Table 1. *iso*DGR peptides as integrin ligands

Analogue	$\alpha_5\beta_1$ in nM	$\alpha_v\beta_3$ in nM	$\alpha_5\beta_1/\alpha_v\beta_3$
c(-*iso*D-G-R-G-G-)	147	106	1.4
c(-*iso*D-G-R-G-**homophe**-)	**18**	93	5
c(-*iso*D-G-R-G-**homoPhe**-)	446	295	2
c(-*iso*D-G-R-G-**f**-)	78	189	2
c(-*iso*D-G-R-**f**-G-)	500	**10.7**	0.02
c(-*iso*D-G-R-G-**phg**-)	**3.3**	518	157
c(-*iso*D-G-R-G-**Phg**-)	**29**	>1000	>34
c(-*iso*D-G-R-**Phg**-G-)	643	**16.4**	0.03
c(-*iso*D-G-R-**phg**-G-)	225	**6.7**	0.03
c(-*iso*D-G-R-G-**A**-G-)	590	**7.4**	80
c(-*iso*D-G-R-G-**a**-G-)	356	43	82

Results and Discussion

The findings of Curnis *at al.*[3] stimulated us to create a library of cyclic peptides containing the *iso*DGR sequence. Biological evaluation of this library showed various new peptides with high activity and selectivity towards the integrin receptor $\alpha_5\beta_1$ or for the $\alpha_V\beta_3$ receptor. Our goal was to introduce an *iso*DGR-sequence into head to tail cyclized pentapeptides. Here, we first surrounded the *iso*DGR-sequence with two flanking glycines. This was done to create a structure similar to the GNGRG loops found in Fn, where they are located in the Fn-I5 and Fn-I7 modules.[6] Furthermore, we subtituted one of the flanking glycines with phenylalanine, phenylglycine, and homophenyl alanine.

Table 1 shows the *iso*DGR peptide flanked by two glycines and a small assortment of peptides which are flanked by variations of phenyl alanine (Phe, Phg and Homophe) in the position next to the *iso*Asp. Surprisingly, our new *iso*DGR peptides show either affinity for the integrin $\alpha_5\beta_1$ or no affinity at all. We observed the highest activity and selectivity towards the integrin receptor $\alpha_5\beta_1$ with 3.3 nM for the cyclic peptides with D-phenylglycin. But the peptide with L-phenylglycin and D-homophenylalanine also showed high activity. After these results, we continued screening in two directions: we now varied the amino acid flanking the Arg and, additionally, synthesized some cyclic hexapeptides. Surprisingly, both show activity for the $\alpha_V\beta_3$ integrin. The comparison of the peptides with phenylglycine on different positions shows different integrin affinity.

Conclusion

We were able to show that it is possible to address the $\alpha_V\beta_3$ and $\alpha_5\beta_1$ integrin ligands selectively using the recently found *iso*DGR sequence. Our library approach resulted in a series of highly active and already quite selective cyclic pentapeptids that could be used as a starting towards a new class of integrin ligands. It is important to point out that it seems that nature uses the enzymatic or non-enzymatic rearrangement of Asn to *iso*Asp as on a switch to regulate adhesion function.

References

1. Hynes RO. *Nat Med* **8**: 918-921, 2002.
2. Takahashi S, Leiss M, Moser M, Ohashi T, Kitao T, Heckmann D, Pfeifer A, Kessler H, Takagi J, Erickson HP, Fässler R. *J Cell Biol* **178**: 167-178, 2007.
3. Curnis F, Longhi R, Crippa L, Cattaneo A, Dondossola E, Bachi A, Corti A. *J Biol Chem* **281**: 36466-36476, 2006.
4. Robinson NE, Robinson AB. *Proc Natl Acad Sci U S A* **98**: 944-949, 2001.
5. Wermuth J, Goodman SL, Jonczyk A, Kessler H. *J Am Chem Soc* **119**: 1328-1335, 1997.
6. Di Matteo P, Curnis F, Longhi R, Colombo G, Sacchi A, Crippa L, Protti MP, Ponzoni M, Toma S, Corti A. *Mol Immunol* **43**: 1509-1518, 2006.

2-18-187

Development of GnRH-III anthracycline conjugates as drug delivery systems for targeted chemotherapy

Manea, Marilena[1]; Szabó, Ildikó[2]; Orbán, Erika[2]; Bősze, Szilvia[2]; Tejeda, Miguel[3]; Gaál, Dezső[3]; Kapuvári, Bence[3]; Csámpai, Antal[4]; Radnai, László[5]; Mező, Gábor[2]

[1]University of Konstanz, Department of Chemistry, Laboratory of Analytical, GERMANY; [2]Eötvös L. University, Research Group of Peptide Chemistry, HUNGARY; [3]National Institute of Oncology, HUNGARY; [4]Eötvös L. University, Institute of Chemistry, HUNGARY; [5]Eötvös L. University, Department of Biochemistry HUNGARY

E-mail: gmezo@elte.hu

Introduction

Targeted chemotherapy has been developed to overcome the drawbacks associated with the application of free anticancer drugs.[1] It is based on the finding that receptors for certain peptide hormones are overexpressed on tumor cells. Consequently, peptide hormones or hormone analogs can be used as targeting moieties to deliver cytotoxic agents directly to tumor cells. Expression of gonadotropin-releasing hormone (GnRH) receptor was identified on different types of tumors.[2] It has been shown that GnRH-III (Glp-His-Trp-Ser-His-Asp-Trp-Lys-Pro-Gly-NH_2) isolated from sea lamprey has antiproliferative activity on numerous tumor cells, and significantly less potency on releasing gonadotropin hormones (LH, FSH); therefore, it is a more selective antitumor agent than the human GnRH derivatives.[3-5] In our work, GnRH-III was used as targeting moiety with own antitumor activity for the preparation of multifunctional drug delivery systems for targeted chemotherapy. Daunorubicin (Dau) and doxorubicin (Dox) as antineoplastic agents were attached to the side chain of ^{8}Lys of GnRH-III through amide, oxime, hydrazone or ester bonds, either directly or by insertion of an enzyme cleavable tetrapeptide spacer. *In vitro* long term antitumor effect of the conjugates on MCF-7 human breast cancer and C26 murine colon carcinoma cell lines was studied. One of the most effective compounds was the oxime bond-linked Dau-GnRH-III conjugate that was selected for further *in vitro* and *in vivo* studies.

Results and Discussion

GnRH-III derivatives containing a spacer attached to the side chain of ^{8}Lys were prepared by solid phase synthesis using mixed Boc/Fmoc strategies. Dau and Dox were attached to the aminooxyacetic acid (Aoa) modified GnRH-III derivative (<EHWSHDWK(Aoa-GFLG)PG-NH_2) via oxime bond (<EHWSHDWK(X=N-O-CH_2-CO)PG-NH_2, X = Dau (1) or Dox (2)). In the case of ester linkage, Dox was protected with Fmoc group on its sugar moiety, and then the ester bond was prepared using glutaric anhydride. The Dox derivative was attached to GnRH-III using BOP reagent, and followed by Fmoc removal (<EHWSHDWK(Dox-O-CO-$(CH_2)_3$-CO)PG-NH_2, (3)). Oxo-group on C^{13} of Dau was used for chemoselective hydrazone bond formation similarly to oxime linkage (<EHWSHDWK(Dau=N-NH-CO-$(CH_2)_2$-CO)PG-NH_2, (4)). Both Dau and Dox were conjugated through amide bond to the NH_2-group of the sugar moiety.

Hydrazone bond is acid sensitive and can be split under lysosomal circumstances, while the ester bond is cleaved easily by esterases. However, the conjugates with oxime linkage might require an enzyme labile spacer for efficient drug release. Therefore, GFLG tetrapeptide spacer was incorporated between the drug and GnRH-III. The enzymatic lability of the conjugate was determined in human serum. The slow cleavage of Leu-Gly bond and of the isopeptide bond between Gly and εNH-group of Lys residue was observed, but even after 24 h the intact conjugate could be also detected.

The structure of Dau-Aoa-OH was studied by ^{1}H- and ^{13}C-NMR, which indicated only "E"-isomer around the oxime bond.

Long-term *in vitro* antitumor effect of the conjugates was studied on MCF-7 human breast and C26 murine colon tumor cell lines. All compounds were more effective on MCF-7 cells and except amide bond containing conjugates the others showed significant antitumor activity (IC50 (μM) on MCF-7: 3.9 (1), 5.4 (2), 0.8 (3), 1.5 (4); on C26: 22.5 (1), 46.1 (2), 4.8 (3)). The *in vitro* antitumor activity of the free drugs (Dau and Dox) was one magnitude higher than that of the conjugates (IC50 (μM) on MCF-7: 0.23 (Dau), 0.07 (Dox); on C26: 1.95 (Dau), 4.51 (Dox). It was also found that the antitumor activity of the compounds was correlated with the intensity of their cellular uptake.

Compound 1 (oxime bond-linked Dau-GnRH-III) was selected for *in vivo* experiments. The conjugate was not toxic up to 15 mg/kg body weight Dau content on BDF-1 healty mice and the weight of the treated mice increased similarly to that of the control animals. In contrast, the mice treated with the same amount of free drug lost their weight rapidly and died between the days 10 and 12 of the experiment.

The *in vivo* antitumor activity of compound 1 was

studied on C26 tumor bearing mice. The results were compared with those obtained for the free drug and GnRH-III(GFLG) hormone analog. Treatment of mice with free Dau 5x2 mg or 1x5 mg/body weight showed 23% and 36% tumor growth inhibition, respectively, but the animals died much earlier than the untreated controls because of the drug toxicity. The conjugate resulted in tumor growth inhibition and longer survival time depending on the dose, the number and the start of treatments. The best results were obtained in the case of two treatments on the days 4 and 7 after tumor transplantation using a dose with 15 mg/kg Dau content. 70-80% tumor growth inhibition was observed during the treatment and still at the end of the experiment 46% inhibition was detected. Also 41% increase of survival was determined to the control in this case. The GnRH-III hormone derivative also showed some inhibitory effect on tumor growth (18%) and longer survival time (14% in average) using the same peptide content as in the conjugate. These results confirm the multivalency of the Dau-GnRH-III conjugate as drug for targeted chemotherapy.

References

1. Dharap SS, Wang Y, Chandna P, Khandare JJ, Qui B, Gunaseelan S, Sinko PJ, Stein S, Farmanfarmaian A, Minko T. *Proc Natl Acad Sci U S A* **102**: 12962-12967, 2005.
2. Nagy A, Schally AV. *Biol Reprod* **73**: 851-859, 2005.
3. Mezõ I, Lovas S, Pályi I, Vincze B, Kálnay A, Turi G, Vadász Zs, Seprõdi J, Idei M, Tóth G, Gulyás É, Ötvös F, Mák M, Horváth JE, Teplán I, Murphy RF. *J Med Chem* **40**: 3353-3358, 1997.
4. Lovas S, Pályi I, Vincze B, Horváth J, Kovács M, Mezõ I, Tóth G, Teplán I, Murphy RF. *J Pept Res* **52**: 384-389, 1998.
5. Kovács M, Vincze B, Horváth JE, Seprõdi J. *Peptides* **28**: 821-829, 2007.

2-18-189

Dimeric α-MSH analogues carrying DOTA for melanoma tumor targeting

Tanner, Heidi; Bapst, Jean-Philippe; Calame, Martine; Eberle, Alex N[1,]*

University Hospital Basel, Department of Biomedicine, SWITZERLAND

[*]E-mail: Alex-N.Eberle@unibas.ch

Introduction

Metastatic melanomas express melanocortin-1 receptors (MC1R), a potential target for radiotherapy of cancer lesions with analogues of α-melanocyte-stimulting hormone (α-MSH) containing suitable chelators such as 1,4,7,10-tetraazacyclododecane-1,4,7,10-tetraacetic acid (DOTA) for incorporation of radiometals.[1] Several DOTA-MSH analogues have been developed displaying high potency *in vitro* and excellent incorporation into tumor lesions *in vivo*.[2,3] In order to further increase the potency of DOTA-MSH compounds, dimeric peptides had been investigated.[4] These studies were based on earlier observations that multimeric MSH-carrier molecules exhibit a markedly increased potency.[5,6] In this paper, we demonstrate that a novel DOTA-MSH dimer with an enzymatic cleavage site has a very high receptor affinity but also an unwanted elevated retention by the kidneys.

Results and discussion

In the course of this study, three linear dimeric analogs were designed containing a slightly modified MSH heptapeptide core sequence (Nle-Asp-His-D-Phe-Arg-Trp) in parallel or antiparallel orientation, a short spacer and the DOTA chelator for incorporation of the radiometal (Fig. 1). *In vitro*, all three peptides were more potent

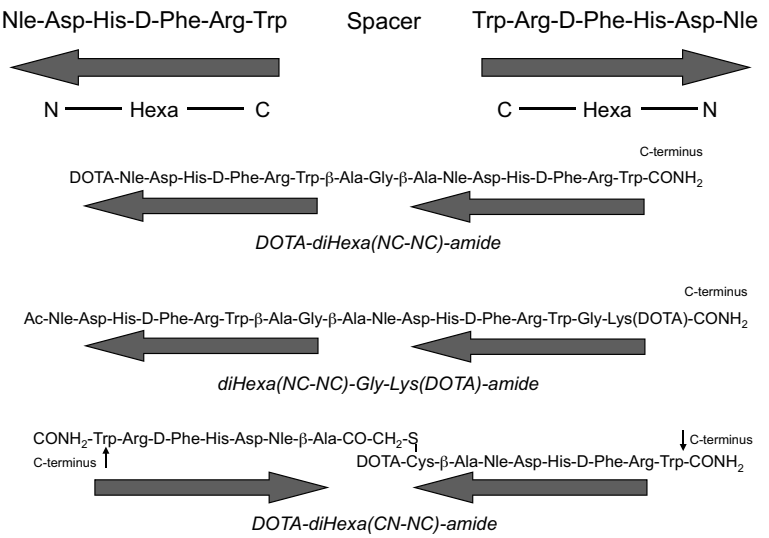

Figure 1. General orientation of the hexapeptide Nle-Asp-His-D-Phe-Arg-Trp sequence in the dimer peptides. DOTA-diHexa(NC-NC)-amide and diHexa(NC-NC)-Gly-Lys(DOTA)-amide contained the two hexapeptides in linear parallel and consecutive N-to-C–spacer–N-to-C orientation; the spacer was *β*-Ala-Gly-*β*-Ala. In DOTA-diHexa(NC-NC)-amide, the DOTA moiety was attached at the N-terminus. In diHexa(NC-NC)-Gly-Lys(DOTA)-amide, the sequence was extended at the C-terminus by a –Gly-Lys-amide containing the DOTA in the ε-amino position of Lys. The DOTA-diHexa(CN-NC)-amide contained the two hexapeptides in antiparallel C-to-N–linker–N-to-C orientation. The linker consisted of a Cys-*β*-Ala attached to the N-terminus of one hexapeptide and, respectively, a *β*-Ala (containing a iodoacetyl group at its amino group) attached to the N-terminus of the other hexapeptide. The hexapeptide dimer was obtained by reacting the SH group of Cys with iodoacetyl of *β*-Ala, leaving the amino group of Cys free for attachment of DOTA.

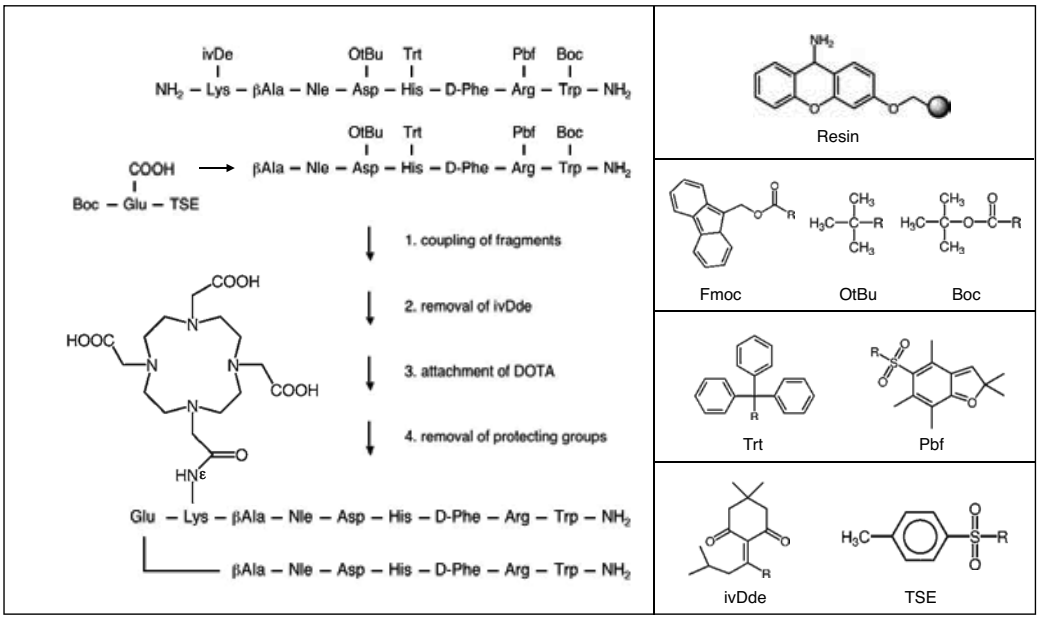

Figure 2. Structure and synthesis of DOTA-MSH diheptapeptide. The general outline of the synthesis is shown on the left, the resin-spacer and the protecting groups on the right.

ligands of the mouse B16-F1 melanoma cell MC1R than DOTA-NAPamide which served as standard.[3] The binding activity of DOTA-diHexa(NC-NC)-amide was 1.75-fold higher, that of diHexa(NC-NC)-Gly-Lys(DOTA)-amide 3.37-fold higher, and that of DOTA-diHexa(CN-NC)-amide 2.34-fold higher. Using human HBL melanoma cells, the binding activity of diHexa(NC-NC)-Gly-Lys(DOTA)-amide was 6-fold higher than that of DOTA-NAP-amide. Uptake by cultured B16-F1 cells was rapid and almost quantitative. *In vivo*, however, the data were less promising: tumor-to-kidney ratios 4 h post-injection were 0.11 for [111In]DOTA-diHexa(NC-NC)-amide, 0.26 for diHexa(NC-NC)-Gly-Lys([111In]DOTA)-amide, and 0.36 for [111In]DOTA-diHexa(CN-NC)-amide, as compared to 1.67 for [111In]DOTA-NAPamide. The novel DOTA-MSH diheptapeptide dimer presented here was of the (CN-NC)-amide type (Fig. 1). The structure and a general outline of its synthesis are displayed in Fig. 2. Basically, the spacer contained a Glu-Lys(DOTA) structural element which in principle can serve as an enzymatic cleavage site in the kidneys, in order to reduce kidney uptake. This spacer element was flanked by a *β*-Ala on both sides, followed by the hexapeptide core sequence of [Nle4, D-Phe7]-α-MSH.[7] In the B16-F1 mouse melanoma binding assay, the IC50 at the MC1R was 0.38 nM, i.e. DOTA-MSH diheptapeptide is one of the most potent DOTA-MSH peptides tested to date. Similarly, the potency in the human HBL melanoma cell assay was also markedly superior to that of DOTA-NAP-amide. The uptake of bound DOTA-MSH diheptapeptide by melanoma cells was rapid and almost quantitative. However, as observed with other short DOTA-MSH dimer peptides, the non-specific uptake by the kidneys was far too high (about 6- to 8-fold higher than that of DOTA-NAPamide), excluding DOTA-MSH diheptapeptide as a candidate for clinical development. In conclusion, it appears that despite the higher affinity to the MC1R of the peptide dimers and their excellent internalization *in vitro*, the uptake by melanoma tumors *in vivo* was lower, possibly because of reduced tissue penetration. More striking however was the marked increase of kidney uptake of the dimers, explaining the unfavorable ratios. Thus, although radiolabeled α-MSH dimer peptides display excellent receptor affinity and internalization, they are no alternative to the monomeric DOTA-NAPamide for *in vivo* application.

References

1. Eberle AN, Froidevaux S. *J Mol Recognit* **16**: 248-54, 2003.
2. Froidevaux S, Calame-Christe M, Tanner H, Sumanovski L, Eberle AN. *J Nucl Med* **43**: 1699-706, 2002.
3. Froidevaux S, Calame-Christe M, Schuhmacher J, Tanner H, Saffrich R, Henze M, Eberle AN. *J Nucl Med* **45**: 116-123, 2004.
4. Bapst JP, Froidevaux S, Calame M, Tanner H, Eberle AN. *J Recept Signal Transduct* **27**: 383-409, 2007.
5. Kriwaczek VM, Eberle AN, Müller M, Schwyzer R. *Helv Chim Acta* **61**: 1232-1240, 1978.
6. Eberle AN. *Biochem Soc Trans* **129**: 113-6, 1981.
7. Sawyer TK, Sanfilippo PJ, Hruby VJ, Engel MH, Heward CB, Burnett JB, Hadley ME. *Proc Natl Acad Sci U S A* **77**: 5754-5758, 1980.

2-19-190

Protein delivery with transportans avoids recycling endosomal route and is not potentiated by EGF

Säälik, Pille[1]; Räägel, Helin[1]; Hansen, Mats[2]; Langel, Ülo[2]; Pooga, Margus[3]

[1]University of Tartu, Institute of Molecular and Cell Biology, ESTONIA; [2]Stockholm University, Department of Neurochemistry and Neurotoxicology, SWEDEN; [3]Estonian Biocentre, ESTONIA

[1]E-mail: pillesk@ut.ee

Introduction

Cell-penetrating peptides (CPP) and the cellular delivery of big hydrophilic cargoes with them has been an attractive subject of research almost two decades. It is now known that for most of the CPP-cargo constructs the main entry to cells is achieved by an endocytic mechanism as visualized by formation of vesicular structures after internalization.[1,2] Still, in spite of the improvement in understanding the capabilities and action mechanisms of CPPs the field meets several questions concerning the trafficking, stability and functionality of the cargo after cellular internalization. We have focused on revealing the internalization mechanisms of cargo delivery and trafficking by three CPPs, transportan (TP), its shorter form TP10 and nonaarginine (Arg_9) using biotinylated peptides and avidin as cargo. Cos-1 and Cos-7 cells were chosen to reveal the endosomal routing of CPP-protein complexes since it has been shown that in these cell lines the endosomes leading to degradation and recycling are differently located in relation to the *trans*-Golgi ring.[3] We also analyzed the acidification of endosomal organelles containing TP- and Arg_9-protein complexes in relation to pH-sensitive marker LysoSensor DND-189 in order to define the pH of the vesicles containing the CPP-cargo constructs. Additionally, the effect of EGF as an inducer of macropinocytosis on the protein cellular delivery mediated by transportans was estimated in HeLa cells.

Results and Discussion

Confocal fluorescence microscopy and FACS analysis indicated that the cellular transport of avidin by biotinylated TP and TP10 was not enhanced by EGF, an inducer of macropinocytosis, and the peptide-protein complexes revealed little overlap with EGF on the plasma membrane as well as inside cells at earlier timepoints. Up to 20-25 minutes, the peptide-protein complexes showed little intracellular overlap with fluorescently-labeled EGF, however, about 30 minutes after the start of incubation the complexes were often detectable in big vesicles marked by EGF, indicating the targeting of CPP-avidin constructs to these structures at later steps during intracellular trafficking. To assess the fraction of EGF internalized by clathrin-mediated endocytosis, colocalization between transferrin and EGF was studied. Transferrin revealed frequent colocalization with EGF at earlier timepoints but the degree of overlap showed no marked increase in time as observed for CPP-avidin complexes. FACS analysis confirmed that the uptake of peptide-protein complexes into HeLa cells in the presence of EGF was not enhanced, corroborating with the results obtained by confocal microscopy.

As the recycling endosomes are reported to locate in the sphere-shaped *trans*-Golgi ring in Cos cell line, we followed the cellular targeting of complexes of TP, TP10 or Arg_9 with avidin in Cos-1 or Cos-7 cells in order to identify the nature of the endosomal structures entrapping the complexes. We found that the complexes are not directed to the recycling pathway in Cos-1 and Cos-7 cells but remain mainly in other populations of endosomes. The peptide-protein complexes containing vesicles were around and in close proximity to the *trans*-Golgi network after 30 min incubation but the overlap of complexes with the *trans*-Golgi network seemed rather coincidental. The involvement of the recycling pathway in intracellular trafficking of the CPP-avidin complexes seemed therefore negligible. Further, we evaluated the role of the endo-lysosomal pathway by identifying the pH of complexes-containing vesicles with the pH-sensitive dye LysoSensor DND-189. Our results indicated that a fraction of avidin complexed to biotinylated TP or Arg_9 is gradually directed to acidic organelles but the acidification of vesicles containing the peptide-protein complexes is slower than compared to dextran-TRITC. Following the internalization and intracellular trafficking of TP-avidin complexes, we found that after internalization, most of TexasRed-labeled avidin with TP (TPb-AvTxR) was equally routed to both low-pH and medium-pH structures. In time, a large proportion of vesicles became more intense of both LysoSensor and TPb-AvTxR signals marking the trafficking of complexes to degradative compartments. Nevertheless, TPb-AvTxR complexes produced the most structures with non-acidic pH while containing a high concentration of the complexes. Conversely, a large amount of TexasRed-avidin complexed to Arg_9 (Arg_9-AvTxR) was found in LysoSensor positive vesicles already after 1h and in time, more vesicles containing stronger Arg_9b-AvTxR signal were trafficked into low-pH structures marking the lysosomes. However, a fraction of vesicles containing intense Arg_9b-AvTxR signal and a more neutral pH

remained constant over time. Additionally, elevation of the concentration of the complexes led to channeling of excess CPP-AvTxR to low-pH containing organelles where most of the complexes were probably destined for degradation.

The cellular uptake of TP-, TP10- and Arg_9-avidin complexes in Cos cells takes place via several different endocytic pathways where internalized complexes avoid the recycling pathway and are directed later to acidic organelles. On the other hand, a significant fraction of vesicles containing the internalized CPP-protein complexes seems to be acidified at a slower rate, suggesting that the used complexes could interfere with the acidification process of the respective vesicles or a different internalization mode could be utilized by the CPP-cargo constructs leading to creation of endosomes, which are not acidified at a typical rate. Hypothesis, that these non-acidic complexes-containing vesicles could allow the efflux of the complexes to the cytosol, needs further confirmation.

Further details of this study can be found in manuscripts (to be published elsewhere).[4,5]

Aknowledgements

This study was supported by Estonian Science Foundation (ESF 7058).

References

1. Richard JP, Melikov K, Vives E, Ramos C, Verbeure B, Gait MJ, Chernomordik LV, Lebleu B. *J Biol Chem* **278:** 585-590, 2003.
2. El-Andaloussi S, Johansson HJ, Lundberg P, Langel Ü. *J Gene Med* **8:** 1262-1273, 2006.
3. Misaki R, Nakagawa T, Fukuda M, Taniguchi N, Taguchi T. *Biochem Biophys Res Commun* **360:** 580-585, 2007.
4. Säälik P, Padari K, Niinep A, Lorents A, Hansen M, Jokitalo E, Langel U, Pooga M. *Bioconjug Chem* **20**: 877–887, 2009.
5. (a) Räägel H, Säälik P, Hansen M, Langel U, Pooga M. *J Control Release* **139**: 108-117, 2009. (b) Räägel H, Säälik P, Pooga M. *Biochim Biophys Acta* (in press), 2010.

2-19-191

Novel intracellular delivery system using pH-dependent fusiogenic peptide

Nakase, Ikuhiko; Kobayashi, Sachiko; Kawabata, Noriko; Futaki, Shiroh*

Kyoto University, Institute for Chemical Research, JAPAN

**E-mail: nakase@scl.kyoto-u.ac.jp*

Introduction

Plasma membranes have numerous essential functions for maintaining cellular homeostasis. However, the membranes are also barriers for intracellular delivery of various therapeutic molecules. For improvement of their translocations, we developed a novel method using GALA peptide and cationic lipid complexes.

GALA, a 30-residue amphipathic peptide with a repeat sequence of glutamic acid-alanine-leucine-alanine (Fig. 1A), was designed to mimic the function of viral fusion protein sequences that mediate escape of virus gene from acidic endosomes to cytosol.[1] GALA peptide has a function to convert its structure from a random coil to an α-helix, when the pH is reduced from 7.0 to 5.0.[1-3] At neutral pH, electrostatic repulsions between the carboxylic acid moieties of glutamic acid are considered to destabilize the helix, whereas the neutralization of these groups promote helix formation at pH 5.0, leading to destabilize lipid membranes. Therefore, when attached with bioactive cargoes, the GALA peptide may serve as intracellular carrier bearing efficient endosomal escape function. However, because of negative charges from glutamic acids (7-residues) in the GALA sequences, access of the peptide on negatively charged cell surface would be not so efficient. To overcome this problem, cationic lipid was employed as an gadhesive h for pasting the GALA peptide onto cell surface to accomplish efficient cellular uptake (Fig. 1B).

Results and discussion

We studied the ability of GALA peptide as a delivery vector using fluorescein as a model of membrane-impermeable low-molecular weight drugs. When HeLa cells were treated with FITC-GALA (1 μM) formed complex with cationic lipid, Lipofectamine 2000 (LF2000), cellular uptake of FITC-GALA was drastically increased. In a time-dependent manner, the FITC-GALA escaped from endosomes, and diffuse fluorescent signals were observed in both cytosol and nucleus in `2 hr treatment of the complexs on cells. In the case of the cells treated with FITC-GALA without the complex formation, internalization of the peptide was very low. These results suggest that cationic lipid helps for pasting the GALA onto cell surface to accomplish efficient cellular uptake of the cargo-conjugated GALA.

As stated above, GALA destabilizes lipid membranes at low pH by conformational change of the peptide. However helical content of GALA is quite sensitive to its surrounding condition such as the existence of cationic lipids, and the lipids might have some effects on the conformational feature. Therefore, we conducted the study of circular dichroism (CD) analysis of GALA in similar condition with cellular uptake experiments, in the presence of egg phosphatidyl-choline (EPC) and LF2000.

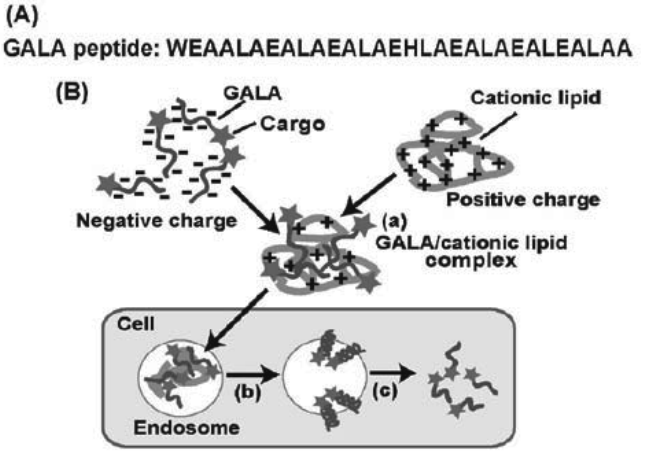

Figure 1. (A) Amino acid sequence of GALA peptide. (B) Scheme of intracellular delivery of cargo-conjugated GALA/cationic lipid complex. (a) Complex of GALA/cationic lipid and cellular uptake, (b) pH-decrease in endosomeendosome and conformational change of GALA, (c) escape of cargo.

As a result, pH-dependent conformational change of GALA was shown to be induced in the presence of LF2000, and GALA promoted its conformation to helix at pH 5.0. Next we synthesized a scrambled-amino acid sequence of GALA (sGALA) as a comparison in order to confirm the importance of comformational feature of GALA for the efficient release from endosomes. In each CD spectra between GALA and sGALA, the helical content of sGALA at pH 5.0 was lower than that of GALA. When cells were treated with FITC-sGALA/LF2000 complex, only punctuate fluorescence signals could be observed, although efficient diffuse fluorescent signals in cells could be observed in the case of FITC-GALA/LF2000 complex.

Next we tried to evaluate the GALA and cationic lipid complexes for efficient delivery of macromolecular proteins into cells as a novel application. FITC-labeled avidin, 68 kDa, was chosen as a protein model, and we synthesized biotinylated-GALA for delivery of FITC-labeled avidin. Neither biotinylated-GALA nor LF2000 could cause the diffusion of FITC-avidin in cytosol, when they were used separately. In these cases, though FITC-avidin could be internalized into cells, only weak punctate fluorescent signals were observed with a confocal microscope. In contrast, when FITC-avidin (250 nM) was mixed with the biotinylated-GALA/LF2000 complexes, diffusion of FITC-avidin in cytosol could be observed. Furthermore, we conducted the experiments for controlling intracellular delivery of the protein. Biotinylated-GALA introduced nuclear-localization signal sequence on its C-terminus brought nuclear import of FITC-avidin, suggesting that degradation of cargo was not proceeded significantly during the intracellular delivery in endosomal pathway, and organelle target of macromolecular protein using this GALA/cationic lipid complex will be able to be further applied. These results support the usefulness of our novel technique for intracellular macromolecular delivery, considered to be a promising technology as wide-applicable system.

References

1. Subbarao NK, Parente RA, Szoka FC Jr, Nadasdi L, Pongracz K. *Biochemistry* **26:** 2964-2972, 1987.
2. Li W, Nicol F, Szoka FC Jr. *Adv Drug Deliv Rev* **56:** 967-985, 2004.
3. Nicol F, Nir S, Szoka FC Jr. *Biophys J* **78:** 818-829, 2000.

2-19-192

Interaction of S4(13)-PV peptide with plasma membrane and cell entry. An electron microscopy view

Koppel, Kaida[1]; Padari, Kärt[1]; Lorents, Annely[1]; Mano, Miguel[2]; Raid, Raivo[1]; Pedroso de Lima, Maria[2]; Pooga, Margus[3,]*

[1]University of Tartu, Institute of Molecular and Cell Biology, ESTONIA; [2]University of Coimbra, Department of Biochemistry PORTUGAL; [3]Estonian Biocentre, ESTONIA

[*]E-mail: mpooga@ebc.ee

Introduction

The S4(13)-PV is a chimeric peptide comprising a sequence derived from the Dermaseptin S4 and the nuclear localization signal (NLS) of SV40 large T antigen.[1] This cell-penetrating peptide (CPP) has been shown to use two different mechanisms for entering cells – the fast penetration directly through the plasma membrane, and the slower mechanism by regulated endocytotic pathways; whereas the endocytosis-dependent mechanism dominates at low and the non-endocytotic at high peptide concentrations.[2] The cellular uptake of CPPs and their cargoes has been mostly studied by using fluorescence and activity based methods, while the almost missing information about the interaction mode of CPPs with the plasma membrane or distribution in cells at the ultrastructural level might help in unravelling the internalization mechanisms of CPPs. Here we characterize the membrane interaction and cellular translocation of cell-penetrating peptide S4(13)-PV and its analogues by using transmission electron microscopy (TEM).

Results and discussion

For visualization of S4(13)-PV in cells by TEM, we tagged the wild-type peptide (S4-wt, ALWKTLLKKVLKAPKKKRKVC-NH_2) and its analogues with reverse NLS (S4-rev, ALWKTLLKKVLKAVKRKKKPC-NH_2) and scrambled sequence (S4-scr, KTLKVAKWLKKAKPLRKLVKC-NH_2) covalently with gold nanoparticles (1.4 nm). After incubation of HeLa cells with peptide-nanogold conjugates the cells were fixed and the gold label was magnified by silver enhancement to the diameter of about 8 - 10 nm.

Both, the S4-wt peptide and its analogue with reverse NLS sequence assemble into spherical clusters upon association with cell surface and insert into cells (Fig. 1A). These clusters have regular shape and rather uniform size of about 50 to 100 nm resembling nanoparticles. The seeds of nanoparticles form already in 10 minutes at 0.1 μM of peptide concentration. At the higher concentrations the S4-wt and S4-rev peptides accumulate on the cell surface in the particular regions of cell membrane where they interfere with the organization of lipid bilayer and

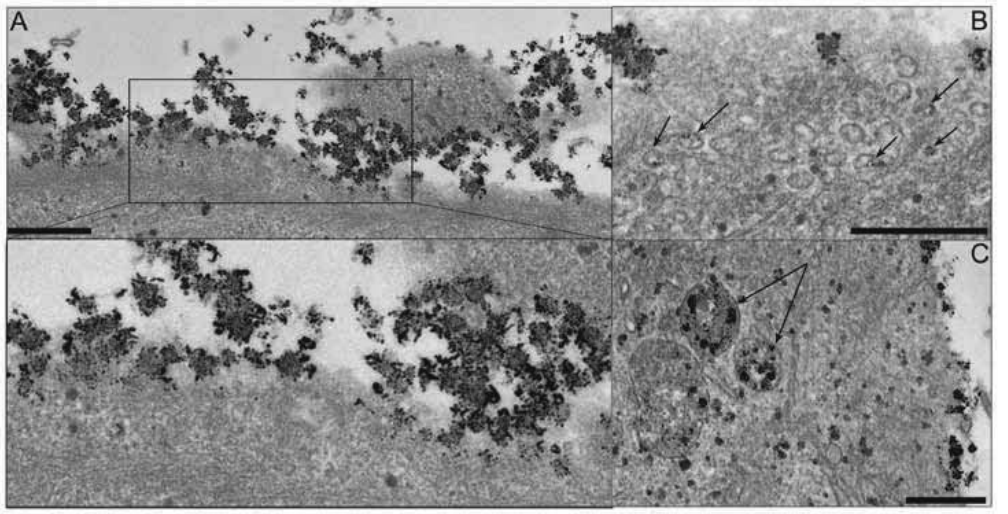

Figure 1. *Interaction of S4-wt-nanogold with cell surface (A) and their intracellular localization (B, C).* HeLa cells were incubated with 0.5 μM (A, B) or 1 μM (C) S4-wt-nanogold conjugates for 1 h. Localization of S4-wt-nanogold particles in small vesicular structures (B) and in multivesicular bodies (C). Bars 500 nm.

insert into cells. Concentration of S4(13)-PV peptides on/in the plasma membrane induces the cellular uptake mostly by vesicular mechanism. Clusters of S4(13)-PV peptides localize initially in small (~80 nm) caveolae-like or non-coated vesicles (Fig. 1B, arrows) and are subsequently targeted to multivesicular bodies (MVB) (Fig. 1C). Surprisingly, even inside the MVB the peptides retain their structural organization for at least 1 h and remain associated with the vesicle´s membrane (Fig. 1C, arrows). The nanoparticles of S4(13)-PV peptides had always the electron-dense background in electron micrographs. Staining of cell surface with Ruthenium Red further increased the background density suggesting that the negatively charged glycosides are incorporated into nanoparticles. This is in agreement with earlier studies demonstrating that cell surface proteoglycans facilitate the cellular uptake of S4(13)-PV peptides and induce CPPs to concentrate as dense aggregates at the cell surface for subsequent internalization.[2,3]

In order to characterize the endocytotic processes involved in the cellular uptake of S4 peptides we assessed the influence of low temperature and dynamin inhibition. At temperatures 4 - 10 °C S4(13)-PV nanoparticles interact with plasma membrane less avidly and their translocation into cells is suppressed but the vesicular uptake is not abolished. Treatment of cells with dynasore (80 μM for 1.5 h) also reduced the formation of vesicles but again did not block it. The S4(13)-PV peptides were still present in small vesicles as well as larger endosomal structures, mainly in the cortical cytoplasm. This suggests that the dynamin-independent poorly understood endocytotic mechanisms are also involved in the translocation process of S4(13)-PV peptides. The peptide with scrambled sequence, in contrary, can not assemble in regular spherical structures and forms bigger aggregates, which enter cells less efficiently. This indicates that the positions of amino acids in the peptide are of the crucial importance for assembly into regular clusters. Moreover, the ability of cell-penetrating peptides to form nanoparticles seems to correlate with their efficiency in cellular uptake.

In conclusion, our study demonstrates that S4(13)-PV peptides interact with the plasma membrane at specific loci of HeLa cells. CPPs form spherical clusters in a cooperative manner on/in the plasma membrane and interfere with the organization of the lipid bilayer leading to their subsequent vesicular uptake by cells.

References

1. Hariton-Gazal E, Feder R, Mor A, Graessmann A, Brack-Werner R, Jans D, Gilon C, Loyter A. *Biochemistry* **41:** 9208-9214, 2002.
2. Mano M, Teodosio C, Paiva A, Simoes S, Pedroso de Lima M C. *Biochem J* **390:** 603-612, 2005.
3. Ziegler A, Seelig J. *Biophys J* **94:** 2142-2149, 2007.

2-19-193

A Modular Strategy for the Design of Apoptogenic Cell Penetrating Peptides

Jones, Sarah; Howl, John*

University of Wolverhampton, RIHS, School of Applied Sciences, UNITED KINGDOM

**E-mail: S.Jones4@wlv.ac.uk*

Introduction

By convention, cell penetrating peptides (CPP) have mostly been utilized as inert, non-toxic vectors for the intracellular delivery of bioactive cargoes. However, our more recent studies have focused upon the identification and application of CPP with intrinsic biological activities. Amongst which has been the design, synthesis and evaluation of CPP with apoptosis inducing activities. These apoptogenic CPP have included the mastoparan analogue mitoparan ([Lys^{5,8}Aib^{10}]mastoparan; Aib = α-aminoisobutyric acid) and a cryptic fragment of human cytochrome *c* Cyt *c*$^{77\text{-}101}$ (*H*-GTKMIFVGIKKKEERADLIAYLKKA-*NH*$_2$). Mitoparan (mitP) is a highly potent mitochondriotoxic peptide that demonstrates a significant intracellular co-localization with mitochondria and, through co-operation with a protein of the mitochondrial permeability transition pore VDAC, this apoptogenic CPP promotes apoptosis of human cancer cells as confirmed by endonuclease and caspase-3 activation and phosphatidylserine translocation.[1] In contrast, Cyt *c*$^{77\text{-}101}$ (*H*-GTKMIFVGIKKKEERADLIAYLKKA-*NH*$_2$) is a moderately potent apoptogenic CPP that demonstrates a strong propensity for co-localization within the endoplasmic reticulum.[2] Using a sychnologic modular design, we have synthesized and evaluated a broad range of chimeric constructs combining apoptogenic CPP (*message*) and peptidyl *address* motifs. The overriding objective of these studies was to enhance cytotoxicity and/or develop target-selective drug delivery vectors. *Address* motifs (Fig. 1) that target both plasma membrane and nuclear envelope protein structures included i) the integrin-specific RGD sequence, ii) a Fas ligand mimetic WEWT[3], iii) heptagastrin (G7; AYGWMDF) that targets a novel membrane binding site on high grade astrocytoma,[4] and iv) a mimetic of FG nucleoporins (Nups).

Results and discussion

Incorporation of peptidyl *address* motifs was achieved by simple N-terminal acylation or via a flexible aminohexanoic acid (Ahx) linker of the parent apoptogen, a strategy that produced modular chimeric constructs with enhanced cytotoxic potencies, compared to the parent apoptogen alone. N-terminal blockade with Z-Gly and inclusion of a D-Phe (*f*) were additional

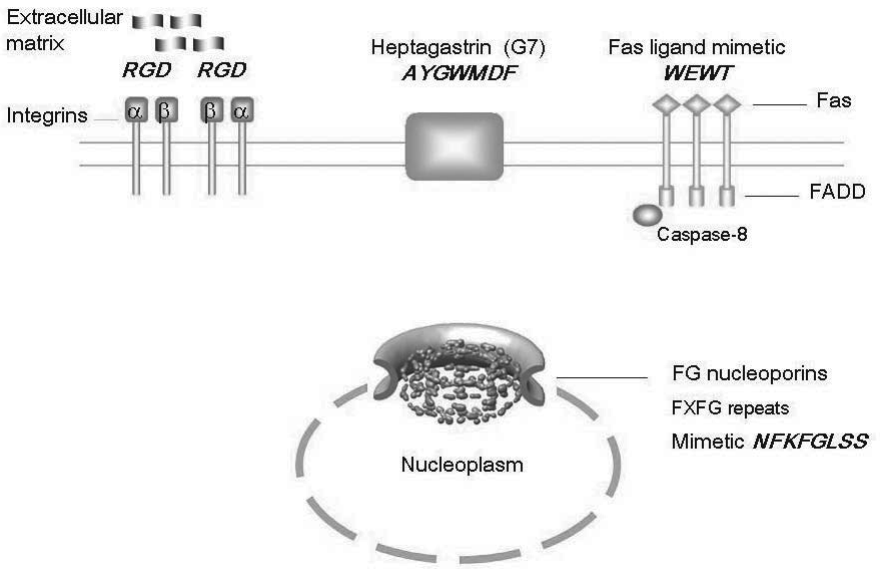

Figure 1. Origins of peptidyl address motifs used to target both plasma membrane and nuclear envelope protein structures. Address motifs are highlighted in bold itallics.

Table 1. LD_{50} values of apoptogenic CPP chimerae. Cell viability was used to determine cytotoxicity and measured by MTT conversion. LD_{50} values are expressed in μM as mean ± S.E.M. from 3 separate experiments performed in triplicate. Values were calculated following 24 h exposure to peptides

Apoptogenic CPP	LD_{50}	
	U373MG	ECV304
MitP	7.92 ± 0.12	6.81 ± 0.05
Z-Gly-RGD*f*-mitP		1.40 ± 0.13
Z-Gly-RGE*f*-mitP		4.71 + 0.05
Z-Gly-RGD*f*-mitP + cyclo(-RGD*f*V) (300nM)		9.17 + 0.07
WEWT(Ahx) mitP		4.44 ± 0.04
G7:mitP	0.92 ± 0.05	
Ac-NFKFGLSS(Ahx)Cyt $c^{77\text{-}101}$	0.73 + 0.08	

modifications aimed at improving the biostability of the integrin-targeted chimera to produce z-Gly-RGD*f*-mitP. As indicated in Table 1 and using ECV304 cells, Z-Gly-RGD*f*-mitP demonstrated an enhanced cytotoxic potency (LD_{50} = 1.40 μM) compared to the mitP alone (LD_{50} = 6.81 μM). Specificity of integrin binding was determined by substitution of the core RGD sequence with RGE, a sequence variant that prevents integrin binding and a subsequent reduction in potency was observed (Table 1). Likewise, a dramatic reduction in potency was witnessed following pre-incubation with the integrin antagonist cyclo(-RGD*f*V) (Table 1). In addition, a moderately enhanced potency compared to mitP was demonstrated with the Fas ligand mimetic chimeric construct WEWT(Ahx)mitP (Table 1). U373MG astrocytoma were used to evaluate the impact of the G7 containing chimeric apoptogen and as indicated in Table 1, the cytotoxic potency of this chimeric construct was much enhanced (LD_{50} = 0.92 μM) compared to mitP alone (LD_{50} = 7.92 μM). The most significant enhancement in cytotoxic potency was obtained using the chimeric construct *Ac*-NFKFGLSS(Ahx)Cyt $c^{77\text{-}101}$, composed of the moderately apoptogenic CPP Cyt $c^{77\text{-}101}$ and a mimetic of FG nucleoporins. FG nucleoporins are components of the nuclear pore complex that control import and export between the cytoplasm and the nucleus and are characterised by multiple FXFG repeat sequences (Fig. 1). $NFKFGLSS^{980\text{-}988}$ was taken from human nucleoporin 153 and as an N-terminal extension of Cyt $c^{77\text{-}101}$, demonstrated a dramatically enhanced potency giving an LD_{50} of 0.73 μM on U373MG astrocytoma compared to the moderately cytotoxic Cyt $c^{77\text{-}101}$, which demonstrates a maximum reduction in cell viability of a mere 35% at 30 μM. In conclusion, apoptogenic CPP can be incorporated into chimeric constructs without impacting upon the bioactivity of the parent apoptogen and offer a promising strategy for the future development of target (tissue/cell)-specific inducers of apoptosis. Moreover, the enhanced potencies of *Ac*-NFKFGLSS(Ahx)Cyt $c^{77\text{-}101}$, Z-Gly-RGD*f*-mitP, and G7:mitP, compared to their parent apoptogenic CPP, are concentrations that are easily achievable *in vivo*.

References

1. Jones S, Martel C, Belzacq-Casagrande AS, Brenner C, Howl J. *Biochim Biophys Acta Molecular Cell Research* **1783:** 849-863, 2008.
2. Howl J, Jones S. *Int J Pept Res Ther* **14**: 359-366, 2008.
3. Yoshimori A, Takasawar R, Hayakawa A, Mizuno M, Yoshida J, Tanuma S. *Apoptosis* **10:** 323-329, 2005.
4. Pannequin J, Oiry C, Morel C, Kucharczak J, Camby I, Kiss R, Gagne D, Galleyrand JC, Martinez J. *J Pharmacol Exp Ther* **302:** 274-282, 2002.

2-20-194

Multifunctional Peptides. Analogues of Tyr-MIF

Lipkowski, Andrzej W; Kosson, Piotr[1]; Tsuda, Yuko[2]; Okada, Yoshio[2]*

[1]Integrated Centre of Excellence of Medicinal Chemistry of Neuropeptides at Medical Research Centre, Polish Academy of Sciences, POLAND; [2]Graduate School of Food and Medicinal Sciences, Kobe Gakuin University, JAPAN

**E-mail: andrzej@lipkowski.org*

Introduction

Multitarget medicines are a new, very promising avenue of drug development.[1] Interestingly, most of the endogenous neuropeptides function through interactions with several receptors and/or regulatory pathways. Tyr-MIF vs. Opioid Peptides Tyr-MIF, endogenous neuropeptide[2] is one of the best examples of such multifunctional molecules. Tyr-MIF interacts with non-opioid, specific receptors and blood-brain-barrier transporter that recognizes Tyr-Pro motive, including opioid endomorphin and morphiceptin. Tyr-MIF itself, expresses very weak affinity to mu opioid receptors. Structure-activity studies suggest that Tyr-MIF that functions as an endogenous analgesic (opioid) plays an important, not fully understood role, as regulatory component of neurohomeostase of pain and stress signals.[3] The available data suggest that this molecule has dual function, weak opioid agonistic dependent on N-terminal tyrosine and antiopioid effect determined by C-terminal fragment, including attenuation the development of tolerance. It is a chance that increasing opioid affinity of Tyr-MIF analogues may result in new generation of analgesics with positive adjunct site effects. (Fig. 1.) Stereo view of overlapped morphine tyramine with tyramine of compounds containing (A) DMT[4] and (B) 6 Htc[5] in solid state. Modification of N-terminal tyramine In contrast to opiate alkaloid, tyramine moiety of the N-terminal tyrosine in neuropeptides exists mainly in conformation that does not fit to opioid receptor binding site. Therefore, in endogenous opioid peptides, additional conformational elements should exist that enhance receptor-peptide complex formation. In recent years, several tyrosine analogues that much more effectively simulate opioid tyramine have been developed, including 2,6-dimethyltyrosine (DMT)[3] or 6-Hydroxy-1,2,3,4-tetrahydro-isoquinoline-3-carboxylic acid (6Htc).[4]

Materials and methods

To test the effect of substitution Tyr opioid function with preservation of all other functional components, the analogues of Tyr-MIF with such opioid enhanced tyrosine residue have been designed, synthesized and tested their affinity to mu opioid receptors.

Results and discussion

Sequence Mu affinity IC50 (nM) Tyr-MIF Tyr-Pro-Leu-Gly-NH2 >1500 DMT-MIF DMT-Pro-Leu-Gly-NH2 32.6 6Htc-MIF 6Htc-Pro-Leu-Gly-NH2 7.9 The replacement of tyrosine residue with DMT and 6Htc resulted with compounds that express high affinity to opioid receptor types. If the analogues preserve their other properties it is a chance that such analogues will be analgesics without dependence development. Further pharmacological studies are under progress.

Table 1. Binding data of Tyr-MIF and its analogues to mu opioid receptors

	Sequence	Mu affinity IC_{50} (nM)
Tyr-MIF	Tyr-Pro-Leu-Gly-NH_2	**>1500**
DMT-MIF	DMT-Pro-Leu-Gly-NH_2	**32.6**
6Htc-MIF	6Htc-Pro-Leu-Gly-NH_2	**7.9**

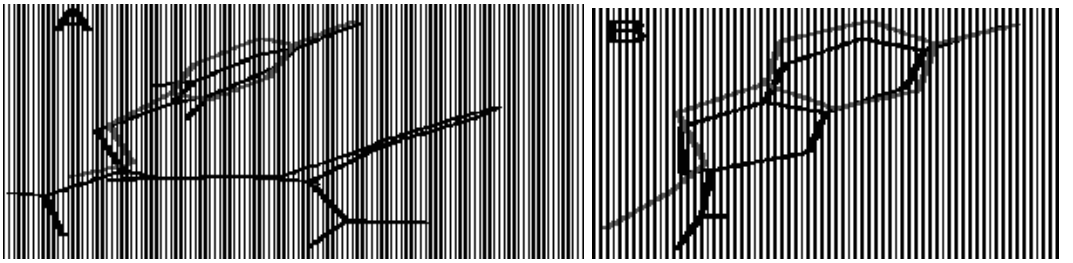

Figure 1. Stereo view of overlapped morphine tyramine with tyramine of compounds containing (A) DMT[4] and (B) 6 Htc[5] in solid state.

Acknowledgements

This work has been partially supported by the European Grant Normolife (LSHC-CT-2006-037733).

References

1. Lipkowski AW, Misicka A, Hruby V.J, Carr DB. *Polish J Chem* **68**: 907-912, 1994.
2. Horvath A, Kastin AJ. *J Biol Chem* **264**: 2175-2179, 1989.
3. Pan W, Kastin AJ. *Peptides* **28**: 2411-2434, 2007.
4. Bryant SD, George C, Flippen-Anderson JL, Deschamps Jr, Salvadori S, Balboni G, Guerrini R, Lazarus LH. *J Med. Chem* **45**: 5506-5513, 2002.
5. Sperlinga E, Kosson O, Urbanczyk-Lipkowska Z, Ronsisvalle G, Carr DB, Lipkowski AW. *Bioorg Med. Chem Lett* **15**: 2467-2469, 2005.

2-20-195

Synthesis of conformationally restricted analogues of GnRH-I and GnRH-III and studies on prostate cancer cell proliferation

Pappa, Eleni V.[1]; Zompra, Aikaterini A.[1]; Magafa, Vassiliki[1]; Diamantopoulou, Zoi[2]; Lamari, Fotini N[1]; Katsoris, Panagiotis[2]; Cordopatis, Paul[1,]*

[1]University of Patras, Department of Pharmacy, GREECE; [2]University of Patras, Department of Biology, GREECE

[*]E-mail: pacord@upatras.gr

Introduction

Mammalian Gonadotropin Releasing Hormone type I (GnRH-I) and the sea lamprey Gonadotropin Releasing Hormone type III (GnRH-III) belong to the class of conserved gonadotropin releasing hormone peptides. In addition to the classic hypophysiotropic action of GnRH-I, it has been shown that many malignant cells, such as prostate cancer cells, secrete GnRH-I and express the GnRH-I receptor/s.[1] GnRH-III has no endocrine activity in mammals even at high doses and has been shown to suppress directly sex hormone-dependent and -independent growth of breast and prostatic cancer cells in vitro.[2,3] In order to study the structure-activity relationship of GnRH-I and III on prostate cancer cells, we synthesized ten new peptide analogues of GnRH-I and five new analogues of GnRG-III. D-Leu6 of Leuprolide was substituted by D-Lys, D-or L-Glu and Ser4 by *N*–Me-Ser. Asp in position 6 of GnRH-III was substituted by Asn and Glu, Pro9 was substituted by α-aminoisobutyric acid (Aib) and Trp3 and/or Trp7 by D-Trp (Table1). Experimental Procedures. GnRH-I, GnRH-III, Leuprolide and the sixteen new analogues of GnRH were assembled on a [3-((Ethyl-Fmoc-amino)-methyl)-1-indol-1-yl] acetyl AM resin and on a Rink Amide MBHA resin[2.3]. Generally, chain extension was carried out using standard Fmoc protocols. The crude peptides were purified by gel filtration chromatography on Sephadex G15 using 15% acetic acid as the eluent. Final purification was achieved by semipreparative HPLC on Supelcosil C18 with a linear gradient from 20 to 60% acetonitrile containing 0.1% TFA for 30 min at a flow rate of 2ml/min and UV detection at 214 and 254 nm. The appropriate fractions were pooled and lyophilized. Analytical HPLC on a C-18 Phase Sep column produced a single peak with at least 98% of the total peak integrals. Electro-spray MS was in agreement with the expected results. Prostate cancer epithelial cells LNCaP (5x103, androgen-dependent) and PC3 (1x104, androgen-independent) were seeded in 48-well plates for 24h in RPMI-1640 medium supplemented with 10% (v/v) FBS and then treated with GnRH peptide analogues in RPMI-1640 medium supplemented with 2% (v/v) FBS. After a 72 h incubation period, cell number was estimated by Crystal violet assay. Adherent cells were fixed with methanol and stained with 0.5% crystal violet in 20% methanol for 20 min. After gentle rinsing with water, the retained dye was extracted with 30% acetic acid, and the absorbance was measured at 590 nm.

Results and Discussion

The overall yield of the synthesis of the new GnRH analogues was in the range of 40-55%. Analogues I-IV and VIII with *N*-Me-Ser in position 4 and side chain modified D-Lys in position 6 exhibited inhibitory effects similar to that of Leuprolide, on the proliferation of LNCaP prostate cancer cells with an exception of the analogue with Ala in the side chain of D-Lys (analogue III). In PC3 cells, the antiproliferative activity of analogues I-IV was lower than that in LNCaP cells. Furthermore, in PC3 cells analogues VII and VIII exhibited inhibitory effects higher than that of analogues I-IV and similar to that of Leuprolide. Substitution of Ser in position 4 of the analogue VII by *N*-Me-Ser, combined with incorporation of D-Lys[Gly(But)] (analogue VIII), did not seem to effect the biological activity in both cell lines. Incorporation of Glu or D-Glu in position 6 maintained the antiproliferative activity of Leuprolide in both prostate cancer cell lines. Substitution of Ser in position 4 of the analogue X by *N*-Me-Ser, combined with D-Glu in position 6 (analogue X), did not seem to affect the biological activity. In comparison to GnRH-I, GnRH-III had similar antiproliferative effect in LNCaP and higher in PC3 cells. Incorporation of Asn or Glu in position 2 (analogues XIII and XIV) reduced the antiproliferative effect in PC3 cells. Substitution of Trp in position 7 with D-Trp alone (analogue XV) also reduced the antiproliferative effect of GnRH-III but, combined with substitution of Trp at position 3 (analogue XVI) antiproliferative effect was higher in both cell lines.

Conclusions

Results indicate that the presence of D-amino acids at position 6 stabilizes the biologically active conformation of GnRH-I. Substitution of Ser in position 4 of GnRH-I by N-Me-Ser can probably provide added stability to enzymic breakdown of the peptide but did not seem to effect the antiproliferative activity of the analogues. The side chain group of Asp in position 6 and stereochemistry of Trp3,7 of GnRH-III are important for the anticancer activity (especially for inhibitory effects on PC3 prostate cancer cells).

Table 1. New analogues of GnRH-I and GnRH-III

Code	GnRH Analogues
GnRH-I	pGlu^{1}-His^{2}-Trp^{3}-Ser^{4}-Tyr^{5}-Gly^{6}-Leu^{7}-Arg^{8}-Pro^{9}-Gly^{10}-NH_2
GnRH-III	pGlu^{1}-His^{2}-Trp^{3}-Ser^{4}-His^{5}-Asp^{6}-Trp^{7}-Lys^{8}-Pro^{9}-Gly^{10}-NH_2
Leuprolide	pGlu^{1}-His^{2}-Trp^{3}-Ser^{4}-Tyr^{5}-D-Leu^{6}-Leu^{7}-Arg^{8}-Pro^{9}-NHEt
I	pGlu^{1}-His^{2}-Trp^{3}-N-Me-Ser^{4}-Tyr^{5}-D-Lys^{6}-Leu^{7}-Arg^{8}-Pro^{9}-NHEt
II	pGlu^{1}-His^{2}-Trp^{3}-N-Me-Ser^{4}-Tyr^{5}-D-Lys^{6}(Gly)-Leu^{7}-Arg^{8}-Pro^{9}-NHEt
III	pGlu^{1}-His^{2}-Trp^{3}-N-Me-Ser^{4}-Tyr^{5}-D-Lys^{6}(Ala)-Leu^{7}-Arg^{8}-Pro^{9}-NHEt
IV	pGlu^{1}-His^{2}-Trp^{3}-N-Me-Ser^{4}-Tyr^{5}-D-Lys^{6}(Sar)-Leu^{7}-Arg^{8}-Pro^{9}-NHEt
V	pGlu^{1}-His^{2}-Trp^{3}-N-Me-Ser^{4}-Tyr^{5}-D-Lys^{6}(a-Me-Val)-Leu^{7}-Arg^{8}-Pro^{9}-NHEt
VI	pGlu^{1}-His^{2}-Trp^{3}-N-Me-Ser^{4}-Tyr^{5}-D-Lys^{6}(N-Me-Val)-Leu^{7}-Arg^{8}-Pro^{9}-NHEt
VII	pGlu^{1}-His^{2}-Trp^{3}-Ser^{4}-Tyr^{5}-D-Lys^{6}[Gly(tBu)]-Leu^{7}-Arg^{8}-Pro^{9}-NHEt
VIII	pGlu^{1}-His^{2}-Trp^{3}-N-Me-Ser^{4}-Tyr^{5}-D-Lys^{6}[Gly(tBu)]-Leu^{7}-Arg^{8}-Pro^{9}-NHEt
IX	pGlu^{1}-His^{2}-Trp^{3}-Ser^{4}-Tyr^{5}-Glu^{6}-Leu^{7}-Arg^{8}-Pro^{9}-NHEt
X	pGlu^{1}-His^{2}-Trp^{3}-Ser^{4}-Tyr^{5}-D-Glu^{6}-Leu^{7}-Arg^{8}-Pro^{9}-NHEt
XI	pGlu^{1}-His^{2}-Trp^{3}-N-Me-Ser^{4}-Tyr^{5}-D-Glu^{6}-Leu^{7}-Arg^{8}-Pro^{9}-NHEt
XII	pGlu^{1}-His^{2}-Trp^{3}-Ser^{4}-His^{5}-Asp^{6}-Trp^{7}-Lys^{8}-Aib^{9}-Gly^{10}-NH_2
XIII	pGlu^{1}-His^{2}-Trp^{3}-Ser^{4}-His^{5}-Asn^{6}-Trp^{7}-Lys^{8}-Pro^{9}-Gly^{10}-NH_2
XIV	pGlu^{1}-His^{2}-Trp^{3}-Ser^{4}-His^{5}-Glu^{6}-Trp^{7}-Lys^{8}-Pro^{9}-Gly^{10}-NH_2
XV	pGlu^{1}-His^{2}-Trp^{3}-Ser^{4}-His^{5}-Asp^{6}-D-Trp^{7}-Lys^{8}-Pro^{9}-Gly^{10}-NH_2
XVI	pGlu^{1}-His^{2}-D-Trp^{3}-Ser^{4}-His^{5}-Asp^{6}-D-Trp^{7}-Lys^{8}-Pro^{9}-Gly^{10}-NH_2

References

1. Emons G, Schally AV. *Hum Reprod* **9**: 1364-1379, 1994.
2. Ravenna L, Salvatori L, Morrone S, Lubrano C, Cardillo MR, Sciarra F, Frati L, Di Silverio F, Petrangeli E. „*J Androl* **21**: 549-557, 2000.
3. Zompra AA, Magafa V, Lamari FN, Nikolopoulou A, Nock B, Maina Th, Spyroulias GA, Karamanos NK, Cordopatis P. *J Pept Res* **13**: 143-149, 2007.

2-21-196

Apoptotic effect of peptides produced by elastase I hydrolysis of bone proteoglycan extract

McLaughlin, Rene[1]; Johnson, Keryn[2]; Harper, Jacquie[1]; Vasudevamurthy, Madhusudan[2,*]
[1]Malaghan Institute of Medical Research, NEW ZEALAND; [2]Industrial Research Limited, NEW ZEALAND

[*]E-mail: m.vasudevamurthy@irl.cri.nz

Introduction

Cancer cells have an ability to evade cell death through down regulation of intrinsic cell death pathways. Usually anticancer therapies focus on triggering cell death through one or more of the three main cell death pathways: apoptosis, necrosis and autophagy. Recently it has been shown that innate immunity polypeptides have an unique mechanism of cancer killing that involves membrane lysis.[1,2] However, the effect of these peptides is dependent on cell type. Some peptides have activity against bacteria and cancer cells, but not against normal mammalian cells, whereas others can kill bacteria as well as both mammalian cancer and non-cancer cells.[3] It has been shown that these peptides kill cells via different mechanisms.[4] For example, host defence peptides may trigger necrosis through a cell membrane lytic effect, as they bind rapidly to the plasma membrane of cancer cells resulting in cell death. Alternatively, internalization of peptides inside eukaryotic cells, can disrupt the mitochondrial membrane resulting in the release of cytochrome c and induction of apoptosis.[4]

The increasing number of cancers resistant to conventional chemotherapy emphasises the potential for developing cytotoxic polypeptides as novel anticancer agents. We have investigated the effect of peptides released by proteolytic hydrolysis of proteoglycan extracts of bones from New Zealand meat industry waste and found that these peptides are biologically active triggering apoptosis in a human leukaemia cell line (HL60).

Materials and Methods

Waste bone fragments from the meat industry were powdered and homogenised using liquid nitrogen and proteoglycans were extracted overnight with guanidinium HCl and then filtered through four layers of muslin cloth. Salts were then removed from the filtrate using dialysis and the proteoglycan extract was freeze-dried. The resulting dried proteoglycan extract was digested overnight with elastase I. The remaining insoluble proteins were removed using a Celite filter and the filtrate collected and freeze-dried. The final freeze-dried product (PGE peptide) contained peptides released from proteolytic hydrolysis and was used to test for biological activity with HL60 cells. HL60 cells were cultured in cRPMI at 37 °C, 5% CO_2. Confluent HL60 cells ($1x10^6$ cells/ml) were incubated in the presence or absence of different concentrations of PGE peptides for 24 hours. Cells treated with 10% DMSO (v/v) were used as a positive control and 10% PBS (v/v) as a negative control. To determine the extent of apoptosis and/or cell death, cells were stained with Annexin-V-FITC and PI respectively and analysed by flow cytometry (BD FACScalibur, FlowJo Version 8.5.2.). Dead cells were identified as AnnV+/PI+, apoptotic cells as AnV+/PI- and necrotic cells as AnV-/PI+. Slides were photographed using Olympus BX51 microscope using differential interference contrast (DIC).

Results and Discussion

The biological activity of a mixture of peptides released through elastase hydrolysis of proteoglycan extract (PGE peptide) was first tested for the ability to induce simple morphological changes. Following treatment with PGE peptides, the cells lost membrane integrity, formed large vacuoles and became spindle shaped (Fig. 1). After

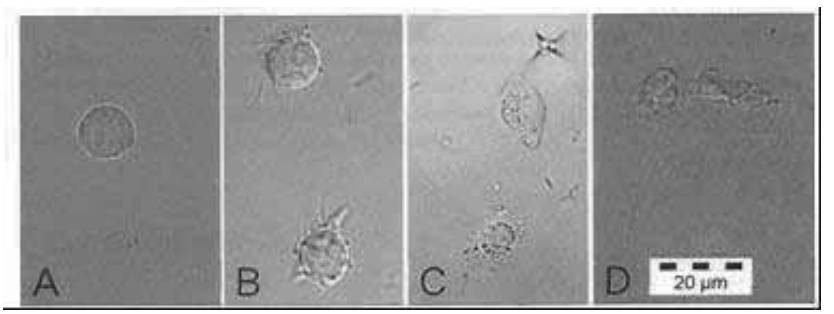

Figure 1. HL60 cells undergo morphological changes when exposed to PGE peptides. A) PBS control. B – D) 1, 4 and 24 hours respectively after PGE treatment. Cells photographed using DIC microscopy. Original magnification = 100x.

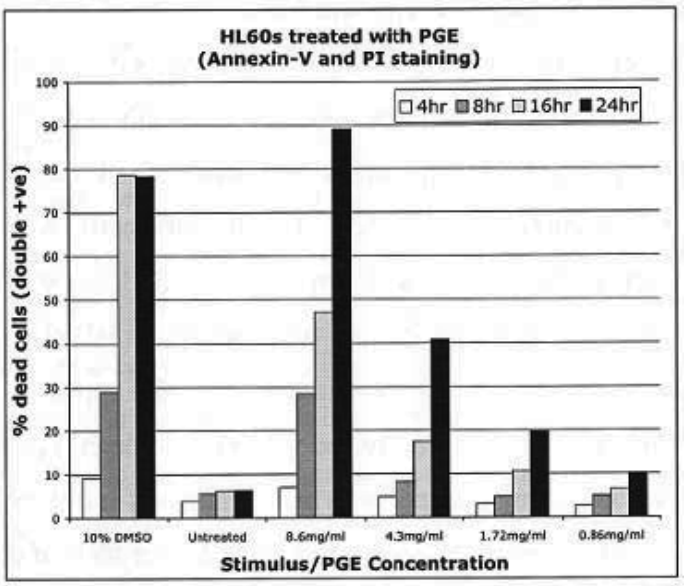

Figure 2. PGE peptides induced cell death is concentration and time dependent.

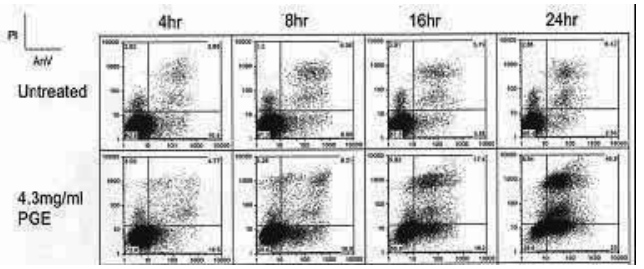

Figure 3. PGE induces cell death by apoptosis.

24 hours the cells displayed the classic popcorn-like morphology associated with apoptotic cell death.

To confirm that the PGE peptide preparation was inducing cell death, the HL60 cells were stained for the expression of markers of apoptosis (Annexin-V) and necrosis (PI) and analysed by flow cytometry. As shown in Fig. 2 the PGE peptides induced cell death in both a concentration and time dependent manner. Centrifugation and resuspension of the PGE peptide-treated cells in fresh media at different timepoints following PGE peptide treatment did not abrogate cell death (data not shown) indicating that once triggered, PGE peptide-induced cell death is not reversible.

To determine whether cell death was occurring via apoptosis or necrosis, HL60 cells treated with 4.3 mg/mL PGE peptides were analysed for the presence of apoptotic (AnV^+/PI^-) and necrotic (AnV^-/PI^+) cells at 4, 8, 16 and 24 hours. Fig. 3 confirms that the cell death was occurring predominantly via apoptosis (AnV^+/PI^-), rather than necrosis, at all time points.

The PGE peptides also induced apoptosis in human monocytic leukemia cells (THP-1) indicating that the cytotoxic effect was not specific to HL60 cells.

Conclusions

Here we have shown that HL60 cells enter the apoptotic cell death pathway when treated with peptides produced by elastase hydrolysis of a bone proteoglycan extract. Further work is required to separate and identify the specific peptide(s) responsible for inducing apoptosis.

References

1. Shadidi M, Sioud M. Selective targeting of cancer cells using synthetic peptides. *Drug Resist Updat* **6**: 363-371, 2003.
2. Leuschner C, Hansel W. Membrane disrupting lytic peptides for cancer treatments. *Curr Pharm Des* **10**: 2299-2310, 2004.
3. Rozek T, Wegener KL, Bowie JH, Olver IN, Carver JA, Wallace JC, Tyler MJ. The antibiotic and anti-cancer active aurien peptides from the Australian bell frogs Litoria aurea and Litoria raniformis and the solution structure of aurien 1.2. *Eur J Biochem* **267**: 5330-5341, 2000.
4. Papo N, Shai Y. Host defense peptides as new weapons in cancer treatment. *Cell Mol Life Sci* **62**: 784-790, 2005..

2-21-197

Opioid peptide-platinum(II) complexes: synthesis, characterization and *in vitro* antitumor activity

Glowinska, Agnieszka[1,]; Tomczyszyn, Aleksandra[1]; Kosson, Piotr[2]; Matalinska, Joanna[2]; Lipkowski, Andrzej W[2]; Misicka, Aleksandra[3]*

[1]University of Warsaw, Faculty of Chemistry, POLAND; [2]Medical Research Centre, Polish Academy of Sciences, POLAND; [3]University of Warsaw, Faculty of Chemistry; Medical Research Centre, Polish Academy of Sciences, POLAND

[*]E-mail: aglowinska@chem.uw.edu.pl

Introduction

Cisplatin belongs to the most powerful and useful anticancer agents. It binds strongly to DNA in regions containing several guanine units, forming Pt-DNA links within strands.[1] Through disrupting base-pairing guanine to cytosine cross-links lead to unwinding of the DNA. As a result cisplatin works against both types of cells, destroying cancer and normal type ones. Therefore more selective delivery system of platinum to cancer cells is still needed.

Based on the evidence of the presence of δ- and μ-opioid receptor types in carcinoma cells[2] we proposed to use opioid peptides as selective carriers for delivering platinum ions to the cancer cells. We designed hybride molecules which combine two fragments. One part of the molecule contains the opioid pharmacophore and the other fragment is designed to form a complex with platinum ion. Biphalin analogue, which is known as a strong antinociceptive agent, has been chosen as an opioid pharmacophore fragment.[3] The other fragment, designed to form complexes of Pt(II), could be described as cisplatin analogue. It consists of a plane square structure containing two cis leaving chloride atoms and bidentate amino acid ligand bound to Pt(II) ion. N-terminal cysteine, histidine or methionine (Xaa) residues have been selected to coordinate Pt(II), as these amino acids are able to coordinate platinum ion by S,N, or N,N atoms.

Results and discussion

Synthesis of the biphalin analog was performed in solution using the standard coupling reagents and protection groups. Then peptide was reacted with complexing agent (K_2PtCl_4) to get the desired compounds I, II and III. Purification of the final compounds was performed using high performance liquid chromatography and isolated products were characterized by mass spectroscopy.

All synthesized compounds showed μ- and δ-receptor affinities in the binding assays in the nanomolar (μ) or micromolar (δ) range, what confirmed that terminal complex unit (Pt) does not interfere with the activity of opioid pharmacophore.

The effect of two synthesized compounds on proliferation of human glioblastoma cells is presented below. The preliminary results indicate that the proliferation T98G cells measured on the 4th day is 50% lower, compared to the control.

Cell growth test: For the assessment of the effect of peptides on cell growth, T98G cells were seeded into 35mm diameter culture dishes and peptides dissolved in medium were added at the concentration 10 μM or 20 μM. Cell numbers were measured every day by harvesting the cells using 0.25% trypsin - 0.02% EDTA and counting the hemacytometer chamber.

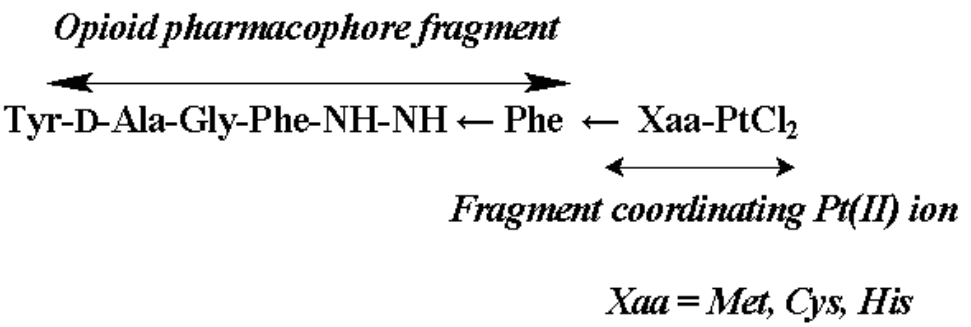

Scheme 1.

Conclusions

The synthesized compounds show bifunctional properties: affinity at the μ and δ opioid receptors and antitumour activity on carcinoma cells. Therefore, the designed hybride compounds are potential analgesics and antitumor compounds. Neuropeptides which receptors exist on cancer cells in higher concentration compare to normal cells could serve as address part of the hybride molecules with increased selectivity for platinum (cisplatin).

Acknowledgements

Project supported by EU grant Normolife (LSHC-CT-2006-037733).

References

1. Cruhl M, van Waardenburg RCAM, Beijnen JH, Schellens JHM. *Canc Treat Rev* **28**: 291-303, 2002.
2. Madar I, Bencherif B, Lever J, Heitmiller RF, Yang SC, Brock M, Brahmer J, Ravert H, Dannals R, Frost JJ. *J Nucl Med* **48**: 207-213, 2007.
3. Lipkowski AW, Misicka A, Davis P, Stropova D, Janders J, Lachwa M, Porreca F, Yamamura HI, Hruby VJ. *Bioorg Med Chem Lett* **9**: 2763-2766, 1999.

2-22-198

Bioinformatic-aided studies of biological activity of food peptides and proteins

Darewicz, Malgorzata; Dziuba, Jerzy*

University of Warmia and Mazury in Olsztyn, Department of Food Biochemistry POLAND

**E-mail: darewicz@uwm.edu.pl*

Introduction

According to the present state of our knowledge, each protein may perform the role of a precursor of biologically active peptides, in addition to its basic functions. Bioactive motifs in protein polypeptide chains are defined as those fragments which remain inactive in sequences of their precursors, but are able to interact with receptors or regulate physiological functions of the body when released by proteolytic enzymes.[1] Their effects may be positive or negative. Peptides obtained from food (e.g. milk, plant, meat or egg) can for example reduce blood pressure, stimulate the immune system, induce smooth muscle contraction, inhibit the activity of proline endopeptidases and HIV proteinase. Researchers display a growing interest in the use of bioactive peptides for therapeutic purposes. Biologically active peptides are also recommended as functional food components. At research laboratories analytical techniques are often combined with computer techniques, especially in such branches of Science as molecular biology or biochemistry which contributed to the development of a new scientific discipline referred to as bioinformatics.[2] At the Department of Food Biochemistry we developed a database of protein and bioactive peptide sequences BIOPEP. This database enables searching for bioactive fragments in polypeptide chains, hierarchical classification of proteins according to algorithms, proteolysis design aimed at bioactive peptide acquisition or removal. The information obtained can be used for designing desirable food properties, as well as predicting biological functions of proteins.[3] The BIOPEP database is available on the Internet at [http://www.uwm.edu.pl/biochemia]. At present BIOPEP include 161 and 1916 sequences of proteins and peptides respectively, and 25 sequences of proteolytic enzymes respectively. The database provides information on 44 types of bioactive peptides. The BIOPEP program offers a proteolysis design option. The value of a protein as a precursor of bioactive peptides is determined on the basis of automatically calculated discriminants: profile of potential biological activity of a given protein; occurrence frequency of bioactive motifs (A); potential activity (B). The profile of potential biological activity of a given protein is defined as a kind and location of bioactive fragments in the precursor sequence. The occurrence frequency of bioactive fragments in the protein chain (A) is defined as follows: A = a/N where: a - number of fragments with a given kind of activity in the protein chain, N - number of amino acids residues. The potential activity (B) of protein fragments (mM^{-1}) is defined as follows: the total sum of number of repetitions of bioactive fragment in the protein chain versus concentration of bioactive peptide corresponding to half of its maximum activity, devided in the number of fragments with a given kind of activity.

Results and discussion

Antihypertensive, immonomodulating and opioid peptides dominate in 161 profiles of potential biological activity of proteins, examined in our studies. An analysis of 44 kinds of peptide activities, included in the BIOPEP database, showed that protein sequences were relatively poor in antibacterial fragments. The richest potential source of bioactive peptides are milk proteins. For instance, in the beta-casein sequence there are 70 fragments corresponding to various bioactive peptides. Most of them show antihypertensive activity. Distriminant A, i.e. the occurrence frequency, is the highest for this kind of activity (A=0.2344). Beta-casein has not been known as a precursor of dipeptidyl peptidase IV inhibitors so far. The analysis of relationships between the kind of activity and structure include evaluation of hydrophobicity and presence of a secondary structure in bioactive fragments of precursor protein sequences. In most cases all forms of secondary structure were present. However, we found that structural motifs of peptides toxic to patients suffering from celiac disease, chemotactic, embryotoxic and dipeptidyl aminopeptidase inhibitors do not contain alpha-helix structure, and are dominated by disordered structure. Almost all bioactive motifs show hydrophilic character (negative hydrophobicity). We characterized proteins as a source of celiac toxic tetrapeptides and their extended motifs. The BIOPEP database (http://www.uwm.edu.pl/biochemia), SWISS-PROT database (http://www.expasy.org), BLAST (http://www.ncbi.nlm.nih.gov/blast) homology searching protocol and PREDICT 7 program were applied. Rich sources of celiac-disease-potentiating peptides were wheat gliadins, barley hordeins and rye secalins as well as low-molecular weight fractions of glutenin. In addition, amino acid sequences with a high degree of identity to the toxic peptides examined were detected in maize zein, oat avenin, protein of rice, yeast and chicken muscles, as well as casein and galanin. The BLAST homology searching protocol proved the existence of high extent of evolutional homology. Random coil and beta-sheet were the only

occuring secondary structure for peptides that were studied. Celiac-toxic peptides were obtained as a result of proteinase K, thermolysin and prolyl endopeptidase. The presence of an active motif in protein and its computer-designed release are verified by mass spectrometry, using a device for advanced analysis of proteins and peptides. For instance in the final stage of our studies isolated and characterized chromatographically antibacterial, infection-preventing lactoferrin was identified by peptide mass fingerprinting (PMF) using a mass spectrometer. The hexapeptide showing antiviral activity, with weight of 802 D and the following sequence: Glu-Asp-Leu-Ile-Trp-Lys, constituting fragment 278-282, was found in trypsin hydrolysate of lactoferrin.

References

1. Dziuba M, Darewicz M. *Food Sci Technol Inter* **13**: 393-404, 2007.
2. Darewicz M, Dziuba J, Minkiewicz P. *Food Sci Technol Inter* **13**:125-133, 2007.
3. Dziuba J, Niklewicz M, Iwaniak A, Darewicz M, Minkiewicz P. *Polimery* **6**: 9-13, 2005.

2-23-199

Search for modulators of VEGF-KDR interaction: hydrocarbon-bridged VEGF derived peptides

García-Aranda, M Isabel[1]; Mirassou, Yasmina[2]; Mirones, Isabel[3]; Alfranca, Arantza[3]; Martín-Martínez, Mercedes[1]; García-López, M Teresa[1]; Jiménez, M Angeles[2]; Redondo, Juan M[3]; Gónzález-Muñiz, Rosario[1]; Pérez de Vega, Mª Jesús[1,]*

[1]Instituto de Química Médica-CSIC, Juan de la Cierva, 3, 28006 Madrid, SPAIN; [2]Instituto de Química Física Rocasolano-CSIC, Serrano, 119, 28006 Madrid, SPAIN; [3]Centro Nacional de Investigaciones Cardiovasculares (CNIC), Melchor Fernández Almagro, 3, 28029 Madrid, SPAIN

[*]E-mail: iqmg313@iqm.csic.es

Angiogenesis, the formation of new blood vessels from existing ones, is an important process in both physiologic and pathologic situations, and its inhibition can be useful in the fight against several diseases, among others cancer, diabetic retinopathy and atherosclerosis. One of the key factors in promoting angiogenesis is the Vascular Endothelial Growth Factor (VEGF), which exerts its biological activity through interaction with specific transmembrane receptors, such as VEGFR-1 (Flt-1), VEGFR-2 (KDR, Flk-1) and VEGFR-3 (Flt-4). KDR is overexpressed in most of the pathologies associated to angiogenesis, therefore, the inhibition of the VEGF-KDR interaction constitutes a valuable approach towards the search for new anti-angiogenic agents.

Directed mutagenesis studies allowed the identification of a possible "hot spot" for the VEGF-KDR interaction. Particularly, residues Arg^{82}, Ile^{83}, Lys^{84}, His^{86} and Glu^{89}, located in a β–hairpin of loop 3, were identified as essential for this interaction.[1-3] According to this, a series of analogues of the $VEGF_{81-91}$ fragment (MRIKPHQGQHI) were designed, in which hydrocarbon bridges were introduced to generate cyclic derivatives, trying to preserve the β–hairpin native structure (Fig. 1, Series 1). Additionally, considering that the β-turn of native $VEGF_{81-91}$ is slightly distorted, due to the presence of an extra amino acid residue, in addition to the bridged undecapeptides, two series of decapeptide analogues have also been prepared (Fig. 1, Series 2 and 3), just by removing the residue Glu^{87} or Gly^{88} in Series 1.

Designed compounds were prepared following typical solid-phase peptide synthesis (SPPS) protocols. The cyclization was achieved by introduction of allylglycine residues into the selected positions, and subsequent olefin cross metathesis reaction on solid phase to give the olefin-bridged (C=C) peptides (Fig. 2). Further on-resin reduction of the so formed double bond led to the corresponding saturated (C-C) analogues (Fig. 2).

The conformational behavior of linear and bridged-peptides was analyzed by NMR, using ^{1}H and ^{13}C chemical shifts deviation and temperature coefficients for NH amide protons. The obtained data showed that linear compounds are not structured, while cyclic derivatives, even if more structured, do not fix the β-hairpin conformation.

All compounds were tested for their capacity to inhibit endothelial proliferation in HUVEC cells incubated with tritiated timidine, using VEGF as stimulus. None of the evaluated compounds showed significant activity in this assay.

As a summary, a convenient procedure for the synthesis of hydrocarbon-bridged conformationally constrained analogues of $VEGF_{81-91}$ has been developed. Most of these cyclic peptides are able to stabilize the β-turn of $VEGF_{81-91}$ fragment, although the β-hairpin structure does not seem to be accurately fixed. None of these VEGF constrained analogues were able to significantly antagonize the VEGF-induced angiogenesis. A possible explanation can be either the lack of defined conformation, as none of the compounds are able to mimic the structure of the native loop, or the lack of the Arg^{82} side chain, one of the important residues of the hot-spot. Work to clarify these questions is in progress.

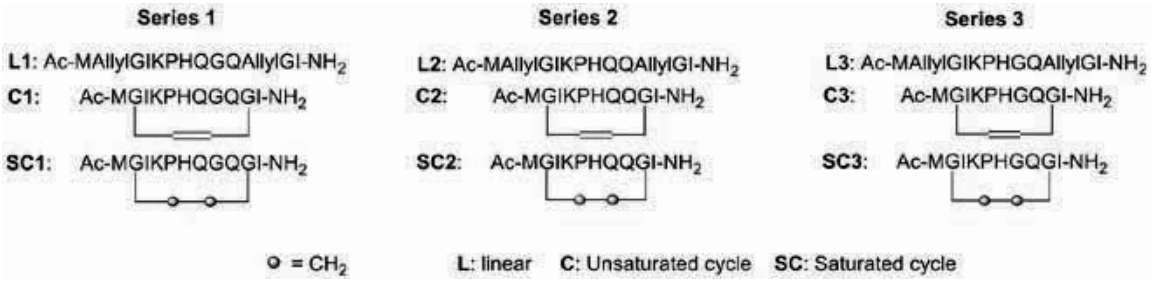

Figure 1. Designed VEGF-derived peptides.

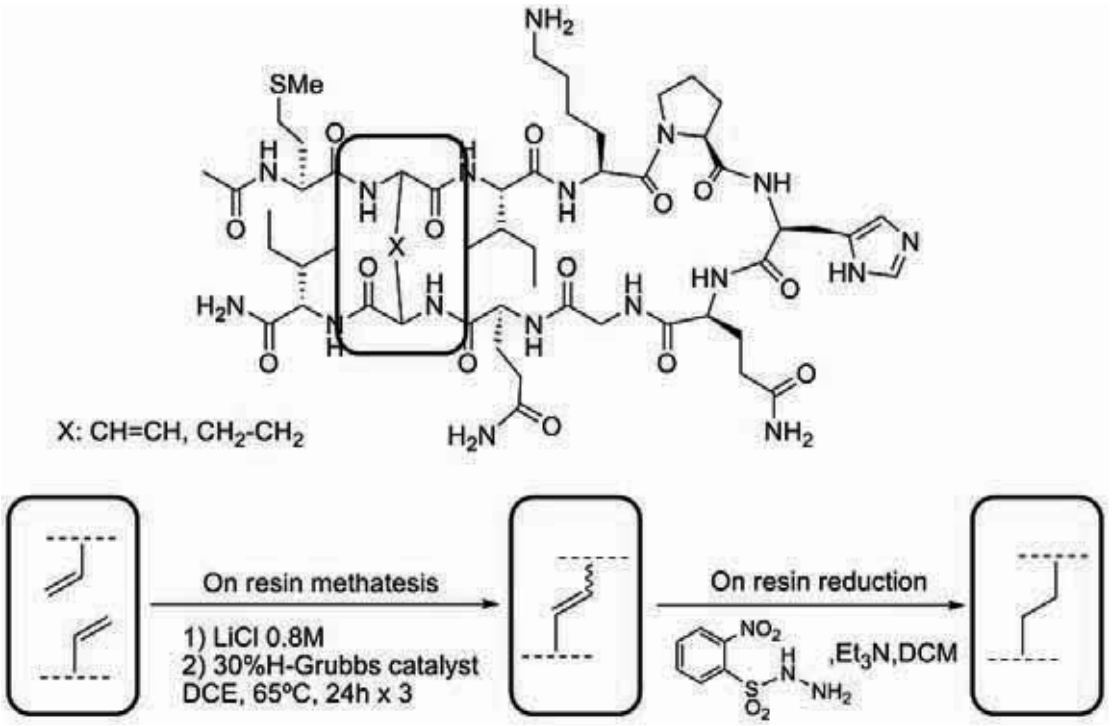

Figure 2. Main steps in the synthesis of VEGF-derived peptides.

Acknowledgements

We thank the CSIC (Proyectos Intramurales: 2005-80F0161 and 2006-80I066) and the CICYT (SAF 2006-01205) for financial support, and the CSIC for the fellowships to M. I. G.-A. and Y. M.

References

1. Keyt BA, Nguyen HV, Berleau LT, Duarte CM, Park J, Chen H, Ferrara N. Identification of Vascular Endothelial Growth Factor Determinants for Binding KDR and FLT-1 Receptors. *J Biol Chem* **271**: 5638-5646, 1996.
2. Fuh G, Li B, Crowley C, Cunningham B, Wells JA. Requirements for Binding and Signaling of the Kinase Domain Receptor for Vascular Endothelial Growth Factor. *J Biol Chem* **273**: 11197-11204, 1998.
3. Fuh G, Wu P, Liang WC, Ultsch M, Lee CV, Moffat B, Wiesmann C. Structure-Function Studies of Two Synthetic Anti-vascular Endothelial Growth Factor Fabs and Comparison with the AvastinTM Fab. *J Biol Chem* **281**: 6625-6631, 2006.

2-23-200

Cyclic peptides comprising constrained amino acids as inhibitors of integrin-ligand interaction

Royo, Soledad[1,]; Conradi, Jens; Sewald, Norbert*
Bielefeld University, Organic and Bioorganic chemistry, GERMANY

[*]E-mail: soledad.royo@uni-bielefeld.de

Introduction

Integrins are heterodimeric cell surface receptors that play an important role in numerous cellular processes, such as migration, growth and differentiation. Integrins mediate cell-cell and cell-matrix adhesion. The binding of integrins to their natural ligands is the molecular basis of physiological as well as of patho-physiological processes. Thus, small molecules capable of interfering with this integrin binding process have pharmacological potential in the therapy of diseases such as cancer, osteoporosis or thrombosis. The amino acid sequence RGD (-Arg-Gly-Asp-), present on many of the natural ligands, is a prominent recognition motif of integrin ligands. Thus, small peptides containing the RGD sequence have emerged as an excellent starting point for the identification, synthesis and development of selective integrin ligands.[1]

The affinity and selectivity of the peptide ligands towards different integrins depend strongly on the secondary structure and the overall three-dimensional shape. Cyclization is frequently used as a method to reduce the accessible conformational space. It results in higher affinity and selectivity, if the receptor-bound conformation is still accessible. Additionally, the incorporation of non-natural conformationally constrained amino acids can greatly affect the secondary structure of the peptide, hindering or inducing a particular conformation. Introduction of a *β*-amino acid, for example, in a cyclic RGD-pentapeptide results in the stabilization of a secondary structure where the *β*-amino acid residue preferably occupies the central sequence position of a pseudo *γ*-turn conformation. Some of these modifications have provided highly active and selective integrin ligands.[2,3]

Results and discussion.

We have synthesized a series of cyclic peptides containing the RGD motif and constrained amino acids with conformational bias (such as α-methylated amino acids, *β*-amino acids or dehydroamino acids). Taking the known $\alpha_v\beta_3$-ligand c-(-Arg-Gly-Asp-D-Phe-Val-) as the starting point, the new cyclic pentapeptides should incorporate a hydrophobic amino acid following Asp, whereas the nature of the residue preceeding Arg can be modified without affecting the activity.[4] Binding to integrin $\alpha_v\beta_3$ is favoured by a non-stretched conformation around the RGD sequence, whereas $\alpha_{IIb}\beta_3$-ligands show the recognition triad in a somewhat elongated conformation. Thus, c-(-Arg-Gly-Asp-D-Phe-Val-) adopts a conformation where Gly occupies the central position of a *γ*-turn and D-Phe is in the i+1 position of a βII'-turn. A similar secondary structure is found for the highly active and selective $\alpha_v\beta_3$-ligand c-(-Arg-Gly-Asp-(+)$^{\beta}$Acc-Val-).[3]

Different aromatic amino acids known to accomodate or induce β-turns have been selected as replacements for D-Phe (Xaa), such as Phe and (αMe)Phe (Fig. 1). In addition, Val has been replaced by other *β*-turn inducers (Yaa), such as Leu, (αMe)Val and Iva. Both *α,β*-dehydroamino acids and *α*-methylated amino acids stabilize *β*-turn and helical structures.[5,6]

All cyclic peptides have been prepared from the side-chain protected linear precursors H-Asp(*t*Bu)-Xaa-Yaa-Arg(Pbf)-Gly-OH, performing the cyclization in solution under pseudo-dilution conditions and using HATU as coupling reagent. The linear peptides have successfully been assembled on a 2-chlorotrityl resin using a *CEM Liberty* microwave peptide synthesizer and Fmoc/*t*Bu chemistry on a semi-automated synthesis. Fmoc

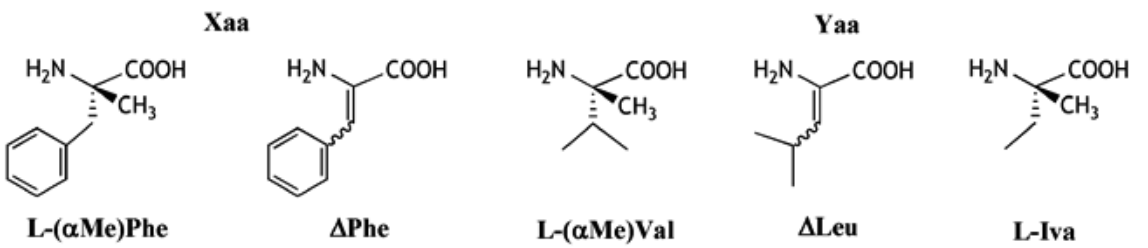

Figure 1. Constrained amino acids incorporated in the RGD peptides.

deprotection and normal couplings are achieved using standard microwave methods and TBTU as coupling reagent. Modified methods with elongated reaction times (one cycle of 600-900 seconds instead of one cycle of 300 seconds) and HATU as coupling reagent are needed for couplings involving constrained amino acids. Double couplings are necessary for the incorporation of the residue following the dehydroamino acids, which are known to be weak nucleophiles. After side-chain deprotection, the cyclic peptides have been purified by RP-HPLC and characterized by MALDI-Tof mass spectrometry and NMR spectroscopy.

A cell adhesion assay has been established for the analysis of the biological activity of the new peptides as integrin ligands. In these assays, the influence of the cyclic RGD peptides on the adhesion of WM115 cancer cells on human vitronectin has been determined. Adhesion of these cells to vitronectin is predominantly mediated by integrin $\alpha_v\beta_3$. As reference for these tests, c-(-Arg-Gly-Asp-D-Phe-Leu-) has been used.[4]

All peptides tested so far are active $\alpha_v\beta_3$-ligands (Table 1). The two cyclic peptides containing dehydroamino acids are active in the nanomolar range. Their affinity to integrin $\alpha_v\beta_3$ is comparable to that of the reference peptide. The peptide containing (αMe)Phe is active only in the low micromolar range. Further tests will be carried out for the other two α-methylated peptides, as well as on a different cell line, expressing integrin $\alpha_5\beta_1$.

Acknowledgments

This work is supported by a Marie Curie Intra-European Fellowship from the 6th Framework Programme. DSM Research is gratefully acknowledged for providing some of the amino acids used in this work.

References

1. Meyer A, Auernheimer J, Modlinger A, Kessler H. *Curr Pharm Des* **12**: 2723-2747, 2006.
2. Schumann F, Mueller A, Koksch M, Mueller G, Sewald N. *J Am Chem Soc* **122**: 12009-12010, 2000.
3. Urman S, Gaus K, Yang Y, Strijowski U, Sewald N, De Pol S, Reiser O. *Angew Chem Int Ed Engl* **46**: 3976-3978, 2007.
4. Haubner R, Gratias R, Diefenbach B, Goodman SL, Jonczyk A, Kessler H. *J Am Chem Soc* **118**: 3461-3472, 1996.
5. Mathur P, Ramakumar S, Chauhan VS. *Biopolymers (Peptide Science)* **76**: 150-161, 2004.
6. Toniolo C, Crisma M, Formaggio F, Peggion C. *Biopolymers (Peptide Science)* **60**: 396-419, 2001.

Table 1. Inhibitory activity of RGD peptides on the interaction between WM115 cells and vitronectin

Peptide	IC_{50}(M)
c-(-Arg-Gly-Asp-DPhe-Leu-)	$5.29 \cdot 10^{-8}$
c-(-Arg-Gly-Asp-ΔPhe-Leu-)	$4.66 \cdot 10^{-8}$
c-(-Arg-Gly-Asp-DPhe-ΔLeu-)	$4.98 \cdot 10^{-8}$
c-(-Arg-Gly-Asp-(αMe)Phe-Val-)	$2.60 \cdot 10^{-6}$

2-23-201

Conjugation of RGD analogs with o-quinone methides of [1,1´]binaphthalenyl and their biological activity

Sarigiannis, Yiannis[1]; Saravanos, Antonios[2]; Stavropoulos, George[1,]; Tsoungas, Peter[3]; Cordopatis, Paul[2]*
[1]University of Patras, Department of Chemistry, GREECE; [2]University of Patras, Department of Pharmacy, GREECE; [3]General Secretariat of Research and Technology, Department of Development and Technology, GREECE

[*]E-mail: G.Stavropoulos@chemistry.upatras.gr

Introduction

The ability of electrophilic carbonyl species to form protein adducts has been implicated in a number of disease processes, including diabetes, atherosclerosis and neurodegenerative diseases. Quinone methides (QMs) represent an extensive class of electrophilic molecules that can form covalent adducts with proteins and can produce toxicological effects via such adduction.[1-4] The asymmetry introduced by the presence of two electronically different substituents, carbonyl and methylidene, on the cyclohexadiene ring imparts a strong dipolar character to quinone methides not found in benzoquinones and quinodimethanes.

The formation of o-quinone methides as reactive intermediates in biologically-active natural products has been reviewed.[2] For example, a proposed reactive quinone methide intermediate generated from the naturally occurring antitumor antibiotic, mitomycin C, is believed to be responsible for DNA alkylation.[5] They also function as efficient heterodienes in Diels–Alder reactions and undergo a variety of self dimerization reactions.[6-8] The significance of QMs rests upon their mode of action being the reactive site of various structures of cellular macromolecules such us DNA or proteins. o-QMs of types 1, prepared by coupling of an appropriately substituted naphthol, are useful intermediates for alkylation / X-linking of simple amino acids right through to cellular macromolecules such as DNA, proteins and peptides. This reaction is already known to be responsible for a broad spectrum of activity of these molecules. These compounds will be also useful tools for the synthesis of non natural amino acids.

Chemistry and Results

Here we present the synthesis of a new series of synthetic o-QMs ([1,1´]Binapthalenyl type). The following scheme represents the procedure for the synthesis of these compounds. The dimerisation of the naphthol group is the crucial synthetic step, which under the described reaction conditions gave the desired product in high yield 83%. (NMR data:α_H(400 MHz, $CDCl_3$): 8.17 (2H, m, ArH); 7.457 (2H, m, ArH); 7.392-7.353 (4H, m, ArH); 7.310 (2H, m, ArH); 6.938-6.918 (2H, m, ArH); 4.088 (6H, s, OCH_3). These compounds will be conjugated to known RGD analogs and investigated for their biological activity as antiplatelet or antitumor agents. Preliminary experiments to this direction with primary amines and pyrrolidine gave encouraging results.

Scheme 1. Synthetic Procedure for the synthesis of o-Quinone Methides

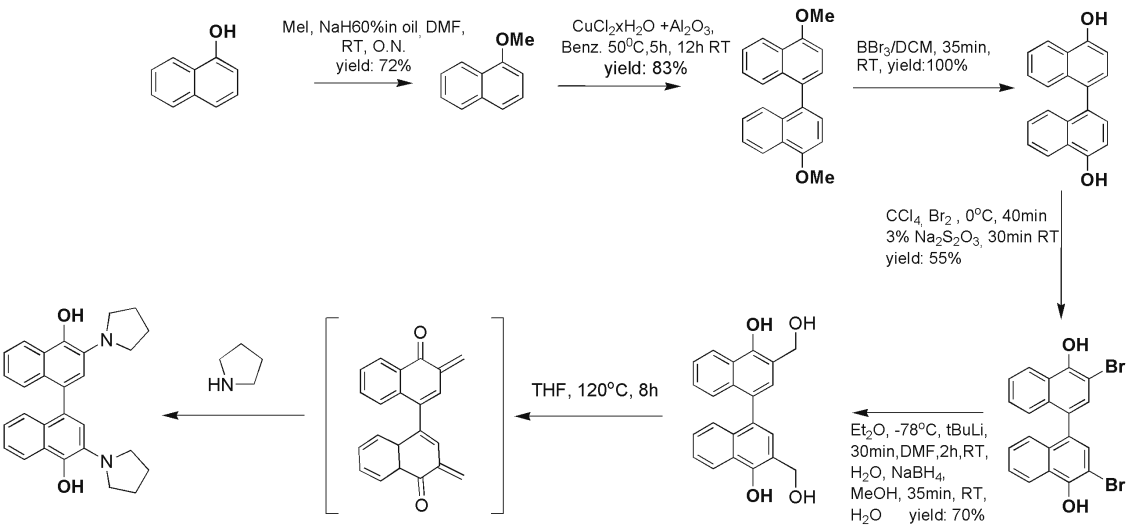

Acknowledgements

We thank the European Social Fund (ESF), Operational Program for Educational and Vocational Training II (EPEAEK II) and particularly the Program PYTHAGORAS II for funding the above work.

References

1. Van De Water RW, Pettus TRR. *Tetrahedron* **58**: 5367-5405, 2002.
2. Zeng Q, Rokita SE. *J Org Chem* **61**: 9080-9081, 1996.
3. Quyang A, Skibo EB. *J Org Chem* **63**: 1983- , 1998.
4. Nikolaou KC, Dai W. *J Am Chem Soc* **114**: 8908-8921, 1992.
5. Qiao GG, Lenghaus K, Solomon DH, Reisinger A, Bytheway I, Wentriep C. *J Org Chem* **63**: 9806-9811, 1998.
6. Vigalok, A, and Milstein, D, *J Am Chem Soc* **119**: 7873-7874, 1997.
7. Amouri H, Besace Y, Le Bras J. *J Am Chem Soc* **120**: 6171- 6172, 1998.
8. Amouri H, Vaissermann J, Rager MN, Grotjahn DB. *Organometallics* **19**: 5143-5148, 2000.

2-23-202

Analysis of POI-PO interaction using fluorescent labeled analogs designed based on "camouflaging substitution"

Yoshida, Rinako[1]; Awada, Chihiro[2]; Takao, Toshifumi[2]; Sato, Takashi[1,]*

[1]Saga University, Dept. of Applied Biochemistry and Food Science, JAPAN; [2]Osaka University, Institute for Protein Research, JAPAN

[*]E-mail: sugartap@cc.saga-u.ac.jp

Introduction

Phenoloxidase (PO) plays essential roles in insect immunity and melanization necessary for maintenance of their life. Regulation of PO is indispensable since too much work of PO lead to death of insect itself. Based on this idea, we have found the Phenol Oxidase Inhibitor (POI) in the hemolymph of housefly pupae that potently (Ki ≈ 10^{-9} M) and selectively inhibited PO.[1] POI contains three disulfide bridges and a novel post translational modified residue; DOPA at the position 32. NMR study revealed the conical shape of POI and the position of residue 32 at the top of the cone structure.[2] Though POI showed very strong affinity to PO, exact Ki has not been determined and thus SAR of POI is still unclear. The reason for this is due to very slow manner in 'off-rate' process in the binding between POI and PO, and thus analysis of POI-PO interaction based on steady-state kinetics is very difficult. Also sensitive measurements are required because these molecules interact in low concentration. Therefore we decided to employ the fluorescent labeled POI and static titration analyses for determination of Kd and SAR study of POI.

Concept of this study

Fluorescent labeling is very useful and important tool for biological analysis such in detection of trace amount of molecule, quantitation, analysis of interaction, molecular imaging and so on. Huge numbers of fluorescent dyes have been innovated and utilized until now, however, introduction of fluorescent groups may considerably affect the characteristics of parent molecule because of their bulky structure and hydrophobicity. Since POI is a small rigid peptide and has very hydrophilic character, introduction of fluorescent groups will change its characteristics largely and it may lead to changing the binding affinity to PO. Similar situation are thought to be happened in most of cases, however, it has been considered as inevitable change coming together with fluorescent labeling. Here, we propose a novel concept for the molecular labeling, "Camouflaging substitution" that enable to introduce chemical groups with least impact to the characteristics of parent molecule. The main subject of this concept is 'functional swapping' that exchange some part of parent molecule, where specific function is not coded, with some functional group(s) that possess major

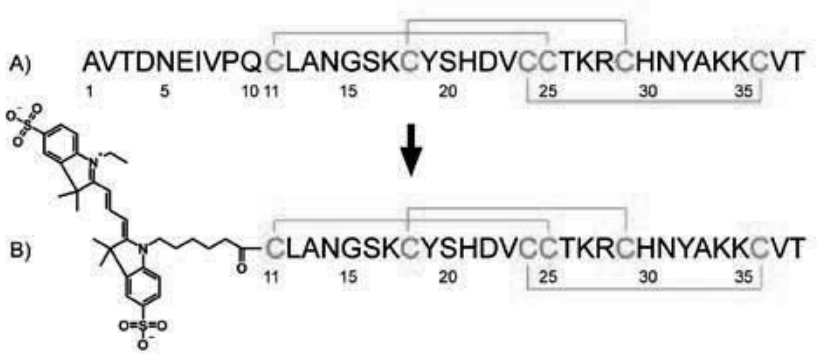

Figure 1. Structure of A) Native POI(1-38) and B) the camouflalog that was truncated N-terminal part of POI containing DNEIVPQ sequence and was labeled with the fluorescent group, Cy3, based on the concept of "camouflaging substitution".

Figure 2. Comparison of the N-terminal structure of POI containing DNEIVPQ sequence (shown in hatching) with Cy3 (shown in lighter hatching). Both structures were obtained by molecular orbital calculation with AM1. The positions of negative charges are indicated by circles.

structural features of swapped part of parent molecule. We reached this idea in the process of fluorescent labeling of POI where we found that the linear structure of fluorescent dye, Cy3, has very similar structural characteristics of N-terminal POI sequence, DNEIVPQ, including the hydrophobicity / hydrophilicity and positions of charged groups. Molecular orbital calculation using AM1 revealed that Cy3 can camouflage the structural features of some peptide chains containing (D/E)XEββPX sequence, where *β*-denotes amino acid residues preferred for *β*-structure (Fig. 2).

Results and discussion

Based on above idea, "Camouflaging substitution" we synthesized the "camouflalog" of POI (Fig. 1) as a reference molecule by the coupling of Cy3-ONSu to [Tyr^{32}]POI(11-38) in neutral pH conditions. Fluorescent group was mainly introduced in N-terminal amino group of POI(11-38) and other products that were modified with their Lys residues were removed by using active NCO-resins.[3] Mini-library of 77 analogs modified with four Lys residues were also prepared for SAR study of POI by employing random labeling of POI(11-38) with Cy3-ONSu to prevent obtaining analogs with irregular disulfide bridging pattern. All the products were purified by RP- / ion-exchange HPLC. Simultaneous measurements of both binding and inhibitory activities are now on going. The binding characteristics were analyzed by employing FRET and fluorescence polarization, and inhibitory activities were assayed by measuring residual PO activities of the mixture for interaction assays. These peptides were then subjected to MS / MS analyses for identification of modified residues. Inspection of tertiary structure of POI revealed that modified residues covered most of all molecular surface, thus quantitative analyses of these results may provide clear-cut SAR of POI.

Camouflaging substitution, could be expanded to other cases?

In this study, we found that Cy3 could be effectively camouflage the N-terminal sequence of POI. Although this is very specific in limited pair of sequence and fluorescent group, we believe that application to other peptides or proteins are possible, e.g. BODIPYs for replacement of β-turn structure. We are trying to synthesize various camouflalogs of other peptides using different fluorescent dye sets to generalize this concept.

References

1. Daquinag AC, Nakamura S, Takao T, Shimonishi Y, Tsukamoto T. *Proc Natl Acad Sci U S A* **92:** 2964-2968, 1995.
2. Sato, T. *et al*. *Biochemistry* **38:** 2179-2188, 1999
3. Mikami T, Takao T. *Anal Chem* **79:** 7910-7915, 2007.

2-23-203

Linear and cyclic synthetic peptide analogs of the A2 subunit (sequence 558-565) of the factor VIIIa blood coagulation and their biological effects

Anastasopoulos, Charalampos[1,]; Sarigiannis, Yiannis[1]; Stavropoulos, George[1]; Liakopoulou-Kyriakides, Maria[2]; Makris, Pantelis[3]*

[1]University of Patras, Department of Chemistry, GREECE; [2]Aristotle University of Thessaloniki, Department of Chemical Engineering, GREECE; [3]Aristotle University of Thessaloniki, AHEPA Hospital, GREECE

[*]E-mail: G.Stavropoulos@chemistry.upatras.gr

Introduction

Platelets aggregation causes clotting in the blood vessels during the blood circulation due to several reasons. Factor VIII (FVIII), a blood coagulation protein, is a key component of the blood coagulation system. The glycoprotein FVIII, in its activated form (FVIIIa), acts as a cofactor to the serine protease factor IXa in the conversion of the zymogen FX to the active enzyme (FXa) and is synthesized in the liver. The role of FVIIIa is to markedly increase the catalytic efficiency of FIXa in the activation of factor X. Activation of FVIII results from limited proteolysis catalyzed by thrombin or FXa, which binds the FVIII substrate over extended interactive surfaces.

The target of the present research is the synthesis and biological evaluation of linear and cyclic head to tail peptides, which are expected to inhibit selectively the maximisation of thrombin production depended on factor IX and accordingly the additional activation of platelets.[1,2] These peptides are based on the regions in which the FVIII interacts with FIX. The full length unprocessed glycoprotein FVIII consists of 2332 amino acid residues and is composed of three distinct domain types in the arrangement A1-A2-B-A3-C1-C2.[3,4]

The role of FVIIIa is to bind FIXa, generating the phospholipid-dependent intrinsic factor Xase complex. The Ser^{558}-Gln^{565} sequence within the A2 subunit has been shown to be crucial for VIIIa-IXa interaction.

Results & Discussion

In an attempt to study this interaction, we synthesized a series of twelve peptide analogs of 558-565 loop of the A2 subunit. The syntheses were carried out by using SPPS on 2-CLTR and Fmoc/tBu methodology. We synthesized tail peptides (No 1-4) and tail peptide analogs (No 6-10) incorporating Asp instead of Asn^{564}.

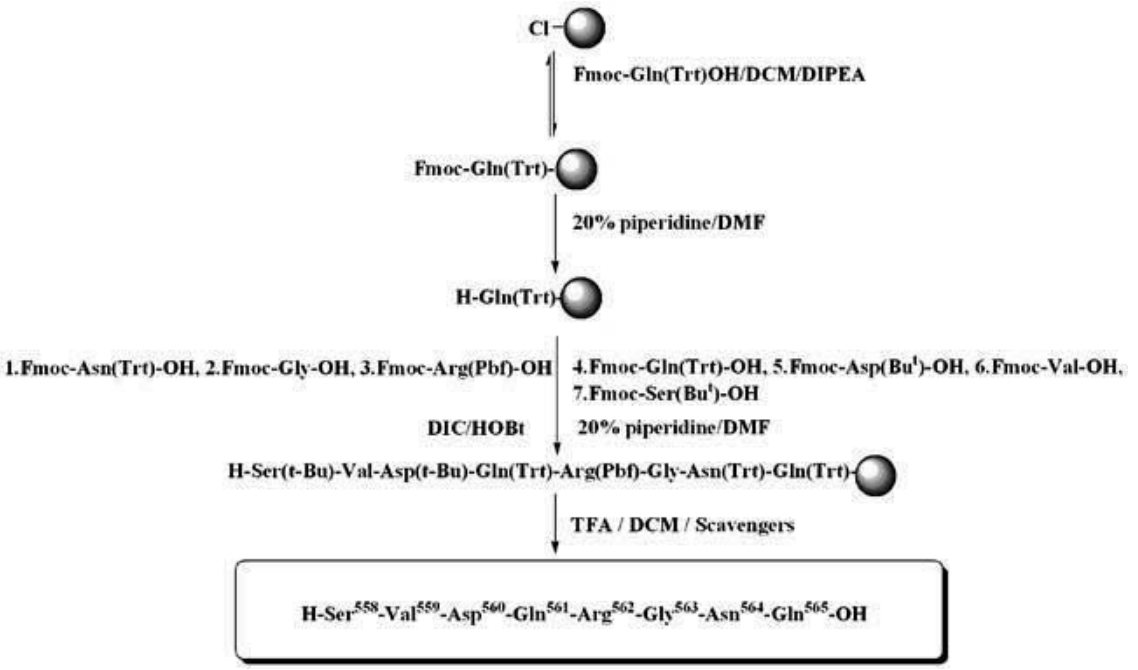

Figure 1. Synthetic route of the peptide sequence Ser^{558}-Gln^{565}.

Table 1. Synthesized analogs of the peptide sequence Ser558- Gln565 and their % inhibition of the FVIIIa activity *in vitro*

	Analogs of the sequence 558-565 of the FVIIIa	% Inhibition of the FVIIIa activity
	rFVIIIa	35.90%
1.	Gly^{563}-**Asn^{564}**-Gln^{565}-OH	9.47%
2.	Arg^{562}-Gly^{563}-**Asn^{564}**-Gln^{565}-OH	10.79%
3.	Gln^{561}-Arg^{562}-Gly^{563}-**Asn^{564}**-Gln^{565}-OH	10.11%
4.	Asp^{560}-Gln^{561}-Arg^{562}-Gly^{563}-**Asn^{564}**-Gln^{565}-OH	10.13%
5.	Ser^{558}-Val^{559}-Asp^{560}-Gln^{561}-Arg^{562}-Gly^{563}-**Asn^{564}**-Gln^{565}-OH	10.72%
6.	Gly^{563}-**Asp^{564}**-Gln^{565}-OH	13.33%
7.	Arg^{562}-Gly^{563}-**Asp^{564}**-Gln^{565}-OH	9.89%
8.	Gln^{561}-Arg^{562}-Gly^{563}-**Asp^{564}**-Gln^{565}-OH	8.84%
9.	Asp^{560}-Gln^{561}-Arg^{562}-Gly^{563}-**Asp^{564}**-Gln^{565}-OH	11.10%
10.	Ser^{558}-Val^{559}-Asp^{560}-Gln^{561}-Arg^{562}-Gly^{563}-**Asp^{564}**-Gln^{565}-OH	12.15%
11.	**Cyclo**(-Ser^{558}-Val^{559}-Asp^{560}-Gln^{561}-**Lys^{562}**-Gly^{563}-**Asp^{564}**Gln^{565})	8.37%
12.	**Cyclo** (-Ser^{558}-Val^{559}-Asp^{560}-Gln^{561}-Arg^{562}-Gly^{563}-**Glu^{564}**-Gln^{565})	10.51%

Also, we synthesized cyclic analogs containing Asp (No 11) or Glu (No 12) instead of $Asn^{564}$and Lys instead of Arg^{562}(No 11). All the compounds are purified (RP-HPLC) and identified (ESI-MS).

Biological Assays

The synthesized peptide analogs were investigated for their inhibitory activity and tested for clotting deficiency by measuring the reduction of the %-value of the FVIIIa that they generate in samples containing recombinant FVIIIa *in vitro*[5] The above results show clearly that smaller peptides like No 1 and No 8, or cyclic ones like No 11, are more active than the natural peptides No 5 and No 10 in reduction of the %-value of the rFVIIIa. Other biological assays of the analogs concerning their clotting deficiency are under investigation.

Acknowledgements

This Research Project is co-financed: 80% by European Union – European Social Fund and 20% by General Secretary of Research & Technology (PENED 03ED569).

References

1. Fay P, Jenkins V. *Blood Reviews* **19**: 15-27, 2005.
2. Obergfell A, Sturm A, Speer C, Walter U, Grossmann R. *Platelets* **17**: 448-453, 2006.
3. Shen BW, Spiegel PC, Chang CH, Huh JW, Lee JS, Kim J, Kim YH, Stoddard BL. *Blood* **111**: 1240-1247, 2008.
4. Bajaj SP, Schmidt AE, Mathur A, Padmanabhan K, Zhong D, Mastri M, Fay PJ. *J Biol Chem* **276**: 16302-16309, 2001.
5. Stoilova-McPhie S, Villoutreix BO, Mertens K, Kemball-Cook G, Holzenburg A. *Blood* **99**: 1215-1222, 2002.

2-23-204

Effect of 4-*R*-Hydroxy-L-proline (Hyp) on peptide conformation and SH3 affinity

Ruzza, Paolo[1,]; Siligardi, Giuliano[2]; Hussain, Rohanah[2]; Calderan, Andrea[1]; Guiotto, Andrea[1]; Biondi, Barbara[1]; Cesaro, Luca[3]; Donella-Deana, Arianna[3]*

[1]CNR - Institute of Biomolecular Chemistry, ITALY; [2]Diamond Light Source, UNITED KINGDOM; [3]University of Padova, Department of Biological Chemistry, ITALY

[*]E-mail: paolo.ruzza@unipd.it

Introduction

Short proline-rich peptides interact with SH3 domains, exhibiting little or no secondary structure before their binding to the cognate protein-targets. Under these conditions the binding process of a proline-rich peptide with the SH3 domain shows unfavorable binding entropy, likely resulting from a loss of rotational freedom on the formation of the PPII helix. With the aim of stabilizing the PPII helix conformation in SH3 binding motifs we have previously replaced the proline residues of the HPK1 proline-rich decapeptide, PPPLPPKPKF (**P2**), either with 4-*R*- or 4-*S*-fluoro-L-proline at different *i, i+3* positions.[1] The interactions of the fluoroproline-peptides with the SH3 domain of cortactin ($SH3_{cort}$) protein were analyzed quantitatively by Non-Immobilized Ligand Interactions Assay by Circular Dichroism (NILIA-CD), whereas CD thermal transitions were measured to correlate their propensity to adopt PPII helix with their affinity for SH3. Results show that the presence of the 4-*R*-fluoroproline residue stabilizes the PPII helix conformation of the peptides in a position-dependent manner, however the induction of a stable peptide conformation does not increase the ligand affinity towards the SH3 domain of cortactin.[1] With the intention of analyzing the effect of the nature of the electron-withdrawing substituent at the 4-position in the proline residue, we replaced the 4-*R*-fluoroproline (Fp) residues by the natural amino acid 4-*R*-hydroxy-proline (Hyp). The interaction with the $SH3_{cort}$ domain, as well as the capability to adopt a PPII-like helix conformation of this new class of peptides were then studied by CD spectroscopy.

Results and Discussion

Peptides were synthesized by manual solid-phase method using Fmoc/HBTU chemistry in 0.05 mmolar scales. Cleavage from the resin and side-chain deprotection were performed by treatment with TFA in presence of anisole-TIS-H_2O as scavengers (95:2.5:2.0:0.5 v/v). Peptides were purified by preparative RP-HPLC and their molecular weight was determined by ESI-MS on a Mariner mass spectrometer instrument.

The interaction of **P2** analogues with the recombinant GST-$SH3_{cort}$ fusion protein was analyzed by NILIA-CD techniques in 20 mM Tris-HCl buffer, pH 7.5, at 20 °C. The binding was monitored by the CD changes of the Trp side-chain of the recombinant protein upon peptide addition. The dissociation constants K_d were determined analyzing the CD data at 294 nm using a non-linear regression method (Table 1).[2] Unexpectedly, the peptides containing two or three Hyp residues (**Hyp-2** and **Hyp-3**) are characterized by K_d values comparable to that displayed by the parent peptide **P2** and lower than that exhibited by the corresponding Fp-peptides (**Fp-2** and **Fp-3**).

In buffer solution, the CD peptide spectra show that, by lowering the temperature, a positive band at about 225 nm is emerging (Fig. 1), consistent with an increased PPII contribution. In addition, an isosbetic point at about 210 nm is present. This is indicative of an equilibrium between two forms: the PPII helix and an irregular conformation. Surprisingly, the peptides containing Hyp residues show an higher propensity to adopt an ordered PPII helix conformation than the corresponding Fp containing

Table 1. Effect of Hyp and Fp residues on the binding to GST-$SH3_{cort}$ protein

Peptide	*Sequence*	K_d (μM)
P2	H-Pro-Pro-Pro-Leu-Pro-Pro-Lys-Pro-Lys-Phe-OH	2.5±1.3
Hyp-2	H-Pro-Pro-**Hyp**-Leu-Pro-**Hyp**-Lys-Pro-Lys-Phe-OH	2.6±0.7
Hyp-3	H-Pro-**Hyp**-Pro-Leu-**Hyp**-Pro-Lys-**Hyp**-Lys-Phe-OH	2.9±0.4
Hyp-5	H-Pro-**Hyp**-**Hyp**-Leu-**Hyp**-**Hyp**-Lys-**Hyp**-Lys-Phe-OH	13.2±1.0
Fp-2	H-Pro-Pro-**Fp**-Leu-Pro-**Fp**-Lys-Pro-Lys-Phe-OH	8.1±1.8
Fp-3	H-Pro-**Fp**-Pro-Leu-**Fp**-Pro-Lys-**Fp**-Lys-Phe-OH	8.3±1.6
Fp-5	H-Pro-**Fp**-**Fp**-Leu-**Fp**-**Fp**-Lys-**Fp**-Lys-Phe-OH	6.6±2.0

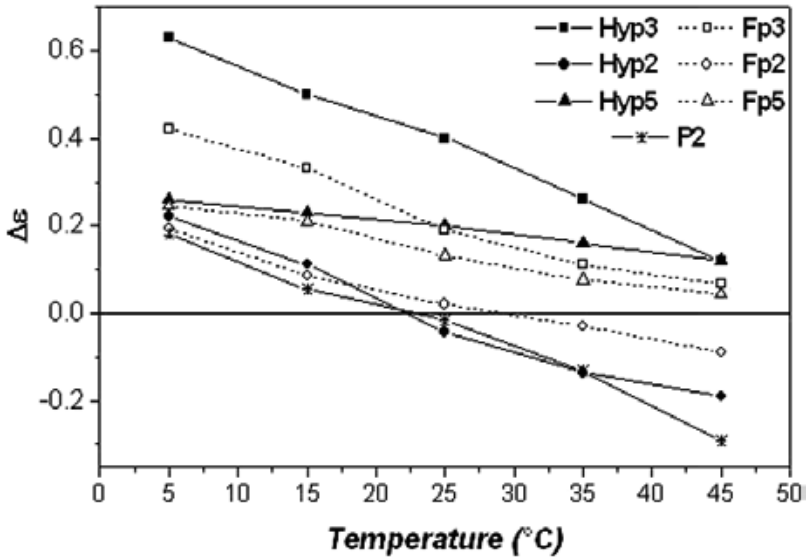

Figure 1. Thermal transition curves of Hyp-, Fp- and P2 peptides.

peptides in contrast to the reported effect involving the electron-withdrawing ability of the substituent in the 4 position of the proline ring to stabilize the pucker of a pyrrolidine ring.

These results provide two different conclusions: the replacement of Pro residues by Hyp into an SH3 binding sequence stabilizes the PPII-like conformation with more ability than the corresponding fluoro-derivative; the effect of Hyp residues on the stabilization of peptide conformation is not sufficient to increase its binding affinity, however it is less detrimental than that of the corresponding fluoro analogues, suggesting that the interaction of the Pro-rich peptides with the SH3 domain is the result of a delicate balance of mutually compensating contributions and that different factors play a role in the binding energetics.

Acknowledgements

Contract grant sponsor: National Research Council of Italy.

References

1. Ruzza P, Rubini C, Siligardi G, Hussain R, Calderan A, Guiotto A, Cesaro L, Brunati AM, Donella-Deana A. Effect of 4-fluoro-L-proline on the SH3 binding affinity. *Biopolymers (Peptide Science)* **88**: 558, 2007.
2. Siligardi G, Hussain R. Biomolecules interactions and competitions by non-immobilised ligand interaction assay by circular dichroism. *Enantiomer* **3**: 77-85, 1998.
3. Eberhardt ES, Panasik N & Raines RT. Inductive effects on the energetics of prolyl peptide bond isomerization: Implications for collagen folding and stability. *J Am Chem Soc* **118**: 12261-12266, 1996.

2-23-205

Binding of Peptides to GPCRs – A Molecular Docking Approach with PSO@Autodock

Namasivayam, Vigneshwaran; Schild, Enrico; Günther, Robert; Beck-Sickinger, Annette G.*

Faculty of BioSciences, Pharmacy and Psychology, University of Leipzig, Institute of Biochemistry, GERMANY

E-mail: {vignesh, robguent}@uni-leipzig.de

Introduction

GPCRs are seven transmembrane domain proteins responsible for signal transduction. They represent one of the largest family of proteins in the human genome and are targets for more than 30% of the drugs currently on the market. Hence, understanding the binding mechanisms of these receptors facilitate the development of novel inhibitors. However, the vast majority of endogenous ligands of these receptors are peptides. In the post-genomic era, molecular docking techniques are becoming more and more popular to investigate binding interaction of ligands to their receptors, provided, the 3D-structure or a reliable model of the protein is known. However, current molecular docking tools have only limited capabilities to handle highly flexible molecules like peptides. Recently, we developed the molecular docking program PSO@Autodock[1] in the framework of AutoDock3[2] for efficient docking of highly flexible ligands to proteins.[1,3] It employs our novel *velocity adaptive and regenerative Constriction Particle Swarm Optimization with local search* (*var*CPSO-ls) algorithm, which requires less than 10% of computing time for the correct prediction of the a peptide-protein complex in comparison to standard docking protocols.[1] Furthermore, an undecapeptide LF20 (KKVYPYPMEPT) with 38 rotatable bonds was successfully docked on the complex structure of Lethal Factor of anthrax (1pww.pdb) with an RMSD value of 1.98 Å, which clearly shows the reliability of PSO@Autodock for docking peptides to proteins.[4]

Here, we employ PSO@Autodock to investigate the binding mode of peptides to the human ghrelin receptor (hGHS). This receptor is involved in growth hormone release and controls food intake and energy expenditure. Recently, an experimental study has determined the substance P derivative rPKPfQwFwLL-NH_2 (small letters indicate D-amino acids) as a potent inverse agonist.[5] Additionally, the N-terminal-amidated Peptide wFwLL-NH_2 has been identified as the core essential for binding to the hGHS receptor. Furthermore, hexapeptides bearing this core peptide act either as inverse agonists or agonists depending on the N-terminal residue: while the peptide with a Lysine is an inverse agonist, that with Alanine is an agonist of the hGHS receptor. To shed light on the underlying mechanism, we performed docking studies employing PSO@Autodock with full flexible treatment of the peptides rPKPfQwFwLL-NH_2, KwFwLL-NH_2 and AwFwLL-NH_2.

Data Preparation and Methods

The molecular docking studies were performed on the theoretical model of hGHS-R1a.[6] For PSO@Autodock, the protein and peptide molecules were prepared using AutoDockTools as described.[1] A grid box of 33.75 Å length was defined around the proposed binding site predicted by the SiteFinder module of MOE 2007.09 (CCG Inc., Montreal, Canada). 50 independents docking runs were performed with a termination criterion of 500,000 evaluation steps with PSO@Autodock. The other parameters were set to the default values.[1]

Docking study on GPCRs

Initially, the substance P derivative rPKPfQwFwLL-NH_2 was docked on the hGHS receptor. The docking results show, that this undecapeptide binds with the N-terminus

Table 1. Comparison of predicted binding energies and measured[5] binding affinities of the investigated peptides with hGHS

Peptide	ΔEbind (kcal/mol)	IC50 - Binding (nM)	Action in hGHS
KwFwLL-NH_2	-25.95	13 ± 2	Inverse agonist
AwFwLL-NH_2	-19.71	53 ± 17	Agonist

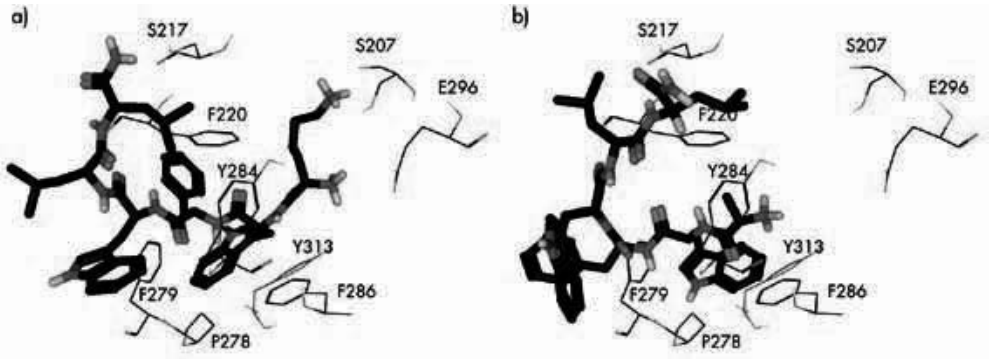

Figure 1. Predicted binding conformation of a) KwFwLL-NH_2 and b) AwFwLL-NH_2 with the important residues of hGHS.

in the binding pocket. The docked conformations of KwFwLL-NH_2 and AwFwLL-NH_2 on hGHS are shown in Fig. 1a and 1b. Both the hexapeptides bind with the N-terminus to the protein similar to the substance P derivative. Furthermore, the core region of the peptide (wFw) is predicted to bind in a hydrophobic region of the pocket formed by the residues F220, F278, Y284, F286 and Y313. The positively charged side chain of the KwFwLL-NH_2 peptide located near to the negatively charged residue E296 and forms H-bonds to S207. Contrarily, the peptide AwFwLL-NH_2 lacking this charge doesn't show similar interactions with the hGHS protein.

Although the investigated hexapeptides bind differently to the receptor, the predicted binding strength is similar, which is in excellent agreement with experimental data[5] (Table 1). Thus, the variation in the binding mode might be the cause of the different mode of action as agonist or inverse agonist.

Conclusion

PSO@Autodock, a simulation based docking method can be applied for flexible docking of peptides including flexible treatment of the backbone, which is not feasible in other docking programs. The docking study here delivers an explanation for the different action of hexapeptides on hGHS by means of distinct binding modes. The results of this study are in excellent agreement with experimental data[5]. Both peptides KwFwLL-NH_2 and AwFwLL-NH_2 bind with the N-terminus in the proposed binding pocket similar to the substance P derivative rPKPfQwFwLL-NH_2 and interact with the hydrophobic core (wFw) at similar sites. In contrast to the peptide KwFwLL-NH_2, the peptide AwFwLL-NH_2 shows further interactions with the receptor, which might be the course of its inverse agonism to the hGHS receptor.

Acknowledegments

Financial support of SFB 610 of the Deutsche Forschungsgemeinschaft is kindly acknowledged.

References

1. Namasivayam V, Günther R. *Chem Biol & Drug Des* **70:** 475-484, 2007.
2. Morris GM, Goodsell DS, Halliday RS, Hart WE, Belew R, Olson AJ. *J Comp Chem* **19:** 1639-1662, 1998.
3. Namasivayam V, Günther R. Proceedings *From Computational Biophysics to Systems Biology (CBSB07), NIC Series* **36:** 239-241, 2007.
4. Namasivayam V, Günther R. Proceedings *From Computational Biophysics to Systems Biology (CBSB08), NIC Series* **40:** 337-340, 2008.
5. Holst B, Mokrosinski J, Lang M, Brandt E, Nygaard R, Frimurer TM, Beck-Sickinger AG, Schwartz TW. *J Biol Chem* **282:**15799-15811, 2007.
6. Pedretti A, Villa M, Pallavicini M, Valoti E, Vistoli G. *J Med Chem* **49:** 3077-3085, 2006.

2-25-206

Peptides from a Phage Display Library Recognize of Modified Nucleosides of Anticodon Domain of Human tRNA^{Lys3}

Rekowski, Piotr[1,]; Mucha, Piotr[1]; Kozlowska, Anna[1]; Ruczynski, Jaroslaw[1]; Agris, Paul F[2]*

[1]Faculty of Chemistry, University of Gdańsk, POLAND; [2]Department of Molecular and Structural Biochemistry North Carolina State University, Raleigh, UNITED STATES

[*]E-mail: piotr.j.rekowski@wp.pl

Many of functions that RNAs perform in the living cell require it's being recognized by and bound to specific proteins. With some exceptions little is known how RNA-binding proteins specifically interact with its cognate RNAs to form functional complexes. Virtually almost no information about contribution of the natural modified nucleosides to RNA-protein interaction is known. However, studies of tRNA with its many modifications have revealed that tRNA modifications are recognition determinants for some aminoacyl-tRNA synthetases and initiation and elongation factors.[1,2]

Because of the great importance of human tRNA^{Lys3} in reverse transcription of HIV, we decided to find and study peptides that specifically recognize modified nucleosides located in the anticodon domain (ASL^{Lys3}) (Fig. 1). We have demonstrated that 15 (or 16) -aa peptides selected from a random phage display library selectively recognized modified ASL^{Lys3}. An analogue of ASL^{Lys3} having two modified nucleosides s^2U_{34} and ψ_{39} (Fig. 1C) has been used for the selection. Affinity of the selected peptides was characterized by fluorescence quenching of the peptides' tryptophans or tyrosines. Peptides bound ASL analogues in micromolar range and exhibited the highest and similar binding affinity for singly and doubly modified ASL^{Lys3}. Unmodified ASL^{Lys3} was bound a few to several times weaker. This shows importance of s^2U_{34} located in the anticodon loop and a minor role of ψ_{39} located in the stem of ASL. Peptide t^K29 (T^1RQQCQKWTL^{10}WCRTVL^{16}-NH_2 showed the highest affinity ($K_d \approx$ 1 μM) for ASL^{Lys3}- s^2U_{34} compared to unmodified ASL^{Lys3} ($K_d \approx$ 25 μM) (Fig. 2). The highest binding selectivity was observed in the presence of Zn^{2+} ions. Thus, modifications contribute identity elements in peptide recognition of the anticodon domain of human tRNA^{Lys3} and may be a new target of antiretroviral therapy.

Acknowledgements

This work was supported by the Ministry of Science and Higher Education (Poland) grant 1542/B/H03/2007/33.

References

1. Curran JF. In *Modification and Editing of RNA*, Grosjean H, Benne R. (Eds), American Society for Microbiology, Washington DC, pp. 493-516, 1998.
2. Mucha P, Szyk A, Rekowski P, Weiss PA, Agris PF. Anticodon domain methylated nucleosides of yeast tRNA^{Phe} isolation and analyses of tRNA^{Phe} are significant recognition determinants in the binding of phage disply selected peptide. *Biochemistry* **40**: 14191-14199, 2001.

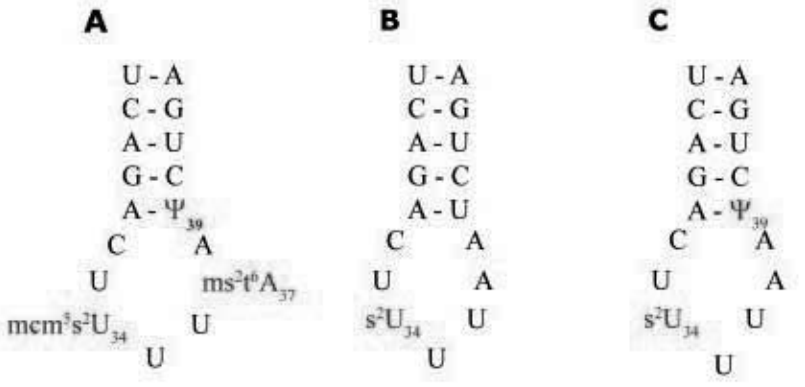

Figure 1. Structure of native (A), singly (B) and doubly modified (C) ASL^{Lys3}. ASL^{Lys3}-s^2U_{34},ψ_{39} (C) was used for peptides selection. Modified nucleosides labels: $mcm^5s^2U_{34}$ - 5-methoxycarbonylmethyl-2-thiouridine, $ms^2t^6A_{37}$ - 2-methylthio-*N*^{6}-threonylcarbamoyladenosine, s^2U_{34} - 2-thiouridine, ψ_{39} – pseudouridine.

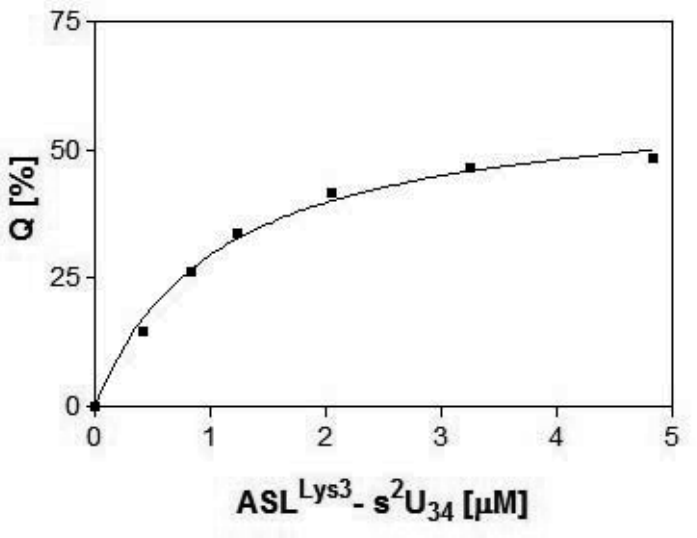

Figure 2. Results of a fluorescence titration of peptide $t^{K}29$ ($T^{1}RQQCQKWTL^{10}WCRTVL^{16}$-$NH_2$) with ASL^{Lys3}-$s^{2}U_{34}$ in the presence of Zn^{2+} ions.

2-25-207

GnRH analogs as carriers for targeted suicide gene delivery

Burov, Sergey[1,]; Yablokova, Tatyana[1]; Dorosh, Marina[1]; Orlov, Sergey[2]; Ignatovich, Irina[2]*

[1]Institute of Macromolecular Compounds RAS, RUSSIAN FEDERATION; [2]Institute of the Experimental Medicine RAMS, RUSSIAN FEDERATION

[*]E-mail: burov@hq.macro.ru

Introduction

Suicide gene therapy represents one of the promising approaches to the cancer treatment. An application of herpes simplex virus thymidine kinase (HSV-TK)/ganciclovir (GCV) system possesses additional advantage due to bystander effect on neighboring cancer cells. So, expression of HSV-TK in 10% of tumor cells in animal models resulted in complete tumor regression after GCV treatment. The efficiency of gene therapy can be additionally improved by the targeting of suicide gene to the cancer cells.

Last years it was shown that GnRH receptors are overexpressed in the most of adenocarcinoma cells in contrast to their low content in normal tissues except for hypophysis.[1] Moreover, there are numerous evidences that GnRH analogues can significantly increase efficiency of suicide gene therapy both *in vitro* and *in vivo*.[2] These data along with peculiarities of signal transduction in tumor cells are in favour of GnRH analogues application as carriers in suicide gene delivery systems.

Results and discussion

Considering that "classical" GnRH analogues have no ability interact with DNA, it was necessary to incorporate DNA-binding moiety into the structure of peptide carrier. Preliminary experiments demonstrated that apart from other cationic peptides (K_8 3, Tat (47-57) and NLS-2) only NLS from large antigen of SV40 (VIII) formed complex with DNA lacking the ability penetrate cellular membrane by the endocytic pathway. Previously it was shown that after cytoplasmic injection, this complex retain capability to reach cell nucleus.[4]

GnRH analogues, containing NLS were synthesized using combination of Boc- and Fmoc-chemistry. Depending on peptide structure (agonist or antagonist) NLS was attached via position 6 or 1 of the natural molecule.

The competition experiments with powerful GnRH agonist "alarelin" demonstrated that internalization of DNA complexes with synthesized peptide carriers is mediated by specific receptor binding. Transfection

Control peptides

"Alarelin"	pGlu-His-Trp-Ser-Tyr-D-Ala-Leu-Arg-Pro-NH-CH_2-CH_3	(I)
[D-Lys^6]-GnRH	pGlu-His-Trp-Ser-Tyr-D-Lys-Leu-Arg-Pro-Gly-NH_2	(II)
"K_8"	H-Tyr-Lys-Ala-Lys-Lys-Lys-Lys-Lys-Lys-Lys-Lys-Trp-Lys-OH	(III)
"GTS-1"	H-Gly-Leu-Phe-Glu-Ala-[$(Leu)_2$-Glu]$_2$-Ser-Leu-Trp-Glu-$(Leu)_3$-Glu-Ala-OH	(IV)
"RGDF-K8"	Arg-Gly-Asp-Phe-OH CO-$(CH_2)_3$-CO-Tyr-Lys-Ala-$(Lys)_8$-Trp-Lys-OH	(V)
Tat (47-57)	H-Tyr-Gly-Arg-Lys-Lys-Arg-Arg-Gln-Arg-Arg-Arg-OH	(VI)
"Fluo-Tat"	Fluo-Gly-Gly-Tyr-Gly-Arg-Lys-Lys-Arg-Arg-Gln-Arg-Arg-Arg-OH	(VII)
"NLS"	H-Pro-Lys-Lys-Lys-Arg-Lys-Val-NH_2	(VIII)
"NLS-2"	H-Arg-Arg-Asn-Arg-Arg-Arg-Arg-OH	(IX)

GnRH-based peptide carriers

Pam-D-Lys(NLS)-Pro-Gly-D-Phe-Pro-Ser-Tyr-D-Lys-Leu-Arg-Pro-Gly-NH_2	(X)
Pam-Pro-Gly-D-Phe-Pro-Ser-Tyr-D-Lys(NLS)-Leu-Arg-Pro-Gly-NH_2	(XI)
Pam_2-D-Lys-Pro-Gly-D-Phe-Pro-Ser-Tyr-D-Lys(NLS)-Leu-Arg-Pro-Gly-NH_2	(XII)
H-D-Lys(NLS)-Pro-Gly-D-Phe-Pro-Ser-Tyr-D-Lys-Leu-Arg-Pro-Gly-NH_2	(XIII)
pGlu-His-Trp-Ser-Tyr-D-Lys(NLS)-Leu-Arg-Pro-Gly-NH_2	(XIV)

Figure 1. Structure of peptides, applied in different formats of gene delivery systems.

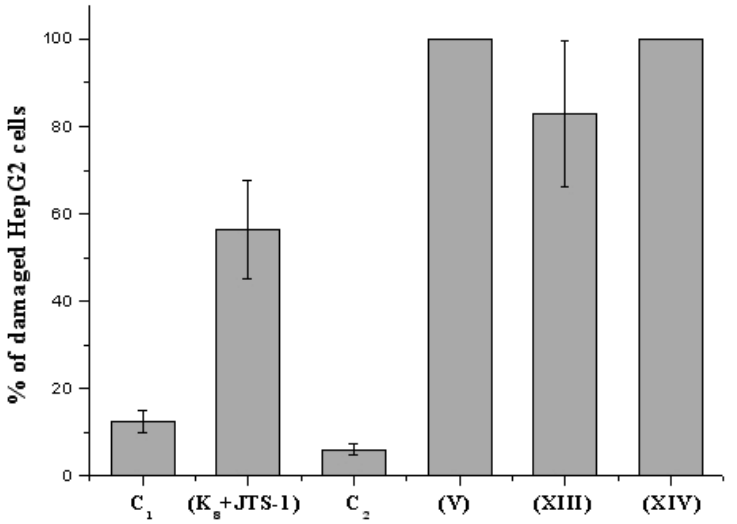

Figure 2. An influence of peptide carrier structure on efficiency of suicide gene therapy *in vitro.*

experiments were performed using plasmides pCMVluc, containing a firefly luciferase coding sequence regulated by human CMV promoter and pST826, containing gene of HSV-1 thymidine kinase. In order to improve selectivity of suicide gene action the last construct includes regulatory region, expressing only in rapidly proliferating cells. The suicide effect of HSV-TK gene was estimated after acyclovir treatment of transfected human HepG2 cells, using luminescent microscopy.

The structure of selected carrier determines the mechanism of peptide/DNA complex penetration via cellular membrane. While complexes of cationic peptides (III), (VI), (VII) and (IX) were internalized by the endocytic pathway, that of NLS (VIII) was unable to pass inside the cells. Addition of peptide (IV), possesses endosomolytic activity,[3] significantly increases transfection efficiency. Complexes of DNA with analogues (V) and (X)-(XIV) were internalized by receptor-mediated endocytosis.

It was shown that application of reference peptide gene delivery system,[3] followed by acyclovir treatment, killed about 50% of cancer cells. Use of cationic peptide, conjugated with RGDF sequence provides high efficiency of treatment, however can not ensure selective action on cancer cells. Nonetheless, similar hybrid structures can represent promising variants of carrier molecules for gene delivery *in vivo*, provided the choice of ligand moiety with high affinity to $\alpha_v\beta_3$ receptors, identified as a marker of angiogenic vascular tissue.

An application of GnRH-based peptide carriers suppressed tumor growth *in vitro* due to specific interaction of peptide/DNA complex with correspondent receptor. The efficiency of suicide gene therapy depended on GnRH analogue structure and was in favor of agonists as compared to antagonists. In contrast to delivery of cytotoxic agents to the cancer cells,[5] peptides (X)-(XII) containing palmitoyl moiety were significantly less effective in transfection experiments as compared to analogues (XIII) and (XIV). Moreover, in the case of compound (XII), peptide/DNA complex possesses cytotoxic activity. These data can reflect specificity of complex structure namely, external position of palmitoyl groups, resulted in damage of cellular membrane.

The best efficiency of tumor cells treatment was obtained using peptide (XIV) as a carrier for suicide gene delivery. Preliminary data of experiments *in vivo* on laboratory animals demonstrated possible practical utility of tested peptides in the course of intravenous administration.

Thus, incorporation of NLS sequence from large antigen of SV40 into the structure of GnRH analogues resulted in new promising peptide carriers, useful for targeted suicide gene delivery to the cancer cells.

References

1. Nechushtan A, Yarkoni S, Marianovsky I, Lorberboum-Galski H. *J Biol Chem*, **272**: 11597-11603, 1997.
2. Gründker C, Nia AH, Emons G. *Mol Cancer Ther* **4**: 225-231, 2005.
3. Gottschalk S, Sparrow JT, Hauer J, Mims MP, Leland FE, Woo SLC, Smith LC. *Gene Ther* **3**: 448-457, 1996.
4. Collas P, Aleström P. *Zebrafish Sci Monitor* **4**: 3, 1996.
5. Burov SV, Iablokova TV, Dorosh MYu, Shkarubskaia ZP, Blank M, Epstein N, Fridkin M. *Bioorg Khim* **32**: 459-466, 2006.

2-28-208

Molecular Modeling of GnRH analogues in DMSO solution using Nuclear Magnetic Resonance (NMR) and Molecular Dynamics (MD)

Laimou, Despina[1]; Mantzourani, Efthimia[1]; Platts, Jamie[2]; Matsoukas, Minos-Timotheos[1]; Troganis, Anastasios[3]; Tselios, Theodore[1,]*

[1]University of Patras, Department of Chemistry, GREECE; [2]Cardiff University, Department of Chemistry, UNITED KINGDOM; [3]University of Ioannina, Department of Biological Applications & Technology, GREECE

[*]E-mail: ttselios@upatras.gr

Introduction

Gonadotropin-Releasing hormone (GnRH) is produced in the hypothalamus under the control of neurotransmitter type compounds[1] and is the central regulator of the reproductive system.[2] GnRH is a decapeptide which interacts with high affinity to the G-protein-coupled receptor (GPCR) on gonadotroph cells through the anterior pituitary gland G-protein-coupled receptor (GPCR) on gonadotroph cells through the anterior pituitary gland, stimulating them to synthesize and release the Luteinizing (LH) and Follicle-Stimulating (FSH) hormones. LH and FSH are responsible for the production of androgens in men, testosterone and dihydrotestosterone (DHT), and estrogens in women. Although the specific role of these steroids is not yet established, the fact that tumors regress as a result of androgen reduction indicates that androgens play a significant role in the development of prostate cancer as well as estrogens for ovarian and breast cancer. For the treatment of sex-hormone-dependent disorders, such as breast and prostate cancer, agonistic GnRH derivatives[3] such as [DLeu[6], NHEt[10]]GnRH (Leuprolide)[4] or [DTrp[6]]GnRH (Triptorelin), as well as antagonists such as the linear decapeptide Cetrorelix (Cetrotide) are clinically and therapeutic valuable.

Leuprolide acetate (pGlu-His-Trp-Ser-Tyr-(D)Leu-Leu-Arg-Pro-NHEt, LPA) is a potent GnRH agonist and is used to treat a wide range of sex hormone related disorders, including prostatic cancer, endometriosis and precosious puberty. Despite its widespread use, only limited information based on spectroscopic evidence regarding the solution conformation of Leuprolide are known.

Results and Discussion

The aim of this study was to characterize the solution conformation of Leuprolide and its modified linear analogue (pGlu-His-Trp-Ser-Tyr(OMe)-(D)Leu-Leu-Arg-Aze-NHEt) in DMSO solution using Nuclear Magnetic Resonance (NMR) and Molecular Dynamics (MD)[5] in order to explore the structural characteristics which are related with its agonistic biological activity. This approach is of value as no crystallographic data is available for the receptor of GnRH. By using both NMR and Molecular Modeling we have characterized the secondary structural preferences of these GnRH analogues Computer calculations were performed on

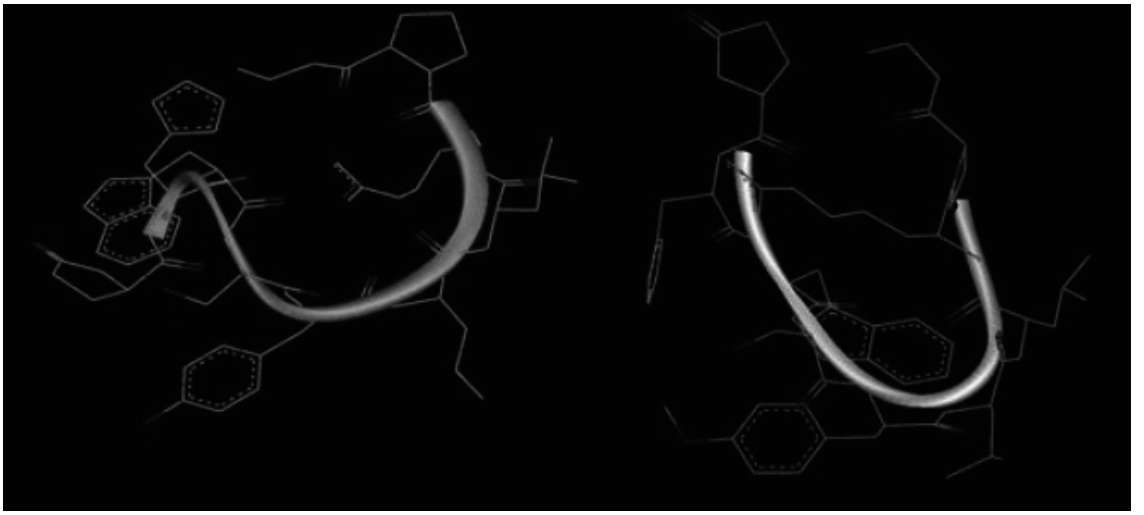

Figure 1. Putative bioactive conformation of Leuprolide and its modified analogue.

a Silicon Graphics O2 workstation using Quanta 2005 and CHARMm force field. Moreover, a Pharmacophore Model was generated by the structural data obtained from NMR and analysis.

In conclusion, the putative bioactive conformations of Leuprolide and its linear modified analogue were compared to the structural characteristics known from the literature. The most important finding is the existence of a type II β-turn[6] in the His^2-Ser^4 segment of Leuprolide and in the Trp^3-$Tyr(OMe)^5$ segment of the modified analogue. Furthermore, there is another bend in the Tyr^5-Arg^8 segment due to a network of hydrogen bonds in which Arg^8 residue participates. This agrees with the U-shape feature adopted by the molecule of Leuprolide when binds to receptor.[7] Pharmacophore Models are revealed indicating the internal distances between the most important for binding and activation of GnRH receptor indole (Trp^3), imidazole (His^2) and guanidine (Arg^8) groups which could be placed to a rigid organic template in order to design and synthesize potent non-peptide analogues.

Acknowledgement

D. Laimou is financial supported by Karatheodoris Grant of University of Patras, Greece.

References

1. Lincoln DW. Gonadotropin-releasing hormone (GnRH): basic physiology. *Endocrinology,* DeGroot LJ *et al* (Eds),WB Saunders Co, Philadelphia, pp. 142-151, 1997.
2. Flanagan CA, Millar RP, Illing N. Advances in understanding gonadotrophin-releasing hormone receptor structure and ligand interactions. *Rev Reprod* **2**: 113-120, 1997.
3. Matsoukas JM, Keramida M. Structure elucidation and conformational analysis of gonadotropin releasing hormone and its novel synthetic analogue [Tyr(OMe)5, DLys6, Aze9NHEt]GnRH: The importance of aromatic clustering in the receptor binding activity. *Eur J Med Chem*, **32**: 927-940, 1997.
4. Meyer JD, Manning MC, Vander Velde DG. Characterization of the solution conformations of leuprolide acetate. *J Pept Res*, **60**: 159-168, 2002.
5. Karplus K, Petsko GA. Molecular dynamics simulations in biology. *Nature* **347**:631-639, 1990.
6. Wilmot CM, Thornton JM. Analysis and prediction of the different types of β-turn in proteins. *J Mol Biol* **203**: 221-232, 1988.
7. Söderhäll JA, Polymeropoulos EE. Antagonist and agonist binding models of the human gonadotropin-releasing hormone receptor, Biochemical and *Biophysical Research Communications* **333** :568-582, 2005.

3-05-001

Cell Adhesive Laminin Peptides for Tissue Engineering

Nomizu, Motoyoshi[1,*]; Otagiri, Dai[2]; Fujimori, Chikara[2]; Hozumi, Kentaro[2]; Kikkawa, Yamato[2]

[1]Tokyo University of Pharmacy and LifeSciences, JAPAN; [2]Tokyo University of Pharmacy and Life Sciences, JAPAN

[*]E-mail: nomizu@ps.toyaku.ac.jp

Introduction

Tissue engineering aims to create functional tissue or organ replacements using various combinations of scaffold materials and cells. Materials provide a support or scaffold for tissue formation. These materials are from either natural resources or chemical products and have little or no biological activity of their own. Consequently, attempts have been made to endow these scaffold materials with biological activity specific for the target organ. Extracellular matrix (ECM) components including laminin, collagen, and fibronectin, and their active peptides are potential candidate for increasing the biological activity and tissue specificity of scaffold materials. Basement membrane, a thin layer of ECM, plays a critical role in tissue regeneration and remodeling. Basememt membrane mimetics are of importance for tissue engineering because of their functions as scaffolds for cells. Laminins are large heterotrimeric glycoproteins, consisting of α, β, and γ chains, and located in the basement membranes of whole bodies like skin, muscle, nerve, kidney, blood vessels, and fat tissues. Laminins play important roles in basement membrane including cell adhesion, migration, proliferation, neurite outgrowth, and angiogenesis. Our goal is to identify cell type-specific sequence from the laminins and to use the biologically active peptides for biomaterials. We have identified various active sequences in the laminins using a systematic screening with more than 2000 synthetic peptides. These peptides are recognized various cellular receptors and have the potential ability to serve as biomaterials for tissue engineering. Previously, we have demonstrated that several laminin active peptide-conjugated chitosan membranes enhanced the biological activity and promoted cell adhesion in a cell-type specific manner.[1,2] Here, we demonstrate that a most active laminin peptide (AG73: RKRLQVQLSIRT)[3]-conjugated chitosan membrane can deliver cells and is applicable for keratinocyte transferring to wound bed.

Results and Discussion

First, we tested whether human keratinocytes would adhere and grow on AG73-chitosan membranes *in vitro*. We found that nearly 80% of the cells were attached to the membranes within 2 h; such rapid cell adhesion is an advantage of the present system. Since keratinocytes fail to bind to the chitosan membrane without peptide, the AG73 peptide sequence plays an essential role in keratinocyte adhesion. Next, we tested whether AG73-chitosan membranes containing keratinocytes could deliver keratinocytes to a wound bed created in mice. The membranes carrying keratinocytes were stable enough for handling with forceps and were inverted so that the side of the membrane with the keratinocytes contacted the muscle fascia exposed on the flanks of nude mice. After 3 or 7 days, the skin flap was reopened and treated wound was examined. The chitosan membranes were easily detached from the fascia, exposing the wound surface. Adjacent to the chitosan membrane, a layer containg leukocytes was observed on both days. Beneath these inflammatory cells were loose fibrous layer containing various connective tissue cells. Sheets or cyst-like spheroids consisting of stratified epithelium were found on the surface of or within the fibrous layer. We then tested the expression of various keratinocyte markers in transplanted cells. An antibody against cytekeratin-1 (sc-17091) clearly reacted on the cytoplasm of both the sheets and spheroids, indicating their keratinocyte origins. Moreover, an antibody against involucrin, which reacted on the granular layer and upper portion of the spinous layer but not the basal layer of epidermis, confirming that transplanted keratinocytes were undergoing cytodifferentitation resembling epidermis. Expression of the laminin-γ2 chain, a specific component of stratified epithelial basement membranes, was seen underneath the keratinocyte layer. These data demonstrate that the transplanted keratinocytes started to differentiate on the wound bed. Recent study revealed syndecan-2 expression in the epidermis of human skin but not epithelial tissues of mouse. Hence, the reactivity of an antibody against syndecan-2 (sc-9492) was tested on mouse and human skin tissues. We found that the syndecan-2 antibody reacted strongly on human epidermis but only faintly on mouse epidermis, indicating the preferential binding of the syndecan-2 antibody to human epidermis. Thus, this antibody was applied to the transplanted keratinocytes to test their origin. The antibody clearly reacted on the stratified keratinocytes on the wound bed, confirming human origin of these cells. There are no reports of using peptide-immobilized materials for the *in vivo* delivery of epithelial cells. These results suggest that the AG73-chitosan membrane is useful as a therapeutic formulation and is applicable as a cell delivery system.[4] Taken together, peptide-chitosan matrix may be a novel and powerful tool for tissue engineering.

References

1. Mochizuki M, Kadoya Y, Wakabayashi Y, Kato K, Okazaki I, Yamada M, Sato T, Sakairi N, Nishi N, Nomizu M. Laminin-1 peptide-conjugated chitosan membranes as a novel approach for cell engineering. *FASEB J* **17**: 867-877, 2003.
2. Mochizuki M, Yamagata N, Philp D, Hozumi K, Watanabe T, Kikkawa Y, Kleinman, HK, Nomizu M. Integrin-Dependent Cell Behavior on ECM Peptide-Conjugated Chitosan Membranes. *Biopolymers* **88**: 122-130, 2007.
3. Suzuki N, Ichikawa N, Kasai S, Yamada M, Nishi N, Morioka H, Yamashita H, Kitagawa Y, Utani A, Hoffman MP, Nomizu M. Syndecan binding sites in the laminin α1chain G domain. *Biochemistry*. **42**: 12625-12633, 2003.
4. Ikemoto S, Mchizuki M, Yamada M, Takeda A, Uchinuma E, Yamashina S, Nomizu M, Kadoya Y. Laminin peptide-conjugated chitosan membrane: Application for keratinocyte delivery in wound skin. J. Biomed. Mater. Res. A. **79**: 716-722, 2006.

3-11-002

Photocurrent generation in peptide-based self-assembled monolayers functionalized with electron transfer antenna chromophores

Gatto, Emanuela[1]; Stella, Lorenzo[1]; Formaggio, Fernando[2]; Toniolo, Claudio[2]; Venanzi, Mariano[1,]*

[1]Department of Chemical Sciences and Technologies, University of Rome "Tor Vergata", 00133 Rome, ITALY; [2]Institute of Biomolecular Chemistry, Padova Unit, CNR, Department of Chemistry, University of Padova, 35131 Padova, ITALY

[*]E-mail: venanzi@uniroma2.it

Introduction

Bio-hybrid devices based on the integration of biological molecules and metal substrates are currently actively explored for potential applications in the areas of molecular recognition, biological sensing, and molecular electronics. Among the biomaterials available, helical peptides have shown peculiar properties in terms of long-range efficiency and directional character of the electron transfer (ET) process. We have recently shown that self-assembled monolayers (SAMs) formed by conformationally-constrained hexapeptides, suitably functionalized with ET antenna chromophores and covalently linked on gold electrodes, are able to generate electronic current upon photoexcitation.[1] We report here on the electrochemical properties and the photocurrent generation efficiency of a series of 3_{10}-helical hexapeptides, primarily formed by Cα-tetrasubstituted residues and covalently linked to gold electrodes through the terminal disulfide of lipoic acid (Lipo). The peptides differ for the antenna chromophore at the C-terminus of the main chain, i.e. an electroactive nitroxide group in SSTOAC and two strongly UV-absorbing chromophores in SSTrp (Trp) and SSPyr (pyrene).

Sequences and acronyms of the peptides investigated:

SSTOAC: Lipo-$(Aib)_3$-Ala-**TOAC**-Ala-OtBu;
SSTrp: Lipo-$(Aib)_3$-Ala-**Trp**-Ala-OtBu;
SSPyr: Lipo-$(Aib)_6$-NH-CH_2-**Pyr**

Results and Discussion

Cyclic voltammetry (CV), ultra-high vacuum scanning tunneling microscopy, and quartz crystal microbalance experiments showed that SSTrp forms a densely-packed self-assembled monolayer on a gold surface. CV experiments confirmed that this is also the case for SSTOAC and SSPyr. Chronoamperometry measurements on SSTOAC demonstrated the directional character of the ET process across the peptide spacer, the rate constant for ET from TOAC to gold being systematically larger than the reverse process. The electrostatic field generated by the lectric dipole associated to the helical chain is responsible for such effect, favoring the ET reaction aligned with it.

This effect is amplified when the antenna chromophores functionalizing SSTrp and SSPyr are photoexcited, giving rise to an electric current, the character of which can be easily switched from anodic to cathodic by simply changing the electron donor (triethanolamine) or acceptor (methylviologen) in the electrochemical cell. A typical example is the cathodic current that the SSPyr SAM generates upon photoexcitation when immersed in a methylviologen (MV^{2+}) solution. The relative action spectrum, i.e. the excitation wavelength dependence of the measured electronic current, and a sketch of the elementary steps of the ET process in the electrochemical cell are reported in Fig. 1. Upon optical excitation of the Pyr antenna, a fast ET from Pyr* to MV^{2+} readily occurs, followed by a slow ET transfer from the gold electrode to the Pyr positive ion through the peptide spacer. This process is strongly affected by the overpotential applied to the work electrode, that, modifying the energy alignment between the Fermi energy level of the gold electrode and the position of the HOMO-LUMO gap of the antenna chromophore, modulates the intensity and, in some cases, even the anodic or cathodic character of the generated current.

Acknowledgement

This project was supported by the Italian Ministry of University and Research (PRIN 2006).

References

1. Gatto E, Stella L, Formaggio F, Toniolo C, Lorenzelli L, Venanzi M. Electroconductive and photocurrent generation properties of self-assembled monolayers formed by functionalized, conformationally-constrained, peptides on gold electrodes. *J Pept Sci* **14**: 184-191, 2008.

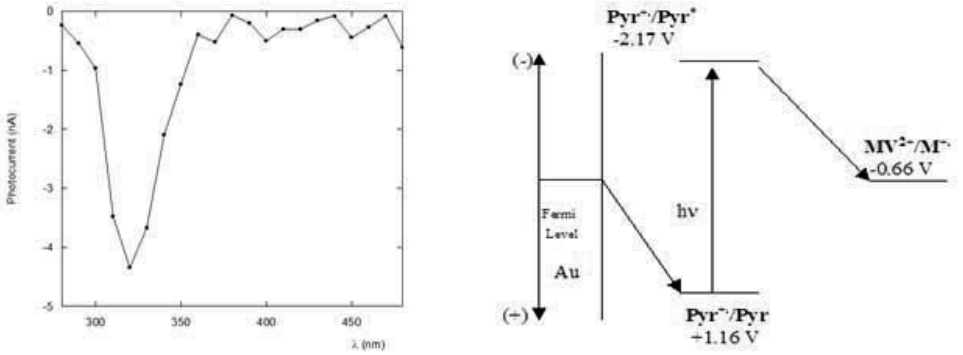

Figure 1. Action spectrum (left) and mechanism (right) of the cathodic photocurrent generation upon photoexcitation of the SAM formed by SSPyr on a gold electrode in a methylviologen solution.

3-13-003

Neoglycopeptides as glycoprobes for lectin-carbohydrate interaction studies by SPR

Jiménez-Castells, Carmen[1]; de la Torre, Beatriz G[1]; Gutiérrez-Gallego, Ricardo[2]; Andreu, David[1,]*

[1]Pompeu Fabra University, Department of Experimental and Health Sciences, SPAIN; [2]IMIM-Hospital del Mar & Pompeu Fabra University, Bioanalysis group & Dept. Exp. and Health Sciences, SPAIN

[*]E-mail: david.andreu@upf.edu

Introduction

Glycan-lectin interactions play a key role in numerous communication processes, such as fertilization, immune response or pathogen anchoring.[1] These, and other recognition processes explain the increasing interest in finding powerful analytical tools to study the mechanisms of these interactions. To study glycan-lectin interactions, surface plasmon resonance (SPR) is a particularly attractive biophysical technique, as it provides both quantitative and qualitative data of the interaction. For interaction studies between lectins and short oligosaccharides, the immobilization of the glycan is preferred. In our group we have designed an immobilization strategy that uses an aminooxy-acetic (Aoa) peptide module (Fig. 1) to which the glycan is conjugated via oxime ligation. The resulting glycopeptide probe is purified and characterized prior to its attachment to the sensor surface.[2]

Here we describe several improvements on the original proof-of-concept design. First, synthesis of the peptide module (**1**) has been optimized, by solving an NH-O over-acylation problem. Boc-Aoa coupling by DIPCDI in combination with short (10 min) reaction times gives a quantitative (97%) formation of **1**, which without further purification can then be conjugated to any glycan **2** with a reducing end.[3]

Secondly, we have explored the applicability of the platform to glycan epitopes containing sialic acid as terminal residue, a very frequent situation in biological contexts. The glycopeptides containing the trisaccharide Neu_5Ac-α-2,6-Gal-β-1,4-GlcNAc and Neu_5Ac-α-2,3-Gal-β-1,4-GlcNAc were synthesized by the general procedure[2], purified by HPLC, characterized by MALDI-TOF MS and tested by SPR against the lectins from *Sambucus nigra* and *Maackia amurensis* (specific for sialyl α-2,6 and α-2,3 linkages, respectively). The results show that the established conditions for oxime ligation and immobilization are compatible with even the most labile sugar residues.

In the third phase of the study, the validity of our glycoprobe for minimal (mono-, disaccharide) sugar epitopes was tested. When these epitopes are ligated to the Aoa-peptide via an oxime function, the glycan unit next to the Aoa results in four different forms (anti, syn, α, β), not all representative of the native situation. We used NMR to determine the relative ratio of the four isomers in the case of a glycoprobe displaying GlcNAc. Well-resolved signals for the anti and syn (oxime) and the β and α anomeric (pyranose) protons were identified and peak integration allowed to determine a 70:30 ratio between the open (anti, syn) and closed (α, β) forms[4]. In this case, the oxime ligation is only 30% effective in displaying the glycan proximal to the peptide core in a cyclic (native-like) conformation. From these data it follows that the sensitivity of the SPR readout for a minimal glycan epitope will be decreased by the under-representation of the native-like cyclic structures in the equilibrium mixture.

A solution to the problem can be found in the work of the Mutter group,[5] who showed that a secondary amine (i.e., *N*-alkylated Aoa) in the ligation reaction imposed a ring conformation in the proximal glycan unit. Accordingly, an *N*(Me)Aoa-peptide module was used in a ligation reaction with GlcNAc and the product was compared, after per-acetylation and MS analysis, to a parallel ligation using the original peptide **1** module. As shown in Fig. 2B (i), the ligation with the Aoa peptide results in two different products, corresponding to the open and closed forms of GlcNAc. In contrast, the ligation with *N*-methylated Aoa peptide (Fig. 2B (ii)) furnishes only one product, corresponding exclusively to the ring form. The existence of only the native-like form in this glycopeptide platform is further corroborated by its much higher SPR response relative to the non-methylated glycopeptide probe when tested against *Erythrina cristagalli agglutinin* (ECA), a lectin with specificity for Gal-β1,4 [Fig. 2C (i,ii)].

In conclusion, we have found satisfactory solutions

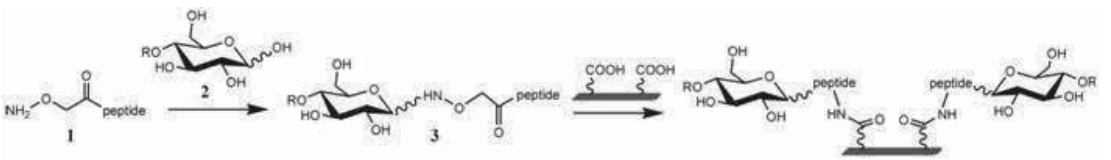

Figure 1. General scheme of glycan-peptide conjugation and surface immobilization via Aoa peptide.

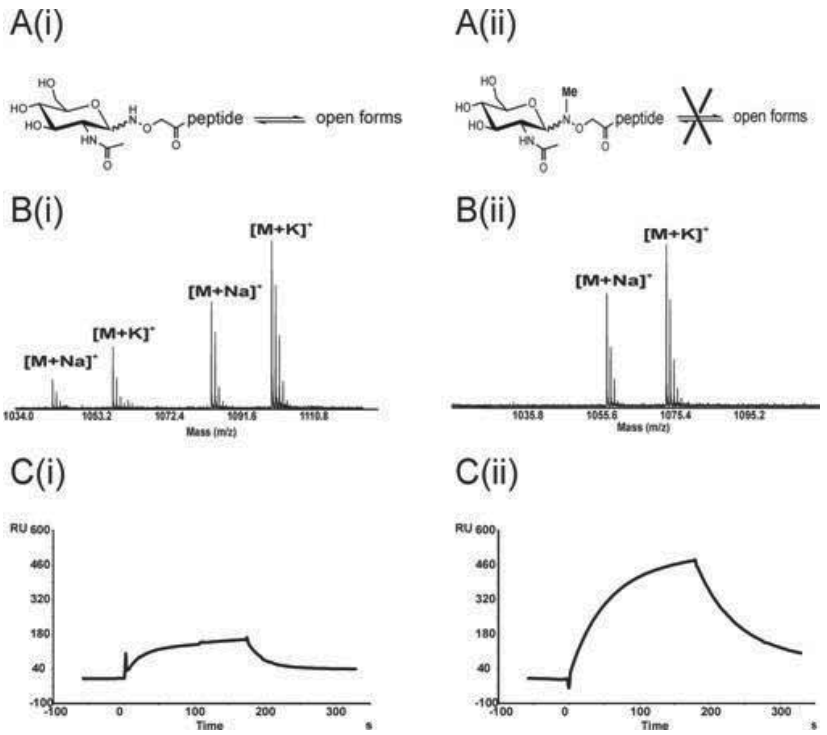

Figure 2. Comparison between the glycoprobe derived from an Aoa peptide (i) and from a *N*(Me)Aoa peptide (ii). A) Scheme of ligation with peptide B) MALDI-TOF MS spectra of their per-acetylated glycopeptides. C) SPR sensorgrams of both glycoprobes displaying the disaccharide Gal-β1,4-GlcNAc against ECA.

to the problems of (i) Aoa overacylation and (ii) low representation of the native-like ring form of the sugar proximal to the peptide when non-methylated Aoa is used. Our neoglycopeptide is shown to be a robust, reliable and versatile platform for sugar display and lectin capture, particularly suited to the study of sugar-protein interactions by SPR methods.

References

1. Gabius, H.G., Siebert, H.C., André, S., Jiménez-Barbero, J., Rüdiger, H. *ChemBioChem* **5:** 740-764, 2004
2. Vila-Perelló, M., Gutiérrez-Gallego, R., Andreu, D. *ChemBioChem* **6:** 1831-1838, 2005
3. Jiménez-Castells, C., de la Torre, B.G., Gutiérrez-Gallego R., Andreu, D. *Bioorg Med Chem Lett* **17:** 5155-5158, 2007
4. Jiménez-Castells, C., de la Torre, B.G., Andreu, D., Gutiérrez-Gallego R. Glycoconj. J. **25**:879-887, 2008
5. Peri, F., Dumy, P., Mutter, M. *Tetrahedron* **54:** 12269-12278, 1998

3-14-004

Involvement of alpha-helix 2 domain in prion protein conformationally-induced diseases

Ronga, Luisa[1]; Palladino, Pasquale[1]; Rossi, Filomena[1]; Pugnière, Martine[2]; Roquet, Françoise[2]; Amblard, Muriel[3]; Martinez, Jean[3]; Benedetti, Ettore[1]

[1]Centro Interuniversitario di Ricerca sui Peptidi Bioattivi, Università degli Studi di Napoli Federico II, ITALY; [2]Centre d'études d'agents Pathogènes Biotechnologies pour la Santé, UMR 5236 CNRS, Universités Montpellier 1 et 2, FRANCE; [3]Institut des Biomolécules Max Mousseron, U.M.R. 5247 CNRS, Universités Montpellier 1 et 2, FRANCE

[1]E-mail: luironga@unina.it

The Transmissible spongiform encephalopathies, also known as prion diseases, are currently classified as conformational diseases. These are disorders in which the native conformation of the protein is reorganized in an abnormal aggregated state.[1] Prion diseases are caused by the conversion of the cellular prion protein into the aggregated and toxic "scrapie" variant (PrP^{Sc}).[2] While the cellular form is characterized by a high alpha helical content, susceptibility to proteolytic digestion and solubility in detergents; the scrapie form is characterized by a prevalent beta-sheet content, resistance to proteolysis and insolubility in detergents. The structure of this protein consists of two distinct domains: an unfolded and flexible N-terminal region and a structured C-globular domain, characterized by the presence of three alpha-helices, two short beta-strands and a disulfide bridge.[3] Despite a large number of studies on PrP^{C}, possible causes of its pathogenic conversion and its role in cellular function still remain unclear. Particularly fascinating is the notion that the protein possesses one or several spots of intrinsic structural flexibility, which might favour conversion into the pathogenic beta-structure. In particular, many characteristics of the peptide fragment 173-195 corresponding to the prion protein helix 2, invariant among various mammalian species, support this hypothesis. First of all, it is able to form amyloid fibrils,[4] it is characterized by an high density of mutations which promote diseases[5] and in addition, it is characterized by a large presence of Thr (^{188}TVTTTT^{193}), beta-branched amino acid, which makes this segment a good candidate to promote a local transition from α to β conformation. Moreover, it has been demonstrated that a very low free-energy separates the α-helical and β-type conformation of this peptide.[6] This evidence denotes the structural ambivalence of helix 2 that could induce local destabilization and concur to protein transformation. Following these arguments, we have investigated the conformational landscape of the human prion protein helix 2 by a comparative study on synthetic peptides derived from this domain. We have demonstrated that a single amino acid replacement in the helix 2 significantly affects the organization of the 173-195 peptide, enhancing the propensity of this region for β-conformation.[7] Furthermore, neurotoxicity assays have shown a link between β-conformation propensity and toxicity.[8,9] We have also demonstrated that the conformational properties of helix 2-derived analogues are affected by pH changes and anion density.[10] It is therefore evident that the intriguing structural properties of the PrP helix 2 make this domain a primary target for therapeutic strategies and a suitable model to rationally design compounds able to block or prevent prion diseases. In this regard, we have synthesized peptide constructs able to interact with the helix 2. The design of these molecules has as a starting point the crystal structure of the complex between an antibody and the sheep PrP which defines the epitope of the antibody that basically consists of the last two turns of the helix 2 of the sheep PrP, which is invariant in the human domain.[11] We have identified the antibody fragments which are able to form hydrogen bonds with the helix 2 C-terminal end in the crystal structure and designed peptide constructs suitable to model this interaction. These peptide constructs were obtained on SynPhase Lanterns[12] linking these two peptide fragments by spacers of different length, rigidity and chemical nature. Subsequently, in order to investigate by fluorescence the affinity of all the Fab constructs for the helix 2 we have functionalized with fluorescein the full length helix 2 peptide. Then we have registered the fluorescence emission spectra of this peptide in the presence of increasing amounts of Fab molecules. The fluorescence intensity decreases as a function of increasing Fab molecules concentration, the fluorescence quenching was then used to evaluate the apparent dissociation constants for each Fab molecule-helix 2 complex. These experiments suggest that all peptide constructs strongly interact with the helix 2-derived fragment ($K_D$values are in the nM range). We have also performed SPR binding experiments with the Prion protein immobilized onto the sensor surface and tested against our peptide constructs and the single Fab peptide sequences. Preliminary results of these SPR experiments with the protein confirm the general trend, initially observed by fluorescence experiments with the helix 2. We have also demonstrated that the affinity of the single peptide fragments is lower compared to that of the entire constructs including the two peptide sequences and the spacer (Fig. 1). In conclusion, we have highlighted the importance of the helix 2 domain as model for rational design compounds able to block or prevent prion diseases and opened interesting perspectives for the use

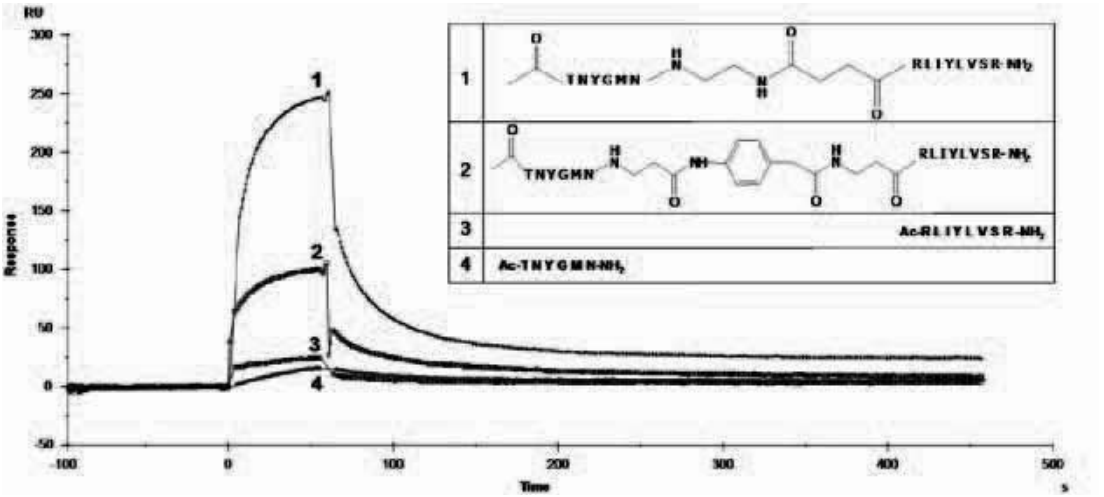

Figure 1. Sensorgrams showing the binding of 1-4 molecules onto immobilized PrP.

of these constructs as therapeutic and diagnostic tools in PrP-associated diseases.

References

1. Temussi PA, Masino L, Pastore A. EMBO J. 22: 355-361, 2003.
2. Prusiner SB. *Proc Natl Acad Sci U S A* **95**: 13363-13383, 1998.
3. Zahn R, Liu A, Lührs T, Riek R, von Schroetter C, López García F, Billeter M, Calzolai L, Wider G, Wüthrich K. *Proc Natl Acad Sci U S A* **97**: 145-150, 2000.
4. Thompson A, White AR, McLean C, Masters CL, Cappai R, Barrow CJ. *J Neurosci Res* **62**: 293-301, 2000.
5. Kuznetsov IB, Rackovsky S. *Protein Sci* **13**: 3230-3244, 2004.
6. Tizzano B, Palladino P, De Capua A, Marasco D, Rossi F, Benedetti E, Pedone C, Ragone R, Ruvo M. *Proteins* **59**: 72-79, 2005.
7. Ronga L, Palladino P, Saviano G, Tancredi T, Benedetti E, Ragone R, Rossi F. *Bioinorg Chem Appl* **10720***:* 1-9, 2007. doi:10.1155/2007/10720
8. Ronga L, Palladino P, Costantini S, Facchiano A, Ruvo M, Benedetti E, Ragone R, Rossi F. *Current Protein & Peptide Science* **8**: 83-90, 2007.
9. Ronga L, Tizzano B, Palladino P, Ragone R, Urso E, Maffia M, Ruvo M, Benedetti E, Rossi F. Chemical Biology & Drug Design 68: 139-147, 2006.
10. Ronga L, Palladino P, Tizzano B, Marasco D, Benedetti E, Ragone R, Rossi F. *J Pept Sci* **12**: 790-795, 2006.
11. Eghiaian F, Grosclaude J, Lesceu S, Debey P, Doublet B, Tréguer E, Rezaei H, Knossow M.*Proc Nat Acad Sci USA* **101**: 10254-10259, 2004.
12. Geysen HM, Meloen RH, Barteling SJ. *Proc Nat Acad Sci USA* **81**: 3998–4002, 1984.

3-15-005

A leptin receptor agonist glycopeptide for leptin replacement therapy

Otvos, Laszlo[1,*]; Cassone, Marco[1]; Wade, John D[2]; Knappe, Daniel[3]; Hoffmann, Ralf[3]; Henry, Belinda[4]; Clarke, Iain[4]; Surmacz, Eva[1]

[1]Temple University, UNITED STATES; [2]Howard Florey Institute, AUSTRALIA; [3]Leipzig University, GERMANY; [4]Monash University, AUSTRALIA

[*]E-mail: otvos@temple.edu

Introduction

Leptin receptor (ObR) modulating biologicals, proteins and peptides, populate the current research literature and clinical trial landscape.[1] However, disadvantageous specificity and pharmacology issues represent a roadblock to the development of leptin agonists for the treatment of various metabolic diseases and leptin antagonists for obesity-related cancer. In the past two years we attempted to provide remedies to these problems by using well-characterized, pharmacologically improved and monofunctional peptide-based therapeutic leads. Inefficient activity of the obesity hormone - leptin in the brain leads to obesity, hyperinsulinemia, and has been linked to infertility, impaired cognitive function, and osteoporosis. Recombinant leptin protein is currently undergoing ten different clinical trials targeting leptin deficiency-related diseases, including lipodystrophy, diet-induced food craving, and hypothalamic amenorrhea. However, many of these trials demonstrated only limited efficacy of the approach.

Results and Discussion

Leptin is produced by adipose tissue and regulates energy balance in the hypothalamus.[2] The existence of disorders related to leptin deficit and leptin overabundance calls for the development of drugs activating or inhibiting the leptin receptor. Most of the earlier studies used full-length native leptin protein or laboratory alanine mutants. The multiple roles that leptin plays in various biological processes suggest that it is not straightforward to obtain true agonists or antagonists that do not change the downstream signaling effect upon varying environmental conditions. Indeed, the emergence of both partial antagonists and weak agonists in the literature may indicate that depending on individual cell context as well as the presence or absence of native, unmodified leptin, the same mutant protein or large subunit can trigger different downstream signaling responses. Thus, their use in human or veterinary therapy might meet regulatory opposition. Our long term goals are to develop full agonist and antagonist peptide ligands of the leptin receptor. Ideally, to antagonize ObR, we envision a short peptide that does not cross the blood-brain barrier (BBB) and is able to inhibit ObR mitogenic signaling in cancer cells with or without native leptin present. On the other hand, to mimic leptin functions under leptin-deficient pathological conditions, we envision a small and monofunctional full agonist possessing BBB penetrating and full signaling abilities in the presence or absence of leptin. To reach our goals, we synthesized individual arms of three proposed bivalent receptor-binding leptin fragments (sites I-III), their reportedly antagonist analogs, and a peptide chimera composed of the two discontinuous site II arms.[3] To assess the pharmacological utility of the leptin fragments, we studied the peptides' ability to stimulate the growth of ObR-positive and ObR-negative cells. The combined site II construct and site III derivatives selectively reversed leptin-induced growth of ObR-positive cells at mid-nanomolar concentrations. However, these peptides appeared to be partial agonists/antagonists as they activated cell growth in the absence of exogenous leptin. Armed with this information, we designed a leptin site III analog that featured non-natural amino acids at terminal positions to decrease proteolysis and a BBB penetration-enhancing carbohydrate moiety. We prepared the peptide both unprotected (E1Free) and protected (E1Ac) forms where the carbohydrate hydroxyl groups were acetylated. E1Free: H-Tyr(I_2)-Ser[β(Glc])-Thr-Glu-Val-Val-Ala-Leu-Ser-Arg-Leu-Dap(Ac)-NH_2, where Dap(Ac) is 2-acetamido-3-amino-propionic acid. E1Free and E1Ac proved to be full agonists to ObR, i.e., stimulated proliferation of different ObR-positive (MCF-7 breast cancer and DU-145 prostate cancer) but not ObR-negative (MCF-10 normal mammary epithelium) cells in the presence or absence of leptin (Fig. 1).

These glycopeptides bound to isolated ObR on solid-phase assays and activated ERK-1/2 signaling in ObR-positive MCF-7 cells at 100 – 150 nM concentrations. The glycopeptides were stable in mouse serum (except the sugar hydroxyl-protecting acetyl groups), readily crossed epithelial/astrocyte cell layers in a blood-brain barrier model, and the free version was distributed into the brain of Balb/c mice after intraperitoneal administration. To prove the proof-of-concept *in vivo*, the efficacy of the free glycopeptide was tested on typical leptin functions in sheep. Voluntary food intake of program-fed animals was reduced by 25% and central infusion increased post-prandial thermogenesis in muscle by 3 degrees C without an effect on core body temperature in summer and winter,

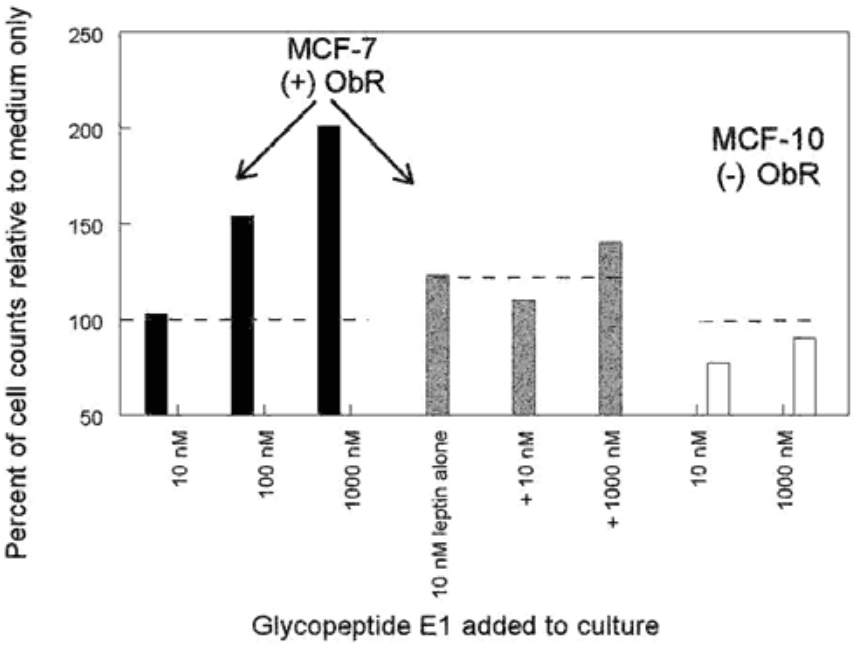

Figure 1. Activity of glycopeptide E1Free on the growth of MCF-7 cells that express the leptin receptor and MCF-10 cells without leptin receptor. MCF-7 cells responded to the peptide with vigorous proliferation regardless whether exogenous leptin protein was present or not, but the growth properties of MCF-10 were not influenced by peptide addition.

but not in the spring season when sheep are resistant to leptin. While this is not the first peptide fragment that reduces appetite *in vivo*,[4] this is the first one that does so by inhibiting ObR. In conclusion, leptin binding site III appears to be suitable for medicinal chemistry manipulations to improve the pharmacological properties of the peptide drug leads. The biological activities and preliminary pharmacological parameters of the site III designer glycopeptides E1Ac and E1Free warrant further studies evaluating their activity in animal models of leptin deficiency or dysfunction. If the sheep data are confirmed in mice, the E1 glycopeptides can proceed further in the drug development process as a therapeutic means in leptin-deficient diseases.

References

1. Lo KM, Zhang J, Sun Y, Morelli B, Lan Y, Lauder S, Brunkhorst B, Webster G, Hallakou-Bozec S, Doare L, Gillies SD. Engineering a pharmacologically superior form of leptin for the treatment of obesity. *Prot Eng Des Sel* **18**: 1-10, 2005.
2. Wauters M, Considine RV, Van Gaal LF. Human leptin: from an adipocyte hormone to an endocrine mediator. *Eur J Endocrinol* **143**: 293-311, 2000.
3. Otvos L, Jr Terrasi M, Cascio S, Cassone M, Abbadessa G, De Pascali F, Knappe D, Stawikowski M, Cudic P, Wade JD, Hoffmann R, Surmacz E. Development of a pharmacologically improved peptide agonist of the leptin receptor. *Biochim Biophys Acta* **1783**: 1745-1754, 2008.
4. Grasso P, Leinung MC, Ingher SP, Lee DL. In vivo effects of leptin-related synthetic peptides on body weight and food intake in female ob/ob mice: Localization of leptin activity to domains between amino acid residues (106-140). *Endocrinology* **138**: 1413-1418, 1997.

3-18-006

Peptide-based immunoassays for biomarkers detection: a challenge for translational research

*Papini, Anna Maria**

Dept. of Organic Chemistry "Ugo Schiff", University of Florence, Interdepartmental Laboratory of Peptide & Protein, ITALY

**E-mail: annamaria.papini@unifi.it*

Introduction

Autoimmune diseases are considered now as a plague. In fact some autoimmune diseases previously considered rare are presently increasing their frequency, possibly because of an earlier diagnosis (e.g. Celiac Disease, Primary Biliary Cirrhosis, etc.). Autoimmune diseases have been considered for a long time to be associated with synergic humoral and cell-mediated immune reactions against one or more of the body's own constituents, even if the role of autoantibodies have been often underscored. This is possibly due to low specific detection assays, such as Indirect Immunofluorescence (IIF) assays or immunoenzymatic assays, e.g. ELISA. It is now accepted that autoantibodies are possibly first actors, thus reliable tests are necessary not only for an early diagnosis and for monitoring disease activity, but also for setting up personalized therapeutic treatments. We started very early to focus our attention on the development of specific autoantibody detection methods on patients'sera, to be used to guide the clinical management of certain autoimmune diseases.[1] It is more and more evident that one single biomarker is not sufficient to set up successful diagnostic and prognostic tools for autoimmune diseases.[2] Different types of autoreactive epitopes can coexist in protein antigens. Using epitope mapping approaches, the epitope on a large polypeptide autoantigen can be narrowed down to small synthetic peptide antigens. Depending on the type of epitope, the peptide may have different clinically relevant features. For example, it can be of prognostic value, it may correlate with disease activity or specific symptoms, and the course of the disease.[3]

Results and Discussion

The hypothesis we have been investigating for years is that in autoimmunity aberrant post-translational modifications (PTMs), i.e. glycosylation, deimination etc., may affect the immunogenicity of self-protein antigens and create neoantigens triggering autoantibodies. This could explain why proteins (both recombinant and isolated), components of target organs or tissues may limit specificity in autoantibody detection. Therefore, synthetic peptides specifically modified (with sugars, citrulline, lipophilic moieties, etc.) are interesting tools to fishing out autoantibodies in patients'sera as disease biomarkers. We have recently proposed a strategy defined "Chemical Reverse Approach".[4] This approach is based on the selection of the optimal Synthetic Antigen Peptides (SAP) guided by autoantibodies circulating in blood. Autoantibody recognition drives selection and optimisation of the best "chemical structure" SAP from defined PTM-peptide libraries. A "Chemical Reverse Approach" can be successfully applied for the development of specific non-invasive diagnostic/ prognostic assays of autoimmune diseases. The SAP is a peptide sequence exposing at the best on the tip of a β-turn structure the epitope (linear or conformational) including specific PTMs selected for optimal autoantibody recognition in patients' sera. The use of synthetic peptides chemically modified by the introduction of specific PTMs can overcome the limitations occurring with recombinant proteins or protein extracts. Moreover, using peptides as SAPs, it is possible to stabilize the bioactive conformational epitope and to assure unique and consistent antigens by efficient synthetic protocols.

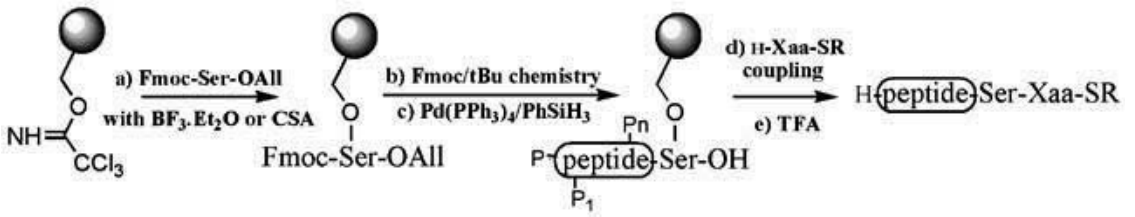

Figure 1.

Characterisation of biomarkers of disease activity can be achieved through immunochemistry studies using conventional assays and innovative techniques based on biosensor or electrochemical devices. Peptide-based immunoenzymatic assays can be translated into different analytical diagnostic platforms (i.e. multiplex, etc.) for efficient detection of autoantibodies as biomarkers of a specific autoimmune disease. Among post and co-traslational modifications, glycosylation plays a crucial role in the immune response. It is interesting to observe that the introduction of precise chemical modifications on side chains of amino acids enables the production of modified molecules mimicking neo-antigens more accurately than recombinant proteins or protein extracts. We successfully applied the "Chemical Reverse Approach" for the development of CSF114(Glc), the first Multiple Sclerosis Antigenic Probe (MSAP). This N-glucosylated peptide is characterized by a type I' β-turn structure exposing at the best the minimal epitope Asn(β-Glc) fundamental for autoantibody recognition in MS.[5] Autoantibody recognition by MS PepKit, the CSF114(Glc)-based ELISA as diagnostic for MS was improved by [Pro7,Asn8(Glc),Thr10]CSF114, which is characterized by a type I β-turn around the minimal epitope Asn(Glc).[6] Sensitivity of MS PepKit detection, is possible by new electrochemical biosensors based on CSF114(Glc) analogues. Preliminary results were obtained by using "Electrochemical labeled modified CSF114(Glc) in Cyclic Voltammetry.[7] An extensive application of our SAP concept was undertaken in the case of Rheumatoid Arthritis by deimination and/or galactosylation[8] or for investigating Primary Biliary Cirrhosis (PBC), by lipoamidation. Lys(Lipoamide) was introduced on the tip of several β-turn structures as peptidomimetics of possible native antigens involved in PBC. Antibody recognition in PBC sera of the protein autoantigen of PDC-E2 used up to now in ELISA, PDH and of its lipoamide modified native β-turn fragment PDH(44-63) were compared with our lipoamide SAPs, as irrelevant β-turn structures.

References

1. Mazzucco S, Matà S,Vergelli M, Fioresi R, Nardi E, Mazzanti B, Chelli M, Lolli F, Ginanneschi M, Pinto F, Massacesi L, Papini AM. *Bioorg Med Chem Lett* **9**: 167-172, 1999.
2. Lolli F, Rovero P, Chelli M, Papini AM. *Expert Rev Neurotherapeutics* **6**: 781-794, 2006.
3. Kessenbrock K, Raijmakers R, Fritzler MJ, Mahler M. *Curr Med Chem* **14**: 2831-2838, 2007.
4. Alcaro M.C. *et al*. *Chemistry Today* **25**: 14, 2007.
5. (a) Papini AM. *Nat Med* **11**: 13, 2005;
   (b) Lolli F, Mulinacci B, Carotenuto A, Bonetti B, Sabatino G, Mazzanti B, D'Ursi AM, Novellino E, Pazzagli M, Lovato L, Alcaro MC, Peroni E, Pozo-Carrero MC,Nuti F, Battistini L, Borsellino G, Chelli M, Rovero P, Papini AM.*Proc Nat Acad Sci USA* **102**: 10273-10278, 2005;
   (c) Lolli F, Mazzanti B, Pazzagli M, Peroni E, Alcaro MC, Sabatino G, Lanzillo R, Brescia Morra V, Santoro L, Gasperini C, Galgani S, D'Elios MM, Zipoli V, Sotgiu S, Pugliatti M, Rovero P, Chelli M, Papini AM. *J Neuroimmunol* **167**: 131-137, 2005.
6. Carotenuto A, Alcaro MC, Saviello MR, Peroni E, Nuti F, Papini AM, Novellino E, Rovero P. *J Med Chem* **51**: 5304, 2008.
7. Real-Fernández F, Colson A, Bayardon J, Nuti F, Peroni E, Meunier-Prest R, Lolli F, Chelli M, Darcel C, Jugé S, Papini AM. *Biopolymers*: *Peptide Science* **90**: 488-495, 2008; *8EP Application 07118566.4*. "Galactosylated peptides, their preparation and use in autoimmune disease diagnosis". Filing date 16/10/2007.

3-18-007

Synthesis and Evaluation of RGD Peptide Analogs Cyclized by Coordination of Oxorhenium and Oxotechnetium Cores for Molecular Imaging of Cancer

*Aufort, Marie; Gonera, Marta; Dubs, Pascaline; Czarny, Bertrand; Thai, Robert; Le Clainche, Loïc; Masella, Michel; Servent, Denis; Dugave, Christophe**

CEA/Saclay/iBiTecS, SIMOPRO, bâtiment 152, FRANCE

**E-mail: christophe.dugave@cea.fr*

Integrins form a family of integral proteins that are involved in cell-cell and cell-matrix adhesion and play an important role in tumor neoangiogenesis, cancer progression and dissemination.[1] Among 25 integrins, 10 bind to RGD sequences and 8 of them are implicated in various cancers. In many cases, integrin overexpression is related to cancer severity and propensity to metastatic processes.[2] Therefore, integrins are interesting targets for the development of anti-neoangiogenic agents such as cilengitide, a RGD cyclopentapeptide which selectively binds integrin $\alpha_V\beta_3$ and has reached phase III clinical trial for the treatment of cancer.[3] Several other tracers, mainly based on the c(RGDfV) peptide,[4] and bearing an exocyclic radiolabel, have been reported in the literature, and some of them have been tested clinically.[5] *In vivo*, most of these compounds display relatively low tumor accumulation as well as side labeling of others tissues that are mainly due to fair metabolic stability and moderate selectivities.

We investigated a new strategy that enables the development of libraries of RGD cyclopeptides with original structures and properties. These peptides of general formula NS_2-X1-X2-X3-R (where X1-X2-X3 is a RGD analog) were cyclized through oxorhenium/oxotechnetium coordination by an NS_2/S motif. Metal coordination was anticipated to give a mixture of up to 4 diastereomers resulting from the particular arrangement of the modified peptide around the metal core.[6]

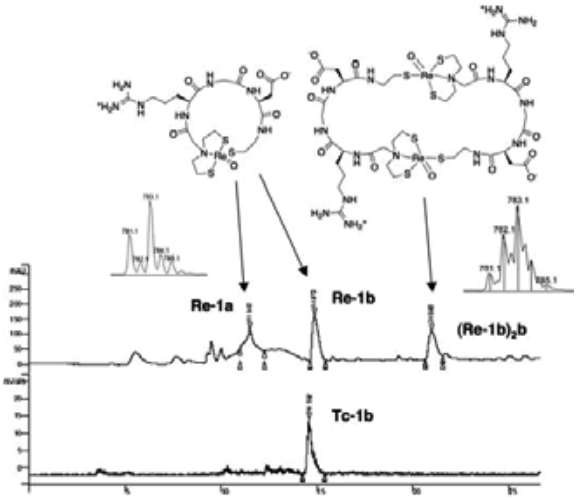

Figure 1

In a preliminary study, peptide **1** containing a RGD sequence along with a 2-aminoethanethiol linker (Fig. 1) was prepared from a (Fmoc-Asp(PEG-PS)-OAllyl) resin as previously reported. Coupling of the N-bis(thioethyl) glycinate at the N-terminus of the peptide was performed using HATU while trityl-thioethyl-2-amine was grafted at the C-terminus after deprotection of the allyl-ester using tetrakis(triphenylphosphine)palladium. Metallation of the purified peptide using tetrabutylammonium tetrachlorooxorhenate gave the corresponding cyclic oxorhenium coordinate **Re-1** which was isolated as a mixture of 2 diastereomeric monomers **Re-1a** and **Re-1b** and 2 dimers (Fig. 1) **$(Re\text{-}1a)_2$** and **$(Re\text{-}1b)_2$**.

Both monomers and one dimer **$(Re\text{-}1b)_2$** were isolated by RP-HPLC and tested as ligands of integrin $\alpha_V\beta_3$ using the standard [^{125}I]iodoechistatin binding assay. **Re-1b** displays the most promising activity (IC_{50} = 86 nM) whereas it binds integrin $\alpha_{IIb}\beta_3$ with a lower affinity (IC_{50} = 1.12 μM) (Table 1). Isomer **Re-1a** and dimer **$(Re\text{-}1b)_2$** have higher IC_{50} values.

Studies of stability of the oxorhenium coordinates in a PBS buffer pH 7.4 showed that complex **Re-1b** is stable for several hours. Conversely, isomer **Re-1a** and dimer **$(Re\text{-}1b)_2$** tend to isomerize to give isomer **Re-1b**. This result suggests that the apparent affinity of these compounds for integrin $\alpha_V\beta_3$ might be essentially related to the formation of isomer **Re-1b** in buffer.

Ab initio calculation, using a polarizable force field and molecular dynamics in a box containing 4000 molecules of water and performed for 10 ns at 300 K, suggested that the distance between the Arg and Asp *β*-methylene moieties are about 6-7 ngström, a distance which is equivalent to that observed in c(RGDfV) peptides.[7,8] This result might account for the specific binding of the oxorhenium coordinate to integrin $\alpha_V\beta_3$.

We prepared a library of 64 peptides NS_2-X1-X2-X3-R (X1 = D/L-Arg; X2 = Gly or βAla; X3 = D/L-Asp/Glu) with R is either 2-aminoethanethiol, 3-aminopropanethiol, 3- or 4-aminothiophenol by parallel peptide synthesis starting from the corresponding thiol-grafted trityl resin. Complexation of the oxorhenium core as described above afforded 48 complexes since 4-aminothiophenol coordinates were difficult to obtain. All compounds were screened towards integrin $\alpha_V\beta_3$ and 4 other compounds

Table 1

IC_{50} (nM ± SD, n = 3)

Initial compds	Products of isomerization	αVβ3	αIIbβ3
c(RGDyV)	-	67 ± 35	675 ± 60
1	$(\mathbf{1})_2$ (100%)	360 ± 220	930 ± 85
Re-1a	**Re-1b** (5%)	930 ± 65	3270 ± 440
Re-1b	Not observed	**86 ± 26**	1120 ± 365
$(\mathbf{Re\text{-}1})_2$**b**	**Re-1a** (traces) + **Re-1b** (25%) + $(\mathbf{Re\text{-}1})_2$**a** (20%)	210 ± 70	4500 ± 430

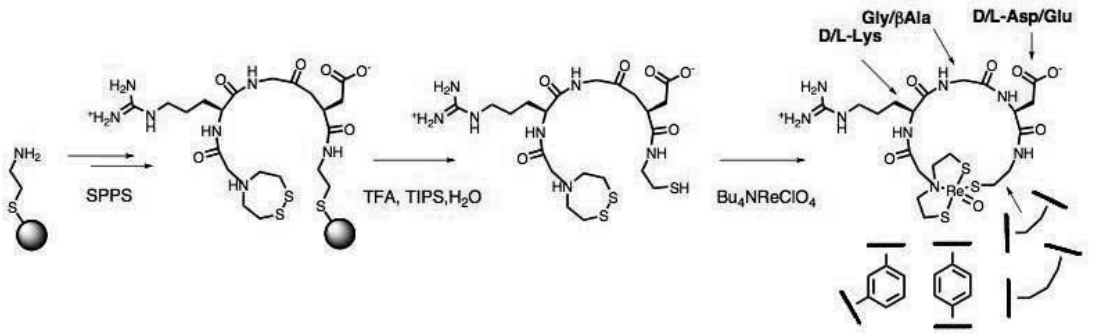

Figure 2

showed a significant binding (IC_{50} < 1 μM), though none of them seems to have a higher affinity for $\alpha_v\beta_3$ than **Re-1b**.

A set of rhenium coordinate (including **Re-1b**), that display varying sequences and linkers, showed satisfactory stabilities in murine plasma except in the 3-aminopropanethiol series. Compound **Re-1b** could be recovered from an U87-MG tumor homogenate provided a proteases inhibitors cocktail was added. Reaction of peptide **1** with oxotechnetium gluconate gave exclusively complex **Tc-1b**, the Tc equivalent to coordinate **Re-1b** that has displayed an interesting activity *in vitro*. This result, originally obtained with 99gTc, was confirmed with the short period γ emitter ^{99m}Tc (T = 6 h, γ 141 Kev). Preliminary experiments carried out in Balb-C nu/nu mice bearing an U87-MG tumor xenograft have shown interesting retention of radioactivity inside the tumor. Complementary experiments to evaluate the biodistribution of the tracers are underway and might lead to the development of new diagnostic agents for the early detection of tumor recurrence and metastasis.

References

1. Hynes RO. *Cell* **110**: 673-687, 2002.
2. Wehrle-Haller B, Imhof BA. *J Pathol* **200**: 481-487, 2003.
3. Smith JW. *Curr Op Invest Drugs* **4**: 741-745, 2003.
4. Haubner R, Fisinger D, Kessler H. *Angew Chem Int Ed Engl* **36**: 1374-1389, 1997.
5. Zhang X, Xiong Z, Wu Y, Cai W, Tseng JR, Gambhir SS, Chen X. *J Nucl Med* **47**: 113-121, 2006.
6. Clavaud C, Heckenroth M, Stricane C, Ménez A, Dugave C. *Bioconjugate Chem* **17**: 807-814, 2006.
7. Masella M, Cuniasse P. *J Chem Phys* **119**: 1866-1873, 2003.
8. Masella M, Borgis D, Cuniasse P. *J Comput Chem* **29**: 1707-1724, 2008.

3-26-008

Synthesis of smart potential MRI contrast reagents that bind aggregated β amyloid for the diagnosis of Alzheimer's disease

Austen, Brian; Mohammed, Yeser; Cheng, Elliott; Matharu, Balpreet*

St George's University of London, Basic Medical Sciences, UNITED KINGDOM

**E-mail: sghk200@sgul.ac.uk*

Definitive diagnosis of Alzheimer's disease (AD) in living patients has been a goal since the first description of the disease in 1906. The ability to separate early AD from other causes of dementia, is extremely important in clinical management. The main pathological feature of AD is the deposition of plaques in the brain, composed primarily of 38-42 residue peptides known collectively as *β*-amyloid (Aβ). It would be of immense diagnostic advantage to be able to image *β*-amyloid deposits in the brains of Alzheimer's patients at various stages of their illness It is known that the course of AD is associated with increased deposition of *β*-amyloid 38-42, into plaques in the brain. And there is considerable evidence that suggests that deposition of Aβ is a cause of the disease. We have recently reported two peptides derived from residues 16-20 of *β*-amyloid, RGKLVFFGR and RGKLVFFGR-NH_2, that are effective inhibitors of fibril or oligomer formation1. As these peptides have affinity for *β*-amyloid, it seemed reasonable to generate *β*-amyloid binding compounds that could be used for diagnosis, from them. Our aim is to produce reagents with increased affinity for A*β* and stability *in vivo*. This has been achieved by retroinversion of the 16-20 binding sequence ie reversing the sense of the sequence and incorporating D- rather than L-amino acids. Retroinversion retains the arrangement of residue side chains for optimal hydrophobic interactions with the target sequence, but also stabilizes the inhibitors against proteolytic degradation *in vivo*. The brain is protected by a tight epethelial layer of cells and astrocyte foot-processes, which together provide a tight physical barrier, that must be traversed for brain-active compounds to function. Some consideration was given to improving the brain penetration of reagents, and to that end an aliphatic amine was attached to the C-terminal carboxyl group to create R1 (Table 1), as amines have been reported to increase blood-brain penetration of peptides2. A truncated all-D version of the cell penetrating peptide sequence of HIV Tat 3 was incorporated C-terminally in R2 (Table 1). In R3, an all-D version of the SynB sequence reported by Drin *et al*.[4] to transport doxorubicin and enkephalin into brain was incorporated C-terminally. In the following description of peptides, lower case represents D-amino acids, whereas upper case represents

Table 1. Synthesised MRI contrast agents for neurodegerative disease

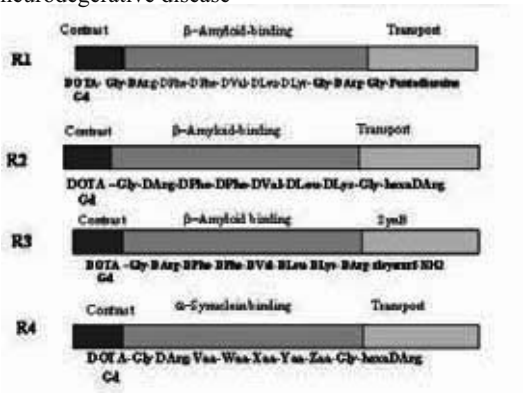

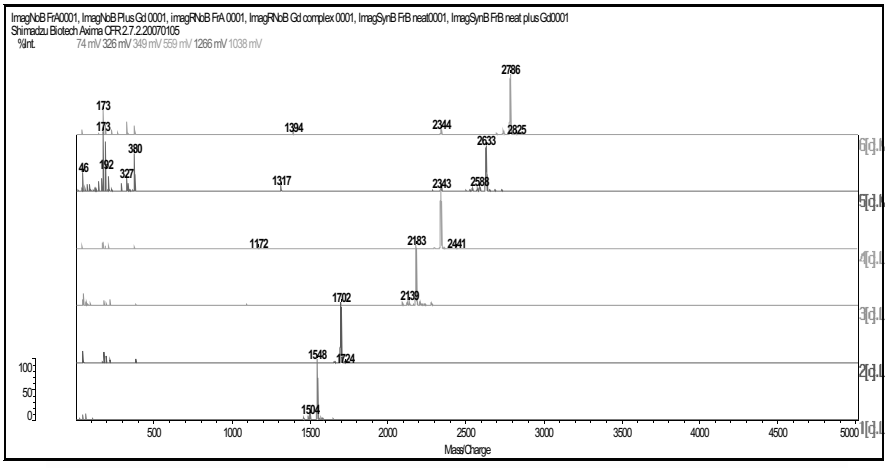

Figure 1. Mass spectra of peptide imaging agents without complexed Gd; R1, R2 and R3, and the respective gadolinium adducts.

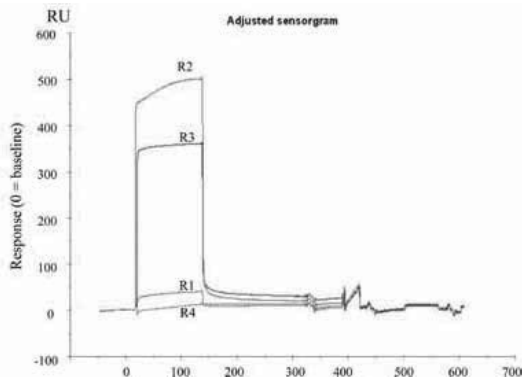

Figure 2. Biacore analysis of binding of +Gd reagents R1, R2, R3 at pH 7.4 and pH 4 to aggregated Aβ40 immobilised at 0.5 mg/ml to a carboxymethyl chip activated with EDC/NHS at pH 4.5. The response from a control surface without Aβ was subtracted.

L-amino acids. A*β*40, A*β*42, IR-Omar-2 (Ac-rGffvlkGr-NH_2), LPFFD and Ac-QKLVFF-NH_2 were synthesized by the optimized Fmoc procedure described previously. The peptide (1,4,7,10-tetraazacyclododecane-1,4,7-tris(acetic acid-t-butyl ester)-10-acetic acid) (DOTA)-GrffvlkGrG-pentadiamine (R1), was synthesized from 4-Formyl-3-methoxyphenoxy}butyric acid (FMBP) NovaGel TM resin (0.55 mequivs) (Nova Biochem), suspended in DCM (8 ml) and trimethylorthoformate (8ml) and stirred overnight under helium agitation with mono-1-butoxycarbonyl, 1,5-diminopentane (Tosyl salt) (Nova) (1g) along with sodium acetoxy borohydride (0.6 g) and DMF (6 ml). The resin was washed with excess DMF, followed by 10% (v/v) DIPEA in DMF, and then DMF. Fmoc-Glycine (1.2 g) and (HATU) (1.5 g) were added and stirring continued overnight. The following residues were coupled from the C-terminus to the N-terminus, using double coupling with HATU for each position as described.[5] Fmoc-D-Arg(Pbf), Fmoc-Gly, Fmoc D-Lys(tBoc), Fmoc-D-Leu, Fmoc-D-Val, Fmoc-D-Phe, Fmoc-D-Phe, Fmoc-D-Arg(Pbf), Fmoc-Gly all from Nova-Biochem, and finally protected DOTA (1,4,7,10-tetraazacyclododecane-1,4,7-tri(acetic acid-t-butyl ester)-10-acetic acid) were coupled.in 4-molar excess using HATU. The peptides (1,4,7,10-tetraazacyclododecane-1,4,7-tris(acetic acid-t-butyl ester)-10-acetic acid) (DOTA)-Grffvlkrrrrrr-NH2 (R2) and (1,4,7,10-tetraazacyclododecane-1,4,7-tris(acetic acid-t-butyl ester)-10-acetic acid) (DOTA)-Grffvlkrrlsysrrf-NH2 (R3) were synthesized on Fmoc-PAL-PEG-PS resin (1.13 g; 0.2 mmoles) by the procedure of El-Agnaf *et al* (2000)5. Protected DOTA (1,4,7,10-tetraazacyclododecane-1,4,7-tri(acetic acid-t-butyl ester)-10-acetic acid) (Macrocyclics, USA) was coupled in 4-fold molar excess at the final step as above. Additional peptides with εBiotinLys residues inserted at position 8 were also synthesized to enable monitoring of binding of reagents. Gadolinium salts of R1, R2 and R3 after deprotection and purification on HPLC as below, were prepared by incubation overnight with a 3-fold molar excess of gadolinium trichloride in 9 ml of water, adjusted to pH 7.0 by the addition of 20 mM NaOH, then purified on a preparative column of Phenomenix C4 in 0.1% TFA with an acetonitrile gradient (GdR1;MH gave 1702 calc 1701) The mass spectra of the imaging agents before and after the addition of gadolinium are shown in Fig. 1. R4 was a control reagent identical to R2, except that the binding sequence ffvlk was changed to an irrelevant pentapeptide, D-amino acid sequence. The reagents and their gadolinium adducts were monitored by MALDI MS analysis on a Kratos Axima after purification by HPLC (Fig. 1), The measured masses were all identical to calculated masses (within 1 mu) in all cases, with gadolinium adducts being 157 mass units higher than their non-complexd peptides. Analysis by surface plasmon resonance (Biacore) (Fig. 2) showed that R1, R2 and R3 have higher affinity to immobilized A*β* aggregates, than the natural sequence peptides described previously (Austen *et al*., 2008), whereas R4 has no affinity. The order of affinities was R2> R3> R1>R4, indicating that the incorporation of multiple cationic residues in R2 and R3 increased affinity ifor A*β* aggregates.

Acknowledgements

We are grateful to St George's University for financial support, the Biomics Unit at sgul for mass spec analyses, and GE Healthcare (Cambridge) for Biacore analysis.

References

1. Austen BM, Paleologou KE, Sumaya AE, Qureshi MM, Allsop D, El-Agnaf OMA. *Biochemistry* **47**: 1984-1992, 2008.
2. Poduslo JF, Curran GL, Kumar A, Frangione B, Soto C. *J Neurobiol* **39**: 371-382, 1999.
3. Wender PA, Mitchell DJ, Pattabiraman K, Pelkey ET, Steinman L, Rothbard JB. *Proc Natl Acad Sci U S A* **97**: 13003-13008, 2000.
4. Drin G, Rousselle C, Scherrmann JM, Rees AR, Temsamani J. *AAPS PharmSci* **4**: E26, 2002.
5. El-Agnaf OM, Mahil DS, Patel BP, Austen BM. *Biochem Biophys Res Commun* **273**: 1003-1007, 2000.

3-03-101

Semi-synthetic approaches to glycosylation of MOG as autoantigen in Multiple Sclerosis disease

Gori, Francesca[1]; Mulinacci, Barbara[2]; Papini, Anna Maria[3]; Rovero, Paolo[2]; Beck-Sickinger, Annette G.[*]

[1]University of Leipzig, Institute of Biochemistry GERMANY; [2]University of Florence, PeptLab, Department of Pharmaceutical Sciences, ITALY; [3]University of Florence, PeptLab, Department of Organic Chemistry, ITALY

[*]E-mail: gori.francesca@gmail.com

Introduction

Post-translational modifications (PTMs), as glycosylation and phosphorilation, can modulate proteins activity and expand the diversity and complexity of their biological functions. In fact glycosylation of secreted proteins plays a crucial role in several immune functions.[1] A number of immune diseases have been associated with PTMs, which can alter the function and immunogenicity of protein antigens (Ags).

The role of autoantibodies (autoAbs) in autoimmune diseases has been reevaluated and it is accepted that a distinct pattern of Multiple Sclerosis (MS) pathology could involve an Ab-mediated demyelination.[2] Previous studies showed that CSF114(Glc),[3,4] a designed glycopeptide characterized by a β-D-glucopyranosyl moiety, is able to detect and isolate specific autoAbs present in the sera of a significant number of MS patients. This synthetic Ag could be considered a mimetic of aberrantly glucosylated myelin proteins triggering autoimmunity in MS, therefore we focused our interest on the role of myelin proteins.

One of these is Myelin Oligodendrocyte Glycoprotein (MOG), a type I integral membrane protein specifically expressed on the outermost lamellae of myelin sheath and considered a putative autoantigen in MS.[5] We decided to study the extracellular domain of MOG (MOG_{ED}) and to obtain this fragment properly glycosylated in order to characterize the molecular mechanisms of Ab-mediated MS and to design new antigenic probes to detect auto-Abs as biomarkers.

The aim of this research is to demonstrate a possible cross-reactivity of this glycoprotein, modified with a well defined glycosyl moiety, with the glycopeptide CSF114(Glc).

Results and Discussion

Production of glycoproteins with recombinant methods presents several difficulties. Thus, the preparation of specific glycoform may benefit from a chemical approach. During these last years several new interesting strategies have been developed to introduce noncanonical amino acids and biological probes into proteins.

The Expressed Protein Ligation is a protein engineering approach that allows synthetic and recombinant poly-peptides to be chemoselectively and regioselectively joined together.[6] This technique is an extension of the Native Chemical Ligation, based on the reaction between a peptide fragment containing a C-terminal thioester group and a second peptide containing a N-terminal Cys residue that generate an amide bond at the ligation junction after a spontaneous intramolecular *S-N* acyl shift.

Studies performed on X-ray crystal structure of MOG_{ED} showed that this protein has a β-hairpin conformation, reminiscent of CSF114(Glc) one, in the segment 98-117.[7] As a consequence we decided to obtain MOG_{ED} synthetically glucosylated in position 104 in order to test it in immunological assays.

The recombinant $rMOG_{ED}$(1-97) has been obtained as C-terminal thioesther using the IMPACT™ system (New England Biolabs) based on the protein splicing, while the peptide fragment [$Gly^{103}Asn^{104}$(Glc)]MOG_{ED}(98-117), bearing a Cys residue at the N-terminus, has been obtained by Solid-Phase Peptide Syntehsis (SPPS). In this way the PTM has been introduced in the peptide sequence following the building-block approach: preformed glycosylated amino-acid building blocks are employed in the stepwise assembly of the peptide backbone.[8] We are exploiting different conditions for the reaction between these two fragments.

An alternative strategy exploits the selective reaction between a glucosyl iodoacetamide derivative and the Cys free thiol of a protein.[9]

A site directed mutation has been performed on the plasmid pQE12$rMOG_{ED}(His)_6$ to introduce a Cys residue at position 31, native site of glycosylation, and to get the mutated $rMOG_{ED}N(31)C(His)_6$ protein by over expression in *E. coli*. After purification and characterization by LC-MS, the protein has been treated with the glycosyl derative and a tryptic digestion has been performed in order to investigate the result of the reaction.

The obtained homogeneously glucosylated protein, carrying a glucosylated side-chain at natural glycosylation site, and the semi-synthetic protein with a well defined PTM will be tested by ELISA to study their ability to detect auto-Abs in MS patient sera, as compared to CSF114(Glc), and to characterize native MS autoantigen(s).

References

1. Daniels MA, Hogquist KA, Jameson SC. *Nat Immunol* **10**: 903-910, 2002.
2. a) Lucchinetti CF, Joseph Parisi J, Bruck W. *Neurol Clin* **23***:* 77-105, 2005; b) Hu W, Lucchinetti CF. *Semin Immunopathol* **31**: 439-453, 2009.
3. Papini AM, Rovero P, Chelli M, Lolli F. *PCT International Patent Application WO 03/000733*.
4. Lolli F, Mulinacci B, Carotenuto A, Bonetti B, Sabatino G, Mazzanti B, D'Ursi AM, Novellino E, Pazzagli M, Lovato L, Alcaro MC, Peroni E, Pozo-Carrero MC, Nuti F, Battistini L, Borsellino G, Chelli M, Rovero P, Papini AM. *Proc Natl Acad Sci U S A* **102**: 10273-10278, 2005.
5. Johns TG, Bernard CCA. *J Neurochem* **72**: 1-9, 1999.
6. a) Muir T. *Ann Rev Biochem* **72**: 249-289, 2003; b) Davies R, Richter MP, Beck-Sickinger AG. *Eur J Biochem* **271**: 663-677, 2004.
7. Breithaupt C, Schubart A, Zander H, Skerra A, Huber R, Linington C, Jacob U. *Proc Natl Acad Sci U S A* **100**: 9446-9451, 2003.
8. Paolini I, Nuti F, Pozo-Carrero MC, Barbetti F, Kolesińska B, Kamiński ZJ, Chelli M, Papini AM. *Tetrahedron Lett* **48**: 2901-2904, 2007.
9. Macmillan D, Bill RM, Sage KA, Fern D, Flitsch SL. *Chemistry & Biology* **8**: 133-145, 2001.

3-03-102

Different proteases immobilized inside chitosan film can catalyze synthesis and hydrolysis of peptide substrates

Bacheva, Anna V[1,]; Macquarrie, Duncan J[2]; Filippova, Irina Yu[1]*

[1]Moscow State University, Chemistry Department, RUSSIAN FEDERATION; [2]Department of Chemistry, Universitry of York, Centre of Excellence in Green Chemistry, UNITED KINGDOM

[*]E-mail: anbach@genebee.msu.ru

Introduction

Growing interest to the peptide substrates, inhibitors and other peptidomimetics required new highly effective synthetic techniques. The important goal of enzymatic peptide bond formation is the optical purity of the peptide, which facilitates the product isolation. Thus using enzymatic condensation as a last step in peptidomimetics production is preferable and reuse of biocatalyst is the necessary condition. Fixing of enzymes on/in suitable insoluble supports has many advantages such as high operational stability, ease of separation, possibility of recycling and improved activity in low water media. As a matrix we choose chitosan, natural hydrophilic polysaccharide. Chitosan has distinct advantages over the other supports due to (a) its renewable nature - it is currently available in large quantities as a waste product from the fishing industry and (b) its excellent film-forming ability, allowing attachment to reactor walls for advanced processing.[1,2]

Results and discussion

The main goal of this work was to create immobilized biocatalyst capable to work both in aqueous and low water media with high efficiency. Serine proteases subtilisin and chymotrypsin, and cysteine protease papain were immobilized onto chitosan. The films of biocatalysts were prepared by drying the mixed solution of chitosan and enzyme in acetate buffer pH 5.6. The biocomposite films were prepared as described in detail.[3,4] It was found that treatment with glutaraldehyde crosslinker gave a material with high stability and good mechanical properties. The novel preparation technique provided for high loading and uniform enzyme distribution. The biocomposites thus obtained showed high amidase activity against specific chromogenic peptide substrates (of subtilisin was tested using Glp-Ala-Ala-Leu-pNA,[3,4] of chymotrypsin - by Glp-Phe-pNA and of papain - by Glp-Phe-Ala-pNA[5]) and protein substrate azacasein. Immobilized subtilisin and chymotrypsin also possess esterase activity against p-nitrophenyl acetate. The amidase, esterase and protease activities of obtained samples were tested and compared with activities of native enzymes. It was shown that proteases after immobilization retain 15-40% of native amidase activity and 20-45% of native protease activity. Esterolytic activity maintained at very high level (75-90%), and this result also assumed presence of diffusion limitation – one can see that the lower the substrate specificity the higher the residual activity. The long-term storage in aqueous buffer and acetonitrile had a little effect on the hydrolytic activity of subtilisin-based biocomposite (Fig. 1).

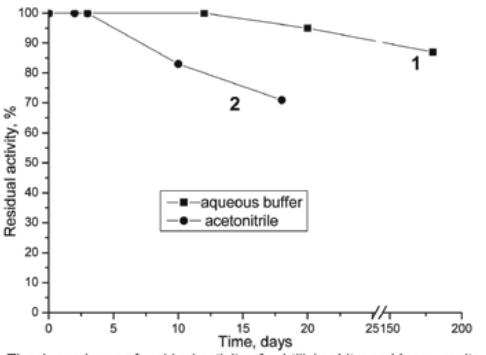

Fig. 1. The dependence of residual activity of subtilisin-chitosan biocomposite on storage time in aqueous buffer (1) and acetonitrile(2)

High stability of subtilisin-chitosan biocomposite in aqueous and organic media indicates that enzyme's molecules are in appropriate microenvironment, maintaining native and active conformation. The dependence of subtilisin/chitosan hydrolytic activity on temperature and pH was studied (Fig. 2,3).

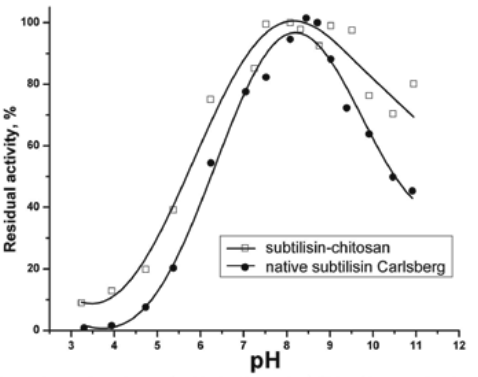

Fig. 2. The pH-dependence of residual activity of subtilisin-chitosan and native subtilisin

pH-dependence of subtilisin-chitosan biocomposite was bell-shaped and range of pH values where subtilisin have maximum activity was more broad comparing native enzyme. Activity was higher at acidic and alkaline pH, especially in the range 3,5-6 and 9-11 (Fig. 2). The dependence of activity on temperature for subtilisin was examined (Fig. 3).

The immobilization often leads to stabilization of enzyme against high temperature. In our case considerable shift of temperature optimum to higher range was achieved. For native subtilisin maximum activity was observed in 30-60 °C, at 70 °C the residual activity was about 70% and at 80 °C enzyme was inactive. For immobilized subtilisin activity increased along with temperature up to 70 °C, and even at 80 °C the residual activity was about 70%. After optimization of biocomposite preparation technique we choose several samples which possess high activity and tested the ability of biocatalytic films of subtilisin and papain immobilized in chitosan to catalyze peptide bond formation were capable to catalyze peptide bond formation in dimethylformamide / acetonitrile (6/4) mixture in reaction Z-Ala-Ala-Leu-OCH_3 + Phe-pNA → Z-Ala-Ala-Leu-Phe-pNA + CH_3OH for subtilisin, Z-Ala-Ala-OCH_3 + Leu-pNA → Z-Ala-Ala-Leu-pNA + CH_3OH for papain. (Table 1).

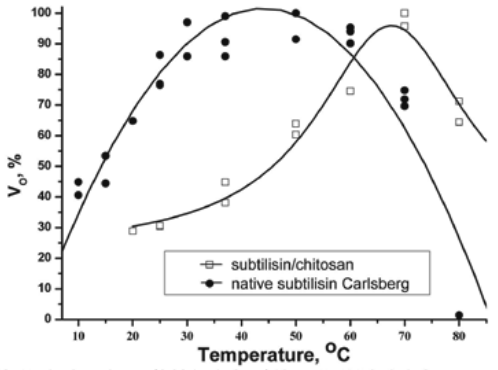

Fig. 3. The dependence of initial velocity of Glp-AAL-pNA hydrolysis on temperature for subtilisin-chitosan biocomposite and native subtilisin Carlsberg

Biocatalytic films catalyzed peptide synthesis with the average [E]/[S] ratio in the syntheses 1/1500, and the product yields reached 60-100% after 24 h of reaction. Thus biocatalytic films prepared in this work are characterized by preparative simplicity, high activity and stability in different media.

Acknowledgements

This work was supported by RFBR # 06-03-33056a.

References

1. Macquarrie DJ, Hardy JJE. *Ind Eng Chem Res* **44**: 8499-8521, 2005.
2. Krajewska B. *Enz Microb Technol* **35**: 126-139, 2004.
3. Macquarrie DJ, Bacheva AV. *Green Chem* **10**: 692-695, 2008.
4. Bacheva AV, Isakov MS, Lysogorskaya EN, Macquarrie DJ, Philippova I Yu. *Russ J Bioorg Chem* **34**: 334-338, 2008.
5. Semashko TA, Lysogorskaya EN, Oksenoit ES, Bacheva AV, Filippova I Yu. *Russ J Bioorg Chem* **34**: 339-343, 2008.

Table 1. Enzymatic peptide synthesis catalyzed by protease-enzyme biocomposites in DMF/acetonitrile mixture

Sample of biocatalyst	Product	Reaction time, h	Yield, %
subtilisin-chitosan biocomposite	Z-AAL-FpNA	2	82
subtilisin-chitosan biocomposite	Z-AAL-FpNA	24	100
papain-chitosan biocomposite	Z-AA-LpNA	2	35
papain-chitosan biocomposite	Z-AA-LpNA	24	61

3-05-103

Cell Adhesion Ability of Self-Assembled Nanofiber Consisting of RGDS-Tagged Amphiphilic Peptide

Higashi, Nobuyuki[1,]; Kawamura, Yoko; Koga, Tomoyuki*

Doshisha University, Department of Molecular Chemistry & Biochemistry JAPAN

[*]E-mail: nhigashi@mail.doshisha.ac.jp

Introduction

The aim of tissue engineering is to replace failed organs with new functional tissue and organs. To realize this, materials are needed, which can direct the growth of cells to generate new tissue. To control and direct cell behavior, a defined biomimetic environments is needed, which surrounds the cells and promotes specific cell interactions. The RGDS sequence has been recognized as the cell attachment site of a large number of adhesive extracellular matrix,[1] and is widely used to modify the surface of biomaterial scaffolds to mediate cell adhesion. Biological adhesion through the RGDS sequence on synthetic substrates is known to depend on epitope density.[2] We have previously reported on a self-assembling amphiphilic triblock peptide consisting of Leu and Lys (L4K8L4). This peptide self-assembled into nanofibers under a specific condition.[3] The purpose of this study is to fabricate a RGDS-carrying nanofiber scaffold towards cell adhesion using a self-assembling technique.

Results and Discussion

A novel, bifunctional peptide (RGDS- L4K8L4) has been designed, consisting of RGDS as cell-adhesive site and L4K8L4 as nanofiber-formable sequence (Fig. 1).

We envisioned that in the assembled nanofibers, the RGDS sequence is displayed at high density along the fiber periphery. The peptide was synthesized by solid phase synthesis using Fmoc-chemitry and purified by HPLC and identified by MALDI-TOF mass spectrometer. The secondary structure and morphology of the peptide in water were first examined by means of circular dichroism (CD) spectroscopy and atomic force microscopy (AFM) observation. As a result, RGDS-L4K8L4 was found to self-assemble into nanofibers at pH 9.6, at which the RGDS-free L4K8L4 had been already described to self-assemble into well-developed nanofiber structure.3 Average fiber height was estimated to be 3 nm and the nanofibers were on the basis of β-sheet motifs. By lowering the pH value to 7.3, the conformational change from β-sheet to random coil structure was caused due to promoting protonation of Lys-residues, giving no aggregation of the peptide. Two types of the peptide-coated polystyrene dishes were prepared; RGDS-L4K8L4 (nanofiber)-coated dish and RGDS-L4K8L4 (random coil)-coated dish, and NIH/3T3 cells were seeded and cultured on them in serum-free medium for 2 h and the cell adhesion behavior and morphology were observed. As a control, the same experiment was performed for the bare polystyrene dish. Cells adhered on the bare

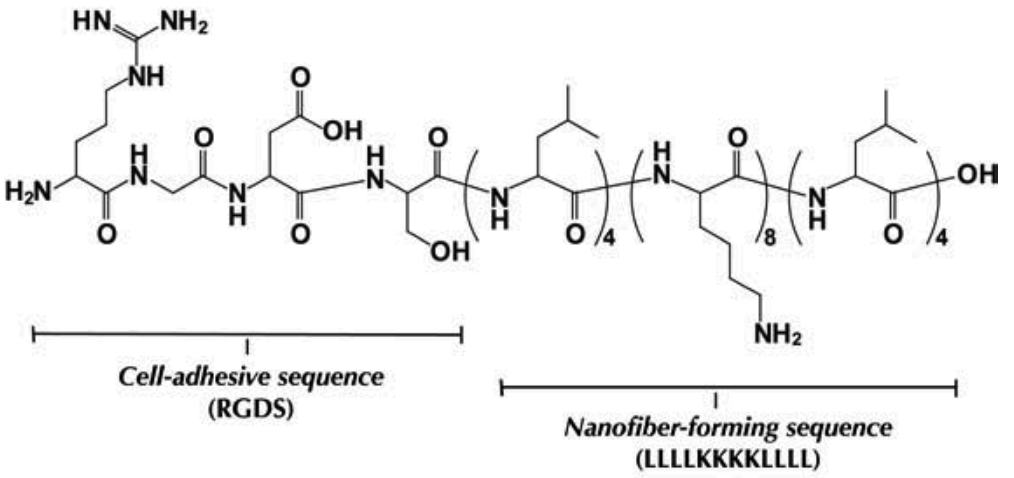

Figure 1. Chemical structure of RGDS-tagging nanofiber formable peptide.

dish probably because of a hydrophobic interaction, but did not spread at all. When cells were seeded on the RGDS-L4K8L4 (random coil)-coated dish, only slight spreading was observed. In contrast, the RGDS-L4K8L4 (nanofiber)-coated dish showed sufficient cell adhesion and well-spreading. Therefore, it is suggested that the cell spreading on the nanofiber-coated dish was facilitated by the interaction between intergrine and the RGDS sequence that would locate densely and regularly at the nanofiber surface.

Acknowledgement

This work was supported in part by a grant-in-aid for scientific research (No. 19710099), and the Academic Frontier Research Project on "New Frontier of Biomedical Engineering Research" from the Ministry of Education, Culture, Sports, Science and Technology, Japan.

References

1. Pierschbacher MD, Ruoslahti E. Influence of stereochemistry of the sequence Arg-Gly-Asp-Xaa on binding specificity in cell adhesion. *J Biol Chem* **262**: 17294-17298, 1987.
2. Houseman BT, Mrksich M. The microenvironment of immobilized Arg-Gly-Asp peptides is an important determinant of cell adhesion. *Miomaterials* **22**: 943-955, 2001.
3. Koga T, Higuchi M, Kinoshita T, Higashi N. Controlled self-assembly of Amphiphilic Oligopeptides into shape-specific nanoarchitectures. *Chem Eur J* **12**: 1360-1367, 2006.

3-06-104

ÄKTA™ oligopilot™ for Automated Solid Phase Peptide Synthesis

Tedebark, Ulf[1,]; Latassa, Daniel[2]; Heinzmann, Etienne[2]; Denker, Per[1]; Holmberg, Lars[1]; Uhlén, Kristina[1]; Karlberg, Per[1]; Werbitzky, Oleg[2]; Strong, Andrew[2]*

[1]GE Healthcare Bio-Sciences AB, Uppsala, SWEDEN; [2]Lonza AG, Visp, SWITZERLAND

[*]E-mail: ulf.tedebark@ge.com

Introduction

Automation and scalability are two of the most important features in Solid Phase Synthesis of peptide therapeutics. Today there is no industry standard for scalable Solid Phase Peptide Synthesis (SPPS) equipped with Process Analytical Technology (PAT) capabilities. GE Healthcare provides scalable and complete solutions for automated solid-phase synthesis of oligonucleotides from small research amounts to full commercial production (1 µmol - 1 mol) based on the ÄKTA™, Oligopilot™ 400 and OligoProcess™ platforms. The UNICORN™ software provides control and monitoring of the processes. GE Healthcare synthesizers are designed around flow-through column reactors, giving faster kinetics and lower solvent and reagent consumption compared to batch synthesizers. Based on experience with scale-up of oligonucleotides, GE Healthcare and Lonza are confident that the flow through-column technology also can be scaled up for peptides to a more cost-efficient process compared to current batch reactor technologies. As a first step in this direction, GE Healthcare has decided to explore the potential of the ÄKTA platform as a peptide synthesizer.

Objectives

GE Healthcare was approached by Lonza to develop a peptide synthesizer based on the ÄKTA platform instrument to compete with the state of the art in the peptide field. The aim is to develop the fluidics, programming and chemistry methods of the ÄKTA system to Lonza's needs for routine production of 0.4 g to 2 g of crude peptide, and later scale up to 2 kg.

System Description

Two prototype synthesizers have been built. These synthesizers, controlled by the UNICORN software, have the capability to perform synthesis using on-line mixing or pre-activation at different programmed times and temperatures of amino acids, coupling reagents, solvents and additives. The GE Healthcare ÄKTA pep synthesizer (prototype) is a flexible and fully automated peptide synthesis system employing flowthrough reactor technology. Compared to batch reactors, the flow-through reactor technology results in lower reagent consumption and enables exact control of reaction rates and contact times, as well as allows smooth scale up. Additional features for the ÄKTA pep synthesizer are column re-circulation and a temperature controlled pre-activation chamber. The system is controlled via an external computer using UNICORN software. The ÄKTA pep synthesizer is equipped with UV-, pressure- and conductivity-monitors. By combining the ÄKTA pep synthesizer's monitoring capabilities with UNICORN, a Process Analytical Technology (PAT) approach can be used.

Applications

The applicability of developing, based on the ÄKTA platform, a first ÄKTA pep prototype for automated solid-phase peptide synthesis was illustrated in the synthesis of peptides varying in lengths and sequence difficulties. Results from manual and automated synthesis are compared, also taking reproducibility and possibility to scale up into regards. The evaluated peptides are ACP[65-74], Fmoc- Leu-Enkephaline and Lonza's CN: 32358

Synthesis of ACP [65-74]

Initial work was devoted to synthesis of the fragment [65-74] (Val-Gln-Ala-Ala-Ile-Asp-Tyr-Ile-Asn-Gly) of the acyl carrier protein using preloaded Primer Support™ 200. This decapeptide has been widely accepted as a model for illustrating the efficiency of a reagent, polymer support or a synthetic condition and testing of peptide synthesizers.[1]

When all AA were dissolved in DMSO,[2] except (Fmoc-Asn(Trt)-OH) which was not soluble in DMSO, and DMSO/NMP 1:1 was used instead, an increase in De-Fmoc values was obtained indicating an overall higher yield and purity of the crude peptide. As can be seen from the HPLC trace, 08pep015b, the purity was increased further to almost 88%. Yield was close to quantitative.

Synthesis of Fmoc-Leu-Enkephalin

Enkephalin, one of several naturally occurring morphine-like substances (endorphins) released from nerve endings of the central nervous system and the adrenal medulla. They act as analgesics and sedatives in the body and appear to affect mood and motivation. Fmoc-Leu-

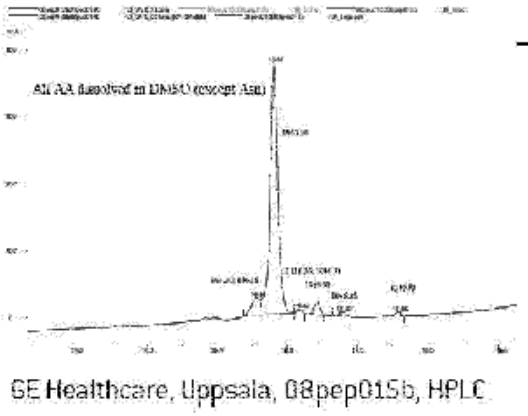

No	Retention (min)	Peak area %
1	16.56	6.51
2	16.81	87.37
3	16.19	1.01
4	16.43	3.04
5	16.78	1.09
6	17.50	0.78

Enkephalin is an opioid peptide that has been found to modulate nociception in the spinal cord.[3] Lonza's initial work was focused on the synthesis of Fmoc-Tyr-Gly-Gly-Phe-Leu-OH. The experimental conditions (not optimized) are described. HPLC and LC-TOF analyses were in agreement with the desired product.

Synthesis of a 12mer peptide

In parallel, Lonza has extended this technology towards the synthesis of a 12mer peptide having a difficult sequence (Lonza CIS-Number: 32358). For confidential reasons, the sequence can not be disclosed. The ASPPS is carried out using a Fmoc-Leu loaded trityl-based-PS200. Preliminary results are promising. The crude peptide could be isolated with a purity of 75% and a yield of nearly 70%. The main peak was in agreement with an internal reference.

Conclusions

Two ÄKTA pep prototype synthesizers have showed initial very promising results towards a scalable automated peptide synthesizer based on proven technology.

Lonza, one of the largest contract manufacturers of synthetic peptides is collaborating with GE to develop the ÄKTA pep synthesizer.

Synthesis and analysis of ACP showed reproducible results between prototypes and sites.

Lonza have obtained similar synthesis performance compared to manual batch synthesis.

Finally the number of options provided by the ÄKTA pep synthesizer in terms of CR and additives, different pre-activation times and temperatures, re-circulation times, low solvent/reagent consumption during synthesis together with PAT capability provided by UNICORN makes the ÄKTA pep attractive as a scalable automated synthesizer.

References

1. Arunan C, Pillai VNR. *Tetrahedron* **56**: 3005-3011, 2000.
2. Hood CA, Feuntes G, Patel H, Menakuru M, Park JH. *J Pept Sci* **14**: 97-101, 2008.
3. Leung MK, Stefano GB. *Proc Natl Acad Sci U S A* **81**: 955-958, 1984.

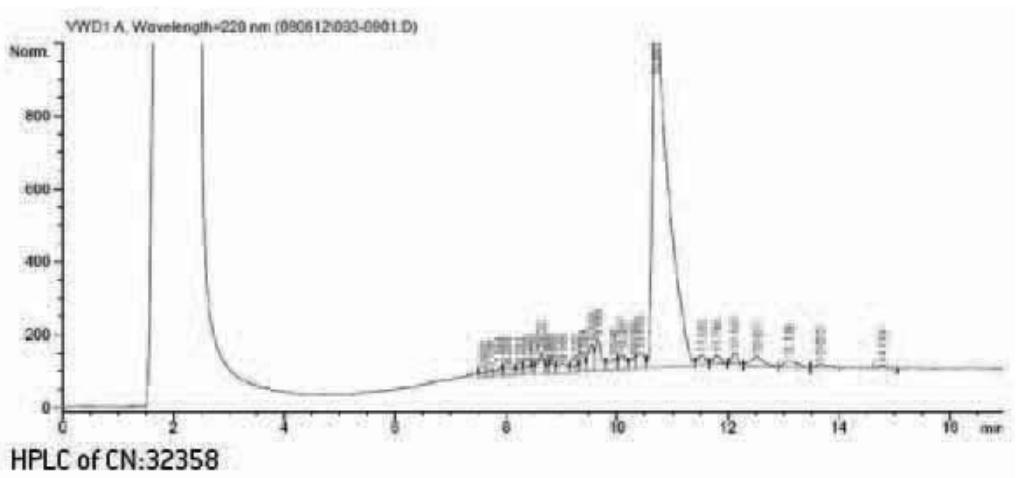

3-07-105

Using the activity-based approach to identify neuropeptide-processing proteases

Sabidó, Eduard[1,]; Tarragó, Teresa[2]; Giralt, Ernest[1]*

[1]University of Barcelona, Department of Organic Chemistry, SPAIN; [2]Institute for Research in Biomedicine, SPAIN

[*]E-mail: eduard.sabido@irbbarcelona.org

Introduction

Neuropeptides comprise neurotransmitters and peptide hormones, which are 3 to 40 amino acids long, involved in intercellular communication, neurotransmission processes and endocrine regulation. They are synthesized in neural tissues and play a key role in several physiological processes including pain, weight and temperature control, memory, anxiety and water balance, among many others.[1]

Neuropeptides are produced from precursor proteins, which include one or more copies of the mature neuropeptides, by selective cleavage at specific sites.[2] Classical biosynthetic cleavage of precursor proteins occurs at basic residues within the consensus sequence Lys/Arg-$(Xxx)_n$-Lys/Arg↓ with n = 0, 2, 4 o 6. This cleavage is performed by a relatively small number of well-known peptidases, including prohormone convertases and cathepsin L. However, the discovery and characterization of new neuropeptides has led to the description of a new non-classical pathway with cleavage occurring at tryptophan, leucine and other amino acids.[3] Neuropeptide-processing peptidases involved in this new non-classical pathway remain largely unknown, despite a few have been recently reported, such as proteins SKI-1/S1P, NARC-1, PPE/ADAM-10 and endothelin-converting enzymes. It is however clear that, many other proteases involved in this kind of neuropeptide maturation remain unknown.[4]

To identify peptidases involved in the non-classical biosynthetic pathway we propose the synthesis of dipeptide phosphonate probes and their use in an activity-based proteomics approach.

Results and discussion

We designed and synthesized several probes based on the chromogranin B-derived neuropeptides described in the literature.[5,6] These probes consisted of amino acids P1 and P2 of the mature neuropeptides, a phosphonate functional group in C_{ter} able to bind the active site of serine proteases, and an N_{ter} alkyne functional group for probe labeling (Fig. 1).

Activity-based probes were used to screen the mouse brain and pituitary proteomes. Protein-bound probes were labeled with biotin or rhodamine by 1,3-dipolar cycloaddition, and the complexes were characterized by in-gel analysis and multidimensional nLC-MS/MS (MudPIT)[7] (Fig. 2A).

The comparison of samples and heat denatured controls allowed the identification of several candidate proteins in the corresponding proteomes (Fig. 2B). These proteins specifically recognize the designed activity-based probes and, therefore, they may be involved in neuropeptide-processing. The liver carboxylesterase N precursor, the serotransferrin precursor, the Ndr2 protein,

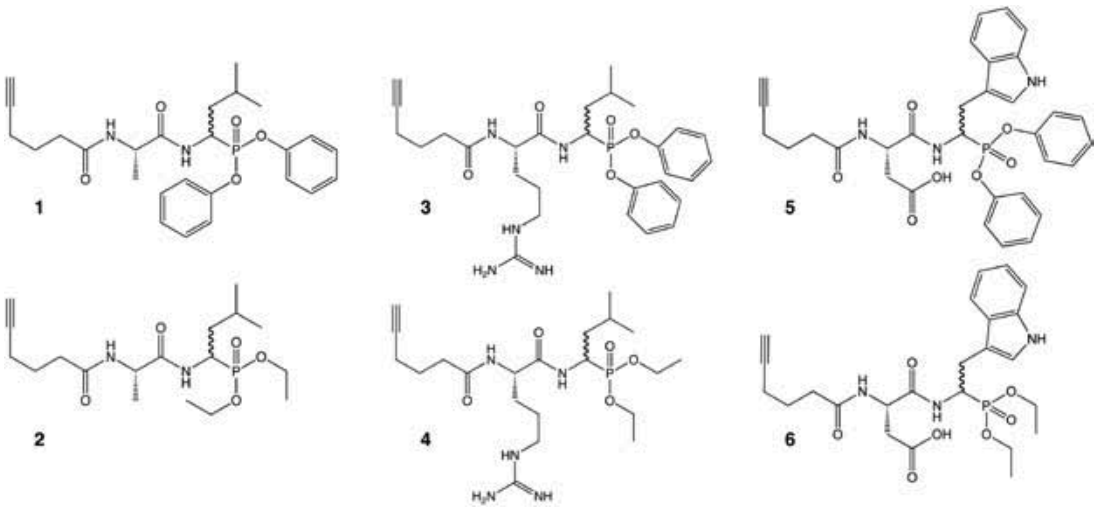

Figure 1. Structure of synthesized phosphonate dipeptidic probes Aha-Ala-Leu^P$(OPh)_2$ (**1**), Aha-Ala-Leu^P$(OEt)_2$ (**2**), Aha-Arg-Leu^P$(OPh)_2$ (**3**), Aha-Arg-Leu^P$(OEt)_2$ (**4**), Aha-Asp-Trp^P$(OPh)_2$ (**5**), Aha-Asp-Trp^P$(OEt)_2$ (**6**).

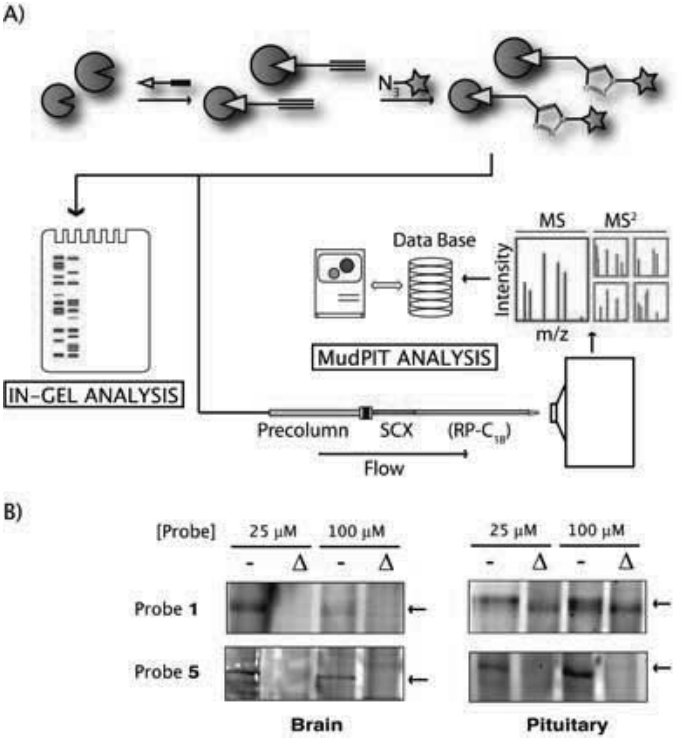

Figure 2. A) Schematic representation of the workflow for proteome characterization both by in-gel analysis and MudPIT analysis. B) Specific protein band detection by fluorescent SDS-PAGE after proteome screening with probes 1 and 5 at 25 µM and 100 µM. δ: heat denatured proteome.

the thimet oligopeptidase and dipeptidyl peptidase III are among these candidate proteins. In order to definitely establish their role in biological tissues, functional studies including cloning of the corresponding gene regions, expression experiments and assays of protein activity as well as colocalization studies are needed.

Acknowledgements

We thank Prof. B. Cravatt for his support and excellent advise in activity-based proteomics. This work was supported by MCYT-FEDER (Bio2005-00295 and NAN2004-09159-C04-02), and the Generalitat de Catalunya (CERBA and 2005SGR-00663).

References

1. Strand FL. Neuropeptides: general characteristics and neuropharmaceutical potential in treating CNS disorders. *Prog Drug Res* **61**: 1-37, 2003.
2. Hook V, Funkelstein L, Lu D, Bark S, Wegrzyn J, Hwang SR. Proteases for processing proneuropeptides into peptide neurotransmitters and hormones. *Annu Rev Pharmacol Toxicol* **48**: 393-423, 2008.
3. Fricker LD. Neuropeptide-processing enzymes: applications for drug discovery. *AAPS J* **7**: E449–55, 2005.
4. A) Rosendahl MS, Ko SC, Long DL, Brewer MT, Rosenzweig B, Hedl E, Anderson L, Pyle SM, Moreland J, Meyers MA, Kohno T, Lyons D, Lichenstein HS. Identification and characterization of a pro-tumor necrosis factor-alpha-processing enzyme from the adam family of zinc metalloproteases. *J Biol Chem* **272**: 24588–24593, 1997. B) Seidah NG, Mowla SJ, Hamelin J, Mamarbachi AM, Benjannet S, Touré BB, Basak A, Munzer JS, Marcinkiewicz J, Zhong M, Barale JC, Lazure C, Murphy RA, Chrétien M, Marcinkiewicz M. Mammalian subtilisin/kexin isozyme SKI-1: A widely expressed proprotein convertase with a unique cleavage specificity and cellular localization. *Proc Natl Acad Sci U S A* **96**: 1321–1326, 1999. C) Bagetta G, Corasaniti MT, Aloe L, Berliocchi L, Costa N, Finazzi-Agrò A, Nisticò G. The secretory proprotein convertase neural apoptosis-regulated convertase 1 (NARC-2): liver regeneration and neuronal differentiation. *Proc Natl Acad Sci U S A* **100**: 928–933, 2003. D) Xu D, Emoto N, Giaid A, Slaughter C, Kaw S, deWit D, Yanagisawa M. ECE-1: a membrane-bound metalloprotease that catalyzes the proteolytic activation of big endothelin-1. *Cell* **78**: 473–485, 1994.
5. Che FY, Yan L, Li H, Mzhavia N, Devi LA, Fricker LD. Identification of peptides from brain and pituitary of Cpe(fat)/Cpe(fat) mice. *Proc Natl Acad Sci U S A* **98**: 9971–9976, 2001.
6. Strub JM, Garcia-Sablone P, Lonning K, Taupenot L, Hubert P, Van Dorsselaer A, Aunis D, Metz-Boutigue MH. Processing of chromogranin B in bovine adrenal medulla. Identification of secretolytin, the endogenous C-terminal fragment of residues 614-626 with antibacterial activity. *Eur J Biochem*, **229**: 356–368, 1995.
7. Washburn MP, Wolters D, Yates JR 3rd. Large-scale analysis of the yeast proteome by multidimensional protein identification technology" *Nat Biotechnol* **19**: 242–247, 2001.

3-07-106

A flow cytometric method to detect internalization of antimicrobial fluorescently-labeled peptides in bacterial cells

*Gennaro, Renato; Benincasa, Monica; Pacor, Sabrina; Carlini, Gianluigi; Tossi, Alessandro; Scocchi, Marco**

University of Trieste, Departement of Life Sciences, ITALY

**E-mail: mscocchi@units.it*

Introduction

Antimicrobial peptides (AMPs) inactivate bacteria via different mechanisms of action. Some AMPs, including the proline-rich antimicrobial peptides (PRPs), kill bacteria without any apparent membrane damage and their bactericidal action is mediated by their internalization into the target cells.[1] Thus, the detection of peptide's localization in the bacterial cells is an important task to understand their mode of action. Immunoelectron transmission microscopy and confocal microscopy are the reference methods to study peptides' uptake but, unfortunately, these techniques are quite complex to perform and time consuming, and the results are sometimes ambiguous. Here we propose a simple and rapid flow cytometric method to assess internalization of the peptides in *E. coli* and other bacteria. The study was performed in parallel on two peptides showing different mechanisms of action: the PRP and cell-penetrating peptide Bac7[1,2] and the membrane-permeabilizing antibiotic polymyxin B.[3] The use of the extracellular quencher Trypan Blue (TB), a dye that is excluded from the membrane barrier of intact cells quenching the extracellular fluorescence[4] allowed us to discriminate between a cell surface and cytoplasmic localization of the peptides.

Results and discussion

Uptake in *E. coli* HB101 cells was investigated by using the fluorescent derivative of a synthetic N-terminal active

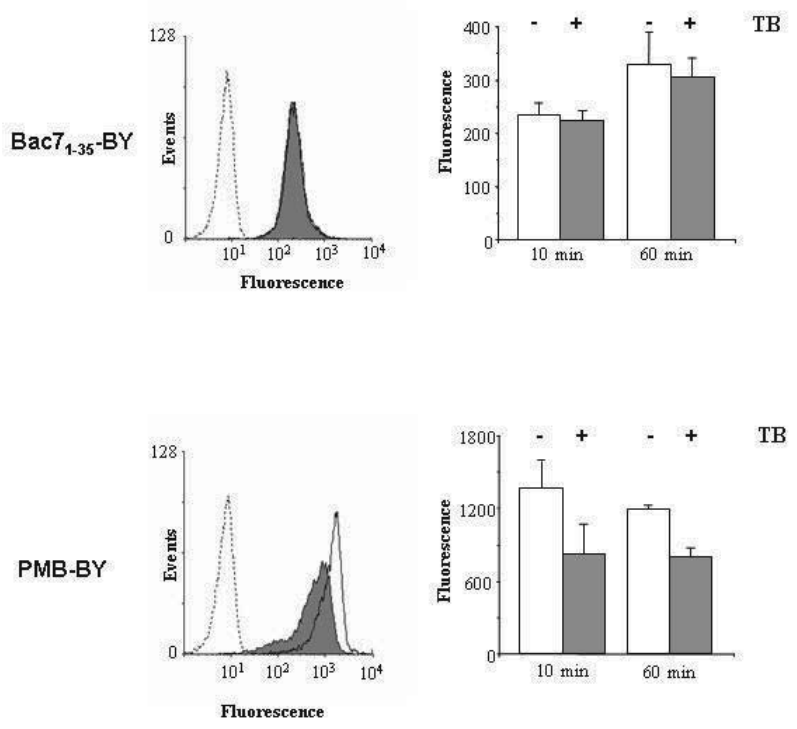

Figure 1. Effect of TB on *E. coli* HB101 cells exposed to Bac7$_{1-35}$-BY or PMB-BY *E. coli* cells (1 x 10^6 CFU/ml) were incubated with 0.25 μM Bac7$_{1-35}$-BY or 0.1 μM PMB-BY, washed with buffered high-salt solution and then analyzed by flow cytometry with (grey histograms) or without (empty histograms) incubation for 10 min with 1 mg/ml of the extracellular quencher TB. A representative experiment (left panels), and the mean of fluorescence intensity ± S.D. of four independent experiments (right panels) are shown.

fragment of Bac7, $Bac7_{1-35}$-BY, prepared by addition of a BODIPY group to a C-terminal cysteine and PMB-BY, a commercial polymyxin B linked to the same fluorophore (Invitrogen). The two peptides showed identical antibacterial activities compared to the corresponding unlabelled peptides (data not shown). They were incubated with 10^6 CFU/ml of *E. coli* HB101 for 10 or 60 min at sub-lethal concentrations so that to ensure the maintenance of an impermeant membrane barrier and, at the same time, to assure peptide detection. The cells were then analyzed by a flow cytometer equipped with an argon laser (488 nm) and with one of the photomultipliers set at 525 nm to detect BODIPY emission. Both peptides were shown to bind efficiently to the cells with PMB-BY. When the cells were washed with high-salt buffered solution, the cell-associated fluorescence decreased significantly, indicating that most of the molecules were weakly bound to the cell surfaces (data not shown). To quantify the portion of fluorescence due to the internalized peptides, the peptide-treated HB101 cells were then analyzed in the presence of TB. Fluorescence signal due to $Bac7_{1-35}$-BY was not significantly reduced (<5%) by addition of the quencher and its value increases with time in agreement with a progressive internalization of the peptide (Fig. 1). In contrast, incubation of the cells with PMB-BY resulted in an approximately 40% reduction of the fluorescence after addition of TB (Fig. 1), in agreement with a more surface-bound state. Overall these results likely indicate that this method is useful to discriminate between molecules such as $Bac7_{1-35}$-BY, associated with the cell and poorly exposed to the quencher consistent with a cytoplasmic localization, and molecules, such as PMB-BY, that appear to be, at least in part, displayed on the bacterial surface and whose fluorescent is promptly quenched.

Analyses have been then extended to *Salmonella enterica* serovar Typhimurium and to *Staphylococcus aureus* which are respectively a Bac7-sensitive and a Bac7-insensitive species.[5] Results of assays carried out under the conditions reported above showed that the fluorescence intensity of peptide-treated cells correlates with their susceptibility towards $Bac7_{1-35}$-BY. In particular, while *S. enterica* cells showed a fluorescence level comparable with *E. coli* cells (not shown), *S. aureus* cells showed no fluorescent at all (Fig. 2), indicating that its insensitivity to Bac7 is likely due to the incapability of the peptide to be internalized into these cells. This method allows to rapidly assess the internalization of peptides into bacterial cells and it is, in principle, also applicable to other types of molecules.

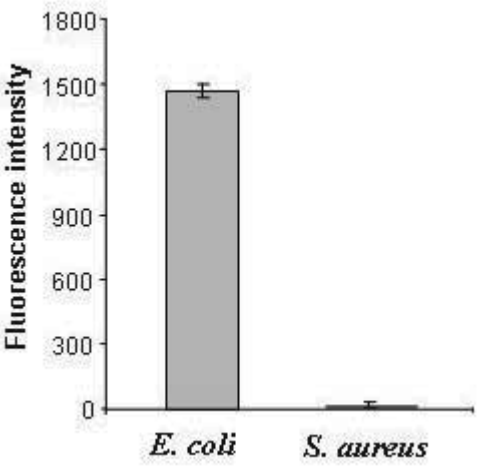

Figure 2. Uptake of $Bac7_{1-35}$-BY in *E. coli* HB101, and *S. aureus* ATCC 25923. Bacterial cells (1 x 10^6 CFU/ml) were incubated with 1 μM $Bac7_{1-35}$-BY for 240 min and analyzed as described in the legend of Fig. 1.

Acknowledgements

This study was supported by grants from the Italian Ministry for University and Research (PRIN 2007), and by Friuli Venezia Giulia Region (LR26/2007 grant 200502027001).

References

1. Gennaro R, Zanetti M, Benincasa M, Podda E, Miani M. *Curr Pharm Des* **8:** 763-778, 2002.
2. Podda E, Benincasa M, Pacor S, Micali F, Mattiuzzo M, Gennaro R, Scocchi M. *Biochim Biophys Acta* **1760:** 1732-1740, 2006.
3. Daugelavicius R, Bakiene E, Bamford DH. *Antimicrob Agents Chemother* **44:** 2969-2978, 2000.
4. Nuutila J, Lilius EM. *Cytometry A* **65:** 93-102, 2005.
5. Benincasa M, Scocchi M, Podda E, Skerlavaj B, Dolzani L, Gennaro R. *Peptides* **25:** 2055-2061, 2004.

3-13-107

Synthesis and Characterization of a Molecular Force Balance based on Peptide Epitopes

David, Ralf; Ho, Dominik; Gaub, Hermann E*

Center for Integrated Protein Science Munich & Center of Nano Science, LMU Munich, Chair for Applied Physics, GERMANY

**E-mail: Ralf.David@physik.uni-muenchen.de*

Single-molecule force spectroscopy provides a powerful tool to investigate biomolecular interactions. An alternative approach recently introduced in our lab,[1] measures forces required for breaking bonds in a differential format by comparison with a known reference bond. This differential force assay has been used to characterize ligand-receptor interaction,[2] DNA-drug interaction[3] and single nucleotide polymorphisms.[4] In the differential force assay, the nanomechanical force sensor -typically a cantilever spring or an optical tweezer- is replaced by a polymeric anchor and a known reference bond combined with a fluorescence label (Fig 1). When the two surfaces are separated, the polymeric anchors are stretched and a force builds gradually up in the chain consisting of the reference and the bond of interest. Finally the weaker of the two bonds ruptures. The ratio of the bondrupture probabilities of the two bonds is directly given by the ratio of the flourescences on both surfaces and can be easily determined by quantitative fluorescence microscopy. Whereas typically dsDNA1 is employed as reference bond, we investigated here the advantages of peptide antibody complexes for this purpose.

In particular, we apply here this molecular force balance approach to the measurements of the bond strengths of peptides and receptors on living cells. The activation of receptors in cells under force promises to give a deeper insight into mechanosensoric events and the mechanotransduction of signals. For the reference system the GCN4-peptide was chosen. This peptide interacts with artificial antibody-fragments and the peptide-antibody interaction is well investigated.[5] The dissociation constant of the GCN4 peptide to the chosen antibody fragment was determined to be 40 pM.[6] As the second bond an -Arg-Gly-Asp- (RGD) motive containing peptide was used. Such peptides can interact with integrines like the integrin $\alpha_V\beta_3$, which is expressed in OVMZ-6 cells.[7] The force balance containing an RGD-peptide on the one hand and the GCN4-peptide on the other hand was made by solid phase peptide synthe sis by the application of the Fmoc-chemistry using a Wang resin as solid support and HOBt and DIC as activating agents in DMF. The RGD-peptide was located at the C-terminal part, then a 3 kD Fmoc-protected polyethylenglykol-spacer was introduced using HATU (*O*-(7-Azabenzotriazo-1-yl)-*N,N,N',N'*-tetramethyluronium hexafluorophosphat). After deprotection a lysine with DDE-protected side change was coupled followed by an aminohexanoic acid spacer. The N-terminal part of the construct consists of a GCN4-peptide either or mutated variants to generate different binding forces to the artificial antibody fragment (Table 1).

The N-terminal tyrosine was introduced as Boc-protected amino acid. After deprotection of the DDE protected lysine by the application of 2% hydrazine in DMF 5(6)-carboxyfluoresceine was linked to the Lys-side chain. After TFA cleavage peptides were purified by HPLC and analyzed by SDS-PAGE applying the protocol given[8] (Fig. 2A).

Since the affinity of the native GCN4 to the antibody fragment is very high, two different leucine residues, either Leu 3 or Leu 10, were replaced by alanine to generate lower binding forces. To investigate the affinity of all three variants, the antibody fragment was detached to a PDMS-stamp as described in Ref[5]. In the first step an amino silane was coupled to the stamp, the amino group enables the attachment of an NHS-PEG-maleimide (5 kD). The antibody fragment was than linked to the maleimide function by the thiol group of the N-terminal Cys-residue. The force balance can then be applied to the stamp in different concentrations (10 nM-10 μM) in order to investigate the affinity of the GCN4 variants to the applied receptor fragment (Fig. 2B). The detection occurred by fluorescence readout. Both mutations lead to a dramatic loss of affinity, whereas the variant Leu3Ala shows at least a weak binding at a concentration of

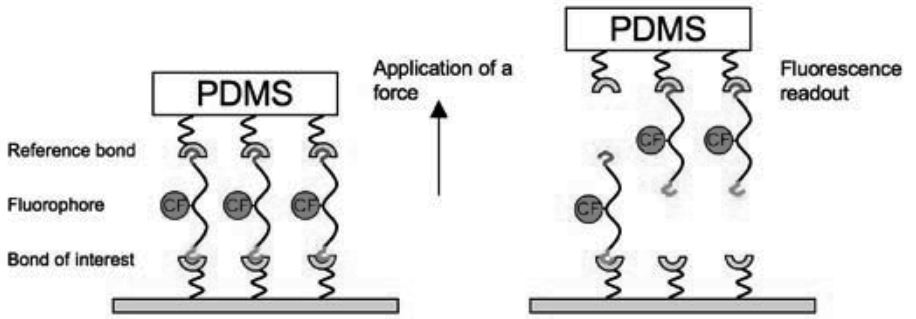

Figure 1. Principle of molecular force balance based on peptide epitopes.

Table 1. Amino acid sequences of the synthesized peptides. The introduced mutations of leucine 3 and 10 of the GCN4-peptide (left) to alanine are coloured red, the CF-labelled lysine is coloured magenta and the RGD-sequence blue

Peptid	Sequence
RGD-GCN4	YHLENEVARLKK-Ahx-K(CF)-PEG-TGRGDSPA
RGD-GCN4 Leu10Ala	YHLENEVARAKK-Ahx-K(CF)-PEG-TGRGDSPA
RGD-GCN4 Leu3Ala	YHAENEVARLKK-Ahx-K(CF)-PEG-TGRGDSPA

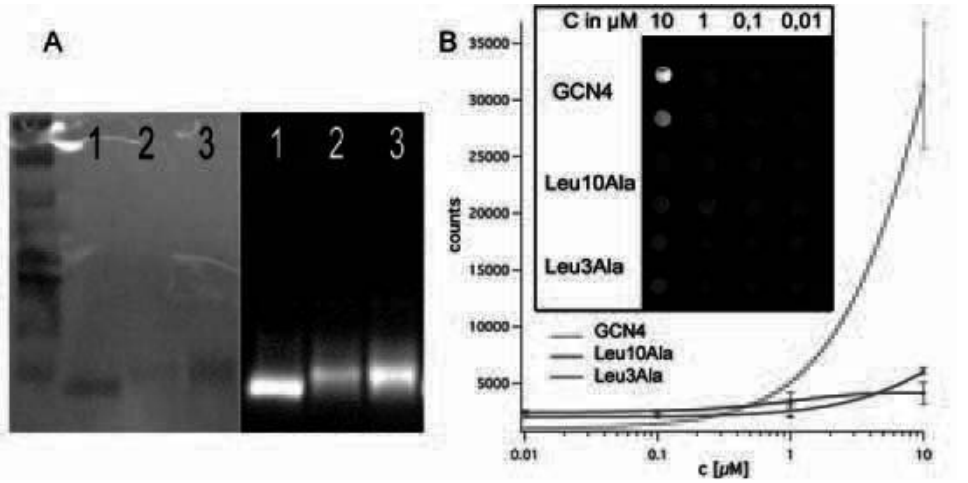

Figure 2. A) Tricine gel after Coomassie-staining (left) and after investigation using a fluorescence scanner (exitation 488 nm, emission 535 nm). 1 - RGD-GCN4 (M = 5483 Da), 2 - RGD-GCN4 Leu10Ala (M = 5455 Da), 3 -RGD-GCN4 Leu3Ala (M = 5455 Da) B) Binding of the peptidic force balances to GCN4 antibody fragments immobilized on PDMS-stamps. Both GCN4 variants Leu3Ala and Leu10Ala show a strongly decreased binding to the immobilized antibody-fragment.

10 µM. First stamping experiments versus cells expressing the RGD-receptor showed, that the RGD-peptide receptor interaction is too weak to compare it with the very strong GCN4-peptide antibody interaction, because all of the CF-labelled constructs remained on the stamp and no fluorescence could be detected on the cells (Data not shown). In order to apply the force balance system for this system, further GCN4 mutations should be generated, which provide a weakening of the interaction and which do not lead to a complete loss off the affinity. Furthermore mutations of the antibody fragment with lower affinity to the GCN4 could be generated.

Acknowledgement

This work was supported by the Nanosystems Initiative Munich.

References

1. Albrecht C, Blank K, Lalic-Mülthaler M, Hirler S, Mai T, Gilbert I, Schiffmann S, Bayer T, Clausen-Schaumann H, Gaub HE. DNA: A Programmable Force Sensor. *Science* **301**: 367-370, 2003.
2. Blank K, Mai T, Gilbert I, Schiffmann S, Rankl J, Zivin R, Tackney C, Nicolaus T, Spinnler K, Oesterhelt F, Benoit M, Clausen-Schaumann H, Gaub HE. A force-based protein biochip. *Proc Nat Acad Sci* **100**: 11356-11360, 2003.
3. Dose C, Ho D, Gaub HE, Dervan PB, Albrecht CH. Recognition of "mirror-image" DNA by small molecules. *Angew Chem* **46**: 8384-8387, 2007.
4. Albrecht CH, Clausen-Schaumann H, Gaub HE. Differential analysis of biomolecular rupture forces. *J Phys Condens Matter* **18**: 581-599, 2006.
5. Morfill J, Blank K, Zahnd C, Luginbühl B, Kühner F, Gottschalk KE, Plückthun A, Gaub HE. Affinity-Matured Recombinant Antibody Fragments Analyzed by Single-Molecule Force Spectroscopy. *Biophys J* **93**: 3583-3590, 2007.
6. Zahnd C, Spinelli S, Luginbühl B, Amstutz P, Cambillau C, Plückthun A. Directed in Vitro Evolution and Crystallographic Analysis of a Peptide-binding Single Chain Antibody Fragment (scFv) with Low Picomolar Affinity. *J Biol Chem* **279**: 18870-18877, 2004.
7. Hapke S, Kessler H, Arroyo de Prada N, Benge A, Schmitt M, Lengyel E, Reuning U. Integrin avb3/Vitronectin Interaction Affects Expression of the Urokinase System in Human Ovarian Cancer Cells. *J Biol Chem* **28**: 26340-26348, 2001.
8. Schagger H, Von Jagow S. Tricine-sodium dodecyl sulfate-polyacrylamide gel electrophoresis for the separation of protein in the range from 1 to 100 kDa. *Anal Biochem* **166**: 368-379, 1987.

3-13-108

Totally synthetic collagen-like gels by intermolecular folding of designed peptides

Yamazaki, Chisato M[1,]; Asada, Shinichi[2]; Kitagawa, Kouki[2]; Koide, Takaki[1]*

[1]Waseda University, Department of Chemistry and Biochemistry JAPAN; [2]Niigata University of Pharmacy and Applied Life Sciences, Faculty of Pharmaceutical Sciences, JAPAN

[*]E-mail: monco1981@toki.waseda.jp

Introduction

Development of artificial collagens to replace the animal-derived collagens presents a challenge in the formation of safer and functional biomaterials. We report here the development of collagen-like gels by means of the self-assembly of chemically synthesized peptides (Fig. 1).

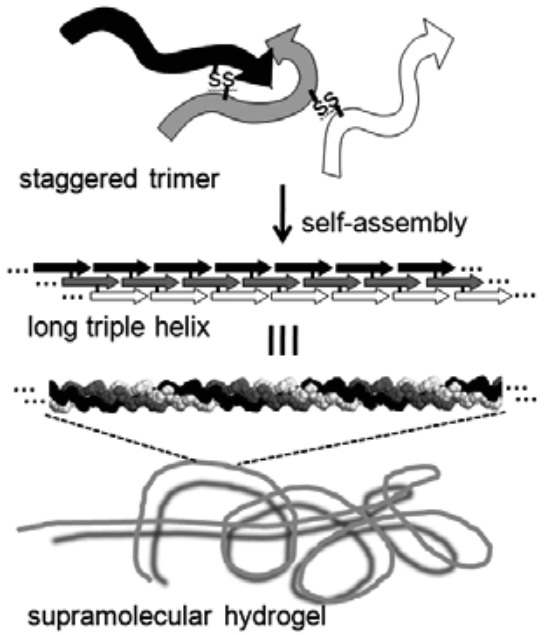

Figure 1. Concept for the formation of artificial collagen gels by self-assembling of staggered trimers.

Results and Discussion

The peptides **1**, **2**, and **3** are disulfide-tethered trimers of 27-mer peptides comprised of collagenous Gly-Pro-Hyp (4-Hydroxyproline) triplet repeats (Fig. 2). Between the adjacent peptide strands, 12 to 18 residue-staggers were introduced to create self-complementary cohesive ends. These self-complementary peptides are able to form elongated supramolecular architectures through spontaneous self-assembling process.[1,2] Peptide **4**, corresponding to the structure of a single-chain precursor of the staggered trimers is a conventional open-chain collagen model that spontaneously trimerizes with forming the triple-helical structure. This peptide was used as an experimental control.

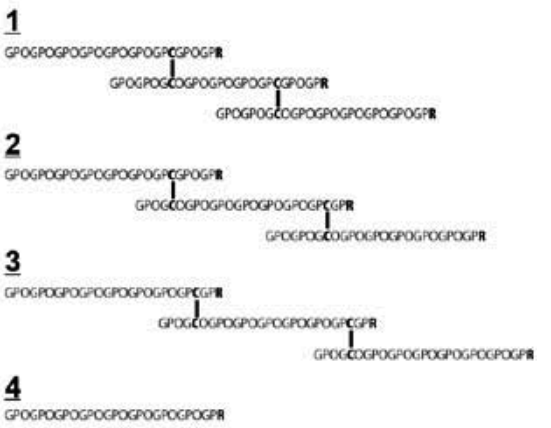

Figure 2. Structure of the staggered trimers synthesized in this study. G, glycine; P, proline; O, 4-hydroxyproline; C, cysteine; R, arginine.

Single-chain precursors of the trimeric peptides were synthesized using the standard *N*-(9-fluorenyl) methoxycarbonyl-based solid-phase method. Heterotrimeric assembly of such peptide strands was achieved by regioselective disulfide bond-formation involving stepwise activation of Cys side-chains.[3]

Circular dichroism spectroscopic analysis showed the existence of collagen-like triple helix in peptide **1**, **2**, and **3**, and the spectra were very similar to that of peptide **4** (data not shown). Since peptide **1**, **2**, and **3** could not fold intramolecularly, these peptides were suggested to form elongating supramolecules *via* intermolecular triple helix-formation as illustrated in Fig. 1. The melting temperatures (T_m) for the triple helices of **1**, **2**, **3**, and **4** were estimated to be 32, 36, 41.5, and 48 °C, respectively (data not shown). It should be noted that the stability of the triple helices of the supramolecules is positively correlated with the length of the chain staggers in the trimeric peptide units.

Upon cooling the aqueous solutions of peptide **1**, **2**, and **3**, peptide hydrogels formed (Fig. 3). On the other hand,

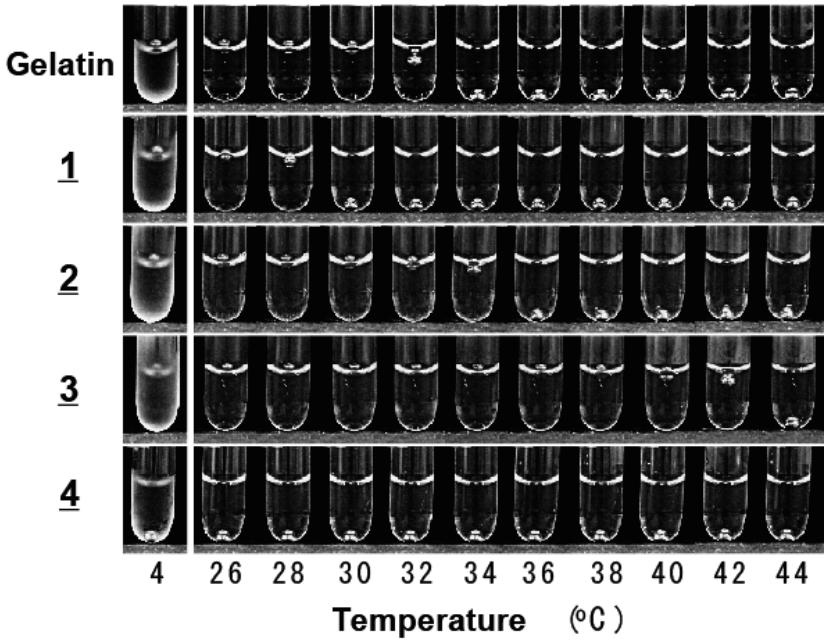

Figure 3. Thermal stability of the peptide hydrogels. A stainless steel ball was placed on the gel surface at 4 °C. The tubes were incubated for 10 minutes at indicated temperatures before taking photographs.

the solution of the corresponding open-chain peptide **4** did not. Similar to gelatin gel, the peptide hydrogels melted at high temperature, and the thermal gel-sol transition was observed to be reversible. These observations also indicated the formation of supramolecular architectures *via* elongating peptide self-assembly concomitant with triple helix-formation.

The thermal stabilities of the hydrogels were analyzed by monitoring the sinking of stainless balls place on the gels. The sol-gel transition temperatures (T_{gel}) for the 10% (w/v) hydrogels of peptides **1**, **2**, and **3** and **gelatin** were estimated to be 29, 36, 43, and 32 °C, respectively (Fig. 3). These T_{gel} values for the peptide hydrogels were positively correlated to the T_m values of triple helices in solution.

The use of synthetic peptides as building blocks will allow further functionalization of the artificial collagen by incorporating specific sequences, such as receptor-binding motifs found in native collagen. This concept for the totally synthetic artificial collagen gel presented here offers a novel strategy toward the development of innovative biomaterials.

Acknowledgement

This work was supported in part by Grant-in-Aid for Scientific Research (No. 19390032) from Japan Society of the Promotion of Science (JSPS), and by the Cosmetology Research Foundation. C. M. Y. thanks the support from The Sasagawa Scientific Research Grant (No. 19-318) of The Japan Scientific Society, Global COE Program of MEXT Japan, and JSPS Research Fellowships for Young Scientists.

References

1. Koide T, Homma DL, Asada S, Kitagawa K. Self-complementary peptides for the formation of collagen-like triple helical supramolecules. *Bioorg Med Chem Lett* **15**: 5230-5233, 2005.
2. Kotch FW, Raines RT. Self-assembly of synthetic collagen triple helices. *Proc Natl Acad Sci U S A* **103**: 3028-3033. 2006.
3. Ottl J, Moroder L. Disulfide-bridged heterotrimeric collagen peptides containing the collagenase cleavage site of collagen type I. synthesis and conformational properties. *J Am Chem Soc* **121**: 653-661, 1999.

3-13-109

Towards a fully synthetic "phage-display like" system for high-throughput screening

Khandadash, Raz[1]; Partouche, Shirly[1]; Margel, Shlomo[2]; Byk, Gerardo[1,]*

[1]Bar Ilan University/Dept. of Chemistry, Laboratory of Nano-Biotechnology, ISRAEL; [2]Bar Ilan University/Dept. of Chemistry, Laboratory of Polymers, ISRAEL

[*]E-mail: bykger@mail.biu.ac.il

Introduction

Phage display random peptide libraries represents the unique available tool for *in vivo* high throughput combinatorial screening.[1] This technology opened new gates towards tissue/cell specific targeting and allowed new strategies for drug targeting and diagnostics. However, this approach is intrinsically limited to the identification of peptides which are prone to be rapidly degraded *in vivo*. A novel strategy for high-throughput identification of targeting non peptide ligands is of great importance for drug discovery, diagnostics, drug delivery and gene delivery.

Results and discussion

The present work aims to develop a new platform for selecting molecules that home to a selected organ or tissue *in vitro* and *in vivo* and methods of identifying them. Finding new specific prostate cancer cell ligands are of particular interest. Thus, ligands targeted to these cells will allow a selective localization of a therapeutic drug in the tumor area. Coupling of these ligands to chemotherapeutic agents, will promote the specific elimination of these rapidly growing tumor cells, thereby resulting in tumor reduction or elimination. Here, we introduce a fully synthetic "phage display like" system aimed at overcoming the intrinsic limitation of phage display libraries to exclusively produce peptides. As a first proof of concept, we have synthesized mono-dispersed cross-linked microspheres with a narrow size distribution of 2 ± 0.2 μm bearing different intensity-levels of FITC suitable for flow-cytometry analysis as mixtures (Fig. 1, left pannel).

The synthetic system possesses also a magnetic arm that can be used for tracing (using MRI) and for separation of microspheres from tissues. In order to assess our screening concept we have synthesized on the microspheres DUP-1, a prostate carcinoma binding peptide (FRPNRAQDYNTN) recently shown to have specificity for tumor cell lines such as PC-3.[2] As negative control a non related peptide called here 15-mer with no affinity for PC-3 cells was also synthesized on the microspheres. These model peptides bound to the microspheres were used as a tumor-selective specific binding prototype: the affinity of the DUP-1 microspheres to PC-3 cells was assayed as compared to naked microspheres and microspheres bearing the non related 15-mer peptide which were administered as mixtures. Naked, DUP-1 and 15-mer microspheres bearing each of them a different intensity FITC-tag, were mixed together and the ratio of each population was measured by passing the mixtures through the flowcytometer prior to incubation with cells. This procedure allowed to obtain the starting ratio. Then, the mixture was incubated on PC-3 cells under classical conditions and washed to eliminate the non specific microspheres. Finally, the cells were lysed and the remaining microspheres analysed by flowcytometry. The ratio of the mixture after incubation was compared to the starting ratio and the ranking of the different microspheres could be established. Results in Fig. 1 (right panel) clearly demonstrate the specific affinity of DUP-1 as compared to 15-mer peptide and naked microspheres. In the next step, we have synthesized two convoluted combinatorial positional peptide libraries derived from DUP-1 on differentially tagged microspheres where [2]Arg and [5]Arg were replaced by a mixture of 19 amino acids at a time (Table 1).

These libraries were screened for binding to prostate cancer model cells PC-3 using flow-cytometry as compared to the DUP-1 microsphere control in the same way. Library I displayed enhanced affinity as compared to DUP-1 and Library II (Fig. 2).

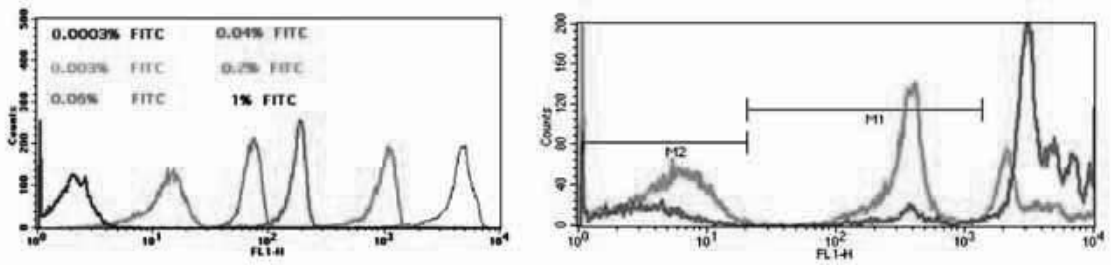

Figure 1. *Typical flowcytometry plots of microspheres.* Left panel: FACS analysis of FITC-intensity tagged microsphere mixtures, right panel: FACS analysis before (clear) and after (dark) incubation of mixture of DUP-1, 15-mer peptide [M1] and PCMS [M2] microspheres.

Table 1. Sequences of convoluted libraries, X stands for 19 amino acids (Cys excluded). Arg2 and Arg5 were replaced by mixture X of 19 natural amino acids.

#	Sequence	Symbol and tag intensity
DUP-1	FRPNRAQDYNTN	SMN-2101-A -0.2% FITC
Library I	FXPNRAQDYNTN	SMN-2101- C- 1% FITC
Library II	FRPNXAQDYNTN	SMN- 2101-B-0.04% FITC

Deconvolution of library I resulted in two peptides with high affinity for PC-3 cells as compared to model peptide DUP-1: ^{2}Ala and ^{2}Lys.

Finally, a small molecules library generated by the known Ugi-reaction[3] was covalently bound to the same tagged microsphere system by attachment of a free amine function in the Ugi molecules to a free carboxylate on the microspheres. These microsphere were analyzed as mixtures including DUP-1 standard microspheres on the same cell-based bioassay using the fluorescent code tags. These experiments allowed us to identify compound 2-D having affinity for PC-3 cells in a competitive manner with DUP-1 peptide (Table 2).

Overall, this work demonstrates that synthetic "phage-like" systems can be developed on the base of nano/microspheres including direct synthesis on them. These "phage like" systems can be used in the future for high throughput *in vitro*/*in vivo* screening of non peptide small molecules.

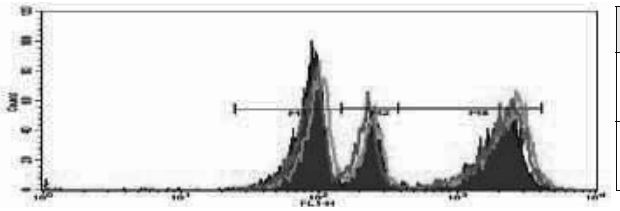

Plot type	Symbol	Marker	% Gated
Before (purple line)	SMN-2101-B	M1	44
	SMN-2101-A	M2	17
	SMN-2101-C	M3	38
After (pink and green plot)	SMN-2101-B	M1	36.6
	SMN-2101-A	M2	19.4
	SMN-2101-C	M3	43

Figure 2. *FACS Screening of Libraries I and II for affinity to PC-3 cells as compared to DUP-1*. Left panel: dark-full plot stands for the initial ratio of the populations, clear empty plots: ratio of populations after incubation with PC-3 cells and repeated washes. Right panel: analysis of results in percentage. Library I gives high score as compared to DUP-1 microspheres.

Table 2. *Ugi library bound to microspheres*. Left panel: Overall affinity ranking obtained by FACS screening on PC-3 cells as compared to DUP-1 microspheres. Right panel: structure of the candidate molecules.

Molecule candidate	Before incubation CL# / DUP	After incubation CL# /DUP	After/ Before
2 A	1.14	0.89	0.78
2 B	1.35	1.16	0.85
2 C	1.12	0.92	0.82
2 D	**1.43**	**1.45**	**1.01**
2 E	1.51	1.45	0.96
2 F	1.63	1.4	0.85
2 G	1.29	0.91	0.70
2 H	1.51	0.92	0.60
2 I	1.84	0.65	0.35
2 J	1.62	1.04	0.64

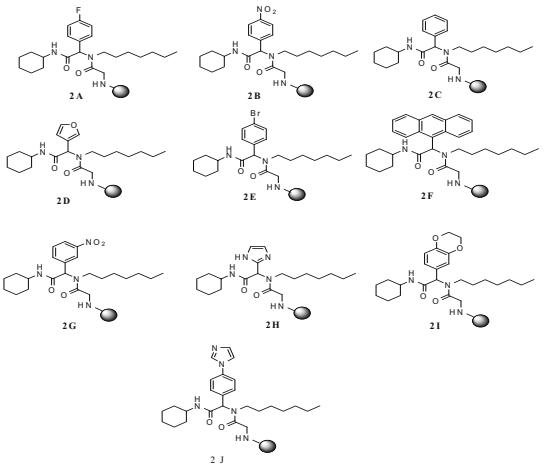

Figure 3.

Acknowledgements

This work was supported in part by U.S.-Israel Bi-National Science Foundation [1998378], by AFIRST Israel/France and by The Marcus Center for Medicinal Chemistry. R. Khandadash is indebted to the President of BIU for a Presidential PhD fellowship.

References

1. Pasqualini R, Koivunen E, Ruoshlati E. *Nature Biotech* **15**: 542-515, 1997.
2. Zitzmann S, Mier W, Schad A, Kinscherf R, Askoxylakis V, Kraemer S, Altmann A, Eisenhut M, Haberkorn U. *Clin Cancer Res* **11**: 139-146, 2005.

3-14-110

Molecular-weight distribution and structural transformation in water-soluble conjugates of poly(acrylic acid) and synthetic peptide

Mansuroglu, Banu; Topuzogullari, Murat; Akdeste, Zeynep*

Yildiz Technical University, Faculty of Chemical and Metallurgical Engineering, Department of Bioengineering, TURKEY

**E-mail: banumansur@gmail.com*

Introduction

Water-soluble and insoluble protein–polyelectrolyte complexes as functional biopolymer systems represent a specific class of polymer–protein compounds that have important applications in various areas. Poly(acrylic acid) (PAA) is a well known bioactive polymer (bioadhesive nano- and microparticles, pH-sensitive PAA grafted poly(vinylidene fluoride) membrane bags, ultrafine cellulose fiber surfaces grafted with PAA for enzyme immobilization, PAA–polyvinylpyrrolidone biopolymeric systems for the treatment of the dry eye, etc. PAA, their alkyl-esters and non-toxic copolymers with vinyl pyrrolidones are strong adjuvant for primary and secondary responses and that they are promising alternatives to the mineral oil-based adjuvants presently used in various veterinary vaccines.[1,2,3] In this study, the interaction between peptide epitops of VP1 protein of foot- and mouth disease (FMDV) and poly(acrylic acid) will be discussed on the basis of the experimental results obtained by the size-exclusion chromatography (SEC) with on-line quadruple detection system: UV absorption (UV), refractive index (RI), right angle light scattering (LS) and viscosity (VIS) detectors and the binding coefficient, i.e., the binding ratio of peptide to poly(acrylic acid).

Results and discussion

PAA was purchased from Sigma-Aldrich and weight average molecular weight (Mw) of this polymer was 100 kDa. Peptides containing the VP1 epitope (170-188) (Trp-Ala-Thr-Asp-Ile-Ser-Glu-Leu-Leu-Val-Arg-Met-Lys-Arg-Ala-Glu-Leu-Tyr-Cys-Pro) were synthesized by using the continuous solid-phase method by Sigma Gynosys. Covalent conjugates of PAA and peptide with different ratios of $C_{Peptide}/C_{PAA}$ was prepared using carbodiimide linker. Covalent conjugates of poly(acrylic acid)-peptide were analyzed using SEC with quadruple detection to study the composition and structure of the molecule. PAA, which has a ratio ($C_{Peptide}/C_{PAA}$) zero, is characterized by one peak (RV=10,9 mL) in all chromatograms and very low UV absorption in the UV

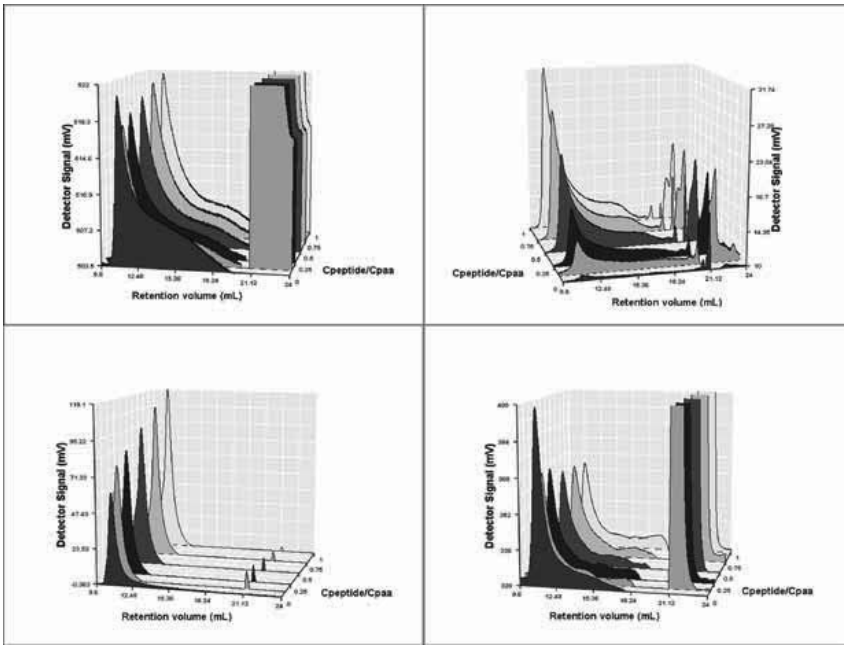

Figure 1. Refractive index (RI), UV (280 nm), Light scattering (LS) and Viscosity (VIS) chromatograms of covalent conjugates of polyacrylic acid-peptide prepared at the ratios of $C_{Peptide}/C_{PAA}$ = 0; 0,1; 0,25; 0,5; 0,75; 1.

chromatogram acquired at 280 nm. After conjugation of PAA with peptide, the system is characterized by two peaks (Fig. 1). The peak (Peak I) eluting firstly from the column has the same retention volume of PAA, and the second peak (Peak II) has a retention volume of 21,5 mL, which shows the unconjugated peptides. In the UV chromatograms of PAA-peptide bioconjugates solutions, peak I has an increased area which is dependent on the UV absorption of peptides bound to the polymer molecules. In addition, areas of peak I in LS chromatograms are increased upon conjugation of PAA and peptide. LS signal is related to the molecular weight of the molecule. It may be assumed from these results that peak I in chromatograms correspond to PAA-Peptide bioconjugates.

Fig. 2 shows the dependency of areas of peak I on the ratio of $C_{Peptide}/C_{PAA}$. In RI chromatograms, peak areas are increased after conjugation which is the result of the change of dn/dc value of the molecule. Signal of RI detector is related to the concentration and the dn/dc value of the solution. Composition of the molecule is one of the effects that change the dn/dc value. Area of peak I in UV chromatograms are increased linearly with increase in the $C_{Peptide}/C_{PAA}$ ratio due to the UV absorption of peptides bound to PAA, while free peptide molecules coexist with PAA-Peptide bioconjugates. Area of peak I in LS chromatograms increases similar to UV chromatograms, which indicates the Mw increase of PAA-peptide bioconjugates. In addition to UV and LS chromatograms, area of peak I is increased in VIS chromatograms, but after the ratio of $C_{Peptide}/C_{PAA}$=0,5 area is decreased. VIS signal is associated with viscosity and concentration of molecules. Viscosity of a polymer solution depends on the size and shape of the molecule.

The values of the weight-average molecular weight, number-average molecular weight and hydrodynamic radius of PAA and PAA-Peptide bioconjugates are shown in Table 1. Molecular weight values of bioconjugates are increased with increased ratio of $C_{Peptide/}C_{PAA}$, which indicates binding of the peptides to poly(acrylic acid) molecules. There is a linear relation between the ratio of $C_{Peptide}/C_{PAA}$ and molecular weight. Hydrodynamic radius of PAA is decreased by the binding of the peptide, but increase in the number of bound peptides caused a slight increase in radius. In addition, polydispersity index of the bioconjugates are decreased by the conjugation of peptide to PAA. a exponent of Mark-Houwink equation is related to the shape of the polymer molecule. Values of a exponent changes between 0 and 2. When value of a exponent is close to 0, molecule becomes sphere-like, a more compact, shape. Binding of peptides to PAA molecule caused a change in the structure of PAA molecule from random-coil to a more compact, sphere-like, shape. Compactization of the polymer chain can be explained by hydrophobic interactions of bound peptide molecules and intra-polymer cross-linking of PAA chain via peptide molecules. The peptide can covalently be linked to two carboxylate groups of PAA chain, since

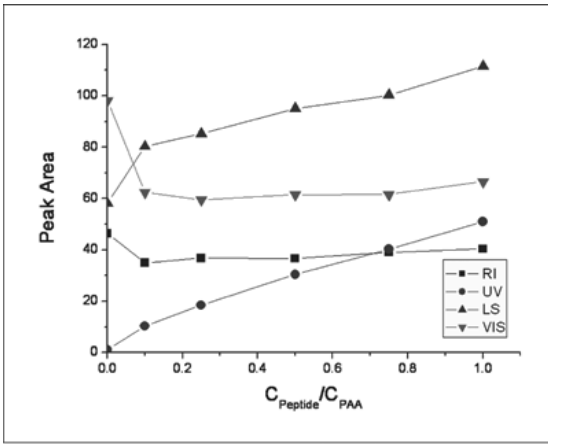

Figure 2. Dependence of peak areas (peak I, RV=10,9 mL) acquired from RI, UV, LS and VIS chromatograms on ratios of $C_{Peptide}/C_{PAA}$.

170-188 sequence of FMDV has two amine groups, N-terminus of the peptide and ε-amino group of lysine residue.

Table 1. Hydrodynamic radius (Rh), Mw, Mn, a exponent of Mark-Houwink equation and polydispersity index (Mw/Mn) values for PAA and PAA-Peptide conjugates.

$C_{peptide}/C_{PAA}$	Rh (nm)	Mw (Da)	Mn (Da)	α	Mw/Mn
0	10,60	102596	23916	0,489	4.25
0,1	9,283	175569	54325	0,374	3,23
0,25	9,186	198138	56551	0,366	3,50
0,5	9,623	257653	98132	0,277	2,63
0,75	9,594	279067	95330	0,286	2,93
1	9,992	302860	123276	0,382	2,46

Acknowledgements

This research was supported by grant from T.R. Prime Ministry State Planning Organization (Project No. 25-DPT-07-04-01.

References

1. Topuzogullari M, Çimen NS, Mustafaeva Z, Mustafaev M. *Eur Pol J* **43**: 2935-2946, 2007.
2. Qian RL, Mhatre R, Krull IS. *J Chromatogr A* **787**: 101–109, 1997.
3. Kendrick BS, Kerwin BA, Chang BS, Philo JS. *Anal Biochem* **299**: 136–146, 2001.

3-15-111

A new stable Copper(III)/Cyclopeptide complex: structural characterization by XANES and EXAFS studies

Pratesi, Alessandro[1,]; Giuli, Gabriele[2]; Cicconi, Maria Rita[2]; Pratesi, Giovanni[3]; Ginanneschi, Mauro[1]*

[1]University of Firenze, PeptLab, Dipartimento di Chimica Organica, ITALY; [2]University of Camerino, Dipartimento di Scienze della Terra, ITALY; [3]University of Firenze, Dipartimento di Scienze della Terra, ITALY

[*]E-mail: alessandro.pratesi@unifi.it

Introduction

Cyclic peptides are important tools in medicinal chemistry, as their constrained geometry allows conformational investigations for structure-activity relationship studies in the characterization of the active site of proteins. In particular, His-containing peptides play an important role in studying copper complexation as they are very often mimicking the binding sites of etalloproteins. We use l or d isomers of His in the sequence to study the stereochemical effects on chelating ability. This amino acid links metals ions, in particular Cu(II), in a strong way, by his imidazolic N^3 (Nπ) which originates a high stably six-membered ring with the relevant peptide NH in the linear sequences at pH > 4.[1,2] A series of 13-membered ring cyclic tetrapeptides was synthesized by the SPPS method, and their copper(II) coordination properties analyzed by X-ray Absorption Spectroscopy (XAS).

Results

In order to specifically assess the effects of the metal binding cavity on the copper binding properties, we synthesized the cyclopeptides showed in Fig. 1. The syntheses were performed by solid-phase peptide technique (SPPS), anchoring the Fmoc-His-Al or Fmoc-Lys-Al side-chains to a trityl-type resin.[3] The linear peptides had NH_2 and COOH groups ready for the cyclization that was performed in the pseudodilution conditions with no evidence of polymerization or cyclooligomerization by-products.[4]

Preliminary investigation of the Cu(II) coordination properties of compounds **1**, **2** and **3** gave evidence of the formation of a stable Cu(III) complex at alkaline pH. Now, through the use of the XAS technique, we confirm the previous results. X-Ray Absorption Spectroscopy data have been collected at the ID26 beamline of the ESRF storage ring (Grenoble, Fr). Cu K-edge XANES (X-ray Absorption Near Edge Structure) and EXAFS (Extended X-ray Absorption Fine Structure) step scan spectra were acquired in fluorescence mode, monitoring the emitted fluorescence signal with a high-purity multi-element Ge detector. Radiation was monochromatised by means of a double-crystal Si(311) monochromator to achieve high-energy resolution at the Cu K-edge. In order to minimize the radiation induced damage of the samples, spectra have been collected at 10 K in a He cryostat, and the intensity of the incident radiation at the sample has been adjusted by means of Al filters. Preliminary time scans allowed to ascertain that the samples suffered no damage within 1300 seconds exposure to the X-ray beam. For each sample 1000 seconds long spectra have been acquired at different sample positions in order not to alter the sample. Average of 10 scans allowed to obtain a good signal to noise ratio for all the samples.

XANES and EXAFS spectra of DK13; LK13 and GK13 peptides were collected at low temperature for studying the oxidation state of copper, the average Cu-N distance, and to get information on the local geometry around copper as a function of the peptides sequency.

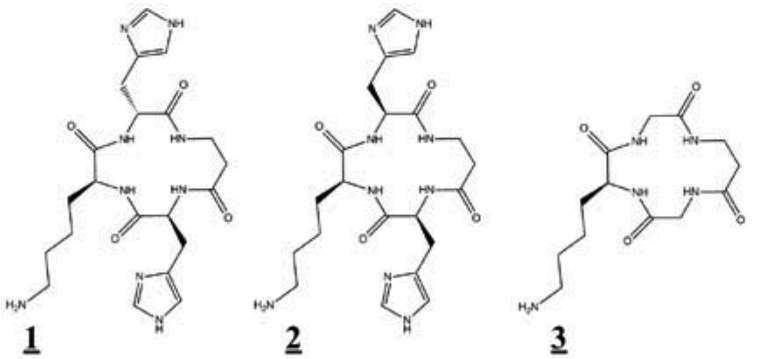

Figure 1. *c*(Lys-dHis-βAla-His) DK13 (1); *c*(Lys-His-βAla-His); LK13 (2); *c*(Gly-βAla-Gly-Lys) GK13 (3).

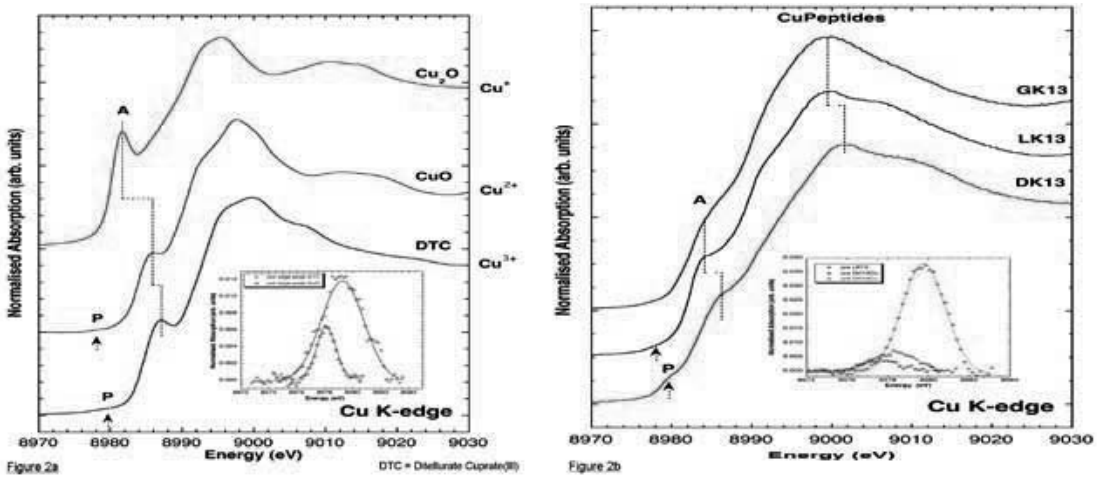

Figure 2. Cu K-edge XANES spectra of selected Cu model compounds with different oxidation state (2a) and Cu K-edge XANES spectra of DK13; LK13 and GK13 copper complexes (2b).

To this aim, also a suite of well characterised copper model compounds with known oxidation state (Cu^{+}, Cu^{2+} and Cu^{3+}) and coordination geometries (linear, tetrahedral, square pyramidal, octahedral) were studied allowing to parametrise pre-edge peak intensity and energy, edge energy, and other spectral features as a function of oxidation state. Moreover, theoretical XANES calculations are being performed on model compounds in order to test how confidently the experimental features can be reproduced. Then, calculations will be carried out on the peptides in order to get information on the local geometry. The model compounds showed a consistent shift in the edge energy as a function of Cu oxidation state. Moreover, there also a shift of a peak in the edge region (labelled A in Fig. 2). However, in order to quantify relative abundances of Cu^{2+} and Cu^{3+} we found that pre-edge peak (labelled P in Fig. 2a-2b inset) is much more useful. In particular, monovalent Cu compounds do not display pre-edge peak (as expected for a d^{10} compound), whereas divalent Cu compounds display a well defined pre-edge peak consistently at 8978 eV (integrated area =0.01) and trivalent model compounds display a pre-edge peak shifted at higher energy (8979.3 eV) and with a higher integrated intensity (0.04). Despite the very low pre-edge peak intensity, the very good signal to noise ratio of the collected spectra allow to discriminate perfectly the pre-edge peaks of the samples investigated.

Discussion

Two of the investigated cyclopeptides (**1** and in less extent **2**) showed pre-edge peak energy position and integrated intensity consistent with those of Cu^{3+} model compounds. Also edge energy is consistent with the presence of trivalent copper complex. While the DK13 favoured the oxidation of Cu(II) to Cu(III), in LK13 the oxidation state seemed to be correlated to the different His stereochemistry (l in this case). The ligand GK13, devoid of the His, did not promoted the oxidation Cu(II) → Cu(III) despite the fact that the size of the ring is the same. This is certainly due to the absence of imidazole rings, that play a key role in copper autooxidation. EXAFS spectra also show well definite oscillations well above noise level up to 10 $Å^{-1}$. EXAFS data analysis and calculation of theoretical XANES spectra are currently in progress in order to get information on the Cu-N inter-atomic distances and Cu coordination geometry.

In conclusion, also on the basis of our previous studies on cyclopeptides/copper systems, we suggest that the copper(III) ion is at the centre of the ligand's cavity being coordinated to four deprotonated amide nitrogens. This donor set would greatly lower the redox potential for the Cu(III)/Cu(II) couple thus allowing easy oxidation of the coordinated copper(II) by atmospheric oxygen.

Acknowledgments

This work was supported by Ente Cassa di Risparmio di Firenze and MIUR funds (Prin 2005).

References

1. Casolaro M, Chelli M, Ginanneschi M, Laschi F, Muniz-Miranda M, Papini AM, Sbrana G. *Spectrochim Acta* **55A**: 1675-1689, 1999.
2. Daniele PG, Zerbinati O, Aruga R, Ostacoli G. *J Chem Soc Dalton Trans* **5**: 1115-1120, 1988.
3. Sabatino G, Chelli M, Mazzucco S, Ginanneschi M, Papini AM. *Tetrahedron Lett* **40**: 809-812, 1999.
4. Pratesi A, Zanello P, Giorgi G, Messori L, Laschi F, Casini A, Corsini M, Gabbiani C, Orfei M, Rosani C, Ginanneschi M. *InOrg Chem* **46**: 10038-10040, 2007.

3-15-112

The role of deiminated protein antigens in the diagnosis of Rheumatoid Arthritis

Magyar, Anna[1,]; Neer, Zsuzsa[2]; Szarka, Eszter[3]; Hudecz, Ferenc[4]; Sarmay, Gabriella[3]*

[1]HAS-ELTE, Research Group of Peptide Chemistry, HUNGARY; [2]Research Group HAS-ELTE, 3Institute of Biology Department of Immunology, HUNGARY; [3]Research Group HAS-ELTE, Institute of Biology Department of Immunology, HUNGARY; [4]ELTE, Institute of Chemistry, HUNGARY

[*]E-mail: magyar@elte.hu

Introduction

Rheumatoid arthritis (RA) is a chronic inflammatory condition. Autoantibodies directed against the citrulline-containing peptide (ACPA) have high specificity of RA. Citrullinated proteins are formed by posttranslational modification, namely by deimination of arginine residues in protein sequences by peptidylarginine deiminase enzymes (PADI). Autoantibodies to deiminated (citrullinated) proteins are the most specific serological markers of RA. Rheumatoid arthritis symptoms develop gradually and it is difficult to date the beginning of the disease precisely. These antibodies are detectable years before the first clinical symptoms of the disease. Many serological markers of RA have been described over the past half century: rheumatoid factor (RF) and antibodies against a range of citrullinated proteins such as filaggrin,[1,2] fibrin[3] and vimentin (anti-Sa antibody).[4] The aim of our study was to identify epitopes of vimentin and filaggrin derived-peptides targeted by RA specific antibodies to provide further information about the nature of the initial autoantigenic substance.

Results and discussion

The identification of regions of interaction between an antigen and antibody is an important area of research in immunology. The correct identification of epitopes not only allows to map where the important regions of an antigen are located in its three-dimensional structure but more importantly, it is instrumental in the diagnosis and prognosis of disease.

Synthesis: we used solid-phase peptide synthesis (Fmoc strategy) on "MULTIPIN NCP" non-cleavable pins (Chiron Technologies) at 66 nmol scale.[5] Identification of the epitope structure of antigenic proteins represents one of the major applications of these technologies. The following side chain protecting groups were used: tBu for Ser and Thr, Trt for Gln, Pbf for Arg. Coupling was performed with DIC/ HOBt in DMF. After the final coupling cycle the Fmoc protecting groups were removed and the N-terminus of the peptides were acetylated using Ac2O-DIEA-DMF=5:1:50 (v/v/v). The side chain protecting groups were cleaved from the peptides with TFA containing 2.5% ethanedithiol and 2.5% anisole. Peptides were prepared in duplicates. Citrullinated peptides and the nonmodified counterparts containing arginine instead of citrulline residues were synthesized in order to compare their respective reactivities (Table 1.).

ELISA experiments: in the "indirect" ELISA experiments (where the different synthetic peptides were covalently attached on the pins' gears) the presence of ACPA was determined using serum samples of RA patients (50 anti-CCP3 (INOVA) positive and 43 anti-CCP3 negative) with definite RA[6] and healthy blood donors (36). *Determination of antibodies:* ELISA protocol of "Noncleavable Peptides Manual" of Mimotopes was followed by some modifications.

Statistical Analysis: we used the ANOVA analysis, for analyzing the specificity of anti-peptide antibody (RA versus each disease and healthy control group) based on clinical results, Pearson correlation test was used. To examine the correlation between the different groups Tukey post hoc test was used.

In this study we have been working with a subset of RA specific peptides containing citrulline (deiminated

Table 1. Sequences of peptides used in the experiments (X= citrulline).

Protein	Arginine containing epitope	Citrulline containing epitope
1. Filaggrin5	^{311}TRGRS^{315}	TXGRS
2. Filaggrin14	^{311}TRGRSRGRSGRSGS^{326}	TXGRSRGRSGRSGS
3. Filaggrin19	^{306}SHQESTRGRSRGRSGRSGS^{326}	SHQESTXGXSXGRSGRSGS
4. Vimentin	^{1}STRSVSSSSYRRMFG^{15}	STXSVSSSSYXXMFG
5. Collagen	^{559}ARGLTGRPGDA^{569}	AXGLTGXPGDA
6. Fibrin-alpha	^{36}GPRVVERHSACKDS^{50}	GPXVVEXHSACKDS
7. Fibrin-beta	^{60}RPAPPPISGGGYRAR^{74}	XPAPPPISGGGYXAX

arginine) which was previously identified as specific targets of the IgG autoantibody response in RA patients. In our system the selected anti-vimentin peptide/ autoantibody is also found in patients with other diseases and therefore is not specific for RA. There was no significant variation in anti-collagen, anti-fibrin-alpha, anti-fibrin-beta antibody concentrations in RA and control patients (Fig. 1A, 1B). Significant change was observed only case of filaggrin5 and filaggrin 19 between the two groups. The determination of epitopes of these proteins could be important for the development of appropriate diagnostics in this most frequent human systemic autoimmune disease.

Acknowledgements

This work was supported by National Office for Research and Technology (RET-06/2006, GVOP-3.1.1.-2004-05-0183/3.0).

References

1. Schellekens GA, de Jong BA, van den Hoogen FH, van de Putte LB, van Venrooij WJ. *J Clin Invest* **101**: 273-281, 1998.
2. Magyar A, Brózik M, Tóbi R, Szabó T, Gergely P, Merétey K, Hudecz F. SPPS London, England, 2005.
3. Chapuy-Regaud S, Nogueira L, Clavel C, Sebbag M, Vincent C, Serre G. *Clin Exp Immunol* **139**: 542-550, 2005.
4. Wernhoff P, Unger C, Bajtner E, Burkhardt H, Holmdahl R. *Int Immunology* **13**: 909-919, 2001.
5. Geysen HM, Rodda SJ, Mason TJ, Tribbick G, Schoofs PG. *J Immunol Methods* **102**: 259-274, 1987.
6. Arnett FC, Edworthy SM, Bloch DA, McShane DJ, Fries JF, Cooper NS, Healey LA, Kaplan SR, Liang MH, Luthra HS *et al*. *Arthritis Rheum* **31**: 315-324, 1988.

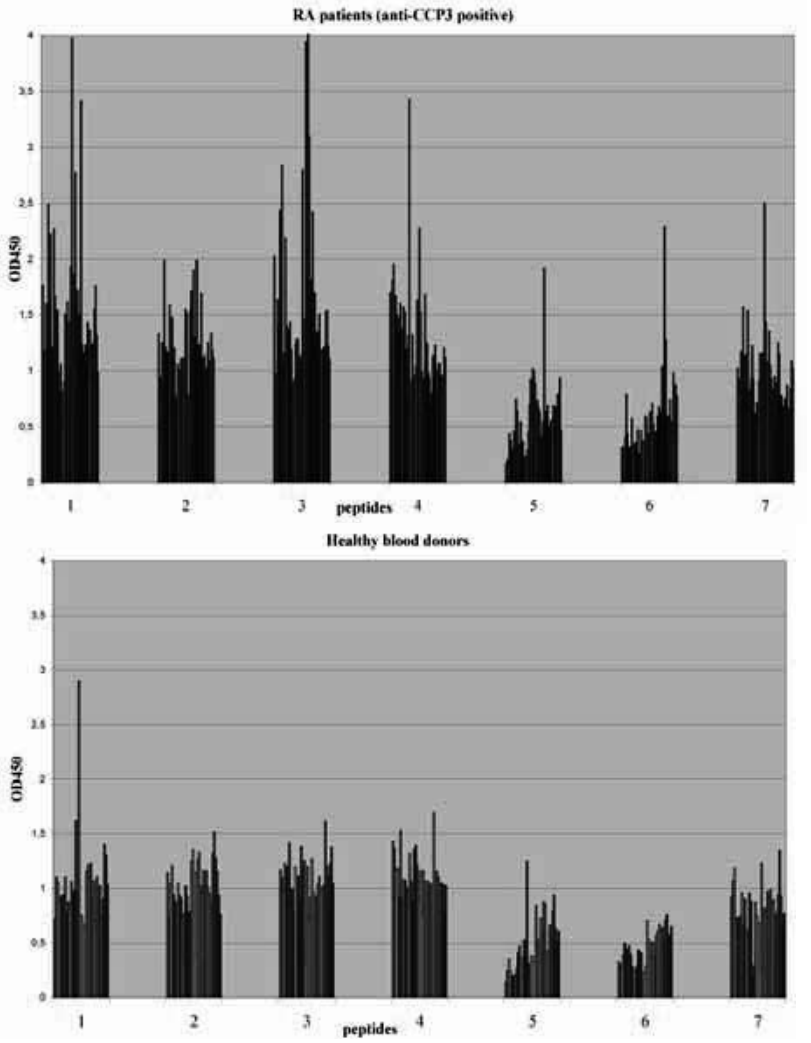

Figure 1. The ELISA results with the peptides using serum samples of anti-CCP3 positive RA patients (A) and healthy blood donors (B).

3-15-113

New selective substrates for detection of cysteine proteinases

Semashko, Tatiana[1,]; Popletaeva, Sofia[2]; Oksenoit, Elena[2]; Lysogorskaya, Elena[2]; Filippova, Irina Yu[2]*

[1]Bioengineering and Bioinformatics Department, Lomonosov Moscow State University, RUSSIAN FEDERATION;
[2]Chemistry Department, Lomonosov Moscow State University, RUSSIAN FEDERATION

[*]E-mail: t.semashko@gmail.com

Introduction

The C1 (papain) family of cysteine proteases is a numerous family of proteases, which contents both widespread plant proteases (papain, bromelain, ficin) and mammalian lysosomal proteases (cathepsins B, L, etc.).[1] At present these enzymes attract great attention in different aspects. Cheap plant enzymes papain, bromelain, ficin are used in medicine, food industry, agriculture, biotechnology, and scientific research. The major cysteine cathepsins play important role in degradation of proteins and, as was recently shown, participate in regulation of some metabolic processes. Selective detection of these enzymes is difficult because determination of their enzymatic activity is carried out using substrates also corresponding to specificity of trypsin-like enzymes.

In this work we have synthesized series of new substrates for detection of C1 family of cysteine proteinases and have studied the selectivity of substrates.

Results and discussion

The design of substrate formula was based on the differences in substrate specificity of papain-like[2] and trypsin-like enzymes. The common substrate structure is A Phe/Val-Ala-B, where A and B are protective or detective groups, Phe, Val - specific amino acids in S_2-subsite of papain-like cysteine proteases, and Ala in S_1-subsite is specific for cysteine proteases and is not suitable for trypsin-like proteases. These compounds are chromogenic Glp-Phe-Ala-pNA (I), Glp-Val-Ala-pNA (II) and fluorogenic Abz-Phe-Ala-pNA (III), Glp-Phe-Ala-AMC (IV) substrates (Abz, pNA, Glp, and AMC are *o*-aminobenzoyl, *p*-nitroanilide, pyroglutamyl, and 4-amino-7-methylcoumaride, respectively).

The peptides were obtained by a combination of chemical and enzymatic synthetic methods according to one universal scheme.[3] Peptide bond formation at the last step was performed by enzymatic technique. Reaction was carried out in organic media using chymotrypsin

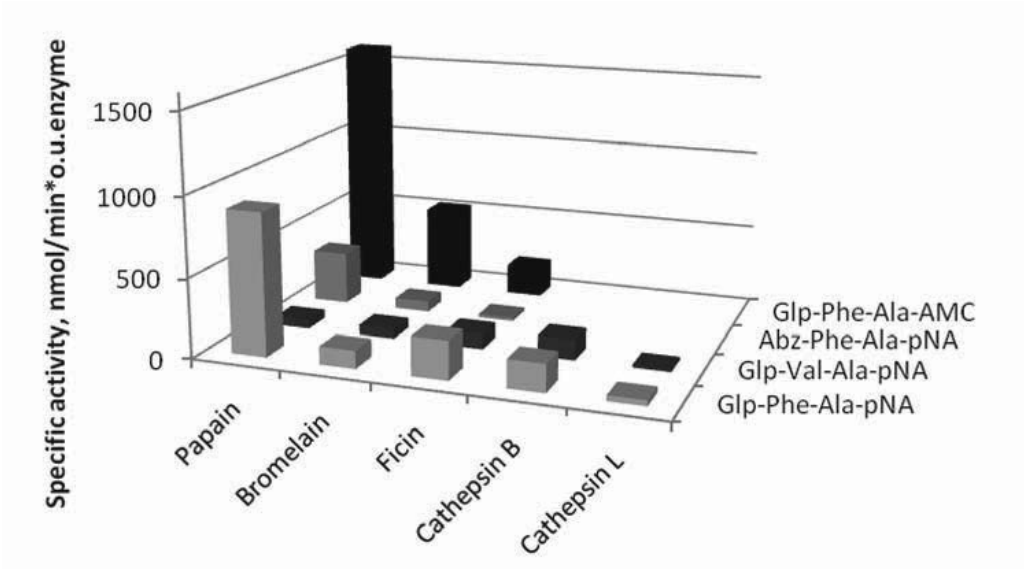

Figure 1. Specific activity of cysteine proteinases against Glp-Phe-Ala-pNA, Glp-Val-Ala-pNA, Abz-Phe-Ala-pNA, Glp-Phe-Ala-AMC.

and subtilisin Carlsberg immobilized on poly(vinyl alcohol) cryogel as a catalysts. Synthesized compounds were characterized by amino acids analysis, HPLC, mass-spectrometry, spectrophotometry (I and II) and fluorimetry (III and IV).

The specific activities of cathepsins B, L and plant enzymes papain, bromelain and ficain (fig. 1) as well as enzymes of other classes - serine (chymotrypsin, trypsin and subtilisin), aspartic (pepsin) and metalloproteinases (thermolysin) - were determined using synthesized substrates and commercial available substrates Z-Phe-Arg-pNA, Z-Arg-Arg-pNA and Bzl-Arg-pNA. It was shown, that three of our substrates Glp-Phe-Ala-pNA, Glp-Val-Ala-pNA and Glp-Phe-Ala-AMC were cleaved only by enzymes of papain family and we could not detect their cleavage by enzymes of other classes.

Acknowledgments

This work has been supported by RFBR grant ¹ 06-03-33056à.

References

1. Rawlings ND, Barrett AJ. *Biochem J* **290**: 215–218, 1993.
2. Choe Y, Leonetti F, Greenbaum DC, Lecaille F, Bogyo M, Brömme D, Ellman JA, Craik CS. *J Biol Chem* **281**: 12824-12832, 2006.
3. Semashko TA, Lysogorskaia EN, Oksenoit ES, Bacheva AV, Filippova I.Yu. *Bioorg Khim* **34**: 376-381, 2008.

3-15-114

Post translational modified peptide-based ELISA to detect autoantibodies in Primary Biliary Cirrhosis

Innocenti, Elisa[1,2]; Peroni, Elisa[1,2,]; Nuti, Francesca[1,2]; Chelli, Mario[1,2]; Rovero, Paolo[1,3]; Selmi, Carlo[4]; Papini, Anna Maria[1,2]*

[1]Interdepartimental Laboratory of Peptide & Protein Chemistry & Biology (PeptLab), Polo Scientifico e Tecnologico of the University of Firenze, ITALY; [2]Dept. of Organic Chemistry 'Ugo Schiff', and CNR-ICCOM, University of Firenze, ITALY; [3]Dept. of Pharmaceutical Sciences, University of Firenze, ITALY; [4]San Paolo School of Medicine, University of Milano, Div. of Internal Medicine, ITALY

[*]E-mail: elperoni@hotmail.com

Introduction

Primary Biliary Cirrhosis (PBC) is an autoimmune cholestatic liver disease that predominantly affects middle-age women. It is histologically characterized by infiltration of lymphocytes in portal tracts and destruction of intrahepatic small bile ducts, causing liver fibrosis and eventually liver failure. The most characteristic feature is the presence of antimitochondrial antibodies (AMA, detected up to now by immunofluorescence assays) positive in 90% of PBC patients long before clinical signs or symptoms appear. The autoantigens in PBC are supposed to be located on the inner mitochondrial membrane and identified as members of the 2-oxo-Acid Dehydrogenase enzyme complexes (2-OADC). Among them, the major autoantigen in PBC is considered to be PDC-E2, which is one of the three component enzymes of the Pyruvate Dehydrogenase Complex (PDC-E2).[1] Aim of the present research is the development of innovative peptide-based diagnostic tools for PBC. As Post-Translational Modified (PTM) synthetic peptides can be useful tools for mimicking neoantigens responsible of the autoimmune response, we propose to take advantage of a unique technology for monitoring peptide epitope modifications and leading to the identification of altered autoantigens that the human host is recognizing as non self. Our approach is aimed to the development of new diagnostic/prognostic tools that can be used in earlier stage PBC patients and possibly monitoring disease activity similarly to what recently reported for multiple sclerosis.[2] More than 95% of PBC patients have detectable levels of autoantibodies to PDC-E2 and in general these react with a region of the molecule containing a lipoamide lysine residue [Lys(ALA)]. It has been hypothesized[3] that the lipoamide in PDC-E2 serves as a xenobiotic target becoming immunogenic and initiates or perpetuates an AMA response.

Results

The use of synthetic peptides chemically modified by the introduction of specific PTMs can overcome the limitations occurring with recombinant proteins or protein extracts. In fact, PTMs can be univocally introduced during peptide synthesis leading to chemically defined molecules mimetics of neo-antigens. Therefore we synthesised different lipoamide-peptides as mimetics of native autoantigens involved in autoantibody recognition:

1. PDH(44-63) fragment, minimal epitope of PDC-E2, bearing the modification on the tip of the β-turn structure in PDC4.

2. The universal scaffold CSF114,[2] a structure based designed β-hairpin peptide, irrelevant for the PDC sequence, modified at position 7 with Lys(ALA).

To this aim, we synthesized the building block Fmoc-Lys(ALA)-OH to introduce the lipoamide residue in synthetic antigenic probes for the development of PBC diagnostic tools. In order to identify the best synthetic antigen, we investigated the antibody recognition in PBC sera compared to normal blood donors'sera by ELISA using the following peptides:

1. [Lys50(ALA)]PDH(44-63) and [Lys50]PDH(44-63).

2. [Lys7(ALA)]CSF114 and [Lys7]CSF114 modifying the universal scaffold CFS114, previously demonstrated to expose at the best PTMs in ELISA as diagnostics of multiple sclerosis.[2]

3. Porcine Pyruvate DeHydrogenase (PHD, Sigma P7032), which is up to now used as an antigen in ELISA to detect autoantibodies in PBC patients' sera.

First of all we didn't observe any false positive with all the peptides. Moreover lipoamide modified peptides showed the best reactivity. In fact [Lys7(ALA)]CSF114 showed the highest reactivity confirming that the β-hairpin structure of CSF114 is possibly able to expose at the best the modification in the solid phase assay conditions.[5] All the synthetic peptide antigenic probes were able to detect by ELISA autoantibodies in 30% of PBC AMA-negative sera. The native protein PDH was unable to detect by ELISA autoantibodies in PBC AMA-negative sera.

Discussion

By our "Chemical Reverse Approach" we developed [Lys50(ALA)]PDH(44-63) and [Lys7(ALA)]CSF114 able to detect antibodies in PBC AMA-positive sera. In particular [Lys50(ALA)]PDH(44-63) and [Lys7(ALA)] CSF114 are able to detect Abs in 30% PBC AMA-negative sera compared to the native antigen PDH (0%). Lys7(ALA)]CSF114 ppossibly exposing lipoamide residue on the tip of a β-turn structure was demonstrated to be able to detect the best antibody titre in PBC patients'sera (increasing sensitivity in PBC diagnostics). These data are in agreement with the hypothesis that an optimal exposition more than the peptide sequence is fundamental for antibody recognition in the solid phase conditions of ELISA (to be confirmed by conformational studies). In conclusion, modified peptides as synthetic probes characterizing families of antibodies in biological fluids are a suitable option for the development of multiple diagnostic/prognostic immunoassays, increasing sensitivity in autoimmunity diagnostics.

References

1a. Ichiki Y, Shimoda S, Ishibashi H, Gershwin M E. *Autoimmunity Rev* **3**: 331-336, 2004.

1b. Howard MJ, Fuller C, Broadhurst RW, Perham RN, Tang J, Quinn J, Diamond AG, Yeaman SJ. *Gastroenterology* **115**: 139-146, 1998. (c) Selmi C, Balkwill DL, Invernizzi P, Ansari AA, Coppel RL, Podda M, Leung PS, Kenny TP, Van De Water J, Nantz MH, Kurth MJ, Gershwin ME. *Hepatology* **38**: 1250-1257, 2003.

2a. Lolli F, Mulinacci B, Carotenuto A, Bonetti B, Sabatino G, Mazzanti B, D'Ursi AM, Novellino E, Pazzagli M, Lovato L, Alcaro MC, Peroni E, Pozo-Carrero MC, Nuti F, Battistini L, Borsellino G, Chelli M, Rovero P, Papini AM. *Proc Natl Acad Sci U S A* **102**: 10273-10278, 2005.

2b. Papini AM. *Nat Med* **11**: 13, 2005.

2c. Papini AM, Rovero P, Chelli M, Lolli F. *US Patent & PCT WO 03/000733 A2*.

2d. Alcaro MC, Lolli F, Migliorini P, Chelli M, Rovero P, Papini AM. *Chemistry Today* **25**: 14-16, 2007.

3. Long SA, Quan C, Van de Water J, Nantz MH, Kurth MJ, Barsky D, Colvin ME, Lam KS, Coppel RL, Ansari A, Gershwin ME. *J Immunol* **167***:* 2956-2963, 2001.

4. Howard MJ, Fuller C, Broadhurst RW, Perham RN, Tang J, Quinn J, Diamond AG, Yeaman SJ. *Gastroenterology* **115**: 139-146, 1998.

5. Carotenuto A, Alcaro MC, Saviello MR, Peroni E, Nuti F, Papini AM, Novellino E, Rovero P. *J Med Chem* **51**: 5304-5309, 2008.

3-15-115

Development of CelluSpot™ method for serodiagnosis of human parvovirus B19 infections

Hepojoki, Jussi[1]; Brandt, Ole[2]; Frank, Ronald[3]; Kaikkonen, Leena[4]; Söderlund-Venermo, Maria[4]; Hedman, Klaus[5]; Lankinen, Hilkka[6]

[1]University of Helsinki, Haartman Institute, FINLAND; [2]INTAVIS Analytical Instruments AG, GERMANY; [3]Helmholtz Centre for Infection Research, Dept. Chemical Biology, GERMANY; [4]University of Helsinki, Haartman Institute, Dept. of Virology, FINLAND; [5]University of Helsinki, Dept. of Virology and HUSLAB, FINLAND; [6]University of Helsinki, Haartman Institute, Dept. of Virology, Peptide and Protein Lab., FINLAND

[*]E-mail: hilkka.lankinen@helsinki.fi

Introduction

Positional peptide arrays in miniaturized formats are expected to enhance the value of peptides in diagnostics of infectious disease and as parts of protein sequences encoded by the infectious agents monitor cause of infection providing profiles of immune responses to the immunogenic regions of expressed proteins. Since immune responses and binding affinities of antibodies vary in magnitude it is potentially a benefit if peptides can be presented in high local concentrations. CelluSpot™ method is a derivative of the well established and highly sensitive SPOT method with the difference that in CelluSpot™ peptides are produced in a soluble form and for that reason CelluSpot peptides are an attractive source in development of diagnostic peptide arrays and assays.[1,2] CelluSpot™ peptide synthesis is carried out on cellulose discs. After synthesis the discs are dissolved in strong acid resulting in peptide-cellulose-complexes with unprotected side chains. The peptide-cellulose is soluble in dimethyl sulfoxide (DMSO) and can be printed with suitable spotter to any surface to which it adheres strongly enough to enable generation of peptide mini and micro arrays.[2] To begin with a peptide array requires assay normalization and large scale sample evaluations for diagnostic tests. We used here our human parvovirus B19 serum banks and previously identified epitope reactivities of B19 capsid proteins as the model[3] to study sensitivity of CelluSpot™ mini arrays in serodiagnostics. An immunodominant B19 acute-phase-specific heptapeptide found in PepSpot epitope-mapping and used in point-of-care diagnostics is shown to be sensitive in CelluSpot™ arrays.

Results and discussion.

PepSpot epitope mapping results using pools of parvovirus B19 acute-phase sera, old immunity sera and negative human sera were revisited to select a mixture of 46 reactive and non-reactive 20-residue peptides covering the primary sequence of both VP1 and VP2 proteins of the parvovirus B19 capsid. Two non-related control peptides (#1 monoclonal antibody epitope to HIV myc and #2 Streptavidin binding peptide) were included and all 48 peptides were presented in duplicates, resulting in total of 96 peptides per array (Fig. 1). The panel consisted of 30 acute-phase (up to 3 months from onset of illness), 30 convalescent-phase (over 3 months after the illness) and 30 parvovirus negative serum samples.

Measured reactivity of each peptide in each array probed with sera of different patients was collected in an Excel table and cumulative reactivity, i.e. the sum of reactivity of each spot for all experiments, was derived. The peptides having lowest cumulative reactivity were

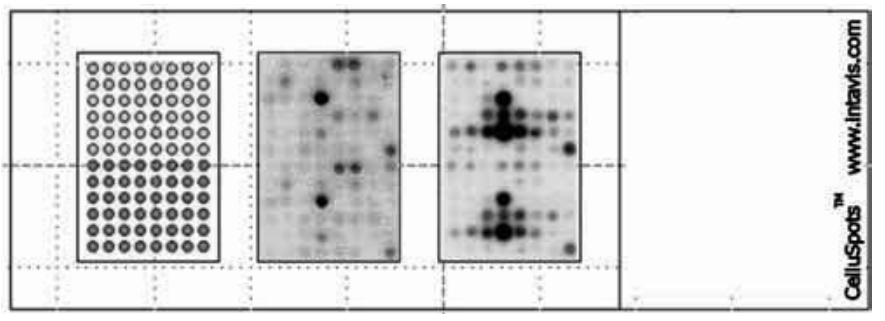

Figure 1. A schematic image of CelluSpot™ peptide array of 3 parallel arrays on microscopic slide. The 1st array describes the location of each sub-array, the 2nd and 3rd array exemplify results of probing the arrays with parvovirus B19 antisera.

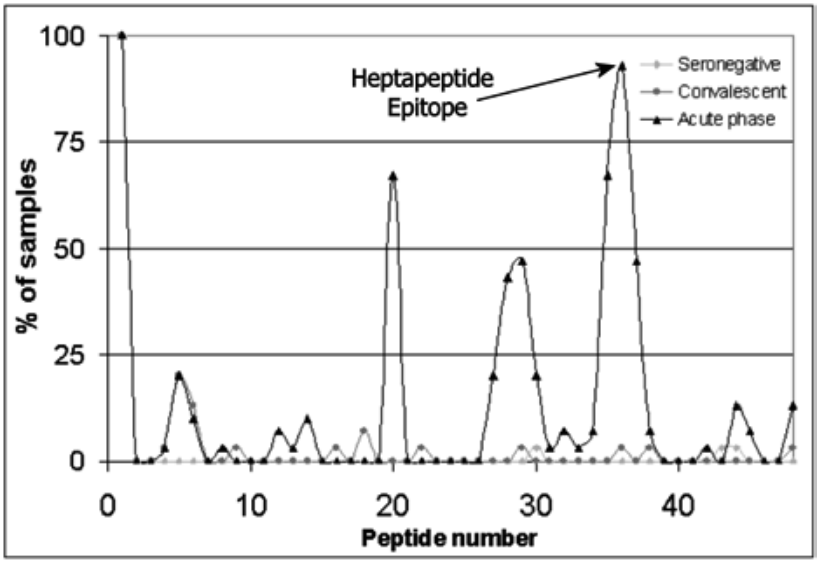

Figure 2. Epitope prevalence in grouped serum samples. X-axis presents individual peptides on array and y-axis % of positive samples in each of the indicated group (seronegative, convalescent and acute-phase).

considered negative, five of which were selected for background calculation. Normalization of CelluSpot assay required the cut-off to be set with negative peptides to 3.29 standard deviation (s) confidence of >99.9%. The average reactivity and standard deviation for the above-determined negative peptides were calculated in each individual experiment and the average value + 3.29s was subtracted from the reactivity of each peptide of the array. After the subtraction of background, the reactivity of each spot measured in two parallels was averaged. If the resulting value was below zero the spot result was assigned to be a negative (0) and if above zero a positive (1) reaction. The CelluSpot™ method can be considered sensitive enough to be useful in serodiagnostics (Fig. 2). From the acute phase patient samples we identified 93% being reactive towards the known acute phase epitope; however a single positive (3%) convalescent patient serum was also found to recognize this peptide representing the most reactive antigenic region of VPI and VP2 in the CelluSpot assay. The presence of other acute-phase specific epitopes needs further evaluation, but the results presented here suggest that the most prevalent acute-phase specific epitope is the KYVTGIN heptapeptide reported earlier.[3]

Acknowledgements

Mrs. Lea Hedman is gratefully acknowledged for her excellent parvovirus antiserum bank supplies and Mrs. Minttu Kaloinen for skilful technical assistance. This research was supported by DAAD (Deutscher Akademischer Austausch Dienst) and The Academy of Finland grant number 107967.

References

1. Frank R. *J Immunol Methods* **267**: 13-26, 2002.
2. Dikmans A, Beutling U, Schmeisser E, Thiele S, Frank R. *QSAR Comb Sci* **25**: 1069-1080, 2006.
3. Kaikkonen L, Lankinen H, Harjunpää I, Hokynar K, Söderlund-Venermo M, Oker-Blom C, Hedman L, Hedman K. *J Clin Microbiol* **37**: 3952-3956, 1999.

3-15-116

Design and synthesis of aminoacyl esters of unprotected saccharides as potent inhibitors of angiotensin converting enzyme (ACE)

Stoineva, Ivanka; Ivanova, Galya; Tchorbanov, Bozidar*

Bulgarian Academy of Sciences, Institute of Organic Chemistry, BULGARIA

**E-mail: istoineva@Yahoo.com*

Angiotensin converting enzyme (ACE) is a vital catalytic component in regulation of blood pressure by modulating rennin –angiotensin system.[1,2] Several synthetic drug and bio-molecules are available for inhibition of ACE and possess antihypertensive effect.[3] Most of the food-derived ACE inhibitors are peptidic in nature.[4] Only a few non-peptidic compounds have been reported to possess the ACE inhibitory activity.[5] Recent investigations have revealed that glycoconjugates possessing an ester bond between the bioactive moiety and one of the sugar hydroxyls are valuable tools in biochemical and medical research. Despite of the ready construction of carbohydrate-ester linkages, there are few reports on enzymatic or chemical synthesis of sugar amino acid esters. In the synthetic design of a newly sugar esters it is very important to control of the degree of substitution and the regiocelectivity is the second important issue. Even with similar physicochemical properties, regioisomers might differ in their toxicity, smell, taste and biodegrability.

In this study, we described a simple method for aminocylation of unprotected sucrose with mildly activated amino acids esters to obtain new compounds with antihypertensive action.

The esters of disaccharide -sucrose are of substantial interest because of their biological and commercial roles. The difference of reactivity between the eight hydroxyl groups in sucrose is a key factor in chemical exploration. In polar solvent as DMF or DMSO the primary position might react faster than secondary ones, if the reaction is sensitive to steric interactions. On the other hand, the reaction might be more sensitive to the activity of the alcohol functions. In this respects, 2^g-OH has been shown to be the most reactive among eight hydroxyl groups of sucrose.

Esterification reactions of unprotected disaccharides -sucrose, were studied with either *N*-benzyloxycarbonyl-L-phenylalanine cyanomethyl ester or *N*-benzyloxycarbonyl-L-proline cyanomethyl ester in dry DMF. The molar proportions of reactants used were sugar: amino acid ester: base, 1: 0.5:4, in all reactions performed.

Analysis of the ^{1}H and ^{13}C NMR spectra of sucrose esters demonstrated that in reaction mixture we have 4 compounds- 2^g-*O*-,3^g-*O*-, 6^g-*O*- and 1^f-*O*-monoacyl sucrose. The crude reaction mixture was purified by high performance liquid chromatography (HPLC). A Biotronic (Germany) HPLC system equipped with NH_2 column and UV detector at 254 $_{nm}$ were used. Sucrose esters were eluted isocratic by 93 % AcCN: 7% H_2O at a flow rate of 1 ml×min^{-1}. Peaks for 3^g-*O*-Phe-sucrose (Rt 15`-20.01 %) , $2^g$-*O*-Phe-sucrose (Rt 22`-55.72 %) , 1^f-*O*-Phe-sucrose (Rt-30`-12.8 %) $6^g$-*O*-Phe-sucrose (Rt 35`-8.57 %) were detected and the peak area of each peak was measured. After purification by HPLC we obtained pure 2^g-*O*- and 3^g-*O*- monoacyl sucrose.

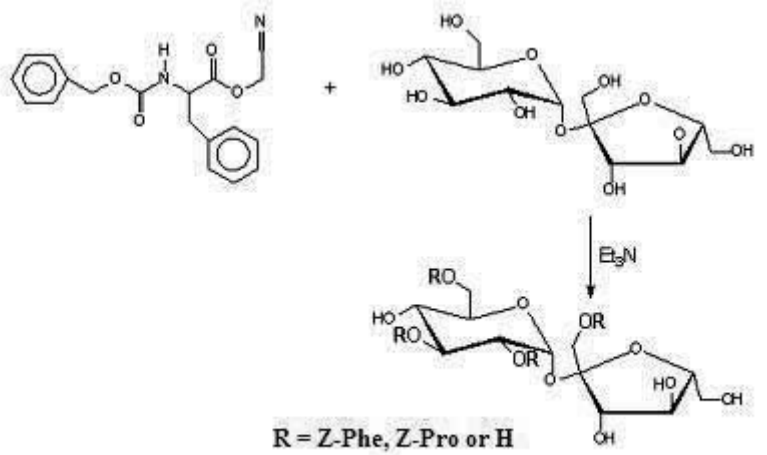

Figure 1.

After deprotection the product possess groups which can accommolated in the hydrophobic S_1 and S_2 site of angiotensin I converting enzyme. The free amino group in the amino acids- carbohydrate ester can also serve as good ligands for Zn^{+2} in the ACE active site. Carbohydrate possess both hydrophobic and hydrophilic groups in their structure and could also bind with enzyme subsite.[6] According Divakar[6] the IC_{50} value for 2-*O*-L-phenylalanyl-D-glucose is 1.0 μM. Our measurements of IC_{50} value of newly synthesized compounds are in progress.

We proposed original and simple method for aminoacylaion of unprotected sucrose with mildly activated amino acids esters. The newly synthesized aminoacyl saccharides are promising compounds as inhibitors of ACE.

Acknowledgements

This work was supported by a Grant X-1608 from the National Fund for Scientific Investigations, Bulgarian Ministry of Education and Sciences.

References

1. Erdos EG. Angiotensin-I converting enzyme. *Circ Res* **36:** 247-255, 1975.
2. Skidgel RA, Erdos EG. Novel activity of human angiotensin I converting enzyme: release of the NH2- and COOH-terminal tripeptides from the luteinizing hormone-releasing hormone. *Proc Natl Acad Sci U S A* **82:** 1025-1029, 1985.
3. Verme-Gibboney C. *Am J Health Syst Pharm* **54:** 2603–2689, 1997.
4. Ariyoshi Y. *Trends Food Sci Technol* **4:** 139-144, 1993.
5. Kamath V, Rajini PS, Lohith K, Somashekar BR, Divakar S. Angiotensin converting enzyme inhibitory activity of amino acid esters of carbohydrates. *Intern J Bio Macromol* **38:** 89-93, 2006.
6. Lohith K, Vijayakumar GR, Somashekar BR, Sivakumar R, Divakar S. Glycosides and amino acyl esters of carbohydrates as potent inhibitors of angiotensin converting enzyme. *Eur J Med* **41:** 1059-1072, 2006.

3-15-117

^{99m}Tc-labeled Tetraamine-Derivatized Cyclic Nonapeptides with Pansomatostatin-like Properties: Synthesis and Comparative Biological Evaluation

Nikolopoulou, Anastasia[1]; Petrou, Christos[2]; Zompra, Aikaterini A[2]; Charalambidis, David[1]; Nock, Berthold Artur[1]; Waser, Beatrice[3]; Cescato, Renzo[3]; Reubi, Jean Claude[3]; Cordopatis, Paul[2]; Maina, Theodosia[1,]*

[1]I/R-RP, NCSR "Demokritos", Molecular Radiopharmacy, GREECE; [2]University of Patras, Department of Pharmacy, GREECE; [3]University of Bern, Institute of Pathology, SWITZERLAND

[*]E-mail: maina_thea@hotmail.com

Introduction

Somatostatin subtype 2(sst_2)-preferring radiolabeled somatostatin analogs - like OctreoScan® ([^{111}In-DTPA^0] octreotide) - have been developed and are currently used with success in targeted diagnostic imaging and radionuclide therapy of sst_2-positive tumors. Nevertheless, recent research efforts are aiming toward new radiolabeled somatostatins having extended $sst_{1\text{-}5}$ affinity profile (pansomatostatins) and may consequently be suitable for broader clinical indications.[1] In a recent study, Reubi *et al*. reported on the cyclic nonapeptide KE108 (Tyr^0-c[(D)Dab-Arg-Phe-Phe-(D)Trp-Lys-Thr-Phe]) exhibiting pansomatostatin properties.[2] However, important data on the overall *in vivo* performance of a radiolabeled KE108-based analog were not included in this study. As a part of our search for useful ^{99m}Tc-based radiopeptides functionalized with acyclic tetraamine chelators (N_4),[3] we synthesized two novel KE108 derivatives: DemoPan 1 ([N_4^0,*des*-Tyr^0]KE108) and DemoPan 2 ([N_4^{-1}]KE108), carrying the N_4 chelator at their N-terminus. The biological properties of resulting (radio)peptides were studied in several *in vitro* models and AR4-2J tumor-bearing Lewis rats.

Results and discussion

DemoPan 1 and DemoPan 2 were synthesized on the solid support, purified by HPLC and lyophilized to afford white solids in ~10% overall yields. ES-MS spectra were consistent with the expected formulae.

The binding properties of new analogs were determined during competition binding assays conducted in rat sst_2-expressing AR4-2J cell-membranes using [^{125}I-Tyr^3]octreotide as radioligand and [Tyr^3]octreotate as reference compound. Results are included in Table 1. The $sst_{1\text{-}5}$ affinity profile of DemoPan 1 and DemoPan 2 was selectively investigated by receptor autoradiography on cell membrane pellet sections each expressing one of the human $sst_{1\text{-}5}$; [^{125}I][Leu^8,(D)Trp^{22},Tyr^{25}]SS-28 was used as radioligand and SS-28, KE108 served as control compounds. Results are summarized in Table 1. DemoPan 1 and DemoPan 2 showed high affinity binding for all five $sst_{1\text{-}5}$ with IC_{50} values found in the low and sub-nanomolar range. Significantly higher affinity for most $sst_{1\text{-}5}$ was shown by DemoPan 2 as compared to DemoPan 1 in accordance to the respective $rsst_2$ results (last column). Both DemoPan 1 and DemoPan 2 exhibited agonistic properties, by inducing sst_2 and sst_3 internalization. However, they were weaker in inducing sst_2 internalization as compared to native SS-28.

Labeling with ^{99m}Tc was performed at ambient temperature in alkaline aqueous medium using $SnCl_2$ as reductant in the presence of citrate anions affording the respective ^{99m}Tc-radiopeptides in >97% yields.

The *in vivo* profile of [^{99m}Tc]DemoPan 1 and [^{99m}Tc] DemoPan 2 was studied in male Lewis rats bearing $rsst_2$-positive AR4-2J tumors. For *in vivo* blockade 100 μg of [Tyr^3]octreotate was injected along with the radioligand. Animals were sacrificed in groups of four at 4 h post-

Table 1. Affinity profiles (IC_{50}s in nM) of bioconjugates for human $sst_{1\text{-}5}$ receptors; [^{125}I][Leu^8,(D)Trp^{22},Tyr^{25}]SS-28 was used as the radioligand; SS-28 and KE108 were used as control compounds. Respective values for the rat sst_2 in AR4-2J cell membranes are included in the last column; [^{125}I-Tyr^3]octreotide served as the radioligand and [Tyr^3] octreotate as control*

Analog	$hsst_1$	$hsst_2$	$hsst_3$	$hsst_4$	$hsst_5$	$rsst_2$
SS-28	2.2; 1.3	3.2; 3.2	4; 4.8	5.2; 4.3	2.6; 1.5	-
KE108	2.6 ± 0.4	0.9 ± 0.1	1.5 ± 0.2	1.6 ± 0.1	0.65 ± 0.1	0.3 ± 0.0*
DemoPan 1	7.5; 4.3	12; 9.5	1.6; 3.5	8.3; 3.9	1.2; 1.2	3.4 ± 0.3
DemoPan 2	0.83; 0.85	2.4; 2.7	1.7; 1.5	3.2; 3.5	0.7; 0.7	0.6 ± 0.1

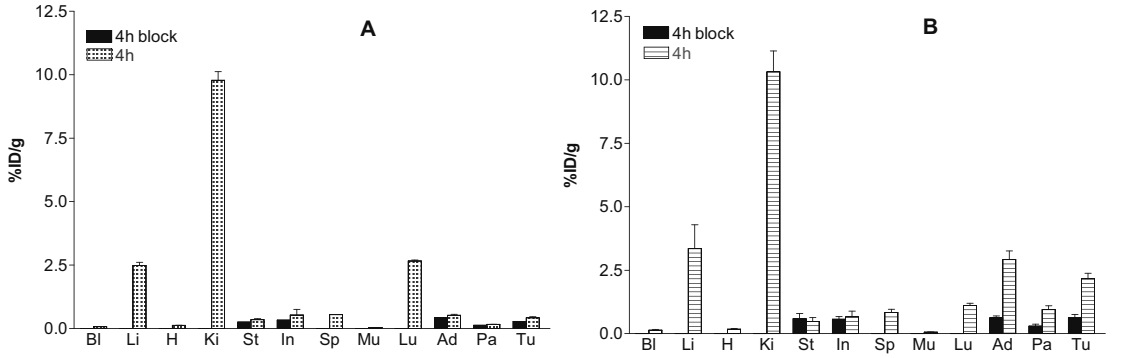

Figure 1. Tissue distribution data of [^{99m}Tc]DemoPan 1 (A) and [^{99m}Tc]DemoPan 2 (B) in AR4-2J tumor bearing Lewis rats at 4 h pi (%ID/g). Bl= blood, Li= liver, He= heart, Ki= kidneys, St= stomach, In= intestines, Sp= spleen, Mu= muscle, Lu= lungs, Pa= pancreas, Ad= adrenals, Tu= AR4-2J tumor; for *in vivo* receptor blockade 100 μg [Tyr^3] octreotate was co-injected with test radiopeptide.

injection (pi) by heart puncture. [^{99m}Tc]DemoPan 1 failed to localize specifically in sst$_2$-expressing organs, such as the pancreas, the adrenals, the stomach and the intestines, but also in the implanted tumor. Furthermore, it showed undesirable high liver and kidney uptake (Fig. 1A). In contrast, [^{99m}Tc]DemoPan 2 exhibited a sst$_2$-mediated accumulation both in these physiological sst$_2$-expressing tissues and in the experimental tumor while displaying similar to [^{99m}Tc]DemoPan 2 liver and kidney values (Fig. 1B).

Functionalization of KE108 with acyclic tetraamines amenable to ^{99m}Tc-labeling may lead to clinically useful radiotracers with pansomatostatin properties. Biodistribution experiments in sst$_2$-positive tumor bearing rats have indicated that careful radiotracer design may further improve the *in vivo* targeting capacity and pharmacokinetics of [^{99m}Tc]DemoPan - related radiopeptides; work in this direction is currently in progress.

Acknowledgements

This work has been supported by GSRT of Greece via the Research Project "Functional and Functionalized Biomolecules in Biodiagnosis and Radiopharmacy" (EPAN 3.3. Excellence in Research).

References

1. Breeman WAP, de Jong M, Kwekkeboom DJ, Valkema R, Bakker WH, Kooij PPM, Visser TJ. *Eur J Nucl Med Mol Imaging* **28:** 1421-1429, 2001.
2. Reubi JC, Eisenwiener KP, Rink H, Waser B, Maecke H. *Eur Pharmacol* **456:** 45-49, 2002.
3. Maina T, Nock B, Nikolopoulou A, Sotiriou P, Loudos G, Maintas D, Cordopatis P, Chiotellis E. *Eur J Nucl Med Mol Imaging* **29:** 742-753, 2002.

3-15-118

Introduction of Hydrophilic Asp-Residue(s) in [^{99m}Tc]Demotate 1: A Structure - Activity Relationships Study

Nock, Berthold Artur[1]; Petrou, Christos[2]; Galanis, Athanassios S.[2]; Nikolopoulou, Anastasia[1]; Waser, Beatrice[3]; Reubi, Jean Claude[3]; Cordopatis, Paul[2]; Maina, Theodosia[1,]*

[1]I/R-RP, NCSR "Demokritos", Molecular Radiopharmacy, GREECE; [2]University of Patras, Department of Pharmacy, GREECE; [3]University of Bern, Institute of Pathology, SWITZERLAND

[*]E-mail: maina_thea@hotmail.com

Introduction

The high density expression of somatostatin receptors (sst_{1-5}), especially of sst_2, has been documented in many neuroendocrine tumors.[1] A part of our research activities is focused on the development of ^{99m}Tc-labeled somatostatin analogs with potential application in the sst_2-targeted tumor imaging.[2,3] We report here on a series of Tate ([Tyr^3,Thr^8]octreotide) analogs, coupled to acyclic tetraamines (N_4) to stably bind the diagnostic radionuclide ^{99m}Tc. Accordingly, introduction of/substitution by hydrophilic Asp residues at the N-/C-terminus of Tate resulted in the following bio-conjugates: Demotate 1: [N_4^0]Tate; Demotate 2: [N_4^{-1},Asp^0]Tate; Demotate 3: [N_4^{-2},Asp^{-1},Asp^0]Tate; Demotate 5: [N_4^0,Asp^1]Tate; Demotate 6: [N_4^0,Asp^8]Tate; and Demotate 7: ([N_4^{-1},Asp^0,Asp^8]Tate. The aim of the study was to evaluate the effects of the negative charge(s) introduced in Tate on the biological behavior of resulting [^{99m}Tc]Demotate 1-7. According to previous reports, introduction of extra-pendant carboxylate group(s) has facilitated the rapid renal clearance of other radiolabeled somatostatin analogs into the urine.[4-6]

Results and discussion

Bioconjugates were synthesized on the solid support, purified by HPLC and lyophilized to afford white solids in a >97% purity. ES-MS spectra were consistent with the expected formulae. Competition binding assays were conducted in rat sst_2-expressing AR4-2J cell-membranes using [^{125}I-Tyr^3]octreotide as radioligand and the IC_{50} values determined (in nM) as follows: Demotate 1: 0.13 ± 0.05; Demotate 2: 0.45 ± 0.05; Demotate 3: 2.30 ± 0.04; Demotate 5: 2.95 ± 0.06; Demotate 6: 0.50 ± 0.04; and Demotate 7: 1.63 ± 0.04.

The sst_{1-5} affinity profile of Demotate 1, Demotate 2, Demotate 3 and Demotate 6 was selectively investigated by receptor autoradiography on cell membrane pellet sections each expressing one of the human sst_{1-5}; [^{125}I][Leu^8,(D)Trp^{22},Tyr^{25}]SS-28 was used as radioligand and SS-28, Tate and OctreoScan® ([In-DTPA^0]octreotide) served as control compounds. Results summarized in Table 1 show the superior affinity of Demotate 1 for the $hsst_2$ which exceeds that of native SS-28.

Labeling of Demotates with ^{99m}Tc was performed at ambient temperature in alkaline aqueous medium using $SnCl_2$ as reductant in the presence of citrate anions affording the respective ^{99m}Tc-radiopeptides in >97% yields. Internalization of [^{99m}Tc]Demotate 1-7 was conducted in AR4-2J cells at 37 ^{0}C; non-specific internalization was determined in the presence of 1 μM Tate. [^{99m}Tc]Demotate 1 internalized rapidly and twice as effectively as [^{99m}Tc]Demotate 2, whereas [^{99m}Tc]Demotate 3, [^{99m}Tc]Demotate 5, [^{99m}Tc]Demotate 6 and [^{99m}Tc]Demotate 7 internalized very poorly.

Table 1. Affinity profiles (IC_{50}s in nM) of bioconjugates for human sst_{1-5} receptors; [^{125}I][Leu^8,(D)Trp^{22},Tyr^{25}]SS-28 was used as the radioligand; SS-28 Tate and OctreoScan® were used as control compounds

Analog	chemical structure	$hsst_1$	$hsst_2$	$hsst_3$	$hsst_4$	$hsst_5$
SS-28	SS-28	2.6±0.6 (10)	2.7±0.3 (10)	3.9±0.9 (10)	3.6±0.4 (10)	2.7±0.4 (10)
OctreoScan®	[In^{III}-DTPA^0]octreotide	>10,000 (5)	22±3.6 (5)	182±13 (5)	>1,000 (5)	237±52 (5)
Tate	[Tyr^3]octreotate	>1,000 (2)	0.95±0.15(2)	>1,000 (2)	765±15 (2)	240±70 (2)
Demotate 1	[N_4^0]Tate	946±401 (3)	0.5±0.07 (3)	93±23 (3)	51±6.9 (3)	7.3±1.4 (3)
Demotate 2	[N_4^{-1},Asp^0]Tate	>1000 (3)	3.2±0.09 (3)	>1000 (3)	267±60 (3)	129±23 (3)
Demotate 3	[N_4^{-2},Asp^{-1},Asp^0]Tate	>1000 (3)	3.1±0.57 (3)	>1000 (3)	73±11 (3)	261±36 (3)
Demotate 6	[N_4^0,Asp^8]Tate	>1000 (2)	6.4; 5.9	541; 233	118; 150	23; 21

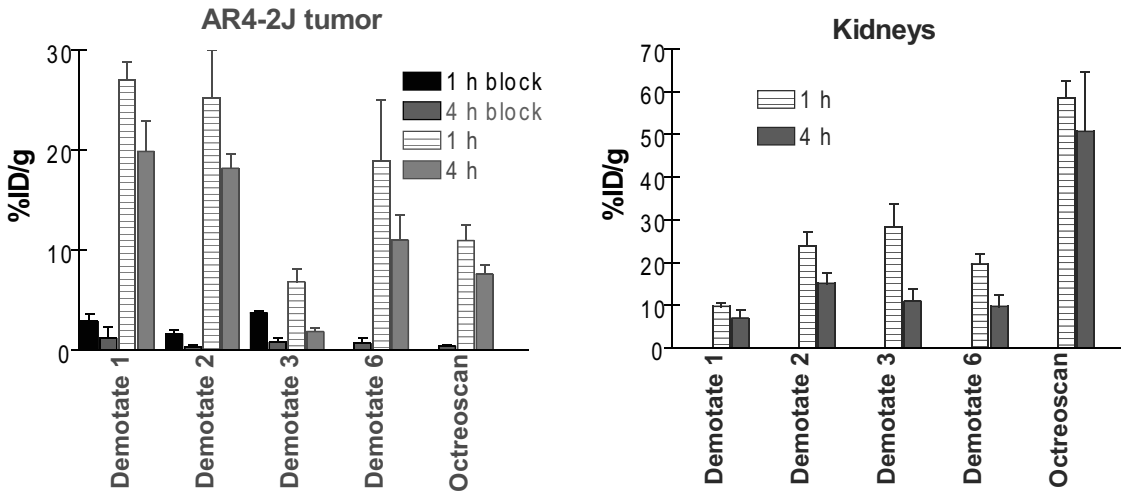

Figure 1. Comparative AR4-2J tumor (left) and kidney (right) uptake of [^{99m}Tc]Demotate 1, [^{99m}Tc]Demotate 2, [^{99m}Tc] Demotate 3, [^{99m}Tc]Demotate 6 and OctreoScan® in tumor-bearing mice; values represent %ID/g tissue; for *in vivo* blockade 100 μg Tate was co-injected in the animals.

The *in vivo* profile of all [^{99m}Tc]Demotates was compared in healthy male Swiss albino mice. Unmodified [^{99m}Tc]Demotate 1 exhibited a clearly superior uptake in all sst_2-target organs (pancreas, adrenals, bowels and stomach). Conversely, the kidney uptake increased for all Asp-derivatized [^{99m}Tc]Demotates, with the exception of [^{99m}Tc]Demotate 5. The latter, however, totally failed to show any *in vivo* sst_2-specific uptake. Biodistribution was further tested selectively for [^{99m}Tc]Demotate 1, [^{99m}Tc]Demotate 2, [^{99m}Tc]Demotate 3, [^{99m}Tc]Demotate 6 and OctreoScan® in mice bearing AR4-2J tumors. As shown in Fig. 1, uptake in the tumor was high for [^{99m}Tc] Demotate 1 and [^{99m}Tc]Demotate 2 (>25% ID/g at 1 h pi), lower for [^{99m}Tc]Demotate 6 (>18% ID/g at 1 h pi), and much lower for [^{99m}Tc]Demotate 3 (~ 6% ID/g at 1 h pi). The commercial agent OctreoScan® performed rather poorly in terms of tumor targeting (>7.5% ID/g at 1 h pi) while by far displaying the highest uptake and retention in the kidneys (>50% ID/g at 1 and 4 h pi).

Introduction of Asp residues at the N-/C-terminus of [^{99m}Tc]Demotate 1 has a great impact on biological properties. Both unlabeled and radiolabeled Demotate analogs showed *in vitro* affinity and internalization profiles very much dependent on the number and position of introduced Asps. *In vivo* results paralleled *in vitro* findings with *in vivo* sst_2-targeting found reduced by introduction of Asp(s). Accordingly, [^{99m}Tc]Demotate 1 showed superior uptake in all sst_2-positive tissues in healthy and in AR4-2J tumor bearing mice. At the same time, unmodified [^{99m}Tc]Demotate 1 exhibited the lowest renal values. In conclusion, [^{99m}Tc]Demotate 1 achieved the highest tumor-to-kidney ratios and turned out to be the best candidate for clinical applications.

Acknowledgements

This work was partially funded by the GSRT via the National Program EPET II: "Cancer Biology: Genetic Analysis & In Vivo Receptor Imaging - Radiotherapy" (Project No: 97EKBAN2-1,2-112) and by Biomedica Life Sciences, S.A.

References

1. Reubi JC, Waser B, Friess H, Buchler M, Laissue J. *Gut* **42:** 1421-1429, 1998.
2. Maina T, Nock B, Nikolopoulou A, Sotiriou P, Loudos G, Maintas D, Cordopatis P, Chiotellis E. *Eur J Nucl Med Mol Imaging* **29:** 742-753, 2002.
3. Decristoforo C, Maina T, Nock B, Gabriel M, Cordopatis P, Moncayo R. *Eur J Nucl Med Mol Imaging* **30:** 1211-1219, 2003.
4. Akizawa H, Arano Y. *Q J Nucl Med* **46:** 206-223, 2002.
5. Akizawa H, Arano Y, Mifune M, Iwado A, Saito Y, Mukai T, Uehara T, Ono M, Fujioka Y, Ogawa K, Kiso Y, Saji H. *Nucl Med Biol* **28:** 761-768, 2001.
6. Akizawa H, Saito M, Tsukamoto I, Ohkura T, Shimizu T, Kitamura Y, Mifune M, Saito Y, Arano Y, Saji H. *Biol Pharm Bull* **30:** 2226-2228, 2007.

3-15-119

Adrenomedullin analogs: potential diagnostic tools for pulmonary circulation imaging

Letourneau, Myriam[1]; Fu, Yan[1]; Nguyen, Quang Trinh[2]; Harel, François[2]; Dupuis, Jocelyn[2]; Fournier, Alain[1,]*

[1]Institut National de la Recherche Scientifique-Institut Armand Frappier, CANADA; [2]Centre de recherche de l'institut de cardiologie de Montréal, CANADA

[*]E-mail: alain.fournier@iaf.inrs.ca

Introduction

Diagnosis and follow up of many pathophysiological states are now achievable in a non-invasive mode through the use of nuclear medicine imaging modalities. Generally, a radiopharmaceutical agent composed of an organic molecule associated with a radionuclide is used as the imaging source and its biodistribution is determined by its physicochemical properties or specific biological interactions. Currently, pulmonary circulation imaging is performed in North America with ^{99m}Tc-labeled albumin macroaggregates (^{99m}Tc-AMA). However, ^{99m}Tc-AMA is a physical imaging agent since it is larger than small pulmonary vessels where it is trapped to allow imaging. This particularity potentially limits its ability to detect minute anatomical vascular defects and does not allow the detection of functionnal perfusion defects. Therefore, a smaller molecular lung selective radiopharmaceutical agent would be a valuable asset in nuclear medicine. Peptides, with their high selectivity towards specific receptors and their small molecular weight, are promising lead compounds. Adrenomedullin (AM), a 52-amino acid peptide belonging to the calcitonin family, has its highest binding site density in lungs and kidneys.[1] Moreover, pulmonary blood vessel binding sites appear to act as AM clearance receptors.[2,3] So, AM could be a potential molecular lung imaging agent. However, upon binding to its receptors, namely AM_1 and AM_2, AM produces different biological activities and particularly a potent vasodilation.[4,5] Structure-activity studies have led us to identify a peptide analog enabling lung imaging and showing reduced hypotensive activity.

Results and discussion

Binding studies performed on dog lung homogenates using peptides of the calcitonin family allowed to pharmacologically characterize these binding sites as AM_1 receptors. Various AM analogs were then synthesized by solid phase peptide synthesis following a standard Fmoc chemistry protocol, purified by reverse phase HPLC and characterized by Maldi-Tof mass spectrometry (Table 1).

Table 1. Synthetic peptide analogs.

AM analogs	Sequences
Analog 1	(13-16)-dPEG$_2$-AM(21-52)
Analog 2	(13-16)-dPEG$_4$-AM(21-52)
Analog 3	**Gly-Gly-Gly-Cys**-dPEG$_4$-AM(21-52)*
Analog 4	**Gly-Gly-ala-Gly-**Cys-dPEG$_4$-AM(21-52)*§
Analog 5	**Gly-Gly-ala-Gly-**dPEG$_4$-AM(22-52)*

*Bold characters form the chelating moieties.
§Cyclized peptide

Two direct ^{99m}Tc labeling approaches were evaluated: through cysteine residues within the peptide sequence and with a chelating moiety added at the N-terminus of the peptide composed of 4 amino acids (GGGC or GGaG). Labelling efficiency was monitored by instant thin layer chromatography on silica gel impregnated paper (Table 2). Solvants were acetone for dosage of free ^{99m}Tc and a mixture of butanol, acetic acid, pyridine and water to determine the amount of labeled peptide. Evaluation of our results indicates that the labeling procedure involving a chelating moiety is more efficient.

Table 2. Minimum dose causing a hypotensive response in dogs and ^{99m}Tc-labeling efficiencies. Results are mean of at least 3 independent evaluations.

Peptides	Minimum hypotensive dose (nmol)	^{99m}Tc-labeling efficiency
AM	6.7	52% *
AM(13-52)	7.7	45% *
AM(22-52)	>140	n/a
Analog 1	14.4	53% *
Analog 2	57.6	75% *
Analog 3	88.0	84% §
Analog 4	>140	88% §
Analog 5	>140	85% §

*Method involving cysteine residues
§Method involving a chelator

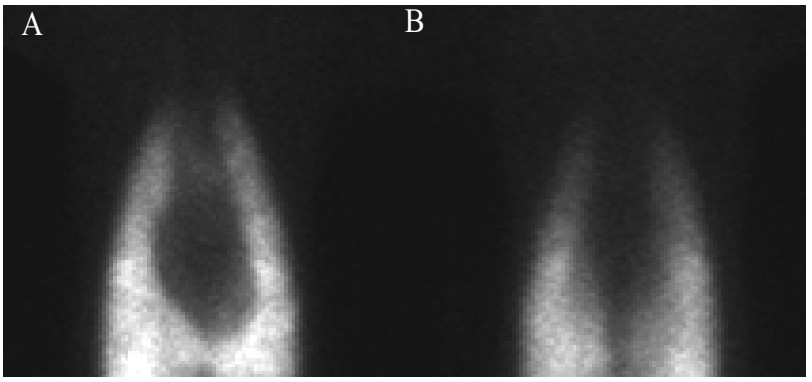

Figure 1. Dog lung imaging 60 min following an i.v. injection of ^{99m}Tc-labeled analog 4 with anterior (a) and posterior (B) views.

Cumulative doses of peptide were injected into the jugular vein of dogs and the delta mean arterial pressure was monitored for 15 min to evaluate the hypotensive response associated with each peptide analog. Results have shown that AM cyclic structure along with residues in the vicinity of the disulfide bridge appear to play an important role in receptor affinity and activation. Moreover, the cyclic structure is essential in maintaining good receptor affinity since a linear peptide such as analog 5 no longer has affinity for lung tissues (results not shown). However, amino acid substitution within this cyclic structure is associated with decreased hypotensive activity. Accordingly, analog 4 was ^{99m}Tc-labeled with high efficiency and was able to produce sharp lung imaging in dogs at a dose not associated with a hypotensive response (Fig. 1). Thus, AM analogs appear to be promising lead molecules for the development of a new molecular imaging agent of the pulmonary circulation.

Acknowledgements

Maryse Bolduc is gratefully acknowledged for her skillful technical assistance. This research was supported by PulmoScience.

References

1. Owji AA, Smith DM, Coppock HA, Morgan DG, Bhogal R, Ghatei MA, Bloom SR. *Endocrinology* **136:** 2127-2134, 1995.
2. Dschietzig T, Azad HA, Asswad L, Bohme C, Bartsch C, Baumann G, Stangl K. *Biochem Biophys Res Commun* **294:** 315-318, 2002.
3. Dupuis J, Caron A, Ruel N. *Clin Sci* (*Lond*) **109:** 97-102 , 2005.
4. Hay DL, Howitt SG, Conner AC, Schindler M, Smith DM, Poyner DR. *Br J Pharmacol* **140:** 477-486, 2003.
5. Gibbons C, Dackor R, Dunworth W, Fritz-Six K, Caron KM. *Mol Endocrinol* **21:** 783-796, 2007.

3-16-120

Production of peptide arrays consisting of labeled structured peptide and glycopeptide libraries for the construction of protein detection systems

Nokihara, Kiyoshi[1]; Hirata, Akiyoshi; Kawasaki, Takayasu; Miyazato, Naeko; Kodama, Yukiko; Ono, Noriko; Sogon, Tetsuya; Suzuki, Kanae; Miyajima, Midori; Kawahira, Noboru; Ohyama, Takafumi

HiPep Laboratories, JAPAN

[*]E-mail: noki@hipep.jp

Introduction

Since high-throughput protein-detection and characterization systems are urgently required, a novel concept has been proposed.[1] This involves visualizing the interaction between proteins and labeled peptides as a bar-code using fluorescent intensities to generate "protein fingerprints". The use of peptide arrays as a "protein-chip Eaffords significant advantages for industrial production and applications, in particularly for practical manufacturing, storage and delivery, compared to arrays with antibodies or recombinant proteins. The following key areas have been successfully investigated: 1) High throughput syntheses and characterization of labeled peptides as capture molecules, 2) Development of novel chip-materials, 3) Use of novel surface chemistries and quality control methods, and 4) Deposition of labeled peptide solutions on to the chip surface. Peptide libraries consisting of several hundred structured peptides with α-helices, β-loops and β-sheets have been prepared in a high-throughput manner and used for protein recognition. The present paper describes a further extension to glycopeptides and their preliminary applications. Protein-protein interactions, which may not occur in a 1:1 manner and can be mimicked by peptide-protein interactions, are based on the recognition of different structural motifs, thus together with statistical methods, such as principal component analysis, these biochips can discriminate the structure of different proteins in analytes. Since peptides can be designed and chemically synthesized by well-established methods, the present micro-array system promises practical production on an industrial scale.

Results and Discussion

Since glycoproteins play an important role in bio-recognition, our designed labeled peptide libraries have recently been expanded to include glycopeptides. Initially ca. 100 *O*-linked glycopeptides were synthesized by the Fmoc-SPPS using a building block strategy.[2,3] The diversity was selected from considerations of their secondary structures, amino acid sequence, four glycoside building blocks (glucosyl-, galactosyl-, mannosyl- and lactosyl-threonine) and one or two sugar side chains. It is known that some toxicant proteins, such as *Ricinus communis* agglutinin (RCA), cholera toxin, Vero toxin, and lectins, such as *Pseudomonas aeruginosa* lectin (PA-I), bind carbohydrate. In preliminary experiments we have used 12 labeled α-helical *O*-glycopeptides together with a non-glycosylated peptide (Table 1) in solution to test their discrimination of sugar-binding proteins. The glycopeptides (1-12), and not the non-glycosylated peptide (13), bind to the two toxicant proteins and show decreased fluorescent intensities (Fig. 1). Different glycoside-side chains gave different responses (Glc, Gal, Lac > Man) and a specific response was observed for peptide 10 towards RCA. Toxicant proteins were also dissolved in 2% milk to mimic biological fluids and nutritional situations. RCA showed a significant response to peptides 1, 11 and 13, whereas PA-1 did not. Binding of RCA to the Lac- and non-glycosylated peptides can be visualized by changes in the fluorescent intensity. RCA binds to Lac-peptide in dose-dependent manner and these differ significantly from the same sequence-peptide without Lac (Fig. 2). Since individual peptides

Table 1. Peptide sequences of the α-helical glycopeptide library (C-terminal amide) used for the present toxicant protein detection (TG: Glucosyl-Thr; TM: Mannosyl-Thr ; TGal: Galactosyl-Thr; TL: Lactosyl-Thr). Cys can be used for immobilization after removal of the Acm group by AgOTf

01	αTAMRA-AT^{G}KAAKAAKKAAKA-GC(Acm)	02	αTAMRA-AKKAAT^{G}AAKKAAKA-GC(Acm)
03	αTAMRA-AKKAAKAAT^{G}KAAKA-GC(Acm)	04	αTAMRA-AT^{M}KAAKAAKKAAKA-GC(Acm)
05	αTAMRA-AKKAAT^{M}AAKKAAKA-GC(Acm)	06	αTAMRA-AKKAAKAAT^{M}KAAKA-GC(Acm)
07	αTAMRA-AT^{Gal}KAAKAAKKAAKA-GC(Acm)	08	αTAMRA-AKKAAT^{Gal}AAKKAAKA-GC(Acm)
09	αTAMRA-AKKAAKAAT^{Gal}KAAKA-GC(Acm)	10	αTAMRA-AT^{L}KAAKAAKKAAKA-GC(Acm)
11	αTAMRA-AKKAAT^{L}AAKKAAKA-GC(Acm)	12	αTAMRA-AKKAAKAAT^{L}KAAKA-GC(Acm)
13	αTAMRA-AKKAAKAAKKAAKA-GC(Acm) ------- *without glycoside*		

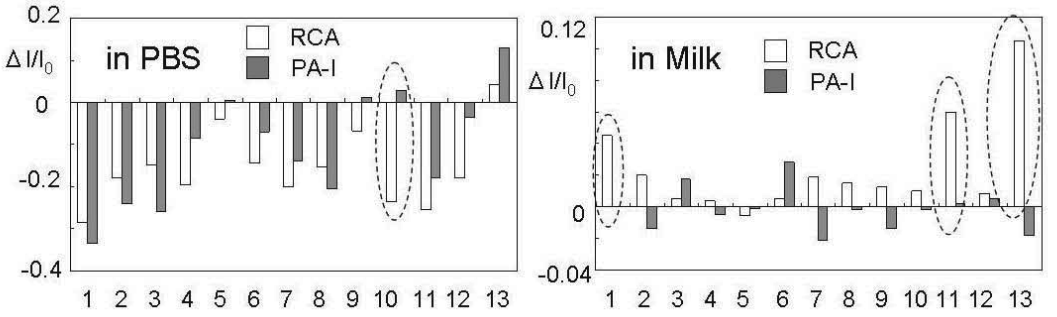

Figure 1. Solution assay of peptide 1 E13 (3.0 μM) with proteins (10 μg/ml, 0.5 μM).

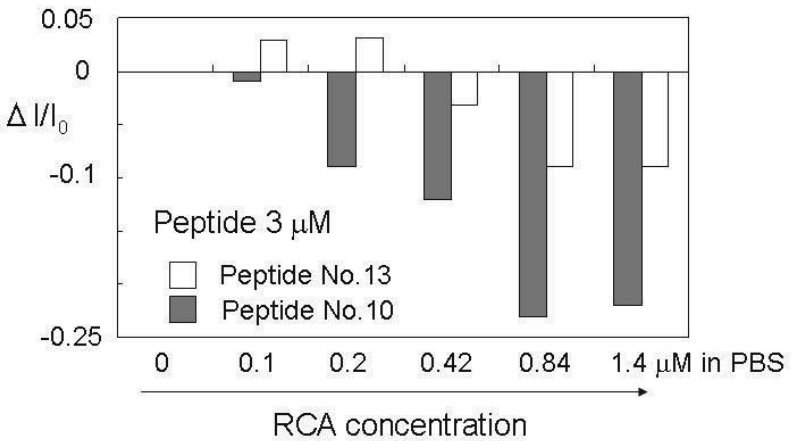

Figure 2. Binding of RCA to the Lac- and non-glycosylated peptides was detected by fluorescent intensity changes.

show different responses to a particular toxicant protein, they can be used for the specific detection of these compounds.

In conclusion the present results suggest that the array constituting the *O*-glycopeptide library shows promise as a toxin detection tool. It can also be envisaged for *in vitro* diagnosis and/or in the area of infection prevention. At present toxicant proteins are detected by a combination of culture and ELISA, a procedure that takes several hours during which time infection may have progressed. Thus a rapid and facile method is required. A carbohydrate array without peptide chains has been reported[4] for the detection of bacterial toxins, although this is impractical since analytes have to be labeled and sensitivities are not significant. At present our detection range is similar to that of ELISA but it is expected that the sensitivity of the arrayed peptide can be further optimized.

Acknowledgements

This work was partially supported by the Research and Development Program for New Bio-industry Initiatives, National Agriculture and Food Research Organization and Bio-Venture Project of Okinawa Prefecture (2004-6), Ministry of Internal Affairs and Communications.

References

1. *JP WO2002/090985*, and reviewed: Nokihara K, Ohyama T, Usui K, Yonemura K, Tomizaki K, Mihara H. *Kobunsi Ronbunshu* **61**: 523-,532 2004.
2. Yang Y-Y, Ficht S, Brik A, Wong C-H. *J Am Chem Soc* **129**: 7690-7701, 2007.
3. Norgren AS, Norberg T, Arvidsson PI. *J Pept Sci* **13**: 717-727, 2007.
4. Ngundi M, Taitt C-R, McMurry S-A, Kahne D, Ligler F-S. *Biosens Bioelectron* **21**: 1195-1201, 2006.

3-16-121

A Compact Disc-sized biochip structured and functionalized by microplasma-based patterned amination as substrate for an automated chemical synthesizer

Franke, Raimo[1,]; Hinze, Alena[2]; Lucas, Nina[3]; Büttgenbach, Stephanus[3]; Klages, Claus-Peter[2]; Frank, Ronald[1]*

[1]Helmholtz Centre for Infection Research GmbH, Department of Chemical Biology, GERMANY; [2]Technische Universität Braunschweig, Institut für Oberflächentechnik, GERMANY; [3]Technische Universität Braunschweig, Institut für Mikrotechnik, GERMANY

[*]E-mail: raimo.franke@helmholtz-hzi.de

Introduction

Micro-arrays are manufactured either by spatial deposition and immobilization of preformed probe molecules or *in situ* by parallel combinatorial chemical synthesis. The latter is carried out by the sequential spatially addressable coupling of activated monomers to an array of chemically reactive sites on a suitably derivatized surface of a planar substrate. Spatially addressable chemical synthesis is achieved either by lithographic masking techniques or by addressable delivery of reagents with suitable pipetting robots. The latter principle was developed by R. Frank and termed SPOT-Synthesis.[1] Previous work in this direction has led to the development of the BioDisc-Synthesizer,[2] which utilizes a novel type of array format based on the Compact Disc information storage medium and rapid (100 Hz) nl-dispensing of reagents with ink jet valves (Fig. 1).

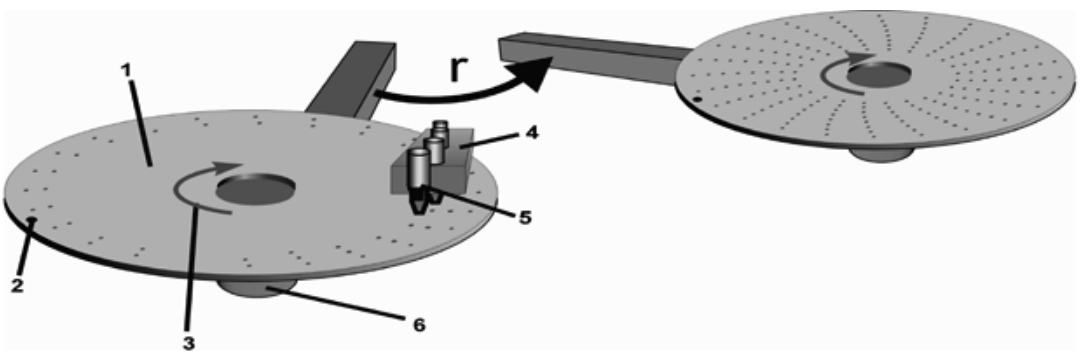

Figure 1. Functional principle of the BioDisc-Synthesizer.[2]

Results and Discussion

We aim at providing an improved substrate disc for the BioDisc-Synthesizer, which will allow for in situ detection by matrix-assisted laser desorption mass spectroscopy (MALDI-MS) of biomolecules captured on the probe array. For this we developed a microstructured surface treatment by atmospheric-pressure microplasmas for local functionalization of a conductive polymer composite disc to generate high density arrays of chemically reactive microsites as anchor spots for spatially addressable chemical array synthesis. Microplasma stamps were used for the area-selective modification of polymer surfaces in the scope of this work.[3] Amino-functionalization by plasma treatment has been conducted in a nitrogen-hydrogen gas mixture (96% N_2 + 4% H_2) at atmospheric pressure with medium frequency excitation (33 kHz), details are described elsewhere.[4] This process allows the separation of the hydrophilic microsites by hydrophobic barriers in order to avoid mixing of reaction solutions during chemical synthesis performed on the rotating substrate disc. In a proof of concept study polypropylene-carbon (PP/C 204) composites, micro-structured and amino-functionalized by plasma treatment, have been utilized to carry out peptide synthesis. Two residues of β-alanine were coupled to the surface using the Fmoc/t-butyl strategy with DIC/HOBt-activation. Unreacted amino groups were capped using acetic anhydride and the N-termini of the peptides were finally biotinylated. Subsequently a bioassay using Cy3-labeled streptavidin as analyte (1:400 diluted in phosphate buffered saline (PBS) containing 1% BSA) was carried out on the composite disc. After 1 h incubation with Cy3-streptavidin, the composite disc was washed with Tris-

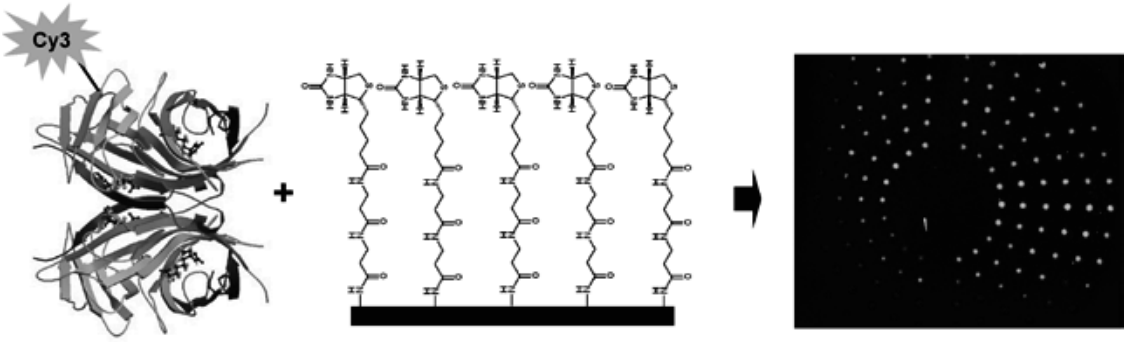

Figure 2. Bioassay on a peptide array, synthesized on plasma-functionalized PP/C.

buffered saline containing 1% of the detergent Tween 20 to wash off any non-specifically bound molecules. Afterwards analysis in a biochip reader (filter setting for Cy3: λ_{ex}= 550 nm, λ_{em}= 570 nm) was performed to detect bound streptavidin molecules. The results presented in Fig. 2 show a strong fluorescence due to the bound Cy3-streptavidin. In conclusion, PP/C-composites, micro-structured and functionalized by plasma treatment, were successfully utilized to carry out chemical synthesis of a peptide array, which was subsequently used to carry out a bioassay on the composite disc surface. Moreover, we could also show that MALDI-ToF-MS can be performed on the conductive PP/C-surface. In the future this will allow the label-free detection of bound analytes, such as antibodies from plasma samples, via mass spectrometry.

Acknowledgements

The authors would like to thank the Institut für Hochspannungstechnik at the TU Braunschweig for providing the PP/C 204 discs. This research is funded by Volkswagen Foundation.

References

1. Frank R. SPOT-synthesis: an easy technique for the positionally addressable, parallel chemical synthesis on a membrane support. *Tetrahedron* **48:** 9217–9232, 1992.
2. Dikmans AJ, Morr M, Zander N, Adler F, Türk G, Frank R. A new compact disc format of high density array synthesis applied to peptide nucleic acids and in situ MALDI analysis. *Mol Divers* **8:** 197-207, 2004.
3. Lucas N, Hinze A, Klages C-P, Büttgenbach S. Design and optimization of dielectric barrier discharge microplasma stamps. *J Phys D: Appl Phys* **41:** 194012-195001, 2008.
4. Lucas N, Franke R, Hinze A, Klages C-P, Frank R, Büttgenbach S. Microplasma stamps for area-selective modification of polymer. *Surfaces Plasma Processes and Polymers* **6**: S370-S374, 2009.

3-19-122

Cellular Activity of Antisense CatLip PNA Conjugates

Shiraishi, Takehiko; Nielsen, Peter E*

Department of Cellular and Molecular Medicine, The Panum Institute, Faculty of Health Sciences,University of Copenhagen, DENMARK

**E-mail: shiraishi@imbg.ku.dk*

Introduction

Bioavailability in general and effective cellular delivery in particular are major challenges for nucleic acid derived gene targeting agents and thus for drug discovery and development of such agents. Conjugation to cationic cell penetrating peptides (such as Tat, Penetratin or oligo-arginines) efficiently improves the cellular uptake of large hydrophilic molecules such as oligonucleotides and peptide nucleic acids (*Proc Nat Acad Sci USA*), but the cellular uptake is predominantly via an unproductive endosomal pathway and therefore mechanisms that promote endosomal escape (or avoid the endosomal route) are required for improving bioavailability. A variety of auxiliary agents (chloroquine (CQ), calcium ions or lipophilic photosensitisers)[1-3] has this effect, but improved, unaided delivery would be highly advantageous in particular for future *in vivo* applications. In order to address whether conjugation of a lipophilic moiety (a fatty acid) to a cationic cell penetrating peptide domain could be a general principle to obtain increased cellular bioavailability we recently made a series of PNA conjugates based on oligo-arginines and Tat-peptide and tested in a luciferase cellular antisense assay (using HeLa pLuc 705 cells).[4]

Results and discussion

We found that simply conjugating a lipid domain (fatty acid) to the cationic peptide (a CatLip conjugate) significantly increases the biological effect of the corresponding PNA (CatLip) conjugates.[4] In particular, PNA-Tat conjugate shows only very weak antisense activity, the analogous conjugate containing a decanoic acid attached to the ε-amino group of a lysine (Tat- Deca-PNA) is dramatically more active. The activity is further enhanced by having two decanoic acids in the conjugate (Deca-Tat-Deca-PNA) resulting in a luciferase activity 150 times higher than that found for the pure Tat-PNA conjugate at 2 μM. We also studied the effect of cleavable linkers (ALALG (peptide linker) or BMB2 (ester linker)[5] between the PNA and the CatLip domain (Fig. 1). The PNA with cleavable ALALG-linker (PNA2782) or with BMB2 linker (PNA 2630) showed slightly higher activity (ca. 2-fold at 4 μM) than ordinary Tat-Deca-PNA (PNA2534). However, so did the PNA with non-cleavable SMCC-linker (PNA2630) (ca. 3-fold at 4 μM). Therefore, we unfortunately or not able to ascribe the increased activity to the cleavability of the linker.

In addition we compared the activities of (D-Arg)$_n$-Deca-*Proc Nat Acad Sci USA* and (L-Arg)$_n$-Deca-*Proc Nat Acad Sci USA* in the absence or the presence of the endosome disruptive agent chloroquine (Fig. 2).

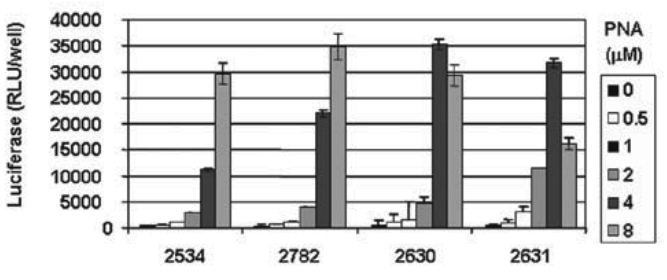

PNA#	Sequence
2534	Tat-Lys(Deca)-Gly-PNA[1]
2782	Tat-Lys(Deca)-ALALG[2]-PNA
2630	Tat-SMCC[3]-Lys(Deca)-BMB2[4]-Gly-PNA
2631	Tat-SMCC-Lys(Deca)-Gly-PNA

[1] PNA sequence, CCTCTTACCTCAGTTACA. [2] ALALG is a peptide cleavable linker (Ala-Leu-Ala-Leu-Gly). [3] SMCC (Succinimidyl 4-[*N*-maleimidomethyl]cyclohexane-1-carboxylate) is heterobifunctional linker. [4] BMB2 (2-([N-Boc-glycyl]oxymethyl)benzoic acid.) is an ester cleavable linker.

Figure 1. Relative cellular luciferase antisense activity in HeLa pLuc705 cells of *Proc Nat Acad Sci USA* conjugated to Tat-peptide and decanoic acidby a direct conjugation or *via* cleavable linkers. Cells were treated with *Proc Nat Acad Sci USA* (2534, 2782, 2630, and 2631) for 4 h in OPTI-MEM medium and incubated further for 24 h in the presence of serum. The cell samples were then subjected to luciferase analysis and shown as relative light units (RLU/well) (n=3. indicated as mean ± SD).

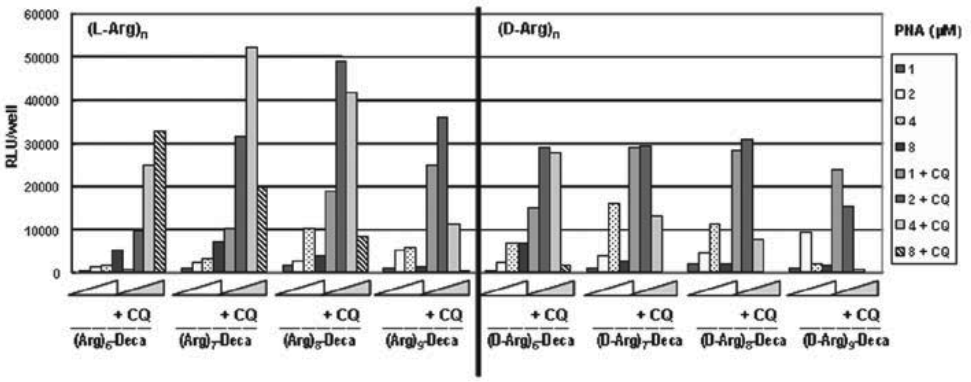

Figure 2. Relative cellular luciferase antisense activity in HeLa pLuc705 cells of *Proc Nat Acad Sci USA* conjugated to oligo-arginine (D or L) and decanoic acid in the absence and presence of the 100 μM chloroquine (CQ). Cells were treated with *Proc Nat Acad Sci USA* for 4 h in OPTI-MEM medium and incubated further for 24 h in the presence of serum. The cell samples were then subjected to luciferase analysis and shown as relative light units (RLU/well).

While *Proc Nat Acad Sci USA* with D-arginines ((D-Arg)$_n$-Deca-PNA) showed higher antisense activities than the corresponding PNA with L-arginines in the absence of CQ, this order was reversed in the presence of CQ, (L-Arg)$_n$-Deca-*Proc Nat Acad Sci USA*. Analogous behavior was observed upon comparison of (L-Arg)$_n$-*Proc Nat Acad Sci USA* and (D-Arg)$_n$-*Proc Nat Acad Sci USA* in combination wth photochemical internalization.[1] The higher nuclear antisense activity of the PNA L-arginine conjugates (compared to than D-arginine) might be explained by the fact that L-arginine chain will be digested by the endosomal proteases while D-arginine chain is stable. These results suggest that liberation of the PNA from the CatLip domain may improve the nuclear antisense activities although the escape from the endosomal compartments itself remains one of the major rate limiting steps.

Acknowledgment

This work was supported by the Lundbeck Foundation, The Danish Cancer Foundation and the European Commission (6th FP EMIL and SNIPER contracts LSHC-CT-2004-503569 & LSHB-CT-2004-005204). The authors would like to acknowledge Ms. Jolanta Ludvigsen and MSc. Nadia Bendifallah for synthesizing the PNA conjugates.

References

1. Shiraishi T, Nielsen PE. *FEBS Letter*s **580**: 1451-1456, 2006.
2. Shiraishi T, Pankratova S, Nielsen PE. *Chemistry & Biology* **12**: 923 -929, 2005.
3. Shiraishi T, Nielsen PE. *Nature Protocols* **1**: 633-636, 2006.
4. Koppelhus U, Shiraishi T, Zachar V, Pankratova S, Nielsen PE. *Bioconjug Chem* **19**: 1526-1534, 2008.
5. Bendifallah N, Kristensen E, Dahl O, Koppelhus U, Nielsen PE. *Bioconjug Chem* **14**: 588-592, 2003; (Erratum in: *Bioconjug Chem* **14**: 848, 2003).

3-26-123

New Strategy for Protein Identification-Improving Signal Intensity and Sensitivity of MALDI Mass Spectrometry by Specific Peptide Derivatization

Cantel, Sonia; Valmalle, Charlène; Subra, Gilles; Enjalbal, Christine; Martinez, Jean

IBMM, Institut des Biomolécules Max Mousseron, Universités Montpellier 1 et 2, Department of Amino Acids, Peptides and Proteins, FRANCE

**E-mail: sonia.cantel@univ-montp2.fr*

Introduction

Biochemical and Molecular Biological approaches are generally used to isolate and characterize a Protein target. Biotinylated (and/or Poly-His) analogues can be designed to purify the binding sites by affinity chromatography. Then, the purified protein extracts are further purified by one or two dimensional chromatography and then submitted to mass spectrometry analysis (nanoLC-MS/MS) after enzymatic digestion.

The resulting PMF (Peptide Mass Fingerprint) for an unknown protein can be compared with all of the PMFs in a database to find the best match, thereby identifying the protein.

There are, however, several technical difficulties involved in determining the PMF for a protein. A typical protein will give rise to at least twenty to thirty peptides after trypsin digestion. Not all of these peptides will appear in the mass spectrum. One factor that is believed to cause incomplete spectra is competition for protonation during the ionization process inducing ion discrimination. Moreover, sensitivity is a problem with conventional protocols for identifying proteins from their PMF.

Derivatization-based strategies to improve the analysis of peptides by enhancement of the MALDI MS signal intensities have been described for UV MALDI ionization.[1] In these technologies, the matrix absorbs the laser UV light and transmits energy to the directly linked protein or peptide molecules, thus promoting their desorption and ionization.

We have recently developed a new technology allowing specific labeling of lysine residues in proteins and easy MALDI-MS detection and identification of labeled peptides following protein hydrolysis.[2] *N*-hydroxysuccinimide ester of α-cyano-4-hydroxycinnamic acid (CHCA) was used as labeling reagent to dramatically increase MALDI signal of Lysine-containing peptides in Cytochrome C proteolytic mixture.

This original approach enables to discriminate labeled peptides of interest among other abundant peptides. We decided to apply this strategy for identification and characterization of peptides within complex mixtures to identify new protein targets and in a strategy of ligand deorphanization (Scheme 1).

Results and Discussion.

In order to investigate the limit of this tool, a chosen model peptide (FPTTTKFAA-OH) was labeled by coupling with CHCA and analyzed by MALDI-MS at different concentrations in a mixture of 5 other non-labeled peptides (Table 1). The labeled peptide allowed a limit of detection corresponding to a relative concentration of 0.002%, indicating a 1000-fold sensitivity increase compared to a non labeled peptide (Fig. 1).

In a second set of experiments, the labeled peptide was tested in a highly complex mixture coming from tryptic hydrolysis of 7 different proteins (Table 2). Within this highly complex mixture the limit of detection corresponding to a relative concentration was 0.02% (Fig. 2). This level of sensitivity should allow detection of a labeled peptide coming from a labeled protein target within a complex mixture of proteins after tryptic hydrolysis.

Scheme 1.Strategy for specific protein identification by mass spectrometry analysis

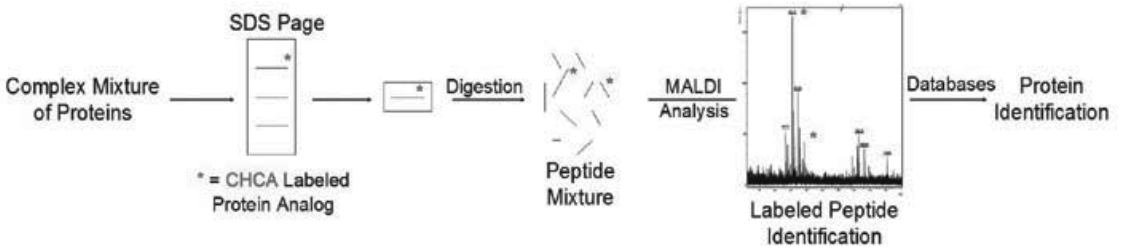

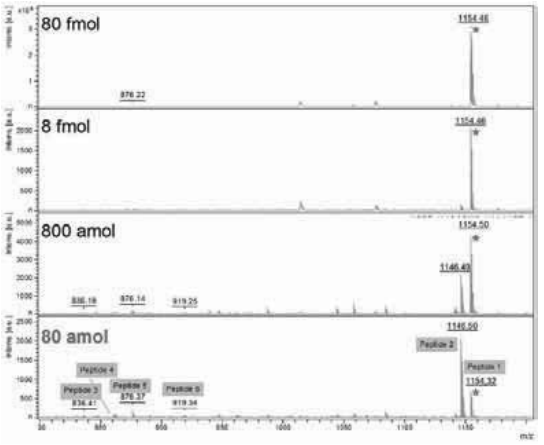

Figure 1. MALDI spectrum of labeled peptide at different concentrations within a peptide mixture.

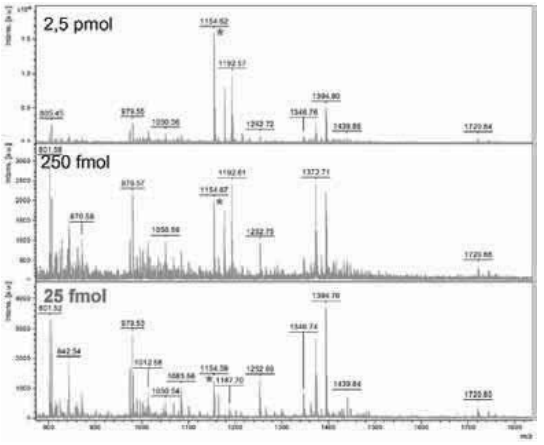

Figure 2. MALDI spectrum of labeled peptide at different concentrations in a tryptic peptide mixture.

In conclusion, we were able to develop a methodology that allowed highly sensitive detection of specific labeled peptides within a complex protein mixture. This technology will be applied to the labeling of ligands with both *α*-cyano-4-hydroxycinnamic acid and a cross-linker (i.e. BPA), followed by cross-linking to the protein target, hydrolysis and MALDI MS detection of the labeled peptide(s). Search in databases will then provide the sequence of the target protein and its characterization. This methodology should allow deorphanization of ligands without extensive purification of the protein target.

References

1. Pashkova A, Moskovets E, Karger BL. Coumarin Tags for Improved Analysis of Peptides by MALDI-TOF MS and MS/MS. *Anal Chem* **76**: 4550-4557, 2004.
2. Lascoux D, Paramelle D, Subra G, Heymann M, Geourjon C, Martinez J, Forest E. Discrimination and Selective Enhancement of Signals in the MALDI Mass Spectrum of a Protein by Combining a Matrix-Based Label for Lysine Residues with a Neutral Matrix. *Angew Chem Int Ed* **119**: 5690-5693, 2007.

3-27-124

Synthesis and evaluation of peptide analogues as functional probes targeting matrix metalloproteinases

Plattner, Hannes Patrik[1]; Collet, Magalie[1]; Hoess, Eva[2]; Lenger, Janina[1]; Pestlin, Gabriele[2]; Sewald, Norbert[1,]*

[1]Bielefeld University, Organic and Bioorganic chemistry, GERMANY; [2]Pensberg, Roche Diagnostics GmbH, GERMANY

[*]E-mail: norbert.sewald@uni-bielefeld.de

Introduction

The isolation and detection of low abundant enzymes and proteins is one of the most challenging tasks in bioanalytical and pharmacological fields, especially if information about their state of activity is required. For this purpose tailored solutions for addressing the members of a protein family are necessary. Peptide chemistry provides established methods to assemble building blocks in order to construct such molecular probes. We chose matrix metalloproteinases (MMP) for validation of such an approach. This protein family processes and degrades various extracellular matrix proteins and possesses a highly conserved catalytic site with a zinc ion in its centre. Most of the known and potent inhibitors are peptidomimetics containing zinc chelating hydroxamate groups (e.g. marimastat).[1,2] Although it binds reversibly, it is potent and active against a wide range of metalloproteinases.

Results and discussion

Molecular probes to target matrix metalloproteinases were designed and synthesized based on a building block strategy. Marimastat was used as head group to target MMP and biotin served as a reporter group to isolate and detect labelled protein. A spacer links both functionalities. A photoreactive group (L-4-benzoylphenylalanine) was additionally introduced into the molecule to form a covalent bond to target the protein upon irradiation[3] and to improve the isolation of MMP with magnetic beads (Fig. 1). This would enable metalloproteinase pulldown on streptavidin-beads combined with a permanent labelling of the metalloproteinases by a biotinylated probe. The selectivity of the probe was tested in activity assays and the IC_{50} values were determined to lie in the nanomolar range. Non-covalent isolation experiments of MMP-9 were successfully performed from buffer solutions to validate

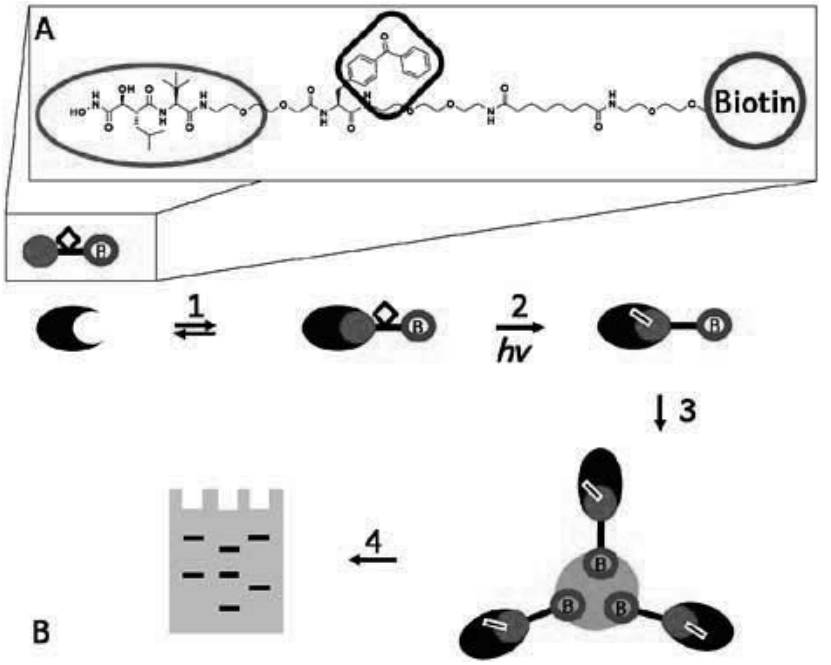

Figure 1. Activity based approach to isolate matrix metalloproteinases.

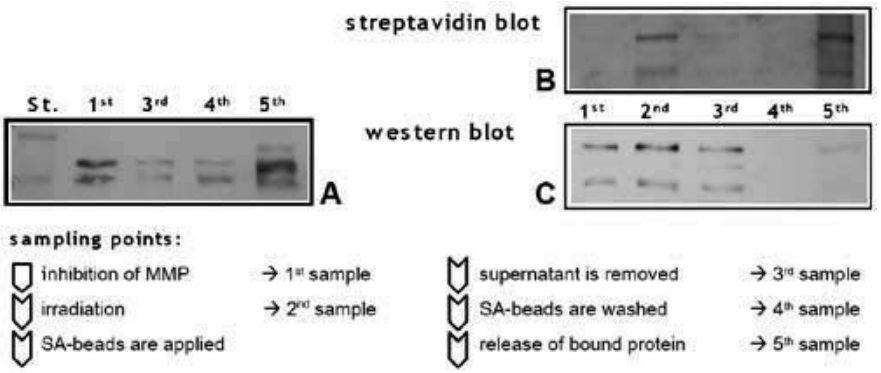

Figure 2. Stages of the pulldown/photocrosslinking experiment with MMP-9. (A) Non-covalent isolation without irradiation and (B/C) with irradiation for covalent biotinylation.

the approach. Western blot analysis (Fig. 2) indicated small amounts of MMP-9 in the supernatant of the beads and in the washing fraction. This can be explained by the reversibility of the protein binding or by the presence of inactive protein. To be able to transfer this approach to more complex mixtures, intensified washing protocols are necessary to remove all unspecific bound protein. The formation of a covalent bond prevents the loss of isolated protein during multiple washing steps. For this purpose the solutions were irradiated at a wavelength of 350 nm after incubation of the proteinase with the probe (Fig. 1). The trifunctional probe (A) was used to target MMP-9 (1) and label it covalently (2). Those complexes were enriched with streptavidin coated beads (3) before denaturing conditions were applied to release the proteins from the beads (4).

Samples were taken after each step of the experiment with purified MMP-9 to monitor the efficiency of pulldown and photocrosslinking. Additionally to the Western blot analysis the efficiency of the labeling experiment was tested. Using horseradish peroxidase conjugated streptavidin the formation of the covalent protein-probe complex can be detected (Fig. 2). The streptavidin blot shows that labeling of the MMP-9 during the irradiation occurs. It also proves the ability to remove biotinylated proteins quantitatively using streptavidin coated beads. The complementary information of the western blot demonstrates an incomplete labeling of the protein. Tests with increased irradiation times suspect a decomposition of the protein as side effect during labeling and cause a dissociation of the probe (results not shown).

Samples were taken (1st) after incubation of MMP-9 with the biotinylated Marimastat probe; (2nd) after photocrosslinking, only B and C; (3rd) after incubation with streptavidin beads the supernatant was analyzed; (4th) the washing solution of the beads and (5th) the released MMP-9.

We have successfully synthesized a biotinylated probe to target MMP-9 based on the activity of the enzyme. A covalent bond could be established using an inhibitor independent photoactive group. The label was used to purify the proteins with streptavidin beads and additionally to stain them in a biotin detection blot.

Acknowledgements

Thanks to Anke Nieß and Peter Schröder for their synthetical assistance and Kai Jenssen for the introduction into this topic. This work was financially supported by Roche Diagnostics GmbH.

References

1. Jenssen K, Sewald K, Sewald N. B*ioconj Chem* **15:** 594-600, 2004.
2. Collet M, Lenger J, Jenssen K, Plattner H. P, Sewald N. *J Biotechnol* **129:** 316-328, 2007.
3. Hagenstein MC, Mussgnug JH, Lotte K, Plessow R, Brockhinke A, Kruse O, Sewald N. *Angew Chem* **115:** 5793-5796, 2003; *Angew Chem Int Ed* Engl **42:** 5635-5638, 2003.

3-28-125

The Potential Stem-Forming Sequence Consists of the 2-Stranded β-Structure in Prion Proteins

Saiki, Masatoshi[1,]; Hidaka, Yuji[1]; Nara, Msayuki[2]; Morii, Hisayuki[3]*

[1]Kinki University, Department of Life Science, School of Science and, JAPAN; [2]Tokyo Medical and Dental University, Laboratory of Chemistry, JAPAN; [3]National Institute of Advanced Industrial Science and Technology (AIST), JAPAN

[*]E-mail: saiki@life.kindai.ac.jp

Introduction

Amyloid fibrils are responsible for several diseases, which are generally termed conformational diseases. Prion diseases have become a serious social issue. Prion protein is known to form amyloids in cells of mammalian brains. Up to date several structural models of fibrils are proposed for respective proteins, but the structure of pathogenic prion is still veiled. Certain fragment peptides of prion were reported to form amyloids with the interaction of single *β*-strand in each peptide. However, it seems difficult to form aggregates by the interaction with only one *β*-strand in each peptide, because of their high structural flexibility of the molecular chain to be stem-forming region. On the other hand, a 2-stranded *β*-structure is presumed to be more stable as a fibril forming intermediate than a single strand. Therefore, the aggregation mechanism of prion protein remains to be further studied on their precursor structures. In the present paper, we focused on the possible precursor region of the stem of aggregates consisting of a 2-stranded *β*-structure as for prion protein.

Results and Discussion

Recently, we have established a novel strategy to determine the amino acid sequence for amyloid formation, based on their essential interactions.[1,2] Probable fibril-forming peptides were obtained by our calculation method at positions from 160 to 230 in the amino acid sequence. In order to confirm whether aggregates of the candidate peptides consist of the 2-stranded *β*-structure, a series of peptides consisting of g10 residues-turn-10 residues h were prepared (Fig. 1).

Several candidate peptides, of which regions are 166-187, 168-189, 170-191, and 178-199, showed the typical enhanced fluorescence intensities in the thioflavin T-binding assay, suggesting the amyloid formation. The fibril forming abilities of these peptides were also examined by electron microscopy (Fig. 2). The result clearly indicates that, among the synthetic peptides based on our calculation method, these peptides possess remarkable amyloid-forming ability.

In order to obtain the structural information of synthetic peptides, we measured CD spectra of these

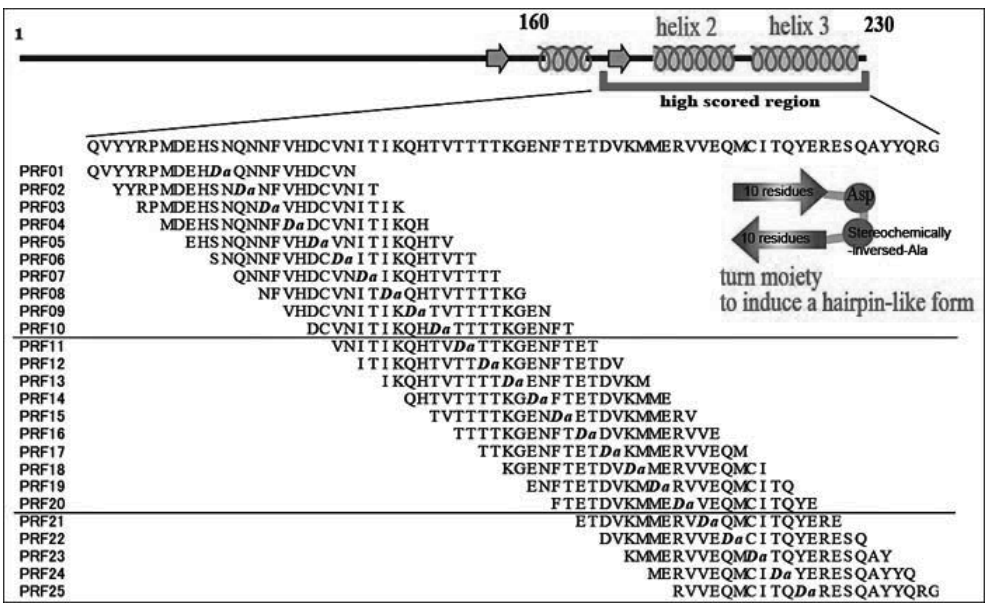

Figure 1. Designed peptides, 10 residues-turn-10 residues, covering the region including predicted sequences with amyloid-forming propensity were synthesized. (ga h indicates stereochemically-inversd Ala).

Figure 2. Electron microscopic images of the peptides, MDEHSNQNNF-Da-DCVNITIKQH and DCVNITIKQH-Da-TTTTKGENFT, with high-scoring sequence for amyloid forming propensity.

peptides. The peptides with little thioflavin T fluorescence showed typical random coil structure. On the other hand, the peptides exhibiting enhanced fluorescence of thioflavin T are likely to have amyloid structure rich in β-structure. In order to confirm whether the peptides bearing β-rich amyloid structure form 2-stranded β-sheet or not, IR spectra were analyzed. IR spectra of these peptides showed the typical bands corresponding to the β-structure in the region of amide-I f band. In addition, the peptide (178-199) exhibited a shoulder band at 1654 cm^{-1} in IR spectrum, reflecting a turn structure. These results revealed that the amyloids of the peptide (178-199) are constructed with the 2-stranded β-structure, which may be formed by intra-molecular hydrogen bonds.

Summarizing the results obtained here, it should be noted that the sequence from 178 to 187, which is common for 4 peptides described above, could be a key region for the transition from a normal to an abnormal structural state of prion.

Acknowledgments

We thank Ms. Emiko Kobayashi (AIST) for her indispensable suggestions and skillful electron microscopic observations of amyloid fibrils.

References

1 Saiki M, Honda S, Kawasaki K, Zhou D, Kaito A, Konakahara T, Morii H. *J Mol Biol* **348:** 983-998, 2005.
2 Saiki M, Konakahara T, Morii H. *Biochem Biophys Res Commun* **343:** 1262-1271, 2006.

4-01-001

CREDEX-MS: Molecular elucidation of carbohydrate recognition peptides in lectins and related proteins by proteolytic excision- mass spectrometry

Przybylski, Michael[1,]; Moise, Adrian[1]; Siebert, Hans-Christian[2]; Gabius, Hans-Joachim[2]*

[1]University of Konstanz, Department of Chemistry, Laboratory of Analytical Chemistry, GERMANY; [2]Department of Physiological Chemistry, Ludwig-Maximilians-University of Munich, Munich, GERMANY

[*]E-mail: michael.przybylski@uni-konstanz.de

Introduction

The emerging relevance of glycan-encoded information in a plethora of biological events directs increasing attention to interaction structures between bioactive glycan determinants and their endogenous receptors, such as lectins.[1] Structures of carbohydrate complexes with lectins and antibodies have been determined in a few cases by X-ray crystallography and NMR, however both methods are limited by large amounts and high purity of material required. We report here a new direct method for molecular mapping of peptide motifs in lectin carbohydrate domains (CRD) by the combination of proteolytic excision of protein-carbohydrate complexes and mass spectrometry (CREDEX: **C**arbohydrate-**RE**cognition-**D**omain-**EX**cision). In a first study, the CREDEX-MS method was applied to the identification of the carbohydrate binding sites of human galectin-3 and galectin-1, for which X-ray crystal structures of their lactose complexes have been determined.[2]

Results and Discussion

Lactose was covalently coupled to epoxy-activated Sepharose, galectins added to the affinity matrix and the lectin-carbohydrate complexes digested using trypsin. After removal of unbound fragments, competitive elution of the remaining affinity-bound gal-peptides was performed with lactose. MALDI-MS analysis of the elution fraction provided the direct identification of specific peptides, gal-3(152-162) and gal-3(177-183); and gal-1(37-48) and gal-1(64-73), respectively. The identified CRD peptides were in complete agreement with the binding sites from the crystal structures [3]. With the same method, two specific, discontinuous gal-3 peptide epitopes, gal-3(152-162) and gal-3(130-144) were identified for blood group tri-A. The specificity of the epitope peptides was confirmed by affinity-MS of the synthetic CRD peptides,[3] and by inhibition studies with gal-3 in two human lymphoma cell lines. Most recent applications to CRD identifications of hitherto unknown lectin-carbohydrate complexes ascertain the CREDEX-MS approach as a powerful tool for the direct determination of CRDs in solution, suggesting a wide range of applications to define contact sites for lectin ligands of human sugar receptors in biological material.[4]

References

1. Gabius H-J. Cell surface glycans: the why and how of their functionality as biochemical signals in lectin-mediated information transfer. *Crit Rev Immunol* **26**: 43-80, 2006.
2. Seetharaman J, Kanigsberg A, Slaaby R, Leffler H, Barondes SH, Rini JM. X-ray crystal structure of the human galectin-3 carbohydrate recognition domain at 2.1-A resolution. *J Biol Chem* **273**: 13047-13052, 1998.
3. Moise A, Siebert HC, Gabius H-J, Przybylski M. *New Biotechnology , Vol 25S, p S19, 2009.* doi:10.1016/j.nbt.2009.06.048
4. Przybylski M, Moise A, Gabius H-J. *Eur Patent application* S9247, 2008.

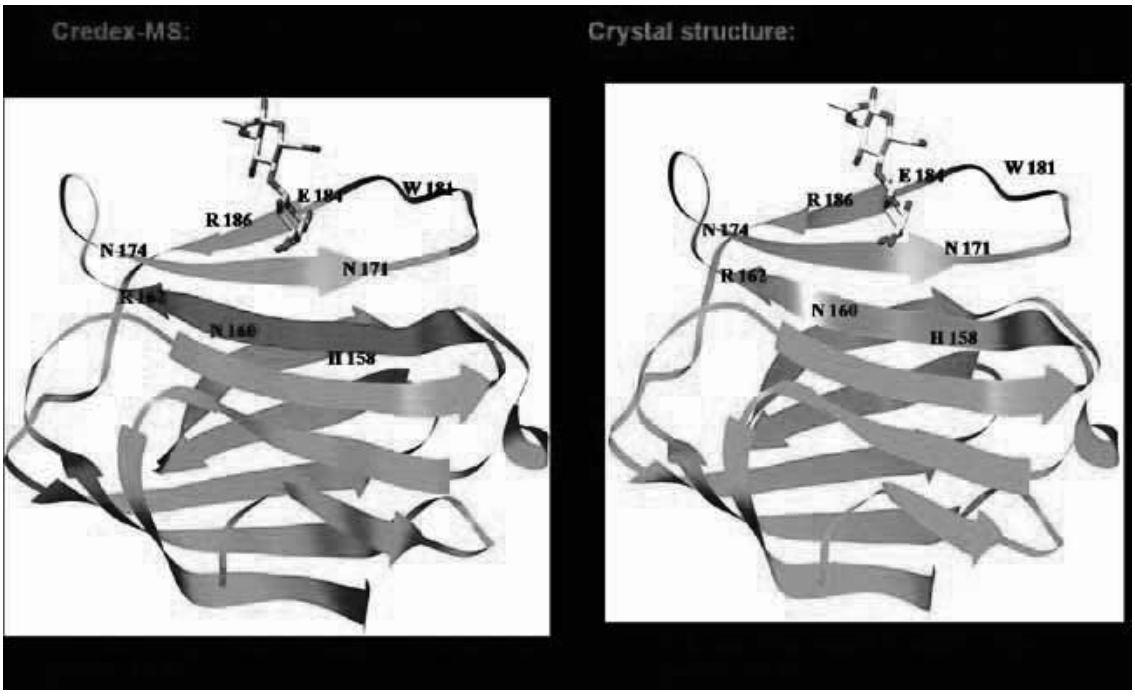

Figure 1. Comparison of the CREDEX-MS results with X-ray crystal structure of the galectin-3 CRDs in complex with LacNAc. Peptides identified by CREDEX-MS are highlighted in red. The peptides comprising the amino acid residues (in bold) that interact directly with the carbohydrate are highlighted in green.

4-07-002

Novel non-peptide ghrelin receptor ligands based on 1,2,4-trisubstituted triazoles

Blayo, Anne-Laure[1]; Moulin, Aline[1]; Demange, Luc[1]; Galleyrand, Jean-Claude[1]; Locatelli, Vittorio[2]; Torsello, Antonio[2]; Perrissoud, Daniel[3]; Salomé, Nicolas[4]; Dickson, Suzanne L.[4]; Martinez, Jean[1]; Fehrentz, Jean-Alain[1,]*

[1]Faculté de Pharmacie, Université Montpellier 1, Institute of Biomolecules Max Mousseron, FRANCE; [2]Universita di Milano-Bicocca, Dipartimento di Medicina Sperimentale, ITALY; [3]Aeterna-Zentaris, GERMANY; [4]Department of Physiology/Endocrinology, The Sahlgrenska Academy at Gothenburg University, Gothenburg, SWEDEN

[*]E-mail: jean-alain.fehrentz@univ-montp1.fr

The central actions of ghrelin include stimulation of appetite and GH secretion. Such properties support the hope that ghrelin receptor antagonists could be useful for the treatment of obesity. However for an efficient anti-obesity activity, an ideal ghrelin antagonist should counteract the orexigenic effect of ghrelin without altering the effect on GH secretion, since GH deficiency is frequently associated with increased adiposity. Starting from compound JMV 1843 (Fig. 1),[1] a potent pseudotripeptide agonist of the ghrelin receptor, we decided to introduce a cyclic structure as scaffold bearing the three major pharmacophores contained in compound JMV 1843.

Several cyclic scaffolds were tested such as piperazines, keto-piperazines, piperidines and triazinones (unpublished results). 1,2,4-triazoles were found to be the best template. We then developed this new series of ghrelin receptor ligands based on 1,2,4-trisubstituted triazoles. In position 4 of the triazole, the best R^1 substitutions were found to be 4-methoxybenzyl or 2,4-dimethoxybenzyl groups; for R^2, a two carbon length chain between position 5 of the triazole and an aromatic group (phenyl or indole) led to ligands presenting the best affinity and various R^3 groups as acylating agents of the primary amine could be introduced and they greatly influence the agonist or antagonist character of the obtained compounds. The systematic screening of over 250 novel compounds for their ability to displace radiolabelled ghrelin and to activate or to inhibit calcium uptake in cells transiently expressing GHS-R1a led to the characterization of compounds acting as ghrelin receptor full agonists, partial agonists or antagonists.[2,3,4] Some results are gathered in Table 1.

These compounds were then investigated for their effects on food intake and GH secretion in animal models. Our results showed that non-peptide compounds characterized as *in vitro* ghrelin receptor antagonists were able *in vivo* to inhibit food intake without altering GH secretion. As an example, JMV 2959 (Fig. 2), exhibited *in vitro* an IC50 of 32 nM and a Kb of 19 nM. When evaluated for its activity on GH secretion after s.c. injection in 10 days old rats, compound JMV 2959 did not have any proper effect on GH release. Furthermore, compound JMV 2959 (160 µg/kg) was not able to modify hexarelin-stimulated GH release (80 µg/kg). Food intake control elicited by this compound was also evaluated on two animal models. In a first model, after one week of training, young-adult male Sprague Dawley rats were administered s.c. with 160 µg/kg of compound JMV 2959 at time -10 min, and/or hexarelin (80 µg/kg) at time 0 to stimulate the feeding behaviour. Immediately after, the animals were returned to their home cages, which contained a known amount of standard rat chow and ad libitum water. Compound JMV 2959 was unable to stimulate food intake when administered alone. Moreover, when administered with hexarelin, cumulative food intake stimulated by hexarelin was totally inhibited even at 6 hours. In a second model, mice were fasted for 16 hours before p.o. administration of the test substance (2 µmole/mouse) as described.[5] Compound JMV 2959

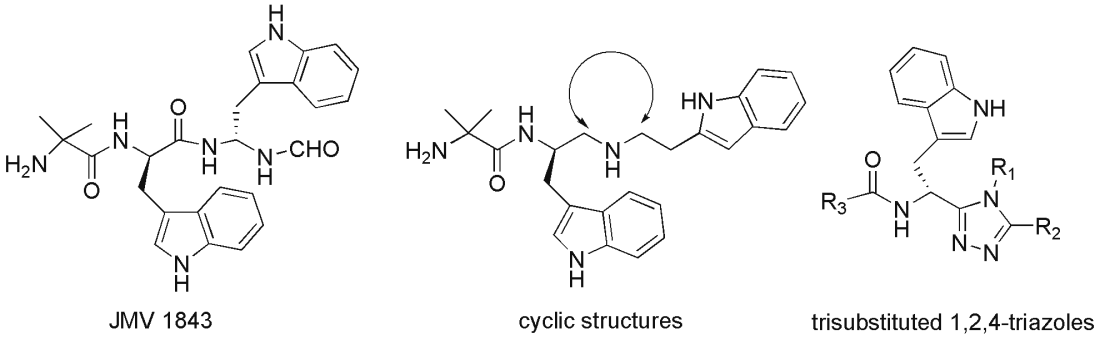

Figure 1. From the pseudopeptide structure (JMV 1843) to the 1,2,4- triazole scaffold.

Table 1. Binding affinity constants and biological activities of trisubstituted 1,2,4-triazoles

R_3	R_2	R_1	IC_{50} (nM)	Biological activity	Kb (nM)	EC_{50} (nM)
Aib	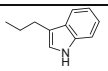		6 ± 3	antagonist	4 ± 1	-
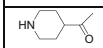	"	"	0.3 ± 0.2	agonist	-	3.0 ± 1.3
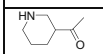	"	"	10 ± 2	agonist	-	2.5 ± 1
	"	"	1.9 ± 0.6	antagonist	102 ± 20	-
	"	"	45 ± 7	antagonist	24 ± 14	-
Gly	"	"	76 ± 20	antagonist	19 ± 6	-

significantly reduced food intake over the 4-hour test period as compared with vehicle (up to -28% from control at time point T + 4 hours).

The dissociated effects of the novel ghrelin receptor ligands on food intake and GH secretion support the role of different subtypes or signaling pathways of the ghrelin receptor in the control of these functions. Our results suggest that some of the compounds described in this study selectively target the mechanism of action of the ghrelin receptor correlated with food intake and not with GH secretion. Further investigations are going on to explain these observations.

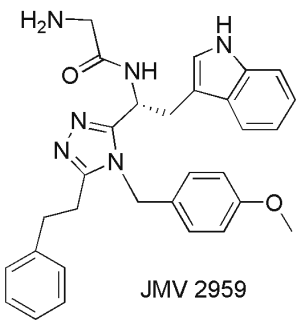

Figure 2. Structure of compound JMV 2959.

References

1. Guerlavais V, Boeglin D, Mousseaux D, Oiry C, Heitz A, Deghenghi R, Locatelli V, Torsello A, Ghé C, Catapano F, Muccioli G, Galleyrand JC, Fehrentz JA, Martinez J. New active series of growth hormone secretagogues. *J Med Chem* **46**: 1191-1203, 2003.
2. Demange L, Boeglin D, Moulin A, Mousseaux D, Ryan J, Bergé G, Gagne D, Heitz A, Perrissoud D, Locatelli V, Torsello A, Galleyrand JC, Fehrentz JA, Martinez J. Synthesis and Pharmacological in Vitro and in Vivo Evaluations of Novel Triazole Derivatives as Ligands of the Ghrelin Receptor. 1. *J Med Chem* **50**: 1939-1957, 2007.
3. Moulin A, Demange L, Bergé G, Gagne D, Ryan J, Mousseaux D, Heitz A, Perrissoud D, Locatelli V, Torsello A, Galleyrand JC, Fehrentz JA, Martinez J. Towards Potent GHS-R1a Ligands Based on Trisubstituted 1,2,4-Triazole Structure. Synthesis and Pharmacological in Vitro and in Vivo Evaluations. 2. *J Med Chem* **50**: 5790-5806, 2007.
4. Moulin A, Demange L, Ryan J, Mousseaux D, Sanchez P, Bergé G, Gagne D, Perrissoud D, Locatelli V, Torsello A, Galleyrand JC, Fehrentz JA, Martinez J. Towards New Potent GHS-R1a Antagonists Based on Trisubstituted 1,2,4-Triazole Structure. 3. Synthesis and Pharmacological in vitro and in vivo Evaluations. *J Med Chem* **51**: 689-693, 2008.
5. Asakawa A, Inui A, Kaga T, Katsuura G, Fujimiya M, Fujino MA, Kasuga M. Antagonism of ghrelin receptor reduces food intake and body weight gain in mice. *Gut* **52**: 947-952, 2003.

4-13-003

The proline-rich antimicrobial peptide dimer A3-APO and its single chain in vivo metabolite represent a new paradigm in microbiology, pharmacology and drug development.

Cassone, Marco[1,]; Vogiatzi, Paraskevi[1]; Wade, John D[2]; Rozgonyi, Ferencz[3]; Szabo, Dora[3]; Kocsis, Bela[3]; Otvos, Laszlo[4]*

[1]Temple University, UNITED STATES; [2]Howard Florey Institute, University of Melbourne, AUSTRALIA; [3]Semmelweiss University, HUNGARY; [4]Temple University, HUNGARY

[*]E-mail: cassone@temple.edu

Introduction

Native Proline-rich antimicrobial peptides are widely diffused in nature. They penetrate or disintegrate bacterial membranes and specifically inhibit the bacterial heat shock protein DnaK, or HSP70, thus showing an interesting, dual and specific mechanism of action. Molecular modeling of the bioactive protein indicates that the peptide binding site is located at the D-E helix region of the carboxy-terminal multihelical lid. DnaK only functions as dimer, and binding the D-E helix region the Proline-rich peptides impair protein refolding activity and kill the bacterial cell. SAR studies of the best-studied native proline-rich peptide pyrrhocoricin identified the Asp[2]-Lys[3] dipeptide and Tyr[6]-Leu-Pro-Arg-Pro[10] pentapeptide fragments as crucial for antibacterial activity.[1]

Results and Discussion

A series of synthetic peptides with variable degrees of homology to the major natural exponents of this class was designed, and among those structural modifications such as the development of dimers were evaluated. To identify which A3-APO analogs bind purified DnaK protein, a dot-blot assay was used. To test the efficacy on several bacterial species, we performed Minimal Inhibitory Concentration (MIC) determination assay in duplicate using a liquid growth inhibition microdilution assay in sterile polypropylene 96-well plates (Nunc F96 microtiter plates), with a final volumeof 100 µl.[2] The lead compound A3-APO was selected for its highest efficacy against several *Enterobacteriaceae* as well as a few Gram-positives such as Staphylococcus saprophyticus. The Minimal Inhibitory Concentrations of A3-APO in undiluted broth ranged from 1 to 8 mg/L for *E. coli*, *K. pneumoniae* and *S. typhimurium*. The peculiar molecular target of A3-APO means it is equally active on Multi-Drug Resistant (MDR) strains. Also, its target is a crucial pathway for maintenance of functional enzymes in the cell. Since resistance to many antibiotics is due to the expression or de novo acquisition of enzymes that degrade conventional antibiotics or bypass their targets, we wondered whether A3-APO could be effective not only alone, but also in synergy with common antibiotics.[3] This aspect was exploited by antimicrobial

Table 1. MICs of several A3APO analogues against selected strains

Bacterial Strain	MIC (µg/ml)						
	A3-APO	Arg5A3	Glu4A3	Lys12A3	Gly11A3	A3 Single chain	A3-desVal
E. coli HK101	2	2	2	2	4	6.5	2
E. coli HK179	2	2	2	2	4	1	2
E. coli SOTE40	8	8	8	8	32	2	2
E. coli 5770	2	2	2	2	4	6.5	1
E. coli HK131	4	4	8	8	32	1	4
E. coli SEQ102	2	2	2	2	4	1	2
E. coli 045-847	4	2	4	4	8	2	2
K. pneumoniae HK 123	4	4	8	8	32	2	16
K. pneumoniae HK 186	8	4	8	8	32	0.25	4
K. pneumoniae HK 127	8	8	8	8	32	0.25	1
K. pneumoniae D12-3132	2	2	2	2	8	0.25	2
K. pneumoniae K6	4	4	8	4	16	2	4
S. typhimurium ATCC 14028	8	4	8	8	16	1	4
S. typhimurium S5	8	8	8	8	16	0.5	4
S. typhimurium G10215	4	4	4	4	8	0.25	2
P. aeruginosa ATCC 39329	8	4	8	4	8	32	8
P. aeruginosa 10	8	8	8	4	8	32	4
S. saprophyticus ATCC 15305	2	2	2	2	2	4	2

combination studies. As expected, through inactivating of resistance enzymes, A3-APO was able to recover *in vitro* the lost activity of conventional antibiotics including chloramphenicol, β-lactams, sulfonamides or trimethoprim with a partial or full synergic effect. However, the synergy appeared to be individual strain and drug combination-dependent. In order to evaluate A3-APO as a candidate for preclinical studies, we tested its stability in mouse serum. A3-APO was rapidly degraded to smaller metabolites, and principally in its monomeric form (Chex1-Arg^{20}). Investigation of the efficacy of this monomer, single chain metabolite demonstrated a surprisingly good activity against *Enterobacteriaceae* strains. While the dimeric structure seemed not to be needed after sequence optimization, we observed that the monomer exhibits even better efficacy than A3-APO, but on a narrower spectrum of species, namely limited to *E. coli*, *Salmonella* and *Klebsiella*, probably due to an improved intracellular target affinity but at the same time less activity on the membrane (Table 1).

Another notable difference between the single chain metabolite (Chex1-Arg20) compared to its prodrug A3-APO was evident when we tested the ability of the two peptides to induce resistance in *K. pneumoniae* when administered at sublethal doses in repeated passages. While A3-APO generated no resistance after 20 passages, the metabolite induced the emergence or resistance with a rapid increase in the MIC already after a few passages, similarly to Ciprofloxacin, one of the most commonly used conventional antibiotics, which is known for its tendency to induce resistance.[4] (Fig. 1). A3-APO was tested in mouse models of sepsis. We used CD-1 female mice pre-treated with 18 mg/kg cisplatin for four days in order to bring the renal Clearence rate to a value comparable to humans, then infected intraperitoneally (ip) with LD90 amount of the extended spectrum ß-lactamase producing, fluoroquinolone-resistant *E. coli* 5770 strain. A total ip dose of 3x10 mg/kg each in four hour intervals led to both blood sterilization and survival improvement, similar to imipenem added at a higher dose. Further experiments using both A3-APO and Chex1-Arg20 along with Imipenem and ciprofloxacin at increasing doses demonstrated a nice dose dependency of both CFU counts in the blood and survival (Fig. 2). A3-APO and its metabolite, with their dual and specific mechanism and pharmacologic properties, represent top candidates for the development of new, peptide based drugs for infectious diseases, a field of Medicine in which the Pharmaceutical industry has not provided, so far, enough answers for our urgent and growing needs.

References

1. Otvos L Jr, O I, Rogers ME, Consolvo PJ, Condie BA, Lovas S, Bulet P, Blaszczyk-Thurin M. Interaction between heat shock proteins and antimicrobial peptides. *Biochemistry* **39**: 14150-14159, 2000.
2. Amsterdam D. Susceptibility testing of antimicrobials in liquid media. *Antibiotics in Laboratory Medicine.* Lorian V (Ed) Lippincott Williams and Wilkins, Philadelphia, PA, USA, 1996, pp 52-111.
3. Otvos L Jr, de Olivier Inacio V, Wade JD, Cudic P. Prior antibacterial peptide-mediated inhibition of protein folding in bacteria mutes resistance enzymes. *Antimicrob Agents Chemother* **50**: 3146-3149, 2006.
4. Cirz RT, Chin JK, Andes DR, de Crécy-Lagard V, Craig WA, Romesberg FE. Inhibition of mutation and combating the evolution of antibiotic resistance. *PLoS Biol* **3**: e176, 1024-1033, 2005.

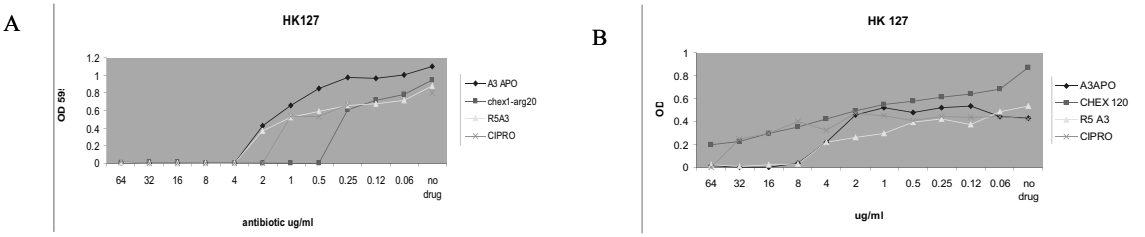

Figure 1. MICs of K. pneumoniae HK127 at baseline (A) and after 15 passages (B).

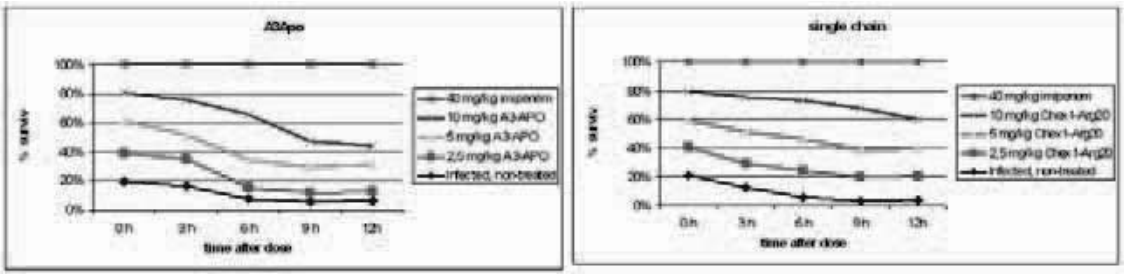

Figure 2. Survival of spetic mice (I. P. infection with *E. coli* 5770) treated with A3-APO, the single chain metabolite, or Imipenem.

4-18-004

Naposomes: A new class of peptide containing supramolecular aggregates as target selective delivery systems.

Morisco, Anna[1]; Accardo, Antonella[2]; Tesauro, Diego[2]; Benedetti, Ettore[1]; Pedone, Carlo[1]; Morelli, Giancarlo[1,]*
[1]University of Naples "Federico II" - CIRPeB, ITALY; [2]University of Naples, ITALY

[*]E-mail: gmorelli@unina.it

In order to increase therapeutic or diagnostic efficacy of the administered drug and reduce potential toxic side effects on non-target organs, the development of schemes aimed at achieving more specific and selective delivery to target cells constitutes a major challenge for many clinical applications. Peptides have been validated as targeting tools in a wide number of applications. Radiolabeled peptides are used in nuclear medicine techniques to perform imaging or to deliver radiotherapeutic doses to cancer tissues, overexpressing cell membrane receptors such as those for somatostatin or bombesin. A more complex objective would be to adopt a similar scheme to deliver supramolecular aggregates, such as micelles or liposomes, to a tissue of interest. To achieve this goal we have developed mixed aggregates (spherical micelles, rod-like micelles and liposomes) with enhanced properties(1,2) (*Naposomes*) as potential target selective nanovectors of drugs and/or contrast agents. Naposomes are obtained assembling together amphiphilc molecules containing, as hydrophilic head, a chelating agent able to coordinate a paramagnetic or a radioactive metal ion; and a bioactive peptide able to recognize cholecistokinin, somatostatin and bombesin receptors. The radioactive ion allows to visualize *in vivo* the aggregates with nuclear medicine techniques. The peptide molecules present in the amphiphilic molecules are CCK8, 7-14-bombesin or octreotide; all of them are derivatized on their N-terminus: it is well know that chemical modifications on this position do not prevent their receptor binding affinity. Four generations of supramolecular aggregates based on different amphiphilic molecules were designed and synthesized by solid phase synthesis, following a Fmoc strategy. The first generation is based on amphilic monomers (compounds **a** and **b** in Fig. 1), containing

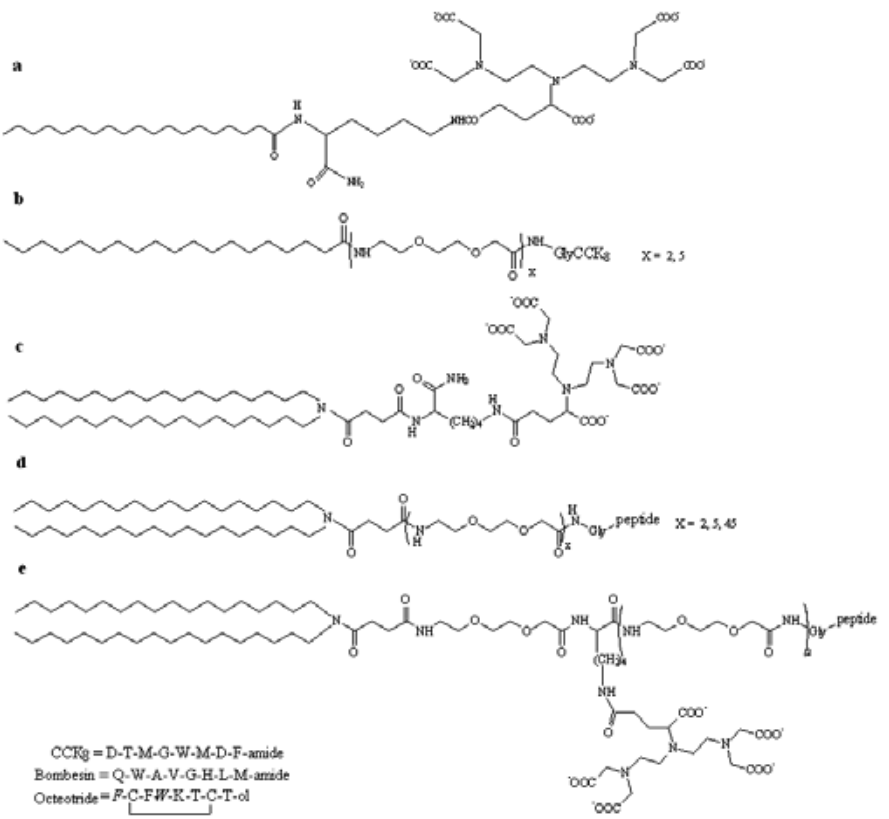

Figure 1

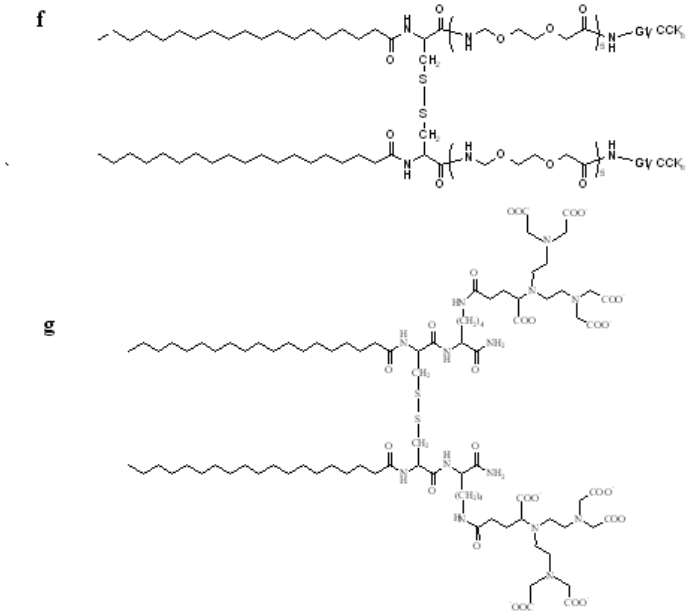

Figure 2

a single C18 hydrocarbon chain. It has the drawback of low *in vivo* aggregate stability and some hemolitic effects, and it was overcame by others generations bearing two lipophilic tails for each monemer. In the second generation of amphiphilic molecules (compounds **c** and **d** in Fig. 1) the two lipophilic tails are linked to the hydrophilic heads by different length ethoxylic moieties. The anionic nature of chelating agent, and the length of the spacers influence size and shape of the aggregates, varying among micelles, bilayers and vescicles. The third generation of aggregates is based on a single monomer (compound **e**) containing the chelating agent, the bioactive peptide and the hydrophobic moiety in the same molecule. The gemini monomers (compounds **f** and **g** in Fig. 2) of the forth generation were obtained coupling together two first generation monomers by a cysteine bridge; they assemble in stable micelles. A complete characterization of chemical-physical properties by dynamic light scattering (DLS), small angle neutron scattering (SANS) fluorescences studies and circular dichroysme, allows to define the exposition of the peptide moiety, the critic micellar concentration of micelles, shape and size of the supramolecular aggregates. The aggregates (micelles, vesicles or liposomes) could entrap on their inner compartment or in the phospholipid bilayer, a pharmaceutical active principle such as the citotoxic drug Doxorubicin. Naposomes could act as: i) Target-selective vehicles for drug-delivery; ii) Target-selective vehicles of contrast agents for imaging techniques; iii) Target-selective vehicles for simultaneous delivery of a drug (in the inner compartment) and a contrast agent (on the aggregate surface, for its visualization); iv) Target-selective delivery system of a drug and a therapeutic active radionuclide. The efficacy of the aggregates were tested *in vitro* and *in vivo* as target selective delivery systems for drugs and contrast agents. In particular liposomes obtained by assembling together second generation monomers at different molar ratios were loaded with Doxorubicin and *in vitro* tested. Higher mortality of cells expressing receptors respect to control cells was observed, thus indicating the efficiency of the exposed peptide in target selective delivery of the drug containing aggregates.

References

1. Accardo A, Tesauro D, Morelli G, Gianolio E, Aime S, Vaccaro M, Mangiapia G,Paduano L, Schillén K. *J Biol Inorg Chem* **12**: 267-276 2007.
2. Accardo A, Tesauro D, Aloj L, Tarallo L, Arra C, Mangiapia G, Vaccaro M, Pedone C, Paduano L, Morelli G. *ChemMedChem* **3**: 594-602 2008.

4-20-005

New approaches to the design, synthesis and biochemical and biophysical evaluation of heteromultivalent ligands for detection and treatment of cancer

Hruby, Victor[1,2,]; Josan, Jatinder[1]; Vagner, Joseph[1,4]; Fernandes, Steve[2]; Handl, Heather[2]; Xu, Liping[2]; Lynch, Ronald[3]; Mash, Eugene[1]; Gillies, Robert [2,4]*

[1]University of Arizona, Tucson, AZ 85721, Department of Chemistry, UNITED STATES; [2]University of Arizona, Tucson, AZ 85721, Biochemistry & Molecular Biophysics, UNITED STATES; [3]University of Arizona, Tucson, AZ 85721, Physiology, UNITED STATES; [4]University of Arizona, Tucson, AZ 85721, BIO5, UNITED STATES

[*]E-mail: hruby@u.arizona.edu

Introduction

Many cancers including melanoma and pancreatic cancer, are highly resistant to treatment especially following metastasis. Detection of these cancers in their early manifestations, especially pancreatic cancer, are still problematic. Furthermore, there is increasing evidence that most cancers have multiple phenotypes, so that any single approach to detection and treatment will fail for some people with that cancer. To overcome these problems we are taking a novel approach which directly addresses the cancer state. We are targeting cancer cells with a single ligand that can target two or more surface proteins (receptors, ion channels, enzymes, cytokines, etc.) that distinguish a cancer cell from normal cells. This requires the development of scaffolds that allow one to place the specific ligands at appropriate distances from each other so as to non-covalently "cross-link" two or more different cell surface proteins, and which also possess imaging and/or therapeutic agents that will not interfere with the binding process. Both thermodynamic and kinetic considerations are critical for obtaining useful ligands.[1,2] Here we report on the design, synthesis, biochemical and biophysical properties of multimeric, multi-heterovalent ligands which demonstrate the crosslinking of two different cell surface proteins, and the viability of this new approach.

Results and discussion

To assemble multi-heterovalent ligands that can crosslink cell surface proteins requires assembly of different pharmacophores on a scaffold that will place these pharmacophores sufficiently separated from each other that they can independently, but simultaneously, interact with different cell surface proteins (in our case G-protein coupled receptors -- GPCRs). Such interactions should lead to both enhanced affinity and selectivity for cells that possess the corresponding receptors. A significant amount of modeling with scaffold components that varied in length and flexibility/rigidity was done. This aspect will not be discussed here except to say that one of the systems we chose for scaffold assembly was scaffolds that contain (Pro-Gly)n sequences (n=3 to 18) and a PEGO linker of structure -NH-$(CH_2)_3$-[*O*-$CH_2CH_2]_3$-CH_2-NH-CO-CH_2-*O*-CH_2-CO-. The former has 9 to 54 atoms and the latter 20 atoms in the backbone structure. The former is semi-rigid, the latter is a more flexible linker system. Both were chosen because of their biocompatibility, relative chemical stability, and synthetic accessibility. A general scheme for the stepwise synthesis of one of these heterobivalent ligands which contain alpha-MSH heptapeptide fragment MSH-7 (Ac-Ser-Nle-Glu-His-DPhe-Arg-Trp-) at the N-terminal and the alpha CCK hexapeptide fragment CCK-6 (-Nle-Gly-Trp-Nle-Asp-Phe-NH_2) at the C-terminal of the molecular assembly is shown in Fig. 1. Full details of the synthetic procedures are being published.[3]

Since multiple reaction steps are required, all steps were optimized and terminating acylation was done when necessary. HPLC purification followed by structural analysis using high resolution mass spectrometry was used3 to evaluate purity and structure. A family of ligands were obtained with different numbers of (PG)3 and PEGO units. Good yields of pure multi-heterovalent complexes were obtained following these procedures.

The biological activities of the heteromultivalent ligand were examined in several ways using binding affinity assays which were obtained by methods previously reported[4] using cell lines that contained only the CCK-2, the hMC4 receptor, or both receptors. Or cell lines that contained both receptors. In the latter case, there was approximately a 2-fold excess of cell surface expressed CCK-2 receptor vs the MC4 receptor. Binding affinities at cells only containing one receptor were accomplished in the normal manner. In the cells with more than one receptor three different binding affinity assays were performed: 1) binding assays for the MC4R in the presence of a CCK-2R antagonist; 2) binding of assays for the CCK-2R in the presence of an MC4R antagonist; and 3) binding assays in which both receptors could be addressed by the heterobivalent ligands. The results obtained are very interesting.

In a stable cell line in which the CCK-2R had about 2 fold greater expression than the MC4R the heterobivalent ligands Ac-MSH-7-$PEGO_{20}$-$[Pro\text{-}Gly]_6$-PEGO-CCK-6-NH_2 (76 atom linker) an 80 fold enhancement in binding vs. binding of Ac-MSH-7 when the CCK-2R receptor was

blocked was observed, while there was no enhancement relative to the CCK-2R binding. On the other hand, when a similar heterobivalent ligand with a fluorescent moiety present for imaging was examined, the cells that contained both receptors were highly fluorescently labeled within three minutes, whereas the cells which contained only the MC4R or the cells that contained only the CCK-2R were barely visible at that time point. These results strongly indicated that our heterobivalent ligands can rapidly crosslink two different cell surface receptors. There is a greatly enhanced binding affinity of the ligands to the two receptors being crosslinked, at least up to the point where the least populated surface receptor is occupied. As expected, the receptor that is more greatly expressed interacts with the heterobivalent ligand as a single valent ligand because no crosslinking is possible since the other receptor is occupied.

These results are consistent with our hypothesis that heterobivalent ligands can non-covalently crosslink two different receptors if properly constructed on a scaffold which is greater than 35±15 Å from each other. Much additional work is necessary to demonstrate the application of this approach for detection and treatment of cancer *in vivo*.

Acknowledgements

This research was supported by a grant from the Arizona Biological Research Commission (ABRC) and by grants from the National Institutes of Health, National Cancer Institute.

References

1. Gillies RJ, Hruby VJ. *Expert Opinion Ther Targets* **7**: 137-139, 2003.
2. Handl HL, Vagner J, Han H, Mash E, Hruby VJ, Gillies RJ. *Expt Opin Ther Targets* **8**: 565-586, 2004.
3. Josan JS, Vagner J, Handl H, Sankaranarayanan HR, Gillies RJ, Hruby VJ. Int *J Pept Res* Ther. **14**: 293-300, 2008.
4. Handl HL, Vagner J, Yamamura HI, Hruby VJ, Gillies RJ. *Anal Biochemistry* **333**: 242-250, 2004.

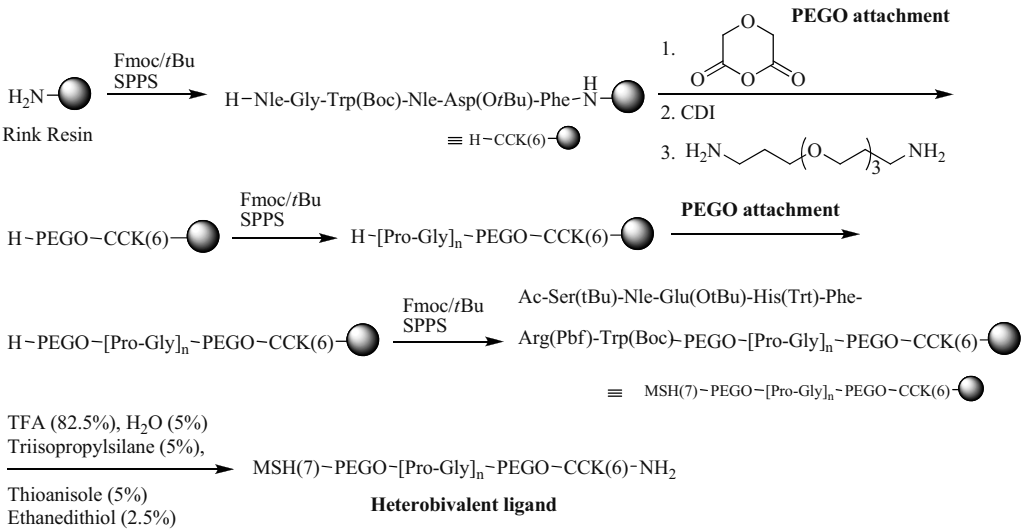

Figure 1. Scheme for heterobivalent ligand synthesis.

4-21-006

Rational Design of Highly Active and Selective $\alpha_5\beta_1$ Integrin Antagonists

Laufer, Burkhardt[1]; Heckmann, Dominik[1]; Meyer, Axel[1]; Marinelli, Luciana[2]; Neubauer, Stefanie[1]; Zahn, Grit[3]; Stragies, Roland[3]; Kessler, Horst[1,]*

[1]Center of Integrated Protein Science at the TU München, Department Chemie, Lichtenbergstrasse 4, 85747 Garching, GERMANY; [2]Dipartimento di Chimica Farmaceutica e Tossicologica, Università di Napoli "Federico II", Via D. Montesano, 49-80131 Napoli, ITALY; 3Jerini AG, Invalidenstrasse 130, 10115 Berlin, GERMANY

[*]Email: horst.kessler@ch.tum.de

Integrins constitute a family of heterodimeric, transmembrane cell adhesion receptors which connect cells to the scaffolding proteins of the extracellular matrix. The pioneering observation that integrins - especially $\alpha_V\beta_3$ and $\alpha_5\beta_1$ - are hallmarks of metastatic cancer and seriously involved in the process of tumor angiogenesis turned them into attractive targets for cancer therapy. Out of that, the inhibition of integrin function is a major challenge in medicinal chemistry. Potent ligands are currently in different stages of clinical trials for the antiangiogenic therapy of cancer and age-related macula degeneration (AMD). Especially the subtype $\alpha_5\beta_1$ has recently been drawn into the focus of research due to its genuine role in angiogenesis.[1] Based on the homology model of Marinelli *et al.*,[2] rational design and the synthesis of high affinity $\alpha_5\beta_1$ binders and the optimization of their activity and selectivity against $\alpha_V\beta_3$ by means of extensive SAR-studies and docking experiments became possible. Starting from a tyrosine scaffold we succeeded in getting compounds with affinities in the low and even sub-nanomolar range and selectivities of 400 fold against $\alpha_V\beta_3$.[3] The insights about the structure-activity-relationship gained from the tyrosine based ligands could then be successfully transferred to ligands bearing an aza-glycine scaffold to yield $\alpha_5\beta_1$ ligands with affinities of even sub-nanomolar range and selectivites exceeding 10^4 fold.[4]

Biological evaluations of the aza-glycine scaffold revealed high $\alpha_5\beta_1$-affinities together with a dramatic increase in selectivity compared to the tyrosine scaffold. The selectivities of 6000 and higher are owed to the rigidity of the diacylhydrazone scaffold compared to the rather flexible tyrosine. The lack of degrees in freedom strongly disfavors alternative binding modes, where the mesitylene moiety is oriented outside the pocket of $\alpha_V\beta_3$. Both arylguanidyl and alkylguanidyl groups show a comparable selectivity (low affinity) against $\alpha_V\beta_3$, which once again points out that only the C-terminal part of the molecule is responsible for the selectivity.

A comparison of virtually all yet published integrin ligands shows that the most conserved functionality is the carboxylic acid. It is involved in the coordination of the bivalent metal cation at the MIDAS site, which is present in all integrins. To our knowledge, the successful substitution of this carboxylic moiety has not yet been reported. A new approach for the substitution of carboxylic acids in integrin ligands is the conversion of the carboxylates into hydroxamic acids, which are known to fulfill a variety of roles in biology and medicine.[5] Hydroxamic acids are overall less acidic but have good

Table 1. Highly active and selective integrin ligands for $\alpha_5\beta_1$

	IC50 α5β1 in nM	IC50 αvβ3 in nM	Selectivity
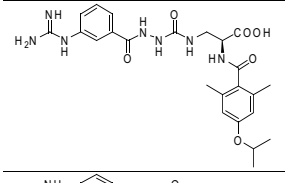	0.96	4750	~ 5000 fold
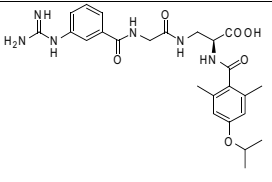	0.86	9600	~11000 fold

coordination properties, which could be useful for the binding of bivalent cations in the MIDAS site. In case of a mainly ionic interaction, a dramatic loss of activity would be expected, while with a mainly coordinative binding, the affinities of carboxyl and hydroxamic acid should be comparable. The substitution of the carboxylic acid by a hydroxamic acid results in new ligands that still show activity in the nanomolar range. As can be seen, the activity in the hydroxamic acids towards $\alpha_5\beta_1$ drops down while there is still high activity towards $\alpha_V\beta_3$. This might be caused by sterical effects as the binding pocket of $\alpha_V\beta_3$ is slightly larger than that one of $\alpha_5\beta_1$.

References

1. Hynes RO. *Nature Medicine* **8**: 918-921, 2002.
2. Marinelli L, Meyer A, Heckmann D, Lavecchia A, Novellino E, Kessler H. *J Med Chem* **48**: 4204-4207, 2005.
3. Heckmann D, Meyer A, Marinelli L, Zahn G, Stragies R, Kessler H. *Angew Chem Int Ed* **46**: 3571-3574, 2007.
4. Heckmann D, Meyer A, Laufer B, Zahn G, Stragies R, Kessler H. *ChemBioChem* **9**: 1397-1407, 2008.
5. Marmion CJ, Griffith D, Nolan KB. *Eur J Inorg Chem* **15**: 3003-3016, 2004.

Compound		IC50 α5β1 in nM	IC50 αvβ3 in nM
1a	Carboxylic acid	46	3.8
1b	Hydroxamic acid	132	<5
2a	Carboxylic acid	0.7	279
2b	Hydroxamic acid	40	13.5

Figure 1. Binding affinities for integrin ligands containing a carboxyl or a hydroxamic acid group.

4-28-007

N-methyl phenylalanine-rich peptides as potential blood brain barrier shuttles

Malakoutikhah, Morteza[1]; Teixidó, Meritxell[1]; Giralt, Ernest[2,]*

[1]Barcelona Science Park, Institute for research in biomedicine, SPAIN; [2]University of Barcelon, Department of Organic Chemistry, SPAIN

[*]E-mail: ernest.giralt@irbbarcelona.org

Introduction

The blood-brain barrier (BBB) is a membrane that protects the brain from harmful substances in circulating blood and regulates the entry of particular molecules from blood into the central nervous system (CNS). This physical and enzymatic barrier is the major bottleneck for the delivery of therapeutic agents to the brain. The BBB is formed by endothelial cells that are sealed through tight junctions, which significantly block paracellular transport. To bypass the BBB and deliver drugs to the brain, several strategies have been used such as: modifying the structure of a drug to increase its permeability by passive diffusion. Another option is to couple a drug to a "Trojan horse", a compound that passes the BBB by receptor-mediated transcytosis (RMT) and can carry the drug across the barrier.[1,3] The concept of Trojan horses can be extended to other mechanisms, in addition to RMT, by means of searching for peptides with the capacity to enter the brain by passive diffusion and shuttle drugs that cannot cross the BBB unaided. These diffusion "Trojan horses", also called BBB-shuttles, have recently been described by our group.[4] *N*-Methylation of amino acids has been proposed as a powerful tool to decrease the number of H-bonds and increase the lipophilicity and permeability of peptides. *N*-Methylamino acids are not rare in nature. *N*-Methylphenylalanine (*N*-MePhe) is present in several natural peptides and proteins.[5] Given these properties and the observation that *N*-MePhe is present in several natural peptides, *N*-MePhe was chosen as a key residue for our design of shuttles that cross the BBB by passive diffusion. For this purpose, several peptide libraries were synthesized and evaluated by PAMPA (parallel artificial membrane permeability assay) and IAMC (immobilized artificial membrane chromatography).

Results and Discussion

Library of Peptides Containing *N*-MePhe. To evaluate the effect of length on peptide permeability, a library of nine peptides, Ac-(*N*-MePhe)$_n$-CONH$_2$ (n = 2-10), which have only *N*-MePhe in their sequences, was synthesized using a solid phase peptide synthesis (SPPS) technique with Fmoc strategy. All peptides were characterized using HPLC, HPLC-MS, MALDI-TOF MS, and HRMS. All peptides showed purity greater than 98%. The PAMPA, a relatively new technique,[6] is an approach based on an artificial membrane system with a microfilter coated by phospholipids, The PAMPA was performed on our nine-peptide library to study the relationship between chain length and permeability of these compounds. In this series of *N*-MePhe oligomers, Peptide with four *N*-MePhe residues showed the greatest transport (16.7%), which was higher than that of Ac-(*N*-MePhe)$_3$-CONH$_2$ (12.5%), an in situ BBB-positive peptide (Table 1).

IAMC is a model of interaction between compounds and a phospholipid.[7] In this approach a phospholipid (phosphatidylcholine) is covalently attached to silica, The capacity factor (k_{IAM}), calculated using the retention time of the test compound, is used to estimate the membrane partition coefficient. k_{IAM} was determined for the nine peptides and controls . For the first three members of the peptide family, an increase in chain length induced higher retention in IAMC and higher PAMPA permeability. The remaining peptides showed very high retention in IAMC and no permeability in PAMPA (except Ac-(*N*-MePhe)$_5$-CONH$_2$), probably because of their size or high lipophilicity.

Evaluation of Terminal Groups. After optimizing peptide length, we evaluated the effect of terminal groups. For this purpose, four peptides with distinct terminal groups were synthesized and studied by PAMPA and IAMC. The findings suggested that acetyl and amide groups were the best options for the N-terminus and C-terminus of our BBB-shuttle, respectively.

Effect of Amino Acid Replacement. To establish the effect of amino acid replacement on peptide permeability, a library consisting of 20 peptides, which differ only in the N-terminal amino acid (4th), was designed and synthesized in solid phase. The peptides were evaluated by PAMPA and IAMC (Table 2). Of all the N-methylated amino acids, N-MePhe showed the greatest transport capacity while Cha and 2Nal were the best unmethylated residues. From this library, we selected combinations of the three best amino acids, namely, Ac-*N*-MePhe-(*N*-MePhe)$_3$-CONH$_2$, Ac-Cha-(*N*-MePhe)$_3$-CONH$_2$, and Ac-2Nal-(*N*-MePhe)$_3$-CONH$_2$, as BBB-shuttles.

Stability Assay in Human Serum.

The stability of our peptides in human serum was tested and compared to that of Ac-(Phe)$_4$-CONH$_2$. The data show a considerable enhancement of stability of the peptides in contact with enzymes because of the use of N-methylated or unusual amino acids. While only 6% of the parent peptide Ac-(Phe)$_4$-CONH$_2$ remained intact after 12 h, 91%, 57%, and 86% of Ac-*N*-MePhe-(*N*-MePhe)$_3$-CONH$_2$, Ac-Cha-(*N*-MePhe)$_3$-CONH$_2$, and Ac-2Nal-(*N*-MePhe)$_3$-CONH$_2$, respectively, remained stable within the same time period.

Table 1. Percentage of transport after 4 h, effective permeability (P_e) in the PAMPA and k_{IAM} of peptides Ac-(*N*-MePhe)$_n$-CONH$_2$ (n=2,3,4,5,6,7,8,9,10) and control compounds (Propranolol, Carbamazepine)

Compound	*P*e (× 10^6) cm/s	Transport (%) (4h)	k_{IAM}
Propranolol	7.4	13.5	1.9
Carbamazepine	10.4	17.7	2.1
Ac-(*N*-MePhe)$_2$-CONH$_2$	3.3	6.8	3.2
Ac-(*N*-MePhe)$_3$-CONH$_2$	6.8	12.5	17.7
Ac-(*N*-MePhe)$_4$-CONH$_2$	13.5	21.7	>128[a]
Ac-(*N*-MePhe)$_5$-CONH$_2$	1.1	2.3	>128[a]
Ac-(*N*-MePhe)$_6$-CONH$_2$	0	0	>128[a]
Ac-(*N*-MePhe)$_7$-CONH$_2$	0	0	>128[a]
Ac-(*N*-MePhe)$_8$-CONH$_2$	0	0	>128[a]
Ac-(*N*-MePhe)$_9$-CONH$_2$	0	0	>128[a]
Ac-(*N*-MePhe)$_{10}$-CONH$_2$	0	0	>128[a]

[a]: Retention time higher than 60 min in the IAMC HPLC column.

Table 2. Percentage of transport after 4 h, effective permeability (Pe) in the PAMPA and kIAM of peptides X-(N-MePhe)3-CONH2 (X=diverse amino acids) and controls (Propranolol, Carbamazepine)

Compound	Pe (× 10^6) cm/s	Transp. %, 4h	k_{IAM}
Propranolol	7.9	16.6	1.9
Carbamazepine	8	16.9	2.1
Ac-Phe-(N-MePhe)3-CONH2	2.3	4.9	43.4
Ac-N-MePhe -(N-MePhe)3-CONH2	6.4	13.4	>128a
Ac-Gly-(N-MePhe)3-CONH2	0.6	1.3	5.3
Ac-N-MeGly-(N-MePhe)3-CONH2	0.7	1.5	9.3
Ac-Phg-(N-MePhe)3-CONH2	0	0	25.9
Ac-N-MePhg-(N-MePhe)3-CONH2	0.7	1.5	>128a
Ac-Cha-(N-MePhe)3-CONH2	2.6	5.5	>128a
Ac-N-MeCha-(N-MePhe)3-CONH2	1.9	4	>128a
Ac-HomoPhe-(N-MePhe)3-CONH2	2.	4.3	>128a
Ac-N-MeHomoPhe-(N-MePhe)3-CONH2	1.8	3.7	>128a
Ac-2Nal-(N-MePhe)3-CONH2	3.1	6.6	>128a
Ac-N-Me2Nal-(N-MePhe)3-CONH2	1.3	2.8	>128a
H-Tic-(N-MePhe)3-CONH2	2.2	4.6	>128a
Ac-Tic-(N-MePhe)3-CONH2	2	4.3	>128a
Ac-Trp-(N-MePhe)3-CONH2	1.8	3.9	87.2
Ac-N-MeTrp-(N-MePhe)3-CONH2	1.4	2.9	>128a
Ac-Tyr-(N-MePhe)3-CONH2	1.1	2.3	10.8
H-1,2,3,4-tetrahydronorharman-3-carboxylic acid-(N-MePhe)3-CONH2	0.6	1.3	13.6
Ac-1,2,3,4-tetrahydronorharman-3-carboxylic acid-(N-MePhe)3-CONH2	1.5	3.2	24.6
Ac-3Pal-(N-MePhe)3-CONH2	1.2	2.5	6.3

a Retention time higher than 60 min in the IAMC HPLC column.

Application of Peptides as BBB-Shuttles. Levodopa, a prodrug to dopamine that has been the most efficacious drug therapy for Parkinson's disease since 1967,[8] was used as a cargo to evaluate the capacity of the three selected peptides to carry drugs through an artificial membrane While levodopa alone did not show permeability in the PAMPA, our peptides carried this drug in this assay and exhibited great permeability and are therefore considered potential candidates as BBB-shuttles to transport drugs to the CNS.

References

1. Temsamani J, Scherrmann JM, Rees AR, Kaczorek M. Brain Drug Delivery Technologies: Novel Approaches for Transporting Therapeutics. P*harm Sci Technol Today* **3**: 155–162, 2003.
2. Witt KA, Gillespie TJ, Huber JD, Egleton RD, Davis TP. Peptide Drug Modifications To Enhance Bioavailability and Blood-Brain Barrier Permeability. *Peptides* **22**: 2329–2343, 2001.
3. Alavijeh MS, Chishty M, Qaiser MZ, Palmer AM. Drug Metabolism and Pharmacokinetics, the Blood-Brain Barrier, and Central Nervous System Drug Discovery. *Neurotherapeutics* **2**: 554–571, 2005.
4. Teixido´ M, Zurita E, Malakoutikhah M, Tarrago´ T, Giralt E. Diketopiperazines as a Tool for the Study of Transport across the Blood-Brain Barrier (BBB) and Their Potential Use as BBB-Shuttles. *J Am Chem Soc* **129**: 11802–11813, 2007.
5. Randazzo A, Debitus C, Gomez-Paloma L. Haliclamide, a Novel Cyclic Metabolite from the Vanuatu Marine Sponge Haliclona Species. *Tetrahedron* **57**: 4443–4446, 2001.
6. Kansy M, Senner F, Gubernator K. Physicochemical High Throughput Screening: Parallel Artificial Membrane Permeation Assay in the Description of Passive Absorption Processes. *J Med Chem* **41**: 1007–1010, 1998.
7. Reichel A, Begley DJ. Potential of Immobilized Artificial Membranes for Predicting Drug Penetration across the Blood-Brain Barrier. *Pharm Res* **15**: 1270–1274, 1998.
8. Hawkins RA, Mokashi A, Simpson IA. An Active Transport System in the Blood-Brain Barrier May Reduce Levodopa Availability. *Exp Neurol* **195**: 267–271, 2005.

4-01-101

Esters of Purine Nucleosides (Abacavir) with Natural and Unnatural Amino Acids -Synthesis and Cytotoxicity in Cell Culture

Stankova Ivanka[1,]; Genova, Petia[2]; Chayrov, Radoslav[1]; Argirova, Radka[2]*

[1]South-West University ''Neofit Rilski", Department of Chemistryersity, BULGARIA; [2]National Center of Infectious and Parasitic Diseases, Dept. of Virology, BULGARIA

[*]E-mail: ivastankova@abv.bg

Introduction

Abacavir (Ziagen)–(*1S,cis*)-4-[2-amino-6-(cyclopropyl-amino)-9H-purin-9-yl]-2-cyclopentene-1-methanol is a synthetic carbocylcilic nucleoside analogue with inhibitory activity against HIV methanol.[1-2] Abacavir is a commonly prescribed HIV drug belonging to the nucleoside reverse transcriptase inhibitor (NRTI) class. The major treatment-limiting side effect associated with its use is an early onset multi-system drug hypersensitivity reaction typically including some combination of rash, fever and gastrointestinal symptoms, occurring within 6 weeks of initiating treatment in approximately 5-8% of abacavir recipients. Hypersensitivity to this syndrome is strongly predicted by the presence of a specific human leukocyte antigen (HLA) allele - HLA-B * 5701 - the dominant risk factor among Caucasian and Hispanic populations. The frequency distribution of this genetic marker in different populations is likely to provide a rational basis for racially-defined differences in susceptibility to the drug. On the other hand, the critical role of HLA-B* 5701 in directing CD8+ T-cell-dependent, HLA-restricted immune response plays a key role in the pathogenesis of abacavir-specific immune responses. In this chapter, we explore a possible way to minimize the side effects of abacavir by modifying the structure of the known drug using various amino acids methanol.[3] The aim of this study is to design and synthesize prodrugs of abacavir using glycine and thiazole containing glycine and to study their anti- HIV activity in cell culture.

Results and Discussion

Synthesis of thiazole containing amino acid

Boc-2-aminomethyl-thiazole-4-carboxylic acid were prepared according to Videnov *et al*.[4]

Synthesis of prodrugs

A mixture of z-Gly-OH, Boc-2-aminomethyl-thiazole-4-carboxylic acid 2 a-b and 1- [3-(di-methylamino) propyl]-3-ethyl carbodiimide hydrochloride (EDC) in dimethylformamide (DMF) with ratio 1:2 EDC/AA was stirred for 1 h at 0 °C under nitrogen atmosphere.[5] A solution of abacavir (1) (Fig. 1) and *4-N*, *N*-(dimethylamino)-pyridine (DMAP) was added to the reaction mixture and stirred for 24 h. Then DMF was evaporated in vacuo and the residue was chromatographed on silica gel, using 1:4 MeOH:CH_2CH_2.

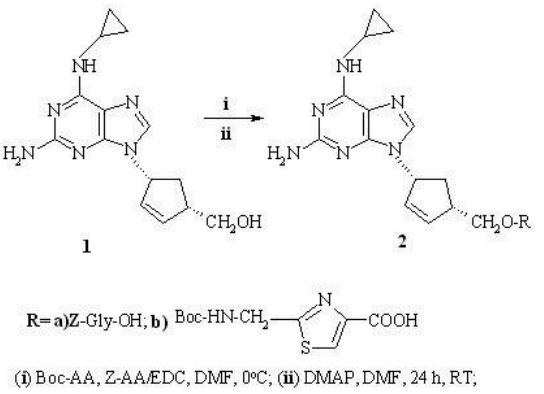

Figure 1. Cytotoxicity of the new compound.

Before study of antiviral activity in cell culture the following parameters were studied: cytotoxic concentration 50-CC50 (concentration preventing death of 50% of MT-4 cells) and maximal nontoxic concentration-MNC (the highest concentration causing no cytotoxicity). CC50 and MNC were detected by MTT assay.[6] The cells used were MT-4 - a classical target for acute HIV infection and MTT assay, kindly provided by Prof. Gianfranco Pancino - Institute Pasteur, Unite de Regulation des Infections Retrovirales, Paris, France.

Acknowledgements

Partial support of this work by the National Found for Scientific Research of Bulgaria (VUL-304/07) is gratefully acknowledged.

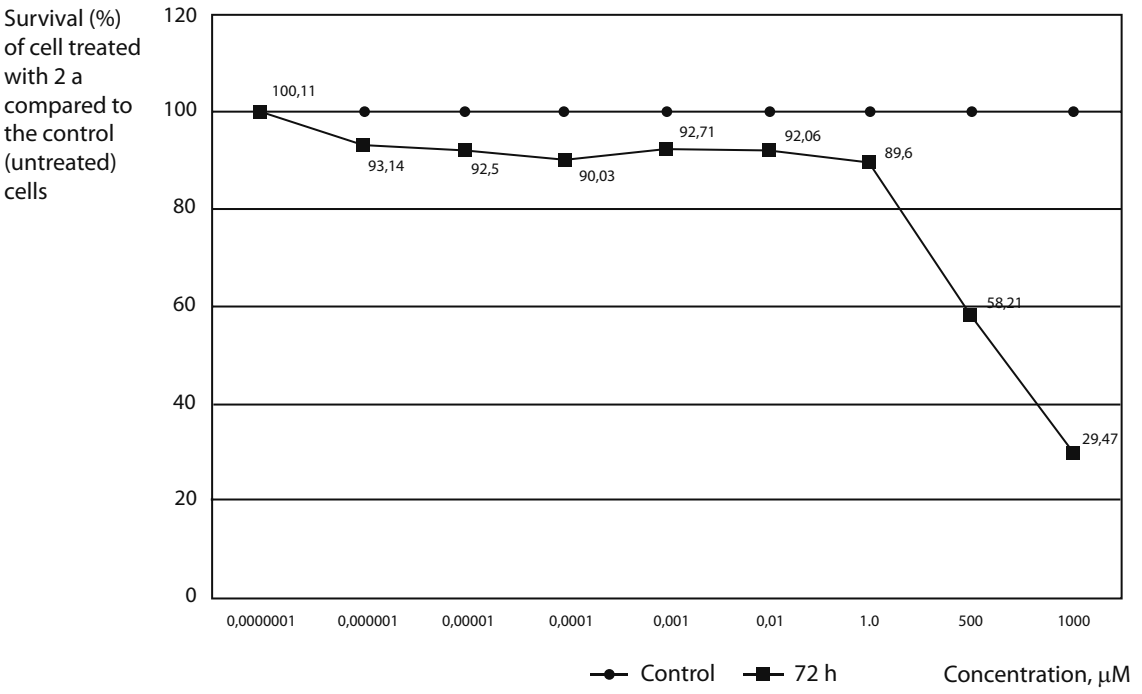

Figure 2. Cytotoxicity of z-Gly-Abacavir on MT-4 cells for 72 h of cultivation . The CC50 was determined to be 650 μÌ and MNC - resp. 0.000 0001 μÌ.

References

1. Daluge SM, Good SS, Faletto MB, Miller WH, St Clair MH, Boone LR, Tisdale M, Parry NR, Reardon JE, Dornsife RE, Averett DR, Krenitsky TA. *Antimicrob Agents Chemother* **41**: 1082–1093, 1997.
2. Faletto MB, Miller WH, Garvey EP, St Clair MH, Daluge SM. *Antimicrob Agents Chemother* **41**: 1099–1107, 1997.
3. Nolan D, Almeida C-A, Phillips E, Mallal S. *Drug Hypersensitivity*. Pichler WJ (ed), Basel, Swizerland, Karger, 2007, pp 95-104.
4. Videnov G, Kaiser D, Kempter C, Jung G. Synthesis of Naturally Occurring Conformationally Resticted Oxazole and Thiazole Containing Di- and Tripeptide Mimetics. *Angew Chem* **108**: 1604-1607; *Angew Chem Int Ed Engl* **35**: 1503-1506, 1996.
5. Boger DL, Miyazaki S, Kim SH, Wu JH, Loiseleur O, Castle SL, Loiseleur O, Jin Q. Total Synthesis of the Vancomycin Aglycon. *J Am Chem Soc* **121**: 10004-10011, 1999; *ibid*: Boger DL, Miyazaki S, Kim SH, Wu JH, Loiseleur O, Castle SL. Diastereoselective Total Synthesis of the Vancomycin Aglycon with Ordered Atropisomer Equilibrations. *pp* 3226-3227.
6. Mossmann T. *J Immunol.Methods* **65**: 55-63, 1983.

4-01-102

Development of N-acyl amino acid bisphosphonate amide derivatives as potent bone metastatic prostate anti-cancer agents

Gera, Lajos[1,]; Wu, Daqing[2]; Seo, Seongil[3]; Chan, Daniel C.[4]; Stewart, John M[1]; Chung, Leland WK[2]*

[1]University of Colorado Health Sciences Center, Department of Biochemistry and Molecular Genetics, UNITED STATES; [2]Emory University School of Medicine, Department of Urology, UNITED STATES; [3]The Catholic University of Korea, Department of Urology, KOREA (DEM.PEOPLE'S REP.); [4]University of Colorado Health Sciences Center, Cancer Center, UNITED STATES

[*]E-mail: lajos.gera@uchsc.edu

Introduction

Lung and prostate cancers are the leading cause of cancer death in the United States. Cisplatin continues to play a major role in lung and metastatic malignancy of prostate cancer chemotherapy in spite of its toxicity. We have developed bradykinin antagonists, as N-terminal acylated-(B10238, B10324), *N*-terminal dimerized (B9870 = CU201 = Breceptin) peptides and a small molecule, a simple acyl-tyrosine-amide derivative (M570) which showed higher cytotoxicity for small cell lung cancer (SHP-77) and prostate cancer (PC3) than the widely used but highly toxic cisplatin (Table 1).[1] To develop novel anticancer agents that specifically target prostate cancer (PCa) bone metastases, we designed analogs of M570 with aminobisphosphonate groups.

Results and Discussion

Our lead anti-cancer compound BKM-570 (F5c-OC2Y-Atmp; F5c: 2,3,4,5,6-pentafluorocinnamic acid, OC2Y: (*O*-2,6-dichlorobenzyl)tyrosine, Atmp: 4-amino-2,2,6,6-tetramethylpiperidine) as a first generation of our anti-cancer small molecules, consists of three parts (Fig. 1): A an acyl group; B a tyrosine amino acid residue and C an amide group. Because recent studies suggest that bisphosphonates may have direct anti-cancer activity it was obvious to conjugate our powerful M570 anti-cancer compound with aminobisphosphonate. We designed the A-B-C analog of M570 replacing the C = Atmp part with aminobisphosphonate (M1644) and we also synthesized an aminobisphosphonate analog with a 4-piperidinyl spacer between B and C (M1740) for structure-activity study. We started the synthesis of M570 and M1644 with the BOP activated coupling of Boc-(*O*-2,6-dichlorobenzyl)-L-tyrosine respectively with 4-amino-2,2,6,6-tetramethylpiperidine or 1-aminomethylenebisphosphonic acid tetraethyl ester. The Boc-groups were deprotected in 50% TFA/DCM and amines acylated with pentafluorocinnamic acid. The synthesis of M1740 started with Boc-(*O*-2,6-dichlorobenzyl)-L-tyrosine BOP activated coupling with 4-piperidone. The reductive amination of the resulting 1-[*N*-Boc-(*O*-2,6-dichlorobenzyl)-L-tyrosyl]-piperidin-4-one and aminomethylbisphosphonic acid tetraethyl ester with sodium cyanoborohydride provided 1-{[*N*-Boc-(*O*-2,6-dichlorobenzyl)]-L-tyrosyl}-4-[bis(diethoxyphosphono)]-methylaminopiperidine. The Boc-deprotected compound was also acylated with pentafluorocinnamic acid using BOP. The crude products were purified by preparative HPLC. Interestingly, M570 effectively inhibited the growth of PCa C4-2 tumors equally with the aminobisphosphonate small molecules (Table 1) but M1740 was effective against bone metastatic prostate cancer *in vivo*. These results suggest that M1740 is a novel promising drug candidate for human PCa bony metastases.

References

1. Gera L, Chan DC, York EJ, Simkeviciene V, Bunn PA Jr. Taraseviciene-Stewart L, Stewart JM. *Peptides 2004* (Proceedings of the Third Intern. and Twenty-Eighth European Peptide Symposium, Prague, Czech Republic). Flegl EM, Slaninova S, Fridkin M, Gilon C (Eds), Kenes Intern., Geneva, Switzerland, 2005, pp 846-847.

Table 1. Structures and activities of selected compounds

Number	Structure	GPI[a] pA_2	SHP-77[b] *in vitro*	SHP-77[c] *in vivo %*	C4-2[d] *in vitro*	PC3[e] *in vivo %*
B9870	SUIM-$(B9430)_2$	8.4	0.15	65	--	78
B10238	F5c-B9430	8.1	50	61	--	--
B10324	F5c-B9958	--	--	86	4	43
M570	F5c-OC2Y-Atmp	5.6	1.8	91	0.5	65
M1644	F5c-OC2Y-$AMDP(OEt)_4$	--	4.3	--	1	--
M1740	F5c-OC2Y-$Pipe[AMDP(OEt)_4]$	--	3.7	--	1	--
Cisplatin		--	--	60	--	39

[a]pA_2 for BK antagonist activity on isolated guinea pig ileum. [b]IC_{50} (μM) for cytotoxicity by MTT test. [c]Per cent inhibition of lung cancer growth of xenografts in nude mice. Compounds were injected i.p. at 5 mg/kg/day for 27 days, except cisplatin (10 mg/kg/week for 4 weeks). [d]IC_{50} (μM) for proliferation of human prostate cancer cell line C4-2 by MTS assay. [e]Per cent inhibition of prostate PC3 in nude mice. Abbreviations: $AMDP(OEt)_4$, 1-aminomethylenebisphosphonic acid tetraethyl ester; B9430, DR-R-P-Hyp-G-Igl-S-DIgl-Oic-R; B9958, K-K-R-P-Hyp-G-CpG-S-DTic-Cpg; CpG, α-cyclopentylglycine; Hyp, *trans*-4-hydroxyproline; Igl, α-(2-indanyl)glycine; Oic, octahydroindole-2-carboxylic acid; Pipe, 4-piperidinyl; SUIM, suberimidyl crosslinker at N-terminus; Tic, tetrahydroisoquinoline-3-carboxylic acid.

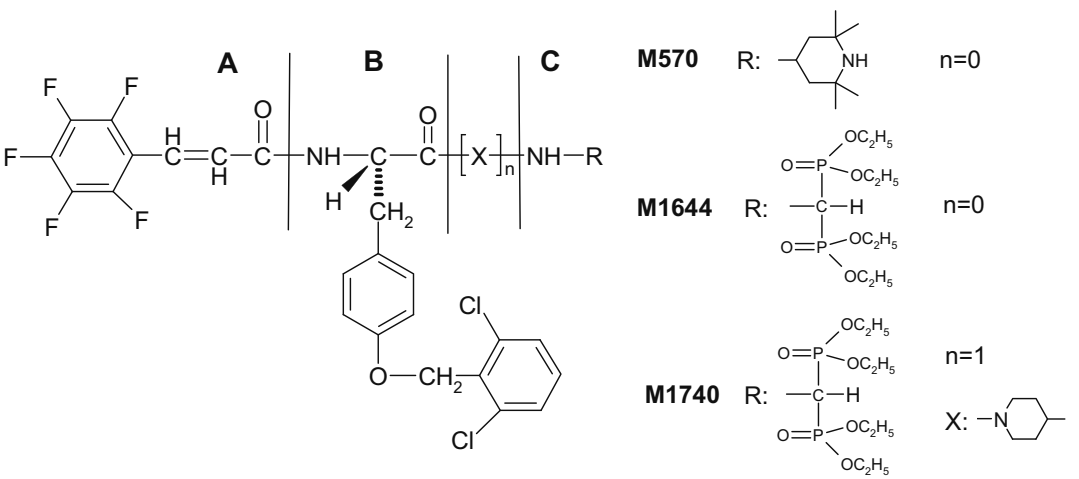

Figure 1. Aminobisphosphonate derivatives of M570.

4-01-103

Novel, potent and selective Angiotensin IV short analogues

Lukaszuk, Aneta[1,]; Demaegdt, Heidi[2]; Karoyan, Philippe[3]; Vanderheyden, Patrick[2]; Vauquelin, Georges[2]; Tourwé, Dirk[1]*

[1]Vrije Universiteit Brussel, Organic Chemistry, BELGIUM; [2]Vrije Universiteit Brussel, Molecular and Biochemical Pharmacology, BELGIUM; [3]Université Pierre & Marie Curie, CNRS/UMR 7613, FRANCE

**E-mail: alukaszu@vub.ac.be*

Introduction

Angiotensin IV: H-Val-Tyr-Ile-His-Pro-Phe-OH (Ang IV) is a bioactive metabolite of Ang II which mediates a wide range of physiological actions such as the ability to improve learning and memory, the stimulation of DNA synthesis and which has vascular and renal actions. It was proposed that Ang IV exerts its effects by binding to AT4 receptors. Those were recently identified as cystinyl aminopeptidase (CAP, also denoted as IRAP).[1] It is still not clear how Ang IV exerts its biological effects. This could be through inhibition of the activity of IRAP or through activating its receptor function.[2] Ang IV is also capable to inhibit the activity of aminopeptidase N (AP-N), which might represent an alternative target for Ang IV.[3,4] We have reported earlier that the β-homo amino acid containing analog H-*β*^{2}hVal-Tyr-Ile-His-Pro-*β*^{3}hPhe-OH (**AL-11**) is a potent, selective and stable Ang IV antagonist, in which the *β*^{2}hVal is responsible for stability and the β^{3}hPhe for selectivity.[5] In this study we shorten Ang IV sequence to reduce the number of breakdown sites and additionally we stabilized compound by introducing *β*^{2}hVal, reduced amide bond and conformational constraints.

Results

Peptide synthesis. Standard solid phase synthesis using Boc- and Fmoc-strategy on Merrifield, Wang or ClTrt resin was pused, followed by HPLC purification and separation of the peptide epimers resulting from the use of racemic eβMePhe. These epimeric peptides are indicated as ”a” and ”b” in the table. Reductive amination was done according to the procedure reported in.[6] (*R*)-*β*^{2}hVal was prepared by asymmetric synthesis.[7] Enzyme assay: Catalytic activity was measured by determining the rate of Leu-pNA cleavage in membrane homogenates of HEK293 cells transient transfected with human IRAP or AP-N in the presence of different concentrations of compound.[5] Results are reported in Table 1.

Stability experiments. Stability experiments were performed by incubating the peptides in the presence and in the absence of metal chelators, with membrane homogenates of CHO-K1 cells which contain endogenous IRAP. The enzymatic activity was determined in the two conditions. Metabolic cleavage is indicated by a drop in potency.

Binding to the AT1 receptor. Affinity of the selected compounds to the AT1 receptor was tested on intact CHO-AT1 cells. Cells were incubated with concentration 10^{-5} of compound and 3H Valsartan (1.5 nM). Non-specific binding was measured with Candesartan (1 μM).

Conclusions

All peptides are able to inhibit the IRAP activity more potently than the AP-N activity. Changes on the C-terminus results in loss of AT1 receptor affinity and induce selectivity. The Pro-deletion pentapeptides H-Val-Tyr-Ile-His-Tic-OH (**AL-29**) and H-Val-Tyr-Ile-His-e*β*MePhe-OH (**AL-32**) were among the most potent and selective analogues. It indicates that Pro is not essential for IRAP inhibition. Further deletion of His results in the potent and selective tetrapeptide H-Val-Tyr-Ile-Tic-OH (**AL-33**). *β*^{2}hVal substitution in **AL-33** to give **AL-35** resulted in a potent and metabolically stable analog, whereas this substitution in **AL-29** resulted in a reduced IRAP affinity (**AL-34**). Reduction of the Val-Tyr amide bond (**AL-36, AL-37**) as in Divalinal[8] resulted in a drop in potency.

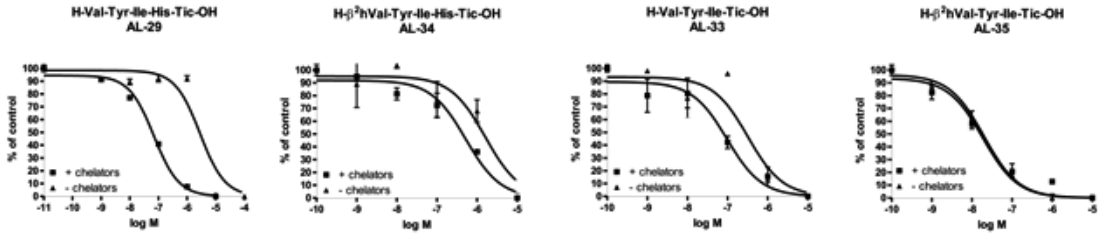

Figure 1.

Table 1. Enzyme activity inhibited by Ang IV short analogues in membranes of transfected HEK 293 cells.

Code	Sequence	HEK293 IRAP pKi ± SD	HEK293 APN pKi ± SD
Ang IV	H-Val-Tyr-Ile-His-Pro-Phe-OH	7.25 ± 0.14	6.08 ± 0.02
AL-11	**H-β²hVal**-Tyr-Ile-His-Pro-**β³hPhe-OH**	7.56 ± 0.21	5.23 ± 0.04
AL-30	H-Val-Tyr-Ile-His-Pro-**Tic-OH**	6,76 ± 0,03	6,20 ± 0,80
AL-29	H-Val-Tyr-Ile-His-**Tic-OH**	7,45 ± 0,29	5,64 ± 0,59
AL-32a	H-Val-Tyr-Ile-His-**eβMePhe-OH**	6,89 ± 0,01	5,77 ± 0,02
AL-32b	H-Val-Tyr-Ile-His-**eβMePhe-OH**	7,21 ± 0,07	5,48 ± 0,04
AL-33	H-Val-Tyr-Ile-**Tic-OH**	7,27 ± 0,21	5,90 ± 0,34
AL-34	**H-β²hVal**-Tyr-Ile-His-**Tic-OH**	5,90 ± 0,09	3,49 ± 0,99
AL-35	**H-β²hVal**-Tyr-Ile-**Tic-OH**	7,16 ± 0,04	4,98 ± 0,04
AL-36	**H-Valψ(CH₂NH)**-Tyr-Ile-His-**Tic-OH**	5,95 ± 0,28	4,00 ± 0,07
AL-37	**H-Valψ(CH₂NH)**-Tyr-Ile-**Tic-OH**	5,25 ± 0,52	3,25 ± 0,84

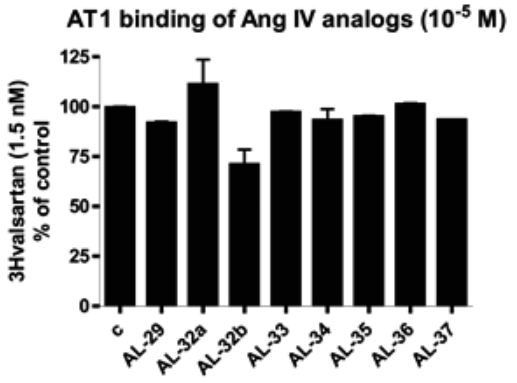

Figure 2.

Acknowledgements

We thank the 'The Fund for Scientific Research-Flanders' (FWO, Belgium) for financial support. Heidi Demaegdt has a grant from the 'Institute for the Promotion of Innovation through Science and Technology' in Flanders (I.W.T.-Vlaanderen).

References

1. Chai SY, Fernando R, Peck G, Ye SY, Mendelsohn F A, Jenkins TA, Albiston AL. *Cell Mol Life Sci* **61**: 2728-2737, 2004.
2. Wright JW, Krebs LT, Stobb JW, Harding JW. *Front Neuroendocrinol* **16**: 23-52, 1995.
3. Garreau I, Chansel D, Vandermeersch S, Fruitier I, Piot JM, Ardaillou R. *Peptides* **19**: 1339-1348, 1998.
4. Moeller I, Allen AM, Chai SY, Zhuo J, Mendelsohn FA. *J Hum Hypertens* **12**: 289-293, 1998.
5. Lukaszuk A, Demaegdt H, Szemenyei E, Toth G, Tymecka D, Misicka A, Karoyan P, Vanderheyden P, Vauquelin G, Tourwe D. *J Med Chem* **51**: 2291-2296, 2008.
6. Sasaki Y, Coy DH. *Peptides* **8**: 119-121, 1987.
7. Moumne R, Denise B, Guitot K, Rudler H, Lavielle S, Karoyan P. *Eur J Org Chem* **12**: 1912-1920, 2007.
8. Sardinia MF, Hanesworth JM, Krebs LT, Harding JW. *Peptides* **14**: 949-954, 1993.

4-01-104

Improving pharmacokinetic properties of radiolabeled bombesin analogues by incorporation of polar groups

Brans, Luc[1]; Maes, Veronique[1]; Garcia-Garayoa, Elisa[2]; Schweinsberg, Christian[2]; Daepp, Simone[2]; Schibli, Roger[2]; Bläuenstein, Peter[2]; Tourwé, Dirk[1]

[1]Vrije Universiteit Brussel, Department of Organic Chemistry, BELGIUM; [2]Paul Scherrer Institute ETH-PSI-USZ, Center for Radiopharmaceutical Science, SWITZERLAND

[*]E-mail: datourwe@vub.ac.be

Introduction

Bombesin (BBS) is a neuropeptide that binds with high affinity to the GRP-receptors which are overexpressed in human cancers such as prostate, breast and pancreas cancer. Therefore, ^{99m}Tc and ^{188}Re radiolabeled BBS(7-14) analogues can serve as tools for the *in vivo* imaging and therapy respectively of these cancers. For the radiolabeling, a (NαHis)Ac chelator was attached to the N-terminus of the BBS analogues.[1] The native BBS(7-14) sequence has been stabilized by replacing Leu^{13} and Met^{14} by Cha and Nle respectively. The βAla-βAla linker between the chelator and the binding sequence resulted in an improved tumor uptake.

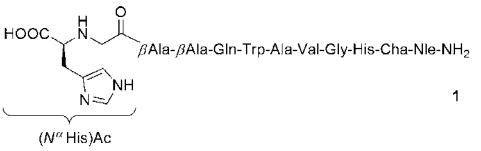

Figure 1: BBS1: (N$^{\alpha}$His)Ac-βAla-βAla-[Cha^{13}, Nle^{14}]BBS(7-14)-NH$_2$

For this BBS1 analogue, different glycation strategies, such as the Maillard reaction, the chemoselective oxime formation and the Cu(I) catalyzed azide-alkyne cycloaddition reaction, were investigated to make this compound more hydrophilic. The binding affinity and biodistribution profile of the resulting glycated BBS analogues were compared with non glycated BBS1.

Results and Discussion

Synthesis of the Glycated Analogs. To improve the pharmacokinetic properties of radiolabeled BBS analogues, we first used the on-resin Maillard reaction between α-D-glucose and the side chain amine of a Lys residue to glycate BBS.[2] However, due to the high reactivity of the secondary amine of the (NαHis)Ac chelator a mixture of a mono- **3** and diglycated **4** peptide was always formed. The only way to obtain a small amount of **3** was to stop the Maillard reaction after 16 h, when only 50% of the starting material **2** was converted. At this stage no double glycated product

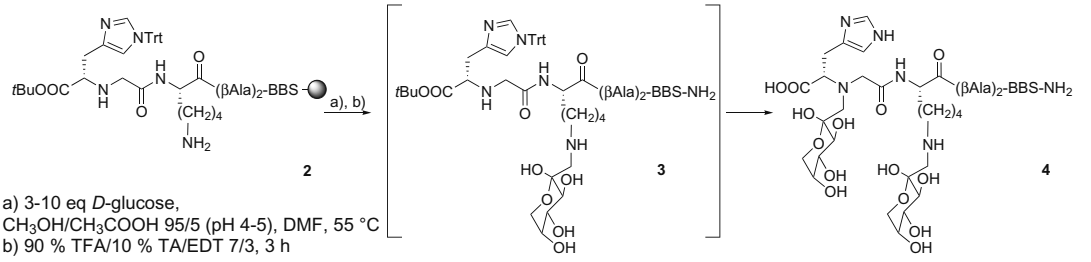

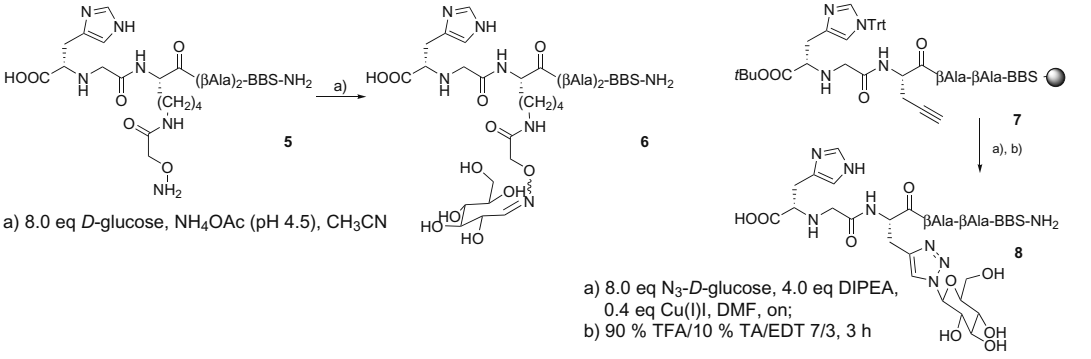

4 was present. The chemoselective reaction between a hydroxylamine (conjugated to the peptide **5**) and an aldehyde (α-D-glucose) in solution solved this double glycation problem. Since **5** and **6** overlap in HPLC it was impossible to separate them. In order to obtain compound **6** in a good purity it was therefore very important to have full conversion; this had to be checked by HPLC/MS. When 8.0 eq of α-D-glucose were used, the reaction time ranged from 16 h to several days to achieve full conversion. Adding additional α-D-glucose helped to obtain full conversion, but even then this reaction lacked reproducibility. The second alternative was based on the Cu(I) catalyzed azide-alkyne cycloaddition reaction between the side chain of propargyl alanine and α-N_3-D-glucose. This type of reaction is the best known example of a "click" reaction and has become very popular recently.[3,4] A "click" reaction is characterized by full conversion, high purity and yield, is very chemoselective and stereospecific and is easy to perform. We used this reaction as a glycation method for **7** and it was carried out on resin. Indeed, this reaction met all our expectations, we obtained **8** as a very pure compound and we did not encounter any of the above described problems.

Results and Discussion

***In Vitro* and *In Vivo* Evaluation.** The affinity of the ^{99m}Tc-labeled glycated BBS analogues for the GRP-receptor was determined on human PC-3 cells. All the glycated analogues exhibited high affinities, comparable to that of analogue **1** (Kd = 0.18 nM). An overview of the Kd values is given in Table 1. It can be concluded that glycation does not affect binding to the GRP receptor.

Table 1. Binding affinities of the glycated BBS-analogues for the GRP-receptor on human PC-3 cells

Compound	Receptor affinity K_d (nM)
1	0.18 ± 0.12
3	0.18 ± 0.03
6	0.16 ± 0.06
8	0.29 ± 0.16

Internalization studies showed a fast uptake into the tumor cells. A plateau was reached (20-40 % dose/mg prot) within 60-120 min. Maximal internalization was similar for **1**, **3** and **8**, whereas **6** showed lower percentages. Externalization of internalized activity was rather similar. After 5 h, still 40 % of the radioactivity remained inside the cell for all analogues. The biodistribution profile of ^{99m}Tc-labeled BBS analogues **1**, **3** and **8** in nude mice bearing PC-3 tumor xenografts was evaluated.[5] The glycated ^{99m}Tc-labeled BBS analogues showed an increased tumor uptake. The uptake of the ^{99m}Tc labeled analogue **8** was a factor 3.5 higher when compared to analogue **3**, at 5 h p.i. The high tumor uptake, together with the fast clearance from kidneys, liver and blood resulted in improved tumor-to-background ratios, especially for analogue **8**. It can be concluded that glycation is of great interest to increase the potential of ^{99m}Tc-labeled BBS analogues for imaging of GRP receptor-positive tumors.

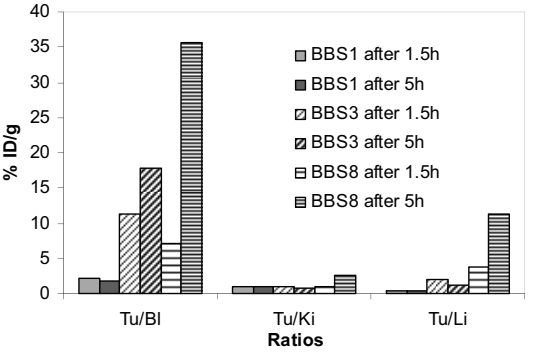

Figure 3. Tumor-to-background ratios for glycated BBS analogues 1, 3 and 8.

Acknowledgments

L. Brans thanks the "Institute for the Promotion of Innovation through Science and Technology in Flandres (IWT-Vlaanderen)" for a grant. V. Maes is a Postdoctoral Researcher of the Fund for Scientific Research-Flanders. This work was funded by a FWO grant (No. G.0036.04) and by an Oncosuisse grant (No. OCS 01311-02-2003).

References

1. Egli A, Alberto R, Tannahill L, Schibli R, Abram U, Schaffland A, Waibel R, Tourwé D, Jeannin L, Iterbeke K, Schubiger PA. Organometallic ^{99m}Tc aquaion labels peptide to an unprecedented high specific activity. *J Nucl Med* **40**: 1913-1917, 1999.
2. Maes V, Tourwe D. Maillard glycation of peptides containing the (NαHis)Ac chelator for ^{99m}Tc(CO)3 labeling. *Int J Pept Res Ther* **12**: 197-202, 2006.
3. Kolb HC, Sharpless KB. The growing impact of click chemistry on drug discovery. *Drug Discov Today* **8**: 1128-1137, 2003.
4. Tornoe CW, Caspar C, Meldal M. Peptidotriazoles on solid phase: [1,2,3]-triazoles by regiospecific copper(I)-catalyzed 1,3-dipolar cycloadditions of terminal alkynes to azides. *J Org Chem* **67**: 3057-3064, 2002.
5. Schweinsberg C, Maes V, Brans L, Bläuenstein P, Tourwe DA, Schubiger PA, Schibli R. Garayoa EG. Novel glycated [^{99m}Tc(CO)$_3$]-labeled bombesin analogues for improved targeting of gastrin-releasing peptide receptor-positive tumors. *Bioconjugate Chem* **19**: 2432-2439, 2008.

4-04-105

Chemical Stability of Some Purine Analogues

Stankova, Ivanka[1,]; Hristov Georgi[1]; Dzimbova, Tatiana[2]*

[1]Department of Chemistry, South-West University ``Neofit Rilski'', Blagoevgrad, BULGARIA;

[2]Institute of Molecular Biology, Bulgarian Academy of Sciences, Sofia, BULGARIA

[*]E-mail: ivastankova@abv.bg

Introduction

Following the discovery of the first effective antiviral compound (idoxuridine) in 1959, nucleoside analogues, especially acyclovir (ACV) for the treatment of herpesvirus infections, have dominated antiviral therapy for several decades. However, ACV and similar acyclic nucleosides suffer from low aqueous solubility and low bioavailability following oral administration. Derivatives of acyclic nucleosides, typically esters, were developed to overcome this problem and valaciclovir, the valine ester of ACV, was among the first of a new series of compounds that were readily metabolized upon oral administration to produce the antiviral nucleoside *in vivo*, thus increasing the bioavailility by several fold.[1,2]

We synthesized and explored antiviral activity (HSV-1, HSV-2) of some esters of acyclovir with amino acid (Gly, Ala, Val, Leu) containing thiazole, oxazole and thiazolyl-thiazole ring. The results showed that modification of acyclovir with amino acids containing (Gly, Val, Leu) thiazole, oxazole and thiazolyl-thiazole ring reduced antiviral effect in comparison with these modification with natural amino acids. Only the inhibitory effect of alanyl ester of acyclovir against HSV-2 was appreciable.[3] The chemical stability of some of them was studied at pH 1.0 and 7.4 and 37 °C. An HPLC method was developed for quantification of the ester concentration.

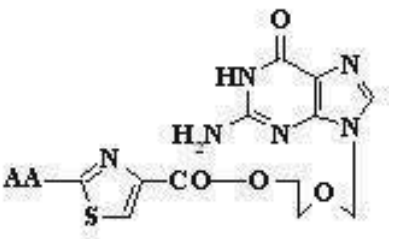

AA=Boc-Val, Gly, Ala, Leu

Figure 1

Results and Discussion

The chemical stability of the Boc-2-aminomethyl-thiazole- (1), Boc-2-Ala-thiazole (2), Boc-2-Val-thiazole- (3) and Boc-2-Leu-thiazole- (4) derivatives of acyclovir was examined at 37 °C at pH 1.0 (0.1M HCl) and pH 7.4 (phosphate buffer) (Fig. 1). Hydrolysis to acyclovir was detected by HPLC using a C 18 reversed-phase column. The mobile phase consisted of acetonitrile/water in ratio 30:70 or 50:50 v/v depending on the polarity of the compounds. It was established that under the described experimental conditions some esters undergo decomposition by hydrolysis. The hydrolysis followed an apparent firs order kinetics, and the rate constant (K) were obtained as slopes from the semilogarithmic plots of the unchanged ester concentration versus time. The chemical stability was assessed by means of the decomposition half-times ($t_{1/2}$=ln 2/K) which values are shown in Table 1.

Table 1. Half-lives (h) of amino acid ester of acyclovir at 37 °C

Coumpound	*pH 1.0*	*pH 7.4*
1	1.1 h	4.9 h
2	1.3 h	7.8 h
3	0.7 h	17.8 h
4	2.6 h	5.0 h

The Boc-2-Val-thiazole-acyclovir (3) and Boc-2-aminomethyl-thiazole-acyclovir (1) were less stable than the Boc-2-Ala-thiazole-acyclovir (2) and Boc-2-Leu-thiazole-acyclovir (4) at pH 1.0. Esters (1) and (4) manifest lower stability at pH 7.4. It was proved that the rest of compounds are stable at the pH 7.4.

Conclusion

The chemical stability of amino acids esters containing thiazole ring of acyclovir was studied in experimental conditions simulating some relevant biological medias (pH 1.0 and 7.4, 37 °C). The order of decreasing stability at neutral media and temperature of 37 °C was 3>>2>4>1. At the same conditions the Boc-2-Val-thiazole-acyclovir (3) was more stable than valacyclovir (t1/2=13 h) - the first effective prodrug of acyclovir.[4] The compound (2) with appreciable effect against HSV-2 exhibited satisfying chemical stability. The correlation with both biological activity and chemical stability suggest that the Boc-2-Ala-thiazole-acyclovir (2) could be attractive for antiviral chemotherapy.

Acknowledgements

Partial support of this work by the National Found for Scientific Research of Bulgaria (VUL-304/07) is gratefully acknowledged.

References

1. De Clercq E, Field J Hugh. Antiviral prodrugs – the development of successful prodrug strategies for antiviral chemotherapy. *British Journal of Pharmacology* **147**: 1–11, 2006.
2. Field HJ, De Clercq E. Antiviral drugs – a short history of their discovery and development. (Balzarini J, Schols D, Baba M, Field HJ, De Clercq E) *Microbiol Today* **31**: 58–61, 2004.
3. Stankova I, Dzimbova T, Shishkov St, Kostova K, Galabov A. Synthesis and biological activity of amino acid ester prodrugs of acyclovir. *Peptides 2006* (Proceedings of the 29th European Peptide Symposium, Gdańsk, Poland). Rolka Krz, Rekowski P, Silberring J (Eds), Kenes International, Geneva, Switzerland, 2007, pp 226-227.
4. Beauchamp LM, Krenitsky TA. Acyclovir prodrugs: the road to valaciclovir. *Drugs Future* **18**: 619-628, 1993.

4-05-106

A Novel Approach to Improve Cellular Delivery of 5-Aminolaevulinic Acid: New 5-ALA-containing Peptide Prodrugs for Photodynamic Therapy

Giuntini, Francesca[1,]; Bourré, Ludovic[2]; MacRobert, Alexander J[2]; Wilson, Michael[3]; Eggleston, Ian M[1]*

[1]University of Bath, Department of Pharmacy and Pharmacology, UNITED KINGDOM; [2]University College of London, National Medical Laser Centre, UNITED KINGDOM; [3]University College of London, UCL Eastman Dental Institute, UNITED KINGDOM

[*]E-mail: fg214@bath.ac.uk

Introduction

Photodynamic therapy (PDT) is a binary therapeutic modality which is currently under investigation for the treatment of several kinds of malignancies[1] and pathogens.[2] It relies on the interaction of two individually harmless components: a photosensitiser and an external radiation. The interaction of a photosensitiser with light of the appropriate wavelength and molecular oxygen results in the generation of cytotoxic species, namely singlet oxygen and/or radicals, and localized destruction of tumours or infected tissue, relative to normal adjacent tissue. The efficacy of this approach has led to approval for clinical use or trials for the treatment of non-melanoma skin cancer, advanced and early lung cancer, oesophagus adenocarcinoma, and palliative treatment of head and neck cancer. It has also received approval for the treatment of precancerous conditions (e.g. Barrett's oesophagus), hyperkeratotic conditions (e.g. actinic keratoses), and age-related macular degeneration. In 5-aminolaevulinic acid photodynamic therapy (5-ALA-PDT), exogenous administration of 5-ALA is employed to generate elevated intracellular levels of the natural photosensitiser protoporphyrin IX (PpIX), via metabolism through the haem biosynthetic pathway.[3] However this approach suffers from several drawbacks associated with 5-ALA's lack of stability at physiological pH and its highly hydrophilic nature, which prevent it from crossing biological membranes and hence limit tissue penetration. 5-ALA delivery with synthetic peptide prodrugs is a promising way to address these problems.[4] In this work we report the synthesis and characterisation of a series of peptide prodrugs of general structure Ac-Xaa-ALA-OR, where Xaa is an alpha amino acid, chosen to provide a prodrug with appropriate lipophilicity and water solubility. In a parallel study, we have also explored the possibility of coupling of 5-ALA and 5-ALA prodrugs to cell penetrating peptides (CPP).[5] The conjugation of one or more molecules of 5-ALA to a CPP sequence represents an interesting approach to enhanced topical delivery of 5-ALA.[6]

Results and discussion

The instability of 5-ALA in basic media is an obstacle for any derivatisation of its amino-group occurring in basic environment. To overcome this problem we performed the coupling with amino acids by adding a solution of base (DIPEA) to a suspension of 5-ALA and an activated amino acid derivative, by slow infusion over 7 hours. This strategy afforded the protected dipeptides (general formula **2**) in excellent yields (72-98%). 22 prodrugs (general formula **4**) containing L- as well as D-amino acids, were obtained after removal of the Boc group, acetylation, and side-chain deprotection, if required.

Scheme 1

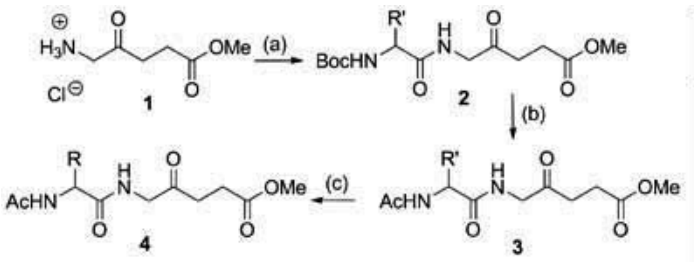

(a): BocXaaOSu, DIPEA, THF, 0°C to r.t, (b): HCl, 1,4-dioxane, then Ac_2O, DIPEA, CH_2Cl_2, 0°C to r.t, (c): eventual side-chain deprotection step

Aa	φ_0 (CH_3OH)	φ_0 (CH_3CN)
Gly	18.77	10.31
Val	41.60	25.64
Leu	50.92	36.67
Met	41.40	28.89
Ser	36.43	14.61
Phe	52.96	34.71
Trp	22.08	37.35
Lys	13.61	8.48
Asp	24.27	19.62

Scheme 2

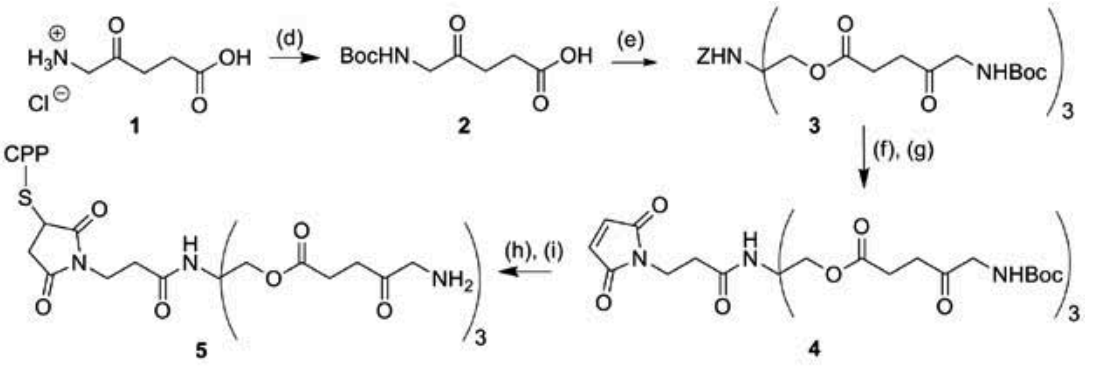

(d) Boc_2O, DIPEA, THF, 0°C to r.t., (74%), (e) *N*-Z-*tris*-hydroxylaminomethane, EDC, DMAP, DMF/DCM r.t., (66%), (f) H_2, Pd/C, HCl, EtOH, r.t., (quant.), (g) maleimidopropionic acid, PyBOP ®, DIPEA, CH_2Cl_2, r.t., (68%), (h) CPP, DMSO, pyridine, (i) TFA, TIS (95/5)

In order to evaluate the hydrolipophilic balance of the new compounds, their chromatographic hydrophobicity index (φ_0) was determined by isocratic RP-HPLC methods.[7] Table 1 (Scheme 1, inset) shows selected examples of φ_0 values determined in MeOH and CH_3CN. The induction of PpIX production exerted by the new prodrugs is currently under evaluation in several cell lines. We previously showed that the conjugation of 5-ALA to a cell penetrating peptide may be used to enhance the cellular delivery of 5-ALA.[6] We wished to expand this approach and explore the possibility of using a CPP sequence to deliver more than one 5-ALA into cells, and to this end, we synthesised a thiol-reactive dendrimeric cargo containing three units of 5-ALA (Scheme 2).[8] 5-Boc-ALA was first esterified to *N*-Z-hydroxylaminomethane, then Z cleavage and subsequent PyBOP® mediated coupling with maleimidopropionic acid yielded the desired compound **4**. We chose to conjugate **4** to the CPP sequences TAT-1, p-Vec, and Tp-10,5 with a cysteinyl residue appended at the C-terminus of each peptide in order to provide the thiol moiety required for the reaction with **4**. The synthesis of the peptides was performed on Rink amide® resin by Fmoc-SPPS, on an automated peptide synthesiser (Activo P11®, ActivoTec, Cambridge, UK).

After cleavage from the resin and purification, the conjugation reaction was carried out in solution with the fully deprotected peptides and excess **4**. Final acidolytic deprotection of the cargo moieties gave the desired conjugates **5**, which were purified by HPLC and their structures confirmed by ESI-MS (TAT-1 conjugate: 820.44 $[M+3H]^{3+}$, Tp10 conjugate: 966.22 $[M+3H]^{3+}$, pVec conjugate: 975.21 $[M+3H]^{3+}$).

Acknowledgements

We thank Biotechnology and Biological Sciences Research Council for financial support (grants BBD0127831 and BBD113291).

References

1. Brown SB, Brown EA, Walker I. *Lancet Oncol*. **5:** 497-508, 2004.
2. Hamblin MR, Hasan T. *Photochem Photobiol Sci* **3:** 436-450, 2004.
3. Peng Q, Warloe T, Berg K, Moan J, Kongshaug M, Giecksky KE, Nesland JM. *Cancer* **79:** 2282-2308, 1997.
4. Rogers LMA, McGivern PG, Butler AR, MacRobert AJ, Eggleston IM. *Tetrahedron* **61:** 6951-6958, 2005.
5. Lundberg P, Langel U. *J Mol Recognit* **16:** 227-233, 2003.
6. Dixon MJ, Bourre L, MacRobert AJ, Eggleston I M. *Bioorg Med Chem Lett* **17:** 4518-4522, 2007.
7. Valko K, Bevan C, Reynolds D. *Anal Chem* **69:** 2022-2029, 1997.
8. Battah SH, Chee CE, Nakanishi H, Gerscher S, MacRobert AJ, Edwards C. *Bioconjugate Chem* **12:** 980-988, 2001.

4-05-107

Determination of Binding Ratio of Hydrofobic Peptide-Polymer Conjugates by Using Fluorescamine Assay

Budama Battal, Yasemin; Derman, Serap; Mansuroglu, Banu; Mustafaeva, Zeynep*

Yildiz Technical University, Bioengineering Department, TURKEY

**E-mail: yaseminbattal@gmail.com*

Introduction

Fluorescamine (4-Phenylspiro-[furan-2(3H),1-phthalan]-3,3'-dione) which heterocyclic dione is a reagent for the detection of primary amines on peptides or completion of coupling reactions in the picomole range. Its reaction with amines is almost instantaneous at room temperature in aqueous media, organic solvents etc. Fluorescamine reacts with primary amines (in peptide, protein etc.) to form highly fluorescent product (fluorophors) whereas the reagent and its degradation products are nonfluorescent.[1,2] This is the basis of a fluorescent protein assay.[3,4] Fluorescamine is used in many sensitive detection methods, for example, characterization of poly-L-lysine (pLL)/DNA complexes post-modified with a multivalent hydrophilic polymer,[5] or synthetic peptide-polymer conjugates. Also it has been used to detect free amino groups on peptides or completion of coupling reactions in solid phase peptide synthesis and not only in aqueous solution but also in organic solvents and on solids.

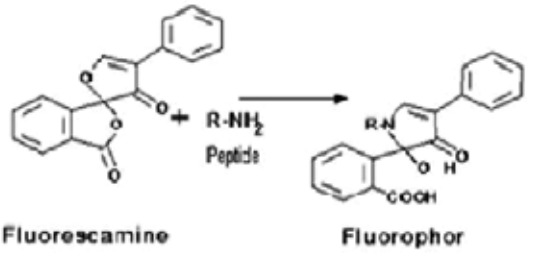

Figure 1. *Reaction of fluorescamine and primary amino groups.* Fluorescamine reacts with the primary amino groups found in terminal amino acids and the e amine of lysine to form fluorophore attribute.

Results and discussion

Peptide epitops of VP1 capsid protein of Foot-and-Mouth-Diseases Virus 40-60 amino acid residues (Val-Lys-Ile-Asn-Asn-Thr-Ser-Pro-The-His-Val-Ile-Asp-Leu-Met-Gln-Thr-His-Gln-His-Gly) were synthesized by Sigma. We synthesized the covalent conjugate of 40-60 amino acid residues with copolymers of acrylic acids and N-vinylpyrolidone (VP\AA) at different ratio of components ($n_{Peptide}/n_{Polymer}$=13,20) and investigated the mechanism of condensation reaction by using different physicochemical analyses as Fluorescence Spectroscopy and Fluorescamine assay. For determination of binding ratio of hydrophobic peptide-polymer conjugates, fluorescent measurements were performed in the presence of fluorescamine at the wavelengths of excitation 390 nm and emission 475 nm. When conjugation reaction completed, the amount of free amino groups had decreased and observed that Fluorescence Intensity had decreased and the estimated degree of primary amino group after conjugation, calculated from fluorescence spectrums.

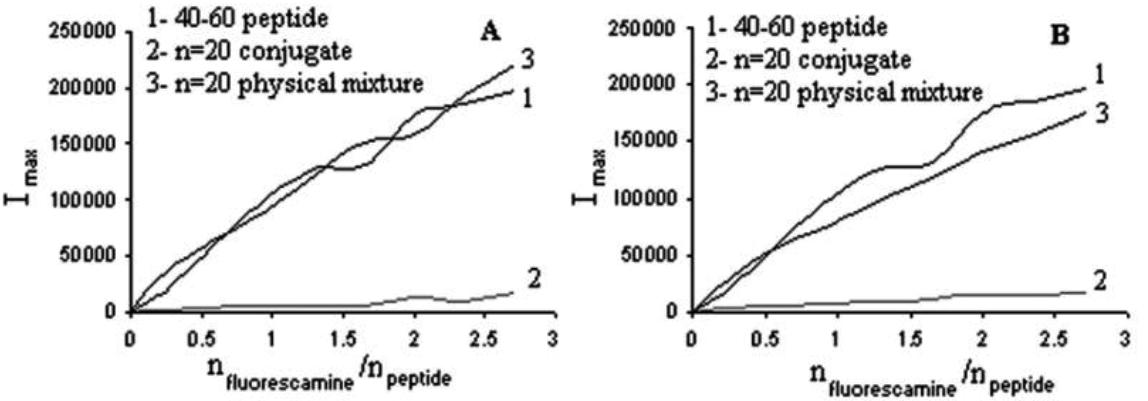

Figure 2. A. Titration of 40-60 peptide, n=20 conjugate and n=20 physical mixture with Fluorescamine. **B.** Titration of 40-60 peptide, n=13 conjugate and n=13 physical mixture with Fluorescamine.

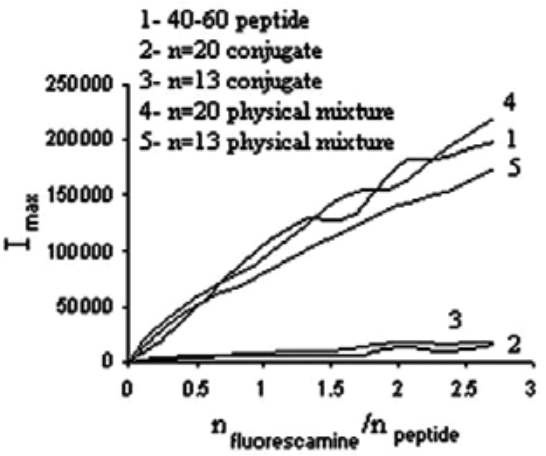

Figure 3. Titration of 40-60 peptide, n=20 conjugate. n=13 conjugate, n=20 physical mixture and n=13 physical mixture with Fluorescamine.

When a constant quantity of peptide solution, by its own and mixed physically with different ratios of the polymer, it has been observed that since it does not react with the amino groups in the structure and does not cover, $n_{fluorescamine}/n_{peptide}$ ratio is found to be 2 for all 3 solutions (peptide, n=13 conjugate and n=20 conjugate). But, it has also been observed that, the fluorescence intensities of the conjugates produced after the peptide making a covalent bond to the polymer using carbodiimide, decrease and $n_{fluorescamine}/n_{peptide}$ ratio is too low.

The reason of this is the polymers carboxyl groups activated by WSC during the conjugation, by reacting with the free amino groups, utilizing conjugation by forming amide bonds. By the formation of conjugation, the number of free amino groups has decreased, and as the number of amino groups that can react with fluorescamine has decreased too, the intensity of fluorescence has decreased.

As seen clearly from the figure, n=20, n=13 Physical Mixture and pure peptide including peptide of constant quantity solutions show the same characteristics as the free amino groups have not reacted and interacted with fluorescamine resulting in fluorophore attribute. But, as the majority of free amino groups have formed amide bonds with the carboxyl groups in the conjugate because of this have not reacted with fluorescamine and have not gained fluorophore attribute. Thus the fluorescence intensities has been measured to be too low as seen in Fig. 3, following the addition of fluorescamine.

Acknowledgements

This research was supported by grant from Republic of Turkey Prime Ministry State Planning Organization (25-DPT-07-04-01).

References

1. *Spectrophotometry and Spectrofluorimetry: A Practical Approach.* Gore M (Ed), Oxford University Press, Incorporated New York, 2000, p 63.
2. http://www.sigmaaldrich.com/etc/medialib/docs/Sigma/Product_Information_Sheet/f9015pis.Par.0001.File.tmp/f9015pis.pdf
3. Böhlen P, Stein S, Dairman W, Udenfriend S. Fluorometric assay of proteins in the nanogram range. *Arch Biochem Biophys*, **155**: 213-220, 1973.
4. Udenfriend S, Stein S, Böhlen P, Dairman W, Leimgruber W, Weigele M. Fluorescamine; a reagent for assay of amino acids, peptides, proteins, and primary amines in picomole range. *Science*, **178**: 871-872, 1972.
5. Read ML, Etrych T, Ulbrich K, Seymour LW. Characterisation of the binding interaction between poly(L-lysine) and DNA using the fluorescamine assay in the preparation of non-viral gene delivery vectors. *FEBS Lett* **461**: 96-100, 1999.

4-07-108

Peptides from CcdB protein as novel inhibitors of DNA gyrase

Marchetto, Reinaldo; Garrido, Saulo S; Barros, Ronaldo S; Trovatti, Eliane; Cotrim, Camila A*
UNESP - Institute of Chemistry - Dept. Biochemistry and Technological Chemistry - Araraquara - SP, BRAZIL

**E-mail: marcheto@iq.unesp.br*

Introduction

Toxin-antitoxin (TA) systems contribute to plasmid stability by a mechanism that relies on the differential stabilities of the antitoxin and toxin proteins and leads to the killing of daughter bacteria that did not receive a plasmid copy at cell division.[1] *Ccd* was the first TA system to be discovered and is located on the F plasmid with CcdB being the toxin and CcdA the antitoxin.[2] CcdB, a 11.7 kDa protein, is known to poison the DNA gyrase, unique type IIA topoisomerase able to introduce negative supercoils into bacterial DNA.[3] The mechanism of the inhibition of the gyrase activity by CcdB is still an object of many debates, but is clear that Arg462 residue of GyrA and the C-terminus of CcdB (Trp99-Ile101) play a crucial role in the gyrase-CcdB interactions.[4] As an approach for a better understanding of this mechanism as well as for development of new gyrase inhibitors, we have synthesized peptide analogues of the CcdB protein and studied its inhibitory activity by supercoiling assays and bacterial growth.

Results and Discussion

The peptide analogues (Fig. 1) were built using the 13 residues C-terminal α-helix, the loop Arg40-Leu50 of the wing sheet, the strand called S6 (residues 68 to 72), the N-terminal β-sheet (Met1 to Leu9) and the residues Gly100 and Ile101 that seem to play a key role in the formation of CcdB-GyrA complex.[4]

The ability of the analogues to inhibit the supercoiling reaction of DNA gyrase was investigated by titrating CcdB analogues into a fixed concentration of enzyme and DNA. The minimum concentration that produced complete inhibition of supercoiling activity was termed the IC_{100}. In standard supercoiling assays at 37 °C with 3.4 nM of gyrase, a relaxed DNA (500 ng) substrate is completely negatively supercoiled in 1 h. *CcdBET2* inhibited this reaction (Fig. 2) with an IC_{100} value of 10 μM.

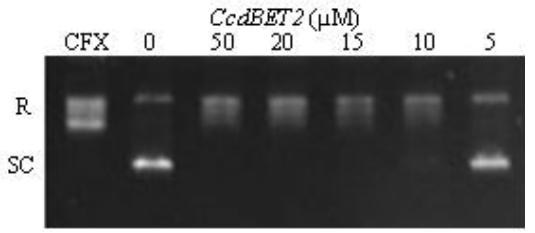

Figure 2. *CcdBET2*-mediated inhibition of DNA supercoiling reactions of DNA gyrase (3.4 nM) from *Escherichia coli*. Controls were no drug (lane 0) and treatment with ciprofloxacin (10 μM), the known topoisomerase inhibitor (lane CFX). R and SC represent relaxed and supercoiled pBR322 DNA, respectively.

The lack of the loop Arg40-Leu50 yielded *CcdBET3* a peptide that was 6-fold weaker than *CcdBET2*, in the supercoiling inhibition. The introduction of the fragment Met64-Val73 into *CcdBET3* resulted in the *CcdBSS1* analogue, which showed the same activity of the *CcdBET3* (Table 1). A higher concentration (60 μM) was required for *CcdBET1* (without the loop and the N-terminal β-sheet) inhibit the supercoiling reaction. The *CcdBET4* analogue, which contains the full amino acid sequence of CcdB devoid of the 67 N-terminal residues, did not inhibit the DNA gyrase (Table 1).

Table 1. Inhibitory activities of peptide analogues of CcdB on bacterial DNA gyrase.

peptide	IC_{100} (μM)
CcdBET1	60
CcdBET2	10
CcdBET3	50
CcdBET4	ND
CcdBSS1	50

^{84}SHRENDIKNAINLMFWGI^{101} (*CcdBET1*)
^{1}MQFKVYTYK^{9}-**Z**-^{40}RLLSDKVSREL^{50}-**Z**-^{84}SHRENDIKNAINLMFWGI^{101} (*CcdBET2*)
^{1}MQFKVYTYK^{9}-**Z**-^{84}SHRENDIKNAINLMFWGI^{101} (*CcdBET3*)
^{68}MASVPVSVIGEEVADLSHRENDIKNAINLMFWGI^{101} (*CcdBET4*)
^{1}MQFKVYTYK^{9}-**Z**-^{44}MTTDMASVPV^{73}-**Z**-^{84}SHRENDIKNAINLMFWGI^{101} (*CcdBSS1*)

Figure 1. The primary structures of the synthesized CcdB analogues (Z = ε-amino hexanoic acid).

From these results it's possible to speculate about of the requirement of the N-terminal sequence (Met1-Lys9) in a probable structure-activity relationship of the peptides synthesized. The best inhibitors (*CcdBET2, CcdBET3* and *CCdBSS1*) share this fragment and the analogue that showed the lesser activity (*CcdBET1*), not includes the Met1-Lys9 sequence in its primary structure. Probably the peptides with the fragment Met1-Lys9 contain enough structural information to induce the formation of an inactive peptide-enzyme complex. Additionally, in *CcdBET2*, the Arg40-Leu50 fragment seems to improve the molecular adjustments of the peptide in the complex, resulting in the most promising peptide inhibitor of the bacterial DNA gyrase. The lack of inhibitory activity observed for *CcdBET4*, analogue devoid of those fragments, corroborates these findings. All peptides in the free form were unable to inhibit the bacterial growth in liquid culture medium, probably due the poor permeability of the bacterial membrane to the peptides. When encapsulated in Liposome (SUV) the peptides, especially *CcdBET2*, showed antimicrobial activity. In this case, the interaction of the liposome with the cell changed the permeability of the membrane and facilitated the release of the peptides inside the cell and consequently the access to its target: DNA gyrase. For *CcdBET2* analogue, the growth inhibition *in vitro* was about 70% for *Pseudomonas sp*, 50% for *Streptococcus agalactae*, *Salmonella sp*. and *Klebsiella pneumoniae*, and about 30% for *Escherichia coli K-12*, *Sthaphilococcus aureus* and *Shigella sp*. The antimicrobial activity and the peculiar primary structure makes of the *CcdBET2* a good start point for the development of the new powerful and specific family of peptide antibiotics inhibitors of DNA gyrase.

Acknowledgments

The authors gratefully acknowledge Brazilian Financial Research Agencies FAPESP and CNPq for their continuous and generous support to this research.

References

1. Hayes F. Toxins-antitoxins: Plamid maintenance, programmed cell death, and cell cycle arrest. *Science* **301**: 1496-1499, 2003.
2. Ogura T, Hiraga S. Mini-F plasmid genes that couple host cell division to plasmid proliferation. *Proc Natl Acad Sci U S A* **80**: 4784-4788, 1983.
3. Reece RJ, Maxwell A. DNA gyrase: structure and function. *Crit Rev Biochem Mol Biol* **26**: 335-375, 1991.
4. Loris R, Dao-Thi M-H, Bahassi EM, Van Melderen L, Poortmans F, Liddington R, Couturier M, Wyns L. Crystal structure of CcdB, a topoisomerase poison from E.coli. *J Mol Biol* **285**: 1667-1677, 1999.

4-07-109

Synthesis and Biological Activity of a Series of Aza-β^3-Pseudopeptides Related to 26RFa, The Endogenous Ligand of GPR103

Le Marec, Olivier[1]; Neveu, Cindy[1]; Tasseau, Olivier[2]; Guilhaudis, Laure[3]; Ségalas-Milazzo, Isabelle[3]; Lefranc, Benjamin[1]; Tena-Sempere, Manuel[4]; Tonon, Marie-Christine[1]; Baudy-Floc'h, Michèle[2]; Vaudry, Hubert[1]; Leprince, Jérôme[1,]*

[1]INSERM U413, Laboratory of Cellular & Molecular Neuroendocrinology, University of Rouen, FRANCE; [2]CNRS UMR 6226, Ciblage et Auto-assemblages Fonctionnels, University of Rennes, FRANCE; [3]CNRS UMR 6014, Laboratory of Nuclear Magnetic Resonance, University of Rouen, FRANCE; [4]Physiology Section, Faculty of Medecine, University of Cordoba, SPAIN

[*]E-mail: jerome.leprince@univ-rouen.fr

Introduction

26RFa, a novel neuropeptide of the RFamide family recently characterized in our laboratory, is the endogenous ligand of the previously orphan receptor GPR103.[1,2,3] In rodents, both 26RFa and GPR103 mRNAs are highly expressed in hypothalamic nuclei involved in the control of energy homeostasis.[4] Intracerebroventricular injection of 26RFa increases food intake and stimulates locomotor activity in mice.[4,5] Recently, it has been shown that GPR103-deficient mice exhibit a phenotype similar to osteoporotic patients characterized notably by a pronounced kyphotic hump and an early arrest of osteogenesis.[6] These data suggest that GPR103 agonists could have a therapeutic value to stimulate food consumption and bone regeneration in anorexic and osteoporotic patients, respectively, whereas GPR103 antagonists may be used to restrict feeding and treat obesity. Analysis of the human 26RFa precursor reveals that it may generate several additional RFa-related-peptides including an N-terminally extended form (43RFa) and a truncated form (26RFa$_{(20-26)}$) the sequence of which has been strictly conserved throughout the vertebrate phylum.[1] 26RFa and 43RFa increase dose-dependently $[Ca^{2+}]_i$ in GPR103-transfected cells while 26RFa$_{(20-26)}$ is significantly less potent than 26RFa.[2] In contrast, it has been demonstrated that, *in vivo*, 26RFa$_{(20-26)}$ mimics the effects of 26RFa, on food intake and on gonadotropin release.[5,7] Molecular modeling under H^1-NMR constraints of 26RFa in methanol shows that the Pro^4-Arg^{17} region encompasses an α-helix whereas the N- and C-terminal extremities of the peptide are disordered. Preliminary results indicate that the C-terminal region of *h*26RFa adopts a γ-turn in DPC micelles and that this γ-turn exhibits major distortions in 26RFa$_{(20-26)}$. This conformational alteration may be responsible for the weak potency of the C-terminal heptapeptide in our *in vitro* model. Previous reports have shown that aza-β^3–amino acids constrain the dihedral angles of pseudopeptidic bounds and rigidify the peptide backbone in a turn conformation.[8] The aim of the present study was to introduce an aza-β^3 residue in the 26RFa$_{(20-26)}$ sequence that may restore the *γ*-turn, in order to increase the biological activity of the heptapeptide.

Results

Human 26RFa (TSGPLGNLAEELNGYSRKKGGFSF-RF-NH_2), 26RFa$_{(20-26)}$ (GGFSFRF-NH_2) and all aza-β^3-moiety-substituted 26RFa$_{(20-26)}$ analogs were synthesized by the conventional solid-phase methodology by using the standard Fmoc procedure. After cleavage from the resin, the peptides and the pseudopeptides were purified by reversed-phase HPLC and their sequence was verified by MALDI-TOF mass spectrometry analysis. To assess the biological activity of *h*26RFa, 26RFa$_{(20-26)}$ and aza-β^3-substituted 26RFa$_{(20-26)}$ analogs, the effect of the peptides on $[Ca^{2+}]_i$ was tested on CHO cells stably expressing human GPR103 by spectrofluorometry using the Flexstation technology. Administration of graded doses of *h*26RFa resulted in a concentration-dependent increase in $[Ca^{2+}]_i$ with a potency (EC_{50}) of 9.7 ± 1.3 nM. 26RFa$_{(20-26)}$ was 75 times less potent than 26RFa (EC_{50} = 750 ± 169 nM) in this Ca^{2+} mobilization assay. Substitution of glycine at position 20 and 21 by aza-β^3–glycine led to analogs that were, respectively, 2 and 5 fold more potent than 26RFa$_{(20-26)}$. The [aza-β^3-Phe^{22}]26RFa$_{(20-26)}$ pseudopeptide exhibited a very weak potency (EC_{50} = 2340 ± 1540 nM). Replacement of the native Ser^{23} by the aza-β^3 surrogate of (*γ*-OH)homoThr (aza-β^3-Hth) generated an analog that was 2 times more potent (EC_{50} = 407 ± 55 nM) than 26RFa$_{(20-26)}$. Finally, the analogs obtained by substitution of each amino acid at position 24 to 26 as well as the bi-substituted analog [aza-β^3-$Phe^{22, 24}$]26RFa$_{(20-26)}$ were totally devoid of activity in our calcium mobilization assay.

Discussion

Modifications of the peptide backbone are used to generate conformationally constrained, stable and active peptides. In the present study, we have sequentially introduced aza-β^3 surrogates of each native amino acid in 26RFa$_{(20-26)}$, and tested the ability of the resulting pseudopeptides to increase $[Ca^{2+}]_i$ in GPR103-transfected cells. As previously shown, 26RFa$_{(20-26)}$ was found to be far less potent and efficient to elevate intracellular calcium levels than *h*26RFa.[2] This observation suggests that the distortions of the γ-turn detected in the 26RFa$_{(20-26)}$ sequence may account for the lower activity as compared

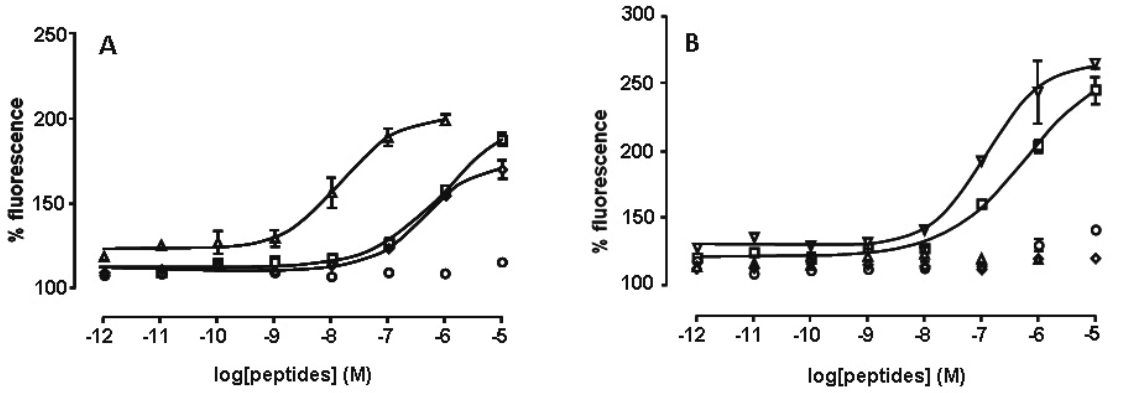

Figure 1. Effects of graded concentrations of (**A**) h26RFa (△), $26RFa_{(20–26)}$ (□), [aza-β^3-Gly^{20}]$26RFa_{(20–26)}$ (◇) and [aza-β^3-Phe^{22,24}]$26RFa_{(20–26)}$ (○) and (**B**) $26RFa_{(20–26)}$ (□), [aza-β^3-Gly^{21}]$26RFa_{(20–26)}$ (▽), [aza-β^3-Phe^{24}]$26RFa_{(20–26)}$ (△), [aza-β^3-Arg^{25}]$26RFa_{(20–26)}$ (◇) and [aza-β^3-Phe^{26}]$26RFa_{(20–26)}$ (○) on [Ca^{2+}], in CHO GPR103-transfected cells. Each value represents the mean amplitue (±SEM) of the calcium response calculated from at least 6 different experiments.

to 26RFa. Three of the hydrazino-pseudopeptides were found to be more potent than the native heptapeptide. In particular, the analog [aza-β^3-Gly^{21}]$26RFa_{(20-26)}$ appeared to be about 5-fold more potent than $26RFa_{(20-26)}$ indicating that the aza-β^3 radical at position 21 may induce a local secondary structure that is favorable to the binding and/or the activation of the receptor. These data constitute the first step towards the development of new GPR103 analogs that could prove useful for the treatment of feeding disorders and/or osteoporosis.

Acknowledgments

This study was supported by Inserm (U413 and PNR-RE), the Research Platform for Cell Imaging (PRIMACEN) and the Conseil Régional de Haute-Normandie.

References

1. Chartrel N, Dujardin C, Anouar Y, Leprince J, Decker A, Clerens S, Do-Régo JC, Vandesande F, Llorens-Cortes C, Costentin J, Beauvillain JC, Vaudry H. *Proc Natl Acad Sci U S A* **100**: 15247-15252, 2003.
2. Jiang Y, Luo L, Gustafson EL, Yadav D, Laverty M, Murgolo N, Vassileva G, Zeng M, Laz TM, Behan J, Qiu P, Wang L, Wang S, Bayne M, Greene J, Monsma F Jr, Zhang FL. *J Biol Chem*,**278**: 27652-27657, 2003.
3. Fukusumi S, Yoshida H, Fujii R, Maruyama M, Komatsu H, Habata Y, Shintani Y, Hinuma S, Fujino M. *J Biol Chem* **278**: 46387-46395, 2003.
4. Takayasu S, Sakurai T, Iwasaki S, Teranishi H, Yamanaka A, Williams SC, Iguchi H, Kawasawa YI, Ikeda Y, Sakakibara I, Ohno K, Ioka RX, Murakami S, Dohmae N, Xie J, Suda T, Motoike T, Ohuchi T, Yanagisawa M, Sakai J. *Proc Natl Acad Sci U S A* **103**: 7438-7443, 2006.
5. Do-Rego JC, Leprince J, Chartrel N, Vaudry H, Costentin J. *Peptides* **27**: 2715-2721, 2006.
6. Baribault H, Danao J, Gupte J, Yang L, Sun B, Richards W, Tian H. *Mol Cell Biol* **26**: 709-717, 2006.
7. Navarro VM, Fernández-Fernández R, Nogueiras R, Vigo E, Tovar S, Chartrel N, Le Marec O, Leprince J, Aguilar E, Pinilla L, Dieguez C, Vaudry H, Tena-Sempere M. *J Physiol* **573**: 237-249, 2006.
8. Cheguillaume A, Lehardy F, Bouget K, Baudy-Floc'h M, Le Grel P. *J Org Chem* **64**: 2924-2927, 1999.

4-07-110

Effect of Synthetic Peptides against Multi-Drug Resistant Bacteria from Otitis Media

Park, Yoonkyung; Jeong, Nari; Park, Hae-Kyun; Kim, Mi-Hyun

Chosun University, KOREA (REP.)

E-mail: kshahm@chosun.ac.kr (Hahm Kyung-Soo)

Introduction

Membrane-active peptides, including a host of antimicrobials and toxins, have been shown to induce the formation of transmembrane pores. Although the molecular mechanisms by which pore formations occur remain to be thoroughly elucidated, the three mechanisms thus far proposed include the barrel-stave, carpet, and toroidal models. In the barrel-stave model, peptide helices form a bundle with a central lumen within the membrane, appearing similar to a barrel in which the helical peptides function as the staves.[1-5] Stomach mucosa that is infected with *Helicobacter pylori*, the bacterial pathogen associated with gastritis and peptic ulcers, typically shows massive infiltration of inflammatory cells and tissue destruction.[6] Persistence of *H. pylori* in the mucosa has been suggested to be facilitated by *H. pylori*-produced cecropin-like peptides with antibacterial properties. Although *H. pylori* itself is resistant to this peptide, the release of these peptides gives a competitive advantage over other microorganisms.[7] The linear -helical peptide that has beenαantimicrobial peptide, HP(2-20), is a cationic isolated from the N-terminal region of the *Helicobacter pylori* ribosomal protein, L1.[8] This peptide possesses several important functional characteristics; it is bactericidal, it is a neutrophil chemoattractant, and it activates phagocyte NADPH oxidase to produce reactive oxygen species.[8]

Results and discussion

Barely 10 years after ciprofloxacin's introduction into otology, the emergence of ciprofloxacin-resistant *P. aeruginosa* (CRPA) have created new therapeutic challenge in otology. A3 is a synthetic antimicrobial peptide derived from HP (2-20), derived from Helicobacter pylori. In previous study, A3 was strong antimicrobial activity *in vitro* test. The peptide A3 showed a strong antimicrobial activity against CRPA *in vivo* and the cochlear tolerance of A3 was studied *in vivo* by topical application to the middle ear in guinea pig model. Twenty guinea pigs (5 groups, each group n=4) were each injected by transtympanic approach with 20 μl of 8 μg/ml, 16 μg/ml, 32 μg/ml, 128 μg/ml of A3, and 0.4% gentamicin sulfate was instillated as a control. Auditory brainstem responses(ABR) to click were measured between 1st and 7th days after injection. Histologic investigation of cochlea was performed by scanning electron microscope and light microscope. Guinea pig injected with A3 8 μg/ml, 16 μg/ml, 32 μg/ml showed no interval changes in response ABR threshold and SEM showed the intact cochlear hair cells. However, 128ug/ml showed slight loss of hair cell in the SEM and increased ABR threshold 10 dB more than A3 32 μg/ml treated group. The control GM treated group showed no detectable ABR threshold, and severe missing of hair cells in the SEM and severe edematous stria vascularis

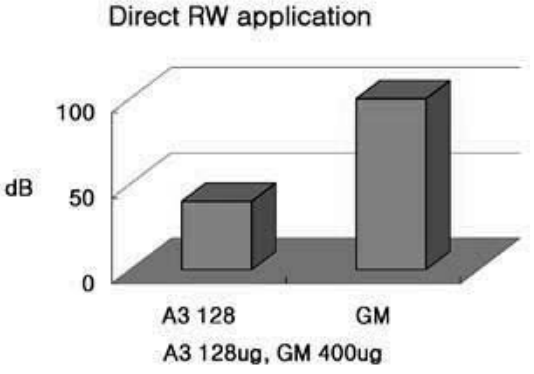

Figure 1. ABR : Direct RW approach. A3 128 ug and GM 400 ug (10ul) using gelfoam to the RW by postauricular app. Avoid trauma to ISJ. Check C-ABR postop 7th day

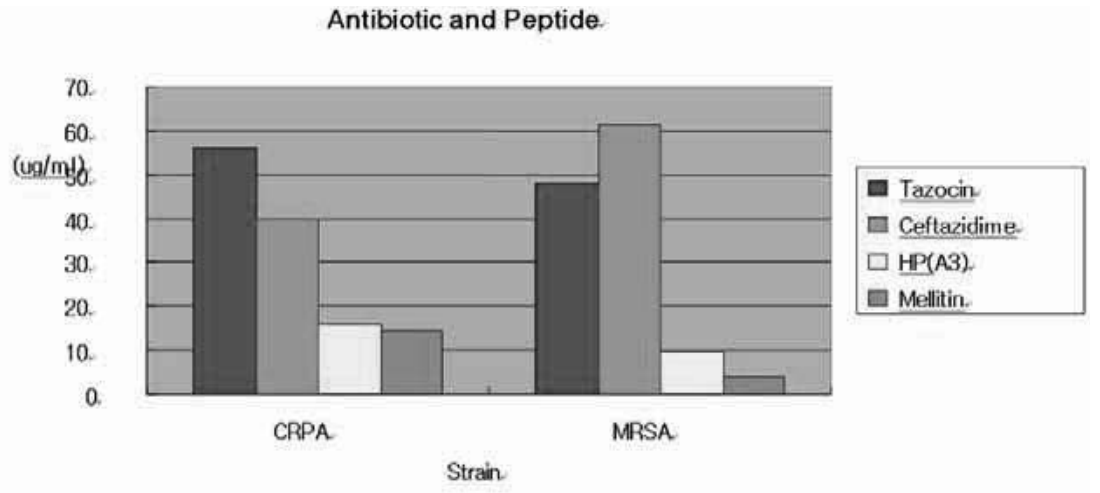

Figure 2. Antibacterial activity: MIC by ELISA.

in the LM. Topical application of A3 to the middle ear is well tolerated without cochlear damage and may be a useful as a new ototopical agent for CRPA otitis media.

Table 1. ABR : Direct RW approach. A3 128 μg and GM 400 μg (10 μl) using gelfoam to the RW by postauricular app. Avoid trauma to ISJ. Check C-ABR postop 7th day

Acknowledgements

This work was supported by grant from the Ministry of Science and Technology, Korea and the Korea Science and Engineering Foundation through the Research Center for Proteineous Materials (R11-2000-083-00000-0), and from the Korea Foundation for International Cooperation of Science & Technology (KICOS) through a grant provided by the Korean Ministry of Science & Technology(MOST) in 2007 (No. K20713000012-07B0100-01210).

References

1. Yang L, Harroun TA, Weiss TM, Ding L, Huang HW. *Biophys J* **81**: 1475-1485, 2001.
2. Ehrenstein G, Lecar H. *Q Rev Biophys* **10**: 1-34, 1977.
3. Dave PC, Billington E, Pan YL, Straus SK. *Biophys J* **89**: 2434-2442, 2005.
4. Lee MT, Chen FY, Huang HW. *Biochemistry* **43**: 3590-3599, 2004.
5. Chen FY, Lee MT, Huang HW. *Biophys J* **84**: 3751-3758, 2003.
6. Allen LA. *J Exp Med* **191**: 1451-1454, 2000.
7. Pütsep K, Brändén CI, Boman HG, Normark S. *Nature* **398**: 671-672, 1999.
8. Bylund J, Christophe T, Boulay F, Nyström T, Karlsson A, Dahlgren C. *Antimicrob Agents Chemother* **45**: 1700-1704, 2001.

4-07-111

Development of biotin-tagged diketopiperazine based anti-microtubule agents and tubulin photoaffinity labeling

Yamazaki, Yuri[1,]; Kohno, Kyoko[2]; Yasui, Hiroyuki[2]; Kiso, Yoshiaki[2]; Neuteboom, Saskia[3]; Barral, Ana M[3]; Potts, Barbara[3]; Lloyd, G Kenneth[3]; Hayashi, Yoshio[1]*

[1]Tokyo University of Pharmacy and Life Sciences, JAPAN; [2]Kyoto Pharmaceutical University, JAPAN; [3]Nereus Pharmaceuticals, UNITED STATES

[*]E-mail: yuyama@ps.toyaku.ac.jp

Introduction

The introduction of anti-microtubule agents such as taxanes and *vinca* alkaloids has revolutionized cancer treatment and improved patient survival time. However, tumors become resistant to these drugs after long-term treatment. Hence, there is a significant need to develop novel anti-microtubule agents. As one of such candidates, natural diketopiperazine, phenylahistin (PLH, halimide) exhibiting colchicine-like anti-microtubule activity,[1,2] has been our focus. We have succeeded in total synthesis of PLH, and performed a structure activity relationship (SAR) study of its derivatives.[3] From this SAR study, a highly potent derivative NPI-2358 (**1**, IC_{50} = 15 nM against HT-29 cells) was developed. Additionally, it was recently shown that NPI-2358 functions as a strong vascular disrupting agents (VDAs) to induce tumor-selective vascular collapse.[4] The therapeutic potential targeting the tumor vascular supply is now widely recognized. Therefore, NPI-2358 is a valuable compound for an antitumor drug, which is currently in Phase I clinical trial in the US. Although NPI-2358 is suggested to recognize around the colchicine binding site on tubulin, its three-dimensional structure could not be superimposed over that of colchicine. In order to understand the precise binding mode of NPI-2358 to tubulin, we planned to develop its biologically active photoaffinity probe. Photoaffinity labeling is well-known as a powerful tool to provide valuable information about the topology of the ligand-binding site on the target proteins. Here, we describe the design and synthesis of a photoaffinity probe and its photolabeling into tubulin.

Results and Discussion

We have established the synthetic route of NPI-2358 and its derivatives. Until now, more than 100 analogues were prepared and screened by HT-29 cytotoxicity assay. Then, a SAR study was performed. As a result, several highly potent derivatives were developed. One of these compounds is KPU-244 (**2**),having a benzophenone structure, which is often used photoaffinity labeling as a photo-reactive group. In cytotoxicty assay, KPU-244 exhibited highly potent activity (IC_{50} = 4 nM against HT-29 cells). Therefore, we designed biotin-tagged[5] KPU-244, KPU-244-B1 (**3**) and KPU-244-B2 (**4**), as a photoaffinity probe, which can be photo-reactive and detected by an avidin-peroxidase system. In the synthesis of **3** and **4**, a biotin-tag was successfully connected at the 4 f position of the benzophenone moiety of **2** via an additional amino-methyl group.

Firstly, to investigate the biological activity of biotin-tagged photoaffinity probe **3**, we performed a binding assay to tubulin according to the intristic fluorescence change of the tryptphan residue in tubulin caused by the binding of compounds. The dissociation constant (K_d) of **3** and **4** to tubulin (0.5 μM) at 37 °C were calculated to be 7.95 and 7.19 μM, respectively, which were about 2 and 5 times lower affinity than those of colchicine (3.32 μM) and NPI-2358 (1.46 μM), respectively. These results indicated that probes **3** and **4** at least possess a significant binding ability to tubulin. Additionally, **3** and **4** at 10 μM exhibited mild but significant inhibition of tubulin polymerization (data not shown). In the citotoxicity

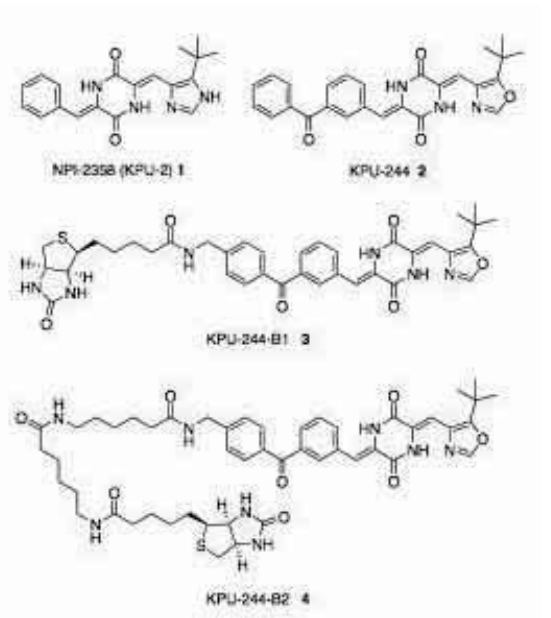

Figure 1. Structures of NPI-2358 (**1**), KPU-244 (**2**) and biotin-tagged photoaffinity probes (**3**, **4**).

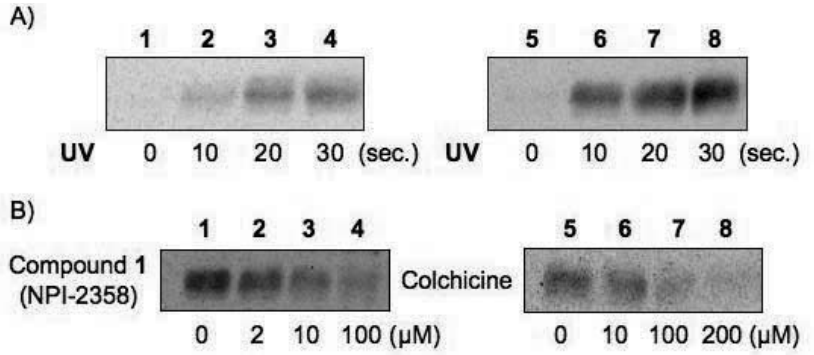

Figure 2. Photoaffinity labeling of tubulin: A) Photoaffinity labeling of tubulin by compounds **3** (2 μM, lanes 1-4) and **4** (2 μM, lanes 5-7) at different irradiation time (0-30 sec). B) Photoaffinity labeling of tubulin by compound **4** (2 μM) in the absence or presence of NPI-2358 (0-100 μM, lanes 1-4) and colchicine (0-200 μM, lanes 5-8).

assay, **3** and **4** also exhibited low citotoxicity against HT-29 human colon cancer cell lines with IC_{50} values of 0.91 and 1.1 μM, respectively. These results suggest that **3** and **4** are able to function as the biologically active photoaffinity probes.

Therefore, secondly, tubulin was photo-irradiated at 365 nm in the absence or presence of probe **3** and **4** on ice after incubation at 37 °C in MES buffer. An aliquot of sample solution was applied to SDS-PAGE and electrically blotted onto nitro-cellulose membrane, followed by detection using the avidin-biotin system. Non-specific labelling was not observed without photo-irradiation (Fig. 2A, lanes 1, 5). However, in the photo-irradiation sample, a significant irradiation-time-dependent labeling was observed (Fig. 2A, lanes 2-4, 6-8). Furthermore, competitive photoaffinity labeling study on probe **4** was examined in the absence or presence of NPI-2358, colchicines or D-biotin. A dose-dependent inhibition was observed in the presence of NPI-2358 (Fig. 2B, lanes 1-4) and colchicine (Fig. 2B, lanes 5-8), whereas no competitive inhibition was observed when D-biotin was used as a negative control (data not shown). These results seem to be reasonable, because, although the three-dimensional structures of anti-microtubule diketopiperazines are different from that of colchicine, the original PLH is known to recognize the colchicine binding site by radio-binding assay.[6] Therefore, these results also indicate that NPI-2358 and its derivatives can recognize the same binding site on tubulin as probe **4**, suggesting that probe **4** functions as a useful chemical probe for the anti-cancer drug candidate. These findings would form a basis for further studies on the precise binding site of NPI-2358 and its microtubule depolymerization mechanism.[7]

Acknowledgments

This research was supported by various grants from MEXT (Ministry of Education, Culture, Sports, Science and Technology), Japan, including the 21st Century COE Program of Kyoto Pharmaceutical University.

References

1. Kanoh K, Kohno S, Katada J, Hayashi Y, Muramatsu M, Uno I. *Biosci. Biotechnol. Biochem* **63**: 1130-1133, 1999.
2. Kanoh K, Kohno S, Katada J, Takahashi J, Uno I, Hayashi Y. *Bioorg Med Chem* **7**: 1451-1457, 1999.
3. Hayashi Y, Orikasa S, Tanaka K, Kanoh K, Kiso Y. *J Org Chem*, **65**, 8402-8405, 2000.
4. Nicholson B, Lloyd GK, Miller BR, Palladino MA, Kiso Y, Hayashi Y, Neuteboom ST. *Anti-Cancer Drugs* **17**: 25-31, 2006.
5. Hofmann K, Kiso Y. *Proc Natl Acad Sci U S A* **73**: 3516-3518, 1976.
6. Kanoh K, Kohno S, Katada J, Takahashi J, Uno I. *J Antibiot* (*Tokyo*) **52**: 134-141, 1999.
7. Yamazaki Y, Kohno K, Yasui H, Kiso Y, Akamatsu M, Nicholson B, Deyanat-Yazdi G, Neuteboom S, Potts B, Lloyd GK, Hayashi Y. *ChemBioChem* **9**: 3074-3081.

4-07-112

New, all non-aromatic vasopressin V1a receptor agonists

Wisniewski, Kazimierz; Galyean, Robert; Schteingart, Claudio; Taki, Hiroe; Alagarsamy, Sudar; Croston, Glenn; Heitzmann, Joshua; Kohan, Arash; Wisniewska, Halina; Laporte, Regent; Riviere, Pierre*

Ferring Research Institute, Inc., UNITED STATES

**E-mail: Kazimierz.Wisniewski@ferring.com*

Introduction

The neurohypophyseal hormone 8-arginine-vasopressin (AVP) is the endogenous ligand for the V1a and the two other subtypes of the vasopressin receptor (V1bR and V2R), and also acts on the oxytocin receptor (OTR). AVP produces arterial vasoconstriction by activation of the V1a receptor subtype (V1aR) located in vascular smooth muscle. This vasopressor effect can be potentially used to treat vasodilatory hypotension in critical care and other conditions.[1] The lack of selectivity of AVP could possibly hamper its use as a vasoconstrictive agent due to unwanted side effects such as V2 receptor mediated antidiuresis and release of coagulation factors. We have recently reported potent and V1a receptor selective analogues of AVP of general structure [Xaa^2,Ile^3,Yaa^4,Zaa^8]VP, where Xaa was an aromatic amino acid residue.[2] In this paper we focus on a series of analogues where Xaa was selected from a collection of cyclic and acyclic non-aromatic amino acids. Although AVP analogues with cyclic aliphatic residues in position 2 have been previously reported,[3] and a few all non-aromatic naturally occurring vasopressin/conopressin analogues were described in the literature,[4] our new analogs appear to be the first examples of all non-aromatic and in some cases fairly potent and selective V1a receptor agonists.

Results and discussion

The first AVP analogs showing improved V1a receptor (V1aR) selectivity in a rat *in vivo* model were reported by Huguenin in the early sixties.[5] The best compound described in that study, [Phe^2,Ile^3,Orn^8]VP, **2**, was retested in our *in vitro* RGA assays at the V1a and related receptors and its improved V1aR selectivity as compared to AVP, **1**, was confirmed. Based on the Huguenin report[5] and our preceding study[2] it was evident that the amino acid residue in position 2 is of key importance for attaining enhanced V1a receptor selectivity. In this study we replaced the aromatic residues in position 2 with some cyclic or acyclic aliphatic ones to examine whether the presence of an aromatic ring in the side chain of position 2 is required for V1aR agonism, or perhaps, generally hydrophobic residues there would be sufficient to preserve biological activity. The analogs were prepared with different side chain lengths in positions 4 and/or 8. The Ala^2 analogue ([Ala^2,Ile^3,Dab^8]VP, **6**) was totally inactive (no significant V1aR agonism *in vitro* up to 1000 nM) as reported previously for [Ala^2]AVP.[6] However, the peptides with bulkier acyclic side chains **7** (R_1 = isobutyl, EC50 = 12.6 nM) and **8** (R_1 = neopentyl, EC50 = 10.7 nM) were found to be reasonably potent as hV1aR agonists. Compounds **9-17** with cyclic aliphatic residues were found to be generally more potent as V1aR agonists than the ones containing acyclic residues. The Cha^2 analogs **15-17** were as potent and selective at the hV1R as their Phe^2 counterparts **3** and **4**. The modifications with 1-aminocyclobutyl-1-carboxylic acid (compounds **9-11**) or cyclopentylalanine (**12-14**) resulted in potent hV1aR agonists only when combined with the Gln^4 and Dab^8 residues (**9** and **12**, respectively). Analogs **6-17** were generally less potent at the rat V1a receptor with a notable exception of compounds **12** (R_1 = cyclopentylmethyl, EC50 = 4.17 nM) and **15** (R_1 = cyclohexylmethyl, EC50 = 2.07 nM) . Following the *in vitro* evaluation, analogues **12**, **15** and **16** and reference compounds **1** (AVP), **2**, **4** and **5** were tested *in vivo* in a rat pressor model. All compounds were found to be effective in raising arterial blood pressure and all non-aromatic analogs **12**, **15** and **16** appeared to be longer acting *in vivo* when compared to **1** and related compounds **2**, **4** and **5**, as demonstrated by slower disappearance of their pressor effect at equieffective doses.

Conclusion

We report here the results of biological evaluation of a new class of all-non aromatic AVP analogs. Some of the compounds display a favorable pharmacological profile as potent and selective V1a receptor agonists and they are efficacious *in vivo* in a rat pressor model. We conclude from this study that the presence of an aromatic amino acid residue in position 2 and 3 is not essential to preserve V1aR agonist activity in these analogs.

Table. Structure and biological activity of compounds synthesized in this study.

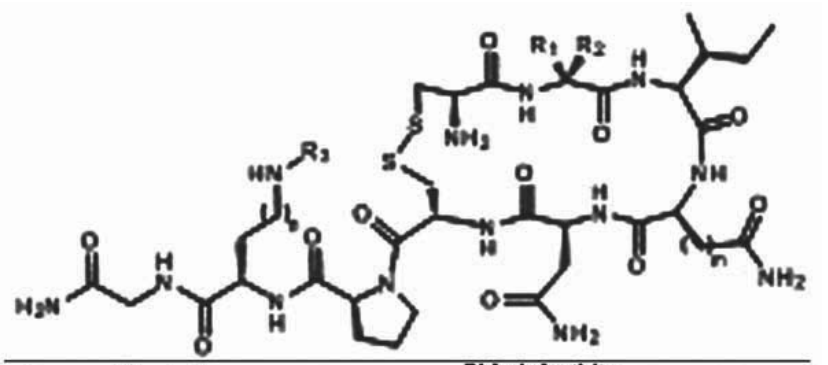

Analog	Structure[a]				Biological activity						In vivo duration relative to 1
					EC50 at receptor [nM]				Selectivity[b]		
	R_1	R_2	m	n	hV1a	hV2	rV1a	rV2	hV2	rV2	
1	AVP				0.23	0.05	0.07	0.03	0.2	0.4	1.0
2	Bzl	H	2	3	0.27	226	0.12	10.0	830	83	2.1
3	Bzl	H	2	2	0.50	66.4	0.14	2.28	130	16	
4	Bzl	H	1	2	2.89	>10000[c]	1.95	70.3	>3400	36	1.3
5	Bzl	H	1	3	1.45	>100[d]	8.20	48.2	>68	5	1.6
6	$-CH_3$	H	2	2	>1000[e]	>100[d]	>1000[e]	>100[d]	N/A	N/A	
7	iBu	H	2	2	12.6	>100[d]	35.8	88.5	>7	2	
8	tAm	H	2	2	10.7	>100[d]	34.2	14.9	>9	0.4	
9	$-(CH_2)_3-$		2	2	0.94	>100[d]	28.5	41.7	>106	1	
10	$-(CH_2)_3-$		1	3	7.92	>100[d]	65.1	>100[d]	>12	>1	
11	$-(CH_2)_3-$		1	2	12.3	>100[d]	22.3	>100[d]	>8	>4	
12	cPeMe	H	2	2	0.80	>100[d]	4.17	16.7	>125	4	2.2
13	cPeMe	H	1	3	7.70	>100[d]	61.5	>100[d]	>12	>1	
14	cPeMe	H	1	2	10.5	>100[d]	140	>100[d]	>9	>0.7	
15	cHxMe	H	2	2	0.23	>100[d]	2.07	11.4	>430	5	2.6
16	cHxMe	H	1	3	1.42	>100[d]	57.1	>100[d]	>70	>1	2.7
17	cHxMe	H	1	2	1.58	>100[d]	94.2	>100[d]	>63	>1	

[a]R_3 for compound **14** is iPr and for all other analogs is H. [b]Ratio EC50(receptor)/EC50(V1aR); [c]Highest concentration tested – 10000 nM; [d]Highest concentration tested – 100 nM; [e]Highest concentration tested – 1000 nM

References

1. Landry DW, Levin HR, Gallant EM, Ashton RC Jr, Seo S, D'Alessandro D, Oz MC, Oliver JA. Vasopressin deficiency contributes to the vasodilation of septic shock. *Circulation* **95**: 1122-1125, 1997.
2. Wisniewski K, Galyean R, Taki H, Alagarsamy S, Croston G, Laporte R, Schteingart CD, Rivière PJ-M. Synthesis and *in vitro* pharmacological profile of potent and selective peptidic V1a receptor agonists. *20th American Peptide Symposium,* Monteral, Canada 2007, Poster P209.
3. Jastrzebska B, Derdowska I, Kowalczyk W, Machova A, Slaninova J, Lammek B. Influence of 1-aminocyclohexane-1-carboxylic acid in position 2 or 3 of AVP and its analogues on their pharmacological properties. *J Pept Res* **62**: 70-77, 2003.
4. Kruszynski M, Manning M, Wo NC and Sawyer W H. Invertebrate neuropeptides resembling vasotocin and some analogs: synthesis and pharmacological properties. *Experientia* **46**: 771-773, 1990.
5. Huguenin RL. Synthesis of Phe2-Orn8-vasopressin and of Phe2-Orn8-oxytocin, two analogs of vasopressin with selective pressor activity. *Helv Chim Acta* **47**: 1934-1941, 1964.
6. Konieczna E, Czaja M, Kasprzykowska R, Kozlowski A, Dzieciol K, Trzeciak HI, Lammek, B. Synthesis and biological activity of arginine-vasopressin analogs modified with L-alanine or L-proline. *Pol J Chem* **68**: 1535-1543, 1994.

4-11-113

The Impact of Lithium Cations on the Peptide Bond

Kunz, Claudia[1,]; Berger, Stefan[2]; Fischer, Günter[3]; Hofmann, Hans-Jörg[1]*

[1]Leipzig University, Institute of Biochemistry GERMANY; [2]Leipzig University, Institute of Analytical Chemistry, GERMANY; [3]Max Planck Research Unit for Enzymology of Protein Folding, GERMANY

[*]E-mail: ckunz@uni-leipzig.de

Introduction

A wide variety of cations are known to be crucial for biological processes. In contrast, on the role of the lithium cation is by far less known. Nevertheless, there is evidence for Li^+ to be involved in signal transduction processes like the IP-3 pathway. Moreover, the application of lithium salts for treatment of neuronal dysfunctions in the case of bipolar disorder proves a physiological influence. The underlying mechanisms to explain these effects are not described up to know. Recently it has been shown that lithium cations influence the isomerisation state of peptide bonds, which is essentially pronounced in the case of the amino acid proline.[1,2] Thus, we can expect that folding and structuring of peptides and proteins and, therefore, their biological function could essentially be influenced by this ion.

To clarify the role of lithium cations at the molecular level, various NMR spectroscopic protocols were established as the basis for extensive investigations of the Li^+ effect on the model peptide Suc-Ala-Ala-Pro-Phe-pNA **1** (Fig. 1) with respect to the *cis*/*trans* populations and possible structuring effects in the hydrophobic solvent trifluoroethanol.

Results and discussion

The initial and, therefore, common step of all NMR spectroscopic approaches was a signal assignment of both isomers employing several 2D methods like COSY, NOESY, and HSQC. The isomer ratios were determined by integration of the corresponding signals. The first studies concentrated on a systematic look at the effect by a stepwise increase of the concentration of LiCl. The measurements show an excessive boost of the *cis* peptide content from about 10% to 65% when LiCl is added up to a concentration of 460 mM (Fig. 2a). Further investigations revealed a strong dependence of this effect on traces of moisture. Amounts of water higher than 4% decrease the *cis* population to its value for pure TFE (Fig. 2b).

Following these observations, NH temperature coefficients were determined which allow insight into hydrogen bond formation. Thus, this method opens up the possibility to monitor structuring events. For this purpose, we observed the NH resonances of all amide bonds (Fig. 1) over a temperature range of 50 K in 1 K steps referenced to TMS.

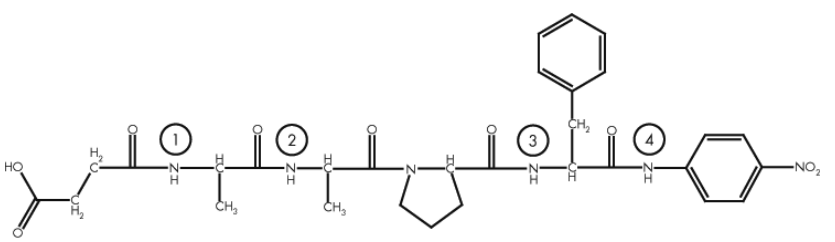

Figure 1. Formula of peptide **1** with the numbering scheme of the amide protons used in Table 1.

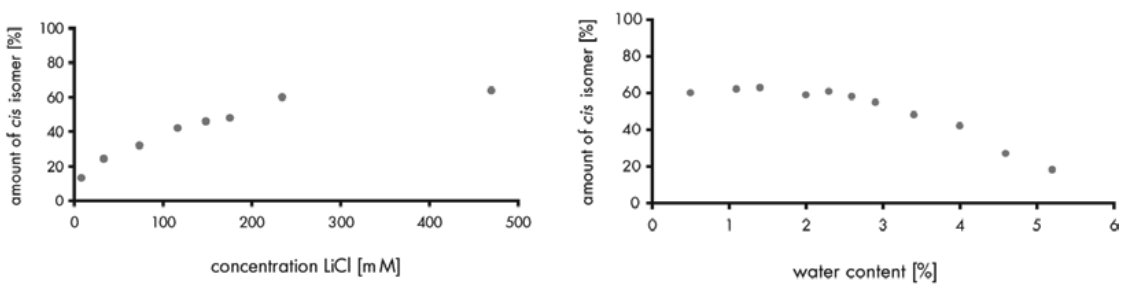

Figure 2. a) Percentage of the *cis* isomer of **1** as a function of the LiCl concentration in TFE. b) Percentage of the *cis* isomer of **1** as a function of the amount of water in a 300 mM LiCl/TFE solution.

Table 1. Temperature coefficients in ppb/K for **1** under different conditions

		1	2	3	4
TFE	*trans*	- 8.6	- 6.4	- 4.9	- 6.6
	cis [a]	–	–	–	–
TFE / LiCl	*trans*	- 6.3	- 3.1	– [a]	- 7.5
	cis	- 7.7	- 3.2	- 2.5	- 7.6

[a] Data not available due to insufficient sensitivity or signal overlapping.

Subsequent analysis of the chemical shift temperature gradients ($\Delta\sigma_{HN}/\Delta T$) of the amide protons (Table 1, see attachment) shows an influence of lithium cations on structuring as can be seen by the shift of the NH resonances of the central amino acids 2 and 3, which indicate them as partners in stable hydrogen bonds. This might be a starting point for a detailed structure analysis in further studies.

Acknowledgements

Support of this work by Deutsche Forschungsgemeinschaft (SFB 610 ”Proteinzustände mit zellbiologischer und medizinischer Relevanz”) is gratefully acknowledged.

References

1. Kessler H, Gehrke M, Lautz J, Köck M, Seebach D, Thaler A. *Biochem Pharmacol* **40**: 169-173, 1990.
2. Kofron J, Kuzmic P, Kishore V, Colon-Bonilla E, Rich D. *Biochemistry* **30**: 6127-6134, 1991.

4-14-114

Microwave Assisted Synthesis of Polyelectrolytic Bioconjugates of Hepatitis B Surface Antigenic Polypeptides and Their Immunological Properties

Mustafaeva, Zeynep[1,]; Ozdemir, Zafer Omer; Iscani, Basak; Karabulut, Erdem; B. Battal, Yasemin*
Chemical and Metallurgical Faculty, Yildiz Technical University, Bioengineering Dept., TURKEY

[*]E-mail: zmustafaeva@yahoo.com

Introduction

Hepatitis B Virus is one of the most common problem and potential danger of all over the world. It is known that the use of proteins and peptide antigens as vaccines has several potential advantages over whole viral or bacterial preparations. To elicit the maximum immunogenic response from synthetic peptide antigens, it is generally necessary to bind the peptide to a carrier protein. Moreover, to realize the full potential of synthetic peptide antigens protein-peptide conjugate will have to be used with an adjuvant. We have developed new approaches for obtaining highly immunogenic peptide conjugate. Synthetic polyelectrolytes were used for the conjugation with peptide molecules in which polyelectrolytes carry out the carrier and adjuvant roles simultaneously. This concept drive us to create new immunogenic bioconjugates of *Hepatitis B* surface antigenic polypeptides (HbsAg) with synthetic polyelectrolytes.[1,2]

Materials and Methods

All chemicals used in this study were obtained from commercial sources. Wang resins, amino acids and coupling reagents were purchased from NovaBiochem. The other chemicals were purchased from Sigma-Aldrich. Vinyl Prylidone-co-Acrylic acid copolymer (VP/AA 25:75, Mw= 80.000) was synthesized according to literature.[3] And used as a polyelectrolyte.

In this study we synthesized *Hepatitis B* Surface Antigenic peptide the region 95-109 of the s gene. The peptide was synthesized in our laboratory with Liberty Automated Microwave Synthesis Workstation (CEM), by using Solid Phase F-moc Chemistry. After synthesis it was cleaved with appropriate cocktail.

Polyelectrolyte-peptide conjugates were synthesized in different ratios by microwave assisted method in water media, using with 1-ethyl-3-(3-dimethylaminopropyl) carbodiimide [4] as an activator. Using microwave energy for this type reaction is a novel method.

Composition and structure of polyelectrolyte-peptide bioconjugates were characterized by GPC and Spectrofluorometry.

Immunization

The immunogenic properties of water-soluble polyelectrolyte-HbsAg peptide conjugates were investigated by intravenous injections on mice. The ELISA procedure was used to assay serum samples. It was obtained that a single immunization of mice with polyelectrolyte-peptide conjugates without classical

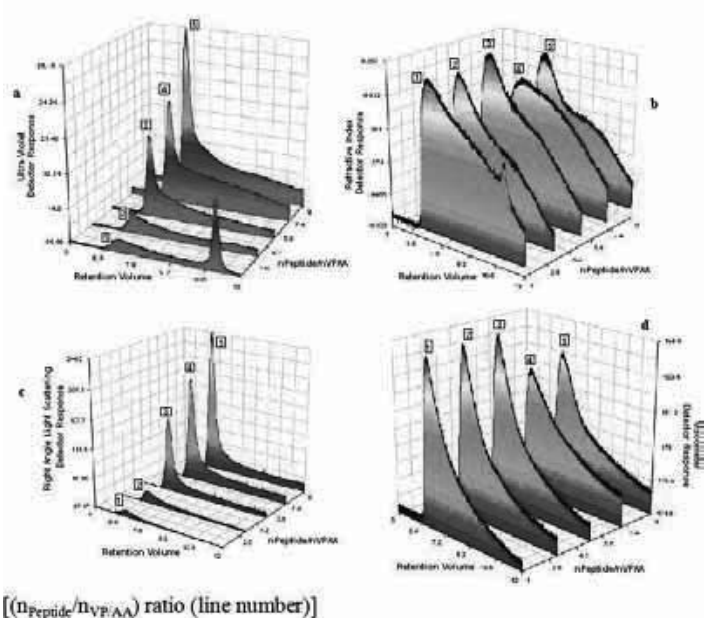

Figure 1. GPC results of the conjugates of VP/AA (25:75) copolymer with Hepatitis B Surface Antigen Peptide (region 95-109) in different molar ratios ($n_{peptide}/n_{VP/AA}$): a] 1 (1), 3 (2), 5 (3), 7 (4), 9 (5), at pH 7 with Ultra Violet detector, b] 1(4), 3 (2), 5 (1), 7 (5), 9 (3), at pH 7 with Refractive Index detector, c] 1(4), 3 (3), 5 (5), 7 (1), 9 (2), at pH 7 with Right Angle Light Scattering detector, d] 1(1), 3 (3), 5 (2), 7 (4), 9 (5), at pH 7 with Viscometer detector. [($n_{Peptide}/n_{VP/AA}$) ratio (line number)].

adjuvants increased the primary and secondary peptide specific immune response to HbsAg.

Acknowledgments

This research was supported by grant from Turkish Republic Prime Ministry State Planning Organization (25-DPT-07-04-01).

References

1. Mustafaev M. Functionally Biopolymer Systems", *Sigma Journal of Engineering and Natural Science* **4**: 1-201, 2004.
2. Mustafaev M, Mustafaeva Z, Ergen E, Uraki Y, Sano Y. *Journal of Bioactive and Compatible Polymers* **17**: 251-269, 2002.
3. Uelzmann H. *Journal of Polymer Science* **33**: 377-379, 1958.
4. Williams A, Ibrahim IT. *Chem Rev* **81**: 589-636, 1981.

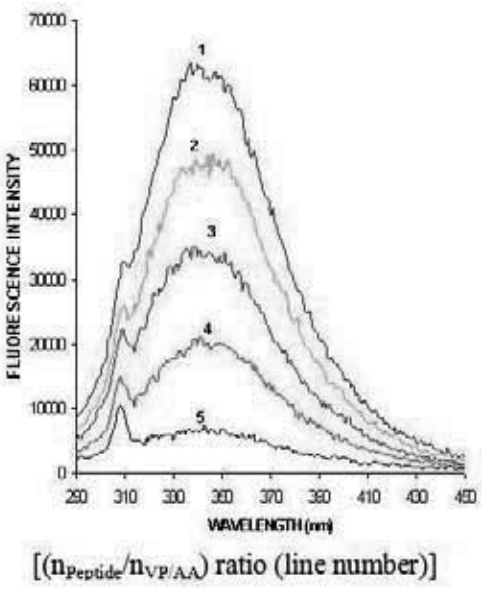

Figure 2. Fluorescence spectra of the conjugates of VP/AA copolymer with Hepatitis B Surface Antigen Peptide (95-109) in different initial ratios ($n_{Peptide}/n_{VP/AA}$): 1(5), 3 (4), 5 (3), 7 (2), 9 (1), at pH 7. Fluorescence intensity rise with the increasing peptide ratio. [($n_{Peptide}/n_{VP/AA}$) ratio (line number)].

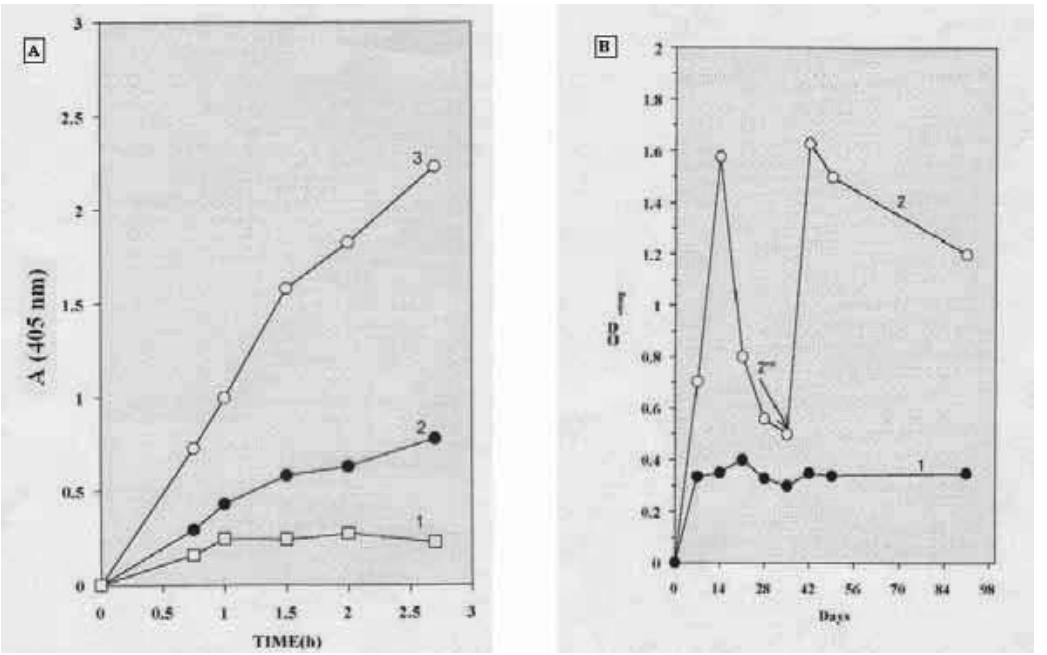

Figure 3. A. A single immunization of mice with polyelectrolye-peptide conjugates without classical adjuvants increased the primary and secondary peptide specific immune response to HbsAg. **B.** The dynamics of formation of antigen-antibody complexes in the blood sera of serum free medium (1) control, normal (2) and Hepatitis B carriers peaples (3). PE-HbsAg conjugates also were used for the detection of HbsAg-specific antibodies in the serum of normal and Hepatitis B virus carriers peaples blood. The enzyme immunoassay method was used for the detection of resulting antigen (PE-HbsAg) –antibody complexes in serum samples.The dynamics of formation of antigen-antibody complexes in the blood sera of serum free medium (1, control), normal (2) and Hepatitis B carriers peaples (3) are shown in Fig. 3B.

4-14-115

Synthesis and utilization of peptide adhesives for medical application

Rawer, Stephan; Schauer, Frieder[2]; Lindequist, Ulrike[3]; Wende, Kristian[3]; Jülich, Wolf-Dieter[3]*

[1]Applied Biosystems Deutschland GmbH, PSM support europe, GERMANY; [2]EMA University Greifswald, Institute for Microbiology, GERMANY; [3]EMA University Greifswald, Institute for Pharmacy, GERMANY

**E-mail: Stephan.rawer@eur.appliedbiosystems.com*

Introduction

Adhesives for medical applications have special requirements in physical and chemical properties, for instance with respect to biological resorption. Degradation characteristics are important for application in surgery. General requirements for the application are biocompatibility, functionality, and the avoidance of carcinogenic, mutagenic, toxic and allergic reactions. In nature mussel adhesive proteins (MAP) are known as adhesives. They are able to form permanent and strong but also flexible bonds with special amino acids like DOPA, tyrosine and lysine. The products are biodegradable and non toxic to the human body and do not exhibit immunogenicity.

Results and Discussion

Mimicking the MAPs, oligopeptides with the structure [Tyr-Lys]n are synthesized. A new adhesive technique based on the polymerisation of such peptides by the help of polyphenoloxidases is described in patent.[1] The peptides and the substrates of polyphenoloxidases as bridge molecules can be varied. We used 12 substrates with different physical and chemical properties. In earlier experiments, a composition of peptides with the structure $[Tyr\text{-}Lys]_n$; n = 4–25 was used as adhesive. To test the required length of the oligopeptide, we synthesized peptides with several defined lengths, $[Tyr\text{-}Lys]_{10}$ and $[Tyr\text{-}Lys]_{15}$, by solid phase peptide synthesis on a 433A peptide synthesizer with UV-monitoring (Applied Biosystems). The cleavage of the resin was done in 95% TFA; 2,5% TIS; 2,5% water for 2 h.

As a specific polyphenoloxidase laccase, produced by the fungus *Myceliophthora thermophila*, was used as to crosslink the peptides with the following substrates:

Aromatic 3,4-dihydroxy-derivatives:
(3,4-dihydroxybenzoic acid,
3,4-dihydroxyphenylacetic acid, hydrocaffeic acid)
2,5-dihydroxy-derivatives:
(2,5-dihydroxybenzoic acid,
2,5-dihydroxybenzoic acid-methylester,
2,5-dihydroxy-benzoic acid -ethylester,
2,5-dihydroxy-benzaldehyd,
2,5-dihydroxy-N-(2-hydroxyethyl)-benzamide)
Other substrates:
(5,8-dihydroxy-1,4-naphthochinone,
trans-ferulic acid, 4-hydroxycinnamic acid,
violuric acid,
2,2´-azino-bis (3-ethylbenzothiazolin-6-sulfonic acid).

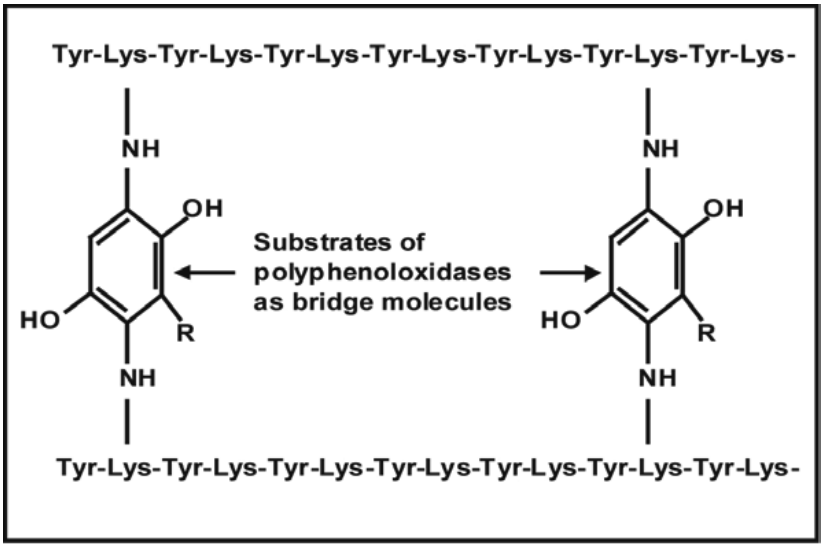

Figure 1. Chemical structure of cross-linking reaction.

Figure 2. a) *SaOS-2 cell* control after acridinorange treatment: Nuclei of cells (green), their nucleoli (light green) and acidic cell organelles (red) within the dark green coloured cytoplasma, 200 fold. **b)** SaOS-2 cells treated with adhesive (250 µg [Lys-Tyr]10, 25 µg DHBA and 1,5 µl laccase), 200-fold. **c** SaOS-2-cells near the adhesive, 50-fold.

Cytotoxicity of all substrates was determined using neutral red uptake assay according to NIH protocol (USA). Briefly, subconfluent human skin HaCaT cells were treated with different concentrations of phenoloxidase substrate in a 96 well plate for 48h. During this time, cells were kept in RPMI with 8% FCS, 37 °C in a humidified 5% CO2-athmosphere. After washing, cells were incubated for 3h with neutral red solution in RPMI. Neutral red was set free with ethanol/water, readout at 550nm and inhibition concentration (50%, IC50) was calculated. The substrates 2,5-dihydroxybenzoic acid, 3,4-dihydroxybenzoic acid and 2,2´-azino-bis(3-ethylbenzothiazolin-6-sulfonic acid did not show any cytotoxicity. In opposite 2,5-dihydroxy-benzaldehyde (DHBA), trans-ferulic acid and 5,8-dihydroxy-1,4-naphthochinone exhibit cytotoxic activity with IC50 values of 697 µM, 186 µM or 41 µM resp. For gathering information on adhesive and cell interaction, different mixtures of peptide, subtrate and laccase were placed in a 24 well plate overnight. Per well, 0,05 mio human bone SaOS-2 cells were seeded in IMDM medium with 10% FCS and kept for 48h at 37 °C in an atmosphere of 5% CO2. After that cells were stained with acridinorange (10 µM, 10 min) and observed by fluorescence microscopy. All resulting adhesives inclusing those with DHBA are not cytotoxic (Fig. 2).

Tests for adhesive properties of the products are in progress. Experiments with modified peptides containing the RGD-sequences to enhance cell adhesion are planned. Due to the broad substrate spectrum of laccase many other aromatics are possible coupling substrates for different amines. They should be tested for toxicity and impact to adhesiveness in the future.

References

1. Schauer F, Jülich W-D, Mikolasch A, Manda K, Lindequist U, Schomburg J, Schultz C, Protor P, Speitling A. Kleber für medizinische Anwendungen und Mittel zur Blutstillung. *PCT-Anmeldung PCT/EP 2007/001131*

4-15-116

Chimeric opioid-neurotensin ligands as new prospective analgesics in chronic pain

Kleczkowska, Patrycja[1]; Ruszczynska-Bartnik, Katarzyna[2]; Kaczorowska, Ewa[2]; Ejchart, Andrzej[2]; Kosson, Piotr[1]; Tourwé, Dirk[3]; Lipkowski, Andrzej W[1]

[1]Integrated Centre of Excellence of Medicinal Chemistry of Neuropeptides at Medical Research Centre, Polish Academy of Sciences, POLAND; [2]Institute of Biochemistry and Biophysics, Polish Academy of Sciences, POLAND; [3]Vrije Universiteit Brussels, Department of Chemistry,Brussels, BELGIUM

[*]E-mail: hazufiel@wp.pl

Introduction

Analgesics have an ability to reduce perception of pain impulses by the central nervous system. Opioid peptides are endogenous modulators of nociceptive signals. Opiate medicines interact with opioid receptors and enhance antinociceptive effects. However, chronic selective activation of the opioid pathway with μ-opioid agonists results in the development of dependence and addiction and induces side effects such as sedation, dysphoria, and constipation. Therefore, there has been proposed the idea to develop multitarget analgesics that could interact with opioid and complementary pathways involved in nociceptive signal transmissions.[1] The presented studies have been focused on development of opioid pharmacophores hybridized with neurotensin pharmacophores.

Materials and methods

In the present study we have synthesized several new opioid hybrids using C-terminal fragment of neurotensin (NT) that has been described to participate as a modulator of signal transmission.[2,4] The decapeptide Tyr-D-Lys-Phe-Phe-Lys-Lys-Pro-Phe-Ile-Leu-OH (AA2066) has been established as a primary hybrid peptide that expressed significant affinity to opioid as well as to neurotensin receptors.[1] To increase receptor affinities and enzymatic stability several analogues have been design and tested. From this set of compounds, two peptide analogues have been chosen for further structure-activity relationship studies which were PK-7 and PK-20. The sequences and binding data are shown below.

It is known that neurotensin itself exerts potent CNS effects like profound analgesia or can enhance pain responses, therefore for those two compounds the antinociceptive effect (tail-flick test) was measured using male Wistar rats. Moreover, preliminary NMR studies (using Varian Inova 400 MHz NMR Spectrometer, temp 25 °C, solution: 90%H_2O/10%D_2O) were performed to detect any structural differences between the two compounds.

Results and discussion

Both peptide analogues applied intrathecally produced analgesia at 0.1 μmol dose. However, the duration of action of those compounds are quite different, PK-20 expressed prolong, over 2 hours analgesic effect. Very likely, this effect is a result of peptide resistance to enzymatic degradation due to an implementation of Dmt and Tle residues.

Acknowledgements

This work has been partially supported by the European Grant Normolife (LSHC-CT-2006-037733).

References

1. Lipkowski AW, Misicka A, Hruby VJ, Carr DB. *Polish J Chem* **68**: 907-912, 1994.
2. Clineschmidt BV, McGuffin JC, Bunting PB. *Eur J Pharmacol* **54**: 129-139, 1979.
3. Coutant J, Curmi PA, Toma F, Monti JP. *Biochemistry* **46**: 5656-5663, 2007.
4. Dobner PR. *Peptides* **27**: 2405-2414, 2006.
5. Xu GY, Deber C. *Int J Peptide Protein Res* **37**: 528-535, 1991.

Table 1. Binding data of two new opioid-neurotensin hybrid peptides

Compound's sequence		IC_{50} (nM ± SEM)
		μ-opioid receptor
AA2066	H-Tyr-D-Lys-Phe-Phe-Lys-Lys-Pro-Phe-Ile-Leu-OH	1.2 ± 0.4
PK-7	H-Tyr-D-Lys-Phe-Phe-Lys-Lys-Pro-Phe-Ile-D-Asp-NH_2	162 ± 4,76
PK-20	H-Dmt-D-Lys-Phe-Phe-Lys-Lys-Pro-Phe-Tle-Leu-OH	9,7 ± 3,09

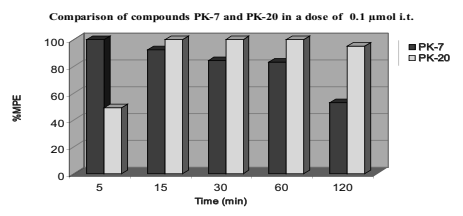

Figure 1. Antinociceptive effect of PK-7 and PK-20 opioid-neurotensin hybrid peptides. Several groups have shown NT as well as its different analogues to exist either as a "flexible random coil",[5] or to have a flexible central region with structured N- and C-termini.[3] In the case of our analogue PK-20 we could identify the existence of some structural proton contacts between several amino acids in the sequence.

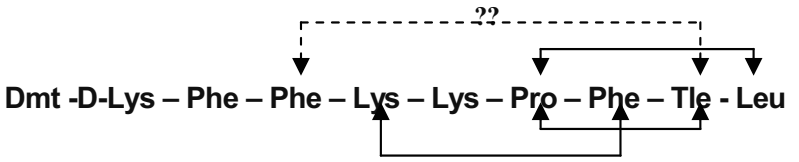

Figure 2. Possible short distance interaction within molecule PK-20, visible in D_2O. The obtained results rationalize further structure-activity relationship studies.

4-16-117

Multi-component fluorescence labeling method for efficient positional screening of peptide library

Kitamatsu, Mizuki; Kuroiwa, Hiroyuki; Sakata, Daisuke; Yamamoto, Takahiro; Inoue, Keisuke; Kishimoto, Yoshiko; Futami, Midori; Sisido, Masahiko*

Okayama University, BioScience and Biotechnology, JAPAN

E-mail: kitamatu@biotech.okayama-u.ac.jp

Peptide library is a general method for screening specific peptides that bind to a target protein. Generally, the method has to fix peptides on large carriers like phage, beads and so on.[1-3] So that these large carriers would affect the binding between peptides and the target protein, it will be difficult for the method to obtain accurate results concerning the binding. In this study, we develop a new precise method that does not need the carriers for screening peptides. The new method (multi-component fluorescent labeling method) uses peptides that connected multiple fluorescent dyes as peptide tag. The peptide that binds to a target protein is identified with specific fluorescence that emitted from the peptides.

To establish this method, we synthesized amino acids containing a fluorescent group in the side chain (fluorescent amino acids = FLAAs) at first. In this report, we could prepare for 36 FLAAs. In consideration of fluorescence intensity and the excitation / emission wavelength of the 36 FLAAs, we chose 15 FLAAs for the method.

With these 15 FLAAs, we synthesized peptides that connected an FLAA (FL-peptides) for screening by solid-phase peptide synthesis (SPPS) technique. A screening peptide moiety of the FL-peptides consists of 8 amino acids. The structure is Ac-EE-FLAA-EE-O(6)-XXXXXXXX-NH_2: where Ac is an acetyl group, E is Glu, O(6) is water-soluble linker that consists of ethylene glycol units, and X represents mixtures of 19 natural amino acids except Cys. We were able to incorporate FLAAs in the peptides by SPPS technique at reactivity from 30 to 100%.

The concentrations of each FL-peptide in a mixture of 15 FL-peptides can be provided by separating the two dimensions fluorescence (2-D FL) spectrum of the mixture by a least-squares method on the basis of the 2-D FL component spectra (2-D FL spectra for each FL-peptide). We measured the mixture containing FL-peptides of the known concentrations, and each concentration of FL-peptides in the mixture could be successfully identified.

In this study, we made choice of EGFR as a target protein. We were based on the multi-component fluorescent labeling method and searched for the peptide that bound to EGFR by combining a positional screening method with gel permeation chromatography. We examined whether there were not the FL-peptides that adsorbed to gel nonspecifically before screening for a sequence of peptide bound to EGFR. As a result, among 15 FL-peptides, it was indicated that 5 FL-pepitdes adsorbed to gel. Finally, we adopted 7 FLAAs for this experiment among 10 FLAAs in this report. The structures of 7 FLAAs are shown in Fig. 1.

We prepared the peptide sub-library that consisted of peptides containing 1 or 2 amino acids that corresponded to 7 FLAAs to decide the 6th position in sequences of the peptides. After the mixture of the library and EGFR was fractionated by gel filtration, we examined quantity of the FL-peptides in each fraction from the 2-D FL spectra. Quantity of the FL-peptides in each fraction was shown in Fig. 2. We also showed an amount of EGFR obtained from each fraction in Fig. 2. The result was shown that some FL-peptides were obtained from fraction 7 containing EGFR. Free FL-peptides were contained in later fractions. These results are suggested that FL-peptides bind to EGFR. In the Fl-peptides, Acd-peptide containing Ser/Thr bound to EGFR most strongly. And TMR-peptide containing Phe/Trp/Tyr bound to EGFR reversibly.

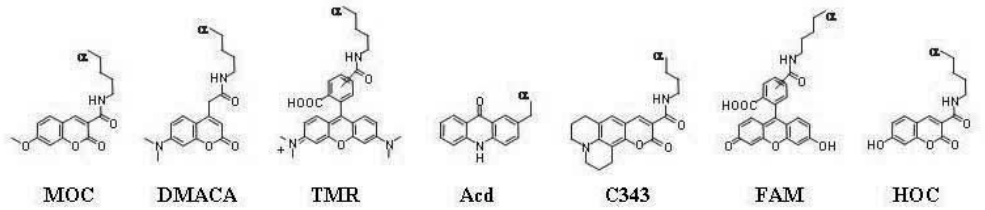

Figure 1. Chemical structures of FLAAs. Side chain structures of FLAAs are shown. These FLAAs are α-amino acids.

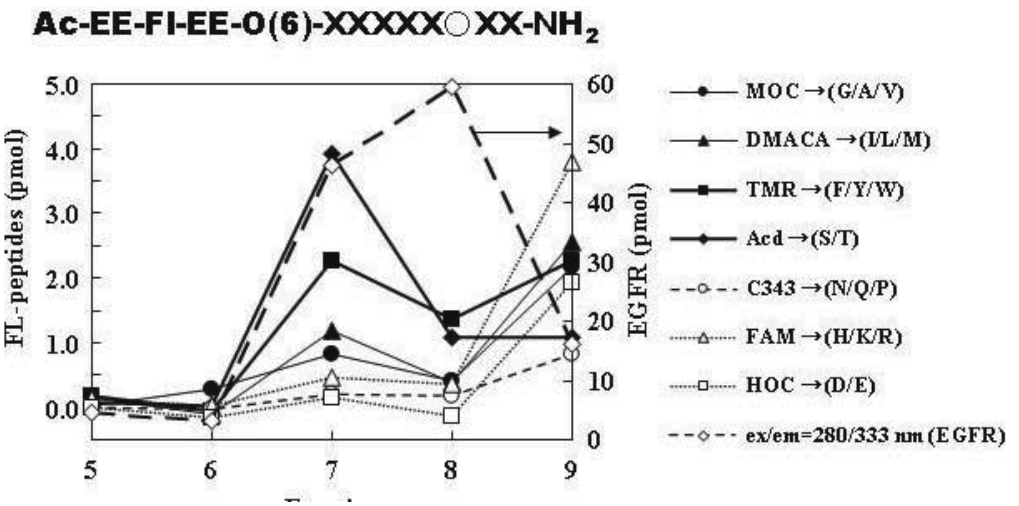

Figure 2. Prot of mole of FL-peptides and EGFR (estimated from fluorescence intensity for ex/em = 280/333 nm) against each fraction by gel filtration.

In this report, we established the new method to screen for a peptide that binds to EGFR. We will clarify complete sequences of 8-mer peptide that binds to EGFR specifically in future.

References

1. Mattheakis LC, Bhatt RR, Dower WJ. *Proc Natl Acad Sci U S A* **91**: 9022-9026, 1994.
2. Hanes J, Plückthun A. *Proc Natl Acad Sci U S A* **94**: 4939-4942, 1997.
3. Hanes J, Jermutus L, Plückthun A. *Methods Enzymol* **328**: 404-430, 2000.

4-17-118

Study of spillover tritium reaction with insulin

Vaskovsky, Boris[1]; Zolotarev, Yurii[2]; Shepel, Elena[1]; Ksenofontov, Alexander[3]; Murashev, Arkadi[1]; Dadayan, Alexander[2]; Semushina, Svetlana[1]; Pakhomova, Irina[1]; Kozik, Valerii[2]; Myasoedov, Nikolai[2]

[1]Shemyakin–Ovchinnikov Institute of Bioorganic chemistry RAS, RUSSIAN FEDERATION; [2]Institute of Molecular Genetics RAS, RUSSIAN FEDERATION; [3]AN Belozersky Institute of Physico-Chemical Biology, Moscow State University, RUSSIAN FEDERATION

[*]E-mail: taeek@ibch.ru

Introduction

Highly tritium-labeled compounds with retained physiological activity can be obtained by the high temperature solid phase catalytic isotope exchange (HSCIE) reaction occurring in solid organic compounds under the action of spillover hydrogen.[1,2] A virtually complete absence of racemization makes this reaction a valuable preparative method. A number of tritium-labeled peptides with completely retained biological activity were obtained using HSCIE.[3,4] The molar radioactivities of these peptides were many times higher than those of labeled preparations obtained by traditional methods, which is particularly important for studying the specific binding. Unlike the label in peptides obtained by traditional methods, the isotope label introduced in peptides using HSCIE is distributed throughout the entire peptide molecule, which allows the monitoring of all the products of peptide biodegradation.

Results and discussion

In the present investigation HSCIE reaction between insulin and spillover tritium was studied. HSCIE reaction with the solid mixture containing 1 mg recombinant human insulin was performed for 10 min at 120 °C using 5% Pd/$BaSO_4$ catalyst. The product of the reaction was purified by HPLC on m, 4 x 150 mm column (Fig. 1). Tritium labeled insulin withμ Kromasil C-18, 7 specific radioactivity 40 Ci/mmol and radiochemical purity of more than 97% was obtained. Performic acid oxidation of cysteine residues and subsequent acid hydrolysis were used to analyze the distribution of tritium. It was demonstrated that specific radioactivity of À and B chains amounted to 8.2 and 31.8 Ci/mmol respectively. All the amino acids contained tritium and its content in His residues of the B chain was equal to 45%. Experiments for the evaluation of the biological activity of tritium labeled insulin were performed on CD-1 6-8-week-

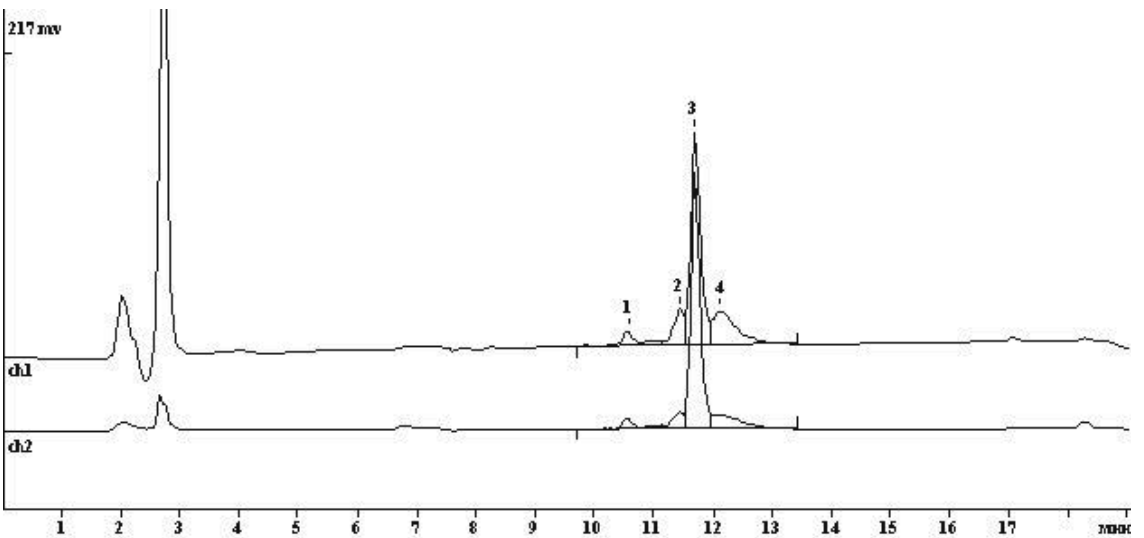

Figure 1. Chromatographic purification of m, 4 x 150 mm column, μ[^{3}H]insulin^3 from reaction mixture. Kromasil C-18, 7 gradient elution with 20-70% acetonitrile in 0.1% TFA, 1 ml/min. Detection at 220 nm /1.0 A (Ch1) and 254 nm /0.1 A (Ch2).

old awake male mice. Activity of labeled insulin was compared with the activity of standard insulin. Insulin was injected subcutaneously at a dose of 0.8 U/kg. Twofold statistically significant lowering of glucose level was observed 40 min after injection (4.9 + 0.4 and 4.3 + 0.3 mmol/l for standard and tritium labeled insulin, respectively). Lowering of the glucose level in animals obtaining labeled insulin was the same, as in animals obtaining standard insulin. Thus, HSCIE reaction of insulin with tritium doesn't change its hypoglycemic activity.

References

1. Zolotarev Yu, Dadayan A, Borisov Yu. *Rus J Bioorg Chem* **31**: 1-17, 2005.
2. Zolotarev Yu, Dadayan A, Bocharov E, Borisov Yu, Vaskovsky B, Dorokhova E, Myasoedov N. *Amino Acids* **24**: 325- 333, 2003.
3. Zolotarev Yu, Dadayan A, Borisov Yu, Dorokhova E, Kozik V, Vtyurin N, Bocharov E, Ziganshin R, Lunina N, Kostrov S, Ovchinnikova T, Myasoedov N. *Bioorg Chem* **31**: 453-463, 2003.
4. Zolotarev Yu, Dadayan A, Kozik V, Ziganshin R, Vaskovsky B, Myasoedov N. *J of Lab Comp and Radiopharm* **50**: 483-486, 2007.

4-19-119

BioShuttle for Temozolomide Transport into Prostate Cancer Cells

Pipkorn, Rüdiger[1,]; Waldeck, Waldemar[2]; Didinger, Bernd[3]; Wießler, Manfred[4]; Braun, Klaus[4]*

[1]German Cancer Research Center, Peptide Synthesis Unit, INF 580, 69120 Heidelberg, GERMANY;

[2]German Cancer Research Center, Dept. Biophysics of Macromolecules, INF 580, D-69120 Heidelberg, GERMANY; [3]University of Heidelberg, Radiation Oncology, INF 110, D-69120 Heidelberg, GERMANY

[4]GermanCancer Research Center, Dept. Molecular Toxicology, INF 280, D-69120 Heidelberg, GERMANY

[*]E-mail: r.pipkorn@dkfz.de

Abstract

Temozolomide (TMZ) an orally applicable chemotherapeutic substance was inefficient in the treatment of symptomatic progressive hormone-refractory prostate cancer (HRPC). This may have different reasons like the short plasma half-life of TMZ, a non adapted application schema and as a result, an insufficient bioavailability. Therefore we built a TMZ-BioShuttle consisting of a transmembrane transporter molecule connected via a disulfide-bridge with a nuclear localization sequence which in turn is attached by a diaryltetratrazine spacer with TMZ. This resulted in a much higher pharmacological effect in the targeted nuclei of DU-145 cells even under reduced doses. The reformulation of TMZ to TMZ-BioShuttle achieved higher cell toxicity while the application dose was simultaneously reduced to 50 µM. The potential of the established TMZ for the treatment of prostate tumors was dramatically enhanced.

Introduction

During the previous decades, established drugs have been redesigned particularly their physicochemical properties. The goal was to optimize the pharmacologic properties and concomitantly minimizing undesired adverse reaction, which hamper the therapeutic outcome. In therapy of glioblastoma multiforme (GBM), the anti cancer drug temozolomide (TMZ) is commonly used. Encouraging data[1] gave reason for expanding the intervention to delicate tumor entities like prostate cancer with TMZ. TMZ spontaneously decomposed at physiological pH to the active compound diazomethane.[2,3] Inauspicious properties of TMZ can result in adverse reactions. Therefore TMZ proves to be a dedicated candidate for re-formulation. After the transport into the cytoplasm across the cellular membrane, the TMZ-NLS peptides conjugate discharges it's TMZ-NLS-Cys-cargo so that a sufficient concentration of pharmacologically active molecules can reach their target site inside the nucleus. We improved the

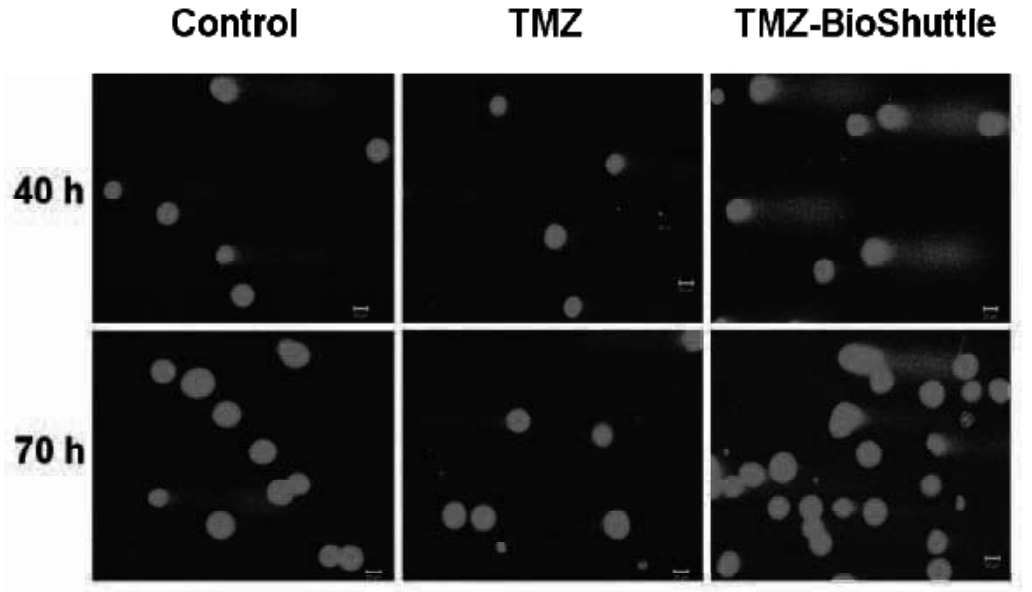

Figure 1. The comet formation of DU-145 prostate cancer cells by treatment with TMZ and TMZ-BioShuttle (final concentration 50 µM) after 40 hours (upper line) and 70 hours (lower line) respectively. The left column exhibits the untreated control cells. The scale bars (white) represent 20 µm.

TMZ transport into the cell nucleus by suitable ligation modes of TMZ with a nuclear address peptide module which in turn is connected to carrier molecules[5] called it TMZ-BioShuttle. The ligation of TMZ to the BioShuttle carrier was carried out by cycloaddition reactions.[4] During biological tests we showed an increased efficiency in the human prostate cancer cell line DU-145.

Materials and Methods

Cell culture and detailed syntheses procedures of the peptide-based BioShuttle modules, the ligation chemistry of the TMZ derivative and the subsequent coupling with the BioShuttle-transporter are described in (Drug Design, Delivery & Therapy, 2008).

Results

Comet formation in DU-145 prostate cancer cells induced by TMZ and TMZ-BioShuttle The metastatic human prostate adenocarcinoma cell line DU-145 (Fig. 1) was used to investigate the pharmacological effect of TMZ and TMZ-BioShuttle. We evaluated the DNA damage and the cell death in the DU-145 cell line after treatment with TMZ and with TMZ-BioShuttle (final concentration of 50 μM). We carried out comet assays in parallel probes (middle column and right column of the Fig. 1). The untreated cultures of DU-145 prostate cancer cells (left column) did not exhibit fragmented DNA.

Two days after treatment with TMZ (final concentration 50 μM), the DU-145 cells seem to be unfazed and no visual change in the phenotype could be observed under the light microscope. Counting the corresponding cell numbers offers, if anything, a hardly detectable decrease of the cell number (from 1.15 to 1.05 × 106 cells) compared to the untreated control with 1.12 × 106 cells. The comet assay study did not indicate a higher sensitivity and exhibited no fragmented DNA in the probes treated with 50 μM TMZ after 40 hours and 70 hours. This is in contrast to the probes treated with TMZ-BioShuttle, exhibiting comets and almost swollen nuclei 40 hours after treatment. 70 hours after TMZ-BioShuttle treatment the probes displayed a deviant behaviour. The cells offer less DNA fragmentation but their nuclei are partly shrunken and disintegrated by damage of chromatin.

Discussion

As definitive treatments of prostate cancer, the leading cause of morbidity and mortality in man, remain surgery and radiation therapy, and hormonal therapy in case of metastatic progress. However the timing of treatment in all stages of this disease remains controversial and new therapies are needed.[6,7] The derivatization of TMZ for coupling to transporter molecules which facilitate the passage across the cell membranes and the use of subcellular address molecules like NLS holds tremendous potential to optimize treatment of genetic diseases. With enhanced cellular delivery of active substances like TMZ into the cell nuclei, as site of pharmacological action, we can expect lower application doses with concomitantly decreased side-effects. The criteria to determine the applicability for targeting including accessibility, specificity, safety and subcellular precision are documented.[8,9] New ways for the synthesis are needed, namely the established solid phase peptide synthesis (SPPS) for synthesis of functional peptides. Reaction-conditions which hampered the chemical reactions for a chemical ligation of peptides in aqueous solution at room temperature could be circumvented using the Diels Alder Reaction (DAR). The BioShuttle delivery and targeting platform, facilitating the transport of DNA derivatives into living cells[5,10] and of diagnostics into the cytoplasm and nuclei of tumor tissues, was documented.[11]

References

1. Mutter N, Stupp R. *Expert Rev Anticancer Ther* **6**: 1187-1204, 2006.
2. Marchesi F, Turriziani M, Tortorelli G, Avvisati G, Torino F, De Vecchis L. *Pharmacol Res* **56**: 275-287, 2007.
3. Danson SJ, Middleton MR. *Expert Rev Anticancer Ther* **1**: 13-19, 2001.
4. Kim EY, Gronewold C, Chatterjee A, von der Lieth C-W, Kliem C, Schmauser B, Wiessler M, Frei E. *ChemBioChem* **6**: 422-431, 2005.
5. Braun K, Peschke P, Pipkorn R, Lampel S, Wachsmuth M, Waldeck W, Friedrich E, Debus J. *J Mol Biol* **318**: 237-243, 2002.
6. Chay C, Smith DC. *Semin Oncol* **28**: 3-12, 2001.
7. Hegeman RB, Liu G, Wilding G, McNeel DG. *Clin Prostate Cancer* **3**: 150-156, 2004.
8. Muzykantov VR. *Expert Opin Drug Deliv* **2**: 909-926, 2005.
9. Braun K, Pipkorn R, Waldeck W. *Curr Med Chem* **12**: 1841-1858, 2005.
10. Braun K, von Brasch L, Pipkorn R, Ehemann V, Jenne J, Spring H, Debus J, Didinger B, Rittgen W, Waldeck W. *Int J Med Sci* **4**: 267-277, 2007.
11. Heckl S, Debus J, Jenne J, Pipkorn R, Waldeck W, Spring H, Rastert R, von der Lieth CW, Braun K. *Cancer Res* **62**: 7018-7024, 2002.

4-19-120

Analogues of the kinin B1 receptor antagonist R-954 bearing *N*-terminal lipid moieties

Neugebauer, Witold; Savard, Martin; Elkara, Sonia; Sirois, Pierre; Gobeil, Fernand Jr*

Universite de Sherbrooke / Faculty of Medecine, Pharmacology Department, CANADA

**E-mail: witold.neugebauer@usherbrooke.ca*

We previously reported the identification of a potent peptide antagonist of the kinin B1 receptor (B1R), the R-954 (Ac-Orn-Arg-Oic-Pro-Gly-(α-Me)Phe-Ser-D-β-Nal-Ile-OH),[1] which holds therapeutic potential as a topical analgesic drug.[2] In an effort to further improve stability and pharmacokinetic (absorption) properties of R-954 while retaining its high antagonistic potency, the latter peptide was extended by a lipid moiety at its N-terminal region. *N*-acylating lipidic moieties comprising either, a ω-amino fatty acids (C-6, C-8, and C-11) or cholic acid (Fig. 1) were coupled on the resin during the solid phase synthesis of the antagonist sequence. Antagonist potencies (IC_{50}) of R-954 analogues were determined by classical *in vitro* rabbit B1R bioassay using the isolated rabbit aorta and compared to the parent peptide R-954. All synthetic analogues were FITC-labelled at their *N*-terminal to examine whether R-954 and its lipopeptide congeners can pass into live HEK-293T cells by confocal microscopy and by fluorescence-activated cell sorting (FACS) technique.

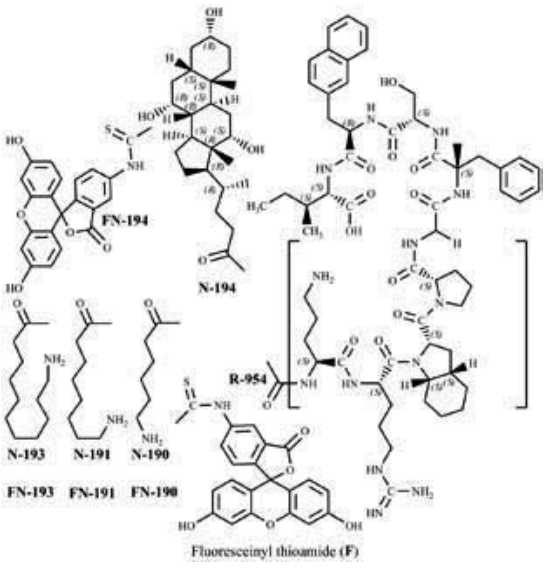

Figure 1. Structures of lipidic derivatives of R-954 and their fluorescein analogues.

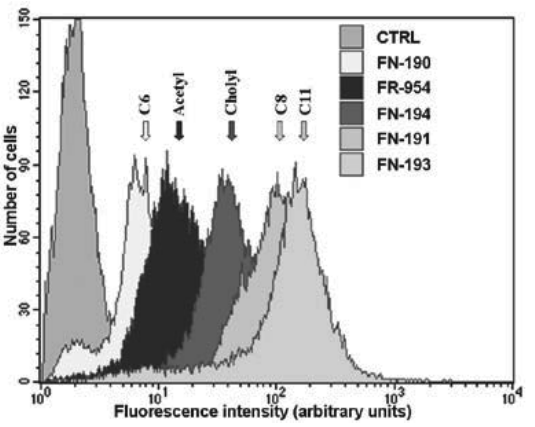

Figure 2. Flow cytometry analysis of B1R antagonist incorporation in HEK 293T.

Methods

Peptide synthesis: Peptides (Fig. 1) were synthesized using Fmoc chemistry on continuous flow system Pioneer Peptide Synthesizer starting with Fmoc-Ile-TentaGel resin (0.24 mmol/g) (Rapp Polymere). Step by step coupling of Fmoc amino acids were performed in amine free DMF using HATU/DIEA (1:1) as coupling agent. We used 3 fold excess of a coupling mixture over resin substitution. Fmoc deprotection was performed with 20% piperidine in DMF. FITC was coupled to the peptides on the resin from pyridine/DCM/DIEA solution over night. Final peptide cleavage and protective group's cleavage were performed with cleavage solution (TFA/water/TIPS=95%:2.5%:2.5%) stirring resin-peptide for 2h. Then acidic solution was filtered off the resin and dropped to diethyl ether. Peptides were precipitated in ether and were centrifuged then dissolved in water and lyophilized. The crude peptides were finally purified by C18 column chromatography in acetonitrile gradient in water with 0.1%TFA. Peptides identities were confirmed by MALDI mass spectrometry and their chromatographic purity verify by analytical HPLC.

Organ bath: Rabbit aortas from New Zealand rabbits were used. Tissue preparation and experimental protocol for vascular contractility bioassays were performed as described[3]. The apparent affinity of each antagonist was evaluated and expressed in terms of IC_{50} (the molar

concentration of an antagonist that makes it necessary to double the concentration of the agonist desArg^9-BK (DBK) needed to elicit the original submaximal response).

Flow cytometry analysis: HEK 293T cells were incubated for 1h at 37 °C with or without 10 μM of the indicated fluorescein-labelled B1R antagonists in serum-free medium. Following incubation, cells were successively washed in PBS, scraped, acid washed (2 min, 4 °C) in a pH 2.5 150 mM NaCl/ 50 mM CH_3COOH solution and washed again in PBS. Finally, cells were resuspended in PBS containing 15 μg/ml of propidium iodide (PI). Fluorescence analysis was performed with a FACScan activated cell sorter (BD BioSciences). PI positive cells were excluded from analysis. A minimum of 10,000 events by sample was processed.

Results and Discussion

Our results showed that the analogue N-190 comprising a 6-amino caproyl acyl component was slightly more potent (IC_{50}: 11 ± 1 nM) than R-954 (IC_{50}: 15 ± 1 nM) against desArg^9-BK-induced contraction; the peptide R-958 comprising no ω-amino group was significantly less active (IC_{50}: 36 ± 1 nM). All other chemical modifications were deleterious to R-954's activity (Table 1). In HEK-293T cells that do not express B1R, major cell incorporation was noticed for the lipopeptides N-191, N-193 and N-194 relative to R-954 as determined by FACS (Fig. 2). The confocal microscopic analysis revealed that a prominent intracellular staining of fluorescently labelled FN-194 and FN-191 more so than the unconjugated FR-954 (not shown). We concluded that *ω*-amino fatty acyls, in particular C8 and C11, as well as lipidic cholyl acyl can possibly be used as vectors for intracellular delivery of peptides into cells.

Acknowledgements

M. Savard is a recipient of a fellowship award from the Fonds de la recherche en sante du Quebec. This study was supported in part by grants from the Canadian Institute of Health Research.

References

1. Neugebauer W, Blais PA, Hallé S, Filteau C, Regoli D, Gobeil F Jr. Kinin B1 receptor antagonists with multi-enzymatic resistance properties. *Can J Physiol Pharmacol* **80**: 287-292, 2002.
2. Gabra BH, Sirois P. Beneficial effect of chronic treatment with the selective bradykinin B1 receptor antagonists, R-715 and R-954, in attenuating streptozotocin-diabetic thermal hyperalgesia in mice. *Peptides* **24**: 1131-1139, 2003.
3. Gobeil F Jr, Charland S, Filteau C, Perron SI, Neugebauer W, Regoli D. Kinin B1 receptor antagonists containing α-methyl-L-phenylalanine: In vitro and in vivo antagonistic activities. *Hypertension* **33**: 823-829, 1999.

Table1. Antagonistic activities of R-954 analogues assessed by the isolated organ bath technique

SEQUENCE		IC_{50} (nM)
AcOrn[Oic^2, (αMe)Phe^5, DβNal^7, Ile^8]DBK	(R-954)	15 ±1
Hexanoyl Orn[Oic^2, (αMe)Phe^5, DβNal^7, Ile^8]DBK	(R-958)	36±1
Ahx Orn[Oic^2, (αMe)Phe^5, DβNal^7, Ile^8]DBK	(N-190)	11±1
F-Ahx Orn[Oic^2, (αMe)Phe^5, DβNal^7, Ile^8]DBK	(FN-190)	3162
Aot Orn[Oic^2, (αMe)Phe^5, DβNal^7, Ile^8]DBK	(N-191)	32 ± 2
F-Aot Orn[Oic^2, (αMe)Phe^5, DβNal^7, Ile^8]DBK	(FN-191)	>1 000
Aud Orn[Oic^2, (αMe)Phe^5, DβNal^7, Ile^8]DBK	(N-193)	>1 000
F-Aud Orn[Oic^2, (αMe)Phe^5, DβNal^7, Ile^8]DBK	(FN-193)	>1 000
Cholyl-Orn[Oic^2, (αMe)Phe^5, DβNal^7, Ile^8]DBK	(N-194)	>1 000
F-Cholyl-Orn[Oic^2, (αMe)Phe^5, DβNal^7, Ile^8]DBK	(FN-194)	>1 000

Values are means ± S.E.M of 3-4 experiments. Ahx: 6-amino-hexanoyl; Aot: 8-amino-octanoyl; Aud:11-amino-undecanoyl; Nal: naphtyl-alanine.

4-19-121

Peptide conjugates of new *in silico* identified drug candidates and first/second line antituberculars - design, synthesis and antimycobacterial effect

Horváti, Kata[1,]; Mező, Gábor[1]; Szabó, Nóra[2,3]; Szabó Ildikó[1]; Grolmusz, Vince[3]; Hudecz, Ferenc[1]; Bősze, Szilvia[1]*

[1]Hungarian Academy of Sciences, Eötvös L. University, Research Group of Peptide Chemistry, HUNGARY; [2]Corden International Kft, Laboratory of Bacteriology, HUNGARY; [3]Department of Computer Science, Eötvös L. University, Protein Information Technology Group, HUNGARY

[*]E-mail: khorvati@gmail.com

Introduction

TB is responsible for more deaths throughout the world than any other infectious disease. It is estimated that more than one-third of the world's population is infected with *Mycobacterium tuberculosis* and over three million people die each year of TB, resulting in the World Health Organization declaring TB a global emergency.[1] Despite the existence of effective chemotherapy the increasing rate of multidrug-resistant TB has led to develop new drugs against the bacteria. High performance *in silico* screening docking method is a cost-effective computational approach to find new promising drug candidates. In the chemotherapy of such intracellular pathogens it is necessary to achieve relatively high levels of the drug in blood to attain therapeutically effective concentration in infected cells, which presumably has several serious side effects on healthy tissues. The elimination of *M. tuberculosis* from infected phagocytes could be more efficient with target cell directed delivery of antituberculars. A particularly promising approach is to conjugate a drug moiety to a peptide based carrier. The conjugates are chemically constructed to target release by hydrolysis (enzymatic and/or chemical) to liberate the active compound. The proposed targeted therapy would be based on cell surface receptors which are expressed mainly on machrophages (i.e. tuftsin receptor).[2,3]

Experimental procedures

New promising drug candidates were identified by a new molecular dynamic docking method using RS-PDB (highly structured and repaired version of PDB)[4] and Zinc (a free database of commercially-available compounds for virtual screening).[5] Antimycobacterial activity of compounds *in vitro* was characterized by the determination of the minimal inhibitory concentration (MIC) using *M. tuberculosis* H_{37}Rv and *M. kansasii* strain with 4-week exposure period in Sula semisynthetic media. The cytostatic effect of compounds was tested on human peripheral blood monomorphonuclear cells (PBMC) and HepG2 human hepatoma cell line by MTT assay. The synthesis of tuftsin receptor-specific peptide conjugates were prepared on MBHA resin using Fmoc/*t*Bu strategy. The first line antitubercular isoniazid (INH) was reacted with glyoxylic acid, the formed hydrazone bond was mildly reduced by $NaCNBH_3$ than coupled to the N-terminal of the peptide. The *p*-aminosalicylic acid (PAS) was conjugated through amide bond on solid phase with DIPC/HOBt coupling reagents. In the case of TB5, a hydroxyl group was esterificated with glutaric acid and than coupled to the peptide on solid phase. TB8 was conjugated through oxime bond.

Results

Sixteen new molecules effective on crucial enzymes of the pathogen and *in vitro* cultured *M. tuberculosis* were identified (Table 1).

Table 1. Minimal inhibitory concentration (MIC) of *in silico* identified molecules

docked ligand	MIC *M. tuberculosis* H_{37}Rv	
	γ (μg/mL)	(mol/L)
TB1	25	5.1×10^{-5}
TB2	5	1.2×10^{-5}
TB3	15	3.1×10^{-5}
TB4	30	6.3×10^{-5}
TB5	20	4.6×10^{-5}
TB6	45	9.4×10^{-5}
TB7	25	5.2×10^{-5}
TB8	**1**	**3.7×10^{-6}**
TB9	45	9.2×10^{-5}
TB10	45	1.1×10^{-4}
TB16	5	1.3×10^{-5}
TB21	40	8.9×10^{-5}
TB22	20	4.2×10^{-5}
TB23	20	4.2×10^{-5}
TB28	60	1.2×10^{-4}
TB29	10	2.1×10^{-5}

Table 2. Minimal inhibitory concentration (MIC) of tutsin peptide – drug conjugates

drug / conjugate	MIC *M. tuberculosis* $H_{37}Rv$	
	γ (μg/mL)	(mol/L)
INH	0.16	1.2×10^{-6}
INH-conjugate	2	1.2×10^{-6}
PAS	0.10	6.5×10^{-7}
PAS-conjugate	no effect	no effect
TB5	20	4.6×10^{-5}
TB5-conjugate	42	7.6×10^{-5}
TB8	1	3.7×10^{-6}
TB8-conjugate	40	3.0×10^{-5}

More than 50% of the tested *in silico* identified compounds were effective against the bacteria. TB8 molecule shows the lowest MIC value (MIC=1 γ; 3.7ó-10^{-6} M). The cytostatic effect of the compounds was tested at concentrations equal to and higher than the MIC value. In the case of TB8 the difference between the IC_{50} (on HepG2 cell line) and MIC value is more than 4 order of magnitude (IC_{50}= 1.2ó-10^{-2} M; MIC=3.7ó-10^{-6} M). Tuftsin derived peptide conjugates of TB5, TB8, INH and PAS molecules were synthesized on solid phase and carefully characterized by ESI-MS, analytical RP-HPLC and amino acid analysis. In the case of PAS the conjugate was not effective against *M. tuberculosis*, while the MIC value of INH-conjugate as well as the free drug exhibited the same value 1.2ó-10^{-6} M. The conjugation of TB5 and TB8 was also a successful approach to get effective compounds against *M. tuberculosis* (Table 2).

Acknowledgments

Supported by NKFP_07_1-TB_INTER-HU; Hungarian Research Fund (T68285, T68358, T49814); GVOP-3.2.1-2004-04-0005/3.0; GVOP-3.2.1-2004-04-0352/3.0.

References

1. *WHO fact sheet* No 104 - Tuberculosis.
2. Krieger M, Herz J. *Ann Rev Biochem* **63**: 601-637, 1994.
3. Taylor PR *et al*. *Ann Rev Immunol* **23**:901-944, 2005.
4. Szabadka Z, Grolmusz V. *Conf Proc IEEE Eng Med Biol Soc* **1**: 5755-5758, 2006.
5. Irwin JJ, Shoichet BK. *J Chem Inf Model* **45**: 177-182, 2005.

4-19-122

CPP or cholesterol conjugation to antisense PNA for cellular delivery

Joshi, Rajendra; Mishra, Ritu; Su, Wu; Engelmann, Joern*

Max-Planck Institute for Biological Cybernetics, High Field Magnetic Resonance Center, Tübingen, GERMANY

**E-mail: rajendra.joshi@tuebingen.mpg.de*

Introduction

Peptide nucleic acids (*Proc Nat Acad Sci USA*) are DNA mimics consisting of the four common bases as in DNA on a pseudopeptide backbone that makes them extremely stable in biological fluids. Antisense PNA can be targeted to mRNA in the cytoplasm in a complementary base pairing manner. In order to achieve efficient mRNA based targeting, endosomal release or direct uptake of *Proc Nat Acad Sci USA* into the cytosol is mandatory. However, relatively poor internalization of these agents is reported for most cells.[1] Several reports suggested cell penetrating peptide (CPP) based delivery systems for PNA delivery into cells.[2] Unfortunately, endosomal capture seems to be a major challenge in these approaches restricting the ability of PNA to bind with mRNA. Recent studies have explored the use of cholesterol-siRNA conjugates to enhance cellular import.[3] In order to attain efficient PNA internalization into cells, we synthesized two different sequences of cholesterol coupled antisense PNA and evaluated their uptake efficacy in comparison to a PNA-CPP conjugate previously reported by our group.[4]

Methods

The synthesis of PNA (anti-dsRed, specifically targeted to mRNA of red fluorescent protein dsRed) conjugated to CPP (D-Tat_{57-49} i.e. rrrqrrkkr) or cholesterol (Fig. 1) was performed in a fully automated synthesizer (peptides&elephants, Germany) using Fmoc continuous solid phase chemistry. All compounds were labeled with fluorescein isothiocyanate (FITC) to confirm the cellular uptake and were characterized by ESI-MS. Cellular uptake was estimated by fluorescence microscopy and spectroscopy in NIH-3T3 mouse fibroblasts plated in 96well plates. Briefly, cells were labelled with conjugates in complete, serum-containing medium for 18h. Afterwards, cell nuclei were counterstained with H33342, a DNA dye, and external fluorescence was quenched with trypan blue followed by repeated washes to ensure that only intracellular fluorescence was detected.

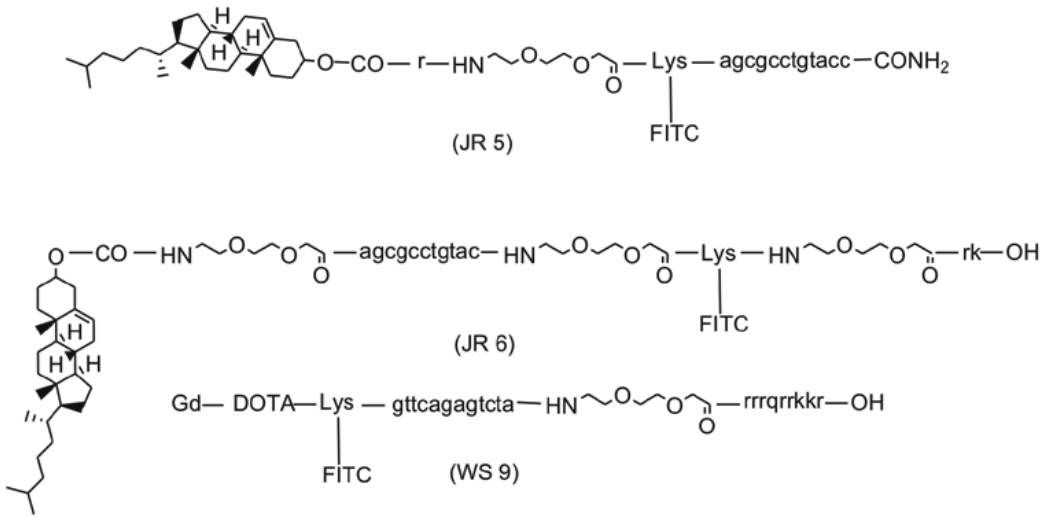

Figure 1. Schematic structure of PNA conjugated to cholesterol (Jr 5 & Jr 6) or CPP (WS 9). Antisense PNA sequence (a: adenine, c: cytosine, g: guanidine, t: thymine); CPP sequence (r: D-arginine, q: D-glutamine, k: D-lysine); Gd: gadolinium; DOTA: 1,4,7,10-tetraazacyclododecane-*N,N',N'',N'''*-tetraacetic acid; FITC: fluorescein isothiocyanate.

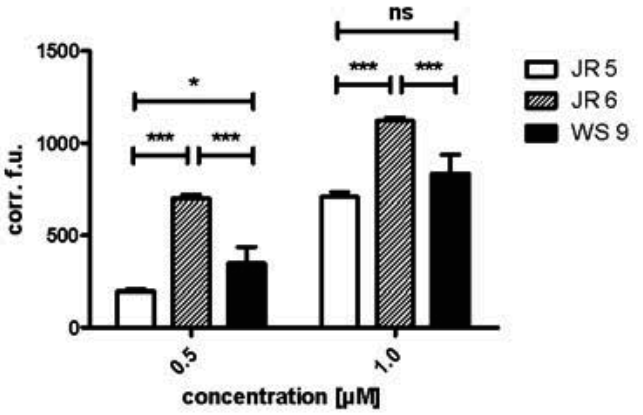

Figure 2. Comparison of cell internalization among Jr 5, Jr 6 and WS 9. ns, not significantly, *p<0.1,***p<0.001, significantly different (Tukey's Multiple Comparison Test).

Results and discussion

The synthesis of PNA, often laborious and lengthy, was made facile by developing and optimizing the Fmoc synthetic scheme for an automated peptide synthesizer. The advantage of this scheme was that all reactions were performed under mild conditions preventing the formation of side products, such as excess coupling on the phenol group of FITC.

Two different conjugates (Jr 5 and Jr 6) were synthesized altering the position of cholesterol, PNA and linkers in order to achieve better aqueous solubility as well as efficient internalization into cells. However, limitation in these syntheses was the removal of cholesterol during the cleavage of the product from the resin. This side reaction was dependent upon incubation time of resin in the cleavage cocktail and could be suppressed to a great extent by choosing the proper reaction time.

The results of fluorescence spectroscopy showed that cholesterol conjugates (Jr 5 & Jr 6) could enter efficiently into 3T3 cells in a concentration dependent manner from 0.5 µM to 2.5 µM (data not shown). However, at concentrations ≥ 2.0 µM, precipitation was observed after 18 h indicating a solubility problem of these conjugates under physiological conditions. Thus, further comparisons with CPP-PNA conjugates were made solely at 0.5 µM and 1 µM. Jr 6 was most efficiently internalized among all three (Fig. 2). This might be either governed by the molecular size or the interaction of cholesterol specifically with cell membrane may play a role in enhancing cellular uptake.

Fluorescence microscopy demonstrated that all the three conjugates were located in vesicles around the cell nucleus indicating a predominantly endosomal uptake mechanism (data not shown).

Conjugate Jr 6 was internalized most efficiently into cells indicating that by the conjugation of cholesterol not only the number of synthetic steps was decreased significantly but also a better internalization was achieved as compared to PNA-CPP. However, cholesterol-PNA conjugates were poorly soluble in aqueous solution at higher concentrations. Nevertheless, it can be expected from the above results that Jr 6 could be a promising delivery agent after further improvements like adding more linkers or residues which enhance solubility in water at physiological pH. In addition, Streptolysin-O, a bacterial protein able to reversibly permeabilize cell membranes, can be used to enhance direct cytosolic uptake into cells as reported elsewhere.[5]

Conclusion

Cholesterol-PNA conjugates need fewer synthetic steps, have a modest molecular size and better or comparable internalization properties as compared to PNA-CPP. However, its applicability on targeting mRNA is still restricted due to endosomal trapping of these conjugates. Nevertheless, the efficient uptake might make it a promising cellular delivery agent after further improvements.

References

1. Kilk K, *Langel Ü. Methods Mol Biol* **298**: 131-141, 2005.
2. Gait MJ. *Cell Mol Life Sci* **60**: 844-853, 2003.
3. Wolfrum C, Shi S, Jayaprakash KN, Jayaraman M, Wang G, Pandey RK, Rajeev KG, Nakayama T, Charrise K, Ndungo EM, Zimmermann T, Koteliansky V, Manoharan M, Stoffel M. *Nature Biotechnology* **25**: 1149-1157, 2007.
4. Su W, Mishra R, Pfeuffer J, Wiesmueller K-H, Ugurbil K, Engelmann J. *Contrast Media Mol Imaging* **2**: 42-49, 2007.
5. Barry EL, Gesek FA, Friedmann PA. *Biotechniques* **15**: 1016-1018, 1020, 1993.

4-20-123

The Evaluation of the Effect of Japanese Herbal (Kampo) Medicines using Bioavtive Peptides as Biomarkers.

Katagiri, Fumihiko; Sato, Yuhki; Itoh, Hiroki; Takeyama, Masaharu*

Oita University Hospital, Department of Clinical Pharmacy, JAPAN

**E-mail: fkata@med.oita-u.ac.jp*

In Western medical science, doctors usually treat patients according to disease diagnosis, while, in eastern medical science, treatment is based on diagnostics called gsho h, which is a unique concept in Japanese herbal (Kampo) medicines and quite different from diagnosis. Kampo medicines are prescribed according to patient constitution, appearance of diseases, position of the disease in the body, and progression of the diseases. Eastern medical science traditionally does not mention causes of diseases, therefore, Kampo medicines are not expected to cure diseases but to improve symptoms. In the West, from clinical trials, patients are grouped according to diseases, and the effectiveness of drugs is evaluated using statistical analysis. It is remarkable that drugs can cause various effects in individuals according to gene polymorphisms. The concept of gsho h is difficult for non-professionals to understand, furthermore, there are responders and non-responders when non-professionals prescribe Kampo medicines. The concept of gsho h focuses on individuals, not diseases, therefore, it is difficult to gain a given effect for everyone by general clinical trials. In many cases, Kampo medicines have been used in the empirical treatment of chronic hypofunction. In recent years, some Kampo medicines have been used to treat experiential gastrointestinal diseases that have been elucidated pharmacologically from the standpoint of gut-regulated hormone levels. One of the gastrointestinal motility regulatory factors has been assumed to be the induction of changes in the levels of peptides such as gastrin, somatostatin and motilin in plasma. In this study, we investigated the effects of five prokinetic Kampo medicines including Pinelliae Tuber and Zingiberis Rhizoma (shohangekabukuryoto, nichinto, ninjinto, rikkunshito, hangeshashinto) on plasma levels of gut-Regulatory Peptides (somatostatin, motilin and gastrin) and compared with that of three dopamine receptor antagonists (metoclopramide, donperidone and itopride), the western prokinetics. Venous blood samples were taken before and 20, 40, 60, 90, 120, 180 and 240 min after administration of drugs. Plasma peptides levels were measured using sensitive enzyme immunoassays. The dopamine receptor antagonists and Kampo medicines caused significant increase of plasma gut-regulatory peptide levels compared with placebo group (Table). In this study, the prokinetic Kampo medicines had similar effects to dopamine D2 receptor antagonists from the standpoint of plasma levels of gut-Regulatory Peptides (somatostatin, motilin and gastrin). Shohangekabukuryoto,

Table 1.

	Somatostatin	Motilin	Gastrin	Pharmacological Effect
Metoclopramide	↑	—	↓	D2 receptor antagonism (central&peripheral)
Donperidone	↑	↑	—	D2 receptor antagonism (mainly peripheral)
Itopride	↑	↑	—	D2 receptor antagonism (peripheral), AChE inhibition
Shohangeka-bukuryoto	↑	—	↓	inhibition of gastric acid, accerelation of gastrointestinal motility
Nichinto	↑	↑	↑	stimulation of gastric acid secretion, improvement of gastrointestinal motility
Ninjinto	↑	↑	↓	improvement of upper gastrointestinal motility
Rikkunshito	↑	—	↑	stimulation of gastric acid secretion and gastric motility
Hangeshashinto	↑↑	↑	↑	stimulation of gastric acid secretion and upper gastrointestinal motility, antidiarrhea

which is used to treat hyperemesis of pregnancy or motor dysfunction, and metoclopramide with a strong antiemetic effect, increased plasma somatostatin levels and inhibited increased plasma gastrin levels. Nichinto, hangeshashinto, donperidone and itopride, which have strong gastrokinetic effects, increased plasma somatostatin and motilin levels. Nichinto and rikkunshito also increased plasma gastrin levels. To evaluate Kampo medicines, pharmacokinetic factors such as concentration in body fluids are not useful. To use physiologically active peptides as biomarkers (pharmacodynamic factors), it is easy to compare and evaluate general and Kampo medicines, and non-professionals can prescribe Kampo medicines similarly to general medicines. To evaluate Kampo medicines using bioactive peptides as biomarkers, it may be possible to cure diseases that are difficult to treat by western medicines. Table. The effects of dopamine receptor antagonists and Kampo medicines on gut-Regulatory Peptides levels

4-20-124

Design and synthesis of a tripartate paclitaxel prodrug for melanoma therapy

Ruzza, Paolo[1,]; Nassi, Alberto[2]; Marchiani, Anna[1]; Rondina, Maria[3]; Rosato, Antonio[3]; Rossi, Carlo Riccardo[3]; Mammi, Stefano[4]; Floreani, Maura[2]; Quintieri, Luigi[2]*

[1]CNR - Institute of Biomolecular Chemistry, ITALY; [2]University of Padova, Department of Pharmacology and Anesthesiology, ITALY; [3]University of Padova, Department of Oncology and Surgical Sciences, ITALY; [4]University of Padova, Department of Chemical Sciences, ITALY

[*]E-mail: paolo.ruzza@unipd.it

Introduction

In an attempt to improve the effectiveness and the selectivity of the anticancer agents, one useful approach might be to develop prodrugs which specifically release the cytotoxic drug in the tumor environment. With this aim, we synthesized a tripartate paclitaxel (PTX) prodrug, potentially useful in the treatment of human melanoma, containing a "targeting domain" bound to PTX by a protease-cleavable peptide linker. The "targeting domain" was represented by an RGD-containing cyclic peptide [c(RGDfK), where f denote a residue of D-Phe] able to bind selectively to $\alpha_V\beta_3$ integrin receptor, which is highly over-expressed by both metastatic human melanoma cells and endothelial cells of tumor vessels. The linker was a short peptide (GRRFA) cleaved by cathepsin B at both lysosomal and extracellular pH values.[1] Cathepsin B is a cysteine protease highly up-regulated in malignant tumors, which is localized in acidic lysosomes and is secreted in extracellular spaces.

Results and Discussion

The N- and C-terminal ends of the linker were opportunely modified to permit the anchorage of the RGD-peptide and PTX, respectively; a succinyl moiety was introduced at the N-terminal position, whereas a 1,2-diaminoethane group, suitable of a 1,6-elimination reaction, was introduced at the C-terminal position. The RGD-containing peptide and the cathepsin B-cleavable linker were synthesized by manual SPPS using Fmoc/HBTU chemistry on H-Gly-2-chlorotrityl resin and 1,2-diaminoethane trityl resin, respectively. The RGD peptide was cleaved from the resin (1% TFA in DCM) and cyclized in a diluted solution using DPPA as the coupling reagent in the presence of an inorganic base. After deprotection of the Lys side-chain from the *iv*Dde protecting group, the cyclic peptide was linked to the carboxy group of succinyl-linker peptide anchored to the resin. At last the RGD-linker peptide was deprotected and cleaved from the resin by treatment with TFA, and then conjugated with PTX modified at the 7-hydroxyl

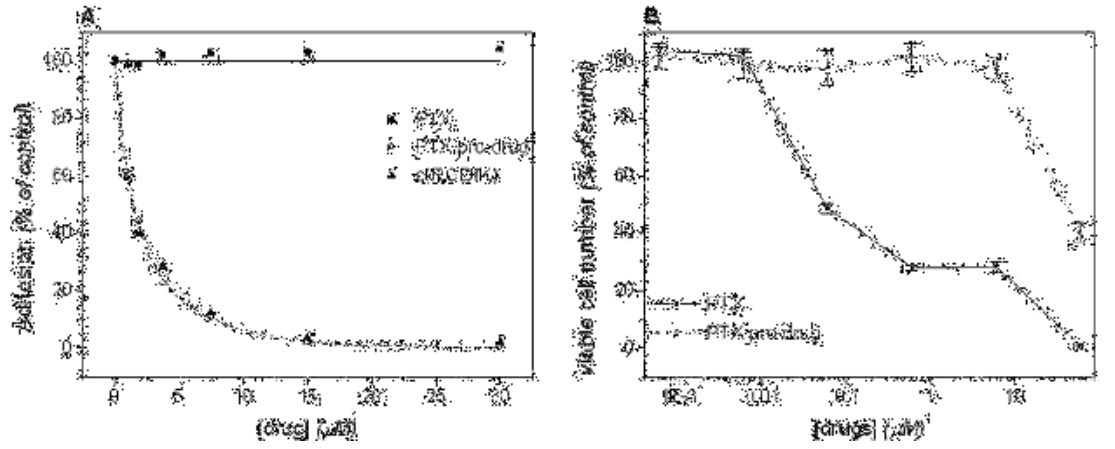

Figure 1. *In vitro* anti-adhesive (Panel A) and cytotoxic (Panel B) effects of paclitaxel (PTX) peptide prodrug toward human melanoma A375 cells. Panel A: A375 cells, preincubated for 15 min in the absence or presence of increasing concentrations of c(RGDfK), free PTX, or PTX prodrug, were seeded in vitronectin-coated 96-well culture plates. After a 1 h-incubation, vitronectin-bound cells were quantified by an MTT test.[3] Panel B: A375 cell viability was evaluated by means of an MTT test upon a 72 hrs-incubation in the absence or presence of increasing concentrations of the PTX prodrug or free PTX.

functionality with 4-nitrophenyl chloroformate.[2] Both c(RGDfK)-linker peptide and the PTX prodrug were purified by RP-HPLC and their identity was confirmed by ESI-MS. NMR experiments carried out in the presence of SDS micelles at 25 °C showed that the molecule adopted an extended conformation, with no interaction between the two ends. This left both ends of the molecule free to interact with its proper partner.

The ability of the synthesized prodrug to bind to $\alpha_V\beta_3$ integrin receptor was evaluated by means of a cell adhesion assay carried out using human melanoma A375 cells. The PTX prodrug completely inhibited, in a concentration-dependent manner, tumor cell adhesion to vitronectin, whereas free PTX was devoid of any anti-adhesive effect (Fig. 1, panel A). The Fig. also shows that the concentration-response curve for the anti-adhesive effect of free c(RGDfK) was superimposable to that of our conjugate, indicating that conjugation of PTX to c(RGDfK) does not modify the affinity of the RGD peptide for $\alpha_V\beta_3$ integrin receptor.

The PTX conjugate showed a significant cytotoxic activity toward A375 cells only at the highest concentration tested (about 60% reduction of cell viability at 60 μM; Fig. 1, panel B). By contrast, as expected, free PTX markedly and concentration-dependently decreased cell viability. Taken together, these data may suggest that PTX was poorly released from the prodrug after cleavage of the cathepsin B-sensitive peptide linker.

In conclusion, our tripartate PTX prodrug answers the purpose of targeting the antitumor drug to the tumor environment, since the RGD-PTX conjugate retains the anti-adhesive effect of the RGD moiety. Unfortunately, this prodrug is provided with a much lower cytotoxic activity than the parent antitumor agent. This result, together with the unsatisfactory stability of the prodrug in human plasma (about 35% of the conjugate was hydrolyzed after 6 hrs of incubation with 50% human plasma in PBS), lead us to design and synthesize novel $\alpha_V\beta_3$ integrin-targeted cathepsin B-cleavable PTX prodrugs, able to efficiently release the active drug and provided with a better stability in plasma.

Acknowledgements

This work was supported by grants from University of Padova (CPDA064182) and Associazione Piccoli Punti, Padova - ONLUS. We thank Indena S.p.A (Milan, Italy) for the gift of paclitaxel.

References

1. Ruzza P, Quintieri L, Osler A, Calderan A, Biondi B, Floreani M, Guiotto A & Borin G. Fluorescent, internally quenched, peptides for exploring the pH-dependent substrate specificity of cathepsin B. *J Pept Sci* **12**: 455-461, 2006.
2. de Groot FMH, van Berkom LWA, Scheeren HW. Synthesis and biological evaluation of 2'-carbamate-linked and 2'-carbonate-linked prodrugs of paclitaxel: Selective activation by the tumor-associated protease plasmin. *J Med Chem* **43**: 3093-3102, 2000.
3. Quintieri L, Rosato A, Napoli E, Sola F, Geroni C, Floreani M & Zanovello P. In vivo antitumor activity and host toxicity of methoxymorpholinyl doxorubicin: Role of cytochrome P450 3A. *Cancer Res* **60**: 3232-3238, 2000.

4-21-125

Synthetic immunoactive fragments of endogenous proteins: selection and application for diagnostics and immunotherapy

Volpina, Olga[1,]; Kamynina, Anna[1]; Shalgunov, Vladimir[1]; Akhidova, Elena[1]; Volkova, Tatyana[1]; Koroev, Dmitriy[1]; Filatova, Margarita[1]; Kormakova, Tatyana[2]; Bobkova, Natalya[3]; Vladimirova, Natalya[4]*

[1]Shemyakin-Ovchinnikov Institute of Bioorganic chemistry, RUSSIAN FEDERATION; [2]Hertzen Moscow Oncological Institute, RUSSIAN FEDERATION; [3]Institute of Cell Biophysics, Russian Academy of Sciences, RUSSIAN FEDERATION; [4]Shemyakin-Ovchinnikov Institute of Bioorganic chemistry, Russian Academy of Sciences, RUSSIAN FEDERATION

[*]E-mail: volpina@ibch.ru

We selected and synthesized immunoactive fragments of four endogenous proteins: nucleophosmin, survivin, prion and α-7 subunit of acetylcholine receptor (AChR). Self-proteins are known to be weakly recognized by immune system, so for the induction of immune response against these proteins we successfully used their synthetic fragments. All synthetic fragments included theoretically predicted T-epitopes to make them able to induce immune response in mice and rabbits in free nonconjugated form.

Nucleolar protein nucleophosmin (NPM), represented in humans by NPM.1 and NPM.2 isoforms, is involved in carcinogenesis, which is often followed by the over-expression of nucleophosmin, the formation of specific oligomers and mutant species carrying alterations in their C-terminal domains.[1] We selected and synthesized two fragments of nucleophosmin, (19-36) and (283-294). The first fragment is present in all forms of NPM and the second fragment is present in normal NPM.1 but not in NPM.2 or mutant species of NPM.1. Antibodies were raised against both peptides. Western blot analysis carried out using affinity purified rabbit antibodies showed that the antibodies raised against the peptides (19-36) and (283-294) detect monomeric and oligomeric forms of nucleophosmin in HeLa cells lysate. At present the ability of the antibodies raised against the peptide (283-294) to distinguish between NPM.1 and NPM.2 isoforms of nucleophosmin is being evaluated.

Another endogenous protein – survivin – belongs to the inhibitory apoptotic protein (IAP) family and is also over-expressed in a variety of human neoplasms.[2] High survivin expression is known to be correlated with aggressive phenotype, weak response to chemotherapy and decreased survival time. Apart from expression level, the localization of survivin within the nucleus or cytoplasm has an important prognostic value. To raise antibodies, we synthesized four synthetic fragments of survivin 2B, namely (1-22), (54-74), (80-88)–(153-165) and (118-144). Immune sera against all these peptides were obtained. Immunohistochemical staining of paraffin embedded sections of tissue samples obtained from patients with infiltrative ductal carcinoma of the breast using affinity purified rabbit antibodies was carried out. The antibodies against peptide (80-88)-(153-165) detected survivin in the cytoplasm but not in the nucleus while antibodies against peptide (54-74) detected survivin both in the nucleus and in the cytoplasm. It was also demonstrated that the immunization with (80-88)–(153-165) impairs the growth of sarcoma S37 tumor in mice. Thus, antibodies against survivin may assist the development of new approaches to tumor disease diagnostics and immunotherapy.

Accumulation of pathogenic isoform of prion protein (PrP^{Sc}) in the brain causes neurodegenerative prion diseases. It is known that anti-prion antibodies can be used for the immunodetection of pathogenic isoform in brain samples and for the immunotherapy of prion disorders.[3,4] We have selected and synthesized seven fragments from four regions of amino acid chain of bovine prion protein. All synthetic peptides in free non-conjugated state were able to induce the formation of anti-peptide antibodies in rabbits. One of the sera obtained against free peptide 106-134 was able to interfere with PrP^{Sc} propagation in prion infected ScN2a neuroblastoma cell culture. In the immunohistochemical test using samples of bovine brain with transmissible spongiform encephalopathy, rabbit antibodies against peptides 214-240 and 106-134 were able to bind to PrP^{Sc}.

Alzheimer's disease (AD) is a neurodegenerative disorder which involves neuronal death, progressive memory loss and cognitive decline. One of the hypotheses of AD neuropathology involves high affinity binding of beta-amyloid with α7 AchR leading to neuronal lysis.[5] We proposed that antibodies against α7 AchR would prevent its interaction with beta-amyloid and the development of neurodegenerative process. In our experiments we used bulbectomized (BE) mice as a model of sporadic AD.[6] These mice posessed behavioral, morphological and biochemical symptoms of neurodegenerative AD-like processes including the loss of spatial memory and increased level of brain beta-amyloid developed as a result of olfactory bulbs removal. Protective effect of immunisation with synthetic fragment (173-193) of extracellular domain of α7 AchR was studied on BE and non-bulbectomized, so called sham-operated (SO) mice. Synthetic fragment (171-199) from meningococcal

protein OMP was used as negative control compound. After double immunization 82% of BE mice immunized with α7 (173-193) peptide demonstrated good spatial memory in Morris water maze while the spatial memory of BE mice immunized with (171-199) peptide proved to be impaired. All SO mice immunized with α7 (173-193) peptide and (171-199) control peptide showed no spatial memory impairment. ELISA showed high levels of antibodies in the blood sera and in the cerebrospinal fluid of BE and SO mice immunized with both peptides. Immunization with α7 (173-193) peptide decreased the level of beta-amyloid in the mice's brain to 11 ng/g of brain tissue compared to 38 ng/g for control mice immunized with (171-199). Thus, we showed that immunization with synthetic fragment (173-193) improves cognitive decline of mice with experimental induñed AD and antibodies against α7 AchR can penetrate blood brain barrier and decrease beta-amyloid level in the mice's brain.

References

1. Grisendi S, Mecucci C, Falini B, Pandolfi PP. Nucleophosmin and cancer. *Nat Rev Cancer* **6**: 493-505, 2006.
2. Li F, Ling X. Survivin study: An update of "What is the next wave?" J Cell Physiol **208**: 476-486, 2006.
3. Schoch G., Seeger H., Bogousslavsky J., Tolnay M., Janzer R.C., Aguzzi A., Glatzel M. Analysis of prion strains by PrPSc profiling in sporadic Creutzfeldt-Jakob disease. *PLoS Medicine* **3**: 0236-0243, 2006.
4. Schwarz A, Kratke O, Burwinkel M, Riemer C, Schultz J, Henklein P, Bamme T, Baier M. Immunisation with a synthetic prion protein-derived peptide prolongs survival times of mice orally exposed to the scrapie agent. *Neurosci Lett* **350**: 187-189, 2003.
5. D'Andrea MR, Nagele RG, Wang HY, Peterson PA, Lee DH. Evidence for neuronal origin of amyloid plaques in Alzheimer's disease. *Histopathology* **38**: 120-134, 2001.
6. Nesterova IV, Bobkova NV, Medvinskaia NI, Samokhin AN, Aleksandrova IYu. Morpho-functional state of neurons in temporal cortex and hippocampus in bulbectomized rats with different level of spatial memory. *Morfologiia* **131**: 32-36, 2007.

4-23-126

Allosteric inhibition and activation of SHP-1 phosphatase by SH2 phosphopeptide ligands

Teichmann, Kathleen; Hampel, Kornelia; Imhof, Diana*

Friedrich-Schiller-University/Center of Molecular Biomedicine, Department of Biochemistry GERMANY

**E-mail: sunandsnow@gmx.de*

Introduction

The tandem SH2 domain (N-SH2, C-SH2) containing protein tyrosine phosphatase SHP-1 regulates signal transduction pathways mediated by a variety of hematopoietic receptors.[1] In the native state, the *N*-SH2 domain interacts with the PTP-domain that in turn renders the enzyme inactive. After the binding of a phosphorylated ligand to the *N*-SH2 domain the PTP domain is released and accessible for substrates.[1-3] Synthetic ligands based on the consensus sequence class 1 and the native high-affinity interaction partner RTK Ros pY2267 (EGLNpY2267MVL-NH2) have previously been shown to bind to the *N*-SH2 domain with considerable high affinity.[3,4] Recently, we identified cyclic compounds that showed an increased binding affinity for the *N*-SH2 domain and partially inhibited Ros-mediated SHP-1 activity.[4,5] These peptide ligands are interesting tools to modulate the catalytic activity of this enzyme. The specificity of the SHP-1 SH2 domains is primarily determined by phosphotyrosine (pY, position 0) and the residues at positions -2, +1 and +3 with a preference for hydrophobic and, in particular, aromatic amino acids at +1 and +3.[3] Furthermore, residues at pY+4 to pY+6 significantly influence the binding affinity to the SH2 domains of SHP-1 and SHP-2.[6] With a series of new linear and cyclic ligands, we investigated different aspects such as ring position and ring size in cyclic peptides as well as whether the gain in binding affinity by recognition elements in pY+4 and pY+5 is retained in ligands gradually truncated at the N-terminus.

Results and discussion

We previously reported that the cyclic compounds 2 and 3 were designed with the intent of reducing the conformational flexibility of the linear lead structure 1 (Table 1). Both peptides showed a higher binding affinity than Ros pY2267 (0.11 and 0.21 μM, respectively, vs. 1.44 μM) and were partially inhibitors of SHP-1 activity.[4,5] These ligands were used as a template for further compounds, e.g. 4 and 5, in which the incorporation of optimal residues at positions pY+1 and pY+3 yielded high-affinity ligands with an increased ability to stimulate SHP-1 activity.[7] In addition to these ligands, peptides 6 and 7 were synthesized in order to provide evidence for the library-determined recognition elements at pY+4 and pY+5.[6] The introduction of motifs WYG (6) and NleFP (7) increased the binding affinity of the corresponding peptides to SHP-1 *N*-SH2 5-fold and 8.5-fold, respectively.[6] These results provided the basis for the design of a series of new ligands (8-16, Table 1) which combine the specific determinants for optimal binding to the *N*-SH2 domain and a motif expected to bind to the surface of the PTP domain. These bivalent peptides have been designed and synthesized[5,7] with the aim to generate inhibitors of the dissociation process of the *N*-SH2/PTP-complex. In contrast to Ros pY2267(1), cyclic peptide 8 reached half-maximal activation already at 12 μM, though this compound activates SHP-1 up to 100 μM and inhibited the phosphatase activity at higher concentrations. In 8, the cyclization between positions pY+2 and pY+4 is obviously not influencing the recognition of the amino acid side chains at pY+1 (Met) and pY+3 (Leu) by the SH2 domain that is a prerequisite for effective ligand binding. However, this seems to be the case for peptides 9, 14 and 15, yet to a different extent. In 9 the conformational restriction seems to interfere with the specificity for the C-terminal residues at pY+4/+5. The same maybe discussed for 16, but this peptide showed a better ability to stimulate SHP-1 than 1, i.e. the C-terminal extension by the PTP-binding motif seems to be preferred over 8. Compound 12 was expected to be less active or inactive, since one of the specificity determinants (pY-2) is missing. This was confirmed by our experiment, thus, the loss of pY-2 is not compensated by the additional specificity for residues pY+4 and +5. In general, the fact that all specificity determinants (pY-2 to pY+5) are present in a peptide ligand leads to compounds that stimulate SHP-1 activity better than the native lead 1, e.g. peptides 8, 10, 11, and 13. Biacore studies are currently under investigation and will reveal, whether inhibiting peptides 9, 12, 14 and 15 show better binding affinities than 1 as found for peptides 2 and 3. Also, Molecular Modeling studies will be extended to characterize differences in the binding of activating and inhibiting compounds.

Table 1. Evaluation of linear and cyclic peptides as effectors of SHP-1 activity.[4,6,7]

Peptide	Sequence	EC_{50}[µM]	K_D [µM] [(a)]
1 Ros pY[2267]	EGLNpYMVL-NH_2	160	1.44±0.45
2	EGLc[K($COCH_2NH$)pYMD]L-NH_2	N.A.[(b)]	0.11±0.01
3	EGLc[K($COCH_2NH$)pYME]L-NH_2	N.A.	0.21±0.07
4	EGLc[K($COCH_2NH$)pYFD]Hfe-NH_2	31	0.06±0.01
5	EGLc[K($COCH_2NH$)pYNleD]Hfe-NH_2	49	0.06±0.01
6	AALNpYAQLWYG-NH_2	N.D.[(c)]	0.28±0-03
7	AALNpYAQLNleFP-NH_2	N.D.	0.17±0.03
KT002	EGLNpYMc[KLD]FP-NH_2	12	- [(d)]
KT003	EGLNpYMc[KLNleFD]-NH_2	272	- [(d)]
KT007	EGLNpYMVLNleFPAPEEE-NH_2	43	- [(d)]
KT008	LNpYMVLNleFPAPEEE-NH_2	35	- [(d)]
KT009	pYMVLNleFPAPEEE-NH_2	N.A.	- [(d)]
KT010	EGLc[KpYMD]LNleFPAPEEE-NH_2	71	- [(d)]
KT012	EGLNpYc[KVD]NleFPAPEEE-NH_2	647	- [(d)]
KT014	EGLNpYMc[KLD]FPAPEEE-NH_2	200	- [(d)]
KT016	EGLNpYMc[KLNleFD]APEEE-NH_2	67	- [(d)]
SPR measurements performed with GST-N-SH2, (b) N.A. not active, (c) not determined, (d) currently under investigation			

Acknowledgements

This work was financially supported by the Deutsche Forschungsgemeinschaft (IM 97/1-2) and the Friedrich Schiller University Jena.

References

1. Sathish JG, Matthews RJ. SHP-1 twelve years on: structure, ligands, substrates and biological roles. *Topics in Current Genetics* **5**: 301-331, 2004.
2. Yang J, Liu L, He D, Song X, Liang X, Zhao Z J, Zhou GW. Crystal Structure of Human Protein-tyrosine Phosphatase SHP-1. *J Biol Chem* **278**: 6516-6520, 2003.
3. Sweeney MC, Wavreille AS, Park J, Butchar JP, Tridandapani S, Pei D. Decoding protein-protein interactions through combinatorial chemistry: sequence specificity of SHP-1, SHP-2, and SHIP SH2 domains. *Biochemistry* **45**: 14932-14947, 2005.
4. Imhof D, Wieligmann K, Hampel K, Nothmann D, Zoda MS, Schmidt-Arras D, Zacharias M, Böhmer FD, Reissmann S. Design and biological evaluation of linear and cyclic phosphopeptide ligands of the N-terminal SH2 domain of protein tyrosine phosphatase SHP-1. *J Med Chem* **48**: 1528-1539, 2005.
5. Imhof D, Nothmann D, Zoda MS, Hampel K, Wegert J, Böhmer FD, Reissmann S. Synthesis of linear and cyclic phosphopeptides as ligands for the N-terminal SH2-domain of protein tyrosine phosphatase SHP-1. *J Pept Sci* **11**: 390-400, 2005.
6. Imhof D, Wavreille A S, May A, Zacharias M, Tridandapani S, Pei D. Sequence specificity of SHP-1 and SHP-2 Src homology 2 domains. Critical roles of residues beyond the pY+3 position. *J Biol Chem* **281**: 20271-20282, 2006.
7. Hampel K, Kaufhold I, Zacharias M, Böhmer F D, Imhof D. Phosphopeptide ligands of the SHP-1 N-SH2 domain: effects on binding and stimulation of phosphatase activity. *ChemMedChem* **8**: 869-877, 2006.

4-23-127

Size and Zeta Potential Analysis of Synthetic Peptide-Carrier Protein Conjugates Depend on the Time

Derman, Serap; Dalgakiran, Eray; Mustafaeva, Zeynep*

Yildiz Tehcnical University, Bioengineering Department, TURKEY

**E-mail: serapacar5@gmail.com*

Introduction

In this study we report the investigation of size and zeta potential of synthetic Peptide-Carrier protein covalent conjugates. Synthetic peptides are not strong immunogens on its own, because of their small size.[1] To use peptides as synthetic vaccines to make them more immunogenic and to generate an immune response and high levels antibodies they have to be coupled to a carrier protein.[2,3] There for in this study we aimed preparation of immunogen and vaccine by conjugation of synthetic peptide antigen of 135-161 (WSKYSTTGERTRGDLGALAARVATQLPA) amino acids sequence of immunogenic VP1 capsid protein of "A type Foot-and-Mouth Disease Virus" and globular macromolecules (Bovine Serum Albumin) with carbodiimide method different molar ratio ($n_{peptide}$/ $n_{protein}$). Zeta potential and size measurements of protein, polymer, peptide-protein or peptide-polymer conjugates were carried out in Zetasizer Nano ZS instrument at 25 °C. All solutions were filtered with 0,2 μm RC-membrane filters (Sartorius) before measurements. M3-PALS (phase analysis light scattering) technique was used for zeta potential analysis and photon correlation spectroscopy (PCS) was used for size analysis. For data analysis, while the viscosity of 0,8872 cP and the refractive index of 1,330 values were used for the solvent for PCS measurements, the viscosity of 0,8872 cP, the dielectric constant of 79 and f(ka)=1,50 values were used for M3-PALS measurements. The number of runs and run durations were chose as automatically.

Results and discussion

In this study we synthesized three different conjugates which $n_{peptide}/n_{BSA}$ ratios are 1, 3 and 5. Zeta potential and size values which belong to conjugates were measured after the 45., 90., 135. ve 180. minutes from beginning of the synthesis. According to the Zeta potential analysis, zeta potential of free BSA found as -15,0 mV while zeta potential of free Peptide found as -13,5 mV at pH 7 (because of carboxyl group's negative charge). After 45. minutes of conjugation, zeta potential values of n=1, 3 and 5 conjugates increased to -7,5, -6,5 and -4,5 mV respectively (Fig. 1). Because BSA and Peptide have negative electrical charges, they must not bind together under normal physical conditions to make such an increase in zeta potential. Therefore, these positive zeta potential shifts show that peptide and BSA amino groups covalently bounded to each other and negatively charged carboxyl groups were decreased.

According to PCS measurements, free peptide is 4,61 nm and free BSA is 8,69 nm in size. After 30 minutes of conjugation, again Z-average sizes of n=1, 3 and 5 conjugates increased to approximately 1,5-2 times of free BSA size (Fig. 2) and longer conjugation times resulted increasing of size.

It is also found that for a constant conjugation time, Z-average sizes of conjugates increased linearly depend on npeptide/nBSA ratio (Table 1) which shows that all amount of added peptides which increases with increasing of npeptide/nBSA ratio were continually draw into conjugate up to ratio 9.

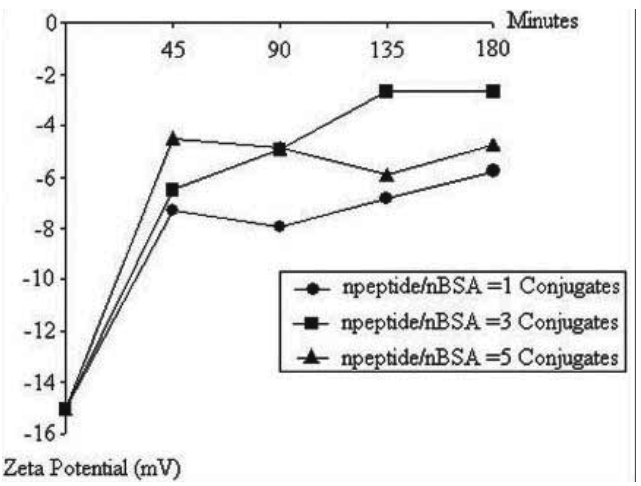

Figure 1. Zeta potential values. Comparison of Zeta potential values of npep/nBSA=1, 3, 5 conjugates depend on the time (Zeta potential values were measured at 45., 90., 135. and 180. min. and graphic was started BSA Zeta potential value which is -15 mV).

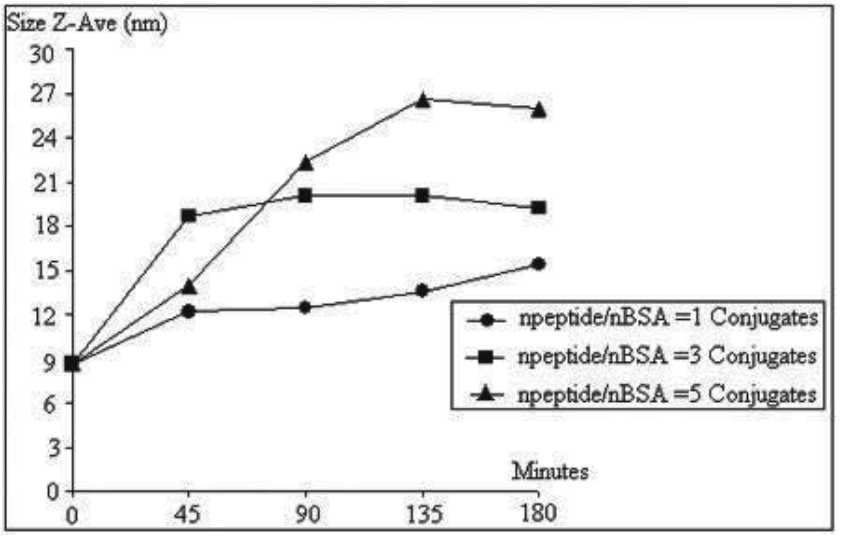

Figure 2. Size values. Comparison of Size values of npep/nBSA=1, 3, 5 conjugates depend on the time (Size values were measured at 45., 90., 135. and 180. min. and graphic was started BSA Size value which is 8,6 nm).

Table 1. Size value of npeptide/nBSA =1, 3, 5, 7 and 9 conjugates

$n_{peptide}/n_{BSA}$ ratio	Size (nm)
n=1	15,4
n=3	19,2
n=5	25,9
n=7	30,1
n=9	35,5

While conjugation reaction we investigate zeta potential and size values changing depend on the time and as a result of the binding carboxyl groups to amino groups we observed that zeta potential approach to zero and size values increased linearly depend on the npeptide/nBSA ratio. This positive shift at Zeta potential (from -15 mV to -2 mV and -6 mV) show that peptide and BSA amino groups covalently bounded to carboxyl group and because of this binding negatively charged carboxyl groups were decreased. All of the results show that two or more molecules bonded each other.

Acknowledgements

This research was supported by grant from Republic of Turkey Prime Ministry State Planning Organization (25-DPT-07-04-01).

References

1. Deen C, Claasen E, Gerritse K, Zegers DN, Boersma JAW. A novel carbodiimide coupling method for synthetic peptides enhanced anti-peptide antibody responses. *J Immunol. Methods* **129**: 119-125, 1990.
2. Beekman NJCM, Schaaper WMM, Turkstra JA, Meloen RH. Highly immunogenic and fully synthetic peptide-carrier constructs targetting GNRH. *Vaccine* **17**: 2043-2050, 1999.
3. Ghosh S, Jackson DC. Antigenic and immunogenic properties of totally synthetic peptide-based anti-fertility vaccines. *Int Immunol* **11**: 1103-1110, 1999.

4-26-128

Peptide drugability: Analytical functionality

De Spiegeleer, Bart[1,]; Van de Wiele, Christophe[2]; Burvenich, Christian[3]; Van Dorpe, Sylvia[1]; Vergote, Valentijn[1]; Baert, Bram[1]; Peremans, Kathelijne[4]; Audenaert, Kurt[5]*

[1]Ghent University / Faculty of Pharmaceutical Sciences, DruQuaR (Drug Quality & Registration) group, BELGIUM; [2]Ghent University / Faculty of Medicine, Department of Nuclear Medicine, BELGIUM; [3]Ghent University / Faculty of Veterinary Medicine, Department of Physiology, BELGIUM; [4]Ghent University / Faculty of Veterinary Medicine, Department of Medical Imaging, BELGIUM; [5]Ghent University / Faculty of Medicine, Department of Psychiatry, BELGIUM

[*]E-mail: bart.despiegeleer@ugent.be

Peptide drugs gain increased interest as a new supra-group of therapeutics between the classic-organic, small-molecule drugs and the large biotechnology-derived bio-drugs. They are used in different therapeutic or diagnostic areas like allergy, anti-infection, oncology, obesity etc. but also as functional excipients (e.g. CPPs). Due to their particular structure and biochemical origin, the pharmaceutical development of a peptide drug poses special challenges.

After the initial synthesis of the active pharmaceutical ingredient (API) or functional excipient, analytical characterisation is aimed at **integrity and purity** evaluation of the compound, which is also required for initial biomedical experiments.[1-3] It is important te be aware of quality differences, e.g. depending on the supplier. We recently found major differences in the HPLC purity profile of human obestatin obtained from 5 different suppliers (Table 1). In this analytical characterisation, sample treatment issues like solubility, adsorption and degradation are important aspects to be looked after for peptide drugs.[4] This is not only important for the original peptides as such, but is also true if radiochemical or fluorophore modified peptides are ex tempore prepared for biomedical studies. An example is given by the indirect iodination through Bolton-Hunter (BH) conjugation of the peptide FPKPEGSQ, yielding the mono-^{125}I-BH-peptide (RT of 7.0 min) , the di-^{125}I-BH-peptide (RT of 16.5 min), but other radiochemical impurities as well.

The **chemical and metabolic stability**, critical parameters for peptides, is to be assessed to obtain kinetic and mechanistic information.[5] In-vitro experiments using peptide-spiked media as well as tissue extracts are performed, followed by HPLC-UV/Fl/MS quantification of the parent peptide and identification of the resulting metabolic and/or degradation products. In this way, for example, the peptide FPKPEGSQ was demonstrated to have a half-life in mouse liver homogenate of 21 minutes (95% C.I.: 16-31 min), with the main metabolic cleavage sites at P^2-K^3 and P^4-E^5.

Functionality is tested in-vitro, using cell- and organ-based protocols including ligand binding studies, as well as in-vivo encompassing ADME and target-organ confirmation like brain behaviour. Saturation experiments with the ^{125}I-BH-peptide FPKPEGSQ did not show significant binding to mouse stomach, spleen, cerebrum, kidney and small intestine tissue extracts, but a significant binding to cerebellum was observed, indicating a potential brain interaction. Next, a multiple-time regression blood-brain barrier influx experiment was performed, showing however no significant influx of this peptide.

Table 1. LC-purity of human obestatin samples from different suppliers (UV @ 195 nm) [(1)]

Supplier	Sum of impurities (%)	Largest impurity (%)	Number of impurities	
			Total	≥ 1.00%
GLB	7.26	2.65	6	3
PB	0.67	0.17	7	0
GPS	6.91	1.66	12	3
PP	6.82	1.99	7	4
CPR	0.34	0.19	3	0

[(1)] *Reporting threshold = 0.05%.*

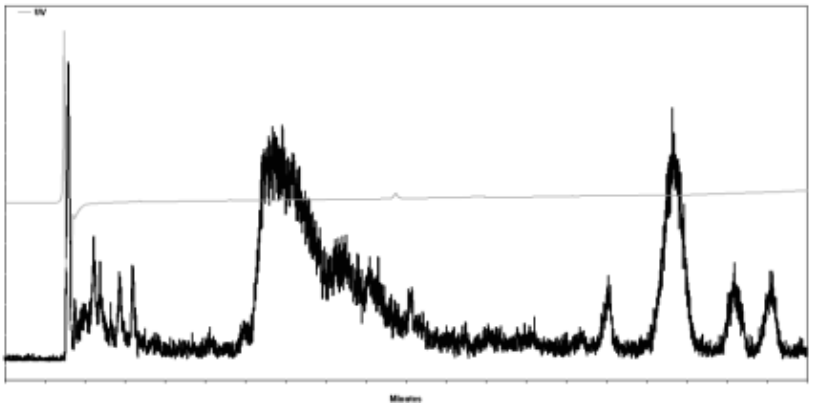

Figure 1. HPLC (UV and RA detection) of synthesis mixture of ^{125}I-BH-FPKPEGSQ.

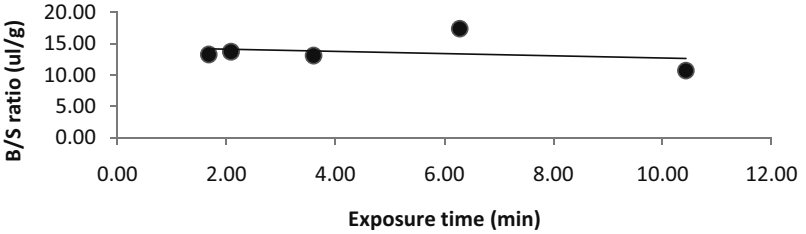

Figure 2. BBB Multiple-time regression of ^{125}I-BH-FPKPEGSQ in mice.

The pharmaceutical drugability information of a peptide thus obtained allows further development decisions, including required drug modifications, synthesis and purification modifications, quality specification settings as well as proof-of-principle drug delivery formulations.

References

1. Vergote V, Baert B, De Spiegeleer B. HPLC analysis and stress stability of peptide drugs. Presented at Barcelona 2008: *6th World Meeting on Pharmaceutics, Biopharmaceutics & Pharmaceutical Technology*.
2. De Spiegeleer B, Vergote V, Pezeshki A *et al*. Impurity profiling quality control testing of synthetic peptides using LC-PDA-Fl and LC-ESI-MS: the obestatin case. *Anal Biochem* **376**: 229-234, 2008.
3. De Spiegeleer B, Vergote V, Burvenich C. Development of quality specifications of peptide drugs. *11th Workshop on Bioactive Peptides*, Naples, Italy, 2008.
4. Pezeshki A, Vergote V, De Spiegeleer B *et al*. Adsorption of peptides at the sample drying step: influence of solvent evaporation technique, vial material and solution additive. *J Pharm Biomed Anal* **49**: 607-612, 2009.
5. Vergote V, Van Dorpe S, De Spiegeleer B *et al*. In vitro metabolic stability of obestatin: kinetics and identification of cleavage products. *Peptides* **29**: 1740-1748, 2008.

5-07-001

Determination of GPCR structures and activation mechanisms with reactive peptide probes

Arsenault, Jason; Clément, Martin; Fillion, Dany; Beaulieu, Marie-Eve; Holleran, Brian; Leduc, Richard; Guillemette, Gaétan; Lavigne, Pierre; Escher, Emanuel[1,]*

Université de Sherbrooke, Pharmacologie, CANADA

[*]E-mail: Emanuel.Escher@USherbrooke.ca

Rational drug design relays largely on the availability of pertinent structural information of the respective drug target. X-ray crystallography provides most of those molecular structures and increasingly, protein NMR. Even high throughput X-ray crystallography of drug targets has become a reality in pharmaceutical industry environment.[1] Those technological and instrumental-analytical advances notwithstanding, the most important drug target family, the seven transmembrane spanning, G-protein coupled receptor (GPCR) family is however extremely resistant to those technological structure determinations. There are over 600 genes in the human genome, coding for individual GPCR, making them extremely promising targets for efficient pharmacotherapy in most disease categories if only highly receptor selective substances can be designed. Until now, some partial GPCR structures from different protein NMR approaches[1,3] and only four such GPCR structures have been successfully obtained from X-ray crystallography:[4-7] Bovine rhodopsin, squid opsin and the adrenergic beta receptors 1 and 2. Due to the inherent mobility and the relatively labile, membrane stabilized tertiary structure of these strongly anisotropic proteins it was necessary to use almost extreme non-physiological crystallization conditions or extensive mutagenesis to stabilize sufficiently the target protein; the beta receptors were stable, ligand binding but unable to elicit signalling. Such a general, inactive receptor structure is already of pertinence for drug design but more so the extent of mobility and its thermodynamics that allows an agonist occupied receptor to undergo the structural changes associated to receptor activation and coupling to the intracellular effectors. Actually, this type of information is not available for this family of drug targets.

In the present contribution a biochemical pathway is outlined that may allow for many peptidergic GPCR to obtain acceptable liganded receptor structures and the relevant structural changes associated with receptor activation. The basic approach is to create within the general GPCR structure spatial restrictions between individual receptor residues in different parts of the protein domains. If sufficient interconnecting restrictions may be determined, inescapable molecular structures within the general GPCR structure are bound to emerge and allow for a determination of a more or less complete receptor structure. By using tools like agonistic or inverse agonistic ligands and constitutively active and inactive receptor mutants besides the wild-type receptor, activation status specific molecular structures of the receptor become accessible. To create those spatial restrictions a variant of the method of photoaffinity labelling was used, the Methionin Proximity Assay (MPA).[8,9] Contrary to the classical approach where photolabels with high-energy, chemically non selective properties were preferred like nitrene or carbene producing precursor analogues, the MPA exploits the chemical selectivity of the benzophenone keto radical. Previous studies with Ang II analogues bearing aromatic azido groups always produced results that were not compatible with a single attachment site[10] and later an exhaustive study with a fluorinated azido analogue showed that the label incorporated into three transmembrane elements simultaneously (TM 3,6 &7).[10] A similar result was observed with a carbene-generating analogue that identified TM 3 and 6.[11] Since benzophenone photoreacts with high selectivity into methionin residues due to its particular photochemistry[9,11,12] the MPA approach was proposed with an iterative X→M mutagenesis strategy. If a mutated M residue finds itself in proximity to the benzophenone residue of the receptor bound ligand, then the photoactivated benzophenone would react with this residue and form a covalent receptor-ligand complex. Upon chemical digestion of this complex, SDS-PAGE can then identify a fragmentation patterns different from the native receptor and thus confirm a ligand-receptor contact.[8,9]

For the human AT1 receptor, its constitutively active mutant N111G-hAT1 and its constitutively inactive mutant N111W-hAT1 the following contact points were obtained with p-benzoyl-phenylalanine (Bpa) modified AngII: Molecular modelling of the liganded hAT1 on the bovine rhodopsin template and minimizing the distances between the individual contact residues and the ligand labelling position resulted in two sets of structures. One is identical for native AT1 and the inactive mutant N111W-hAT1 and the other for the constitutively active mutant series on the N111G- template. A significant shift of the upper part of the TM elements 6 and 7, a parallel displacement of TM 1 and 2 and, most interestingly a movement of intracellular helix 8, commonly associated to G-protein interaction[13,14] are evident (see Fig.). Since the main photolabelling analogue [Sar1, Bpa8]AngII is a

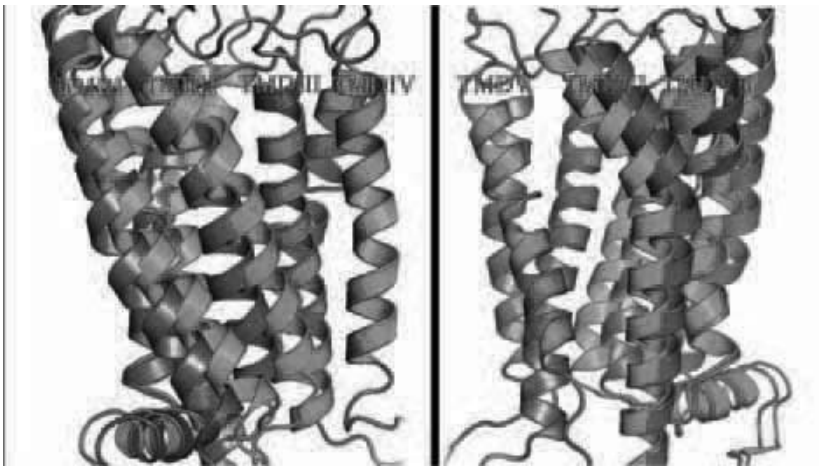

Figure 1. Molecular modelling overlay of hAT1 in the inactive (green) and active conformations (blue). Transmembrane domains are indicated in red.

neutral antagonist of competitive nature, it does not shift the receptor equilibrium towards an active or inactive form as an agonist or an inverse agonist, respectively, would do. The obtained structural changes observed between the two structures should therefore reflect the structural change observed during receptor activation.

Conclusion

The MPA approach can produce through experimentally obtained receptor-ligand contact points the molecular structures of peptidergic receptors and, if constitutively active mutants are available, event the structural changes of receptor activation.

Acknowledgements

Supported by grants of the Canadian Institutes of Health Research.

References

1. Sugahara M *et al*. High-throughput crystallization-to-structure pipeline at RIKEN SPring-8 Center. *J Struct Funct Genomics* **9**: 21-28, 2008.
2. Conner M *et al*. Functional and biophysical analysis of the C-terminus of the CGRP-receptor; a family B GPCR. *Biochemistry* **47**: 8434-8444, 2008.
3. Arevalo E *et al*. Biosynthesis and biophysical analysis of domains of a yeast G protein-coupled receptor. *Biopolymers* **71**: 516-531, 2003.
4. Palczewski K *et al*. Crystal structure of rhodopsin: A G protein-coupled receptor. *Science* **289**: 739-745, 2000.
5. Park JH *et al*. Crystal structure of the ligand-free G-protein-coupled receptor opsin. *Nature* **454**: 183-187, 2008.
6. Rasmussen SG *et al*. Crystal structure of the human beta2 adrenergic G-protein-coupled receptor. *Nature* **450**: 383-387, 2007.
7. Cherezov V *et al*. High-resolution crystal structure of an engineered human beta2-adrenergic G protein-coupled receptor. *Science* **318**: 1258-1265, 2007.
8. Clement M *et al*. Determining the environment of the ligand binding pocket of the human angiotensin II type I (hAT1) receptor using the methionine proximity assay. *J Biol Chem* **280**: 27121-27129, 2005.
9. Rihakova L *et al*. Methionine proximity assay, a novel method for exploring peptide ligand-receptor interaction. *J Recept Signal Transduct Res* **22**: 297-313, 2002.
10. Gagnon T *et al*. Synthesis of an agonistic, difluoro-azido photolabel of angiotensin II and labeling of the AT1 receptor: transmembrane domains 3, 6, and 7 form the ligand-binding pocket. *J Recept Signal Transduct Res* **26**: 435-451, 2006.
11. Fillion D *et al*. Stereospecific synthesis of a carbene-generating angiotensin II analogue for comparative photoaffinity labeling: improved incorporation and absence of methionine selectivity. *J Med Chem* **49**: 2200-2209, 2006.
12. Arsenault J *et al*. Temperature-dependent variations of ligand-receptor contact points in hAT(1). *J Pept Sci* **13**: 575-580, 2007.
13. Swift S *et al*. Role of the PAR1 receptor 8th helix in signaling: the 7-8-1 receptor activation mechanism. *J Biol Chem* **281**: 4109-4116, 2006.
14. Shimamura T *et al*. Crystal structure of squid rhodopsin with intracellularly extended cytoplasmic region. *J Biol Chem* **283**: 17753-17756, 2008.

5-22-101

Protein-oligopeptide fragmentomics

Zamyatnin, Alexander[1,2,]*

[1]A.N.Bach Institute of Biochemistry Russian Academy of Sciences, Moscow, RUSSIAN FEDERATION; [2]Universidad Tecnica Federico Santa Maria, Departamento de Informatica, Valparaiso, CHILE

[*]E-mail: aaz@inbi.ras.ru

Introduction

The term "fragmentomics" was used at first for consideration of oligopeptide and protein fragments that were true biomarkers.[1] However, protein fragmentation has been used long in protein chemistry for obtaining protein primary structures. Natural fragmentation of specialized precursors of oligopeptides and proteins was also well known. Therefore it was necessary to find a more general definition of the term "fragmentomics". We proposed to define fragmentomics as an area of researches where structure and functions of the set of molecular fragments was studied.[2] Thus, complete set of fragments could be named as fragmentom. Within the framework of fragmentomics the theoretical structural-functional analysis of all possible fragments of several food protein molecules has been performed with the purpose of determination of their sites which could be potential sources of the regulatory oligopeptides. The data on the primary structures of meat and milk proteins from public protein databases, information from EROP-Moscow (**E**ndogenous **R**egulatory **O**ligo**P**eptides) database[3] data on structures and functions of the natural oligopeptides, and special computer program complex were used. Food protein fragment amino acid residues were compared with all data of natural oligopeptide database (more than 7000 entries).

Results and discussion

Fragmentoms of bovine casein (CS), human cytochrome b (CH b), bovine hemoglobin (HB), human α-lactoalbumin (α-LA), bovine β-lactoglobulin (β-LG), and human lactoferrin (LF) were studied. It has found out that a lot of natural regulatory oligopeptides elucidated in other sources represent exact structures of food protein fragments. Amino acid residue sequences of more than 100 different food protein fragments were identical to many natural oligopeptides. Table 1 demonstrates 82 oligopeptides with known type of functional activity. Total amount of putative regulatory oligopeptide sequences in all the six food proteins was 242. These fragments could contain from 2 to 7 amino acid sequences and represented 6 different functional types. Enzyme inhibitors were the main part of revealed natural non-food protein oligopeptides. Except for this, many natural oligopeptides being identical to food protein fragments were not characterized functionally (have been not shown in Table 1). Some fragments were presented several times in one food protein. For example tripeptide sequence JQK (J - pyroglutamic residue formed from glutamine, Q, at N-terminal) was met 9 times in all chains of bovine casein molecule. Thus, the method allowed to reveal new potentially active sites of protein amino acid sequences yet not investigated experimentally. Food protein fragments as putative oligopeptides could participate in regulation of all regulatory systems: nervous, endocrine, and immune. Hence food proteins could most likely act, not only as proteins, but as a source of fragments possessing regulatory functions. It is possible that food protein fragments could be considered as exogenous regulatory structures. A great deal of evidence indicated that regulation could be simultaneously performed at all levels of the systems of a living organism, and digestion played a significant role in such regulation. These data supported the hypothesis that a functionally continuous continuum of natural oligopeptides of both endogenous and exogenous structures existed and confirmed deep relationship between the basic regulatory systems.

Acknowledgements

This study was supported by the "Molecular and Cellular Biology" program for the basic research of Presidium of the Russian Academy of Sciences, Grant No. 10P and by Chilean National Science and Technology Research Fund FONDECYT, Grant No. 1080504.

References

1. Lopez M, Kuzdzal1 S, Mikulskis A, Sarracino D, O'Gorman M, Fishman D, Rosenblatt K, Whiteley G, Petricion E, Liotta L. *17th International Mass Spectrometry Conference.* Abstract Book, ThP-057, 2006.
2. Zamyatnin AA. *Biofizika* **53:** 725-733, 2008.
3. Zamyatnin AA, Borchikov AS, Vladimirov MG, Voronina OL. *Nucl Acids Res* **34:** D261-D266, 2006 .

Table 1. Structures and functions of the natural oligopeptides identical to food protein fragments.

EROP □	OLIGOPEPTIDE NAME	FUNCTION	SEQUENCE*	CS	CH b	HB	□-LA	□□LG	LF	SUM
E02335	Development regulating peptide Hym311 (hydra)	development regulator	+FW-		1	1				2
E04069	ACEI 4 (wheat)	enzyme inhibitor	+AF-	1	2	1			3	7
E01340	ACEI 11 (Japanese sardine)	enzyme inhibitor	+AKK-				1			1
E02856	ACEI (bovine)	enzyme inhibitor	+ALPMHIR-					1		1
E04540	ACEI (human)	enzyme inhibitor	+AW-	1		1				2
E04098	ACEI 3 (Tatarian buckwheat)	enzyme inhibitor	+AY-	2	1					3
E05453	ACEI (edible mushroom)	enzyme inhibitor	+GEP-	1						1
E01431	ACEI 1.1 (bonito)	enzyme inhibitor	+IKP-		1					1
E07046	ACEI IPP (bovine)	enzyme inhibitor	+IPP-	2						2
E04103	ACEI 10 (Tatarian buckwheat)	enzyme inhibitor	+ITF-		1					1
E01434	ACEI 3.1 (bonito)	enzyme inhibitor	+IW-		1				1	2
E01439	ACEI 7 (bonito)	enzyme inhibitor	+IY-						1	1
E01332	ACEI 2 (Japanese sardine)	enzyme inhibitor	+KW-		1			1		2
E01831	Bitter peptide 2 (soybean)	enzyme inhibitor	+LF-	1	6		1	1	5	14
E04102	ACEI 9 (Tatarian buckwheat)	enzyme inhibitor	+LGI-		1					1
E01438	ACEI 6.1 (bonito)	enzyme inhibitor	+LKP-					1		1
E06531	ACEI 4 (oriental sesame)	enzyme inhibitor	+LQP-	1						1
E06533	AACEI 6 (oriental sesame)	enzyme inhibitor	+LSA-		1	1				2
E06530	ACEI 3 (oriental sesame)	enzyme inhibitor	+LVY-	1						1
E01336	ACEI 6 (Japanese sardine)	enzyme inhibitor	+LY-	2	4				1	7
E01333	ACEI 3 (Japanese sardine)	enzyme inhibitor	+MF-	1	2	1	1			5
E04101	ACEI 8 (Tatarian buckwheat)	enzyme inhibitor	+PSY-	1						1
E01341	ACEI 12 (Japanese sardine)	enzyme inhibitor	+RVY-					1		1
E01334	ACEI 4 (Japanese sardine)	enzyme inhibitor	+RY-	4	1				1	6
E04068	ACEI 1 (wheat)	enzyme inhibitor	+TF-	1	2	1				4
E01331	ACEI 1 (Japanese sardine)	enzyme inhibitor	+VF-	2				1	1	4
E04097	ACEI 1 (Tatarian buckwheat)	enzyme inhibitor	+VK-	3		4			3	10
E07045	ACEI VPP (bovine)	enzyme inhibitor	+VPP-						1	1
E06385	ACEI WL (soybean)	enzyme inhibitor	+WL-		1		2			3
E01337	ACEI 7 (Japanese sardine)	enzyme inhibitor	+YL-	6	1			1	3	11
E07062	ACEI m (marine shrimp)	enzyme inhibitor	+YLLF-					1		1
E01003	ACEI 5 (snake: jararaca)	enzyme inhibitor	JQK-	9						9
E04099	ACEI 6 (Tatarian buckwheat)	enzyme inhibitor	+YQ-	8						8
E06239	Gonadin Q (rat)	hormone	+EQPz	1						1
E02538	Serum amyloid A peptide 5 (human)	hormone	+GLP-	1						1
E00244	Tyrotropin-releasing hormone [2-3] (pig)	hormone	+HP-	4	1					5
E00285	Hypothalamic peptide IV (pig)	hormone	+YF-	1	2	1			3	7
E00823	TRH-related peptide (human)	hormone	JEPz	2					2	4
E00284	Hypothalamic peptide III (pig)	hormone, enzyme inhibitor	+VW-						1	1
E02539	Serum amyloid A-derived peptide 6 (human)	hormone, transporter	+LP-	8	3	2	1	1		15
E01883	Casein fragment (human)	immunomodulator	+GLF-		1		1			2
E01884	Casein fragment (bovine)	immunomodulator	+LLY-	1						1
E07051	Antihypertensive peptide AFL (Chlorella vulgaris)	neuropeptide	+AFL-	1						1
E06395	Anti-hypertensive peptide beta-Lactosin B (human)	neuropeptide	+ALPM-					1		1
E00596	DE Peptide (rat)	neuropeptide	+DE-	2		1		1	4	8
E01600	Bioactive peptide 3 (hibernating ground squirrel)	neuropeptide	+DY-				1	1		2
E07052	Antihypertensive peptide FAL (Chlorella vulgaris)	neuropeptide	+FAL-	1					1	2
E01598	Bioactive peptide 1 (hibernating ground squirrel)	neuropeptide	+FK-			2		1	3	6
E01801	Bradykinin [8-9] (bovine)	neuropeptide	+FR-	1	1				1	3
E02182	APGWamide-related peptide (common cuttlefish)	neuropeptide	+GWz		1				2	3
E04738	Neuropeptide-like peptide, NLP-32-4 (nematode)	neuropeptide	+GYGG-				1			1
E00983	ECUM inhibitory tripeptide (human)	neuropeptide	+HGK-						1	1
E07055	Antihypertensive peptide IAE (Spirulina platensis)	neuropeptide	+IAE-					1	1	2
E07050	Antihypertensive peptide PPK (pig)	neuropeptide	+PPK-	1						1
E01800	Bradykinin [6-7] (bovine)	neuropeptide	+SP-	3	3				4	10
E00798	Mosquito neuropeptide II (yellowfever mosquito)	neuropeptide	+TRFz		1					1
E07057	Antihypertensive peptide VAF (Spirulina platensis)	neuropeptide	+VAF-						2	2
E01599	Bioactive peptide 2 (hibernating ground squirrel)	transporter	+AL-	3	3	6	2	4	3	21
E01761	Hemoglobin beta chain [026-028] (bovine)	transporter	+ALG-		1					1
E06287	Transporter DtpT 1 (Lysteria monocytogenes)	transporter	+LA-	1	7	4	1	2	6	21
E06288	Transporter DtpT 2 (Lysteria monocytogenes)	transporter	+LGG-		1					1
	TOTAL:	**6 functional types**	**62 different sequences**	**78**	**52**	**26**	**12**	**20**	**54**	**242**

* Standard one-letter code is used. Additional abbreviations: J — pyroglutamic residue, "+" — N-terminal ($^{+}NH_3$— group), "—" — C-terminal (—COO^{-} group).

5-22-102

Folding patterns for double helices in α-peptides

Schramm, Peter; Hofmann, Hans-Jörg*

Leipzig University, Faculty of BioSciences, Pharmacy, and Psychology, Institute of Biochemistry GERMANY

**E-mail: schramm@uni-leipzig.de*

Introduction

Many studies deal with the folding of double helices in nucleic acids. In contrast, much lesser attention has been given to double helices in peptides. Nevertheless, the investigation of peptides with alternating L- and D-α-amino acids, like Gramicidin A, shows various double helix patterns with antiparallel and parallel arrangements of the two strands.[1] These double helices possess dimer periodicity (1:1 alternation). It might be interesting to know which double helices patterns with dimer periodicity exist in α-peptides at all.

Generally, double helices with parallel and antiparallel orientation of the two strands can be expected. Both helix types can only be formed with strands of the same handedness. Parallel and antiparallel β-sheet structures represent borderline cases of double helices. In these structures the interacting amino acids of the two strands are facing. To get helical screws, one must allow for hydrogen bonding interactions between amino acids in different positions of the sequences. In antiparallel double helices, hydrogen bonding occurs always between amino acid pairs, in parallel double helices, the two hydrogen bonding functionalities of an amino acid of one stand are directed to two different amino acids of the other strand. Following these principles, we get the patterns with the nearest neighbour distances between the two strands for parallel and antiparallel double helices in Fig. 1.

In antiparallel type 1 helices, the hydrogen bonds are directed from an even-numbered amino acid of one strand to an odd-numbered amino acid of the other strand and vice versa. In antiparallel type 2 helices, the hydrogen bonds are between the even-numbered amino acids and the odd-numbered amino acids of the two strands, respectively. Based on these types, we can systematically create further double helices, where the hydrogen bonds between the two strands are formed in larger intervals along the sequences. When considering the next two extension steps of the hydrogen bond patterns between the two strands, 6 parallel and 14 antiparallel (6 derived from type 1 and 8 derived from type 2) double helices could principally be possible. These have to be verified by quantum chemical calculations. In this preliminary study, we present the results for antiparallel double helices.

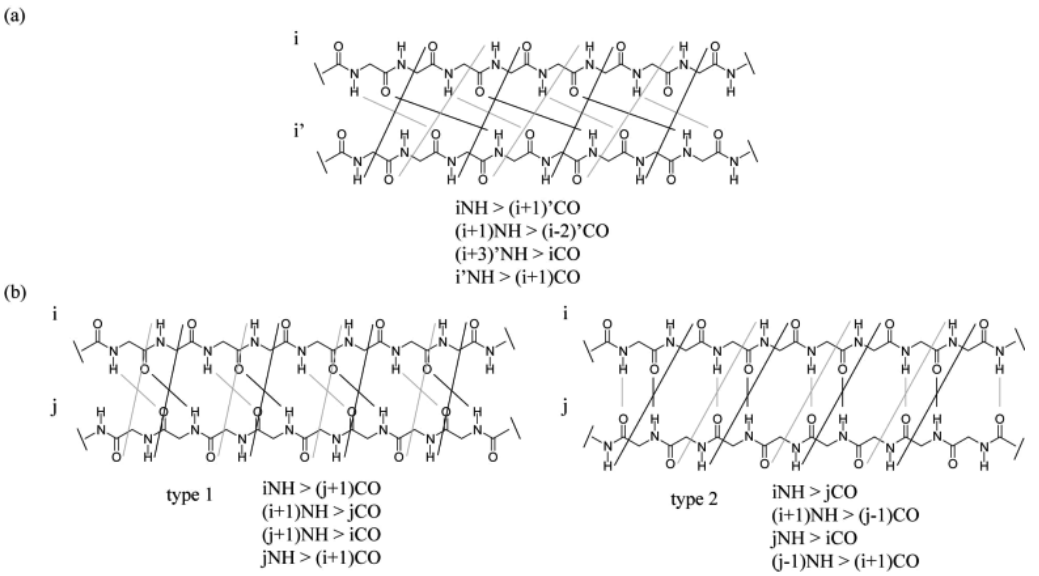

Figure 1. Nearest neighbour hydrogen bonding patterns in double helices with parallel (a) and antiparallel strands (b). The strands of antiparallel helices have opposite direction, but are counted in the same direction.

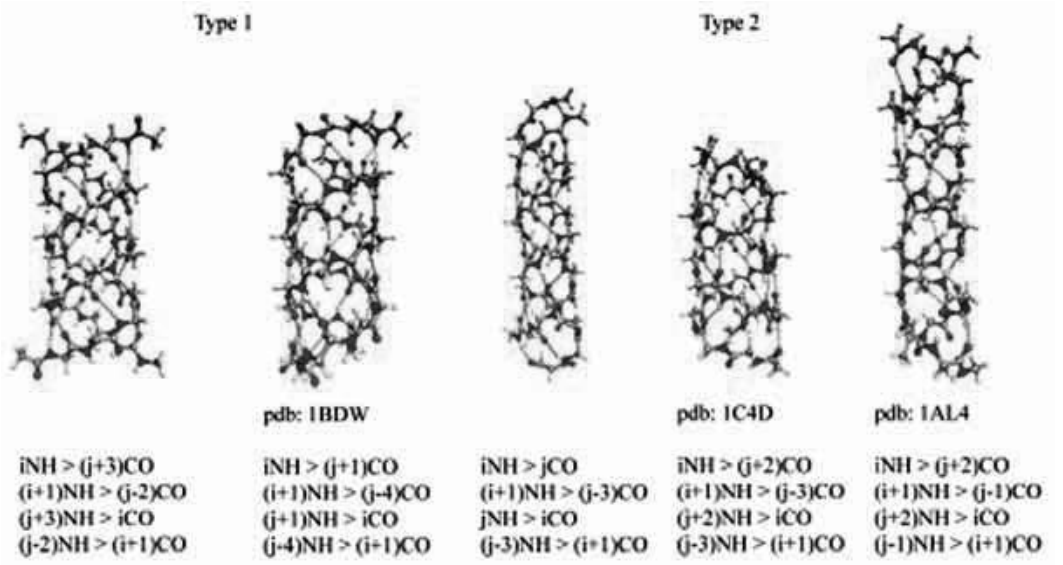

Figure 2. The five most stable antiparallel double helices in α-peptides.[2-4]

Results and discussion

A systematic structure investigation employing ab initio MO theory considering the formal possibilities of hydrogen bonding between two *α*-peptide strands provides an overview on the possible double helix types and their energetic relationships. In detail, the following steps have to be performed. The first step is the generation of different hydrogen bonding patterns for double helices in *α*-peptides according to Fig. 1. Then the geometry optimization of these structures was performed at the HF/6-31G* level of ab initio MO theory. Our calculations confirm all 14 antiparallel double helices predicted for both types. Fig. 2 shows the five most stable helices.

Three of these double helices were also found in experiment. Investigation of side chain influence and a comparable search for parallel double helices is under work.

Acknowledgements

Support of this work by Deutsche Forschungsgemeinschaft (Project HO2346/1-3) is gratefully acknowledged.

References

1. Urry DW, Goodall MC, Glickson JD, Mayers DF. *Proc Nat Acad Sci USA* **68**: 1907-1911, 1971.
2. Burkhart BM, Li N, Langs DA, Pangborn WA, Duax WL. *Proc Nat Acad Sci USA* **95**: 12950-12955, 1998.
3. Burkhart BM, Grassman RM, Langs DA, Pangborn WA, Duax WL. *Biophys J* **75**: 2135-2146, 1998
4. Wallace BA. *RCSB-Protein Data Base*: pdb-Code: 1C4D, 2000.

5-24-103

Cryptic signal: A novel signaling mechanism involving cryptides

Mukai, Hidehito[1,]; Ueki, Nobuhiko[2]; Wakamatsu, Kaori[3]; Kiso, Yoshiaki[1]*

[1]Kyoto Pharmaceutical University, 21st Century COE Program, JAPAN; [2]Mitsubishi Kagaku Institute of Life Sciences, Laboratory of Peptide Signal Engineering, JAPAN; [3]Faculty of Engineering, Gunma University, Department of Biological and Chemical Engineering, JAPAN

[*]E-mail: hmukai-endo@umin.ac.jp

Introduction

It is well known that physiological Regulatory Peptides that act as hormones and neurotransmitters are produced by the specific cleavage of their precursor proteins that per se have no biological functions. During these processes, many fragmented peptides are also produced from the same precursor proteins. It is expected that they may have various unexpected biological activities, but their biological functions have not been investigated in depth. The neutrophil-activating peptides we recently purified turned out to be the peptides that are cleaved from mitochondrial proteins by proteolysis,[1-4] suggesting that fragmented peptides produced by maturation and degradation of functional proteins may also have various biological functions.[5-7] Therefore, we named such functional cryptic peptides hidden in protein sequences *cryptides*, and those cryptides that are derived from mitochondrial proteins "*mitocryptides*" in particular.[3-5] It was also indicated the presence of many cryptides, presumably derived from mitochondrial proteins, that activate neutrophils.[3,4] In the present study, therefore, we tried to identify such neutrophil-activating cryptides systematically and investigated the signaling mechanisms induced by them.

Results and discussion

We identified mitocryptides by the combined investigation with "dry" and "wet" experiments. Namely, the peptide sequences that activate G proteins were predicted based on the distribution of positively charged and hydrophobic residues and the specific cleavage by mitochondrial processing peptidases.[5,8] These predicted peptides were chemically synthesized, and their activities to induce β-hexosaminidase release from neutrophilic/granulocytic differentiated HL-60 cells were examined. As a result, more than forty peptides including mitocryptide (MCT)-3 were identified as neutrophil-activating cryptides. Moreover, the mixture of MCT peptides at the concentrations that did not cause the stimulation by each peptide markedly promoted *β*-hexosaminidase release in the differentiated HL-60 cells, indicating the presence of novel accumulative signaling mechanisms by those mitocryptides whose primary structures are not homologous (Fig. 1).

It is thought that the biologically active peptides which have different amino-acid sequences bind to different receptors, and induce the independent signaling (additive signal, right). In the present study, the presence of the alternative signaling mechanism, which active peptides having the common physicochemical properties bind to the common receptors, was proposed. See text in detail.

To characterize their receptors, N-biotynylated MCT-3 with Cys residue at C-terminus was incubated with neutrophilic/granulocytic differentiated HL-60 cells and molecules that cross-linked with the peptide were purified using streptavidin beads.[9] Five protein bands including HSP-70 were identified as specific binding proteins for MCT-3 by SDS gel-electrophoresis. Moreover, the crosslink between MCT-3 and its binding proteins were prevented by the presence of other mitocryptides whose primary structures were apparently unrelated to MCT-3. We are now characterizing unidentified binding proteins.

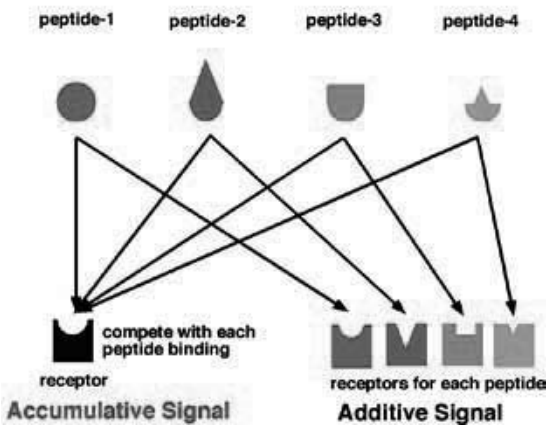

Figure 1. Comparison of the novel accumulative signaling mechanisms and the gclassical h additive signaling mechanisms.

Experimental procedures

All peptide derivatives used in the present study were synthesized by the solid-phase method using Fmoc strategy. HL-60 cells, a cell line derived from human acute leukemia cells, were cultured in RPMI-1640 medium containing 10% fetal bovine serum at 5% CO2 and 37 °C in a humidified atmosphere. To differentiate HL-60 cells into neutrophilic/granulocytic cells, they were treated with 500 μM dibutyryl cyclic adenosine monophosphate for 72 h. The activity of the peptides was measured as described previously.[3,4] In brief, to stimulate the cells with synthetic peptides, cells were washed 3 times with ice-cold HEPES-buffered Hanks solution containing 0.1% bovine serum albumin (HBHS)[3], and cytochalasin B and DNase I were then added, each to a final concentration of 5 μg/ml. Each tube containing cell suspension (90 μl) was preincubated at 37 °C for 10 min, and the synthetic peptide solutions (10 μl) were added to each tube. The samples were incubated at 37 °C for 10 min to stimulate the cells. Immediately after the 10-min incubation, 200 μl of ice-cold reaction quenching buffer was added to the cell suspensions to stop the stimulation. Then, the tubes were centrifuged for 60 sec at 4 °C and 5,000 rpm, and the activities of β-hexosaminidase in the supernatant were measured. To identify the proteins which bind to the active peptides, biotinylated peptides with Cys residue at C-terminus were incubated with the differentiated HL-60 cells for 10 min at 37 °C, and the cells were solubilized after washing with HBHS. Then, proteins with biotynilated peptides were purified using streptavidine beads, and analyzed by SDS gel-electrophoresis.

Acknowledgements

This study was supported by a research grant from the Special Research Project on the Circulation Biosystem, the University of Tsukuba, the Naito Foundation, Mitsubishi Chemical Corporation, JT Inc., and a Grant-in-Aid for Scientific Research (No. 06680605) from the Ministry of Education, Culture, Sports, Science and Technology of Japan.

References

1. Mukai H, Hokari Y, Seki T, Nakano H, Takao T, Shimonishi Y, Nishi Y, Munekata E. *Peptides: The Wave of the Future* 2001: 1014-1015.
2. Mukai H, Matsuo Y, Kamijo R, Wakamatsu K. *Peptide Revolution: Genomics and Therapeutics 2003* (18th American Peptide Symposium), Chorev M Sawyer T (Eds), American Peptide Society, Boston, MA, U.S.A., 2004, pp 553-555.
3. Mukai H, Hokari Y, Seki T, Takao T, Kubota M, Matsuo Y, Tsukagoshi H, Kato M, Kimura H, Shimonishi Y, Kiso Y, Nishi Y, Wakamatsu K, Munekata E. *J Biol Chem* 283: 30596-30605, 2008.
4. Mukai H, Seki T, Nakano H, Hokari Y, Takao T, Kawanami M, Kiso Y, Shimonishi Y, Nishi Y, Munekata E. *J Immunol* **182**: 5072-5080, 2009.
5. Ueki N, Someya K, Matsuo Y, Wakamatsu K, Mukai H. *Biopolymers (Peptide Science)* **88**: 190-198, 2007.
6. Mukai H, Kikuchi M, Fukuhara S, Kiso Y, Munekata E. *Biochem Biophys Res Commun* 375: 22-26, 2008
7. Mukai H, Suzuki Y, Kiso Y, Munekata E. *Protein Pept Lett* **15**: 931-937, 2008.
8. Mukai H, Munekata E, Higashijima T. *J Biol Chem* **267**: 16237-16243, 1992.
9. Hofmann K, Kiso Y. *Proc Natl Acad Sci U S A* **73**: 3516-3518, 1976; Hofmann K, Finn FM, Kiso Y. *J Am Chem Soc* **100**: 3580-3590, 1978.

5-28-104

The binding of peptides containing tyrosine residue to β-cyclodextrin

Czaplewski, Cezary; Czaplewska, Paulina; Romankiewicz, Justyna; Wiczk, Wiesław*

University of Gdańsk, Faculty of Chemistry, POLAND

**E-mail: czarek@sun1.chem.univ.gda.pl*

Introduction

Cyclodextrins are cyclic oligomers of 1,4-linked, α-D-glucose monomers that have a hydrophilic exterior and a hydrophobic center. This enables cyclodextrins to form inclusion complexes with various organic molecules.[1] Aromatic amino acid residues bind to *β*-cyclodextrin with deep penetration of the cyclodextrin cavity. In case of oligopeptides binding depends on the peptide conformation.[2] The formation of *β*-cyclodextrin inclusion complexes with three peptides of sequences shown in Table 1 was investigated experimentally using steady-state fluorescence spectroscopy and theoretically by molecular dynamic simulations. The objective of this study is to develop an understanding of how these peptides bind to *β*-cyclodextrin.

Results and discussion

The three peptides studied consist of eighteen amino acids and the tyrosine residues are located at the position 1, 2 or 4. Selected sequences are fragments of NOTCH receptors.[3] The free energy along the reaction pathway (potential of mean force, PMF) delineating the inclusion of tyrosine's aromatic ring into *β*-cyclodextrin was computed using umbrella sampling molecular dynamic simulation. Two different solvation models were used: implicit generalized Born (GB) solvation and explicit water model. There is a good agreement between experimental results of steady-state fluorescence spectroscopy and molecular dynamic simulations with both solvation models. Only for NOTCH2 and NOTCH3 peptides enhancements in tyrosine fluorescence on adding cyclodextrin was observed. No changes in emission spectra were observed for NOTCH1. The titration of NOTCH2 peptide with cyclodextrin gives linear dependence of fluorescence intensity as function of cyclodextrin concentration, which only allows estimation of binding constant as close to zero. Therefore experiments show that out of three peptides studied only NOTCH3 binds strongly to *β*-cyclodextrin with binding constant similar to that of AcTyrNHMe.

Theoretical studies using both explicit water and implicit GB solvation show that NOTCH3 interacts with *β*-cyclodextrin stronger than other two peptides. The differences between PMFs for NOTCH3 and other two peptides are more distinct in case of explicit water simulations. The PMF for NOTCH3 peptide interaction with *β*-cyclodextrin has low free energy minimum, around 4 kcal/mol for explicit water simulations and 3 kcal/mol for implicit solvent simulation, for deep penetration of the cavity of *β*-cyclodextrin by tyrosine sidechain (distance between the center of tyrosine ring and central plane of *β*-cyclodextrin is close to zero). For other two peptides minima on PMFs are shallower and shifted to larger distances, which shows that tyrosine ring is only partially buried in the *β*-cyclodextrin cavity. The theoretical association constant and the corresponding association free energy were derived by integrating the free energy profiles over a representative ordering parameter. Theoretical association constant for NOTCH3 is much higher than for other two peptides and is the same order of magnitude as experimental value.

The binding of cyclodextrins depends on accessibility of tyrosine sidechain and only sequnce of NOTCH3 peptide allows for deep and tight penetration of tyrosyl group within the *β*-cyclodextrin cavity. The binding of cyclodextrins with phenolic compounds involves nonspecific van der Waals and hydrophobic interactions and depends on accessibility of tyrosine sidechain.

Table 1. Sequences of peptides studied, experimental and theoretical association constants and association free energies of their complexes with *β*-cyclodextrin

label	sequence	K_{exp} [dm³/mol]	Kt_{heor} [dm³/mol]	ΔG_{theor} [kcal/mol]
NOTCH1	YKIEAVQSETVEPPPPAQ	- [a]	0.98	0.01
NOTCH2	TLSYPLVSVVSESLTPER	0 [b]	0.7	0.2
NOTCH3	PYPLRDVRGEPLEPPEPS	80	34	-2.1

[a] no changes in fluorescence spectra as function of added β-CD
[b] linear dependence of fluorescence intensity as function of added β-CD

Methods

The free energy profiles were calculated using umbrella sampling molecular dynamics (MD) with the Weighted Histogram Analysis Method (WHAM).[4] In umbrella sampling simulations restraints were imposed on the distances d_1,d_2,d_3 between center of Tyr ring and three selected oxygen atoms of cyclodextrin. Molecular dynamic simulations, using AMBER 9 package[5] of 2ns

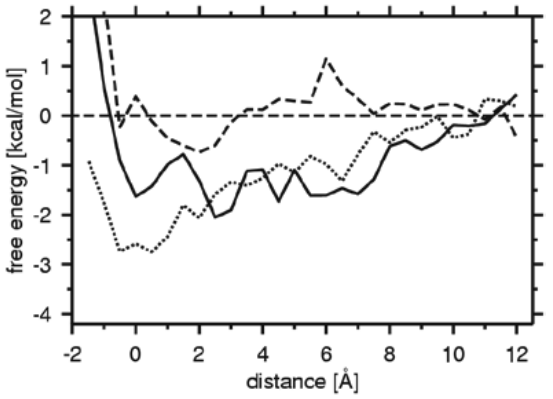

Figure 1. Free energy profiles obtained from implicit solvent (GB) simulations for inclusion of NOTCH1 (solid line), NOTCH2 (dashed line) and NOTCH3 (dotted line) into *β*-cyclodextrin cavity.

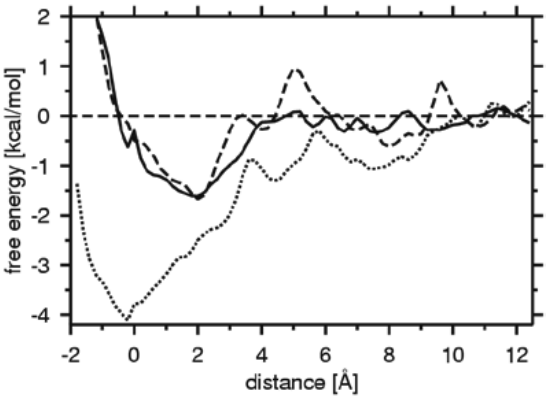

Figure 2. Free energy profiles obtained from explicit solvent simulations for inclusion of NOTCH1 (solid line), NOTCH2 (dashed line) and NOTCH3 (dotted line) into *β*-cyclodextrin cavity.

using explicit TIP3P water model[6] and 1ns using implicit GB solvation[7] were performed for 24 windows with a harmonic restraining potential with the force constant 2 kcal/mol/Å, and the equilibrium distance for a given window equal to 3.5, 4.0, 15.0 Å for windows 1 to 24. Using the weighted histogram analysis method (WHAM)[4] free energy profiles were projected as function of distance x between center of Tyr ring and plane π in the center of cyclodextrin molecule. Plane π is defined by seven oxygen atoms from cyclodextrin ring marked as spheres on Fig. 3.

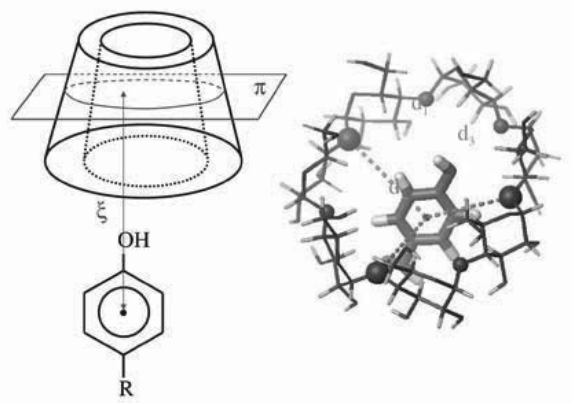

Figure 3. A schematic representation of restrains used in umbrella sampling simulations.

Acknowledgments

This work is supported by grant DS 8372-4-0138-8 from the Polish Ministry of Science and Higher Education. This research is conducted by using the resources of our Beowulf cluster at the Molecular Modeling Group Faculty of Chemistry University of Gdańsk and the Informatics Center of the Metropolitan Academic Network (TASK) in Gdańsk.

References

1. Rekharsky MV, Inoue Y. *Chem Rev* **98**: 1875-1917, 1998.
2. Bekos EJ, Gardella Jr JA, Bright FV. *J Incl Phenom Mol Rec Chem* **26**: 185-195, 1996.
3. Baron M. *Semin Cell Dev Biol* **14**: 113-119, 2003.
4. Kumar S, Bouzida D, Swendsen RH, Kollman PA, Rosenberg JM. *J Comput Chem* **13**: 1011-1021, 1992.
5. Case DA, Darden TA, Cheatham TE, III, Simmerling CL, Wang J, Duke RE, Luo R, Merz KM, Pearlman DA, Crowley M, Walker RC, Zhang W, Wang B, Hayik S, Roitberg A, Seabra G, Wong KF, Paesani F, Wu X, Brozell S, Tsui V, Gohlke H, Yang L, Tan C, Mongan J, Hornak V, Cui G, Beroza P, Mathews DH, Schafmeister C, Ross WS, Kollman PA, *AMBER 9*, University of California, San Francisco, 2006.
6. Jorgensen WL, Chandrasekhar J, Madura J, Klein ML. *J Chem Phys* **79**: 926-935, 1983.
7. Tsui V, Case DA. *Biopolymers* (*Nucl Acid Sci*) **56**: 275-291, 2001.

6-07-001

Artificial intelligence delivers superb antibiotics for superbugs

Jenssen, Håvard[1,]; Hilpert, Kai[1]; Fjell, Christopher D[1]; Waldbrook, Matt[1]; Mullaly, Sarah D[1]; Volkmer, Rudolf[2]; Cherkasov, Artem[1]; Hancock, Robert EW[1]*

[1]University of British Columbia, CANADA; [2]Humboldt-Universität zu Berlin, GERMANY

[*]E-mail: jenssen@cmdr.ubc.ca

Introduction

There is currently an alarming spread of so-called "Superbugs", bacterial strains that are resistant to multiple or all antibiotics.[1] A new drug class that has demonstrated promising results in inhibiting many of these Superbugs is founded on the naturally occurring cationic antimicrobial host defense peptides (12-50 residues, rich in R/K and hydrophobic residues).[2] Despite this promising potential, peptide antibiotics have shown limited success to date. To overcome the challenges in the design and optimization of antimicrobial peptides, we utilized here experimental data from large random 9-mer peptide libraries in combination with the descriptive power of atomic-resolution chemical descriptors and the predictive ability of an artificial neural net approach. By combining these disciplines we were able to design and correctly predict the biological activity of large pools of potent antimicrobial peptide candidates capable of combating life-threatening, multi-drug resistant pathogens.

Results and Discussion

Two computer-selected semi-random cellulose peptide libraries (Set-A; 943- and Set-B; 500 peptides) were iteratively designed by moderately adjusting the amino acid composition of Set-B to the preferences indicated by the best Set-A peptides. The antibacterial activity was measured by *lux* assay, demonstrating high antibacterial activity for 28% of the peptides in Set-A and 53% in Set-B. Thus the amino acid composition of the Set-B peptides was used for semi-random computer generation of 100K virtual 9-mer peptides. We abstracted from the conventional amino acid level and calculated a number of 'inductive' chemical descriptors.[3] To relate chemical descriptors to antimicrobial activity of the peptides in the two tested 9-mer libraries, we employed the method of artificial neural networks. The 10-fold cross validated atomic-based QSAR models for Set-A, Set-B and Set-A+B resulted in a total of 30 neural net models, which were utilized to predict the activity of all 100K virtual peptides. The peptides were sorted by hypothetical activity based on voting (predicted 5% most active) and overall ranking, and sorted into four quartiles of 25K peptides (Q1-Q4), expected to contain high-activity, medium–, low– and inactive entries, respectively. To evaluate the developed structure-activity models, 50 peptide candidates were selected from each quartile and their activities were tested against *P. aeruginosa* using the *lux* assay, demonstrating a remarkable correlation to the antibacterial activity predicted by the QSAR model. Antibacterial testing of the 200 peptides also demonstrated an excellent distribution of their activity levels, matching the predicted activity levels in the 4 quartiles (Table 1). Importantly peptides from each quartile had similar charge, hydrophobicity, and amphipathicity, each of which have been considered to be critical determinants for antimicrobial activity.[4] Two peptide candidates from Q1 were selected, synthesized on solid phase and tested for antibacterial activity using standard MIC assays, revealing broad spectrum activity against several multi-drug resistant pathogens (Table 2). The peptides were tested *in vivo* in a well-established[5] mouse model of invasive *Staphylococcus aureus*, in comparison to a control peptide MX-226 (currently most advanced antimicrobial peptide in clinical trails). Female CD1 mice were infected intraperitoneally (IP) with ~10^9 bacteria of *S. aureus*, and injected IP with peptides (4 mg/kg) 4h post-infection. Peritoneal counts 24h later demonstrated a 2.5-$\log_{10}$ bacterial reduction in the presence of HHC-10 and a 1-$\log_{10}$ reduction for HHC-36 ($p<0.001$ by Chi-square analysis with a 95% confidence interval for both), while MX-226 demonstrated no significant effect.

Conclusions

We have demonstrated here that QSAR methodology combined with an artificial neural net approach can significantly accelerate the discovery of antimicrobial peptides, even from semi-random starting points based on diverse peptide sequences.

Table 1. Numbers of Peptides having particular Relative IC_{50} values (50% inhibition values in μM) of 200 representative peptides from the 100K peptide virtual library separated into four quartiles Q1-Q4 (Q1 being predicted as most active)

	Rel. IC_{50}			
Quartile	<0.5	0.5-2.0	25 > 2.0	>25
Q1	47	3	-	-
Q2	32	16	1	1
Q3	2	6	38	4
Q4	-	-	44	6

Table 2. Activities against multi-resistant Superbugs, HHC-10 and HHC-36, compared to control peptide MX-226 as well as the highly utilized antibiotic ciprofloxacin. NB; the table gives MIC values (μM) measured in 3-5 replicates against MDR (multidrug resistant), ESBL (extended spectrum β-lactamases producing), MRSA (methicillin resistant *S. aureus*), and VRE (vancomycin-resistant Enterococci) pathogens

Bacterium	MIC (μM)			
	MX-226	HHC-10	HHC-36	Ciprofloxacin
P. aeruginosa (MDR)	153	1.5	1.4	97
E. coli (ESBL)	38	1.5	2.7	>386
K. pneumonia (ESBL)	76	6.2	22	193
S. aureus (MRSA)	19	1.5	1.4	6.0
E. faecium (VRE)	76	1.5	1.3	386

Acknowledgements

We gratefully acknowledge financial support from the Canadian Institutes for Health Research (CIHR) and the Foundation of the National Institutes of Health and CIHR through the Grand Challenges in Global Health Initiative.

References

1. Hancock REW. The end of an era? *Nature Reviews Drug Discovery* **6**: 28, 2007.
2. Hancock REW, Sahl HG. Antimicrobial and host-defense peptides as new anti-infective therapeutic strategies. *Nat Biotechnol* **24**: 1551-1557, 2006.
3. Cherkasov A. Inductive QSAR descriptors, distinguishing compounds with antibacterial activity by artificial neural network. *Int J Mol Sci* **6**: 63-86, 2005.
4. Jenssen H, Gutteberg TJ, Lejon T. Modelling of anti-HSV activity of lactoferricin analogues using amino acid descriptors. *J Pept Sci* **11**: 97-103, 2005.
5. Scott MG *et al*. An anti-infective peptide that selectively modulates the innate immune response. *Nat Biotechnol* **25**: 465-472, 2007.

6-01-101

Design and synthesis of asymmetric β-Sandwich Proteins

*Fritzemeier, Kai; Haehnel, Wolfgang**

University of Freiburg, Institute of Biology II / Biochemistry GERMANY

**E-mail: haehnel@uni-freiburg.de*

Computational design has been successful in creating proteins as well as changing their function.[1,2] The tight packing of the hydrophobic core of proteins with a selection of amino acid sidechain conformations (rotamers) provides a basic concept of protein design.

We have developed a program termed ProPac to optimize the packing in the hydrophobic core of proteins with a given backbone. The program is adopted to the possibilities of peptide chemistry e.g. the coupling of identical fragments on a template generating symmetric parts in the sequence. Our program was tested by repacking the core of ten natural proteins, and compared with the program ROSETTA.[3] The output of both programs was very close to the natural sequences and showed slightly different but equivalent variations of residues. We have focused on the design of a *β*-sandwich protein. Characteristic for a *β*-sandwich are the H-bonds between neighboring strands on a tightly packed hydrophobic core and a tendency of aggregation.

Starting with a backbone with two anti-parallel four-stranded sheets derived from the *β*-sandwich of the µ2 Adaptin subunit (1BW8.PDB) the program ProPac was used to pack cores with different symmetries. In a first approach a hydrophobic core was optimized to be assembled from two identical antiparallel *β*-sheets which avoids the conformational memory. The molecule was synthesized from four *β*-hairpins selectively coupled to a cyclic decapeptide template (TASP)[4] via bromoacetylated amino groups (N-terminus or C-terminal diaminopropionic acid) to orthogonally deprotected cysteines of the template.

Iteratively increasing the number of positive surface residues reduced the aggregation of the proteins from large aggregates (1600 kDa) to stable dimers.[5] The *β*-structure was consistent with CD- and FTIR (Fourier transform infrared) spectra. Guanidinium chloride dependent reversible unfolding indicates a free energy near – 25 kJ/mol.

In a second approach the design was modified to partial asymmetric sandwiches assembled from three different hairpins (*c.f.* **A** in the scheme). To our knowledge such a *β*-structure has not yet been designed. ProPac was used to calculate large sets of hydrophobic cores. 5000 cores with lowest energy were used for further sequence selection. The selected molecules included a tryptophane with the intention to determine the folding energy by fluorescence measurements. Glycines were limited to a maximum of three. The remaining protein cores and the backbone were energy minimized using the CHARMM package and then selected for a maximum number of hydrogen bonds and no holes which could harbor a water molecule in the hydrophobic core. The surface was the previously optimized one.

CD and FTIR spectra of this protein termed BetaMOP-4 confirmed *β*-fold, fluorescence measurements show a free energy of folding of -20 kJ/mol. The molecule is the first synthetic *β*-sandwich molecule showing a defined fold in NMR. The crosspeaks in 2D-COSY experiments show a typical *β*-sheet distribution, extending well into the characteristic regions >8.5 ppm (for amide protons) and >5.0 ppm (for Hα signals). The structure is stable up to more than 80 °C as indicated by 1D-NMR. The folding of BetaMOP-4 compared to the symmetric molecules BetaMOP-1, -2, -3 and the symmetric betabellins[6] seem to indicate that *β*-sandwiches from identical sheets may not fold into defined structures.

The rather tedious assembly of four *β*-hairpins on the peptide template led us to simplify the synthesis of *β*-sandwiches by directed coupling of two four-stranded antiparallel *β*-sheets (*c.f.* **B** in the scheme). This allows the fast synthesis of completely asymmetric *β*-sandwiches. The core of these proteins was designed by an iterative calculation. To find an optimal crosslink between the two *β*-sheets all rotamers of crosslinks (bromoacetylated diaminopropionic acid and bromoacetylated diaminobutyric acid coupled to a cystein) were tested. Ten backbones with different crosslinker rotamers were packed and selected as described for the partially symmetric molecule. After a molecular dynamics simulation and a second packing calculation the cores with the highest number of hydrogen bonds, no holes and good results in procheck were selected for further analysis. Molecular dynamics was used to evaluate the stability of the folds. The best two cores were selected for synthesis. To analyze the contribution of the surface and the hydrophobic core to the folding free energy both cores were synthesized with two different surfaces. In addition to the symmetric surface an asymmetric one was designed with amino acids based on statistically determined probabilities in natural proteins. At the new surface the excess of positive charges was reduced from +7 to +4.

All molecules show *β*-structure in CD. Preliminary data suggest that the fraction of *β*-folding is determined by the hydrophobic core. The folding free energies of the molecules suggest an additive contribution of the

hydrophobic core and the surface. One of our remaining goals is to find a correlation between the experimentally determined protein stability and the parameters used for the selection of the residues in the hydrophobic core and at the surface.

Acknowledgements

NMR measurements were done by Dr. G. Gemmecker and Prof. Dr. H. Kesser (Technical University of Munich).

References

1. Kuhlman B, Dantas G, Ireton G, Varani G, Stoddard B, Baker D. *Science* **302**: 1364–1368, 2003.
2. Looger L, Dwyer M, Smith J, Hellinga H. *Nature* **423**: 185–190, 2003.
3. Kuhlman B, Baker D. *Proc Natl Am Soc U S A* **97**: 10383-10338, 2000.
4. Mutter M, Altman E, Altman H, Hersperger R, Koziej P, Nebel K, Tuchscherer G, Vuilleumier S. *Helv Chim Acta* **71**: 835–847, 1988.
5. Fritzemeier K, Haehnel W. *Peptides 2004* (*Proceedings of the Third Intern. and Twenty-Eighth European Peptide Symposium, Prague, Czech Republic*). Flegl EM, Slaninova S, Fridkin M, Gilon C (Eds), Kenes Intern., Geneva, Switzerland, 2005, pp 716-171.
6. Lim A, Makhov A, Bond J, Inouye H, Connors L, Griffith J, Erickson B, Kirschner D, Costello C. *J Struct Biol* **130**: 363-370, 2000.

6-07-102

NMR solution structure analysis of the active and inactive fragments of pheromone biosynthesis-activating neuropeptide (PBAN) from the silkmoth *Bombyx mori*

Nagata, Koji[1,]; Okada, Akitoshi[2]; Ohtsuka, Jun[1]; Takahashi, Mihoko[1]; Kawai, Takeshi[1]; Sugisaka, Arisa[1]; Hull, J Joe[3]; Moto, Ken-ichi[3]; Matsumoto, Shogo[3]; Nagasawa, Hiromichi[1]; Tanokura, Masaru[1]*

[1]The University of Tokyo, Grad. Sch. of Agric. Life Sci., JAPAN; [2]The University of Tokyo, Grad. Sch. of Sci., JAPAN; [3]RIKEN, Mol. Entomol. Lab., JAPAN

[*]E-mail: aknagata@mail.ecc.u-tokyo.ac.jp

Introduction

In most moths, the sex pheromone production is regulated by pheromone biosynthesis-activating neuropeptide (PBAN), a 33-34 amino acid neuropeptide that is released from the subesophageal ganglion into the hemolymph in response to physiological and environmental cues.[1] PBAN exerts its pheromonotropic effects by binding to PBANR, a member of the rhodopsin-like family of G protein-coupled receptors (GPCR) that is predominantly expressed in the pheromone-producing cells of the female pheromone gland.[2] The structure-activity relationship studies for *Bombyx mori* PBAN have revealed that the shortest peptide with pheromonotropic activity is the C-terminal pentapeptide-amide, PBAN(29-33)-NH_2 (FSPRL-NH_2), and that the C-terminal amide group is required for the pheromonotropic activity of PBAN.[3] In this study, we have analyzed the solution structures of the C-terminal decapeptides derived from *Bombyx mori* PBAN with an amidated and a free C-termini by two-dimensional NMR.

Results and discussion

The decapeptides, PBAN(24-33)-NH_2 and -OH, were synthesized by Fmoc-based solid-phase synthesis. The sample for NMR measurements contained 10 mM PBAN(24-33)-NH_2 or -OH dissolved in (1) 50 mM sodium phosphate buffer (pH 6.0)/100 mM NaCl/0.02% NaN_3 in 90% (v/v) H_2O/10% (v/v) D_2O (buffer A), (2) 500 mM dodecyl phosphocholine (DPC)-d_{38} in buffer A, or (3) 30% (v/v) 2,2,2-trifluoroethanol (TFE)-d_3 in buffer A. DQF-COSY, TOCSY (mixing time, 50 ms) and NOESY (mixing time, 100, 200, 300, 400, or 500 ms) spectra recorded at 25 °C on a Unity Inova 500-MHz spectrometer (Varian). The acquired NMR data were processed, displayed and analyzed with the softwares, NMRPipe, NMRDraw and Sparky. All the observed proton resonances were assigned by the conventional sequential assignment procedure. In buffer A, very few NOE cross-peaks were detected for both the peptides even with a long mixing time as 500 ms, which indicated that both the peptides did not take a specific conformation in aqueous solution at pH 6.0. But in the presence of DPC-d_{38} micelles or 30% (v/v) TFE-d_3 in buffer A, many NOE cross-peaks were observed for both the peptides, which indicated that both the peptides adopted specific conformations under these solvent conditions. Solution structures of these peptides were calculated using interproton distance restraints derived from cross-peak intensities in the NOESY spectrum (mixing time, 200 ms). The cross-peak intensities were translated to interproton distances using the macro CALIBA implemented in the program CYANA. Pseudoatom corrections were added to the upper bound distance restraints involving degenerate protons from methylene groups and aromatic rings. Solution structures were calculated with ca. 100 NOE-derived distance restraints by torsion angle dynamics using the program CYANA. Twenty conformers with the lowest CYANA target functions were used to represent the solution conformation of these peptides (Fig. 1). The RMS deviations of atomic coordinates of the 20 structures range 0.001-0.038 nm for the backbone atoms and 0.038-0.127 nm for all the non-hydrogen atoms.

In the presence of DPC micelles, the two peptides took a similar β-turn structure at the C-terminal SPRL segment. Their β-turns, however, belonged to different types: types II and III in PBAN(24-33)-NH_2 and -OH, respectively. Types II and III β-turns have the same value for φ_{i+1} (-60°), but different values for ψ_{i+1} (120° and -30°), φ_{i+2} (80° and -60°), and ψ_{i+2} (0° and -30°), where the residues at positions i+1 and i+2 correspond to Pro^{31} and Arg^{32} of PBAN. In 30% (v/v) TFE, the two peptides took distinctly different conformations. PBAN(24-33)-NH_2 took a type-I β-turn at the C-terminal SPRL segment. In contrast, PBAN(24-33)-OH did not take a β-turn, but instead took an extended conformation. The NMR structural analyses thus indicated the C-terminal amide group contributed to the stabilization of the β-turn formed by the C-terminal SPRL segment, although its types are different depending on the solvent used (types II and I in the presence of DPC micelles and 30% (v/v) TFE, respectively). Several reports already showed that the C-terminal segment of PBAN adopted the β-turn structure.[4-8] Our results have demonstrated for the first time that the C-terminal amide group of PBAN contributes to the stabilization of the β-turn formed by the C-terminal SPRL segment. When the amide group is lost, the β-turn structure is abolished in 30% (v/v) TFE or the type of the β-turn changes from type II to type III in the presence of

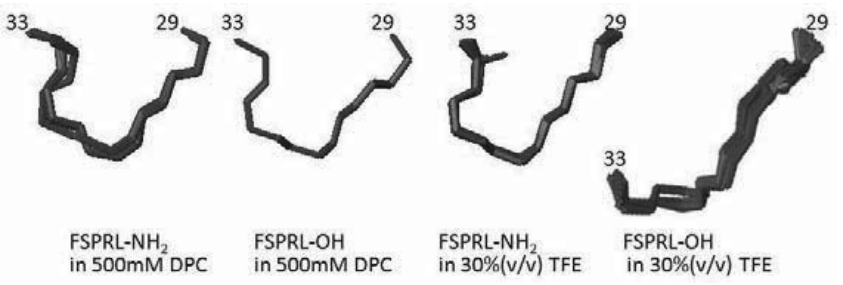

Figure 1. NMR structures of PBAN(24-33)-NH_2 and -OH in DPC micelles and 30% (v/v) TFE. The C-terminal five residues (FSPRL), the minimal length for the PBAN activity, are shown.

DPC micelles. It was shown that the C-terminal β-turn of PBAN in 30% (v/v) TFE was type I',[8] but our results have shown that the β-turn is its mirror image, type I. The reason for this inconsistency is unclear.

In summary, the NMR structural studies of the active and inactive fragments of PBAN, PBAN(24-33)-NH_2 and -OH, have revealed that these decapeptides do not adopt a specific conformation in phosphate buffer (pH 6.0), but they adopt specific conformations at the C-terminal SPRL segment under an amphiphilic condition and in a water/alcohol mixed solvent. PBAN(24-33)-NH_2 takes types II and I β-turns, while PBAN(24-33)-OH takes type III β-turn and an extended conformation in the presence of DPC micelles and in 30% (v/v) TFE, respectively. The different conformations of the peptide fragments with an amidated and a free C-termini indicate that the C-terminal amide group contributes to the stabilization of the β-turn structure, which is probably important for exerting the PBAN activity.

Acknowledgements

This research was supported by Targeted Proteins Research Program (TPRP) from the Ministry of Education, Culture, Sports, Science and Technology of Japan.

References

1. Kitamura A, Nagasawa H, Kataoka H, Inoue T, Matsumoto S, Ando T, Suzuki A. *Biochem Biophys Res Commun* **163:** 520-526, 1989.
2. Hull JJ, Ohnishi A, Moto K, Kawasaki Y, Kurata R, Suzuki MG, Matsumoto S. *J Biol Chem* **279:** 51500-51507, 2004.
3. Nagasawa H, Kuniyoshi H, Arima R, Kawano T, Ando T, Suzuki A. Arch Insect Biochem Physiol **25:** 261-270, 1994.
4. Nachman RJ, Roberts VA, Dyson HJ, Holman GM, Tainer JA. *Proc Natl Acad Sci U S A* **88:** 4518-4522, 1991.
5. Nachman RJ, Kuniyoshi H, Roberts VA, Holman GM, Suzuki A. *Biochem Biophys Res Commun* **193:** 661-666, 1993.
6. Wang YS, Kempe TG, Raina AK, Mazzocchi PH. *Int J Peptide Protein Res* **43:** 277-283, 1994.
7. Nachman RJ, Roberts VA, Holman GM, Beier RC. *Reg Peptides* **57:** 359-370, 1995.
8. Clark BA, Prestwich GD. *Int J Peptide Protein Res* **47:** 361-368, 1996.

6-07-103

Membrane interactions of primate antimicrobial cathelicidins LL37 and RL37

Morgera, Francesca[1]; Antcheva, Nikolinka[1]; Scaini, Denis[2]; Pacor, Sabrina[1]; Vaccari, Lisa[2]

[1]University of Trieste, Department of Life Sciences, ITALY; [2]ELETTRA Synchrotron Light Laboratory, Trieste, ITALY

E-mail: atossi@units.it (Tossi, Alessandro)

Introduction

Cathelicidins are a family of vertebrate host defence peptides with the capacity to inactivate microbes and to modulate host immune and healing processes.[1] LL-37, the only human cathelicidin, displays a broad-spectrum, medium sensitive antimicrobial activity *in vitro* accompanied by some cytotoxicity, and a strong capacity to modulate host cells at lower concentrations. These activities likely all involve interaction with biological membranes at some point, and are related to its amphipathic, helical structure. They are modulated by its tendency to structure and aggregate under physiological conditions, due to the presence of numerous intramolecular salt-bridges.[2] These are evolved features that are absent in some primate orthologues, which structure only in the presence of membranes.[3]

Results and discussion

The structural and aggregational behaviour of human hssLL37 and orthologues from orang-utan (ppyLL-37) and rhesus macaque (mmuRL-37) (Table 1) were investigated under different conditions and in the presence of model membranes. CD spectroscopy confirmed that hss and ppyLL-37 (Fig. 1), with an excess of intramolecular electrostatic attractions over repulsions, were structured, and likely aggregated, in phosphate buffered saline (PBS), while RL-37, with repulsions > attractions, remained random-coiled. All three peptides were fully structured in the presence of 50% TFE or SDS micelles, as well as in the presence of anionic anionic (PG/dPG) LUVs. With zwitterionic (PC:SM:Ch) LUVs, hss- and ppyLL-37 maintained a similar helicity as in PBS, while RL-37 remained random coiled. All peptides were monomeric in the presence of TFE or SDS micelles, as indicated by a $[\theta]_{222}/[\theta]_{208}$ ratio < 1,[4] and RL-37 remained so also in the presence of anionic LUVs, whereas hss and ppyLL-37 may remain aggregated in the presence of biological membranes (ratio ≥ 1 for anionic or neutral LUVs). ATR-FTIR spectroscopy, in the presence of supported PG bilayers, confirms that both LL-37 and RL-37 interact with the anionic membrane in a structured form, with sharp amide I bands respectively centred at 1652 and 1656 cm^{-1}, typically assigned to a helical structure. CN stretching frequencies with symmetric and antisymmetric modes shifted to about 1635 and 1685 cm^{-1}, respectively, are consistent with intramolecular side-chain salt-bridging occurring within a relatively hydrophobic environment.[5] Broadening of lipid acyl bands and a shift in the CH_2 antisymmetric and symmetric stretching modes upon peptide binding indicate that both peptides insert into and perturb the membrane. mmuRL-37 however shows greater shifts in amide bands and acyl stretching modes than LL-37, suggesting deeper insertion and a greater effect on the lipid order. AFM measurements on the supported lipid bilayer indicated different morphological effects on the membrane, with RL-37 destroying phase homogeneity and producing amorphous lesions of varying sizes, while LL-37 preserves phase homogeneity and produces smaller, homogeneous hole-like lesions. Given the AFM tip resolution limits (10 nm), the size of these holes (< 10 nm) and the positive membrane curvature around them is consistent with the formation of toroidal pores.

Table 1. Sequence and physico-chemical properties of LL-37 orthologues

peptide	sequence*	q	<H>‡	μH‡	attractions§ repulsions	% helix	
						(PBS)	(TFE)
LL-37	LLGDFFRKSKEKIGKEFKRIVQRIKDFLRNLVPRTES	+6	-1.83	0.59	9/7	30	70
*ppy*LL-37	LLGDFFRKAREKIGEEFKRIVQRIKDFLRNLVPRTES	+4	-1.70	0.59	11/5	65	65
*mmu*RL37	RLGNFFRKVKEKIGGGLKKVGQKIKDFLGNLVPRTAS	+8	-1.66	0.56	4/5	<5	73

*Conserved residues in orthologues relative to human LL-37 are shaded grey; qCharge; ‡Mean hydrophobicity and relative hydrophobic moment, calculated as described;[3] §Intermolecular side-chain attractions and repulsions, as derived.[3]

Flow cytometric measurements of *E. coli* cells in the presence of both PI and the membrane potential probe DiBAC4(3) indicated that mmuRL-37 permeabilized cells somewhat more efficiently than LL-37 and depolarised them much more rapidly, whereas dye release experiments with anionic PG/DPG LUVs loaded with the ANTS/DPX fluorescent dye/quencher pair indicated a permeabilising capacity with trend ppyLL-37 > hssLL-37 > mmuRL-37. The apparent inconsistency of permeabilisation data with real and model membranes may be explained by a greater tendency of hss and ppyLL-37 to bind non-productively with non-membrane components than mmuRL-37. Assays in medium ranging from 5% to 50% Tryptic soy broth showed an unvaried antimicrobial potency for mmuRL-37 under all conditions (full growth inhibition of 106 CFU by 0.5-1 μM peptide), while ppy and hssLL-37 lost activity in higher medium (full growth inhibition required 5-10 μM peptide). mmuRL-37 is more active on both G+ and G- bacteria than the LL-37 orthologues under all conditions, indicating it is less affected by interaction with bacterial outer cell-wall components (LPS, peptidoglycan).

The evolution of primate cathelicidin leads to sequence variations that determine distinct structuring capacities for different orthologues and result in different modes of membrane interaction and different types of membrane lesions. Some orthologues are random-coil in physiological solution and structure only at the bacterial surface. This ensures a potent, broad-spectrum activity *in vitro* that is relatively insensitive to salt or medium effects, or interaction with cell wall components, ultimately resulting in membrane damage by an apparent carpet-like mechanism. Others have gained a salt-dependent capacity to structure and aggregate in solution, and their activity affected by medium in a manner that apparently reduces their direct antimicrobial potency. This may however be compensated by a better capacity to interact in a productive manner with eukaryotic membranes, in agreement with the many reported activities of human LL-37 on host immune cells.[6] It is tempting to speculate that RL-37-like orthologues have been selected to have primarily a directly antimicrobial defensive activity, while LL-37-like ones have somewhat sacrificed this capacity to gain in host-cell modulating functions.

Acknowledgements

F. Morgera is supported by an Elettra Ph.D grant. Research was supported by FGV LR26-2008, EU FR6 project COOP-CT-2005-018191 and PRIN 2007.

References

1. Zanetti M. *J Leukoc Biol* **75**: 39-48, 2004.
2. Oren Z, Lerman JC, Gudmundsson GH, Agerberth B, Shai Y. *Biochem J* **341**: 501-513, 1999 .
3. Zelezetsky I, Pontillo A, Puzzi L, Antcheva N, Segat, L, Pacor S, Crovella S, Tossi A. *J Biol Chem*. **281**: 19861-19871, 2006.
4. Lau SYM, Taneja AK, Hodges RS. *J Biol Chem* **259**: 13253-13261, 1984.
5. Braiman MS, Briercheck DM,Kriger KM. *J Phys Chem* **103**: 4744-4750, 1999.
6. Tomasinsig L, Pizzirani C, Skerlavaj B, Pellegatti P, Gulinelli S, Tossi A, Di Virgilio F, Zanetti M. *J Biol Chem* **283**: 30471-30481, 2008.

6-11-104

Azobenzene-mediated photomodulation of a collagen triple helix monitored by IR spectroscopy

Lorenz, Lisa[1]; Kusebauch, Ulrike[2]; Moroder, Luis[2,]; Wachtveitl, Josef[1]*

[1]Johann Wolfgang Goethe-University, Institute of Physical and Theoretical Chemistry, GERMANY; [2]Max Planck Institute of Biochemistry Bioorganic chemistry, GERMANY

[*]E-mail: moroder@biochem.mpg.de

Introduction

Following previous studies on the use of photoresponsive molecular switches to induce conformational transitions in model peptides,[1] our most recent efforts were addressed to the design and synthesis of a photoswitchable collagen triple helix. As shown in Fig. 1, by replacing in suitable positions of the Ac-(Gly-Pro-Hyp)$_7$-Gly$_2$-NH$_2$ collagenous peptide a Pro and Hyp residue with (*4S*)-mercaptoproline (Mpc), respectively (**1**), a side chain-to-side chain cross-linking of the collagen peptide was afforded with a purposely designed azobenzene derivative. For an optimal transfer of the geometrical changes of the azobenzene chromophor, upon photoisomerization, to the collagen peptide the rigid but-2-ynyl spacer was selected. As expected from modeling studies, self-association of the side-chain bridged collagen model peptide **2** into a stable triple helix was observed with the *trans*-azobenzene clamp, while its photoisomerization to the *cis* isomeric state leads to unfolding processes as well assessed by NMR conformational analysis.[2] In the present study, temperature and light-induced unfolding was analyzed by FTIR to identify optimal conditions for subsequent time-resolved monitoring of unfolding pathways by ultrafast FTIR spectroscopy.

Results and Discussion

Incorporation of the two (*4S*)-Mpc residues in Ac-(Gly-Pro-Hyp)$_7$-Gly$_2$-NH$_2$ leads to a decrease of the thermal stability of the triple helix by 8.5 °C in aqueous solution.[3] Intramolecular cross-bridging of peptide **1** with the azobenzene clamp reduces significantly the water solubility and in EG/H$_2$O (1:1) a T_m of 55 °C was determined by CD for **2** compared to a T_m of 60 °C for the parent peptide **1** in this solvent. The identical T_m value of 55 °C was obtained for **2** in EG/H$_2$O (1:1) by following the IR intensity at 1645 cm^{-1}. The relatively weak destabilization of the triple helix by the azobenzene clamp agrees with results of MD simulations and confirms the correct design of the photoswitchable collagen molecule. The azobenzene chromophore in **2** retains its ability to undergo a fully reversible *cis/trans* photoisomerization, but the amplitude of this process and thus also the extent of light-induced unfolding of the triple helix is severely limited at room temperature by the structural restraints imparted by the supercoiled fold.[2] This would suggest that interacting forces of the triple helix overpower the conformational preferences of the chromophore. However, with increasing temperature the azobenzene clamp is relieved from these conformational restraints and its *trans*-to-*cis* and *cis*-to-*trans* photoisomerization becomes fully functional in terms of inducing unfolding and refolding of the triple-helical structure, respectively (Fig. 2A). At temperatures near the melting point the maximum effects are reached (Fig. 2B).

Ac-(Gly-Pro-Hyp)$_2$-Gly-(4*S*)-Mpc-Hyp-Gly-Pro-Hyp-Gly-Pro-(4*S*)-Mpc-(Gly-Pro-Hyp)$_2$-Gly$_2$-NH$_2$ (**1**)

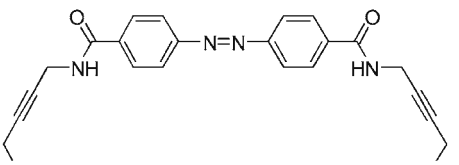

Ac-(Gly-Pro-Hyp)$_2$-Gly-(4*S*)-Mpc-Hyp-Gly-Pro-Hyp-Gly-Pro-(4*S*)-Mpc-(Gly-Pro-Hyp)$_2$-Gly$_2$-NH$_2$ (**2**)

Figure 1. A Pro residue in position X and a Hyp residue in position Y of the collagen (Gly-Xaa-Yaa) triplets were replaced with (4*S*)-Mpc in an i and i+7 sequence interval and the resulting collagen peptide **1** was cross-reacted at the two thiol functions with 4,4′-(diazene-1,2-diyl)bis(*N*-(4-iodobut-2-ynyl)benzamide to produce peptide **2**.

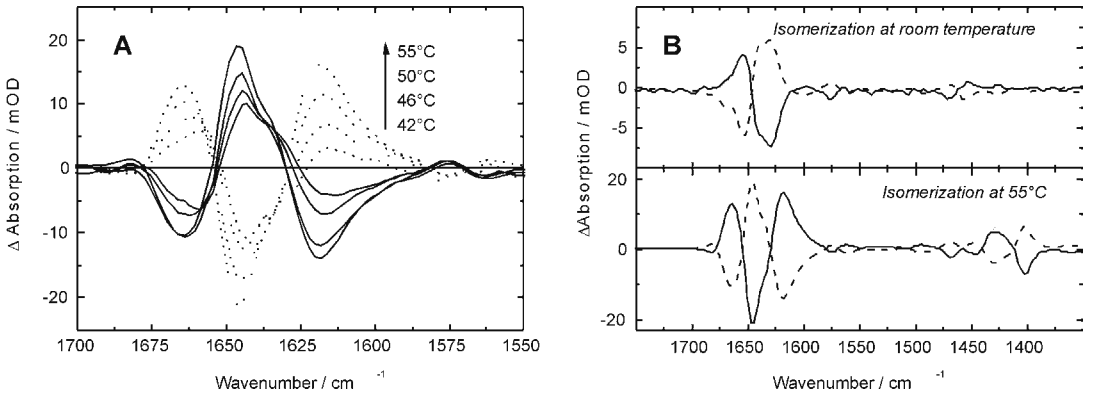

Figure 2. A) Absorbtion changes induced by photoisomerization of the azobenzene moiety in function of temperature; *trans*-to-*cis* (—) and *cis*-to-*trans* (·····). (B) Difference spectra of *trans*-to-*cis* (—) and *cis*-to-*trans* (·····) isomerization at room temperature (top) and at the melting temperature (bottom).

The results confirm that photomodulation of the collagen triple helix is reversible and that the efficiency of the photoisomerization increases with temperature reaching a maximum value shortly below the melting point. With IR spectroscopy the optimal temperatures were identified, which are required for structure destabilization at sufficient extents to enable unfolding by the weak driving force of the azobenzene clamp. Under these optimized conditions the chromophore is capable of photo-controlling the complex triple-helical structure, thus allowing for time-resolved monitoring of its unfolding process.

Acknowledgements

The study was partly supported by the Deutsche Forschungsgemeinschaft (SFB 533, A8).

References

1. Renner C, Moroder L. Azobenzene as conformational switch in model peptides. *ChemBioChem* **7**: 868-878, 2006.
2. Kusebauch U, Cadamuro SA, Musiol H-J, Lenz MO, Wachtveitl J, Moroder L, Renner C. Photo-controlled folding and unfolding of a collagen triple helix. *Angew Chem Int Ed* **45**: 7015-7018, 2006.
3. Cadamuro SA, Reichold R, Kusebauch U, Musiol H-J, Renner C, Tavan P, Moroder L. Conformational properties of 4-mercaptoproline and related derivatives. *Angew Chem Int Ed* **47**: 2143-2146, 2008.

6-11-105

Are V57 mutants of amyloidogenic protein - human cystatin C more or less resistant to denaturation conditions?

Jankowska, Elzbieta; Orlikowska, Marta; Radulska, Adrianna; Szymańska, Aneta*
University of Gdańsk, POLAND

**E-mail: elaj@chem.univ.gda.pl*

Introduction

Cystatins are natural inhibitors of cysteine proteases – hydrolytic enzymes widely distributed in animals, plants and microorganisms. Human cystatin C (hCC) has been also recognized as an amyloidogenic protein directly involved in formation of pathological fibrillar aggregates which deposit in brain arteries of elderly persons causing cerebral amyloid angiopathy.[1]

The overall 3D architecture of monomeric human cystatin C is not determined yet but it could be predicted from the already resolved structure of its dimeric form.[2] Dimeric cystatin C is created through an exchange of 'subdomains' between two molecules (3D domain swapping) and consists of two identical subunits reconstituting to the great extent the fold of the monomeric chicken analogue of hCC.

The dimerization process of human cystatin C affects mostly the so-called L1 loop (residues 55-59, QIVAG) which occurred to be a hinge region in the 3D domain swapping event. To check an effect of greater or decreased stability of this loop on dimerization and aggregation propensity of human cystatin C, we designed and constructed hCC mutants with Val57 residue replaced by Asp, Asn or Pro, respectively. Structural studies of these mutants and their thermal denaturation process have been performed by means of CD and FTIR spectroscopies.

Results and discussion

CD spectra recorded at room temperature indicate that replacing of Val57 with Asp or Asn residues does not change the protein structure significantly. Only proline mutant seems to have slightly less helical fold than wild-type hCC. The main minimum on all spectra recorded at 95 °C is shifted from 208 to about 202 nm, that is to the wavelength characteristic of random coil conformation. At the same time the overall shape of the spectra change significantly, although in the case of hCC V57D mutant this change is not so great as for the rest studied proteins suggesting greater thermal stability of this mutant. Nevertheless, thermal denaturation occurred to be an irreversible process for every studied cystatin C variant.

Only one main transition point is visible on the melting curves recorded at 218 nm (Fig. 1A) what indicates a cooperative transformation of the *β*-structure in both wild-type and mutated hCC. One transition point appears also on the melting curves recorded at 222 nm but only for the mutated proteins whereas the temperature-induced structural changes proceeding in the α-helical region of wild-type human cystatin C are clearly not a simple two-state process (Fig. 1B). The conducted studies reveal also that the *β*-structure of wild-type cystatin C has essentially the same stability as the equivalent region in its Asn and Asp mutants (Fig. 1A). The helical curve (Fig. 1B), however, indicates lower stability of the wild-type form in comparison with V57D and V57N variants. Not only the unfolding process connected with the thermal denaturation of hCC wt helical region starts at a slightly lower temperature, but also the main transition depicted

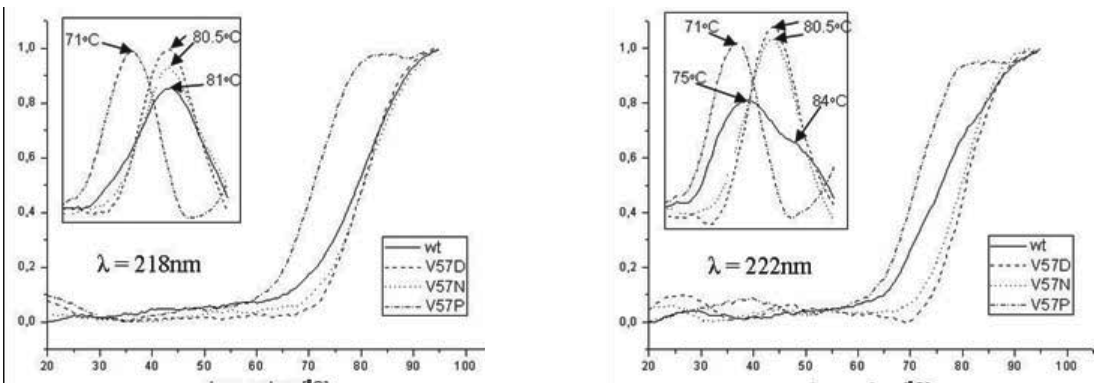

Figure 1. Melting curves of the *β*-sheet (A) and *α*-helical region (B), insets: the 1st derivative of the melting curves recorded at 218 and 222 nm, respectively.

as a maximum on the first derivative curve (Fig. 1B, inset) appears about 5 °C earlier than for Asp and Asn mutants. The lowest thermal stability was detected in the case of Pro variant, for which a melting temperature was lower by 10 °C than for V57D and V57N mutants.

Structural information in FT-IR method is predominantly derived from an analysis of so-called amide I band (1600-1700 cm^{-1}) composed mainly of a peptide backbone carbonyl bond (C=O) stretching vibration.[3] Thermal denaturation of wild-type cystatin C causes changes in a shape and position of this band. A red shift of the amide I band starts at 80 °C, and at 90 °C the second maximum at a lower wavenumber arises concomitantly with a decrease in the old maximum intensity. The band transformations are probably caused by the protein aggregation since massive precipitation was observed in the sample heated to 80 °C.

Under a broad contour of the amide I band several overlapping bands due to different secondary structure elements are hidden.[4] Derivation makes possible to distinguish between individual components and assign each of them to a specific conformational type. The most clearly visible on the derivative curves of wild-type and mutated cystatin C are components at about 1690 and 1630 cm^{-1} connected with the β-structure. Heating causes gradual decrease of the intensity of these bands, especially of the latter one. At the same time a new minimum, at a lower wavenumber starts to appear. It is positioned at about 1620 cm^{-1} and, according to literature, connected with creation of the β-sheet aggregates.[5] It seems that Asp mutant displays lower propensity to create the β-sheet aggregates than wild-type cystatin C. The 2nd derivative curve for hCC V57D variant suggests that even at 90 °C the native β-structure is still present although aggregating species also start to appear.

To summarize, our studies allow to establish that: structures of all but V57P mutant of hCC are similar at room temperature; Pro mutant is less helical than all the rest studied proteins and about 10 °C less thermally stable than Asn and Asp mutants; Asp mutant is the most stable among the studied proteins; Asn and Asp mutation make visible improvement in stability of the helical region of hCC.

Acknowledgements

This work was supported by Polish Ministry of Higher Education grant No 4233/H03/2007/32.

References

1. Olafsson I, Grubb A. Hereditary cystatin C amyloid angiopathy. *Amyloid* **7**: 70-79, 2000.
2. Janowski R, Kozak M, Jankowska E, Grzonka Z, Grubb A, Abrahamson M, Jaskólski M. Human cystatin C, an amyloidogenic protein, dimerizes through three-dimensional domain swapping. *Nature* Struct. Biol. **8**: 316-320, 2001.
3. Fabian H, Naumann D, Misselwitz R, Ristau O, Gerlach D, Welfle H. Secondary structure of streptokinase in aqueous solution: a Fourier transform infrared spectroscopic study. *Biochemistry* **31**: 6532-6538, 1992.
4. Casal HL, Köhler U, Mantsch HH. Structural and conformational changes of beta-lactoglobulin B: an infrared spectroscopic study of the effect of pH and temperature. *Biochim Biophys Acta* **957**: 11-20, 1988.
5. Mohney BK, Petri ET, Uvarova V, Walker GC. Infrared Absorption and Ultraviolet-Circular Dichroism Spectral Studies of Thermally Induced Unfolding of Apomyoglobin. *Appl Spectrosc* **54**: 9-14, 2000.

6-11-106

Molecular dynamics study of β-peptides: Using computer simulation to correct and interpret experimental data

*Gattin, Zrinka; van Gunsteren, Wilfred F**

ETH, Laboratory of Physical Chemistry, SWITZERLAND

**E-mail: wfvgn@igc.phys.chem.ethz.ch*

Introduction

β-peptides offer the possibility to investigate the folding-unfolding equilibrium in the context of very small systems, therefore they have also been the subject of a number of investigations based on atomistic molecular dynamics (MD) simulations which revealed that the folding-unfolding equilibrium of *β*-peptides typically occurs on time scale of nanosecond to tens of nanoseconds.

How the backbone bound heteroatoms (OH, NH_2, F) influence the structure of a peptide is little known by now, both experimentally as well as theoretically. We performed several MD studies on the conformational behavior of centrally placed *β*HAla(*α*-F) and *β*HAla(*α*-OH), as function of configuration at *Cα* to investigate the influence of different configuration on secondary structure formation and stability. All *β*-peptides were simulated in methanol solution.

Results and discussion

The four investigated *β*-heptapeptides carry different configurations at *Cα* of the centrally placed amino acid residue. For peptide **3** (*S,S*) and peptide **4** (*S,R*) the centrally placed amino acid residue is *β*HAla(*α*-F) whereas for peptide **6** (*S,S*) and peptide **7** (*S,R*) is *β*HAla(*α*-OH) amino acid residue.

The MD results for peptides **3** and **4** are in agreement with primary, i.e. measured, experimental data (NOEs and ^{3}J-values), but the conformational interpretation that we can infer from the MD trajectories contradicts the molecular conformations derived from the experimental data[1] by single-structure refinement (SSR) using the program X-PLOR. The reason for this contradiction is likely to rest in the absence of long-range NOEs for peptides **3** and **4**.

SSR in vacuo based on only local and limited number of atom-atom distance bounds can easily lead to a non-representative structure for the molecule. In contrast, the MD simulations using a thermodynamically equilibrated force field (FF) and explicit solvent molecules lead, even without using the experimental data as restraints, to conformational ensembles that better satisfy these experimentally measured data. Among the structures of the five most populated conformational clusters of the MD trajectories of peptide **3** (Fig. 1) and of peptide **4** (which

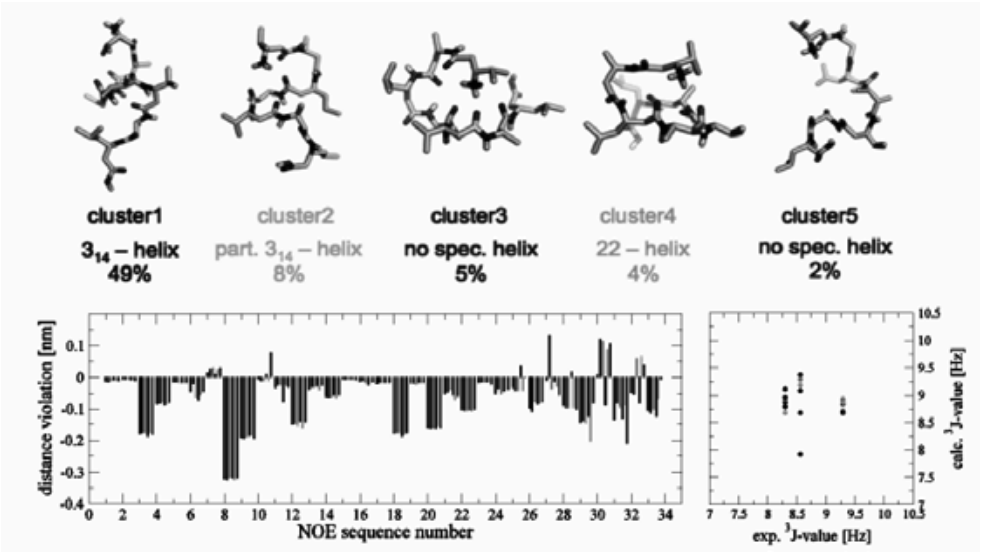

Figure 1. Upper part: The central member structures of the five most populated clusters with the corresponding population [in %] and a description of the type of helicity. Bottom part: NOE distance violations and ^{3}J-coupling constants (HN-H*β*) calculated for the MD trajectory structures (black) and for the five most populated clusters for peptide **3**.

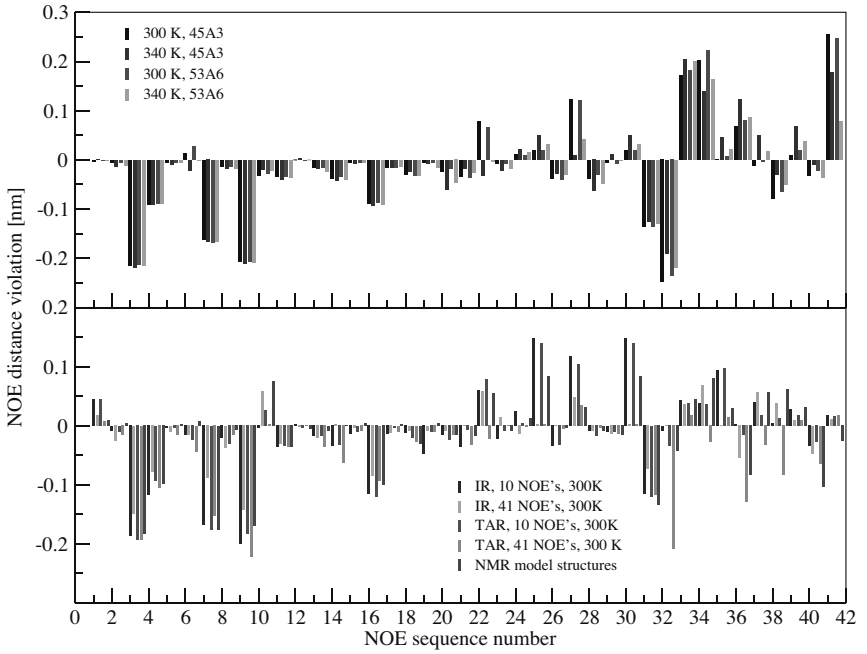

Figure 2. NOE distance violations calculated from the unrestrained MD simulations, upper panel, and from the distance restraining MD simulations, bottom panel.

comprise more than 60% of all trajectory structures) there are structures that satisfy the given NOE upper bounds.[2]

The unrestrained simulations of peptides **6** and **7** were performed at two temperatures, 300 K and 340 K, with two GROMOS FFs, 45A3 and 53A6. The NOE distance restraining simulations, instantaneous (IR) and time-averaged (TAR), were performed only at 300 K for peptide **6**, restraining the structures to either 10 long-range or to all 41 NOE distance upper bounds, whereas for peptide **7** restraining was performed to the 19 long-range NOE distance upper bounds, both at 300 K and 340 K. In all restraining simulations the 45A3 FF was used.

The unrestrained MD simulations show more 3_{14}-helical structure for peptide **6** than for peptide **7**, in line with observations for the correspondingly Me-substituted β-heptapeptide. The application of NOE upper bound distance restraints, either IR or using TAR, decreases the 3_{14}-helical character for peptide **6** and increases it for peptide **7**. For peptide **6** the dominant conformation is different for the IR and TAR ensembles on the one hand compared to the set of 10 NMR model structures resulting from SSR using X-PLOR on the other hand[3]. This is not surprising in view of the few NOE bounds involving residues of the carboxy terminal of peptide **6** (Fig. 2), and the fact that the X-PLOR calculations are performed for a molecule in vacuo. The GROMOS FFs clearly populate different conformers. For peptide **7**, with its more even distribution of NOE bounds over the molecule, the GROMOS IR and TAR ensembles show a dominant conformer much alike the one of the set of NMR model structures.

The MD simulations reported illustrate some of the problematic aspects of structure refinement based on NMR data: conformational and/or time averaging and insufficient number of experimental data. The lack of NOE data for the carboxy terminal residues of peptide **6** increased the importance of using an accurate FF and inclusion of solvent degrees of freedom: for peptide **6** the instantaneous restrained simulations showed better agreement with the primary, i.e. measured, experimental data than the set of 10 NMR model structures derived using SSR in vacuo with X-PLOR. The results for peptide **7** illustrate that a simple SSR approach as employed in X-PLOR yields the dominant conformation for cases where one conformation reaches a certain level of dominance and sufficient and well distributed atom-atom distance bounds are available. For peptide **6**, clearly a multi-conformational case, the agreement with the experimental data improved upon using time-averaging, especially regarding ^{3}J-values. The unrestrained simulations, however, did not produce a very good fit to the experimental data, which may hint at FF inadequacies.

References

1. Mathad RI, Gessier F, Seebach D, Jaun B. *Helv Chim Acta* **88**: 266-280, 2005.
2. Gattin Z, van Gunsteren WF. *J Phys Chem. B* **113**: 8695–8703, 2009.
3. Gattin Z, Schwartz J, Mathad RI, Jaun B, van Gunsteren WF. *Chemistry* **15**: 6389-6398, 2009.

6-11-107

Nanomolar aggregation of amyloid β peptides covalently and site-specifically modified by cholesterol oxidation products

Usui, Kenji[1]; Powers, Evan[2]; Paulsson, Johan[2]; Siegel, Sarah[2]; Kelly, Jeffery[2,]*
[1]Tokyo Institute of Technology, Department of Bioengineering, JAPAN; [2]The Scripps Research Institute, Department of Chemistry, UNITED STATES

[*]E-mail: jwk@scripps.edu

Aging, associated with decreasing protein homeostasis (proteostasis) capacity and increasing oxidative stress, is a prominent risk factor for amyloid diseases.[1,2] Alzheimer's disease (AD) involves intra- and extracellular amyloid formation by the amyloid bata peptide (Aβ). However, it is a mystery how Aβ can aggregate *in vivo* even though its physiological concentration (PC) is much lower than its critical concentration (CC) for aggregation. We have proposed that covalent modification of Aβ by small oxidative metabolites can explain how Aβ can form amyloid at its PC.[3-5] The aldehyde-bearing cholesterol oxidation product 1(2),[6] which can modify Aβ by Schiff-base formation, is an example of the products that could affect AD onset. However, significant questions about the modification persist, including: Does modification by 1(2) lower the CC of Aβ aggregation into the PC range? And, how does this modification enhance Aβ aggregation? In this study, these questions are answered by studying chemically synthesized analogs of Aβ that are site-specifically modified by 1(2). We chemically synthesized analogs of Aβ40 modified with 1(2) at D1 (Aβ1(2)D1), K16 (Aβ1(2)K16) or K28 (Aβ1(2)K28). Note that the hydrolytically unstable Schiff-base linkage was reduced to a secondary amine in each Aβ1(2) conjugate (Fig. 1). At first, aggregation reactions of Aβ variants carried out at 10 μM were monitored by Thioflavin-T (TfT) fluorescence. Microfibrillar aggregates appeared in the aggregation reactions of all of the Aβ1(2) conjugates with no lag phase. In contrast, aggregates of unmodified Aβ40 appeared more slowly. The conversion to microfibrillar aggregates was fastest for Aβ1(2)D1, followed by Aβ1(2)K16 and then by Aβ1(2)K28. The CC for aggregation is equivalent to the concentration of monomeric protein left in solution when aggregation reaches equilibrium. We used a chaotrope denaturation strategy to estimate the CCs of Aβ1(2) conjugates, because the values are so low that they cannot be determined directly. The critical concentrations of Aβ1(2)D1, Aβ1(2)K16, and Aβ1(2)K28 shown in Fig. 2A are the same within experimental error, averaging about 4 nM. This value is much lower than those of Aβ40 and Aβ42. The aggregation kinetics of Aβ variants at 500 nM monitored by light scattering (LS) are plotted in Fig. 2B. Unmodified Aβ40 and Aβ42 did not aggregate on the time scale of the experiment (2 h). In contrast, all of the Aβ1(2) conjugates showed evidence of aggregation. Unlike the thermodynamic results described above, the aggregation kinetics of Aβ1(2) conjugates depended strongly on the modification site: the rank ordering of aggregation rates was Aβ1(2)K16 > Aβ1(2)K28 > Aβ1(2)D1. Aβ1(2)K16 and Aβ1(2)K28 still aggregated at 100 nM and 50 nM. The aggregates from low concentration LS time courses were examined by immuno-EM to ensure that the particles detected by LS were aggregates composed of Aβ1(2) (Fig. 2C). The samples were incubated with a monoclonal anti-Aβ antibody followed by protein A conjugated to gold particles. No aggregates were observed in samples of Aβ40 and 42 at 500 nM. In contrast, amorphous aggregates were detected at 500 nM for Aβ1(2)D1, at 20 nM for Aβ1(2)K16, and at 100 nM for Aβ1(2)K28. These results are consistent with the LS results described above. Modification of Aβ by 1(2) at the different sites has a similar effect on the thermodynamic propensity for aggregation, but different effects on the aggregation kinetics. Aβ1(2)K16 formed amorphous aggregates fastest at the lowest concentrations. In contrast, TfT positive aggregation at higher concentration was fastest for Aβ1(2)D1. The influence of modification site on the nature of the aggregates suggests that amorphous aggregation and

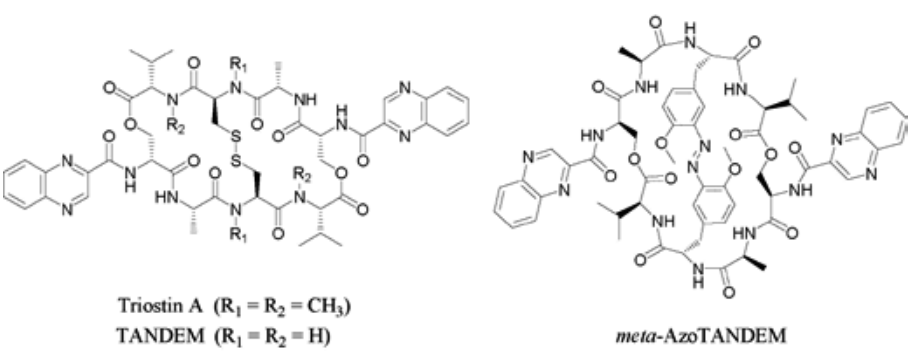

Figure 1. Oxidative cholesterol metabolites and their Aβ conjugates.

Scheme 1. Total synthesis of *meta*-AzoTANDEM

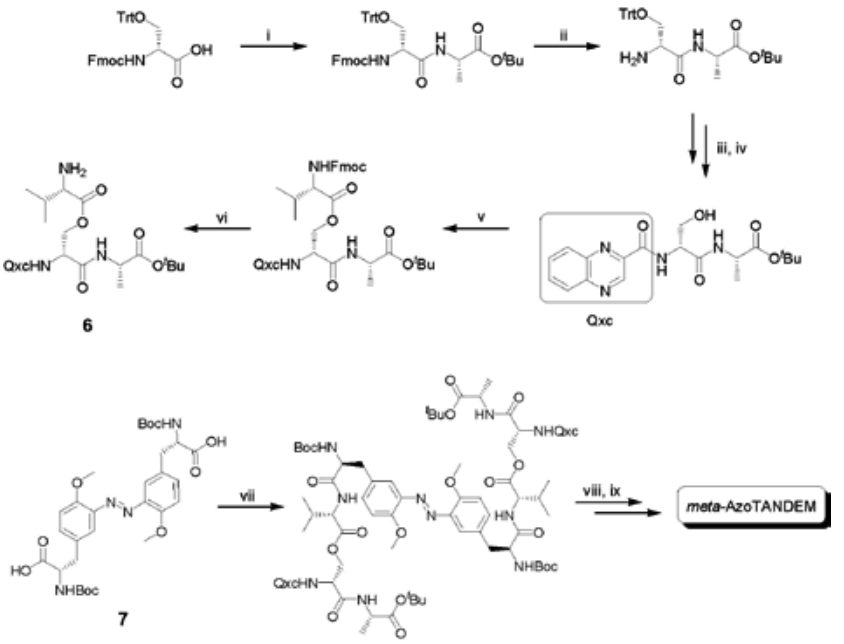

Reagents and conditions: (i) H-Ala-O^{t}Bu·HCl, HATU, HOAt, DIPEA, DMF; (ii) 20 % Diethylamine, DCM; (iii) QxcCl, Triethylamine, DCM; (iv) 2% TFA in DCM; (v) Fmoc-Val-OH, HATU, HOAt, DIPEA, DMF; (vi) 7% Piperazine in DCM; (vii) **6**, HATU, HOAt, DIPEA, DMF; (viii) 50% TFA in DCM; (ix) HATU, HOAt, DIPEA, DMF.

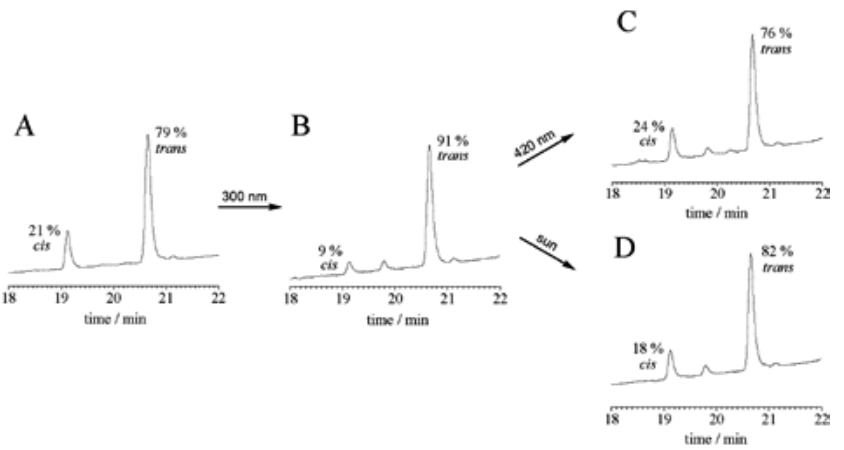

Figure 2. (A) Determination of CCs for Aβ variants. (B) Aggregation kinetics of Aβ variants at 500 nM monitored by LS. (C) Immuno-EM images of aggregates formed (or not formed) by Aβ 1(2) and Aβ40.

fibrillization place different conformational demands on Aβ. Furthermore, these studies may partially explain how Aβ can aggregate at nM PCs when the CC of unmodified Aβ is in the μM range. It also suggests that inhibiting Aβ modification by aberrant metabolites could be a viable preventative strategy against AD.

References

1. Balch WE, Morimoto RI, Dillin A, Kelly JW. *Science* **319**: 916-919, 2008.
2. Cohen E, Bieschke J, Perciavalle RM, Kelly JW, Dillin A. *Science* **313**: 1604-1610, 2006.
3. Bieschke J *et al*. *Acc Chem Res* **39**: 611-619, 2006.
4. Bieschke J, Zhang Q, Powers ET, Lerner RA, Kelly JW. *Biochemistry* **44**: 4977-4983, 2005.
5. Zhang Q, Powers ET, Nieva J, Huff ME, Dendle MA, Bieschke J, Glabe CG, Eschenmoser A, Wentworth P Jr, Lerner RA, Kelly JW. *Proc Natl Acad Sci U S A* **101**: 4752-4757, 2004.
6 . Wentworth P Jr, Nieva J, Takeuchi C, Galve R, Wentworth AD, Dilley RB, DeLaria GA, Saven A, Babior BM, Janda KD, Eschenmoser A, Lerner RA. *Science* **302**: 1053-1056, 2003.

6-11-108

Hairpin peptide inhibitors of amyloid fibril formation

Huggins, Kelly; Andersen, Niels*

University of Washington, Chemistry Department, UNITED STATES

E-mail: khuggins@u.washington.edu

Introduction

Amyloid fibrils have been suggested as the cause and/or result of many different diseases including Alzheimer's, Parkinson's and Type II diabetes. Their mechanism/ pathway of formation has been a major focus of many studies aimed at developing inhibitors that may prevent onset of fibril formation, limit the formation of toxic intermediates, and/ or decrease the overall amount of aggregates or fibrils that can form.

Inhibitors to date include small molecules such as polyphenols and peptides analogous to a part or all of the fibril forming peptide,[1,2,6] as well as a 56-residue mini-protein (an analogue of the B1 domain of protein G) with solvent exposed residues on two of its beta strands that is effective against Aβ1-40 fibril formation.[3]

The successful evolution of such a structured mini-protein to a potent inhibitor, lead to the question of whether isolated, structured hairpin peptides could present the features necessary to inhibit amyloid formation. These hairpins offer further minimized systems with possible exposed sites/residues on each beta strand that can bind to aggregation prone peptides/proteins and prevent fibril formation.

The incorporation of aromatic residues such as Trp and/ or Tyr in small peptides has provided amyloidogenesis inhibitors. Some examples include: SNWKWWPDGIFD (effective against Poly Glu fibrils),[4] GTXEGKX-NH_2, where X = W or Y, (Y being less potent than W substitutions, against Aβ 1-40/42 fibrils).[5] We view the evolved GB1 analogue as another example; presumably its potency against Aβ1-40 fibrillization results in large part from W and Y substitutions at solvent-exposed sites.[3]

The prominence of aromatic residues in previous peptide inhibitors of amyloidogenesis prompted us to introduce Trp and Tyr residues at differing positions in a previously optimized 16-residue β-hairpin (MrH),[7] as shown in Scheme 1. The resulting hairpin peptides were at least 60% folded under the conditions used for amyloid inhibition studies and did not aggregate up to 1-2 mM concentration based on Nuclear Magnetic Resonance (NMR) studies.

The amyloidogenic system examined was human pancreatic amylin (hAM), a 37-residue peptide associated with type-II diabetes. Inhibitors of hAM to date include phenol red, peptide analogues of the full length hAM[6] as well as a peptide fragment analogue of the amyloidogenic sequence.[2]

Results and Discussion

The assay conditions used (8 μM hAM in 2% HFIP, 5mM phosphate buffer at pH 7.2) for this study allowed for a reasonable and reproducible lag time. The α/coil to β structure transition (at 55±20 minutes in the absence of inhibitors) was monitored by circular dichroism (CD); fibril formation was monitored by the enhancement of Thioflavin T (ThT) fluorescence, onset time 61±14 minutes. Inhibitors effectiveness determinations are based on increased lag time relative to the uninhibited hAM controls.

hAM analogues: Our first studies with the assay were made with full length hAM analogues and fragments (Scheme 1); all of which (at up to 8:1 peptide to hAM molar ratios) were ineffective as inhibitors. This result was most surprising for the I26P and F23P hAM fragment (hAMF) mutants since previous studies indicate that I26 and F23 play crucial roles in the onset of fibril formation: in the full sequence, the I26P mutant is a potent inhibitor.[6] This may indicate that either our conditions require more potent inhibitors for effects to be seen, or that the N-terminal sequence of hAM is required for binding to and inhibiting fibril formation in this case.

***MrH β-hairpins*:** The MrH β-hairpins, on the other hand, showed interesting results. The lag times resulting on addition of effective hairpins are shown in Table 1, and the effect of these inhibitors are illustrated in Fig. 1 (ThT assays) and Fig. 2 (CD assays). The ranking of relative potency of the MrH hairpins as hAM inhibitors is shown below and is based on the onset of aggregation observed

```
hAM(17-33):          -VHSSNNFGAILSSTNVG-
Pramlintide(17-33):  -VHSSNNFGPILPPTNVG-
Rat Amylin(17-33):   -VRSSNNLGPVLPPTNVG-
hAMF        :         VHSSNNFGAILSSTNYG-NH2
hAMF I26P   :         VHSSNNFGAPLSSTNYG-NH2
hAMF F23P   :         VHSSNNPGAILSSTNYG-NH2

MrH Hairpin
     1          6          12       16
     K-K-L-T-V-S-I-pG-K-K-I-T-V-S-A
S6W,K11W - WWS2      V5W,I12W - WWS3
T4W,T13W - WWS4      S6Y,K11Y - YYS2
V5Y,I12Y - YYS3      T4Y,T13Y - YYS4
L3Y,V14Y - YYS5      L3Y      - YS5
D-Pro8N (p8N)- WWS2(NG)
```

Scheme 1. List and sequence of inhibitors tested against hAM. Top: partial sequences are shown for hAM, Pramlintide and Rat hAM and the full sequences are shown for hAMF; mutations for ham analogues and fragments are shown in blue. Bottom: MrH sequences and nomenclature used in this study. Red highlights reverse turn region in hairpin, S2/4= strand residues on one face of hairpin (even sites) and S3/5= strand residues on opposite face (odd sites)

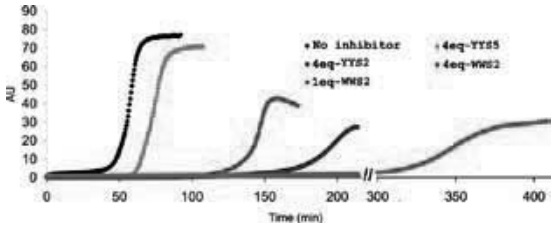

Figure 2. Circular Dichroism spectra monitoring b state formation: A. hAM without inhibitor, B. 1 molar eq of WWS2, C. 4 molar eq of WWS3. Intense minima at 217 nm represent full fibril formation. Onset of fibril formation was recorded at the point of transition to beta sheet signal at ~217 nm. For WWS3, transition occurred between 117-145 min.

at 2 molar equivalents (or, as needed, 6 molar eq):

WWS2 > YYS2 > WWS4 ≥ YYS4 > YYS5 ≥ WWS3 ≥ WWS2(NG) >> YYS3, YS5

Trp has a greater inhibitory effect than Tyr at comparable positions within the hairpin, which is consistent with previous studies.[5] Inhibition appears to be most effective when the aryl residues are on one face of the hairpin (S2/4, even sites).

The most potent inhibitor, WWS2, has cross-strand Trp's which are in an edge-to-face (EtF) interaction geometry. As a probe of the stereoselectivity of this feature, inhibition trials were extended to a truncated analogue, Pr-WIpGKWTG-NH_2 (data not shown), which has been shown to have a reversed FtE orientation.[7] This truncated peptide was ineffective up to 6 molar equivalents. This suggests the importance of sequence and/or aryl/aryl geometries in binding to and inhibiting hAM aggregation.

WWS2(NG), which retains the EtF geometry of the Trps, was effective only at 6 molar equivalents (Table 1). This result was surprising given the comparable structure and fold stability to WWS2. The turn D-Pro-Gly unit may play an additional role in binding and inhibition of hAM amyloidogenesis.

Acknowledgements

NSF (CHE-065031) and NIH (GM059658) grants, Amylin Pharmaceuticals Inc. and Halocarbon Products Corp.

Table 1. Summary of β-hairpin inhibition of hAM aggregation, lag time measures in min. The times required for the appearance of the β-signature in CD assays are shown in parentheses

Peptide	1 eq	2eq	4 eq	6eq
WWS2	151±42 (*150*)	253±52 (*300*)	344±28	N/D
WWS4	(*114*)	82±33 (*95*)	155±11	333
WWS2 (NG)	--	--	--	130
WWS3	--	--	98±10	107±33
YYS2	139	201±42 (66-*81*)	190	303±37
YYS4	--	157±43 (*150*)	180	156±18
YYS5	--	--	71±6	159±33

References

1. Porat Y, Abramowitz A *et al.* Inhibition of amyloid fibril formation by polyphenols: Structural Similarity and aromatic interactions as a common inhibitor. *Chem Biol Drug Design* **67**: 27-37, 2006.
2. Porat Y, Mazor Y *et al*. Inhibition of Islet amyloid polypeptide fibril formation: A potential role for heteroaromatic interaction. *Biochemistry*. **43**: 14454-14462, 2004.
3. Smith TJ, Stains CI *et al.* Inhibition of beta-amyloid fibrillization by directed evolution of a bets-sheet presenting miniature protein. *J Am Chem Soc.* **128**: 14456-14457, 2006.
4. Nagai Y, Tucker T *et al*. Inhibtion of polyglutamine protein aggregation and cell death by novel peptides identified by phage display screening. *J Biol Chem* **14**: 332-340, 2007.
5. Sato T, Pascal K-C. Inhibitors of Amyloid Toxicity based on β-sheet packing of Aβ 40 and Aβ 42 *Biochemistry* **45**: 5503-5516, 2006.
6. Abedini, A., Meng, F. and Raleigh , D.P. A single-point mutation converts the highly amyloidogenic human islet amyloid polypeptide into a potent fibrillization inhibitor. *J Mol Biol* **355**: 274-281, 2007.
7. Eidenschink LA, Kier BL *et al*. Very short peptides with stable folds: Building on the inter-relationship of Trp/Trp, Trp/cation, and Trp/backbone-amide interaction geometries. *Proteins: Struct Funct Bioinf* **75**: 308-322, 2009.

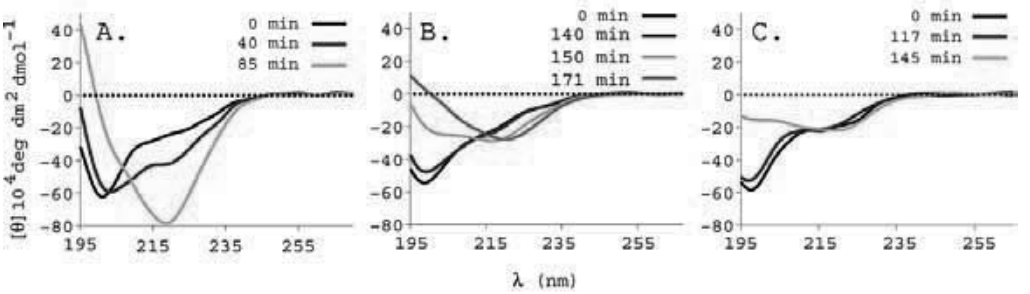

Figure 2. Circular Dichroism spectra monitoring β state formation: A. hAM without inhibitor, B. 1 molar eq of WWS2, C. 4 molar eq of WWS3. Intense minima at 217 nm represent full fibril formation. Onset of fibril formation was recorded at the point of transition to beta sheet signal at ~217nm. For WWS3, transition occurred between 117-145 min.

6-11-109

Structural Studies on the Membrane-Reconstituted Transmembrane-Juxtamembrane Region of ErbB2/Neu(647-693)

Matsushita, Chihiro[1,]; Sato, Takeshi[1]; Furukawa, Yusuke[1]; Smith, Steven O[2]; Aimoto, Saburo[1]*
[1]Institute for Protein Research, Osaka University, Japan, JAPAN; [2]Stony Brook University, United States, UNITED STATES

[1]Institute for Protein Research, Osaka University, JAPAN; [2]Stony Brook University, UNITED STATES

[*]E-mail: chihiro@protein.osaka-u.ac.jp

Introduction

We are interested in the activation mechanism of receptor tyrosine kinases (RTKs), especially how the transmembrane (TM) and the intracellular juxtamembrane (JM) regions couple ligand binding to tyrosine phosphorylation. Growth factor binding to RTK leads to the autophosphorylation of tyrosine residues in the intracellular region. Many of molecular details concerning the mechanism of the receptor activation depend on crystal structures of the extracellular and the intracellular region of RTKs. Much less is known about how TM and JM regions change their structures upon ligand binding leading to intracellular tyrosine phosphorylation. Recently, we have performed a structural study on a TM-JM region of EGFR (ErbB1).[1] We have shown that the TM helix breaks at the membrane interface and the unfolded JM region binds electrostatically to the membrane. We also have shown that the complex of Ca^{2+} with calmodulin (Ca^{2+}/CaM) binds to the positively charged JM region and pulls this region off the membrane. These results are consistent with an electrostatic engine model postulated by McLaughlin and coworkers[2] for the autoinhibition and activation of the EGFR. Results emphasize a functional importance of the JM region in activation mechanism of RTK. However, still, the link between the structural changes in TM and in JM remained to be elucidated.

One of the RTKs that we are focusing on is the rat Neu (ErbB2) receptor, which is one of the four members of ErbB receptor family. It has been known that this RTK with a mutation in the transmembrane region (V664E) is a potent transforming oncogene product. Although there is no ligand identified for Neu, structural studies on this mutant provide valuable information on the active form of RTKs. Thus we decided to compare structure of the wild type and the mutant sequence of TM-JM region of Neu receptor. Structure of the consecutively active V664E mutant must represent an active form of the receptor.

In this research, as an initial step towards the structure comparison, we performed solid state NMR experiments to obtain structural information on the wild type TM-JM sequence of Neu receptor. Also, we performed fluorescence experiments to see whether the electrostatic engine model is applicable to Neu receptor.

Results and discussion

A key feature in the Fig. 1 is the secondary structure of the TM-JM peptide. In order to address where the TM helix breaks and forms random coil or extended structure, we have performed cross polarization magic angle spinning (CPMAS) experiment to obtain 13C spectra of the TM-JM peptide, Neu(647-693), containing specific backbone

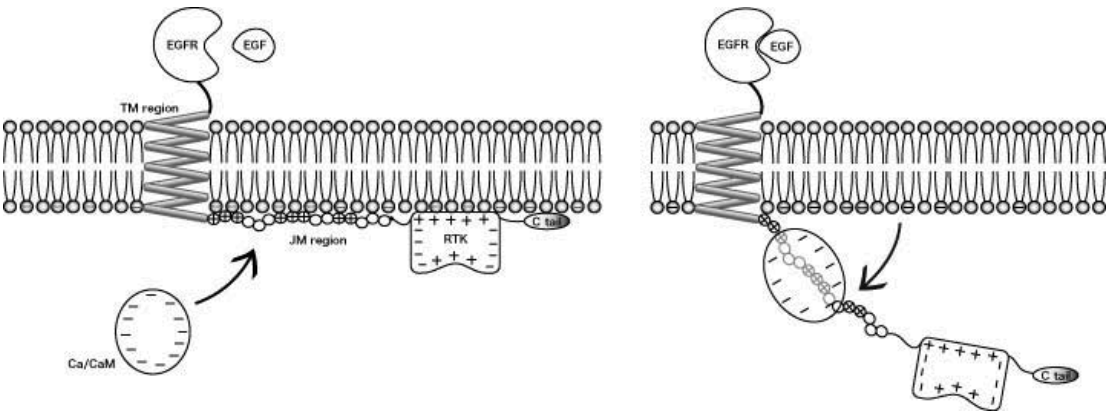

Figure 1. Electrostatic Engine Model. *Left:* The unfolded JM region has eight basic amino residues and it binds to the acidic lipid bilayer through nonspecific electrostatic interaction. *Right:* Negative charged Ca/CaM binds to the JM region and pulls the JM region off the membrane, which leads to inter molecular association of kinase domains for the autophosphorylation.

13C labels at the putative TM-JM boundary. The TM-JM peptide was reconstituted into 1,2-Dimyristoyl-sn-Glycero-3-phosphocholine (DMPC) /1,2-Dimyristoyl-sn-Glycero-3-[Phospho-rac-(1-glycerol)] (DMPG) multilamellar vesicles for these experiments. The carbonyl carbon ^{13}C chemical shifts have been shown to be sensitive to secondary structure.[3] The results suggested that the TM sequence spans cell membrane in helical secondary structure that breaks at the cytoplasmic membrane surface.

Another feature in the model is that the JM region binds to the lipid bilayer through an electrostatic interaction which is diminished by an addition of Ca^{2+}/CaM in the system. Villalobo and coworkers have shown that Neu receptor binds to Ca^{2+}/CaM.[4] We have performed fluorescence energy transfer (FRET) experiment to see the contact between the JM region and the membrane. Alexa568, as a donor, was introduced to the side chain of Cys at the C-terminal of the TM-JM peptide. This fluorescence labeled peptide was reconstituted in lipid bilayers containing 1-Palmitoyl-2-Oleoyl-sn-Glycero-3-Phosphocholine (POPC), 1-Palmitoyl-2-Oleoyl-sn-Glycero-3-[Phospho-L-Serine] (POPS) and 1,1'-dioctadecyl-3,3,3',3'-tetramethyl-indodicarbocyanine perchlorate(DiD) as an acceptor. We have observed FRET between Alexa568 and DiD. Also, as we add sphingosine, an amphipathic membrane-permeable base, to the system, the signal intensity from DiD has decrease, suggesting that the JM region bind to the membrane through the electrostatic interaction. Decrease in the fluorescence intensity from DiD was also observed as we add Ca^{2+}/CaM in the system, suggesting that Ca^{2+}/CaM pulls the JM region off the membrane.

Experiments are in progress to establish if there is an orientational dependence of the TM helices for Ca^{2+}/CaM binding to the JM sequence and for structural change in the JM region.

References

1. Sato T, Pallavi P, Golebiewska U, McLaughlin S, Smith SO. *Biochemistry* **45**: 12704-12714, 2006.
2. McLaughlin S, Smith SO, Hayman MJ, Murray D. *J Gen Physiol* **126**: 41-53, 2005.
3. Saito H, Tuzi S, Naito A. *Annu Rep NMR Spectrosc* **36**: 79-121, 1998.
4. Li H, Sabchez-Torres J, DelCarpino A, Salas V, Villalobo A. *Biochem J* **381**: 257-266, 2004.

6-11-110

An End-cap for Enhancing Hairpin Stability

Kier, Brandon; Andersen, Niels*
University of Washington, Department of Chemistry, UNITED STATES

**E-mail: sciguy@u.washington.edu*

Introduction

α-Helix capping motifs are textbook biochemistry; they are common in natural proteins and for decades they have been employed in peptide helix design strategies to improve stability and reduce fraying.[1] Capping moieties stabilize a helix by providing H-bonding partners for free backbone amides or carbonyls, countering the helix macrodipole, or employing a hydrophobic staple. A hairpin cap would be very useful; ideally it would increase stability and reduce fraying via strong, end-specific interactions that locked the two termini together. To date, the only candidates for end-specific β-hairpin caps are terminal ion pairs[2] and cyclization[3] (a disulfide or amide bond covalently linking the termini to form a second turn).

We designed a series of stable, 6-10 residue "capped loop" microprotein hairpins.[4] These peptides are of the formula (Ac/Pr)-W^{1}I^{2} (N/p) ^{3}G^{4} (I/L/K) ^{5}W^{6}T^{7}G^{8} (-NH_2/PS) (Pr= propionyl, p=D-Pro), and incorporate a very strong set of capping interactions (W/W cross strand interaction,[5] WTG indole/amide interaction, and bifurcated Thr to Ac H-bonds) flanking a tight, two residue turn. The capping motif exhibited a distinct CSD (Chemical Shift Deviation) profile by NMR; the chemical shifts of the W6 Hε3 and Hβ3 protons (**1**) and G8 HN (**2**) proton are far upfield of their expected random coil positions. Furthermore, the hydroxyl proton for T7 (**3**) is NMR-visible due to a bifurcated H-bond with the acetyl (or Pr) carbonyl.

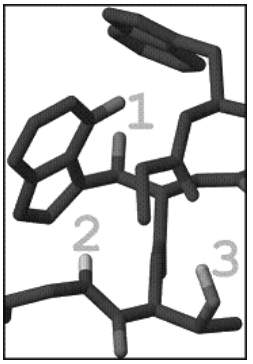

Figure 1.

In our other systems with a stabilizing W/W interaction flanking a tight turn, mutating the turn Gly to D- or L-Ala was destabilizing (data not shown.) However, in the Ac-WIpGKWTG-NH_2 microprotein (Tm≈65 °C) the orientation of the indole rings was reversed[6] (C-term Trp interacting with a terminal Gly amide instead of N-term Trp interacting with turn amides) and the <><>Gs for Gly4 to L-Ala and G4 to D-Ala mutations were nearly zero. This tolerance of turn mutations suggested that the turn and cap were not directly interacting, and thus the peptide would tolerate insertions between the loop and the cap which would produce longer hairpins.

Results and discussion

We now report that this motif can be used to stabilize hairpins of any length, so long as the capping tryptophan residues are at non-H-bonding positions. The bar graph illustrates this using diagnostic CSDs (The C-term W Hε3 and C-term G HN are diagnostics of the capping motif; the turn G <>δHα and inward pointing amide proton of the 2nd residue give turn and strand populations, respectively. When the capping motif was placed an odd

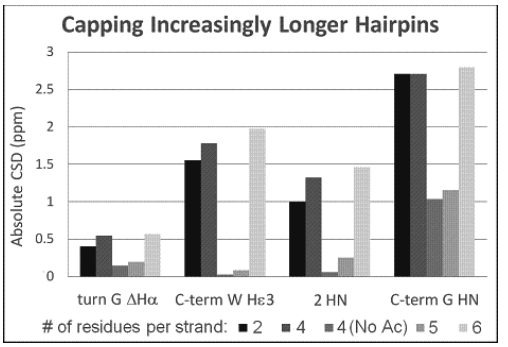

Figure 2.

2: Ac-W----INGK----WTG-NH_2
4a: Ac-W--VTINGKKI--WTG-NH_2
4b: ---W--VTINGKKI--WTG-NH_2
5: Ac-W-TVTINGKKIT-WTG-NH_2
6: Ac-WLSVTINGKTIKVWTG-NH_2

Figure 3.

number of residues from the turn (W/W pair occupying H-bonding positions), hairpin formation was not observed and the shift of the terminal Gly HN was about the same as that seen for random-coil aryl-amide interactions (eg. in tripeptide Ac-WTG-NH_2).

The general format (Ac/Pr)-W…XZG… must be followed, where X is optimally Trp (Phe or Tyr are tolerated) and Z is optimally Thr (Ser, Val, and Abu – Thr minus the OH – were all shown to be slightly less stable; data not shown.) The cap is amenable to C-terminal extensions; peptides of the formula Pr-W…WTGPS motifs are slightly better folded than their Ac-W…WTG-NH_2 counterparts. However, N-terminal extensions disrupt the capping interaction, and removal of the Ac (or Pr) to leave a free amine at the N-terminus causes catastrophic destabilization.

Lys and Arg were employed at positions diagonal to Trp1 to produce stabilizing pi-cation interactions. Ala mutations were only modestly deleterious, suggesting that "free" diagonal pi-cation interactions provide a greater net benefit that those associated with a capping interaction. (~0.2 kJ/mol vs. the 0.35-0.08 kJ/mol determined by Waters *et al*.).[7]

This capping motif should prove useful in expanding possibilities for stable beta hairpin design and stabilizing biologically relevant loop sequences as well as *in vitro* and in silico folding studies. These applications are being examined.

Acknowledgements

This research was supported by a grant from the NSF (National Science Foundation, USA; grant # GM059658).

References

1. Chakrabartty A, Doig AJ, Baldwin RL. *Proc Natl Acad Sci U S A*. **90**: 11332-11336, 1993.
2. Fesinmeyer RM, Hudson FM, Andersen NH. *J Am Chem Soc* **126**: 7238-7243, 2004; Olsen KA, Fesinmeyer RM, Stewart JM, Andersen NH. *Proc Natl Acad Sci U S A*. **102**: 15483-15487, 2005.
3. Gibbs AC, Kondejewski LH, Gronwald W, Nip AM, Hodges RS, Sykes BD, Wishart DS. *Nat Struct Biol* **5**: 284-88, 1998; Russell SJ, Blandl T, Skelton NJ, Cochran AG. *J Am Chem Soc* **125**: 388-395, 2003.
4. Kier BL, Andersen NH. *J Am Chem Soc* **130**: 14675-14683, 2008.
5. Cochran AG, Skelton NJ, Starovasnik MA. *Proc Natl Acad Sci U S A* **98**: 5578-83, 2001; Andersen NH, Olsen KA, Fesinmeyer RM, Tan X, Hudson FM, Eidenschink L, Farazi SR. *J Am Chem Soc* **128**: 6101-6110, 2006.
6. Eidenschink L, Kier B, Huggins KNL, Andersen NH. *Proteins: Struct Funct Bioinf* **75**: 308-322, 2009.
7. Tatko D, Waters ML. *Prot Sci* **12**: 2443-2452, 2003.

6-12-111

Interaction of the minimal active peptide sequence of human growth hormone releasing factor with negatively charged liposomes

Thomas, Lars; Weigelt, Heiko; Köhler, Guido; Zschörnig, Olaf [*]

University of Leipzig, Institute for Medical Physics and Biophysics, GERMANY

[*]*E-mail: zsco@medizin.uni-leipzig.de*

Introduction

The most bioactive peptides such as hormones and neurotransmitters do not exist in an ordered structure in aqueous solution. The conformation of the peptide changes from this flexible unordered structure into an inherent one, only when it reaches a biomembrane. On this basis it is important to investigate peptides like growth hormone releasing factor (GHRF) in the presence of phospholipid bilayers. Human GHRF is an amidated peptide consisting of 44 amino acids residues. A lot of studies have shown that the residues at the N-terminal part are the active core of the peptide. The residues YADAIFTNSYRKVLGQLSARKALQDISR (1-29) possess almost full activity *in vivo* and *in vitro*. We studied the interaction of human GHRF (AA 1-29) with phospholipid membranes. The interaction of GHRF (AA 1-29) with liposomes was investigated fluorescence spectroscopy. To detect a fluorescence signal the peptide were labelled at the first, 15th, 24th and 29th position with Dansyl. The dansyl fluorescence intensity of human GHRF (AA 1-29) at different lipid peptide ratios were analysed using a model, which includes the hydrophobic and the electrostatic interaction between the peptide and the phospholipid membrane[1]. The hydrophobic binding constant of GHRF(AA 1-29) and its effective charge were determined using this model. All results indicate, that the binding of GHRF (AA 1-29) to phospholipid membranes is increased strongly by increase of the surface charge density of the liposomes. The peptide is arranged parallel to the membrane surface and is localized in membrane-water-interface of the liposomes.

Results and Discussion

Using neutral liposomes made of pure phosphatidylcholine, no changes of the fluorescence properties of different dansyl labelled GHRF (AA1-29) could be observed. This

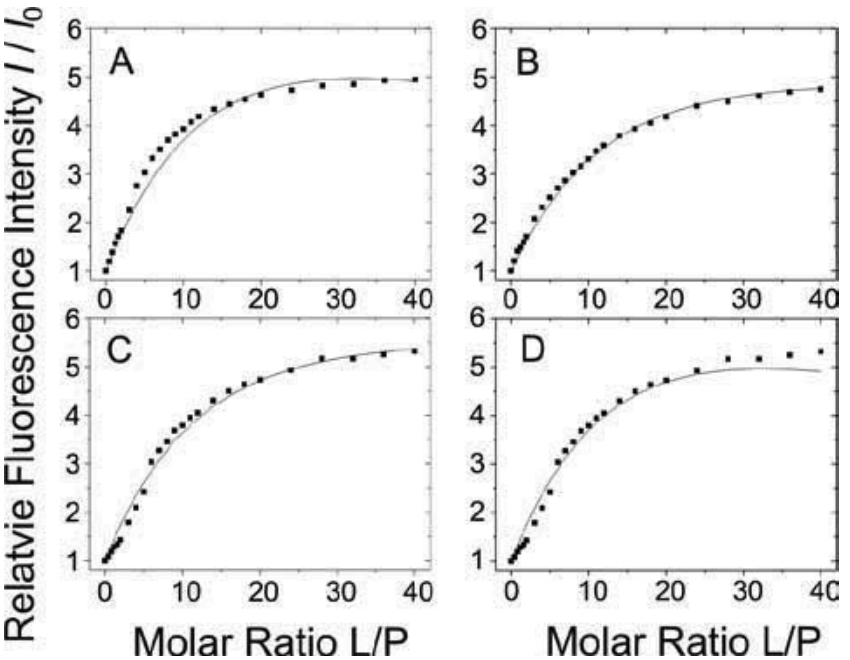

Figure 1. Normalized Dansyl fluorescence emission intensity of different GHRF analogs at 520 nm for different lipid peptide ratios, acquired at pH 7.4 and a temperature of 25 °C. The used liposomes were composed of 1:1 mixture of PS and PC. The used GHRF analogs were 1-Dansyl GHRF (A), 15-Dansyl GHRF (B), 24-Dansyl GHRF (C) and 29-Dansyl GHRF.

indicates a complete absence of GHRF binding to neutral phospholipid membrane surfaces. In the presence of negatively charged membrane surfaces binding of dansyl labeled GHRF (AA1-29) could be observed.

The normalized fluorescence intensities I/I_0 of the four Dansyl-labelled GHRF peptides at 520 nm for different lipid peptide ratios (binding curve) are shown in Fig. 1. The liposomes were composed of a 1:1 mixture of PS and PC. The line represents the best fit of the data using the described model. All used GHRF analogs show nearly identical binding properties. Therefore the amino acid exchange for the labeling has only negligible effects on peptide binding. The hydrophobic binding energy δG_H of all Dansyl-labelled GHRF peptides to the lipid membrane was calculated to be –35 kJ/mol. Due to ion binding, the effective charge of the peptide was reduced to 2 e, which is about 50% of the expected net charge of the peptide at the used pH value of 7.4. The electrostatic binding energy $\delta G_E = z_{eff} F\psi$ can be calculated from the effective charge of the peptide z_{eff} and surface potential ψ. It amounts to -10 kJ/mol for the used conditions. Methods The fluorescence spectra were acquired on a Fluoromax 2 spectrometer (Jobin Yvon, Edison NJ, USA). An excitation wavelength of 340 nm for Dansyl was used. The fluorescence emission were observed between 480 and 550 nm. The binding curves were acquired as follows: Certain amounts of the liposomes in buffer solution were titrated to a peptide solution with a concentration of 10 µM to achieve the desired lipid-peptide-ratio. The lipid-peptide-ratio were increased by adding further liposome stock solution to the lipid peptide solution. The fluorescence spectra were accumulated 5 times to get a reasonable signal to noise ratio. Additionally, fluorescence spectrum of each liposome concentration were acquired in the absence of peptide. These background spectra were subtracted from the original spectra to minimize the effect of light straggling due to the LUV. The background corrected fluorescence intensity at 520 nm were used for the calculation for membrane bound fraction of peptide according to Ladokhin *et al.*[2]: $f_b=(I-I_o)/(I_\infty-I_o)$ whereas fb is the membrane bound fraction of the peptide, I the fluorescence intensity of the peptide at certain lipid peptide ratio, I_0 the fluorescence intensity in the absence of lipid and I_∞ the fluorescence intensity when all peptide is bound to the membrane. This value is unknown and has to be calculated from the fit of the data.

References

1. Thomas L, Scheidt HA, Bettio A, Beck-Sickinger AG, Huster D, Zschörnig O. *Eur Biophys J* **38**: 663-677, 2009.
2. Ladokhin AS, Jayasinghe S, White SH. *Anal Biochem* **285:** 235-245, 2000.

6-12-112

Artificial esterases formed by self-organization of N-lipidated tripeptides of a catalytic triad immobilized on cellulose

Fraczyk, Justyna; Kujawska, Nina; Kamiński, Zbigniew J*

Technical University of Łódź, Institute of Organic Chemistry, POLAND

E-mail: jfraczyk@gmail.com

Introduction

Supramolecular structures formed by N-lipidated oligopeptides immobilized in a regular pattern on a cellulose surface are able to recognize the shape and properties of a ligand, then binding selectively guest molecules matching the requirements of a binding pocket.[1] Due to the conformational flexibility of both interacting partners, the relative orientation of the functional groups of a ligand as well as that of the binding cavities could be readjusted to the most energetically favored conformation. Our previous studies have documented that process of binding guest molecules is reversible and competitive.

Results and Discussion

The catalytic activity of the library was measured by spectrophotometric determination of amount of p-nitrophenol formed from Z-Ala-Aib-ONp in buffered aqueous methanol in the presence of appropriate N-lipidated peptides (Fig. 3).

Results have shown that most supramolecular structures with a variation of a Glu, His, Ser tripeptide motif inside the binding pockets revealed significant hydrolytic activity at room temperature even in the case of the relatively uncreative substrate Z-Ala-Aib-ONp with a reactive center in the close proximity of *α,α*-disubstituted Aib

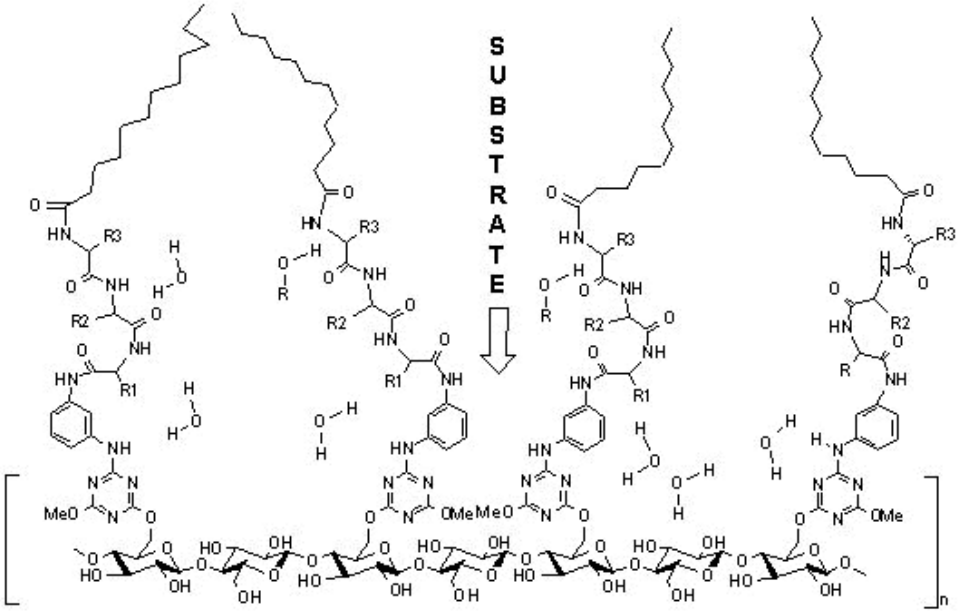

Figure 1. Binding of the substrate.

Therefore, it was supposed that under favorable circumstances the host structure could operate as a catalyst if suitable molecular fragments were incorporated into the binding pocket.

In order to verify this hypothesis, we prepared a library of 36 supramolecular structures with a catalytic triad His Asp (Glu) Ser inside the binding pockets using 4-(4,6-dimethoxy-1,3,5-triaz-2-yl)-4-methylmorpholinium tetrafluoroborate as a coupling reagent.[2]

residue. In the structures of the most catalytically active constructs, ~His-Glu-Ser-10-undecenoyl, ~His-Ser-Glu-10-undecenoyl and ~Ser-His-Glu-ricinoyl fragments were enclosed. Taking into account the substantial acceleration of the reaction rate under relatively mild reaction conditions, catalysts formed by the self-organization of N-lipidated tripeptides of a catalytic triad immobilized on cellulose could be considered artificial enzymes (chemzymes) emulating esterases.

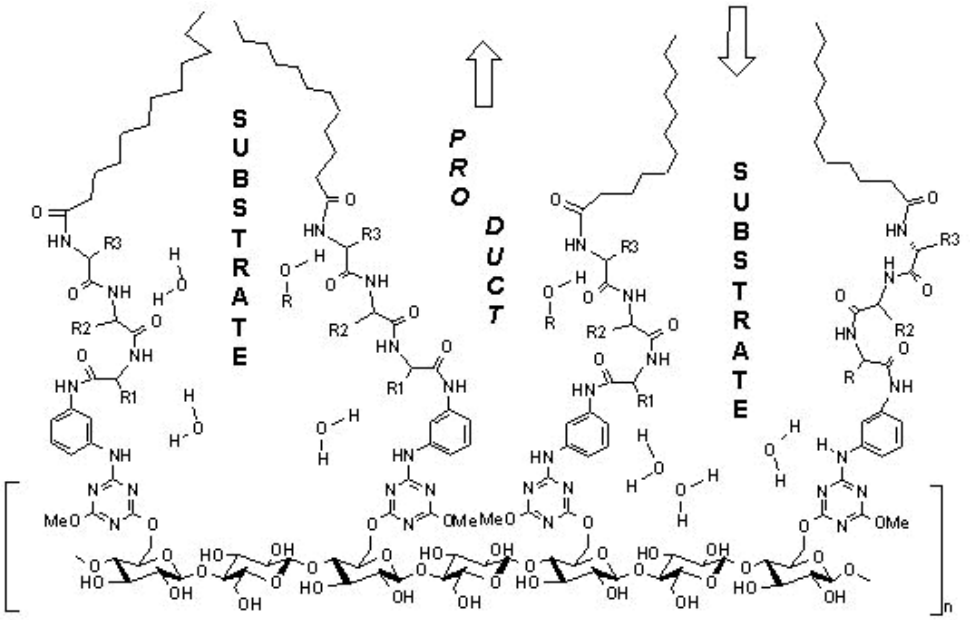

Figure 2. Release of product assisted by substrate binding.

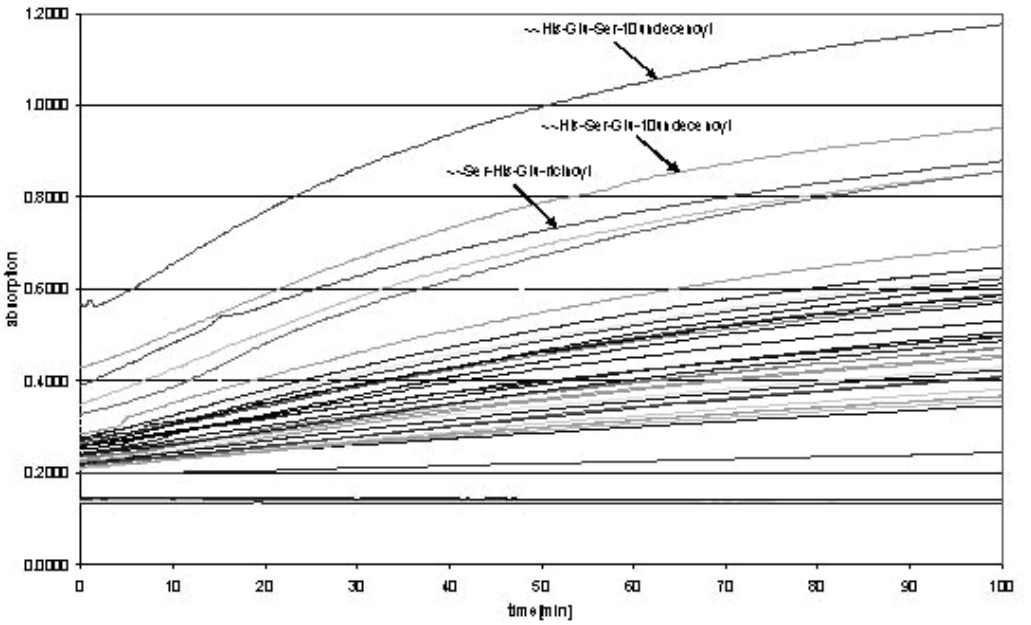

Figure 3. The rate of hydrolysis of Z-Ala-Aib-ONp and corresponding blank data obtained in the absence of catalytic structures.

Acknowledgement

This work was supported by Ministry of Science and Higher Education, Grant 2 P05F 031 30.

References

1. Frczyk J, Kamiński ZJ. *J Comb Chem* **10**: 934-990, 2008.
2. Kamiński ZJ, Kolesińska B, Kolesińska J, Sabatino G, Chelli M, Rovero P, Błaszczyk M, Główka ML, Papini AM. *J Am Chem Soc* **127**: 16912-16920, 2005.

6-12-113

A comparative study on lipid affinity of cell penetrating peptides in presence or absence of cargo

Biondi, Barbara; Calderan, Andrea; Guiotto, Andrea; Ruzza, Paolo*

CNR - Institute of Biomolecular Chemistry, ITALY

**E-mail: barbara.biondi@unipd.it*

Introduction

A growing number of natural and/or synthetic peptides have been discovered with cell membrane penetrating capability and considered as targeting structures for delivery of bioactive compounds into various cell types.

Although CPPs show an highly variable structure some general features, as abundance of positive charges, especially from arginine residues, and the presence of bulky hydrophobic aminoacids, have been suggested to be essential for an efficient cellular uptake. Even if the mechanism is still unclear , the most common hypotheses propose that translocation occurs via endocytosis or macropynocytosis followed by partial escape from the endocytotic vesicles of lysosomes.

The ability to disturb the membrane, or to bind and thereby recruit specific membrane component, is important to awaken endocytotic machinery; consequently studying CPPs in model membrane could become important to understand peptide-membrane interaction on a molecular level, explaining how CPPs may translocate a membrane without destroying it and how peptide-membrane interactions come into play in shuttling CPPs via different routes with different efficiency.

In this work we try to connect structural and chemical characteristics of CPPs to the capability to interact with model membrane in order to obtain a biophysical classification that could predict the behavior in cell systems. Using fluorescence and CD spectroscopies we studied the interaction of different CPPs (Antennapedia, kFGF, Tat and oligoarginines peptides), and their chimeric conjugates with HS1pY^{396} peptide (corresponding to the sequence 392-401 of HS1 protein), with small unilayer vesicles (SUVs) of different charge density.

Results and Discussion

The peptides were synthesized by solid-phase method on an Advanced ChemTech 348ω synthetizer using Fmoc chemistry.

The binding of peptide to phospholipid of different composition was evaluated using carboxyfluorescein labeled peptides. Carboxyfluorescein emission is

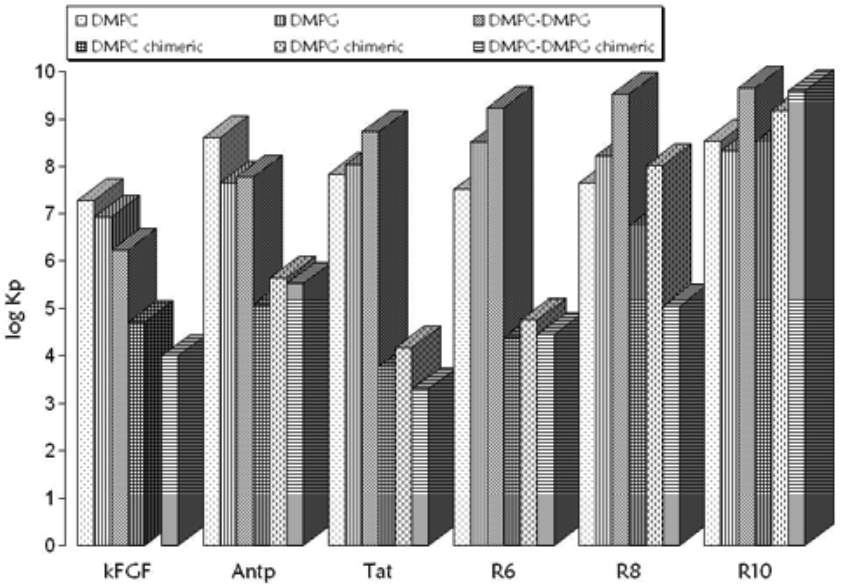

Figure 1. Values of log Kp for the different peptides.

sensitive to environment change, showing a quenching of the fluorescence emission when is in a more hydrophobic environment after addition of phospholipid.[1]

Spectroscopic titrations of peptides with SUVs were performed adding appropriate aliquots of SUVs (DMPC, DMPG or DMPC-DMPG 3:1 molar ratio) to a solution of peptide in TRIS-HCl buffer (5 mM, pH 6.8).

Fluorescence quenching induced by phospholipid addition was used both to generate the binding isotherm of the labeled peptides and to calculate the related partition coefficients (K_p). In Fig. 1 we report the values of $\log K_p$ for the different CPPs and chimeric peptides.

In addition, peptides mediated membrane leakage has been evaluated by fluorescence detection of calcein release from DMPC/DMPG 3:1 SUVs.[2]

All peptides show a leakage percentage less than 25% at a high peptide/lipid ratio. The comparison of conformational properties of CPPs and HS1pY-conjugates has been evaluated by CD spectroscopy both in membrane mimetic environment and bound to phospholipid vesicles. Results evidence that the conformation of CPPs is destabilized by the addition of cargo.

To assess the cell penetration ability of the chimeric phospho-peptides into mammalian cells the carboxy fluoresceinyl labeled HS1pY peptide and its CPP-conjugates have been tested. The phospho-peptides were added (12.5 μM) to the incubation medium of CHO (Chinese hamster ovary) cells for 30 min, 1 h at 4 °C and 2 h at 37 °C; cells were washed and peptide internalization was analyzed by confocal microscopy. In the conditions examined all the chimeric peptides, with the exception of R6-HS1pY and kFGF-HS1pY, penetrate in the ovarian cells.

These results provide three different conclusions:

i) increasing the number of basic residues (arginine) the affinity of CPPs for phospholipids increase and there is a minor effect of cargo, as is pointed out by the Kp values of R8-HS1pY and R10-HS1pY;

ii) on the other hand the affinity of CPP and CPP-cargo toward phospholipids is not related to the internalization capability, therefore the mechanism of cell penetration is independent of the affinity CPP-phospholipids;

iii) membrane leakage studies confirm the atoxicity of our CPPs and chimeric conjugates, in fact the release of calcein is very low compared to the values reported for antimicrobic peptides.

Acknowledgements

Contract grant sponsor: National Research Council of Italy.

References

1. Ruzza P, Elardo S, Calderan A, Donella-Deana A, Crisma M, Brunati A, Massimino ML, Pinna LA, Borin G. Conformational studies of chimeric cell penetrating peptides in membrane mimicking environment. *Peptides 2002* (Proceedings of the 27th European Peptide Symposium, Napoli, Italy) Benedetti E, Pedone C (Eds), Eldizioni Ziino, Napoli, 2002, pp 876-877.
2. Belokoneva OS, Villegas E, Corzo G, Dai L, Nakajima T. The hemolytic activity of six arachnid cationic peptides is affected by the phosphatidylcholine-to-sphingomyelin ratio in lipid bilayers. *BBA-Biomembranes* **1617**: 22-30, 2003.

6-12-114

Kinetic Study of Liposome Adsorption to a Peptide-modified Au Electrode for Applications in Biomembrane Sensors

Kasuya, Yuzo[1,]; Nosaka, Shizuka[2]; Yamada, Daisuke[2]; Ikeda, Yasuyuki[1]; Matsumura, Kazunari[2]*

[1]Graduate School of Engineering, Shibaura Institute of Technology, JAPAN; [2]Faculty of Engineering, Shibaura Institute of Technology, JAPAN

[*]E-mail: i022031@sic.shibaura-it.ac.jp

Introduction

Specific binding of biomolecules to membrane receptor is deeply involved in a cellular process. Since membrane-bound molecules such as membrane proteins are labile in solution compared to those in lipids environment, analytical devices based on artificial membrane systems that permits the functional reconstitution of them have been studied during the past decade.[1] Immobilization of intact liposomes on solid surface has attracted attention because liposome which preserves internal space and membrane dynamics is more potent plasma membrane mimics than planar lipids bilayer. To prepare a stable liposome adlayer, we have proposed an immobilizing method based on small peptide modification of solid surface.[2] Here we present investigating the kinetics of liposome adsorption to surface-bound synthetic peptides and applications of our method in detection of protein-glycolipid interactions on membrane surface using quartz crystal microbalance (QCM).

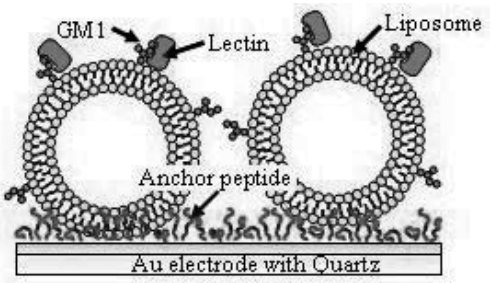

Figure 1. Immobilized-liposome sensor using peptide-modified Au electrode for monitoring protein-glycolipid interaction on membrane surface.

Results and discussion

The study of liposome adsorption to surface-bound peptides was performed according to the following procedure. A cleaned Au electrode was modified with various amphiphilic peptides which have terminus Cys residue for binding to Au surface. Adsorbed mass changes upon injection of liposome suspension were monitored by QCM. The densities of surface-bound peptides were adjusted to 0.67 pmol/mm^2 by the addition of an appropriate concentration of peptide solution.

The QCM measurements revealed that the Ac-A5W2K9C peptides immobilize liposomes consisted of phosphatidylcholine (PC), phosphatidylserine (PS) and cholesterol (chol) at a density of 23-25 ng/mm^2 with maximum at 100 nm vesicle size between 50 nm to 1000 nm. These adsorbed masses, which are six-fold amount of molecular assembly expected for formation of planar lipids bilayer, indicate the encapsulation of solution by intact liposome. AFM study also showed that the surface-bound peptides kept a single flattened vesicular structure of liposome without fusion. It is noteworthy that desorption of immobilized liposome from the peptidic surface was not observed for buffer exchanges while the initial adsorption processes could be described by Langmuir adsorption kinetics. The peptides which have diminished electrostatic segment or lack Trp residue such as WK4A5C, K4WA5C, K5A5C modestly immobilized liposomes at a density of 5 ng/mm^2. Moreover, electrostatically adsorbed lipid vesicles on K5A5C were easily removed from electrode. These results show two findings: firstly, the solid surfaces modified with small peptides which have appropriate hydrophilicity dose not cause fusion or disruption of liposome ; and secondly, penetration of the hydrophobic segment including Trp residue into liposome membrane lead to irreversible adsorption process.

High association and low dissociation rate constant were yielded for liposome adsorption to transmembrane peptides, especially Ac-A5W2K9C-modified Au (Fig. 2). In contrast, high dissociation rate constant was observed when the liposomes were adsorbed to K5A5C-modified Au surface, although association rate is comparable to WK4A5C and K4WA5C. The result means that a penetration activity of peptide driven by the Trp dominates a dissociation process of adsorbed liposome and electrostatic attractive force contributes an association process. The both of rate constants were decreased with increasing vesicle size regardless of the peptide sequence. However, the binding constants for liposome adsorption to transmembrane peptide showed bell-shape profile with maximum at 100 nm similar to the size dependence for immobilized amounts of liposome.

But the non-transmembrane peptide as K5A5C showed simple decreasing with particle size.

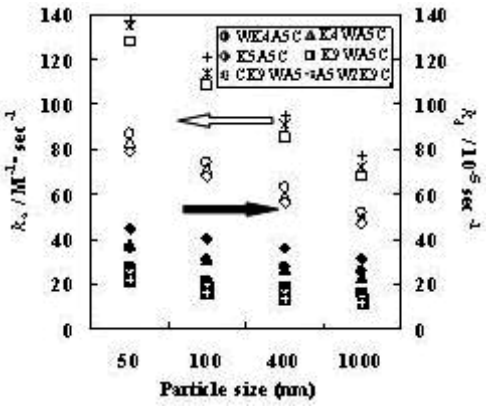

Figure 2. Association and dissociation rate constants for liposome adsorption to the surface-bound peptides.

To validate our approach, we monitored the well-studied interactions of lectins with monosialoganglioside GM1 (GM1) at liposome surface immobilized with K9WA5C (Fig. 1). The obvious frequency decrease was observed with a stepwise injection of peanut agglutinin (PNA), maackia amurensis agglutinin (MAA) and wheat germ agglutinin (WGA) to GM1-doped vesicles. The binding constants (K_a) and the maximum binding amounts (δm_{max}) were obtained from the binding isotherm (Table 1). For PNA-GM1 interactions, the value of δm_{max} share similarity with the findings obtained from liposomal affinity chromatography[3] rather than those from QCM study of a planar lipid membrane doped with glycolipids.[4] The δm_{max} of WGA to GM1-doped liposome was a third of that obtained from PNA experiment, corresponding to the difference of molecular weight. All the binding parameters were easily determined without any labeled molecules, and the availability of our method was proven.

Table 1. Maximum adsorbed masses and binding constants of lectin binding to glycolipid

lectins	Δm_{max} (ng / mm^2)	K_a ($\times 10^6$ M^{-1})
PNA	2.3 ± 0.1	3.2 ± 0.4
MAA	1.5 ± 0.1	2.4 ± 0.1
WGA	0.8 ± 0.1	1.2 ± 0.2

Here we demonstrate that our approach based on peptides-modification is applicable to monitoring of biomolecular interactions occur at membrane surface. This method is no need to specially doped tethered molecules for immobilization of liposomes on solid surface. Moreover, the liposomes can be mounted at sufficient densities without transformation to lipid bilayer. These are great advantages for development of liposomal sensor to study the ligand-transmembrane receptor interactions.

References

1. a) Stenlund P, Babcock GJ, Sodroski J, Myszka DG. *Anal Biochem* **316**: 243-250, 2003.
   b) Morita S, Nukui M, Kuboi R. *J Colloid Interface Sci* **298**: 672-678, 2006.
   d) Yoshina-Ishii C, Miller GP, Kraft ML, Kool ET, Boxer SG. *J Am Chem Soc* **127**: 1356-1357, 2005.
2. Kasuya Y, Ohtaka M, Tsukamoto K, Ikeda Y, Matsumura K. *Chemistry Letters* **37**: 588-589, 2008.
3. Mansson J-E, Olofsson S. *FEBS Lett* **156**: 249-252, 1983.
4. Steinem C, Janshoff A, Wegener J, Ulrich W-P, Willenbrink W, Sieber M, Galla H-J. *Biosens Bioelectron* **12**: 787-808, 1997.

6-17-115

Fraternal twins ! γ-peptide and oligoureas are isosteric, isostructural foldamers endowed with yet distinct biomolecular recognition properties.

Claudon, Paul[1,]; Violette, Aude[1]; Lamour, Karen[1]; Fournel, Sylvie[1]; Heurtault, Béatrice[2]; Godet, Julien[3]; Jamart-Grégoire, Brigitte[4]; Averlant-Petit, Marie-Christine[4]; Briand, Jean-Paul[1]; Duporail, Guy[3]; Monteil, Henri[5]; Guichard, Gilles[1]*

[1]CNRS, IBMC, UPR9021, immunologie et chimie thérapeutique, FRANCE; [2]CNRS/ULP, chimie enzymatique et vectorisation, FRANCE; [3]CNRS/ULP, photophysique des interactions biomoléculaires, FRANCE; [4]CNRS/INPL, Laboratoire de chimie physique macromoléculaire, FRANCE; [5]ULP, Institut de bactériologie, FRANCE

[*]E-mail: G.guichard@ibmc.u-strasbg.fr

Introduction

In the field of peptidomimetics, there has been a sustained interest towards the design of non-natural oligomeric backbones with new folding patterns. Over the past 12 years, the amide linkage has become the quintessential motif to elaborate folding oligomers. Aliphatic and aromatic oligoamides (peptoids, *β*-, *γ*-peptides) have provided numerous helical-folded structures, many of which have shown interesting biological activities.[1] Interestingly, substituting urea for the CH_2-CO-NH units in the γ^4-peptide backbone represents a spectacular case of isosteric and iso-structural replacement. Detailed NMR studies of the resulting oligoureas revealed a helical fold very similar to that reported for the cognate γ^4-peptides.[2,3]

How such isosteric and isostructural oligoamide and oligourea backbones compare in biomolecular recognition events is an interesting question that we attempted to address in the present work. Notably the two systems were compared for their antimicrobial activity, membrane interaction and disruption properties. Both *γ*-peptides and oligoureas designed to mimic globally amphiphilic *α*-helical host-defense peptides have been synthesized and tested.

Results

Antibacterial activity of **1** and **2** was determined against *E. coli, P. aeruginosa* and *S. aureus.* Whereas **1** exhibited minimal inhibitory concentrations (MICs) very similar to that found for melittin, a honeybee toxin, peptide **2**, was virtually inactive (MIC and MBC > 256 µg mL-1) on both gram positive and gram negative bacteria. These results thus reveal a surprising functional dichotomy between the two isostructural systems and underscore the unique antibacterial of amphiphilic oligourea helices. To question whether the functional difference between oligourea and oligoamide backbones results from differential membrane disruption activities, we have undertaken detailed physicochemical investigations using negatively charged phospholipid membranes as model systems.

The restricted mobility of the indole moiety upon interaction with the membrane was inferred from an increase in fluorescence anisotropy. Titration of **1** and **2** with EYPC/EYPG LUVs was used to quantify the binding of both oligomers to vesicles (Fig. 2).

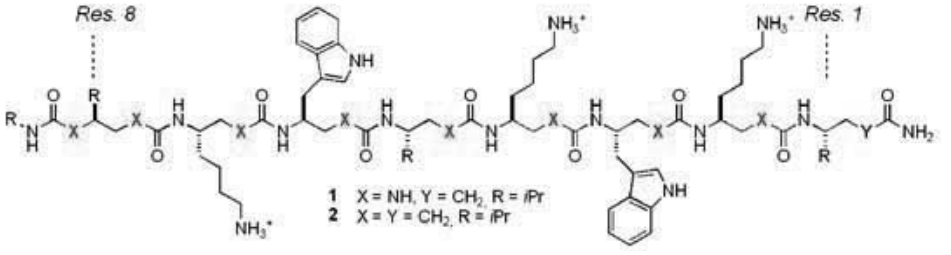

Figure 1. Sequence of oligourea and *γ*-peptide compared for biological activities and physical properties.

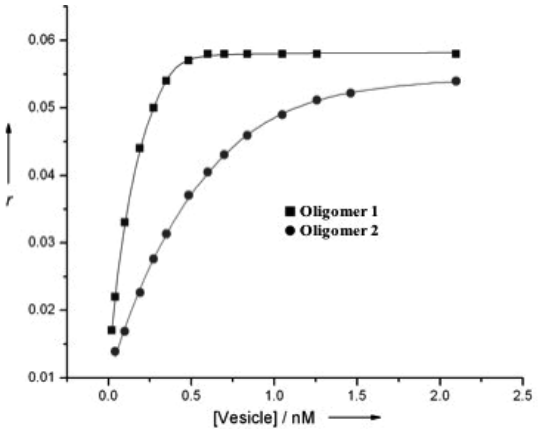

Figure 2. Fluorescence anisotropy (r) of oligourea **1** and γ-peptide **2** measured at increasing vesicle concentration (EYPC/EYPG 70:30 molar ratio).

The apparent dissociation constants ($1.4 \cdot 10^{-7}$ $molL^{-1}$ for **1** and $9 \cdot 10^{-7}$ $molL^{-1}$ for **2**) calculated by curve fitting using a receptor-ligand binding model indicates that γ-peptide **2** has a 6-fold lower affinity for the membrane than oligourea **1**.

The time course of the leakage of encapsulated carboxyfluorescein was detected by its increase in fluorescence intensity at 518 nm (Fig. 4). Whereas γ-peptide **2** was not able to induce significant efflux of carboxyfluorescein at 4.16 μM even after prolonged time, very fast and strong carboxyfluorescein release was observed when LUVs were treated with more polar oligourea **1** at the same concentration.

This series of experiments further confirms the differential membrane disruption properties exhibited by isostructural oligoamide and oligourea backbones.

Acknowledgments

This research was supported in part by CNRS, ANR, Région Alsace, and ImmuPharma. CIFRE fellowships from ImmuPharma and the Agence Nationale pour la Recherche Technique (ANRT) for PC is gratefully acknowledged.

References

1. Le Grel G. *Foldamers.* Huc I, Hecht S (Eds), Wiley-VCH Verlag, Weinheim, 2007, pp 35-74.
2. Semetey V, Rognan D, Hemmerlin C, Graff R, Briand J-P, Marraud M, Guichard G. *Angew Chem Int Ed* **41**: 1893-1895, 2002.
3. Violette A, Averlant-Petit MC, Semetey V, Hemmerlin C, Casimir R, Graff R, Marraud M, Briand J-P, Rognan D, Guichard G. *J Am Chem Soc* **127**: 2156-2164, 2005.

6-17-116

Temperature dependant methionine proximity assay highlights conformational variations occurring through the mechanism of peptidergic GPCR activation

Arsenault, Jason[1,]; Clément, Martin; Leduc, Richard; Guillemette, Gaétan; Lavigne, Pierre; Escher, Emanuel*

Université de Sherbrooke, Pharmacologie, CANADA

[*]E-mail: Jason.arsenault@usherbrooke.ca

G protein coupled receptors are invaluable for cell signal transduction mediated by external stimulus. Pharmacological efforts towards these targets are of primordial importance albeit few efforts have resulted in structural characterisation, even though rational drug design necessitates such information. Recent advances in crystallisation of the β-adrenergic receptor[1] have been highly insightful and such a structure corroborates our results on the human Angiotensin II type 1 receptor (hAT1) using the Methionine Proximity Assay (MPA) in identifying ligand receptor contact points.[2,3] Unfortunately, physical methods such as crystallography are still far from routine procedures and are limited to a static picture of a given receptor. In the present contribution we propose a cost effective method that permits analysis of conformational variations of different receptor states through an energy landscape, spanning from low energy conformations to conformations at physiological temperatures.[4] Our precise temperature controlled methodology requires a temperature stabilised photoreaction environment for the samples, which are inserted alongside hermetic UV lamps and, submerged in a circulating isothermal fluid.[4] Shown in Fig. 1, the CNBr digestion of a temperature dependant photolabelling experiment of the N111G/H256M hAT1 double mutant, demonstrates increased intrareceptor fluctuations at higher temperature which permits the tagging of methionine residues that are not accessible at lower temperatures (Fig. 1). Ligand accessibility can be classified from easily accessible (low temperature photolabelling) to less accessible residues (higher temperature photolabelling).

Photolabelling, MPA mutants constructed on the WT receptor, the constitutively active receptor (N111G) and a corresponding non-activable mutant (N111W) across the temperature range reveals activation-status dependant labelling patterns. This activation-status dependant labelling pattern may allow quantifying and identifying structural changes occurring during receptor activation. These temperature dependant changes can be normalised by dividing the TMDVII radioactive signal with the TMDVI signal. The H256M mutant and double mutants, depending on the proportion of active versus inactive conformation, have an altered methionine accessibility pattern (data not shown). This mutant thus indicates a loss of accessibility to position 256 compared to TMDVII when the receptor is in the active conformation

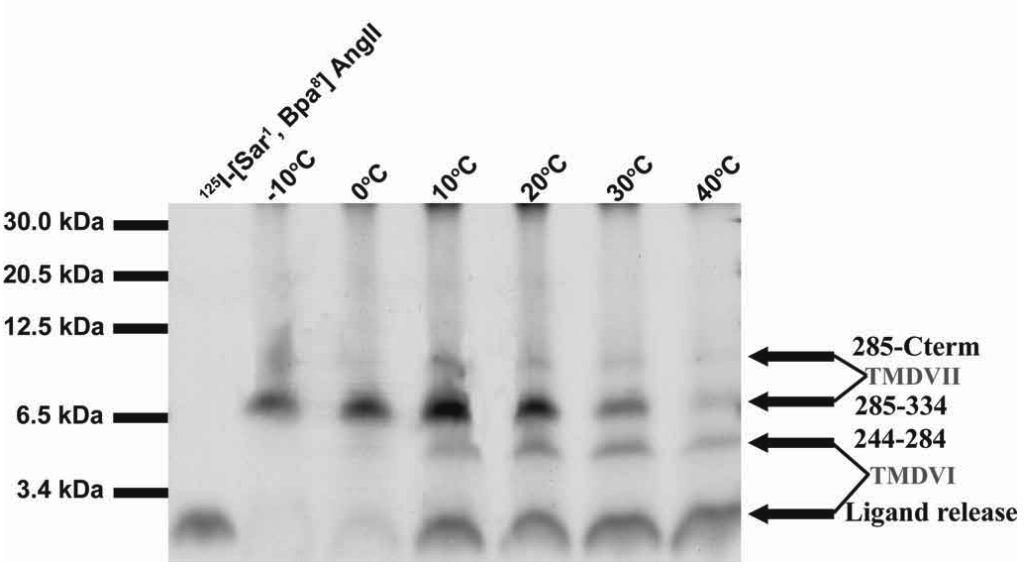

Figure 1. Temperature dependant methionine proximity assays of the N111G/H256M hAT1.

Figure 2. Ligand binding domains as seen by temperature dependant methionine proximity assays. An inactive conformation favours residues closers to the extracellular region, while an active conformation favours tagging of residues deeper within the transmembrane regions closer to the intracellular region. In the overlap figure the inactive (green) conformation is overlapped by the active (blue) conformation.

(N111G/H256M). In correlation with the other residues (data not shown), we propose an outwards movement of TMDVI during activation. Another observable event is the deeper ligand penetration inside the receptor. In the inactive receptor residue 260 is the most accessible, determined by the highest methionine specific tagging, but opposingly residue 249 is the most accessible in the constitutively active mutant.

These ligand dependant conformational changes would thus alter the intracellular loops and C-terminal portions of the receptor to transduce the signal and activate the G protein. We have elaborated a cost effective method to determine conformational changes occurring through receptor activation as well as thermodynamic stability of methionine mutants. An increased physiological temperature augments the range of motions permitted by the photoprobe (Bpa) and receptor complex, while opposingly lower temperature photolabelling highlights a more rigid, lower energy conformation. It is thus crucial that future photoaffinity labelling be done under temperature controlled conditions to highlight either physiological significance or lower energy conformational precision. Further understanding of GPCR conformations, activation and, thermodynamics are fundamentally important for rational drug designs.

References

1. Rasmussen SG, Choi HJ, Rosenbaum DM, Kobilka TS, Thian FS, Edwards PC, Burghammer M, Ratnala VR, Sanishvili R, Fischetti RF, Schertler GF, Weis WI, Kobilka BK. *Nature* **450**: 383-387, 2007.
2. Clément M, Martin SS, Beaulieu ME, Chamberland C, Lavigne P, Leduc R, Guillemette G, Escher E. *J Biol Chem* **280**: 27121-27129, 2005.
3. Rihakova L, Deraët M, Auger-Messier M, Pérodin J, Boucard AA, Guillemette G, Leduc R, Lavigne P, Escher E. *J Recept Signal Transd Res* **22**: 297-313, 2002.
4. Arsenault J, Renaud MP, Clément M, Fillion D, Guillemette G, Leduc R, Lavigne P, Escher E. *J Pept Sci* **13**: 575-580, 2007.

6-26-117

New analytical methodology for the characterization of synthetic polypeptides

*Miramon, Hélène; Cottet, Hervé; Martinez, Jean; Cavelier, Florine**

IBMM-UMR CNRS UM1 UM2 5247, FRANCE

**E-mail: florine@univ-montp2.fr*

Introduction

Our laboratory has developed a series of synthetic polymers which are elicitor *ie.* plant protector with an original mode of action: no direct attack of pathogenic agents but stimulation of the natural defenses of the entire plant. These polymers result from Ring Opening Polymerization of *N*–Carboxy Anhydride of L-alanine (20 eq) initiated by alaninol[1] (Scheme 1).

Although the ratio Monomer/Initiator (M/I) was defined, the length of polypeptides varied because the polymerization was not controlled. The mixture of poly(alanine)s $(Ala)_n$-Alol) with different lengths was difficult to analyse considering important solubility problem in common organic solvents and water. These tendencies are due to the ability of $(Ala)_n$-Alol to form intra-chain (α-helix) and inter-chain (β-sheet) H-bonds.[2] However, to have a full characterization of polypeptides, the determination of DP and molecular weight distributions can't be ignored. For example, NMR in deuterated TFA was possible and permitted to analyse end group and to determine DP_n by integration of central chain methylene in relation to the methylene of the initiator: the DP_n was 17. However, the success of DP_n determination based on end group required that polymerization initiation resulted from alaninol only, which was not the case. Indeed, polypeptides other than $(Ala)_n$-Alol were present and not differenciated. Unfortunately, NMR was not adapted to analyse the complex mixture of polypeptides with probable secondary products. MALDI-TOF mass spectrometry is a useful technique to visualize the molecular weight distribution of hardly soluble polypeptides. However, due to mass discrimation during ionisation, it was impossible to quantify the proportion of different chain lengths of polypeptides. To obtain more detailed characterizations, it was necessary to separate the polypeptides by chain length. Size Exclusion Chromatography was also considered but it was not possible to use such columns refereed to solubility problem in authorized solvents.

Results and discussion

We developed a separative method by Capillary Zone Electrophoresis (CZE) in new solvents mixtures based on HFIP. HFIP is a breaking H-bonds which enables to solubilize proteins and synthetic polypeptides. It's transparent to UV and allows CZE separations to be performed at all common wavelengths of analysis. It's miscible with water and has a low viscosity. Few publications deal with the use of HFIP for the separation of peptides by CZE.[3] To ensure oligomeric ionization of $(Ala)_n$-Alol in such a non-dissociating solvent with low dielectric constants, a solution of acid in water had to be added to the electrolyte. The proportion of aqueous acid in HFIP has been determined on the basis of the balance between ionization and solubility. The best ratio has been established as 80/20 (HFIP/Acidic water).

Results with different electrolyte conditions are displayed in Fig. 1. The first electropherogram (A) exhibited a separation using formic acid [0.4 M] in HFIP/water (80/20 v/v) mixture. In these conditions, polypeptides are separated according to the chain length up to DP=30. Two families of different functionalities were visible. Unfortunately, because of loss of efficiency for high DP due to polypeptide adsorption onto capillary

Scheme 1. Polymerization of NCA Ala

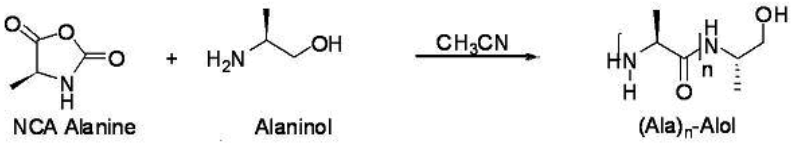

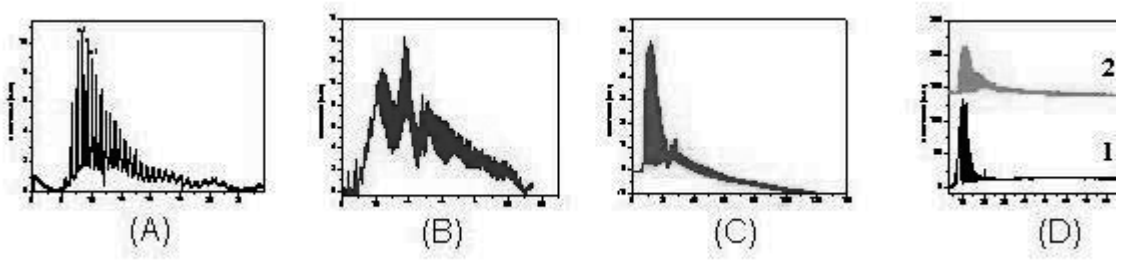

Figure 1. CZE characterization of $(Ala)_n$-Alol obtained at room temperature. Time scale electropherogram. Electrophoretic conditions: fused-silica capillary 33.5 cm (25 cm to the detector) × 50 mm id. Applied voltage: +30 kV. Hydrodynamic injection: 17 mbar, 3 s. UV detection at 200 nm. Temperature: 25 °C. Sample: 20 g L^{-1} in HFIP ((M/I=20 for A, B, C and D 2 and M/I = 5 for D 1) (A): Electrolyte is based on formic acid [0.4 M] in HFIP/water (80/20 v/v) mixture. (B): Electrolyte is based on formic acid [0.4 M] in HFIP/water (80/20 v/v) mixture with 0.5 % HEC (C) and (D): Electrolyte is based on orthophosphoric acid [0.04 M] in HFIP/water (80/20 v/v) mixture.

wall, these electrolyte conditions were not adapted to polypeptides with high chain length. However, it's well known in CZE separation of protein that addition of cellulose derivatives prevents adsorption.[4,5] Several tests conducted with formic acid [0.4 M] in HFIP/water (80/20 v/v) mixture with 0.5 % HEC allowed us to visualize longer chains until DP = 120 (B). But, the asymmetry of the peaks of low DP and the resolution precluded DP determination. An improvement of resolution has been obtained with orthophosphoric acid [0.04 M] in HFIP/water (80/20 v/v) mixture (C).

Several samples containing polypeptides with different M/I ratio (5/1 and 20/1) have been analysed to confirm the pertinence and reliability of CZE. The number average DP, weight average DP and molecular polydispersity were found to be 6,7 and 1.1 for the first sample and 9, 18 and 2 for the second sample respectively (D). In conclusion, a size-based separation of $(Ala)_n$-Alol has been achieved by CZE using HFIP/water mixtures. Best analytical results were obtained in the presence of cellulose derivatives and phosphoric acid for electrolyte mixture. This technique allowed us to characterize the entire molar mass distribution of hardly soluble $(Ala)_n$-Alol.

References

1. Cavelier F, Besnard O, Martinez J. *Patent* **2 832 409 n° 01 14 084** Published April 2006.
2. Kricheldorf HR, Mutter M, Maser F, Mueller D, Foerster H. *Biopolymers* **22**: 1357-1372, 1983.
3. Bossi A, Righetti PG. *Journal of Chromatography A* **840**: 117-129, 1999.
4. Gilges M, Kleemiss MH, Schmburg G. *Analytical Chemistry* **29**: 1460-1466, 1994.
5. Verzola B, Gelfi C, Righetti PG. *Journal of Chromatography A* **874**: 293-303, 2000.

6-28-118

Conformational analysis of the new temporin analogues: Gln^{3}TA and Pro^{3}TL

Saviello, Maria Rosaria[1,]; Cavalli, Andrea[2]; Malfi, Stefania[1]; Campiglia, Pietro[3]; Gomez-Monterrey, Isabel Maria[4]; Mangoni, Maria Luisa[5]; Novellino, Ettore[1]; Grieco, Paolo[1]; Carotenuto, Alfonso[1]*

[1]University of Naples "Federico II", Dept. Chimica Farmaceutica e Toss., ITALY; [2]University of Bologna, Dept. Scienze Farmaceutiche, ITALY; [3]University of Salerno, Dept Scienze Farmaceutiche., ITALY; [4]University of Naples, Dept. Chimica Farmaceutica e Toss., ITALY; [5]University of Rome, II Facolta' di Medicina e Chirurgia, ITALY

[*]E-mail: mariarosaria.saviello@unina.it

Introduction

Temporins are antimicrobial peptides (AMP's) isolated from the skin of Red European frog "Rana temporaria". They are active particularly against Gram-positive bacteria, Candida species, fungi. They have the ability to bind and permeate both artificial and biological membranes. By spectroscopic means, we have recently investigated two members of this AMP family Temporin L (FVQWFSKFLGRIL-NH_2) and Temporin A (FLPLIGRVLSGIL-NH_2).[1] At the same time, we developed two new analogues of these peptides named Pro^{3}TL (FVPWFSKFLGRIL-NH_2) and Gln^{3}TA (FLQLIGRVLSGIL-NH_2). Biological data indicate that Pro^{3}TL has a higher antimicrobial activity and a lower hemolytic activity than the native peptide TL. In contrast, Gln^{3}TA has a higher ability to lyse human red blood cells and a similar antimicrobial activity to the native peptide TA. The conformational behavior of the new analogues was investigated in membrane mimetic environment (SDS and DPC micelles) by spectroscopic and computational methods; and paramagnetic probes (16-doxylstearic acid and Mn^{2+}) were used to understand their positioning relative to surface and interior of the SDS and DPC micelles. To investigate the interactions of this analogues with the micelles we are studying their behavior also by molecular dynamics simulation in an explicit solvated peptide-dodecylphosphocholine and peptide-sodium dodecylsulfate systems. These simulations provide a realistic picture of the interactions between the peptide and models of bacterial and mammalian membranes.

NMR spectroscopy and spin-label experiments

The samples for NMR spectroscopy were prepared by dissolving the appropiate amount of peptide to obtain a concentration of 1-2 mM peptides and 200 mM SDS or DPC. Nmr spectra were recorded on a Varian Unity INOVA 700 MHz spectrometer at a temperature of 298.1 K. The qualitative and quantitative analyses of DQF-COSY, TOCSY, and NOESY spectra were obteined using the interactive program package XEASY. The NMR samples for spin-label experiments were prepared by dissolving 2 mM of peptides in 200 mM deuterated SDS solution in H_2O/D_2O 90:10. Assuming an SDS micelle aggregation number of 56, this corrisponds to a micelle concentration of 3.6 mM. The 16-doxylstearic acid and Mn^{2+} were added to the samples at a concentration of one spin label per micelle.

Table 1. Sequences of Analyzed Peptides

TA	H-FLPLIGRVLSGIL-NH_2
GLN^3-TA	H-FLQLIGRVLSGIL-NH_2
TL	H-FVQWFSKFLGRIL-NH_2
PRO^3-TL	H-FVPWFSKFLGRIL-NH_2

NMR analysis

NMR analysis reveals that peptides adopt a random coil conformation in water solution and prefer a helical

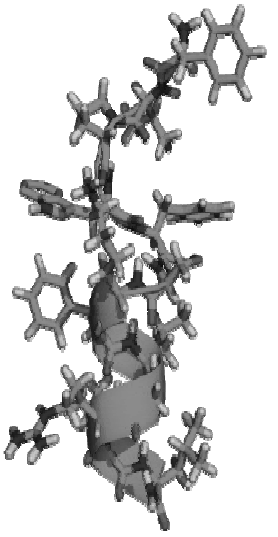

Figure 1. Lowest energy conformer of PRO^{3}TL in DPC solution. Heavy atoms are shown with different colors (C, green; N, blue; O, red). Backbone atoms is evidenced as a ribbon.

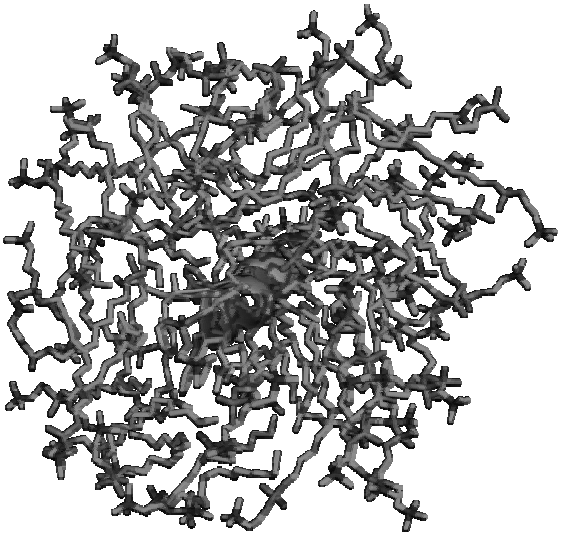

Figure 2. Gln^{3}TA in DPC micelle.

conformation in membrane mimetic environments. Diagnostic NMR parameters observed for Gln^{3}TA both in SDS and DPC solution indicate a conformational propensity toward helical structure along the entire sequence. Pro^{3}TL shows helical conformation along residues 6-13 while β-turns structures at the N-terminal residues are observed (Fig.1).

Spin-label and molecular dynamics

Spin–label experiments shows that, in contrast with the native peptide TL, Pro^{3}TL is located at the lipid-water interface, parallel to the membrane, when it interacts with zwitterionic DPC micelle, which can explain its reduced hemolitic activity. Gln^{3}TA adopts a topological orientation perpendicular to membrane when bound to the zwitterionic DPC micelle, with the N-terminus located close to the center of the micelle, again in accordance with biological data. We are studying these interaction by molecular dynamics simulation. We placed both peptides in the center of SDS and DPC micelles core with the micelle center of mass overlapping with the center of mass of the peptides (Fig.2). Preliminary results are in agreement with the experimental ones.

Future views

On the basis of the NMR and simulation results, we will design other analogues of TA and TL aiming to improve their pharmacological profiles and to reduce their side effects.

References

1. Carotenuto A, Malfi S, Saviello MR, Campiglia P, Gomez-Monterrey I, Mangoni ML, Gaddi LM, Novellino E, Grieco P. A Different Molecular Mechanism Underlying Antimicrobial and Hemolytic Actions of Temporins A and L. *J Med Chem* **51**: 2354-2362, 2008.

6-28-119

Synthesis and characterization of the collagen model peptides containing 4(*S*)-hydroxyproline

Motooka, Daisuke[1,]; Kawahara, Kazuki[2]; Sato, Nozomi[1]; Nakamura, Shota[3]; Uchiyama, Susumu[4]; Doi, Masamitsu[5]; Nishiuchi, Yuji[6]; Nakazawa, Takashi[7]; Yoshida, Takuya[2]; Ohkubo, Tadayasu[2]; Nishi, Yoshinori[1]; Kobayashi, Yuji[1]*

[1]Osaka University of Pharmaceutical Sciences, JAPAN; [2]Graduate School of Pharmaceutical Sciences, Osaka University, JAPAN; [3]Research Institute for Microbial Diseases, Osaka University, JAPAN; [4]Graduate School of Engineering, Osaka University, JAPAN; [5]Department of Materials Science, Wakayama National College of Technology, JAPAN; [6]Peptide Institute Inc., JAPAN; [7]Department of Chemistry, Nara Women fs University, JAPAN

[*]E-mail: m07954@gly.oups.ac.jp

Introduction

The sequence of the collagen molecule has a characteristic repeat of X-Y-Gly, where X and Y are often imino acids, Pro or Hyp^{R} (4(*R*)-hydroxyproline). Studies on various collagen model peptides (X-Y-Gly)$_{10}$ have shown that Hyp^{R} at the Y position stabilizes the collagen triple helical structure, whereas Hyp^{R} at X position or 4(*S*)-Hyp (Hyp^{S}) at both X and Y positions destabilizes it. Similar effects on the stabilities of triple helices are provided by the substitution of fluoroproline. However, there is an exception that (fPro^{S}-Pro-Gly)$_{10}$ takes a triple helix at 4 °C, whereas the counterpart, (Hyp^{S}-Pro-Gly)$_{10}$, is in a single coil state.[1] Although the difference has been explained by the steric hindrance of hydroxyl group in *S* configuration, [2] judging from the volumes of OH group and F atom, this hindrance by OH group could not obstruct the triple helix formation so strongly. Therefore, even though apparently (Hyp^{S}-Pro-Gly)$_{10}$ is not capable of triple helix formation, we expected that (Hyp^{S}-Pro-Gly)$_{n}$ with higher degree of polymerization would be able to form a triple helix and proved this using (Hyp^{S}-Pro-Gly)$_{15}$.

Results and Discussion

(Hyp^{S}-Pro-Gly)$_{15}$ was synthesized by solid-phase coupling of Fmoc-Hyp^{S}(Bu^{t})-Pro-Gly-OH units. The synthesis of these units was carried out by solution-phase techniques. Fmoc-Hyp^{S}(Bu^{t})-OH was synthesized from Boc-Hyp^{R}-OH as described in the reference.[3] Couplings were carried out on an Alko-PEG resin. The synthesis scale was 0.18 mmol. Fmoc-tripeptide unit was activated with HATU (4.0 eq)/DIEA (8.0 eq) in DMF. Cleavage of the peptide resin proceeded for 1 h using a TFA/water/triisopropylsilane mixture (95:2.5:2.5). The peptide was purified by high performance liquid chromatography (HPLC) on a ZORBAX C18 column. We employed the peptide that has proven more than 97% pure as judged by HPLC. The molecular weight of the peptide was determined by MALDI-TOF mass spectrometry. The peptides were dissolved in 100 mM aqueous AcOH. In order to make sure the peptides form triple helices, after keeping a stock solution of a peptide for 1h at 90 °C to complete the dissociation into the monomer, the solution was gradually cooled to room temperature, kept for a day and then cooled down and equilibrated at 4 °C

Measurements of CD spectra were carried out on an Aviv Model 202 spectropolarimeter. Spectra were obtained with a cell of 1mm path length by averaging 8 scans from 190 to 260 nm. The peptides were dissolved in 100mM AcOH at a concentration of 45 μM. (Hyp^{S}-Pro-Gly)$_{15}$ showed a spectrum indicating that the peptide forms the triple helix at 4 °C. However (Hyp^{S}-Pro-Gly)$_{10}$ did not show such a spectrum (Fig. 1). This has clearly shown that the thermal stability of the collagen model peptide with the sequence of Hyp^{S}-Pro-Gly: depends on the degree of polymerization and thus the existence of Hyp^{S} at X position does not interfere with the triple helix formation.

In order to compare the thermal stabilities of (Pro-Pro-Gly)$_{15}$ and (Hyp^{S}-Pro-Gly)$_{15}$, DSC measurements were carried out on a VP-DSC calorimeter. Each peptide was dissolved in 100 mM AcOH at concentrations of ca. 1.3 mM. Degassed peptide solutions were heated at a heating rate of 0.1 K min^{-1} from 40 to 80 °C and 4 to 70 °C, respectively. For both peptide solutions, the heat capacity curves at the second and the third scan completely overlapped without refilling the solution. This indicates that the transitions are reversible. The curves in Fig.2 were subjected to least square fitting to estimate the thermodynamic parameters as shown in Fig.3.

$T_{1/2}$ values were determined to be 63.1 °C and 22.4 °C, respectively. The reduced stability of (Hyp^{S}-Pro-Gly)$_{15}$ compared to (Pro-Pro-Gly)$_{15}$ was attributed to the smaller ΔH and larger $T\Delta S$ in the conformational free energy change. In order to understand the mechanism how the existence of Hyp^{S} contributes to the thermal stabilities of the triple helix, we are now carrying out the DSC and X-ray analyses on a series of the model peptides containing Hyp^{S} with the fixed degree of polymerization (n=15).

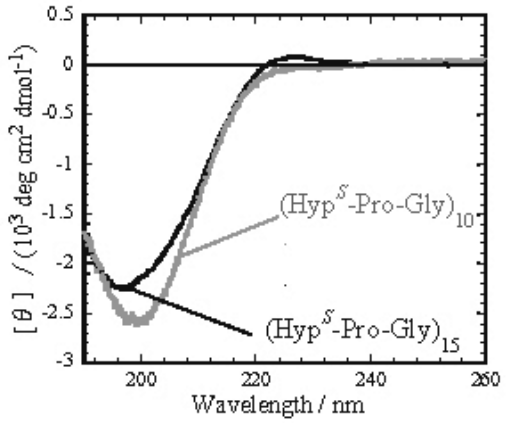

Fig.1 CD spectra of $(Hyp^S\text{-Pro-Gly})_n$ (n=10,15).

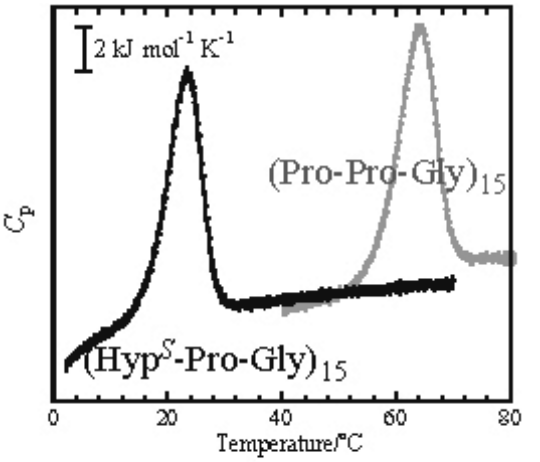

Fig.2 Molar heat capacity of $(Pro\text{-}Pro\text{-}Gly)_{15}$ and $(Hyp^S\text{-}Pro\text{-}Gly)_{15}$.

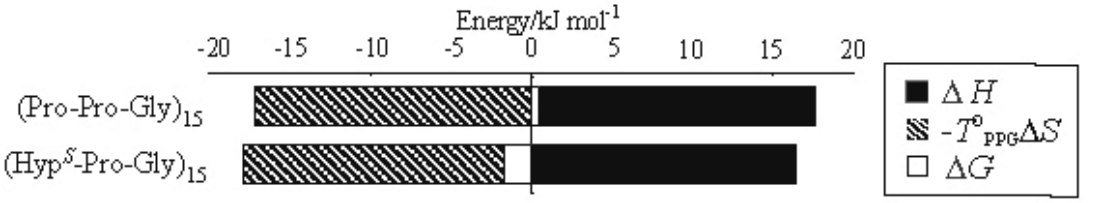

Fig.3 Comparison of thermodynamic parameters of transition of collagen model peptides per tripeptide unit. T^o_{ppG} refers to T^o = 71.9°C for $(Pro\text{-}Pro\text{-}Gly)_{10}$

Acknowledgements

We thank Dr. Kumiko Yoshizawa-Kumagaye (Peptide Institute Inc.) for the characterization of the model peptides with mass spectrometry.

References

1. Doi M, Nishi Y, Uchiyama S, Nishiuchi Y, Nakazawa T, Ohkubo T, Kobayashi Y. *J Am Chem Soc* **125**: 9922-9923, 2003.
2. Vitagliano L, Berisio R, Mazzarella L, Zagari A. *Biopolymers* **58**: 459-464, 2001.
3. Nishi Y, Uchiyama S, Doi M, Nishiuchi Y, Nakazawa T, Ohkubo T, Kobayashi Y. *Biochemistry* **44**: 6034-6042, 2005.

7-13-001

β-sheet antimicrobial peptide cateslytin generates rigid domains for membrane permeation

Jean-François, Frantz[1]; Elezgaray, Juan[1]; Metz-Boutigue, Marie-Hélène[2]; Dufourc, Erick[1,]*

[1]Université Bordeaux1/IECB/CBMN UMR5248, FRANCE; [2]Université louis pasteur strasbourg/ISERM U 575, FRANCE

[*]E-mail: e.dufourc@iecb.u-bordeaux.fr

Cateslytin, a five positively charged arginine-rich peptide (bCgA, RSMRLSFRARGYGFR), coming from the secretion of Chromogranin A during stress, was recently shown to possess interesting antimicrobial properties.[1] To investigate its specificity against bacteria, several physical techniques have been used. Circular dichroism (CD), polarized ATR (Attenuated Total Reflectance) and ^{1}H high-resolution magic angle sample spinning (HR-MAS) NMR were used to monitor changes on peptide secondary structure both in solution and in membrane media. ^{2}H and ^{31}P solid state NMR were applied to follow changes in membrane structure and dynamics. To mimic globally neutral mammalian membranes, 1,2-dimyristoyl-sn-glycero-3-phosphocholine (DMPC) water dispersions (large multilamellar or unilamellar vesicles, MLV or LUV) were prepared. To come close to the negative phospholipids charge of Candida albicans, a fungus whose growth is perturbed by Cateslytin, DMPC/DMPS (1,2-dimyristoyl-sn-glycero-3-phosphoserine) (1:1) or DMPC/DMPG (1,2-dimyristoyl-sn-glycero-3-phosphoglycerol), (1:1) MLV were made. ^{2}H-NMR experiments were performed with chain perdeuterated phospholipids. DMPC-^{2}H54/DMPS and DMPC/DMPS-^{2}H54 systems were prepared to follow the respective role of zwitterionic vs. charged lipids in a mixed membrane. Possible pore formation was investigated by both patch clamp experiments and molecular simulations. There are three major outcomes of our study. (i) Cateslytin adopts a dominant *β*-sheet character upon interaction with negatively charged membranes. (ii) Membranes regions of increased rigidity are observed only with negatively charged systems. (iii) Cateslytin forms channel in the zwitterionic part of the membrane. These finding will be discussed below. Cateslytin Switches from Random Coil in Water and Neutral Membranes to *β*-Sheet Aggregates on Negatively Charged Membranes. As many other short peptides, Cateslytin appears to be random coiled in solution.[2] Surprisingly, it keeps this unfolding state when applied to zwitterionic membranes, and becomes *β*-sheet structured only on negatively charged membranes, Fig. 1.

Figure 1. Circular Dichroism spectra of cateslytin in water, pH 7 (triangles), LUV of DMPC, Ri (lipid/peptide molar ratio) =15 (circles), and LUV of DMPC/DMPS (1:1), Ri =15 (squares). LUVs are in buffer, pH 7.4. *β* = *β*-sheets, r = random coil. 8 scans were accumulated at a scan speed of 15 nm/min, T = 25 °C. Polarized ATR-FTIR, indicated that these *β*-sheets are anti-parallel, highly aggregated and mainly oriented in the membrane plane.[2] These results are in favour of a catalyser role played by negatively charged membranes. Ordered Lipid Domains Are Induced by Cateslytin on "Bacterial-like" Membranes. Upon Cateslytin addition, no change is observed on NMR spectra of DMPC membranes (Fig. 2). On the contrary, when adding Cateslytin on DMPC/DMPS, ^{2}H-NMR spectra depict typical pattern of more ordered domains for all negatively charged lipids after addition of peptide.[2] The neutral lipids are splitted in two populations. As shown on Fig. 3 insert, where the lower spectrum is obtained by the subtraction of 50% of the middle spectrum (DMPC-^{2}H54/DMPS without peptide) from the upper spectrum (DMPC-^{2}H54/DMPS with peptide), meaning that 50% of the DMPC have the same rigidity of membrane without peptides and the other 50% have the same rigidity of the negatively charged lipid rigid domains.[2] Evidence of Channel Formation in the Zwitterionic Part of the Membrane. Both Patch-clamp and molecular simulation demonstrate that this peptide is able to form a channel of 0.25 nS conductance, corresponding to a 1 nm diameter channel.[3] The simulations on a 200 ns time scale show that a single peptide is able to form a pore as suggested in the DTP (disordered toroidal pore) model.[4] In addition, Patch clamp experiments are in favour of a more organised structure on longer time scales displaying a voltage-dependant channel fingerprint.

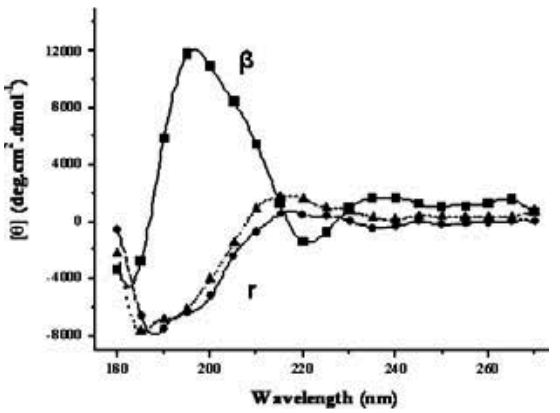

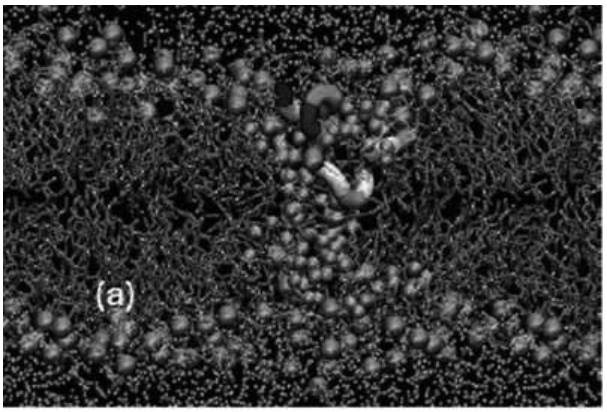

Figure 2. Side view of the pore formed after 12 ns molecular dynamics. The bilayer is represented by the position of the phosphate groups (purple beads), fatty acil chains are in light brown. Water molecules (orange) in the vicinity of the pore are also shown, other water molecules are in blue. Only the peptide that participate in the pore are represented as blue-green-yellow ribbons (residue color code: blue, basic; green, polar; yellow, non-polar). Biological implications. Assembling the above discussed findings into a molecular model leads to the schematics of Fig. 3. Upon strong electrostatic interaction between basic residues and acidic lipid head groups at membrane surfaces, as found in bacterial systems, Cateslytin, which is unstructured in solution, aggregates as patches of anti-parallel amphipatic β-sheets. These highly positively charged patches of peptide trigger an accumulation of negatively charged lipids that form ordered domains where the lipid anisotropic diffusion is greatly lowered. The presence of these domains generates zones of different rigidity and thickness and consequently phase boundary defects that could promote leakage through a DTP-like channel. Thus, cateslytin could pass across membranes and interact with crucial biological pathways, as do other arginine-rich peptides.

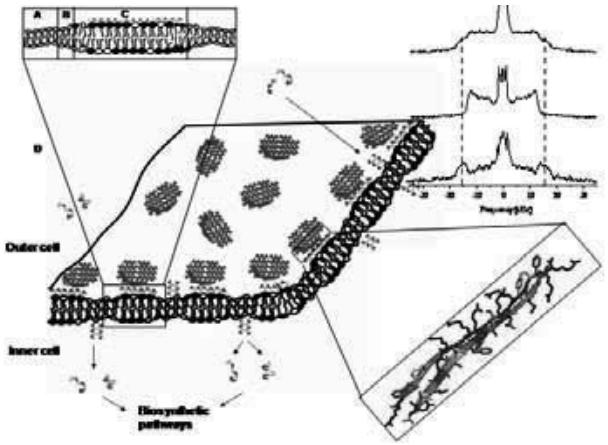

Figure 3. Model for cateslytin interaction with bacterial-like membrane domains. Peptides are unstructured in solution (D) and adopt a b-sheet conformation upon interaction with negatively-charged membranes (C). At the membrane, the peptides aggregate to form b-sheet plates (right lower insert) leading to rigid (thicker) domain formation (C) enriched in negatively-charged lipids (left upper insert). Amino acids are coloured in function of their hydrophobicity: basic residues (arginines) are in blue; polar residues are in cyan and hydrophobic residues are in red. Right upper insert: ^{2}H-NMR spectra evidencing rigid domains formation (see text).

References

1. Briolat J, Wu SD, Mahata SK, Gonthier B, Bagnard D, Chasserot-Golaz S, Helle KB, Aunis D, Metz-Boutigue MH. New antimicrobial activity for the catecholamine release-inhibitory peptide from chromogranin A. *Cell Mol Life Sci* **62**: 377-385, 2005.
2. Jean-François F, Castano S, Desbat B, Odaert B, Roux M, Metz-Boutigue MH, Dufourc EJ. Aggregation of Cateslytin beta-Sheets on Negatively Charged Lipids Promotes Rigid Membrane Domains. A New Mode of Action for Antimicrobial Peptides ? *Biochemistry* **47**: 6394–6402, 2008.
3. Jean-François F, Elezgaray J, Bergson P, Vacher P, Dufourc EJ. Pore formation induced by an antimicrobial peptide: electrostatic effects. *Biophys J* **95**: 5748-5756, 2008.
4. Leontiadou H, Mark AE, Marrink SJ. Antimicrobial peptides in action. *J Am Chem Soc* **128**: 12156-12161, 2006.

7-01-101

Degradation product of desmopressin in phosphate/citrate buffer

*Nylander, Bo; Malm, Mattias; Walhagen, Karin; Nilsson, Anders**
Ferring Pharmaceuticals A/S, DENMARK

**E-mail: anders.nilsson@ferring.com*

Introduction

Ferring is marketing two different nasal spray formulations of desmopressin **(1)**, one buffered, MINIRIN nasal spray RTS (phosphate/citrate buffer, pH 5; RTS=room temperature storage) and one unbuffered, MINIRIN nasal spray CS (pH 4 adjusted with HCl; CS=cold storage). In the buffered formulation there are five main degradation products with *m/z* 1070.4 (+1 Da compared to desmopressin). Four of them are the expected hydrolysis products [Glu^4]-, [Asp^5]-, [β-Asp^5]- and [Gly^9-OH] desmopressin. The fifth degradation product (compound **(2)**, Fig. 1) with a much lower relative retention time in the LC-UV system has been identified.

Results and discussion

A three years old buffered formulation containing compound **(2)** was treated with TCEP (Tris-(2-carboxyethyl)-phosphine) for 20 h at room temperature and analysed with a LC-MS method. The sample showed the expected mass numbers *m/z* 1071.4 and 1072.4 from desmopressin and the known hydrolysis products, respectively, but also two smaller peaks with *m/z* 439.2 and 656.3. None of the degradation products with *m/z* 1070.4 were observed. The reaction between compound **(2)** and TCEP indicated that compound **(2)** contains an S-S-bond. MS and MS/MS analysis indicated that *m/z* 439.2 and 656.3 could be the sodium salt of Mpa(H)-Tyr-Phe-OH **(5)** and the protonated molecular ion of pGlu-Asn-Cys(H)-Pro-D-Arg-Gly-NH_2 **(6)**, respectively. Therefore compound **(2)** could be [seco-3/4,pGlu^4]desmopressin (Fig. 2) which was synthesized and found to co-elute with compound **(2)** in MINIRIN nasal spray RTS.

Compound **(2)** is a major degradation product in MINIRIN nasal spray RTS but is not observed in MINIRIN nasal spray CS. Another difference between the two formulations is that much more [β-Asp^5] desmopressin is formed in the RTS formulation (Table 1). The pH value of the RTS formulation is higher and it contains a phosphate buffer. These parameters are known to be important for the degradation of Asn via the aspartimide route[1,2] [Structure **(4)]**, Fig. 2) which results in formation of [β-Asp^5]desmopressin. Therefore in analogy with the aspartimide route we believe that an imide, a pGlu derivative [Structure **(3)]**, Fig. 2) is formed. On cleavage of this imide either [Glu^4]- or [seco-3/4,pGlu^4]desmopressin is formed.

References

1. Patel K, Borchardt RT. *Pharm Res* **7**: 703-711, 1990.
2. Capasso S, Mazzarella L, Zagari A. *Peptide Res* **4**: 234-238, 1991.

Table 1. Hydrolysis products in MINIRIN nasal spray RTS and CS[1)].

Type	Batch	[seco-3/4,pGlu^4]	[Asp^5]	[β-Asp^5]	[Glu^4]	[Gly^9-OH]
CS	GC 8852[2)]	-	0.11%[3)] (12%)[4)]	0.03% (3%)	0.48% (51%)	0.32% (34%)
RTS	GE 8960[2)]	0.60 % (19 %)	0.27% (9%)	0.99% (31%)	0.77% (24%)	0.52% (17%)

1) LC-UV method: Zorbax SB-C18, mobile phase 25 mM NH_4OAc/MeCN 85/15, pH 4.6
2) Both batches have been stored for about 3 years.
3) Percentage of the desmopressin peak area.
4) In brackets percentage of the total amount of hydrolysis products.

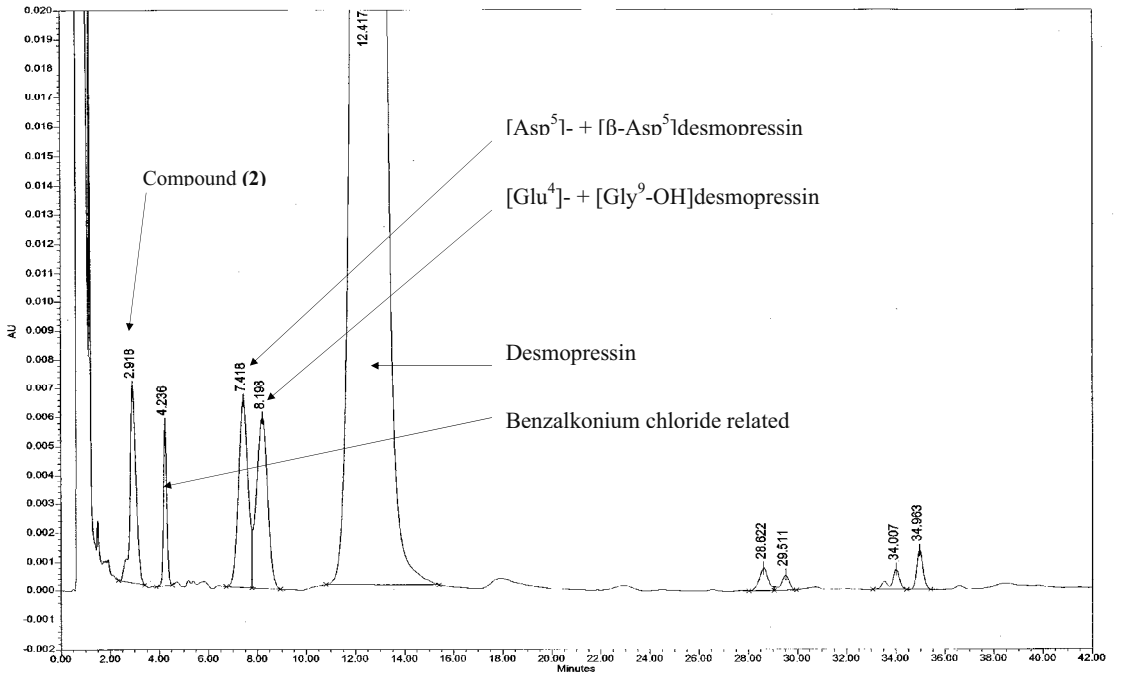

Figure 1. Analysis of MINIRIN nasal spray RTS 0.1 mg/ml, batch AB5579, after storage at 25 °C/60% RH for 3.5 years. LC-UV method: Merck Lichrospher RP-18, mobile phase 0.067M KH_2PO_4/ Na_2HPO_4, pH 7.0/ MeCN.

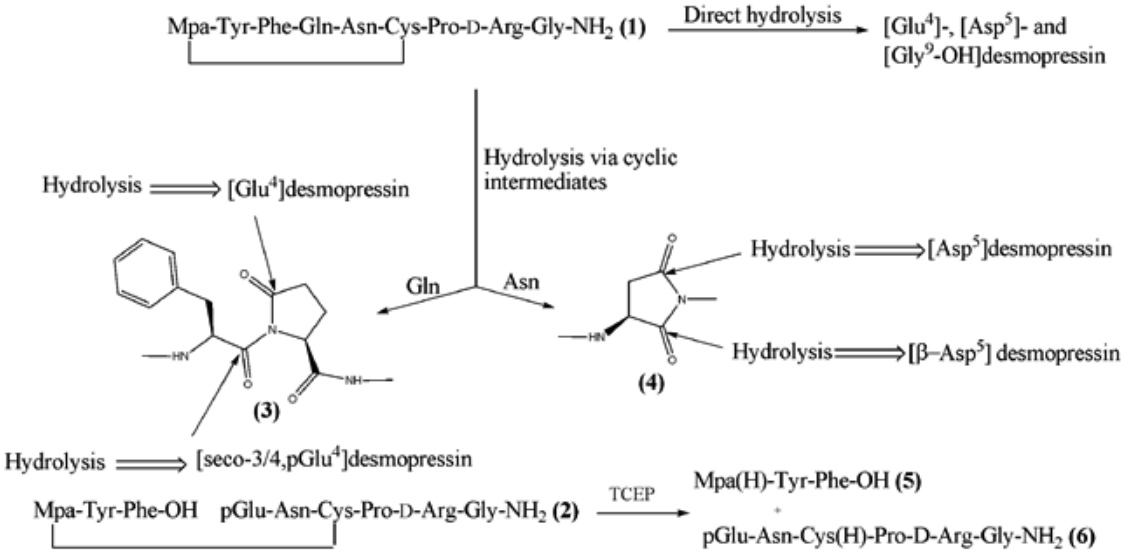

Figure 2. Hydrolysis products of desmopressin and treatment of [seco-3/4,pGlu^4]desmopressin with TCEP.

7-01-102

Unusual Cleavage of Tripeptides Containing Pipecolic Acid

*Islam, Md. Nurul; Shankar, Sonu Ram; Kato, Tamaki; Nishino, Norikazu**

Graduate School of Life Science and Systems Engineering, Kyushu Institute of Technology, JAPAN

**E-mail: nishino@life.kyutech.ac.jp*

Introduction

Pipecolic acid (Pip), a widespread natural non-proteinogenic amino acid, and its derivatives occur in numerous natural and synthetic products with important biological properties. For example, biologically important natural products such as immunosuppressant FK506,[1] histone deacetylase inhibitor apicidin,[2] trapoxins etc. contain Pip moiety. It also has found widespread utility as a proline mimic and β-turn inducer in many designed peptides and synthetic drug candidates,[3] as a building block in organic synthesis,[4] and is receiving current attention for application as an organo-catalyst.[5] Replacement of proline for its higher homologue Pip in peptides is reported to go along with a significant change in bioactivity and leads to interesting model compounds for studies on peptide conformations.[6] Comparative investigations of Pip residues to other cyclic amino acids, especially proline, incorporated in peptides give detailed insight into local mechanisms of peptide folding processes according to ring size.[7]

During the preparation of Fmoc-L-Pip-L-Pip-Gly-OH, the building block of a model collagen peptide, from Fmoc-L-Pip-L-Pip-Gly-O^{t}Bu by the treatment with TFA, unexpectedly Fmoc-L-Pip-D/L-Pip-OH diastereo-mixture were found as major products. The formation of Fmoc-L-Pip-D/L-Pip-OH indicates the cleavage of Pip-Gly bond and the mechanism involves racemization. Amide bonds are generally known to be stable towards TFA treatment and HCl/dioxane treatment. So, acid stability of peptides containing Pip becomes important.

Results and discussion

A series of Fmoc-di/tripeptides (Table 1) with and without Pip have been designed and synthesized to investigate the stability toward acid treatment. Fmoc protection was chosen as this is commonly employed protection in solid phase synthesis. Benzyl protection was chosen for its acid stability. Synthesis was carried out according to Scheme 1. Acid stability test of protected di/tripeptides in 4 M HCl/dioxane at room temperature was carried out by means of HPLC analysis.

Although compounds **1** and **6** contain Pip residue at N-terminal and at both N and C-terminal, respectively, these are stable. Compounds **2-5**, **7** and **8** contain Pip residue at the center, and are unstable due to the cleavage of C-terminal peptide bond. It was confirmed by MALDI TOF MS analysis and HPLC coinjection that the Fmoc-dipeptide thus formed was Fmoc-L-X-D/L-Pip-OH (X= Pro, Pip, Gly, Ala), which indicates the involvement of racemization mechanism. Compounds **5** and **7** have Pip residue at the center and at C-terminal, and are highly unstable. On the other hand, compounds **9** and **10** contain 1, 2, 3, 4-tetrahydro-3-isoquinolinecarboxylic acid (D-Tic) residue, which has six member ring like Pip, and are stable. Also protected dipeptides containing Pip (**11-13**) are stable towards 4 M HCl/dioxane. The change in

Table 1. Results of stability test for protected di/ tripeptides in 4 M HCl/dioxane at room temperature (22-23 ^{0}C).

Protected di/tripeptides	No.	Stability	Bonds cleaved	Kinetics followed	Rate constant/ min.$^{-1}$
Fmoc-L-Pip-L-Pro-Gly-OBzl	**1**	Stable	--	--	--
Fmoc-L-Pro-L-Pip-Gly-OBzl	**2**	Unstable	Pip-Gly	1st order	0.0078
Fmoc-L-Pip-L-Pip-Gly-OBzl	**3**	Unstable	Pip-Gly	1st order	0.0092
Fmoc-L-Pip-L-Pip-L-Ala-OBzl	**4**	Unstable	Pip-Ala	1st order	0.0068
Fmoc-L-Pip-L-Pip-L-Pip-OBzl	**5**	Unstable	Pip-Pip*	ND**	--
Fmoc-L-Pip-Gly-L-Pip-OBzl	**6**	Stable	--	--	--
Fmoc-Gly-L-Pip-L-Pip-OBzl	**7**	Unstable	Pip-Pip	ND**	--
Fmoc-L-Ala-L-Pip-Gly-OBzl	**8**	Unstable	Pip-Gly	1st order	0.0050
Fmoc-D-Pro-D-Tic-Gly-OBzl	**9**	Stable	--	--	--
Fmoc-D-Ala-D-Tic-Gly-OBzl	**10**	Stable	--	--	--
Fmoc-L-Pip-L-Pip-OBzl	**11**	Stable	--	--	--
Fmoc-L-Pip-Gly-OBzl	**12**	Stable	--	--	--
Fmoc-L-Pip-L-Ala-OBzl	**13**	Stable	--	--	--

*C-terminal Pip-Pip bond, **Not determined as cleavage almost completed within 30 min.

Scheme 1. a) Synthesis of compounds 1, 2, 3, 9 and 10; b) Synthesis of compounds 4, 5, 6, 7 and 8

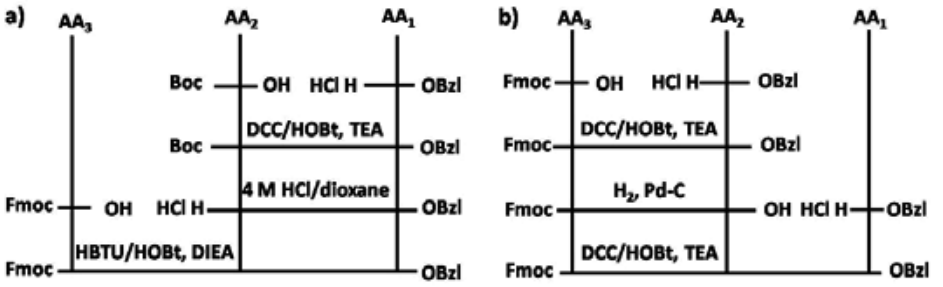

concentration of compounds **2-4** and **8** during the course of observation were fitted with the kinetic equation and was found well agreement with first order rate equation.

Conclusion

Among the protected di/tripeptides listed in Table 1, only tripeptides containing Pip at the center are unstable due to the cleavage of Pip-X bond (X= amino acid residue). Conformation of the tripeptides containing Pip at the center may facilitate the cleavage process. The cleavage mechanism involves racemization. Presence of Pip both at the center and at C-terminal also favors the cleavage process.

References

1. Tanaka H, Kuroda A, Marusawa H, Hatanaka H, Kino T, Goto T, Hashimoto M. *J Am Chem Soc* **109:** 5031-5033, 1987.
2. Singh SB, Zink DL, Liesch JM, Mosley RT, Dombrowski AW, Bills GF, Darkin-Rattray SJ, Schmatz DM, Goetz MA. *J Org Chem* **67:** 815-825, 2002.
3. Hanessian S, Papeo G, Angiolini M, Fettis K, Baretta M, Munro A. *J Org Chem* **68:** 7204-7218, 2003.
4. Sardine FJ, Rapoport H. *Chem Rev* **99:** 3329-3366, 1999.
5. Cheoug PH-Y, Zhang H, Thayumanavan R, Tanaka F, Houk KN, Barbas CF III. *Org Lett* **8:** 811-814, 2006.
6. Williams M, Kowaluk EA, Arneric SP. *J Med Chem* **42:** 1481-1500, 1999.
7. Hanessian S, McNaughton-Smith G, Lombart H-G, Lubell WD. *Tetrahedron* **53:** 12789-12854, 1997.

7-02-103

Analysis of protein-protein interaction sites without natively folded protein samples: fiction or fact?

Malešević, Miroslav[1,]; Pöhlmann, Angela[1]; Lücke, Christian[1]; Träger, Mario[1]; Jahreis, Günther[1]; Hernandez-Alvarez, Birte[1]; Bordusa, Frank[2]; Fischer, Günter[1]*

[1]Max Planck Research Unit for Enzymology of Protein Folding, Weinbergweg 22, 06120 Halle/Saale, GERMANY; [2]Institute of Biochemistry and Biotechnology, Martin Luther University Halle-Wittenberg, Kurt-Mothes-Str. 3, 06120 Halle/Saale, GERMANY

[*]E-mail: miroslav@enzyme-halle.mpg.de

Introduction

Protein-protein and protein-ligand interactions control many essential processes in living organisms. The understanding of those interactions provides insights into fundamental events in the life cycle of plants, animals and microorganisms. Among other things, peptide libraries prepared by spot synthesis on different solid carriers are powerful biotechnological tools for the study of these interactions (Fig. 1A).[1] Such assays, where peptides or any other compound class are simultaneously and in parallel synthesized at distinct positions on a solid carrier, have found manifold applications in biological and pharmaceutical research. However, soluble native protein probes and a method for their identification are an absolute prerequisite in these types of arrays. The recently developed IANUS (Induced orgANization of strUcture by matrix-assisted togethernesS) peptide array has the potential to evolve into a protein-free method for detection of protein-protein interaction sites.[2] With this assay, protein-protein and protein-ligand interactions can be represented by and investigated as peptide-peptide interactions using peptide pairs immobilized on a solid support (Fig. 1B). However, two main obstacles had to be overcome for successful implementation of this array: (i) identification of interacting peptide pairs and (ii) the library size.

Results and discussion

To date, two methods for the identification of interacting peptides in a library have been developed. In the first one, a protein (e.g. streptavidin) competes for peptide binding (e.g. to the streptavidin ligand Strep-tag II) with a neighbor peptide in a pair (Fig. 2A). In this case the binding of Strep-tag II (Stt II) to a soluble streptavidin probe is decreased due to the existence of competitive interactions with the neighboring immobilized peptide epitope derived from streptavidin.[2] This peptide-peptide interaction, however, could be intra- or intermolecular. Fluorescence resonance energy transfer (FRET) is a well-known method for distance determination in biomolecular studies. FRET could also be used to study the peptide-peptide interactions in IANUS peptide array (Fig. 2B).

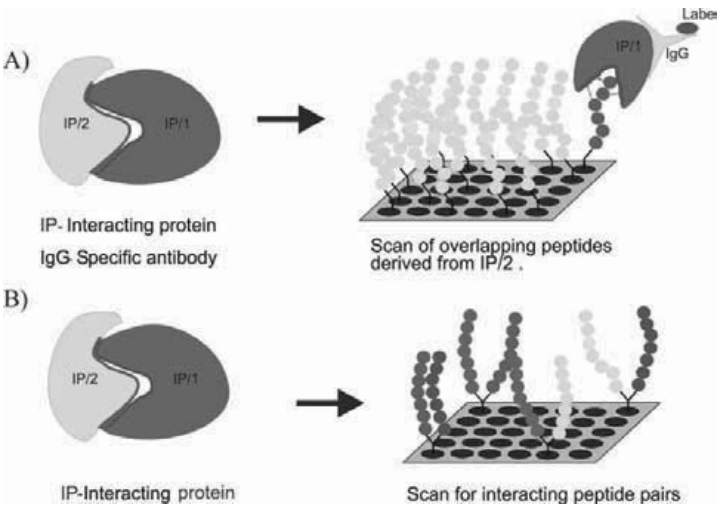

Figure 1. A) Study of protein-protein interactions using a peptide array. B) Study of protein-protein interactions using the IANUS peptide array.

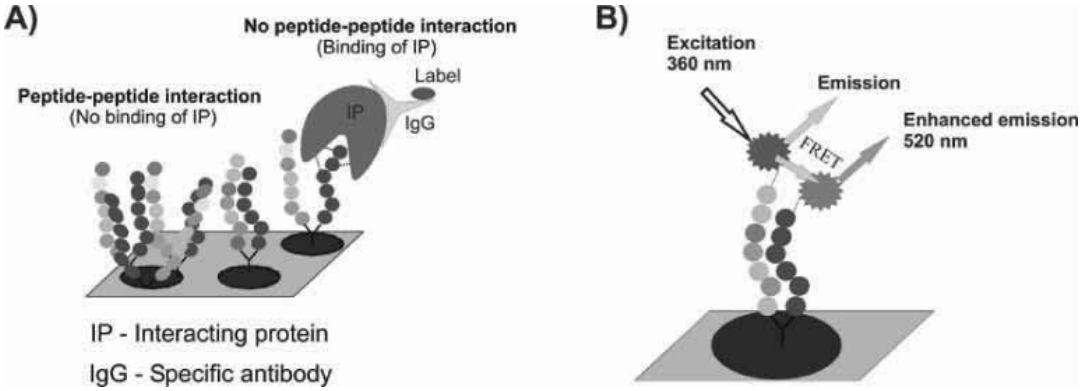

Figure 2. Methods for detection of peptide-peptide interactions. A) Competition in each spot between a native protein and a neighboring peptide for binding to the native ligand. B) Identification of interacting peptide pairs using FRET.

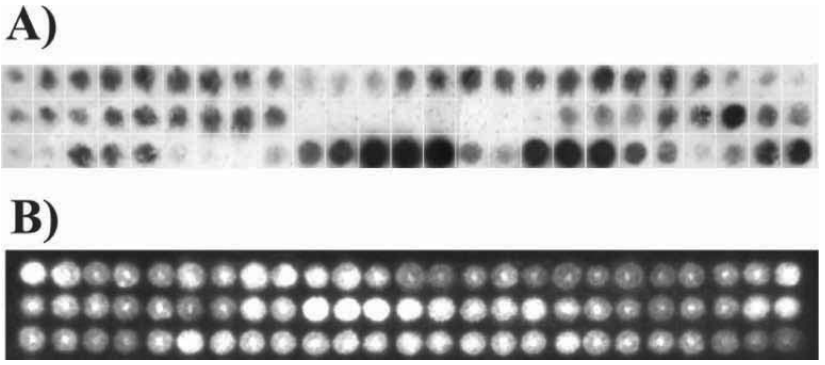

Figure 3. Comparison of results obtained by both methods for detection of peptide-peptide interactions in the IANUS peptide array. A) The competition between a protein and neighbor peptide for the native ligand produces a lower intensity spot. B) Fluorescence intensity higher than the standard deviation from average fluorescence was found for interacting peptide pairs.

Using a standard spot-technique, the streptavidin scans were synthesized on one side of the orthogonal protected linker[3] which was attached to the derivatised cellulose membrane and the Stt II peptide on the another side. Subsequently, peptide pairs attached to the cellulose membrane were probed with streptavidin and any bound streptavidin was detected (Fig. 3A). Examination of the streptavidin-Stt II IANUS peptide pairs involving N-terminally dansyl labeled streptavidin peptides and N-terminally fluorescein-labeled Stt II showed that IANUS-positive spots usually have a high fluorescence intensity at 510-530 nm (Fig. 3B).

The protein-protein interaction between parvulin 10 (Par10) and the small subunit (AhpC) of the alkyl hydroperoxide reductase, both from *E. coli*, was also studied using the IANUS peptide array. In this case, to screen all possible peptide combinations (overlapping 12-mer peptides scanning through the entire protein sequences with a frame shift of 2 amino acids) of both proteins, a library of 3696 peptide pairs would be needed. However, the three-dimensional structure of Par10 in solution is already known and AhpC was screened for interactions with only the putative binding sequence of Par10 (L49-F61), thus dramatically reducing the size of the peptide library. All peptides indicated by the IANUS peptide array as part of the AhpC interacting regions were able to inhibit Par10 catalytic activity in a PPIase assay. Moreover, NMR measurements of Par10 in presence of the inhibitory peptide indeed emphasized binding of the peptide to the Par10 binding pocket.

References

1. Frank R. *Tetrahedron* **48**: 9217-9232, 1992.
2. Yu C, Malesevic M, Jahreis G, Schutkowski M, Fischer G, Schiene-Fischer C. *Angew Chem Int Ed* **44**: 1408-1412, 2005.
3. Malesevic M, Lücke C, Jahreis G, *Peptides 2004* (*Proceedings of the Third International and Twenty-Eighth European Peptide Symposium*), Kenes International, Geneva, Switzerland, 2005, pp 391-392.

7-05-104

Improved expressed protein ligation method for consecutive coupling of polypeptide fragments

Tömböly, Csaba[1,]; Welker, Ervin[2]*

[1]Biological Research Centre of the Hungarian Academy of Sciences, Institute of Biochemistry HUNGARY;
[2]Biological Research Centre of the Hungarian Academy of Sciences, Institutes of Biochemistry and Enzymolgy, HUNGARY

[*]E-mail: tomboly@brc.hu

Introduction

After genome sequencing, there is a growing demand for specially engineered proteins, that is proteins enriched with chemical information, and for novel methods with which such selective protein modifications become available. Expressed protein ligation[1,2] (EPL) is the method of choice for the semisynthetic preparation of unique protein derivatives not available by recombinant methods, and when the protein fragments extend the size accessible by solid phase peptide synthesis. This ligation technique makes the introduction of extra chemical information, that is a special covalent modification, into a well-defined part of the protein sequence possible. Nevertheless, ligation of large protein fragments remains a challenge. We demonstrate here an improved EPL method that facilitates the ligation of any combination of large recombinant protein fragments, domains and/or synthetic peptides. Furthermore, the consecutive ligation of such fragments is also feasible. The building blocks of the method are N-terminal Cys protected protein/peptide thioesters, that are coupled in native chemical ligation[3] (NCL) reactions, and the N-terminal Cys protection is removed with an immobilized aminopeptidase before the next coupling (Scheme 1).

Results and Discussion

The semisynthesis of multidomain proteins, protein chimeras, and homogenous proteins with covalent modification in the middle of the sequence requires the ligation of more than two polypeptides. In order to achieve it, the protection of the N-terminal reactive group – the Cys residue – of any inner fragments is necessary (Scheme 1). Careful selection of the protection–deprotection scheme for the step-by-step NCL reactions is vital when the aim is the semisynthesis of functional proteins. N-terminal intein fusions and proteolytic cleavage sequences[2] including methionine.[4,5] as the shortest one, have already been considered for the preparation of the N-terminal Cys possessing ligation partner. In the case of Met, the *in vivo* Met-aminopeptidase activity can partially unmask the N-terminal Cys during the protein expression step, and as a result, a mixture of polypeptide thioesters with Met-Cys and Cys N-terminus is obtained. To minimize this, we used the dipeptide Met-Met for the N-terminal Cys protection, because the wild type enzyme is not able to cleave off the first Met when the penultimate residue is also a Met. This way the probability of the *in vivo* loss of the Met residues is very low and the total protection of the N-terminal Cys is achieved. For the cleavage of this Cys protection, our strategy explores a mutant form of a yeast methionine aminopeptidase I (MetAP I) that, in contrast to the wild type enzyme, cleaves off the N-terminal Met when the penultimate residue is also a Met. The method was optimized with model peptides and then with the modified *E. coli* maltose-binding protein (MBP)[6] as a model protein (Fig. 1). The peptides and peptide thioesters were prepared by solid- phase peptide synthesis using the in situ neutralization protocol,[7] while the MBP derivatives were prepared.

Scheme 1. Strategy for the consecutive ligation of protein fragments

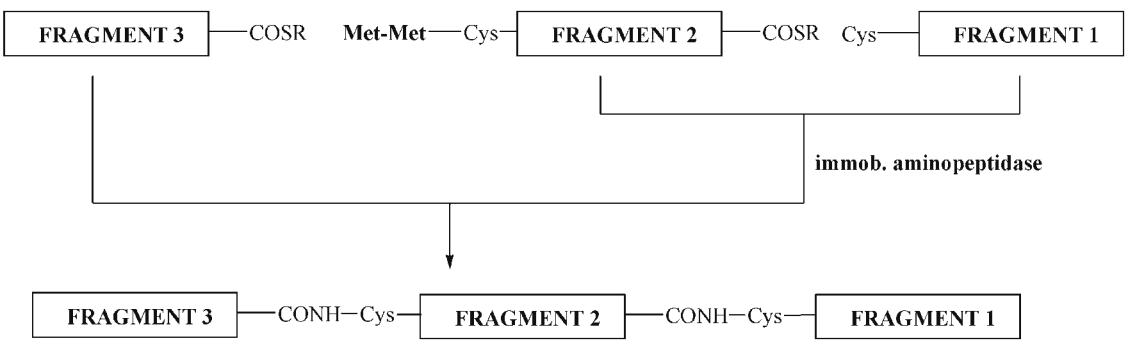

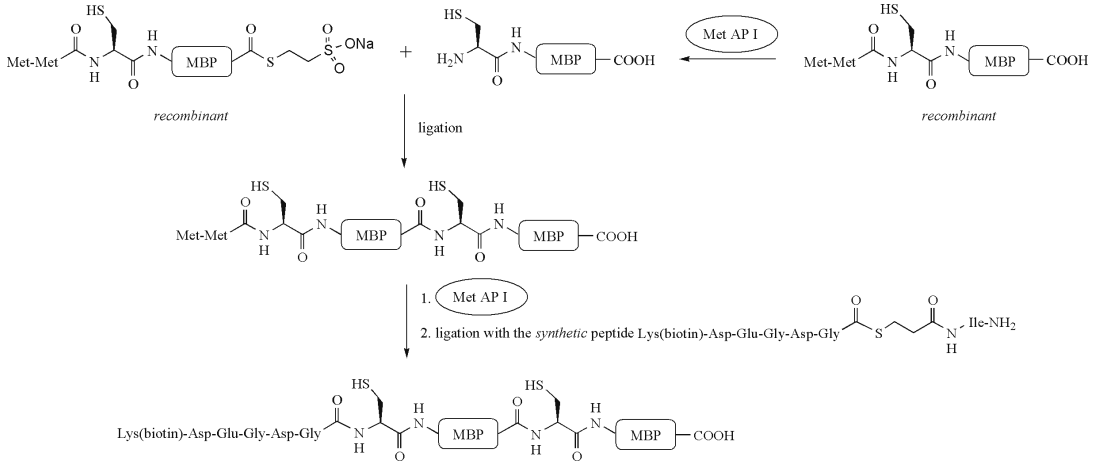

Figure 1. Semisynthesis of a biotinylated MBP dimer by expression as Mxe GyrA intein and CBD fusions6 in *E.coli* (BL21) followed by chitin affinity purification and thiolysis.

The mutant MetAP I was expressed as a GST fusion in *E.coli*, and after affinity purification it was used in a GSH-Sepharose bound form. This quasi-immobilized enzyme fusion showed sufficient proteolytic activity and makes its separation from the digestion reaction mixture easier. The enzyme activity was investigated by digestion of the peptides X-Gly-Gly-Trp-Phe-NH_2 (X= Met, Met-Met, Met-Cys, Met-Met-Cys) and Met-Met-Cys-Lys-Ala-Ser-Asn-Met-Gly-NH_2. The enzymatic reactions were followed by RP-HPLC, and it turned out that the N-terminal Cys residue was unmasked within 1-5 min quantitatively under reducing conditions. Furthermore, the quasi-immobilized enzyme retained the proteolytic activity in the presence of up to 2 M urea. The digestion of the recombinant model protein, Met-Met-Cys-MBP-COOH[6] was followed by the RP-HPLC measurement of Met, that was isolated from the digestion mixture, in GITC-derivative form. The protein content determined by the Bradford method was in agreement with the measured Met content. The consecutive ligation was started with a 10 min digestion of the Met-Met-Cys-MBP-COOH,[6] then it was ligated with the thioester derivative Met-Met-Cys-MBP-COSR for 16 h (Fig. 1). Afterwards, the unreacted Cys-MBP-COOH was quenched with a high molar excess of the thioester Lys(biotin)-Asp-Glu-Gly-Asp-Gly-COS$(CH_2)_2$-CONH-Ile-NH_2, and the biotinylated C-terminal protein monomer was removed by streptavidin affinity chromatography. The formation of the protein dimer was proved by MALDI MS and SDS PAGE experiments. The crude dimeric protein Met-Met-Cys-MBP-Cys-MBP-COOH was then digested with the MetAP I for 10 min in the presence of 2 M urea, followed by the addition of the thioester Lys(biotin)-Asp-Glu-Gly-Asp-Gly-COS$(CH_2)_2$-CONH-Ile-NH_2. The formation of the trimeric product composed of two recombinant and one synthetic fragments was verified by the SDS PAGE analysis of the streptavidin Sepharose phase of the affinity purification. In conclusion, our novel Cys protection–deprotection strategy widen the scope of both NCL and EPL, as large protein fragments' N-terminal reactive residue can be deprotected with an enzyme that is more specific than the currently used Factor Xa or TEV proteases. Acknowledgements This work was supported by the OTKA F049222 grant and János Bolyai Fellowship (Cs.T.).

References

1. Muir TW, Sondhi D, Cole PA. *Proc Natl Acad Sci U S A* **95**: 6705-6710, 1998.
2. Muralidharan V, Muir TW. *Nature Methods* **3**: 429-348, 2006.
3. Dawson PE, Muir TW, Clark-Lewis I, Kent SBH. *Science* **266**: 776-779, 1994.
4. Iwai H, Plückthun A. *FEBS Lett* **459**: 166-72, 1999.
5. Camarero JA, Fushman D, Cowburn D, Muir TW. *Bioorg Med Chem* **9**: 2479-2484, 2001.
6. It is expressed using a modified MYB5 vector (NEB).
7. Schnolzer M, Alewood P, Jones A, Alewood D, Kent SBH. *Int J Pept Protein Res* **40**: 180-193, 1992.

7-10-105

Cellular peptidomics: peptide sets produced by rat hepatocytes in vitro

Sazonova, Olga; Yatskin, Oleg; Khachin, Dmitry; Kudryavtsev, Denis; Karelin, Andrei; Ivanov, Vadim*

Shemyakin-Ovchinnikov Institute of Bioorganic chemistry Russian Academy of Sciences, Laboratory of Peptide Chemistry, RUSSIAN FEDERATION

E-mail: olgavsazonova@gmail.com

Introduction

Earlier we have carried out a series of studies on protein degradation in erythrocytes.[1-2] We have shown that erythrocytes contain fragments of hemoglobin derived from about 0.5 % of cellular hemoglobin and specifically release some fragments of hemoglobin and other proteins into the surrounding medium. Mature erythrocytes neither synthesize proteins nor are secretory cells. In contrast, the primary function of hepatocytes is synthesis and secretion of various proteins, including plasma carrier and regulatory proteins. Analysis of the secreted proteome of primary hepatocytes in 3D culture resulted in identification of about 200 proteins, some of them isolated from the conditioned medium as fragments.[3]

In the present work we analyzed the secreted and intracellular peptidomes of rat tumor and primary normal hepatocytes in 2D culture. As with erythrocytes, the supernatants were obtained after 3 h of incubation with the hepatocytes. The intracellular peptides were extracted from organellae-free cytoplasmic fraction of hepatocytes, to exclude lysosomal proteolysis products (as erythrocytes lack lysosomes, mainly proteasome-generated peptides were our aim).

Results and discussion

To obtain supernatants, hepatocytes (normal or HTC rat hepatoma cells) were stabilized in culture for several days after de-freezing or isolation. The cells were thoroughly washed with incubation buffer (KHB with slight modificatioins) and then incubated in a fresh portion of the buffer for 3 h. Cells and the debris were sedimented from the supernatants. Peptides were extracted from the supernatants by solid-phase extraction, and then peptide fractions corresponding to 1.5-5.0 kDa and 0.5-1.5 kDa molecular weight ranges were analyzed by RP-HPLC. Fractions corresponding to predominant chromatographic peaks were analyzed by MALDI MS. The levels of low molecular components in the supernatants of both normal and tumor hepatocytes were low, which did not allow any reliable molecular weight determination. Moreover, the intensiveness of the components' accumulation in primary cell culture was lower than it could be expected in functional hepatocytes. It could be due to the dedifferentiated state of the normal hepatocytes in 2D culture. Primary hepatocytes in 2D cultures rapidly loose liver-specific functions; In our case, though the hepatocytes had been incubated in a

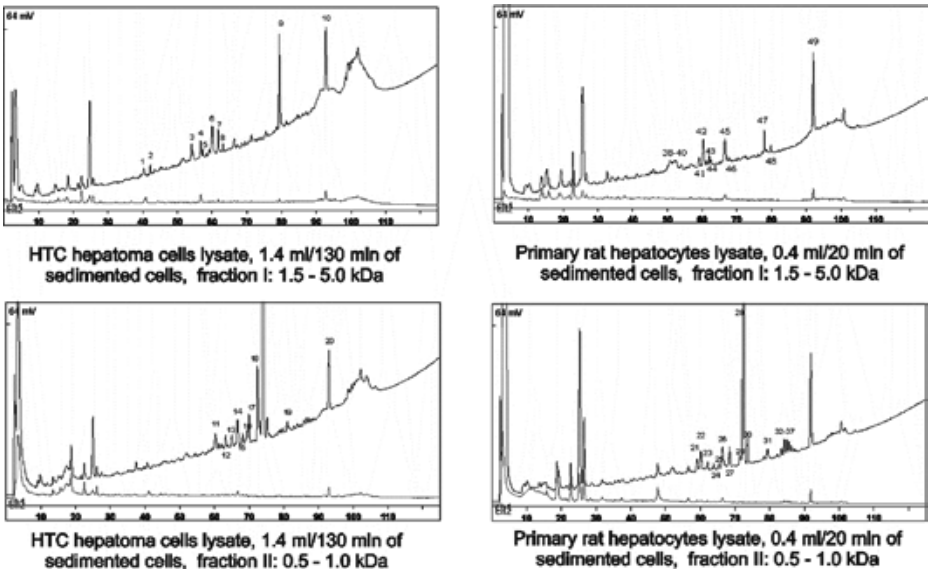

Figure 1. RP-HPLC of the low molecular weight fractions obtained from lysates of rat hepatocytes.

medium maintaining the differentiated phenotype and their morphology was typical of hepatic cells, at day 4 of incubation (when the supernatants were obtained) they expressed intermediate filament protein vimentin, which is a fibroblastic marker.

To obtain hepatocyte lysates, tumor cells were harvested from culture flasks, normal cells were lysed immediately after isolation. The cells (normal or tumor) were thoroughly washed with cold PBS. The cells were lysed in 10 x volume of a hypotonic lysis buffer A containing protease inhibitors, DTT, phosphatase inhibitor orthovanadate and 0.5% of Igepal. The nuclei and organelles were sedimented from the lysates in two steps; the integrity of the nuclei was confirmed using Hoechst 33342 dye. Peptide-protein material was extracted from the lysates by solid-phase extraction and then fractionated by size-exclusion chromatography. Peptide fractions corresponding to 1.5-5.0 kDa and 0.5-1.5 kDa molecular weight ranges were analyzed by RP-HPLC (Fig. 1). Fractions corresponding to predominant chromatographic peaks were analyzed by MALDI MS. During the hepatocyte lysis procedure, we removed all organelles from the cytoplasm, in the first place, lysosomes, to obtain free cytoplasmic peptides, i. e., those that could act as intracellular autocrine regulators or to be liberated to intracellular space upon cellular membrane damage.

The summary content of low molecular weight components per mL of cellular volume in both tumor and normal hepatocytes was estimated as being 100 – 1000 times smaller than in erythrocytes containing hemoglobin fragments whose level reaches more than 1 nmole/mL of sedimented cells. Molecular weights were established for 20 of 30 analyzed individual peaks in the both HTC lysate fractions and for 29 of 36 peaks in normal hepatocytes lysate fraction II (see Table 1). MS/MS is in process; to date, ubiquitin fragment (53-76) was identified in fraction 47. It seems likely that, non-respectively of cell phenotype, cellular cytoplasm normally contains small amounts of peptides, presumably proteasome products.

Acknowledgements

This work was supported by RAS Presidium grant "Molecular and Cellular Biology"; Russian President grant "Scientific schools" # 5737.2008.4; RFBR grant # 08-04-00550-a.

References

1. Ivanov V, Karelin A, Yatskin O. *Biopolymers* **80**: 332-346, 2005.
2. Filippova M, Khachin D, Sazonova O, Blishchenko E, Iatskin O, Nazimov I, Karelin A, Ivanov V, Rasstrigin N, Pivnik A. *Bioorg Khim* **34**: 160-170, 2008.
3. Farkas D, Bhat VB, Mandapati S, Wishnok JS, Tannenbaum SR. *Chem Res Toxicol* **18**: 1132-1139, 2005.

Table 1. Molecular weights of low molecular weight components isolated from the lysates (cytoplasmic fraction) of rat hepatocytes.

HTC hepatoma cells		Primary normal rat hepatocytes		Primary normal rat hepatocytes	
#	Molecular weights	#	Molecular weights	#	Molecular weights
1	547.27	21	529.18, 735.50	41	1097.7, 2226.2, 6070.0
2	3150.55	22	513.13, 779.55	42	6236.0
3	877.56	23	535.19	43	6180.0
4	965.65	24	427.91, 579.30, 601.20, 688.60, 710.50, 853.70	44	6180.0
5	4935.15, 2235.31	25	623.40, 853.70, 579.20, 688.5	45	999.7
6	1097.77	26	594.15, 667.40, 716.50, 835.60	46	2520.6
7	1141.85	27	702.46	47	2726.6, 8567.0
8	823.63	28	686.44	48	2533.5, 9957.0
9	1416.04, 1572.27	29	686.44		
10	1330.00	30	684.45, 686.40		
11	735.43	31	700.53, 664.50		
12	823.54, 877.64	32	591.30		
13	867.59	33	635.44		
14	911.65, 955.69	34	679.50, 714.50		
15	702.44, 999.75	35	723.43		
16	1043.69	36	767.6		
17	724.38	37	811.6		
18	670.70	38	1909.0, 6330.0		
19	700.47	39	6665.0		
20	1094.83	40	6648.0		

7-11-106

Spectroscopic characterization of doppel peptide fragments and their complex species with Cu (II)

La Mendola, Diego[1]; Magrì, Antonio[1,]; Bonomo, Raffaele P[2]; Rizzarelli, Enrico[2]; Hansson, Orjan[3]*

[1]C.N.R. Istituto di Biostrutture e Bioimmagini (IBB), Unità Operativa di Catania, ITALY; [2]Università degli studi di Catania, Dipartimento di Scienze Chimiche, ITALY; [3]University of Gothenburg, Department of Chemistry, SWEDEN

[*]E-mail: leotony@unict.it

Introduction

The Doppel protein is encoded by a gene located 16-20 Kb downstream from that encoding the prion (Doppel, downstream prion protein-like).[1] It shares 25% identity with the C-terminal two-thirds of prion and an almost superimposible three-dimensional fold. Both proteins are able to selectively bind Cu(II) *in vitro*. One histidine residue has been identified as Doppel-Cu(II) binding site and an enhancement of α-helical content of the whole protein has been observed after copper complexation.[1,2] It has been supposed that such an effect might be due to the involvement of a carboxyl group of aspartate side chain and one or more deprotonated amide nitrogens from the amino acid residues located in the loop between the second and third helices.[2] The unambiguous characterization of the Cu (II) coordination binding site has not been yet achieved. In order to investigate the coordination environment of copper we have synthesized the peptide fragment of human Dpl encompassing residues 122-130 with blocked N- and C-termini. Furthermore, single point mutation of the aspartate residue with asparagine in the Dpl-Ac122-130NH_2 (Dpl) peptide allowed the role of carboxyl group side chain in copper(II) coordination to be evaluated.

Dpl 122-130: Ac-KPDNKLHQQ-NH_2 (Dpl)
DplN: Ac-KPNNKLHQQ-NH_2 (DplN)

Results and Discussion

In the CD spectra, both peptides show a random coil conformation in the overall investigated pH range. The Cu (II) binding and the formation of a 1:1 complex species induces conformational changes more remarkable in the region of basic pH. Until pH 5, no differences are observed in the shape of band which has the minimum centred at 198 nm in the Dpl system. At pH=6, a conformational change is observed. After this pH value, a marked red shift of the minimum is observed. The subtraction of the Cu(II)-Dpl system CD spectra with the parent ligand suggest an increase of a turn structure determined by Cu (II) binding with the likely involvement of amide nitrogen atoms from the peptide backbone. In the Cu-DplN system, until pH=7, no evident changes of the CD spectra are observed. Increasing the pH, two phenomena are observed: a red-shift of minimum towards 202 nm and the presence of two isodichroic points at 205 nm and 225. Also in this case the difference spectra suggest an increase of turn

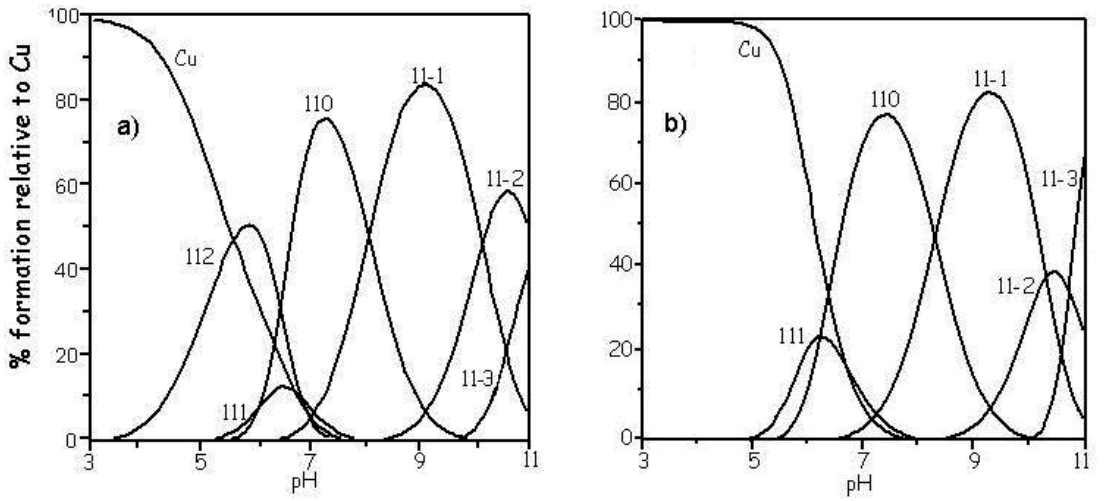

Figure 1. Species distribution diagrams of the Cu(II) complexes in aqueous solution with (a) Dpl and (b) DplN polypeptides.

conformation of peptide as result of involvement in Cu (II) coordination of backbone amide nitrogen atoms. Finally, the comparison of CD data between the two peptides indicate that Dpl starts to coordinate Cu (II) at lower pH than DplN. The absence of definite isodichroic points for Dpl suggest the presence of more Cu (II) complex species in comparison with Asn-Asp mutated peptide fragment. Potentiometric measurements confirm that Dpl starts to bind Cu (II) before than the DplN as shown in species distribution diagrams (Fig. 1).

The first complex species formed by Dpl is $CuLH_2$ in which the imidazole nitrogen of histidine and carboxyl group of aspartate residue are coordinated to the metal ion. It's important to point out that this complex species results to be predominant up to neutral pH 6-6.5. It's possible to assume the formation of a 20-membered macrochelate in which the aspartate side chain carboxylate group is coordinated. This hypothesis is confirmed by EPR parameters ($g_{\|}$ = 2.332 and $A_{\|}$ = 162 x10^{-4} cm^{-1}). In the CD spectra recorded in the visible region, an extremely low intensity was detected, confirming that metal ion is coordinated by donor atoms belonging to side chains, more distant from chiral centres of peptide backbone. Moreover, the UV-Vis parameters (λ_{max} = 706 nm and ε = 25) are compatible with this coordination mode. A indubitable evidence is provided by the absence of an analogous copper complex species in the mutated peptide DplN in wich the carboxylate side chain is not present. The EPR parameters found for the $CuLH_2$ complex species of Dpl are very similar to those found for the Cu (II) complex species with the entire protein at acidic pH. At neutral pH, in both systems, the CuL complex species is predominant. In the CD spectra, the presence of a band at 345 nm and a shoulder around 290-310 nm clearly indicate the involvement in Cu (II) coordination of both imidazole and amide nitrogen atoms. In the Cu-Dpl system, the pK of the second amide deprotonation is lower than that of the first amide nitrogen atom, while an opposite and more usual trend is observed in the Cu-DplN system. This effect is due to the carboxylate direct involvement in the $CuLH_2$ species formation as above reported. The EPR parameters obtained for CuL complex species of Cu-Dpl confirm this hypothesis. In this case, this Cu (II) complex species has not an equivalent in the EPR results reported for the entire protein. In the pH range between 7-8 another species is formed $CuLH_{-1}$, which is predominant at pH higher than 8. in the UV-Vis spectra, a blue shift in the λ_{max} was observed and in the the CD spectra, an increase of the intensity of the N- $\rightarrow$ Cu (II) charge transfer band at 310 nm was recorded. Then the EPR parameters suggest that a third amide was depronated participating to the coordination of the Cu (II) (N_{Im}, 3xN-). The Hamiltonian parameters recorded for the CuLH complex species are similar to those of principal copper complex species reported for the entire protein at neutral pH. This suggests that the coordination mode for the copper bound to doppel protein may involve four nitrogen atoms. At basic pH, potentiometric data indicate that in both systems amino lysine side chains are depronated but are not directly involved in the copper (II) coordination. This sentence is confirmed by no spectral changes observed by spectroscopic techniques.

References

1. Quin K, Coomaraswamy J, Mastrangelo P, Yang Y, Lugowski S, Petromilli C, Prusiner SB, Fraser PE, Goldberg JM, Chakrabartty A, Westaway D. The PrP-like Protein Doppel Binds Copper. *J Biol Chem* **278**: 8888-8896, 2003.
2. Cereghetti GM, Negro A, Vinck E, Massimino ML, Sorgato MC, Van Doorslear S. Copper(II) Binding to the Human Doppel Protein May Mark Its Functional Diversity from the Prion Protein. *J Biol Chem* **279**: 36497-36503, 2004.

7-11-107

Angiotensin-I/captopril competitive interaction studies with 46-residues catalytic site maquettes of angiotensin-I converting enzymes through NMR studies

Tsami, Natalia[1]; Galanis, Athanassios S[1]; Spyroulias, Georgios A[1]; Pairas, George[1]; Manessi-Zoupa, Evy[2,]; Cordopatis, Paul[2]*

[1]University of Patras, Department of Pharmacy,, GREECE; [2]University of Patras, Department of Pharmacy, GREECE

[*]E-mail: E.Manesi@chemistry.upatras.gr

Introduction

Angiotensin-I converting enzyme (ACE) somatic form bears two catalytic domains with two Zn metal ions, while the testis form bears remarkable similarity to the aminoacid sequence of ACE C-catalytic domain and only one Zn metal ion. However, both exhibit their hydrolytic activity to vasoactive peptides such as angiotensin I (AngI) and bradykinin (BK), though with different efficacy.[1] In order to study experimentally the possible interaction and binding events between the ACE active site(s) and known ACE substrates or inhibitors, we constructed peptide-based catalytic site maquettes (CSM). 46-residue peptides were synthesized through solid-phase peptide synthesis having the aminoacid sequence that correspond to the ACE Val380-Ala425 N- domain segment and to the Val978-Ala1023 C-domain segment and enzyme's active sites were reconstructed through addition of zinc metal ion in solution. The resulting complexes have the metal ion bound in a native-like mode, as manifested by previously reported NMR data.

Results and discussion

The NMR solution structure of the Zn(II)-loaded ACEC-36 is present in Fig. 4. The peptide construct exhibits three regions, one at each terminus and one in the intermediate spacer, having á-helix structure. These data are fully consistent with the pattern of sequential NOEs (Fig. 1). Consequently, NMR data suggest that both Zn-binding motifs are found in helical (C-terminal motif) or in helix-like (N-terminal motif) conformation as has been observed for other gluzincin metallopeptidases crystal structures.[2-4]

ACE CSM and AI/BK or Captorpil interaction was also performed and monitored through NMR spectroscopy. The reconstituted peptides were titrated separately by Captopril and Angiotensin-I with a molar ratio ACE:Captopril/AngI 1:15 and 1:5, respectively. Titration was followed by ^{1}H NMR spectroscopy (Fig. 2) and spectral changes (chemical shifts, line broadening, etc.) were recorded and analyzed. After the end of AngI titration the solution of interacting peptides was titrated with Captopril and the titration was followed by ^{1}H NMR spectroscopy. At the end of each titration 2D homonuclear 1H-1H TOCSY and NOESY spectra were recorded.

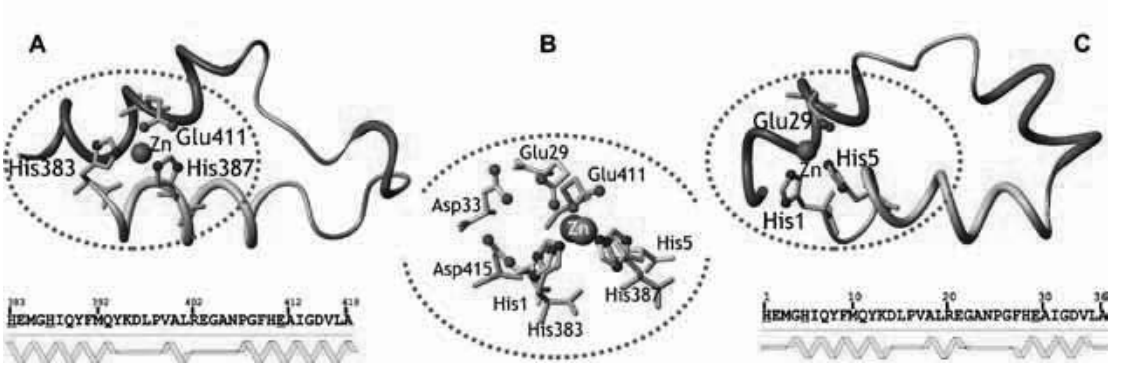

Figure 1. (A) Domain of the active zinc-binding site of ACE testis crystal structure and schematic representation of helical fragments (B) Best fit of the Zn(II) ligands and the structurally important Asp residue of the second metal binding motif. (C) Representative model of the family of 30 NMR structures of ACEc-36 CSM that corresponds to the respective domain of ACE testis crystal structure and schematic representation of helical fragment. Figures were generated with MOLMOL.[5]

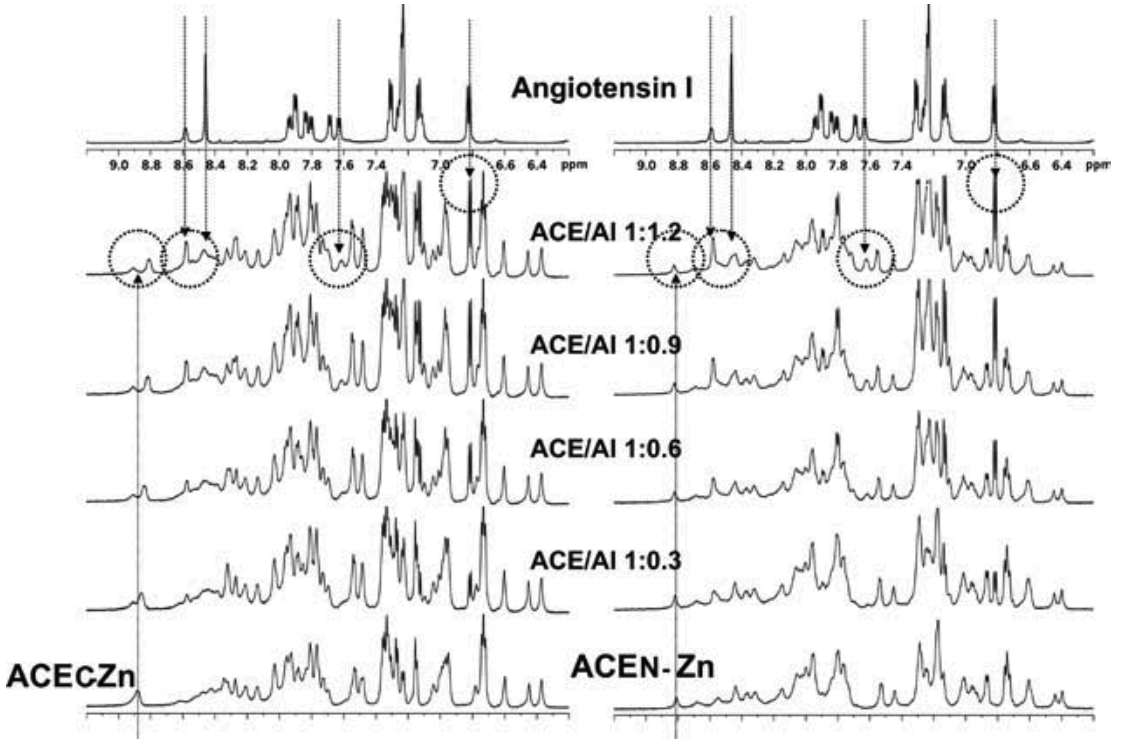

Figure 2. Enzyme-substrate interaction: NMR studies of Angiotensin-I interaction with ACE-Zn active sites.

Conclusion

Elucidation of the enzyme-peptide interaction plays an important role in order to understand the physical and structural determinants that determine peptide substrate selectivity and binding. Additionally, these data can offer new insight in structure-based design of the novel ACE inhibitors with specific inhibition of the two catalytic sites of somatic isoform. These catalytic sites differ slightly in amino acid composition, exhibiting in some cases different specificity and activity against natural substrates as AI and BK.

References

1. Inagami T. *Essays Biochem* **28**: 147-164, 1994.
2. Spyroulias GA, Galanis AS, Pairas G, Manessi-Zoupa E, Cordopatis P. *Curr Topics Med Chem* **4**: 403-429, 2004.
3. Galanis AS, Spyroulias GA, Pierattelli R, Tzakos A, Troganis A, Gerothanassis IP, Pairas G, Manessi-Zoupa Å, Cordopatis P. *Biopolymers* **69**: 244-252, 2003.
4. Galanis AS, Spyroulias GA, Pairas G, Manessi-Zoupa E, Cordopatis P. *Biopolymers* **6**: 512-526, 2004.
5. Koradi R, Billeter M, Wüthrich K. *J Mol Graphics* **14**: 51-55, 1996.

7-11-108

The influence of human cystatin C hinge loop L1 on its dimerization and oligomerization propensities.

Szymańska, Aneta[1,]; Czaplewska, Paulina[1]; Jankowska, Elzbieta[1]; Radulska, Adrianna[1]; Wahlbom, Maria[2]; Grubb, Anders[2]; Liberek, Krzysztof[3]; Rodziewicz-Motowidło, Sylwia[1]*

[1]University of Gdańsk, Faculty of Chemistry, Department of Organic Chemistry, POLAND; [2]University Hospital, Department of Clinical Chemistry, SWEDEN; [3]University of Gdańsk, Inter-Collegiate Faculty of Biotechnology, Department of Molecular and Cellular Biology, POLAND

[*]E-mail: aneta@chem.univ.gda.pl

Introduction

Three-dimensional (3D) domain swapping process is one of the molecular mechanisms involved in formation of oligomers and fibrils of several amyloidogenic proteins.[1] It was proposed that domain swapping-prone proteins have some common "hot spots" in their structure that facilitate the process.[2] One of these common motives are so called "hinge loops" - turns connecting protein subdomains showing enhanced propensity for unfolding due to conformational constraints.[3] Human cystatin C (hCC), the main inhibitor of cysteine proteases in human body, is one of the amyloidogenic proteins containing such structure.[4] hCC is small (120 amino acids long), basic protein which was shown to dimerize and oligomerize[5] through the domain swapping. hCC contains a highly conserved loop L1, connecting two β strands which, together with the *α*-helix, create a structural unit that undergoes the domain swapping process. Experimental and theoretical[6] studies revealed that this region of cystatin fold is conformationally unstable. The main destabilization is connected with Val57 residue, located near the top of the loop. Values of the φ and ψ angles for this residue are not optimal, which can account for the propensity of the protein to undergo the domain swapping. In order to asses the influence of this destabilization on the dimerization of the hCC, mutants in which Val residue was substituted by residues favored in this position of β-turns[7] like Asp and Asn were obtained. Additionally, since hCC is one of the proteins undergoing 3D domain swapping which does not contain proline residue in the hinge loop, in order to verify the "hinge proline hypothesis",[8] proline residue was introduced in position 57. All obtained mutants were analyzed to asses their ability to form dimers and higher oligomers.

Results and discussion.

Dimerization of hCC variants.

At physiological conditions hCC wt is a monomeric protein. *In vitro* dimerization of cystatin C can be induced by, among others, supplementing of the protein solution with mild denaturant like guanidinium hydrochloride.[5] Addition of GuaHCl to 0.5 M followed by incubation of protein samples showed that the hCC mutants display distinct propensities for dimer formation comparing to the control native protein. Both mutants containing conformationally favorable amino acid residues (hCC V57D and hCC V57N) remained mostly monomeric during the time of incubation. For the control wt protein slow increase of dimer content was observed. Further increase of the denaturant concentration to 1.0 M had minor impact on the dimerization propensities of the discussed mutants, whereas the wild type protein showed significant destabilization and dimerization (above 75%).

On the other hand, proline mutant incubated without and at lower GuaHCl concentration was predominantly dimeric, even when freshly dissolved in the assay buffer, and the amount of dimer did not change significantly with incubation time. This observation confirms the „proline-hinge" hypothesis according to which proline favors extended conformations of protein thus facilitating dimerization process.

Oligomerization of hCC variants.

Incubation of hCC samples at oligomerization-promoting, acidic conditions[5] and subsequent analysis by gel filtration revealed that all studied proteins are capable of forming oligomers higher than dimers. The main oligomeric form had retention time of about 11 minutes which is expected for hexameric assemble of the protein. Additionally, for the wt protein formation of higher oligomers, with the molecular mass higher than 100 kD was observed.

The microscopic picture obtained for hCC wt revealed the presence of a new type of structural forms. In addition to doughnut-shaped oligomers reported by us before[5], electron micrographs demonstrated rod-like objects with the outer diameter of 17±1.5 nm and length of 100±15 nm. This kind of structures was not observed before. We hypothesize that it may correspond to the pre-fibrillar intermediate of hCC formed by the protein undergoing the domain swapping in the propagated manner at the point proceeding its transformation to insoluble fibril. The other possibility is that the observed rods can be constituted by the „doughnuts" stacked on each other.

Dimensions of the observed specimenn (the outer diameter bigger than the one of typical amyloid fibril and shorter length) suggest that additional conformational change is necessary in order to form the mature fibril.

For hCC mutants analogous structures were not observed, what may suggest the important role of the domain swapping capability of a particular protein in their formation. Additionally, the lack of the rod-like oligomers for hCC V57P which is predominantly dimeric may strengthen the hypothesis of the propagated manner of the domain exchange process. Dimer formed by this mutant may be too stable to undergo opening and further oligomerization in the „run-away" mode.

Conclusions

By applying rational mutagenesis approach we have confirmed the important role of the hinge loop region of human cystatin C in its dimerization and oligomerization process. Substitution of conformationally constrained Val residue by more favorable Asp and Asn stabilized the protein in the closed state thus preventing opening of the molecule and its subsequent dimerization. On the contrary, introduction of Pro residue in the same position favored the open conformation of hCC and facilitated the domain swapping.

Stabilization of the protein in monomeric or dimeric form did not abolish completely its oligomerization and protein assembles higher than dimers were observed. The mechanism of their formation is not certain and additional studies are necessary, but at that point it seems that propagated domain swapping may play some role in this process.

Acknowledgements

Work supported by Polish Ministry of Science and Higher Education grant N204 161 32/4233 (to AS and S R-M) and grant N204 023435 (to AR).

References

1. Bennet MJ, Sawaya MR, Eisenberg D. *Structure* **14**: 811-824, 2006.
2. Ding F, Prutzman KC, Campbell S, Dokholyan NV. *Structure* **14**: 5-14, 2006.
3. Liu Y, Eisenberg D. *Protein Science* **11**: 1285-1299, 2002.
4. Grubb AO. *Adv Clin Chem* **35**: 63-99, 2000.
5. Wahlbom M, Wang X, Lindström V, Carlemalm E, Jaskolski M, Grubb A. *Biol Chem* **282**: 18318-18326, 2007.
6. Rodziewicz-Motowidło S, Iwaszkiewicz J, Sosnowska R, Czaplewska P, Sobolewski E, Szymańska A, Stachowiak K, Liwo A. *Biopolymers* **91**:373-383, 2009.
7. Wilmot CM, Thornton JM. *J Mol Biol* **203**: 221-232, 1988.
8. Bergdoll M, Remy M-H, Cagnon Ch, Masson J-M, Dumas P. *Structure* **5**: 391–401, 1997.

7-12-109

1,4-DHP-lipid forms rod like micellae

Liepina, Inta[1,4,*]; Plotniece, Aiva[1]; Czaplewski, Cezary[2]; Liwo, Adam[2]; Pajuste, Karlis[1]; Ose, Velta[3]; Duburs, Gunars[1]

[1]Latvian Institute of Organic Synthesis, LATVIA; [2]University of Gdańsk, 80-952 Gdańsk, Faculty of Chemistry, POLAND; [3]Latvian Biomedical Research and Study Centre, LATVIA; [4]Center of Drug Research, University of Helsinki, FINLAND

[*]E-mail: inta@osi.lv

Abstract

The cationic amphiphilic lipid tipe compound 1,1'-{[3,5-bis(dodecyloxycarbonyl)-4-phenyl-1,4-dihydropyridin-2,6-diyl]dimethylene} bispyridinium dibromide (1,4-DHP lipid) (charge +2), is a gene transfection agent. The electronic structure of 1,4-DHP lipid molecule was investigated by ab initio quantum mechanics, and the supramolecular structure formed by 1,4-DHP lipid molecules in water was investigated by means of molecular dynamics simulation, AMBER force field, version AMBER 8.0. During the molecular dynamics simulations of 10 ns of MD 1,4-DHP lipid formed a worm-like micellae, which was preserved during the time course of 32 ns of MD simulations. Result was confirmed with the electron microscopy showing extended, rod-like structures.

Keywords: lipid, gene transfection, rod-like structure, worm-like micellae, molecular dynamics.

Introduction

Synthetic cationic lipids are becoming increasingly popular as gene transfection agents due to their minimal toxicity, absence of immunological problems, possible large scale production. A large number of lipids with variations in the hydrophilic and hydrophobic regions were generated. Unfortunately they still have less efficiency when compared with viral vectors. Recently we synthesized novel group of gene transfection agents comprising partially hydrogenated cyclic heterocyclic 1,4-dihydropyridine moiety as active linker. 1,4-DHP derivatives are well-known antihypertensive agents, cardiovascular drugs.[1] Appropriately decorated with substituents, they may possess bioprotective properties.[2] The cationic amphiphilic lipid type compound 1,1'-{[3,5-bis(dodecyloxycarbonyl)-4-phenyl-1,4-dihydropyridin-2,6-diyl]dimethylene} bispyridinium dibromide (1,4-DHP lipid, charge q=+2) has gene transfection activity.[3,4] This compound is more active than DOTAP and PEI 25 (liposomal and polymeric gene transfection agents). The sharp increase of the 1,4-DHP cycle N-H acidity (up to pKa ≈7-8) is due to 2- and 6-pyridiniomethyl groups and conjugated alkoxycarbonyl substituents in positions 3 and 5 of the 1,4-DHP cycle. N-H acidity is the basis for its buffering activity in this novel type of gene transfection agents. The electronic structure of 1,4-DHP lipid molecule was investigated by ab initio quantum mechanics, and the supramolecular structure formed by 1,4-DHP lipid molecules was investigated by means of molecular dynamics simulation. Methods 1,4-DHP lipid molecule was minimized by Sybyl, Tripos force field in vacuo. As it was expected that in water or lipid bilayer the fatty acid tails must be not in the fully extended state, but close to each other, the structure with bent fatty acid tails was chosen as the starting structure for lipid supramolecular structure calculations. 1,4-DHP lipid structure was calculated by Restricted Hartree-Fock (RHF) ab initio quantum mechanics, 6-31G* bases set, to obtain the charges for molecular dynamics using RESP algorithm (electrostatical potential based method using charge restrains for determining atom-centered charges). 72 molecules of 1,4-DHP-lipid initially were put in a periodic lipid bilayer-water box, with a small amount of excessive water on the lipid edges to ensure the mobility of lipid molecules. There were 72 DHP-lipid molecules, 144 counterions of chlorine ions and 4401 water molecules in the system DHP-lipid-water box. The total number of atoms in the system is 22491. The 1,4-DHP-lipid – water box were subjected to molecular dynamics, (AMBER force field, version 8.0, NTP protocol (constant number of particles, constant temperature, constant pressure)). Temperature was risen gradually from T=10 K by step of 10 degrees till 300 K. Calculations were performed for 326212 ps.

Results and Discussion

After 35 ns of the MD simulation few lipid molecules turned with their charged heads to the side of the lipid bilayer and after 100 ns a profound worm-like micelle structure began to form. The worm-like micelle structure becomes more perfect during the course of simulation of 300 ns. The results of MD simulation were confirmed by electron microscopy, showing the interwinding worm-like structures.[5] The total energy become stable at 49 ns. The size of the periodic box has changed from the dimensions of x= 70 Å, y = 55 Å, z = 103 Å at the start of molecular dynamics, to x= 102 Å, y = 46 Å, z = 48 Å at 318039 ps, The worm-like micellae axes - the longer dimension, is in the x-axes direction, but y- axes and z-axes dimensions

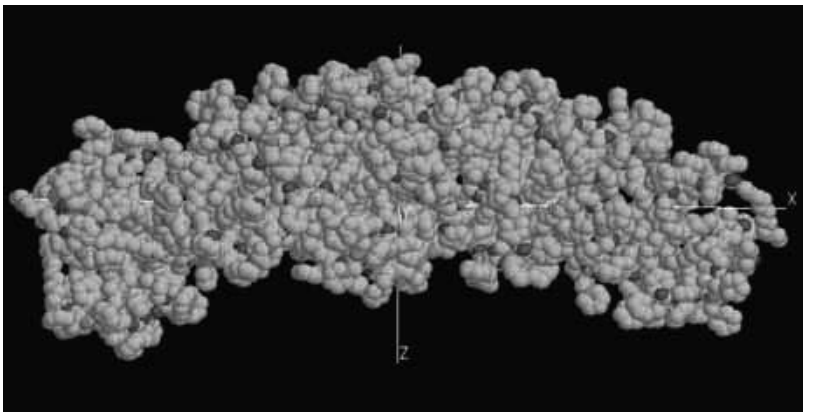

Figure 1. Snapshot of the 1,4-DHP-lipid - water box at the temperature 300 K 110673 ps of MD run, space fill representation, colored by atom type. At this stage of MD run the worm-like micellae has formed.

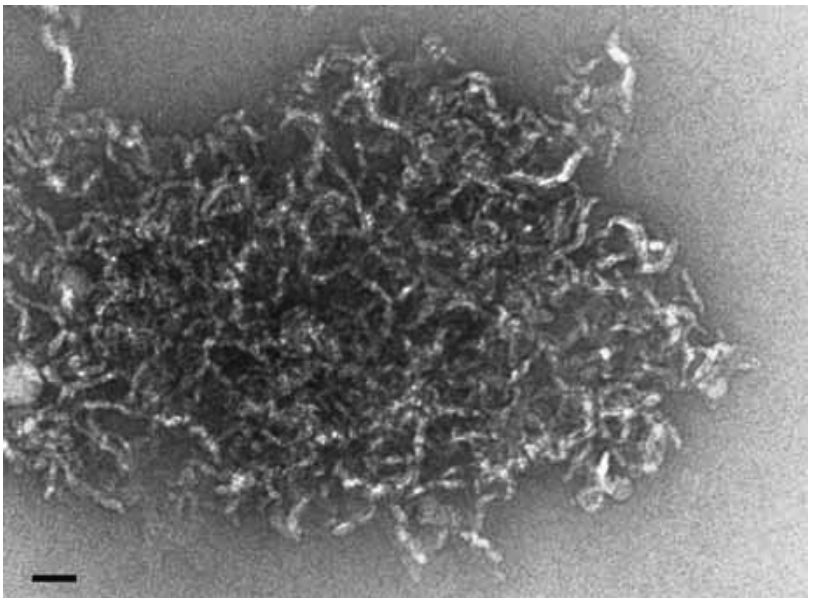

Figure 2. Electron microscopy of the 1,4-DHP lipid, bar 10 nm.

are similar, which is explainable with the top view of the worm-like micellae, having approximately the same diameter in all directions.

Conclusion

Conclusion is that one of the gene transfection agent 1,4-DHP lipid structures is a worm-like, rod-like micellae, and we could expect that such the micellaes are capable to form a lipoplex for the DNA transfection.

Acknowledgments

This work was supported by Stipend of Finland Academy of Sciences for IL, and by Latvian Science Council Grant 05.1768. Calculations were performed on computers of the Gdańsk Academic Computer Centre TASK.

References

1. Triggle DJ. L-type calcium channels. In *Voltage-gated ion channels as drug targets*. Triggle DJ, Gopalakrishnan M, Rampe D, Zheng W (Eds), Wiley-VCH Verlag GmbH & Co. KGaA, Weinheim, 2006, pp 100-122.
2. Duburs G, Vigante B, Plotniece A, Krauze A, Sobolevs A, Briede J, Klusa V, Velena A. Dihydropyridine derivatives as bioprotectors. *Chemica OGGI/Chemistry Today* Vol.26, N2, 68-70, 2008.
3. Hyvonen Z, Plotniece A, Reine I, Chekavichus B, Duburs G, Urtti A. Novel cationic amphiphilic 1,4-dihydropyridine derivatives for DNA delivery. *Biochim Biophys Acta* **1509**: 451-466, 2000.
4. Hyvonen Z, Ronkko S, Toppinen M-R, Jaaskelainen I, Plotniece A, Urtti A. Dioleoyl phosphatidylethanolamine and PEG-lipid conjugates modify DNA delivery mediated by 1,4-dihydropyridine amphiphiles. *Journal of Controlled Release* **99**: 177-190, 2004.
5. Velta Ose, Privat communication.

7-14-110

Self-assembling cyclic peptides for peptide nanotube formation

Kato, Tamaki[1,]; Yoshizaki, Mai[1]; Nishio, Natsuko[1]; Kuwahara, Junko[2]; Nishino, Norikazu[1]*

[1]Graduate School of Life Sciences and Systems Engineering, Kyushu Institute of Technology, JAPAN; [2]Faculty of Engineering, Fukuoka Institute of Technology, JAPAN

[*]E-mail: tmkato@life.kyutech.ac.jp

Introduction

Advancements in nanotechnology have led to many scientific developments to discover new materials and their properties at micrometer and nanometer levels. Recently, biodegradable substances have attracted attention. Among them, peptide nanotubes are of interest in materials, medicine and more. In 1993, Ghadiri *et al*. reported peptide nanotube for the first time.[1-3] Cyclic peptide nanotubes are formed by self-assembly of cyclic peptides with alternating L- and D-amino acids. However, peptide nanotube self-assembly phenomenon has not yet been made cleared. Intermolecular electrostatic interaction is one of the important driving forces to assemble cyclic peptides to peptide nanotubes.[4] Herein, a series of cycilc hexapeptides, *cyclo*(-L-Lys-Gly-)$_3$, *cyclo*(-L-Glu-Gly-)$_3$, *cyclo*(-L-Lys-D-Ala-)$_3$, *cyclo*(-D-Glu-L-Ala-)$_3$, *cyclo*(-L-Trp-D-Lys-)$_3$, and *cyclo*(-L-Trp-D-Glu-)$_3$, were designed.

Results and discussion

Cyclic hexapeptides *cyclo*(-Lys-Xxx-)$_3$ and *cyclo*(-Glu-Xxx)$_3$ were designed and synthesized. We utilized standard fluorenylmethoxycarbonyl (Fmoc) protected solid-phase automated peptide synthesis (SPPS) to construct side chain protected linear peptides on preloaded 2-chlorotrityl chloride resin (Cl-Trt(2-Cl)-Resin). Cleavage of the linear peptides from the resin was achieved by acetic acid at room temperature. Cyclization of them in DMF was carried out with *O*-(7-azabenzotriazol-1-yl)-1,1,3,3-tetramethyluronium hexafluorophosphate (HATU) (1.5 eq.) and diisopropylethylamide (DIEA) (2.5 eq.) in high dilution (1 mM). Yields of protected cyclic hexapeptides were 50%-68%. Thereafter, side chain protecting groups were removed by trifluoroacetic acid (TFA) on ice bath, and the cyclic hexapeptides were purified by Gel Filtration (LH-20) or preparative HPLC.

Turbidity study revealed that the ability of self-assembly formation of the 1:1 mixture of *cyclo*(-L-Trp-D-Lys-)$_3$ and *cyclo*(-L-Trp-D-Glu-)$_3$ in aqueous solution is (peptide concentration 500 μM) extremely higher than that of each individual positively or negatively charged cyclic peptides. This result indicates that self-assembly formation needs both negatively and positively charged peptides. In addition, 1: 1 mixtures of *cyclo*(-L-Trp-D-Lys-)$_3$ and *cyclo*(-L-Trp-D-Glu-)$_3$ in aqueous solution with 200 mM NaCl did not show such high abilities.

Fluorescence studies using *cyclo*(-L-Trp-D-Lys-)$_3$ and *cyclo*(-L-Trp-D-Glu-)$_3$ indicated that the self-assembly formation consisted of two stages (peptide concentration 25 μM) (Fig. 2). In the first stage, Trp fluorescence increased. The peptide nanotube formation caused by electrostatic interactions between positively and negatively charged peptides might change the Trp surroundings to hydrophobic environment from hydrophilic aqueous atmosphere. In the second stage, bundle formation of peptide nanotube might cause Trp fluorescence decrease by concentration quenching.

Transmission electron microscope (TEM) experiments showed that mixtures of *cyclo*(-Lys-Xxx-)$_3$ and *cyclo*(-Glu-Xxx-)$_3$ formed fibrous structures (Fig. 3). TEM images indicated that, the diameters of the nanotubes were approximately 2-5 nm. Diameters of similar cyclic peptides were found to be approximately 1 nm.[5] These results also supported the bundle formation of peptide nanotubes. Conformations of monomer cyclic

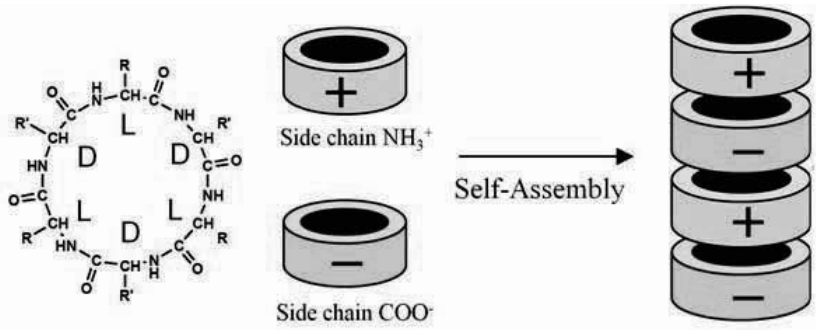

Figure 1. Proposed design of nanotube by formation of salt-bridged cyclic peptides.

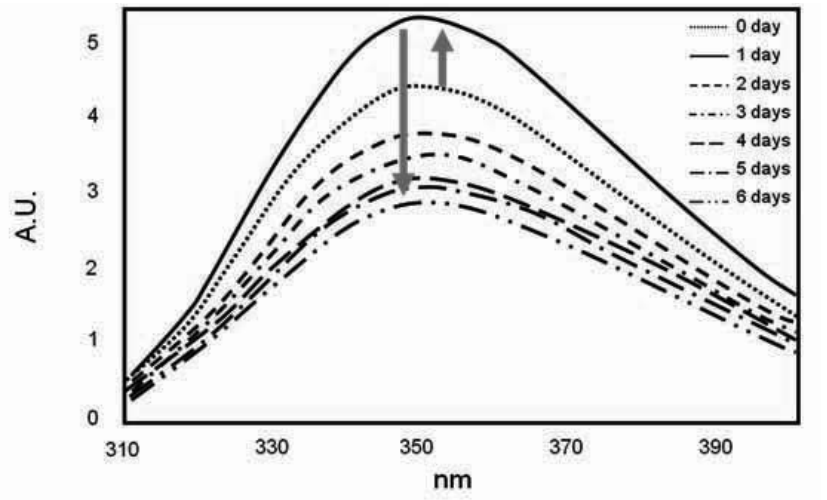

Figure 2. Fluorescence spectra of *cyclo*(-L-Trp-D-Lys-)$_3$ + *cyclo*(-L-Trp-D-Glu-)$_3$.

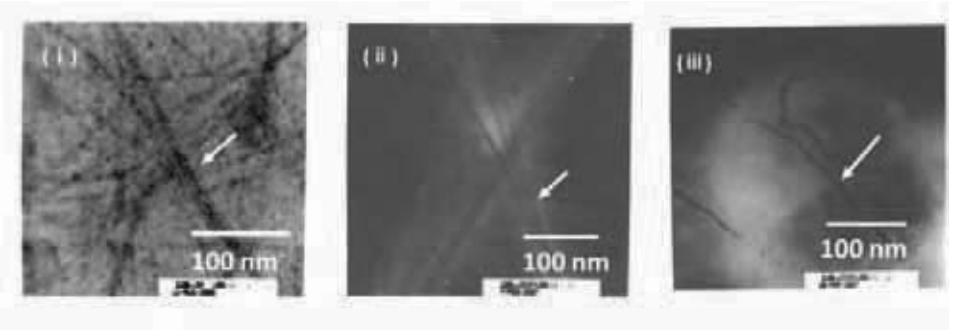

Figure 3. TEM images of fibrous structures formed by (i) *cyclo*(-L-Lys -Gly-)$_3$ and *cyclo*(-L-Glu-Gly)$_3$, (ii) *cyclo*(-L-Lys-D-Ala-)$_3$ and *cyclo*(-D-Glu-L-Ala-)$_3$, and (iii) *cyclo*(-L-Trp-D-Lys-)3$_3$ and *cyclo*(-L-Trp-D-Glu-)$_3$.

hexapeptides were calculated using MOE system based on NMR observation (Data not shown). Estimated formation of peptide nanotubes is consisted with the bundle structure.

Acknowledgements

The help pertaining to TEM measurements by Mr. Noboru Wakayama (Kyushu Institute of Technology, Center for Instrumental Analysis) is gratefully acknowledged.

References

1. Ghadiri MR, Granja Jr, Milligan RA, McRee DE, Khazanovich N. *Nature* **366**: 324-327, 1993.
2. Hartgerink JD, Granja Jr, Milligan RA, Ghadiri MR. *J Am Chem Soc* **118**: 43-50, 1996.
3. Clark TD, Buriak JM, Kobayashi K, Isler MP, McRee DE, Ghadiri MR. *J Am Chem Soc* **120**: 8949-8962, 1998.
4. Rosenthal-Aizman K, Svensson G, Unden A. *J Am Chem Soc* **126**: 3372-3373, 2004.
5. Okamoto H, Yamada T, Miyazaki H, Nakanishi T, Takeda K, Usui K, Obataya I, Mihara H, Azehara H, Mizutani W, Hashimoto K, Yamaguchi H, Hirayama Y. *Japanese Journal of Applied Physics* **44**: 8240-8248, 2005.

7-14-111

Control of duplex formation and columnar self-assembly with heterogeneous amide/urea macrocycles

Fischer , Lucile[1]; Decossas, Marion[1]; Briand, Jean-Paul[1]; Didierjean, Claude[2]; Guichard, Gilles[1,]*

[1]CNRS, Institute of Molecular and Cellular Biology, FRANCE; [2]Université Henri Poincaré, LCM3B, FRANCE

[*]E-mail: g.guichard@ibmc.u-strasbg.fr

Introduction

Owing to their diversity in size and shape, easy access, and biocompatibility, peptides represent versatile units for the construction of H-bonded tubular assemblies and other biomimetic materials with potentially useful applications.[1,2] So-called peptide nanotubes (PNTs) have been obtained through multiple and complementary approaches including the formation of i) hollow β-helices, ii) barrel-hoop motifs from stacked macrocyclic peptides, iii) barrel-stave motifs from rigid-rod peptide conjugates, iv) helical pores from cationic, zwitterionic and dendritic dipeptides and v) large tubes from linear and cyclic amphiphilic peptides. Originally designed from α-peptides made of D- and L-amino acids,[3] flat macrocyclic systems forming cylindrical *β*-sheetlike assemblies have diversified to include oligoamides made from higher amino acid homologs (e.g. *β*-peptides)[4] as well as peptide hybrids (e.g. *α,β*-peptides)[5]. Tubular sheet-like assemblies however are not restricted to oligoamides. The urea group for example which shares a number of features with the amide linkage, i.e. rigidity, planarity, polarity, and hydrogen bonding capacity is an interesting surrogate. We and other have demonstrated that macrocyclic biotic and abiotic *N,N'*-linked oligoureas have a unique propensity to self-organize into polar H-bonded nanotubes.[6] We have now investigated cyclooligomerization of chiral dipeptide-derived building blocks **1** as a general strategy to generate self-assembling hybrid urea/amide macrocycles (**2**). Herein, we show that high level of hierarchical and directional control can been achieved in these systems.

Results and discussion

A series of four enantiopure 14-membered C_2 symmetric macrocycles (**2a-2d**) have been prepared starting from homochiral *N*MeLeu-Leu, *N*MeVal-Val, Pro-Val and Pro-Phe dipeptide sequences, respectively. Single crystals of **2a** and **2b** suitable for X-ray crystallographic analysis were grown by slow evaporation of a solution of acetonitrile and methanol. The crystal structures were solved in the $P1$ and $I4_1$ space groups, respectively. In both structures, the main chain adopts a rectangular shape of 3.8 Å x 4.8 Å. The amide and urea groups are perpendicular to the mean plane of the ring and their carbonyl groups point in opposite directions. By analogy to partially *N*-methylated D,L-*α*-peptides, cyclic urea/amide oligomers self assemble in an antiparallel manner to form H-bonded dimers maintained by a set of four strong H-bonds between urea carbonyls and amide NHs. Both dimers of **2a** and **2b** form columnar stacks parallel to the b-axis and c-axis, respectively, with a mean distance between H-bonded dimers of ca 4.5 Å (Fig. 1a and 1b). Column stabilization in **2b** is essentially driven by weak CH•••O=C bonds between methyl groups and

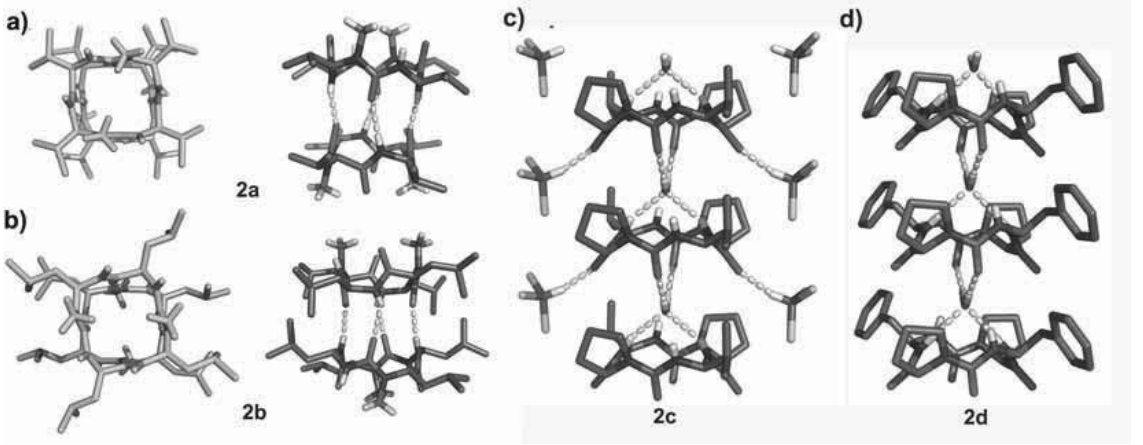

Figure 1. (a,b) Representations of cyclindrical H-bonded dimers of **2a** and **2b**; (c,d) Representations of the crystal structures of **2c** and **2d** showing the bridging water molecules and their binding mode to upper and lower rings.

amide carbonyl of two H-bonded dimers as well as by van der Waals interactions between interdigitated *i*Bu side chains of adjacent columns. A different mode of column stabilization is used in the structure of **2a** where two H-bonded dimers are interconnected by two bridging water molecules.

Susbtituting proline for the *N*-methyl amino acids in urea/amide cyclodimers had dramatic consequences on both ring geometry and self-assembly properties of resulting cyclodimers. Compound **2c** crystallized from $CHCl_3$ in the $P2_12_12$ space group. Crystals of **2c** obtained by slow evaporation of a mixture of acetonitrile and water exhibited the $I4_1$ space group. Both **2c** and **2d** present a very similar rectangular shape of 3.8 Å x 4.8 Å. In contrast to **2a** and **2b**, gem-diaminoalkyl residues in **2c** and **2d** feature negative pseudo Phi angle values and as a result, amide and urea NH-groups are now pointing on one side of the ring, the carbonyl groups being sequestered on the other side. This novel ring geometry in **2c** and **2d** led to the formation of a novel type of columnar arrangement in the crystal (Fig. 1c and 1d). Although backbone-backbone H-bonding is not observed, rings are linked in a parallel orientation via bridging water molecules. Noteworthy, TEM imaging of **2d** revealed another level of hierarchical organization with the formation of well defined tubular nanostructures of 20 nm to 1.2 µm diameter. Herein, we have describeed biotic macrocyclic amide/urea hybrids with partially *N*-alkylated backbones **2** as new candidates for the formation of H-bonded columnar and tubular ensembles. Depending on the level of backbone pre-organization, columnar or tubular arrangements with either *parallel* or *antiparallel* growing modes can thus be selected.

Acknowledgements

This research was supported in part by Centre National de la recherche Scientifique (CNRS), and Agence Nationale pour la Recherche (grant number NT05_4_42848). The authors thank Roland Graff and Lionel Allouche for their assistance with 2D NMR measurements and the "plateforme RIO d'imagerie cellulaire Strasbourg Esplanade" for the use of the TEM.

References

1. Gao X, Matsui H. *AdV Mater* **17**: 2037-2050, 2005.
2. Ulijn RV, Smith AM. *Chem Soc Rev* **37**: 664-665, 2008.
3. Bong DT, Clark TD, Granja Jr, Ghadiri MR. *Angew Chem Int Ed* **40**: 988-1011, 2001.
4. Seebach D, Matthews JL, Meden A, Wessels T, Baerlocher C, McCusker LB. *Helv Chim Acta* **80**: 173-182, 1997.
5. Karle I, Handa BK, Hassall CH. *Acta Cryst* ***B31***: 555-560, 1975.
6. Semetey V, Didierjean C, Briand JP, Aubry A, Guichard G. *Angew Chem Int Ed* **41**: 1895-1898, 2002.

7-17-112

Site-specific labelling of proteins using an engineered intein

Aranko, A. Sesilja; Iwai, Hideo*

University of Helsinki, Institute of Biotechnology, FINLAND

**E-mail: sesilja.aranko@helsinki.fi*

Introduction

Site-specific labelling of proteins is an important mean to study protein functions, interactions, and microenvironment such as structural changes. However, labelling of proteins with any fluorescent label or stable isotope in a site- or region-specific manner is generally challenging and labour-intensive. Protein splicing using inteins is one of promising approaches to explore protein ligation for site-specific labelling. Protein splicing is a post-translational modification in which an intein catalyzes ligation of flanking protein sequences and the concomitant self-excision from the precursor protein. Protein splicing can also take place in *trans*, thereby ligating two separate polypeptide chains by a split intein.[1,2] Thus, protein *trans*-splicing enables protein ligation of diverse protein fragments of interest by fusing them to halves of a split intein. We have engineered a naturally split intein, DnaE intein from *Nostoc punctiforme* (*Npu*),[3] to facilitate protein ligation using synthetic peptides. Here, highly efficient fluorescent labelling of proteins has been demonstrated in a site-specific manner by protein ligation using the newly engineered intein. Moreover, protein *trans*-splicing approach could be extended to dual site-specific labelling using an additional intein.

Site-specific fluorescent labelling using protein *trans*-splicing

*Npu*DnaE intein was engineered to be split at a new site, thereby bearing a short C-terminal intein (IntC), which is appropriate for chemical synthesis. The engineered short C-terminal intein was chemically synthesized with the modification of the side-chain of lysine residue in the C-extein by a dansyl group. Thus, the peptide containing the C-terminal intein was site-specifically labelled with a dansyl (Dns) group by the chemical synthesis. The site-specific Dns-labelling was achieved by mixing the two precursors, namely, the fusion protein of Smt3 and the N-terminal fragment of split *Npu*DnaE intein (H6-Smt3-IntN) and the Dns-labelled peptide containing C-terminal intein (IntC). The fluorescent label was site-specifically attached to the protein of interest (H6-Smt3) by protein ligation upon protein trans-splicing (Fig. 1a).

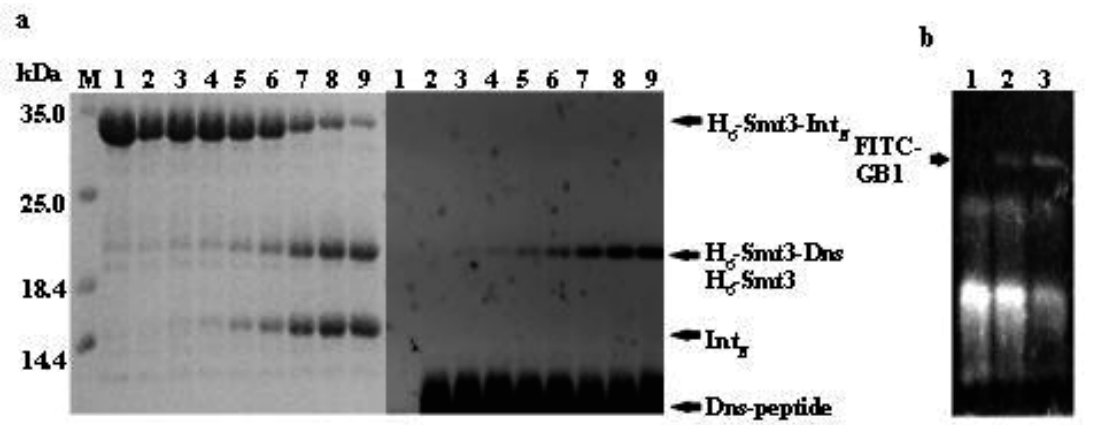

Figure 1. a) C-terminal site labelling. SDS-PAGE analysis confirm the *in vitro* ligation of H6-Smt3-*Npu*DnaE<> and dansyl (Dns)-labelled peptide. Lanes 1–9 indicate the samples collected during *in vitro* ligation. Lane 1, Smt3-*Npu*DnaE-Int<> alone; lanes 2–9, 1 min, 2 min, 10 min, 30 min, 1 h, 2 h, 4 h and 24 hours after starting the reaction, respectively. M indicates molecular mass marker. H6-Smt3-*Npu*DnaE-Int<> , H6-Smt3-Dns, H6-Smt3 and *Npu*DnaE-Int<> are indicated by arrows. b) N-terminal site labelling. *In vitro* ligation of N-terminally modified peptide using split *Ssp*DnaB-Int.5 Lanes 1–3 indicate samples collected. Lane 1, 0 h; lane 2, 4 h; and line 3, 24 hours after starting the reaction, respectively. FITC-labelling of GB1 as the result of ligation is indicated by an arrow. The reactions in a and b were performed at 25 °C and stopped by mixing samples with 1×SDS Buffer. The 18% SDS-PAGE gel was stained with Coomassie Blue (a, left panel). Fluorescent label was visualized by UV-light (a, right panel, and b).

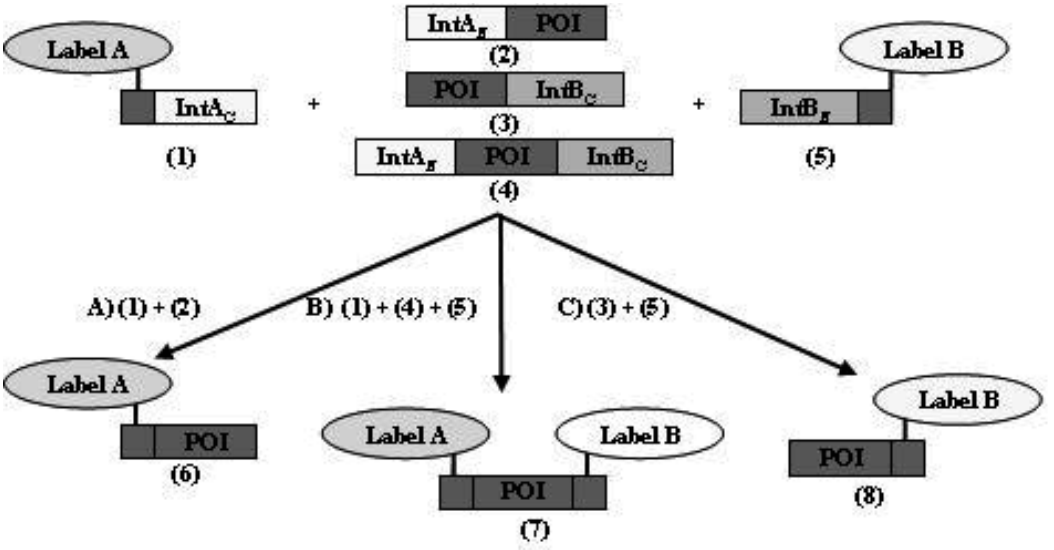

Figure 2. Schematic representation of the principle of site-specific fluorescent labelling of proteins. A) C-terminal labelling. B) Dual labelling. C) N-terminal labelling. POI stands for the protein of interest.

Site-specific dual labelling

Dual labelling could be achieved by protein *trans*-splicing when it is applied with two different inteins. Artificially split *Ssp*DnaB intein was used for the site-specific labeling of the N-terminus of the protein (GB1). The FITC-labelled peptide containing the N-terminal half of the split *Ssp*DnaB was chemically synthesized. The peptide was mixed with the fusion protein containing the C-terminal half of split *Ssp*DnaB and GB1. Upon protein *trans*-splicing, POI was labelled with FITC by protein ligation (Fig. 1b, Fig. 2). Thus, we demonstrated that both N- and C-terminal sites of the proteins could be labelled in site-specific manners. It should be possible to achieve dual-labelling of a protein by combining the N- and C-terminal site labelling demonstrated here.

Conclusions

Site-specific labelling is a valuable tool for studies of protein structure, function, and interactions. Therefore, an efficient and simple method for site-specific labelling of proteins will be of significant importance. Here, we demonstrated site-specific fluorescence labelling of proteins using protein *trans*-splicing. The label can be attached at either an N-terminal or C-terminal side of a protein depending on the split intein used. Site-specific labelling by protein *trans*-splicing is "traceless" as the split intein is removed after protein *trans*-splicing. It is, therefore, suitable for studies of proteins with small chemical probes. Protein *trans*-splicing mediated site-specific labelling is simple to perform and can be achieved at low concentrations. The engineered *Npu*DnaE intein is especially promising for protein labelling due to fast *trans*-splicing reaction and its high yield.

Acknowledgment

This work is supported by the grants from Sigrid Jusélius Foundation, Biocentrum Helsinki, and the Academy of Finland (118385).

References

1. Wu H, Hu Z, Liu X-Q. Protein trans-splicing by a split intein encoded in a split DnaE gene of Synechocystis sp. PCC6803. *Proc Natl Acad Sci U S A*. **95.**: 9226–31, 1998.
2. Paulus H. Protein splicing and related forms of protein autoprocessing. *Ann Rev Biochem* **69**: 447-96, 2000.
3. Iwai H, Züger S, Jin J, Tam PH . Highly efficient protein trans-splicing by a naturally split DnaE intein from Nostoc punctiforme. *FEBS Lett* **580**: 1853-1858, 2006.
4. Muona M, Aranko AS, Iwai, H. Segmental isotopic labelling of a multi-domain protein by protein ligation using protein trans-splicing. *ChemBioChem* **9**: 2958-2961, 2008.
5. Ludwig C, Pfeiff M, Linne U, Mootz HD. Ligation of a synthetic peptide to the N terminus of a recombinant protein using semisynthetic protein trans-splicing. *Angew Chem Int Ed* **45**: 5218-5221, 2006.

7-18-113

Fluorescent agonists for the human vasopressin V_{1b} receptor

Guillon, Gilles[1]; Murat, Brigitte[1]; Corbani, Maithe[1]; Boulay, Vera[1]; Stoev, Stoytcho[2]; Manning, Maurice[2,]*
[1]Université Montpellier I & II, 34094 Montpellier Cedex 5, Institut de Genomique Fonctionnelle, UMR5203-CNRS, U661INSERM, FRANCE; [2]The University of Toledo College of Medicine, Toledo, OH, 43614 USA

[*]E-mail: maurice.manning@utoledo.edu

Introduction

Fluorescent ligands selective for a given receptor family or a given receptor subtype are very useful pharmacological tools for investigating receptor localization and trafficking, receptor molecular structural analysis and developing new receptor-selective high-throughput ligand screening assays. Although many fluorescent V_{1a}, V_2 and OT receptor ligands were discovered,[1,2] to date there are no reported highly selective fluorescent V_{1b} receptor agonists. This is due to the fact that until recently, the design of peptides which are selective for the V_{1b} receptor has proved to be highly elusive. We recently reported that d[Leu^4, Lys^8]VP (A) is the first selective agonist for the rat vasopressin (VP) V_{1b} receptor.[3,4] It was also shown to be less selective for the human V_{1b} receptor due to its relative weak OT/V_{1b} selectivity[5] and Table 1. We now report the synthesis and some pharmacological properties of three fluorescent $hV_{1b}R$ ligands (peptides 1-3), based on modifications of the Lys^8 residue in d[Leu^4, Lys^8]VP (A), with Alexa 488 (peptide 1), Antraniloyl (Atn) (peptide 2) and Alexa 647 (peptide 3).

Results and discussion

The human V_{1b}, V_2 , V_{1a} and OT receptor affinities of peptides 1-3, together with those of their parent analogue d[Leu^4, Lys^8]VP (A)[3-5] are given in Table 1. The addition of the Alexa 488 and Atn fluorophores to d[Leu^4, Lys^8]VP (A) to give d[Leu^4, Lys(Alexa 488)^8]VP (peptide 1), K_i = 1.2 nM and d[Leu^4, Lys(Atn)^8]VP (peptide 2), K_i = 0.65 nM, does not decrease the affinity for the V_{1b} receptor of the parent peptide (A) (K_i = 0.52). By contrast, the addition of the Alexa 647 fluorophore to d[Leu^4, Lys^8] VP (A) to give d[Leu^4, Lys(Alexa 647)^8]VP (peptide 3), K_i = 186 nM, drastically reduced the affinity for the hV_{1b} receptor. This is probably due to the molecular size of the Alexa 647 which is about twice that of Alexa 488. All three fluorescent peptides 1-3 exhibited excellent $V_{1a}R$ /$V_{1b}R$ and V_2R /$V_{1b}R$ selectivities. While fluorescent peptides 1 – 3 exhibit diminished affinities for the hOTR relative to the $hV_{1b}R$, they did not exhibit the same striking gains in $V_{1b}R$/OTR selectivities as for the V_{1a} and V_2 receptors.

Functional experiments were performed in an AtT20 cell line stably transfected with the V_{1b} receptor with d[Leu^4, Lys(Alexa 488)^8]VP (peptide 1). The K_{act} values are as follows: for the parent peptide d[Leu^4, Lys^8]VP (A) K_{act} = 1.3 nM; for AVP K_{act} = 2.2 nM and for d[Leu^4, Lys(Alexa 488)^8]VP (peptide 1) K_{act} = 2.9 nM. These data show that the fluorescent peptide d[Leu^4, Lys(Alexa 488)^8]VP (peptide 1) possesses a K_{act} in the same range as AVP and d[Leu^4, Lys^8]VP (A), which suggests that, as observed for the binding data, the attachment of Alexa 488 fluorophore to d[Leu^4, Lys^8]VP (A) does not modify its K_{act}. Moreover, the maximal phospholipase C activation observed for the fluorescent peptide 1, is similar to those obtained either with AVP or d[Leu^4, Lys^8] VP (A). Thus, the d[Leu^4, Lys(Alexa 488)^8]VP (peptide 1) is a full V_{1b} agonist.

Conclusions

We report here the first fluorescent agonists for the human vasopressin V_{1b} receptor. These peptides were designed by using as a lead our recently discovered highly promising potent and selective V_{1b} agonist d[Leu^4, Lys^8]VP (A)[3-5]. Modification of the Lys^8 residue of (A) with Alexa 488, Antraniloyl (Atn) and Alexa 647 fluorophores resulted in peptides 1 – 3 (Table 1). Addition of Alexa 488 or Atn to d[Leu^4, Lys^8]VP (A) (peptides 1 and 2) does not

Table 1. Fluorescent Agonists for the Human V_{1b} Receptors.

		Affinity (K_i) (nM)			
No.	**Peptide**	**hV_{1b}-R**	**hV_{1a}-R**	**hV_2-R**	**hOT-R**
A	d[Leu^4,Lys^8]VP[a]	0.52	69	6714	29
1	d[Leu^4,Lys(Alexa 488)^8]VP[b]	1.2	258	>10^6	30
2	d[Leu^4,Lys(Atn)^8]VP[b]	0.65	346	>10^6	21
3	d[Leu^4,Lys(Alexa 647)^8]VP[b]	186	>10^6	>10^6	36

[a]Data from references 4,5. [b]This presentation.

statistically modify the affinity of the parent peptide (A) for the $hV_{1b}R$. The addition of Alexa 647 fluorophore to d[Leu^4, Lys^8]VP (A) (peptide 3) significantly reduces its $V_{1b}R$ affinity. All fluorescent peptides (1-3) exhibit moderate affinities for the hOT receptor and very weak affinities for the hV_{1a} and hV_2 receptors. Functional assays with the most promising fluorescent peptide d[Leu^4, Lys(Alexa 488)^8]VP (1) show that it is a full V_{1b} agonist.

In summary, the new fluorescent hV_{1b} receptor agonists presented here promise to be useful tools for the studies on the human V_{1b} receptor. Their value is even greater due to the fact that, to date, no selective radioiodinated ligands for the V_{1b} receptor have been reported. Moreover, fluorescent ligands offer a safer, more powerful and more versatile alternative to radioligands in molecular pharmacology and drug discovery.

Acknowledgements

We thank Ms. Ann Chlebowski for the expert help in the preparation of this manuscript. Supported by NIH Grant GM-25280 and the Institut National de la Santé et de la Recherche Médicale.

References

1. Manning M., Stoev S, Chini B, Durroux T, Mouillac B, Guillon G. *Progress in Brain Res 2008.* Neumann I.D, Landgraf R (Eds), Vol 170, pp 473-512.
2. Albizu L, Teppaz G, Seyer R, Bazin H, Ansanay H, Manning M, Mouillac B, Durroux T. *J Med Chem* **50**: 4976-85, 2007.
3. Pena A, Murat B, Trueba M, Ventura MA, Wo NC, Szeto HH, Cheng LL, Stoev S, Guillon G, Manning M. *J Med Chem* **50**: 835-47, 2007.
4. Pena A, Murat B, Trueba M, Ventura MA, Bertrand G, Cheng LL, Stoev S, Szeto HH, Wo NC, Brossard G, Serradeil-Le Gal C, Manning M, Guillon G. *Endocrinology* **148**: 4136-4146, 2007.
5. Guillon.G, Murat B, Pena A, Trueba M, Wo NC, Szeto H, Stoev S, Cheng LL, Manning M. *Peptides 2006* (Proceedings of the 29th European Peptide Symposium, Gdańsk, Poland). Rolka K, Rekowski P, Silberring J (Eds), Kenes International, Geneva, Switzerland, 2007, pp 742-743.

7-25-114

DNA-peptide interaction forces on the single molecule level

Wollschläger, Katrin[1,]; Gaus, Katharina[1]; Körnig, André[2]; Eckel, Rainer[2]; Wilking, Sven David[1]; Lovas, Zsuzsa[3]; Majer, Zsuzsa[3]; Becker, Anke[4]; Ros, Robert[2]; Anselmetti, Dario[2]; Sewald, Norbert[1]*

[1]Bielefeld University, Organic and Bioorganic chemistry, GERMANY; [2]Bielefeld University, Biophysics and Applied NanoSciences, GERMANY; [3]Eötvös Loránd University, Institute of Chemistry, HUNGARY; [4]Bielefeld University, Genetics, GERMANY

[*]E-mail: katrin.wollschlaeger@uni-bielefeld.de

DNA-protein interactions are a key element in the regulation of cellular processes. Transcription factors are able to recognize their cognate DNA sequences and regulate the expression of proteins. During the last decade, single molecule experiments experienced increasing attention. The specific DNA binding of the transcription factor PhoB from *E. coli* represents a suitable model system. DNA binding of different epitopes of PhoB has been investigated on the single molecule using atomic force spectroscopy (AFM) and with ensemble methods like electrophoretic mobility shift assays (EMSA) and surface plasmon resonance (SPR). Structural information of the DNA-protein complex is obtained using circular dichroism (CD) studies.

Structurally, PhoB belongs to the family of winged helix-turn-helix proteins and controls the expression of genes involved in phosphate metabolism. It is composed of a transactivation domain (amino acids 1-127) and a DNA binding domain (DBD, amino acids 123-229).[1] After phosphorylation of the transactivation domain, the protein binds to specific DNA sequences containing a TGTCA consensus sequence. Structural information of the DBD was derived from available X-ray single crystal and NMR solution structures of the DBD both free and in complex with DNA.[2] Experiments with a PhoB/PhoR deficient strain show that the PhoB DBD without regulatory domain is also able to bind to DNA and to activate transcription.[3] C-terminally modified protein epitopes representing parts of the DNA binding domain of PhoB were

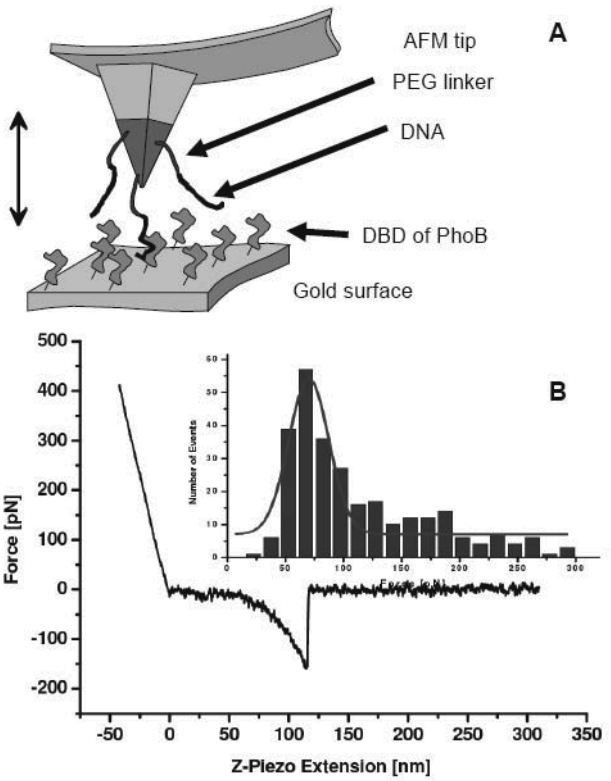

Figure 1. A) Schematic AFM force spectroscopy setup. B) typical AFM single molecule force curve diagram with force histogram (insert).

Table 1. Dissociation rate constant (k_{off}) for the peptide/protein DNA complexes; $\tau = 1/k_{off}$: complex lifetime.

	k_{off} [s^{-1}] peptide PhoB (190-209)	τ [s]	k_{off} [s^{-1}] protein PhoB (127-229)	τ [s]
wildtype	3.1 ± 2.1	0.32	0.0025 ± 0.0021	400
R193A	0.071 ± 0.053	14	0.012 ± 0.008	83
H198A	49.5 ± 21.2	0.020	0.760 ± 0.250	1
R203A	—	—	—	—

chemically synthesized using microwave assisted solid phase peptide synthesis. The binding contributions of peptide PhoB(190-229) are compared to the complete DNA binding domain PhoB(127-229). This protein was purified using intein mediated protein splicing, while an additional cysteine residue was ligated to the protein by intein mediated ligation.[4] Kinetic off-rates were obtained in single molecule dynamic force spectroscopy experiments. In such an experiment the binding partners are covalently bound to either the AFM tip or the surface (Fig. 1A). The dissociation of a DNA-protein complex can be monitored during a cycle when the tip is approached to and retracted from the surface (Fig. 1B). Sequence specific DNA-binding of both peptide and protein was proven in competition experiments with soluble Pho box DNA or soluble PhoB proteins. Such competition experiments employed free wild type peptide PhoB(190-209) as competitor to the wild type protein PhoB(127-229) for binding to the Pho box DNA, which yielded a decreased binding probability of 55%. Alanine scans of strategic residues revealed the contributions of single amino acid residues for peptides and proteins.[4, 5]

The complete loss of affinity to DNA for the peptide and protein mutants R203A demonstrates the importance of this amino acid for DNA-protein interaction. These results were also confirmed using ensemble methods like EMSA and SPR. Structural investigations of the peptides, the proteins and DNA/protein complexes were performed using circular dichroism measurements. The CD spectra show no major differences between the wild type proteins and and corresponding alanine mutants. The CD spectra of the wild type peptide PhoB(190-209) and its alanine point mutants display no differences, while titration with 2,2,2-trifluoroethanol (TFE) indicate a high tendency to form α-helices. Differential CD spectra, calculated by subtracting either the protein or DNA spectra from the protein-DNA complex spectrum, reveal a significant change in the DNA structure but no change in protein structure upon complex formation. In line with NMR and crystal structure analysis, this indicates that the DNA is being bent upon complex formation. According to previous reports, the overall folding of the unbound DNA binding domain is maintained in the complex with only local differences being observed.

Acknowledgment: This project was supported by DFG (SFB 613).

References

1. Makino K, Amemura M, Kawamoto T, Kimura S, Shinagawa H, Nakata A, Suzuki M. *J Mol Biol* **259**: 15-26, 1996.
2. Okamura H, Shinagawa H, Nagadoi A, Makino K, Nishimura YJ. *J Mol Biol* **295**: 1225-1236, 2000.
3. Ellison DW, McCleary WR. *J Bacteriol* **182**: 6592-6597, 2000.
4. Wollschläger K, Gaus K, Körnig A, Eckel R, Wilking SD, McIntosh M, Majer Z, Becker A, Ros R, Anselmetti D, Sewald N. *Small* **5**: 484-495, 2009.
5. Eckel R, Wilking SD, Becker A, Sewald N, Ros R, Anselmetti D. *Angew Chem* **117**: 3989-2993, 2005; *Angew Chem Int Ed* **44**: 3921-3924, 2005.

7-27-115

Hemoglobin peptides in mammalian tissues: facts or artifacts?

Yatskin, Oleg; Karelin, Andrei; Ivanov, Vadim*
Shemyakin-Ovchinnikov Institute of Bioorganic chemistry, Russian Academy of Sciences, RUSSIAN FEDERATION

E-mail: Oleg.Yatskin@mail.ru

In our early papers describing analysis of tissue extracts for endogenous peptides we used the acid extraction procedure in 1 M or 10% acetic acid.[1] Although short time acid extraction procedure at low temperatures is a standard technique for peptide isolation from tissues, this approach does not exclude proteolysis induced by tissue proteases. Moreover, our recent studies[2] demonstrated that rapid pepstatin-dependent hemoglobin degradation in acidified erythrocyte lysate takes place leading to peptides previously reported as endogenous intraerythrocyte components.

In this paper we describe large-scale isolation and identification of rat brain, heart, lung and spleen peptidome components, performed with a special attention to its endogeneity. The extracts were prepared from snap-frozen organs both in the presence and in absence of protease inhibitors (10^{-6} M pepstatin A, 10^{-4} M PMSF, 2 mM EDTA). Peptide pools were isolated using size-exclusion chromatography and analyzed using PR-HPLC and MALDI MS. It was established that the peptide composition (with respect to predominant components) of tissue acid extracts is stable in the presence of protease inhibitors. The absence of inhibitors led to appearance of novel peptides and did not affect the concentration of predominant peptide components detected in samples prepared with protease inhibitors. Therefore, the latter were considered as present in the tissues prior to extraction, i.e. as endogenous.

The majority of predominant peptide components (>80% of endogenous peptides and >65% of extraction artifacts) were found common in the studied tissues. The structures of 105 peptides (both endogenous and artifacts) were established by MS/MS analysis. The predominance of hemoglobin fragments in the tissue peptidome was confirmed (69% of identified endogenous peptides). The set of hemoglobin peptides (N- and C-terminal fragment groups) was found very similar to that isolated from human erythrocytes.[2] The tissue levels of these peptides (up to 10 nmol/g) were estimated as generally exceeding the concentrations of intraerythrocyte ones, so the mechanism of hemoglobin peptide transfer from erythrocytes to tissues still unclear. The endogenous fragments of some other proteins (thymosin, serum albumin, enzymes) were also found in the tissues.

The attempts of other authors to freeze the *in vivo* peptide profile by the microwave irradiation focused on the brain of the living animal[3] were reported to result in dramatic decrease of total peptide content, in significant changes of individual neuropeptide levels, and complete disappearance of previously detected fragments of functional proteins, especially hemoglobin.[4] These changes were ascribed to the rapid (< 90 s) postmortem degradation of tissue proteins being blocked by the protease microwave denaturation. On the basis of these findings, the *in vivo* focused microwave irradiation was suggested as a preferred sample-preparation technique, and all the fragments of tissue proteins were considered as post-sampling artifacts interfering with the neuropeptidomic analysis.[5] We believe that the available data do not always accord with such conclusion and call for a more balanced view.

For example, some hemoglobin fragments were found later in the microwave-irradiated brain tissues by other groups.[6, 7] Second, in a number of reports relatively high (within several hours) stability of tissue peptide material against post-mortem changes has been demonstrated. Finally, the absence of peptide material in the microwaved samples can be explained by reasons other than protease inactivation, such as formation of insoluble peptide-protein aggregates caused by deep denaturation and leading to peptide loss. In general, the problem of peptide formation and degradation in the postmortem tissues requires further detailed study.

It follows from the results obtained that the protease-inactivating measures taken in this work (inhibitors, pH < 3.5) seem sufficient for preventing the in-tissue peptide pattern from changes in the process of tissue homogenization and peptide extraction. At the same time, with respect to endogeneity problem, this approach has obvious limitations. The stability of tissue homogenates in the presence of protease inhibitors was strictly proven only for the predominant (i.e. corresponding to quantifiable HPLC peaks) peptide components. Therefore, the endogeneity of minor (< 10 pmol/g of wet tissue in our case) components cannot be assured in this way and therefore requires further consideration. Nevertheless, basing on the characteristic rates of peptide post-mortem generation or degradation, the presence of predominant (at least, most abundant) peptide components in the protease-inactivated tissue extracts can be reliably extrapolated to the *in vivo* presence in the tissues in comparable concentrations. Generally, one has to accept that the results of peptidomic studies strongly depend on sample preparation procedures involved, such as extraction conditions and primary treatment of peptide fraction. Apparently, there is a growing need for developing a unified approach to sample handling in peptidomic studies that would allow the meaningful

coordination of international efforts in that rapidly growing area.

Acknowledgements

This study was supported by Russian Academy of Sciences Presidium grant “Molecular & Cellular Biology”.

References

1. Karelin AA, Philippova MM, Yatskin ON, Kalinina OA, Nazimov IV, Blishchenko EY, Ivanov VT. Peptides comprising the bulk of rat brain extracts: isolation, amino acid sequences and biological activity. *J Pept Sci* **6**: 345-354, 2000.
2. Ivanov VT, Karelin AA, Yatskin ON. Generation of peptides by human erythrocytes: facts and artifacts. *Biopolymers* **80**: 332-346, 2005.
3. Svensson M, Sköld K, Svenningsson P, Andren PE. Peptidomics-based discovery of novel neuropeptides. *J Proteome Res* **2**: 213-219, 2003.
4. Sköld K, Svensson M, Kaplan A, Björkesten L, Aström J, Andren PE. A neuroproteomic approach to targeting neuropeptides in the brain. *Proteomics* **2**: 447-454, 2002.
5. Svensson M, Sköld K, Nilsson A, Fälth M, Svenningsson P, Andrén PE. Neuropeptidomics: expanding proteomics downwards. *Biochem Soc Trans* **35**: 588-593, 2007.
6. Che FY, Lim J, Pan H, Biswas R, Fricker LD. Quantitative neuropeptidomics of microwave-irradiated mouse brain and pituitary. *Mol Cell Proteomics* **4**: 1391-1405, 2005.
7. Dowell JA, Heyden WV, Li L. Rat neuropeptidomics by LC-MS/MS and MALDI-FTMS: Enhanced dissection and extraction techniques coupled with 2D RP-RP HPLC. *J Proteome Res* **5**: 3368-3375, 2006.

7-28-116

Photoswitchable DNA bis-intercalators — structure and activity

Gaus, Katharina[1]; Wollschläger, Katrin[1]; Zobel, Ansgar[1]; Nieß, Anke[1]; Korff, Gerrit[1]; Juodaityte, Jovita[1]; Kleimann, Christoph[2]; Sischka, Andy[2]; Anselmetti, Dario[2]; Sewald, Norbert[1,]*
[1]Bielefeld University, Organic and Bioorganic chemistry, GERMANY; [2]Bielefeld University, Experimental Biophysics and Applied NanoScience, GERMANY

[*]E-mail: norbert.sewald@uni-bielefeld.de

Triostin A is a naturally occurring quinoxaline depsipeptide antibiotic originally isolated from Streptomyces S-2-210. With its two quinoxaline moieties it bis-intercalates into DNA in a GC selective manner. Triostin A contains the N-methylated amino acids L-valine and L-cysteine. The unmethylated TANDEM binds AT selectively due to a change in the hydrogen bond pattern.[1] Substitution of the disulfide bridge of TANDEM by an azobenzene moiety leads to the photoswitchable analog AzoTANDEM. Peptide synthesis with appropriate protecting groups gives Qxc-D-Ser(Val)-Ala-OtBu, which can be coupled to the photoisomerizable amino acid,[2] 4,4'-Diazendiyldi(*N*-*tert*-butoxycarbonyl)-phenylalanine, to give a linear precursor. Cyclization using pseudo-high dilution results in the bicyclic molecule.

Photoswitchability could be successfully investigated and quantified using UV, CD and NMR spectroscopy as well as HPLC. The trans isomer predominates in the thermodynamic equilibrium, about 80 % of AzoTANDEM are trans-configured at the azobenzene moiety in this state. Irradiation at 350 nm increases the content of the cis isomer considerably, resulting in a photostationary state with approximately 70 % of the cis and 30 % of the trans isomer. If kept in the dark, this state is relatively stable and the thermal equilibration is slow. A ratio of 50 % trans and 50 % cis is only attained after 2 days.

DNA binding studies were carried out using a high precision optical tweezers system for single-molecule detection,[3] which allows the measurement of mechanical properties of DNA molecules without and with binding ligands by stretching a single double-stranded DNA molecule. Unaffected dsDNA produces a characteristic overstretching plateau of 64 pN. Bis-intercalation of binding ligands alters the mechanical properties of DNA complex, which is indicated by vanishing of the overstretching plateau. This could be observed for Triostin A and -DNA. The TANDEM analog had a less pronounced influence on the stretching behavior -DNA.

In order to determine the three-dimensional structure, conformational analysis by NMR spectroscopy in combination with molecular dynamics calculations was performed. In this process, distance restraints were obtained from NMR spectra measured in DMSO-D_6 and applied in distance geometry/simulated annealing calculations, generating 1000 structures. These structures were clustered according to their torsion angles,[4] the central structure of the major cluster was subsequently submitted to restrained molecular dynamics calculations, where the restraints still have to be fulfilled in a time-scale average. After another torsion angle clustering step, unrestrained molecular dynamics calculations were carried out, to obtain a structural proposal. As it is possible to distinguish between cis- and trans-isomer in NMR spectra due to the difference in the chemical shifts, structures of both isomers were investigated.

In TANDEM, the quinoxaline moieties are oriented in parallel to each other and the cyclic backbone is bridged by the disulfide bond on the short side. In contrast, the longer side of the backbone is bridged by the azobenzene moiety in trans configuration of the photoswitchable TANDEM analog. In this isomer, the quinoxaline moieties are closer to each other than in the cis configuration. The backbone is also more flexible for the cis isomer, and the shorter side of the backbone is bridged by the azobenzene moiety. In summary, the introduction of an azobenzene unit significantly changes the conformation of the molecule but brings about photoswitchability. Due to the rigidity of the TANDEM backbone, photo-isomerization has a large influence on the positions of the quinoxaline moieties.

Acknowledgment

This work was supported by the DFG (SFB 613). K. Gaus gratefully acknowledges the financial support (PhD grant) by the International NRW Graduate School of Bioinformatics and Genome Research.

References

1. Addess K J, Sinsheimer J S, Feigon J. *Biochemistry* **32**: 2498-2508, 1992.
2. Juodaityte J, Sewald N. *J Biotechnol* **112**: 127-138, 2004.
3. Sischka A, Tönsing K, Eckel R, Wilking SD, Sewald N, Ros R, Anselmetti D. *Biophys J* **88**: 404-411, 2005.
4. Guthöhrlein E W, Maleševic M, Majer Z, Sewald N. *Biopolymers* **88**: 829-839, 2007.

7-29-117

Melanocollagen type I – structure, obtaining and application

Przybylski, Józef; Rogala, Piotr; Siemaszko-Przybylska, Krystyna*

3-Helisa Ltd, POLAND

**E-mail: jozef.przybylski@3-helisa.pl*

Introduction

This paper presents biologically active nanomelanocollagen obtained from fish skins by means of lactic acid-catalysed hydration according to a patent by J. Przybylski and co-workers; Polish Patent PL190737 and US Patent 7285638 B2.

Biologically active nanomelanocollagen combines the properties of intact collagen in the form of Biopolymers of collagen nanoparticles and melanin nanoparticles.

Structure of biologically active collagen

In the process of our work we realised that collagen is not only produced by vertebrates but by lower organisms like sponges, clams, annelida (earthworms), too.

We realised that the collagen structure theory proposed in scientific literature is not sufficient because nothing is known about the first-order structure and that the higher-order structures are destroyed during preparatory steps before analyses. The amino acid composition of collagen quoted up to date does reflect the reality.

We formulated a new hypothesis concerning the structures of collagen and melanin. We were guided by the following premises:

1. Biosynthesis of collagen takes place in cells that produce and process mostly endogenous amino acids. There are 8–10 of those, according to different sources: Cys, Gly, Asp, Gln, Arg, Glu, Asn, Ala, Cys
2. According to our hypothesis there are only 8 endogenous amino acids in collagen, with cysteine present twice, in positions 1 and 9.
3. The Cys residues are linked via a 1–9 peptide bond. In the position opposite to the formed 1–9 peptide bond there is an Arg residue, while on the left and right of its chain there are Gln and Glu residues. In further positions on both sides there are residues of Asn and Asp, of Gly and Ala, with Cys residues on both C- and N-termini.
4. We calculate that circle has 9xC-C(0,077+0,077) nm=9x0,154nm=1,368nm & 18xC-N(0,077+0,07) nm=18x0,147nm=2,646nm totality=Circle=4,032nm Diameter: 1,284nm

Each subsequent circle is shifted in relation to the previous and next ones by one average -NH-CH(R)-CO- system bond, i.e. by 0,22nm, which corresponds to the angle of 40°.

Figure 1. Hydration.

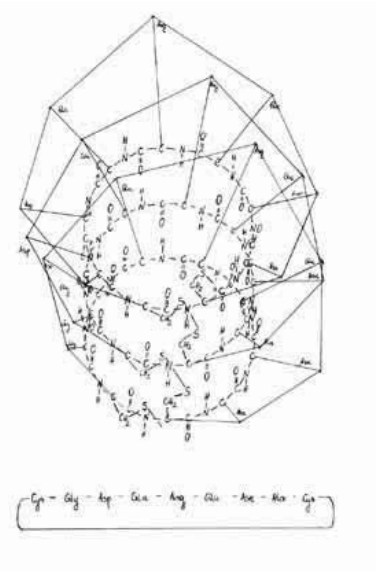

Figure 2. Circle.

The whole of information about biosynthesis and structure of collagen, research procedures and results are available on the website which is inserted in the end of this article.

We would like to emphasise the spatial structure of these proteins and the possibility of destroying their structure by employing improper isolation conditions, as well as usually destructive preparatory conditions

Melanin: its origin and hypothetical structure

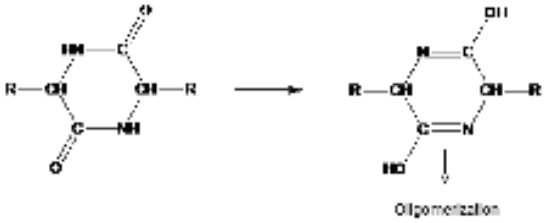

Figure 3. Diketopiperazines.

Electric conductivity for different collagens

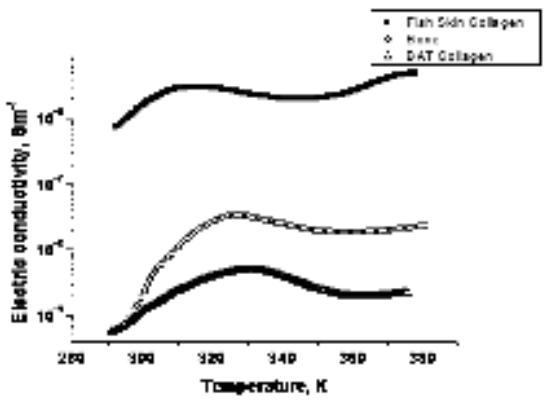

Figure 4. Electric conductivity vs. temperature.

preceding space structure determination. This aspect is underlined, as this may – and often does – lead to experimental results reflecting the properties of degradation products of the system investigated.

Conclusion

1. The lactic acid-catalysed hydration method allows for obtaining collagen and melanin in the form of particles of unaltered spatial structure from natural materials.
2. Nanomelanocollagen obtained by hydration is used:
– in hydrated form: in medicine, *in vivo* and *in vitro* transplantology, cosmetology;
– as film: 3D image generation, computer Science;
– as lyophilizate: in computer Science.
3. Free melanin – nanomelanin, as well as collagen-bound melanin – nanomelanocollagen, find application in neurology, neurosurgery, neurological rehabilitation and computer Science as AI nanoprocessors.
4. Hydration which is presented in this publication is the only effective method to obtain biologically active collagen.

Acknowledgements

We hereby thank our friends for help in conducting some of the experiments
Anna Szaniawska PhD. DSc – professor, v-ce President University of Gdańsk
Maciej Wolowicz PhD. DSc – professor, v-ce Dean Faculty of Oceanology University of Gdańsk
Leszek Kubisz PhD, DSc – professor Medical University of Poznań
Agnieszka Kruszyna MSc. – 3-Helisa Ltd, Gdynia, Poland
Monika Mazik MSc. – 3-Helisa Ltd, Gdynia, Poland
Piotr Przybylski student – Polish Navy Academy, Gdynia, Poland

References

1. Lee CH *et al*. Biomedical application of collagen. Review. *Int J Pharm* **221**: 1–22, 2001.
2. Hervieu GJ *et al*. The distribution of the mRNA and protein products of the melanin-concentrating hormone (MCH) receptor gene, slc-1, in the central nervous system of the rat. *Eur J Neurosci* **12**: 1194–1216, 2000.
3. Francke F *et al*. Immunohistochemical distribution of MIZIP and its co-expression with the Melanin-concentrating hormone receptor 1 in the adult rodent brain. *Mol Brain Res* **139**: 31–41, 2005.
4. Capozzi V, *et al*. Optical and photoelectronic properties of melanin. *Thin Solid Films* **511–512**: 362–366, 2006.
5. Subianto S *et al*. Electrochemical synthesis of melanin free-standing films. *Polymer* **46**: 11505–11509, 2005.
6. Boswell T, *et al*. Recent developments in our understanding of the avian melanocortin system: Its involvement in the regulation of pigmentation and energy homeostasis. Review. *Peptides* **26**: 1733 –1743, 2005.

The full text is available on our website:
http://www.3-helisa.pl/research

7-29-118

2-Alkyl-2-carboxyazetidines as reverse turns inducers when incorporated at (i+2) position of model peptides

Baeza, José Luis[1]; Pérez de Vega, Mª Jesús[1]; Gerona-Navarro, Guillermo[1]; Infantes, Lourdes[2]; García-López, M Teresa[1]; Gónzález-Muñiz, Rosario[1]; Martín-Martínez, Mercedes[1,]*

[1]CSIC. Juan de la Cierva 3, 28006 Madrid, Instituto de Química Médica, SPAIN; [2]CSIC. Serrano, 119, 28006 Madrid, Instituto de Química Física "Rocasolano", SPAIN

[*]E-mail: mercedes@iqm.csic.es

Introduction

Reverse turns, γ and β, are defined as tri (γ) and tetrapeptide (β) sequences that give rise to a reversal in the peptide chain, and which are frequently stabilized by an H-bond between the CO of the first residue and the NH of the last one. Turns have been shown to be relevant in biomolecular recognition events, and turn-like hot-spots have been found within several peptide-protein and protein-protein interaction surfaces.[1,2] Thus, there is an interest in developing scaffolds able to mimic or induce these types of secondary peptide structure.

We have previously described that the skeleton of 2-alkyl-2-carboxyazetidine is able to induce γ-turns when incorporated at the i+1 position of model peptides,[3] whereas Pro tends to be at this position in type I and II β-turns.[4] On the other hand, several studies have shown that type VI β-turns are favoured when Pro residues are at the i+2 position and the preceding amide bond is in a *cis* conformation.[4] As part of our studies on azetidine-2-carboxilate derivatives, we report the conformational behaviour of the azetidine restricted amino acids when incorporated at the i+2 position of model peptides (R^3-CO-Ala-Azx-NH-R^2), and the comparison with the corresponding peptides incorporating Pro or α-MePro.

Results and discussion

The synthesis of model peptides **6**-**10** was carried following standard procedures for the preparation of peptides in solution (Scheme 1).

Molecular dynamic were performed with the simplest derivatives **6a**,**b** using AMBER as the force field. These studies shown that the 2-carboxyazetidines preferentially induce γ-turns, with the characteristic $CO^{i+1\cdots}HN^{i+3}$ H-bond, and with the dihedral angles corresponding to an inverse γ-turn. β-Turn-like conformations are also observed, but they are present in lower number and higher energy compared with γ-turn ones.

Conformational studies of these peptides in solution were obtained from ^{1}H-NMR experiments. In particular, Ala-Azx *trans*-conformers of peptides incorporating 2-alkyl-2-carboxyazetidines at the i+2 position, **6b**,**c**, **7b**,**c** and **8c**, have absolute values of the temperature coefficients of the NH-Me amide protons lower than 3 ppb/K, indicative of their involvement in intramolecular H-bonds (γ- or β-turn-like conformations). On the contrary, none of the amide protons of neither the *trans* isomers of peptides incorporating Pro and α-MePro, **9** and **10**, nor those having an Azg residue, **6a** and **7a**, are involved in H-bonds. Concerning the *cis* isomers of

Scheme 1

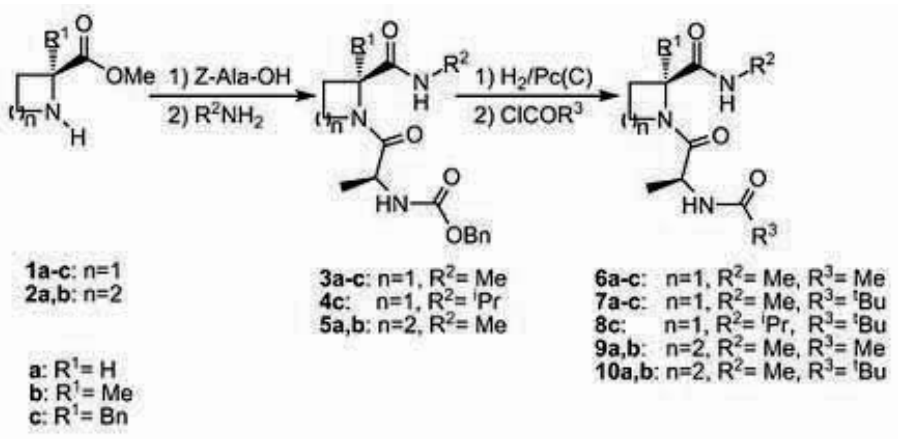

peptides **6**-**10**, only Pro-derived compound **10a** might have an H-bond characteristic of a β-turn conformation.

The crystal structure of Piv-Ala-(*S*)-Azf-NH^{i}Pr (**8c**) have been solved by X-ray diffraction studies and, in agreement with the molecular modelling studies, shows an intramolecular H-bond between the CO(Ala) and the HN-^{i}Pr, characteristic of a γ-turn conformation. Fig. 1 shows a dimer of two molecules of **8c** stabilized by an intermolecular H-bond between the NH(Ala) of one monomer and the oxygen of the CO(Ala) group of the other.

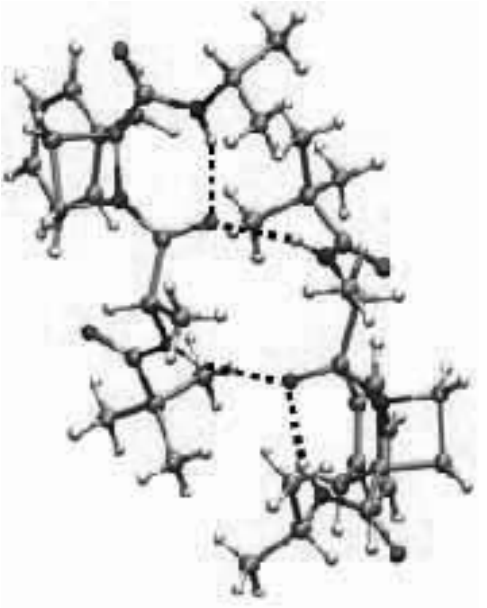

Figure 1

In conclusion, the 2-alkyl-2-carboxyazetidine skeleton, when incorporated into short peptide sequences, prompted them to adopt γ-turn conformations. It is worth to point out the positive influence of the 2-alkylation of the azetidine nucleus upon the capacity to promote these conformations. Thus, 2-alkyl-2-carboxyazetidines could be useful chemical tools to study the bioactive conformation of biologically relevant peptides.

Acknowledgments

This work has been supported by the CICYT (SAF 2006-01205). J.L.B. is a predoctoral fellow from the Spanish Ministry of Education and Science.

References

1. Tyndall JDA, Tyndall JD, Pfeiffer B, Abbenante G, Fairlie DP. *Chem Rev* **105**: 793-826, 2005.
2. Panasik N Jr, Fleming PJ, Rose GD. *Protein Sci.* **14**: 2910-2914, 2005.
3. Baeza JL, Gerona-Navarro G, Pérez de Vega MJ, García-López MT, Gónzález-Muñiz R, Martín-Martínez M. *J Org Chem* **73**: 1704-1715, 2008.
4. Guruprasad K, Rajkumar S. *J Biosci* **25**: 143-156, 2000.
5. Nomenclature proposed for our azetidine containing derivatives: the first two letters (Az) indicate the azetidine ring while the third letter is the one letter symbol for the corresponding amino acid. Azg: azetidine-2-carboxylate (Gly-derived azetidine), Aza: Ala-derived azetidine, Azf: Phe-derived azetidine, and Azx indicates an azetidine containing any amino acid side-chain at position 2.

7-07-119

Determining the location of antimicrobial peptides inside lipid bilayers by combined fluorescence spectroscopy and molecular dynamics simulations

Stella, Lorenzo; Bocchinfuso, Gianfranco[1]; Grande, Giacinto[1]; Orioni, Barbara[1]; Venanzi, Mariano[1]; Kim, Jin-Young[2]; Park, Yoonkyung[2,3]; Hahm, Kyung-Soo[2,3]; De Zotti, Marta[4]; Formaggio, Fernando[4]; Toniolo, Claudio[4]; Palleschi, Antonio[1]*

[1]*Department of Sciences and Chemical Technologies, University of Rome "Tor Vergata", 00133 Rome, ITALY*
[2]*Research Center for Proteineous Materials, Chosun University, 501-759 Gwangju, KOREA*
[3]*Department of Cellular Molecular Medicine, Chosun University, 501-759 Gwangju, KOREA*
[4]*Institute of Biomolecular Chemistry, Padova Unit, CNR, Department of Chemistry, University of Padova, 35131 Padova, ITALY*

**E-mail: stella@stc.uniroma2.it*

Introduction

Several bioactive peptides, such as antimicrobial, cell-penetrating or fusogenic peptides, exert their biological function by interacting with cellular membranes. Therefore, structural data on the location of these molecules inside lipid bilayers are very important for a detailed understanding of their mechanism of action. Fluorescence spectroscopic methods are particularly suited to the study of peptide-membrane association, but give only low-resolution information on peptide position in the lipid bilayer. Molecular dynamics (MD) simulations, on the other hand, can provide a very detailed picture of the peptide-membrane interaction, but need to be validated by quantitative comparison with experimental data. We applied several fluorescence approaches, together with MD simulations, to study two very different antimicrobial peptides: PMAP-23, a member of the cathelicidin family and the lipopeptaibol trichogin GA IV.

PMAP-23 is an amphiphilic cationic peptide, 23-residue long. Trichogin is only 10 amino acid residue long, neutral and very hydrophobic. Both peptides are helical when associated to membranes, with an amphiphilic arrangement of the side chains. To perform the spectroscopic studies, a variety of peptide analogues containing a single fluorophore were synthesized. In all cases, their membrane-perturbing activities were comparable with those of the parent peptides, suggesting that they can be considered reliable model systems.

Results and Discussion

Fluorescence spectra, depth-dependent quenching experiments, and peptide-translocation assays were employed to determine the location of the two peptides inside lipid bilayers, in particular as a function of the peptide/lipid ratio. Trichogin undergoes a cooperative

PMAP-23	RIIDLLWRVRRPQKPKFVTVWVR
PMAP-W7	RIIDLLWRVRRPQKPKFVTVFVR
PMAP-W21	RIIDLLFRVRRPQKPKFVTVWVR
Trichogin	Oct-UGLUGGLUGI-Lol
F0	**Fmoc**-UGLUGGLUGI-L-OMe
F10	Oct-UGLUGGLUG-**Dab(Fmc)**-L-OMe
A3	Oct-UG-**Aal**-UGGLUG-**Dab(Boc)**-L-OMe

* U = Aib = α-aminoisobutyric acid; Oct = n-octanoyl; Lol = L-leucinol; OMe = methoxy; Fmoc = fluorenyl-9-methyloxycarbonyl; Dab=2,4-diaminobutyric acid; Fmc = fluorenyl-9-methylcarbonyl; Aal = β-(1-azulenyl)-alanine; Boc=tert-butyloxycarbonyl.

transition, driven by peptide concentration, from an inactive state, where the peptide is monomeric and parallel to the membrane surface, to an active species, where trichogin is aggregated and inserted into the bilayer.[1] This peptide can diffuse through the membrane even at concentrations where it is not perturbing the bilayer permeability. Furthermore, it does not modify membrane order (e.g., as indicated by the lack of effects on the thermotropic lipid phase transition) at all concentrations investigated. PMAP-23, on the other hand, remains associated to the membrane surface at all concentrations considered, is not able to translocate across the bilayer at concentrations below its activity threshold, and induces a strong perturbation in the membrane order, broadening the gel to liquid-crystal phase transition.

MD simulations were performed by a "minimum bias" approach, starting from a random mixture of one peptide molecule, 128 lipids and more than 5000 water molecules, and following the spontaneous self-assembly of the lipid bilayer, which took place in approximately 100 ns. Two independent simulations were performed for each peptide, with comparable results. The final membrane-bound 3D-structure of both peptides was in quantitative agreement with the position of the fluorescent labels determined by depth-dependent quenching experiments. PMAP-23 caused a significant perturbation of the membrane, by forcing the insertion of charged lipid polar heads in the apolar portion of the membrane and by displacing several lipid molecules from the membrane leaflet to which it was associated. By contrast, the surface-bound state of trichogin did not cause any significant effects on lipid order or on the distribution of phospholipid molecules between the two lipid layers. Interestingly, an additional simulation, with the trichogin molecule positioned in a transmembrane orientation, indicated that the peptide might be able to distort the bilayer in order to span it from one side to the other, despite its relatively short main-chain length.

Overall, coupled fluorescence experiments and MD simulations provide a clear insight into the mechanism of action of these two antimicrobial peptides, and allowed a clear-cut differentiation between their different mechanisms of action. In the two case studies, all available data suggest a carpet-like mechanism for the cationic peptide PMAP-23, while a barrel-stave model for the hydrophobic lipopeptaibol trichogin.

Acknowledgements

This project was supported by the Italian Ministry of Foreign Affairs, the Italian Ministry of University and Research (PRIN 2006) and by the Korean Ministry of Science and Technology (MOST). Computational resources were kindly made available by the Fermi and CASPUR Research Centers (Rome).

References

1. Stella L, Mazzuca C, Venanzi M, Palleschi A, Didonè M, Formaggio F, Toniolo C, Pispisa B. *Biophys J* **86:** 936-945, 2004; Mazzuca C, Stella L, Venanzi M, Formaggio F, Toniolo C, Pispisa B. *Biophys J* **88:** 3411-3421, 2005; Gatto E, Mazzuca C, Stella L, Venanzi M, Toniolo C, Pispisa B. *J Phys Chem B* **110:** 22813-22818, 2006.

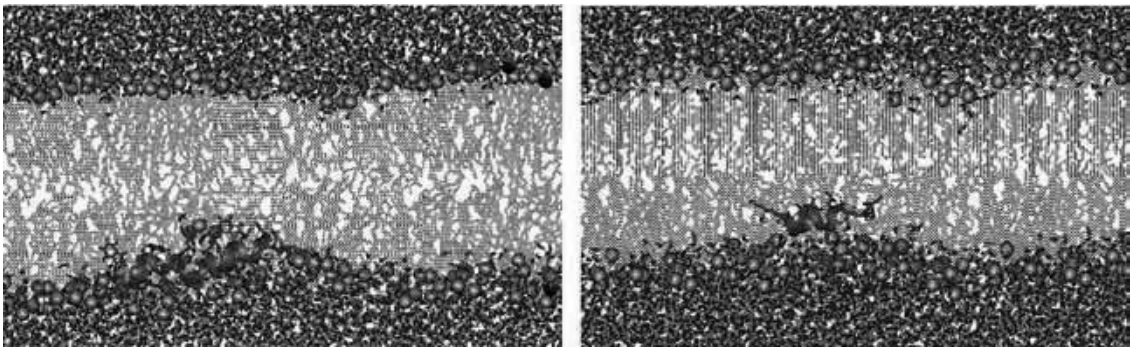

Figure 1. Structures of the membrane-associated peptides at the end of the simulations. Left panel: PMAP-23 in a POPC/POPG 2:1 bilayer; right panel: trichogin GA IV in a POPC membrane.

Alphabetical index of authors